

The neglected goat: a methodological approach to the understanding of the role of this species in English medieval husbandry

Lenny Salvagno

**A thesis submitted for the degree of
Doctor of Philosophy**

Department of Archaeology
University of Sheffield

December 2015

Abstract

The study of the goat has been largely disregarded by British archaeologists, partly because there is a methodological problem related to the difficulty of distinguishing goat remains from those of the more common sheep, and partly because the relative rarity of this species during the Middle Ages has contributed to the perception that this animal was not important.

Despite the fact that different methodological approaches have been proposed, problems still affect our ability to correctly differentiate sheep and goat bones. The most commonly used approach relies on morphological traits that have been established by analysing goat specimens from many different parts of the world, and not all of them may necessarily apply to British populations. In addition, these criteria are based on morphological differences whose assessment may be highly subjective.

The development of a more objective methodology is of paramount importance in order to address the various historical and archaeological questions concerning the role of the English medieval goat. For instance, why is the goat commonly recorded in the Domesday Book when it appears to be so scarce in the contemporary archaeological record? Is it under-represented in the archaeological record or over-represented in the Domesday Book? Why is the goat, when identified in English medieval animal bones assemblages, almost exclusively represented by horncores?

This study provides a new methodology that is based on a combination of two approaches: morphological and biometric. Through the study of modern reference material, a short-list of reliable morphological criteria has been defined and a new biometrical approach focused on translating, whenever possible, morphological differences into Biometrical Indices, has been tested for a variety of mainly post cranial bones. This has permitted the development of a more objective tool for the assessment of archaeological sheep/goat identification. The new protocol has then been then applied to three English sheep and goat medieval assemblages so that a reassessment of the role this animal played in the Middle Ages could be carried out. The results obtained have confirmed what many researchers have previously observed: the goat was not a very common animal. When identified, it is mainly represented by horncores, which are more numerous than those of the sheep; when postcranial bones are considered, sheep by far outnumber goat. It is likely that the abundance of goat horns is a consequence of an international trade in goat skins (containing horns) while only a relatively small number of goats lived on British soil, probably to be used for small scale household consumption.

A mia zia Lucy

(to my aunty Lucy)

e a tutti quelli che hanno sempre creduto e credono in me.

(and to all those who have believed and still believe in me)

Acknowledgements

The completion of this project would not have been possible without the help of a number of amazing people - colleagues and friends - who have supported me throughout this journey. Useful advice, great references and fruitful discussions on relevant topics, as well as words of encouragement, have all contributed to making this experience very special.

First and foremost, my most deep gratitude goes to my supervisor Umberto Albarella. He made me feel part of the group from the beginning and believed in me throughout out the PhD journey. He has been a very caring, supportive and dedicated supervisor. I never felt abandoned, neglected or lost. Umberto has my admiration not only because he is a great zooarchaeologist and academic but also because he is a great moral example. I have never met such a principled person.

A thank you also goes to my second supervisor Hugh Willmott who has been a great support and has offered useful advice.

Many people at a number of institutions arranged access to modern and archaeological collections and their contributions have made my study visits truly unique:

In Portsmouth, thanks go to Polydora Baker and Fay Louise who provided access to the Fort Cumberland English Heritage sheep and goat modern collection, from which the bulk of my modern sheep data comes. They also provided me with some unpublished sheep and goat data, which have been useful for my research.

In Cardiff, a big thank you goes to Peter Howlett who made the English goat collection of Barbara Noddle hosted at the National Museum of Wales available to me.

In York, I am grateful to Terry O'Connor who gave me access to the sheep and goat skeletons hosted at the Zooarchaeology Laboratory of the University of York.

In Germany, a big thank you goes to Renate Schafberg who opened the doors of the amazing Julius Kuhn Museum in Halle to me, where I gathered most of my modern goat data (and could touch original notes written by Boessneck!).

Again in Germany, but this time at the Institute of Zoology at the University of Kiel, I would like to thank Cheryl Makarewicz and Renate Lücht who gave me access to the German sheep and goat specimens they have.

Regarding the archaeological material, thanks go to Tim Thorpe, Oliver Bone and Dayna Woolbright who have given me access to the animal bones assemblage from King's Lynn and helped me sort out chronology problems.

In Lincoln, I am grateful to Antony Lee who has granted me access to the huge animal bone assemblage from Flaxengate and has patiently helped me to select the boxes for the contexts I was interested in.

In Northampton, a thank you goes to Paul Robinson who has given me access to the animal bone assemblage from Woolmonger Street/Kingswell Street and to Jim Brown and Iain Soden who gave me useful information to sort out chronology issues.

Finally, a big thank you goes to Christopher Grimbley, the technician of the University of Sheffield, who took care of all the journeys to pick up and return the archaeological material I have studied.

A number of other people have contributed, at different stages of my research, to make the PhD experience even more unforgettable, as such I would like to thank:

Simon Davis, who provided me with interesting papers, useful discussions on my results and fruitful suggestions.

All the tutors at MASH (Maths and Statistics help), of the University of Sheffield, and in particular Ellen Marshall who patiently helped me with the statistical parts of my research and answered the countless questions I had, even though statistics applied to archaeology was out of her comfort zone. Thanks also go to Jean Russell who helped me at the very beginning with the explorative statistical analysis.

A huge thank you also goes to all past and present members of the Zooarchaeology Laboratory at the Department of Archaeology, University of Sheffield. You have been a great team to work with and a constant source of encouragement and inspiration. In particular, a special thank you goes to Claudia Minniti and Beatrice Pertini Vacca who welcomed me when I arrived, to Lizzie Wright and Angela Trentacoste, who always had a nice word of encouragement, to Silvia Valenzuela Llamas, Kim Vickers, Sarah Viner-Daniels, Idoia Grau and Hannah Russ, who have always made their experience available to me, but also to Giorgos Kazantzis, Laura Llorente, Marian Galindo, Cristina Barrachina and Jane Ford with whom I have shared laughs and concerns.

Many people have crossed my path in Sheffield and some of them have contributed to making me a different and better person. Veronica Velazques. You have been a very good friend, a fun

person to be around and a constant source of encouragement. The days we spent in Sheffield together are those which I remember with most joy. Pablo Silva Rodriguez. Pablo you have been an amazing flatmate and a very precious friend, the memories of our beer together and morning pancakes will always accompany me. Siba Ayyubb. Siba, I enjoyed your company so much! I hope we will meet again for a pizza and a horror movie for the sake of the old times. Also: Nadja Barkova, Marcia Vera, Isabelle Solange, David Mennear, Vanessa Campanacho, and Chris Shimwell. Thank you all for sharing with me your time and being such loving and caring friends!

A special thank you goes also to Neya Willmott. Neya, thank you for your time, your laughs, your advice and your lovely company.

I am also grateful to Roberta Montesana who has shared with me frustrations, hate, love, desperation, laughs, songs, coffees and much more. Your support and understanding has been precious to me.

I would also like to thank all my Italian students who have always been very interested in my research and have always been incredibly supportive. Among those: Julia Kaye, Sharon Hannaford, Mary Chenoweth, Sally Green, Patricia Stubbs, Rona Treeby and Elsa Lucas.

Other people have supported me from Italy and should not be forgotten. First of all, Umberto Tecchiati, my former supervisor but also precious colleague and friend. He has always encouraged me to continue with zooarchaeology and to take paths which I did not consider before. I thank you Umberto for having been consistently present in my life despite distances and, above all, to have been so wise to suggest me to leave Italy for another country, where I could grow and develop as a researcher.

It would not have been thinkable for me to undertake a PhD in England if it had not been for the support of my family and in particular of my parents Laura and Alfredo. Thank you mum and dad, for having been such good parents and inspiring examples. You have always encouraged me to follow my dreams even though this meant to live in another and ‘far away’ country.

Finally, a special mention must go to Phillip, my boyfriend, to whom I owe my deepest gratitude. He has been supporting me emotionally through this experience and has always been there when I needed. He knows about English medieval goats as much as I do! Phill, I will never be grateful enough for your support.

This project was made possible through a Scholarship given by the Arts and Humanities Research Council (AHRC) and a Faculty Post-Graduate Scholarship from the University of Sheffield. In addition, a number of smaller grants were received to assist me with the costs of

data collection trips and participation in several conferences. These, were received from the AHRC and Learned Societies (through the University of Sheffield).

List of Contents

ABSTRACT	I
ACKNOWLEDGEMENTS	V
LIST OF TABLES	XIII
LIST OF FIGURES	XXXI
CHAPTER 1 INTRODUCTION AND BACKGROUND	1
1.1 RESEARCH QUESTIONS AND THESIS STRUCTURE	1
1.1.2 <i>Description of the structure of the thesis</i>	3
1.2 TAXONOMY	4
1.3 METHODOLOGICAL BACKGROUND	5
1.3.1 <i>Morphological approach</i>	6
1.3.1.1 Post-cranial bones	6
1.3.1.2 Mandibular teeth	15
1.3.2 <i>Non morphological approaches</i>	19
1.3.3 <i>Biometrical approach</i>	21
1.3.4 <i>Conclusions</i>	27
1.4 THE MEDIEVAL ENGLISH GOAT: SETTING THE SCENE.....	28
1.4.1 <i>The historical evidence for the medieval goat</i>	29
1.4.2 <i>Zooarchaeological evidence for the medieval goat</i>	31
CHAPTER 2 STUDY OF THE MORPHOLOGICAL TRAITS AND BIOMETRY OF THE MODERN MATERIAL	41
2.1 METHODS	41
2.1.1 <i>Introduction</i>	41
2.1.2 <i>Morphological Approach</i>	42
2.1.3 <i>Biometrical approach</i>	66
2.1.4 <i>The Recording Protocol</i>	83
2.2 MATERIALS	85
2.3 INTER-OBSERVER ERROR AND INTRA-OBSERVER ERROR: CONSISTENCY TESTS	94
2.3.1 <i>Reliability Tests</i>	97
2.3.2 <i>Inter-Observer Error: Inter Correlation Coefficient</i>	106
2.3.3 <i>Intra-Observer Error: Inter Correlation Coefficient</i>	116
2.3.4 <i>Conclusions</i>	122
2.4 MORPHOLOGICAL RESULTS.....	124
2.4.1 <i>Reliability of the morphological diagnostic traits</i>	124

2.4.2 Influence of sex.....	152
2.4.3 Influence of age.....	179
2.4.4 Conclusions.....	205
2.5 BIOMETRIC RESULTS	210
2.5.1 Descriptive Statistics	210
2.5.2 Bivariate plots	217
2.5.3 Allometric shape analysis as expressed by Biometrical Indices.....	253
2.5.4 Statistical Analyses: Mann Whitney U test and Multivariate Approaches.....	273
2.5.5 Mann Whitney U-test and Manova	274
2.5.6 Discriminant Analysis	279
2.5.7 Principal Component Analysis	317
2.5.8 Conclusions.....	361
2.6 DISCUSSION OF THE STUDY OF THE MODERN MATERIAL: MORPHOLOGICAL AND BIOMETRICAL APPROACH	364

CHAPTER 3 REEVALUATION OF THE ROLE OF THE GOAT IN MEDIEVAL ENGLAND 369

3.1 THE ARCHAEOLOGICAL SITES	369
3.2 KING'S LYNN (1050-1800 AD).....	371
3.2.1 Introduction.....	371
3.2.2 Archaeological Investigations	371
3.2.3 Activities at King's Lynn.....	374
3.2.4 What does the zooarchaeological evidence say?.....	375
3.2.5 Reevaluation of King's Lynn sheep/goat bone material: methodology	378
3.2.6 Morphological Approach: Results	379
3.2.7 Shape analysis as expressed by Biometrical Indices.....	384
3.2.8 DA predictions of the sheep/goat assemblage from King's Lynn	447
3.2.9 Discriminant Analysis on the King's Lynn material in toto	503
3.2.10 Discussion.....	529
3.2.10.1 An assessment of the new methodology	530
3.2.10.2 The King's Lynn case study	536
3.3 MEDIEVAL AND POST-MEDIEVAL FLAXENGATE (C. LATE 11 TH CENTURY; LATE 14 TH - MIDDLE 16 TH CENTURY AD)	538
3.3.1 Introduction.....	538
3.3.2 Archaeological Investigations	539
3.3.3 What does the zooarchaeological evidence say?.....	540
3.3.4 Reevaluation of Flaxengate sheep/goat bone material: methodology.....	542
3.3.5 Morphological Approach: Results	542
3.3.6 Shape analysis as expressed by Biometrical Indices.....	545
3.3.7 Discriminant Analysis	581
3.3.8 Discussion.....	609
3.3.8.1 An assessment of the new methodology	610
3.3.8.2 The Flaxengate case study	614

3.4. WOOLMONGER /KINGSWELL STREET, NORTHAMPTON (c. 1000-1550 AD)	615
3.4.1 Introduction	615
3.4.2 Archaeological Investigations.....	616
3.4.3 Trade activities at Northampton	619
3.4.4 What does the zooarchaeological evidence say?	620
3.4.5 Reevaluation of Woolmonger/ Kingswell Street sheep/goat bone material: methodology...	623
3.4.6 Morphological Approach: Results.....	623
3.4.7 Shape analysis as expressed by Biometrical Indices	627
3.4.8 Discriminant Analysis.....	673
3.4.9 Discussion	700
3.4.9.1 An assessment of the new methodology	701
3.4.9.2 The Woolmonger/Kingswell Street case study.....	706
3.5 DISCUSSION OF THE APPLICATION OF THE NEW METHODOLOGY ON ARCHAEOLOGICAL ASSEMBLAGES.....	707
3.6 REASSESSMENT OF THE ROLE OF THE GOAT IN MEDIEVAL ENGLISH HUSBANDRY AND ECONOMY: A BEGINNING.	711
3.7 FUTURE DEVELOPMENTS: THE WAY IS PAVED	715
CHAPTER 4 CONCLUSIONS	717
REFERENCES	725
APPENDICES	741
APPENDIX I: THE IMPORTANCE OF THE GOAT IN THE HUMAN PAST	741
1.1 THE DOMESTICATION OF THE GOAT: BACKGROUND, DYNAMICS, PLACE AND TIME	741
1.2 THE WILD PROGENITOR OF THE DOMESTIC GOAT.....	743
1.3 DIFFERENCES AND SIMILARITIES WITH THE SHEEP	744
APPENDIX II: BLAND AND ALTMAN PLOTS AS INTEGRATION OF THE ICC (INTER-OBSERVER ERROR)	747
APPENDIX III: DESCRIPTIVE STATISTICS FOR THE MODEN SHEEP AND GOAT MATERIAL	793
APPENDIX IV: ASSUMPTIONS FOR DISCRIMINANT ANALYSIS AND PRINCIPAL COMPONENT ANALYSIS	857
APPENDIX V: PRINCIPAL COMPONENT ANALYSIS: BRIEF GLOSSARY	859
APPENDIX VI: DISCRIMINANT ANALYSIS: HOW TO USE IT TO PREDICT NEW ARCHAEOLOGICAL CASES.....	861
RAW DATA (CD).....	INSIDE BACK COVER

List of Tables

TABLE 1.1 LIST OF SPECIES OF <i>CAPRA</i> WITH THEIR COMMON NAME.....	5
TABLE 1.2 LIST OF THE MAJOR STUDIES ON THE TOPIC WITH A BRIEF DESCRIPTION OF SAMPLE USED, THE ANATOMICAL ELEMENTS CONSIDERED, THE MORPHOLOGY AND/OR BIOMETRY APPROACHES ADOPTED.	14
TABLE 1.3 ELEMENTS, INDICES AND SUMMARY RESULTS FROM FERNÁNDEZ (2001).	24
TABLE 1.4 NUMBERS OF GOAT FLOCKS AS REPORTED BY THE DOMESDAY BOOK (IMAGE REPRINTED FROM DARBY, H.C. <i>DOMESDAY ENGLAND</i> , COPYRIGHT 1977, CAMBRIDGE: CAMBRIDGE UNIVERSITY PRESS, WITH PERMISSION FROM CAMBRIDGE UNIVERSITY PRESS).	30
TABLE 2.1 REFERENCE FOR THE MORPHOLOGICAL TRAITS CHOSEN FOR THIS STUDY.....	44
TABLE 2.2 MORPHOLOGICAL CHARACTERISTICS ADOPTED FOR THE HORNCORE (TRAIT 1: IMAGE REPRINTED FROM SCHMID, E. <i>ATLAS OF ANIMAL BONES: FOR PREHISTORIANS, ARCHAEOLOGISTS AND QUATERNARY GEOLOGISTS</i> . AMSTERDAM: ELSEVIER, COPYRIGHT 1972, BY PERMISSION OF JOERG SCHIBLER. TRAIT 2: IMAGES REPRINTED FROM BOESSNECK, J. OSTEOLOGICAL DIFFERENCES BETWEEN SHEEP (<i>OVIS ARIES</i> LINNÉ) AND GOAT (<i>CAPRA HIRCUS</i> LINNÉ). IN <i>SCIENCE IN ARCHAEOLOGY: A SURVEY OF PROGRESS AND RESEARCH</i> , EDS. D. BROTHWELL AND E. HIGGS, 331-358, COPYRIGHT 1969. LONDON: THAMES AND HUDSON, WITH PERMISSION FROM THAMES AND HUDSON).....	45
TABLE 2.3 MORPHOLOGICAL CHARACTERISTICS ADOPTED FOR THE 3 RD DECIDUOUS PREMOLAR (IMAGES REPRINTED FROM PAYNE, S. MORPHOLOGICAL DISTINCTIONS BETWEEN THE MANDIBULAR TEETH OF YOUNG SHEEP, <i>OVIS</i> , AND GOATS, <i>CAPRA</i> . <i>JOURNAL OF ARCHAEOLOGICAL SCIENCE</i> 12: 139-147, COPYRIGHT 1985, WITH PERMISSION FROM ELSEVIER).	46
TABLE 2.4 MORPHOLOGICAL CHARACTERISTICS ADOPTED FOR THE 4 TH DECIDUOUS PREMOLAR (IMAGES REPRINTED FROM PAYNE, S. MORPHOLOGICAL DISTINCTIONS BETWEEN THE MANDIBULAR TEETH OF YOUNG SHEEP, <i>OVIS</i> , AND GOATS, <i>CAPRA</i> . <i>JOURNAL OF ARCHAEOLOGICAL SCIENCE</i> 12: 139-147, COPYRIGHT 1985, WITH PERMISSION FROM ELSEVIER).	46
TABLE 2.5 MORPHOLOGICAL CHARACTERISTICS ADOPTED FOR THE 3 RD PERMANENT PREMOLAR (IMAGES REPRINTED FROM HALSTEAD, P., P. COLLINS AND V. ISAKKIDOU. SORTING THE SHEEP FROM THE GOATS: MORPHOLOGICAL DISTINCTIONS BETWEEN THE MANDIBLES AND MANDIBULAR TEETH OF ADULT <i>OVIS</i> AND <i>CAPRA</i> . <i>JOURNAL OF ARCHAEOLOGICAL SCIENCE</i> 29: 545-553, COPYRIGHT 2002, WITH PERMISSION FROM ELSEVIER).	47
TABLE 2.6 MORPHOLOGICAL CHARACTERISTICS ADOPTED FOR THE 4 TH PERMANENT PREMOLAR (IMAGES REPRINTED FROM HALSTEAD, P., P. COLLINS AND V. ISAKKIDOU. SORTING THE SHEEP FROM THE GOATS: MORPHOLOGICAL DISTINCTIONS BETWEEN THE MANDIBLES AND MANDIBULAR TEETH OF ADULT <i>OVIS</i> AND <i>CAPRA</i> . <i>JOURNAL OF ARCHAEOLOGICAL SCIENCE</i> 29: 545-553, COPYRIGHT 2002, WITH PERMISSION FROM ELSEVIER).	48
TABLE 2.7 MORPHOLOGICAL CHARACTERISTICS ADOPTED FOR THE 3 RD MOLAR (IMAGES REPRINTED FROM HALSTEAD, P., P. COLLINS AND V. ISAKKIDOU. SORTING THE SHEEP FROM THE GOATS: MORPHOLOGICAL DISTINCTIONS BETWEEN THE MANDIBLES AND MANDIBULAR TEETH OF ADULT <i>OVIS</i> AND <i>CAPRA</i> . <i>JOURNAL OF ARCHAEOLOGICAL SCIENCE</i> 29: 545-553, COPYRIGHT 2002, WITH PERMISSION FROM ELSEVIER).	49
TABLE 2.8 MORPHOLOGICAL CHARACTERISTICS ADOPTED FOR THE MANDIBULA (IMAGES REPRINTED FROM HALSTEAD, P., P. COLLINS AND V. ISAKKIDOU. SORTING THE SHEEP FROM THE GOATS: MORPHOLOGICAL DISTINCTIONS BETWEEN THE	

MANDIBLES AND MANDIBULAR TEETH OF ADULT <i>OVIS</i> AND <i>CAPRA</i> . <i>JOURNAL OF ARCHAEOLOGICAL SCIENCE</i> 29: 545-553, COPYRIGHT 2002, WITH PERMISSION FROM ELSEVIER).	49
TABLE 2.9 MORPHOLOGICAL CHARACTERISTICS ADOPTED FOR THE SCAPULA (IMAGES REPRINTED FROM BOESSNECK, J. OSTEOLOGICAL DIFFERENCES BETWEEN SHEEP (<i>OVIS ARIES</i> LINNÉ) AND GOAT (<i>CAPRA HIRCUS</i> LINNÉ). IN <i>SCIENCE IN ARCHAEOLOGY: A SURVEY OF PROGRESS AND RESEARCH</i> , EDS. D. BROTHWELL AND E. HIGGS, 331-358, COPYRIGHT 1969. LONDON: THAMES AND HUDSON, WITH PERMISSION FROM THAMES AND HUDSON).	50
TABLE 2.10 MORPHOLOGICAL CHARACTERISTICS ADOPTED FOR THE DISTAL HUMERUS (TRAITS 1 AND 2: IMAGES REPRINTED FROM BOESSNECK, J. OSTEOLOGICAL DIFFERENCES BETWEEN SHEEP (<i>OVIS ARIES</i> LINNÉ) AND GOAT (<i>CAPRA HIRCUS</i> LINNÉ). IN <i>SCIENCE IN ARCHAEOLOGY: A SURVEY OF PROGRESS AND RESEARCH</i> , EDS. D. BROTHWELL AND E. HIGGS, 331-358, COPYRIGHT 1969. LONDON: THAMES AND HUDSON, WITH PERMISSION FROM THAMES AND HUDSON. TRAIT 3 TO 5: IMAGES REPRINTED FROM ZEDER, M.A. AND H.A. LAPHAM. ASSESSING THE RELIABILITY OF CRITERIA USED TO IDENTIFY POSTCRANIAL BONES IN SHEEP, <i>OVIS</i> , AND GOATS, <i>CAPRA</i> . <i>JOURNAL OF ARCHAEOLOGICAL SCIENCE</i> 37: 2887-2905, COPYRIGHT 2010, WITH PERMISSION FROM ELSEVIER). ..	51
TABLE 2.11 MORPHOLOGICAL CHARACTERISTICS ADOPTED FOR THE PROXIMAL RADIUS (IMAGES REPRINTED FROM ZEDER, M.A. AND H.A. LAPHAM. ASSESSING THE RELIABILITY OF CRITERIA USED TO IDENTIFY POSTCRANIAL BONES IN SHEEP, <i>OVIS</i> , AND GOATS, <i>CAPRA</i> . <i>JOURNAL OF ARCHAEOLOGICAL SCIENCE</i> 37: 2887-2905, COPYRIGHT 2010, WITH PERMISSION FROM ELSEVIER).	53
TABLE 2.12 MORPHOLOGICAL CHARACTERISTICS ADOPTED FOR THE PROXIMAL ULNA (IMAGES REPRINTED FROM BOESSNECK, J. OSTEOLOGICAL DIFFERENCES BETWEEN SHEEP (<i>OVIS ARIES</i> LINNÉ) AND GOAT (<i>CAPRA HIRCUS</i> LINNÉ). IN <i>SCIENCE IN ARCHAEOLOGY: A SURVEY OF PROGRESS AND RESEARCH</i> , EDS. D. BROTHWELL AND E. HIGGS, 331-358, COPYRIGHT 1969. LONDON: THAMES AND HUDSON, WITH PERMISSION FROM THAMES AND HUDSON).	54
TABLE 2.13 MORPHOLOGICAL CHARACTERISTICS ADOPTED FOR THE METAPODIALS (TRAITS 1, 2, 5: IMAGES REPRINTED FROM FROM BOESSNECK, J. OSTEOLOGICAL DIFFERENCES BETWEEN SHEEP (<i>OVIS ARIES</i> LINNÉ) AND GOAT (<i>CAPRA HIRCUS</i> LINNÉ). IN <i>SCIENCE IN ARCHAEOLOGY: A SURVEY OF PROGRESS AND RESEARCH</i> , EDS. D. BROTHWELL AND E. HIGGS, 331-358, COPYRIGHT 1969. LONDON: THAMES AND HUDSON, WITH PERMISSION FROM THAMES AND HUDSON. TRAITS 3, 4 AND 6: IMAGES REPRINTED FROM ZEDER, M.A. AND H.A. LAPHAM. ASSESSING THE RELIABILITY OF CRITERIA USED TO IDENTIFY POSTCRANIAL BONES IN SHEEP, <i>OVIS</i> , AND GOATS, <i>CAPRA</i> . <i>JOURNAL OF ARCHAEOLOGICAL SCIENCE</i> 37: 2887-2905, COPYRIGHT 2010, WITH PERMISSION FROM ELSEVIER). ..	55
TABLE 2.14 MORPHOLOGICAL CHARACTERISTICS ADOPTED FOR THE DISTAL TIBIA (TRAITS 1, 2, 5 AND 6: IMAGES REPRINTED FROM ZEDER, M.A. AND H.A. LAPHAM. ASSESSING THE RELIABILITY OF CRITERIA USED TO IDENTIFY POSTCRANIAL BONES IN SHEEP, <i>OVIS</i> , AND GOATS, <i>CAPRA</i> . <i>JOURNAL OF ARCHAEOLOGICAL SCIENCE</i> 37: 2887-2905, COPYRIGHT 2010, WITH PERMISSION FROM ELSEVIER. TRAITS 3 AND 4: IMAGES REPRINTED FROM KRATOCHVÍL, Z. SPECIES CRITERIA ON THE DISTAL SECTION OF THE TIBIA IN <i>OVIS AMMON</i> F. <i>ARIES</i> L. AND <i>CAPRA AEGAGRUS</i> F. <i>HIRCUS</i> L. <i>ACTA VETERINARIA</i> (BRNO), COPYRIGHT 1969, 38: 483-490. LICENSE AT: HTTPS://CREATIVECOMMONS.ORG/LICENSES/BY/4.0/).	57
TABLE 2.15 MORPHOLOGICAL CHARACTERISTICS ADOPTED FOR THE ASTRAGALUS (TRAITS 1, 2, 3 AND 6: IMAGES REPRINTED FROM BOESSNECK, J. OSTEOLOGICAL DIFFERENCES BETWEEN SHEEP (<i>OVIS ARIES</i> LINNÉ) AND GOAT (<i>CAPRA HIRCUS</i>	

LINNÉ). IN <i>SCIENCE IN ARCHAEOLOGY: A SURVEY OF PROGRESS AND RESEARCH</i> , EDS. D. BROTHWELL AND E. HIGGS, 331-358, COPYRIGHT 1969. LONDON: THAMES AND HUDSON, WITH PERMISSION FROM THAMES AND HUDSON.	
TRAITS 4 AND 5: IMAGES REPRINTED FROM ZEDER, M.A. AND H.A. LAPHAM. ASSESSING THE RELIABILITY OF CRITERIA USED TO IDENTIFY POSTCRANIAL BONES IN SHEEP, <i>OVIS</i> , AND GOATS, <i>CAPRA</i> . <i>JOURNAL OF ARCHAEOLOGICAL SCIENCE</i> 37: 2887-2905, COPYRIGHT 2010, WITH PERMISSION FROM ELSEVIER).....	59
TABLE 2.16 MORPHOLOGICAL CHARACTERISTICS ADOPTED FOR THE CALCANEUM (TRAITS 1 AND 2: IMAGES REPRINTED FROM ZEDER, M.A. AND H.A. LAPHAM. ASSESSING THE RELIABILITY OF CRITERIA USED TO IDENTIFY POSTCRANIAL BONES IN SHEEP, <i>OVIS</i> , AND GOATS, <i>CAPRA</i> . <i>JOURNAL OF ARCHAEOLOGICAL SCIENCE</i> 37: 2887-2905, COPYRIGHT 2010, WITH PERMISSION FROM ELSEVIER. TRAIT 3: IMAGE REPRINTED FROM BOESSNECK, J. OSTEOLOGICAL DIFFERENCES BETWEEN SHEEP (<i>OVIS ARIES</i> LINNÉ) AND GOAT (<i>CAPRA HIRCUS</i> LINNÉ). IN <i>SCIENCE IN ARCHAEOLOGY: A SURVEY OF PROGRESS AND RESEARCH</i> , EDS. D. BROTHWELL AND E. HIGGS, 331-358, COPYRIGHT 1969. LONDON: THAMES AND HUDSON, WITH PERMISSION FROM THAMES AND HUDSON).....	61
TABLE 2.17 MORPHOLOGICAL CHARACTERISTICS ADOPTED FOR THE 1 ST PHALANX (IMAGES REPRINTED FROM BOESSNECK, J. OSTEOLOGICAL DIFFERENCES BETWEEN SHEEP (<i>OVIS ARIES</i> LINNÉ) AND GOAT (<i>CAPRA HIRCUS</i> LINNÉ). IN <i>SCIENCE IN ARCHAEOLOGY: A SURVEY OF PROGRESS AND RESEARCH</i> , EDS. D. BROTHWELL AND E. HIGGS, 331-358, COPYRIGHT 1969. LONDON: THAMES AND HUDSON, WITH PERMISSION FROM THAMES AND HUDSON).....	63
TABLE 2.18 MORPHOLOGICAL CHARACTERISTICS ADOPTED FOR THE 2 ND PHALANX (IMAGES REPRINTED FROM ZEDER, M.A. AND H.A. LAPHAM. ASSESSING THE RELIABILITY OF CRITERIA USED TO IDENTIFY POSTCRANIAL BONES IN SHEEP, <i>OVIS</i> , AND GOATS, <i>CAPRA</i> . <i>JOURNAL OF ARCHAEOLOGICAL SCIENCE</i> 37: 2887-2905, COPYRIGHT 2010, WITH PERMISSION FROM ELSEVIER).....	64
TABLE 2.19 MORPHOLOGICAL CHARACTERISTICS ADOPTED FOR THE 3 RD PHALANX (IMAGES REPRINTED FROM BOESSNECK, J. OSTEOLOGICAL DIFFERENCES BETWEEN SHEEP (<i>OVIS ARIES</i> LINNÉ) AND GOAT (<i>CAPRA HIRCUS</i> LINNÉ). IN <i>SCIENCE IN ARCHAEOLOGY: A SURVEY OF PROGRESS AND RESEARCH</i> , EDS. D. BROTHWELL AND E. HIGGS, 331-358, COPYRIGHT 1969. LONDON: THAMES AND HUDSON, WITH PERMISSION FROM THAMES AND HUDSON).....	65
TABLE 2.20 LIST OF THE SCORES GIVEN FOR EACH MORPHOLOGICAL TRAITS EVALUATED.	65
TABLE 2.21 REFERENCES FOR THE CHOSEN MEASUREMENTS WITH REFERENCE TO THE MORPHOLOGICAL TRAITS THEY TRANSLATE. MEASUREMENTS IN WHICH THE AUTHORS NAME IS CITED WITH AN ASTERISK ARE THOSE THAT HAVE BEEN SLIGHTLY MODIFIED FROM THE ORIGINAL VERSION, WHILE THOSE ONLY REPRESENTED BY AN ASTERISK HAVE BEEN NEWLY DEvised BY THE AUTHOR.	68
TABLE 2.22 MEASUREMENTS TAKEN ON TEETH (DP ₄ : IMAGE REPRINTED FROM PAYNE, S. MORPHOLOGICAL DISTINCTIONS BETWEEN THE MANDIBULAR TEETH OF YOUNG SHEEP, <i>OVIS</i> , AND GOATS, <i>CAPRA</i> . <i>JOURNAL OF ARCHAEOLOGICAL SCIENCE</i> 12: 139-147, COPYRIGHT 1985, WITH PERMISSION FROM ELSEVIER. M ₃ : IMAGE REPRINTED FROM HALSTEAD, P., P. COLLINS AND V. ISAKKIDOU. SORTING THE SHEEP FROM THE GOATS: MORPHOLOGICAL DISTINCTIONS BETWEEN THE MANDIBLES AND MANDIBULAR TEETH OF ADULT <i>OVIS</i> AND <i>CAPRA</i> . <i>JOURNAL OF ARCHAEOLOGICAL SCIENCE</i> 29: 545-553, COPYRIGHT 2002, WITH PERMISSION FROM ELSEVIER).....	70
TABLE 2.23 MEASUREMENTS TAKEN ON THE MANDIBLE (IMAGES REPRINTED FROM HALSTEAD, P., P. COLLINS AND V. ISAKKIDOU. SORTING THE SHEEP FROM THE GOATS: MORPHOLOGICAL DISTINCTIONS BETWEEN THE MANDIBLES AND MANDIBULAR TEETH OF ADULT <i>OVIS</i> AND <i>CAPRA</i> . <i>JOURNAL OF ARCHAEOLOGICAL SCIENCE</i> 29: 545-553, COPYRIGHT 2002, WITH PERMISSION FROM ELSEVIER).....	71

TABLE 2.24 MEASUREMENTS TAKEN ON THE HORNCORE (IMAGES REPRINTED FROM SCHMID, E. <i>ATLAS OF ANIMAL BONES: FOR PREHISTORIANS, ARCHAEOLOGISTS AND QUATERNARY GEOLOGISTS</i> . AMSTERDAM: ELSEVIER, COPYRIGHT 1972, WITH PERMISSION FROM JOERG SCHIBLER).....	71
TABLE 2.25 MEASUREMENTS TAKEN ON THE SCAPULA (IMAGE REPRINTED FROM BOESSNECK, J. OSTEOLOGICAL DIFFERENCES BETWEEN SHEEP (<i>OVIS ARIES</i> LINNÉ) AND GOAT (<i>CAPRA HIRCUS</i> LINNÉ). IN <i>SCIENCE IN ARCHAEOLOGY: A SURVEY OF PROGRESS AND RESEARCH</i> , EDS. D. BROTHWELL AND E. HIGGS, 331-358, COPYRIGHT 1969. LONDON: THAMES AND HUDSON, WITH PERMISSION FROM THAMES AND HUDSON).	72
TABLE 2.26 MEASUREMENTS TAKEN ON THE DISTAL HUMERUS (IMAGE 1: REPRINTED FROM BOESSNECK, J. OSTEOLOGICAL DIFFERENCES BETWEEN SHEEP (<i>OVIS ARIES</i> LINNÉ) AND GOAT (<i>CAPRA HIRCUS</i> LINNÉ). IN <i>SCIENCE IN ARCHAEOLOGY: A SURVEY OF PROGRESS AND RESEARCH</i> , EDS. D. BROTHWELL AND E. HIGGS, 331-358, COPYRIGHT 1969. LONDON: THAMES AND HUDSON, WITH PERMISSION FROM THAMES AND HUDSON. IMAGE 2: REPRINTED FROM ZEDER, M.A. AND H.A. LAPHAM. ASSESSING THE RELIABILITY OF CRITERIA USED TO IDENTIFY POSTCRANIAL BONES IN SHEEP, <i>OVIS</i> , AND GOATS, <i>CAPRA</i> . <i>JOURNAL OF ARCHAEOLOGICAL SCIENCE</i> 37: 2887-2905, COPYRIGHT 2010, WITH PERMISSION FROM ELSEVIER. IMAGE 3 (FIG. 32E): REPRINTED FROM VON DEN DRIESCH, A. <i>A GUIDE TO THE MEASUREMENT OF ANIMAL BONES FROM ARCHAEOLOGICAL SITES</i> . PEABODY MUSEUM BULLETINS, VOL. 1. COPYRIGHT 1976 WITH PERMISSION FROM THE PRESIDENT AND FELLOWS OF HARVARD COLLEGE).	73
TABLE 2.27 MEASUREMENTS TAKEN ON THE RADIUS (IMAGE REPRINTED FROM ZEDER, M.A. AND H.A. LAPHAM. ASSESSING THE RELIABILITY OF CRITERIA USED TO IDENTIFY POSTCRANIAL BONES IN SHEEP, <i>OVIS</i> , AND GOATS, <i>CAPRA</i> . <i>JOURNAL OF ARCHAEOLOGICAL SCIENCE</i> 37: 2887-2905, COPYRIGHT 2010, WITH PERMISSION FROM ELSEVIER). ...	73
TABLE 2.28 MEASUREMENTS TAKEN ON THE ULNA (IMAGES (FIGS. 33B AND 33E): REPRINTED FROM VON DEN DRIESCH, A. <i>A GUIDE TO THE MEASUREMENT OF ANIMAL BONES FROM ARCHAEOLOGICAL SITES</i> . PEABODY MUSEUM BULLETINS, VOL. 1. COPYRIGHT 1976 WITH PERMISSION FROM THE PRESIDENT AND FELLOWS OF HARVARD COLLEGE).....	74
TABLE 2.29 MEASUREMENTS TAKEN ON THE METAPODIALS (IMAGE 1: REPRINTED FROM ZEDER, M.A. AND H.A. LAPHAM. ASSESSING THE RELIABILITY OF CRITERIA USED TO IDENTIFY POSTCRANIAL BONES IN SHEEP, <i>OVIS</i> , AND GOATS, <i>CAPRA</i> . <i>JOURNAL OF ARCHAEOLOGICAL SCIENCE</i> 37: 2887-2905, COPYRIGHT 2010, WITH PERMISSION FROM ELSEVIER. IMAGE 2: REPRINTED FROM BOESSNECK, J. OSTEOLOGICAL DIFFERENCES BETWEEN SHEEP (<i>OVIS ARIES</i> LINNÉ) AND GOAT (<i>CAPRA HIRCUS</i> LINNÉ). IN <i>SCIENCE IN ARCHAEOLOGY: A SURVEY OF PROGRESS AND RESEARCH</i> , EDS. D. BROTHWELL AND E. HIGGS, 331-358, COPYRIGHT 1969. LONDON: THAMES AND HUDSON, WITH PERMISSION FROM THAMES AND HUDSON).....	75
TABLE 2.30 MEASUREMENTS TAKEN ON THE TIBIA (IMAGE REPRINTED FROM KRATOCHVÍL, Z. SPECIES CRITERIA ON THE DISTAL SECTION OF THE TIBIA IN <i>OVIS AMMON</i> F. <i>ARIES</i> L. AND <i>CAPRA AEGAGRUS</i> F. <i>HIRCUS</i> L. <i>ACTA VETERINARIA</i> (BRNO), COPYRIGHT 1969, 38: 483-490. LICENSE AVAILABLE AT: HTTPS://CREATIVECOMMONS.ORG/LICENSES/BY/4.0/)...	76
TABLE 2.31 MEASUREMENTS TAKEN ON THE ASTRAGALUS (IMAGES REPRINTED FROM BOESSNECK, J. OSTEOLOGICAL DIFFERENCES BETWEEN SHEEP (<i>OVIS ARIES</i> LINNÉ) AND GOAT (<i>CAPRA HIRCUS</i> LINNÉ). IN <i>SCIENCE IN ARCHAEOLOGY: A SURVEY OF PROGRESS AND RESEARCH</i> , EDS. D. BROTHWELL AND E. HIGGS, 331-358, COPYRIGHT 1969. LONDON: THAMES AND HUDSON, WITH PERMISSION FROM THAMES AND HUDSON).	76
TABLE 2.32 MEASUREMENTS TAKEN ON THE CALCANEUM (IMAGE 1 (FIG. 42B): REPRINTED FROM VON DEN DRIESCH, A. <i>A GUIDE TO THE MEASUREMENT OF ANIMAL BONES FROM ARCHAEOLOGICAL SITES</i> . PEABODY MUSEUM BULLETINS, VOL. 1. COPYRIGHT 1976 WITH PERMISSION FROM THE PRESIDENT AND FELLOWS OF HARVARD COLLEGE. IMAGES 2 AND 3:	

REPRINTED FROM ZEDER, M.A. AND H.A. LAPHAM. ASSESSING THE RELIABILITY OF CRITERIA USED TO IDENTIFY POSTCRANIAL BONES IN SHEEP, *OVIS*, AND GOATS, *CAPRA*. *JOURNAL OF ARCHAEOLOGICAL SCIENCE* 37: 2887-2905, COPYRIGHT 2010, WITH PERMISSION FROM ELSEVIER. IMAGE 4: REPRINTED FROM BOESSNECK, J. OSTEOLOGICAL DIFFERENCES BETWEEN SHEEP (*OVIS ARIES* LINNÉ) AND GOAT (*CAPRA HIRCUS* LINNÉ). IN *SCIENCE IN ARCHAEOLOGY: A SURVEY OF PROGRESS AND RESEARCH*, EDS. D. BROTHWELL AND E. HIGGS, 331-358, COPYRIGHT 1969. LONDON: THAMES AND HUDSON, WITH PERMISSION FROM THAMES AND HUDSON)..... 77

TABLE 2.33 MEASUREMENTS TAKEN ON THE 3RD PHALANX..... 78

TABLE 2.34 TOTAL NUMBER OF SHEEP AND GOAT SPECIMENS INCLUDED IN THE STUDY ALONG WITH THE DESCRIPTION OF THEIR COMPLETENESS..... 86

TABLE 2.35 GOAT SPECIMENS INCLUDED IN THE SAMPLE STUDIED. THE INFORMATION GIVEN IN THIS TABLE (BREED, SEX AND AGE) IS AS PROVIDED BY THE COLLECTION DATA-BASES..... 86

TABLE 2.36 SHEEP SPECIMENS INCLUDED IN THE SAMPLE STUDIED. THE INFORMATION GIVEN IN THIS TABLE (BREED, SEX AND AGE) IS AS PROVIDED BY THE COLLECTION DATA-BASES CONSULTED..... 90

TABLE 2.37 FORM PROVIDED TO THE GROUP FOR RECORDING THE MEASUREMENTS. THE FORM INCLUDED ALL THE MEASUREMENTS, EVEN THOUGH SOME OF THEM COULD NOT BE TAKEN ON THE SELECTED SPECIMENS..... 95

TABLE 2.38 MEAN, STANDARD DEVIATION (SD) AND COEFFICIENT OF VARIATION (CV) FOR EACH MEASUREMENT FOR EACH OF THE SPECIMENS CALCULATED FROM THE MEASUREMENTS PROVIDED BY THE EIGHT OPERATORS. THE MEASUREMENTS HIGHLIGHTED WITH AN ASTERISK ARE THOSE WHICH COULD NOT BE TAKEN ON ALL THE FOUR SPECIMENS. THE ‘NUMBER OF SPECIMENS’ COLUMN INDICATES THE NUMBER OF SPECIMENS FOR WHICH A MEASUREMENT HAS BEEN TAKEN. 98

TABLE 2.39 LIST OF THE MEASUREMENTS WHICH PROVIDED THE LOWEST CV VALUES PER SPECIES. 102

TABLE 2.40 LIST OF THE MEASUREMENTS WHICH PROVIDED THE HIGHEST CV VALUES PER SPECIES..... 103

TABLE 2.41 ICC VALUE AND 95% CONFIDENCE INTERVAL VALUES FOR DIFFERENT MEASUREMENTS TAKEN ON DIFFERENT ANATOMICAL ELEMENTS..... 106

TABLE 2.42 ICC VALUE AND 95% CONFIDENCE INTERVAL VALUES FOR DIFFERENT MEASUREMENTS TAKEN ON DIFFERENT ANATOMICAL ELEMENTS..... 116

TABLE 2.43 MATCHINGS OF MORPHOLOGICAL IDENTIFICATIONS WITH ACTUAL TAXA. C= *CAPRA*, O= *OVIS*, CL= *CAPRA*-LIKE, OL= *OVIS*-LIKE, OC= *OVIS/CAPRA*. 125

TABLE 2.44 MORPHOLOGICAL TRAITS WHICH HAVE PROVIDED A HIGH PERCENTAGE OF TAXON ATTRIBUTIONS FOR GOAT (>90%)..... 126

TABLE 2.45 MORPHOLOGICAL TRAITS WHICH PROVIDED A HIGH PERCENTAGE OF TAXON ATTRIBUTIONS FOR SHEEP (>90%). 126

TABLE 2.46 MORPHOLOGICAL TRAITS FOR THE GOAT GROUP WHICH PROVIDE A HIGH SCORE (>95%) ONLY WHEN DIFFERENT CATEGORIES WERE COMBINED (C+CL). 127

TABLE 2.47 MORPHOLOGICAL TRAITS FOR THE GOAT GROUP, WHICH PROVIDE A HIGH SCORE (>95%) ONLY WHEN DIFFERENT CATEGORIES WERE COMBINED (O+OL). 127

TABLE 2.48 NUMBER OF MODERN SPECIMENS ACCORDING TO THEIR SEX FOR EACH TAXON. 153

TABLE 2.49 GOAT. SCORES EXPRESSED IN PERCENTAGES GIVEN TO DIFFERENT MORPHOLOGICAL CHARACTERISTICS OF DIFFERENT CRANIAL AND POST-CRANIAL BONES ACCORDING TO THE SEX OF THE ANIMALS..... 153

TABLE 2.50 SHEEP. SCORES EXPRESSED IN PERCENTAGES, GIVEN TO DIFFERENT MORPHOLOGICAL CHARACTERISTICS OF DIFFERENT CRANIAL AND POST-CRANIAL BONES, ACCORDING TO THE SEX OF THE ANIMAL.....	154
TABLE 2.51 GOAT. LIST OF MORPHOLOGICAL TRAITS PER ELEMENT PER SEX, WHICH HAVE PROVIDED A HIGH INITIAL PERCENTAGE (>90%) OF SPECIES ATTRIBUTIONS (C) AND A HIGH PERCENTAGE (>95%) WHEN THE INTERMEDIATE CATEGORY (CL) WAS ADDED.....	155
TABLE 2.52 SHEEP. LIST OF MORPHOLOGICAL TRAITS PER ELEMENT PER SEX, WHICH HAVE PROVIDED A HIGH INITIAL PERCENTAGE (>90%) OF SPECIES ATTRIBUTIONS (O) AND A HIGH PERCENTAGE (>95%) WHEN THE INTERMEDIATE CATEGORY (OL) WAS ADDED.	156
TABLE 2.53 SUMMARY OF THE AGE CATEGORIES ESTABLISHED BY PAYNE (1973; 1987) AND USED FOR THIS ANALYSIS. ...	179
TABLE 2.54 NEW AGE GROUPS COMBINING DIFFERENT PAYNE’S AGE CATEGORIES. THE SPECIMENS PRESENT ARE BOTH THOSE FOR WHICH THE AGE WAS ESTABLISHED THROUGH PAYNE’S METHOD AND THOSE FOR WHICH THE AGE AT DEATH WAS KNOWN.....	179
TABLE 2.55 GOAT. SCORES EXPRESSED IN PERCENTAGES GIVEN TO DIFFERENT MORPHOLOGICAL CHARACTERISTICS OF DIFFERENT CRANIAL AND POST-CRANIAL BONES ACCORDING TO AGE GROUPS.	180
TABLE 2.56 SHEEP. SCORES EXPRESSED IN PERCENTAGES GIVEN TO DIFFERENT MORPHOLOGICAL CHARACTERISTICS OF DIFFERENT CRANIAL AND POST-CRANIAL BONES ACCORDING TO AGE GROUPS.	181
TABLE 2.57 SUMMARY OF THE RELIABILITY OF THE MORPHOLOGICAL TRAITS FOR THE TWO SPECIES WITH INFORMATION REGARDING THE FACTORS CAN INFLUENCE THEM. RELIABILITY IS EXPRESSED IN SCORES: ***= > 90% PERCENTAGE OF SPECIES IDENTIFICATION (C OR O), **= >= 60% OF SPECIES IDENTIFICATION; *= <60% OF SPECIES ATTRIBUTION. THE OVERALL RELIABILITY IS, BY AND LARGE, THE MEAN BETWEEN THE RELIABILITY SCORES OF THE TWO SPECIES.	207
TABLE 2.58 COEFFICIENTS OF VARIATION AND STANDARD VALUES IN TENTHS OF MILLIMETER FOR EACH MEASUREMENT.	210
TABLE 2.59 CV VALUES FOR THE GOAT GROUP REARRANGED FROM THE HIGHEST TO THE LOWEST.	212
TABLE 2.60 CV VALUES FOR THE SHEEP GROUP REARRANGED FROM THE HIGHEST TO THE LOWEST.	213
TABLE 2.61 MEDIAN, EFFECT SIZE, MANN-WHITNEY U TEST AND BONFERRONI ADJUSTMENT RESULTS, CALCULATED FOR EACH RATIO INDEX ON EACH SKELETAL ELEMENT INCLUDED IN THE STUDY. THE PROBABILITY LEVEL WAS DETERMINED AS SIGNIFICANT WHEN $P<0.05$ (*) AND HIGHLY SIGNIFICANT WHEN $P<0.01$ (**).....	274
TABLE 2.62 RESULTS FROM MANOVA FOR EACH COMBINATION OF RATIOS USED IN THE ALLOMETRIC SHAPE ANALYSIS (SECTION 2.5.3). P VALUE SIGNIFICANT A $P<0.001=***$	278
TABLE 2.63 PERCENTAGE OF CORRECT CLASSIFICATIONS BY ELEMENT AND SPECIES FROM LINEAR DISCRIMINANT ANALYSIS.	280
TABLE 2.64 CANONICAL CORRELATION COEFFICIENT FOR THE HORNCORE.	281
TABLE 2.65 WILKS' LAMBDA TEST FOR THE HORNCORE.....	281
TABLE 2.66 STRUCTURE MATRIX FOR THE HORNCORE SHOWING THE CANONICAL VARIATE CORRELATION COEFFICIENTS. ...	282
TABLE 2.67 TOLERANCE TEST FOR THE HORNCORE.....	283
TABLE 2.68 CLASSIFICATION RESULTS FOR THE HORNCORE.....	283
TABLE 2.69 LIST OF THE SET OF MEASUREMENTS OF THE HORNCORE DROPPED FROM THE ANALYSIS ALONG WITH THEIR PERCENTAGE OF CORRECT ATTRIBUTIONS.	284
TABLE 2.70 CANONICAL CORRELATION COEFFICIENT FOR THE SCAPULA.	285

TABLE 2.71 WILKS' LAMBDA TEST FOR THE SCAPULA.....	285
TABLE 2.72 STRUCTURE MATRIX FOR THE SCAPULA SHOWING THE CANONICAL VARIATE CORRELATION COEFFICIENTS.....	286
TABLE 2.73 CLASSIFICATION RESULTS FOR THE SCAPULA.	286
TABLE 2.74 LIST OF THE SET OF MEASUREMENTS ON THE SCAPULA DROPPED FROM THE ANALYSIS ALONG WITH THEIR PERCENTAGE OF CORRECT ATTRIBUTIONS.....	288
TABLE 2.75 CANONICAL CORRELATION COEFFICIENT FOR THE HUMERUS.....	288
TABLE 2.76 WILKS' LAMBDA TEST FOR THE HUMERUS.	289
TABLE 2.77 STRUCTURE MATRIX FOR THE HUMERUS SHOWING THE CANONICAL VARIATE CORRELATION COEFFICIENTS.....	289
TABLE 2.78 CLASSIFICATION RESULTS FOR THE HUMERUS.	290
TABLE 2.79 LIST OF THE SET OF MEASUREMENTS OF THE HUMERUS DROPPED FROM THE ANALYSIS ALONG WITH THEIR PERCENTAGE OF CORRECT ATTRIBUTIONS.....	290
TABLE 2.80 CANONICAL CORRELATION COEFFICIENT FOR THE RADIUS.	292
TABLE 2.81 WILKS' LAMBDA TEST FOR THE RADIUS.	292
TABLE 2.82 STRUCTURE MATRIX FOR THE RADIUS SHOWING THE CANONICAL VARIATE CORRELATION COEFFICIENTS.....	292
TABLE 2.83 CLASSIFICATION RESULTS FOR THE RADIUS.	293
TABLE 2.84 LIST OF THE SET OF MEASUREMENTS OF THE RADIUS DROPPED FROM THE ANALYSIS ALONG WITH THEIR PERCENTAGE OF CORRECT ATTRIBUTIONS.....	294
TABLE 2.85 CANONICAL CORRELATION COEFFICIENT FOR THE ULNA.	295
TABLE 2.86 WILKS' LAMBDA TEST FOR THE ULNA.	295
TABLE 2.87 STRUCTURE MATRIX FOR THE ULNA SHOWING THE CANONICAL VARIATE CORRELATION COEFFICIENTS.....	295
TABLE 2.88 CLASSIFICATION RESULTS FOR THE ULNA.	296
TABLE 2.89 LIST OF THE SET OF MEASUREMENTS OF THE ULNA DROPPED FROM THE ANALYSIS ALONG WITH THEIR PERCENTAGE OF CORRECT ATTRIBUTIONS.....	297
TABLE 2.90 CANONICAL CORRELATION COEFFICIENT FOR THE METACARPAL.....	298
TABLE 2.91 WILKS' LAMBDA TEST FOR THE METACARPAL.	298
TABLE 2.92 STRUCTURE MATRIX FOR THE METACARPAL SHOWING THE CANONICAL VARIATE CORRELATION COEFFICIENTS.....	299
TABLE 2.93 CLASSIFICATION RESULTS FOR THE METACARPAL.	300
TABLE 2.94 LIST OF THE SET OF MEASUREMENTS ON THE METACARPAL DROPPED FROM THE ANALYSIS ALONG WITH THEIR PERCENTAGE OF CORRECT ATTRIBUTIONS.....	300
TABLE 2.95 CANONICAL CORRELATION COEFFICIENT FOR THE METATARSAL.....	302
TABLE 2.96 WILKS' LAMBDA TEST FOR THE METATARSAL.	302
TABLE 2.97 STRUCTURE MATRIX FOR THE METATARSAL SHOWING THE CANONICAL VARIATE CORRELATION COEFFICIENTS.....	302
TABLE 2.98 CLASSIFICATION RESULTS FOR THE METATARSAL.	303

TABLE 2.99 LIST OF THE SET OF MEASUREMENTS ON THE METATARSAL DROPPED FROM THE ANALYSIS ALONG WITH THEIR PERCENTAGE OF CORRECT ATTRIBUTIONS.	304
TABLE 2.100 CANONICAL CORRELATION COEFFICIENT FOR THE TIBIA.	305
TABLE 2.101 WILKS' LAMBDA TEST FOR THE TIBIA.	305
TABLE 2.102 STRUCTURE MATRIX FOR THE TIBIA SHOWING THE CANONICAL VARIATE CORRELATION COEFFICIENTS.	306
TABLE 2.103 CLASSIFICATION RESULTS FOR THE TIBIA.	306
TABLE 2.104 LIST OF THE SET OF MEASUREMENTS ON THE TIBIA DROPPED FROM THE ANALYSIS ALONG WITH THEIR PERCENTAGE OF CORRECT ATTRIBUTIONS.	307
TABLE 2.105 CANONICAL CORRELATION COEFFICIENT FOR THE ASTRAGALUS.	308
TABLE 2.106 WILKS' LAMBDA TEST FOR THE ASTRAGALUS.	308
TABLE 2.107 STRUCTURE MATRIX FOR THE ASTRAGALUS SHOWING THE CANONICAL VARIATE CORRELATION COEFFICIENTS.	309
TABLE 2.108 CLASSIFICATION RESULTS FOR THE ASTRAGALUS.	309
TABLE 2.109 LIST OF THE SET OF MEASUREMENTS ON THE ASTRAGALUS DROPPED FROM THE ANALYSIS ALONG WITH THEIR PERCENTAGE OF CORRECT ATTRIBUTIONS.	310
TABLE 2.110 CANONICAL CORRELATION COEFFICIENT FOR THE CALCANEUM.	311
TABLE 2.111 WILKS' LAMBDA TEST FOR THE CALCANEUM.	311
TABLE 2.112 STRUCTURE MATRIX FOR THE CALCANEUM SHOWING THE CANONICAL VARIATE CORRELATION COEFFICIENTS.	312
TABLE 2.113 CLASSIFICATION RESULTS FOR THE CALCANEUM.	312
TABLE 2.114 LIST OF THE SET OF MEASUREMENTS ON THE CALCANEUS DROPPED FROM THE ANALYSIS ALONG WITH THEIR PERCENTAGE OF CORRECT ATTRIBUTIONS.	313
TABLE 2.115 CANONICAL CORRELATION COEFFICIENT FOR THE 3 RD PHALANX.	314
TABLE 2.116 WILKS' LAMBDA TEST FOR THE 3 RD PHALANX.	314
TABLE 2.117 STRUCTURE MATRIX FOR THE 3 RD PHALANX SHOWING THE CANONICAL VARIATE CORRELATION COEFFICIENTS.	315
TABLE 2.118 CLASSIFICATION RESULTS FOR THE 3 RD PHALANX.	316
TABLE 2.119 KMO AND BARTLETT'S TEST FOR MEASUREMENTS TAKEN ON THE HORNCORES.	318
TABLE 2.120 CORRELATION MATRIX FOR THE HORNCORE.	319
TABLE 2.121 TOTAL VARIANCE EXPLAINED FOR THE HORNCORE.	319
TABLE 2.122 COMPONENT MATRIX FOR THE HORNCORE.	320
TABLE 2.123 KMO AND BARTLETT'S TEST FOR THE MEASUREMENTS TAKEN ON THE SCAPULA.	321
TABLE 2.124 CORRELATION MATRIX FOR THE SCAPULA.	322
TABLE 2.125 TOTAL VARIANCE EXPLAINED FOR THE SCAPULA.	322
TABLE 2.126 COMPONENT MATRIX FOR THE SCAPULA.	323
TABLE 2.127 ROTATED COMPONENT MATRIX FOR THE SCAPULA.	325
TABLE 2.128 KMO AND BARTLETT'S TEST FOR THE MEASUREMENTS TAKEN ON THE HUMERUS.	326
TABLE 2.129 CORRELATION MATRIX FOR THE HUMERUS.	326
TABLE 2.130 TOTAL VARIANCE EXPLAINED FOR THE HUMERUS.	327

TABLE 2.131 COMPONENT MATRIX FOR THE HUMERUS.....	327
TABLE 2.132 ROTATED COMPONENT MATRIX FOR THE HUMERUS.	328
TABLE 2.133 KMO AND BARTLETT'S TEST FOR THE MEASUREMENTS TAKEN ON THE RADIUS.	330
TABLE 2.134 CORRELATION MATRIX FOR THE RADIUS.	330
TABLE 2.135 TOTAL VARIANCE EXPLAINED FOR THE RADIUS.....	330
TABLE 2.136 COMPONENT MATRIX FOR THE RADIUS.	331
TABLE 2.137 ROTATED COMPONENT MATRIX FOR THE RADIUS.	333
TABLE 2.138 KMO AND BARTLETT'S TEST FOR MEASUREMENTS TAKEN ON THE ULNA.....	335
TABLE 2.139 CORRELATION MATRIX FOR THE ULNA.	335
TABLE 2.140 TOTAL VARIANCE EXPLAINED FOR THE ULNA.	335
TABLE 2.141 COMPONENT MATRIX FOR THE ULNA.	336
TABLE 2.142 ROTATED COMPONENT MATRIX FOR THE ULNA.....	337
TABLE 2.143 KMO AND BARTLETT'S TEST FOR THE MEASUREMENTS TAKEN ON THE METACARPAL.	338
TABLE 2.144 CORRELATION MATRIX FOR THE METACARPAL.....	338
TABLE 2.145 TOTAL VARIANCE EXPLAINED FOR THE METACARPAL.....	339
TABLE 2.146 COMPONENT MATRIX FOR THE METACARPAL.....	340
TABLE 2.147 ROTATED MATRIX FOR THE METACARPAL.....	341
TABLE 2.148 KMO AND BARTLETT'S TEST FOR MEASUREMENTS TAKEN ON THE METATARSAL.	345
TABLE 2.149 CORRELATION MATRIX FOR THE METATARSAL.....	345
TABLE 2.150 TOTAL VARIANCE EXPLAINED FOR THE METATARSAL.....	346
TABLE 2.151 COMPONENT MATRIX FOR THE METATARSAL.....	347
TABLE 2.152 ROTATED COMPONENT MATRIX FOR THE METATARSAL.	348
TABLE 2.153 KMO AND BARTLETT'S TEST FOR THE MEASUREMENT TAKEN ON THE TIBIA.....	349
TABLE 2.154 CORRELATION MATRIX FOR THE TIBIA.....	350
TABLE 2.155 TOTAL VARIANCE EXPLAINED FOR THE TIBIA.....	350
TABLE 2.156 COMPONENT MATRIX FOR THE TIBIA.....	351
TABLE 2.157 ROTATED COMPONENT MATRIX FOR THE TIBIA.	351
TABLE 2.158 KMO AND BARTLETT'S TEST FOR THE MEASUREMENTS TAKEN ON THE ASTRAGALUS.	353
TABLE 2.159 CORRELATION MATRIX FOR THE ASTRAGALUS.	353
TABLE 2.160 TOTAL VARIANCE EXPLAINED FOR THE ASTRAGALUS.	354
TABLE 2.161 COMPONENT MATRIX FOR THE ASTRAGALUS.	355
TABLE 2.162 ROTATED COMPONENT MATRIX FOR THE ASTRAGALUS.....	355
TABLE 2.163 KMO AND BARTLETT'S TEST FOR THE MEASUREMENTS TAKEN ON THE CALCANEUM.	357
TABLE 2.164 CORRELATION MATRIX FOR THE CALCANEUM.....	358
TABLE 2.165 TOTAL VARIANCE EXPLAINED FOR THE CALCANEUM.....	358
TABLE 2.166 COMPONENT MATRIX FOR THE CALCANEUM.....	359
TABLE 2.167 ROTATED COMPONENT MATRIX FOR THE CALCANEUM.	359
TABLE 2.168 LIST OF THE MOST IMPORTANT MEASUREMENTS PER ANATOMICAL ELEMENT ACCORDING TO THE DIFFERENT ANALYSES ADOPTED.	362

TABLE 3.1 DIVISION INTO CHRONOLOGICAL PERIODS FOR THE SITES EXCAVATED AT KING'S LYNN (CLARKE AND CARTER 1977).....	373
TABLE 3.2 NISP FOR THE THREE CATEGORIES IDENTIFIED FOR PHASE I (1050-1250).....	379
TABLE 3.3 NISP FOR THE THREE CATEGORIES IDENTIFIED FOR PHASE II (1250-1350).	381
TABLE 3.4 NISP FOR THE THREE CATEGORIES IDENTIFIED FOR PHASE III (1350-1550).	382
TABLE 3.5 NISP FOR THE THREE CATEGORIES IDENTIFIED FOR PHASE IV (1550-1880).....	383
TABLE 3.6 NISP FOR THE THREE CATEGORIES IDENTIFIED AMONG THE UNSTRATIFIED BONES.....	383
TABLE 3.7 RESULTS FROM THE DISCRIMINANT ANALYSIS WHEN APPLIED ON THE ARCHAEOLOGICAL HORNCORES OF PHASE I. A = PERCENTAGE OF CORRECT ATTRIBUTIONS RELATED TO THE MODERN MATERIAL (SELECTED ORIGINAL GROUPED CASES); B = PERCENTAGE OF CORRECT ATTRIBUTIONS RELATED TO THE ARCHAEOLOGICAL MATERIAL (UNSELECTED ORIGINAL GROUPED CASES); D = PERCENTAGE OF CORRECT ATTRIBUTIONS WHEN CROSS-VALIDATION WAS APPLIED. SAME TERMINOLOGY IS ADOPTED IN ALL THE FOLLOWING TABLES.	448
TABLE 3.8 RESULTS FROM THE DISCRIMINANT ANALYSIS WHEN APPLIED ON THE ARCHAEOLOGICAL SCAPULAE OF PHASE I.	449
TABLE 3.9 RESULTS FROM THE DISCRIMINANT ANALYSIS WHEN APPLIED ON THE ARCHAEOLOGICAL HUMERI OF PHASE I.	450
TABLE 3.10 RESULTS FROM THE DISCRIMINANT ANALYSIS WHEN APPLIED ON THE ARCHAEOLOGICAL RADII OF PHASE I, EXCLUDING VARIABLES GL AND SD.	451
TABLE 3.11 RESULTS FROM THE DISCRIMINANT ANALYSIS WHEN APPLIED ON THE ARCHAEOLOGICAL ULNAE OF PHASE I.	452
TABLE 3.12 RESULTS FROM THE DISCRIMINANT ANALYSIS WHEN APPLIED ON THE ARCHAEOLOGICAL ULNAE OF PHASE I, EXCLUDING THE VARIABLES B AND L.....	453
TABLE 3.13 RESULTS FROM THE DISCRIMINANT ANALYSIS WHEN APPLIED ON THE ARCHAEOLOGICAL METACARPALS OF PHASE I.	454
TABLE 3.14 RESULTS FROM THE DISCRIMINANT ANALYSIS WHEN APPLIED ON THE ARCHAEOLOGICAL METACARPALS OF PHASE I, EXCLUDING THE VARIABLES GL AND SD.	454
TABLE 3.15 RESULTS FROM THE DISCRIMINANT ANALYSIS WHEN APPLIED ON THE ARCHAEOLOGICAL METATARSALS OF PHASE I.	455
TABLE 3.16 RESULTS FROM THE DISCRIMINANT ANALYSIS WHEN APPLIED ON THE ARCHAEOLOGICAL METATARSALS OF PHASE I, EXCLUDING VARIABLES GL AND SD.	456
TABLE 3.17 RESULTS FROM THE DISCRIMINANT ANALYSIS WHEN APPLIED ON THE ARCHAEOLOGICAL TIBIAE OF PHASE I.	457
TABLE 3.18 RESULTS FROM THE DISCRIMINANT ANALYSIS WHEN APPLIED ON THE ARCHAEOLOGICAL TIBIAE OF PHASE I, EXCLUDING THE VARIABLE GL.	457
TABLE 3.19 RESULTS FROM THE DISCRIMINANT ANALYSIS WHEN APPLIED ON THE ARCHAEOLOGICAL TIBIAE OF PHASE I, EXCLUDING THE VARIABLES GL AND SD.	458
TABLE 3.20 RESULTS FROM THE DISCRIMINANT ANALYSIS WHEN APPLIED ON THE ARCHAEOLOGICAL ASTRAGALI OF PHASE I.....	459

TABLE 3.21 RESULTS FROM THE DISCRIMINANT ANALYSIS WHEN APPLIED ON THE ARCHAEOLOGICAL CALCANEAE OF PHASE I.....	459
TABLE 3.22 RESULTS FROM THE DISCRIMINANT ANALYSIS WHEN APPLIED ON THE ARCHAEOLOGICAL HORNCORES OF PHASE II.	460
TABLE 3.23 RESULTS FROM THE DISCRIMINANT ANALYSIS WHEN APPLIED ON THE ARCHAEOLOGICAL HORNCORES OF PHASE II, EXCLUDING E AND F VARIABLES.....	461
TABLE 3.24 RESULTS FROM THE DISCRIMINANT ANALYSIS WHEN APPLIED ON THE ARCHAEOLOGICAL SCAPULAE OF PHASE II.	461
TABLE 3.25 RESULTS FROM THE DISCRIMINANT ANALYSIS WHEN APPLIED ON THE ARCHAEOLOGICAL HUMERI OF PHASE II.	462
TABLE 3.26 RESULTS FROM THE DISCRIMINANT ANALYSIS WHEN APPLIED ON THE ARCHAEOLOGICAL RADII OF PHASE II.	463
TABLE 3.27 RESULTS FROM THE DISCRIMINANT ANALYSIS WHEN APPLIED ON THE ARCHAEOLOGICAL RADII OF PHASE II, EXCLUDING VARIABLES GL AND SD.	463
TABLE 3.28 RESULTS FROM THE DISCRIMINANT ANALYSIS WHEN APPLIED ON THE ARCHAEOLOGICAL ULNAE OF PHASE II.	464
TABLE 3.29 RESULTS FROM THE DISCRIMINANT ANALYSIS WHEN APPLIED ON THE ARCHAEOLOGICAL ULNAE OF PHASE II, EXCLUDING VARIABLES B AND L.....	465
TABLE 3.30 RESULTS FROM THE DISCRIMINANT ANALYSIS WHEN APPLIED ON THE ARCHAEOLOGICAL METACARPALS OF PHASE II.	465
TABLE 3.31 RESULTS FROM THE DISCRIMINANT ANALYSIS WHEN APPLIED ON THE ARCHAEOLOGICAL METACARPALS OF PHASE II, EXCLUDING VARIABLES GL AND SD.....	466
TABLE 3.32 RESULTS FROM THE DISCRIMINANT ANALYSIS WHEN APPLIED ON THE ARCHAEOLOGICAL METATARSALS OF PHASE II.....	467
TABLE 3.33 RESULTS FROM THE DISCRIMINANT ANALYSIS WHEN APPLIED ON THE ARCHAEOLOGICAL METATARSALS OF PHASE II, EXCLUDING VARIABLES GL AND SD.	467
TABLE 3.34 RESULTS FROM THE DISCRIMINANT ANALYSIS WHEN APPLIED ON THE ARCHAEOLOGICAL TIBIAE OF PHASE II, EXCLUDING VARIABLE GL.	468
TABLE 3.35 RESULTS FROM THE DISCRIMINANT ANALYSIS WHEN APPLIED ON THE ARCHAEOLOGICAL TIBIAE OF PHASE II, EXCLUDING VARIABLES GL AND SD.....	469
TABLE 3.36 RESULTS FROM THE DISCRIMINANT ANALYSIS WHEN APPLIED ON THE ARCHAEOLOGICAL ASTRAGALI OF PHASE II.....	469
TABLE 3.37 RESULTS FROM THE DISCRIMINANT ANALYSIS WHEN APPLIED ON THE ARCHAEOLOGICAL CALCANEAE OF PHASE II.	470
TABLE 3.38 RESULTS FROM THE DISCRIMINANT ANALYSIS WHEN APPLIED ON THE ARCHAEOLOGICAL CALCANEAE OF PHASE II, EXCLUDING VARIABLES SB AND GL.	471
TABLE 3.39 RESULTS FROM THE DISCRIMINANT ANALYSIS WHEN APPLIED ON THE ARCHAEOLOGICAL HORNCORES OF PHASE III.	471
TABLE 3.40 RESULTS FROM THE DISCRIMINANT ANALYSIS WHEN APPLIED ON THE ARCHAEOLOGICAL HORNCORES OF PHASE III, EXCLUDING VARIABLES E AND F.	472

TABLE 3.41 RESULTS FROM THE DISCRIMINANT ANALYSIS WHEN APPLIED ON THE ARCHAEOLOGICAL SCAPULAE OF PHASE III.	473
TABLE 3.42 RESULTS FROM THE DISCRIMINANT ANALYSIS WHEN APPLIED ON THE ARCHAEOLOGICAL HUMERI OF PHASE III.	473
TABLE 3.43 RESULTS FROM THE DISCRIMINANT ANALYSIS WHEN APPLIED ON THE ARCHAEOLOGICAL RADII OF PHASE III.	474
TABLE 3.44 RESULTS FROM THE DISCRIMINANT ANALYSIS WHEN APPLIED ON THE ARCHAEOLOGICAL RADII OF PHASE III, EXCLUDING VARIABLES GL AND SD.	475
TABLE 3.45 RESULTS FROM THE DISCRIMINANT ANALYSIS WHEN APPLIED ON THE ARCHAEOLOGICAL ULNAE OF PHASE III.	475
TABLE 3.46 RESULTS FROM THE DISCRIMINANT ANALYSIS WHEN APPLIED ON THE ARCHAEOLOGICAL ULNAE OF PHASE III, EXCLUDING VARIABLES B AND L.	476
TABLE 3.47 RESULTS FROM THE DISCRIMINANT ANALYSIS WHEN APPLIED ON THE ARCHAEOLOGICAL METACARPALS OF PHASE III.	477
TABLE 3.48 RESULTS FROM THE DISCRIMINANT ANALYSIS WHEN APPLIED ON THE ARCHAEOLOGICAL METACARPALS OF PHASE III, EXCLUDING VARIABLES GL AND SD.	477
TABLE 3.49 RESULTS FROM THE DISCRIMINANT ANALYSIS WHEN APPLIED ON THE ARCHAEOLOGICAL TIBIAE OF PHASE III, EXCLUDING VARIABLE GL.	478
TABLE 3.50 RESULTS FROM THE DISCRIMINANT ANALYSIS WHEN APPLIED ON THE ARCHAEOLOGICAL TIBIAE OF PHASE III, EXCLUDING VARIABLES GL AND SD.	479
TABLE 3.51 RESULTS FROM THE DISCRIMINANT ANALYSIS WHEN APPLIED ON THE ARCHAEOLOGICAL ASTRAGALI OF PHASE III.	479
TABLE 3.52 RESULTS FROM THE DISCRIMINANT ANALYSIS WHEN APPLIED ON THE ARCHAEOLOGICAL CALCANEA OF PHASE III.	480
TABLE 3.53 RESULTS FROM THE DISCRIMINANT ANALYSIS WHEN APPLIED ON THE ARCHAEOLOGICAL HORNCORES OF PHASE IV.	481
TABLE 3.54 RESULTS FROM THE DISCRIMINANT ANALYSIS WHEN APPLIED ON THE ARCHAEOLOGICAL CALCANEI OF PHASE IV, EXCLUDING E AND F VARIABLES.	481
TABLE 3.55 RESULTS FROM THE DISCRIMINANT ANALYSIS WHEN APPLIED ON THE ARCHAEOLOGICAL SCAPULAE OF PHASE IV.	482
TABLE 3.56 RESULTS FROM THE DISCRIMINANT ANALYSIS WHEN APPLIED ON THE ARCHAEOLOGICAL HUMERI OF PHASE IV.	483
TABLE 3.57 RESULTS FROM THE DISCRIMINANT ANALYSIS WHEN APPLIED ON THE ARCHAEOLOGICAL RADII OF PHASE IV.	483
TABLE 3.58 RESULTS FROM THE DISCRIMINANT ANALYSIS WHEN APPLIED ON THE ARCHAEOLOGICAL RADII OF PHASE IV, EXCLUDING VARIABLES GL AND SD.	484
TABLE 3.59 RESULTS FROM THE DISCRIMINANT ANALYSIS WHEN APPLIED ON THE ARCHAEOLOGICAL ULNAE OF PHASE IV.	485
TABLE 3.60 RESULTS FROM THE DISCRIMINANT ANALYSIS WHEN APPLIED ON THE ARCHAEOLOGICAL ULNAE OF PHASE IV, EXCLUDING B AND L VARIABLES.	485

TABLE 3.61 RESULTS FROM THE DISCRIMINANT ANALYSIS WHEN APPLIED ON THE ARCHAEOLOGICAL METACARPALS OF PHASE IV.....	486
TABLE 3.62 RESULTS FROM THE DISCRIMINANT ANALYSIS WHEN APPLIED ON THE ARCHAEOLOGICAL METACARPALS OF PHASE IV, EXCLUDING VARIABLES GL AND SD.	486
TABLE 3.63 RESULTS FROM THE DISCRIMINANT ANALYSIS WHEN APPLIED ON THE ARCHAEOLOGICAL METATARSALS OF PHASE IV.	487
TABLE 3.64 RESULTS FROM THE DISCRIMINANT ANALYSIS WHEN APPLIED ON THE ARCHAEOLOGICAL METATARSALS OF PHASE IV, EXCLUDING VARIABLES GL AND SD.	488
TABLE 3.65 RESULTS FROM THE DISCRIMINANT ANALYSIS WHEN APPLIED ON THE ARCHAEOLOGICAL TIBIAE OF PHASE IV.....	488
TABLE 3.66 RESULTS FROM THE DISCRIMINANT ANALYSIS WHEN APPLIED ON THE ARCHAEOLOGICAL TIBIAE OF PHASE IV, EXCLUDING VARIABLE GL.	489
TABLE 3.67 RESULTS FROM THE DISCRIMINANT ANALYSIS WHEN APPLIED ON THE ARCHAEOLOGICAL TIBIAE OF PHASE IV, EXCLUDING VARIABLES GL AND SD.	490
TABLE 3.68 RESULTS FROM THE DISCRIMINANT ANALYSIS WHEN APPLIED ON THE ARCHAEOLOGICAL ASTRAGALI OF PHASE IV.	490
TABLE 3.69 RESULTS FROM THE DISCRIMINANT ANALYSIS WHEN APPLIED ON THE ARCHAEOLOGICAL CALCANEA OF PHASE IV.	491
TABLE 3.70 RESULTS FROM THE DISCRIMINANT ANALYSIS WHEN APPLIED ON THE UNSTRATIFIED ARCHAEOLOGICAL HORNCORES.....	492
TABLE 3.71 RESULTS FROM THE DISCRIMINANT ANALYSIS WHEN APPLIED ON THE ARCHAEOLOGICAL UNSTRATIFIED HORNCORES, EXCLUDING VARIABLES E AND F.	492
TABLE 3.72 RESULTS FROM THE DISCRIMINANT ANALYSIS WHEN APPLIED ON THE UNSTRATIFIED ARCHAEOLOGICAL SCAPULAE.	493
TABLE 3.73 RESULTS FROM THE DISCRIMINANT ANALYSIS WHEN APPLIED ON THE UNSTRATIFIED ARCHAEOLOGICAL HUMERI.	494
TABLE 3.74 RESULTS FROM THE DISCRIMINANT ANALYSIS WHEN APPLIED ON THE UNSTRATIFIED ARCHAEOLOGICAL RADII.	494
TABLE 3.75 RESULTS FROM THE DISCRIMINANT ANALYSIS WHEN APPLIED ON THE UNSTRATIFIED ARCHAEOLOGICAL RADII, EXCLUDING VARIABLES GL AND SD.	495
TABLE 3.76 RESULTS FROM THE DISCRIMINANT ANALYSIS WHEN APPLIED ON THE UNSTRATIFIED ARCHAEOLOGICAL ULNAE.	496
TABLE 3.77 RESULTS FROM THE DISCRIMINANT ANALYSIS WHEN APPLIED ON THE UNSTRATIFIED ARCHAEOLOGICAL ULNAE, EXCLUDING VARIABLES B AND L.....	496
TABLE 3.78 RESULTS FROM THE DISCRIMINANT ANALYSIS WHEN APPLIED ON THE UNSTRATIFIED ARCHAEOLOGICAL METACARPALS.	497
TABLE 3.79 RESULTS FROM THE DISCRIMINANT ANALYSIS WHEN APPLIED ON THE UNSTRATIFIED ARCHAEOLOGICAL METACARPALS, EXCLUDING VARIABLES GL AND SD.....	497
TABLE 3.80 RESULTS FROM THE DISCRIMINANT ANALYSIS WHEN APPLIED ON THE UNSTRATIFIED ARCHAEOLOGICAL METATARSALS.....	498

TABLE 3.81 RESULTS FROM THE DISCRIMINANT ANALYSIS WHEN APPLIED ON THE UNSTRATIFIED ARCHAEOLOGICAL METATARSALS, EXCLUDING GL AND SD VARIABLES.....	499
TABLE 3.82 RESULTS FROM THE DISCRIMINANT ANALYSIS WHEN APPLIED ON THE UNSTRATIFIED ARCHAEOLOGICAL TIBIAE.....	500
TABLE 3.83 RESULTS FROM THE DISCRIMINANT ANALYSIS WHEN APPLIED ON THE UNSTRATIFIED ARCHAEOLOGICAL TIBIAE, EXCLUDING VARIABLE GL.....	500
TABLE 3.84 RESULTS FROM THE DISCRIMINANT ANALYSIS WHEN APPLIED ON THE UNSTRATIFIED ARCHAEOLOGICAL TIBIAE, EXCLUDING VARIABLES GL AND SD.	501
TABLE 3.85 RESULTS FROM THE DISCRIMINANT ANALYSIS WHEN APPLIED ON THE UNSTRATIFIED ARCHAEOLOGICAL ASTRAGALI.	501
TABLE 3.86 RESULTS FROM THE DISCRIMINANT ANALYSIS WHEN APPLIED ON THE UNSTRATIFIED ARCHAEOLOGICAL CALCANEA.	502
TABLE 3.87 RESULTS FROM THE DISCRIMINANT ANALYSIS WHEN APPLIED ON THE UNSTRATIFIED ARCHAEOLOGICAL CALCANEA, EXCLUDING VARIABLES GL AND SB.....	503
TABLE 3.88 RESULTS FROM THE DISCRIMINANT ANALYSIS WHEN APPLIED ON ALL THE ARCHAEOLOGICAL HORNCORES.	504
TABLE 3.89 RESULTS FROM THE DISCRIMINANT ANALYSIS WHEN APPLIED ON ALL THE ARCHAEOLOGICAL HORNCORES, EXCLUDING VARIABLES E AND F.	504
TABLE 3.90 RESULTS FROM THE DISCRIMINANT ANALYSIS WHEN APPLIED ON ALL THE ARCHAEOLOGICAL SCAPULAE.	507
TABLE 3.91 RESULTS FROM THE DISCRIMINANT ANALYSIS WHEN APPLIED ON ALL THE ARCHAEOLOGICAL HUMERI.....	508
TABLE 3.92 RESULTS FROM THE DISCRIMINANT ANALYSIS WHEN APPLIED ON ALL THE ARCHAEOLOGICAL RADII.....	510
TABLE 3.93 RESULTS FROM THE DISCRIMINANT ANALYSIS WHEN APPLIED ON ALL THE ARCHAEOLOGICAL RADII, EXCLUDING VARIABLES GL AND SD.	510
TABLE 3.94 RESULTS FROM THE DISCRIMINANT ANALYSIS WHEN APPLIED ON ALL THE ARCHAEOLOGICAL ULNAE.....	513
TABLE 3.95 RESULTS FROM THE DISCRIMINANT ANALYSIS WHEN APPLIED ON ALL THE ARCHAEOLOGICAL ULNAE, EXCLUDING VARIABLES B AND L.	513
TABLE 3.96 RESULTS FROM THE DISCRIMINANT ANALYSIS WHEN APPLIED ON ALL THE ARCHAEOLOGICAL METACARPALS.	516
TABLE 3.97 RESULTS FROM THE DISCRIMINANT ANALYSIS WHEN APPLIED ON ALL THE ARCHAEOLOGICAL METACARPALS, EXCLUDING VARIABLES GL AND SD.....	516
TABLE 3.98 RESULTS FROM THE DISCRIMINANT ANALYSIS WHEN APPLIED ON ALL THE ARCHAEOLOGICAL METATARSALS.	518
TABLE 3.99 RESULTS FROM THE DISCRIMINANT ANALYSIS WHEN APPLIED ON ALL THE ARCHAEOLOGICAL METATARSALS, EXCLUDING VARIABLES GL AND SD.....	519
TABLE 3.100 RESULTS FROM THE DISCRIMINANT ANALYSIS WHEN APPLIED ON ALL THE ARCHAEOLOGICAL TIBIAE.	521

TABLE 3.101 RESULTS FROM THE DISCRIMINANT ANALYSIS WHEN APPLIED ON ALL THE ARCHAEOLOGICAL TIBIAE, EXCLUDING VARIABLE GL.	522
TABLE 3.102 RESULTS FROM THE DISCRIMINANT ANALYSIS WHEN APPLIED ON ALL THE ARCHAEOLOGICAL TIBIAE, EXCLUDING VARIABLES GL AND SD.	522
TABLE 3.103 RESULTS FROM THE DISCRIMINANT ANALYSIS WHEN APPLIED ON ALL THE ARCHAEOLOGICAL ASTRAGALI.	525
TABLE 3.104 RESULTS FROM THE DISCRIMINANT ANALYSIS WHEN APPLIED ON ALL THE ARCHAEOLOGICAL CALCANEA.	527
TABLE 3.105 RESULTS FROM THE DISCRIMINANT ANALYSIS WHEN APPLIED ON ALL THE ARCHAEOLOGICAL CALCANEA, EXCLUDING GL AND SB VARIABLES.	527
TABLE 3.106 PERCENTAGES OF CORRECT REATTRIBUTIONS FOR THE MODERN MATERIAL AND FOR THE ARCHAEOLOGICAL MATERIAL (WHOLE ASSEMBLAGE) PROVIDED BY THE DA. AN ASTERISK MARK SMALL SAMPLE SIZES (LESS THAN 10 SPECIMENS).	529
TABLE 3.107 SUMMARY TABLE OF THE RESULTS OBTAINED FROM THE MORPHOLOGICAL APPROACH AND THE BIOMETRICAL APPROACH IN THE FORM OF BOTH BIOMETRICAL INDICES (BI) AND DISCRIMINANT ANALYSIS (DA), WHEN THE SHEEP/GOAT ASSEMBLAGE FROM KING'S LYNN WAS CONSIDERED <i>IN TOTO</i> . THE SPECIMENS CONSIDERED AS 'MISCLASSIFIED' ARE THOSE WHICH, AS THEY FALL ON OR BEYOND THE GROUP CENTROID LINE OF THE OPPOSITE SPECIES, ARE MORE LIKELY TO REPRESENT A MORPHOLOGICAL MISCLASSIFICATION. THE EXPECTATIONS ARE BASED ON THE RESULTS PROVIDED BY THE MODERN MATERIAL; IF THE ARCHAEOLOGICAL MATERIAL HAS GIVEN A HIGHER PERCENTAGE OF CONSISTENT ATTRIBUTIONS THAN THE MODERN, THE EXPECTATIONS ARE EXCEEDED.	532
TABLE 3.108 NISP FOR PHASE T VII OF THE THREE IDENTIFIED CATEGORIES.	542
TABLE 3.109 NISP FOR PHASE S VII OF THE THREE IDENTIFIED CATEGORIES.	543
TABLE 3.110 NISP FOR PHASE S VIII OF THE THREE IDENTIFIED CATEGORIES.	544
TABLE 3.111 RESULTS FROM THE DISCRIMINANT ANALYSIS WHEN APPLIED ON THE ARCHAEOLOGICAL HORNCORES. A = PERCENTAGE OF CORRECT ATTRIBUTIONS RELATED TO THE MODERN MATERIAL (SELECTED ORIGINAL GROUPED CASES); B = PERCENTAGE OF CORRECT ATTRIBUTIONS RELATED TO THE ARCHAEOLOGICAL MATERIAL (UNSELECTED ORIGINAL GROUPED CASES); D = PERCENTAGE OF CORRECT ATTRIBUTIONS WHEN CROSS-VALIDATION WAS APPLIED. SAME TERMINOLOGY IS ADOPTED IN ALL THE FOLLOWING TABLES.	582
TABLE 3.112 RESULTS FROM THE DISCRIMINANT ANALYSIS WHEN APPLIED ON THE ARCHAEOLOGICAL HORNCORES EXCLUDING MEASUREMENTS A AND B.	582
TABLE 3.113 RESULTS FROM THE DISCRIMINANT ANALYSIS WHEN APPLIED ON THE ARCHAEOLOGICAL HORNCORES (EXCLUDING MEASUREMENTS E AND F).	583
TABLE 3.114 RESULTS FROM THE DISCRIMINANT ANALYSIS WHEN APPLIED ON THE ARCHAEOLOGICAL SCAPULAE.	586
TABLE 3.115 RESULTS FROM THE DISCRIMINANT ANALYSIS WHEN APPLIED ON THE ARCHAEOLOGICAL HUMERI.	588
TABLE 3.116 RESULTS FROM THE DISCRIMINANT ANALYSIS WHEN APPLIED ON THE ARCHAEOLOGICAL RADII.	589

TABLE 3.117 RESULTS FROM THE DISCRIMINANT ANALYSIS WHEN APPLIED ON THE ARCHAEOLOGICAL RADII (MEASUREMENTS GL AND SD EXCLUDED).....	590
TABLE 3.118 RESULTS FROM THE DISCRIMINANT ANALYSIS WHEN APPLIED ON THE ARCHAEOLOGICAL ULNAE.....	593
TABLE 3.119 RESULTS FROM THE DISCRIMINANT ANALYSIS WHEN APPLIED ON THE ARCHAEOLOGICAL ULNAE (EXCLUDING MEASUREMENTS B AND L).....	593
TABLE 3.120 RESULTS FROM THE DISCRIMINANT ANALYSIS WHEN APPLIED ON THE ARCHAEOLOGICAL METACARPALS.	596
TABLE 3.121 RESULTS FROM THE DISCRIMINANT ANALYSIS WHEN APPLIED ON THE ARCHAEOLOGICAL METACARPALS (EXCLUDING MEASUREMENTS GL AND SD).....	596
TABLE 3.122 RESULTS FROM THE DISCRIMINANT ANALYSIS WHEN APPLIED ON THE ARCHAEOLOGICAL METATARSALS.	599
TABLE 3.123 RESULTS FROM THE DISCRIMINANT ANALYSIS WHEN APPLIED ON THE ARCHAEOLOGICAL METATARSALS.	599
TABLE 3.124 RESULTS FROM THE DISCRIMINANT ANALYSIS WHEN APPLIED ON THE ARCHAEOLOGICAL TIBIAE (EXCLUDING MEASUREMENT GL).....	602
TABLE 3.125 RESULTS FROM THE DISCRIMINANT ANALYSIS WHEN APPLIED ON THE ARCHAEOLOGICAL TIBIAE (EXCLUDING MEASUREMENT GL AND SD).	602
TABLE 3.126 RESULTS FROM THE DISCRIMINANT ANALYSIS WHEN APPLIED ON THE ARCHAEOLOGICAL ASTRAGALI.	605
TABLE 3.127 RESULTS FROM THE DISCRIMINANT ANALYSIS WHEN APPLIED ON THE ARCHAEOLOGICAL CALCANEA.	607
TABLE 3.128 PERCENTAGES OF CORRECT REATTRIBUTIONS FOR THE MODERN MATERIAL AND FOR THE ARCHAEOLOGICAL MATERIAL (WHOLE ASSEMBLAGE) PROVIDED BY THE DA. AN ASTERISK MARK SMALL SAMPLE SIZES (LESS THAN 10 SPECIMENS).....	610
TABLE 3.129 SUMMARY TABLE OF THE RESULTS OBTAINED FROM THE MORPHOLOGICAL APPROACH AND THE BIOMETRICAL APPROACH IN THE FORM OF BOTH BIOMETRICAL INDICES (BI) AND DISCRIMINANT ANALYSIS (DA), WHEN THE SHEEP/GOAT ASSEMBLAGE FROM FLAXENGATE WAS CONSIDERED <i>IN TOTO</i> . THE SPECIMENS CONSIDERED AS ‘MISCLASSIFIED’ ARE THOSE WHICH, AS THEY FALL ON OR BEYOND THE GROUP CENTROID LINE OF THE OPPOSITE SPECIES, ARE MORE LIKELY TO REPRESENT A MORPHOLOGICAL MISCLASSIFICATION. THE EXPECTATIONS ARE BASED ON THE RESULTS PROVIDED BY THE MODERN MATERIAL; IF THE ARCHAEOLOGICAL MATERIAL HAS GIVEN A HIGHER PERCENTAGE OF CONSISTENT ATTRIBUTIONS THAN THE MODERN, THE EXPECTATIONS ARE EXCEEDED.....	611
TABLE 3.130 CHRONOLOGY OF THE SITE WITH A BRIEF DESCRIPTION OF THE MAIN FEATURES FOUND (FOLLOWING BROWN 2008 AND SODEN 1998-1999).	617
TABLE 3.131 CHRONOLOGICAL PHASES USED IN THIS STUDY.	618
TABLE 3.132 NISP FOR THE THREE IDENTIFIED CATEGORIES FOR PHASE I.	623
TABLE 3.133 NISP FOR THE THREE IDENTIFIED CATEGORIES FOR PHASE II.	624
TABLE 3.134 NISP FOR THE THREE IDENTIFIED CATEGORIES FOR PHASE III.....	625
TABLE 3.135 NISP FOR THE THREE IDENTIFIED CATEGORIES AMONGST THE UNSTRATIFIED SPECIMENS. .	626

TABLE 3.136 RESULTS FROM THE DISCRIMINANT ANALYSIS WHEN APPLIED ON ALL THE ARCHAEOLOGICAL HORNCORES.....	674
TABLE 3.137 RESULTS FROM THE DISCRIMINANT ANALYSIS WHEN APPLIED ON ALL THE ARCHAEOLOGICAL HORNCORES, EXCLUDING VARIABLES E AND F.....	675
TABLE 3.138 RESULTS FROM THE DISCRIMINANT ANALYSIS WHEN APPLIED ON ALL THE ARCHAEOLOGICAL SCAPULAE.....	677
TABLE 3.139 RESULTS FROM THE DISCRIMINANT ANALYSIS WHEN APPLIED ON ALL THE ARCHAEOLOGICAL HUMERI.....	678
TABLE 3.140 RESULTS FROM THE DISCRIMINANT ANALYSIS WHEN APPLIED ON ALL THE ARCHAEOLOGICAL RADII.....	680
TABLE 3.141 RESULTS FROM THE DISCRIMINANT ANALYSIS WHEN APPLIED ON ALL THE ARCHAEOLOGICAL RADII, EXCLUDING VARIABLES GL AND SD.....	680
TABLE 3.142 RESULTS FROM THE DISCRIMINANT ANALYSIS WHEN APPLIED ON ALL THE ARCHAEOLOGICAL ULNAE.....	683
TABLE 3.143 RESULTS FROM THE DISCRIMINANT ANALYSIS WHEN APPLIED ON ALL THE ARCHAEOLOGICAL ULNAE, EXCLUDING VARIABLES B AND L.....	683
TABLE 3.144 RESULTS FROM THE DISCRIMINANT ANALYSIS WHEN APPLIED ON ALL THE ARCHAEOLOGICAL METACARPALS.....	685
TABLE 3.145 RESULTS FROM THE DISCRIMINANT ANALYSIS WHEN APPLIED ON ALL THE ARCHAEOLOGICAL METACARPALS, EXCLUDING VARIABLES GL AND SD.....	686
TABLE 3.146 RESULTS FROM THE DISCRIMINANT ANALYSIS WHEN APPLIED ON ALL THE ARCHAEOLOGICAL METATARSALS.....	688
TABLE 3.147 RESULTS FROM THE DISCRIMINANT ANALYSIS WHEN APPLIED ON ALL THE ARCHAEOLOGICAL METATARSALS, EXCLUDING VARIABLES GL AND SD.....	689
TABLE 3.148 RESULTS FROM THE DISCRIMINANT ANALYSIS WHEN APPLIED ON ALL THE ARCHAEOLOGICAL TIBIAE.....	691
TABLE 3.149 RESULTS FROM THE DISCRIMINANT ANALYSIS WHEN APPLIED ON ALL THE ARCHAEOLOGICAL TIBIAE, EXCLUDING VARIABLE GL.....	691
TABLE 3.150 RESULTS FROM THE DISCRIMINANT ANALYSIS WHEN APPLIED ON ALL THE ARCHAEOLOGICAL TIBIAE, EXCLUDING VARIABLES GL AND SD.....	692
TABLE 3.151 RESULTS FROM THE DISCRIMINANT ANALYSIS WHEN APPLIED ON ALL THE ARCHAEOLOGICAL ASTRAGALI.....	695
TABLE 3.152 RESULTS FROM THE DISCRIMINANT ANALYSIS WHEN APPLIED ON ALL THE ARCHAEOLOGICAL CALCANEA.....	697
TABLE 3.153 RESULTS FROM THE DISCRIMINANT ANALYSIS WHEN APPLIED ON ALL THE ARCHAEOLOGICAL CALCANEA, EXCLUDING GL AND SB VARIABLES.....	697
TABLE 3.154 PERCENTAGES OF CORRECT REATTRIBUTIONS FOR THE MODERN MATERIAL AND FOR THE ARCHAEOLOGICAL MATERIAL (WHOLE ASSEMBLAGE) PROVIDED BY THE DA. AN ASTERISK MARK SMALL SAMPLE SIZES (LESS THAN 10 SPECIMENS).....	700
TABLE 3.155 SUMMARY TABLE OF THE RESULTS OBTAINED FROM THE MORPHOLOGICAL APPROACH AND THE BIOMETRICAL APPROACH IN THE FORM OF BOTH BIOMETRICAL INDICES (BI) AND DISCRIMINANT	

ANALYSIS (DA), WHEN THE SHEEP/GOAT ASSEMBLAGE FROM WOOLMONGER/KINGSWELL STREET WAS CONSIDERED *IN TOTO*. THE SPECIMENS CONSIDERED AS ‘MISCLASSIFIED’ ARE THOSE WHICH, AS THEY FALL ON OR BEYOND THE GROUP CENTROID LINE OF THE OPPOSITE SPECIES, ARE MORE LIKELY TO REPRESENT A MORPHOLOGICAL MISCLASSIFICATION. THE EXPECTATIONS ARE BASED ON THE RESULTS PROVIDED BY THE MODERN MATERIAL; IF THE ARCHAEOLOGICAL MATERIAL HAS GIVEN A HIGHER PERCENTAGE OF CONSISTENT ATTRIBUTIONS THAN THE MODERN, THE EXPECTATIONS ARE EXCEEDED..... 702

TABLE 3.156 LIST OF THE MORPHOLOGICAL TRAIT PER ANATOMICAL ELEMENT WHICH HAVE RESULTED TO BE PARTICULARLY USEFUL IN THE IDENTIFICATION OF THE ARCHAEOLOGICAL MATERIAL. 708

TABLE 3.157 LIST OF THE BI THAT HAVE PROVEN MOST SUCCESSFUL IN SEPARATING ARCHAEOLOGICAL SHEEP AND GOATS..... 709

List of Figures

<p>FIGURE 1.1 DIAGNOSTIC CHARACTERISTICS ON THE DISTAL TIBIA (1=GOAT; 2=SHEEP; C=LATERAL SIDE; D= MEDIAL SIDE; E= DISTAL ARTICULAR SURFACE. IMAGE REPRINTED FROM KRATOCHVÍL, Z. SPECIES CRITERIA ON THE DISTAL SECTION OF THE TIBIA IN <i>OVIS AMMON F. ARIES L. AND CAPRA AEGAGRUS F. HIRCUS L. ACTA VETERINARIA</i> (BRNO), COPYRIGHT 1969, 38: 483-490. LICENCE AVAILABLE AT: HTTPS://CREATIVECOMMONS.ORG/LICENSES/BY/4.0/).</p>	8
<p>FIGURE 1.2 INDEX ADOPTED ON THE DISTAL METAPODIALS AND MORPHOLOGICAL TRAITS CONSIDERED FOR EACH BONE FOLLOWING GROMOVA 1953 AND BOESSNECK <i>ET AL.</i> 1964 (IMAGE REPRINTED FROM HOLE, F. THE CONTEXT OF THE CAPRINE DOMESTICATION IN THE ZAGROS REGION. IN <i>THE ORIGINS AND SPREAD OF AGRICULTURE AND PASTORALISM IN EURASIA</i>, ED. D.R. HARRIS, 263-281, COPYRIGHT 1996. LONDON: UNIVERSITY COLLEGE OF LONDON PRESS, WITH PERMISSION FROM KENT FLANNERY, JOYCE MARCUS AND FRANK HOLE).</p>	9
<p>FIGURE 1.3 SOME MORPHOLOGICAL TRAITS ON THE FOURTH DECIDUOUS LOWER PREMOLAR (DP₄) PROPOSED BY PAYNE (IMAGE REPRINTED FROM PAYNE, S. MORPHOLOGICAL DISTINCTIONS BETWEEN THE MANDIBULAR TEETH OF YOUNG SHEEP, <i>OVIS</i>, AND GOATS, <i>CAPRA. JOURNAL OF ARCHAEOLOGICAL SCIENCE</i> 12: 139-147, COPYRIGHT 1985, WITH PERMISSION FROM ELSEVIER). 5-7 ARE RESPECTIVELY MESIAL, BUCCAL AND DISTAL VIEWS OF A DP₄ OF A KID; 8-10 MESIAL, BUCCAL AND DISTAL VIEWS OF A DP₄ OF A LAMB.</p>	16
<p>FIGURE 1.4 SEQUENCE SHOWING THE CHANGES OF THIRD AND FOURTH PERMANENT LOWER PREMOLARS (P₃ AND P₄) ACCORDING TO WEAR STAGES (IMAGE (FIG. 2) REPRINTED FROM HELMER, D. DISCRIMINATION DES GENRES <i>OVIS</i> ET <i>CAPRA</i> À L'AIDE DES PRÉMOLAIRES INFÉRIEURES 3 ET 4 ET INTERPRÉTATION DES ÂGES D'ABATTAGE: L'EXEMPLE DE DIKILI TASH (GRÈCE). <i>ANTHROPOZOOLOGICA</i> 31: 29-38, COPYRIGHT 2000. COPYRIGHT PUBLICATIONS SCIENTIFIQUES DU MUSÉUM NATIONAL D'HISTOIRE NATURELLE, PARIS).</p>	17
<p>FIGURE 1.5 MEASUREMENTS SUGGESTED BY PAYNE (1969) AS EFFECTIVE FOR DISCRIMINATING SHEEP FROM GOAT, ON THE DISTAL METACARPAL BONE (IMAGE REPRINTED FROM PAYNE, S. A METRICAL DISTINCTION BETWEEN SHEEP AND GOAT METACARPAL. IN <i>THE DOMESTICATION AND EXPLOITATION OF PLANTS AND ANIMALS</i>, EDS. P.J. UCKO AND G.W. DIMBLEBY, 295-306, COPYRIGHT 1969. LONDON: DUCKWORTH, WITH PERMISSION FROM SEBASTIAN PAYNE). ...</p>	22
<p>FIGURE 1.6 PROXIMAL ARTICULATION OF GOAT (LEFT) AND SHEEP (RIGHT) SHOWING THE POINTS AT WHICH THE MEASUREMENTS WERE TAKEN BY ROWLEY-CONWY (IMAGE REPRINTED FROM ROWLEY-CONWY, P. IMPROVED SEPARATION OF NEOLITHIC METAPODIALS OF SHEEP (<i>OVIS</i>) AND GOATS (<i>CAPRA</i>) FROM ARENE CANDIDE CAVE, LIGURIA, ITALY. <i>JOURNAL OF ARCHAEOLOGICAL SCIENCE</i> 25: 251-258, COPYRIGHT 1998, WITH PERMISSION FROM ELSEVIER).</p>	23
<p>FIGURE 1.7 PERCENTAGE OF OCCURRENCE OF IDENTIFIED GOAT SPECIMENS BY BODY PART IN POST-IRON AGE PERIOD-SITES (IMAGE REPRINTED FROM ALBARELLA, U., WITH T. PIRNIE AND S. VINER. (UNPUBLISHED). <i>ANIMALS OF OUR PAST: A REVIEW OF THE ZOOARCHAEOLOGY OF CENTRAL ENGLAND</i>, WITH PERMISSION FROM UMBERTO ALBARELLA).</p>	33
<p>FIGURE 1.8 PERCENTAGE OCCURRENCE OF ROMAN, SAXON, MEDIEVAL, AND POST-MEDIEVAL PERIOD-SITES CONTAINING IDENTIFIED GOAT SPECIMENS, BY BODY PART AND SITE TYPE (IMAGE REPRINTED FROM ALBARELLA, U., WITH T. PIRNIE AND S. VINER. (UNPUBLISHED). <i>ANIMALS OF OUR PAST: A REVIEW OF THE ZOOARCHAEOLOGY OF CENTRAL ENGLAND</i>, WITH PERMISSION FROM UMBERTO ALBARELLA).</p>	35
<p>FIGURE 1.9 PERCENTAGE OF IDENTIFIED GOAT SPECIMENS BY BODY PART FROM SITES ORGANISED BY SUB-REGION (WEST SITES=39; CENTRAL SITES=87; EAST SITES 59. GRAPH REDRAW FROM ALBARELLA 2003).</p>	37

FIGURE 2.1 LEFT MANDIBLE OF A MODERN SPECIMEN OF SHEEP FROM THE REFERENCE COLLECTION OF KIEL (N. 22339) SHOWING THE RIDGE ON THE INTER-ALVEOLAR EDGE OF THE BONE.	79
FIGURE 2.2 LEFT HORNCORE OF A MODERN SHEEP SPECIMEN FROM THE REFERENCE COLLECTION OF PORTSMOUTH (N. 2832) SHOWING A BARELY VISIBLE SEPARATION BETWEEN THE HORN AND THE SKULL.	80
FIGURE 2.3 LEFT SCAPULA OF A MODERN SHEEP SPECIMEN FROM THE REFERENCE COLLECTION OF PORTSMOUTH (N. 3282) SHOWING THE PRESENCE OF A PECTEN ON THE CAUDAL SIDE OF THE NECK. IT IS ALSO POSSIBLE TO SEE THE ROUNDED AREA AT THE BASE OF THE SPINE MENTIONED IN THE TEXT. .	80
FIGURE 2.4 DISTAL RIGHT ARTICULATION OF THE HUMERUS OF A MODERN SHEEP SPECIMEN FROM THE REFERENCE COLLECTION OF PORTSMOUTH (N. 1496) SHOWING THE LACK OF LANDMARKS IN THE REGION WHERE BE IS TAKEN.	81
FIGURE 2.5 LEFT <i>OLECRANON</i> OF AN ULNA FROM A MODERN SPECIMEN OF SHEEP FROM THE REFERENCE COLLECTION OF KIEL (N. 22339) WHICH SHOWS HOW THE MEDIAL SIDE OF THE BONE CAN BE CONVEX IN <i>OVIS</i>	81
FIGURE 2.6 LEFT ASTRAGALUS (FRONTAL AND MEDIAL SIDE) OF A MODERN SPECIMEN OF GOAT FROM THE REFERENCE COLLECTION OF HALLE (N. CSWD 2) SHOWING THE LATERAL PROJECTION OF THE RIDGE.	82
FIGURE 2.7 <i>CALCANEAE</i> FROM A MODERN SPECIMEN OF GOAT (RIGHT, N. 1315) AND SHEEP (LEFT, N. 1496) FROM THE REFERENCE COLLECTION OF PORTSMOUTH SHOWING HOW THE MORPHOLOGY OF THE AREA WHERE THE ARTICULAR FACET OF THE <i>OS MALLEOLARE</i> ATTACHES CAN VARY.	82
FIGURE 2.8 CV FOR EACH OF THE FOUR SPECIMENS FOR ALL THE DIFFERENT MEASUREMENTS.	105
FIGURE 2.9 HORNCORE TRAIT 1 (SECTION): NUMBER OF SPECIMENS ATTRIBUTED TO THE DIFFERENT CATEGORIES FOR THE TWO SPECIES (CH= <i>CAPRA HIRCUS</i> ; OA= <i>OVIS ARIES</i> ; SCORES ON HORIZONTAL AXIS: C= <i>CAPRA</i> ; CL= <i>CAPRA-LIKE</i> ; OC= <i>OVIS/CAPRA</i> ; OL= <i>OVIS-LIKE</i> ; O= <i>OVIS</i>).	129
FIGURE 2.10 HORNCORE TRAIT 2 (CURVATURE): NUMBER OF SPECIMENS ATTRIBUTED TO THE DIFFERENT CATEGORIES FOR THE TWO SPECIES. FOR DETAILS SEE FIG. 2.9.	130
FIGURE 2.11 THIRD DECIDUOUS LOWER PREMOLAR DP ₃ , TRAIT 1 (OVERALL SHAPE): NUMBER OF SPECIMENS ATTRIBUTED TO THE DIFFERENT CATEGORIES FOR THE TWO SPECIES. FOR DETAILS SEE FIG. 2.9.	130
FIGURE 2.12 THIRD DECIDUOUS LOWER PREMOLAR DP ₃ , TRAIT 2 (METACONOID): NUMBER OF SPECIMENS ATTRIBUTED TO THE DIFFERENT CATEGORIES FOR THE TWO SPECIES. FOR DETAILS SEE FIG. 2.9.	130
FIGURE 2.13 FOURTH DECIDUOUS LOWER PREMOLAR DP ₄ , TRAIT 1 (CROWN ASPECT): NUMBER OF SPECIMENS ATTRIBUTED TO THE DIFFERENT CATEGORIES FOR THE TWO SPECIES. FOR DETAILS SEE FIG. 2.9.	131
FIGURE 2.14 FOURTH DECIDUOUS LOWER PREMOLAR DP ₄ , TRAIT 2 (PRESENCE/ABSENCE OF BASAL SWELLING): NUMBER OF SPECIMENS ATTRIBUTED TO THE DIFFERENT CATEGORIES FOR THE TWO SPECIES. FOR DETAILS SEE FIG. 2.9.	131
FIGURE 2.15 FOURTH DECIDUOUS LOWER PREMOLAR DP ₄ , TRAIT 3 (PRESENCE/ABSENCE OF INTERLOBAR PILLAR): NUMBER OF SPECIMENS ATTRIBUTED TO THE DIFFERENT CATEGORIES FOR THE TWO SPECIES. FOR DETAILS SEE FIG. 2.9.	131
FIGURE 2.16 FOURTH DECIDUOUS LOWER PREMOLAR DP ₄ , TRAIT 4 (ENAMEL DEVELOPMENT): NUMBER OF SPECIMENS ATTRIBUTED TO THE DIFFERENT CATEGORIES FOR THE TWO SPECIES. FOR DETAILS SEE FIG. 2.9.	132
FIGURE 2.17 THIRD PERMANENT LOWER PREMOLAR P ₃ , TRAIT 1 (OVERALL SHAPE): NUMBER OF SPECIMENS ATTRIBUTED TO THE DIFFERENT CATEGORIES FOR THE TWO SPECIES. FOR DETAILS SEE FIG. 2.9.	132

FIGURE 2.18 THIRD PERMANENT LOWER PREMOLAR P_3 , TRAIT 2 (MIDDLE VERTICAL RIDGE): NUMBER OF SPECIMENS ATTRIBUTED TO THE DIFFERENT CATEGORIES FOR THE TWO SPECIES. FOR DETAILS SEE FIG. 2.9.....	132
FIGURE 2.19 THIRD PERMANENT LOWER PREMOLAR P_3 , TRAIT 3 (MESIAL-BUCCAL ANGLE): NUMBER OF SPECIMENS ATTRIBUTED TO THE DIFFERENT CATEGORIES FOR THE TWO SPECIES. FOR DETAILS SEE FIG. 2.9.....	133
FIGURE 2.20 FOURTH PERMANENT LOWER PREMOLAR P_4 , TRAIT 1 (OVERALL SHAPE): NUMBER OF SPECIMENS ATTRIBUTED TO THE DIFFERENT CATEGORIES FOR THE TWO SPECIES. FOR DETAILS SEE FIG. 2.9.	133
FIGURE 2.21 FOURTH PERMANENT LOWER PREMOLAR P_4 , TRAIT 2 (MESIO-LINGUAL RIB): NUMBER OF SPECIMENS ATTRIBUTED TO THE DIFFERENT CATEGORIES FOR THE TWO SPECIES. FOR DETAILS SEE FIG. 2.9.....	133
FIGURE 2.22 FOURTH PERMANENT LOWER PREMOLAR P_4 , TRAIT 3 (MESIO-BUCCAL ANGLE): NUMBER OF SPECIMENS ATTRIBUTED TO THE DIFFERENT CATEGORIES FOR THE TWO SPECIES. FOR DETAILS SEE FIG. 2.9.....	134
FIGURE 2.23 THIRD LOWER MOLAR M_3 , TRAIT 1 (MESIAL FACE): NUMBER OF SPECIMENS ATTRIBUTED TO THE DIFFERENT CATEGORIES FOR THE TWO SPECIES. FOR DETAILS SEE FIG. 2.9.....	134
FIGURE 2.24 THIRD LOWER MOLAR M_3 , TRAIT 2 (BUCCAL EDGE ANGLE): NUMBER OF SPECIMENS ATTRIBUTED TO THE DIFFERENT CATEGORIES FOR THE TWO SPECIES. FOR DETAILS SEE FIG. 2.9.....	134
FIGURE 2.25 THIRD LOWER MOLAR M_3 , TRAIT 3 (DIRECTION OF CENTRAL CUSP): NUMBER OF SPECIMENS ATTRIBUTED TO THE DIFFERENT CATEGORIES FOR THE TWO SPECIES. FOR DETAILS SEE FIG. 2.9.....	135
FIGURE 2.26 THIRD LOWER MOLAR M_3 , TRAIT 4 (SYMMETRY AND SHAPE OF CUSPS): NUMBER OF SPECIMENS ATTRIBUTED TO THE DIFFERENT CATEGORIES FOR THE TWO SPECIES. FOR DETAILS SEE FIG. 2.9.	135
FIGURE 2.27 THIRD LOWER MOLAR M_3 , TRAIT 5 (DISTAL FLUTE): NUMBER OF SPECIMENS ATTRIBUTED TO THE DIFFERENT CATEGORIES FOR THE TWO SPECIES. FOR DETAILS SEE FIG. 2.9.....	135
FIGURE 2.28 MANDIBLE, TRAIT 1 (PRESENCE/ABSENCE OF FORAMEN): NUMBER OF SPECIMENS ATTRIBUTED TO THE DIFFERENT CATEGORIES FOR THE TWO SPECIES. FOR DETAILS SEE FIG. 2.9.....	136
FIGURE 2.29 MANDIBLE, TRAIT 2 (HOLLOW): NUMBER OF SPECIMENS ATTRIBUTED TO THE DIFFERENT CATEGORIES FOR THE TWO SPECIES. FOR DETAILS SEE FIG. 2.9.....	136
FIGURE 2.30 SCAPULA, TRAIT 1 (GLENOID TUBERCLE): NUMBER OF SPECIMENS ATTRIBUTED TO THE DIFFERENT CATEGORIES FOR THE TWO SPECIES. FOR DETAILS SEE FIG. 2.9.....	136
FIGURE 2.31 SCAPULA, TRAIT 2 (SHAPE OF GLENOID CAVITY): NUMBER OF SPECIMENS ATTRIBUTED TO THE DIFFERENT CATEGORIES FOR THE TWO SPECIES. FOR DETAILS SEE FIG. 2.9.....	137
FIGURE 2.32 HUMERUS, TRAIT 1 (LATERAL EPICONDYLE): NUMBER OF SPECIMENS ATTRIBUTED TO THE DIFFERENT CATEGORIES FOR THE TWO SPECIES. FOR DETAILS SEE FIG. 2.9.....	137
FIGURE 2.33 HUMERUS, TRAIT 2 (GROVE AT THE POSTERIOR SIDE OF THE LATERAL EPICONDYLE): NUMBER OF SPECIMENS ATTRIBUTED TO THE DIFFERENT CATEGORIES FOR THE TWO SPECIES. FOR DETAILS SEE FIG. 2.9.....	137
FIGURE 2.34 HUMERUS, TRAIT 3 (PIT ON THE LATERAL EPICONDILAR SURFACE): NUMBER OF SPECIMENS ATTRIBUTED TO THE DIFFERENT CATEGORIES FOR THE TWO SPECIES. FOR DETAILS SEE FIG. 2.9.....	138
FIGURE 2.35 HUMERUS, TRAIT 4 (CREST-LIKE PROCESS ON LATERAL BORDER OF EPICONDILAR SURFACE): NUMBER OF SPECIMENS ATTRIBUTED TO THE DIFFERENT CATEGORIES FOR THE TWO SPECIES. FOR DETAILS SEE FIG. 2.9.	138
FIGURE 2.36 HUMERUS, TRAIT 5 (ANGLE AT THE DISTAL PART OF THE MEDIAL EPICONDYLE): NUMBER OF SPECIMENS ATTRIBUTED TO THE DIFFERENT CATEGORIES FOR THE TWO SPECIES. FOR DETAILS SEE FIG. 2.9.....	139

FIGURE 2.37 RADIUS, TRAIT 1 (ASPECT OF THE LATERAL TUBEROSITY): NUMBER OF SPECIMENS ATTRIBUTED TO THE DIFFERENT CATEGORIES FOR THE TWO SPECIES. FOR DETAILS SEE FIG. 2.9.	139
FIGURE 2.38 RADIUS, TRAIT 2 (OVERALL ASPECT OF THE PROXIMAL END): NUMBER OF SPECIMENS ATTRIBUTED TO THE DIFFERENT CATEGORIES FOR THE TWO SPECIES. FOR DETAILS SEE FIG. 2.9.	139
FIGURE 2.39 ULNA, TRAIT 1 (PROJECTION OF LATERAL CORONOID PROCESS): NUMBER OF SPECIMENS ATTRIBUTED TO THE DIFFERENT CATEGORIES FOR THE TWO SPECIES. FOR DETAILS SEE FIG. 2.9.	140
FIGURE 2.40 ULNA, TRAIT 2 (SHAPE OF THE <i>OLECRANON</i>): NUMBER OF SPECIMENS ATTRIBUTED TO THE DIFFERENT CATEGORIES FOR THE TWO SPECIES. FOR DETAILS SEE FIG. 2.9.	140
FIGURE 2.41 METACARPAL AND METATARSAL, TRAIT 1 (DIMENSION OF THE PERIPHERAL PART OF THE TROCHLEAR CONDYLES) NUMBER OF SPECIMENS ATTRIBUTED TO THE DIFFERENT CATEGORIES FOR THE TWO SPECIES. FOR DETAILS SEE FIG. 2.9.	140
FIGURE 2.42 METACARPAL AND METATARSAL, TRAIT 2 (DEFINITION OF THE PERIPHERAL PART OF THE TROCHLEAR CONDYLES) NUMBERS OF SPECIMENS ATTRIBUTED TO THE DIFFERENT CATEGORIES FOR THE TWO SPECIES. FOR DETAILS SEE FIG. 2.9.	141
FIGURE 2.43 METACARPAL AND METATARSAL, TRAIT 3 (ASPECT OF THE PERIPHERAL PART OF THE TROCHLEAR CONDYLES) NUMBER OF SPECIMENS ATTRIBUTED TO THE DIFFERENT CATEGORIES FOR THE TWO SPECIES. FOR DETAILS SEE FIG. 2.9.	141
FIGURE 2.44 METACARPAL AND METATARSAL, TRAIT 4 (DIRECTION OF <i>VERTICILLI</i>) NUMBER OF SPECIMENS ATTRIBUTED TO THE DIFFERENT CATEGORIES FOR THE TWO SPECIES. FOR DETAILS SEE FIG. 2.9.	142
FIGURE 2.45 METACARPAL AND METATARSAL, TRAIT 5 (DEVELOPMENT OF THE FOSSAE ON THE PROXIMAL PART OF THE DISTAL TROCHLEAR CONDYLES) NUMBER OF SPECIMENS ATTRIBUTED TO THE DIFFERENT CATEGORIES FOR THE TWO SPECIES. FOR DETAILS SEE FIG. 2.9.	142
FIGURE 2.46 METATARSAL, TRAIT 6 (ASPECT OF THE JUNCTION ON THE ANTERIOR ASPECT OF THE DISTAL DIAPHYSIS ABOVE THE DISTAL EPIPHYSIS) NUMBER OF SPECIMENS ATTRIBUTED TO THE DIFFERENT CATEGORIES FOR THE TWO SPECIES. FOR DETAILS SEE FIG. 2.9.	143
FIGURE 2.47 TIBIA, TRAIT 1 (DORSAL PROMINENCE) NUMBER OF SPECIMENS ATTRIBUTED TO THE DIFFERENT CATEGORIES FOR THE TWO SPECIES. FOR DETAILS SEE FIG. 2.9.	143
FIGURE 2.48 TIBIA, TRAIT 2 (MEDIAL MALLEOLUS) NUMBER OF SPECIMENS ATTRIBUTED TO THE DIFFERENT CATEGORIES FOR THE TWO SPECIES. FOR DETAILS SEE FIG. 2.9.	144
FIGURE 2.49 TIBIA, TRAIT 3 (PRESENCE/ABSENCE OF THE INTERRUPTION ON THE PLANTAR LIMBUS) NUMBER OF SPECIMENS ATTRIBUTED TO THE DIFFERENT CATEGORIES FOR THE TWO SPECIES. FOR DETAILS SEE FIG. 2.9.	144
FIGURE 2.50 TIBIA, TRAIT 4 (LATERAL PROFILE) NUMBER OF SPECIMENS ATTRIBUTED TO THE DIFFERENT CATEGORIES FOR THE TWO SPECIES. FOR DETAILS SEE FIG. 2.9.	145
FIGURE 2.51 TIBIA, TRAIT 5 (SHAPE OF THE ANTERIOR SIDE OF THE MALLEOLUS) NUMBER OF SPECIMENS ATTRIBUTED TO THE DIFFERENT CATEGORIES FOR THE TWO SPECIES. FOR DETAILS SEE FIG. 2.9.	145
FIGURE 2.52 TIBIA, TRAIT 6 (ASPECT OF THE MEDIAL MALLEOLUS) NUMBER OF SPECIMENS ATTRIBUTED TO THE DIFFERENT CATEGORIES FOR THE TWO SPECIES. FOR DETAILS SEE FIG. 2.9.	146
FIGURE 2.53 ASTRAGALUS, TRAIT 1 (DEPTH OF THE SULCUS OF THE TROCHLEA) NUMBER OF SPECIMENS ATTRIBUTED TO THE DIFFERENT CATEGORIES FOR THE TWO SPECIES. FOR DETAILS SEE FIG. 2.9.	146

FIGURE 2.54 ASTRAGALUS, TRAIT 2 (INCLINATION OF THE LATERAL PART OF THE TROCHLEA) NUMBER OF SPECIMENS ATTRIBUTED TO THE DIFFERENT CATEGORIES FOR THE TWO SPECIES. FOR DETAILS SEE FIG. 2.9.....	147
FIGURE 2.55 ASTRAGALUS, TRAIT 3 (SHAPE OF THE MEDIAL RIDGE) NUMBER OF SPECIMENS ATTRIBUTED TO THE DIFFERENT CATEGORIES FOR THE TWO SPECIES. FOR DETAILS SEE FIG. 2.9.....	147
FIGURE 2.56 ASTRAGALUS, TRAIT 4 (SHAPE OF THE DISTAL ARTICULAR SURFACE ON THE LATERAL ASPECT) NUMBER OF SPECIMENS ATTRIBUTED TO THE DIFFERENT CATEGORIES FOR THE TWO SPECIES. FOR DETAILS SEE FIG. 2.9.	147
FIGURE 2.57 ASTRAGALUS, TRAIT 5 (ASPECT OF THE PROXIMO-PLANTAR PROJECTION ON THE MEDIAL ARTICULAR RIDGE OF THE TROCHLEA) NUMBER OF SPECIMENS ATTRIBUTED TO THE DIFFERENT CATEGORIES FOR THE TWO SPECIES. FOR DETAILS SEE FIG. 2.9.....	148
FIGURE 2.58 ASTRAGALUS, TRAIT 6 (ASPECT AND DIRECTION OF THE ARTICULAR SURFACE ON THE PLANTAR SIDE) NUMBER OF SPECIMENS ATTRIBUTED TO THE DIFFERENT CATEGORIES FOR THE TWO SPECIES. FOR DETAILS SEE FIG. 2.9.	148
FIGURE 2.59 CALCANEUM, TRAIT 1 (OVERALL ASPECT) NUMBER OF SPECIMENS ATTRIBUTED TO THE DIFFERENT CATEGORIES FOR THE TWO SPECIES. FOR DETAILS SEE FIG. 2.9.....	148
FIGURE 2.60 CALCANEUM, TRAIT 2 (LENGTH OF THE <i>OS MALLEOLARE</i> VS LENGTH OF THE ENTIRE PROCESS) NUMBER OF SPECIMENS ATTRIBUTED TO THE DIFFERENT CATEGORIES FOR THE TWO SPECIES. FOR DETAILS SEE FIG. 2.9.	149
FIGURE 2.61 CALCANEUM, TRAIT 3 (PRESENCE/ABSENCE OF THE JUNCTION BETWEEN THE TWO INTERNAL ARTICULAR SURFACES) NUMBER OF SPECIMENS ATTRIBUTED TO THE DIFFERENT CATEGORIES FOR THE TWO SPECIES. FOR DETAILS SEE FIG. 2.9.	149
FIGURE 2.62 1 ST PHALANX, TRAIT 1 (SHAPE OF THE GROOVE IN THE PROXIMAL END) NUMBER OF SPECIMENS ATTRIBUTED TO THE DIFFERENT CATEGORIES FOR THE TWO SPECIES. FOR DETAILS SEE FIG. 2.9.	149
FIGURE 2.63 1 ST PHALANX, TRAIT 2 (PRESENCE OF THE SCARS FOR THE MUSCULAR LIGAMENTS ON THE POSTERIOR SIDE) NUMBER OF SPECIMENS ATTRIBUTED TO THE DIFFERENT CATEGORIES FOR THE TWO SPECIES. FOR DETAILS SEE FIG. 2.9.	150
FIGURE 2.64 1 ST PHALANX, TRAIT 3 (ASPECT OF THE POSTERIOR SIDE) NUMBER OF SPECIMENS ATTRIBUTED TO THE DIFFERENT CATEGORIES FOR THE TWO SPECIES. FOR DETAILS SEE FIG. 2.9.....	150
FIGURE 2.65 1 ST PHALANX, TRAIT 4 (SHAPE OF THE DISTAL ARTICULATION) NUMBER OF SPECIMENS ATTRIBUTED TO THE DIFFERENT CATEGORIES FOR THE TWO SPECIES. FOR DETAILS SEE FIG. 2.9.	151
FIGURE 2.66 2 ND PHALANX, TRAIT 1 (ASPECT OF THE AXIAL PART OF THE POSTERIOR SIDE OF THE DISTAL ARTICULATION) NUMBER OF SPECIMENS ATTRIBUTED TO THE DIFFERENT CATEGORIES FOR THE TWO SPECIES. FOR DETAILS SEE FIG. 2.9.	151
FIGURE 2.67 2 ND PHALANX, TRAIT 2 (ASPECT OF THE RIDGE OF THE POSTERIOR SIDE OF THE DISTAL ARTICULATION) NUMBER OF SPECIMENS ATTRIBUTED TO THE DIFFERENT CATEGORIES FOR THE TWO SPECIES. FOR DETAILS SEE FIG. 2.9.	151
FIGURE 2.68 3 RD PHALANX, TRAIT 1 (PRESENCE/ABSENCE OF A SADDLE ON THE DORSAL EDGE) NUMBER OF SPECIMENS ATTRIBUTED TO THE DIFFERENT CATEGORIES FOR THE TWO SPECIES. FOR DETAILS SEE FIG. 2.9.....	152
FIGURE 2.69 3 RD PHALANX, TRAIT 2 (SHAPE OF THE SOLE) NUMBER OF SPECIMENS ATTRIBUTED TO THE DIFFERENT CATEGORIES FOR THE TWO SPECIES. FOR DETAILS SEE FIG. 2.9.....	152
FIGURE 2.70 HORNCORE, TRAIT 1 (SECTION) NUMBER OF SPECIMENS ATTRIBUTED TO THE DIFFERENT CATEGORIES FOR THE DIFFERENT GENDERS FOR THE TWO SPECIES (C= <i>CAPRA</i> ; CL= <i>CAPRA-LIKE</i> ; OC= <i>OVIS/CAPRA</i> ; OL= <i>OVIS-LIKE</i> ; O= <i>OVIS</i> . ON THE HORIZONTAL AXIS: CH= <i>CAPRA HIRCUS</i> ; OA= <i>OVIS ARIES</i> ; ♂= MALE; ♀= FEMALE; ♂♀= CASTRATE).	157

FIGURE 2.71 HORNCORE, TRAIT 2 (CURVATURE) NUMBER OF SPECIMENS ATTRIBUTED TO THE DIFFERENT CATEGORIES FOR THE DIFFERENT GENDERS FOR THE TWO SPECIES. FOR DETAILS SEE FIG. 2.70.	158
FIGURE 2.72 THIRD DECIDUOUS LOWER PREMOLAR DP ₃ , TRAIT 1 (OVERALL SHAPE) NUMBER OF SPECIMENS ATTRIBUTED TO THE DIFFERENT CATEGORIES FOR THE DIFFERENT GENDERS FOR THE TWO SPECIES. . FOR DETAILS SEE FIG. 2.70.	158
FIGURE 2.73 THIRD DECIDUOUS LOWER PREMOLAR DP ₃ , TRAIT 2 (APPEARANCE OF THE METACONOID) NUMBER OF SPECIMENS ATTRIBUTED TO THE DIFFERENT CATEGORIES FOR THE DIFFERENT GENDERS FOR THE TWO SPECIES. . FOR DETAILS SEE FIG. 2.70.	158
FIGURE 2.74 FOURTH LOWER DECIDUOUS PREMOLAR DP ₄ , TRAIT 1 (CROWN ASPECT) NUMBER OF SPECIMENS ATTRIBUTED TO THE DIFFERENT CATEGORIES FOR THE DIFFERENT GENDERS FOR THE TWO SPECIES. FOR DETAILS SEE FIG. 2.70.	159
FIGURE 2.75 FOURTH LOWER DECIDUOUS PREMOLAR DP ₄ , TRAIT 2 (PRESENCE/ABSENCE BASAL SWELLING) NUMBER OF SPECIMENS ATTRIBUTED TO THE DIFFERENT CATEGORIES FOR THE DIFFERENT GENDERS FOR THE TWO SPECIES. FOR DETAILS SEE FIG. 2.70.	159
FIGURE 2.76 FOURTH LOWER DECIDUOUS PREMOLAR DP ₄ , TRAIT 3 (PRESENCE/ABSENCE INTER-LOBAR PILLAR) NUMBER OF SPECIMENS ATTRIBUTED TO THE DIFFERENT CATEGORIES FOR THE DIFFERENT GENDERS FOR THE TWO SPECIES. FOR DETAILS SEE FIG. 2.70.	159
FIGURE 2.77 FOURTH LOWER DECIDUOUS PREMOLAR DP ₄ , TRAIT 4 (ENAMEL DEVELOPMENT IN MEDIAL AND DISTAL FACE) NUMBER OF SPECIMENS ATTRIBUTED TO THE DIFFERENT CATEGORIES FOR THE DIFFERENT GENDERS FOR THE TWO SPECIES. FOR DETAILS SEE FIG. 2.70.	160
FIGURE 2.78 THIRD LOWER PREMOLAR P ₃ , TRAIT 1 (OVERALL SHAPE) NUMBER OF SPECIMENS ATTRIBUTED TO THE DIFFERENT CATEGORIES FOR THE DIFFERENT GENDERS FOR THE TWO SPECIES. FOR DETAILS SEE FIG. 2.70.....	160
FIGURE 2.79 THIRD LOWER PREMOLAR P ₃ , TRAIT 2 (ASPECT MIDDLE VERTICAL RIDGE) NUMBER OF SPECIMENS ATTRIBUTED TO THE DIFFERENT CATEGORIES FOR THE DIFFERENT GENDERS FOR THE TWO SPECIES. FOR DETAILS SEE FIG. 2.70.	160
FIGURE 2.80 THIRD LOWER PREMOLAR P ₃ , TRAIT 3 (ASPECT MESIAL-BUCCAL ANGLE) NUMBER OF SPECIMENS ATTRIBUTED TO THE DIFFERENT CATEGORIES FOR THE DIFFERENT GENDERS FOR THE TWO SPECIES. FOR DETAILS SEE FIG. 2.70.	161
FIGURE 2.81 FOURTH LOWER PREMOLAR P ₄ , TRAIT 1 (OVERALL SHAPE) NUMBER OF SPECIMENS ATTRIBUTED TO THE DIFFERENT CATEGORIES FOR THE DIFFERENT GENDERS FOR THE TWO SPECIES. FOR DETAILS SEE FIG. 2.70.....	161
FIGURE 2.82 FOURTH LOWER PREMOLAR P ₄ , TRAIT 2 (ASPECT OF THE MESIO-LINGUAL RIB) NUMBER OF SPECIMENS ATTRIBUTED TO THE DIFFERENT CATEGORIES FOR THE DIFFERENT GENDERS FOR THE TWO SPECIES. FOR DETAILS SEE FIG. 2.70.	161
FIGURE 2.83 FOURTH LOWER PREMOLAR P ₄ , TRAIT 3 (ASPECT OF THE MESIO-BUCCAL ANGLE) NUMBER OF SPECIMENS ATTRIBUTED TO THE DIFFERENT CATEGORIES FOR THE DIFFERENT GENDERS FOR THE TWO SPECIES. FOR DETAILS SEE FIG. 2.70.	162
FIGURE 2.84 THIRD LOWER MOLAR M ₃ , TRAIT 1 (ASPECT MESIAL FACE) NUMBER OF SPECIMENS ATTRIBUTED TO THE DIFFERENT CATEGORIES FOR THE DIFFERENT GENDERS FOR THE TWO SPECIES. FOR DETAILS SEE FIG. 2.70.....	162
FIGURE 2.85 THIRD LOWER MOLAR M ₃ , TRAIT 2 (ASPECT BUCCAL EDGE ANGLE) NUMBER OF SPECIMENS ATTRIBUTED TO THE DIFFERENT CATEGORIES FOR THE DIFFERENT GENDERS FOR THE TWO SPECIES. FOR DETAILS SEE FIG. 2.70.....	162
FIGURE 2.86 THIRD LOWER MOLAR M ₃ , TRAIT 3 (DIRECTION OF CENTRAL CUSP) NUMBER OF SPECIMENS ATTRIBUTED TO THE DIFFERENT CATEGORIES FOR THE DIFFERENT GENDERS FOR THE TWO SPECIES. FOR DETAILS SEE FIG. 2.70.....	163

FIGURE 2.87 THIRD LOWER MOLAR M_3 , TRAIT 4 (SYMMETRY AND SHAPE OF CUSPS) NUMBER OF SPECIMENS ATTRIBUTED TO THE DIFFERENT CATEGORIES FOR THE DIFFERENT GENDERS FOR THE TWO SPECIES. FOR DETAILS SEE FIG. 2.70.....	163
FIGURE 2.88 THIRD LOWER MOLAR M_3 , TRAIT 4 (ASPECT OF THE DISTAL FLUTE) NUMBER OF SPECIMENS ATTRIBUTED TO THE DIFFERENT CATEGORIES FOR THE DIFFERENT GENDERS FOR THE TWO SPECIES. FOR DETAILS SEE FIG. 2.70.	163
FIGURE 2.89 MANDIBLE, TRAIT 1 (PRESENCE/ABSENCE OF THE FORAMEN) NUMBER OF SPECIMENS ATTRIBUTED TO THE DIFFERENT CATEGORIES FOR THE DIFFERENT GENDERS FOR THE TWO SPECIES. FOR DETAILS SEE FIG. 2.70.	164
FIGURE 2.90 MANDIBLE, TRAIT 2 (POSTERIOR GROOVE) NUMBER OF SPECIMENS ATTRIBUTED TO THE DIFFERENT CATEGORIES FOR THE DIFFERENT GENDERS FOR THE TWO SPECIES. FOR DETAILS SEE FIG. 2.70.	164
FIGURE 2.91 SCAPULA, TRAIT 1 (SHAPE OF THE GLENOID TUBERCULE) NUMBER OF SPECIMENS ATTRIBUTED TO THE DIFFERENT CATEGORIES FOR THE DIFFERENT GENDERS FOR THE TWO SPECIES. FOR DETAILS SEE FIG. 2.70.	164
FIGURE 2.92 SCAPULA, TRAIT 2 (SHAPE OF THE GLENOID CAVITY) NUMBER OF SPECIMENS ATTRIBUTED TO THE DIFFERENT CATEGORIES FOR THE DIFFERENT GENDERS FOR THE TWO SPECIES. FOR DETAILS SEE FIG. 2.70.	165
FIGURE 2.93 HUMERUS, TRAIT 1 (SHAPE OF THE LATERAL EPICONDYLE) NUMBER OF SPECIMENS ATTRIBUTED TO THE DIFFERENT CATEGORIES FOR THE DIFFERENT GENDERS FOR THE TWO SPECIES. FOR DETAILS SEE FIG. 2.70.	165
FIGURE 2.94 HUMERUS, TRAIT 2 (ASPECT OF THE GROOVE ON THE POSTERIOR SIDE OF THE LATERAL EPICONDYLE) NUMBER OF SPECIMENS ATTRIBUTED TO THE DIFFERENT CATEGORIES FOR THE DIFFERENT GENDERS FOR THE TWO SPECIES. FOR DETAILS SEE FIG. 2.70.	165
FIGURE 2.95 HUMERUS, TRAIT 3 (ASPECT OF THE PIT ON THE LATERAL EPICONDYLE SURFACE) NUMBER OF SPECIMENS ATTRIBUTED TO THE DIFFERENT CATEGORIES FOR THE DIFFERENT GENDERS FOR THE TWO SPECIES. FOR DETAILS SEE FIG. 2.70.....	166
FIGURE 2.96 HUMERUS, TRAIT 4 (PRESENCE/ABSENCE OF A LATERAL THICKENING ON THE LATERAL BORDER OF EPICONDYLAR SURFACE) NUMBER OF SPECIMENS ATTRIBUTED TO THE DIFFERENT CATEGORIES FOR THE DIFFERENT GENDERS FOR THE TWO SPECIES. FOR DETAILS SEE FIG. 2.70.....	166
FIGURE 2.97 HUMERUS, TRAIT 5 (ASPECT OF THE ANGLE OF THE DISTAL PART OF THE MEDIAL EPICONDYLE) NUMBER OF SPECIMENS ATTRIBUTED TO THE DIFFERENT CATEGORIES FOR THE DIFFERENT GENDERS FOR THE TWO SPECIES. FOR DETAILS SEE FIG. 2.70.	167
FIGURE 2.98 RADIUS, TRAIT 1 (ASPECT OF THE LATERAL TUBEROSITY) NUMBER OF SPECIMENS ATTRIBUTED TO THE DIFFERENT CATEGORIES FOR THE DIFFERENT GENDERS FOR THE TWO SPECIES. FOR DETAILS SEE FIG. 2.70.	167
FIGURE 2.99 RADIUS, TRAIT 2 (OVERALL ASPECT OF THE PROXIMAL ARTICULAR SURFACE) NUMBER OF SPECIMENS ATTRIBUTED TO THE DIFFERENT CATEGORIES FOR THE DIFFERENT GENDERS FOR THE TWO SPECIES. FOR DETAILS SEE FIG. 2.70. ...	168
FIGURE 2.100 ULNA, TRAIT 1 (PROJECTION OF THE LATERAL CORONOID PROCESS) NUMBER OF SPECIMENS ATTRIBUTED TO THE DIFFERENT CATEGORIES FOR THE DIFFERENT GENDERS FOR THE TWO SPECIES. FOR DETAILS SEE FIG. 2.70.	168
FIGURE 2.101 ULNA, TRAIT 2 (OVERALL SHAPE OF THE <i>OLECRANON</i>) NUMBER OF SPECIMENS ATTRIBUTED TO THE DIFFERENT CATEGORIES FOR THE DIFFERENT GENDERS FOR THE TWO SPECIES. FOR DETAILS SEE FIG. 2.70.	169
FIGURE 2.102 METACARPAL AND METATARSAL, TRAIT 1 (DIMENSION OF THE PERIPHERAL PART OF THE TROCHLEAR CONDYLES) NUMBER OF SPECIMENS ATTRIBUTED TO THE DIFFERENT CATEGORIES FOR THE DIFFERENT GENDERS FOR THE TWO SPECIES. FOR DETAILS SEE FIG. 2.70.....	169

FIGURE 2.103 METACARPAL AND METATARSAL, TRAIT 2 (DEFINITION OF THE PERIPHERAL PART OF THE TROCHLEAR CONDYLES) NUMBER OF SPECIMENS ATTRIBUTED TO THE DIFFERENT CATEGORIES FOR THE DIFFERENT GENDERS FOR THE TWO SPECIES. FOR DETAILS SEE FIG. 2.70.	169
FIGURE 2.104 METACARPAL AND METATARSAL, TRAIT 3 (ASPECT OF THE PERIPHERAL PART OF THE TROCHLEAR CONDYLES) NUMBER OF SPECIMENS ATTRIBUTED TO THE DIFFERENT CATEGORIES FOR THE DIFFERENT GENDERS FOR THE TWO SPECIES. FOR DETAILS SEE FIG. 2.70.	170
FIGURE 2.105 METACARPAL AND METATARSAL, TRAIT 4 (DIRECTION OF THE <i>VERTICILLI</i>) NUMBER OF SPECIMENS ATTRIBUTED TO THE DIFFERENT CATEGORIES FOR THE DIFFERENT GENDERS FOR THE TWO SPECIES. FOR DETAILS SEE FIG. 2.70....	170
FIGURE 2.106 METACARPAL AND METATARSAL, TRAIT 5 (DEVELOPMENT OF THE <i>FOSSAE</i> ON THE PROXIMAL PART OF THE DISTAL TROCHLEAR CONDYLES) NUMBER OF SPECIMENS ATTRIBUTED TO THE DIFFERENT CATEGORIES FOR THE DIFFERENT GENDERS FOR THE TWO SPECIES. FOR DETAILS SEE FIG. 2.70.	170
FIGURE 2.107 METATARSAL, TRAIT 6 (DEVELOPMENT OF THE <i>FOSSAE</i> ON THE PROXIMAL PART OF THE DISTAL DIAPHYSIS ABOVE THE DISTAL EPIPHYSIS) NUMBER OF SPECIMENS ATTRIBUTED TO THE DIFFERENT CATEGORIES FOR THE DIFFERENT GENDERS FOR THE TWO SPECIES. FOR DETAILS SEE FIG. 2.70.	171
FIGURE 2.108 TIBIA, TRAIT 1 (DORSAL PROMINENCE) NUMBER OF SPECIMENS ATTRIBUTED TO THE DIFFERENT CATEGORIES FOR THE DIFFERENT GENDERS FOR THE TWO SPECIES. FOR DETAILS SEE FIG. 2.70.....	171
FIGURE 2.109 TIBIA, TRAIT 2 (MEDIAL MALLEOLUS) NUMBER OF SPECIMENS ATTRIBUTED TO THE DIFFERENT CATEGORIES FOR THE DIFFERENT GENDERS FOR THE TWO SPECIES. FOR DETAILS SEE FIG. 2.70.....	171
FIGURE 2.110 TIBIA, TRAIT 3 (PRESENCE/ABSENCE INTERRUPTION ON PLANTAR LIMBUS) NUMBER OF SPECIMENS ATTRIBUTED TO THE DIFFERENT CATEGORIES FOR THE DIFFERENT GENDERS FOR THE TWO SPECIES. FOR DETAILS SEE FIG. 2.70....	172
FIGURE 2.111 TIBIA, TRAIT 4 (LATERAL PROFILE) NUMBER OF SPECIMENS ATTRIBUTED TO THE DIFFERENT CATEGORIES FOR THE DIFFERENT GENDERS FOR THE TWO SPECIES. FOR DETAILS SEE FIG. 2.70.	172
FIGURE 2.112 TIBIA, TRAIT 5 (SHAPE OF THE ANTERIOR SIDE OF THE <i>MALLEOLUS</i>) NUMBER OF SPECIMENS ATTRIBUTED TO THE DIFFERENT CATEGORIES FOR THE DIFFERENT GENDERS FOR THE TWO SPECIES. FOR DETAILS SEE FIG. 2.70.....	172
FIGURE 2.113 TIBIA, TRAIT 6 (ASPECT OF THE MEDIAL <i>MALLEOLUS</i>) NUMBER OF SPECIMENS ATTRIBUTED TO THE DIFFERENT CATEGORIES FOR THE DIFFERENT GENDERS FOR THE TWO SPECIES. FOR DETAILS SEE FIG. 2.70.....	173
FIGURE 2.114 ASTRAGALUS, TRAIT 1 (DEPTH OF THE SULCUS OF THE TROCHLEA) NUMBER OF SPECIMENS ATTRIBUTED TO THE DIFFERENT CATEGORIES FOR THE DIFFERENT GENDERS FOR THE TWO SPECIES. FOR DETAILS SEE FIG. 2.70.....	173
FIGURE 2.115 ASTRAGALUS, TRAIT 2 (INCLINATION OF THE LATERAL PART OF THE TROCHLEA) NUMBER OF SPECIMENS ATTRIBUTED TO THE DIFFERENT CATEGORIES FOR THE DIFFERENT GENDERS FOR THE TWO SPECIES. FOR DETAILS SEE FIG. 2.70.	173
FIGURE 2.116 ASTRAGALUS, TRAIT 3 (SHAPE OF THE MEDIAL RIDGE) NUMBER OF SPECIMENS ATTRIBUTED TO THE DIFFERENT CATEGORIES FOR THE DIFFERENT GENDERS FOR THE TWO SPECIES. FOR DETAILS SEE FIG. 2.70.....	174
FIGURE 2.117 ASTRAGALUS, TRAIT 4 (SHAPE ON THE DISTAL ARTICULAR SURFACE ON THE LATERAL ASPECT) NUMBER OF SPECIMENS ATTRIBUTED TO THE DIFFERENT CATEGORIES FOR THE DIFFERENT GENDERS FOR THE TWO SPECIES. FOR DETAILS SEE FIG. 2.70.	174
FIGURE 2.118 ASTRAGALUS, TRAIT 5 (ASPECT OF THE PROXIMO-PLANTAR PROJECTION ON THE MEDIAL ARTICULAR RIDGE OF THE TROCHLEA) NUMBER OF SPECIMENS ATTRIBUTED TO THE DIFFERENT CATEGORIES FOR THE DIFFERENT GENDERS FOR THE TWO SPECIES. FOR DETAILS SEE FIG. 2.70.	174

FIGURE 2.119 ASTRAGALUS, TRAIT 6 (ASPECT OF THE DIRECTION OF THE ARTICULAR SURFACE ON THE PLANTAR SIDE) NUMBER OF SPECIMENS ATTRIBUTED TO THE DIFFERENT CATEGORIES FOR THE DIFFERENT GENDERS FOR THE TWO SPECIES. FOR DETAILS SEE FIG. 2.70.	175
FIGURE 2.120 CALCANEUS, TRAIT 1 (OVERALL ASPECT) NUMBER OF SPECIMENS ATTRIBUTED TO THE DIFFERENT CATEGORIES FOR THE DIFFERENT GENDERS FOR THE TWO SPECIES. FOR DETAILS SEE FIG. 2.70.	175
FIGURE 2.121 CALCANEUS, TRAIT 2 (LENGTH OF THE <i>OS MALLEOLARE</i> VS LENGTH OF THE ENTIRE PROCESS) NUMBER OF SPECIMENS ATTRIBUTED TO THE DIFFERENT CATEGORIES FOR THE DIFFERENT GENDERS FOR THE TWO SPECIES. FOR DETAILS SEE FIG. 2.70.	175
FIGURE 2.122 CALCANEUS, TRAIT 3 (PRESENCE/ABSENCE OF THE JUNCTION BETWEEN THE TWO INTERNAL ARTICULAR SURFACES) NUMBER OF SPECIMENS ATTRIBUTED TO THE DIFFERENT CATEGORIES FOR THE DIFFERENT GENDERS FOR THE TWO SPECIES. FOR DETAILS SEE FIG. 2.70.....	176
FIGURE 2.123 1 ST PHALANX, TRAIT 1 (SHAPE OF THE GROVE ON THE PROXIMAL END) NUMBER OF SPECIMENS ATTRIBUTED TO THE DIFFERENT CATEGORIES FOR THE DIFFERENT GENDERS FOR THE TWO SPECIES. FOR DETAILS SEE FIG. 2.70.....	176
FIGURE 2.124 1 ST PHALANX, TRAIT 2 (PRESENCE OF THE SCARS OF THE MUSCULAR LIGAMENTS ON THE POSTERIOR SIDE) NUMBER OF SPECIMENS ATTRIBUTED TO THE DIFFERENT CATEGORIES FOR THE DIFFERENT GENDERS FOR THE TWO SPECIES. FOR DETAILS SEE FIG. 2.70.....	176
FIGURE 2.125 1 ST PHALANX, TRAIT 3 (ASPECT OF THE POSTERIOR SIDE) NUMBER OF SPECIMENS ATTRIBUTED TO THE DIFFERENT CATEGORIES FOR THE DIFFERENT GENDERS FOR THE TWO SPECIES. FOR DETAILS SEE FIG. 2.70.	177
FIGURE 2.126 1 ST PHALANX, TRAIT 4 (SHAPE OF THE DISTAL ARTICULATION) NUMBER OF SPECIMENS ATTRIBUTED TO THE DIFFERENT CATEGORIES FOR THE DIFFERENT GENDERS FOR THE TWO SPECIES. FOR DETAILS SEE FIG. 2.70.	177
FIGURE 2.127 2 ND PHALANX, TRAIT 1 (ASPECT OF THE AXIAL PART OF THE POSTERIOR SIDE OF THE DISTAL ARTICULATION) NUMBER OF SPECIMENS ATTRIBUTED TO THE DIFFERENT CATEGORIES FOR THE DIFFERENT GENDERS FOR THE TWO SPECIES. FOR DETAILS SEE FIG. 2.70.....	177
FIGURE 2.128 2 ND PHALANX, TRAIT 2 (ASPECT OF THE RIDGE ON THE POSTERIOR EDGE OF THE DISTAL ARTICULATION) NUMBER OF SPECIMENS ATTRIBUTED TO THE DIFFERENT CATEGORIES FOR THE DIFFERENT GENDERS FOR THE TWO SPECIES. FOR DETAILS SEE FIG. 2.70.	178
FIGURE 2.129 3 RD PHALANX, TRAIT 1 (PRESENCE/ABSENCE OF A SADDLE ON THE DORSAL EDGE) NUMBER OF SPECIMENS ATTRIBUTED TO THE DIFFERENT CATEGORIES FOR THE DIFFERENT GENDERS FOR THE TWO SPECIES. FOR DETAILS SEE FIG. 2.70.....	178
FIGURE 2.130 3 RD PHALANX, TRAIT 2 (SHAPE OF THE SOLE) NUMBER OF SPECIMENS ATTRIBUTED TO THE DIFFERENT CATEGORIES FOR THE DIFFERENT GENDERS FOR THE TWO SPECIES. FOR DETAILS SEE FIG. 2.70.	178
FIGURE 2.131 HORNCORE, TRAIT 1 (SECTION) NUMBER OF SPECIMENS ATTRIBUTED TO THE DIFFERENT CATEGORIES FOR THE DIFFERENT AGE-GROUPS FOR THE GOAT (LEFT) AND THE SHEEP (RIGHT). LEGEND: G1= AGE GROUP 1; G2= AGE GROUP 2; G3= AGE GROUP 3; G4= AGE GROUP 4. ON THE HORIZONTAL AXIS: C= <i>CAPRA</i> ; CL= <i>CAPRA-LIKE</i> ; CO= <i>CAPRA/OVIS</i> ; OL= <i>OVIS-LIKE</i> ; O= <i>OVIS</i>	183
FIGURE 2.132 HORNCORE, TRAIT 2 (CURVATURE) NUMBER OF SPECIMENS ATTRIBUTED TO THE DIFFERENT CATEGORIES FOR THE DIFFERENT AGE-GROUPS FOR THE GOAT (LEFT) AND THE SHEEP (RIGHT). FOR DETAILS SEE FIG. 2.131.	184

FIGURE 2.133 MANDIBLE, TRAIT 1 (PRESENCE/ABSENCE OF THE FORAMEN) NUMBER OF SPECIMENS ATTRIBUTED TO THE DIFFERENT CATEGORIES FOR THE DIFFERENT AGE-GROUPS FOR THE GOAT (LEFT) AND THE SHEEP (RIGHT). FOR DETAILS SEE FIG. 2.131.....	184
FIGURE 2.134 MANDIBLE, TRAIT 2 (ASPECT OF THE HOLLOW) NUMBER OF SPECIMENS ATTRIBUTED TO THE DIFFERENT CATEGORIES FOR THE DIFFERENT AGE-GROUPS FOR THE GOAT (LEFT) AND THE SHEEP (RIGHT). FOR DETAILS SEE FIG. 2.131.	184
FIGURE 2.135 THIRD DECIDUOUS LOWER PREMOLAR DP ₃ , TRAIT 1 (OVERALL ASPECT) NUMBER OF SPECIMENS ATTRIBUTED TO THE DIFFERENT CATEGORIES FOR THE DIFFERENT AGE-GROUPS FOR THE GOAT (LEFT) AND THE SHEEP (RIGHT). FOR DETAILS SEE FIG. 2.131.	185
FIGURE 2.136 THIRD DECIDUOUS LOWER PREMOLAR DP ₃ , TRAIT 2 (APPEARANCE OF THE METACONOID) NUMBER OF SPECIMENS ATTRIBUTED TO THE DIFFERENT CATEGORIES FOR THE DIFFERENT AGE-GROUPS FOR THE GOAT (LEFT) AND THE SHEEP (RIGHT). FOR DETAILS SEE FIG. 2.131.	185
FIGURE 2.137 FOURTH DECIDUOUS LOWER PREMOLAR DP ₄ , TRAIT 1 (CROWN ASPECT) NUMBER OF SPECIMENS ATTRIBUTED TO THE DIFFERENT CATEGORIES FOR THE DIFFERENT AGE-GROUPS FOR THE GOAT (LEFT) AND THE SHEEP (RIGHT). FOR DETAILS SEE FIG. 2.131.	185
FIGURE 2.138 FOURTH DECIDUOUS LOWER PREMOLAR DP ₄ , TRAIT 2 (PRESENCE/ABSENCE BASAL SWELLING) NUMBER OF SPECIMENS ATTRIBUTED TO THE DIFFERENT CATEGORIES FOR THE DIFFERENT AGE-GROUPS FOR THE GOAT (LEFT) AND THE SHEEP (RIGHT). FOR DETAILS SEE FIG. 2.131.	186
FIGURE 2.139 FOURTH DECIDUOUS LOWER PREMOLAR DP ₄ , TRAIT 3 (PRESENCE/ABSENCE INTER-LOBAR PILLAR) NUMBER OF SPECIMENS ATTRIBUTED TO THE DIFFERENT CATEGORIES FOR THE DIFFERENT AGE-GROUPS FOR THE GOAT (LEFT) AND THE SHEEP (RIGHT). FOR DETAILS SEE FIG. 2.131.	186
FIGURE 2.140 FOURTH DECIDUOUS LOWER PREMOLAR DP ₄ , TRAIT 4 (ENAMEL DEVELOPMENT ON MEDIAL AND DISTAL FACE) NUMBER OF SPECIMENS ATTRIBUTED TO THE DIFFERENT CATEGORIES FOR THE DIFFERENT AGE-GROUPS FOR THE GOAT (LEFT) AND THE SHEEP (RIGHT). FOR DETAILS SEE FIG. 2.131.....	186
FIGURE 2.141 THIRD LOWER PREMOLAR P ₃ , TRAIT 1 (OVERALL ASPECT) NUMBER OF SPECIMENS ATTRIBUTED TO THE DIFFERENT CATEGORIES FOR THE DIFFERENT AGE-GROUPS FOR THE GOAT (LEFT) AND THE SHEEP (RIGHT). FOR DETAILS SEE FIG. 2.131.....	187
FIGURE 2.142 THIRD LOWER PREMOLAR P ₃ , TRAIT 2 (ASPECT MIDDLE VERTICAL RIDGE) NUMBER OF SPECIMENS ATTRIBUTED TO THE DIFFERENT CATEGORIES FOR THE DIFFERENT AGE-GROUPS FOR THE GOAT (LEFT) AND THE SHEEP (RIGHT). FOR DETAILS SEE FIG. 2.131.	187
FIGURE 2.143 THIRD LOWER PREMOLAR P ₃ , TRAIT 3 (ASPECT MESIAL-BUCCAL ANGLE) NUMBER OF SPECIMENS ATTRIBUTED TO THE DIFFERENT CATEGORIES FOR THE DIFFERENT AGE-GROUPS FOR THE GOAT (LEFT) AND THE SHEEP (RIGHT). FOR DETAILS SEE FIG. 2.131.	187
FIGURE 2.144 FOURTH LOWER PREMOLAR P ₄ , TRAIT 1 (OVERALL SHAPE) NUMBER OF SPECIMENS ATTRIBUTED TO THE DIFFERENT CATEGORIES FOR THE DIFFERENT AGE-GROUPS FOR THE GOAT (LEFT) AND THE SHEEP (RIGHT). FOR DETAILS SEE FIG. 2.131.....	188
FIGURE 2.145 FOURTH LOWER PREMOLAR P ₄ , TRAIT 2 (ASPECT OF THE MESIO-LINGUAL RIB) NUMBER OF SPECIMENS ATTRIBUTED TO THE DIFFERENT CATEGORIES FOR THE DIFFERENT AGE-GROUPS FOR THE GOAT (LEFT) AND THE SHEEP (RIGHT). FOR DETAILS SEE FIG. 2.131.....	188

FIGURE 2.146 FOURTH LOWER PREMOLAR P ₄ , TRAIT 3 (ASPECT OF THE MESIO-BUCCAL ANGLE) NUMBER OF SPECIMENS ATTRIBUTED TO THE DIFFERENT CATEGORIES FOR THE DIFFERENT AGE-GROUPS FOR THE GOAT (LEFT) AND THE SHEEP (RIGHT). FOR DETAILS SEE FIG. 2.131.	188
FIGURE 2.147 THIRD LOWER MOLAR M ₃ , TRAIT 1 (ASPECT MESIAL FACE) NUMBER OF SPECIMENS ATTRIBUTED TO THE DIFFERENT CATEGORIES FOR THE DIFFERENT AGE-GROUPS FOR THE GOAT (LEFT) AND THE SHEEP (RIGHT). FOR DETAILS SEE FIG. 2.131.	189
FIGURE 2.148 THIRD LOWER MOLAR M ₃ , TRAIT 2 (ASPECT BUCCAL EDGE ANGLE) NUMBER OF SPECIMENS ATTRIBUTED TO THE DIFFERENT CATEGORIES FOR THE DIFFERENT AGE-GROUPS FOR THE GOAT (LEFT) AND THE SHEEP (RIGHT). FOR DETAILS SEE FIG. 2.131.	189
FIGURE 2.149 THIRD LOWER MOLAR M ₃ , TRAIT 3 (DIRECTION OF CENTRAL CUSP) NUMBER OF SPECIMENS ATTRIBUTED TO THE DIFFERENT CATEGORIES FOR THE DIFFERENT AGE-GROUPS FOR THE GOAT (LEFT) AND THE SHEEP (RIGHT). FOR DETAILS SEE FIG. 2.131.	189
FIGURE 2.150 THIRD LOWER MOLAR M ₃ , TRAIT 4 (SYMMETRY AND SHAPE OF THE CUSPS) NUMBER OF SPECIMENS ATTRIBUTED TO THE DIFFERENT CATEGORIES FOR THE DIFFERENT AGE-GROUPS FOR THE GOAT (LEFT) AND THE SHEEP (RIGHT). FOR DETAILS SEE FIG. 2.131.	190
FIGURE 2.151 THIRD LOWER MOLAR M ₃ , TRAIT 5 (ASPECT OF THE DISTAL FLUTE) NUMBER OF SPECIMENS ATTRIBUTED TO THE DIFFERENT CATEGORIES FOR THE DIFFERENT AGE-GROUPS FOR THE GOAT (LEFT) AND THE SHEEP (RIGHT). FOR DETAILS SEE FIG. 2.131.	190
FIGURE 2.152 SCAPULA, TRAIT 1 (SHAPE OF THE GLENOID TUBERCLE) NUMBER OF SPECIMENS ATTRIBUTED TO THE DIFFERENT CATEGORIES FOR THE DIFFERENT AGE-GROUPS FOR THE GOAT (LEFT) AND THE SHEEP (RIGHT). FOR DETAILS SEE FIG. 2.131.	190
FIGURE 2.153 SCAPULA, TRAIT 2 (SHAPE OF THE GLENOID CAVITY) NUMBER OF SPECIMENS ATTRIBUTED TO THE DIFFERENT CATEGORIES FOR THE DIFFERENT AGE-GROUPS FOR THE GOAT (LEFT) AND THE SHEEP (RIGHT). FOR DETAILS SEE FIG. 2.131.	191
FIGURE 2.154 HUMERUS, TRAIT 1 (SHAPE OF THE LATERAL EPICONDYLE) NUMBER OF SPECIMENS ATTRIBUTED TO THE DIFFERENT CATEGORIES FOR THE DIFFERENT AGE-GROUPS FOR THE GOAT (LEFT) AND THE SHEEP (RIGHT). FOR DETAILS SEE FIG. 2.131.	191
FIGURE 2.155 HUMERUS, TRAIT 2 (ASPECT OF THE GROOVE ON THE POSTERIOR SIDE OF THE LATERAL CONDYLE) NUMBER OF SPECIMENS ATTRIBUTED TO THE DIFFERENT CATEGORIES FOR THE DIFFERENT AGE-GROUPS FOR THE GOAT (LEFT) AND THE SHEEP (RIGHT). FOR DETAILS SEE FIG. 2.131.	191
FIGURE 2.156 HUMERUS, TRAIT 3 (ASPECT OF THE PIT ON THE LATERAL EPICONDILAR SURFACE) NUMBER OF SPECIMENS ATTRIBUTED TO THE DIFFERENT CATEGORIES FOR THE DIFFERENT AGE-GROUPS FOR THE GOAT (LEFT) AND THE SHEEP (RIGHT). FOR DETAILS SEE FIG. 2.131.	192
FIGURE 2.157 HUMERUS, TRAIT 4 (ABSENCE/PRESENCE OF THE THICKENING ON THE LATERAL BORDER OF THE EPICONDILAR SURFACE) NUMBER OF SPECIMENS ATTRIBUTED TO THE DIFFERENT CATEGORIES FOR THE DIFFERENT AGE-GROUPS FOR THE GOAT (LEFT) AND THE SHEEP (RIGHT). FOR DETAILS SEE FIG. 2.131.	192
FIGURE 2.158 HUMERUS, TRAIT 5 (ASPECT ON THE ANGLE OF THE DISTAL PART OF THE MEDIAL EPICONDYLE) NUMBER OF SPECIMENS ATTRIBUTED TO THE DIFFERENT CATEGORIES FOR THE DIFFERENT AGE-GROUPS FOR THE GOAT (LEFT) AND THE SHEEP (RIGHT). FOR DETAILS SEE FIG. 2.131.	192

FIGURE 2.159 RADIUS, TRAIT 1 (ASPECT OF THE LATERAL TUBEROSITY) NUMBER OF SPECIMENS ATTRIBUTED TO THE DIFFERENT CATEGORIES FOR THE DIFFERENT AGE-GROUPS FOR THE GOAT (LEFT) AND THE SHEEP (RIGHT). FOR DETAILS SEE FIG. 2.131.	193
FIGURE 2.160 RADIUS, TRAIT 2 (OVERALL ASPECT OF THE PROXIMAL ARTICULAR SURFACE) NUMBER OF SPECIMENS ATTRIBUTED TO THE DIFFERENT CATEGORIES FOR THE DIFFERENT AGE-GROUPS FOR THE GOAT (LEFT) AND THE SHEEP (RIGHT). FOR DETAILS SEE FIG. 2.131.	193
FIGURE 2.161 ULNA, TRAIT 1 (PROJECTION OF THE LATERAL CORONOID PROCESS) NUMBER OF SPECIMENS ATTRIBUTED TO THE DIFFERENT CATEGORIES FOR THE DIFFERENT AGE-GROUPS FOR THE GOAT (LEFT) AND THE SHEEP (RIGHT). FOR DETAILS SEE FIG. 2.131.	193
FIGURE 2.162 ULNA, TRAIT 2 (OVERALL SHAPE OF THE <i>OLECRANON</i>) NUMBER OF SPECIMENS ATTRIBUTED TO THE DIFFERENT CATEGORIES FOR THE DIFFERENT AGE-GROUPS FOR THE GOAT (LEFT) AND THE SHEEP (RIGHT). FOR DETAILS SEE FIG. 2.131.	194
FIGURE 2.163 METACARPAL, TRAIT 1 (DIMENSION OF THE PERIPHERAL PART OF THE TROCHLEAR CONDYLES) NUMBER OF SPECIMENS ATTRIBUTED TO THE DIFFERENT CATEGORIES FOR THE DIFFERENT AGE-GROUPS FOR THE GOAT (LEFT) AND THE SHEEP (RIGHT). FOR DETAILS SEE FIG. 2.131.	194
FIGURE 2.164 METATARSAL, TRAIT 1 (DIMENSION OF THE PERIPHERAL PART OF THE TROCHLEAR CONDYLES) NUMBER OF SPECIMENS ATTRIBUTED TO THE DIFFERENT CATEGORIES FOR THE DIFFERENT AGE-GROUPS FOR THE GOAT (LEFT) AND THE SHEEP (RIGHT). FOR DETAILS SEE FIG. 2.131.	194
FIGURE 2.165 METACARPAL, TRAIT 2 (DEFINITION OF THE PERIPHERAL PART OF THE TROCHLEAR CONDYLES) NUMBER OF SPECIMENS ATTRIBUTED TO THE DIFFERENT CATEGORIES FOR THE DIFFERENT AGE-GROUPS FOR THE GOAT (LEFT) AND THE SHEEP (RIGHT). FOR DETAILS SEE FIG. 2.131.	195
FIGURE 2.166 METATARSAL, TRAIT 2 (DEFINITION OF THE PERIPHERAL PART OF THE TROCHLEAR CONDYLES) NUMBER OF SPECIMENS ATTRIBUTED TO THE DIFFERENT CATEGORIES FOR THE DIFFERENT AGE-GROUPS FOR THE GOAT (LEFT) AND THE SHEEP (RIGHT). FOR DETAILS SEE FIG. 2.131.	195
FIGURE 2.167 METACARPAL, TRAIT 3 (ASPECT OF THE PERIPHERAL PART OF THE TROCHLEAR CONDYLES) NUMBER OF SPECIMENS ATTRIBUTED TO THE DIFFERENT CATEGORIES FOR THE DIFFERENT AGE-GROUPS FOR THE GOAT (LEFT) AND THE SHEEP (RIGHT). FOR DETAILS SEE FIG. 2.131.	195
FIGURE 2.168 METATARSAL, TRAIT 3 (ASPECT OF THE PERIPHERAL PART OF THE TROCHLEAR CONDYLES) NUMBER OF SPECIMENS ATTRIBUTED TO THE DIFFERENT CATEGORIES FOR THE DIFFERENT AGE-GROUPS FOR THE GOAT (LEFT) AND THE SHEEP (RIGHT). FOR DETAILS SEE FIG. 2.131.	196
FIGURE 2.169 METACARPAL, TRAIT 4 (DIRECTION OF THE <i>VERTICILLI</i>) NUMBER OF SPECIMENS ATTRIBUTED TO THE DIFFERENT CATEGORIES FOR THE DIFFERENT AGE-GROUPS FOR THE GOAT (LEFT) AND THE SHEEP (RIGHT). FOR DETAILS SEE FIG. 2.131.	196
FIGURE 2.170 METATARSAL, TRAIT 4 (DIRECTION OF THE <i>VERTICILLI</i>) NUMBER OF SPECIMENS ATTRIBUTED TO THE DIFFERENT CATEGORIES FOR THE DIFFERENT AGE-GROUPS FOR THE GOAT (LEFT) AND THE SHEEP (RIGHT). FOR DETAILS SEE FIG. 2.131.	196
FIGURE 2.171 METACARPAL, TRAIT 5 (DEVELOPMENT OF THE <i>FOSSAE</i> ON THE PROXIMAL PART OF THE DISTAL TROCHLEAR CONDYLES) NUMBER OF SPECIMENS ATTRIBUTED TO THE DIFFERENT CATEGORIES FOR THE DIFFERENT AGE-GROUPS FOR THE GOAT (LEFT) AND THE SHEEP (RIGHT). FOR DETAILS SEE FIG. 2.131.	197

FIGURE 2.172 METATARSAL, TRAIT 5 (DEVELOPMENT OF THE <i>FOSSAE</i> ON THE PROXIMAL PART OF THE DISTAL TROCHLEAR CONDYLES) NUMBER OF SPECIMENS ATTRIBUTED TO THE DIFFERENT CATEGORIES FOR THE DIFFERENT AGE-GROUPS FOR THE GOAT (LEFT) AND THE SHEEP (RIGHT). FOR DETAILS SEE FIG. 2.131.	197
FIGURE 2.173 METATARSAL, TRAIT 6 (ASPECT OF THE JUNCTION ON THE ANTERIOR ASPECT OF THE DISTAL DIAPHYSIS ABOVE THE DISTAL EPIPHYSIS) NUMBER OF SPECIMENS ATTRIBUTED TO THE DIFFERENT CATEGORIES FOR THE DIFFERENT AGE-GROUPS FOR THE GOAT (LEFT) AND THE SHEEP (RIGHT). FOR DETAILS SEE FIG. 2.131.	197
FIGURE 2.174 TIBIA, TRAIT 1 (DORSAL PROMINENCE) NUMBER OF SPECIMENS ATTRIBUTED TO THE DIFFERENT CATEGORIES FOR THE DIFFERENT AGE-GROUPS FOR THE GOAT (LEFT) AND THE SHEEP (RIGHT). FOR DETAILS SEE FIG. 2.131.	198
FIGURE 2.175 TIBIA, TRAIT 2 (MEDIAL MALLEOLUS) NUMBER OF SPECIMENS ATTRIBUTED TO THE DIFFERENT CATEGORIES FOR THE DIFFERENT AGE-GROUPS FOR THE GOAT (LEFT) AND THE SHEEP (RIGHT). FOR DETAILS SEE FIG. 2.131.	198
FIGURE 2.176 TIBIA, TRAIT 3 (PRESENCE/ABSENCE OF THE INTERRUPTION ON THE PLANTAR LIMBUS) NUMBER OF SPECIMENS ATTRIBUTED TO THE DIFFERENT CATEGORIES FOR THE DIFFERENT AGE-GROUPS FOR THE GOAT (LEFT) AND THE SHEEP (RIGHT). FOR DETAILS SEE FIG. 2.131.	198
FIGURE 2.177 TIBIA, TRAIT 4 (LATERAL PROFILE) NUMBER OF SPECIMENS ATTRIBUTED TO THE DIFFERENT CATEGORIES FOR THE DIFFERENT AGE-GROUPS FOR THE GOAT (LEFT) AND THE SHEEP (RIGHT). FOR DETAILS SEE FIG. 2.131.	199
FIGURE 2.178 TIBIA, TRAIT 5 (SHAPE OF THE ANTERIOR SIDE OF THE <i>MALLEOLUS</i>) NUMBER OF SPECIMENS ATTRIBUTED TO THE DIFFERENT CATEGORIES FOR THE DIFFERENT AGE-GROUPS FOR THE GOAT (LEFT) AND THE SHEEP (RIGHT). FOR DETAILS SEE FIG. 2.131.	199
FIGURE 2.179 TIBIA, TRAIT 6 (ASPECT OF THE MEDIAL <i>MALLEOLUS</i>) NUMBER OF SPECIMENS ATTRIBUTED TO THE DIFFERENT CATEGORIES FOR THE DIFFERENT AGE-GROUPS FOR THE GOAT (LEFT) AND THE SHEEP (RIGHT). FOR DETAILS SEE FIG. 2.131.	199
FIGURE 2.180 ASTRAGALUS, TRAIT 1 (DEPTH OF THE SULCUS OF THE TROCHLEA) NUMBER OF SPECIMENS ATTRIBUTED TO THE DIFFERENT CATEGORIES FOR THE DIFFERENT AGE-GROUPS FOR THE GOAT (LEFT) AND THE SHEEP (RIGHT). FOR DETAILS SEE FIG. 2.131.	200
FIGURE 2.181 ASTRAGALUS, TRAIT 2 (INCLINATION OF THE LATERAL PART OF THE TROCHLEA) NUMBER OF SPECIMENS ATTRIBUTED TO THE DIFFERENT CATEGORIES FOR THE DIFFERENT AGE-GROUPS FOR THE GOAT (LEFT) AND THE SHEEP (RIGHT). FOR DETAILS SEE FIG. 2.131.	200
FIGURE 2.182 ASTRAGALUS, TRAIT 3 (SHAPE OF THE MEDIAL RIDGE) NUMBER OF SPECIMENS ATTRIBUTED TO THE DIFFERENT CATEGORIES FOR THE DIFFERENT AGE-GROUPS FOR THE GOAT (LEFT) AND THE SHEEP (RIGHT). FOR DETAILS SEE FIG. 2.131.	200
FIGURE 2.183 ASTRAGALUS, TRAIT 4 (SHAPE OF THE DISTAL ARTICULAR SURFACE OF THE LATERAL ASPECT) NUMBER OF SPECIMENS ATTRIBUTED TO THE DIFFERENT CATEGORIES FOR THE DIFFERENT AGE-GROUPS FOR THE GOAT (LEFT) AND THE SHEEP (RIGHT). FOR DETAILS SEE FIG. 2.131.	201
FIGURE 2.184 ASTRAGALUS, TRAIT 5 (ARTICULAR RIDGE OF THE TROCHLEA) NUMBER OF SPECIMENS ATTRIBUTED TO THE DIFFERENT CATEGORIES FOR THE DIFFERENT AGE-GROUPS FOR THE GOAT (LEFT) AND THE SHEEP (RIGHT). FOR DETAILS SEE FIG. 2.131.	201
FIGURE 2.185 ASTRAGALUS, TRAIT 6 (ASPECT AND DIRECTION OF THE ARTICULAR SURFACE ON THE PLANTAR SIDE) NUMBER OF SPECIMENS ATTRIBUTED TO THE DIFFERENT CATEGORIES FOR THE DIFFERENT AGE-GROUPS FOR THE GOAT (LEFT) AND THE SHEEP (RIGHT). FOR DETAILS SEE FIG. 2.131.	201

FIGURE 2.186 CALCANEUS, TRAIT 1 (OVERALL ASPECT) NUMBER OF SPECIMENS ATTRIBUTED TO THE DIFFERENT CATEGORIES FOR THE DIFFERENT AGE-GROUPS FOR THE GOAT (LEFT) AND THE SHEEP (RIGHT). FOR DETAILS SEE FIG. 2.131.....	202
FIGURE 2.187 CALCANEUS, TRAIT 2 (LENGTH OF THE <i>OS MALLEOLARE</i> VS LENGTH OF THE ENTIRE PROCESS) NUMBER OF SPECIMENS ATTRIBUTED TO THE DIFFERENT CATEGORIES FOR THE DIFFERENT AGE-GROUPS FOR THE GOAT (LEFT) AND THE SHEEP (RIGHT). FOR DETAILS SEE FIG. 2.131.	202
FIGURE 2.188 CALCANEUS, TRAIT 3 (PRESENCE/ABSENCE OF THE JUNCTION BETWEEN THE TWO INTERNAL ARTICULAR SURFACES) NUMBER OF SPECIMENS ATTRIBUTED TO THE DIFFERENT CATEGORIES FOR THE DIFFERENT AGE-GROUPS FOR THE GOAT (LEFT) AND THE SHEEP (RIGHT). FOR DETAILS SEE FIG. 2.131.....	202
FIGURE 2.189 1 ST PHALANX, TRAIT 1 (SHAPE OF THE GROOVE ON THE PROXIMAL END) NUMBER OF SPECIMENS ATTRIBUTED TO THE DIFFERENT CATEGORIES FOR THE DIFFERENT AGE-GROUPS FOR THE GOAT (LEFT) AND THE SHEEP (RIGHT). FOR DETAILS SEE FIG. 2.131.	203
FIGURE 2.190 1 ST PHALANX, TRAIT 2 (PRESENCE OF THE SCARS FOR THE MUSCULAR LIGAMENTS ON THE POSTERIOR SIDE) NUMBER OF SPECIMENS ATTRIBUTED TO THE DIFFERENT CATEGORIES FOR THE DIFFERENT AGE-GROUPS FOR THE GOAT (LEFT) AND THE SHEEP (RIGHT). FOR DETAILS SEE FIG. 2.131.....	203
FIGURE 2.191 1 ST PHALANX, TRAIT 3 (ASPECT OF THE POSTERIOR SIDE) NUMBER OF SPECIMENS ATTRIBUTED TO THE DIFFERENT CATEGORIES FOR THE DIFFERENT AGE-GROUPS FOR THE GOAT (LEFT) AND THE SHEEP (RIGHT). FOR DETAILS SEE FIG. 2.131.	203
FIGURE 2.192 1 ST PHALANX, TRAIT 4 (SHAPE OF THE DISTAL ARTICULATION) NUMBER OF SPECIMENS ATTRIBUTED TO THE DIFFERENT CATEGORIES FOR THE DIFFERENT AGE-GROUPS FOR THE GOAT (LEFT) AND THE SHEEP (RIGHT). FOR DETAILS SEE FIG. 2.131.....	204
FIGURE 2.193 2 ND PHALANX, TRAIT 1 (ASPECT OF THE AXIAL PART OF THE POSTERIOR SIDE OF THE DISTAL ARTICULATION) NUMBER OF SPECIMENS ATTRIBUTED TO THE DIFFERENT CATEGORIES FOR THE DIFFERENT AGE-GROUPS FOR THE GOAT (LEFT) AND THE SHEEP (RIGHT). FOR DETAILS SEE FIG. 2.131.....	204
FIGURE 2.194 2 ND PHALANX, TRAIT 2 (ASPECT OF THE RIDGE ON THE POSTERIOR SIDE OF THE DISTAL ARTICULATION) NUMBER OF SPECIMENS ATTRIBUTED TO THE DIFFERENT CATEGORIES FOR THE DIFFERENT AGE-GROUPS FOR THE GOAT (LEFT) AND THE SHEEP (RIGHT). FOR DETAILS SEE FIG. 2.131.	204
FIGURE 2.195 3 RD PHALANX, TRAIT 1 (PRESENCE/ABSENCE OF A SADDLE ON THE DORSAL EDGE) NUMBER OF SPECIMENS ATTRIBUTED TO THE DIFFERENT CATEGORIES FOR THE DIFFERENT AGE-GROUPS FOR THE GOAT (LEFT) AND THE SHEEP (RIGHT). FOR DETAILS SEE FIG. 2.131.	205
FIGURE 2.196 3 RD PHALANX, TRAIT 2 (SHAPE OF THE SOLE) NUMBER OF SPECIMENS ATTRIBUTED TO THE DIFFERENT CATEGORIES FOR THE DIFFERENT AGE-GROUPS FOR THE GOAT (LEFT) AND THE SHEEP (RIGHT). FOR DETAILS SEE FIG. 2.131.	205
FIGURE 2.197 MAXIMUM DIAMETER AT THE BASE OF THE HORNCORE PLOTTED AGAINST THE LENGTH.....	218
FIGURE 2.198 MAXIMUM DIAMETER AT THE BASE OF THE HORNCORE PLOTTED AGAINST THE LENGTH OF THE OUTER CURVATURE.	218
FIGURE 2.199 MAXIMUM DIAMETER OF THE HORNCORE TAKEN AT THE MIDDLE PLOTTED AGAINST THE LENGTH.....	219
FIGURE 2.200 MAXIMUM DIAMETER OF THE HORNCORE TAKEN AT THE MIDDLE PLOTTED AGAINST THE LENGTH OF THE OUTER CURVATURE.	219
FIGURE 2.201 MAXIMUM DIAMETER PLOTTED AGAINST THE MINIMUM DIAMETER TAKEN AT THE BASE OF THE HORNCORE.....	220

FIGURE 2.202 MAXIMUM DIAMETER PLOTTED AGAINST THE MINIMUM DIAMETER TAKEN AT THE MIDDLE OF THE HORNCORE.	221
FIGURE 2.203 MAXIMUM DIAMETER OF THE HORNCORE PLOTTED AGAINST THE MINIMUM DIAMETER AT THE BASE. ANIMALS ARE DIVIDED BY SEX.	222
FIGURE 2.204 MAXIMUM DIAMETER PLOTTED AGAINST THE MINIMUM DIAMETER AT THE BASE OF THE HORNCORE. ANIMALS ARE DIVIDED BY SEX.	222
FIGURE 2.205 MAXIMUM DIAMETER AT THE BASE PLOTTED AGAINST THE GREATEST LENGTH OF THE HORNCORE. ANIMALS ARE DIVIDED BY SEX.	223
FIGURE 2.206 MAXIMUM DIAMETER AT THE BASE PLOTTED AGAINST THE LENGTH OF THE OUTER CURVATURE OF THE HORNCORE. ANIMALS ARE DIVIDED BY SEX.	223
FIGURE 2.207 MAXIMUM DIAMETER AT THE MIDDLE OF THE HORNCORE PLOTTED AGAINST THE GREATEST LENGTH. ANIMALS ARE DIVIDED BY SEX.	224
FIGURE 2.208 MAXIMUM DIAMETER AT THE MIDDLE OF THE HORNCORES PLOTTED AGAINST THE LENGTH OF THE OUTER CURVATURE. ANIMALS ARE DIVIDED BY SEX.	224
FIGURE 2.209 LENGTH OF THE OUTER CURVATURE PLOTTED AGAINST THE MAXIMUM LENGTH OF THE HORNCORE.	225
FIGURE 2.210 LENGTH OF THE OUTER CURVATURE PLOTTED AGAINST THE MAXIMUM LENGTH OF THE HORNCORE. SPECIMENS ARE DIVIDED BY SEX.	226
FIGURE 2.211 GREATEST BREADTH OF THE GLENOID CAVITY PLOTTED AGAINST THE GREATEST LENGTH OF THE <i>PROCESSUS</i> <i>ARTICULARIS</i> (IMAGE OF SCAPULA (FIG. 31B): REPRINTED FROM VON DEN DRIESCH, A. <i>A GUIDE TO THE MEASUREMENT</i> <i>OF ANIMAL BONES FROM ARCHAEOLOGICAL SITES</i> . PEABODY MUSEUM BULLETINS, VOL. 1, COPYRIGHT 1976 WITH PERMISSION FROM THE PRESIDENT AND FELLOWS OF HARVARD COLLEGE).....	227
FIGURE 2.212 GREATEST BREADTH OF THE GLENOID CAVITY PLOTTED AGAINST THE SHORTEST DISTANCE FROM THE SPINE TO THE EDGE OF THE GLENOID CAVITY.	228
FIGURE 2.213 GREATEST LENGTH OF THE GLENOID CAVITY PLOTTED AGAINST THE GREATEST LENGTH OF THE <i>PROCESSUS ARTICULARIS</i>	228
FIGURE 2.214 SHORTEST DISTANCE FROM THE SPINE TO THE EDGE OF THE GLENOID CAVITY PLOTTED AGAINST THE SMALLEST LENGTH OF THE <i>COLLUM SCAPULAE</i>	229
FIGURE 2.215 SHORTEST DISTANCE FROM THE SPINE TO THE EDGE OF THE GLENOID CAVITY PLOTTED AGAINST THE GREATEST LENGTH OF THE <i>PROCESSUS ARTICULARIS</i>	229
FIGURE 2.216 DIAMETER OF THE TROCHLEAR CONSTRICTION PLOTTED AGAINST THE MEDIO LATERAL WIDTH OF THE TROCHLEA.	230
FIGURE 2.217 HEIGHT OF THE TROCHLEA PLOTTED AGAINST ITS MEDIO LATERAL WIDTH.	231
FIGURE 2.218 BREADTH FROM THE LATERAL CREST TO THE CAPITULUM PLOTTED AGAINST THE MEDIO LATERAL WIDTH OF THE TROCHLEA.	231
FIGURE 2.219 HEIGHT OF THE TROCHLEA PLOTTED AGAINST THE BREADTH FROM THE LATERAL CREST TO THE <i>CAPITULUM</i>	232
FIGURE 2.220 BREADTH OF THE <i>EPICONDYLUS LATERALIS</i> PLOTTED AGAINST THE DISTAL WIDTH.	232
FIGURE 2.221 BREADTH OF THE <i>EPICONDYLUS LATERALIS</i> PLOTTED AGAINST THE DEPTH OF THE DISTAL END.....	233
FIGURE 2.222 DIAMETER OF THE TROCHLEAR CONSTRICTION PLOTTED AGAINST THE BREADTH FROM THE LATERAL CREST TO THE <i>CAPITULUM</i>	233

FIGURE 2.223 BREADTH OF THE <i>EPICONDYLUS LATERALIS</i> PLOTTED AGAINST THE MEDIO LATERAL WIDTH OF THE TROCHLEA.	234
FIGURE 2.224 BREADTH OF THE PROXIMAL ARTICULATION PLOTTED AGAINST THE BREADTH OF THE <i>FACIES ARTICULARIS</i> <i>PROXIMALIS</i>	235
FIGURE 2.225 GREATEST LENGTH PLOTTED AGAINST THE SMALLEST WIDTH OF THE SHAFT (IMAGE OF RADIUS: REPRINTED FROM SCHMID, E. <i>ATLAS OF ANIMAL BONES: FOR PREHISTORIANS, ARCHAEOLOGISTS AND QUATERNARY GEOLOGISTS</i> . AMSTERDAM: ELSEVIER, COPYRIGHT 1972, WITH PERMISSION FROM JOERG SCHIBLER).....	235
FIGURE 2.226 DEPTH ACROSS THE <i>PROCESSUS ANCONAEUS</i> TO THE CAUDAL BORDER PLOTTED AGAINST THE GREATEST BREADTH ACROSS THE CORONOID PROCESS.....	236
FIGURE 2.227 SMALLEST DEPTH OF THE <i>OLECRANON</i> PLOTTED AGAINST GREATEST BREADTH ACROSS THE CORONOID PROCESS.	237
FIGURE 2.228 LENGTH OF THE <i>OLECRANON</i> PLOTTED AGAINST ITS BREADTH.	237
FIGURE 2.229 DIAMETER OF THE MEDIAL TROCHLEA PLOTTED AGAINST THE WIDTH OF THE MEDIAL CONDYLE.	238
FIGURE 2.230 DIAMETER OF THE LATERAL TROCHLEA PLOTTED AGAINST THE WIDTH OF THE LATERAL CONDYLE.	238
FIGURE 2.231 DIAMETER OF THE <i>VERTICILLUS</i> AT THE MEDIAL CONDYLE PLOTTED AGAINST THE DIAMETER OF THE MEDIAL TROCHLEA.....	239
FIGURE 2.232 DIAMETER OF THE <i>VERTICILLUS</i> AT THE LATERAL CONDYLE PLOTTED AGAINST THE DIAMETER OF THE LATERAL TROCHLEA.	240
FIGURE 2.233 GREATEST LENGTH PLOTTED AGAINST THE SMALLEST WIDTH OF THE SHAFT (IMAGE OF METACARPAL: REPRINTED FROM SCHMID, E. <i>ATLAS OF ANIMAL BONES: FOR PREHISTORIANS, ARCHAEOLOGISTS AND QUATERNARY GEOLOGISTS</i> . AMSTERDAM: ELSEVIER, COPYRIGHT 1972, WITH PERMISSION FROM JOERG SCHIBLER).....	240
FIGURE 2.234 GREATEST LENGTH PLOTTED AGAINST THE BREADTH AT THE FUSION POINT OF THE DISTAL END.....	241
FIGURE 2.235 GREATEST LENGTH PLOTTED AGAINST THE BREADTH OF THE DISTAL END.	241
FIGURE 2.236 GOAT. GREATEST LENGTH PLOTTED AGAINST THE BREADTH OF THE DISTAL END. SPECIMENS DIVIDED BY SEX.	242
FIGURE 2.237 SHEEP. GREATEST LENGTH PLOTTED AGAINST THE BREADTH OF THE DISTAL END. SPECIMENS DIVIDED BY SEX.	242
FIGURE 2.238 DIAMETER OF THE <i>VERTICILLUS</i> AT THE MEDIAL CONDYLE PLOTTED AGAINST THE DIAMETER OF THE MEDIAL TROCHLEA.....	243
FIGURE 2.239 DIAMETER OF THE <i>VERTICILLUS</i> AT THE LATERAL CONDYLE PLOTTED AGAINST THE DIAMETER OF THE LATERAL TROCHLEA.....	244
FIGURE 2.240 GREATEST LENGTH PLOTTED AGAINST THE SMALLEST WIDTH OF THE SHAFT.	244
FIGURE 2.241 GREATEST LENGTH PLOTTED AGAINST THE BREADTH AT THE FUSION POINT OF THE DISTAL END.....	245
FIGURE 2.242 GREATEST LENGTH PLOTTED AGAINST THE BREADTH OF THE DISTAL END.	245
FIGURE 2.243 GOAT. GREATEST LENGTH PLOTTED AGAINST THE BREADTH OF THE DISTAL END. SPECIMENS ARE DIVIDED BY SEX.....	246

FIGURE 2.244 SHEEP. GREATEST LENGTH PLOTTED AGAINST THE BREADTH OF THE DISTAL END. SPECIMENS ARE DIVIDED BY SEX.	246
FIGURE 2.245 DEPTH OF THE MEDIAL SIDE PLOTTED AGAINST THE DEPTH OF THE LATERAL SIDE OF THE DISTAL END.	247
FIGURE 2.246 DEPTH OF THE LATERAL SIDE PLOTTED AGAINST THE BREADTH OF THE DISTAL END.	248
FIGURE 2.247 GREATEST LENGTH PLOTTED AGAINST THE SMALLEST WIDTH OF THE SHAFT (IMAGE OF TIBIA: REPRINTED FROM SCHMID, E. <i>ATLAS OF ANIMAL BONES: FOR PREHISTORIANS, ARCHAEOLOGISTS AND QUATERNARY GEOLOGISTS</i> . AMSTERDAM: ELSEVIER, COPYRIGHT 1972, WITH PERMISSION FROM JOERG SCHIBLER).	248
FIGURE 2.248 BREADTH OF THE DISTAL END PLOTTED AGAINST THE GREATEST LENGTH OF THE LATERAL PART (IMAGE OF ASTRAGALUS (FIG. 41D): REPRINTED FROM VON DEN DRIESCH, A. <i>A GUIDE TO THE MEASUREMENT OF ANIMAL BONES FROM ARCHAEOLOGICAL SITES</i> . PEABODY MUSEUM BULLETINS, VOL. 1, COPYRIGHT 1976 WITH PERMISSION FROM THE PRESIDENT AND FELLOWS OF HARVARD COLLEGE).	249
FIGURE 2.249 HEIGHT AT THE CENTRAL CONSTRICTION PLOTTED AGAINST THE GREATEST DEPTH OF THE LATERAL HALF (IMAGE OF LATERAL ASTRAGALUS (FIG. 41E): REPRINTED FROM VON DEN DRIESCH, A. <i>A GUIDE TO THE MEASUREMENT OF ANIMAL BONES FROM ARCHAEOLOGICAL SITES</i> . PEABODY MUSEUM BULLETINS, VOL. 1. COPYRIGHT 1976 WITH PERMISSION FROM THE PRESIDENT AND FELLOWS OF HARVARD COLLEGE).	249
FIGURE 2.250 HEIGHT AT THE CENTRAL CONSTRICTION PLOTTED AGAINST THE BREADTH OF THE DISTAL END.	250
FIGURE 2.251 MAXIMUM BREADTH OF THE PLANTAR TROCHLEA PLOTTED AGAINST THE GREATEST DEPTH OF THE LATERAL HALF.	250
FIGURE 2.252 LENGTH OF THE ARTICULAR FACET OF THE <i>OS MALLEOLARE</i> PLOTTED AGAINST LENGTH TAKEN FROM THE ARTICULAR FACET OF THE <i>OS MALLEOLARE</i> TO THE END OF THE ARTICULATION-FREE PART OF THE PROCESS (IMAGE OF CALCANEUM: REPRINTED FROM ZEDER, M.A. AND H.A. LAPHAM. ASSESSING THE RELIABILITY OF CRITERIA USED TO IDENTIFY POSTCRANIAL BONES IN SHEEP, <i>OVIS</i> , AND GOATS, <i>CAPRA</i> . <i>JOURNAL OF ARCHAEOLOGICAL SCIENCE</i> 37: 2887-2905, COPYRIGHT 2010, WITH PERMISSION FROM ELSEVIER).	251
FIGURE 2.253 LENGTH OF THE ARTICULAR FACET OF THE <i>OS MALLEOLARE</i> PLOTTED AGAINST THE BREADTH OF ITS ARTICULAR SURFACE.	251
FIGURE 2.254 GREATEST LENGTH PLOTTED AGAINST THE DEPTH OF THE <i>SUBSTENTACULUM TALI</i>	252
FIGURE 2.255 LENGTH OF THE ARTICULAR FACET OF THE <i>OS MALLEOLARE</i> PLOTTED AGAINST THE DEPTH OF THE <i>SUBSTENTACULUM TALI</i>	252
FIGURE 2.256 DIAGONAL LENGTH OF THE SOLE PLOTTED AGAINST THE MIDDLE BREADTH OF THE SOLE (IMAGE OF 3 RD PHALANX (FIG. 48C): REPRINTED FROM VON DEN DRIESCH, A. <i>A GUIDE TO THE MEASUREMENT OF ANIMAL BONES FROM ARCHAEOLOGICAL SITES</i> . PEABODY MUSEUM BULLETINS, VOL. 1, COPYRIGHT 1976 WITH PERMISSION FROM THE PRESIDENT AND FELLOWS OF HARVARD COLLEGE).	253
FIGURE 2.257 MAXIMUM DIAMETER TAKEN AT THE BASE PLOTTED AGAINST A RATIO BETWEEN THE LENGTH AND THE LENGTH OF THE OUTER CURVATURE OF THE HORNCORE.	254
FIGURE 2.258 RATIO BETWEEN THE LENGTH AND THE LENGTH OF THE OUTER CURVATURE PLOTTED AGAINST THE RATIO BETWEEN THE MAXIMUM DIAMETER TAKEN AT THE BASE AND THE LENGTH OF THE OUTER CURVATURE OF THE HORNCORE.	255

FIGURE 2.259 RATIO BETWEEN THE SHORTEST DISTANCE FROM THE BASE OF SPINE TO THE EDGE OF THE GLENOID CAVITY AND THE BREADTH OF THE GLENOID CAVITY PLOTTED AGAINST THE RATIO BETWEEN THE SHORTEST DISTANCE FROM THE BASE OF THE SPINE TO THE EDGE OF THE GLENOID CAVITY AND THE LENGTH OF THE GLENOID CAVITY.	256
FIGURE 2.260 RATIO BETWEEN THE GREATEST LENGTH OF THE <i>PROCESSUS ARTICULARIS</i> AND THE LENGTH OF THE GLENOID CAVITY PLOTTED AGAINST THE RATIO BETWEEN THE GREATEST LENGTH OF THE <i>PROCESSUS ARTICULARIS</i> AND THE BREADTH OF THE GLENOID CAVITY.	256
FIGURE 2.261 RATIO BETWEEN THE SHORTEST DISTANCE FROM THE BASE OF THE SPINE TO THE EDGE OF THE GLENOID CAVITY (ASG) AND THE SMALLEST LENGTH OF THE <i>COLLUM SCAPULAE</i> (SLC) PLOTTED AGAINST THE RATIO BETWEEN GREATEST LENGTH OF THE <i>PROCESSUS ARTICULARIS</i> (GLP) AND THE BREADTH OF THE GLENOID CAVITY (BG).	257
FIGURE 2.262 RATIO BETWEEN THE MEDIO LATERAL WIDTH OF THE TROCHLEA AND ITS HEIGHT PLOTTED AGAINST THE MEDIO LATERAL WIDTH OF THE TROCHLEA AND THE DIAMETER OF THE TROCHLEAR CONSTRICTION.	258
FIGURE 2.263 RATIO BETWEEN THE BREADTH OF THE CAPITULUM AND THE DISTAL WIDTH PLOTTED AGAINST THE RATIO BETWEEN THE BREADTH OF THE CAPITULUM AND THE MEDIO LATERAL WIDTH OF THE TROCHLEA.	259
FIGURE 2.264 RATIO BETWEEN THE BREADTH OF THE <i>CAPITULUM</i> AND THE DIAMETER OF THE TROCHLEA CONSTRICTION PLOTTED AGAINST THE RATIO BETWEEN THE BREADTH OF THE <i>CAPITULUM</i> AND THE MEDIO LATERAL WIDTH OF THE TROCHLEA.	259
FIGURE 2.265 RATIO BETWEEN THE BREADTH OF THE <i>EPICONDYLE LATERALIS</i> AND THE MEDIO LATERAL WIDTH OF THE TROCHLEA PLOTTED AGAINST THE RATIO BETWEEN THE BREADTH OF THE <i>EPICONDYLE LATERALIS</i> AND THE WIDTH OF THE DISTAL END.	260
FIGURE 2.266 RATIO BETWEEN THE GREATEST LENGTH OF THE <i>FACIES ARTICULARIS PROXIMALIS</i> AND THE GREATEST BREADTH OF THE PROXIMAL END PLOTTED AGAINST THE DEPTH OF THE PROXIMAL END.	261
FIGURE 2.267 RATIO BETWEEN THE BREADTH ACROSS THE CORONOID PROCESS AND THE DEPTH ACROSS THE <i>PROCESSUS ANCONAEUS</i> TO THE CAUDAL BORDER PLOTTED AGAINST THE BREADTH ACROSS THE CORONOID PROCESS AND THE SMALLEST DEPTH OF THE <i>OLECRANON</i>	262
FIGURE 2.268 RATIO BETWEEN THE DIAMETER OF THE MEDIAL TROCHLEA AND THE WIDTH OF THE MEDIAL CONDYLE PLOTTED AGAINST THE RATIO BETWEEN THE DIAMETER OF THE MEDIAL TROCHLEA AND THE DIAMETER OF THE <i>VERTICILLUS</i> AT THE MEDIAL CONDYLE.	263
FIGURE 2.269 RATIO BETWEEN THE WIDTH OF THE LATERAL CONDYLE AND THE DIAMETER OF THE LATERAL TROCHLEA PLOTTED AGAINST THE RATIO BETWEEN THE DIAMETER OF THE LATERAL CONDYLE AND THE DIAMETER OF THE <i>VERTICILLUS</i> ON THE LATERAL CONDYLE.	263
FIGURE 2.270 RATIO BETWEEN THE GREATEST BREADTH OF THE DISTAL END WITH THE GREATEST LENGTH PLOTTED AGAINST THE RATIO BETWEEN THE SMALLEST WIDTH OF THE SHAFT AND THE GREATEST LENGTH.	264
FIGURE 2.271 RATIO BETWEEN THE DIAMETER OF THE MEDIAL TROCHLEA AND THE WIDTH OF THE MEDIAL CONDYLE PLOTTED AGAINST THE RATIO BETWEEN THE DIAMETER OF THE MEDIAL TROCHLEA AND THE DIAMETER OF THE <i>VERTICILLUS</i> AT THE MEDIAL CONDYLE.	266
FIGURE 2.272 RATIO BETWEEN THE WIDTH OF THE LATERAL CONDYLE AND THE DIAMETER OF THE LATERAL TROCHLEA PLOTTED AGAINST THE RATIO BETWEEN THE DIAMETER OF THE LATERAL CONDYLE AND THE DIAMETER OF THE <i>VERTICILLUS</i> ON THE LATERAL CONDYLE.	266

FIGURE 2.273 RATIO BETWEEN THE GREATEST BREADTH OF THE DISTAL END WITH THE GREATEST LENGTH PLOTTED AGAINST THE RATIO BETWEEN THE SMALLEST WIDTH OF THE SHAFT AND THE GREATEST LENGTH.	267
FIGURE 2.274 BREADTH OF THE DISTAL END PLOTTED AGAINST THE RATIO BETWEEN THE DEPTH OF THE MEDIAL (A) AND LATERAL (B) SIDE.	267
FIGURE 2.275 RATIO BETWEEN HEIGHT AT THE CENTRAL CONSTRICTION AND THE GREATEST DEPTH OF THE LATERAL HALF PLOTTED AGAINST A RATIO BETWEEN THE BREADTH OF THE DISTAL END AND THE GREATEST LENGTH OF THE LATERAL HALF.	268
FIGURE 2.276 RATIO BETWEEN HEIGHT AT THE CENTRAL CONSTRICTION AND THE GREATEST DEPTH OF THE LATERAL HALF PLOTTED AGAINST THE RATIO BETWEEN THE BREADTH OF THE DISTAL END AND THE HEIGHT AT THE CENTRAL CONSTRICTION.	269
FIGURE 2.277 RATIO BETWEEN BREADTH OF THE DISTAL END AND THE GREATEST DEPTH OF THE LATERAL HALF PLOTTED AGAINST THE RATIO BETWEEN THE BREADTH OF THE DISTAL END AND THE GREATEST DEPTH OF THE LATERAL HALF. ..	269
FIGURE 2.278 RATIO BETWEEN THE BREADTH OF THE DISTAL END AND THE HEIGHT AT THE CENTRAL CONSTRICTION AND THE RATIO BETWEEN HEIGHT AT THE CENTRAL CONSTRICTION AND THE GREATEST DEPTH OF THE LATERAL HALF.	270
FIGURE 2.279 RATIO BETWEEN THE LENGTH AND THE BREADTH OF THE ARTICULAR FACET OF THE <i>OS MALLEOLARE</i> PLOTTED AGAINST THE RATIO BETWEEN THE LENGTH OF THE ARTICULAR FACET OF THE <i>OS MALLEOLARE</i> AND THE LENGTH TAKEN FROM THE ARTICULAR FACET OF THE <i>OS MALLEOLARE</i> TO THE END OF THE ARTICULATION-FREE PART OF THE PROCESS.	271
FIGURE 2.280 RATIO BETWEEN THE DEPTH OF THE <i>SUBSTENTACULUM TALII</i> AND THE LENGTH OF THE ARTICULAR FACET OF THE <i>OS MALLEOLARE</i> PLOTTED AGAINST THE RATIO BETWEEN THE LENGTH AND THE BREADTH OF THE ARTICULAR FACET OF THE <i>OS MALLEOLARE</i>	271
FIGURE 2.281 RATIO BETWEEN THE DEPTH OF THE <i>SUBSTENTACULUM TALII</i> AND THE LENGTH OF THE ARTICULAR FACET OF THE <i>OS MALLEOLARE</i> PLOTTED AGAINST THE RATIO BETWEEN THE LENGTH AND THE BREADTH OF THE ARTICULAR FACET OF THE <i>OS MALLEOLARE</i>	272
FIGURE 2.282 DIAGONAL LENGTH OF THE SOLE PLOTTED AGAINST THE RATIO BETWEEN THE DIAGONAL LENGTH OF THE SOLE AND THE MIDDLE BREADTH.	272
FIGURE 2.283 HORNCORE: SCATTERPLOT OF THE INDIVIDUAL DISCRIMINANT SCORES.	284
FIGURE 2.284 SCAPULA: SCATTERPLOT OF THE INDIVIDUAL DISCRIMINANT SCORES.	287
FIGURE 2.285 HUMERUS: SCATTERPLOT OF THE INDIVIDUAL DISCRIMINANT SCORES.	291
FIGURE 2.286 RADIUS: SCATTERPLOT OF THE INDIVIDUAL DISCRIMINANT SCORES.	294
FIGURE 2.287 ULNA: SCATTERPLOT OF THE INDIVIDUAL DISCRIMINANT SCORES.	297
FIGURE 2.288 METACARPAL: SCATTERPLOT OF THE INDIVIDUAL DISCRIMINANT SCORES.	301
FIGURE 2.289 METATARSAL: SCATTERPLOT OF THE INDIVIDUAL DISCRIMINANT SCORES.	304
FIGURE 2.290 TIBIA: SCATTERPLOT OF THE INDIVIDUAL DISCRIMINANT SCORES.	307
FIGURE 2.2.291 ASTRAGALUS: SCATTERPLOT OF THE INDIVIDUAL DISCRIMINANT SCORES.	310
FIGURE 2.292 CALCANEUM: SCATTERPLOT OF THE INDIVIDUAL DISCRIMINANT SCORES.	313
FIGURE 2.293 3 RD PHALANX: MBS PLOTTED AGAINST DLS SHOWS THE PRESENCE OF MULTICOLLINEARITY.	315
FIGURE 2.294 3 RD PHALANX: SCATTERPLOT OF THE INDIVIDUAL DISCRIMINANT SCORES.	317
FIGURE 2.295 HORNCORE: SCATTERPLOT OF THE INDIVIDUAL COMPONENT SCORES.	321

FIGURE 2.296 SCAPULA: SCATTERPLOT OF THE INDIVIDUAL DISCRIMINANT SCORE FOR COMPONENT I AND COMPONENT II.	323
FIGURE 2.297 SCAPULA: SCATTERPLOT OF THE INDIVIDUAL COMPONENT SCORES FOR COMPONENT I.	324
FIGURE 2.298 SCAPULA: ROTATED VARIABLE LOADING FOR COMPONENT I AND II.....	325
FIGURE 2.299 HUMERUS: INDIVIDUAL COMPONENT SCORES FOR COMPONENT I AND II.	328
FIGURE 2.300 HUMERUS: ROTATED VARIABLE LOADINGS FOR EACH COMPONENT.	329
FIGURE 2.301 RADIUS: SCATTERPLOT OF THE INDIVIDUAL COMPONENT SCORES FOR COMPONENT I AND II.	332
FIGURE 2.302 RADIUS: INDIVIDUAL COMPONENT SCORES OF COMPONENT II AND III.....	332
FIGURE 2.303 RADIUS: INDIVIDUAL COMPONENT SCORES FOR COMPONENT III AND I.	333
FIGURE 2.304 RADIUS: ROTATED VARIABLE LOADINGS FOR EACH COMPONENT.....	334
FIGURE 2.305 ULNA: SCATTERPLOT OF THE INDIVIDUAL DISCRIMINANT SCORES FOR COMPONENT I AND II.....	337
FIGURE 2.306 ULNA: ROTATED VARIABLE SCORES FOR EACH COMPONENT.	338
FIGURE 2.307 METACARPAL: ROTATED VARIABLE SCORES FOR EACH COMPONENT.	342
FIGURE 2.308 METACARPAL: SCATTERPLOT OF THE INDIVIDUAL COMPONENT SCORES FOR COMPONENTS I AND II.	343
FIGURE 2.309 METACARPAL: SCATTERPLOT OF THE INDIVIDUAL COMPONENT SCORES FOR COMPONENTS II AND III.....	344
FIGURE 2.310 METACARPAL: SCATTERPLOT OF THE INDIVIDUAL COMPONENT SCORES FOR COMPONENTS I AND III.....	344
FIGURE 2.311 METATARSAL: ROTATED VARIABLE SCORES FOR EACH COMPONENT.....	348
FIGURE 2.312 METATARSAL: SCATTERPLOT OF THE INDIVIDUAL COMPONENT SCORES FOR COMPONENTS I AND II.	349
FIGURE 2.313 TIBIA: ROTATED VARIABLE LOADINGS FOR EACH COMPONENT.	352
FIGURE 2.314 TIBIA: SCATTERPLOT OF THE INDIVIDUAL COMPONENT SCORES FOR COMPONENTS I AND II.	352
FIGURE 2.315 ASTRAGALUS: ROTATED VARIABLE LOADINGS FOR EACH COMPONENT.....	356
FIGURE 2.316 ASTRAGALUS: SCATTERPLOT OF THE INDIVIDUAL COMPONENT SCORES FOR COMPONENTS I AND II.....	357
FIGURE 2.317 CALCANEUM: ROTATED VARIABLE LOADINGS FOR EACH COMPONENT.....	360
FIGURE 2.318 CALCANEUM: SCATTERPLOT OF THE INDIVIDUAL COMPONENT SCORES FOR COMPONENTS I AND II.	360
FIGURE 3.1 MAP OF CENTRAL ENGLAND. THE RED STARS REPRESENT THE POSITION ON THE MAP OF THE ARCHAEOLOGICAL SITES ANALYSED (MAP FROM HTTPS://WWW.GOOGLE.COM/MAPS/@53.043617,-1.3465121,8z).	369
FIGURE 3.2 MAP OF THE LOCATION OF KING’S LYNN AND THE INVESTIGATED AREAS (IMAGE REPRINTED FROM CLARKE, H. AND A. CARTER, EDS. <i>EXCAVATION IN KING’S LYNN 1963-1970</i> . MEDIEVAL ARCHAEOLOGY MONOGRAPH SERIES 7, COPYRIGHT 1977. LONDON: SOCIETY FOR MEDIEVAL ARCHAEOLOGY WITH PERMISSION FROM HELEN CLARKE).	373
FIGURE 3.3 MAP OF THE INTERNATIONAL TRADE (IN POTTERY AND OTHER GOODS) BETWEEN KING’S LYNN AND SEVERAL INLAND AND FOREIGN CITIES ON THE LEFT. ON THE RIGHT IS A MAP SHOWING THE SOURCE ATTRIBUTION OF THE MEDIÆVAL POTTERY FOUND AT KING’S LYNN (IMAGES REPRINTED FROM CLARKE, H. AND A. CARTER, EDS. <i>EXCAVATION IN KING’S LYNN 1963-1970</i> , MEDIEVAL ARCHAEOLOGY MONOGRAPH SERIES 7, COPYRIGHT 1977. LONDON: SOCIETY FOR MEDIEVAL ARCHAEOLOGY, WITH PERMISSION FROM HELEN CLARKE).	375
FIGURE 3.4 TABLE OF NISP (NUMBER OF IDENTIFIED SPECIMENS), MNI (MINIMUM NUMBER OF INDIVIDUALS) AND AGE CLASSES FOR THE DOMESTIC SPECIES FOR EACH CHRONOLOGICAL PERIOD AT KING’S LYNN, AS IDENTIFIED BY NODDLE (IMAGE REPRINTED FROM NODDLE, B.A. MAMMAL BONE. IN <i>EXCAVATION IN KING’S LYNN 1963-1970</i> , H. CLARKE AND A. CARTER, 378-399, COPYRIGHT 1977. THE SOCIETY FOR MEDIEVAL ARCHAEOLOGY MONOGRAPH SERIES 7. LONDON: SOCIETY FOR MEDIÆVAL ARCHAEOLOGY, WITH PERMISSION FROM HELEN CLARKE).	377

FIGURE 3.5 NISP AND MNI FOR SHEEP AND GOAT IN PHASE I ACCORDING TO NODDLE 1977 (IMAGE REPRINTED FROM NODDLE, B.A. MAMMAL BONE. IN <i>EXCAVATION IN KING'S LYNN 1963-1970</i> , H. CLARKE AND A. CARTER, 378-399, COPYRIGHT 1977. THE SOCIETY FOR MEDIEVAL ARCHAEOLOGY MONOGRAPH SERIES 7. LONDON: SOCIETY FOR MEDIEVAL ARCHAEOLOGY, WITH PERMISSION FROM HELEN CLARKE).	379
FIGURE 3.6 NISP AND MNI FOR SHEEP AND GOAT IN PHASE II ACCORDING TO NODDLE (IMAGE REPRINTED FROM NODDLE, B.A. MAMMAL BONE. IN <i>EXCAVATION IN KING'S LYNN 1963-1970</i> , H. CLARKE AND A. CARTER, 378-399, COPYRIGHT 1977. THE SOCIETY FOR MEDIEVAL ARCHAEOLOGY MONOGRAPH SERIES 7. LONDON: SOCIETY FOR MEDIEVAL ARCHAEOLOGY, WITH PERMISSION FROM HELEN CLARKE).	380
FIGURE 3.7 NISP AND MNI FOR SHEEP AND GOAT IN PHASE III ACCORDING TO NODDLE (IMAGE REPRINTED FROM NODDLE, B.A. MAMMAL BONE. IN <i>EXCAVATION IN KING'S LYNN 1963-1970</i> , H. CLARKE AND A. CARTER, 378-399, COPYRIGHT 1977. THE SOCIETY FOR MEDIEVAL ARCHAEOLOGY MONOGRAPH SERIES 7. LONDON: SOCIETY FOR MEDIEVAL ARCHAEOLOGY, WITH PERMISSION FROM HELEN CLARKE).	381
FIGURE 3.8 NISP AND MNI FOR SHEEP AND GOAT IN PHASE IV ACCORDING TO NODDLE (IMAGE REPRINTED FROM NODDLE, B.A. MAMMAL BONE. IN <i>EXCAVATION IN KING'S LYNN 1963-1970</i> , H. CLARKE AND A. CARTER, 378-399, COPYRIGHT 1977. THE SOCIETY FOR MEDIEVAL ARCHAEOLOGY MONOGRAPH SERIES 7. LONDON: SOCIETY FOR MEDIEVAL ARCHAEOLOGY, WITH PERMISSION FROM HELEN CLARKE).	382
FIGURE 3.9 MAXIMUM DIAMETER TAKEN AT THE BASE PLOTTED AGAINST A RATIO BETWEEN THE LENGTH AND THE LENGTH OF THE OUTER CURVATURE OF THE HORNCORE. THE MODERN DATA ARE REPRESENTED BY THE SQUARE EMPTY SYMBOL, BLUE FOR MODERN GOATS, RED FOR MODERN SHEEP, WHILE THE ARCHAEOLOGICAL MATERIAL IS REPRESENTED BY THE FILLED DOT SYMBOL: BLUE FOR GOATS, RED FOR SHEEP AND GREEN FOR SHEEP/GOAT.	385
FIGURE 3.10 RATIO BETWEEN THE LENGTH AND THE LENGTH OF THE OUTER CURVATURE PLOTTED AGAINST THE RATIO BETWEEN THE MAXIMUM DIAMETER TAKEN AT THE BASE AND THE LENGTH OF THE OUTER CURVATURE OF THE HORNCORE. SYMBOLS EXPLAINED IN FIG. 3.9.	385
FIGURE 3.11 RATIO BETWEEN THE GREATEST LENGTH OF THE <i>PROCESSUS ARTICULARIS</i> AND THE LENGTH OF THE GLENOID CAVITY PLOTTED AGAINST THE RATIO BETWEEN THE GREATEST LENGTH OF <i>THE PROCESSUS ARTICULARIS</i> AND THE BREADTH OF THE GLENOID CAVITY. SYMBOLS EXPLAINED IN FIG. 3.9.	386
FIGURE 3.12 RATIO BETWEEN THE SHORTEST DISTANCE FROM THE BASE OF THE SPINE TO THE EDGE OF THE GLENOID CAVITY AND THE SMALLEST LENGTH OF THE <i>COLLUM SCAPULAE</i> PLOTTED AGAINST THE RATIO BETWEEN THE GREATEST LENGTH OF THE <i>PROCESSUS ARTICULARIS</i> AND THE BREADTH OF THE GLENOID CAVITY. SYMBOLS EXPLAINED IN FIG. 3.9.	386
FIGURE 3.13 RATIO BETWEEN THE MEDIO LATERAL WIDTH OF THE TROCHLEA AND ITS HEIGHT PLOTTED AGAINST THE MEDIO LATERAL WIDTH OF THE TROCHLEA AND THE DIAMETER OF THE TROCHLEAR CONSTRICTION. SYMBOLS EXPLAINED IN FIG. 3.9.	387

FIGURE 3.14 RATIO BETWEEN THE BREADTH OF THE <i>CAPITULUM</i> AND THE DISTAL WIDTH PLOTTED AGAINST THE RATIO BETWEEN THE BREADTH OF THE <i>CAPITULUM</i> AND THE MEDIO LATERAL WIDTH OF THE TROCHLEA. SYMBOLS EXPLAINED IN FIG. 3.9.	387
FIGURE 3.15 RATIO BETWEEN THE BREADTH OF THE <i>CAPITULUM</i> AND THE DIAMETER OF THE TROCHLEA CONSTRICTION PLOTTED AGAINST THE RATIO BETWEEN THE BREADTH OF THE <i>CAPITULUM</i> AND THE MEDIO LATERAL WIDTH OF THE TROCHLEA. SYMBOLS EXPLAINED IN FIG. 3.9.	388
FIGURE 3.16 RATIO BETWEEN THE BREADTH OF THE EPICONDYLE <i>LATERALIS</i> AND THE MEDIO LATERAL WIDTH OF THE TROCHLEA PLOTTED AGAINST THE RATIO BETWEEN THE BREADTH OF THE EPICONDYLE <i>LATERALIS</i> AND THE WIDTH OF THE DISTAL END. SYMBOLS EXPLAINED IN FIG. 3.9.	388
FIGURE 3.17 RATIO BETWEEN THE GREATEST LENGTH OF THE <i>FACIES ARTICULARIS PROXIMALIS</i> AND THE GREATEST BREADTH OF THE PROXIMAL END PLOTTED AGAINST THE DEPTH OF THE PROXIMAL END. SYMBOLS EXPLAINED IN FIG. 3.9.	389
FIGURE 3.18 RATIO BETWEEN THE BREADTH ACROSS THE CORONOID PROCESS AND THE DEPTH ACROSS THE <i>PROCESSUS ANCONAEUS</i> TO THE CAUDAL BORDER PLOTTED AGAINST THE BREADTH ACROSS THE CORONOID PROCESS AND THE SMALLEST DEPTH OF THE OLECRANON. SYMBOLS EXPLAINED IN FIG. 3.9.	389
FIGURE 3.19 METACARPAL. RATIO BETWEEN THE DIAMETER OF THE MEDIAL TROCHLEA AND THE WIDTH OF THE MEDIAL CONDYLE PLOTTED AGAINST THE RATIO BETWEEN THE DIAMETER OF THE <i>VERTICILLUS</i> AT THE MEDIAL CONDYLE AND THE DIAMETER OF THE MEDIAL TROCHLEA. SYMBOLS EXPLAINED IN FIG. 3.9.	390
FIGURE 3.20 METACARPAL. RATIO BETWEEN THE WIDTH OF THE LATERAL CONDYLE AND THE DIAMETER OF THE LATERAL TROCHLEA PLOTTED AGAINST THE RATIO BETWEEN THE DIAMETER OF THE LATERAL CONDYLE AND THE DIAMETER OF THE <i>VERTICILLUS</i> ON THE LATERAL CONDYLE. SYMBOLS EXPLAINED IN FIG. 3.9.	391
FIGURE 3.21 METATARSAL. RATIO BETWEEN THE DIAMETER OF THE MEDIAL TROCHLEA AND THE WIDTH OF THE MEDIAL CONDYLE PLOTTED AGAINST THE RATIO BETWEEN THE DIAMETER OF THE <i>VERTICILLUS</i> AT THE MEDIAL CONDYLE AND THE DIAMETER OF THE MEDIAL TROCHLEA. SYMBOLS EXPLAINED IN FIG. 3.9.	391
FIGURE 3.22 METATARSAL. RATIO BETWEEN THE WIDTH OF THE LATERAL CONDYLE AND THE DIAMETER OF THE LATERAL TROCHLEA PLOTTED AGAINST THE RATIO BETWEEN THE DIAMETER OF THE <i>VERTICILLUS</i> ON THE LATERAL CONDYLE AND THE DIAMETER OF THE LATERAL CONDYLE. SYMBOLS EXPLAINED IN FIG. 3.9.	392
FIGURE 3.23 BREADTH OF THE DISTAL END PLOTTED AGAINST THE RATIO BETWEEN THE DEPTH OF THE MEDIAL (A) AND LATERAL (B) SIDE. SYMBOLS EXPLAINED IN FIG. 3.9.	392
FIGURE 3.24 RATIO BETWEEN HEIGHT AT THE CENTRAL CONSTRICTION AND THE GREATEST DEPTH OF THE LATERAL HALF PLOTTED AGAINST A RATIO BETWEEN THE BREADTH OF THE DISTAL END AND THE GREATEST LENGTH OF THE LATERAL HALF. SYMBOLS EXPLAINED IN FIG. 3.9.	393
FIGURE 3.25 RATIO BETWEEN HEIGHT AT THE CENTRAL CONSTRICTION AND THE GREATEST DEPTH OF THE LATERAL HALF PLOTTED AGAINST THE RATIO BETWEEN THE BREADTH OF THE DISTAL END AND THE HEIGHT AT THE CENTRAL CONSTRICTION. SYMBOLS EXPLAINED IN FIG. 3.9.	393

FIGURE 3.26 RATIO BETWEEN BREADTH OF THE DISTAL END AND THE GREATEST DEPTH OF THE LATERAL HALF PLOTTED AGAINST THE RATIO BETWEEN THE BREADTH OF THE DISTAL END AND THE GREATEST DEPTH OF THE LATERAL HALF. SYMBOLS EXPLAINED IN FIG. 3.9.	394
FIGURE 3.27 RATIO BETWEEN THE BREADTH OF THE DISTAL END AND THE HEIGHT AT THE CENTRAL CONSTRICTION AND THE RATIO BETWEEN HEIGHT AT THE CENTRAL CONSTRICTION AND THE GREATEST DEPTH OF THE LATERAL HALF. SYMBOLS EXPLAINED IN FIG. 3.9.	394
FIGURE 3.28 RATIO BETWEEN THE LENGTH AND THE BREADTH OF THE ARTICULAR FACET OF THE <i>OS MALLEOLARE</i> PLOTTED AGAINST THE RATIO BETWEEN THE LENGTH OF THE ARTICULAR FACET OF THE <i>OS MALLEOLARE</i> AND THE LENGTH TAKEN FROM THE ARTICULAR FACET OF THE <i>OS MALLEOLARE</i> TO THE END OF THE ARTICULATION-FREE PART OF THE PROCESS. SYMBOLS EXPLAINED IN FIG. 3.9.....	395
FIGURE 3.29 RATIO BETWEEN THE DEPTH OF THE <i>SUBSTENTACULUM TALI</i> AND THE LENGTH OF THE ARTICULAR FACET OF THE <i>OS MALLEOLARE</i> PLOTTED AGAINST THE RATIO BETWEEN THE LENGTH AND THE BREADTH OF THE ARTICULAR FACET OF THE <i>OS MALLEOLARE</i> . SYMBOLS EXPLAINED IN FIG. 3.9.	395
FIGURE 3.30 RATIO BETWEEN THE DEPTH OF THE <i>SUBSTENTACULUM TALI</i> AND THE LENGTH OF THE ARTICULAR FACET OF THE <i>OS MALLEOLARE</i> PLOTTED AGAINST THE RATIO BETWEEN THE LENGTH AND THE BREADTH OF THE ARTICULAR FACET OF THE <i>OS MALLEOLARE</i> . SYMBOLS EXPLAINED IN FIG. 3.9.	396
FIGURE 3.31 MAXIMUM DIAMETER TAKEN AT THE BASE PLOTTED AGAINST A RATIO BETWEEN THE LENGTH AND THE LENGTH OF THE OUTER CURVATURE OF THE HORNCORE. SYMBOLS EXPLAINED IN FIG. 3.9.	396
FIGURE 3.32 RATIO BETWEEN THE LENGTH AND THE LENGTH OF THE OUTER CURVATURE PLOTTED AGAINST THE RATIO BETWEEN THE MAXIMUM DIAMETER TAKEN AT THE BASE AND THE LENGTH OF THE OUTER CURVATURE OF THE HORNCORE. SYMBOLS EXPLAINED IN FIG. 3.9.	397
FIGURE 3.33 RATIO BETWEEN THE GREATEST LENGTH OF THE <i>PROCESSUS ARTICULARIS</i> AND THE LENGTH OF THE GLENOID CAVITY PLOTTED AGAINST THE RATIO BETWEEN THE GREATEST LENGTH OF THE <i>PROCESSUS ARTICULARIS</i> AND THE BREADTH OF THE GLENOID CAVITY. SYMBOLS EXPLAINED IN FIG. 3.9.	397
FIGURE 3.34 RATIO BETWEEN THE SHORTEST DISTANCE FROM THE BASE OF THE SPINE TO THE EDGE OF THE GLENOID CAVITY AND THE SMALLEST LENGTH OF THE <i>COLLUM SCAPULAE</i> PLOTTED AGAINST A RATIO BETWEEN THE GREATEST LENGTH OF THE <i>PROCESSUS ARTICULARIS</i> AND THE BREADTH OF THE GLENOID CAVITY. SYMBOLS EXPLAINED IN FIG. 3.9.....	398
FIGURE 3.35 RATIO BETWEEN THE MEDIO LATERAL WIDTH OF THE TROCHLEA AND ITS HEIGHT PLOTTED AGAINST THE MEDIO LATERAL WIDTH OF THE TROCHLEA AND THE DIAMETER OF THE TROCHLEAR CONSTRICTION. SYMBOLS EXPLAINED IN FIG. 3.9.	398
FIGURE 3.36 RATIO BETWEEN THE BREADTH OF THE <i>CAPITULUM</i> AND THE DISTAL WIDTH PLOTTED AGAINST THE RATIO BETWEEN THE BREADTH OF THE <i>CAPITULUM</i> AND THE MEDIO LATERAL WIDTH OF THE TROCHLEA. SYMBOLS EXPLAINED IN FIG. 3.9.....	399
FIGURE 3.37 RATIO BETWEEN THE BREADTH OF THE <i>CAPITULUM</i> AND THE DIAMETER OF THE TROCHLEAR CONSTRICTION PLOTTED AGAINST THE RATIO BETWEEN THE BREADTH OF THE <i>CAPITULUM</i> AND THE MEDIO LATERAL WIDTH OF THE TROCHLEA. SYMBOLS EXPLAINED IN FIG. 3.9.	399

FIGURE 3.38 RATIO BETWEEN THE BREADTH OF THE EPICONDYLE <i>LATERALIS</i> AND THE MEDIO LATERAL WIDTH OF THE TROCHLEA PLOTTED AGAINST THE RATIO BETWEEN THE BREADTH OF THE EPICONDYLE <i>LATERALIS</i> AND THE WIDTH OF THE DISTAL END. SYMBOLS EXPLAINED IN FIG. 3.9.	400
FIGURE 3.39 RATIO BETWEEN THE GREATEST LENGTH OF THE <i>FACIES ARTICULARIS PROXIMALIS</i> AND THE GREATEST BREADTH OF THE PROXIMAL END PLOTTED AGAINST THE DEPTH OF THE PROXIMAL END. SYMBOLS EXPLAINED IN FIG. 3.9.	400
FIGURE 3.40 RATIO BETWEEN THE BREADTH ACROSS THE CORONOID PROCESS AND THE DEPTH ACROSS THE <i>PROCESSUS ANCONAEUS</i> TO THE CAUDAL BORDER PLOTTED AGAINST THE BREADTH ACROSS THE CORONOID PROCESS AND THE SMALLEST DEPTH OF THE OLECRANON. SYMBOLS EXPLAINED IN FIG. 3.9.	401
FIGURE 3.41 METACARPAL. RATIO BETWEEN THE DIAMETER OF THE MEDIAL TROCHLEA AND THE WIDTH OF THE MEDIAL CONDYLE PLOTTED AGAINST THE RATIO BETWEEN THE DIAMETER OF THE <i>VERTICILLUS</i> AT THE MEDIAL CONDYLE AND THE DIAMETER OF THE MEDIAL TROCHLEA. SYMBOLS EXPLAINED IN FIG. 3.9.	402
FIGURE 3.42 METACARPAL. RATIO BETWEEN THE WIDTH OF THE LATERAL CONDYLE AND THE DIAMETER OF THE LATERAL TROCHLEA PLOTTED AGAINST THE RATIO BETWEEN THE DIAMETER OF THE <i>VERTICILLUS</i> THE LATERAL CONDYLE AND THE DIAMETER OF THE LATERAL CONDYLE. SYMBOLS EXPLAINED IN FIG. 3.9.	402
FIGURE 3.43 METACARPAL. RATIO BETWEEN THE GREATEST BREADTH OF THE DISTAL END WITH THE GREATEST LENGTH PLOTTED AGAINST THE RATIO BETWEEN THE SMALLEST WIDTH OF THE SHAFT AND THE GREATEST LENGTH. SYMBOLS EXPLAINED IN FIG. 3.9.....	403
FIGURE 3.44 METATARSAL. RATIO BETWEEN THE DIAMETER OF THE MEDIAL TROCHLEA AND THE WIDTH OF THE MEDIAL CONDYLE PLOTTED AGAINST THE RATIO BETWEEN THE DIAMETER OF THE <i>VERTICILLUS</i> AT THE MEDIAL CONDYLE AND THE DIAMETER OF THE MEDIAL TROCHLEA. SYMBOLS EXPLAINED IN FIG. 3.9.	403
FIGURE 3.45 METATARSAL. RATIO BETWEEN THE WIDTH OF THE LATERAL CONDYLE AND THE DIAMETER OF THE LATERAL TROCHLEA PLOTTED AGAINST THE RATIO BETWEEN THE DIAMETER OF THE <i>VERTICILLUS</i> ON THE LATERAL CONDYLE AND THE DIAMETER OF THE LATERAL CONDYLE. SYMBOLS EXPLAINED IN FIG. 3.9.....	404
FIGURE 3.46 METATARSAL. RATIO BETWEEN THE GREATEST BREADTH OF THE DISTAL END WITH THE GREATEST LENGTH PLOTTED AGAINST THE RATIO BETWEEN THE SMALLEST WIDTH OF THE SHAFT AND THE GREATEST LENGTH. SYMBOLS EXPLAINED IN FIG. 3.9.....	404
FIGURE 3.47 BREADTH OF THE DISTAL END PLOTTED AGAINST THE RATIO BETWEEN THE DEPTH OF THE MEDIAL (A) AND LATERAL (B) SIDE. SYMBOLS EXPLAINED IN FIG. 3.9.....	405
FIGURE 3.48 RATIO BETWEEN HEIGHT AT THE CENTRAL CONSTRICTION AND THE GREATEST DEPTH OF THE LATERAL HALF PLOTTED AGAINST A RATIO BETWEEN THE BREADTH OF THE DISTAL END AND THE GREATEST LENGTH OF THE LATERAL HALF. SYMBOLS EXPLAINED IN FIG. 3.9.	405
FIGURE 3.49 RATIO BETWEEN HEIGHT AT THE CENTRAL CONSTRICTION AND THE GREATEST DEPTH OF THE LATERAL HALF PLOTTED AGAINST THE RATIO BETWEEN THE BREADTH OF THE DISTAL END AND THE HEIGHT AT THE CENTRAL CONSTRICTION. SYMBOLS EXPLAINED IN FIG. 3.9.....	406

FIGURE 3.50 RATIO BETWEEN BREADTH OF THE DISTAL END AND THE GREATEST DEPTH OF THE LATERAL HALF PLOTTED AGAINST THE RATIO BETWEEN THE BREADTH OF THE DISTAL END AND THE GREATEST DEPTH OF THE LATERAL HALF. SYMBOLS EXPLAINED IN FIG. 3.9.	406
FIGURE 3.51 RATIO BETWEEN THE BREADTH OF THE DISTAL END AND THE HEIGHT AT THE CENTRAL CONSTRICTION AND THE RATIO BETWEEN HEIGHT AT THE CENTRAL CONSTRICTION AND THE GREATEST DEPTH OF THE LATERAL HALF. SYMBOLS EXPLAINED IN FIG. 3.9.	407
FIGURE 3.52 RATIO BETWEEN THE LENGTH AND THE BREADTH OF THE ARTICULAR FACET OF THE <i>OS MALLEOLARE</i> PLOTTED AGAINST THE RATIO BETWEEN THE LENGTH OF THE ARTICULAR FACET OF THE <i>OS MALLEOLARE</i> AND THE LENGTH TAKEN FROM THE ARTICULAR FACET OF THE <i>OS MALLEOLARE</i> TO THE END OF THE ARTICULATION-FREE PART OF THE PROCESS. SYMBOLS EXPLAINED IN FIG. 3.9.....	407
FIGURE 3.53 RATIO BETWEEN THE DEPTH OF THE <i>SUBSTENTACULUM TALI</i> AND THE LENGTH OF THE ARTICULAR FACET OF THE <i>OS MALLEOLARE</i> PLOTTED AGAINST THE RATIO BETWEEN THE LENGTH AND THE BREADTH OF THE ARTICULAR FACET OF THE <i>OS MALLEOLARE</i> . SYMBOLS EXPLAINED IN FIG. 3.9.	408
FIGURE 3.54 RATIO BETWEEN THE DEPTH OF THE <i>SUBSTENTACULUM TALI</i> AND THE LENGTH OF THE ARTICULAR FACET OF THE <i>OS MALLEOLARE</i> PLOTTED AGAINST THE RATIO BETWEEN THE LENGTH AND THE BREADTH OF THE ARTICULAR FACET OF THE <i>OS MALLEOLARE</i> . SYMBOLS EXPLAINED IN FIG. 3.9.	408
FIGURE 3.55 MAXIMUM DIAMETER TAKEN AT THE BASE PLOTTED AGAINST A RATIO BETWEEN THE LENGTH AND THE LENGTH OF THE OUTER CURVATURE OF THE HORNCORE. SYMBOLS EXPLAINED IN FIG. 3.9.	409
FIGURE 3.56 RATIO BETWEEN THE LENGTH AND THE LENGTH OF THE OUTER CURVATURE PLOTTED AGAINST THE RATIO BETWEEN THE MAXIMUM DIAMETER TAKEN AT THE BASE AND THE LENGTH OF THE OUTER CURVATURE OF THE HORNCORE. SYMBOLS EXPLAINED IN FIG. 3.9.	409
FIGURE 3.57 RATIO BETWEEN THE GREATEST LENGTH OF THE <i>PROCESSUS ARTICULARIS</i> AND THE LENGTH OF THE GLENOID CAVITY PLOTTED AGAINST THE RATIO BETWEEN THE GREATEST LENGTH OF THE <i>PROCESSUS ARTICULARIS</i> AND THE BREADTH OF THE GLENOID CAVITY. SYMBOLS EXPLAINED IN FIG. 3.9.	410
FIGURE 3.58 RATIO BETWEEN THE SHORTEST DISTANCE FROM THE BASE OF THE SPINE TO THE EDGE OF THE GLENOID CAVITY AND THE SMALLEST LENGTH OF THE <i>COLLUM SCAPULAE</i> PLOTTED AGAINST THE RATIO BETWEEN THE GREATEST LENGTH OF THE <i>PROCESSUS ARTICULARIS</i> AND THE BREADTH OF THE GLENOID CAVITY. SYMBOLS EXPLAINED IN FIG. 3.9.	410
FIGURE 3.59 RATIO BETWEEN THE MEDIO LATERAL WIDTH OF THE TROCHLEA AND ITS HEIGHT PLOTTED AGAINST THE MEDIO LATERAL WIDTH OF THE TROCHLEA AND THE DIAMETER OF THE TROCHLEAR CONSTRICTION. SYMBOLS EXPLAINED IN FIG. 3.9.	411
FIGURE 3.60 RATIO BETWEEN THE BREADTH OF THE <i>CAPITULUM</i> AND THE DISTAL WIDTH PLOTTED AGAINST THE RATIO BETWEEN THE BREADTH OF THE <i>CAPITULUM</i> AND THE MEDIO LATERAL WIDTH OF THE TROCHLEA. SYMBOLS EXPLAINED IN FIG. 3.9.	411
FIGURE 3.61 RATIO BETWEEN THE BREADTH OF THE <i>CAPITULUM</i> AND THE DIAMETER OF THE TROCHLEAR CONSTRICTION PLOTTED AGAINST THE RATIO BETWEEN THE BREADTH OF THE <i>CAPITULUM</i> AND THE MEDIO LATERAL WIDTH OF THE TROCHLEA. SYMBOLS EXPLAINED IN FIG. 3.9.	412

FIGURE 3.62 RATIO BETWEEN THE BREADTH OF THE <i>EPICONDYLE LATERALIS</i> AND THE MEDIO LATERAL WIDTH OF THE TROCHLEA PLOTTED AGAINST THE RATIO BETWEEN THE BREADTH OF THE <i>EPICONDYLE LATERALIS</i> AND THE WIDTH OF THE DISTAL END. SYMBOLS EXPLAINED IN FIG. 3.9.	412
FIGURE 3.63 RATIO BETWEEN THE GREATEST LENGTH OF THE <i>FACIES ARTICULARIS PROXIMALIS</i> AND THE GREATEST BREADTH OF THE PROXIMAL END PLOTTED AGAINST THE DEPTH OF THE PROXIMAL END. SYMBOLS EXPLAINED IN FIG. 3.9.	413
FIGURE 3.64 RATIO BETWEEN THE BREADTH ACROSS THE CORONOID PROCESS AND THE DEPTH ACROSS THE <i>PROCESSUS ANCONAEUS</i> TO THE CAUDAL BORDER PLOTTED AGAINST THE BREADTH ACROSS THE CORONOID PROCESS AND THE SMALLEST DEPTH OF THE OLECRANON. SYMBOLS EXPLAINED IN FIG. 3.9.	413
FIGURE 3.65 METACARPAL. RATIO BETWEEN THE DIAMETER OF THE MEDIAL TROCHLEA AND THE WIDTH OF THE MEDIAL CONDYLE PLOTTED AGAINST THE RATIO BETWEEN THE DIAMETER OF THE <i>VERTICILLUS</i> AT THE MEDIAL CONDYLE AND THE DIAMETER OF THE MEDIAL TROCHLEA. SYMBOLS EXPLAINED IN FIG. 3.9.	414
FIGURE 3.66 METACARPAL. RATIO BETWEEN THE WIDTH OF THE LATERAL CONDYLE AND THE DIAMETER OF THE LATERAL TROCHLEA PLOTTED AGAINST THE RATIO BETWEEN THE DIAMETER OF THE <i>VERTICILLUS</i> ON THE LATERAL CONDYLE AND THE DIAMETER OF THE LATERAL CONDYLE. SYMBOLS EXPLAINED IN FIG. 3.9.	414
FIGURE 3.67 METACARPAL. RATIO BETWEEN THE GREATEST BREADTH OF THE DISTAL END WITH THE GREATEST LENGTH PLOTTED AGAINST THE RATIO BETWEEN THE SMALLEST WIDTH OF THE SHAFT AND THE GREATEST LENGTH. SYMBOLS EXPLAINED IN FIG. 3.9.	415
FIGURE 3.68 BREADTH OF THE DISTAL END PLOTTED AGAINST THE RATIO BETWEEN THE DEPTH OF THE MEDIAL (A) AND LATERAL (B) SIDE. SYMBOLS EXPLAINED IN FIG. 3.9.	415
FIGURE 3.69 RATIO BETWEEN HEIGHT AT THE CENTRAL CONSTRICTION AND THE GREATEST DEPTH OF THE LATERAL HALF PLOTTED AGAINST A RATIO BETWEEN THE BREADTH OF THE DISTAL END AND THE GREATEST LENGTH OF THE LATERAL HALF. SYMBOLS EXPLAINED IN FIG. 3.9.	416
FIGURE 3.70 RATIO BETWEEN HEIGHT AT THE CENTRAL CONSTRICTION AND THE GREATEST DEPTH OF THE LATERAL HALF PLOTTED AGAINST THE RATIO BETWEEN THE BREADTH OF THE DISTAL END AND THE HEIGHT AT THE CENTRAL CONSTRICTION. SYMBOLS EXPLAINED IN FIG. 3.9.	416
FIGURE 3.71 RATIO BETWEEN BREADTH OF THE DISTAL END AND THE GREATEST DEPTH OF THE LATERAL HALF PLOTTED AGAINST THE RATIO BETWEEN THE BREADTH OF THE DISTAL END AND THE GREATEST DEPTH OF THE LATERAL HALF. SYMBOLS EXPLAINED IN FIG. 3.9.	417
FIGURE 3.72 RATIO BETWEEN THE BREADTH OF THE DISTAL END AND THE HEIGHT AT THE CENTRAL CONSTRICTION AND THE RATIO BETWEEN HEIGHT AT THE CENTRAL CONSTRICTION AND THE GREATEST DEPTH OF THE LATERAL HALF. SYMBOLS EXPLAINED IN FIG. 3.9.	417
FIGURE 3.73 RATIO BETWEEN THE LENGTH AND THE BREADTH OF THE ARTICULAR FACET OF THE <i>OS MALLEOLARE</i> PLOTTED AGAINST THE RATIO BETWEEN THE LENGTH OF THE ARTICULAR FACET OF THE <i>OS MALLEOLARE</i> AND THE LENGTH TAKEN FROM THE ARTICULAR FACET OF THE <i>OS MALLEOLARE</i> TO THE END OF THE ARTICULATION-FREE PART OF THE PROCESS. SYMBOLS EXPLAINED IN FIG. 3.9.	418
FIGURE 3.74 RATIO BETWEEN THE DEPTH OF THE <i>SUBSTENTACULUM TALI</i> AND THE LENGTH OF THE ARTICULAR FACET OF THE <i>OS MALLEOLARE</i> PLOTTED AGAINST THE RATIO BETWEEN THE LENGTH AND	

THE BREADTH OF THE ARTICULAR FACET OF THE <i>OS MALLEOLARE</i> . SYMBOLS EXPLAINED IN FIG. 3.9.	418
FIGURE 3.75 RATIO BETWEEN THE DEPTH OF THE <i>SUBSTENTACULUM TALII</i> AND THE LENGTH OF THE ARTICULAR FACET OF THE <i>OS MALLEOLARE</i> PLOTTED AGAINST THE RATIO BETWEEN THE LENGTH AND THE BREADTH OF THE ARTICULAR FACET OF THE <i>OS MALLEOLARE</i> . SYMBOLS EXPLAINED IN FIG. 3.9.	419
FIGURE 3.76 MAXIMUM DIAMETER TAKEN AT THE BASE PLOTTED AGAINST A RATIO BETWEEN THE LENGTH AND THE LENGTH OF THE OUTER CURVATURE OF THE HORNCORE. SYMBOLS EXPLAINED IN FIG. 3.9.	419
FIGURE 3.77 RATIO BETWEEN THE LENGTH AND THE LENGTH OF THE OUTER CURVATURE PLOTTED AGAINST THE RATIO BETWEEN THE MAXIMUM DIAMETER TAKEN AT THE BASE AND THE LENGTH OF THE OUTER CURVATURE OF THE HORNCORE. SYMBOLS EXPLAINED IN FIG. 3.9.	420
FIGURE 3.78 RATIO BETWEEN THE GREATEST LENGTH OF THE <i>PROCESSUS ARTICULARIS</i> AND THE LENGTH OF THE GLENOID CAVITY PLOTTED AGAINST THE RATIO BETWEEN THE GREATEST LENGTH OF THE <i>PROCESSUS ARTICULARIS</i> AND THE BREADTH OF THE GLENOID CAVITY. SYMBOLS EXPLAINED IN FIG. 3.9.	420
FIGURE 3.79 RATIO BETWEEN THE SHORTEST DISTANCE FROM THE BASE OF THE SPINE TO THE EDGE OF THE GLENOID CAVITY AND THE SMALLEST LENGTH OF THE <i>COLLUM SCAPULAE</i> PLOTTED AGAINST A RATIO BETWEEN THE GREATEST LENGTH OF THE <i>PROCESSUS ARTICULARIS</i> AND THE BREADTH OF THE GLENOID CAVITY PLOTTED AGAINST THE RATIO BETWEEN. SYMBOLS EXPLAINED IN FIG. 3.9.	421
FIGURE 3.80 RATIO BETWEEN THE MEDIO LATERAL WIDTH OF THE TROCHLEA AND ITS HEIGHT PLOTTED AGAINST THE MEDIO LATERAL WIDTH OF THE TROCHLEA AND THE DIAMETER OF THE TROCHLEAR CONSTRICTION. SYMBOLS EXPLAINED IN FIG. 3.9.	422
FIGURE 3.81 RATIO BETWEEN THE BREADTH OF THE <i>CAPITULUM</i> AND THE DISTAL WIDTH PLOTTED AGAINST THE RATIO BETWEEN THE BREADTH OF THE <i>CAPITULUM</i> AND THE MEDIO LATERAL WIDTH OF THE TROCHLEA. SYMBOLS EXPLAINED IN FIG. 3.9.	422
FIGURE 3.82 RATIO BETWEEN THE BREADTH OF THE <i>CAPITULUM</i> AND THE DIAMETER OF THE TROCHLEAR CONSTRICTION PLOTTED AGAINST THE RATIO BETWEEN THE BREADTH OF THE <i>CAPITULUM</i> AND THE MEDIO LATERAL WIDTH OF THE TROCHLEA. SYMBOLS EXPLAINED IN FIG. 3.9.	423
FIGURE 3.83 RATIO BETWEEN THE BREADTH OF THE <i>EPICONDYLE LATERALIS</i> AND THE MEDIO LATERAL WIDTH OF THE TROCHLEA PLOTTED AGAINST THE RATIO BETWEEN THE BREADTH OF THE <i>EPICONDYLE LATERALIS</i> AND THE WIDTH OF THE DISTAL END. SYMBOLS EXPLAINED IN FIG. 3.9.	423
FIGURE 3.84 RATIO BETWEEN THE GREATEST LENGTH OF THE <i>FACIES ARTICULARIS PROXIMALIS</i> AND THE GREATEST BREADTH OF THE PROXIMAL END PLOTTED AGAINST THE DEPTH OF THE PROXIMAL END. SYMBOLS EXPLAINED IN FIG. 3.9.	424
FIGURE 3.85 RATIO BETWEEN THE BREADTH ACROSS THE CORONOID PROCESS AND THE DEPTH ACROSS THE <i>PROCESSUS ANCONAEUS</i> TO THE CAUDAL BORDER PLOTTED AGAINST THE BREADTH ACROSS THE CORONOID PROCESS AND THE SMALLEST DEPTH OF THE OLECRANON. SYMBOLS EXPLAINED IN FIG. 3.9.	425
FIGURE 3.86 METACARPAL. RATIO BETWEEN THE DIAMETER OF THE MEDIAL TROCHLEA AND THE WIDTH OF THE MEDIAL CONDYLE PLOTTED AGAINST THE RATIO BETWEEN THE DIAMETER OF THE <i>VERTICILLUS</i> AT	

THE MEDIAL CONDYLE AND THE DIAMETER OF THE MEDIAL TROCHLEA. SYMBOLS EXPLAINED IN FIG. 3.9.	426
FIGURE 3.87 METACARPAL. RATIO BETWEEN THE WIDTH OF THE LATERAL CONDYLE AND THE DIAMETER OF THE LATERAL TROCHLEA PLOTTED AGAINST THE RATIO BETWEEN THE DIAMETER OF THE <i>VERTICILLUS</i> ON THE LATERAL CONDYLE AND THE DIAMETER OF THE LATERAL CONDYLE. SYMBOLS EXPLAINED IN FIG. 3.9.	426
FIGURE 3.88 METACARPAL. RATIO BETWEEN THE GREATEST BREADTH OF THE DISTAL END WITH THE GREATEST LENGTH PLOTTED AGAINST THE RATIO BETWEEN THE SMALLEST WIDTH OF THE SHAFT AND THE GREATEST LENGTH. SYMBOLS EXPLAINED IN FIG. 3.9.....	427
FIGURE 3.89 METATARSAL. RATIO BETWEEN THE DIAMETER OF THE MEDIAL TROCHLEA AND THE WIDTH OF THE MEDIAL CONDYLE PLOTTED AGAINST THE RATIO BETWEEN THE DIAMETER OF THE <i>VERTICILLUS</i> AT THE MEDIAL CONDYLE AND THE DIAMETER OF THE MEDIAL TROCHLEA. SYMBOLS EXPLAINED IN FIG. 3.9.	427
FIGURE 3.90 METATARSAL. RATIO BETWEEN THE WIDTH OF THE LATERAL CONDYLE AND THE DIAMETER OF THE LATERAL TROCHLEA PLOTTED AGAINST THE RATIO BETWEEN THE DIAMETER OF THE <i>VERTICILLUS</i> ON THE LATERAL CONDYLE AND THE DIAMETER OF THE LATERAL CONDYLE. SYMBOLS EXPLAINED IN FIG. 3.9.	428
FIGURE 3.91 METATARSAL. RATIO BETWEEN THE GREATEST BREADTH OF THE DISTAL END WITH THE GREATEST LENGTH PLOTTED AGAINST THE RATIO BETWEEN THE SMALLEST WIDTH OF THE SHAFT AND THE GREATEST LENGTH. SYMBOLS EXPLAINED IN FIG. 3.9.....	428
FIGURE 3.92 BREADTH OF THE DISTAL END PLOTTED AGAINST THE RATIO BETWEEN THE DEPTH OF THE MEDIAL (A) AND LATERAL (B) SIDE. SYMBOLS EXPLAINED IN FIG. 3.9.	429
FIGURE 3.93 RATIO BETWEEN HEIGHT AT THE CENTRAL CONSTRICTION AND THE GREATEST DEPTH OF THE LATERAL HALF PLOTTED AGAINST A RATIO BETWEEN THE BREADTH OF THE DISTAL END AND THE GREATEST LENGTH OF THE LATERAL HALF. SYMBOLS EXPLAINED IN FIG. 3.9.	430
FIGURE 3.94 RATIO BETWEEN HEIGHT AT THE CENTRAL CONSTRICTION AND THE GREATEST DEPTH OF THE LATERAL HALF PLOTTED AGAINST THE RATIO BETWEEN THE BREADTH OF THE DISTAL END AND THE HEIGHT AT THE CENTRAL CONSTRICTION. SYMBOLS EXPLAINED IN FIG. 3.9.	430
FIGURE 3.95 RATIO BETWEEN BREADTH OF THE DISTAL END AND THE GREATEST DEPTH OF THE LATERAL HALF PLOTTED AGAINST THE RATIO BETWEEN THE BREADTH OF THE DISTAL END AND THE GREATEST DEPTH OF THE LATERAL HALF. SYMBOLS EXPLAINED IN FIG. 3.9.	431
FIGURE 3.96 RATIO BETWEEN THE BREADTH OF THE DISTAL END AND THE HEIGHT AT THE CENTRAL CONSTRICTION AND THE RATIO BETWEEN HEIGHT AT THE CENTRAL CONSTRICTION AND THE GREATEST DEPTH OF THE LATERAL HALF. SYMBOLS EXPLAINED IN FIG. 3.9.	431
FIGURE 3.97 RATIO BETWEEN THE LENGTH AND THE BREADTH OF THE ARTICULAR FACET OF THE <i>OS MALLEOLARE</i> PLOTTED AGAINST THE RATIO BETWEEN THE LENGTH OF THE ARTICULAR FACET OF THE <i>OS MALLEOLARE</i> AND THE LENGTH TAKEN FROM THE ARTICULAR FACET OF THE <i>OS MALLEOLARE</i> TO THE END OF THE ARTICULATION-FREE PART OF THE PROCESS. SYMBOLS EXPLAINED IN FIG. 3.9.	432
FIGURE 3.98 RATIO BETWEEN THE DEPTH OF THE <i>SUBSTENTACULUM TALII</i> AND THE LENGTH OF THE ARTICULAR FACET OF THE <i>OS MALLEOLARE</i> PLOTTED AGAINST THE RATIO BETWEEN THE LENGTH AND	

THE BREADTH OF THE ARTICULAR FACET OF THE <i>OS MALLEOLARE</i> . SYMBOLS EXPLAINED IN FIG. 3.9.	432
FIGURE 3.99 RATIO BETWEEN THE DEPTH OF THE <i>SUBSTENTACULUM TALII</i> AND THE LENGTH OF THE ARTICULAR FACET OF THE <i>OS MALLEOLARE</i> PLOTTED AGAINST THE RATIO BETWEEN THE LENGTH AND THE BREADTH OF THE ARTICULAR FACET OF THE <i>OS MALLEOLARE</i> . SYMBOLS EXPLAINED IN FIG. 3.9.	433
FIGURE 3.100 MAXIMUM DIAMETER TAKEN AT THE BASE PLOTTED AGAINST A RATIO BETWEEN THE LENGTH AND THE LENGTH OF THE OUTER CURVATURE OF THE HORNCORE. SYMBOLS EXPLAINED IN FIG. 3.9.....	433
FIGURE 3.101 RATIO BETWEEN THE LENGTH AND THE LENGTH OF THE OUTER CURVATURE PLOTTED AGAINST THE RATIO BETWEEN THE MAXIMUM DIAMETER TAKEN AT THE BASE AND THE LENGTH OF THE OUTER CURVATURE OF THE HORNCORE. SYMBOLS EXPLAINED IN FIG. 3.9.	434
FIGURE 3.102 RATIO BETWEEN THE GREATEST LENGTH OF THE <i>PROCESSUS ARTICULARIS</i> AND THE LENGTH OF THE GLENOID CAVITY PLOTTED AGAINST THE RATIO BETWEEN THE GREATEST LENGTH OF THE <i>PROCESSUS ARTICULARIS</i> AND THE BREADTH OF THE GLENOID CAVITY. SYMBOLS EXPLAINED IN FIG. 3.9.....	434
FIGURE 3.103 RATIO BETWEEN THE SHORTEST DISTANCE FROM THE BASE OF THE SPINE TO THE EDGE OF THE GLENOID CAVITY AND THE SMALLEST LENGTH OF THE <i>COLLUM SCAPULAE</i> PLOTTED AGAINST A RATIO BETWEEN THE GREATEST LENGTH OF THE <i>PROCESSUS ARTICULARIS</i> AND THE BREADTH OF THE GLENOID CAVITY. SYMBOLS EXPLAINED IN FIG. 3.9.....	435
FIGURE 3.104 RATIO BETWEEN THE MEDIO LATERAL WIDTH OF THE TROCHLEA AND ITS HEIGHT PLOTTED AGAINST THE MEDIO LATERAL WIDTH OF THE TROCHLEA AND THE DIAMETER OF THE TROCHLEAR CONSTRICTION. SYMBOLS EXPLAINED IN FIG. 3.9.	435
FIGURE 3.105 RATIO BETWEEN THE BREADTH OF THE <i>CAPITULUM</i> AND THE DISTAL WIDTH PLOTTED AGAINST THE RATIO BETWEEN THE BREADTH OF THE <i>CAPITULUM</i> AND THE MEDIO LATERAL WIDTH OF THE TROCHLEA. SYMBOLS EXPLAINED IN FIG. 3.9.....	436
FIGURE 3.106 RATIO BETWEEN THE BREADTH OF THE <i>CAPITULUM</i> AND THE DIAMETER OF THE TROCHLEAR CONSTRICTION PLOTTED AGAINST THE RATIO BETWEEN THE BREADTH OF THE <i>CAPITULUM</i> AND THE MEDIO LATERAL WIDTH OF THE TROCHLEA. SYMBOLS EXPLAINED IN FIG. 3.9.	436
FIGURE 3.107 RATIO BETWEEN THE BREADTH OF THE <i>EPICONDYLE LATERALIS</i> AND THE MEDIO LATERAL WIDTH OF THE TROCHLEA PLOTTED AGAINST THE RATIO BETWEEN THE BREADTH OF THE <i>EPICONDYLE LATERALIS</i> AND THE WIDTH OF THE DISTAL END. SYMBOLS EXPLAINED IN FIG. 3.9.....	437
FIGURE 3.108 RATIO BETWEEN THE GREATEST LENGTH OF THE <i>FACIES ARTICULARIS PROXIMALIS</i> AND THE GREATEST BREADTH OF THE PROXIMAL END PLOTTED AGAINST THE DEPTH OF THE PROXIMAL END. SYMBOLS EXPLAINED IN FIG. 3.9.....	437
FIGURE 3.109 RATIO BETWEEN THE BREADTH ACROSS THE CORONOID PROCESS AND THE DEPTH ACROSS THE <i>PROCESSUS ANCONAEUS</i> TO THE CAUDAL BORDER PLOTTED AGAINST THE BREADTH ACROSS THE CORONOID PROCESS AND THE SMALLEST DEPTH OF THE OLECRANON. SYMBOLS EXPLAINED IN FIG. 3.9.....	438
FIGURE 3.110 METACARPAL. RATIO BETWEEN THE DIAMETER OF THE MEDIAL TROCHLEA AND THE WIDTH OF THE MEDIAL CONDYLE PLOTTED AGAINST THE RATIO BETWEEN THE DIAMETER OF THE <i>VERTICILLUS</i>	

AT THE MEDIAL CONDYLE AND THE DIAMETER OF THE MEDIAL TROCHLEA. SYMBOLS EXPLAINED IN FIG. 3.9.	439
FIGURE 3.111 METACARPAL. RATIO BETWEEN THE WIDTH OF THE LATERAL CONDYLE AND THE DIAMETER OF THE LATERAL TROCHLEA PLOTTED AGAINST THE RATIO BETWEEN THE DIAMETER OF THE <i>VERTICILLUS</i> ON THE LATERAL CONDYLE AND THE DIAMETER OF THE LATERAL CONDYLE. SYMBOLS EXPLAINED IN FIG. 3.9.	439
FIGURE 3.112 METACARPAL. RATIO BETWEEN THE GREATEST BREADTH OF THE DISTAL END WITH THE GREATEST LENGTH PLOTTED AGAINST THE RATIO BETWEEN THE SMALLEST WIDTH OF THE SHAFT AND THE GREATEST LENGTH. SYMBOLS EXPLAINED IN FIG. 3.9.	440
FIGURE 3.113 METATARSAL. RATIO BETWEEN THE DIAMETER OF THE MEDIAL TROCHLEA AND THE WIDTH OF THE MEDIAL CONDYLE PLOTTED AGAINST THE RATIO BETWEEN THE DIAMETER OF THE <i>VERTICILLUS</i> AT THE MEDIAL CONDYLE AND THE DIAMETER OF THE MEDIAL TROCHLEA. SYMBOLS EXPLAINED IN FIG. 3.9.	440
FIGURE 3.114 METATARSAL. RATIO BETWEEN THE WIDTH OF THE LATERAL CONDYLE AND THE DIAMETER OF THE LATERAL TROCHLEA PLOTTED AGAINST THE RATIO BETWEEN THE DIAMETER OF THE <i>VERTICILLUS</i> ON THE LATERAL CONDYLE AND THE DIAMETER OF THE LATERAL CONDYLE. SYMBOLS EXPLAINED IN FIG. 3.9.	441
FIGURE 3.115 METATARSAL. RATIO BETWEEN THE GREATEST BREADTH OF THE DISTAL END WITH THE GREATEST LENGTH PLOTTED AGAINST THE RATIO BETWEEN THE SMALLEST WIDTH OF THE SHAFT AND THE GREATEST LENGTH. SYMBOLS EXPLAINED IN FIG. 3.9.	441
FIGURE 3.116 BREADTH OF THE DISTAL END PLOTTED AGAINST THE RATIO BETWEEN THE DEPTH OF THE MEDIAL (A) AND LATERAL (B) SIDE. SYMBOLS EXPLAINED IN FIG. 3.9.	442
FIGURE 3.117 RATIO BETWEEN HEIGHT AT THE CENTRAL CONSTRICTION AND THE GREATEST DEPTH OF THE LATERAL HALF PLOTTED AGAINST A RATIO BETWEEN THE BREADTH OF THE DISTAL END AND THE GREATEST LENGTH OF THE LATERAL HALF. SYMBOLS EXPLAINED IN FIG. 3.9.	443
FIGURE 3.118 RATIO BETWEEN HEIGHT AT THE CENTRAL CONSTRICTION AND THE GREATEST DEPTH OF THE LATERAL HALF PLOTTED AGAINST THE RATIO BETWEEN THE BREADTH OF THE DISTAL END AND THE HEIGHT AT THE CENTRAL CONSTRICTION. SYMBOLS EXPLAINED IN FIG. 3.9.	443
FIGURE 3.119 RATIO BETWEEN BREADTH OF THE DISTAL END AND THE GREATEST DEPTH OF THE LATERAL HALF PLOTTED AGAINST THE RATIO BETWEEN THE BREADTH OF THE DISTAL END AND THE GREATEST DEPTH OF THE LATERAL HALF. SYMBOLS EXPLAINED IN FIG. 3.9.	444
FIGURE 3.120 RATIO BETWEEN THE BREADTH OF THE DISTAL END AND THE HEIGHT AT THE CENTRAL CONSTRICTION AND THE RATIO BETWEEN HEIGHT AT THE CENTRAL CONSTRICTION AND THE GREATEST DEPTH OF THE LATERAL HALF. SYMBOLS EXPLAINED IN FIG. 3.9.	444
FIGURE 3.121 RATIO BETWEEN THE LENGTH AND THE BREADTH OF THE ARTICULAR FACET OF THE <i>OS MALLEOLARE</i> PLOTTED AGAINST THE RATIO BETWEEN THE LENGTH OF THE ARTICULAR FACET OF THE <i>OS MALLEOLARE</i> AND THE LENGTH TAKEN FROM THE ARTICULAR FACET OF THE <i>OS MALLEOLARE</i> TO THE END OF THE ARTICULATION-FREE PART OF THE PROCESS. SYMBOLS EXPLAINED IN FIG. 3.9.	445
FIGURE 3.122 RATIO BETWEEN THE DEPTH OF THE <i>SUBSTENTACULUM TALII</i> AND THE LENGTH OF THE ARTICULAR FACET OF THE <i>OS MALLEOLARE</i> PLOTTED AGAINST THE RATIO BETWEEN THE LENGTH AND	

THE BREADTH OF THE ARTICULAR FACET OF THE <i>OS MALLEOLARE</i> . SYMBOLS EXPLAINED IN FIG. 3.9.	445
FIGURE 3.123 RATIO BETWEEN THE DEPTH OF THE <i>SUBSTENTACULUM TALI</i> AND THE LENGTH OF THE ARTICULAR FACET OF THE <i>OS MALLEOLARE</i> PLOTTED AGAINST THE RATIO BETWEEN THE LENGTH AND THE BREADTH OF THE ARTICULAR FACET OF THE <i>OS MALLEOLARE</i> . SYMBOLS EXPLAINED IN FIG. 3.9.	446
FIGURE 3.124 DIAGRAM OF THE INDIVIDUAL DISCRIMINANT SCORES ATTRIBUTED TO THE ARCHAEOLOGICAL MATERIAL BY DA FOR THE HORNCORE.	505
FIGURE 3.125 DIAGRAM OF THE INDIVIDUAL DISCRIMINANT SCORES ATTRIBUTED TO THE ARCHAEOLOGICAL MATERIAL BY DA FOR THE HORNCORE WHEN VARIABLES E AND F WERE EXCLUDED.	506
FIGURE 3.126 DIAGRAM OF THE INDIVIDUAL DISCRIMINANT SCORES ATTRIBUTED TO THE ARCHAEOLOGICAL MATERIAL BY DA FOR THE SCAPULA. BLUE ARROWS INDICATE THE POSITION OF THE TWO ARCHAEOLOGICAL GOATS.	507
FIGURE 3.127 DIAGRAM OF THE INDIVIDUAL DISCRIMINANT SCORES ATTRIBUTED TO THE ARCHAEOLOGICAL MATERIAL BY DA FOR THE HUMERUS.	509
FIGURE 3.128 DIAGRAM OF THE INDIVIDUAL DISCRIMINANT SCORES ATTRIBUTED TO THE ARCHAEOLOGICAL MATERIAL BY DA FOR THE RADIUS.	511
FIGURE 3.129 DIAGRAM OF THE INDIVIDUAL DISCRIMINANT SCORES ATTRIBUTED TO THE ARCHAEOLOGICAL MATERIAL BY DA FOR THE RADIUS WHEN VARIABLES GL AND SD WERE EXCLUDED.	512
FIGURE 3.130 DIAGRAM OF THE INDIVIDUAL DISCRIMINANT SCORES ATTRIBUTED TO THE ARCHAEOLOGICAL MATERIAL BY DA FOR THE ULNA.	514
FIGURE 3.131 DIAGRAM OF THE INDIVIDUAL DISCRIMINANT SCORES ATTRIBUTED TO THE ARCHAEOLOGICAL MATERIAL BY DA FOR THE ULNA WHEN VARIABLES B AND L WERE EXCLUDED.	515
FIGURE 3.132 DIAGRAM OF THE INDIVIDUAL DISCRIMINANT SCORES ATTRIBUTED TO THE ARCHAEOLOGICAL MATERIAL BY DA FOR THE METACARPAL.	517
FIGURE 3.133 DIAGRAM OF THE INDIVIDUAL DISCRIMINANT SCORES ATTRIBUTED TO THE ARCHAEOLOGICAL MATERIAL BY DA FOR THE METACARPAL WHEN VARIABLES GL AND SD WERE EXCLUDED.	518
FIGURE 3.134 DIAGRAM OF THE INDIVIDUAL DISCRIMINANT SCORES ATTRIBUTED TO ARCHAEOLOGICAL MATERIAL BY DA FOR THE METATARSAL.	520
FIGURE 3.135 DIAGRAM OF THE INDIVIDUAL DISCRIMINANT SCORES ATTRIBUTED TO THE ARCHAEOLOGICAL MATERIAL BY DA FOR THE METATARSAL WHEN VARIABLES GL AND SD WERE EXCLUDED.	520
FIGURE 3.136 DIAGRAM OF THE INDIVIDUAL DISCRIMINANT SCORES ATTRIBUTED TO THE ARCHAEOLOGICAL MATERIAL BY DA FOR THE TIBIA.	523
FIGURE 3.137 DIAGRAM OF THE INDIVIDUAL DISCRIMINANT SCORES ATTRIBUTED TO THE ARCHAEOLOGICAL MATERIAL BY DA FOR THE TIBIA WHEN VARIABLE GL WAS EXCLUDED.	524

FIGURE 3.138 DIAGRAM OF THE INDIVIDUAL DISCRIMINANT SCORES ATTRIBUTED TO THE ARCHAEOLOGICAL MATERIAL BY DA FOR THE TIBIA WHEN VARIABLES GL AND SD WERE EXCLUDED.	524
FIGURE 3.139 DIAGRAM OF THE INDIVIDUAL DISCRIMINANT SCORES ATTRIBUTED TO THE ARCHAEOLOGICAL MATERIAL BY DA FOR THE ASTRAGALUS.	526
FIGURE 3.140 DIAGRAM OF THE INDIVIDUAL DISCRIMINANT SCORES ATTRIBUTED TO THE ARCHAEOLOGICAL MATERIAL BY DA FOR THE CALCANEUM.	528
FIGURE 3.141 DIAGRAM OF THE INDIVIDUAL DISCRIMINANT SCORES ATTRIBUTED TO THE ARCHAEOLOGICAL MATERIAL BY DA FOR THE CALCANEUM WHEN VARIABLES GL AND SB WERE EXCLUDED.	528
FIGURE 3.142 GOAT HORNCORES FROM KING’S LYNN. ON THE LEFT: CUT AND CHOP MARKS AT THE BASE OF THE HORNCORE, EVIDENCE FOR THE REMOVAL OF THE KERATINOUS SHEATH WHICH COVERED THE BONY CORE. ON THE RIGHT: EXAMPLE OF GOAT HORNCORE WITH TIP SAWN.	536
FIGURE 3.143 LOCATION MAP OF THE SITE IN RELATION TO MODERN STREETS (IMAGE REPRINTED FROM PERRING, D. <i>EARLY MEDIEVAL OCCUPATION AT FLAXENGATE LINCOLN</i> . THE ARCHAEOLOGY OF LINCOLN, IX-1. LONDON: COUNCIL FOR BRITISH ARCHAEOLOGY FOR THE LINCOLN ARCHAEOLOGICAL TRUST, COPYRIGHT 1981, WITH PERMISSION FROM CITY OF LINCOLN COUNCIL).	538
FIGURE 3.144 NUMBER OF FRAGMENTS BY PHASES IDENTIFIED BY O’CONNOR (IMAGE REPRINTED FROM O’CONNOR, T. <i>ANIMAL BONES FROM FLAXENGATE, LINCOLN C. 870-1500</i> . THE ARCHAEOLOGY OF LINCOLN, XVIII-1. LONDON: COUNCIL FOR BRITISH ARCHAEOLOGY FOR THE LINCOLN ARCHAEOLOGICAL TRUST, COPYRIGHT 1982, WITH PERMISSION FROM TERRY O’CONNOR).	540
FIGURE 3.145 MAXIMUM DIAMETER TAKEN AT THE BASE PLOTTED AGAINST A RATIO BETWEEN THE LENGTH AND THE LENGTH OF THE OUTER CURVATURE OF THE HORNCORE. THE MODERN DATA ARE REPRESENTED BY THE SQUARE EMPTY SYMBOL, BLUE FOR MODERN GOATS, RED FOR MODERN SHEEP, WHILE THE ARCHAEOLOGICAL MATERIAL IS REPRESENTED BY THE FILLED DOT SYMBOL: BLUE FOR GOATS, RED FOR SHEEP AND GREEN FOR SHEEP/GOAT.....	545
FIGURE 3.146 MAXIMUM DIAMETER TAKEN AT THE MIDDLE PLOTTED AGAINST A RATIO BETWEEN THE LENGTH AND THE LENGTH OF THE OUTER CURVATURE OF THE HORNCORE. SYMBOLS EXPLAINED IN FIG. 3.145.	546
FIGURE 3.147 RATIO BETWEEN THE LENGTH AND THE LENGTH OF THE OUTER CURVATURE PLOTTED AGAINST THE RATIO BETWEEN THE MAXIMUM DIAMETER TAKEN AT THE BASE AND THE LENGTH OF THE OUTER CURVATURE OF THE HORNCORE. SYMBOLS EXPLAINED IN FIG. 3.145.....	546
FIGURE 3.148 RATIO BETWEEN THE LENGTH AND THE LENGTH OF THE OUTER CURVATURE PLOTTED AGAINST THE RATIO BETWEEN THE MAXIMUM DIAMETER TAKEN AT THE MIDDLE AND THE LENGTH OF THE OUTER CURVATURE OF THE HORNCORE. SYMBOLS EXPLAINED IN FIG. 3.145.....	547
FIGURE 3.149 RATIO BETWEEN THE GREATEST LENGTH OF THE <i>PROCESSUS ARTICULARIS</i> AND THE LENGTH OF THE GLENOID CAVITY PLOTTED AGAINST THE RATIO BETWEEN THE GREATEST LENGTH OF THE <i>PROCESSUS ARTICULARIS</i> AND THE BREADTH OF THE GLENOID CAVITY. SYMBOLS EXPLAINED IN FIG. 3.145.	547

FIGURE 3.150 RATIO THE SHORTEST DISTANCE FROM THE BASE OF THE SPINE TO THE EDGE OF THE GLENOID CAVITY AND THE SMALLEST LENGTH OF THE <i>COLLUM SCAPULAE</i> PLOTTED AGAINST A RATION BETWEEN THE GREATEST LENGTH OF THE <i>PROCESSUS ARTICULARIS</i> AND THE BREADTH OF THE GLENOID CAVITY. SYMBOLS EXPLAINED IN FIG. 3.145.....	548
FIGURE 3.151 RATIO BETWEEN THE MEDIO LATERAL WIDTH OF THE TROCHLEA AND ITS HEIGHT PLOTTED AGAINST THE MEDIO LATERAL WIDTH OF THE TROCHLEA AND THE DIAMETER OF THE TROCHLEAR CONSTRICTION. SYMBOLS EXPLAINED IN FIG. 3.145.....	549
FIGURE 3.152 RATIO BETWEEN THE BREADTH OF THE <i>CAPITULUM</i> AND THE DISTAL WIDTH PLOTTED AGAINST THE RATIO BETWEEN THE BREADTH OF THE <i>CAPITULUM</i> AND THE MEDIO LATERAL WIDTH OF THE TROCHLEA. SYMBOLS EXPLAINED IN FIG. 3.145.	549
FIGURE 3.153 RATIO BETWEEN THE BREADTH OF THE <i>CAPITULUM</i> AND THE DIAMETER OF THE TROCHLEA CONSTRICTION PLOTTED AGAINST THE RATIO BETWEEN THE BREADTH OF THE <i>CAPITULUM</i> AND THE MEDIO LATERAL WIDTH OF THE TROCHLEA. SYMBOLS EXPLAINED IN FIG. 3.145.	550
FIGURE 3.154 RATIO BETWEEN THE BREADTH OF THE EPICONDYLE <i>LATERALIS</i> AND THE MEDIO LATERAL WIDTH OF THE TROCHLEA PLOTTED AGAINST THE RATIO BETWEEN THE BREADTH OF THE EPICONDYLE <i>LATERALIS</i> AND THE WIDTH OF THE DISTAL END. SYMBOLS EXPLAINED IN FIG. 3.145.	550
FIGURE 3.155 RATIO BETWEEN THE GREATEST LENGTH OF THE <i>FACIES ARTICULARIS PROXIMALIS</i> AND THE GREATEST BREADTH OF THE PROXIMAL END PLOTTED AGAINST THE DEPTH OF THE PROXIMAL END. SYMBOLS EXPLAINED IN FIG. 3.145.....	551
FIGURE 3.156 RATIO BETWEEN THE BREADTH ACROSS THE CORONOID PROCESS AND THE DEPTH ACROSS THE <i>PROCESSUS ANCONAEUS</i> TO THE CAUDAL BORDER PLOTTED AGAINST THE BREADTH ACROSS THE CORONOID PROCESS AND THE SMALLEST DEPTH OF THE OLECRANON. SYMBOLS EXPLAINED IN FIG. 3.145.....	551
FIGURE 3.157 METACARPAL. RATIO BETWEEN THE DIAMETER OF THE MEDIAL TROCHLEA AND THE WIDTH OF THE MEDIAL CONDYLE PLOTTED AGAINST THE RATIO BETWEEN THE DIAMETER OF THE <i>VERTICILLUS</i> AT THE MEDIAL CONDYLE AND THE DIAMETER OF THE MEDIAL TROCHLEA. SYMBOLS EXPLAINED IN FIG. 3.145.....	552
FIGURE 3.158 METACARPAL. RATIO BETWEEN THE WIDTH OF THE LATERAL CONDYLE AND THE DIAMETER OF THE LATERAL TROCHLEA PLOTTED AGAINST THE RATIO BETWEEN THE DIAMETER OF THE LATERAL CONDYLE AND THE DIAMETER OF THE <i>VERTICILLUS</i> ON THE LATERAL CONDYLE. SYMBOLS EXPLAINED IN FIG. 3.145.	553
FIGURE 3.159 METACARPAL. RATIO BETWEEN THE GREATEST BREADTH OF THE DISTAL END WITH THE GREATEST LENGTH PLOTTED AGAINST THE RATIO BETWEEN THE SMALLEST WIDTH OF THE SHAFT AND THE GREATEST LENGTH. SYMBOLS EXPLAINED IN FIG. 3.145.	553
FIGURE 3.160 METATARSAL. RATIO BETWEEN THE DIAMETER OF THE MEDIAL TROCHLEA AND THE WIDTH OF THE MEDIAL CONDYLE PLOTTED AGAINST THE RATIO BETWEEN THE DIAMETER OF THE <i>VERTICILLUS</i> AT THE MEDIAL CONDYLE AND THE DIAMETER OF THE MEDIAL TROCHLEA. SYMBOLS EXPLAINED IN FIG. 3.145.....	554
FIGURE 3.161 METATARSAL. RATIO BETWEEN THE WIDTH OF THE LATERAL CONDYLE AND THE DIAMETER OF THE LATERAL TROCHLEA PLOTTED AGAINST THE RATIO BETWEEN THE DIAMETER OF THE	

VERTICILLUS ON THE LATERAL CONDYLE AND THE DIAMETER OF THE LATERAL CONDYLE. SYMBOLS EXPLAINED IN FIG. 3.145.	554
FIGURE 3.162 METATARSAL. RATIO BETWEEN THE GREATEST BREADTH OF THE DISTAL END WITH THE GREATEST LENGTH PLOTTED AGAINST THE RATIO BETWEEN THE SMALLEST WIDTH OF THE SHAFT AND THE GREATEST LENGTH. SYMBOLS EXPLAINED IN FIG. 3.145.	555
FIGURE 3.163 BREADTH OF THE DISTAL END PLOTTED AGAINST THE RATIO BETWEEN THE DEPTH OF THE MEDIAL (A) AND LATERAL (B) SIDE. SYMBOLS EXPLAINED IN FIG. 3.145.	555
FIGURE 3.164 RATIO BETWEEN HEIGHT AT THE CENTRAL CONSTRICTION AND THE GREATEST DEPTH OF THE LATERAL HALF PLOTTED AGAINST A RATIO BETWEEN THE BREADTH OF THE DISTAL END AND THE GREATEST LENGTH OF THE LATERAL HALF. SYMBOLS EXPLAINED IN FIG. 3.145.	556
FIGURE 3.165 RATIO BETWEEN HEIGHT AT THE CENTRAL CONSTRICTION AND THE GREATEST DEPTH OF THE LATERAL HALF PLOTTED AGAINST THE RATIO BETWEEN THE BREADTH OF THE DISTAL END AND THE HEIGHT AT THE CENTRAL CONSTRICTION. SYMBOLS EXPLAINED IN FIG. 3.145.	556
FIGURE 3.166 RATIO BETWEEN BREADTH OF THE DISTAL END AND THE GREATEST DEPTH OF THE LATERAL HALF PLOTTED AGAINST THE RATIO BETWEEN THE BREADTH OF THE DISTAL END AND THE GREATEST DEPTH OF THE LATERAL HALF. SYMBOLS EXPLAINED IN FIG. 3.145.	557
FIGURE 3.167 RATIO BETWEEN THE BREADTH OF THE DISTAL END AND THE HEIGHT AT THE CENTRAL CONSTRICTION AND THE RATIO BETWEEN HEIGHT AT THE CENTRAL CONSTRICTION AND THE GREATEST DEPTH OF THE LATERAL HALF. SYMBOLS EXPLAINED IN FIG. 3.145.	557
FIGURE 3.168 RATIO BETWEEN THE LENGTH AND THE BREADTH OF THE ARTICULAR FACET OF THE OS MALLEOLARE PLOTTED AGAINST THE RATIO BETWEEN THE LENGTH OF THE ARTICULAR FACET OF THE OS MALLEOLARE AND THE LENGTH TAKEN FROM THE ARTICULAR FACET OF THE OS MALLEOLARE TO THE END OF THE ARTICULATION-FREE PART OF THE PROCESS. SYMBOLS EXPLAINED IN FIG. 3.145.	558
FIGURE 3.169 RATIO BETWEEN THE DEPTH OF THE SUBSTENTACULUM TALII AND THE LENGTH OF THE ARTICULAR FACET OF THE OS MALLEOLARE PLOTTED AGAINST THE RATIO BETWEEN THE LENGTH AND THE BREADTH OF THE ARTICULAR FACET OF THE OS MALLEOLARE. SYMBOLS EXPLAINED IN FIG. 3.145.	558
FIGURE 3.170 RATIO BETWEEN THE DEPTH OF THE SUBSTENTACULUM TALII AND THE LENGTH OF THE ARTICULAR FACET OF THE OS MALLEOLARE PLOTTED AGAINST THE RATIO BETWEEN THE LENGTH AND THE BREADTH OF THE ARTICULAR FACET OF THE OS MALLEOLARE. SYMBOLS EXPLAINED IN FIG. 3.145.	559
FIGURE 3.171 GREATEST DIAGONAL LENGTH OF THE SOLE PLOTTED AGAINST A RATIO BETWEEN THE GREATEST DIAGONAL LENGTH OF THE SOLE AND THE MIDDLE BREADTH OF THE SOLE. SYMBOLS EXPLAINED IN FIG. 3.145.	559
FIGURE 3.172 RATIO BETWEEN THE GREATEST LENGTH OF THE PROCESSUS ARTICULARIS AND THE LENGTH OF THE GLENOID CAVITY PLOTTED AGAINST THE RATIO BETWEEN THE GREATEST LENGTH OF THE PROCESSUS ARTICULARIS AND THE BREADTH OF THE GLENOID CAVITY. SYMBOLS EXPLAINED IN FIG. 3.145.	560
FIGURE 3.173 RATIO BETWEEN THE SHORTEST DISTANCE FROM THE BASE OF THE SPINE TO THE EDGE OF THE GLENOID CAVITY AND THE MINIMUM LENGTH OF THE COLLUM SCAPULAE PLOTTED AGAINST A	

RATIO THE GREATEST LENGTH OF THE <i>PROCESSUS ARTICULARIS</i> AND THE BREADTH OF THE GLENOID CAVITY. SYMBOLS EXPLAINED IN FIG. 3.145.....	560
FIGURE 3.174 RATIO BETWEEN THE MEDIO LATERAL WIDTH OF THE TROCHLEA AND ITS HEIGHT PLOTTED AGAINST THE MEDIO LATERAL WIDTH OF THE TROCHLEA AND THE DIAMETER OF THE TROCHLEAR CONSTRICTION. SYMBOLS EXPLAINED IN FIG. 3.145.....	561
FIGURE 3.175 RATIO BETWEEN THE BREADTH OF THE <i>CAPITULUM</i> AND THE DISTAL WIDTH PLOTTED AGAINST THE RATIO BETWEEN THE BREADTH OF THE <i>CAPITULUM</i> AND THE MEDIO LATERAL WIDTH OF THE TROCHLEA. SYMBOLS EXPLAINED IN FIG. 3.145.....	561
FIGURE 3.176 RATIO BETWEEN THE BREADTH OF THE <i>CAPITULUM</i> AND THE DIAMETER OF THE TROCHLEA CONSTRICTION PLOTTED AGAINST THE RATIO BETWEEN THE BREADTH OF THE <i>CAPITULUM</i> AND THE MEDIO LATERAL WIDTH OF THE TROCHLEA. SYMBOLS EXPLAINED IN FIG. 3.145.....	562
FIGURE 3.177 RATIO BETWEEN THE BREADTH OF THE EPICONDYLE <i>LATERALIS</i> AND THE MEDIO LATERAL WIDTH OF THE TROCHLEA PLOTTED AGAINST THE RATIO BETWEEN THE BREADTH OF THE EPICONDYLE <i>LATERALIS</i> AND THE WIDTH OF THE DISTAL END. SYMBOLS EXPLAINED IN FIG. 3.145.....	562
FIGURE 3.178 RATIO BETWEEN THE GREATEST LENGTH OF THE <i>FACIES ARTICULARIS PROXIMALIS</i> AND THE GREATEST BREADTH OF THE PROXIMAL END PLOTTED AGAINST THE DEPTH OF THE PROXIMAL END. SYMBOLS EXPLAINED IN FIG. 3.145.....	563
FIGURE 3.179 RATIO BETWEEN THE BREADTH ACROSS THE CORONOID PROCESS AND THE DEPTH ACROSS THE <i>PROCESSUS ANCONAEUS</i> TO THE CAUDAL BORDER PLOTTED AGAINST THE BREADTH ACROSS THE CORONOID PROCESS AND THE SMALLEST DEPTH OF THE OLECRANON. SYMBOLS EXPLAINED IN FIG. 3.145.....	563
FIGURE 3.180 METACARPAL. RATIO BETWEEN THE DIAMETER OF THE MEDIAL TROCHLEA AND THE WIDTH OF THE MEDIAL CONDYLE PLOTTED AGAINST THE RATIO BETWEEN THE DIAMETER OF THE <i>VERTICILLUS</i> AT THE MEDIAL CONDYLE AND THE DIAMETER OF THE MEDIAL TROCHLEA. SYMBOLS EXPLAINED IN FIG. 3.145.....	564
FIGURE 3.181 METACARPAL. RATIO BETWEEN THE WIDTH OF THE LATERAL CONDYLE AND THE DIAMETER OF THE LATERAL TROCHLEA PLOTTED AGAINST THE RATIO BETWEEN THE DIAMETER OF THE LATERAL CONDYLE AND THE DIAMETER OF THE <i>VERTICILLUS</i> ON THE LATERAL CONDYLE. SYMBOLS EXPLAINED IN FIG. 3.145.....	564
FIGURE 3.182 METACARPAL. RATIO BETWEEN THE GREATEST BREADTH OF THE DISTAL END WITH THE GREATEST LENGTH PLOTTED AGAINST THE RATIO BETWEEN THE SMALLEST WIDTH OF THE SHAFT AND THE GREATEST LENGTH. SYMBOLS EXPLAINED IN FIG. 3.145.....	565
FIGURE 3.183 METATARSAL. RATIO BETWEEN THE DIAMETER OF THE MEDIAL TROCHLEA AND THE WIDTH OF THE MEDIAL CONDYLE PLOTTED AGAINST THE RATIO BETWEEN THE DIAMETER OF THE <i>VERTICILLUS</i> AT THE MEDIAL CONDYLE AND THE DIAMETER OF THE MEDIAL TROCHLEA. SYMBOLS EXPLAINED IN FIG. 3.145.....	565
FIGURE 3.184 METATARSAL. RATIO BETWEEN THE WIDTH OF THE LATERAL CONDYLE AND THE DIAMETER OF THE LATERAL TROCHLEA PLOTTED AGAINST THE RATIO BETWEEN THE DIAMETER OF THE <i>VERTICILLUS</i> ON THE LATERAL CONDYLE AND THE DIAMETER OF THE LATERAL CONDYLE. SYMBOLS EXPLAINED IN FIG. 3.145.....	566

FIGURE 3.185 METATARSAL. RATIO BETWEEN THE GREATEST BREADTH OF THE DISTAL END WITH THE GREATEST LENGTH PLOTTED AGAINST THE RATIO BETWEEN THE SMALLEST WIDTH OF THE SHAFT AND THE GREATEST LENGTH. SYMBOLS EXPLAINED IN FIG. 3.145.....	566
FIGURE 3.186 BREADTH OF THE DISTAL END PLOTTED AGAINST THE RATIO BETWEEN THE DEPTH OF THE MEDIAL (A) AND LATERAL (B) SIDE. SYMBOLS EXPLAINED IN FIG. 3.145.....	567
FIGURE 3.187 RATIO BETWEEN HEIGHT AT THE CENTRAL CONSTRICTION AND THE GREATEST DEPTH OF THE LATERAL HALF PLOTTED AGAINST THE RATIO BETWEEN THE BREADTH OF THE DISTAL END AND THE HEIGHT AT THE CENTRAL CONSTRICTION. SYMBOLS EXPLAINED IN FIG. 3.145.....	567
FIGURE 3.188 RATIO BETWEEN THE LENGTH AND THE BREADTH OF THE ARTICULAR FACET OF THE <i>OS MALLEOLARE</i> PLOTTED AGAINST THE RATIO BETWEEN THE LENGTH OF THE ARTICULAR FACET OF THE <i>OS MALLEOLARE</i> AND THE LENGTH TAKEN FROM THE ARTICULAR FACET OF THE <i>OS MALLEOLARE</i> TO THE END OF THE ARTICULATION-FREE PART OF THE PROCESS. SYMBOLS EXPLAINED IN FIG. 3.145.	568
FIGURE 3.189 RATIO BETWEEN THE DEPTH OF THE <i>SUBSTENTACULUM TALII</i> AND THE LENGTH OF THE ARTICULAR FACET OF THE <i>OS MALLEOLARE</i> PLOTTED AGAINST THE RATIO BETWEEN THE LENGTH AND THE BREADTH OF THE ARTICULAR FACET OF THE <i>OS MALLEOLARE</i> . SYMBOLS EXPLAINED IN FIG. 3.145.	568
FIGURE 3.190 RATIO BETWEEN THE DEPTH OF THE <i>SUBSTENTACULUM TALII</i> AND THE LENGTH OF THE ARTICULAR FACET OF THE <i>OS MALLEOLARE</i> PLOTTED AGAINST THE RATIO BETWEEN THE LENGTH AND THE BREADTH OF THE ARTICULAR FACET OF THE <i>OS MALLEOLARE</i> . SYMBOLS EXPLAINED IN FIG. 3.145.	569
FIGURE 3.191 RATIO BETWEEN THE GREATEST LENGTH OF THE <i>PROCESSUS ARTICULARIS</i> AND THE LENGTH OF THE GLENOID CAVITY PLOTTED AGAINST THE RATIO BETWEEN THE GREATEST LENGTH OF THE <i>PROCESSUS ARTICULARIS</i> AND THE BREADTH OF THE GLENOID CAVITY. SYMBOLS EXPLAINED IN FIG. 3.145.	569
FIGURE 3.192 RATIO BETWEEN THE SHORTEST DISTANCE FROM THE BASE OF THE SPINE TO THE EDGE OF THE GLENOID CAVITY AND THE SMALLEST LENGTH OF THE <i>COLLUM SCAPULAE</i> PLOTTED AGAINST THE GREATEST LENGTH OF THE <i>PROCESSUS ARTICULARIS</i> AND THE BREADTH OF THE GLENOID CAVITY. SYMBOLS EXPLAINED IN FIG. 3.145.	570
FIGURE 3.193 RATIO BETWEEN THE MEDIO LATERAL WIDTH OF THE TROCHLEA AND ITS HEIGHT PLOTTED AGAINST THE MEDIO LATERAL WIDTH OF THE TROCHLEA AND THE DIAMETER OF THE TROCHLEAR CONSTRICTION. SYMBOLS EXPLAINED IN FIG. 3.145.	570
FIGURE 3.194 RATIO BETWEEN THE BREADTH OF THE <i>CAPITULUM</i> AND THE DISTAL WIDTH PLOTTED AGAINST THE RATIO BETWEEN THE BREADTH OF THE <i>CAPITULUM</i> AND THE MEDIO LATERAL WIDTH OF THE TROCHLEA. SYMBOLS EXPLAINED IN FIG. 3.145.	571
FIGURE 3.195 RATIO BETWEEN THE BREADTH OF THE <i>CAPITULUM</i> AND THE DIAMETER OF THE TROCHLEAR CONSTRICTION PLOTTED AGAINST THE RATIO BETWEEN THE BREADTH OF THE <i>CAPITULUM</i> AND THE MEDIO LATERAL WIDTH OF THE TROCHLEA. SYMBOLS EXPLAINED IN FIG. 3.145.....	571
FIGURE 3.196 RATIO BETWEEN THE BREADTH OF THE EPICONDYLE <i>LATERALIS</i> AND THE MEDIO LATERAL WIDTH OF THE TROCHLEA PLOTTED AGAINST THE RATIO BETWEEN THE BREADTH OF THE EPICONDYLE <i>LATERALIS</i> AND THE WIDTH OF THE DISTAL END. SYMBOLS EXPLAINED IN FIG. 3.145.	572

FIGURE 3.197 RATIO BETWEEN THE GREATEST LENGTH OF THE <i>FACIES ARTICULARIS PROXIMALIS</i> AND THE GREATEST BREADTH OF THE PROXIMAL END PLOTTED AGAINST THE DEPTH OF THE PROXIMAL END. SYMBOLS EXPLAINED IN FIG. 3.145.....	572
FIGURE 3.198 RATIO BETWEEN THE BREADTH ACROSS THE CORONOID PROCESS AND THE DEPTH ACROSS THE <i>PROCESSUS ANCONAEUS</i> TO THE CAUDAL BORDER PLOTTED AGAINST THE BREADTH ACROSS THE CORONOID PROCESS AND THE SMALLEST DEPTH OF THE OLECRANON. SYMBOLS EXPLAINED IN FIG. 3.145.....	573
FIGURE 3.199 METACARPAL. RATIO BETWEEN THE DIAMETER OF THE MEDIAL TROCHLEA AND THE WIDTH OF THE MEDIAL CONDYLE PLOTTED AGAINST THE RATIO BETWEEN THE DIAMETER OF THE <i>VERTICILLUS</i> AT THE MEDIAL CONDYLE AND THE DIAMETER OF THE MEDIAL TROCHLEA. SYMBOLS EXPLAINED IN FIG. 3.145.....	574
FIGURE 3.200 METACARPAL. RATIO BETWEEN THE WIDTH OF THE LATERAL CONDYLE AND THE DIAMETER OF THE LATERAL TROCHLEA PLOTTED AGAINST THE RATIO BETWEEN THE DIAMETER OF THE <i>VERTICILLUS</i> THE LATERAL CONDYLE AND THE DIAMETER OF THE LATERAL CONDYLE. SYMBOLS EXPLAINED IN FIG. 3.145.....	574
FIGURE 3.201 METACARPAL. RATIO BETWEEN THE GREATEST BREADTH OF THE DISTAL END WITH THE GREATEST LENGTH PLOTTED AGAINST THE RATIO BETWEEN THE SMALLEST WIDTH OF THE SHAFT AND THE GREATEST LENGTH. SYMBOLS EXPLAINED IN FIG. 3.145.	575
FIGURE 3.202 METATARSAL. RATIO BETWEEN THE DIAMETER OF THE MEDIAL TROCHLEA AND THE WIDTH OF THE MEDIAL CONDYLE PLOTTED AGAINST THE RATIO BETWEEN THE DIAMETER OF THE <i>VERTICILLUS</i> AT THE MEDIAL CONDYLE AND THE DIAMETER OF THE MEDIAL TROCHLEA. SYMBOLS EXPLAINED IN FIG. 3.145.....	575
FIGURE 3.203 METATARSAL. RATIO BETWEEN THE WIDTH OF THE LATERAL CONDYLE AND THE DIAMETER OF THE LATERAL TROCHLEA PLOTTED AGAINST THE RATIO BETWEEN THE DIAMETER OF THE <i>VERTICILLUS</i> ON THE LATERAL CONDYLE AND THE DIAMETER OF THE LATERAL CONDYLE. SYMBOLS EXPLAINED IN FIG. 3.145.....	576
FIGURE 3.204 METATARSAL. RATIO BETWEEN THE GREATEST BREADTH OF THE DISTAL END WITH THE GREATEST LENGTH PLOTTED AGAINST THE RATIO BETWEEN THE SMALLEST WIDTH OF THE SHAFT AND THE GREATEST LENGTH. SYMBOLS EXPLAINED IN FIG. 3.145.	576
FIGURE 3.205 BREADTH OF THE DISTAL END PLOTTED AGAINST THE RATIO BETWEEN THE DEPTH OF THE MEDIAL (A) AND LATERAL (B) SIDE. SYMBOLS EXPLAINED IN FIG. 3.145.	577
FIGURE 3.206 RATIO BETWEEN HEIGHT AT THE CENTRAL CONSTRICTION AND THE GREATEST DEPTH OF THE LATERAL HALF PLOTTED AGAINST A RATIO BETWEEN THE BREADTH OF THE DISTAL END AND THE GREATEST LENGTH OF THE LATERAL HALF. SYMBOLS EXPLAINED IN FIG. 3.145.	577
FIGURE 3.207 RATIO BETWEEN HEIGHT AT THE CENTRAL CONSTRICTION AND THE GREATEST DEPTH OF THE LATERAL HALF PLOTTED AGAINST THE RATIO BETWEEN THE BREADTH OF THE DISTAL END AND THE HEIGHT AT THE CENTRAL CONSTRICTION. SYMBOLS EXPLAINED IN FIG. 3.145.	578
FIGURE 3.208 RATIO BETWEEN BREADTH OF THE DISTAL END AND THE GREATEST DEPTH OF THE LATERAL HALF PLOTTED AGAINST THE RATIO BETWEEN THE BREADTH OF THE DISTAL END AND THE GREATEST DEPTH OF THE LATERAL HALF. SYMBOLS EXPLAINED IN FIG. 3.145.	578

FIGURE 3.209 RATIO BETWEEN THE BREADTH OF THE DISTAL END AND THE HEIGHT AT THE CENTRAL CONstriction AND THE RATIO BETWEEN HEIGHT AT THE CENTRAL CONstriction AND THE GREATEST DEPTH OF THE LATERAL HALF. SYMBOLS EXPLAINED IN FIG. 3.145.	579
FIGURE 3.210 RATIO BETWEEN THE LENGTH AND THE BREADTH OF THE ARTICULAR FACET OF THE <i>OS MALLEOLARE</i> PLOTTED AGAINST THE RATIO BETWEEN THE LENGTH OF THE ARTICULAR FACET OF THE <i>OS MALLEOLARE</i> AND THE LENGTH TAKEN FROM THE ARTICULAR FACET OF THE <i>OS MALLEOLARE</i> TO THE END OF THE ARTICULATION-FREE PART OF THE PROCESS. SYMBOLS EXPLAINED IN FIG. 3.145.	579
FIGURE 3.211 RATIO BETWEEN THE DEPTH OF THE <i>SUBSTENTACULUM TALI</i> AND THE LENGTH OF THE ARTICULAR FACET OF THE <i>OS MALLEOLARE</i> PLOTTED AGAINST THE RATIO BETWEEN THE LENGTH AND THE BREADTH OF THE ARTICULAR FACET OF THE <i>OS MALLEOLARE</i> . SYMBOLS EXPLAINED IN FIG. 3.145.	580
FIGURE 3.212 RATIO BETWEEN THE DEPTH OF THE <i>SUBSTENTACULUM TALI</i> AND THE LENGTH OF THE ARTICULAR FACET OF THE <i>OS MALLEOLARE</i> PLOTTED AGAINST THE RATIO BETWEEN THE LENGTH AND THE BREADTH OF THE ARTICULAR FACET OF THE <i>OS MALLEOLARE</i> . SYMBOLS EXPLAINED IN FIG. 3.145.	580
FIGURE 3.213 DIAGRAM OF THE INDIVIDUAL DISCRIMINANT SCORES ATTRIBUTED TO THE MODERN AND ARCHAEOLOGICAL MATERIAL BY DA FOR THE HORNCORES.	584
FIGURE 3.214 DIAGRAM OF THE INDIVIDUAL DISCRIMINANT SCORES ATTRIBUTED TO THE MODERN AND ARCHAEOLOGICAL MATERIAL BY DA FOR THE HORNCORES (MEASUREMENTS A AND B EXCLUDED).	584
FIGURE 3.215 DIAGRAM OF THE INDIVIDUAL DISCRIMINANT SCORES ATTRIBUTED TO THE MODERN AND ARCHAEOLOGICAL MATERIAL BY DA FOR THE HORNCORES (MEASUREMENTS E AND F EXCLUDED).	585
FIGURE 3.216 DIAGRAM OF THE INDIVIDUAL DISCRIMINANT SCORES ATTRIBUTED TO THE MODERN AND ARCHAEOLOGICAL MATERIAL BY DA FOR THE SCAPULA.	587
FIGURE 3.217 DIAGRAM OF THE INDIVIDUAL DISCRIMINANT SCORES ATTRIBUTED TO THE MODERN AND ARCHAEOLOGICAL MATERIAL BY DA FOR HUMERI.	588
FIGURE 3.218 DIAGRAM OF THE INDIVIDUAL DISCRIMINANT SCORES ATTRIBUTED TO THE MODERN AND ARCHAEOLOGICAL MATERIAL BY DA FOR THE RADIUS.	591
FIGURE 3.219 DIAGRAM OF THE INDIVIDUAL DISCRIMINANT SCORES ATTRIBUTED TO THE MODERN AND ARCHAEOLOGICAL MATERIAL BY DA FOR THE RADIUS (MEASUREMENTS GL AND SD EXCLUDED).	592
FIGURE 3.220 DIAGRAM OF THE INDIVIDUAL DISCRIMINANT SCORES ATTRIBUTED TO THE MODERN AND ARCHAEOLOGICAL MATERIAL BY DA FOR THE ULNA.	594
FIGURE 3.221 SCATTERPLOT OF THE INDIVIDUAL DISCRIMINANT SCORES ATTRIBUTED TO THE MODERN AND ARCHAEOLOGICAL MATERIAL BY DA FOR THE ULNA (EXCLUDING MEASUREMENTS B AND L).	595
FIGURE 3.222 DIAGRAM OF THE INDIVIDUAL DISCRIMINANT SCORES ATTRIBUTED TO THE MODERN AND ARCHAEOLOGICAL MATERIAL BY DA FOR THE METACARPAL.	597
FIGURE 3.223 DIAGRAM OF THE INDIVIDUAL DISCRIMINANT SCORES ATTRIBUTED TO THE MODERN AND ARCHAEOLOGICAL MATERIAL BY DA FOR THE METACARPAL (EXCLUDING MEASUREMENTS GL AND SD).	598

FIGURE 3.224 DIAGRAM OF THE INDIVIDUAL DISCRIMINANT SCORES ATTRIBUTED TO THE MODERN AND ARCHAEOLOGICAL MATERIAL BY DA FOR THE METATARSAL.....	600
FIGURE 3.225 DIAGRAM OF THE INDIVIDUAL DISCRIMINANT SCORES ATTRIBUTED TO THE MODERN AND ARCHAEOLOGICAL MATERIAL BY DA FOR THE METATARSAL (EXCLUDING MEASUREMENTS GL AND SD).	601
FIGURE 3.226 DIAGRAM OF THE INDIVIDUAL DISCRIMINANT SCORES ATTRIBUTED TO THE MODERN AND ARCHAEOLOGICAL MATERIAL BY DA FOR THE TIBIA (EXCLUDING MEASUREMENT GL).	603
FIGURE 3.227 DIAGRAM OF THE INDIVIDUAL DISCRIMINANT SCORES ATTRIBUTED TO THE MODERN AND ARCHAEOLOGICAL MATERIAL BY DA FOR THE TIBIA (EXCLUDING MEASUREMENTS GL AND SD). ..	604
FIGURE 3.228 DIAGRAM OF THE INDIVIDUAL DISCRIMINANT SCORES ATTRIBUTED TO THE MODERN AND ARCHAEOLOGICAL MATERIAL BY DA FOR THE ASTRAGALUS.....	606
FIGURE 3.229 DIAGRAM OF THE INDIVIDUAL DISCRIMINANT SCORES ATTRIBUTED TO THE MODERN AND ARCHAEOLOGICAL MATERIAL BY DA FOR THE CALCANEUM.....	608
FIGURE 3.230 LOCATION OF THE SITES AND OF MINOR FIELDWORKS (BROWN 2008). RED ARROWS INDICATE THE AREAS WHERE 1994-1997 (LEFT) AND 2005 (RIGHT) EXCAVATIONS OCCURRED (IMAGE REPRINTED FROM BROWN, J. EXCAVATIONS AT THE CORNER OF KINGSWELL STREET AND WOOLMONGER STREET, NORTHAMPTON. <i>NORTHAMPTONSHIRE ARCHAEOLOGY</i> 35: 173-214, COPYRIGHT 2008, WITH PERMISSION FROM NORTHAMPTONSHIRE ARCHAEOLOGY, NOW MOLA NORTHAMPTON).....	618
FIGURE 3.231 LIST OF THE WRITTEN RESOURCES AND THE ARCHAEOLOGICAL EVIDENCE ATTESTING CRAFTS AT THE SITE (IMAGE REPRINTED FROM SODEN, I. A HISTORY OF URBAN REGENERATION: EXCAVATIONS IN ADVANCE OF DEVELOPMENT OFF ST PETER’S WALK, NORTHAMPTON, 1994-7. <i>NORTHAMPTONSHIRE ARCHAEOLOGY</i> 28: 61-127, COPYRIGHT 1998-99, WITH PERMISSION FROM IAIN SODEN).	619
FIGURE 3.232 LIST OF THE SPECIES IDENTIFIED AT THE SITE BY ARMITAGE IN 1998-1999 (RIGHT). PERCENTAGES OF THE MAIN SPECIES BASED ON NISP AT THE SITE (IMAGE REPRINTED FROM ARMITAGE, P. FAUNAL REMAINS. IN A HISTORY OF URBAN REGENERATION: EXCAVATIONS IN ADVANCE OF DEVELOPMENT OFF ST PETER’S WALK, NORTHAMPTON, 1994-97, I. SODEN, 102-106, COPYRIGHT 1998-99. <i>NORTHAMPTONSHIRE ARCHAEOLOGY</i> 28, WITH PERMISSION FROM PHILIP ARMITAGE).	621
FIGURE 3.233 LIST OF THE IDENTIFIED SPECIES FROM THE 2005 EXCAVATION (IMAGE REPRINTED FROM ARMITAGE, P. MAMMAL, BIRD AND FISH BONES. IN EXCAVATIONS AT THE CORNER OF KINGSWELL STREET AND WOOLMONGER STREET, NORTHAMPTON, J. BROWN, 206-208, COPYRIGHT 2008. <i>NORTHAMPTONSHIRE ARCHAEOLOGY</i> 35, WITH PERMISSION FROM PHILIP ARMITAGE).....	622
FIGURE 3.234 MAXIMUM DIAMETER TAKEN AT THE BASE PLOTTED AGAINST A RATIO BETWEEN THE LENGTH AND THE LENGTH OF THE OUTER CURVATURE OF THE HORNCORE. THE MODERN DATA ARE REPRESENTED BY THE SQUARE EMPTY SYMBOL, BLUE FOR MODERN GOATS, RED FOR MODERN SHEEP, WHILE THE ARCHAEOLOGICAL MATERIAL IS REPRESENTED BY THE FILLED DOT SYMBOL: BLUE FOR GOATS, RED FOR SHEEP AND GREEN FOR SHEEP/GOAT.	627

FIGURE 3.235 RATIO BETWEEN THE LENGTH AND THE LENGTH OF THE OUTER CURVATURE PLOTTED AGAINST THE RATIO BETWEEN THE MAXIMUM DIAMETER TAKEN AT THE BASE AND THE LENGTH OF THE OUTER CURVATURE OF THE HORNCORE. SYMBOLS EXPLAINED IN FIG. 3.234.....	627
FIGURE 3.236 RATIO BETWEEN THE GREATEST LENGTH OF THE <i>PROCESSUS ARTICULARIS</i> AND THE LENGTH OF THE GLENOID CAVITY PLOTTED AGAINST THE RATIO BETWEEN THE GREATEST LENGTH OF THE <i>PROCESSUS ARTICULARIS</i> AND THE BREADTH OF THE GLENOID CAVITY. SYMBOLS EXPLAINED IN FIG. 3.234.	628
FIGURE 3.237 RATIO BETWEEN THE SHORTEST DISTANCE FROM THE BASE OF THE SPINE TO THE EDGE OF THE GLENOID CAVITY AND THE SMALLEST LENGTH OF THE <i>COLLUM SCAPULAE</i> PLOTTED AGAINST THE RATIO BETWEEN THE GREATEST LENGTH OF THE <i>PROCESSUS ARTICULARIS</i> AND THE BREADTH OF THE GLENOID CAVITY. SYMBOLS EXPLAINED IN FIG. 3.234.	628
FIGURE 3.238 RATIO BETWEEN THE MEDIO LATERAL WIDTH OF THE TROCHLEA AND ITS HEIGHT PLOTTED AGAINST THE MEDIO LATERAL WIDTH OF THE TROCHLEA AND THE DIAMETER OF THE TROCHLEAR CONSTRICTION. SYMBOLS EXPLAINED IN FIG. 3.234.	629
FIGURE 3.239 RATIO BETWEEN THE BREADTH OF THE <i>CAPITULUM</i> AND THE DISTAL WIDTH PLOTTED AGAINST THE RATIO BETWEEN THE BREADTH OF THE <i>CAPITULUM</i> AND THE MEDIO LATERAL WIDTH OF THE TROCHLEA. SYMBOLS EXPLAINED IN FIG. 3.234.	629
FIGURE 3.240 RATIO BETWEEN THE BREADTH OF THE <i>CAPITULUM</i> AND THE DIAMETER OF THE TROCHLEA CONSTRICTION PLOTTED AGAINST THE RATIO BETWEEN THE BREADTH OF THE <i>CAPITULUM</i> AND THE MEDIO LATERAL WIDTH OF THE TROCHLEA. SYMBOLS EXPLAINED IN FIG. 3.234.....	630
FIGURE 3.241 RATIO BETWEEN THE BREADTH OF THE EPICONDYLE <i>LATERALIS</i> AND THE MEDIO LATERAL WIDTH OF THE TROCHLEA PLOTTED AGAINST THE RATIO BETWEEN THE BREADTH OF THE EPICONDYLE <i>LATERALIS</i> AND THE WIDTH OF THE DISTAL END. SYMBOLS EXPLAINED IN FIG. 3.234.	630
FIGURE 3.242 RATIO BETWEEN THE GREATEST LENGTH OF THE <i>FACIES ARTICULARIS PROXIMALIS</i> AND THE GREATEST BREADTH OF THE PROXIMAL END PLOTTED AGAINST THE DEPTH OF THE PROXIMAL END. SYMBOLS EXPLAINED IN FIG. 3.234.	631
FIGURE 3.243 RATIO BETWEEN THE BREADTH ACROSS THE CORONOID PROCESS AND THE DEPTH ACROSS THE <i>PROCESSUS ANCONAEUS</i> TO THE CAUDAL BORDER PLOTTED AGAINST THE BREADTH ACROSS THE CORONOID PROCESS AND THE SMALLEST DEPTH OF THE OLECRANON. SYMBOLS EXPLAINED IN FIG. 3.234.	631
FIGURE 3.244 METACARPAL. RATIO BETWEEN THE DIAMETER OF THE MEDIAL TROCHLEA AND THE WIDTH OF THE MEDIAL CONDYLE PLOTTED AGAINST THE RATIO BETWEEN THE DIAMETER OF THE <i>VERTICILLUS</i> AT THE MEDIAL CONDYLE AND THE DIAMETER OF THE MEDIAL TROCHLEA. SYMBOLS EXPLAINED IN FIG. 3.234.	632
FIGURE 3.245 METACARPAL. RATIO BETWEEN THE WIDTH OF THE LATERAL CONDYLE AND THE DIAMETER OF THE LATERAL TROCHLEA PLOTTED AGAINST THE RATIO BETWEEN THE DIAMETER OF THE LATERAL CONDYLE AND THE DIAMETER OF THE <i>VERTICILLUS</i> ON THE LATERAL CONDYLE. SYMBOLS EXPLAINED IN FIG. 3.234.....	632
FIGURE 3.246 METATARSAL. RATIO BETWEEN THE DIAMETER OF THE MEDIAL TROCHLEA AND THE WIDTH OF THE MEDIAL CONDYLE PLOTTED AGAINST THE RATIO BETWEEN THE DIAMETER OF THE <i>VERTICILLUS</i>	

AT THE MEDIAL CONDYLE AND THE DIAMETER OF THE MEDIAL TROCHLEA. SYMBOLS EXPLAINED IN FIG. 3.234.....	633
FIGURE 3.247 METATARSAL. RATIO BETWEEN THE WIDTH OF THE LATERAL CONDYLE AND THE DIAMETER OF THE LATERAL TROCHLEA PLOTTED AGAINST THE RATIO BETWEEN THE DIAMETER OF THE <i>VERTICILLUS</i> ON THE LATERAL CONDYLE AND THE DIAMETER OF THE LATERAL CONDYLE. SYMBOLS EXPLAINED IN FIG. 3.234.....	633
FIGURE 3.248 METATARSAL. RATIO BETWEEN THE GREATEST BREADTH OF THE DISTAL END WITH THE GREATEST LENGTH PLOTTED AGAINST THE RATIO BETWEEN THE SMALLEST WIDTH OF THE SHAFT AND THE GREATEST LENGTH. SYMBOLS EXPLAINED IN FIG. 3.234.	634
FIGURE 3.249 BREADTH OF THE DISTAL END PLOTTED AGAINST THE RATIO BETWEEN THE DEPTH OF THE MEDIAL (A) AND LATERAL (B) SIDE. SYMBOLS EXPLAINED IN FIG. 3.234.	634
FIGURE 3.250 RATIO BETWEEN HEIGHT AT THE CENTRAL CONSTRICTION AND THE GREATEST DEPTH OF THE LATERAL HALF PLOTTED AGAINST A RATIO BETWEEN THE BREADTH OF THE DISTAL END AND THE GREATEST LENGTH OF THE LATERAL HALF. SYMBOLS EXPLAINED IN FIG. 3.234.	635
FIGURE 3.251 RATIO BETWEEN HEIGHT AT THE CENTRAL CONSTRICTION AND THE GREATEST DEPTH OF THE LATERAL HALF PLOTTED AGAINST THE RATIO BETWEEN THE BREADTH OF THE DISTAL END AND THE HEIGHT AT THE CENTRAL CONSTRICTION. SYMBOLS EXPLAINED IN FIG. 3.234.	635
FIGURE 3.252 RATIO BETWEEN BREADTH OF THE DISTAL END AND THE GREATEST DEPTH OF THE LATERAL HALF PLOTTED AGAINST THE RATIO BETWEEN THE BREADTH OF THE DISTAL END AND THE GREATEST DEPTH OF THE LATERAL HALF. SYMBOLS EXPLAINED IN FIG. 3.234.	636
FIGURE 3.253 RATIO BETWEEN THE BREADTH OF THE DISTAL END AND THE HEIGHT AT THE CENTRAL CONSTRICTION AND THE RATIO BETWEEN HEIGHT AT THE CENTRAL CONSTRICTION AND THE GREATEST DEPTH OF THE LATERAL HALF. SYMBOLS EXPLAINED IN FIG. 3.234.	636
FIGURE 3.254 RATIO BETWEEN THE LENGTH AND THE BREADTH OF THE ARTICULAR FACET OF THE <i>OS MALLEOLARE</i> PLOTTED AGAINST THE RATIO BETWEEN THE LENGTH OF THE ARTICULAR FACET OF THE <i>OS MALLEOLARE</i> AND THE LENGTH TAKEN FROM THE ARTICULAR FACET OF THE <i>OS MALLEOLARE</i> TO THE END OF THE ARTICULATION-FREE PART OF THE PROCESS. SYMBOLS EXPLAINED IN FIG. 3.234..	637
FIGURE 3.255 RATIO BETWEEN THE DEPTH OF THE <i>SUBSTENTACULUM TALI</i> AND THE LENGTH OF THE ARTICULAR FACET OF THE <i>OS MALLEOLARE</i> PLOTTED AGAINST THE RATIO BETWEEN THE LENGTH AND THE BREADTH OF THE ARTICULAR FACET OF THE <i>OS MALLEOLARE</i> . SYMBOLS EXPLAINED IN FIG. 3.234.	637
FIGURE 3.256 RATIO BETWEEN THE DEPTH OF THE <i>SUBSTENTACULUM TALI</i> AND THE LENGTH OF THE ARTICULAR FACET OF THE <i>OS MALLEOLARE</i> PLOTTED AGAINST THE RATIO BETWEEN THE LENGTH AND THE BREADTH OF THE ARTICULAR FACET OF THE <i>OS MALLEOLARE</i> . SYMBOLS EXPLAINED IN FIG. 3.234.	638
FIGURE 3.257 GREATEST DIAGONAL LENGTH OF THE SOLE PLOTTED AGAINST A RATIO BETWEEN THE GREATEST DIAGONAL LENGTH OF THE SOLE AND THE MIDDLE BREADTH OF THE SOLE. SYMBOLS EXPLAINED IN FIG. 3.234.	638
FIGURE 3.258 RATIO BETWEEN THE GREATEST LENGTH OF THE <i>PROCESSUS ARTICULARIS</i> AND THE LENGTH OF THE GLENOID CAVITY PLOTTED AGAINST THE RATIO BETWEEN THE GREATEST LENGTH OF THE	

<i>PROCESSUS ARTICULARIS</i> AND THE BREADTH OF THE GLENOID CAVITY. SYMBOLS EXPLAINED IN FIG. 3.234.	639
FIGURE 3.259 RATIO BETWEEN THE SHORTEST DISTANCE FROM THE BASE OF THE SPINE TO THE EDGE OF THE GLENOID CAVITY AND THE SMALLEST LENGTH OF THE <i>COLLUM SCAPULAE</i> PLOTTED AGAINST A RATIO BETWEEN THE GREATEST LENGTH OF THE <i>PROCESSUS ARTICULARIS</i> AND THE BREADTH OF THE GLENOID CAVITY. SYMBOLS EXPLAINED IN FIG. 3.234.	640
FIGURE 3.260 RATIO BETWEEN THE MEDIO LATERAL WIDTH OF THE TROCHLEA AND ITS HEIGHT PLOTTED AGAINST THE MEDIO LATERAL WIDTH OF THE TROCHLEA AND THE DIAMETER OF THE TROCHLEAR CONSTRICTION. SYMBOLS EXPLAINED IN FIG. 3.234.	641
FIGURE 3.261 RATIO BETWEEN THE BREADTH OF THE <i>CAPITULUM</i> AND THE DISTAL WIDTH PLOTTED AGAINST THE RATIO BETWEEN THE BREADTH OF THE <i>CAPITULUM</i> AND THE MEDIO LATERAL WIDTH OF THE TROCHLEA. SYMBOLS EXPLAINED IN FIG. 3.234.	641
FIGURE 3.262 RATIO BETWEEN THE BREADTH OF THE <i>CAPITULUM</i> AND THE DIAMETER OF THE TROCHLEAR CONSTRICTION PLOTTED AGAINST THE RATIO BETWEEN THE BREADTH OF THE <i>CAPITULUM</i> AND THE MEDIO LATERAL WIDTH OF THE TROCHLEA. SYMBOLS EXPLAINED IN FIG. 3.234.	642
FIGURE 3.263 RATIO BETWEEN THE BREADTH OF THE EPICONDYLE <i>LATERALIS</i> AND THE MEDIO LATERAL WIDTH OF THE TROCHLEA PLOTTED AGAINST THE RATIO BETWEEN THE BREADTH OF THE EPICONDYLE <i>LATERALIS</i> AND THE WIDTH OF THE DISTAL END. SYMBOLS EXPLAINED IN FIG. 3.234.	642
FIGURE 3.264 RATIO BETWEEN THE GREATEST LENGTH OF THE <i>FACIES ARTICULARIS PROXIMALIS</i> AND THE GREATEST BREADTH OF THE PROXIMAL END PLOTTED AGAINST THE DEPTH OF THE PROXIMAL END. SYMBOLS EXPLAINED IN FIG. 3.234.	643
FIGURE 3.265 RATIO BETWEEN THE BREADTH ACROSS THE CORONOID PROCESS AND THE DEPTH ACROSS THE <i>PROCESSUS ANCONAEUS</i> TO THE CAUDAL BORDER PLOTTED AGAINST THE BREADTH ACROSS THE CORONOID PROCESS AND THE SMALLEST DEPTH OF THE OLECRANON. SYMBOLS EXPLAINED IN FIG. 3.234.	643
FIGURE 3.266 METACARPAL. RATIO BETWEEN THE DIAMETER OF THE MEDIAL TROCHLEA AND THE WIDTH OF THE MEDIAL CONDYLE PLOTTED AGAINST THE RATIO BETWEEN THE DIAMETER OF THE <i>VERTICILLUS</i> AT THE MEDIAL CONDYLE AND THE DIAMETER OF THE MEDIAL TROCHLEA. SYMBOLS EXPLAINED IN FIG. 3.234.	644
FIGURE 3.267 METACARPAL. RATIO BETWEEN THE WIDTH OF THE LATERAL CONDYLE AND THE DIAMETER OF THE LATERAL TROCHLEA PLOTTED AGAINST THE RATIO BETWEEN THE DIAMETER OF THE <i>VERTICILLUS</i> THE LATERAL CONDYLE AND THE DIAMETER OF THE LATERAL CONDYLE. SYMBOLS EXPLAINED IN FIG. 3.234.	645
FIGURE 3.268 METACARPAL. RATIO BETWEEN THE GREATEST BREADTH OF THE DISTAL END WITH THE GREATEST LENGTH PLOTTED AGAINST THE RATIO BETWEEN THE SMALLEST WIDTH OF THE SHAFT AND THE GREATEST LENGTH. SYMBOLS EXPLAINED IN FIG. 3.234.	645
FIGURE 3.269 METATARSAL. RATIO BETWEEN THE DIAMETER OF THE MEDIAL TROCHLEA AND THE WIDTH OF THE MEDIAL CONDYLE PLOTTED AGAINST THE RATIO BETWEEN THE DIAMETER OF THE <i>VERTICILLUS</i> AT THE MEDIAL CONDYLE AND THE DIAMETER OF THE MEDIAL TROCHLEA. SYMBOLS EXPLAINED IN FIG. 3.234.	646

FIGURE 3.270 METATARSAL. RATIO BETWEEN THE WIDTH OF THE LATERAL CONDYLE AND THE DIAMETER OF THE LATERAL TROCHLEA PLOTTED AGAINST THE RATIO BETWEEN THE DIAMETER OF THE <i>VERTICILLUS</i> ON THE LATERAL CONDYLE AND THE DIAMETER OF THE LATERAL CONDYLE. SYMBOLS EXPLAINED IN FIG. 3.234.....	646
FIGURE 3.271 BREADTH OF THE DISTAL END PLOTTED AGAINST THE RATIO BETWEEN THE DEPTH OF THE MEDIAL (A) AND LATERAL (B) SIDE. SYMBOLS EXPLAINED IN FIG. 3.234.	647
FIGURE 3.272 RATIO BETWEEN HEIGHT AT THE CENTRAL CONSTRICTION AND THE GREATEST DEPTH OF THE LATERAL HALF PLOTTED AGAINST A RATIO BETWEEN THE BREADTH OF THE DISTAL END AND THE GREATEST LENGTH OF THE LATERAL HALF. SYMBOLS EXPLAINED IN FIG. 3.234.	647
FIGURE 3.273 RATIO BETWEEN HEIGHT AT THE CENTRAL CONSTRICTION AND THE GREATEST DEPTH OF THE LATERAL HALF PLOTTED AGAINST THE RATIO BETWEEN THE BREADTH OF THE DISTAL END AND THE HEIGHT AT THE CENTRAL CONSTRICTION. SYMBOLS EXPLAINED IN FIG. 3.234.	648
FIGURE 3.274 RATIO BETWEEN BREADTH OF THE DISTAL END AND THE GREATEST DEPTH OF THE LATERAL HALF PLOTTED AGAINST THE RATIO BETWEEN THE BREADTH OF THE DISTAL END AND THE GREATEST DEPTH OF THE LATERAL HALF. SYMBOLS EXPLAINED IN FIG. 3.234.	648
FIGURE 3.275 RATIO BETWEEN THE BREADTH OF THE DISTAL END AND THE HEIGHT AT THE CENTRAL CONSTRICTION AND THE RATIO BETWEEN HEIGHT AT THE CENTRAL CONSTRICTION AND THE GREATEST DEPTH OF THE LATERAL HALF. SYMBOLS EXPLAINED IN FIG. 3.234.	649
FIGURE 3.276 RATIO BETWEEN THE LENGTH AND THE BREADTH OF THE ARTICULAR FACET OF THE <i>OS MALLEOLARE</i> PLOTTED AGAINST THE RATIO BETWEEN THE LENGTH OF THE ARTICULAR FACET OF THE <i>OS MALLEOLARE</i> AND THE LENGTH TAKEN FROM THE ARTICULAR FACET OF THE <i>OS MALLEOLARE</i> TO THE END OF THE ARTICULATION-FREE PART OF THE PROCESS. SYMBOLS EXPLAINED IN FIG. 3.234..	649
FIGURE 3.277 RATIO BETWEEN THE DEPTH OF THE <i>SUBSTENTACULUM TALI</i> AND THE LENGTH OF THE ARTICULAR FACET OF THE <i>OS MALLEOLARE</i> PLOTTED AGAINST THE RATIO BETWEEN THE LENGTH AND THE BREADTH OF THE ARTICULAR FACET OF THE <i>OS MALLEOLARE</i> . SYMBOLS EXPLAINED IN FIG. 3.234.	650
FIGURE 3.278 RATIO BETWEEN THE DEPTH OF THE <i>SUBSTENTACULUM TALI</i> AND THE LENGTH OF THE ARTICULAR FACET OF THE <i>OS MALLEOLARE</i> PLOTTED AGAINST THE RATIO BETWEEN THE LENGTH AND THE BREADTH OF THE ARTICULAR FACET OF THE <i>OS MALLEOLARE</i> . SYMBOLS EXPLAINED IN FIG. 3.234.	650
FIGURE 3.279 GREATEST DIAGONAL LENGTH OF THE SOLE PLOTTED AGAINST A RATIO BETWEEN THE GREATEST DIAGONAL LENGTH OF THE SOLE AND THE MIDDLE BREADTH OF THE SOLE. SYMBOLS EXPLAINED IN FIG. 3.234.....	651
FIGURE 3.280 RATIO BETWEEN THE GREATEST LENGTH OF THE <i>PROCESSUS ARTICULARIS</i> AND THE LENGTH OF THE GLENOID CAVITY PLOTTED AGAINST THE RATIO BETWEEN THE GREATEST LENGTH OF <i>THE PROCESSUS ARTICULARIS</i> AND THE BREADTH OF THE GLENOID CAVITY. SYMBOLS EXPLAINED IN FIG. 3.234.....	651
FIGURE 3.281 RATIO BETWEEN THE MEDIO LATERAL WIDTH OF THE TROCHLEA AND ITS HEIGHT PLOTTED AGAINST THE MEDIO LATERAL WIDTH OF THE TROCHLEA AND THE DIAMETER OF THE TROCHLEAR CONSTRICTION. SYMBOLS EXPLAINED IN FIG. 3.234.....	652

FIGURE 3.282 RATIO BETWEEN THE BREADTH OF THE <i>CAPITULUM</i> AND THE DISTAL WIDTH PLOTTED AGAINST THE RATIO BETWEEN THE BREADTH OF THE <i>CAPITULUM</i> AND THE MEDIO LATERAL WIDTH OF THE TROCHLEA. SYMBOLS EXPLAINED IN FIG. 3.234.	652
FIGURE 3.283 RATIO BETWEEN THE BREADTH OF THE <i>CAPITULUM</i> AND THE DIAMETER OF THE TROCHLEAR CONSTRICTION PLOTTED AGAINST THE RATIO BETWEEN THE BREADTH OF THE <i>CAPITULUM</i> AND THE MEDIO LATERAL WIDTH OF THE TROCHLEA. SYMBOLS EXPLAINED IN FIG. 3.234.	653
FIGURE 3.284 RATIO BETWEEN THE BREADTH OF THE <i>EPICONDYLE LATERALIS</i> AND THE MEDIO LATERAL WIDTH OF THE TROCHLEA PLOTTED AGAINST THE RATIO BETWEEN THE BREADTH OF THE <i>EPICONDYLE LATERALIS</i> AND THE WIDTH OF THE DISTAL END. SYMBOLS EXPLAINED IN FIG. 3.234.	653
FIGURE 3.285 RATIO BETWEEN THE GREATEST LENGTH OF THE <i>FACIES ARTICULARIS PROXIMALIS</i> AND THE GREATEST BREADTH OF THE PROXIMAL END PLOTTED AGAINST THE DEPTH OF THE PROXIMAL END. SYMBOLS EXPLAINED IN FIG. 3.234.	654
FIGURE 3.286 METACARPAL. RATIO BETWEEN THE DIAMETER OF THE MEDIAL TROCHLEA AND THE WIDTH OF THE MEDIAL CONDYLE PLOTTED AGAINST THE RATIO BETWEEN THE DIAMETER OF THE <i>VERTICILLUS</i> AT THE MEDIAL CONDYLE AND THE DIAMETER OF THE MEDIAL TROCHLEA. SYMBOLS EXPLAINED IN FIG. 3.234.	654
FIGURE 3.287 METACARPAL. RATIO BETWEEN THE WIDTH OF THE LATERAL CONDYLE AND THE DIAMETER OF THE LATERAL TROCHLEA PLOTTED AGAINST THE RATIO BETWEEN THE DIAMETER OF THE <i>VERTICILLUS</i> ON THE LATERAL CONDYLE AND THE DIAMETER OF THE LATERAL CONDYLE. SYMBOLS EXPLAINED IN FIG. 3.234.	655
FIGURE 3.288 METACARPAL. RATIO BETWEEN THE GREATEST BREADTH OF THE DISTAL END WITH THE GREATEST LENGTH PLOTTED AGAINST THE RATIO BETWEEN THE SMALLEST WIDTH OF THE SHAFT AND THE GREATEST LENGTH. SYMBOLS EXPLAINED IN FIG. 3.234.	655
FIGURE 3.289 METATARSAL. RATIO BETWEEN THE DIAMETER OF THE MEDIAL TROCHLEA AND THE WIDTH OF THE MEDIAL CONDYLE PLOTTED AGAINST THE RATIO BETWEEN THE DIAMETER OF THE <i>VERTICILLUS</i> AT THE MEDIAL CONDYLE AND THE DIAMETER OF THE MEDIAL TROCHLEA. SYMBOLS EXPLAINED IN FIG. 3.234.	656
FIGURE 3.290 METATARSAL. RATIO BETWEEN THE WIDTH OF THE LATERAL CONDYLE AND THE DIAMETER OF THE LATERAL TROCHLEA PLOTTED AGAINST THE RATIO BETWEEN THE DIAMETER OF THE <i>VERTICILLUS</i> ON THE LATERAL CONDYLE AND THE DIAMETER OF THE LATERAL CONDYLE. SYMBOLS EXPLAINED IN FIG. 3.234.	656
FIGURE 3.291 BREADTH OF THE DISTAL END PLOTTED AGAINST THE RATIO BETWEEN THE DEPTH OF THE MEDIAL (A) AND LATERAL (B) SIDE. SYMBOLS EXPLAINED IN FIG. 3.234.	657
FIGURE 3.292 RATIO BETWEEN HEIGHT AT THE CENTRAL CONSTRICTION AND THE GREATEST DEPTH OF THE LATERAL HALF PLOTTED AGAINST A RATIO BETWEEN THE BREADTH OF THE DISTAL END AND THE GREATEST LENGTH OF THE LATERAL HALF. SYMBOLS EXPLAINED IN FIG. 3.234.	657
FIGURE 3.293 RATIO BETWEEN HEIGHT AT THE CENTRAL CONSTRICTION AND THE GREATEST DEPTH OF THE LATERAL HALF PLOTTED AGAINST THE RATIO BETWEEN THE BREADTH OF THE DISTAL END AND THE HEIGHT AT THE CENTRAL CONSTRICTION. SYMBOLS EXPLAINED IN FIG. 3.234.	658

FIGURE 3.294 RATIO BETWEEN BREADTH OF THE DISTAL END AND THE GREATEST DEPTH OF THE LATERAL HALF PLOTTED AGAINST THE RATIO BETWEEN THE BREADTH OF THE DISTAL END AND THE GREATEST DEPTH OF THE LATERAL HALF. SYMBOLS EXPLAINED IN FIG. 3.234.	658
FIGURE 3.295 RATIO BETWEEN THE BREADTH OF THE DISTAL END AND THE HEIGHT AT THE CENTRAL CONSTRICTION AND THE RATIO BETWEEN HEIGHT AT THE CENTRAL CONSTRICTION AND THE GREATEST DEPTH OF THE LATERAL HALF. SYMBOLS EXPLAINED IN FIG. 3.234.	659
FIGURE 3.296 GREATEST DIAGONAL LENGTH OF THE SOLE PLOTTED AGAINST A RATIO BETWEEN THE GREATEST DIAGONAL LENGTH OF THE SOLE AND THE MIDDLE BREADTH OF THE SOLE. SYMBOLS EXPLAINED IN FIG. 3.234.	659
FIGURE 3.297 MAXIMUM DIAMETER TAKEN AT THE BASE PLOTTED AGAINST A RATIO BETWEEN THE LENGTH AND THE LENGTH OF THE OUTER CURVATURE OF THE HORNCORE. SYMBOLS EXPLAINED IN FIG. 3.234.	660
FIGURE 3.298 RATIO BETWEEN THE LENGTH AND THE LENGTH OF THE OUTER CURVATURE PLOTTED AGAINST THE RATIO BETWEEN THE MAXIMUM DIAMETER TAKEN AT THE BASE AND THE LENGTH OF THE OUTER CURVATURE OF THE HORNCORE. SYMBOLS EXPLAINED IN FIG. 3.234.	660
FIGURE 3.299 RATIO BETWEEN THE GREATEST LENGTH OF THE <i>PROCESSUS ARTICULARIS</i> AND THE LENGTH OF THE GLENOID CAVITY PLOTTED AGAINST THE RATIO BETWEEN THE GREATEST LENGTH OF THE <i>PROCESSUS ARTICULARIS</i> AND THE BREADTH OF THE GLENOID CAVITY. SYMBOLS EXPLAINED IN FIG. 3.234.	661
FIGURE 3.300 RATIO BETWEEN THE SHORTEST DISTANCE FROM THE BASE OF THE SPINE TO THE EDGE OF THE GLENOID CAVITY AND THE SMALLEST LENGTH OF THE <i>COLLUM SCAPULAE</i> PLOTTED AGAINST A RATIO BETWEEN THE GREATEST LENGTH OF THE <i>PROCESSUS ARTICULARIS</i> AND THE BREADTH OF THE GLENOID CAVITY. SYMBOLS EXPLAINED IN FIG. 3.324.	661
FIGURE 3.301 RATIO BETWEEN THE MEDIO LATERAL WIDTH OF THE TROCHLEA AND ITS HEIGHT PLOTTED AGAINST THE MEDIO LATERAL WIDTH OF THE TROCHLEA AND THE DIAMETER OF THE TROCHLEAR CONSTRICTION. SYMBOLS EXPLAINED IN FIG. 3.234.	662
FIGURE 3.302 RATIO BETWEEN THE BREADTH OF THE <i>CAPITULUM</i> AND THE DISTAL WIDTH PLOTTED AGAINST THE RATIO BETWEEN THE BREADTH OF THE <i>CAPITULUM</i> AND THE MEDIO LATERAL WIDTH OF THE TROCHLEA. SYMBOLS EXPLAINED IN FIG. 3.234.	662
FIGURE 3.303 RATIO BETWEEN THE BREADTH OF THE <i>CAPITULUM</i> AND THE DIAMETER OF THE TROCHLEAR CONSTRICTION PLOTTED AGAINST THE RATIO BETWEEN THE BREADTH OF THE <i>CAPITULUM</i> AND THE MEDIO LATERAL WIDTH OF THE TROCHLEA. SYMBOLS EXPLAINED IN FIG. 3.234.	663
FIGURE 3.304 RATIO BETWEEN THE BREADTH OF THE <i>EPICONDYLE LATERALIS</i> AND THE MEDIO LATERAL WIDTH OF THE TROCHLEA PLOTTED AGAINST THE RATIO BETWEEN THE BREADTH OF THE <i>EPICONDYLE LATERALIS</i> AND THE WIDTH OF THE DISTAL END. SYMBOLS EXPLAINED IN FIG. 3.234.	663
FIGURE 3.305 RATIO BETWEEN THE GREATEST LENGTH OF THE <i>FACIES ARTICULARIS PROXIMALIS</i> AND THE GREATEST BREADTH OF THE PROXIMAL END PLOTTED AGAINST THE DEPTH OF THE PROXIMAL END. SYMBOLS EXPLAINED IN FIG. 3.234.	664
FIGURE 3.306 RATIO BETWEEN THE BREADTH ACROSS THE CORONOID PROCESS AND THE DEPTH ACROSS THE <i>PROCESSUS ANCONAEUS</i> TO THE CAUDAL BORDER PLOTTED AGAINST THE BREADTH ACROSS THE	

CORONOID PROCESS AND THE SMALLEST DEPTH OF THE OLECRANON. SYMBOLS EXPLAINED IN FIG. 3.234.	664
FIGURE 3.307 METACARPAL. RATIO BETWEEN THE DIAMETER OF THE MEDIAL TROCHLEA AND THE WIDTH OF THE MEDIAL CONDYLE PLOTTED AGAINST THE RATIO BETWEEN THE DIAMETER OF THE <i>VERTICILLUS</i> AT THE MEDIAL CONDYLE AND THE DIAMETER OF THE MEDIAL TROCHLEA. SYMBOLS EXPLAINED IN FIG. 3.234.	665
FIGURE 3.308 METACARPAL. RATIO BETWEEN THE WIDTH OF THE LATERAL CONDYLE AND THE DIAMETER OF THE LATERAL TROCHLEA PLOTTED AGAINST THE RATIO BETWEEN THE DIAMETER OF THE <i>VERTICILLUS</i> ON THE LATERAL CONDYLE AND THE DIAMETER OF THE LATERAL CONDYLE. SYMBOLS EXPLAINED IN FIG. 3.234.	666
FIGURE 3.309 METACARPAL. RATIO BETWEEN THE GREATEST BREADTH OF THE DISTAL END WITH THE GREATEST LENGTH PLOTTED AGAINST THE RATIO BETWEEN THE SMALLEST WIDTH OF THE SHAFT AND THE GREATEST LENGTH. SYMBOLS EXPLAINED IN FIG. 3.234.	666
FIGURE 3.310 METATARSAL. RATIO BETWEEN THE DIAMETER OF THE MEDIAL TROCHLEA AND THE WIDTH OF THE MEDIAL CONDYLE PLOTTED AGAINST THE RATIO BETWEEN THE DIAMETER OF THE <i>VERTICILLUS</i> AT THE MEDIAL CONDYLE AND THE DIAMETER OF THE MEDIAL TROCHLEA. SYMBOLS EXPLAINED IN FIG. 3.234.	667
FIGURE 3.311 METATARSAL. RATIO BETWEEN THE WIDTH OF THE LATERAL CONDYLE AND THE DIAMETER OF THE LATERAL TROCHLEA PLOTTED AGAINST THE RATIO BETWEEN THE DIAMETER OF THE <i>VERTICILLUS</i> ON THE LATERAL CONDYLE AND THE DIAMETER OF THE LATERAL CONDYLE. SYMBOLS EXPLAINED IN FIG. 3.234.	667
FIGURE 3.312 METATARSAL. RATIO BETWEEN THE GREATEST BREADTH OF THE DISTAL END WITH THE GREATEST LENGTH PLOTTED AGAINST THE RATIO BETWEEN THE SMALLEST WIDTH OF THE SHAFT AND THE GREATEST LENGTH. SYMBOLS EXPLAINED IN FIG. 3.234.	668
FIGURE 3.313 BREADTH OF THE DISTAL END PLOTTED AGAINST THE RATIO BETWEEN THE DEPTH OF THE MEDIAL (A) AND LATERAL (B) SIDE. SYMBOLS EXPLAINED IN FIG. 3.234.	669
FIGURE 3.314 RATIO BETWEEN HEIGHT AT THE CENTRAL CONSTRICTION AND THE GREATEST DEPTH OF THE LATERAL HALF PLOTTED AGAINST A RATIO BETWEEN THE BREADTH OF THE DISTAL END AND THE GREATEST LENGTH OF THE LATERAL HALF. SYMBOLS EXPLAINED IN FIG. 3.234.	669
FIGURE 3.315 RATIO BETWEEN HEIGHT AT THE CENTRAL CONSTRICTION AND THE GREATEST DEPTH OF THE LATERAL HALF PLOTTED AGAINST THE RATIO BETWEEN THE BREADTH OF THE DISTAL END AND THE HEIGHT AT THE CENTRAL CONSTRICTION. SYMBOLS EXPLAINED IN FIG. 3.234.	670
FIGURE 3.316 RATIO BETWEEN BREADTH OF THE DISTAL END AND THE GREATEST DEPTH OF THE LATERAL HALF PLOTTED AGAINST THE RATIO BETWEEN THE BREADTH OF THE DISTAL END AND THE GREATEST DEPTH OF THE LATERAL HALF. SYMBOLS EXPLAINED IN FIG. 3.234.	670
FIGURE 3.317 RATIO BETWEEN THE BREADTH OF THE DISTAL END AND THE HEIGHT AT THE CENTRAL CONSTRICTION AND THE RATIO BETWEEN HEIGHT AT THE CENTRAL CONSTRICTION AND THE GREATEST DEPTH OF THE LATERAL HALF. SYMBOLS EXPLAINED IN FIG. 3.234.	671
FIGURE 3.318 RATIO BETWEEN THE LENGTH AND THE BREADTH OF THE ARTICULAR FACET OF THE <i>OS MALLEOLARE</i> PLOTTED AGAINST THE RATIO BETWEEN THE LENGTH OF THE ARTICULAR FACET OF THE	

OS MALLEOLARE AND THE LENGTH TAKEN FROM THE ARTICULAR FACET OF THE OS MALLEOLARE TO THE END OF THE ARTICULATION-FREE PART OF THE PROCESS. SYMBOLS EXPLAINED IN FIG. 3.234..	671
FIGURE 3.319 RATIO BETWEEN THE DEPTH OF THE SUBSTENTACULUM TALI AND THE LENGTH OF THE ARTICULAR FACET OF THE OS MALLEOLARE PLOTTED AGAINST THE RATIO BETWEEN THE LENGTH AND THE BREADTH OF THE ARTICULAR FACET OF THE OS MALLEOLARE. SYMBOLS EXPLAINED IN FIG. 3.234.	672
FIGURE 3.320 RATIO BETWEEN THE DEPTH OF THE SUBSTENTACULUM TALI AND THE LENGTH OF THE ARTICULAR FACET OF THE OS MALLEOLARE PLOTTED AGAINST THE RATIO BETWEEN THE LENGTH AND THE BREADTH OF THE ARTICULAR FACET OF THE OS MALLEOLARE. SYMBOLS EXPLAINED IN FIG. 3.234.	672
FIGURE 3.321 GREATEST DIAGONAL LENGTH OF THE SOLE PLOTTED AGAINST A RATIO BETWEEN THE GREATEST DIAGONAL LENGTH OF THE SOLE AND THE MIDDLE BREADTH OF THE SOLE. SYMBOLS EXPLAINED IN FIG. 3.234.	673
FIGURE 3.322 DIAGRAM OF THE INDIVIDUAL DISCRIMINANT SCORES ATTRIBUTED TO THE ARCHAEOLOGICAL MATERIAL BY DA FOR THE HORNCORE.	676
FIGURE 3.323 DIAGRAM OF THE INDIVIDUAL DISCRIMINANT SCORES ATTRIBUTED TO THE ARCHAEOLOGICAL MATERIAL BY DA FOR THE HORNCORE WHEN VARIABLES E AND F WERE EXCLUDED.	676
FIGURE 3.324 DIAGRAM OF THE INDIVIDUAL DISCRIMINANT SCORES ATTRIBUTED TO THE ARCHAEOLOGICAL MATERIAL BY DA FOR THE SCAPULA.	678
FIGURE 3.325 DIAGRAM OF THE INDIVIDUAL DISCRIMINANT SCORES ATTRIBUTED TO THE ARCHAEOLOGICAL MATERIAL BY DA FOR THE HUMERUS.	679
FIGURE 3.326 DIAGRAM OF THE INDIVIDUAL DISCRIMINANT SCORES ATTRIBUTED TO THE ARCHAEOLOGICAL MATERIAL BY DA FOR THE RADIUS.	681
FIGURE 3.327 DIAGRAM OF THE INDIVIDUAL DISCRIMINANT SCORES ATTRIBUTED TO THE ARCHAEOLOGICAL MATERIAL BY DA FOR THE RADIUS WHEN VARIABLES GL AND SD WERE EXCLUDED.	682
FIGURE 3.328 DIAGRAM OF THE INDIVIDUAL DISCRIMINANT SCORES ATTRIBUTED TO THE ARCHAEOLOGICAL MATERIAL BY DA FOR THE ULNA.	684
FIGURE 3.329 DIAGRAM OF THE INDIVIDUAL DISCRIMINANT SCORES ATTRIBUTED TO THE ARCHAEOLOGICAL MATERIAL BY DA FOR THE ULNA WHEN VARIABLES B AND L WERE EXCLUDED.	684
FIGURE 3.330 DIAGRAM OF THE INDIVIDUAL DISCRIMINANT SCORES ATTRIBUTED TO THE ARCHAEOLOGICAL MATERIAL BY DA FOR THE METACARPAL.	687
FIGURE 3.331 DIAGRAM OF THE INDIVIDUAL DISCRIMINANT SCORES ATTRIBUTED TO THE ARCHAEOLOGICAL MATERIAL BY DA FOR THE METACARPAL WHEN VARIABLES GL AND SD WERE EXCLUDED.	687
FIGURE 3.332 DIAGRAM OF THE INDIVIDUAL DISCRIMINANT SCORES ATTRIBUTED TO ARCHAEOLOGICAL MATERIAL BY DA FOR THE METATARSAL.	689
FIGURE 3.333 DIAGRAM OF THE INDIVIDUAL DISCRIMINANT SCORES ATTRIBUTED TO THE ARCHAEOLOGICAL MATERIAL BY DA FOR THE METATARSAL WHEN VARIABLES GL AND SD WERE EXCLUDED.	690

FIGURE 3.334 DIAGRAM OF THE INDIVIDUAL DISCRIMINANT SCORES ATTRIBUTED TO THE ARCHAEOLOGICAL MATERIAL BY DA FOR THE TIBIA.	693
FIGURE 3.335 DIAGRAM OF THE INDIVIDUAL DISCRIMINANT SCORES ATTRIBUTED TO THE ARCHAEOLOGICAL MATERIAL BY DA FOR THE TIBIA WHEN VARIABLE GL WAS EXCLUDED. THE BLUE ARROW INDICATES THE POSITION OF THE ARCHAEOLOGICAL GOAT.	694
FIGURE 3.336 DIAGRAM OF THE INDIVIDUAL DISCRIMINANT SCORES ATTRIBUTED TO THE ARCHAEOLOGICAL MATERIAL BY DA FOR THE TIBIA WHEN VARIABLES GL AND SD WERE EXCLUDED. THE BLUE ARROW INDICATES THE POSITION OF THE ARCHAEOLOGICAL GOAT.	694
FIGURE 3.337 DIAGRAM OF THE INDIVIDUAL DISCRIMINANT SCORES ATTRIBUTED TO THE ARCHAEOLOGICAL MATERIAL BY DA FOR THE ASTRAGALUS.	696
FIGURE 3.338 DIAGRAM OF THE INDIVIDUAL DISCRIMINANT SCORES ATTRIBUTED TO THE ARCHAEOLOGICAL MATERIAL BY DA FOR THE CALCANEUM.	698
FIGURE 3.339 DIAGRAM OF THE INDIVIDUAL DISCRIMINANT SCORES ATTRIBUTED TO THE ARCHAEOLOGICAL MATERIAL BY DA FOR THE CALCANEUM WHEN VARIABLES GL AND SB WERE EXCLUDED.	699

Chapter 1 Introduction and background

1.1 Research questions and thesis structure

“Many historical essays and books begin with the claim that their subject has been neglected, but in the case of the medieval goat this really is the case. The evidence is scattered and thin, and although historians and archaeologists have devoted some space to this animal there is no study of any length” (Dyer 2004: 20).

The study of the goat (*Capra hircus*) has been largely disregarded by British archaeologists, and this neglect is due to a number of different reasons. In part it is a methodological problem, related to the difficulty of distinguishing goat remains from those of the more common sheep (*Ovis aries*). At the same time, the relative scarcity of this species in the archaeological records for the Middle Ages (c. 1066-1500) has contributed to the perception that this animal was not important, and therefore not worth analysing in detail.

There are in fact, various important historical and archaeological questions related to the medieval goat that call for an answer, but their understanding is dependent on our ability to identify goat bones accurately. Both historical (Dyer 2004) and archaeological (Albarella 1997) sources indicate a gradual decline of this species in the course of the Middle Ages. Although some hypotheses for this decline have been raised, the dynamics, extent and timing are still far from understood. In addition, from the study of English medieval bone assemblages an intriguing pattern emerges; on the one hand, a scarcity of goat bones and teeth is recorded but, on the other, there is a much greater abundance of horncores. This has led to different hypotheses, such as the possibility of an international trade in goat skins (Albarella 2003). In more general terms, the overall role that the goat played in English medieval husbandry is still far from clear. The goat is, for instance, more commonly recorded in the 11th-century Domesday Book than one would expect from its occurrence in the archaeological record (Albarella 1999). Whether the reason behind this discrepancy is due to an overestimation in the written sources, or an under-recording of goat bones by zooarchaeologists, is unclear.

Medieval bone assemblages have been studied by a wide variety of researchers, each possessing highly variable skills in identifying goat bones, and also at different times when different identification criteria were available. The most commonly used morphological criteria for sheep/goat postcranial identification were published over 40 years ago (e.g. Boessneck 1969; Boessneck *et al.* 1964; Kratochvíl 1969), but identification methods based on teeth are much more recent (Halstead *et al.* 2002; Payne 1985). All these criteria have recently been subjected

to various refinements and verifications (e.g. Fernández 2001; Fernández 2002; Zeder and Lapham 2010; Zeder and Pilaar 2010).

Despite these contributions, problems still affect the ability of zooarchaeologists to correctly differentiate the two species. For instance, many of the adopted criteria have been established by analysing goat specimens from many different parts of the world, and not all of them necessarily apply to British populations. A further problem is that many criteria are based on morphological differences whose assessment may be highly subjective (visibility and reliability of known morphological traits vary according to different factors: breed and age of the animals, ability and experience of the observer, as well as the completeness of reference collections). In addition, since archaeological reports often include the two taxa (sheep and goat) in a single sheep/goat category, with no or little attempt to separate the two, it is very difficult to compare sites reliably and also get a realistic overview of the importance of the goat in different regions and at different times in England.

A review of the literature concerning the role that the goat played during the Middle Ages in England, have led to the formulation of the following aims for this thesis:

1. To determine to what extent the published morphological criteria generally used for the separation of sheep and goat bones are applicable to breeds and populations from England.
2. To establish the degree of influence of factors such as sex and age on the visibility and reliability of morphological criteria.
3. To translate morphological features into biometrical indices, focusing, as much as possible, on central and northern European modern animals.
4. To provide a baseline of modern sheep and goat morphometric data useful to zooarchaeologists.
5. To provide a new methodology based on morphometry, which will:
 - I. represent an objective tool for the identification of sheep and goat archaeological bones.
 - II. have the potential to be applied beyond the Middle Ages as an additional *Ovis* and *Capra* identification tool.
6. To start a re-assessment of the role that the goat played during the Middle Ages in England by re-analysing a number of English medieval sheep and goat bone assemblages with a proposed new methodology.

7. To reconsider the hypotheses regarding the potential trade in goat horns and skins with the continent during the medieval period.

1.1.2 Description of the structure of the thesis

This thesis is divided into two correlated parts: Part I (Chapters 1 and 2) focuses on the development of a new methodology through the study of modern sheep and goat material. Part II (Chapters 3 and 4) presents the application of such new methodology on a number of English medieval sheep and goat assemblages, thus assessing the reliability of previous identifications and estimating the abundance of the goat in such case studies.

Part I of the thesis starts with an opening section on taxonomy (Section 1.2). The methodological background is outlined in Section 1.3 in order to contextualise the research questions of the project. In the same Section the limits of previous approaches (morphological, biometrical and bio-molecular) are highlighted and the benefits of the proposed new methodology are discussed. An evaluation of the historical and archaeological issues regarding the goat in the English medieval period follows (Section 1.4), beginning with a consideration of the evidence from written sources (Section 1.4.1). The archaeological evidence follows, and an overview of the relative frequency of goats during the Middle Ages is provided. A brief explanation of the main hypotheses concerning the decline of the goat is also included, followed by the analysis of the anatomical representation of this animal in medieval archaeological assemblages (Section 1.4.2).

Chapter 2 is divided into two main sections. The first part is dedicated to an in-depth description of the methods and materials (Sections 2.1 and 2.2). The morphological traits selected from published literature are presented (Section 2.1.2), along with the measurements which form the new recording protocol. Traditional as well as newly devised measurements (Section 2.1.3) are described together with the adopted recording protocol (Section 2.1.4). Section 2.2 is dedicated to the description of the modern sheep and goat specimens making up the modern samples: the full set of information regarding the modern animals is provided, including age, sex, breed and degree of completeness. In section 2.3 the results of the Inter and Intra-Observer Error trial, conducted to verify the replicability and reliability of the measurements included in the new recording protocol, are presented.

The second part of Chapter 2 focuses on the presentation of the results from the analysis of the modern material. Section 2.4 presents the study of the reliability of the chosen morphological traits, leading to a proposed short-list of the most diagnostic and reliable traits. An evaluation of the effects of sex and age on the reliability and visibility of such traits is also attempted (Section

2.4.2 and 2.4.3). The following section (Section 2.5) presents the results of the biometrical analysis: linear measurements and biometrical indices are presented first (Section 2.5.2 and 2.5.3). Statistical analysis then follows (Section 2.5.4). The results from the Mann-Whitney U test and Manova test (Section 2.5.5) along with Discriminant Analysis (Section 2.5.6) and Principal Component Analysis (Section 2.5.7) are then outlined on an element by element basis. Finally, in Section 2.6, general considerations about the results obtained from the application of the new methodology on modern material are summarised.

Part II of the thesis starts with Chapter 3, which focuses on the application of the new methodology to a number of medieval English archaeological sheep/goat assemblages. The first case study is the port and town of King's Lynn in Norfolk. The re-examination of the sheep and goat remains from the site is presented and discussed in Section 3.2. The second case study is represented by the site of Flaxengate, Lincoln. Only some key contexts have been chosen from this site and the results are presented in Section 3.3. Finally, the results from the analysis of the third sheep/goat bones assemblage studied, Woolmonger/Kingswell Street in Northampton, are outlined in Section 3.4. Section 3.5 presents a discussion of the level of success of the new methodological approach on the archaeological material. Section 3.6 re-assesses the likely role that the goat had in medieval England, in light of the presented results. The thesis proceeds with an evaluation of how the research could be expanded and improved (Section 3.7).

The thesis concludes with Chapter 4, which summarises the results obtained by this project.

1.2 Taxonomy

The domestic goat *Capra hircus*, belongs to the mammalian order Artiodactyla, suborder Ruminantia, family Bovidae, sub-family Caprinae, tribe Caprini, genus *Capra*. The sheep (*Ovis aries*) is also included in the tribe Caprini, and is therefore closely related to the goat.

The genus *Capra* includes several species (Corbet 1978; Corbet and Hill 1980 in Mason 1984: 87; Willson and Reeder 2005), as shown by Table 1.1.

Table 1.1 List of species of *Capra* with their common name.

Scientific Name	Common name
<i>Capra aegagrus</i>	the bezoar or wild goat, the animal which is recognized as the ancestor of the domestic goat
<i>Capra ibex</i>	the alpine ibex
<i>Capra caucasica</i>	the west Caucasian tur, sometimes regarded as a subspecies of <i>Capra ibex</i> (<i>C.i. severtzoi</i>);
<i>Capra cylindricornis</i>	the tur of the eastern Caucasus
<i>Capra pyrenaica</i>	the Spanish ibex or Spanish wild goat
<i>Capra falconeri</i>	the markhor
<i>Capra nubiana</i>	the Nubian ibex
<i>Capra sibirica</i>	the Siberian ibex
<i>Capra wallie</i>	the Wallia ibex

The tribe Caprini includes five genera. Apart from *Ovis* and *Capra*, the tribe also includes the tahr of the genus *Hemitragus*, and two species closely related to *Capra*, *Ammotragus lervia* (Barbary sheep) and *Pseudois nayaur* (blue sheep) (Gray 1972 in Mason 1984:87; Schaffer and Reed 1972). The tahrs are divided into three species, *Hemitragus jayakari* (Arabian tahr, mainly found in the mountains of Oman), *Hemitragus jemlahicus* (Himalayan tahr) and *Hemitragus hylocrius* (Nilgiri tahr, common in the Nilgiri hills of southern India).

The Rocky Mountain goat, *Oreamnos americanus* is regarded as belonging to the sub-family Caprinae, along with *Rupicapra rupicapra* (Walker 1975); they both belong to the same tribe Rupicaprini (Rideout and Hoffman 1975).

1.3 Methodological background

The difficulty in distinguishing between sheep and goat bones is very well known to zooarchaeologists. One of the most commonly adopted approaches to distinguish the bones of the two animals is based on the study of morphological differences. Despite the usefulness of this approach, some limitations have also been identified (e.g. the method is highly subjective, the visibility and reliability of the morphological traits vary according to many factors). Consequently, researchers have moved in different directions in order to find new methods which could make sheep/goat identification easier and more reliable.

In this section the different methodological approaches developed are explored and discussed, and the contribution of this research to the problem is outlined.

1.3.1 Morphological approach

Boessneck (1969: 331) in his well-known paper “Osteological differences between sheep (*Ovis aries* Linnè) and goat (*Capra hircus* Linnè)” stated: “*It is well known that to distinguish between the bones of sheep and goat presents great difficulties*”. His contribution, along with other pioneering works (i.e. Cornevin and Lesbre 1891; Gromova 1953; Hildebrand 1955) paved the way for the development of many other studies, which operated in two main directions. On the one hand, the focus was on providing new diagnostic morphological traits and checking their reliability on a variety of modern and archaeological samples, while, on the other, the awareness of the limits the morphological approach entailed, led to the development of studies aimed at finding new and more objective methods for resolving the identification issue.

1.3.1.1 Post-cranial bones

The paper by Cornevin and Lesbre (1891) is probably the earliest study that brought to light the problem of sheep and goat identification. In their research, the authors took into consideration a number of cranial and postcranial elements from a sample of modern sheep and goats. The analysis carried out included the observation and study of some morphological characteristics considered diagnostic by the authors, along with the application of a series of indices that relied heavily on the length of the bones. The study revealed that, while there were only few morphological traits in teeth that could aid species identification, for other anatomical parts the results were more promising. The cranium and horncore showed diagnostic features and the same was the case for atlas, axis and the other vertebrae. Some other elements, as for example the humerus and the radius, were considered to be useful. Metapodials were observed to have distinctive morphological traits and the ratio between length and width was also proposed as a good indicator for species discrimination. The shape of the 3rd phalanx was also regarded to be diagnostic.

A later study, authored by Gromova (1953), identified morphological traits as well as some biometrical indices. Hildebrand's study (1955) had a more general purpose but it still represents a valuable contribution to the issue of sheep/goat identification. The author presents a description of morphological differences not only between sheep and goat but also between these two species and deer, with the goal of establishing identification keys to be used independently from a comparative collection. Hildebrand proposed some new morphological features, excluded those that had proven to be unreliable and reinstated the reliability of some other traits. Moreover, he proposed the use of ratios of measurements as an additional tool that could be used in combination with morphological features. The study concludes that only some skeletal parts (i.e. metacarpal, scapula, pelvis and ulna) bear diagnostic features. The effort put into the use of biometry and ratios is praiseworthy, although they are used in an obscure way. The author does not really explain how the measurements were exactly taken; he provides only

some data (i.e. mean, number of specimens, coefficient of variation) leaving the reader to deal with formulae that are difficult to use. In addition, the lack of diagrams or scatterplots used as a visual aid to demonstrate the effectiveness of the ratios makes understanding of the biometry section difficult. Hildebrand based his observation on a small modern sample for which background information (such as age, sex and breed) was often omitted. Even though the skeletal elements he took into consideration were exclusively postcranial, a great variety of elements was examined. Although such a wide *spectrum* of anatomical elements greatly enriches our knowledge of which body part is most diagnostic, it reveals the extent to which the study was not designed as an aid for the zooarchaeologist, since it includes anatomical parts that are not usually well preserved in archaeological assemblages.

The study conducted by Boessneck and colleagues (Boessneck *et al.* 1964), along with its later shortened English version (Boessneck 1969) provided a complete analysis of the morphology of cranial and post-cranial bone of sheep and goat, with the specific aim of providing a tool to zooarchaeologists.

The study mainly takes into consideration a wide range of morphological characteristics, which are described in a standardized way, but also some measurements and ratios. A wide and heterogeneous sample of modern skeletons of domestic sheep and goat forms the core of the study. The skeletal elements considered were mainly postcranial (of which only a few were excluded such as the distal end of the tibia considered to lack diagnostic features); the only cranial elements included were the horncores. As the whole paper is built around the idea of finding identification keys suitable for archaeological material, the researchers also applied their method to archaeological assemblages from the Celtic *Oppidum* of Manching and the Roman *Emporium* of Magdalensberg, in addition to other archaeological assemblages, to test the criteria. Unfortunately, the results obtained from the application of the method on archaeological assemblages did not receive enough attention in the publication: the results, in fact, are not fully shown, so the paper does not provide a clear idea of the extent to which the features noted on modern specimens could be reliably applied.

Later studies tried to check the reliability of the criteria proposed by previous literature, as well as introduce new ones. Schramm (1967), for instance, used a fairly large modern sample to evaluate the work of Gromova (1953) and Boessneck *et al.* (1964), but also proposed some new metric indices. Many skeletal elements are considered in this study, but biometrical indices were calculated only for the atlas and the scapula.

The gap left by the previous authors regarding the tibia was soon filled by Kratochvíl (1969), who focused his attention on the morphology of the distal articulation of this skeletal element. On the basis of observations on modern and archaeological material Kratochvíl, *contra* previous authors, regarded the distal tibia as diagnostic and suggested some identification criteria.

Although his archaeological sample is large (n=200) he provides little details about its nature, and the drawings in his paper are schematic (Fig. 1.1). Nonetheless, Kratochvíl's is a useful paper, filling a gap left by previous literature and highlighting the diagnostic value of a bone that is commonly found on archaeological sites.

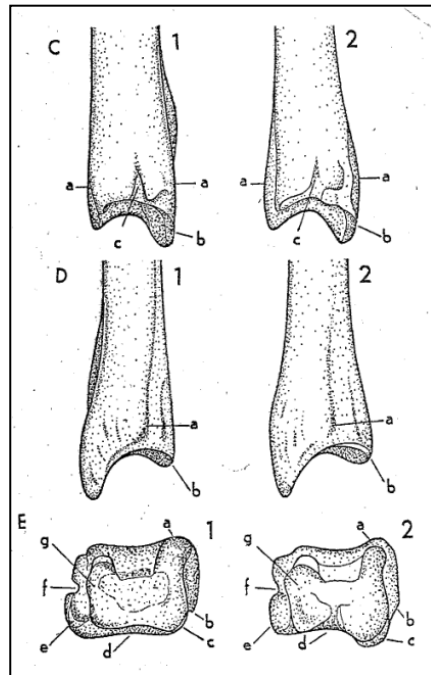


Figure 1.1 Diagnostic characteristics on the distal tibia (1=goat; 2=sheep; C=lateral side; D= medial side; E= distal articular surface. Image reprinted from Kratochvíl, Z. Species criteria on the distal section of the tibia in *Ovis ammon* F. aries L. and *Capra aegagrus* F. hircus L. *Acta Veterinaria* (Brno), copyright 1969, 38: 483-490. Licence available at: <https://creativecommons.org/licenses/by/4.0/>).

The increased interest in sheep/goat identification meant that researchers from all over the world started to routinely attempt a separation between the two taxa using most anatomical elements (Buitenhuis 1995: 141). An early archaeological application is represented by the analysis of the faunal remains from Deh Luran Plain (Hole 1969). The author used both morphological characteristics and biometrical indices with the main aim of investigating the origins of domestication in the Fertile Crescent. The author mostly focused on horncores, distal metapodials and 3rd phalanges as these were considered the most diagnostic elements at that time. Other criteria and elements were examined but the author did not feel confident enough to use them, as attested by this quote: “some (characteristics) may be reliable, but we did not trust our own ability to detect the subtle difference involved” (Hole 1969: 270). Although only a few anatomical elements were considered the results were promising, with good clustering of the two species obtained when Gromova's distal metapodial biometric indices (Fig. 1.2) were used.

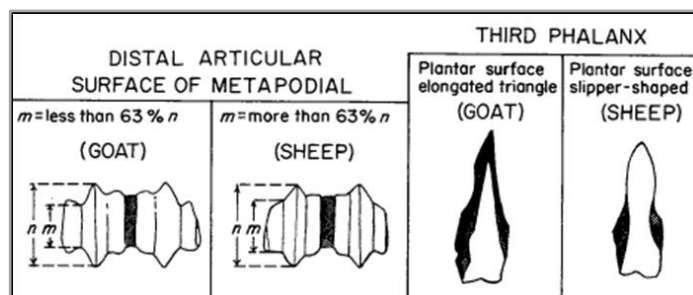


Figure 1.2 Index adopted on the distal metapodials and morphological traits considered for each bone following Gromova 1953 and Boessneck *et al.* 1964 (image reprinted from HOLE, F. The context of the caprine domestication in the Zagros region. In *The origins and spread of agriculture and pastoralism in Eurasia*, ed. D.R. HARRIS, 263-281, copyright 1996. London: University College of London press, with permission from Kent Flannery, Joyce Marcus and Frank Hole).

In terms of the morphological approach, Hole managed to get good results for the horncore but less for the 3rd phalanx.

Another contribution which deserves to be mentioned is Gabler's dissertation, presented in 1985 at the University of Munich. His study dealt with the osteological differences between the Barbary sheep (*Ammotragus lervia*), the domestic sheep (*Ovis aries*) and the domestic goat (*Capra hircus*). The research, conducted on a small sample size, highlighted the morphological differences on the post cranial bones of these species (with a particular focus on the traits useful for identifying Barbary sheep). The author also used biometry but only to investigate size differences, reaching the conclusion that the Barbary sheep is easier to identify as it is always bigger than *Ovis aries* and *Capra hircus*.

The research conducted by Prummel and Frisch (1986) evaluated previously proposed criteria and suggested new ones. In order to accomplish the first task, the authors tested the diagnostic traits on two large early medieval assemblages from north-east Europe - Haithabu and Oldenburg (Holstein, Germany). The results showed that while some criteria worked, others failed. Useful features for discriminating the two species were noticed on several elements (skull, scapula, humerus, radius, ulna, metapodials, femur, tibia, calcaneum and astragalus), which were proposed as the most diagnostic body parts. To contribute to the future development of the morphological approach, the researchers proposed some new diagnostic features on the pelvis, with the intent to establish the sex of sheep, and on metapodials to determine the body size of both species. These new traits, although they represent a valuable addition to zooarchaeological methods, do not actively contribute to improving our ability to distinguish sheep and goat.

A few years later, Clutton-Brock *et al.* (1990) published a study whose aim was to categorize the osteological traits specific to the Soay sheep. The study sample was of a large collection of Soay sheep, a breed from the Scottish Western Isles, broadly unimproved and therefore

representing a potentially useful proxy to past animals. The sheep included in the sample were also reproductively isolated, so that any variation was due to individual differences or sexual dimorphism rather than artificial selection or breeding strategies. Attention was focused on testing the morphological traits of several cranial and post cranial elements. For each element, different morphological characteristics, mainly taken from previous studies (Boessneck *et al.* 1964), were recorded as sheep-like, goat-like or intermediate. A small sample of goats from Scotland was then used for comparison. The result of the study suggested that only a few traits were valid for species identification, when used on their own. These included morphological characteristics of the skull, axis, scapula, femur, metatarsal and the 3rd phalanx. The authors also attempted to use some of the biometrical indices (following Boessneck *et al.* 1964); since the results are highly relevant to this research, they will be discussed in greater detail later in this chapter. The authors concluded that, despite the unreliability of several of the morphological criteria, when morphology is combined with biometry, identifications to species level could be made with a higher degree of confidence.

Helmer and Rocheteau (1994) provided further methodological advancement with the proposal of some new morphological diagnostic criteria. In this study, additional taxa were included (i.e. roe deer, chamois and gazelle). Only two anatomical elements, the scapula and the humerus, were considered as the study was presented as the first part of a larger project in which other elements would have eventually been discussed. The authors briefly described the morphological traits along with accurate drawings, providing a useful aid in understanding the suggested differences. The morphological traits considered were then successively tested on the animal bone assemblage from the pre-Neolithic site of Cafer Höyük (Turkey). Unfortunately, the application of the method on archaeological material is not explained in detail, so that the reader is not informed about the number of bones considered or the result obtained.

Buitenhuis (1995) published a study aimed at testing the reliability of already known morphological traits by using a quantitative approach. Wild and domestic modern sheep and goat material was used by focusing on just one anatomical element, the scapula. Firstly, the standard morphological approach was adopted so that six morphological features out of 11 were considered and scored in their own terms (curved, straight, etc.). The results from this scoring system were that, it was impossible to state with certainty to which species specimens with mixed scores-values belonged to. Statistics (Principal Component Analysis) were also employed to better investigate the traits and the extent to which they contributed to the separation of the specimens. Two functions were found, one linked to the shape of the *collum* and the *processus* of the scapula, the second describing the articulation. The coefficients calculated, when plotted, showed a separation between genera in both wild and domestic animals. Buitenhuis ran a further test that indicated that sex did not bias the visibility of morphological characteristics, but age did. Nevertheless, this influence was shown not to unduly compromise the separation between

the two species. Aware of the importance of applying and testing this new approach on archaeological material, Buitenhuis applied the same method on archaeological *scapulae* from three archaeological sites: the pre-ceramic Neolithic site of Asikli Höyük in central Anatolia, the early Neolithic site of Bouqras in Syria and the late Neolithic/late Chalcolithic site of Ilipinar in north-west Anatolia. The output revealed that the method was successful only in some cases. In an attempt to explore all the available tools, the author also applied some biometrical indices on the scapula, such as those suggested by Boessneck *et al.* (1964), namely ASG:SLC, GLP:BG and Ld:HS (for the definition of the measurements see Boessneck *et al.* 1964). These indices, when applied to recent comparative material, gave unsatisfactory results as the separation was not really clear. The same results were unfortunately obtained with some of the archaeological material: the separation between the taxa was ambiguous, due to the interference of size.

It was in the extensive study by Fernández (2001) on the morphological differences between different Eurasian ruminants (i.e. sheep, goat, roe deer and chamois) that a full analytical review of the reliability of the morphological differences known from previous literature was accomplished, along with the introduction of some new criteria. She analysed a sample composed of modern specimens for which some information was provided. Fernández took into consideration several body parts (i.e. humerus, radius, ulna, metacarpals, femur, and tibia, along with some tarsal bones such as the astragalus, calcaneum and the scapho-cuboid), whose morphological characteristics she scored as 'strong', 'intermediate' or 'weak'. She then identified the characteristics that were more reliable with the ultimate outcome being represented by a list of morphological traits with their quantified degree of reliability. This list, in the specific case of sheep and goat distinction, included 38 potentially useful characteristics which are located on the distal articulation of the humerus, the proximal articulation of the radius, the astragalus and the calcaneum. In addition to the extensive analysis of the morphological traits, Fernández applied some previously published and some new metric criteria, mainly used to translate morphological traits into biometrical indices. The biometrical approach adopted by Fernández, of importance for this dissertation, will be discussed in greater detail later in this chapter. Overall, it can be said that Fernández's study represents the most detailed analyses of the morphological characteristics useful for distinguishing between different caprine species that has been published since Boessneck *et al.* (1964); as such it represents a significant contribution to the development of the research. Her technique, as well as those proposed by Buitenhuis (1995) and Clutton-Brock *et al.* (1990), permits the quantification of the probability of making an incorrect assessment according to which morphological features have been used.

Subsequently, Fernández (2002) published a shortened version of the morphological approach she presented in her unpublished doctoral thesis. Fernández' brief contribution, which focussed on just a few elements (distal end of humerus, proximal end of radius and ulna, distal end of

femur and proximal end of tibia), is due to the fact that her method was applied on the Switzerland archaeological material by Velarde. Unfortunately, the extent to which the method can be applied to archaeological material reliably is not really reported. The reader is only provided with the final results of the analysis, which indicates that of 1726 caprine fragments 9% could be attributed to sheep and 2% to goat, while the rest of the bones could not be distinguished. A difficulty was the presence of young individuals, which were difficult to assign to species level. Unfortunately, in this paper no attempt was made to use Fernández' biometrical indices; a pity as testing the indices on other archaeological material would have assessed the potential of her approach.

Zeder and Lapham's (2010) more recent attempt to assess the reliability of sheep/goat identification criteria indicates that the issue is still very much alive – and contentious. They used a large and heterogeneous sample of modern domestic and wild sheep and goat. A selection of the most promising anatomical elements was chosen and the observed criteria derived mainly from previous literature (Boessneck 1969; Boessneck *et al.* 1964; Gromova 1953; Helmer & Rochetau 1994; Kratochvíl 1969; Prummel and Friesch 1986) and the experience and observation of the authors. Each characteristic was scored using a scale which included three categories: 'consistent with goat', 'consistent with sheep' and 'not clearly identifiable'. The results from the testing on the modern material revealed that the characteristics were reliable especially in goats while in sheep they were often less strongly expressed; nevertheless, the output was very positive in both taxa. The only element which performed poorly was the distal tibia. To add strength to their study, a blind test was also run: different anatomical elements were given to a group of researchers to identify to species using the same morphological criteria. The results of the blind test agreed in general with what was achieved through the analysis of the modern material carried out by Zeder and Lapham; nevertheless the higher variability in the blind test showed that training is necessary before attempting to apply the criteria on archaeological assemblages. As this study was included as part of a wider research project on the domestication of sheep and goat in the Fertile Crescent, the influence of sex, age and status (feral, wild, domestic) on the morphological features was also investigated, with the result that sex and status did not affect the reliability of the features. A different result was obtained when age was considered: when the sample was divided into different age classes the results revealed that all the elements performed well in all the age classes apart from classes A and B, namely animals younger than one year for which there were more indeterminate assignments. If the modern sample is taken into consideration, two observations can be made. First of all, the sample is clearly biased toward the sheep group which is significantly more numerous. The results of the analysis show that the characteristics are generally more reliable in goat than in sheep and this might have been influenced by the higher variability represented in the larger sheep group. Secondly, doubts about the applicability

of this study on assemblages of later historical periods, where the animals were only domestic, could arise as most of the modern animals making up the sample were wild.

Finally, it is worth mentioning another study, though this has remained unpublished for many years. Spearheaded by English Heritage, particularly in the person of Sebastian Payne, a 'sheep/goat working party' was established in the late 1980s (pers. comm.). It had two main purposes:

- to establish which morphological criteria from the known literature were used and considered reliable by zooarchaeologists;
- to identify the measurements that, chosen according to factors such as usefulness, frequency of occurrence on archaeological material and high reproducibility, could contribute to the sheep and goat identification; this should eventually led to the elaboration of a short and standardised list of measurements which could be used internationally.

It was and still is generally known that, among zooarchaeologists, differences are present regarding not only the anatomical parts considered helpful when dealing with sheep/goat distinction, but also the degree of reliability attributed to the known morphological criteria by different researchers. As a consequence, the zooarchaeologists involved in the 'sheep/goat working party' decided to circulate a survey among a number of experienced colleagues in England, with the specific aim of finding out which anatomical elements were considered to be more useful for distinguishing the two species and, how reliable the specialists considered the identifications assessed through the use of these elements. The results revealed that the skeletal elements mostly used were the horncores and the distal metapodial bones. Several researchers expressed a preference for the deciduous fourth lower premolar (dP₄), distal humerus, proximal radius and third phalanx. The other skeletal parts were used only rarely or not considered at all. Despite evidence of moderate consensus, among the 24 anatomical parts considered, the fourth lower deciduous premolar (dP₄) and the distal tibia were the elements about which the surveyed researchers were least in agreement. In addition, when the opinions of the surveyed researchers on the reliability of the traits were considered, the output clearly showed a relationship between frequencies of elements used for identification and estimates of reliability: horncore and metapodials were still the elements which were thought to be the most reliable by the researchers interviewed. The study also included an investigation of which measurements were most useful for species identification and an analysis of the definition and reproducibility of those measurements, the results of which will be explored in the next section.

Table 1.2 List of the major studies on the topic with a brief description of sample used, the anatomical elements considered, the morphology and/or biometry approaches adopted.

Paper	Species	Sample	Info	Elements		Morphol. criteria	Biometry	Archaeol. application	New traits
				Cranial	Post-Cranial				
Cornevin and Lesbire 1891	Domestic and wild sheep and goat	-	Some	Yes	Yes	Yes	Some	-	-
Gromova 1957		-				Yes	Some		-
Hildebrand 1955	Sheep; Goat; Deer	Small (< 30)	Some	No	Yes	Yes	Some	-	Some
Boessneck <i>et al.</i> 1964; 1969	Sheep; Goat	Large	Some	Yes	Yes (tibia not included)	Yes	Some	Yes but not explained	Some
Schramm 1967	Sheep; Goat	Acceptable	Some	Yes	Yes	Yes	Some	-	-
Kratochvíl 1969	Domestic and wild sheep and goat	Small (<30)	-	No	Only distal tibia	Yes	-	Yes but not explained	Yes
Clutton-Brock <i>et al.</i> 1990	Sheep (Soay); Goats	Large	Known	Yes	Yes	Yes	Some	-	-
Hole 1969	Sheep; Goat	-	-	No	Only some	Yes	Some	Yes	-
Prummel and Frisch 1986	Sheep; Goat	Large but only archaeological	-	Yes	Yes	Yes	-	Yes	Some new traits but not focused on sheep/goat separation
Helmer and Rocheteau 1994	Sheep; Goat; Wild caprines	-	Only breed	No	Only humerus	Yes	-	Yes but not explained	-
Buitenhuis 1995	Domestic and wild sheep and goat	Acceptable	Only species	No	Only Scapula	Yes, also statistic is used	Yes	Yes	-
Fernández 2001	Sheep; Goat; Roe deer; Chamois	Large but some species are not highly represented (goats)	Yes	No	Yes	Yes	Yes	Yes	Yes
Fernández 2002	Sheep; goat	Large but only archaeological	-	No	Yes	Yes	-	Yes	-
Zeder <i>et al.</i> 2010	Sheep; Goat	Large but biased toward sheep and wild specimens	Some	No	Yes	Yes	-	-	-
English Heritage (forthcoming)	Sheep; Goat	Small (<30)	-	Yes	Yes	Yes	Yes	-	-

From the above review (see also Tab. 1.2) it can be seen that, although most papers have been written and developed as independent pieces of work all aimed to solve the same identification problems, the conclusions reached by different researchers at different times are very similar. First of all, no individual traits that allow an entirely unambiguous separation between the two species. It is, however, often the case that a combination of traits can increase the probability of a specific identification. Secondly, all researchers were aware of the fact that some of the criteria tend to be less clear or consistent, and therefore less reliable. They also realised that the

degree of reliability is influenced not only by the variability of the samples but also by the experience of the researcher. This is the reason why many authors highly recommend training and previous practice before starting to study any kind of material, as a ‘trained eye’ is more efficient in identifying the traits and in attributing them to the right *taxon*. Finally, as a consequence of the high subjectivity of this approach, a number of researchers have recommended the use of biometry, as an additional tool to be used for increasing the probability of assessing sheep/goat identification accurately.

Some common limits to these previous studies can be identified, and they concern mainly three categories: the method, the analysed sample and the application to archaeological material. Regarding the method, as soon as the limitations of the traditional morphological approach emerged, many researchers tried to focus on finding more objective means for identification purposes. Biometry, indices and statistical analysis were applied on sheep/goat bones but often, when these tools were applied, they were not fully explored or were not explained in detail. If the nature of the sample used is considered, two main problems can be detected: the lack of any information about the origin, age, sex and life history of some of the modern animals studied and the heterogeneous nature of the samples. Although the inclusion of specimens of different age, sex and breed has the potential to represent all possible variation, it also does not allow the limitation of these variables. The heterogeneity issue is, in some cases, worsened by the inclusion of wild specimens (often making up a high proportion of the sample). Wild specimens can present characteristics that can be more obvious or simply divergent from those shown by their domestic counterparts; the study of the morphological characteristics on the wild species is important especially if dealing with archaeological sites where domestication first appeared but, at the same time, in other contexts, this can be a cause of confusion and bias. Despite the aforementioned heterogeneity of the samples used, a pattern can be identified which is the tendency to avoid studying young animals. These are, in fact, believed to be less reliable as, because of their young age, characteristics are thought to be less well defined; this is, however, an issue that has not yet been properly addressed. Lastly, one of the main critiques that can be made to the previous studies is that the method has often not been extensively applied to the archaeological material (or, when it was, no details were given of the results), in order to check whether the characteristics are as visible and reliable as they were on modern material. This is an important drawback, especially if the study itself is aimed to help zooarchaeologists in dealing with the identification of sheep and goat from archaeological assemblages.

1.3.1.2 Mandibular teeth

Following the development of the previously mentioned studies, several researchers focused their efforts on identifying morphological features on sheep and goat teeth, with a particular interest in mandibular teeth, as mandibles tend to survive deposition better than maxillae (Binford and Betram 1977; Lyman 1984); as such mandibular teeth represent a valuable source

of information with the potential to contribute to identification of the two closely related species.

The most commonly applied method for discriminating mandibular teeth of young sheep and goat is the one designed by Payne (1985). He focuses his attention on a small sample of modern specimens (12 for each species) belonging to Greek breeds. The teeth taken into consideration were: first deciduous incisor (dI₁), second deciduous lower premolar (dP₂), third deciduous premolar (dP₃) and, fourth deciduous premolar (dP₄) and first lower molar (M₁). On these the author describes several morphological traits he considers useful for sheep/goat identification (see Fig. 1.3 for some traits identified on the dP₄).

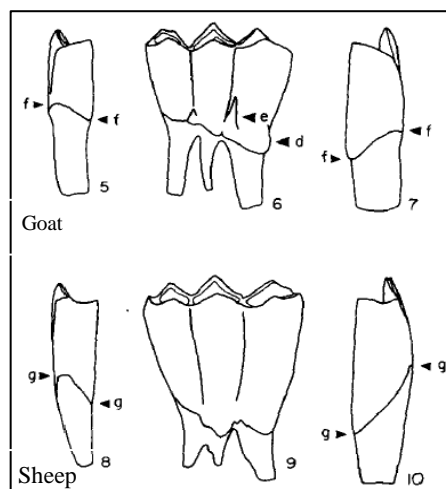


Figure 1.3 Some morphological traits on the fourth deciduous lower premolar (dP₄) proposed by Payne (image reprinted from PAYNE, S. Morphological distinctions between the mandibular teeth of young sheep, *Ovis*, and goats, *Capra*. *Journal of Archaeological Science* 12: 139-147, copyright 1985, with permission from Elsevier). 5-7 are respectively mesial, buccal and distal views of a dP₄ of a kid; 8-10 mesial, buccal and distal views of a dP₄ of a lamb.

The outcomes of the study were promising as some morphological traits were revealed to be successful on the modern material; nevertheless some caution is suggested by the author himself. Payne, in fact, strongly suggests the consideration of a combination of traits when assessing identification. The author was also aware of the small size of his sample but he believed in the potential of the identified traits. Unfortunately, he did not try to assess the effectiveness of his observations on archaeological material. A limitation of this method is that the visibility of some characteristics can be linked to different factors, for example some traits can be visible only if the tooth is loose. An even greater limitation is represented by the degree of wear of the tooth: if the abrasion is heavy, the visibility of the characteristic can be compromised or even impossible to assess, as Payne himself acknowledged.

Helmer (2000) published a paper focused on the study of permanent lower teeth and proposed diagnostic traits detectable on the third permanent lower premolar (P₃) and the fourth permanent

lower premolar (P₄). The criteria were tested on a sample of 40 modern mandibles of sheep and goat specimens with very promising results, as the traits permitted differentiation of the two species. Later, the author applied the new method on an early Neolithic archaeological sample from Greece - Dikili Tash - to evaluate if the traits were also effective on archaeological material. By making a comparison between the relative presence of sheep and goat established through the analysis of the postcranial bones, and the relative presence of the two taxa defined through the study of the permanent premolars, the results showed that the output from the two approaches was consistent. As a consequence, the validity of the traits on permanent teeth for sheep/goat differentiation was confirmed. In agreement with Payne, Helmer suggests that more than one characteristic is considered when evaluating identification. While some traits presented by Payne are not visible if the tooth is in jaw, Helmer's traits are mainly located on the occlusal surface so they are more likely to be recognisable even in non-loose teeth. Despite this advantage, the influence of the tooth wear on the ability to assess the criteria still represents a constraint of the method; a problem the author is aware of (Fig. 1.4).

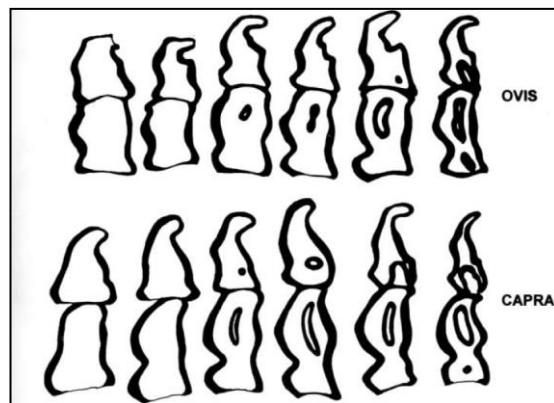


Figure 1.4 Sequence showing the changes of third and fourth permanent lower premolars (P₃ and P₄) according to wear stages (image (Fig. 2) reprinted from Helmer, D. *Discrimination des genres Ovis et Capra à l'aide des prémolaires inférieures 3 et 4 et interprétation des âges d'abattage: l'exemple de Dikili Tash (Grèce). Anthropozoologica* 31: 29-38, copyright 2000. Copyright Publications Scientifiques du Muséum national d'Histoire naturelle, Paris).

A more extensive study of the morphology of permanent teeth in sheep and goats was published slightly later (Halstead *et al.* 2002). In their paper the authors studied a large sample of mandibles of modern wild and domestic sheep and goats, in order to allow, in combination with the use of the criteria proposed by Payne for the deciduous teeth, identification of sheep and goat teeth from a wider age span. They establish criteria by looking at the permanent lower teeth - some similar to those identified by Helmer (2000) - but new traits on the permanent lower molars and on the mandibular *ramus* are also illustrated. The output of the study shows that the tested criteria were reliable. The authors warn the reader about the presence of specimens with

intermediate appearance or with inconsistent characteristics but, in most cases, the teeth could unambiguously be attributed to species. In order to test their method, the researchers applied it to various archaeological materials from Greece, Ireland and Scotland and the results confirmed that they could be used with some confidence on archaeological specimens too. The main problem experienced during the study of the archaeological material was the fragmentation of the material and the degree of wear of the teeth: factors which evidently limit the visibility of the morphological features. It must also be added that while the characteristics are well defined, accurately described and easily observable (Halstead *et al.* 2002), many intermediate forms can be found so that, even if a combination of traits is used, assessing the identification remains challenging.

A different kind of contribution is represented by Balasse and Ambrose's (2005) attempt to distinguish sheep and goat through staple carbon isotopes. The isotopic approach was, however, coupled with a study of the tooth morphological characteristics, based on Halstead *et al.* (2002) and some newly proposed criteria. These newly introduced traits proved to be reliable but they can only be seen on loose teeth. Also of interest in this paper are the results obtained from testing the morphological traits used by Halstead *et al.* on the Kenyan population of modern sheep and goats. Most of the traits on the first and second lower molars M_1 and M_2 proved to be unreliable, while better results were obtained from the permanent lower premolars and third lower molars (M_3).

The whole dental morphological issue was subsequently reviewed by Zeder and Pilaar (2010). A large sample of sheep and goat domestic and wild modern specimens was analysed. The criteria adopted were mainly those proposed by previous studies, with the addition of only a few new criteria. All the morphological characteristics were scored according to a scale which included: 'goat', 'sheep' and 'sheep/goat'. The final assignment was then made by taking into account all the scored traits. The results of the study revealed that certain teeth could not be reliably assigned to species: in older animals, molars appeared to be more unreliable than premolars, with the first lower molar (M_1) being the least reliable permanent tooth in goats. The traits on the mandibular ramus also did not provide good results: they were less reliable than the criteria on teeth, especially in sheep. Of the deciduous teeth, the most unreliable traits were those on the fourth deciduous lower premolar (dP_4), the assessed characteristic of which did not perform well in either species. Better results were given by the third deciduous lower premolar (dP_3) which seemed to be the only reliable tooth for discriminating younger caprines. It has to be mentioned that study was conducted on modern material, which means that the teeth evaluated were in jaws. Because of the nature of the material, some traits, such as the line between the root and the crown in the dP_4 , which is considered to be a reliable trait (Payne 1985), could not be assessed. Therefore the low reliability of the dP_4 is more likely to be due to the nature of the material than the limitation of the method. The study also revealed that while

the criteria were more effective on sheep, they were less reliable on goat; in fact, in the latter group, traits were more likely to be assigned to the sheep/goat category or to the wrong category. Regarding the effect of age on the reliability of these criteria, the authors claim that the identification of teeth of younger animals is highly unreliable, the identification of animals with a moderate state of wear is easier than erupting or highly worn teeth and that old animals, with heavy tooth wear, are difficult to classify.

While the paper by Zeder and Pilaar (2010) provides an assessment of the reliability of the diagnostic morphological traits on teeth in modern material, the publication by Gillis *et al.* 2011 filled the gap relating to the testing of these same traits on archaeological material. The authors tested the morphological diagnostic traits for mandibular teeth, taken from the previous literature, on a very unusual archaeological assemblage, made up of 90 almost complete sheep and 13 goat specimens from a burial site in Sudan, dated to the 3rd and 2nd millennia BC. The aim was to test not only the reliability of the traits but also their efficiency. 38 criteria were tested and the results demonstrated that the criteria performed better on deciduous teeth than those on the permanent premolars and molars; the determination of isolated permanent teeth was shown to be fairly reliable (P₃, M₁ and M₂) even though variation in the results was recorded according to the age and species of the animals. The authors compared also their results with the results obtained by Zeder and Pilaar (2010) and what emerged was that, for most criteria in both studies, there were similarities, especially concerning the efficiency and reliability of some traits.

1.3.2 Non morphological approaches

More recently, to overcome the limits inherent to the morphological method and in order to provide a tool that could permit an unambiguous taxonomic assignment, several non-morphological studies have been conducted.

One of the first attempts to distinguish the two species, by looking at methods other than morphology, was carried out by Grine *et al.* in 1986. A study conducted on a sample of first lower permanent molars (M₁), from 20 caprine specimens was carried out in order to see if the analysis of the enamel ultrastructure, through the use of a scanning electron microscope, could reveal differences between the two species. The results showed that it was impossible to distinguish between the two closely related species on the basis of qualitative characteristics, such as enamel formation pattern, as both species have the same prism packing pattern. Nevertheless, when quantitative parameters were considered, some differences that could allow discrimination between the two species were found. Unfortunately, this technique has not been tested on an archaeological sample and, as a consequence, we do not know to what extent it would be successful on old material. Even though the authors claim that it is not a destructive method, as the processes involved in sample preparation are reversible, the preparation requires

a considerable amount of time and implies the use of sophisticated equipment which would be very expensive to acquire.

Some years later, the first attempt to use molecular methods was conducted by Loreille and colleagues (1997). mtDNA was extracted from a small sample of sheep and goat bones from an archaeological assemblage in order to establish to which species they belonged. The results from this study showed that two different mtDNA sequences, without any intermediate sequence presenting a mixture of them, were found for the two species. The identification made through the mtDNA analysis agreed with the identification made through a morphological approach with the only difference that, in some cases where morphological traits could not be assessed because of their absence, the mtDNA analysis could establish which species the bones belonged. As such, this kind of analysis was shown to be useful not just as a tool for assessing the identity of bones but also as a test of the identification made through the traditional approach.

A further genetic study was undertaken by Bar-Gal and colleagues (2003). The study, focused on ancient DNA analysis, was carried out on caprine bones from a Neolithic site in Israel in order to discriminate between the two species. The results obtained were successful and showed the potential of this new method. However, the bio-molecular method introduced by Bar-Gal *et al.* along with the study conducted by Loreille *et al.*, presents some problems that must be taken into consideration. Firstly, DNA can survive only in specific conditions (e.g. if state of preservation is very good). Secondly, the procedure must be carried out carefully in order to avoid contamination, which can affect the results. Finally, it is a destructive method which also requires considerable time and special equipment, which is usually expensive.

Balasse and Ambrose (2005) presented the result of a study of stable carbon isotope ratios, applied to modern sheep and goat mandibles from Kenya. The identification of these two species by using carbon isotopes is based on the assumption that sheep and goat have different feeding behaviour; while the sheep is a grazing animal and feeds on grass, the goat is a browsing animal whose diet is based on herbs, bushes and trees. As a consequence, the ratio of $^{13}\text{C}/^{14}\text{C}$ isotopes, naturally present in grass and bushes at different levels, should be different for the two *taxa*. Despite the successful results this work produced, some disadvantages must be highlighted. The most limiting one is that this method can only be applied in areas dominated where C_3 and C_4 grassland environment are both present. In addition, this kind of analysis requires specific tools and is time consuming. Finally, it is a destructive method, it requires the tooth to be extracted from the mandible and drilled out in various areas of the crown to extract samples.

More recently, a successful attempt at using collagen peptide analysis was made by Buckley and colleagues (2010). They extracted a single collagen peptide from modern specimens of sheep

and goats from different breeds and then tested the presence of these markers on Neolithic animal bone assemblages from Turkey. The bio-molecular method was shown to have potential and also some advantages over other non-morphological methods. For example, the collagen peptide markers are not subject to degradation as with DNA, there is not such a high danger of contamination and the method appears to be easy, quick, cheap and requires only a small sample.

The potential of the new molecular approach has been confirmed by the latest research but, unfortunately, most of the time these methods do not represent an accessible means of study because of their high costs and destructive nature. In a standard research and commercial environment, there are rarely sufficient financial resources to be invested in isotopic or DNA studies. In addition, these analyses are time consuming, they require particular laboratories, specialists and scientific tools, which have a high cost and are not always easy to obtain. For these reasons, and also because the methodology proposed by this project represents an easier and more immediate option which can be applied routinely without additional costs, bio-molecular investigations are not considered further, though they can have their value in specific contexts.

1.3.3 Biometrical approach

The first attempt at translating morphological traits into biometrical indices was conducted by Boessneck *et al.* in 1964. Even though their paper focused on identifying morphological traits, attention was also given to testing biometrical indices on modern reference material. For instance, by looking at the different shape of the *collum scapulae* of sheep and goat, they suggested an index based on two measurements, which were demonstrated to be effective (Boessneck *et al.* 1964: 59). On the metapodials, two indices were found to be particularly effective as they measure particularly useful distinguishing features: one was based on the length and the distal breadth of the metapodial bones; the other was based on the ratio between the size of the trochlear condyles and the size of the *verticulli* (this latter is more effective on the metacarpal than the metatarsal). The ratio between the greatest width and the greatest length of the *os malleolare* in the calcaneum was also revealed to be effective. However, the biometrical component of the work was only very cursorily dealt with, which explains why, in following decades, that paper has almost exclusively been used for its morphological potential.

The study conducted by Payne (1969) on the distal metacarpal was the first to focus exclusively on morphometry. Payne suggests two measurements (Fig. 1.5) that can be taken on the distal articulation in order to discriminate the two taxa in archaeological assemblages. He applied the protocol on a modern collection and subsequently on archaeological material from sites dated to different periods, located respectively in England and Greece. Despite the author's cautious comment that there was no strong separation into two defined clusters, the absence of overlap

between the two groups (sheep and goat) is indicative of a successful result. Payne's biometrical study on metacarpal bones not only represents a milestone toward the creation of a new and more objective method for distinguishing between *Capra* and *Ovis*, but it also provided the momentum for a series of further studies in which his indices, and some new ones, were applied to a variety of archaeological, as well as modern collections, with the aim exploring the potential of the biometrical approach.

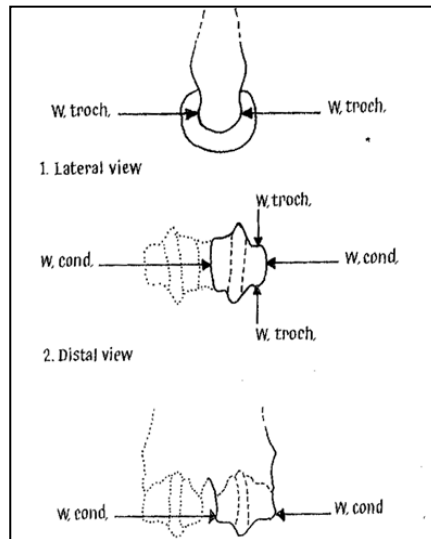


Figure 1.5 Measurements suggested by Payne (1969) as effective for discriminating sheep from goat, on the distal metacarpal bone (image reprinted from PAYNE, S. A metrical distinction between sheep and goat metacarpal. In *The domestication and exploitation of plants and animals*, eds. P.J. UCKO and G.W. DIMBLEBY, 295-306, copyright 1969. London: Duckworth, with permission from Sebastian Payne).

An example of the impact that Payne's paper had on research is represented by the study carried out by Rowley-Conwy (1998) on the Neolithic metapodial bones of sheep and goat from the Arene Candide cave in Italy. The author had several goals:

- to see if a separation between the two species could be obtained by using a metrical method applied not only on metacarpals but also on metatarsals;
- to compare the effectiveness of Payne's and Boessneck's indices on the distal end of the metacarpals and establish which of the two shows a clearer separation between sheep and goat;
- to propose some new measurements applicable on the proximal articulation of the metatarsals.

The assemblage Rowley-Conwy studied comprised several almost complete metacarpals and metatarsals, already assigned to *taxon* through morphological study. Payne's and Boessneck's biometrical indices were applied to assess their effectiveness and to see if the morphological identification was confirmed by metrical analysis. The output was that both Payne's and Boessneck's methods worked well on distal metacarpal bones, though Payne's method was shown to be more effective. Both medial and lateral condyles of the distal end of the metacarpal

were effective for the separation of the two species, which means that if one of the two condyles was missing or damaged, identification to species could still be achieved. The results for the distal metatarsals were less clear, confirming what Boessneck had noticed before (1969: 355): the lateral condyles were not particularly helpful for the proposed distinction, while the medial condyles worked better. Nevertheless, metatarsals could also be used with a certain degree of confidence. The new index proposed (Fig. 1.6) was elaborated by taking into account previously recognised morphological differences on the proximal end of the metatarsal. When applied to the Arene Candide sample, it was shown to be effective; unfortunately the extent to which these new measurements work on other populations has yet to be investigated.

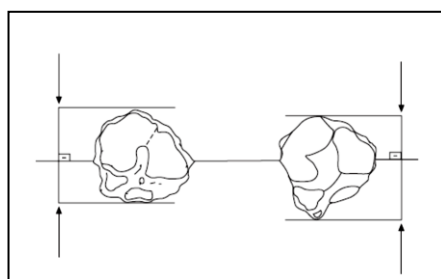


Figure 1.6 Proximal articulation of goat (left) and sheep (right) showing the points at which the measurements were taken by Rowley-Conwy (image reprinted from ROWLEY-CONWY, P. Improved separation of Neolithic metapodials of sheep (*Ovis*) and goats (*Capra*) from Arene Candide cave, Liguria, Italy. *Journal of Archaeological Science* 25: 251-258, copyright 1998, with permission from Elsevier).

A further application of the biometrical approach proposed by Boessneck and colleagues, was published in 1990 by Clutton-Brock *et al.* in their analytical study of Soay sheep. The principal purpose of this study, as discussed before, was an assessment of which morphological traits were more obvious in Soay sheep and which of those were the most effective for differentiating this breed from goats. In this broader context, the authors tested most of the Boessneck's indices and other new indices with the results that, on a selected sample of Soay sheep, only some of the indices used were shown to be genuinely effective. The successful indices were related to measurements taken on the humerus (the index is based on height of condyle/distal width), the ulna (*olecranon* length/depth and *olecranon* width/depth), the metapodials (width of the shaft/length and measurements on the distal condyles, following Boessneck *et al.* 1964) and the calcaneum (length of the lateral process/length of the condyle, following Boessneck *et al.* 1964).

A later and useful contribution to the biometrical approach is represented by the already mentioned research conducted by Fernández (2001). Table 1.3 summarises the list of anatomical elements and indices considered by Fernández in her study.

Table 1.3 Elements, indices and summary results from Fernández (2001).

Element	Index	Results on modern material	Results on archaeological material
Scapula	Smallest length of the <i>collum scapulae</i> /distance from the spine to the edge of the glenoid cavity	Effective. But identification possibilities are limited to the extreme cases (Fernández 2001: 352)	Variability among the sample has an influence, as such the separation between the two groups is blurred (Fernández 2001: 355)
	Smallest length of the <i>collum scapulae</i> /greatest length of the <i>processus articularis</i>	Separation good enough for most of the sample. Sample is small, results have to be taken with caution (Fernández 2001: 356)	Higher variability of the archaeological goats compared to the modern material (Fernández 2001: 357)
	Greatest length of the <i>processus articularis</i> /breadth of the glenoid cavity	Limited utility, only the extreme values are discriminant. Sample is small, results have to be taken with caution (Fernández 2001: 358)	Index resulted to be not useful (Fernández 2001: 360)
Humerus	Height of the trochlea at the central constriction/breadth of the trochlea	Both effective. Second index is better as measurements are easier to take (Fernández 2001: 364)	Both effective in discriminating the two species (Fernández 2001: 366)
	Height of the trochlea/ breadth of the trochlea		
	Anterior-posterior maximum depth of the medial epicondyle/ breadth of the trochlea	Good to distinguish roe deer and chamois from caprines (Fernández 2001: 367)	-
	Height of the trochlea at the central constriction /anterior-posterior maximum depth of the medial epicondyle	Good to distinguish the genus <i>Capra</i> from <i>Rupicapra</i> (Fernández 2001: 367)	-
	Height of the trochlea/anterior-posterior maximum depth of the medial epicondyle	Utility for distinguishing chamois from the other caprines (Fernández 2001: 368)	-
	Anterior-posterior minimum depth at the base of the diaphysis/anterior-posterior maximum depth of the medial epicondyle	Utility for distinguishing chamois from sheep (Fernández 2001: 368)	-
Radius	Depth of the proximal articulation/length of the proximal articulation	Utility for distinguishing ibex from chamois (Fernández 2001: 369)	-
	Maximum depth of the proximal articulation/length of the proximal articulation	Utility for distinguishing chamois from sheep. Small sample results must be taken with caution (Fernández 2001: 369)	-
	Depth of the proximal articulation /breadth of the <i>facies articularis</i>	Utility for distinguishing ibex from chamois (Fernández 2001: 369)	-
	Breadth of the <i>facies articularis</i> /breadth of the proximal articulation	Sheep have average value for this index higher than the other species (Fernández 2001: 370)	-
			-

Element	Index	Results on modern material	Results on archaeological material
Ulna	Breadth across the coronoid process/depth across the <i>processus anconaeus</i>	Utility for distinguishing ibex from chamois. Second index more useful than the first (Fernández 2001: 371)	
	Breadth across the coronoid process/smallest depth of the <i>olecranon</i>		-
	Breadth of the <i>olecranon</i> tuberosity /length of the <i>olecranon</i>	Utility for distinguishing sheep from chamois. First index better than the second (Fernández 2001: 372)	-
	Length of the <i>olecranon</i> tuberosity/ length of the <i>olecranon</i>		-
	Smallest depth of the <i>olecranon</i> / length of the <i>olecranon</i>	Not useful (Fernández 2001: 372)	-
Tibia	Distal breadth/distal depth of the medial side	Useful to distinguish chamois from ibex and sheep (Fernández 2001: 373)	-
Astragalus	Distal breadth/greatest length of the medial half	Useful to distinguish chamois and sheep (Fernández 2001: 374)	-
	Depth of the lateral half/ distal breadth		
	Depth of the medial half/ distal breadth	Useful to distinguish chamois and ibex (Fernández 2001: 374)	-
	Greatest length of the medial half/greatest length of the lateral half	Useful to distinguish chamois and ibex (Fernández 2001: 374)	-
Calcaneum	Length of the process/length of the condyle	Useful to distinguish chamois and ibex on one side, and sheep and goat on the other. Caution is suggested (Fernández 2001: 375)	-
Metapodial bones (proximal articulation)	Depth of the proximal articulation/breadth of the proximal articulation	In metacarpal useful for distinguishing ibex from chamois. In metatarsal useful for distinguishing sheep from chamois (Fernández 2001: 376)	-
Metapodial bones (distal articulation)	Depth of the distal end/breadth of the distal end	In both metacarpal and metatarsal good index for distinguishing sheep from chamois	-
	Diameter of the external part of the medial condyle/diameter of the medial <i>verticillus</i>	In metacarpal useful for distinguishing sheep from goat but sample used is very small. In metatarsal is useful to distinguish ibex from chamois (Fernández 2001: 378)	-
	Diameter of the external part of the lateral condyle/ diameter of the lateral <i>verticillus</i>	For the metacarpal can be used for distinguishing between chamois and sheep. For metatarsal is useful to distinguish chamois and ibex (Fernández 2001: 379)	-
	Diameter of the external part of the medial condyle/width of the	Useful for distinguishing between sheep and goat	-

Element	Index	Results on modern material	Results on archaeological material
	medial condyle		
	Diameter of the external part of the lateral condyle /width of the lateral condyle	but sample very small. Metacarpal works better than metatarsal, medial trochlea better than lateral (Fernández 2001: 379). In both bones the indices are also useful for distinguishing between chamois and ibex (Fernández 2001: 379)	-

Despite the fact that Fernández' study represents a valuable contribution to the sheep and goat differentiation issue, she only compares indices based on linear measurements and not indices based on ratios of measurements. In this way absolute size influences the results and tends to cloud differentiations based on shape (size in itself is certainly not a useful measure of sheep/goat separation). There is also no statistical analysis of the biometric patterns which, considering the very small goat sample utilised (n=4/5), makes the results rather uncertain.

Very recently, a study was conducted by Salami *et al.* (2011) with the purpose of providing a new biometrical means to differentiate *Ovis* and *Capra*. The authors unfortunately focus their attention only on two specific Nigerian breeds of sheep and goat (for a total of 30 individuals) of which they studied the pelvis and limb bones. The parameters they took into account were weight, length and diameter of the proximal articulation, mid-shaft and distal articulation. The results showed that significant statistical difference existed in the length of all the long bones examined between the two species, but length is rarely a measurement that is available on archaeological bones. The difference in weight and diameter of the mid-shaft and distal articulation were shown to be highly significant between the two species only on the tibia. As a consequence, the length of the tibia, along with the entire morphometry of this element, has been put forward as important for the differentiation of the two specific breeds of sheep and goat used for this study.

Finally, the recently accepted thesis by Haruda (2014) on morphological variations existing in archaeological sheep and goat from different geographic areas has to be mentioned. The study has in fact shown that local environment influences inherited morphological traits in sheep and goat. Haruda conducted a GMM (Geometric Morphometrics) study of ankle bones from a number of archaeological sheep and goat Bronze Age Central Asian assemblages located in different geographic areas. The analysis revealed that across all sites, different morphological sheep phenotypes were present. The analysis, however, failed to detect the same phenotypic variety in the archaeological goats as well as, in elucidating qualitative traits for distinguishing the astragali of sheep and goat ankle bones.

1.3.4 Conclusions

The contributions as well as the limitations of the morphological approach to the separation of sheep and goat specimens from archaeological sites have been discussed. Despite the usefulness of this approach, the need for a more objective biometrical tool to be used in tandem with the morphological criteria should be obvious. Some examples of successful biometrical applications have been presented, but there is potential for a much more extensive approach.

This project intends to contribute to use both morphological and biometric methods. Through the study of a large modern sample of English and (mainly) central European sheep and goats, a list of the morphological criteria which will have been proven to be more visible and reliable, will be obtained. This study, focused on particular breeds considered as reasonable proxies for the un-improved English medieval animals, will lead to a new set of morphological criteria, which rely on previous work, but critically select those that seem more promising for an application to the medieval English archaeological material.

In addition, and most crucially, biometrical analysis will be carried out with the main purpose of translating morphological differences into measurements. This will lead to the elaboration of a series of biometrical indices for a variety of cranial and postcranial bones. This biometrical study, supported also by the use of statistical tools, will attempt to fill the gap of knowledge on sheep and goat morphometry left by previous studies.

The combination of the two approaches represents the core of this new ‘study tool’, which has the potential to:

1. limit the subjectivity inherent to the more traditional approaches
2. be specifically effective for archaeological material from central and northern Europe, but potentially applicable to other geographic areas.

1.4 The medieval English goat: setting the scene

The English Middle Ages, which include about five centuries, are conventionally identified as the period beginning in 1066 AD, date of the Norman Conquest, and ending in c.1500 AD. It is divided into different sub-periods (Hills 1999):

- Early medieval 1066-1250 AD;
- High medieval 1250-1400 AD;
- Late medieval 1400-1500 AD.

The medieval period is an age characterised by a series of highly significant events and, as such, witnessed huge transformations in England. The 12th and 13th centuries are characterised by a rise in population that led to the expansion of cultivable lands at the expenses of pasture. This phase ended with a climatic deterioration, which led to progressively cooler weather and a series of harvest failures. The crisis culminated in 1315 when one of the most devastating events of the Middle Ages occurred: the great famine which resulted in the loss of c. 10% of the population (Kershaw 1973). But the 14th century is also marked by another traumatic event, the advent of the Black Death (1348-1350), which resulted in the decimation of the population. As a consequence of the decreased population, the demand for food dropped, and the market in grain consequently suffered. Animal husbandry became more prominent and, major areas, previously used for cultivation, were once again converted to pasture (Thirsk 1997; Thomas 2005b; Williamson 2002). Severe recession characterises the period following the plague and a long time will pass before the population could grow again (in the 16th century) (Wrigley and Schofield 1981). All these events had a profound impact at both economic and social levels. Agriculture and husbandry were deeply affected, bringing significant transformations and preparing the ground for the phenomenon known as the ‘Agricultural Revolution’ (Albarella 1997; Albarella and Davis 1996; Thomas 2005b; Thomas *et al.* 2013 for a revised analysis).

To understand the complexity of the medieval historical events it is important to combine different lines of evidence, such as those produced by archaeological and historical research. Concerning medieval husbandry, both archaeological and historical evidence agree on the fact that it was dominated by the use of cattle, sheep, pig and horse (Albarella 1997; Dyer 1994; Grant 1984; Grant 1988; Sykes 2006; Thirsk 1967; Thomas 2005b). Cattle were mostly used as traction animals. This role did not change until the (gradual) introduction, in the Later Middle Ages, of the horse as the main animal used for agricultural activities (Langdon 1986). This introduction determines a shift in the role of cattle: from main ploughing animals to main meat and milk producer. Sheep in the Early Middle Ages were bred for their meat, milk and wool, but by the 13th century the emphasis was mainly on wool production. English wool acquired the

status of the best wool in Europe and became extensively traded. Pigs, due to their inability to provide secondary products, were almost exclusively used as meat and fat providers (Albarella 2006).

1.4.1 The historical evidence for the medieval goat

Written sources for the Middle Ages do provide valuable information, though the quality of the available evidence, which includes survey texts, tax assessments, manorial accounts, archives and charters (Dyer 2004; Thomas 2002) is variable. Nevertheless, the impression that one gains is that the goat was mainly valued as a milk producer. Goat dairy products and, to a lesser extent, meat could represent a valuable additional contribution to the family economy; milk, cheese and butter surplus, along with (occasional) kids, would have been sold at the market. The meat of older goats was more likely to be consumed by the lower levels of the society, while kid meat was consumed by the higher levels, as attested by several monasteries' and lords' accounts (Dyer 2004; Dyer 2006; Noodle 1994; Wilson 1973) as well as archaeological evidence (Albarella and Davis 1996; Sykes 2006; Thomas 2005).

During the Early Middle Ages goats are rather frequently mentioned in place names (for example Gaterigg - goat's ridge - in North Riding or Gatescarth - goats' pass - in Westmorland) dating back to the period (Dyer 2004: 22). Even more significant is the evidence from the Domesday Book, completed in 1086 (Darby 1977), which provides many details about the numbers of goats present in some English counties. The impression gained is that goats, though far less common than sheep, were present in fairly high numbers (Tab. 1.4) (Albarella 1999; Dyer 1991, 2004; Hallam 1988). Nonetheless, the Domesday Book is not representative of the whole of England (animal numbers only survive for eight counties: Cambridgeshire, Cornwall, Devon, Dorset, Essex, Norfolk, Somerset and Suffolk).

Table 1.4 Numbers of goat flocks as reported by the Domesday Book (image reprinted from Darby, H.C. *Domesday England*, copyright 1977, Cambridge: Cambridge University Press, with permission from Cambridge University Press).

	Norfolk	Suffolk	Essex	Cambridge	Dorset	Somerset	Devon	Cornwall
Sheep	46,176	37,817	47,013	20,512	22,025	46,868	50,024	13,059
Wethers	—	—	—	—	297	948	155	240
Swine	8,082	9,789	13,323	4,591	1,501	6,980	3,694	513
Goats	3,015	4,348	3,642	225	800	4,482	7,246	926
Cows	23	9	160	2	59	123	23	55
Calves	—	—	77	—	—	—	—	—
Oxen	—	—	—	—	9	—	—	—
Bull	—	—	—	—	—	—	—	1
<i>Animalia</i>	2,102	3,052	3,808	958	521	4,343	7,341	1,092
Horses	50	127	3	—	—	—	—	—
Rounceys	767	527	793	170	123	448	159	21
Mares	56	—	21	11	13	35	1	12
Wild mares	—	—	—	24	12	318	155	352
Forest mares	139	114	—	—	—	38	162	58
Foals	25	—	103	7	12	—	—	—
<i>Hercararius</i>	—	—	—	1	—	—	—	—
Mules	1	—	1	1	—	—	—	—
Donkeys	2	2	26	24	1	3	2	—
Foals	—	—	—	2	—	—	—	—

After the 11th century, a drop in goat numbers is attested by evidence such as manorial accounts and archival documents. During the 13th and early 14th centuries, a period in which a higher number of written resources is available, goats are so scarcely mentioned that this species seems to be almost completely absent (Dyer 2004; Woolgar 2006). Nevertheless, this situation does not reflect the complete reality, and in the western and northern regions of England the goat continues to be present. Records such as the Berkeley Castle accounts (1346 AD) and the Alkington accounts (1311-12 AD) in Gloucestershire and the Bolton Priory estate account (1296-97 AD) in North Yorkshire (Dyer 2004: 27-28) all attest to the enduring presence of this animal. The usefulness of this kind of written documents is exceptional but it has limits as well, which have to be taken into consideration.

Written sources refer mainly to the higher levels of the society, but goats were animals of potentially low economic value, and were therefore likely to be owned by peasants, of whom less is known. This lack of information can partially be compensated by an analysis of the tax records. What emerges is that these animals were confined to specific localities, the west and north of the country, and were rare (Dyer 2004). In addition, several documents referring to the trespasses of goats, attest to the extent to which the voracious eating habits of this animal, made it unwanted (Dyer 1991, 2004; Fussell 1936).

During the 15th and 16th centuries, written sources mentioning goats are even scantier than in previous periods. The trend observed for the earlier periods seems, nevertheless, to repeat itself:

the presence of goats in the north and west areas of England persists, but to a smaller scale (Dyer 2004).

1.4.2 Zooarchaeological evidence for the medieval goat

Medieval archaeological sites on which goat bones have been found are scattered over many parts of the country. Nevertheless, the overall impression gained from the literature is that the goat was not really a common farmyard animal in medieval England. Regardless of the geographical areas, a common pattern is present across all English medieval sites: the number of remains belonging to *Capra* is always extremely low compared to other domestic animals, and it is particularly low when compared to the most commonly found *Ovis* bones. Whenever sheep and goat are mentioned in the same report, sheep is almost invariably and overwhelmingly the most common species (Albarella *et al.* unpublished).

Due to the perceived rarity of the goat, but also to the difficulties that distinguishing between sheep and goat entails, an attempt to separate these two *taxa* has not always been made by zooarchaeologists (less than 25% of studies for the Iron Age period according to Albarella *et al.* unpublished). In the cases in which a discrimination between the two *taxa* is carried out, the numbers related to the goat are so low that raw data are often omitted and further information are often excluded from the report. An example of such attitude is given by the report on the animal bones from Saxon and medieval Hereford, written by Baxter (unpublished). In his report the author mentions that 78% of the caprine remains have been attributed to sheep and 22% to goats - these latter are mainly represented by horncores and metapodials - but no raw numbers are given.

In many cases, attempts to differentiate have not been carried out at all, so that the two *taxa* appear combined in the communal category sheep/goat. The report written by Hamilton-Dyer's on the faunal remains excavated at the Saxon and medieval site of Barking Abbey (2002) is an example. The author does not include a methodology section so that the reader neither knows if a discrimination between sheep and goat was attempted nor on which traits it was based. All caprine remains are included in the generic category of sheep/goat.

Sometimes, zooarchaeologists are so certain about the absence of the goat that all the remains are attributed to the sheep. An example of this is given by Gebbels' report (1976) on the faunal remains found at the medieval site of Great Yarmouth. The author does not mention any attempt to discriminate *Ovis* from *Capra*. Furthermore, on the list of identified species only '*Ovis sp.*' appears, while even the safe sheep/goat category is absent.

These are only a few examples of a widespread attitude. This limits the possibility to assess accurately the presence of the goat in medieval England, but also the possibility to quantify the relative proportions of sheep and goat.

More recently, thanks to an increased awareness of the methodological problems related to sheep and goat identification, and to a renewed interest in the role of the rarer animals in the medieval archaeological record, more attention has been dedicated in trying to better understand the role that the goat had in medieval England.

An interesting contribution to the topic is provided by Noddle. According to Noddle (1994: 120) the presence of goat varies, as there are English medieval sites where only a few goat bones have been found and others where several have been unearthed. At Exeter (Devon, Maltby 1979), Lincoln (Lincolnshire, O'Connor 1982), Winchester (Hampshire, Serjeantson and Rees 2009) and York (Bond and O'Connor 1999) goat remains are rare but, at Hereford (Herefordshire, Noddle and Harcourt 1985), King's Lynn (Norfolk, Noddle 1977), Southampton (Hampshire, Bourdillon and Coy 1980), Monmouth and Chepstow (Monmouthshire) on the Welsh border (Noddle and Harcourt 1985; Noddle 1991, 1994) and at Perth, Aberdeen and Elgin in Scotland (Hodgson 1980 in Noddle 1994; Hodgson 1983) a larger number have been found.

Noddle's assertion does, however, require verification, particularly as no other authors have indicated such a prominence of the goat in the archaeological record. The absence of an objective methodology used for identification purposes (see Section 1.4), along with the dearth of comprehensive reviews of the archaeological records for the goat nationwide, has limited the possibility of reaching a realistic overview of the importance of this animal in different regions and at different times in England. Nevertheless, relatively recent works have started clarifying the situation (Albarella 1997, 2003; Stallibrass 1995).

If we consider the archaeological evidence in chronological order, for the Saxon period (400-1066 AD) assemblages are usually dominated by cattle, sheep and pig remains (with some variations according to the status of the site), which represent the main domestic animals. Sheep remains are always overwhelmingly more common than goat remains (Albarella *et al.* unpublished; Holmes unpublished; Stallibrass 1995).

Another trend which has emerged from the Albarella *et al.* (unpublished) review is that the goat appears to be present in a higher proportion during the Saxon period than during the previous Roman period, reaching its peak in the Late Saxon period (Fig. 1.7). The phenomenon of an increase in the presence of goat during the course of the Saxon period has also been noted by Noddle (1980) at North Elmham in Norfolk (8th-15th century) and Crabtree (1989) at West Stow in Suffolk (5th-7th century). For the south and the northern areas of the country, such a trend has not been observed however (Holmes unpublished; Stallibrass 1995). Nevertheless, this may reflect the lack of archaeological evidence on it.

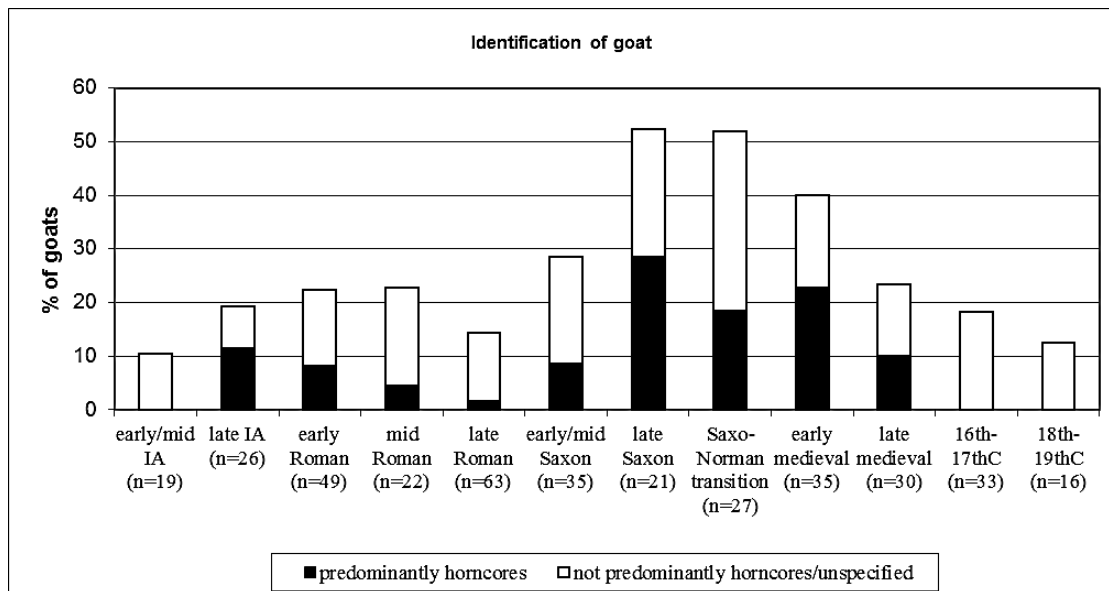


Figure 1.7 Percentage of occurrence of identified goat specimens by body part in post-Iron Age period-sites (Image reprinted from ALBARELLA, U., with T. PIRNIE and S. VINER. (unpublished). *Animals of our past: a review of the zooarchaeology of Central England*, with permission from Umberto Albarella).

According to Albarella *et al.* (unpublished) *Capra* remains appear to be more common in Late Saxon urban rather than rural sites, consistent with finds for the Roman period (Fig. 1.8). This pattern is mainly due to accumulations of goat horncores in towns, such as Thetford in Norfolk (Clutton-Brock 1976). These assemblages, interpreted as the result of industrial activities, are more likely to reflect an interest in horn-working rather than other industrial activities (tanning), which are less well represented chronologically in this period. Accumulations of horncores have also been recorded by Holmes (unpublished) in the south but none of them include goat horncores (only cattle horncores are mentioned). Nevertheless, the existence of goat horncores is reported at Mawgan Porth, Cornwall (Clutton-Brock 1976).

The archaeological evidence for the medieval period is different. A decrease in goat numbers seems to be suggested by written evidence (see above) and is also supported by the archaeological record (Albarella 1997, 1999, 2003; Stallibrass 1995) (Fig. 1.7). Some researchers have suggested that, as a consequence of population pressure in the 12th and 13th centuries, areas previously left uncultivated due to poor soil and used as a primary communal grazing source for the goat herds of villages or estates, declined (Clutton-Brock 1976; Noddle 1994). Others suggest that, when land enclosure became common, the number of goats fell as a consequence of their voracious nature; goats were perceived as hedge destroyers (Albarella 1997; Burke 1834; Dyer 2004; Noddle 1994). The decline of the goat has also been linked to its changing importance as a milk producer. In the 14th century, when farmers developed the techniques to produce milk from cows without the presence of a calf, they became the primary source of dairy products, leading to a decrease in demand for goat's milk and, consequently, to a

decrease in the number of goats (Albarella 1997; Noddle 1994). It is still uncertain which of these factors were key to the decline in goat importance, but it is possible that they all contributed.

During this period the presence of goat kids seems to be common to a number of high status medieval sites. At Launceston Castle in Cornwall (Albarella and Davis 1996) as well as at Dudley Castle in West Midlands (Thomas 2002) a number of kid bones have been in fact identified and has been interpreted as consumption of kid flesh.

The pattern observed during the Saxon period, namely that a larger number of goat horncores deposits are found in the more urban sites (in the Saxon period 47.8%, in the medieval period 19.6%) whilst goat bones have more frequently been recorded in the rural sites, is also attested for the medieval period (Albarella 1999, 2003; Albarella *et al.* unpublished) (Fig. 1.8). In this period, however, the tanning industry had become predominant, while horn trade declined (Albarella 2003), and therefore such accumulations are more likely to be linked to the former activity.

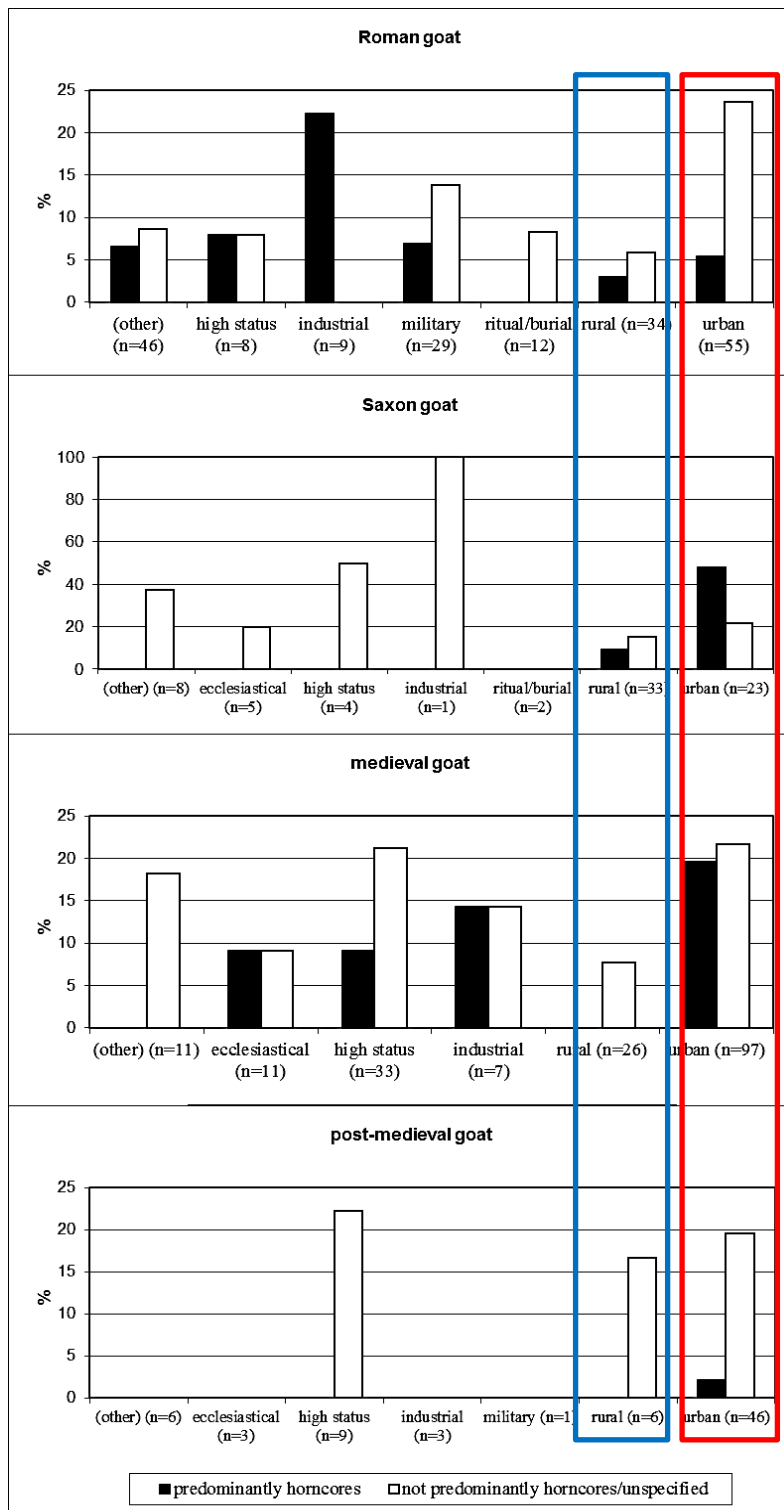


Figure 1.8 Percentage occurrence of Roman, Saxon, medieval, and post-medieval period-sites containing identified goat specimens, by body part and site type (Image reprinted from ALBARELLA, U., with T. PIRNIE and S. VINER. (unpublished). *Animals of our past: a review of the zooarchaeology of Central England*, with permission from Umberto Albarella).

As Figure 1.8 shows, accumulations of goat horncores (and very occasionally foot bones) have

been found at various sites in England. Despite that, the frequency of horncore-dominated goat assemblages decreases when moving from east to west. This is due to the fact that the eastern regions of the country, which were the most urbanised, are those which have revealed the highest concentration of such deposits.

At the site of Harrison Street in Hereford (Hertfordshire, 15th century) (Baxter unpublished) 22% of the caprines remains (against the 78% attributed to the sheep) have been identified as goats. The goat assemblage consisted mainly of horncores and metapodials (numbers not given). At the site of Skeldergate in York (Yorkshire, 11th-12th century) (O'Connor 1984), 34 complete goat horncores were found along with very few postcranials (numbers not given). At the site of Hornpot Lane in York (Yorkshire, 14th century) (Wenham 1964), 500 horncores mainly from oxen and goats were recovered (no further details are given). Furthermore, 66 complete goat horncores were unearthed at the site of Empire Cinema in Bedford (Bedfordshire, 11th-12th century) (Grant 1983), and an accumulation of goat horncores were also found at the site of St Johns Street 29-39 in Bedford (Bedfordshire, 11th-13th century) (Grant 1979) (numbers are not given). Noddle (1975) also mentions accumulations of goat horncores at the sites of St. Mary in Bristol and King's Lynn in Norfolk (in both cases numbers are not given). Specific deposits indicating the use of goat skins and horns in the southern and northern regions of England are scantier, while deposits of cattle horncores are much more frequently reported (Holmes unpublished; Stallibrass 1995).

Since horncores bear very clear morphological traits, allowing sheep and goat to be easily distinguished, the possibility needs to be considered that an over-representation of these elements may be related to an identification bias. However, this bias would not explain why other easily identifiable anatomical elements, such as metapodials, are almost completely absent from the English medieval archaeological record (Albarella 2003).

To sum up, the overall archaeological evidence explored so far indicates that goat bones are scarce in medieval England, regardless of status and geographical location. In the east in particular there is a strong bias in favour of horncores, while post cranial bones and teeth are always rare (Fig. 1.9).

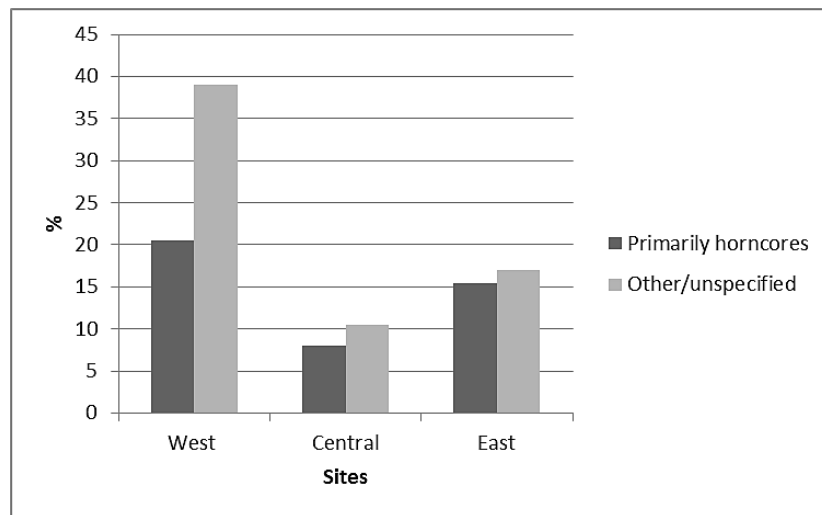


Figure 1.9 Percentage of identified goat specimens by body part from sites organised by sub-region (west sites=39; central sites=87; east sites 59. Graph redraw from Albarella 2003).

In urbanised and industrially specialised centres (mostly located on the east coast), the goat is likely to have mainly been used for its skin and, to a lesser degree, its horns. The absence/under-representation of goat postcranial bones points toward the hypothesis of a trade in goat skins with southern Europe, where this species was more abundant (Albarella 1999, 2003; Noddle 1994).

According to Prummel (1978) and Schmid (1969), when the skins were prepared for further treatments, which eventually led to the final transformation of skin into leather, the foot bones and hoof were retained. This raises the question of why this material is usually missing from the archaeological record in England. With the hypothesis of a trade in goat skins in mind, this anomaly reinforces the theory of long distance trade, for which it would have been useful to eliminate as much weight as possible in order for the goods to be more easily stored and traded. It follows from this supposition that the part of the skin most suitable to be discarded were indeed the foot bones, which were not considered as valuable source of working material as the horncores (Albarella 2003; Noddle 1994). Schmid (1974) argues that keeping the horn would also have provided a means for establishing the age of the animal the skin belonged to. Clearly the horns, probably sold or given to other manufacturers, had a value, but were definitely of secondary use to the skins (Noddle 1994).

Similar situation has been identified in other countries (Albarella 1999; Noddle 1994). Sites such as Dorestad and s'-Hertogenbosch-Gertru in the Netherlands (Prummel 1982) have produced accumulations of goat horncores and, in the case of the latter site, also goat metapodials, something unknown at English sites. In Germany, at the site of Haithabu (Reichstein and Tiessen 1974) a few goat bones along with several remains of goat leather have

been discovered. At other German sites the proportion of goat to sheep is about 1:10; these include Ulm-Weinhof (Anschutz 1966) and Werttenburg (Kühnhold 1971; Schatz 1963). At the Norwegian site of Gamlebyen, accumulations of goat metapodials (but no horncores) have been found; for this site, historical sources also mention the existence of an import trade in goat skins (Lie 1988 in Noddle 1994: 120).

The hypothesis that a trade in goat *horns*, rather than *skins*, could have existed thus explaining the over-representation of this element, has also been evaluated (Albarella 2003). Nevertheless, considering that: 1) no documentary evidence has been found to support this idea; 2) the horn-working industry during the Middle Ages was in decline while the leather industry was developing and 3) documents exist proving the existence of a commerce in goat skins in England and in other countries, it is more plausible that the trade was focused on goat skins rather than horns.

Despite the fact that no documentation has yet been found that specifically refers to a goat skin trade between the more urbanised east of England and other European countries, a series of documents confirming the movement of goat skins from Ireland to western England (Clarkson 1966) does exist and seems to support the idea that a similar trade could have existed in the eastern part of the country. In addition, written records confirming the presence of a contemporary international trade in goat skins in other countries (as in the Norwegian case mentioned earlier), makes this supposition even more plausible (Albarella 2003; Noddle 1994).

The situation discussed above in relation to urban industrial sites cannot be applied to rural sites (or to urban sites outside industrialised areas), for which no evidence of goat horncore accumulations exists. *Capra* remains have been recorded in a few rural sites, among which are the 12th-early 13th century Boteler's Castle, Oversley Warwickshire (Pinter-Bellows 1997) and the site of Walton, Aylesbury, Buckinghamshire dated to the 12th century (Noddle 1976). At both, a small number of goat bones were unearthed and concentrations of goat horncores were not found, suggesting that goat was only occasionally used and was husbanded rather than used in industrial activities. Unfortunately, our knowledge of rural faunal assemblages is scant. In fact, the western and more rural areas of the country remain, to this day, insufficiently documented (Albarella *et al.* unpublished). This is, at least to some degree, because investigations have mainly been focused on large urban centres, leaving rural villages in need of greater attention (Stallibrass 1995). This dearth of information prevents us from undertaking an in-depth study of regional patterns.

During the Post-medieval period (16th century to the present day) further goat decline is attested (Albarella 1997; Noddle 1994; Stallibrass 1995), a trend also supported by documentary evidence. This is the period in which a phenomenon known as the "Agricultural Revolution", which marks, among other phenomena, the beginning of a new husbandry system, starts to

clearly manifest itself. Zooarchaeological studies, as well as 17th century written records attest to the occurrence of important changes in the type and way sheep and goat were used. Zooarchaeologically, these changes in husbandry are detected through an increase in size of the main domestic animals which took place in different regions of England at a different pace for each species (Albarella 1997: 21; Davis and Beckett 1999: 6; Thomas 2013: 3324). The reasons behind such increase are nowadays still unknown but may be linked to environmental as well as genetic factors, i.e. the introduction of new morphotypes/breeds of sheep/goat (Albarella 1997; Davis and Beckett 1999; Thomas 2013). In the case of domestic sheep and goat, this phenomenon, which according to Thomas' studies (2013: 3319) can be dated back as early as the 14th century, could blur some of the criteria used for identifications, making the distinction more challenging (Maltby 1979).

It is clear that there are still important gaps in the historical and archaeological evidence that preclude us from reliably assessing the role of the goat in the English Middle Ages. Paramount to an improvement of current knowledge is the necessity to gain greater confidence in the identification of sheep and goat bones. This dissertation aims to contribute to the matter by proposing a new methodology to distinguish between the bones of sheep and goat. The new methodology will allow more confidence in the identification of the two species and will represent the basis on which a re-assessment of the role of the English medieval goat can be undertaken.

Chapter 2 Study of the morphological traits and biometry of the modern material

2.1 Methods

2.1.1 Introduction

In the previous chapter (Chapter 1, Section 1.3), the different approaches adopted in the past for tackling the issue of sheep/goat identification have been discussed. The critical evaluation of the currently available morphological approaches has allowed us to understand and assess their contributions and limitations. The main problem with a purely morphological approach is that the ability to distinguish between the two closely related taxa is highly subjective.

Pioneering biometrical studies, however, also exist and their potential and applicability to archaeological material has been demonstrated (Fernández 2001; Onar *et al.* 2008; Payne 1985; Rowley-Conwy 1998). Nevertheless, there is scope for a much more extensive biometrical approach to sheep/goat identification.

This project tackles sheep/goat identification by adopting both morphological and biometrical approaches. This is achieved by studying modern reference collections of sheep and goats of known age and sex, mainly belonging to British and central European breeds. This sample was chosen for its potential in representing a better proxy for English medieval animals than the Near East and eastern Mediterranean animals predominately used in previous studies. On this selected sample, morphological and biometrical data were collected with two main goals. The first concerns morphological traits; as many zooarchaeologists know, not all traits identified in previous literature are reliably and consistently identifiable in animals from different regions and breeds. A selection of morphological traits has been recorded to find out which can be more reliably recognised and correctly classified in the selected sample, and eventually applied to archaeological material.

The second goal is to test a new methodology based on biometry, which can be used in combination with the morphological approach, thus enhancing the possibility of identification to species level. This new method is based on measurements which are designed to translate biometrically some of the morphological characteristics used to distinguish *Ovis aries* and *Capra hircus*. Some of the used measurements have previously been used in the literature, while others have been created *ad hoc* for this project.

In the following sections, the morphological traits selected from previous studies are presented, along with an explanation of how the scoring process was carried out on the modern material

(Section 2.1.2). A description of the measurements that make up the new biometrical method follows (Section 2.1.3), along with a brief explanation of how the recording protocol was applied (Section 2.1.4). Finally, a detailed description of the modern sample included in the study, along with information regarding age, sex, breed (when known) and degree of completeness of the animals, is provided (Section 2.2).

2.1.2 Morphological Approach

It has already been mentioned that, despite its unquestionable potential, the morphological approach can be problematic. The visibility and reliability of known morphological traits vary according to different factors such as the breed and age of the animals, the ability and experience of the observer as well as the completeness of one's reference collection.

Because of these issues, the morphological criteria used to identify the two species have recently been reviewed by Zeder and Lapham (2010 post cranial bones) and Zeder and Pilaar (2010 mandibular teeth). This research supplements such previous work by conducting a parallel study on the reliability of selected morphological characteristics on a (relatively) controlled sheep and goat modern sample.

The advantages of testing morphological criteria on modern material first and, subsequently, on archaeological specimens, are several. First of all, modern collections often host complete skeletons in good conditions of preservation, so that the visibility of the characteristics should be at its best. Secondly, in modern collections, important information such as sex, age and breed of the specimens are sometimes, permitting greater understanding of influence of the size and shape. Thirdly, the study of modern material permits preliminary results on the validity of the new methodology adopted and makes it possible to improve the protocol before applying it to the archaeological material. Finally, the collected modern data represent a useful baseline that can be used in future studies.

The anatomical elements included in the study were selected by taking into account several factors. The first was based on the fact that the aim of the project is the application of the method to archaeological material, which is usually fragmented. It is known from previous studies that, because of their differing densities, some skeletal elements are better able to survive deposition (Binford and Betram 1977; Lyman 1984) and, as a consequence, they are more frequently represented in archaeological assemblages. Those elements have preferentially been chosen for the study.

The second factor is related to the fact that some anatomical elements bear more diagnostic traits than others. Horncores and metapodials for example are the skeletal elements most easily assigned to species level due to their distinctive morphologies.

For the reasons outlined above, the following skeletal elements have been selected:

- Cranium:
 - Horncores
 - Mandible
 - Mandibular teeth
- Postcranial:
 - Glenoid cavity and articulation of the Scapula
 - Distal articulation of the Humerus
 - Proximal articulation of the Radius
 - Proximal articulation of the Ulna
 - Distal articulation of the Metacarpal
 - Distal articulation of the Metatarsal
 - Distal articulation of the Tibia
 - Astragalus
 - Calcaneum
 - 1st, 2nd and 3rd Phalanx

The selection of the morphological characteristics was made after a thorough evaluation of the previous literature. In addition, a pilot study was carried out on the sheep and goat specimens hosted at the Zooarchaeology Laboratory of the University of Sheffield. This collection, mainly composed of English and Mediterranean specimens, was used as trial/training material and assisted with the refinement of the criteria to be included in the protocol.

Tables 2.1 to 2.19 provide the reference from which the morphological characteristics have been selected and a brief description of the traits.

Table 2.1 Reference for the morphological traits chosen for this study.

Element	References
Horncore	Clutton-Brock <i>et al.</i> 1990; Schmid 1972.
Deciduous 3 rd lower premolar dP ₃	Payne 1985.
Deciduous 4 th lower premolar dP ₄	Payne 1985.
Permanent lower 3 rd premolar P ₃	Halstead <i>et al.</i> 2002; Helmer 2000.
Permanent lower 4 th premolar P ₄	Halstead <i>et al.</i> 2002; Helmer 2000.
Permanent lower 3 rd molar M ₃	Balasse and Ambrose 2005; Halstead <i>et al.</i> 2002; Helmer 2000.
Mandible	Halstead <i>et al.</i> 2002.
Scapula	Boessneck 1969; Boessneck <i>et al.</i> 1964; Helmer and Rocheteau 1994; Prummel and Frisch 1986.
Distal Humerus	Boessneck 1969; Boessneck <i>et al.</i> 1964; Helmer and Rochetau 1994; Prummel and Frisch 1986; Zeder and Lapham 2010.
Proximal Radius	Boessneck 1969; Boessneck <i>et al.</i> 1964; Prummel and Friesch 1986; Zeder and Lapham 2010.
Proximal Ulna	Boessneck 1969; Boessneck <i>et al.</i> 1964; Prummel and Frisch 1986.
Distal Metapodial	Boessneck 1969; Boessneck <i>et al.</i> 1964; Prummel and Frisch 1986; Zeder and Lapham 2010.
Distal Tibia	Kratochvil 1969; Prummel and Frisch 1986; Zeder and Lapham 2010.
Astragalus	Boessneck 1969; Boessneck <i>et al.</i> 1964; Prummel and Frisch 1986; Zeder and Lapham 2010.
Calcaneum	Boessneck 1969; Boessneck <i>et al.</i> 1964; Prummel and Frisch 1986; Zeder and Lapham 2010.
1 st Phalanx	Boessneck 1969; Boessneck <i>et al.</i> 1964; Zeder and Lapham.
2 nd Phalanx	Boessneck 1969; Boessneck <i>et al.</i> 1964; Zeder and Lapham.
3 rd Phalanx	Boessneck 1969; Boessneck <i>et al.</i> 1964.

Table 2.2 Morphological characteristics adopted for the horncore (trait 1: image reprinted from SCHMID, E. *Atlas of animal bones: for prehistorians, archaeologists and quaternary geologists*. Amsterdam: Elsevier, copyright 1972, by permission of Joerg Schibler. Trait 2: images reprinted from BOESSNECK, J. *Osteological differences between sheep (*Ovis aries* Linné) and goat (*Capra hircus* Linné)*. In *Science in archaeology: a survey of progress and research*, eds. D. BROTHWELL and E. HIGGS, 331-358, copyright 1969. London: Thames and Hudson, with permission from Thames and Hudson).

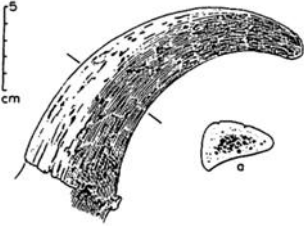
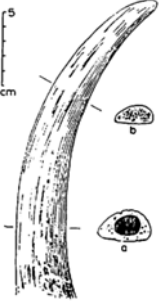
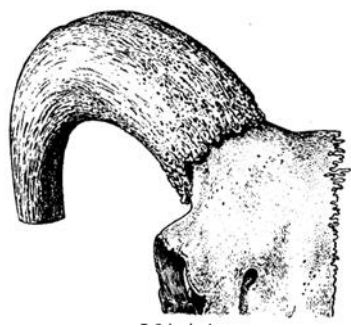

<u>Horncore</u>	
<i>Ovis aries</i> (sheep)	<i>Capra hircus</i> (goat)
TRAIT 1: SECTION	
	
TRAIT 2: CURVATURE	
	
<p>The section of the horn is more or less triangular.</p> <p>In males: horns have a D shape with the anterior edge more rounded and broader than the tapered posterior edge. It curves tightly outwards and backwards spiralling around the ears with the tip pointed forward.</p> <p>In females: the horns are less robust and much shorter than in males, they have sharp keel-shaped anterior and posterior edges and are generally flattened medio-laterally. The tip of the horn is rounded (Clutton-Brock <i>et al.</i> 1990: 10-14; Schmid 1972: 90).</p>	<p>The section of the horn is more or less plano-convex. The horncores are relatively narrower than those of the sheep and rise vertically from the top of the head. They do not curve as tightly as in sheep. The tip is sharp. (Clutton-Brock <i>et al.</i> 1990: 10-14; Schmid 1972: 90).</p>

Table 2.3 Morphological characteristics adopted for the 3rd deciduous premolar (images reprinted from PAYNE, S. Morphological distinctions between the mandibular teeth of young sheep, *Ovis*, and goats, *Capra*. *Journal of Archaeological Science* 12: 139-147, copyright 1985, with permission from Elsevier).

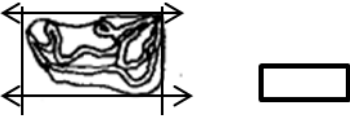
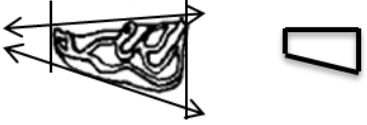


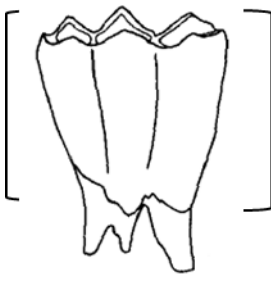
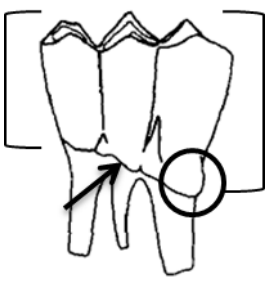
3rd Deciduous Premolar	
<i>Ovis aries</i>	<i>Capra hircus</i>
TRAIT 1: OVERALL SHAPE	
	
The tooth is heavier and squared in shape (Payne 1985: 143).	The tooth is narrower and triangular in shape (Payne 1985: 143).
TRAIT 2: APPEARANCE OF THE METACONOID	
	
The metaconoid, especially if the tooth is not heavily worn, is strongly defined and linked by a short ridge running bucco-distally to connect with the distal part of the tooth (Payne 1985: 143).	The metaconoid tends to be weaker and is linked by a ridge running bucco-mesially to connect with a more mesial part of the crown (Payne 1985: 143).

Table 2.4 Morphological characteristics adopted for the 4th deciduous premolar (images reprinted from PAYNE, S. Morphological distinctions between the mandibular teeth of young sheep, *Ovis*, and goats, *Capra*. *Journal of Archaeological Science* 12: 139-147, copyright 1985, with permission from Elsevier).

4th Deciduous Premolar	
<i>Ovis aries</i>	<i>Capra hircus</i>
TRAIT 1: CROWN ASPECT	
TRAIT 2: PRESENCE OR ABSENCE OF BASAL SWELLING	
TRAIT 3: PRESENCE OR ABSENCE OF THE INTER-LOBAR PILLAR	
	
The crown is more hypsodont, relatively higher-crowned, and is less prone to a basal swelling. The Inter-lobar pillar is often absent between the middle and distal lobes (Payne 1985: 143).	The crown is less strongly hypsodont, relatively lower-crowned with more basal swelling at the buccal-distal corner. The Inter-lobar pillar is often present, especially between the middle and distal lobes (Payne 1985: 143).
TRAIT 4: ENAMEL DEVELOPMENT ON MEDIAL AND DISTAL FACE	

4th Deciduous Premolar			
<i>Ovis aries</i>		<i>Capra hircus</i>	
Mesial view	Distal view	Mesial view	Distal view
The base of the enamel on the medial and distal face of the tooth rises more steeply (Payne 1985: 143).		The base of the enamel on the medial and distal face of the tooth rises less steeply (Payne 1985: 143).	

Table 2.5 Morphological characteristics adopted for the 3rd permanent premolar (images reprinted from HALSTEAD, P., P. COLLINS and V. ISAKKIDOU. Sorting the sheep from the goats: morphological distinctions between the mandibles and mandibular teeth of adult *Ovis* and *Capra*. *Journal of Archaeological Science* 29: 545-553, copyright 2002, with permission from Elsevier).

3rd Permanent Premolar	
<i>Ovis aries</i>	<i>Capra hircus</i>
TRAIT 1: OVERALL SHAPE	
The tooth tends to be broader and squared in shape (Halstead <i>et al.</i> 2002: 547).	The tooth tends to be longer and slender, rectangular in shape. (Halstead <i>et al.</i> 2002: 547)
TRAIT 2: ASPECT MIDDLE VERTICAL RIDGE	
A strongly developed vertical ridge is present in the middle of the lingual face. The lingual edge of the occlusal face is clearly “stepped” (Halstead <i>et al.</i> 2002: 547; Helmer 2000: 31).	A less developed vertical ridge is present in the middle of the lingual face. The lingual edge of the occlusal face usually forms a more or less straight line inclining buccally in a posterior-anterior direction (Halstead <i>et al.</i> 2002: 547; Helmer 2000: 31).
TRAIT 3: ASPECT MESIAL-BUCCAL ANGLE	

3rd Permanent Premolar	
<i>Ovis aries</i>	<i>Capra hircus</i>
The mesial part of the buccal face slopes inwards lingually and in a less strongly posterior-anterior direction. The mesial face is typically perpendicular to the axis of the mandible; as a result, the mesio-buccal quarter of the tooth tends towards a right angle (Halstead <i>et al.</i> 2002: 547).	The mesial part of the buccal face slopes inwards lingually and in a more strongly posterior-anterior direction. The mesial face often slopes anteriorly in a bucco-lingual direction; as a result, the mesio-buccal quarter of the tooth tends towards a more open angle (Halstead <i>et al.</i> 2002: 547).

Table 2.6 Morphological characteristics adopted for the 4th permanent premolar (images reprinted from HALSTEAD, P., P. COLLINS and V. ISAKKIDOU. Sorting the sheep from the goats: morphological distinctions between the mandibles and mandibular teeth of adult *Ovis* and *Capra*. *Journal of Archaeological Science* 29: 545-553, copyright 2002, with permission from Elsevier).







4th Permanent Premolar	
<i>Ovis aries</i>	<i>Capra hircus</i>
TRAIT 1: OVERALL SHAPE	
	
The tooth tends to be broader and squared in shape (Halstead <i>et al.</i> 2002: 547).	The tooth tends to be longer and slender, rectangular in shape (Halstead <i>et al.</i> 2002: 547).
TRAIT 2: ASPECT OF THE MESIO-LINGUAL RIB	
	
The mesio-lingual corner is typically marked by a vertical rib projecting lingually (Halstead <i>et al.</i> 2002: 547).	The rib on the mesio-lingual corner is weak or absent (Halstead <i>et al.</i> 2002: 547).
TRAIT 3: ASPECT OF THE MESIO-BUCCAL ANGLE	
	
The mesio-buccal quarter of the tooth forms an angle closer to a right angle (Halstead <i>et al.</i> 2002: 547; Helmer 2000: 31).	The mesio-buccal quarter of the tooth forms an open angle (Halstead <i>et al.</i> 2002: 547; Helmer 2000: 31).

Table 2.7 Morphological characteristics adopted for the 3rd molar (images reprinted from HALSTEAD, P., P. COLLINS and V. ISAKKIDOU. Sorting the sheep from the goats: morphological distinctions between the mandibles and mandibular teeth of adult *Ovis* and *Capra*. *Journal of Archaeological Science* 29: 545-553, copyright 2002, with permission from Elsevier).









3rd Molar	
<i>Ovis aries</i>	<i>Capra hircus</i>
TRAIT 1: ASPECT MESIAL FACE	
	
The flange of the medial face tends to be broader (Halstead <i>et al.</i> 2002: 548-549).	The flange of the medial face tends to be narrower (Halstead <i>et al.</i> 2002: 548-549).
TRAIT 2: ASPECT BUCCAL EDGE ANGLE	
	
The mesial part of the buccal edge of the mesial buccal cusp is typically convex (Halstead <i>et al.</i> 2002: 548-549).	The mesial part of the buccal edge of the mesial buccal cusp is concave or flat (Halstead <i>et al.</i> 2002: 548-549).
TRAIT 3: DIRECTION OF CENTRAL CUSP	
TRAIT 4: SYMMETRY AND SHAPE OF THE CUSPS	
	
The buccal edge of the disto-buccal and the centro-buccal cusps are relatively symmetrical. They tend to have a rounded “arcaded” appearance (Halstead <i>et al.</i> 2002: 548-549).	The buccal edge of the disto-buccal and the centro-buccal cusps often points strongly in a posterior direction. They tend to be pointed with a “triangular” appearance (Halstead <i>et al.</i> 2002: 548-549).
TRAIT 5: ASPECT OF THE DISTAL FLUTE	
	
The distal margin of the distal cup has a buccally defined “flute” (Halstead <i>et al.</i> 2002: 548-549).	The distal margin of the distal cup rarely has a buccally defined “flute” (Halstead <i>et al.</i> 2002: 548-549).

Table 2.8 Morphological characteristics adopted for the mandibula (images reprinted from HALSTEAD, P., P. COLLINS and V. ISAKKIDOU. Sorting the sheep from the goats: morphological distinctions between the mandibles and mandibular teeth of adult *Ovis* and *Capra*. *Journal of Archaeological Science* 29: 545-553, copyright 2002, with permission from Elsevier).

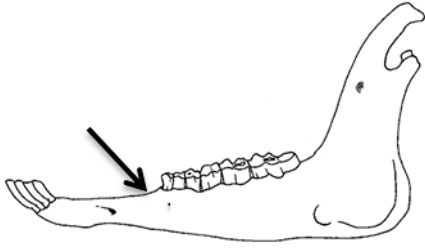
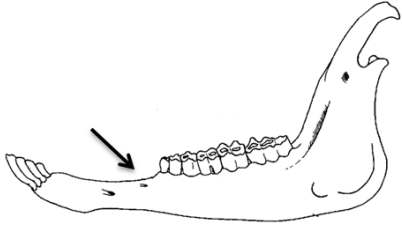
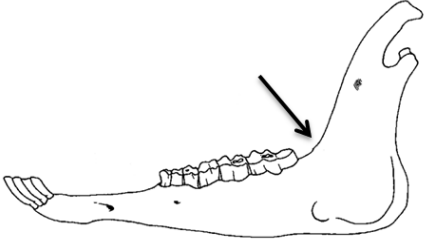
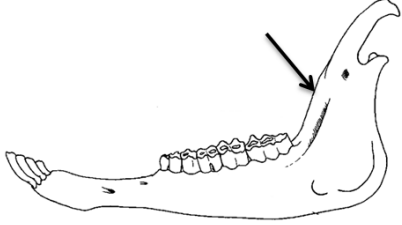
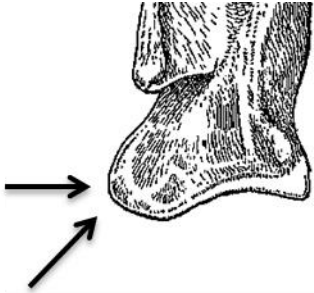
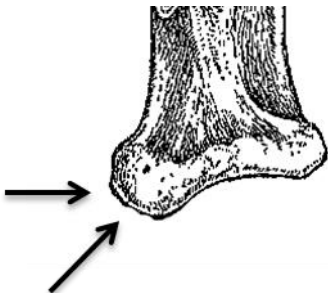
Mandibula	
<i>Ovis aries</i>	<i>Capra hircus</i>
TRAIT 1: PRESENCE/ABSENCE OF THE FORAMEN	
	
On the face of the mandible, a foramen is frequently found below P ₂ -P ₄ (Halstead <i>et al.</i> 2002: 549).	On the face of the mandible, a foramen is absent or less commonly present but anterior to the P ₂ (Halstead <i>et al.</i> 2002: 549).
TRAIT 2: ASPECT OF THE HOLLOW	
	
Behind the M ₃ , the lateral face of the mandible has a slightly pronounced or absent hollow (Halstead <i>et al.</i> 2002: 549).	Behind the M ₃ , the lateral face of the mandible has a more pronounced hollow (Halstead <i>et al.</i> 2002: 549).

Table 2.9 Morphological characteristics adopted for the scapula (images reprinted from BOESSNECK, J. Osteological differences between sheep (*Ovis aries* Linné) and goat (*Capra hircus* Linné). In *Science in archaeology: a survey of progress and research*, eds. D. BROTHWELL and E. HIGGS, 331-358, copyright 1969. London: Thames and Hudson, with permission from Thames and Hudson).

Scapula	
<i>Ovis aries</i>	<i>Capra hircus</i>
TRAIT 1: SHAPE OF THE GLENOID TUBERCULE	
	
The superglenoid tubercle is more developed and reaches further down beyond the glenoid cavity. Viewed laterally, it appears more rounded-off (Boessneck 1969: 337; Boessneck <i>et al.</i> 1964: 56-61; Helmer and Rocheteau 1994: 8; Prummel and Frisch 1986: 569)	The superglenoid tubercle is less developed and reaches less far down the glenoid cavity. (Boessneck 1969: 337; Boessneck <i>et al.</i> 1964: 56-61; Helmer and Rocheteau 1994: 8; Prummel and Frisch 1986: 569)
TRAIT 2: SHAPE OF THE GLENOID CAVITY	

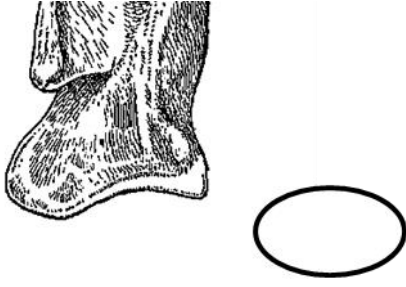


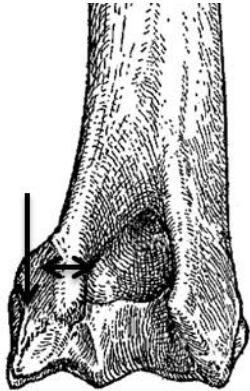
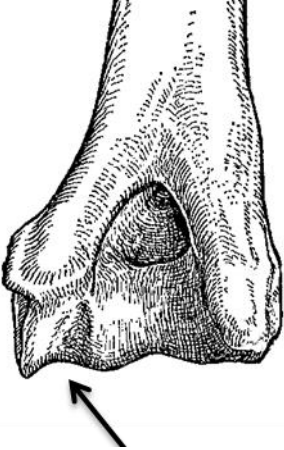
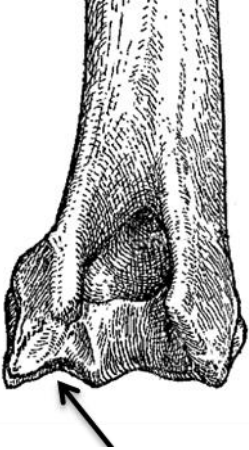
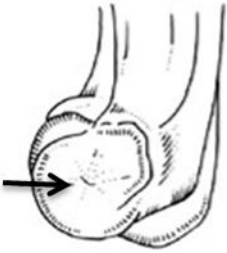

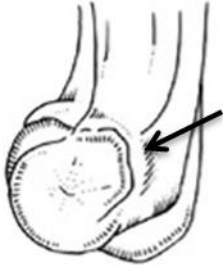

	
The glenoid cavity is elliptical in shape. (Boessneck 1969: 337; Boessneck <i>et al.</i> 1964: 56-61; Prummel and Frisch 1986: 569)	The glenoid cavity is circular in shape. (Boessneck 1969: 337; Boessneck <i>et al.</i> 1964: 56-61; Prummel and Frisch 1986: 569)

Table 2.10 Morphological characteristics adopted for the distal humerus (traits 1 and 2: images reprinted from BOESSNECK, J. Osteological differences between sheep (*Ovis aries* Linné) and goat (*Capra hircus* Linné). In *Science in archaeology: a survey of progress and research*, eds. D. BROTHWELL and E. HIGGS, 331-358, copyright 1969. London: Thames and Hudson, with permission from Thames and Hudson. Trait 3 to 5: images reprinted from ZEDER, M.A. and H.A. LAPHAM. Assessing the reliability of criteria used to identify postcranial bones in sheep, *Ovis*, and goats, *Capra*. *Journal of Archaeological Science* 37: 2887-2905, copyright 2010, with permission from Elsevier).

Humerus: distal articulation	
<i>Ovis aries</i>	<i>Capra hircus</i>
TRAIT 1: SHAPE OF THE LATERAL EPICONDYLE	
	
The epicondyle <i>lateralis</i> is larger and robust, it projects more laterally and it runs obliquely (Boessneck 1969: 341; Boessneck <i>et al.</i> 1964: 61-67; Helmer and Rocheteau 1994:17; Prummel and Frisch 1986: 569-570)	The epicondyle <i>lateralis</i> is thinner. It projects less laterally and it runs straight (Boessneck 1969: 341; Boessneck <i>et al.</i> 1964: 61-67; Helmer and Rocheteau 1994:17; Prummel and Frisch 1986: 569-570).
TRAIT 2: ASPECT OF THE GROOVE AT THE POSTERIOR SIDE ON THE LATERAL CONDYLE	

<u>Humerus: distal articulation</u>	
<i>Ovis aries</i>	<i>Capra hircus</i>
	
The groove of the posterior aspect of the lateral condyle is continuous and unbroken right up to the lateral condyle (Zeder and Lapham 2010: 2889).	The groove on the posterior aspect of the lateral condyle is bisected by a raised ridge running lateral medially just below the lateral epicondyle (Zeder and Lapham 2010: 2889).
TRAIT 3: ASPECT OF THE PIT ON THE LATERAL EPICONDILAR SURFACE	
	
The pit of the lateral epicondyle is surrounded by a more strongly developed epicondylar surface which is broad and shallow (Boessneck 1969: 341; Boessneck <i>et al.</i> 1964: 61-67; Zeder and Lapham 2010: 2889).	The pit of the lateral epicondyle is less developed, sharply defined and deep (Boessneck 1969: 341; Boessneck <i>et al.</i> 1964: 61-67; Zeder and Lapham 2010: 2889).
TRAIT 4: PRESENCE/ABSENCE OF A THICKENING ON THE LATERAL BORDER OF THE EPICONDILAR SURFACE (crest-like process)	
	
The trochlear surface often shows a granular thickening at the end of the lateral border (Boessneck 1969: 341; Boessneck <i>et al.</i> 1964: 61-67; Helmer and Rocheteau 1994: 18; Prummel and Frisch 1986: 569-570; Zeder	The granular thickening at the end of the lateral border of the trochlear surface is absent or slightly pronounced (Boessneck 1969: 341; Boessneck <i>et al.</i> 1964: 61-67; Helmer and Rocheteau 1994: 18; Prummel and Frisch

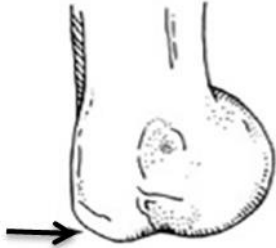
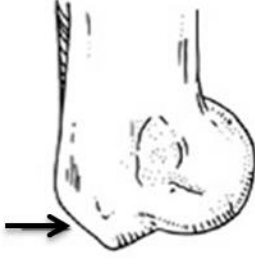
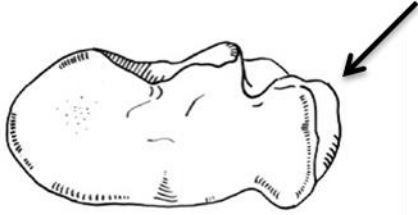
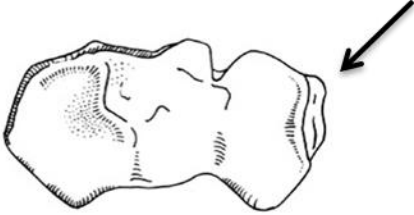
<u>Humerus: distal articulation</u>	
<i>Ovis aries</i>	<i>Capra hircus</i>
and Lapham 2010: 2889).	1986: 569-570; Zeder and Lapham 2010: 2889).
TRAIT 5: ASPECT OF THE ANGLE ON THE DISTAL PART OF THE MEDIAL EPICONDYLE	
	
The distal part of the medial epicondyle ends in an angle that is between a right and obtuse angle (Boessneck 1969: 341; Boessneck <i>et al.</i> 1964: 61-67; Helmer and Rocheteau 1994:16; Prummel and Frisch 1986: 569-570; Zeder and Lapham 2010: 2889).	The distal part of the medial epicondyle ends in an angle that is oblique and looks like it has been cut off (Boessneck 1969: 341; Boessneck <i>et al.</i> 1964: 61-67; Helmer and Rocheteau 1994: 16; Prummel and Frisch 1986: 569-570; Zeder and Lapham 2010: 2889).

Table 2.11 Morphological characteristics adopted for the proximal radius (images reprinted from ZEDER, M.A. and H.A. LAPHAM. Assessing the reliability of criteria used to identify postcranial bones in sheep, *Ovis*, and goats, *Capra*. *Journal of Archaeological Science* 37: 2887-2905, copyright 2010, with permission from Elsevier).

<u>Radius: proximal articulation</u>	
<i>Ovis aries</i>	<i>Capra hircus</i>
TRAIT 1: ASPECT OF THE LATERAL TUBEROSITY	
	
A stronger development of the lateral bicipital tuberosity is visible (Boessneck 1969: 342; Boessneck <i>et al.</i> 1964: 70-71; Prummel and Frisch 1986: 570; Zeder and Lapham 2010: 2890).	The development of the lateral bicipital is weak (Boessneck 1969: 342; Boessneck <i>et al.</i> 1964: 70-71; Prummel and Frisch 1986: 570; Zeder and Lapham 2010: 2890).
TRAIT 2: OVERALL ASPECT OF THE PROXIMAL ARTICULAR SURFACE	

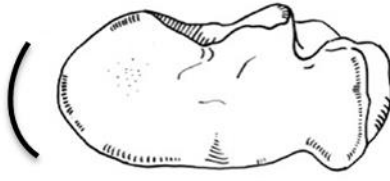
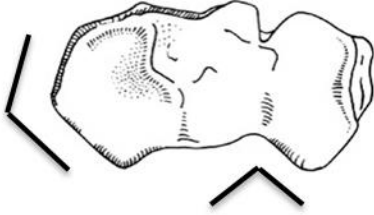
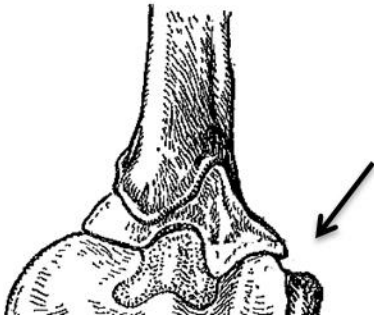
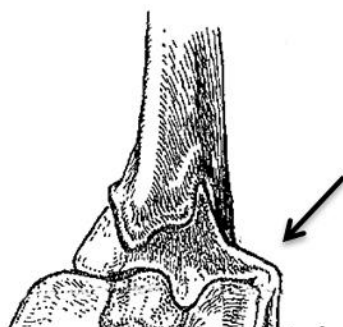
Radius: proximal articulation	
<i>Ovis aries</i>	<i>Capra hircus</i>
	
The medial margin of the proximal articular surface is oval or rounded in shape. The central margin of the articular surface is level with both the lateral and medial margins (Boessneck 1969: 342; Boessneck <i>et al.</i> 1964: 70-71; Prummel and Frisch 1986: 570; Zeder and Lapham 2010: 2890).	The medial margin of the proximal articular surface is angular and squared in shape. The central margin of the articular surface is indented and more angular with a V shape (Boessneck 1969: 342; Boessneck <i>et al.</i> 1964: 70-71; Prummel and Frisch 1986: 570; Zeder and Lapham 2010: 2890).

Table 2.12 Morphological characteristics adopted for the proximal ulna (images reprinted from BOESSNECK, J. Osteological differences between sheep (*Ovis aries* Linné) and goat (*Capra hircus* Linné). In *Science in archaeology: a survey of progress and research*, eds. D. BROTHWELL and E. HIGGS, 331-358, copyright 1969. London: Thames and Hudson, with permission from Thames and Hudson).

Ulna: Olecranon and proximal articulation	
<i>Ovis aries</i>	<i>Capra hircus</i>
TRAIT 1: PROJECTION OF THE LATERAL CORONOID PROCESS	
	
The lateral coronoid process of the ulna does not project so far and it does not unite with the radius (Boessneck 1969: 342; Boessneck <i>et al.</i> 1964: 70; Prummel and Frisch 1986: 570).	The lateral coronoid process of the ulna grows together with the lateral facet of the radius and, with it, forms a laterally projecting edge (Boessneck 1969: 342; Boessneck <i>et al.</i> 1964: 70; Prummel and Frisch 1986: 570).
TRAIT 2: OVERALL SHAPE OF THE OLECRANON	

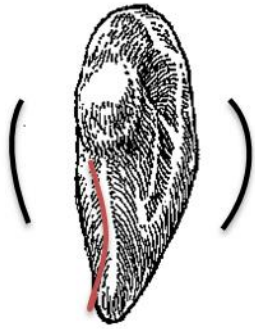
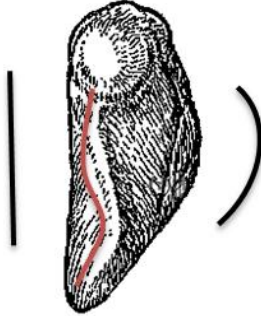
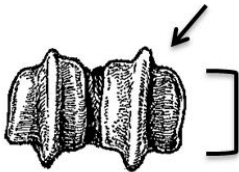

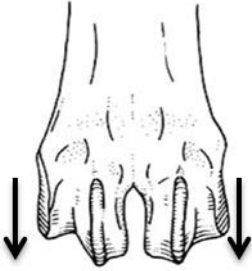
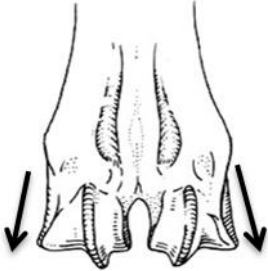
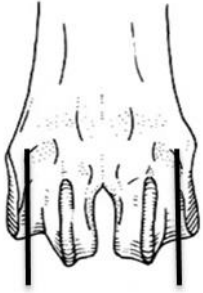


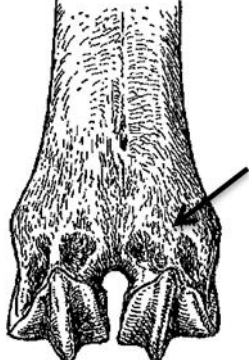
<u>Ulna: Olecranon and proximal articulation</u>	
<i>Ovis aries</i>	<i>Capra hircus</i>
	
<p>The <i>olecranon</i> is shorter. The inner side is slightly curved. On the <i>tuber olecrani</i>, a laterally sloping, smoother face and its terminating border are absent (Boessneck 1969: 343; Boessneck <i>et al.</i> 1964: 74).</p>	<p>The <i>olecranon</i> is longer. Its tuber is thicker. The outer side is more strongly curved and the inner edge, viewed from above, is straight or even slightly bent. On the <i>tuber olecrani</i> a laterally sloping smoother face can be seen. Its partial lateral termination is formed by a more distinct border which runs dorso-volarly (Boessneck 1969: 343; Boessneck <i>et al.</i> 1964: 74).</p>

Table 2.13 Morphological characteristics adopted for the metapodials (traits 1, 2, 5: images reprinted from BOESSNECK, J. Osteological differences between sheep (*Ovis aries* Linné) and goat (*Capra hircus* Linné). In *Science in archaeology: a survey of progress and research*, eds. D. BROTHWELL and E. HIGGS, 331-358, copyright 1969. London: Thames and Hudson, with permission from Thames and Hudson. Traits 3, 4 and 6: images reprinted from ZEDER, M.A. and H.A. LAPHAM. Assessing the reliability of criteria used to identify postcranial bones in sheep, *Ovis*, and goats, *Capra*. *Journal of Archaeological Science* 37: 2887-2905, copyright 2010, with permission from Elsevier).

<u>Metapodials: distal articulation</u>	
<i>Ovis aries</i>	<i>Capra hircus</i>
TRAIT 1: DIMENSION OF THE PERIPHERAL PART OF THE TROCHLEAR CONDYLES	
TRAIT 2: DEFINITION OF THE PERIPHERAL PART OF THE TROCHLEAR CONDYLES	
	
<p>The peripheral parts of the trochlear condyles are relatively bigger. The <i>verticilli</i> on the trochlea are less sharp edged (Boessneck 1969: 354-355; Boessneck <i>et al.</i> 1964: 115-116; Zeder and Lapham 2010: 2892).</p>	<p>The peripheral parts of the trochlear condyles are relatively smaller. They are more sharply defined against the axial part of the trochlear condyle and are more deeply notched-in immediately adjoining the <i>verticillus</i>. The <i>verticilli</i> of the trochlea are sharply defined and steeper (Boessneck 1969: 354-355; Boessneck <i>et al.</i> 1964: 115-116; Zeder and Lapham 2010: 2892).</p>
TRAIT 3: ASPECT OF THE PERIPHERAL PART OF THE TROCHLEAR CONDYLES	

Metapodials: distal articulation	
<i>Ovis aries</i>	<i>Capra hircus</i>
	
The peripheral parts of the trochlear condyles are flatter (Zeder and Lapham 2010: 2892).	The peripheral parts of the trochlear condyles go outward from the axial part of the bone (Zeder and Lapham 2010: 2892).
TRAIT 4: DIRECTION OF THE VERTICILLI	
	
The axial halves of the trochlear condyles with the <i>verticilli</i> run almost parallel in a proximal direction (Boessneck 1969: 355; Boessneck <i>et al.</i> 1964: 107; Prummel and Frisch 1986: 571; Zeder and Lapham 2010: 2892).	The axial halves of the trochlear condyles with the <i>verticilli</i> diverge more strongly in a proximal direction (Boessneck 1969: 355; Boessneck <i>et al.</i> 1964: 107; Prummel and Frisch 1986: 571; Zeder and Lapham 2010: 2892).
TRAIT 5: DEVELOPMENT OF THE FOSSAE ON THE PROXIMAL PART OF THE DISTAL TROCHLEAR CONDYLES	
	
The <i>fossae</i> which join on to the distal trochlear condyles proximally, two each dorsally and volarly or plantarly over each	The <i>fossae</i> which join on to the distal trochlear condyles proximally, two each dorsally and volarly or plantarly over each trochlea, are


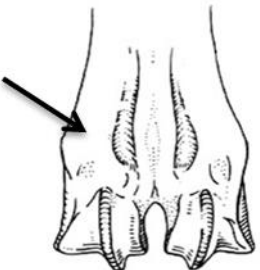

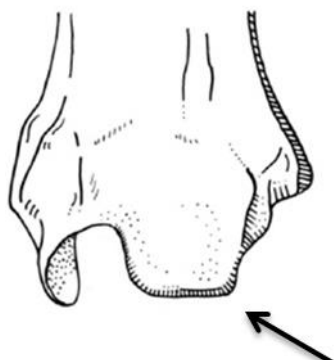

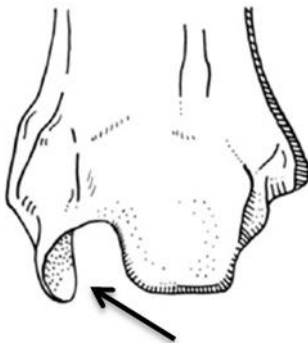
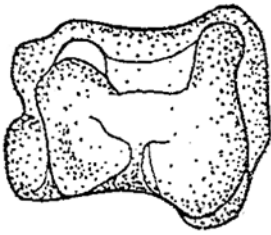
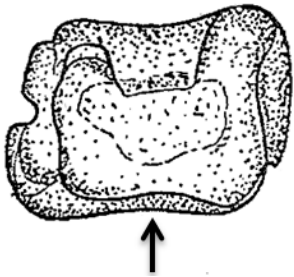
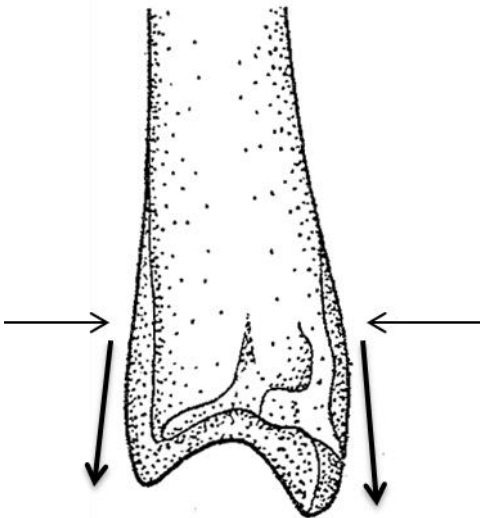
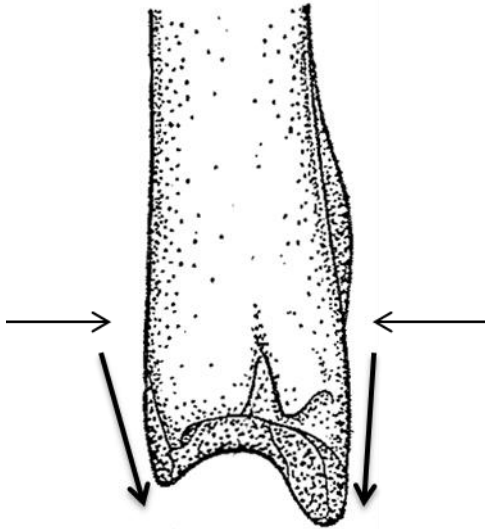
<u>Metapodials: distal articulation</u>	
<i>Ovis aries</i>	<i>Capra hircus</i>
trochlea, are less strongly developed (Boessneck 1969: 355; Boessneck <i>et al.</i> 1964: 107).	strongly developed (Boessneck 1969: 355; Boessneck <i>et al.</i> 1964: 107).
TRAIT 6: ASPECT OF THE JUNCTION ON THE ANTERIOR ASPECT OF THE DISTAL DAIPHYSIS ABOVE THE DISTAL EPIPHYSIS (METATARSAL ONLY)	
	
The junction between the 3 rd and the 4 th metatarsals on the anterior aspect of the distal diaphysis right above the distal epiphysis is flat and not indented (Boessneck <i>et al.</i> 1964: 117-119; Zeder and Lapham 2010: 2892).	The junction between the 3 rd and the 4 th metatarsals on the anterior aspect of the distal diaphysis right above the distal epiphysis is grooved with two prominent ridges on either side (Boessneck <i>et al.</i> 1964: 117-119; Zeder and Lapham 2010: 2892).

Table 2.14 Morphological characteristics adopted for the distal tibia (traits 1, 2, 5 and 6: images reprinted from ZEDER, M.A. and H.A. LAPHAM. Assessing the reliability of criteria used to identify postcranial bones in sheep, *Ovis*, and goats, *Capra*. *Journal of Archaeological Science* 37: 2887-2905, copyright 2010, with permission from Elsevier. Traits 3 and 4: Images reprinted from Kratochvíl, Z. Species criteria on the distal section of the tibia in *Ovis ammon* F. *aries* L. and *Capra aegagrus* F. *hircus* L. *Acta Veterinaria* (Brno), copyright 1969, 38: 483-490. License at: <https://creativecommons.org/licenses/by/4.0/>).

<u>Tibia: distal articulation</u>	
<i>Ovis aries</i>	<i>Capra hircus</i>
TRAIT 1: DORSAL PROMINENCE	
	
The contour of the dorsal prominence is laterally more tortuous (Kratochvíl 1969: 485).	The periphery of the articular surface is, in the medial section, more regularly circular and fuses with the medial contour of the distal prominence. The contour of the dorsal prominence is laterally more ptotic (Kratochvíl 1969: 485).
TRAIT 2: MEDIAL MALLEOLUS	

<u>Tibia: distal articulation</u>	
<i>Ovis aries</i>	<i>Capra hircus</i>
	
If viewed from the anterior side, the medial malleolus is straight so that the articular surface faces laterally (Kratochvíl 1969: 485; Zeder and Lapham 2010: 2891).	If viewed from the anterior side, the medial malleolus is twisted so that more of the articular surface is exposed to view (Kratochvíl 1969: 485; Zeder and Lapham 2010: 2891).
TRAIT 3: PRESENCE/ABSENCE OF THE INTERRUPTION ON THE PLANTAR LIMBUS	
	
The plantar <i>limbus</i> of the articular surface is deeply curved and very often interrupted (Kratochvíl 1969: 488; Prummel and Frisch 1986: 573).	The plantar <i>limbus</i> of the articular surface is less curved and rarely interrupted. (Kratochvíl 1969: 488; Prummel and Frisch 1986: 573).
TRAIT 4: LATERAL PROFILE	
	
When viewed on the lateral side, the medial section of the tibia can be seen. The lateral	When viewed on the lateral side, the medial section is covered. The lateral profile runs

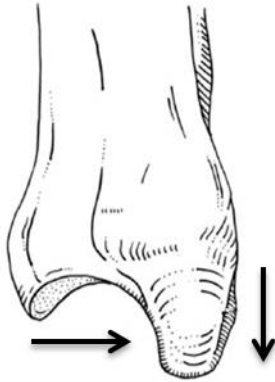

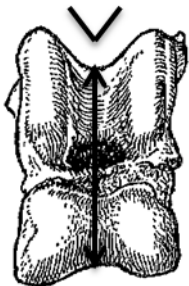
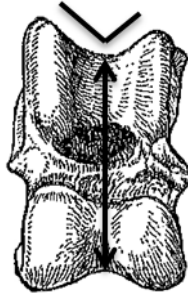
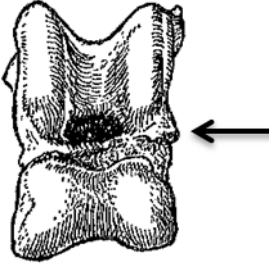
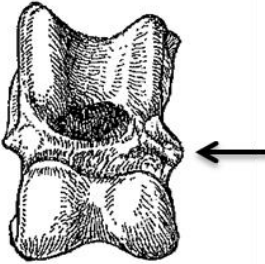
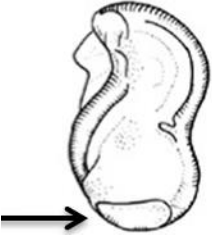

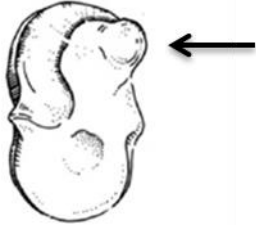
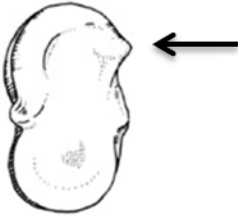
<u>Tibia: distal articulation</u>	
<i>Ovis aries</i>	<i>Capra hircus</i>
profile runs internally but with an obtuse angle (Kratochvíl 1969: 488).	internally forming an acute angle (Kratochvíl 1969: 488).
TRAIT 5: SHAPE OF THE ANTERIOR SIDE OF THE MALLEOLUS	
TRAIT 6: ASPECT OF THE MEDIAL MALLEOLUS	
	
When viewed from the medial aspect, the medial malleolus is rounded on its anterior side, and slopes gradually on its posterior side. It appears bulbous, bulging out convexly in a medial direction (Zeder and Lapham 2010: 2891).	When viewed from the medial aspect, the medial malleolus is angular on its anterior side, and slopes steeply on its posterior side. It is flat and concave (Zeder and Lapham 2010: 2891).

Table 2.15 Morphological characteristics adopted for the astragalus (traits 1, 2, 3 and 6: images reprinted from BOESSNECK, J. Osteological differences between sheep (*Ovis aries* Linné) and goat (*Capra hircus* Linné). In *Science in archaeology: a survey of progress and research*, eds. D. BROTHWELL and E. HIGGS, 331-358, copyright 1969. London: Thames and Hudson, with permission from Thames and Hudson. Traits 4 and 5: images reprinted from ZEDER, M.A. and H.A. LAPHAM. Assessing the reliability of criteria used to identify postcranial bones in sheep, *Ovis*, and goats, *Capra*. *Journal of Archaeological Science* 37: 2887-2905, copyright 2010, with permission from Elsevier).

<u>Astragalus</u>	
<i>Ovis aries</i>	<i>Capra hircus</i>
TRAIT 1: DEPTH OF THE SULCUS OF THE TROCHLEA	
TRAIT 2: INCLINATION OF THE LATERAL PART OF THE TROCHLEA	
	
The sulcus between the two ridges of the trochlea is deeper. The trochlea or its lateral articular ridge stands straight without an angle (Boessneck 1969: 350; Boessneck <i>et al.</i> 1964:	The sulcus between the two ridges of the trochlea is less deep. The trochlea or its lateral articular ridge is inclined slightly medially with reference to the head (Boessneck 1969:

Astragalus	
<i>Ovis aries</i>	<i>Capra hircus</i>
101-103).	350; Boessneck <i>et al.</i> 1964: 101-103).
TRAIT 3: SHAPE OF THE MEDIAL RIDGE	
	
When viewed from the anterior aspect, the medial articular ridge is less strongly expressed and more horizontally oriented (Boessneck 1969: 352; Boessneck <i>et al.</i> 1964: 101-103; Zeder and Lapham 2010: 2893).	When viewed from the anterior aspect, the medial articular ridge is strongly expressed and angled obliquely in a distal direction (Boessneck 1969: 352; Boessneck <i>et al.</i> 1964: 101-103; Zeder and Lapham 2010: 2893).
TRAIT 4: SHAPE OF THE DISTAL ARTICULAR SURFACE ON THE LATERAL ASPECT	
	
When viewed from the lateral aspect, the distal articular surface is semi-circular in shape with a straight proximal edge that runs across the entire lateral face of the bone (Prummel and Frisch 1986: 574; Zeder and Lapham 2010: 2893).	When viewed from the lateral aspect, the distal articular surface forms a tear-drop shape, with a convex proximal edge that does not extend to either the plantar or the dorsal edge of the lateral face of the bone (Prummel and Frisch 1986: 574; Zeder and Lapham 2010: 2893).
TRAIT 5: ASPECT OF THE PROXIMO-PLANTAR PROJECTION ON THE MEDIAL ARTICULAR RIDGE OF THE TROCHLEA	
	
The proximo-plantar projection of the medial articular ridge of the trochlea forms a large and bulbous lobe (Boessneck 1969: 352; Boessneck <i>et al.</i> 1964: 101-103; Prummel and Frisch 1986: 574; Zeder and Lapham 2010: 2893).	The proximo-plantar projection of the medial articular ridge of the trochlea is smaller and flatter and may be more pointed (Boessneck 1969: 352; Boessneck <i>et al.</i> 1964: 101-103; Prummel and Frisch 1986: 574; Zeder and Lapham 2010: 2893).
TRAIT 6: ASPECT AND DIRECTION OF THE ARTICULAR SURFACE ON THE	

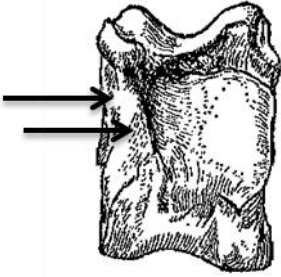
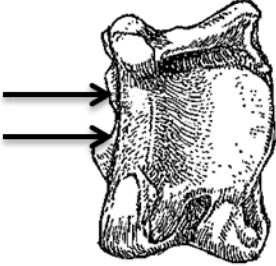

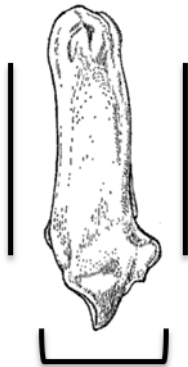
<u>Astragalus</u>	
<i>Ovis aries</i>	<i>Capra hircus</i>
PLANTAR SIDE	
	
<p>The articular surface on the plantar side of the bone goes up higher proximally-medially in a plantar direction. The medial edge of the articular surface usually projects noticeably over the lateral edge. A pad or thickening connecting piece runs from the medial edge of the articulation to the plantar lobe of the medial articular ridge (Boessneck 1969: 352; Boessneck <i>et al.</i> 1964: 101-103; Prummel and Frisch 1986: 574; Zeder and Lapham 2010: 2893).</p>	<p>The medial edge of the articular surface and the lateral edge project roughly equally in a plantar direction. The pad or thickening connecting piece is absent or just slightly indicated (Boessneck 1969: 352; Boessneck <i>et al.</i> 1964: 101-103; Prummel and Frisch 1986: 574; Zeder and Lapham 2010: 2893).</p>

Table 2.16 Morphological characteristics adopted for the calcaneum (traits 1 and 2: images reprinted from ZEDER, M.A. and H.A. LAPHAM. Assessing the reliability of criteria used to identify postcranial bones in sheep, *Ovis*, and goats, *Capra*. *Journal of Archaeological Science* 37: 2887-2905, copyright 2010, with permission from Elsevier. Trait 3: image reprinted from BOESSNECK, J. Osteological differences between sheep (*Ovis aries* Linné) and goat (*Capra hircus* Linné). In *Science in archaeology: a survey of progress and research*, eds. D. BROTHWELL and E. HIGGS, 331-358, copyright 1969. London: Thames and Hudson, with permission from Thames and Hudson).

<u>Calcaneum</u>	
<i>Ovis aries</i>	<i>Capra hircus</i>
TRAIT 1: OVERALL ASPECT	
	
<p>It is shorter and thicker. The depth of the body of the bone increases more in a distal direction (Boessneck 1969: 352; Boessneck <i>et al.</i> 1964: 104-105; Prummel and Frisch 1986: 574).</p>	<p>It is longer and slimmer and slightly curved plantarly. The depth of the body of the bone increases less strongly in a distal direction (Boessneck 1969: 352; Boessneck <i>et al.</i> 1964: 104-105; Prummel and Frisch 1986: 574).</p>

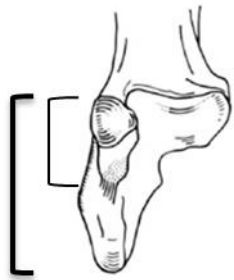

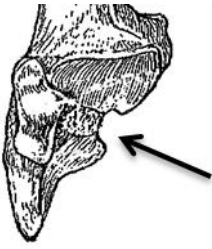
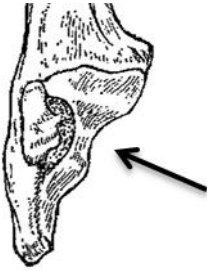


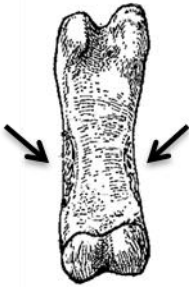
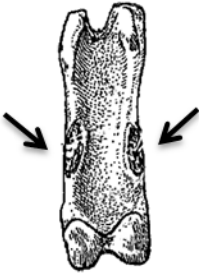


Calcaneum	
<i>Ovis aries</i>	<i>Capra hircus</i>
TRAIT 2: LENGTH OF THE OS MALLEOLARE VS LENGTH OF THE ENTIRE PROCESS	
	
The length of the articular facet for <i>os malleolare</i> on the lateral process is greater than half of the length of the entire process (Boessneck 1969: 353; Boessneck <i>et al.</i> 1964: 104-105; Zeder and Lapham 2010: 2894).	The length of the articular facet for <i>os malleolare</i> on the lateral process is less than half of the length of the entire process (Boessneck 1969: 353; Boessneck <i>et al.</i> 1964: 104-105; Zeder and Lapham 2010: 2894).
TRAIT 3: PRESENCE/ABSENCE OF THE JUNCTION BETWEEN THE TWO INTERNAL ARTICULAR SURFACES	
	
The two articular surfaces of the calcaneum, the narrow one on the medial side of the later process for the lateral side of the ankle-bone and, the large one on the <i>substentaculum tali</i> for the plantar face of the calcaneum, do not join together (Boessneck 1969: 353; Boessneck <i>et al.</i> 1964: 104-105; Prummel and Frisch 1968: 574; Zeder and Lapham 2010: 2894).	The two articular surfaces of the calcaneum, the narrow one on the medial side of the later process for the lateral side of the ankle-bone and, the large one on the <i>substentaculum tali</i> for the plantar face of the calcaneum, often join together (Boessneck 1969: 353; Boessneck <i>et al.</i> 1964: 104-105; Prummel and Frisch 1968: 574; Zeder and Lapham 2010: 2894).

Table 2.17 Morphological characteristics adopted for the 1st phalanx (images reprinted from BOESSNECK, J. Osteological differences between sheep (*Ovis aries* Linné) and goat (*Capra hircus* Linné). In *Science in archaeology: a survey of progress and research*, eds. D. BROTHWELL and E. HIGGS, 331-358, copyright 1969. London: Thames and Hudson, with permission from Thames and Hudson).

1st phalanx	
<i>Ovis aries</i>	<i>Capra hircus</i>
TRAIT 1: SHAPE OF THE GROOVE OF THE PROXIMAL END	
	
The groove between the peripheral and axial articulations of the proximal end is shallow and U shaped (Boessneck 1969: 356; Boessneck <i>et al.</i> 1964: 119-121; Zeder and Lapham 2010: 2895).	The groove between the peripheral and axial articulations of the proximal end is deeper and V shaped (Boessneck 1969: 356; Boessneck <i>et al.</i> 1964: 119-121; Zeder and Lapham 2010: 2895).
TRAIT 2: PRESENCE OF THE SCARS FOR THE MUSCULAR LIGAMENTS ON THE POSTERIOR SIDE	
	
The originating points for ligaments on the posterior side toward the distal end are absent or only visible as a flat scar or outline (Boessneck 1969: 356; Boessneck <i>et al.</i> 1964: 119-121; Zeder and Lapham 2010: 2895).	The originating points for ligaments on the posterior side toward the distal end are raised and pronounced (Boessneck 1969: 356; Boessneck <i>et al.</i> 1964: 119-121; Zeder and Lapham 2010: 2895).
TRAIT 3: ASPECT OF THE POSTERIOR SIDE	
	
The posterior side of the body of the bone is mostly flat or convex (Boessneck 1969: 356; Boessneck <i>et al.</i> 1964: 119-121).	The posterior side of the body of the bone is concave or more rarely flat (Boessneck 1969: 356; Boessneck <i>et al.</i> 1964: 119-121).


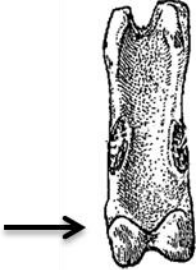
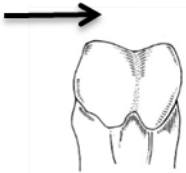

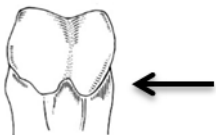
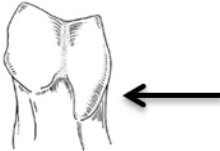
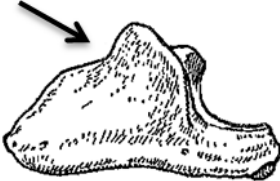
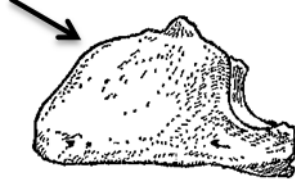
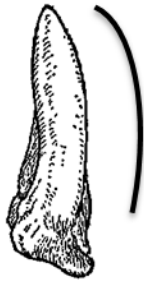
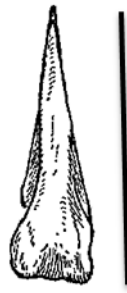
1st phalanx	
<i>Ovis aries</i>	<i>Capra hircus</i>
TRAIT 4: SHAPE OF THE DISTAL ARTICULATION	
	
The posterior edge of the distal articular surface is open or straight so that the articular sections of the distal end are hardly distinguished from one another (Boessneck 1969: 356; Boessneck <i>et al.</i> 1964: 119-121; Zeder and Lapham 2010: 2895).	The posterior edge of the distal articular surface forms a V with its vertex at the articular groove between the articular sections of the distal end (Boessneck 1969: 356; Boessneck <i>et al.</i> 1964: 119-121; Zeder and Lapham 2010: 2895).

Table 2.18 Morphological characteristics adopted for the 2nd phalanx (images reprinted from ZEDER, M.A. and H.A. LAPHAM. Assessing the reliability of criteria used to identify postcranial bones in sheep, *Ovis*, and goats, *Capra*. *Journal of Archaeological Science* 37: 2887-2905, copyright 2010, with permission from Elsevier).

2nd phalanx	
<i>Ovis aries</i>	<i>Capra hircus</i>
TRAIT 1: ASPECT OF THE AXIAL PART OF THE POSTERIOR SIDE OF THE DISTAL ARTICULATION	
	
The axial part and peripheral halves of the distal trochlear condyle both project only slightly distally, giving the articular end a symmetrical appearance (Boessneck 1969: 357; Boessneck <i>et al.</i> 1964: 121-123; Zeder and Lapham 2010: 2896).	The axial part and peripheral halves of the distal trochlear condyle project more distally, giving the articular end an asymmetrical appearance (Boessneck 1969: 357; Boessneck <i>et al.</i> 1964: 121-123; Zeder and Lapham 2010: 2896).
TRAIT 2: ASPECT OF THE RIDGE ON THE POSTERIOR EDGE OF THE DISTAL ARTICULATION	
	
The posterior edge of the distal articular surface is straight or only slightly indented and the peripheral and axial halves of the articular	The posterior edge of the distal articular surface is more sharply indented and the peripheral and axial halves of the articular

2nd phalanx	
<i>Ovis aries</i>	<i>Capra hircus</i>
surface are relatively symmetrical (Boessneck 1969: 357; Boessneck <i>et al.</i> 1964: 121-123; Zeder and Lapham 2010: 2896).	surface form a ridge that continues toward the proximal end giving the distal articular surface an asymmetrical appearance (Boessneck 1969: 357; Boessneck <i>et al.</i> 1964: 121-123; Zeder and Lapham 2010: 2896).

Table 2.19 Morphological characteristics adopted for the 3rd phalanx (images reprinted from BOESSNECK, J. Osteological differences between sheep (*Ovis aries* Linné) and goat (*Capra hircus* Linné). In *Science in archaeology: a survey of progress and research*, eds. D. BROTHWELL and E. HIGGS, 331-358, copyright 1969. London: Thames and Hudson, with permission from Thames and Hudson).

3rd phalanx	
<i>Ovis aries</i>	<i>Capra hircus</i>
TRAIT 1: PRESENCE/ABSENCE OF A SADDLE ON THE DORSAL EDGE	
	
The dorsal edge is generally blunter. The <i>processus extensorius</i> is relatively large and, in front of it, there is a saddle (Boessneck 1969: 358; Boessneck <i>et al.</i> 1964: 123-124)	It looks like it has been pressed flat between two fingers in the anterior half. A sharp dorsal edge is formed with an extremely variable course. The <i>processus extensorius</i> is relatively small (Boessneck 1969: 358; Boessneck <i>et al.</i> 1964: 123-124).
TRAIT 2: SHAPE OF THE SOLE	
	
The side edges of the sole surface are more curved, the outside edge convex, the inner edge in its anterior third also convex but in the middle part concave (Boessneck 1969: 357; Boessneck <i>et al.</i> 1964: 123-124).	The narrow sole surface forms an isosceles triangle with a very short base. The sole surface stands almost vertically to the sagittal plane from proximo-axial to disto-peripheral direction (Boessneck 1969: 357; Boessneck <i>et al.</i> 1964: 123-124).

Every chosen morphological trait has been observed, recorded on an access worksheet, and scored by using the scale shown in Table 2.20.

Table 2.20 List of the scores given for each morphological traits evaluated.

Code	Meaning
C	Consistent with <i>Capra</i> ; when the characteristic could be attributed unambiguously to <i>Capra</i>
O	Consistent with <i>Ovis</i> ; when the characteristic could be attributed unambiguously to <i>Ovis</i>
CL	<i>Capra</i> -like; when the characteristic can be attributed to <i>Capra</i> with a certain degree of confidence
OL	<i>Ovis</i> -like; when the characteristic can be attributed to <i>Ovis</i> with a certain degree of confidence
O/C	Not clearly identifiable; when the characteristic cannot be attributed to <i>Capra</i> or <i>Ovis</i>
NA	(Not Available) The characteristic is not visible because the bone is broken in the region where the trait should be visible or, in the case of teeth, when the tooth is too heavily worn

2.1.3 Biometrical approach

The aim of the biometrical approach is to give zooarchaeologists a (relatively) new and alternative tool for distinguishing the two species, but particularly to present the proposed identifications in a more objective way that is open to scrutiny. All methods have their inevitable limitations and a combination of the two approaches, biometrical and morphological, is proposed.

The biometrical method can be used both as a tool to verify identifications based on morphology or to attempt identifications for specimens that could not be attributed to species on the basis of morphological traits.

As previously mentioned, biometry has been used in the past on both modern and archaeological material and, the results obtained have revealed its potential (Davis in press; Fernández 2001; Onar *et al.* 2008; Payne 1969; Rowley-Conwy 1998). Nevertheless, as the method was applied only to a limited selection of anatomical elements, further analysis is desirable. This project applies the biometrical approach to a variety of cranial and post cranial elements, in the hope of finding other indices that can be used for sheep/goat distinction, thus supplementing and extending the information provided by previous research.

Like for the morphological criteria, a selection of anatomical elements and related measurements was made. Some of the criteria used for the selection are the same as for the morphology approach (Section 2.1.2), but, in addition, the choice of measurements was made according to:

- a critical analysis of previous studies focused on biometry;
- a selection of important morphological criteria on the selected body parts that could be translated relatively easily into measurements.

Measurements suggested in previous studies (Davis in press; Fernández 2001; Payne 1969), as well as some of those routinely taken by zooarchaeologists (cf. von den Driesch manual 1976)

have been selected. To these, new measurements designed to describe biometrically diagnostic morphological differences have also been devised and recorded. The following anatomical elements have been selected for the biometrical approach:

- Cranium:
 - Horncores
 - Mandible
 - Loose mandibular teeth
- Postcranial:
 - Glenoid cavity and articulation of the Scapula
 - Distal articulation of the Humerus
 - Proximal articulation of the Radius
 - Proximal articulation of the Ulna
 - Distal articulation of the Metacarpal
 - Distal articulation of the Metatarsal
 - Distal articulation of the Tibia
 - Astragalus
 - Calcaneum
 - 3rd Phalanx

The anatomical elements selected are essentially the same which were chosen for the morphological study, with the exception of the 1st and 2nd phalanx. These elements have been included in the morphological study because they bear valuable morphological traits but they have been excluded from the biometrical study because these criteria were not easily translatable into measurements.

Although teeth in the mandible were not excluded from the study, loose teeth were generally preferred. This choice was made for two main reasons. Firstly, loose teeth are more common in archaeological assemblages than complete mandibles with rows of teeth still in place. Secondly, because the measurements on the tooth are taken (later in this section) in an area which is often hidden (either by the mandible bone or by the contact with the other teeth) if the tooth is still *in situ* and/or not completely erupted. In both cases the results are the same: measurements cannot be taken as positioning the calliper correctly and consistently is not possible.

Table 2.21 shows respectively the reference from which the measurements have been adopted and a description of which morphological differences they try to translate. Tables 2.22 to 2.33 explain and display how to take the measurements. Pictures are provided only for the new measurements and those that have been slightly modified from the previous literature.

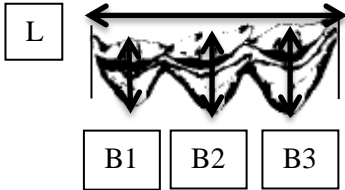
Table 2.21 References for the chosen measurements with reference to the morphological traits they translate. Measurements in which the authors name is cited with an asterisk are those that have been slightly modified from the original version, while those only represented by an asterisk have been newly devised by the author.

Element	Measurements	Bibliography	Morphological trait translated	
Cranial elements	dP ₃	B	von den Driesch 1976*	Shape of the tooth (dP _{3.1})
		L	von den Driesch 1976*	
	dP ₄	B1	*	Shape of the tooth
		B2	*	
		B3	*	
		L	von den Driesch 1976*	
	P ₃	B	von den Driesch 1976*	Shape of the tooth (P _{3.1})
		L	von den Driesch 1976*	
	P ₄	B	von den Driesch 1976*	Shape of the tooth (P _{4.1})
		L	von den Driesch 1976*	
	M ₃	B1	*	Shape of the tooth
		B3	*	
		L	von den Driesch 1976*	
	Mandible	H	*	Position and presence of the foramen on the face of the mandible (Mandible.1)
		B	*	
		PF	*	
	Horncores	A	von den Driesch 1976	Section of the base (Hc.1)
		B	von den Driesch 1976	
		C	*	Section of the middle of the horncore (Hc.1)
		D	*	
E		*	Curvature Section of the base (Hc.2)	
F		von den Driesch 1976		
Scapula	BG	von den Driesch 1976	Shape of the glenoid cavity (Sc.2)	
		von den Driesch 1976		
	GLP	von den Driesch 1976	Shape of the area between the neck, the spine and the glenoid cavity	
	SLC	von den Driesch 1976		
	ASG	English Heritage forthcoming Fernández 2001, *		
Humerus	BT	Payne and Bull 1988	Shape of the trochlea and the distal end	
	Bd	von den Driesch 1976		

Element	Measurements	Bibliography	Morphological trait translated	
	HT	Davis 1996;	Shape of the lateral epicondyle (Hu.1)	
	HTC	Payne and Bull 1988;		
	BE	*		
	Dd	Fernàndez 2001, *		
	BEI	*		
Post-cranial elements	Radius	Bp	von den Driesch 1976	Shape of the proximal end (Ra.1 and 2)
		BFp	von den Driesch 1976	
		Dp	Fernàndez 2001; *	Shape of the bone
		GL	von den Driesch 1976	
		SD	von den Driesch 1976	
	Ulna	B	Fernàndez 2001; *	Shape of the <i>olecranon</i> (Ul.2)
		L	Fernàndez 2001; *	
		DPA	von den Driesch 1976	Shape of the <i>processus anconaeus</i> (Ul.1)
		BPC	von den Driesch 1976	
		SDO	von den Driesch 1976	
	Tibia	Bd	von den Driesch 1976	Shape of the distal end
		Dd(a)	von den Driesch 1976*	
		Dd(b)	*	
	Astragalus	Bd	von den Driesch 1976	Shape of the bone
		GLm	von den Driesch 1976	
		GLI	von den Driesch 1976	
		Dm	von den Driesch 1976	
		DI	von den Driesch 1976	
		H	*	
		BpT	*	Projection of the medial edge of the articular surface and the lateral edge (Ast.6)
	Calcaneum	BS	von den Driesch 1976*	Shape of the bone (Cc.1)
		GL	von den Driesch 1976	
		c	Fernàndez 2001; *	Relationship between the articular facet of the <i>os malleolare</i> and the entire process (Cc.2)
d		Fernàndez 2001;		

Element	Measurements	Bibliography	Morphological trait translated
		*	
	B	Boessneck 1969 Boessneck <i>et al.</i> 1964,	Breadth of the <i>os malleolare</i>
	DS	English Heritage forthcoming	
	Gd	Albarella and Payne 2005	
Metapodials	GL	von den Driesch 1976	Shape of the bone
	SD	von den Driesch 1976	
	BatF	Davis 1996	
	BFd	Davis 1996	
	a	Payne 1969; Davis 1996	Relative dimension of the medial and lateral trochlea and of the <i>verticilli</i> (Mc/Mt.1 and 2)
	b	Payne 1969; Davis 1996;	
	1	Payne 1969*; Davis 1996*	
	2	Davis 1996	
	3	Davis 1996	
	4	Payne 1969*; Davis 1996*	
	5	Davis 1996	
	6	Davis 1996	
	3 rd Phalanx	DLS	von den Driesch 1976
MBS		von den Driesch 1976	

Table 2.22 Measurements taken on teeth (dP₄: image reprinted from PAYNE, S. Morphological distinctions between the mandibular teeth of young sheep, *Ovis*, and goats, *Capra*. *Journal of Archaeological Science* 12: 139-147, copyright 1985, with permission from Elsevier. M₃: image reprinted from HALSTEAD, P., P. COLLINS and V. ISAKKIDOU. Sorting the sheep from the goats: morphological distinctions between the mandibles and mandibular teeth of adult *Ovis* and *Capra*. *Journal of Archaeological Science* 29: 545-553, copyright 2002, with permission from Elsevier).

Description of the measurements		
dP ₃	B = greatest breadth; L = greatest length.	
dP ₄	B1; B2; B3 = greatest breadth of the first, second and third pillar; L = greatest length.	
P ₃	B = greatest breadth; L = greatest length.	
P ₄	B = greatest breadth; L = greatest length.	

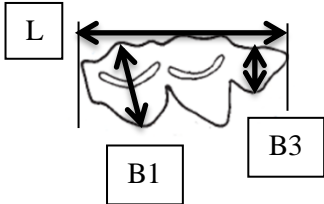
Description of the measurements		
M ₃	<p>B1; B3= greatest breadth of the first and third pillar; L= greatest length.</p>	

Table 2.23 Measurements taken on the mandible (images reprinted from HALSTEAD, P., P. COLLINS and V. ISAKKIDOU. *Sorting the sheep from the goats: morphological distinctions between the mandibles and mandibular teeth of adult Ovis and Capra. Journal of Archaeological Science* 29: 545-553, copyright 2002, with permission from Elsevier).

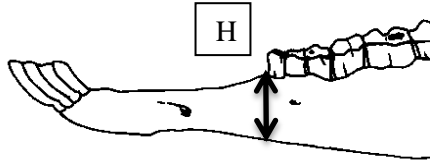
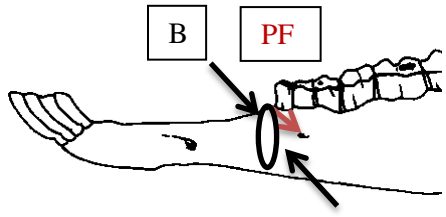
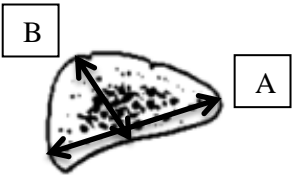
Description of the measurements		
<p>H= Height of the mandible from the alveolus of the dP₂/P₂ to the basal edge of the <i>ramus mandibulare</i>.</p>		
<p>B= breadth of the mandible taken close to the alveolus of the dP₂/P₂.</p> <p>PF= position of the foramen taken from the dP₂/P₂ alveolus. The measurement will have a <u>plus</u> before the value if the foramen is located on the space between the canine and the premolar where the dP₂/P₂ alveolus is, a <u>minus</u> if located after the dP₂/P₂ alveolus. Callipers have to be placed on the anterior edge of the dP₂/P₂ alveolus.</p>		

Table 2.24 Measurements taken on the horncore (images reprinted from SCHMID, E. *Atlas of animal bones: for prehistorians, archaeologists and quaternary geologists*. Amsterdam: Elsevier, copyright 1972, with permission from Joerg Schibler).

Description of the measurements		
<p>A= Maximum diameter of the horncore at the base.</p>		
<p>B= Minimum diameter of the horncore at the base.</p>		

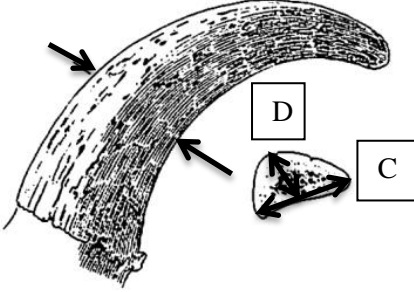
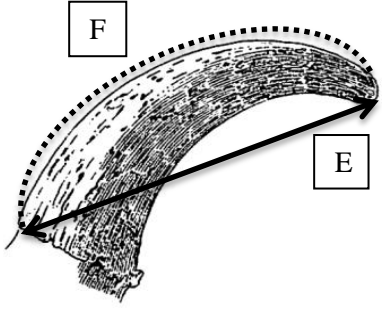
Description of the measurements	
C= Maximum diameter taken at the middle of the horncore length.	<p>Later view of the horn</p> 
D= Minimum diameter taken at the middle of the horncore length.	
E= Length of the horncore from the antero-medial edge of the base to the tip.	
F= Length of the outer curvature of the horncore taken with a tape measure.	

Table 2.25 Measurements taken on the scapula (image reprinted from BOESSNECK, J. Osteological differences between sheep (*Ovis aries* Linné) and goat (*Capra hircus* Linné). In *Science in archaeology: a survey of progress and research*, eds. D. BROTHWELL and E. HIGGS, 331-358, copyright 1969. London: Thames and Hudson, with permission from Thames and Hudson).

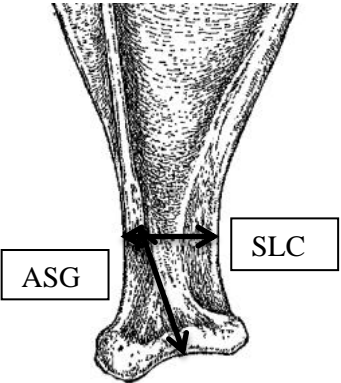
Description of the measurements	
BG= breadth of the glenoid cavity.	
LG= length of the glenoid cavity.	
GLP= greatest length of the <i>processus articularis</i> .	
ASG= shortest distance from the base of the spine to edge of glenoid cavity.	
SLC= the smallest length of the <i>collum scapulae</i> .	

Table 2.26 Measurements taken on the distal humerus (image 1: reprinted from BOESSNECK, J. Osteological differences between sheep (*Ovis aries* Linné) and goat (*Capra hircus* Linné). In *Science in archaeology: a survey of progress and research*, eds. D. BROTHWELL and E. HIGGS, 331-358, copyright 1969. London: Thames and Hudson, with permission from Thames and Hudson. Image 2: reprinted from ZEDER, M.A. and H.A. LAPHAM. Assessing the reliability of criteria used to identify postcranial bones in sheep, *Ovis*, and goats, *Capra*. *Journal of Archaeological Science* 37: 2887-2905, copyright 2010, with permission from Elsevier. Image 3 (Fig. 32e): reprinted from von den Driesch, A. *A guide to the measurement of animal bones from archaeological sites*. Peabody Museum Bulletins, vol. 1. Copyright 1976 with permission from the President and Fellows of Harvard College).

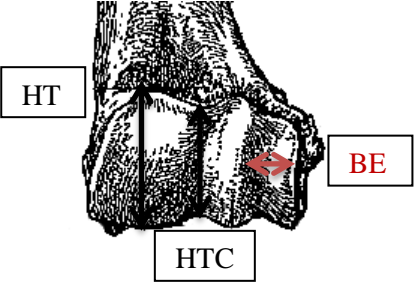
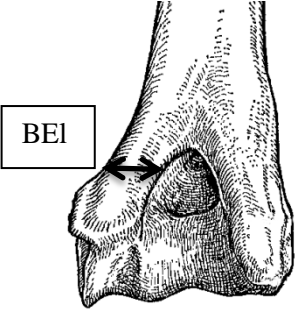
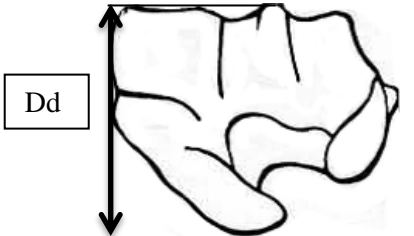
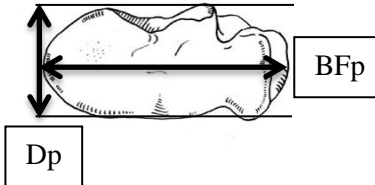
Description of the measurements	
BT = greatest breadth of the trochlea taken on the edges.	
Bd = greatest breadth of the distal end.	
HT = greatest height of the trochlea.	
HTC = diameter of the trochlea at central constriction.	
BE = breadth of the <i>capitulum</i> .	
BEI = breadth of the epicondyle <i>lateralis</i> taken on a depth of 2/3 mms from the lateral margin.	
Dd = depth of the distal end.	

Table 2.27 Measurements taken on the radius (image reprinted from ZEDER, M.A. and H.A. LAPHAM. Assessing the reliability of criteria used to identify postcranial bones in sheep, *Ovis*, and goats, *Capra*. *Journal of Archaeological Science* 37: 2887-2905, copyright 2010, with permission from Elsevier).

Description of the measurements	
Bp = greatest breadth of the proximal end.	

Description of the measurements	
BFp = greatest breadth of the <i>facies articularis proximalis</i> .	
Dp = depth of the proximal end.	
GL = greatest length.	
SD = smallest breadth of the diaphysis.	

Table 2.28 Measurements taken on the ulna (images (Figs. 33b and 33e): reprinted from von den Driesch, A. *A guide to the measurement of animal bones from archaeological sites*. Peabody Museum Bulletins, vol. 1. Copyright 1976 with permission from the President and Fellows of Harvard College).


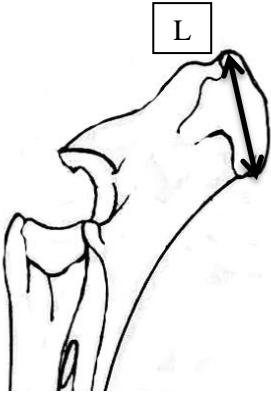
Description of the measurements	
B = breadth of the <i>olecranon</i> taken by keeping the arms of the callipers parallel to the medial face.	
L = length of the <i>olecranon</i> .	
BPC = greatest breadth across the coronoid process.	
DPA = depth across the <i>processus anconaeus</i> .	
SDO = smallest depth of the <i>olecranon</i> .	

Table 2.29 Measurements taken on the metapodials (image 1: reprinted from ZEDER, M.A. and H.A. LAPHAM. Assessing the reliability of criteria used to identify postcranial bones in sheep, *Ovis*, and goats, *Capra*. *Journal of Archaeological Science* 37: 2887-2905, copyright 2010, with permission from Elsevier. Image 2: reprinted from BOESSNECK, J. Osteological differences between sheep (*Ovis aries* Linné) and goat (*Capra hircus* Linné). In *Science in archaeology: a survey of progress and research*, eds. D. BROTHWELL and E. HIGGS, 331-358, copyright 1969. London: Thames and Hudson, with permission from Thames and Hudson).

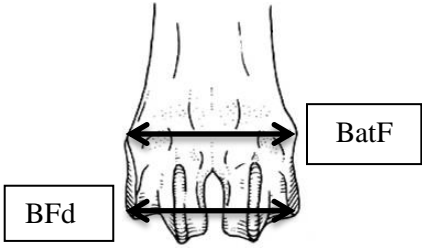
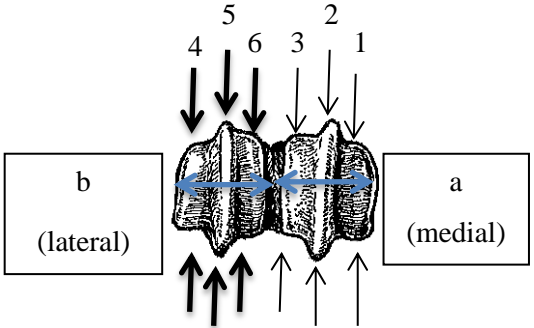
Description of the measurements	
BatF= breadth of the distal end in the point of fusion with the diaphysis.	
BFd= breadth of the distal articulation.	
a= medio-lateral width of the medial condyle.	
b= medio-lateral width of the lateral condyle.	
1= diameter of the external trochlea of the medial condyle. Callipers need to be positioned at the external edge of the trochlea.	
2= diameter of the <i>verticillus</i> on the medial condyle.	
3= diameter of the internal trochlea of the medial condyle.	
4= diameter of the external trochlea of the lateral condyle. Callipers need to be positioned at the external edge of the trochlea.	
5= diameter of the <i>verticillus</i> of the lateral condyle.	
6= diameter of internal trochlea of the lateral condyle.	
GL= greatest length.	
SD= smallest breadth of the diaphysis.	

Table 2.30 Measurements taken on the tibia (image reprinted from Kratochvíl, Z. Species criteria on the distal section of the tibia in *Ovis ammon* F. *aries* L. and *Capra aegagrus* F. *hircus* L. *Acta Veterinaria* (Brno), copyright 1969, 38: 483-490. License available at: <https://creativecommons.org/licenses/by/4.0/>).

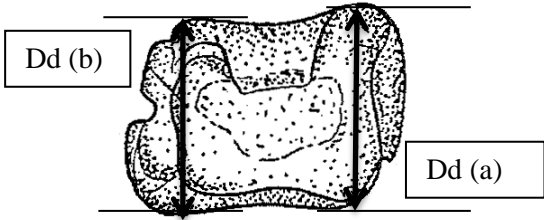
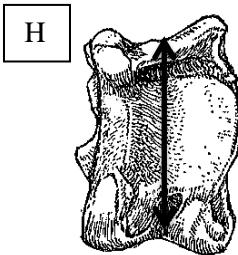
Description of the measurements	
Bd = greatest breadth of the distal end.	
Dd (a) = depth of the distal end on the medial side.	
Dd (b) = depth of the distal end on the lateral side.	
GL = greatest length.	
SD = smallest breadth of the diaphysis.	

Table 2.31 Measurements taken on the astragalus (images reprinted from BOESSNECK, J. Osteological differences between sheep (*Ovis aries* Linné) and goat (*Capra hircus* Linné). In *Science in archaeology: a survey of progress and research*, eds. D. BROTHWELL and E. HIGGS, 331-358, copyright 1969. London: Thames and Hudson, with permission from Thames and Hudson).

Description of the measurements	
Bd = greatest breadth of the distal end.	
GLm = greatest length of the medial half.	
Dm = greatest depth of the medial half.	
GLl = greatest length of the lateral half.	
DI = greatest depth of the lateral half.	
H = height at the central constriction.	
BpT = smallest breadth of the plantar trochlea.	

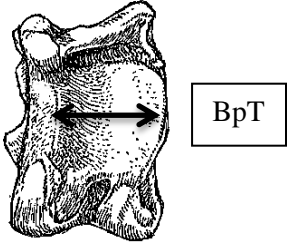
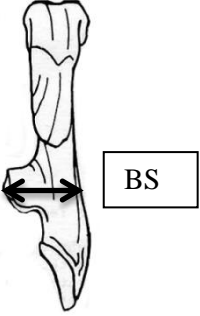
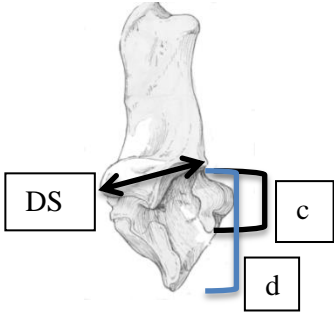
Description of the measurements	
	

Table 2.32 Measurements taken on the calcaneum (image 1 (Fig. 42b): reprinted from von den Driesch, A. *A guide to the measurement of animal bones from archaeological sites*. Peabody Museum Bulletins, vol. 1. Copyright 1976 with permission from the President and Fellows of Harvard College. Images 2 and 3: reprinted from ZEDER, M.A. and H.A. LAPHAM. Assessing the reliability of criteria used to identify postcranial bones in sheep, *Ovis*, and goats, *Capra*. *Journal of Archaeological Science* 37: 2887-2905, copyright 2010, with permission from Elsevier. Image 4: reprinted from BOESSNECK, J. Osteological differences between sheep (*Ovis aries* Linné) and goat (*Capra hircus* Linné). In *Science in archaeology: a survey of progress and research*, eds. D. BROTHWELL and E. HIGGS, 331-358, copyright 1969. London: Thames and Hudson, with permission from Thames and Hudson).

Description of the measurements	
BS = breadth taken at the height of the <i>substantaculum tali</i> .	
GL =greatest length.	
c = length of the articular facet.	
d =length from the articular facet to the articulation-free part of the process.	
DS = greatest depth of the <i>substantaculum tali</i> .	
B = breadth of the articular surface for the <i>os malleolare</i> .	

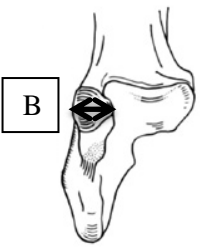
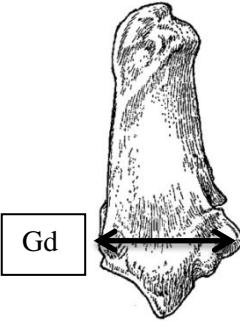
Description of the measurements	
	
Gd = greatest breadth of the distal part (taken from the surface of the <i>os malleolare</i> to the plantar side in its maximum point of expansion).	

Table 2.33 Measurements taken on the 3rd phalanx.

Description of the measurements	
DLS = greatest diagonal length of the sole	
MBS = middle breadth of the sole	

The reliability of measurements as a tool of study in archaeology has been investigated by multiple researchers (Davis 1996; Johnstone 2004; Lyman & VanPool 2009; Popkin *et al.* 2012; Simpson *et al.* 1960; Write 2014). In zooarchaeology, the importance of measurements as a tool of investigation became even clearer after the introduction of the guide for measuring animal bone from archaeological sites, published by Angela von den Driesch (1976). Von den Driesch and, more recently, also Lyman and VanPool in their paper on the use of metric data in archaeology (2009), give a list of the characteristics measurements must have in order to be reliable: comparability, standardisation, and measurability. These important concepts will be analysed in further depth in another section (Section 2.3). In this section, the problem of measurability will be discussed as experienced by the author during the study.

Measurability is defined as the possibility of taking measurements in a precise way (i.e. the precision is the similarity of repeated measurements of the same specimens, *sensu* Lyman & VanPool 2009: 487). As von den Driesch acknowledges in her book (1976: 6), some elements are more precisely measureable than others because they feature easily and precisely defined points.

During the data collection phase of this project and afterwards, when the data from the modern material were analysed, it became clear that this phenomenon was affecting some of the measurements included in the recording protocol. A list of the measurements affected follows along with an explanation of why the problem occurred.

While the other measurement taken on the mandible (PF) has well defined landmarks where to position the callipers, in B and H (breadth and height of the mandible taken close to the *alveolus* of the dP_2/P_2), clear fixed points on the bone are not so easily recognizable (Fig. 2.1). In addition, in the case of H, the process of taking the measurement is made even harder by the fact that the surface of the mandible has a crest on the inter-alveolar border which makes it difficult to hold the callipers firmly.

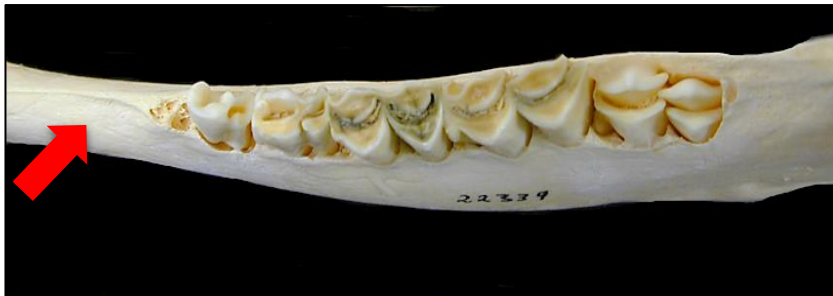


Figure 2.1 Left mandible of a modern specimen of sheep from the reference collection of Kiel (n. 22339) showing the ridge on the inter-alveolar edge of the bone.

Some imprecision was recorded when A and B were taken, mainly due to the problem of identifying where the horncore starts on the skull and, consequently, where to position the callipers (Fig. 2.2). In some specimens the area of transition from the skull to the horncore is not clearly marked with a bony ring as in other species. As a result, some confusion may occur. For C and D, the problem was related to the fact that a universal definition of “taken at the middle of the horncore” is difficult to provide; this location will always depend on the size and shape of the individual specimen.

Finally, E and F share with A and B the problem of establishing where the horncore starts, but, in the case of F, the fact that the measurement is taken with a tape and then transferred to callipers to make it readable, inevitably influences the measurability. This process is extremely imprecise, no matter the care put into the task.



Figure 2.2 Left horncore of a modern sheep specimen from the reference collection of Portsmouth (n. 2832) showing a barely visible separation between the horn and the skull.

ASG measures the shortest distance from the base of the spine to the edge of the glenoid cavity (Fig. 2.3). Because of the nature of the area measured, the arms of the callipers do not grip the surfaces but may only be located close to the region where the crest arises, so that the tool cannot be held firmly. In addition, the area at the base of the spine is not measurement-friendly: it is a rounded area on which the callipers cannot be held without difficulty. In the case of SLC, the problem is that a pecten may sometimes be present on the neck of the scapula. In this case, the callipers have been positioned in the region below the pecten so that the bulging area is left out of the measurement (after English Heritage forthcoming).

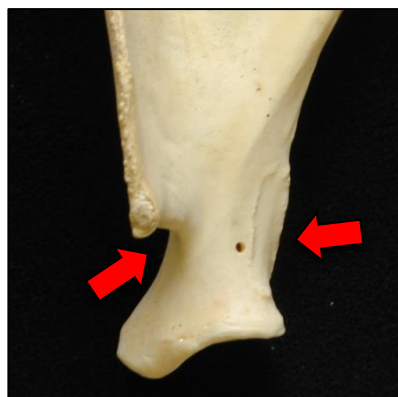


Figure 2.3 Left scapula of a modern sheep specimen from the reference collection of Portsmouth (n. 3282) showing the presence of a pecten on the caudal side of the neck. It is also possible to see the rounded area at the base of the spine mentioned in the text.

The difficulty in taking BE (breadth of the *capitulum*) is due to the fact that no clear landmarks are detectable, especially on the medial part of the *capitulum* (Fig. 2.4). In this area, the callipers cannot be held firmly as the arms do not grip a surface; they can only be held close to the part of the bone to measure. For BEI, the problem is the definition of the measurement and the nature of the area where it is taken. BEI is the breadth of the lateral epicondyle taken on a depth of 2/3 mm. 2/3 millimetre cannot be precisely measured (as it would be very impractical and would require too much time), in addition the area has no clear landmarks showing where to consistently position the callipers. As a consequence, taking this measurement consistently was difficult.

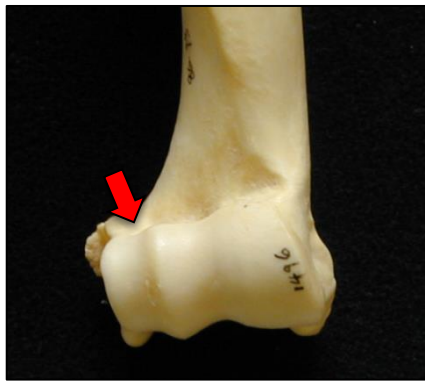


Figure 2.4 Distal right articulation of the humerus of a modern sheep specimen from the reference collection of Portsmouth (n. 1496) showing the lack of landmarks in the region where BE is taken.

B (breadth of the *olecranon* taken by keeping the callipers parallel to the medial surface) is particularly difficult to take in sheep as the shape of the medial surface of the *olecranon* is such that there is not a straight surface on which to hold the callipers (Fig. 2.5). As a result, the measurement cannot be taken in a very consistent way.



Figure 2.5 Left *olecranon* of an ulna from a modern specimen of sheep from the reference collection of Kiel (n. 22339) which shows how the medial side of the bone can be convex in *Ovis*.

The problem for Dm (greatest depth of the medial half) affects mainly goats as, in this region, goats have a developed ridge which runs medio-laterally and projects out (Fig. 2.6). When the arms of the callipers are positioned, they cannot be held firmly as the bone has a tendency to swing around the two points of contact the medial surface has with the callipers' arms, as von den Driesch (1976: 89) notes.

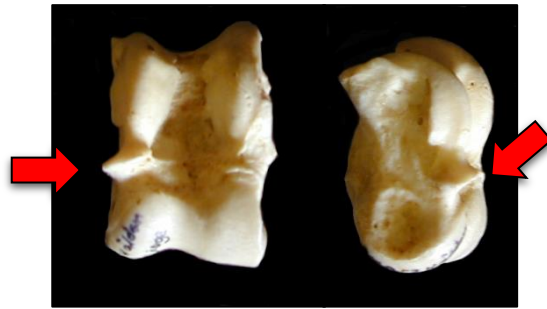


Figure 2.6 Left astragalus (frontal and medial side) of a modern specimen of goat from the reference collection of Halle (n. Cswd 2) showing the lateral projection of the ridge.

A problem emerged regarding measurement of c (i.e. the length of the articular facet) (Fig. 2.7). The beginning of this area, which is clearly visible on the bone (a line defines the articular facet), may, in some specimens, coincide with the area that projects out, forming the *os malleolare*, but, in other specimens, the beginning of the articular facet is visible before it starts to project out. It was decided, for the sake of consistency, to take c on the area where the articular facet starts to project out in all specimens.



Figure 2.7 *Calcanea* from a modern specimen of goat (right, n. 1315) and sheep (left, n. 1496) from the reference collection of Portsmouth showing how the morphology of the area where the articular facet of the *os malleolare* attaches can vary.

The measurability issue that some measurements have raised has not led to the omission of all of them from the adopted protocol, though it must be borne in mind during interpretation. As the main purpose of this project is finding Biometrical Indices (BI) for sheep/goat identification, the measurements which have proved to be effective for the identification have been retained, while those which have shown not to have potential in discriminating have been discarded.

2.1.4 The Recording Protocol

A system was created which consists of four main database structures. Two tables were set up for recording teeth and mandible data and two for recording the post-cranial bones. Each pair of database structures contains a table which was designed to collect the measurements and another used for recording morphological traits. The tables were then joined together in order to link the morphological traits and the measurements to the specimen. This link between tables was also useful in order to avoid information redundancy.

The anatomical parts of the skeleton were recorded when the chosen area was present and preserved almost completely, that is, when a fractured/missing part did not affect the possibility of taking at least a measurement or of making observations of the morphological characteristics.

The side of teeth and bones was recorded. It was decided to record only one side, the left, of every specimen. If the left side was not available (there were no significant differences between right and left side), the right side was measured and scored in order to have as many complete specimens as possible.

The degree of fusion was also recorded. Only fused and fusing bones were included in the analysis and measured. The decision to exclude the un-fused bones was made prior to starting due to the following factors:

because the morphological criteria are less well defined on immature bones;
because, after several attempts during the research, it was clear that taking measurements on unfused epiphyses was more complicated and time consuming than using adult bones;
because of the difficulty of finding enough immature and juvenile modern specimens for a representative study.

If fused and un-fused bones belonged to the same specimen, only the fused skeletal elements were recorded and measured. If recordable elements were fused together (i.e. radius and ulna), they were recorded and measured separately; reference to each other was made in the comments.

Regarding teeth, the degree of tooth wear was recorded following Payne (1973, 1987) and measurements were taken only when there was sufficient enamel preserved.

All the measurements were taken in millimetres, with only one decimal point (i.e. they are approximated to the tenth of millimetre) by using digital callipers. Exception was made for those measurements taken with the measuring box or measuring tape, which have no decimal point (i.e. they are approximated to the millimetre).

2.2 Materials

A detailed description of the material making up the modern reference sample is provided in this section. The reasons behind the selection of British and central European breed samples have already been mentioned. Nevertheless, some Mediterranean and Near East specimens have been included in the analysis in order to increase the sample size, especially for the goat group, as British modern goat specimens were very difficult to obtain.

Different institutions have been visited in order to collect a wide sample of modern sheep and goat specimens. As far as sheep are concerned, the core of the modern sample derives from the collection hosted at Historic England in Portsmouth. The Fort Cumberland modern collection was chosen because it could provide a wide number of specimens of different age and sex, of Shetland and Soay breeds. These breeds are considered of particular interest because they retain some primitive traits; as unimproved animals, they are considered breeds that better resemble the medieval animals (Clutton-Brock *et al.* 1990; Davis 1996). In addition to the large sample from the Historic England collection, several other sheep specimens belonging to different breeds were included. Some Mediterranean specimens hosted at the University of Sheffield and some German, Alpine and Near Eastern breeds were recorded at the Natural History Museum of Berlin and at the Zooarchaeology Laboratory at the University of Kiel (Germany).

For the goat the situation was more complicated. Studying goats from British breeds would have represented the perfect scenario but, now as in the past, goats are not particularly common in Britain. Because of this lack of modern specimens, the attention was focused on central European goats. As mentioned for the sheep modern sample, different institutions were visited: the Zooarchaeology Laboratory at the University of Sheffield, the Zooarchaeology Laboratory at the University of York, the Natural History Museum in Berlin (Germany), the Museum of Natural Science “Julius Kühn” in Halle (Germany), the Zooarchaeology Laboratory of the University of Kiel (Germany) and the Barbara Noddle English goat sample at the National Museum of Cardiff. As a consequence, the goat sample is more heterogeneous in term of breeds than the sheep sample. It includes in fact, mainly modern German morphotypes (Black Forest goat, German Improved white goat, Langensalza goat) along with some English (Old English goat, Feral Galloway, Feral Rhum/Rum, Bagot goat, Northumberland goat), a few Alpine (Balkan goat, Grisons Chamois-coloured goat, Saanen goat, Sardinian goat, Toggenburg goat, Valais Blackneck goat) and Near East specimens (Bezoar goat, Angora goat, Damara goat, Damascus goat, Mamber goat). The presence among the sample of a dwarf goat must be also mentioned.

Table 2.34 Total number of sheep and goat specimens included in the study along with the description of their completeness.

Species	Total Number	Complete	Almost complete	Incomplete
<i>Ovis aries</i>	78	37	41	0
<i>Capra hircus</i>	79	28	47	4
Total	157	65	88	4

Table 2.34 gives the total number for each species included in this study with the description of their completeness. The categories of ‘complete’, ‘almost complete’ and ‘incomplete’ have been created as a rough guide. ‘Complete’ were regarded to be those specimens in which all the elements could be recorded. In this category the specimens that were polled (i.e. in which the lack of horns since birth is natural. This condition affects only females in some breeds, in others both sexes; Ryder 1983: 37) were also included if the horncores were the only missing part. The category of ‘almost complete’ was used for those specimens in which only two elements were missing, while ‘incomplete’ was used to define those specimens in which more than two elements were missing.

Table 2.35 Goat specimens included in the sample studied. The information given in this table (breed, sex and age) is as provided by the collection data-bases.

Species	ID Number	Location	Origin	Breed	Sex	Skeleton	Age
<i>Capra hircus</i>	90	Sheffield University	Halkidiki, Macedonia, Greece	-	♀	Almost Complete	11 years
<i>Capra hircus</i>	91	Sheffield University	Macedonia, Greece	-	♂	Complete	7 years
<i>Capra hircus</i>	94	Sheffield University	Halkidiki, Macedonia, Greece	-	♀	Complete	-
<i>Capra hircus</i>	502	Sheffield University	Katerini, Greece	-	-	Almost Complete	-
<i>Capra hircus</i>	762	Sheffield University	Assiros, Greece	-	-	Almost Complete	-
<i>Capra hircus</i>	784	Sheffield University	Assiros, Greece	-	♀	Almost Complete	-
<i>Capra hircus</i>	790	Sheffield University	Assiros, Greece	-	-	Almost Complete	-
<i>Capra hircus</i>	808	Sheffield University	Kartere, Greece	-	♂	Complete	-
<i>Capra hircus</i>	1053	Sheffield University	Mystras, Greece	-	-	Almost Complete	-
<i>Capra hircus</i>	1581	Sheffield University	Tony Legge Collection*	-	-	Almost Complete	-
TOTAL NUMBER OF SPECIMENS FROM SHEFFIELD						10	
<i>Capra hircus</i>	45dg	English Heritage, Portsmouth	Scotland	-	-	Complete	-
<i>Capra hircus</i>	1315	English Heritage, Portsmouth	-	Toggenburg	♂	Almost Complete	3.5 years
<i>Capra hircus</i>	1631	English Heritage, Portsmouth	Cyprus	Damascus	♀	Almost Complete	7 months

Species	ID Number	Location	Origin	Breed	Sex	Skeleton	Age
<i>Capra hircus</i>	2199	English Heritage, Portsmouth	England	Old English	♂	Almost Complete	15 months
<i>Capra hircus</i>	2774	English Heritage, Portsmouth	Durham	Bagot	♂	Almost Complete	2 years 7 months
<i>Capra hircus</i>	3318	English Heritage, Portsmouth	Islay, Hebrides	Feral	♂	Almost Complete	Adult
<i>Capra hircus</i>	3323	English Heritage, Portsmouth	Islay, Hebrides	Feral	♂	Complete	Adult
<i>Capra hircus</i>	501	English Heritage, Portsmouth	Whipsnade Zoo, Bedfordshire	White goat	♂	Almost Complete	2 years
<i>Capra hircus</i>	502	English Heritage, Portsmouth	-	White goat	♂	Complete	Unknown
TOTAL NUMBER OF SPECIMENS FROM PORTSMOUTH						9	
<i>Capra hircus</i>	511	York University	-	Saanen	♀	Almost Complete	2 years
<i>Capra hircus</i>	512	York University	-	Saanen Anglo-Nubian	♂	Almost Complete	7 months
<i>Capra hircus</i>	515	York University	-	Unknown	♀	Complete	4 years
<i>Capra hircus</i>	544	York University	-	Saanen	♀	Incomplete	Adult
<i>Capra hircus</i>	700	York University	-	-	♂	Almost Complete	Adult
TOTAL NUMBER OF SPECIMENS FROM YORK						5	
<i>Capra hircus</i>	112004011	National Museum Cardiff	Noddle Collection	Feral Rhum	-	Almost Complete	-
<i>Capra hircus</i>	112004012	National Museum Cardiff	Noddle Collection	Feral Rhum	-	Almost Complete	-
<i>Capra hircus</i>	112004016	National Museum Cardiff	Noddle Collection	-	-	Almost Complete	-
<i>Capra hircus</i>	112004019	National Museum Cardiff	Noddle Collection	-	-	Almost Complete	-
<i>Capra hircus</i>	112004020	National Museum Cardiff	Noddle Collection	Feral	-	Almost Complete	-
<i>Capra hircus</i>	112004021	National Museum Cardiff	Noddle Collection	Feral	-	Almost Complete	-
<i>Capra hircus</i>	112004022	National Museum Cardiff	Noddle Collection	Feral	-	Almost Complete	-
<i>Capra hircus</i>	112004032	National Museum Cardiff	Noddle Collection	Welsh goat	♀	Almost Complete	8 months
<i>Capra hircus</i>	112004033	National Museum Cardiff	Noddle Collection	Feral Rhum	-	Almost Complete	-
<i>Capra hircus</i>	112004034	National Museum Cardiff	Noddle Collection	Feral Rhum	-	Almost Complete	-
<i>Capra hircus</i>	112004035	National Museum Cardiff	Noddle Collection	Feral Galloway	-	Almost Complete	-
<i>Capra hircus</i>	112004036	National Museum Cardiff	Noddle Collection	Golden Guernsey	-	Almost Complete	-

Species	ID Number	Location	Origin	Breed	Sex	Skeleton	Age
<i>Capra hircus</i>	112004040	National Museum Cardiff	Noddle Collection	Northumberland goat	-	Almost Complete	-
<i>Capra hircus</i>	1120040401	National Museum Cardiff	Noddle Collection	Northumberland goat	-	Almost Complete	-
<i>Capra hircus</i>	112004080	National Museum Cardiff	Noddle Collection	-	-	Almost Complete	-
<i>Capra hircus</i>	112004081	National Museum Cardiff	Noddle Collection	-	-	Complete	-
TOTAL NUMBER FROM CARDIFF						16	
<i>Capra hircus</i>	C igz 3 (82)	Julius Kahn Museum, Halle	-	Langensalzer	♀	Complete	Adult
<i>Capra hircus</i>	C igz 1 (83)	Julius Kahn Museum, Halle	-	Langensalzer	♂	Complete	Adult
<i>Capra hircus</i>	C swd 2	Julius Kahn Museum, Halle	-	Schwarzwald	♀	Complete	8 years 11 months
<i>Capra hircus</i>	C frb 1	Julius Kahn Museum, Halle	-	Freiburger	♀	Complete	Adult
<i>Capra hircus</i>	C 3	Julius Kahn Museum, Halle	-	Weißer	♀	Complete	Adult
<i>Capra hircus</i>	C bdn 2	Julius Kahn Museum, Halle	-	Bundener	♀	Almost Complete	Adult
<i>Capra hircus</i>	C bdn 3	Julius Kahn Museum, Halle	-	Bundener	♀	Complete	Adult
<i>Capra hircus</i>	C bdn 4	Julius Kahn Museum, Halle	-	Bundener	♀	Complete	(bought 25/10/1886 dead 06/05/1888)
<i>Capra hircus</i>	C19	Julius Kahn Museum, Halle	-	-	♀	Complete	-
<i>Capra hircus</i>	Cd 1	Julius Kahn Museum, Halle	-	-	Hermaprodite	Complete	Adult
<i>Capra hircus</i>	C saa 3	Julius Kahn Museum, Halle	-	Saanen	♀	Complete	3 years 2 months
<i>Capra hircus</i>	C ggb 1	Julius Kahn Museum, Halle	-	Guggisberger	♂	Complete	2 years 7 months
<i>Capra hircus</i>	C appz 1	Julius Kahn Museum, Halle	-	Appenzeller	♀	Almost Complete	Adult
<i>Capra hircus</i>	C saa 6	Julius Kahn Museum, Halle	-	Saanen	♀	Complete	Adult
<i>Capra hircus</i>	C saa 7	Julius Kahn Museum, Halle	-	Saanen	♀	Complete	2 years 1 month
<i>Capra hircus</i>	C saa 1	Julius Kahn Museum, Halle	-	Saanen	♂	Complete	3 years 5 months
<i>Capra hircus</i>	C wal 6	Julius Kahn Museum, Halle	-	Walliser	♂	Almost Complete	4 years 2 months

Species	ID Number	Location	Origin	Breed	Sex	Skeleton	Age
<i>Capra hircus</i>	C wal 8	Julius Kahn Museum, Halle	-	Walliser	♀	Almost Complete	2 years 9 months
<i>Capra hircus</i>	C saa 2	Julius Kahn Museum, Halle	-	Saanen	♀	Complete	3 years 5 months
<i>Capra hircus</i>	C wal 7	Julius Kahn Museum, Halle	-	Walliser	♂	Incomplete	2 years 6 months
<i>Capra hircus</i>	C blk 2	Julius Kahn Museum, Halle	-	Balkan	♀	Complete	(bought 1916-dead 1917)
TOTAL NUMBER OF SPECIMENS FROM HALLE							21
<i>Capra hircus</i>	1912	Zoologisches museum Kiel	-	Zwerg	♀	Almost Complete	Adult
<i>Capra hircus</i>	7176	Zoologisches museum Kiel	-	Ziegenbock	♂	Complete	Adult
<i>Capra hircus</i>	7535	Zoologisches museum Kiel	-	Saanen	♂	Almost Complete	Adult
<i>Capra hircus</i>	18719	Zoologisches museum Kiel	-	Weißer Deutsche Edelziege	♀	Almost Complete	Adult
<i>Capra hircus</i>	19506	Zoologisches museum Kiel	-	Damara	♀	Complete	Adult
<i>Capra hircus</i>	22221	Zoologisches museum Kiel	-	-	-	Almost Complete	Adult
<i>Capra hircus</i>	22222	Zoologisches museum Kiel	-	-	♂	Incomplete	Adult
<i>Capra hircus</i>	30447	Zoologisches museum Kiel	-	Walliser Schwarzhals	♀	Almost Complete	11 years
<i>Capra hircus</i>	33040	Zoologisches museum Kiel	-	Weißer Deutsche Edelziege	♂	Almost Complete	Adult
TOTAL NUMBER OF SPECIMENS FROM KIEL							9
<i>Capra hircus</i>	100	Naturkunde museum, Berlin	-	Bezoar	♂	Almost Complete	-
<i>Capra hircus</i>	1556	Naturkunde museum, Berlin	-	-	♀	Almost Complete	8 years
<i>Capra hircus</i>	1854	Naturkunde museum, Berlin	-	Angora	♀	Almost Complete	-
<i>Capra hircus</i>	3638	Naturkunde museum, Berlin	-	-	♂	Almost Complete	-
<i>Capra hircus</i>	4487	Naturkunde museum, Berlin	-	Beden	♀	Almost Complete	-
<i>Capra hircus</i>	6945	Naturkunde museum, Berlin	-	Mamber	♀	Almost Complete	-
<i>Capra hircus</i>	6998	Naturkunde museum, Berlin	-	Sardinische Heidschnucke	♂	Complete	-
<i>Capra hircus</i>	7555	Naturkunde museum, Berlin	-	-	-	Complete	-
<i>Capra hircus</i>	94892	Naturkunde museum, Berlin	-	-	-	Incomplete	¾ of a year
TOTAL NUMBER OF SPECIMENS FROM BERLIN							9
TOTAL NUMBER OF GOAT				79			

Table 2.36 Sheep specimens included in the sample studied. The information given in this table (breed, sex and age) is as provided by the collection data-bases consulted.

Species	ID Number	Location	Origin	Breed	Sex	Skeleton	Age
<i>Ovis aries</i>	4	Sheffield University	-	-	-	Almost Complete	Sub-adult
<i>Ovis aries</i>	5	Sheffield University	Sheffield	Blackface	-	Almost Complete	-
<i>Ovis aries</i>	20	Sheffield University	Oaker farm	-	♀	Complete	Adult
<i>Ovis aries</i>	21	Sheffield University	Peak District, Derbyshire	-	-	Almost Complete	Adult
<i>Ovis aries</i>	23	Sheffield University	-	-	-	Almost Complete	-
<i>Ovis aries</i>	28	Sheffield University	-	-	-	Almost Complete	Adult
<i>Ovis aries</i>	29	Sheffield University	Sheffield	-	-	Almost Complete	Sub-adult
<i>Ovis aries</i>	43	Sheffield University	Flag Fen, Peterborough, Cambridgeshire	Soay	♂	Complete	Elderly
<i>Ovis aries</i>	45	Sheffield University	Flag Fen, Peterborough, Cambridgeshire	Soay	♀	Complete	Adult
<i>Ovis aries</i>	48	Sheffield University	Graves Park rare Breeds Centre, Sheffield	White-faced woodland	♀	Almost Complete	6-7 years
<i>Ovis aries</i>	50	Sheffield University	Graves Park, Sheffield	Portland	♀	Complete	5 years
<i>Ovis aries</i>	66	Sheffield University	-	-	-	Almost Complete	Adult
<i>Ovis aries</i>	191	Sheffield University	Flag Fen, Peterborough, Cambridgeshire	Soay	♀	Complete	More than 8 years
<i>Ovis aries</i>	193	Sheffield University	Flag Fen, Peterborough, Cambridgeshire	Soay	♀	Complete	More than 8 years
<i>Ovis aries</i>	220	Sheffield University	Langdale, Lake District	Herdwick	-	Almost Complete	-
<i>Ovis orientalis</i>	251	Sheffield University	Flag Fen, Peterborough, Cambridgeshire	-	♀	Almost Complete	Adult
<i>Ovis aries</i>	410	Sheffield University	2km outside Krithia, on road to Assiros	-	-	Complete	-
<i>Ovis aries</i>	436	Sheffield University	Biggin Dale, Hartington, Derbyshire	-	-	Almost Complete	-
<i>Ovis aries</i>	500	Sheffield University	Quarry near Korinos, Katerini, Greece	-	-	Almost Complete	-
<i>Ovis aries</i>	501	Sheffield University	Quarry near Korinis, Katerini, Greece	-	-	Almost Complete	-
<i>Ovis aries</i>	505	Sheffield University	Quarry near Korinis, Katerini, Greece	-	♀	Almost Complete	-
<i>Ovis aries</i>	637	Sheffield University	Picos de Europa, Spain	-	-	Incomplete	-
<i>Ovis aries</i>	668	Sheffield University	Merv, Turkmenistan	Afghan Arabi? (local name)	-	Almost Complete	-
<i>Ovis aries</i>	711	Sheffield University	Beeley Moor, Chatsworth, Derbyshire	-	-	Almost Complete	Adult
<i>Ovis aries</i>	819	Sheffield University	Langdale, Lake District	Herdwick	-	Complete	-

Species	ID Number	Location	Origin	Breed	Sex	Skeleton	Age
<i>Ovis aries</i>	928	Sheffield University	Assiros, Greece	-	-	Almost Complete	Juvenile
TOTAL SPECIMENS FROM SHEFFIELD						26	
<i>Ovis aries</i>	1307	English Heritage, Portsmouth	-	Soay	♀	Complete	12 years
<i>Ovis aries</i>	1310	English Heritage, Portsmouth	-	Soay	♀	Almost Complete	21-25 months
<i>Ovis aries</i>	1311	English Heritage, Portsmouth	-	Soay	♀	Complete	10 years
<i>Ovis aries</i>	1317	English Heritage, Portsmouth	ex. Woburn	Soay	♀	Complete	54 months
<i>Ovis aries</i>	1487	English Heritage, Portsmouth	Hirta, St. Kilda	Soay	♂	Complete	Adult
<i>Ovis aries</i>	1488	English Heritage, Portsmouth	Hoy, Orkney	Shetland	♀	Complete	4 years and 7 months
<i>Ovis aries</i>	1490	English Heritage, Portsmouth	Hoy, Orkney	Shetland	♀	Complete	79 months
<i>Ovis aries</i>	1491	English Heritage, Portsmouth	Hoy, Orkney	Shetland	♀	Complete	4 years and 7 months
<i>Ovis aries</i>	1494	English Heritage, Portsmouth	Hoy, Orkney	Shetland	♀	Complete	6 years and 7 months
<i>Ovis aries</i>	1496	English Heritage, Portsmouth	Hoy, Orkney	Shetland	♀	Complete	67 months
<i>Ovis aries</i>	1540	English Heritage, Portsmouth	-	Soay	♂?	Almost Complete	-
<i>Ovis aries</i>	1553	English Heritage, Portsmouth	Hoy, Orkney	Shetland	♂♀	Almost Complete	24 months
<i>Ovis aries</i>	1555	English Heritage, Portsmouth	Hoy, Orkney	Shetland	♂♀	Almost Complete	39 months
<i>Ovis aries</i>	1556	English Heritage, Portsmouth	Hoy, Orkney	Shetland	♂♀	Almost Complete	27 months
<i>Ovis aries</i>	1558	English Heritage, Portsmouth	Hoy, Orkney	Shetland	♂♀	Almost Complete	30.5 months
<i>Ovis aries</i>	1585	English Heritage, Portsmouth	Hoy, Orkney	Shetland	♂♀	Almost Complete	52.5 months
<i>Ovis aries</i>	1587	English Heritage, Portsmouth	Hoy, Orkney	Shetland	♂♀	Almost Complete	45 months
<i>Ovis aries</i>	1588	English Heritage, Portsmouth	Hoy, Orkney	Shetland	♂♀	Almost Complete	52.5 months
<i>Ovis aries</i>	1591	English Heritage, Portsmouth	Hoy, Orkney	Shetland	♂	Almost Complete	22 months
<i>Ovis aries</i>	1593	English Heritage, Portsmouth	Hoy, Orkney	Shetland	♂	Almost Complete	28 months
<i>Ovis aries</i>	1594	English Heritage, Portsmouth	Hoy, Orkney	Shetland	♂	Almost Complete	24 months

Species	ID Number	Location	Origin	Breed	Sex	Skeleton	Age
<i>Ovis aries</i>	2224	English Heritage, Portsmouth	-	Soay	♀	Almost Complete	42 months
<i>Ovis aries</i>	2228	English Heritage, Portsmouth	-	Soay	♀	Complete	41 months
<i>Ovis aries</i>	2229	English Heritage, Portsmouth	-	Soay	♀	Complete	41 months
<i>Ovis aries</i>	2582	English Heritage, Portsmouth	Hoy, Orkney	Shetland	♂	Complete	23 months
<i>Ovis aries</i>	2777	English Heritage, Portsmouth	Cambridgeshire	Shetland	♀	Complete	6.75 years
<i>Ovis aries</i>	2778	English Heritage, Portsmouth	-	Soay	♀	Complete	45 months
<i>Ovis aries</i>	2801	English Heritage, Portsmouth	Durham	Soay	♂♀	Complete	35 months
<i>Ovis aries</i>	2806	English Heritage, Portsmouth	Suffolk	Soay	♀	Complete	10 years
<i>Ovis aries</i>	2832	English Heritage, Portsmouth	Cambridgeshire	Soay	♂♀	Complete	13 years
<i>Ovis aries</i>	2866	English Heritage, Portsmouth	-	Shetland	♂♀	Almost Complete	2 years and 8 months
<i>Ovis aries</i>	2868	English Heritage, Portsmouth	-	Shetland	♂♀	Almost Complete	20 months
<i>Ovis aries</i>	2938	English Heritage, Portsmouth	-	Shetland	♂♀	Almost Complete	18 months
<i>Ovis aries</i>	2943	English Heritage, Portsmouth	-	Shetland	♂♀	Almost Complete	3 years and 7 months
<i>Ovis aries</i>	2944	English Heritage, Portsmouth	-	Shetland	♂♀	Almost Complete	2 years and 7 months
<i>Ovis aries</i>	2978	English Heritage, Portsmouth	Hoy, Orkney	Shetland	♂♀	Almost Complete	45 months
<i>Ovis aries</i>	3217	English Heritage, Portsmouth	Hoy, Orkney	Shetland	♂♀	Almost Complete	c. 941 days
<i>Ovis aries</i>	3218	English Heritage, Portsmouth	Hoy, Orkney	Shetland	♂♀	Almost Complete	941 days
<i>Ovis aries</i>	3272	English Heritage, Portsmouth	St Kilda	Soay	♂	Complete	31 months
<i>Ovis aries</i>	3281	English Heritage, Portsmouth	Hoy, Orkney	Shetland	♂	Complete	2 years and 7 months
<i>Ovis aries</i>	3282	English Heritage, Portsmouth	Hoy, Orkney	Shetland	♂	Complete	2 years and 7 months
<i>Ovis aries</i>	3283	English Heritage, Portsmouth	Hoy, Orkney	Shetland	♂	Complete	31 months
<i>Ovis aries</i>	3288	English Heritage, Portsmouth	Hoy, Orkney	Shetland	♂	Complete	2 years and 7 months

Species	ID Number	Location	Origin	Breed	Sex	Skeleton	Age
<i>Ovis aries</i>	3289	English Heritage, Portsmouth	Hoy, Orkney	Shetland	♂	Complete	2 years and 7 months
<i>Ovis aries</i>	3420	English Heritage, Portsmouth	Butser Iron Age Farm	Soay	♀	Complete	Adult
TOTAL NUMBER OF SPECIMENS FROM PORTSMOUTH						45	
<i>Ovis aries</i>	15815	Zoologisches museum Kiel	-	Heidschnucke	♀	Almost Complete	-
<i>Ovis aries</i>	21640	Zoologisches museum Kiel	-	Ostfriesisches Milch	♀	Complete	-
<i>Ovis aries</i>	22339	Zoologisches museum Kiel	-	Blu Domane	♀	Complete	-
<i>Ovis aries</i>	22639	Zoologisches museum Kiel	-	Heidschnucke Romanow	♂	Almost Complete	14/16 months
<i>Ovis aries</i>	22711	Zoologisches museum Kiel	-	Heidschnucke	♂	Almost Complete	-
<i>Ovis aries</i>	23629	Zoologisches museum Kiel	-	Deutsches Weißköpfiges Fleischschaf	♀	Complete	2 years
<i>Ovis aries</i>	31005	Zoologisches museum Kiel	-	Rotkopf	♀	Complete	-
TOTAL NUMBER OF SPECIMENS FROM KIEL						7	
TOTAL NUMBER OF SHEEP						78	

From Tables 2.35 and 2.36 it can be seen that, while the sheep sample is mainly dominated by Shetland and Soay breeds, the goat sample is more heterogeneous. The total sample size is of 157 animals, 79 goats and 78 sheep (Tab. 2.34). Most of them are complete or almost complete (only two body parts missing), while only a few specimens were incomplete.

2.3 Inter-Observer Error and Intra-Observer Error: consistency tests

Despite the process of generating measurements affects and influences most branches of archaeology, the topic has rarely been subjected to critical review. Due to the numerical nature of measurements, it is commonly thought that they represent an entirely objective tool and, as a consequence, are immune to observer fallibility (Lyman and VanPool 2009: 486). Nonetheless, recent studies (Davis 1996; Johnstone 2004; Lyman and VanPool 2009; Popkin *et al.* 2012; Write 2013) have acknowledged that several potentially biasing factors must be taken into consideration when measurements are taken. Measurements, to be considered as an effective and reliable study tool, must be adequately reported, comparable (they must be taken in the same way by everyone) and standardized (the measured dimension has to be defined precisely; Lyman and VanPool 2009: 487; Simpson *et al.* 1960: 21-22).

Since the new protocol devised for this project includes some new and some revised measurements from the previous literature, the need to have it tested by other researchers was considered important for many reasons. First of all, it was essential to verify whether the measurements contributing to the new protocol could easily be taken by anyone. Secondly, it was important to test whether the instructions concerning how to take the measurements, especially for the newly introduced ones, were clear to whoever was using the protocol for the first time (standardization). Thirdly, having them tested by a team of zooarchaeologists would reinforce the value/reliability of my research tool.

Considering the fact that one of the aims of this project is to propose a method which could be used by anyone, an Inter-Observer Error test (i.e. when the same measurement, taken more than once, is recorded differently by different people) was conducted.

Nevertheless, measurements not only need to be reproducible over time and repeatably by different people, but also by a single individual. For this reason, an Intra-Observer Error test (i.e. when the same measurement, is recorded repeatedly by the same person) was carried out. In addition, as previous studies have suggested that the Intra-Observer Error is generally lower (Johnstone 2004; Popkin *et al.* 2012; Ulijaszek and Lourie 1994; Utermohle and Zegura 1982) than the Inter-Observer Error, carrying out this further test was considered an additional means to check the reliability of the measurements themselves.

For the Inter-Observer Error test, the new recording protocol was presented to a group of eight colleagues, including the writer, all of them experienced zooarchaeologists. The trial included four skeletons, two sheep and two goats belonging to the Zooarchaeology Laboratory of the University of Sheffield. These specimens were chosen according to their completeness and, as a

consequence, the possibility of taking most of the required measurements. Only one side of the animal was measured, the left. Whenever the left bone was not available, it was replaced with its right counterpart. All my colleagues were provided with a copy of the recording protocol in which a written description and a visual aid of how to take the measurements correctly were included. In addition, callipers, ropes, measuring boxes and a form on which to record the measurements (Tab. 2.37), were provided. The author was present on most of the occasions while the colleagues were carrying out the test, to provide extra help in case of doubts and to collect suggestions and opinions. Very few questions were asked during the trial, which was interpreted as evidence of the ease of applicability of the measurements.

The Intra-Observer Error was conducted on the same specimens used for the Inter-Observer Error. All four specimens were repeatedly measured - a total of four times per specimen - over several days. Measurements were taken only on post-cranial elements and horncores. This choice was made because the results from the Inter-Observer Error test, which was conducted before the Intra-Observer test, revealed the inconsistency of the measurements taken on the cranial elements.

Table 2.37 Form provided to the group for recording the measurements. The form included all the measurements, even though some of them could not be taken on the selected specimens.

Element		Specimen 1 (goat n.0762)	Specimen 2 (goat n.0094)	Specimen 3 (sheep n.0043)	Specimen 4 (sheep n.0045)
dP ₃	B				
	L				
dP ₄	B1				
	B2				
	B3				
	L				
P ₃	B				
	L				
P ₄	B				
	L				
M ₃	B1				
	B3				
	L				
Mandible	H				
	B				
	PF				
Horncores	A				
	B				
	C				
	D				
	E				
	F				
Scapula	BG				
	LG				
	GLP				
	SLC				
	ASG				
Humerus	BT				
	Bd				
	HT				
	HTC				
	BE				

	Dd				
	BEI				
Radius	Bp				
	BFp				
	Dp				
	GL				
	SD				
Ulna	B				
	L				
	BPC				
	DPA				
	SDO				
Metacarpal	GL				
	SD				
	BatF				
	BFd				
	a				
	b				
	1				
	2				
	3				
	4				
	5				
	6				
Metatarsal	GL				
	SD				
	BatF				
	BFd				
	a				
	b				
	1				
	2				
	3				
	4				
Tibia	Bd				
	Dd(a)				
	Dd(b)				
	GL				
	SD				
Astragalus	Bd				
	GLm				
	GLl				
	Dm				
	DI				
	H				
	BpT				
Calcaneum	SB				
	GL				
	C				
	D				
	B				
	DS				
	Gd				
3 rd Phalanx	DLS				
	MBS				

2.3.1 Reliability Tests

Once the data were recorded by the eight operators as well as by the author, they were transferred to an SPSS statistics data editor in order to run a reliability test. The aim of both tests was to verify the reliability of the recording protocol rather than the recorders. Prior to discussing the specifics of the chosen test, I will clarify what, statistically is meant by ‘reliability’ and why it differs from the concept of ‘agreement’.

Reliability and agreement are in fact, often confused and used interchangeably but they refer to different concepts. Reliability refers to reproducibility, namely the degree to which repeated measurements provide the same results, while agreement measures how close the results of the repeated measurements are (de Vet *et al.* 2006: 1033). In the context of this research, reliability is intended as the repeatability or consistency of the measurements (as defined by Bruton *et al.* 2000: 94).

Many methods for testing reliability can be used, such as Correlation Coefficients (i.e. Pearson’s), ICC, SEM (Standard Error of Measurements), Coefficient of Variation (CV), Bland and Altman’s 95% limits of agreement (1986). For this study the Interclass Correlation Coefficient test was chosen for three main reasons:

1. ICC is commonly used for helping to establish and quantify reproducibility (Rankin and Stokes 1998: 187-199); it is useful for estimating inter-rater reliability on quantitative data because it is more flexible than, for example, the Pearson correlation test (r) (Bruton *et al.* 2000: 96).
2. ICC is preferable to the more commonly used Coefficient of Variation (CV), which is no longer considered useful to estimate reliability (Bruton *et al.* 2000; Rankin and Stokes 1998). ICC is in fact considered the most appropriate reliability parameter for repeated measurements on a continuous scale (de Vet *et al.* 2006: 1037).
3. Since I had a wide range of data, eight observers, and four specimens on each of which an average of 40 measurements were taken, all the other techniques explored were either too complicated to compute manually (SEM) or they simply could not be applied for the above explained reasons

For the Inter-Observer Error, the ICC type applied (2,1) included a ‘Two-Way Random’ model, which was chosen because it is the model used when many raters, which are considered representative of a larger population, score each case only once (Landers 2011). ‘Absolute agreement’ was adopted as specificity rather than ‘consistency’ because, while consistency looks only at the ranking (i.e. the process of transforming raw scores into numbers that represent their position on an ordered list of those scores; Field 2009: 792) without considering the raters’

systematic variability, the absolute agreement looks not only at the order of the scores but also at the values to which the scores are linked (Field 2009: 788). Even though the ICC has been pointed as the best options, it has some disadvantages which make it unsuitable for use in isolation. Taking this into account, the ICC test was performed along with Bland and Altman plots (Appendix I, Fig. A1.1 to A1.79), so that an alternative and supportive way of exploring the reliability of the measurements was conducted.

For the Intra-Observer Error, the ICC type (1,1) adopted included a ‘One Way Random’ model, which is the option to select when you have the same rater, considered as representative of a larger population, measuring each case in several occasions (Landers 2011).

As with other kinds of reliability coefficients, for ICC there is not a standard cut-off for establishing the acceptance of the level of reliability: it ranges usually from 0 to 1 where values closer to 1 are the most reliable.

The results from the tests follow on an element by element basis. Some preliminary statistical data which include Mean, Standard Deviation (SD) and Coefficient of Variation (CV) for each measurement for each specimen are given in Table 2.38.

Table 2.38 Mean, Standard Deviation (SD) and Coefficient of Variation (CV) for each measurement for each of the specimens calculated from the measurements provided by the eight operators. The measurements highlighted with an asterisk are those which could not be taken on all the four specimens. The ‘number of specimens’ column indicates the number of specimens for which a measurement has been taken.

Element		Number of Specimens	Goat Specimen 1			Goat Specimen 2		
			MEAN	SD	CV	MEAN	SD	CV
P ₃	B*	2	5.9	0.6	10.9	6.3	0.6	10.3
	L*	2	7.9	0.7	9.4	8.2	0.4	5.0
P ₄	B*	1	7.1	0.5	6.7	-	-	-
	L*	1	10.0	0.5	4.9	-	-	-
Mandible	H*	2	14.7	0.7	4.8	14.6	0.8	5.1
	B*	2	10.8	0.4	3.4	8.9	0.6	6.3
Horncores	A	2	29.6	2.8	9.5	18.1	1.1	6.0
	B	2	22.9	3.1	13.3	14.7	1.8	12.7
	C	2	21.1	1.6	7.5	14.2	0.6	4.8
	D	2	16.2	1.6	9.7	13.5	1.7	16.3
	E*	2	161.8	4.9	3.0	117.6	6.2	5.2
	F*	2	187.5	8.1	4.3	136.4	11.2	8.2
Scapula	BG	2	24.4	0.3	1.0	24.9	0.4	1.7
	LG	2	37.0	0.6	1.7	26.1	1.0	3.8
	GLP	2	29.4	2.7	9.3	34.3	0.3	0.9
	SLC	2	23.5	0.4	1.8	20.2	0.2	1.2
	ASG	2	24.9	2.6	10.4	28.5	3.2	11.4
Humerus	BT	2	31.4	0.6	1.8	31.2	0.4	1.3
	Bd	2	34.8	0.4	1.2	32.9	0.3	0.8
	Dd	2	19.7	0.3	1.7	19.5	0.4	2.3
	BE	2	14.1	0.3	2.1	14.5	0.4	2.6
	BEI	2	9.3	1.1	11.7	10.1	0.9	9.3
	HTC	2	26.7	0.6	2.1	28.3	0.6	2.1
	HT	2	6.2	0.3	4.1	5.5	0.9	16.9
Radius	Bp	2	32.9	0.1	0.4	32.0	0.7	2.1
	BFp	2	30.3	0.5	1.8	30.6	0.8	2.6
	Dp	2	17.3	0.7	3.8	16.0	0.2	1.5
	GL*	1	205.1	87.9	42.9	-	-	-

Element		Number of Specimens	Goat Specimen 1			Goat Specimen 2		
Ulna	SD*	1	20.2	0.4	2.0	-	-	-
	B*	1	11.8	1.5	12.5	-	-	-
	L*	1	26.8	0.7	2.8	-	-	-
	BPC*	1	28.7	1.0	3.4	-	-	-
	DPA*	1	21.2	0.1	0.7	-	-	-
Metacarpal	SDO*	1	23.8	0.6	2.4	-	-	-
	GL	2	119.7	0.5	0.4	122.9	0.9	0.7
	SD	2	17.2	0.2	1.2	15.2	0.1	0.9
	BatF	2	29.3	0.4	1.5	26.8	0.1	0.4
	BFd	2	29.9	0.1	0.3	28.0	0.2	0.7
	a	2	13.7	0.7	5.3	12.8	0.2	1.2
	b	2	13.6	0.5	3.6	12.6	0.2	1.6
	1	2	10.3	0.5	4.4	9.9	0.4	4.2
	2	2	17.1	0.2	1.0	16.6	0.1	0.6
	3	2	14.0	0.1	1.1	13.6	0.1	0.7
	4	2	10.4	1.5	14.7	9.9	1.6	16.2
	5	2	17.2	1.0	6.0	16.4	0.1	0.5
Metatarsal	6	2	13.6	1.6	12.0	13.1	1.4	10.8
	GL	2	129.8	0.4	0.3	131.2	1.4	1.1
	SD	2	13.7	0.1	0.9	12.1	0.2	1.3
	BatF	2	26.7	0.2	0.7	23.7	0.1	0.5
	BFd	2	27.4	0.1	0.3	24.8	0.2	0.7
	a	2	12.7	0.4	3.3	11.5	0.2	2.1
	b	2	11.8	0.2	2.1	11.1	0.2	1.4
	1	2	10.2	0.4	3.4	9.4	0.3	3.7
	2	2	16.9	0.1	0.4	15.9	0.2	1.5
	3	2	13.7	0.1	0.6	13.3	0.1	0.7
	4	2	10.0	1.3	12.9	9.7	1.5	15.8
	5	2	16.1	0.3	2.0	15.4	0.2	1.2
Tibia	6	2	13.3	1.5	11.6	12.8	1.4	11.0
	Bd	2	27.9	0.4	1.3	24.5	1.7	7.1
	Dd(a)	2	21.9	0.6	2.8	19.5	0.2	1.3
	Dd(b)	2	19.0	0.7	3.6	17.5	0.5	2.9
	GL*	1	234.2	0.5	0.2	-	-	-
Astragalus	SD	2	17.4	0.4	2.1	14.0	0.2	1.7
	Bd	2	20.4	0.2	1.1	18.7	0.1	0.5
	GLm	2	29.6	0.0	0.2	29.3	0.2	0.6
	GLI	2	27.5	0.1	0.5	27.5	0.2	0.7
	Dm	2	15.5	0.3	2.1	15.1	0.3	2.2
	DI	2	17.6	0.8	4.5	16.6	0.1	0.6
	H	2	23.8	0.3	1.3	23.8	0.3	1.3
Calcaneum	BpT	2	13.9	0.4	3.2	12.1	0.3	2.2
	SB	2	61.4	0.1	0.2	60.4	0.6	1.0
	GL	2	16.6	2.2	13.1	16.7	0.6	3.9
	c	2	11.1	1.1	10.1	10.8	0.5	4.5
	d	2	22.1	1.0	4.6	22.3	0.8	3.7
	B	2	7.1	0.5	7.5	6.2	0.3	4.1
	DS	2	19.3	0.4	2.2	18.8	0.2	1.1
3 rd Phalanx	Gd	2	24.2	1.2	4.8	23.8	1.2	5.1
	DLS	2	37.5	0.1	0.2	36.7	0.4	1.1
CV MEAN	MBS	2	6.6	0.3	4.0	5.7	0.2	3.6
			4.7			3.4		
Element		Number of Specimens	Sheep Specimen 3			Sheep Specimen 4		
			MEAN	SD	CV	MEAN	SD	CV
P ₃	B*	0	-	-	-	-	-	-
	L*	0	-	-	-	-	-	-
P ₄	B*	1	-	-	-	5.9	0.5	7.7
	L*	1	-	-	-	8.8	0.5	5.1
Mandible	H*	0	-	-	-	-	-	-
	B*	0	-	-	-	-	-	-
Horncores	A	2	50.2	3.3	6.6	31.6	4.7	14.7

Element		Number of Specimens	Goat Specimen 1			Goat Specimen 2		
	B	2	43.4	4.3	9.9	21.9	4.6	20.8
	C	2	43.0	4.0	9.3	28.3	5.0	17.7
	D	2	31.6	5.4	17.0	18.6	4.8	25.6
	E*	1	-	-	-	86.3	4.2	4.9
	F*	1	-	-	-	104.7	4.8	4.6
Scapula	BG	2	21.2	0.4	2.0	19.7	0.2	1.0
	LG	2	24.5	0.4	1.6	23.1	0.8	3.4
	GLP	2	32.9	0.2	0.5	30.5	0.1	0.2
	SLC	2	20.1	0.5	2.7	17.1	0.7	4.2
	ASG	2	22.5	3.5	15.5	20.4	1.4	7.1
Humerus	BT	2	29.5	0.4	1.4	26.2	0.5	1.9
	Bd	2	31.8	0.5	1.7	28.8	1.1	3.8
	Dd	2	18.8	0.6	3.3	17.0	0.4	2.4
	BE	2	14.5	0.3	2.3	12.3	0.7	5.9
	BEI	2	8.0	0.8	10.2	7.6	0.8	10.7
	HTC	2	24.8	0.3	1.2	21.9	0.1	0.5
	HT	2	8.2	0.8	10.0	6.1	0.6	9.5
Radius	Bp	2	32.9	0.4	1.1	29.1	0.2	0.5
	BFp	2	29.4	0.5	1.5	26.0	0.9	3.3
	Dp	2	16.7	0.2	1.1	14.7	0.1	1.0
	GL*	2	179.6	87.6	48.8	171.2	87.5	51.1
	SD*	2	17.8	1.7	9.4	17.3	1.1	6.5
Ulna	B*	2	10.7	0.4	3.3	9.1	0.4	4.0
	L*	2	23.8	1.0	4.1	21.4	1.1	5.2
	BPC*	2	27.7	0.4	1.6	25.0	0.4	1.7
	DPA*	2	21.9	0.2	0.9	18.3	0.1	0.7
	SDO*	2	24.0	0.6	2.4	19.8	0.5	2.7
Metacarpal	GL	2	126.4	0.5	0.4	115.3	0.3	0.2
	SD	2	14.3	0.6	4.3	12.1	0.2	1.8
	BatF	2	25.0	0.4	1.7	22.7	0.2	0.9
	BFd	2	24.8	0.4	1.6	22.7	0.3	1.5
	a	2	11.4	0.3	2.9	10.5	0.1	1.1
	b	2	11.0	0.2	2.2	10.0	0.0	0.5
	1	2	11.2	0.2	2.0	9.9	0.2	1.7
	2	2	16.2	0.3	1.5	14.6	0.1	0.4
	3	2	13.6	0.1	0.9	12.2	0.3	2.1
	4	2	10.6	1.6	15.2	9.7	1.0	10.0
	5	2	15.9	0.2	1.4	14.0	0.1	0.7
6	2	13.3	1.0	7.9	11.8	1.0	8.4	
Metatarsal	GL	2	135.2	1.1	0.8	126.8	0.5	0.4
	SD	2	11.9	0.1	1.0	10.8	0.3	2.8
	BatF	2	22.9	0.2	0.7	21.3	0.1	0.7
	BFd	2	23.8	0.6	2.5	21.9	0.5	2.4
	a	2	11.2	0.1	0.8	10.2	0.2	1.9
	b	2	10.2	0.1	1.0	9.5	0.1	1.4
	1	2	10.4	0.2	2.3	9.4	0.1	1.3
	2	2	16.2	0.1	0.7	14.6	0.0	0.3
	3	2	13.1	0.2	1.8	11.9	0.2	1.6
	4	2	10.0	1.2	12.2	9.2	1.1	12.4
	5	2	15.3	0.1	1.0	13.7	0.1	0.5
6	2	12.6	1.3	10.4	11.6	1.2	10.4	
Tibia	Bd	2	25.7	0.3	1.2	23.4	0.5	2.0
	Dd(a)	2	20.6	0.6	2.7	18.3	0.3	1.4
	Dd(b)	2	17.7	0.5	3.0	16.2	0.3	1.6
	GL*	2	198.4	0.3	0.1	185.1	0.3	0.2
	SD	2	14.4	1.1	7.9	12.8	0.8	6.6
Astragalus	Bd	2	17.9	0.2	0.9	16.3	0.1	0.7
	GLm	2	27.3	0.3	1.0	24.0	0.4	1.6
	GLl	2	27.3	0.3	1.2	23.9	0.2	0.9
	Dm	2	15.9	1.1	6.6	14.5	0.9	6.0
	Dl	2	16.6	1.1	6.9	15.2	0.9	5.8
	H	2	22.9	0.5	2.3	19.8	0.1	0.7
	BpT	2	12.2	0.6	5.3	11.2	0.3	3.0

Element		Number of Specimens	Goat Specimen 1			Goat Specimen 2		
Calcaneum	SB	2	54.2	0.4	0.7	48.8	0.3	0.6
	GL	2	16.5	0.7	4.4	15.8	1.8	11.6
	c	2	11.0	1.2	10.8	10.2	0.7	6.7
	d	2	20.5	1.7	8.2	18.7	1.1	6.1
	B	2	6.3	0.2	2.7	5.8	0.1	2.3
	DS	2	18.5	0.5	2.8	15.9	0.5	3.2
	Gd	2	22.0	0.9	4.0	19.7	0.7	3.8
3 rd Phalanx	DLS	2	29.4	0.3	1.0	27.2	0.2	0.6
	MBS	2	6.8	0.3	4.2	6.1	0.3	4.6
CV MEAN			4.2			4.6		

Since measurements with a higher Mean tend to have a higher Standard Deviation (the Standard Deviation is the estimate of the average variability of a set of data and, as it is the square root of the variance, it is heavily based on the Mean), the Coefficient of Variation (CV) was considered as this was much less dependent on the measurement size. CV values in fact, attest not only the variability of the spread of the data (Sauro 2004-2015), but they can also provide some preliminary ideas about the performance of a method: if the CV value is low, this means that a little difference was present between the results given by the different observers. This would be an indication that the measurements were taken fairly consistently.

By comparing the CV Mean values for each specimen presented in Table 2.38, it can be seen that three of the four produced similar means, whereas this is lower for specimen 2. It is generally accepted that CVs of 5% or less usually attest to a good method performance, while CVs of 10% and higher, indicate poor performance (Westgard 2009). Most of the measurements making up the new recording protocol (Tab. 2.38) have CV values that are lower than 5%. In particular, the measurements which provided the lowest CV values are, as shown by Table 2.39, those already known from previous literature (von den Driesch 1976) to be well defined (for example the humerus BT, following Payne and Bull 1988; the astragalus Bd, GLm and GLl; GL, SD, BatF and BFd on the metapodials). Their low CV values indicate that the raters' scores were close to one another; as a consequence, the measurements were taken fairly consistently by the different operators.

Figure 2.38 shows the CV value for each measurement taken on the four specimens and it can be seen that similar patterns affect the results for all the sheep and goat specimens:

- measurement B on the 3rd lower premolar shows CV values higher than 10 for both specimens on which it could be measured, which means that the taking of measurements was inconsistent.
- high CV values are provided by all the measurements of the horncore for all the specimens. Especially high values are those related to the maximum and minimum

diameter at the base and at the middle of the horncore (A and B; C and D) (The highest values are those obtained for specimen 4);

- a high CV has also been noticed for the scapula ASG in all specimens. Conversely, the scapula GLP measurement provided a high score only in specimen 1;
- in the humerus, the measurements which provided the highest CVs were BEI and HT, consistently high in all the four specimens;
- for the radius, the pattern involves mainly GL which has providing exceptionally high CVs for all specimens. To a lesser degree SD also provided high CVs (only for specimen 3 and 4);
- for the calcaneum, high CV values are given mainly by GL (for specimen 1 and 4), ‘c’ (for specimen 1 and 3) and then ‘d’ and B (these latter had a high CV value only in one of the four specimens);
- finally, for the metapodials, measurement 4 and 6 have constantly provided high CV values in all specimens.

The high CV values (CV>5%) indicate that the measurements were taken with a low degree of consistency by the raters. The inconsistency can be due to different factors: the difficulty of defining accurately a measurement, the difficult for it to be taken consistently because of the nature of the bone itself and, finally, because a human error occurred (typing mistake, calibration problem, etc.). These factors could have influenced the results but, while the presence of a degree of variation due to the nature of the measurement or the nature of the element itself is important to this research, the presence of extreme outliers (scores which are very different from the others; Field 2009: 791) is usually an indicator of human errors. As the goal of this Inter-Observer Error analysis is to test how easily and consistently replicable the measurements are, the inclusion of outliers due to human error could undermine the reliability of the method for biases which are not related to the measurements themselves but to the raters; therefore they must be excluded.

Table 2.39 List of the measurements which provided the lowest CV values per species.

Lowest CV values (<2)		
Element	Measurement per species	
	Goat	Sheep
Sc	BG	-
	SLC	-
	-	GLP
Hu	BT	BT
	Bd	-
	-	HTC
Ra	-	Bp
	-	Dp
Ul	-	BPC
	-	-
	-	DPA

Lowest CV values (<2)		
Element	Measurement per species	
Mc	GL	GL
	SD	SD
	BatF	BatF
	BFd	BFd
	2	2
	3	-
-	5	
Mt	GL	GL
	SD	SD
	-	a
	-	b
	BatF	BatF
	BFd	BFd
	2	2
	3	3
5	5	
Ti	-	Bd
	-	GL
Ast	Bd	Bd
	GLm	GLm
	GLl	GLl
	H	-
Cc	SB	SB
3 rd Ph	DLS	DLS

Table 2.40 List of the measurements which provided the highest CV values per species.

Highest CV values (>5)		
Element	Measurement per species	
	Goat	Sheep
P ₃	B	-
Hc	A	A
	B	B
	-	C
	D	D
Sc	ASG	ASG
Hu	BEI	BEI
	-	HT
Ra	-	GL
	-	SD
Ti	-	SD
Mc	4	4
	6	6
Mt	4	4
	6	6
Ast	-	Dm
	-	Dl
Cc	-	c
	-	d

Most measurements that have provided high CV values (Tab. 2.40) are difficult to be defined accurately or/and to take consistently (for example: A, B, C and D on the horncore, ASG on the scapula, BEI on the humerus, 4 and 6 on the metapodials). As such, the high variability shown is hardly surprising.

The reason behind the extremely high CV values related to well-defined measurements, such as GL in radius, must be different. In this case, the problem was made clear when the raw data

were analysed: one rater had given consistent extremely high values for this measurement, influencing heavily the Mean and, as a consequence the Standard Deviation (SD) and the CV. If the extreme scores given by this rater are excluded from the analysis, the values for radius GL for each specimen changes radically:

- Specimen 1: Mean 174.0, SD 0.7, CV 0.4 versus Mean 205.1, SD 87.9, CV 42.9;
- Specimen 3: Mean 148.6, SD 0.9, CV 0.6 versus Mean 179.6, SD 87.6 and CV 48.8;
- Specimen 4: Mean 140.3, SD 0.8, CV 0.6 versus Mean 171.2, SD 87.5 and CV 51.1.

The extreme values present for this measurement were clearly due to a human error. Consequently, they were excluded from further analysis and the same approach has been used for other measurements for which extremely different values, given by mistake, were provided. All these cases were acknowledged but excluded from the analysis in order to evaluate the performance of the method rather than the raters.

The overall impression, based on the preliminary analysis of the CV values, is that most measurements have been taken with a fairly good degree of consistency by the raters (low CV values). Nevertheless some inconsistency has been noted and it seems to follow clear patterns (related to specific measurements on specific problematic area of the bones). As mentioned above the CV is, however, a useful indicator of variability rather than a reliability test, therefore the Inter Correlation Coefficient test will be considered now.

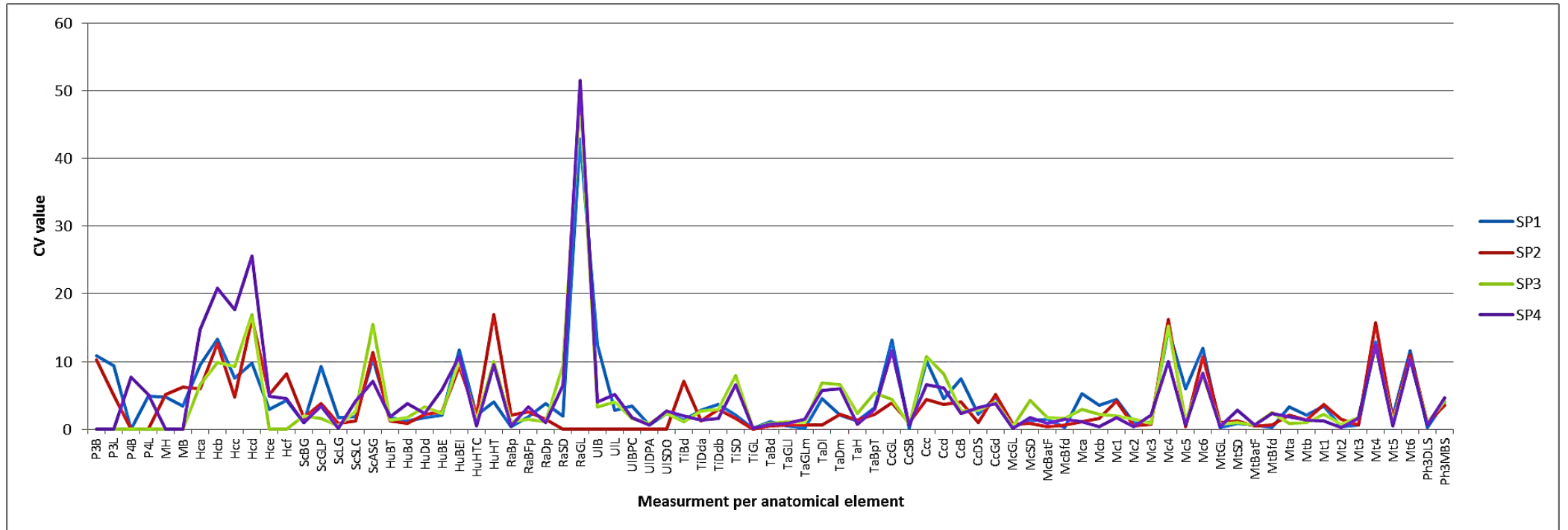


Figure 2.8 CV for each of the four specimens for all the different measurements.

2.3.2 Inter-Observer Error: Inter Correlation Coefficient

Table 2.41 shows the Inter Correlation Coefficient for each measurement taken on different elements for the four modern sheep and goat specimens. The analysis of the results on an element by element basis follows.

Table 2.41 ICC value and 95% Confidence Interval values for different measurements taken on different anatomical elements.

Lower P₃			
Intraclass Correlation Coefficient measurement B			
	Intraclass Correlation Value	95% Confidence Interval	
		Lower Bound	Upper Bound
Single Measures	.134	-.019	.995
Intraclass Correlation Coefficient measurement L			
Single Measures	.031	-.051	.989
Lower P₄			
Intraclass Correlation Coefficient measurement B			
	Intraclass Correlation Value	95% Confidence Interval	
		Lower Bound	Upper Bound
Single Measures	.774	.312	1.000
Intraclass Correlation Coefficient measurement L			
Single Measures	.031	-.051	.989
Mandible			
Intraclass Correlation Coefficient measurement H			
	Intraclass Correlation Value	95% Confidence Interval	
		Lower Bound	Upper Bound
Single Measures	-.018	-.036	.931
Intraclass Correlation Coefficient measurement B			
Single Measures	.887	.533	1.000
Horncore			
Intraclass Correlation Coefficient measurement A			
	Intraclass Correlation	95% Confidence Interval	
		Lower Bound	Upper Bound
Single Measures	.944	.783	.996
Intraclass Correlation Coefficient measurement B			
Single Measures	.923	.703	.994
Intraclass Correlation Coefficient measurement C			
Single Measures	.934	.779	.995
Intraclass Correlation Coefficient measurement D			
Single Measures	.851	.570	.988

Intraclass Correlation Coefficient measurement E			
Single Measures	.969	.825	1.000
Intraclass Correlation Coefficient measurement F			
Single Measures	.925	.649	1.000
Intraclass Correlation Coefficient for A without outliers			
	Intraclass Correlation Value	95% Confidence Interval	
		Lower Bound	Upper Bound
Single Measures	.996	.983	1.000
Interclass Correlation Coefficient for B without outliers			
Single Measures	.995	.982	1.000
Interclass Correlation Coefficient for C without outliers			
Single Measures	.993	.973	.999
Interclass Correlation Coefficient for D without outliers			
Single Measures	.959	.860	.997
Interclass Correlation Coefficient for E without outliers			
Single Measures	.964	.890	.988
Interclass Correlation Coefficient for F without outliers			
Single Measures	.949	.864	.982
Scapula			
Intraclass Correlation Coefficient measurement BG			
	Intraclass Correlation Value	95% Confidence Interval	
		Lower Bound	Upper Bound
Single Measures	.982	.936	.999
Intraclass Correlation Coefficient measurement GLP			
Single Measures	.757	.435	.979
Intraclass Correlation Coefficient measurement LG			
Single Measures	.982	.936	.999
Intraclass Correlation Coefficient measurement SLC			
Single Measures	.962	.868	.997
Intraclass Correlation Coefficient measurement ASG			
Single Measures	.592	.244	.956
Humerus			
Intraclass Correlation Coefficient measurement BT			
	Intraclass Correlation Value	95% Confidence Interval	
		Lower Bound	Upper Bound
Single Measures	.963	.872	.997
Intraclass Correlation Coefficient measurement Bd			
Single Measures	.935	.793	.995
Intraclass Correlation Coefficient measurement Dd			
Single Measures	.871	.638	.990
Intraclass Correlation Coefficient measurement BE			
Single Measures	.827	.537	.986
Intraclass Correlation Coefficient measurement BEI			

Single Measures	.586	.231	.954
Intraclass Correlation Coefficient measurement HTC			
Single Measures	.975	.912	.998
Intraclass Correlation Coefficient measurement HT			
Single Measures	.731	.400	.975
Radius			
Intraclass Correlation Coefficient measurement Bp			
	Intraclass Correlation Value	95% Confidence Interval	
		Lower Bound	Upper Bound
Single Measures	.956	.853	.997
Intraclass Correlation Coefficient measurement BFp			
Single Measures	.905	.717	.993
Intraclass Correlation Coefficient measurement Dp			
Single Measures	.897	.695	.992
Intraclass Correlation Coefficient measurement GL			
Single Measures	.039	.006	.615
Intraclass Correlation Coefficient for GL without outlier			
Single Measures	.997	.994	.999
Intraclass Correlation Coefficient measurement SD			
Single Measures	.780	.437	.981
Ulna			
Intraclass Correlation Coefficient measurement B			
	Intraclass Correlation Value	95% Confidence Interval	
		Lower Bound	Upper Bound
Single Measures	.684	.290	.989
Intraclass Correlation Coefficient measurement L			
Single Measures	.891	.572	.997
Intraclass Correlation Coefficient measurement SDO			
Single Measures	.942	.783	.998
Intraclass Correlation Coefficient measurement BPC			
Single Measures	.888	.615	.997
Intraclass Correlation Coefficient measurement DPA			
Single Measures	.990	.956	1.000
Metacarpal			
Intraclass Correlation Coefficient measurement GL			
	Intraclass Correlation Value	95% Confidence Interval	
		Lower Bound	Upper Bound
Single Measures	.985	.943	.999
Intraclass Correlation Coefficient measurement SD			
Single Measures	.974	.911	.998
Intraclass Correlation Coefficient measurement BatF			
Single Measures	.987	.953	.999
Intraclass Correlation Coefficient measurement BFd			

Single Measures	.992	.972	.999
Intraclass Correlation Coefficient measurement a			
Single Measures	.922	.758	.994
Intraclass Correlation Coefficient measurement b			
Single Measures	.968	.893	.998
Intraclass Correlation Coefficient measurement 1			
Single Measures	.749	.422	.977
Intraclass Correlation Coefficient measurement 2			
Single Measures	.979	.923	.998
Intraclass Correlation Coefficient measurement 3			
Single Measures	.955	.845	.997
Intraclass Correlation Coefficient measurement 4			
Single Measures	.056	-.003	.536
Intraclass Correlation Coefficient for 4 without outliers			
Single Measures	.648	.269	.965
Intraclass Correlation Coefficient measurement 5			
Single Measures	.863	.621	.989
Intraclass Correlation Coefficient measurement 6			
Single Measures	.261	.056	.840
Intraclass Correlation Coefficient for 6 without the outliers			
Single Measures	.975	.911	.998
Metatarsal			
Intraclass Correlation Coefficient measurement GL			
	Intraclass Correlation Value	95% Confidence Interval	
		Lower Bound	Upper Bound
Single Measures	.930	.779	.995
Intraclass Correlation Coefficient measurement SD			
Single Measures	.975	.911	.998
Intraclass Correlation Coefficient measurement BatF			
Single Measures	.995	.983	1.000
Intraclass Correlation Coefficient measurement BFd			
Single Measures	.969	.891	.998
Intraclass Correlation Coefficient measurement a			
Single Measures	.939	.804	.995
Intraclass Correlation Coefficient measurement b			
Single Measures	.975	.909	.998
Intraclass Correlation Coefficient measurement 1			
Single Measures	.780	.447	.981
Intraclass Correlation Coefficient measurement 2			
Single Measures	.980	.930	.999
Intraclass Correlation Coefficient measurement 3			

Single Measures	.957	.856	.997
Intraclass Correlation Coefficient measurement 4			
Single Measures	.070	.010	.537
Intraclass Correlation Coefficient for 4 without outliers			
Single Measures	.697	.342	.972
Intraclass Correlation Coefficient measurement 5			
Single Measures	.959	.862	.997
Intraclass Correlation Coefficient measurement 6			
Single Measures	.212	.043	.799
Intraclass Correlation Coefficient for 6 without outliers			
Single Measures	.896	.689	.992
Tibia			
Intraclass Correlation Coefficient measurement Bd			
	Intraclass Correlation Value	95% Confidence Interval	
		Lower Bound	Upper Bound
Single Measures	.810	.522	.984
Intraclass Correlation Coefficient measurement Dd(a)			
Single Measures	.919	.746	.994
Intraclass Correlation Coefficient measurement Dd(b)			
Single Measures	.825	.544	.985
Intraclass Correlation Coefficient measurement GL			
Single Measures	1.000	.999	1.000
Intraclass Correlation Coefficient measurement SD			
Single Measures	.876	.636	.990
Astragalus			
Intraclass Correlation Coefficient measurement Bd			
	Intraclass Correlation Value	95% Confidence Interval	
		Lower Bound	Upper Bound
Single Measures	.991	.968	.999
Intraclass Correlation Coefficient measurement GLI			
Single Measures	.984	.942	.999
Intraclass Correlation Coefficient measurement DI			
Single Measures	.577	.230	.954
Intraclass Correlation Coefficient measurement GLm			
Single Measures	.991	.967	.999
Intraclass Correlation Coefficient measurement Dm			
Single Measures	.336	.057	.896
Intraclass Correlation Coefficient measurement H			
Single Measures	.966	.885	.998
Intraclass Correlation Coefficient measurement BpT			
Single Measures	.860	.617	.989
Calcaneum			
Intraclass Correlation Coefficient measurement GL			

	Intraclass Correlation Value	95% Confidence Interval	
		Lower Bound	Upper Bound
Single Measures	.006	-.062	.540
Intraclass Correlation Coefficient for GL without the outliers			
Single Measures	.462	.189	.687
Intraclass Correlation Coefficient measurement SB			
Single Measures	.995	.983	1.000
Intraclass Correlation Coefficient measurement c			
Single Measures	.112	-.010	.720
Intraclass Correlation Coefficient measurement d			
Single Measures	.652	.297	.965
Intraclass Correlation Coefficient measurement B			
Single Measures	.757	.418	.978
Intraclass Correlation Coefficient measurement DS			
Single Measures	.923	.756	.994
Intraclass Correlation Coefficient measurement Gd			
Single Measures	.799	.459	.983
3rd Phalanx			
Intraclass Correlation Coefficient measurement DLS			
	Intraclass Correlation Value	95% Confidence Interval	
		Lower Bound	Upper Bound
Single Measures	.997	.991	1.000
Intraclass Correlation Coefficient measurement MBS			
Single Measures	.771	.445	.980

- 3rd lower premolar

The measurements for this element could only be taken on two specimens (both goats) as, in the other specimens, the tooth was missing. Both measurements have very wide confidence intervals (i.e. a range of values around the statistics that are believed to contain, with a probability of 95%, the population value. Field 2009: 783) and ICC values which are far from being close to 1 (Tab. 2.41). As a consequence, they cannot be considered as taken consistently by the raters.

- 4th lower premolar

The measurements could be taken on only two specimens (a sheep and a goat), as the tooth was not present in some of the mandibles. Table 2.41 shows that B has an ICC value which is closer to 1, thus it can be considered acceptable. On the other hand, L has a very low coefficient, closer to 0 suggesting that the measurement has not been taken as consistently as B.

- Mandible

H and B on the mandible could be taken on two specimens (goats), as the other two presented a pathology in the region where these measurements should be taken. PF was excluded from the analysis as it could be taken on only one specimen, thus it was not representative of the sample. The ICC value for H is small, negative and very far from 1 while the value for B is closer to 1. Consequently B has been taken in a more consistent way than H (Tab. 2.41).

In teeth and mandibles, the difference of variation that has been noted among the raters can be due to the different way measurements have been taken. In fact, in the description provided on the protocol, it was not clearly explained where to position the calliper, so that some colleagues may have taken the measurement on the occlusal surface of the tooth as suggested by von den Driesch (1976: 52-57) and not above enamel junction. Taking the measurement in this area (which is not where the crown of the tooth shrinks to connect with the root but the area just above it) allows greater consistency as it can be taken also on heavily worn teeth. We must also consider that the approximation to the tenth of millimetre applied to the measurements, has a greater influence on smaller measurements.

- Horncore

A, B, C, and D on the horncore were taken on all four specimens while E and F only on two (a sheep and a goat) because the horncores were not complete in some cases. Table 2.41 shows that all measurements have provided very high ICC scores (close to 1). It is surprising to note that, despite the fact that E and F may be difficult measurements to take (i.e. no clear and constant landmarks are present and recognizable on the bone indicating where to position the callipers), they have given good results attesting that, although some practical problems may occur, they can be taken in a relatively consistent way.

The use of Bland and Altman plots has revealed the presence of some outliers (Appendix I, Figs. A1.7-A1.12). In order to evaluate their influence ICC was recalculated for all the measurements, leaving out the anomalous values given by one of the raters (rater 1) (Tab. 2.41). The results improve substantially when the outliers are taken out showing how sensitive this test is to the presence of extreme values.

- Scapula

The complete set of measurements could be taken for the scapula on all specimens. All the ICC scores are closer to 1 than 0, attesting to the consistency of these measurements (Tab. 2.41). ASG (mainly) and GLP have clearly the lowest scores and widest confidence intervals, showing that they have been taken less consistently than the other measurements. A possible reason for

the inconsistency of ASG is that the area of the bone where the callipers should be placed is hard to define (see Chapter 2, Section 2.1.3).

- Humerus

All the measurements could be taken on all specimens. Almost all the ICC scores (Tab. 2.41) are high and closer to 1. BEI is the least consistent measurement as its score is the lowest; nevertheless it is still closer to 1 than 0, indicating a certain degree of consistency. The lower consistency of BEI may have been caused by the difficulty of positioning the callipers in the right way: there are no clear landmarks to take as fixed points at the lateral epicondyle to position the callipers. Some variation is present also for measurements HT, Dd and BE, though to a lesser extent than BEI. Thus, the overall reliability is not affected.

- Radius

Bp, BFp, Dp and SD were taken on all specimens, while GL was taken only on three (two sheep and one goat) as the distal end of this bone for one specimen was not fused, thus the measurement could not be taken. Table 2.41 shows that most of the values obtained are very high and closer to 1 than 0, supporting the idea that these measurements were taken consistently. GL is the only measurement which, as it has the lowest coefficient, has been taken with less consistency by the raters. SD, despite having a lower coefficient than the other measurements (Bp, BFp and Dp), shows a certain degree of consistency. The inconsistency found for GL is due to the fact that rater 1 has consistently taken measurements completely differently than the other raters, affecting the overall result. This pattern is made even clearer by Figure A1.28 (Appendix I).

As previously observed with the horncore measurements, if the outliers are excluded from the analysis the result changes significantly: the ICC value for GL is closer to 1 than 0, as such, it has indeed been taken in a consistent way by the different raters (Tab. 2.41).

- Ulna

All the measurements could be taken on only three specimens (two sheep and one goat) as the *olecranon* was not fused for one specimen. The ICC values (Tab. 2.41) are, for the measurements on the ulna as well, close to 1, showing a high level of consistency. Measurement B has the lowest coefficient and a wider confidence interval than the other measurements, attesting to the fact that it was taken less consistently than all the others. An explanation for that can be found in the fact that measurement B is taken in an area which is rounded and bumpy, especially in sheep. It is therefore very difficult to position the callipers in a consistent way (see also Chapter 2 Section 2.1.3).

- Metacarpal

All of the measurements related to the metacarpal could be taken on all the four specimens. The ICC values (Tab. 2.41) are very high for almost all the measurements demonstrating that consistency was adopted while colleagues were taking them. The measurements which have been taken less consistently are 1, 4 and 6, which have lowest coefficients in comparison to all the others. The reason behind the inconsistency of 1 and 4 might be that the description regarding where to position the calliper on the external trochlea of the medial and lateral condyles is unclear. As a consequence, some colleagues have taken it more medially (as suggested by Davis 1996 and Payne 1969), rather than on the external edge as originally intended.

In the case of measurement 4 and 6 (Appendix I, Figs. A1.44 and A1.46), there are some extreme outliers which can explain the lower result given by the ICC test. In order to understand the extent to which the outliers influence the results, a new ICC test was run excluding the extreme values provided by some raters. The results show that the ICC for measurement 4, and even more in the case of measurement 6, is closer now to 1 than 0, making the measurement more reliable and consistently taken. Nonetheless some variability is still noticeable (especially for measurement 4) (Tab. 2.41).

The Bland and Altman plots have revealed an interesting pattern among the raters (Appendix I, Figs. A1.35-A1.46): rater 1 has given markedly different scores for most of the measurements. This may relate to an error in calliper calibration. In the case of the metacarpal, a problem of identification/confusion of medial and lateral condyle may also have occurred. Nevertheless, as the raters were all experienced zooarchaeologists, and the bones not fragmented, this last hypothesis appears to be unlikely.

- Metatarsal

As with the metacarpal, the full set of measurements of the metatarsal could be taken on all specimens. Table 2.41 shows the same pattern observed for the metacarpal: measurements 4 and 6 have the widest intervals and the lowest coefficients obtained, suggesting that they were taken less consistently than all the other measurements (raters were more consistent in taking GL, SD, BatF, BFd, a, b, 2, 3 and 5). Overall, most of the measurements taken on this anatomical element have shown consistency. The reason behind the low ICC given for the metacarpal can also be applied to the metatarsal as the shape of these bones is very similar.

The Bland and Altman scatterplots (Appendix I, Figs. A1.56-A1.58) have revealed some patterns related to measurements 4 and 6, for which outliers have been identified. Consequently,

a new ICC test was run with the exclusion of the outliers for measurement 4 and 6. The values increase significantly (Tab. 2.41) showing that measurements 4 and 6 were taken with a certain degree of consistency.

- Tibia

Bd, Dd(a), Dd(b) and SD have been taken on three specimens while GL only on two, as the proximal end of one of the specimens was not fused, as such the measurement could not be taken. Table 2.41 shows that all the measurements have relatively high coefficients - in particular Dd(a), SD, Dd(b) and Bd (in decreasing order) - confirming that they have been taken consistently.

- Astragalus

All measurements could be taken on all specimens chosen. If we consider the ICC values, DI and Dm scores are lower than the other measurements, showing that these measurements have been taken with less consistency by the raters. This can be explained by the shape of the lateral and medial side of the astragalus: they are not regular surfaces (particularly the medial side in goat) and, as such, they are difficult to measure in a consistent way (see also Chapter 2, Section 2.1.3). A better performance was given by Bd, GLm, GLm, H and, to a lesser extent, BpT; all these measurements have coefficients which are high and close to 1 (Tab. 2.41).

- Calcaneum

The full set of measurements could be taken on all the chosen specimens. Table 2.41 indicates that GL and c have very low coefficients. B and d show some degree of inconsistency, but the overall result is acceptable. Better performance was given by SB, DS and Gd. The reason behind the low performance of GL, which is a straightforward and routinely taken measurement (von den Driesch 1976: 90-91), is not clear. For c on the other hand, the problem could be the shape of the articular facet. Boessneck himself (1969: 353) defines this measurement as imprecise.

Scatterplot A1.71 (Appendix I), related to measurement GL, shows the presence of some outliers (rater 1 and 3). If the outliers are left out of the analysis, the ICC value increases as shown by Table 2.41. Nevertheless the score is still low showing that this measurement has not been taken consistently by the raters.

- 3rd Phalanx

All the measurements were taken on the specimens. The ICC values in Table 2.41 show that both values are satisfactory. Nevertheless, DLS seems to have been taken more consistently than MBS as the former has a score closer to 1 than the latter.

2.3.3 Intra-Observer Error: Inter Correlation Coefficient

Table 2.42 shows the results of the Intra-Observer Error test (ICC). Results are presented for each measurement taken by the same rater (author) on the same four modern sheep and goat specimens used for the Inter-Observer Error test.

Table 2.42 ICC value and 95% Confidence Interval values for different measurements taken on different anatomical elements.

Horncore			
Intraclass Correlation Coefficient measurement A			
	Intraclass Correlation	95% Confidence Interval	
		Lower Bound	Upper Bound
Single Measures	1.000	.998	1.000
Intraclass Correlation Coefficient measurement B			
Single Measures	1.000	.999	1.000
Intraclass Correlation Coefficient measurement C			
Single Measures	1.000	.999	1.000
Intraclass Correlation Coefficient measurement D			
Single Measures	1.000	.999	1.000
Intraclass Correlation Coefficient measurement E			
Single Measures	1.000	1.000	1.000
Intraclass Correlation Coefficient measurement F			
Single Measures	1.000	1.000	1.000
Scapula			
Intraclass Correlation Coefficient measurement BG			
	Intraclass Correlation	95% Confidence Interval	
		Lower Bound	Upper Bound
Single Measures	.995	.978	1.000
Intraclass Correlation Coefficient measurement GLP			
Single Measures	.998	.990	1.000
Intraclass Correlation Coefficient measurement LG			
Single Measures	.998	.993	1.000
Intraclass Correlation Coefficient measurement SLC			
Single Measures	.975	.893	.998
Intraclass Correlation Coefficient measurement ASG			
Single Measures	.992	.967	.999
Humerus			

Intraclass Correlation Coefficient measurement BT			
	Intraclass Correlation	95% Confidence Interval	
		Lower Bound	Upper Bound
Single Measures	.995	.978	1.000
Intraclass Correlation Coefficient measurement Bd			
Single Measures	.999	.994	1.000
Intraclass Correlation Coefficient measurement Dd			
Single Measures	.999	.997	1.000
Intraclass Correlation Coefficient measurement BE			
Single Measures	.985	.934	.999
Intraclass Correlation Coefficient measurement BEI			
Single Measures	.975	.895	.998
Intraclass Correlation Coefficient measurement HTC			
Single Measures	.989	.951	.999
Intraclass Correlation Coefficient measurement HT			
Single Measures	.990	.957	.999
Radius			
Intraclass Correlation Coefficient measurement BFp			
	Intraclass Correlation	95% Confidence Interval	
		Lower Bound	Upper Bound
Single Measures	.996	.982	1.000
Intraclass Correlation Coefficient measurement Bp			
Single Measures	.961	.840	.997
Intraclass Correlation Coefficient measurement Dp			
Single Measures	.968	.869	.998
Intraclass Correlation Coefficient measurement GL			
Single Measures	.999	.995	1.000
Intraclass Correlation Coefficient measurement SD			
Single Measures	.997	.986	1.000
Ulna			
Intraclass Correlation Coefficient measurement B			
	Intraclass Correlation	95% Confidence Interval	
		Lower Bound	Upper Bound
Single Measures	.989	.942	1.000
Intraclass Correlation Coefficient measurement L			
Single Measures	.995	.974	1.000
Intraclass Correlation Coefficient measurement SDO			
Single Measures	.985	.935	.999
Intraclass Correlation Coefficient measurement BPC			
Single Measures	.993	.970	1.000
Intraclass Correlation Coefficient measurement DPA			
Single Measures	.993	.971	1.000
Metacarpal			

Intraclass Correlation Coefficient measurement GL			
	Intraclass Correlation	95% Confidence Interval	
		Lower Bound	Upper Bound
Single Measures	.998	.989	1.000
Intraclass Correlation Coefficient measurement SD			
Single Measures	.998	.991	1.000
Intraclass Correlation Coefficient measurement BatF			
Single Measures	.993	.968	.999
Intraclass Correlation Coefficient measurement BFd			
Single Measures	.998	.991	1.000
Intraclass Correlation Coefficient measurement a			
Single Measures	.998	.991	1.000
Intraclass Correlation Coefficient measurement b			
Single Measures	.997	.985	1.000
Intraclass Correlation Coefficient measurement 1			
Single Measures	.982	.921	.999
Intraclass Correlation Coefficient measurement 2			
Single Measures	.995	.980	1.000
Intraclass Correlation Coefficient measurement 3			
Single Measures	.991	.959	.999
Intraclass Correlation Coefficient measurement 4			
Single Measures	.968	.867	.998
Intraclass Correlation Coefficient measurement 5			
Single Measures	.997	.986	1.000
Intraclass Correlation Coefficient measurement 6			
Single Measures	.991	.960	.999
Metatarsal			
Intraclass Correlation Coefficient measurement GL			
	Intraclass Correlation	95% Confidence Interval	
		Lower Bound	Upper Bound
Single Measures	.999	.996	1.000
Intraclass Correlation Coefficient measurement SD			
Single Measures	.993	.969	1.000
Intraclass Correlation Coefficient measurement BatF			
Single Measures	.999	.994	1.000
Intraclass Correlation Coefficient measurement BFd			
Single Measures	.987	.944	.999
Intraclass Correlation Coefficient measurement 1			
Single Measures	.985	.935	.999
Intraclass Correlation Coefficient measurement 2			
Single Measures	.995	.979	1.000
Intraclass Correlation Coefficient measurement 3			
Single Measures	.998	.991	1.000

Intraclass Correlation Coefficient measurement 4			
Single Measures	.946	.789	.996
Intraclass Correlation Coefficient measurement 5			
Single Measures	.996	.981	1.000
Intraclass Correlation Coefficient measurement 6			
Single Measures	.997	.985	1.000
Tibia			
Intraclass Correlation Coefficient measurement Bd			
	Intraclass Correlation	95% Confidence Interval	
		Lower Bound	Upper Bound
Single Measures	.998	.991	1.000
Intraclass Correlation Coefficient measurement Dd(a)			
Single Measures	.995	.977	1.000
Intraclass Correlation Coefficient measurement Dd(b)			
Single Measures	.991	.959	.999
Intraclass Correlation Coefficient measurement GL			
Single Measures	1.000	.999	1.000
Intraclass Correlation Coefficient measurement SD			
Single Measures	.995	.978	1.000
Astragalus			
Intraclass Correlation Coefficient measurement Bd			
	Intraclass Correlation	95% Confidence Interval	
		Lower Bound	Upper Bound
Single Measures	.988	.949	.999
Intraclass Correlation Coefficient measurement GLI			
Single Measures	.999	.997	1.000
Intraclass Correlation Coefficient measurement DI			
Single Measures	.993	.968	.999
Intraclass Correlation Coefficient measurement GLm			
Single Measures	.999	.996	1.000
Intraclass Correlation Coefficient measurement Dm			
Single Measures	.992	.963	.999
Intraclass Correlation Coefficient measurement H			
Single Measures	.995	.979	1.000
Intraclass Correlation Coefficient measurement BpT			
Single Measures	.992	.964	.999
Calcaneum			
Intraclass Correlation Coefficient measurement GL			
	Intraclass Correlation	95% Confidence Interval	
		Lower Bound	Upper Bound
Single Measures	.999	.997	1.000
Intraclass Correlation Coefficient measurement SB			
Single Measures	.994	.973	1.000

Intraclass Correlation Coefficient measurement c			
Single Measures	.984	.930	.999
Intraclass Correlation Coefficient measurement d			
Single Measures	.990	.955	.999
Intraclass Correlation Coefficient measurement B			
Single Measures	.971	.880	.998
Intraclass Correlation Coefficient measurement DS			
Single Measures	.997	.985	1.000
Intraclass Correlation Coefficient measurement Gd			
Single Measures	.971	.878	.998
3 rd Phalanx			
Intraclass Correlation Coefficient measurement DLS			
	Intraclass Correlation	95% Confidence Interval	
		Lower Bound	Upper Bound
Single Measures	1.000	.998	1.000
Intraclass Correlation Coefficient measurement MBS			
Single Measures	.989	.953	.999
One-way random effects model where people effects are random.			

- Horncore

Table 2.42 shows that all measurements on the horncores have provided very high ICC scores confirming the results obtained from the Inter-Observer Error.

- Scapula

All the ICC scores for all measurements taken on the scapula are closer to 1 than 0, attesting to their consistency (Tab. 2.42). ASG has provided a higher ICC score than the one obtained with the Inter-Observer Error, showing that it can be taken consistently. SLC is the measurement on the scapula which has given the lowest score (ICC= 0.975) however, as the score is far closer to 1 than 0, it has been taken consistently.

- Humerus

All the ICC scores (Tab. 2.42) of the measurements taken on the humerus are high and close to 1. BEI, consistently with what observed with the Inter-Observer Error, has the lowest score (ICC= 0.975); nevertheless, as it is far closer to 1 than 0, it has been taken with consistency.

- Radius

Table 2.42 shows that all the values obtained are very high and closer to 1 than 0, supporting the idea that the measurements on the radius were taken consistently. The measurements which

gave the lowest ICC scores for the radius are Bp (ICC= 0.961) and Dp (ICC= 0.968). As both values are far closer to 1 than 0 they can be considered consistently taken.

- Ulna

The ICC values (Tab. 2.42) are, for the measurements on the ulna as well, close to 1, showing a high level of consistency. Partially consistent with what observed with the Intra-Observer Error test, measurement B (ICC= 0.989) and SDO (ICC= 0.985) have provided the lowest coefficients. Nevertheless, as the coefficients are still very high and closer to 1 than 0, both measurements show to have been taken with consistency.

- Metacarpal

All of the measurements related to the metacarpal have provided high ICC values (Tab. 2.42) demonstrating that they were taken with consistency by the author. The measurements which have given the lowest ICC values are 1 and 4 (respectively ICC= 0.982 and 0.968), consistently with what observed with the Inter-Observer Error. Nevertheless, these values are still very high showing that the author has taken them consistently.

- Metatarsal

Very similar results have been obtained from the metatarsal (Table 2.42) Measurements 4 and 6 have the lowest coefficients (respectively ICC= 0.985 and 0.946), suggesting that they were taken less consistently than all the other measurements. Nevertheless, their ICC scores are far closer to 1 than 0, thus have been taken consistently.

- Tibia

All measurements taken on the tibia have provided very high ICC scores, confirming that they have all been taken consistently.

- Astragalus

Table 2.42 shows that all measurements taken on the astragalus have been taken consistently by the author as the ICC values are all close to 1. The pattern observed for the Inter-Observer Error, according to which D1 and Dm were the less consistently taken measurements, is not confirmed here.

- Calcaneum

All measurements taken on the calcaneum have provided high ICC values. Consistently with what observed for the Inter-Observer test, measurement c has given one of the lowest values

(ICC= 0.984). B and Gd have also given slightly lower results (respectively ICC= 0.971 and 0.971) compared to the others. Nevertheless, they are far closer to 1 than 0, suggesting that they have been taken consistently.

- 3rd Phalanx

All the measurements taken on the 3rd phalanx have given satisfactory ICC values.

2.3.4 Conclusions

The study of the Inter-Observer Error has revealed some interesting trends. The analysis of the Coefficient of Variation (CV) has indicated a fairly high level of consistency in the way most measurements were taken by the eight raters– most CV values were lower than 5%.

Of the measurements proposed, some gave good results (i.e. measurements on the radius, ulna, tibia and 3rd phalanx) while some others were taken less consistently (i.e. all measurements on the horncore, especially A, B, C and D; tooth measurements; ASG on the scapula; BEI and HT on the humerus; 4 and 6 on the metapodials; c and d on the calcaneum).

The more appropriately used Inter Correlation Coefficient test (ICC) revealed that the measurements that were taken less consistently by a number or different raters were mainly those described by previous literature, with only a few newly introduced measurements.

The measurements which gave the lowest ICC values with the Inter-Observer Error test, namely were taken less consistently, were:

- B and L on P₃;
- L in P₄;
- H and B on the Mandible;
- ASG in Scapula;
- BEI in Humerus;
- Dl and Dm in the Astragalus;
- c in the Calcaneum.

Different reasons have been identified to explain such inconsistency. The first is related to the nature of the surface or area in which the measurements are taken: it is difficult to measure consistently bones that do not provide clear landmarks or a straight surface on which to place the callipers (as in the case of ASG in the scapula, BEI in the humerus, Dl and Dm in the astragalus). The second reason is that some problems may have occurred because the

measurement was not sufficiently well defined, leaving room for doubt (as in the case of BEI in the humerus and c in the calcaneum).

Similar trends have been observed when the Intra-Observer Error test was conducted. Notably all measurements, even though to a different degree, gave higher ICC values compared to the values given by the Inter-Observer Error. This confirms what observed by previous researchers (Johnstone 2004; Popkin *et al.* 2012; Ulijaszek and Lourie 1994; Utermohle and Zegura 1982), namely that the Intra-Observer Error is generally lower than the Inter-Observer Error.

The measurements which gave the lowest ICC values with the Intra-Observer Error were:

- ASG and SLC in Scapula;
- BEI in Humerus;
- Bp and Dp in Radius;
- 4 in the Metapodials;
- B in the Calcaneum.

In conclusion, both tests show that there is strong evidence for the repeatability of the measurements making up the new recording protocol. Even though some measurements have revealed to be slightly more problematic to be taken consistently (disregarding the influence of extreme outliers due to human error), the overall results are successful; thus there is no need to exclude any measurement from the recording protocol.

Nevertheless, it is important to make sure that the explanation of how to take the measurements, especially those which have provided lower ICC values, is as clear as possible. It must also be accepted that, because of the nature of some bones themselves, some measurements can be subject to more variability than others.

2.4 Morphological results

Analytical studies of the reliability of known and new morphological criteria for distinguishing sheep and goat specimens have been carried out in the past by a variety of researchers (Clutton-Brock *et al.* 1990; Fernàndez 2001; Zeder and Lapham 2010; Zeder and Pilaar 2010). As most of these studies were carried out on highly heterogeneous modern samples - variable in terms of age, sex and breed - testing the morphological traits on a more homogenous sample was identified as an important step. The aims for such a study were:

1. to check and identify which, among the known morphological traits, were more visible and reliable on English and central European sheep and goat modern specimens;
2. to investigate the extent to which the visibility and reliability of the morphological traits are affected by factors such as age and sex;
3. to create a shortlist of more reliable traits that could be used to analyse English medieval sheep/goat assemblages.

The list of the morphological traits that have been evaluated and the reasons why they were chosen have already been explained. The descriptions of each of the morphological features have been outlined in Chapter 2 (Section 2.1.2) along with the scoring system used to record each trait (Chapter 2, Tab. 2.20).

In the following sections the results of the study of the morphological traits on the modern material are presented. The first section is focused on establishing which morphological features are more reliable for species identification (Section 2.4.1). A study of the influence that sex (Section 2.4.2) and age (Section 2.4.3) can have on the visibility and reliability of the traits follows.

2.4.1 Reliability of the morphological diagnostic traits

Table 2.42 presents the results when the reliability of the morphological traits was tested to see which elements and features were more successful in identifying each species. A list of the anatomical elements, morphological traits and number of specimens is provided, along with the percentage of correct matchings given per *taxon*. The first column presents the percentage of correct matches when the morphological trait was successfully attributed to the *taxon* the specimen belonged to. The second and third column show the percentages, for each species, when a combination of scores was taken into account (for example: C (*Capra*) + CL (*Capra*-like) and, C (*Capra*) + CL (*Capra*-like) + OC (*Ovis/Capra*). For instance, the difference in percentage between the first and second column in characteristic 2 for the mandible is due to the fact that some of the *Capra* specimens were classified as *Capra* like. In the third column the

specimens classified as *Ovis/Capra* also contribute to the percentage. The results are also displayed with the use of charts (Figs. 2.9 to 2.69).

Table 2.42 shows that some traits have achieved higher percentages (>90%) of successful species assignment in both species. Tables 2.43 and 2.44 display the list of these more successful traits, respectively for goat and sheep.

Table 2.43 Matchings of morphological identifications with actual taxa. C= *Capra*, O= *Ovis*, CL= *Capra*-like, OL= *Ovis*-like, OC= *Ovis/Capra*.

	Anatomical Elements	Morphological Trait	N. of Specimens		<i>Capra hircus</i>			<i>Ovis aries</i>		
			C	O	% of matching			% of matching		
					C	C + CL	C+CL+OC	O	O+OL	O+OL+OC
Cranial bones	Horncore	1	36	30	100	100	100	100	100	100
		2	36	30	100	100	100	100	100	100
	Mandible	1	62	71	22.6	22.6	96.8	43.7	43.7	81.7
		2	58	69	69	94.8	100	91.3	98.6	100
	dP ₃	1	6	9	83.3	100	100	55.6	88.9	88.9
		2	4	5	25	50	100	0	20	100
	dP ₄	1	3	5	0	0	100	20	20	100
		2	4	7	0	50	50	100	100	100
		3	6	8	83.3	100	100	100	100	100
		4	4	5	75	75	100	60	60	100
	P ₃	1	52	49	63.5	80.8	82.7	40.8	71.4	85.7
		2	52	49	76.9	84.6	98.1	63.3	83.7	91.8
		3	52	49	82.7	92.3	96.2	57.1	71.4	85.7
	P ₄	1	52	55	36.5	63.5	88.5	63.6	94.5	98.2
		2	52	55	40.4	59.6	84.5	67.3	87.3	100
		3	52	55	59.6	88.5	94.2	70.9	94.5	98.2
	M ₃	1	47	58	36.2	57.4	97.9	0	1.7	34.5
		2	48	58	25	50	89.6	39.7	56.9	100
		3	49	58	61.2	85.7	98	39.7	51.7	56.9
		4	49	58	28.6	75.5	98	5.2	32.8	89.7
		5	46	55	91.3	95.7	97.8	50.9	65.6	78.2
	Scapula	1	74	73	58.1	85.1	90.5	91.8	100	100
		2	74	73	82.4	89.2	94.6	60.3	68.5	72.6
	Humerus	1	76	71	76.3	100	100	94.4	100	100
		2	76	71	47.4	78.9	93.4	64.8	91.5	100
		3	76	71	78.9	88.2	96.1	64.8	91.5	100
		4	76	71	73.7	80.3	85.5	78.9	91.5	93
		5	76	70	85.5	96.1	98.7	97.1	100	100
Radius	1	74	72	85.1	91.9	94.6	100	100	100	
	2	74	72	81.1	87.8	95.9	83.3	97.2	97.2	
Ulna	1	59	59	86.4	94.9	96.6	74.6	76.3	76.3	
	2	56	58	57.1	92.9	96.4	63.8	94.8	96.6	
Metacarpal	1	58	62	93.1	98.3	98.3	98.4	100	100	
	2	58	62	70.7	93.1	98.3	53.2	87.1	96.8	
	3	58	62	22.4	74.1	100	33.9	75.8	96.8	
	4	58	62	79.3	96.6	96.6	91.9	100	100	
	5	58	62	94.8	98.3	98.3	85.5	87.1	93.5	
Metatarsal	1	62	64	85.5	98.4	98.4	98.4	100	100	
	2	62	64	71.0	96.8	100	34.4	77.1	96.9	
	3	62	64	16.1	64.5	96.8	21.9	66.2	90.6	
	4	62	64	79	95.2	98.4	93.8	100	100	
	5	62	64	96.8	100	100	82.8	84.4	90.6	
	6	62	64	93.5	95.2	98.4	98.4	98.4	98.4	
Tibia	1	72	69	58.3	75	79.2	75.4	82.6	84.1	
	2	72	69	77.8	93.1	95.8	49.3	59.4	65.2	
	3	72	69	63.9	70.8	75	31.9	69.6	76.8	
	4	70	69	71.4	84.3	90	88.4	98.5	100	
	5	71	69	45.1	90.1	95.8	37.7	88.4	100	
	6	72	69	72.2	95.8	98.6	65.2	97.1	98.6	
Astragalus	1	73	73	53.4	80.8	90.4	93.2	98.7	100	
	2	74	73	97.3	98.6	100	28.8	50.7	61.6	
	3	73	73	87.7	97.3	98.6	76.7	91.8	91.8	

Anatomical Elements	Morphological Trait	N. of Specimens		<i>Capra hircus</i>			<i>Ovis aries</i>			
		C	O	% of matching			% of matching			
				C	C + CL	C+CL +OC	O	O+OL	O+OL +OC	
		4	74	73	37.8	54.1	63.5	91.8	97.3	98.6
		5	74	71	78.4	91.9	95.9	84.9	97.3	97.3
		6	74	73	90.5	100	100	74.0	98.7	100
	Calcaneum	1	61	62	83.6	96.7	100	58.1	80.6	88.7
		2	61	62	86.9	95.1	98.4	90.3	98.4	100
		3	60	62	73.3	78.3	80	90.3	98.4	100
	1 st Phalanx	1	68	68	72.1	91.2	94.1	66.2	72.1	79.4
		2	69	69	50.7	82.6	94.2	85.5	92.8	98.6
		3	69	69	10.1	27.5	60.9	91.3	94.2	100
		4	69	69	82.6	98.6	100	75.4	91.3	95.7
	2 nd Phalanx	1	66	67	90.9	95.5	97	37.3	52.2	56.7
		2	67	67	70.1	94	98.5	82.1	91	92.5
	3 rd Phalanx	1	67	69	74.6	85.1	89.6	87	95.7	100
		2	67	69	71.6	82.1	92.5	94.2	100	100

Table 2.44 Morphological traits which have provided a high percentage of *taxon* attributions for goat (>90%).

GOAT				
Anatomical Element	Morphological Trait	% of matching		
		C	C+CL	C+CL+OC
Horncore	1	100	100	100
	2	100	100	100
M ₃	5	91.3	95.7	97.8
Metacarpal	1	93.1	98.3	98.3
	5	94.8	98.3	98.3
Metatarsal	5	96.8	100	100
	6	93.5	95.2	98.4
Astragalus	2	97.3	98.6	100
	6	90.5	100	100
2 nd Phalanx	1	90.9	95.5	97

Table 2.45 Morphological traits which provided a high percentage of *taxon* attributions for sheep (>90%).

SHEEP				
Anatomical element	Morphological Trait	% of matching		
		O	O+OL	O+OL+OC
Horncore	1	100	100	100
	2	100	100	100
Mandible	2	91.3	98.6	100
dP ₄	2	100	100	100
	3	100	100	100
Scapula	1	91.8	100	100
Humerus	1	94.4	100	100
	5	97.1	100	100
Radius	1	100	100	100
Metacarpal	1	98.4	100	100
	4	91.9	100	100
Metatarsal	1	98.4	100	100
	4	93.8	100	100
	6	98.4	98.4	98.4
Astragalus	1	93.2	98.7	100
	4	91.8	97.3	98.6
Calcaneum	2	90.3	98.4	100
	3	90.3	98.4	100
1 st Phalanx	3	91.3	94.2	100
2 nd Phalanx	2	94.2	100	100

Two patterns can be noticed. First of all, the horncore is the only anatomical element which has provided 100% of morphological identifications in both species for both traits. This element is clearly highly diagnostic. The other elements that have provided good results in both species are the metapodials; in particular trait 1 in the metacarpal and 6 in the metatarsal. These results are consistent with previous literature.

Some other morphological traits, as shown in Tables 2.43 and 2.44, have provided high identification percentages for only on one of the two species. Overall, the species for which a higher number of traits and elements have provided high percentages of *taxon* attributions is, in this study, the sheep. Thus, the morphological traits in this sample were more variable for the goat group than the sheep group. These outcomes do not agree with what Zeder and Lapham (2010: 2904) stated in their study. According to the two researchers, traits in goat were easier to detect because they were more strongly expressed while in sheep they were more subtle. This different result might be due to the fact that while the samples of modern sheep and goats studied by Zeder and Lapham were both highly heterogeneous with the presence of a high number of wild goats (37 out of 49) - for which the traits may have been more strongly expressed - the modern samples in this study were more homogeneous, as both groups were exclusively made up of domestic animals. Such homogeneity is particularly true for the sheep, whose sample is almost completely represented by two British breeds. It therefore makes sense that the morphological traits could be more consistently observed in the sheep sample, whereas the goat sample was more heterogeneous.

Some morphological traits have not provided very high percentages of specific attributions, but the matching gets much higher (>95%) when more tentative identifications (*Capra*-like and *Ovis*-like) are added. These are shown in Table 2.45 for goat and in Table 2.46 for sheep.

Table 2.46 Morphological traits for the goat group which provide a high score (>95%) only when different categories were combined (C+CL).

GOAT				
Anatomical Element	Morphological Trait	% of matching		
		C	C + CL	C+CL+OC
dP ₃	1	83.3	100	100
dP ₄	3	83.3	100	100
	1	76.3	100	100
Humerus	5	85.5	96.1	98.7
Metacarpal	4	79.3	96.6	96.6
	1	85.5	98.4	98.4
	2	71	96.8	100
Metatarsal	4	79	95.2	98.4
Tibia	6	72.2	95.8	98.6
Astragalus	3	87.7	97.3	98.6
	1	83.6	96.7	100
Calcaneum	2	86.9	95.1	98.4
1 st Phalanx	4	82.6	98.6	100

Table 2.47 Morphological traits for the goat group, which provide a high score (>95%) only when different categories were combined (O+OL).

SHEEP				
Anatomical Element	Morphological Trait	% of matching		
		O	O+OL	O+OL+OC
Radius	2	83.3	97.2	97.2
Tibia	4	88.4	98.5	100
	6	65.2	97.1	98.6
Astragalus	5	84.9	97.3	97.3
	6	74	98.7	100
3 rd Phalanx	1	87	95.7	100

These traits, despite not providing 100% accuracy, are still useful. Some traits that provide 90% of correct attributions to sheep (i.e. dP₄ trait 3, humerus traits 1 and 5, metacarpal trait 4, metatarsal trait 1 and 4 and, calcaneus trait 2) (Tab. 2.44), reach a high score also in goat, but only when the *Capra*-like category is added. This confirms on the one hand the higher degree of variability in goat and, on the other, that some traits are ‘symmetrical’ as they have given reasonably good results in both species.

Those traits that provide high identification percentages only when the category *Ovis/Capra* is added (C+CL <70%) appear to be less reliable. These include:

1. Mandible, trait 1;
2. dP₃, trait 2;
3. dP₄, trait 1, 2 and 4;
4. P₄, trait 1 and 2;
5. M₃, trait 1 and 2;
6. Metatarsal, trait 3;
7. Astragalus trait 4;
8. 1st Phalanx, trait 3.

While for sheep (O+OL<70%) are:

1. Mandible, trait 1;
2. dP₃, trait 2;
3. dP₄, trait 1 and 4;
4. M₃, all traits;
5. Scapula, trait 2;
6. Tibia trait 2 and 3;
7. Metatarsal, trait 3;
8. Astragalus, trait 2;
9. 2nd Phalanx, trait 1.

Traits on teeth and mandible performed poorly in both species. This is in agreement with the results obtained by Zeder and Lapham (2010). Nevertheless, a distinction has to be made as the

degree of reliability of some traits can be linked to different factors. In teeth an important issue affecting the probability of correct identification is represented by the degree of wear. In addition, some morphological traits (such as 1, 2 and 3 in dP₄, and trait 5 on M₃) are located in positions that can be difficult or impossible to see when the tooth is embedded in the jaw – an issue that affects in particular the un-fragmented modern reference material.

As concerns trait 2 on the scapula, the difficulty may be age-related. In sheep the elliptical shape of the glenoid cavity turns into a more circular shape as the animal gets older, making the separation with the goat more challenging. For the tibia there is much variability making identifications sometimes difficult (as also observed by Zeder and Pilaar 2010). A high degree of variation has also been noted in trait 3 on the metapodials, traits 2 and 4 on the astragalus and trait 1 on the 1st and 2nd phalanx.

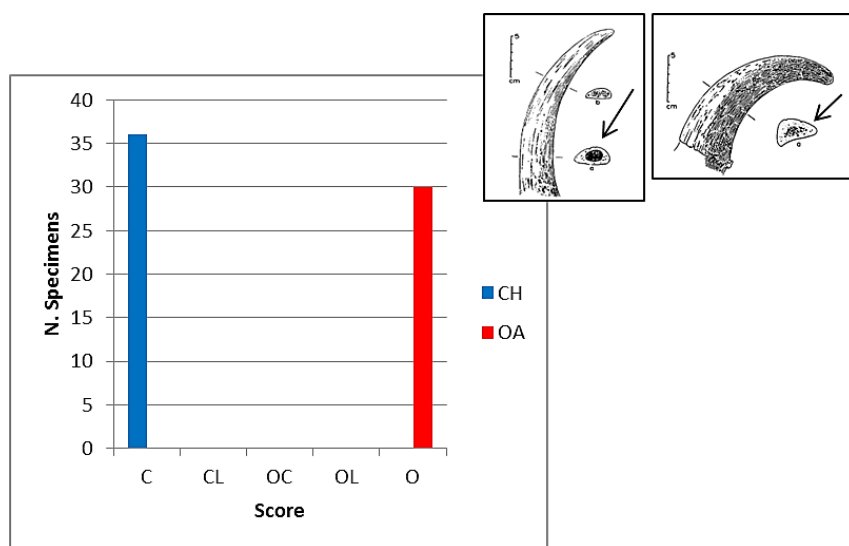


Figure 2.9 Horncore trait 1 (section): number of specimens attributed to the different categories for the two species (CH=*Capra hircus*; OA= *Ovis aries*; scores on horizontal axis: C= *Capra*; CL= *Capra-like*; OC= *Ovis/Capra*; OL= *Ovis-like*; O= *Ovis*).

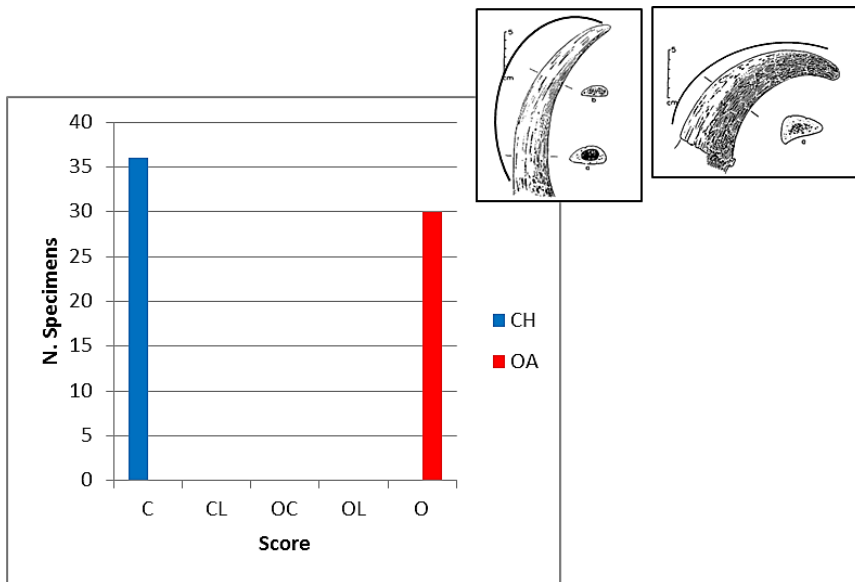


Figure 2.10 Horncore trait 2 (curvature): number of specimens attributed to the different categories for the two species. For details see Fig. 2.9.

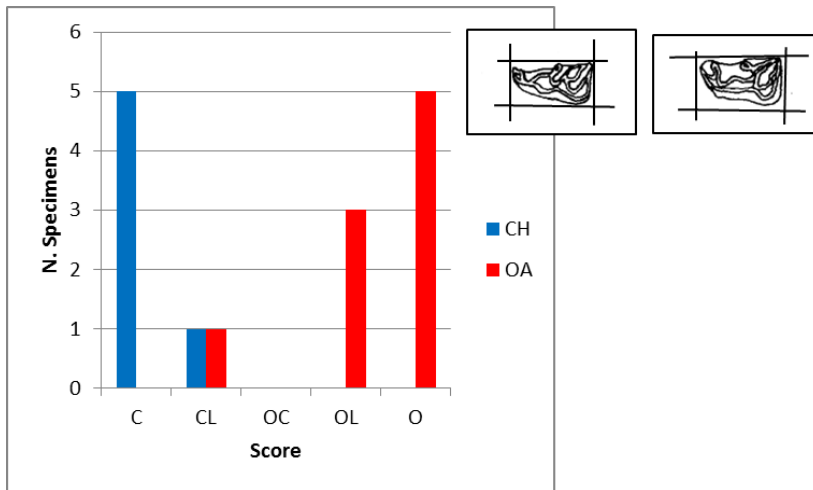


Figure 2.11 Third deciduous lower premolar dP₃, trait 1 (overall shape): number of specimens attributed to the different categories for the two species. For details see Fig. 2.9.

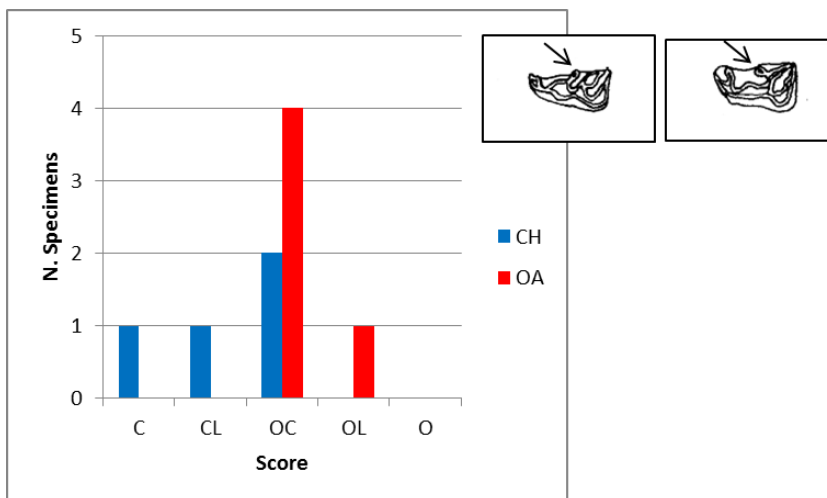


Figure 2.12 Third deciduous lower premolar dP₃, trait 2 (metaconoid): number of specimens attributed to the different categories for the two species. For details see Fig. 2.9.

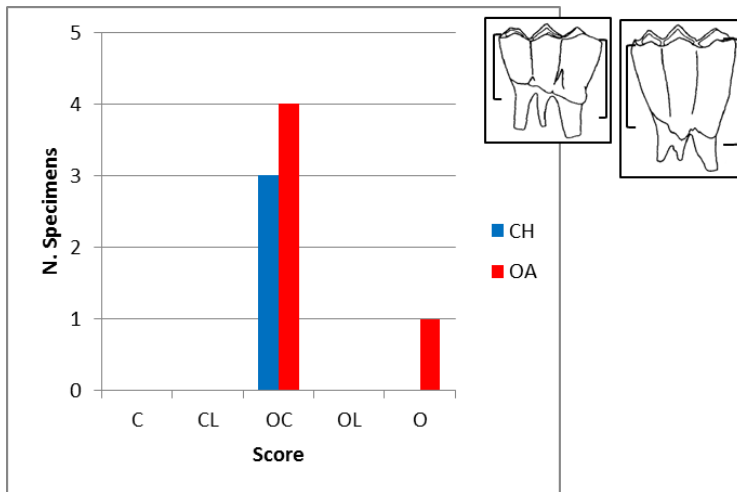


Figure 2.13 Fourth deciduous lower premolar dP₄, trait 1 (crown aspect): number of specimens attributed to the different categories for the two species. For details see Fig. 2.9.

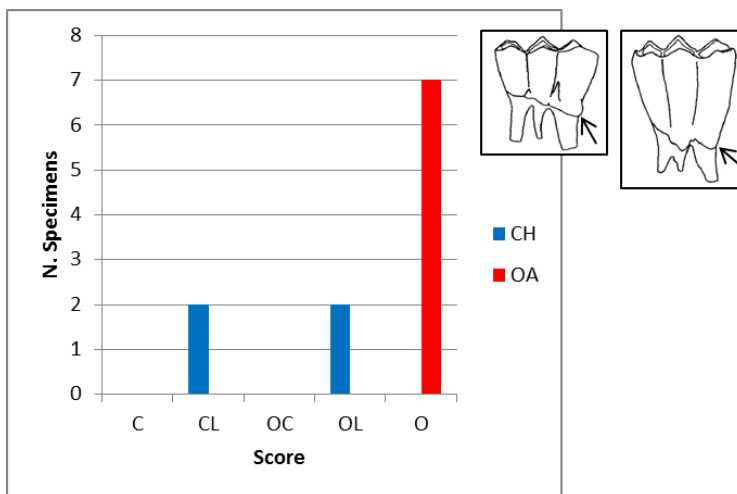


Figure 2.14 Fourth deciduous lower premolar dP₄, trait 2 (presence/absence of basal swelling): number of specimens attributed to the different categories for the two species. For details see Fig. 2.9.

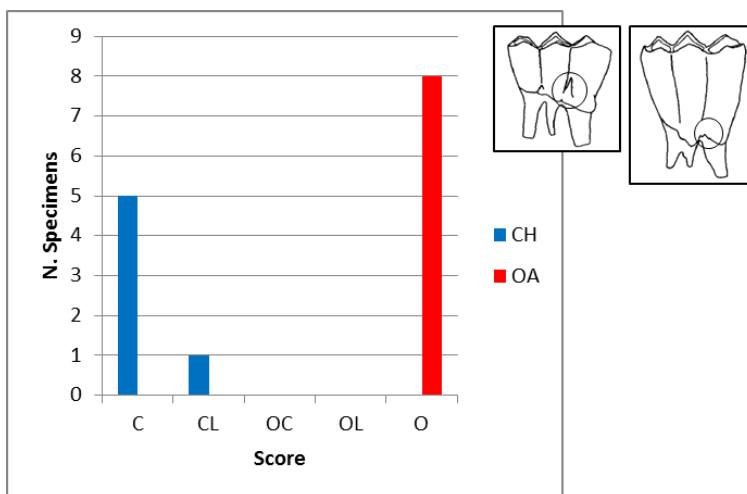


Figure 2.15 Fourth deciduous lower premolar dP₄, trait 3 (presence/absence of interlobar pillar): number of specimens attributed to the different categories for the two species. For details see Fig. 2.9.

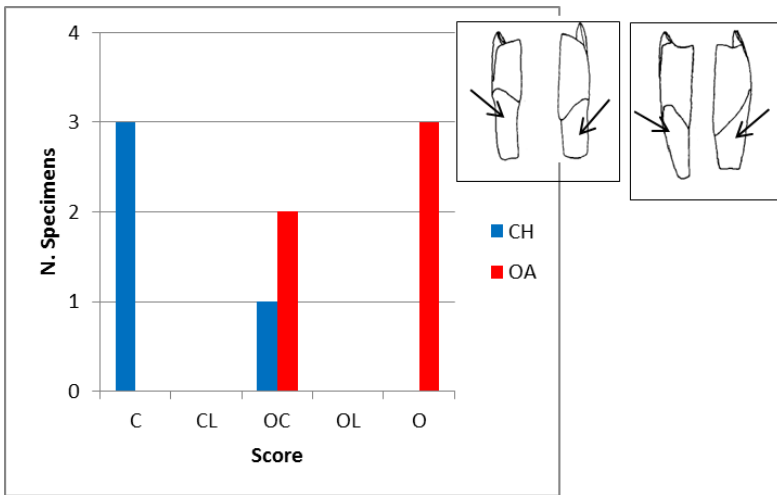


Figure 2.16 Fourth deciduous lower premolar dP₄, trait 4 (enamel development): number of specimens attributed to the different categories for the two species. For details see Fig. 2.9.

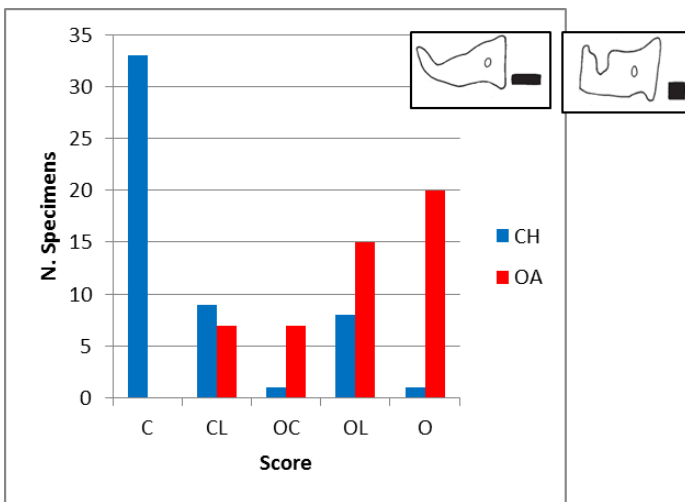


Figure 2.17 Third permanent lower premolar P₃, trait 1 (overall shape): number of specimens attributed to the different categories for the two species. For details see Fig. 2.9.

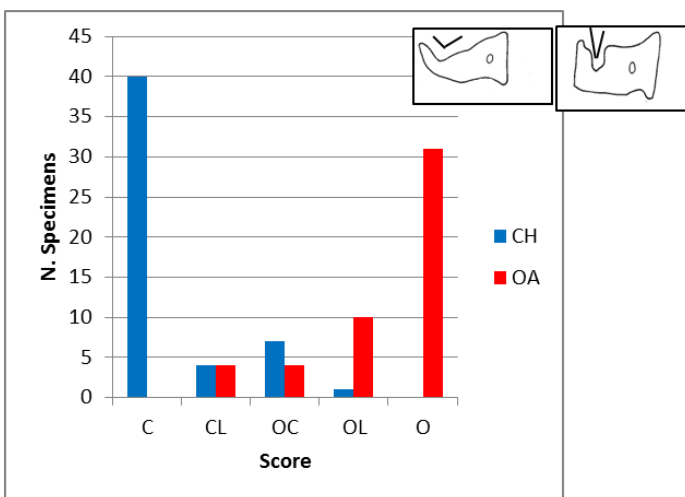


Figure 2.18 Third permanent lower premolar P₃, trait 2 (middle vertical ridge): number of specimens attributed to the different categories for the two species. For details see Fig. 2.9.

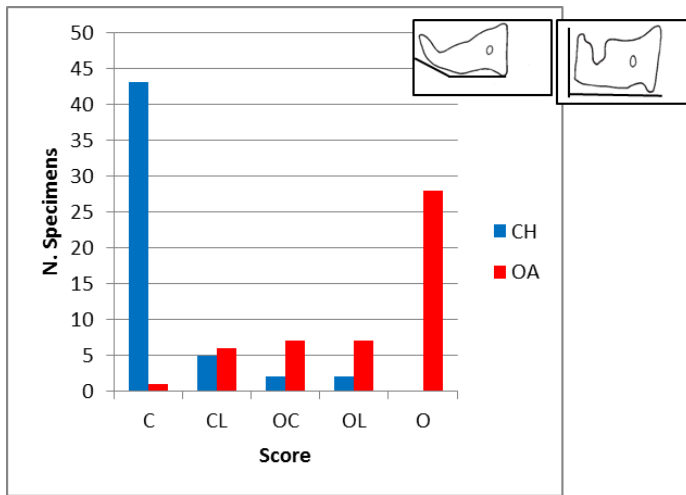


Figure 2.19 Third permanent lower premolar P₃, trait 3 (mesial-buccal angle): number of specimens attributed to the different categories for the two species. For details see Fig. 2.9.

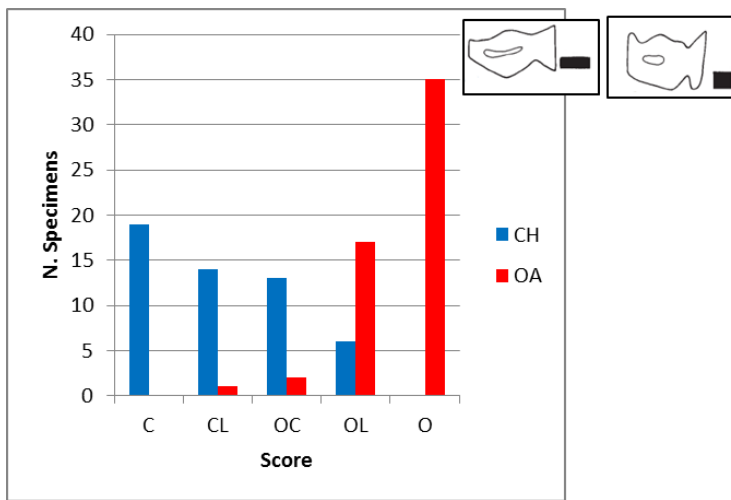


Figure 2.20 Fourth permanent lower premolar P₄, trait 1 (overall shape): number of specimens attributed to the different categories for the two species. For details see Fig. 2.9.

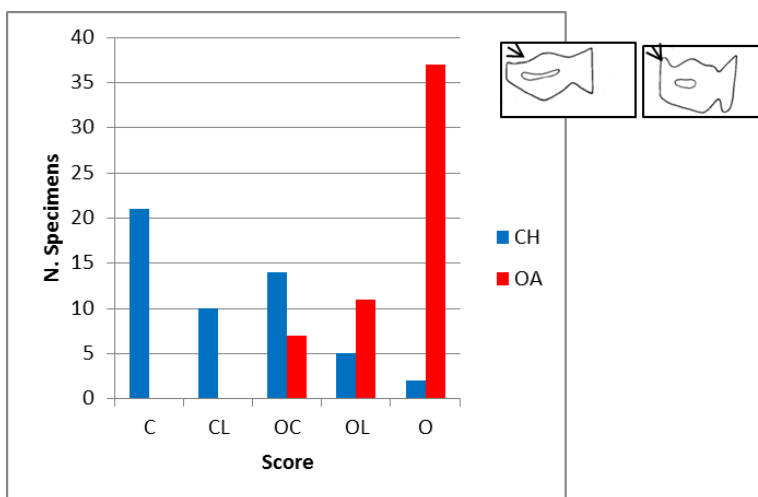


Figure 2.21 Fourth permanent lower premolar P₄, trait 2 (mesio-lingual rib): number of specimens attributed to the different categories for the two species. For details see Fig. 2.9.

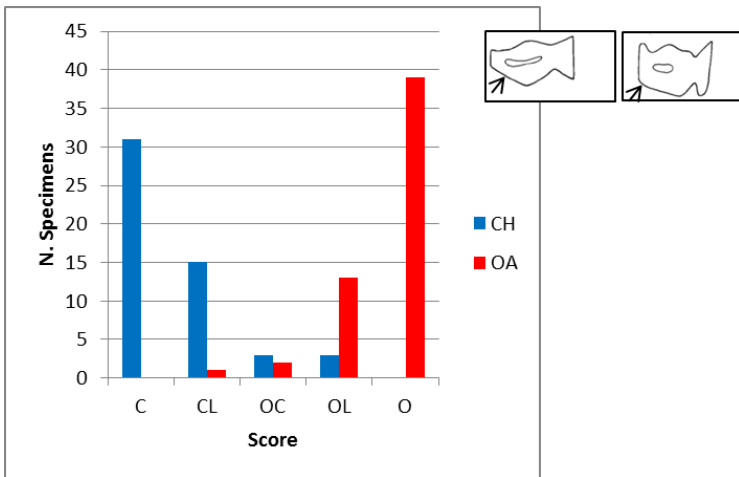


Figure 2.22 Fourth permanent lower premolar P₄, trait 3 (mesio-buccal angle): number of specimens attributed to the different categories for the two species. For details see Fig. 2.9.

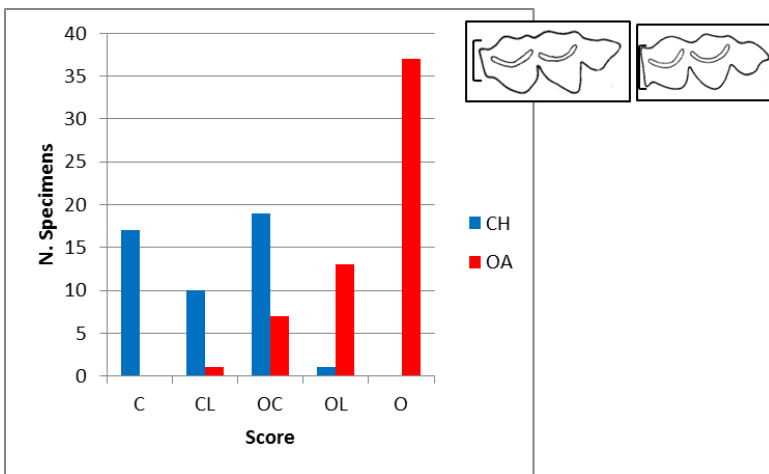


Figure 2.23 Third lower molar M₃, trait 1 (mesial face): number of specimens attributed to the different categories for the two species. For details see Fig. 2.9.

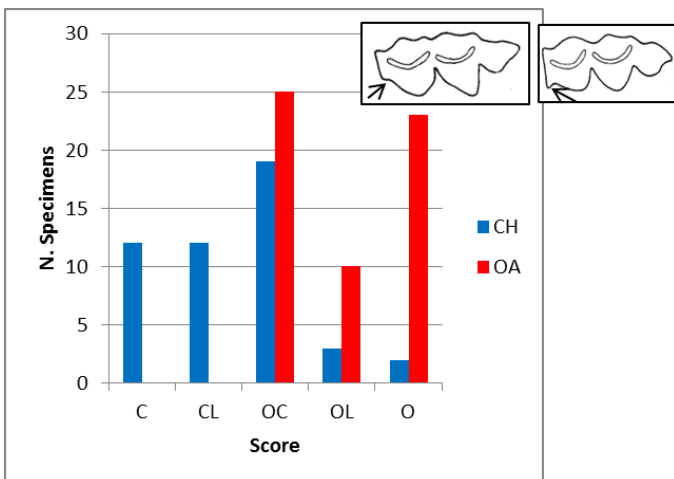


Figure 2.24 Third lower molar M₃, trait 2 (buccal edge angle): number of specimens attributed to the different categories for the two species. For details see Fig. 2.9.

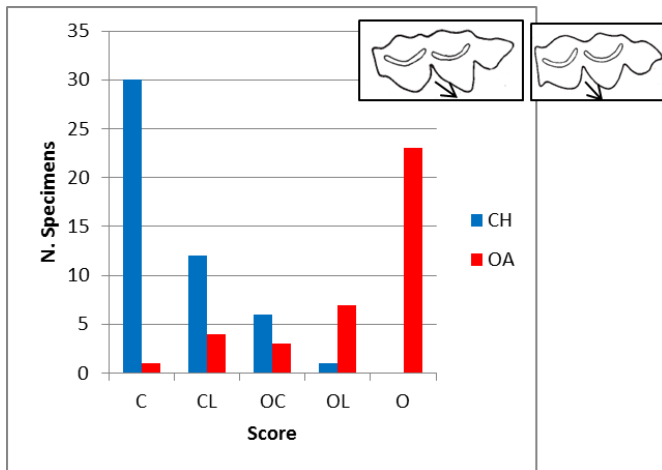


Figure 2.25 Third lower molar M₃, trait 3 (direction of central cusp): number of specimens attributed to the different categories for the two species. For details see Fig. 2.9.

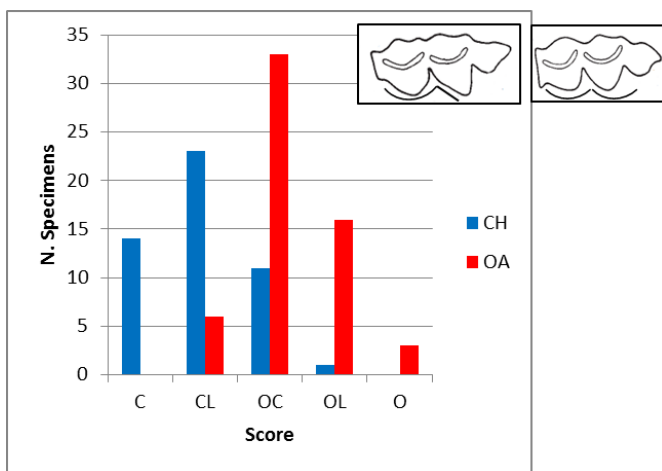


Figure 2.26 Third lower molar M₃, trait 4 (symmetry and shape of cusps): number of specimens attributed to the different categories for the two species. For details see Fig. 2.9.

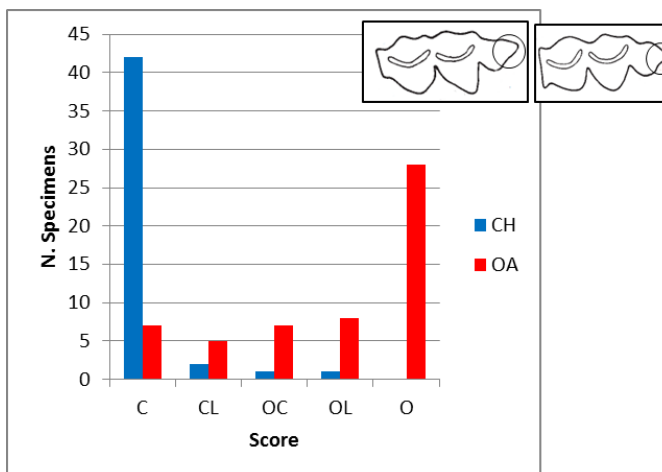


Figure 2.27 Third lower molar M₃, trait 5 (distal flute): number of specimens attributed to the different categories for the two species. For details see Fig. 2.9.

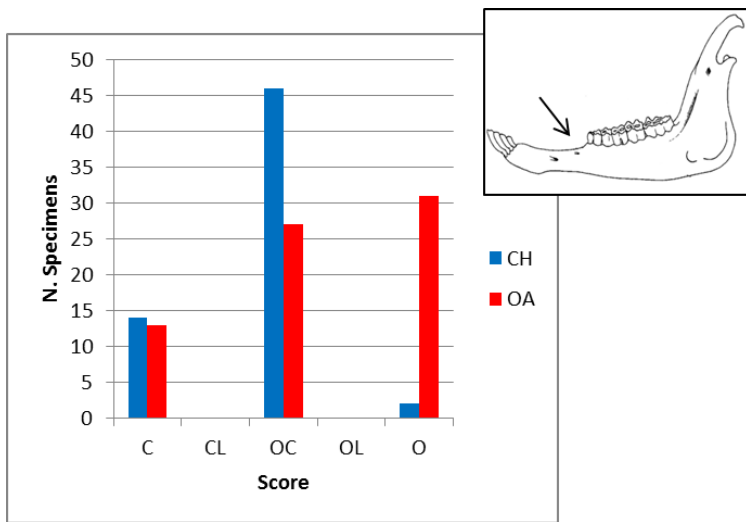


Figure 2.28 Mandible, trait 1 (presence/absence of foramen): number of specimens attributed to the different categories for the two species. For details see Fig. 2.9.

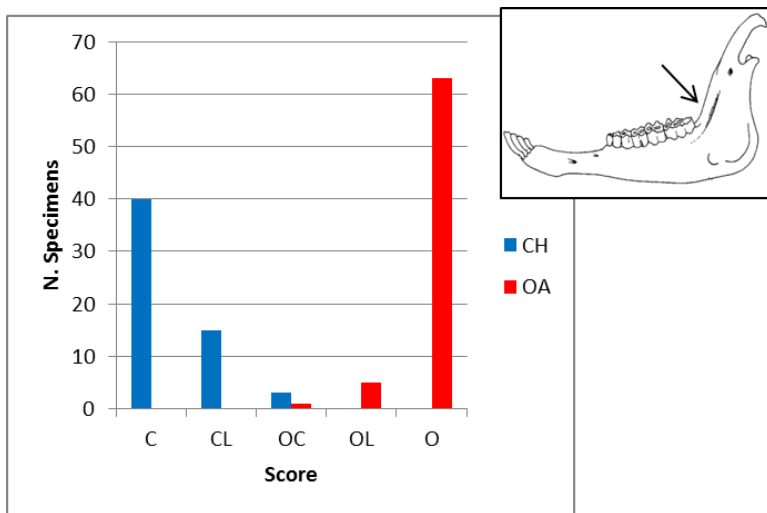


Figure 2.29 Mandible, trait 2 (hollow): number of specimens attributed to the different categories for the two species. For details see Fig. 2.9.

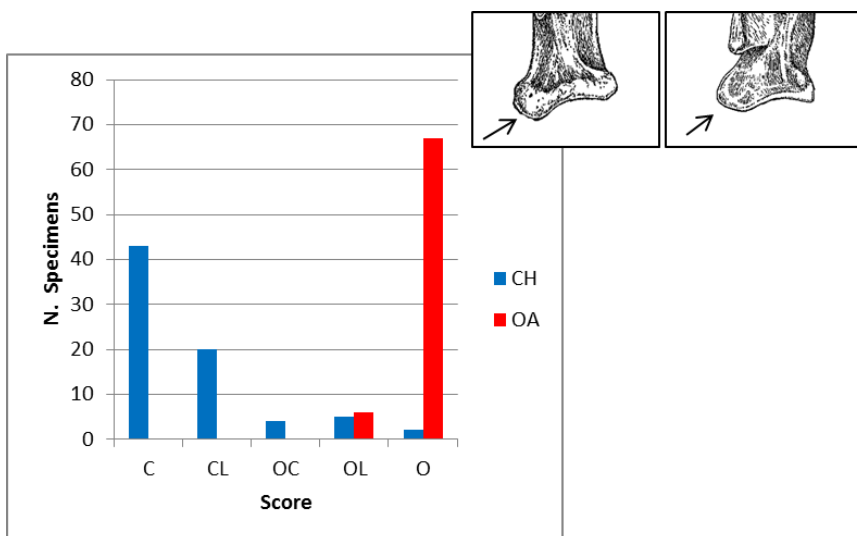


Figure 2.30 Scapula, trait 1 (glenoid tubercle): number of specimens attributed to the different categories for the two species. For details see Fig. 2.9.

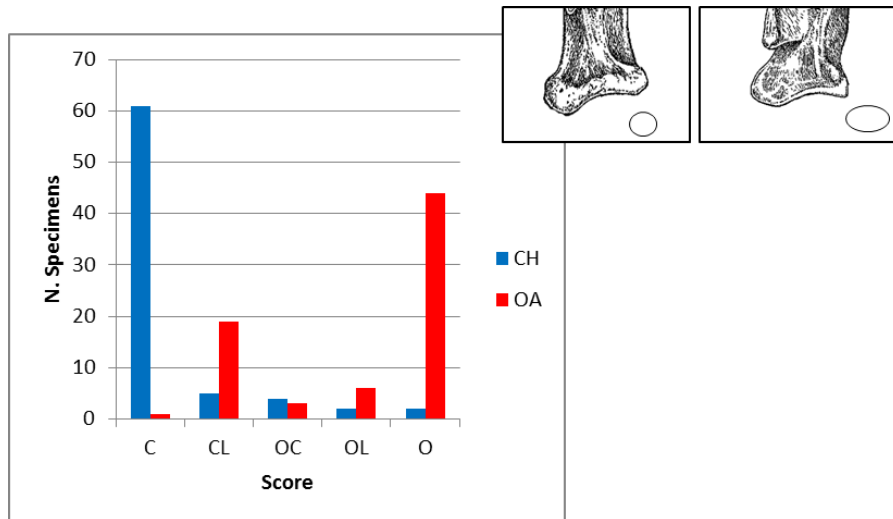


Figure 2.31 Scapula, trait 2 (shape of glenoid cavity): number of specimens attributed to the different categories for the two species. For details see Fig. 2.9.

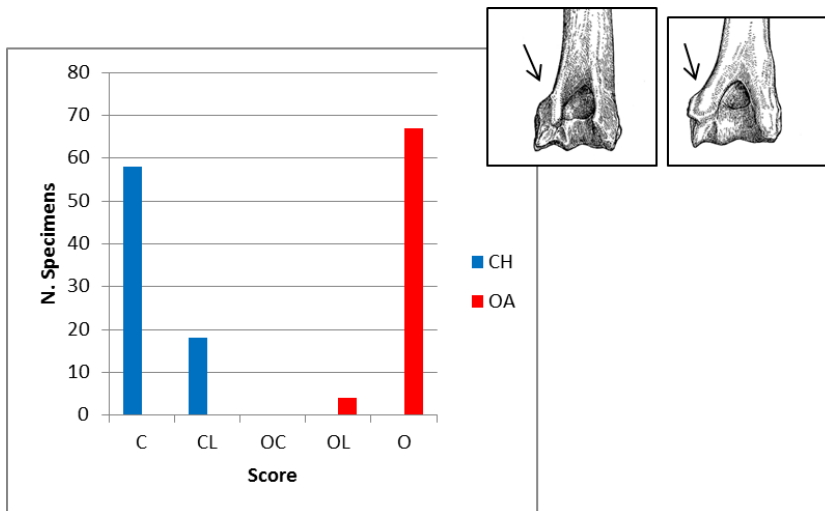


Figure 2.32 Humerus, trait 1 (lateral epicondyle): number of specimens attributed to the different categories for the two species. For details see Fig. 2.9.

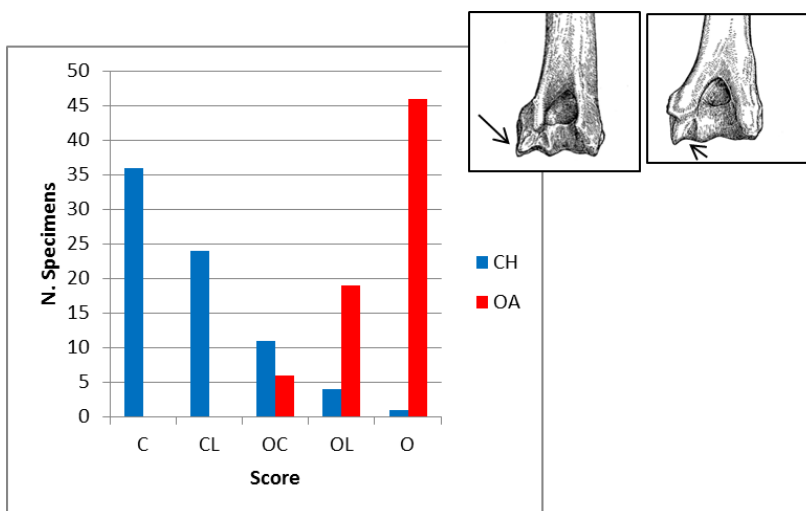


Figure 2.33 Humerus, trait 2 (groove at the posterior side of the lateral epicondyle): number of specimens attributed to the different categories for the two species. For details see Fig. 2.9.

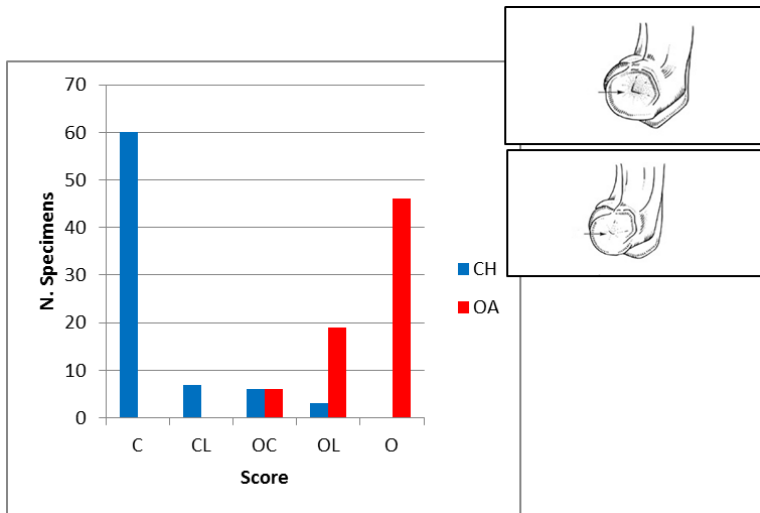


Figure 2.34 Humerus, trait 3 (pit on the lateral epicondilar surface): number of specimens attributed to the different categories for the two species. For details see Fig. 2.9.

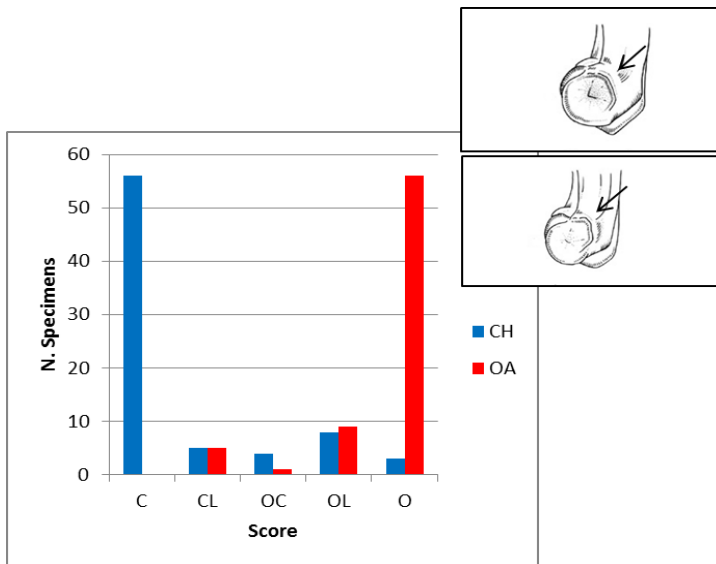


Figure 2.35 Humerus, trait 4 (crest-like process on lateral border of epicondilar surface): number of specimens attributed to the different categories for the two species. For details see Fig. 2.9.

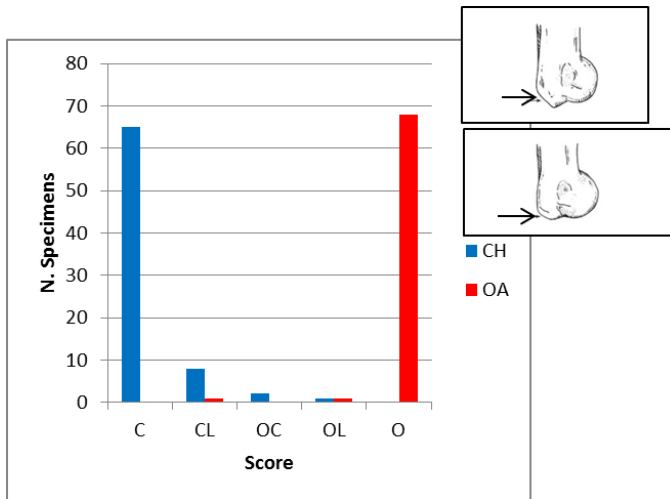


Figure 2.36 Humerus, trait 5 (angle at the distal part of the medial epicondyle): number of specimens attributed to the different categories for the two species. For details see Fig. 2.9.

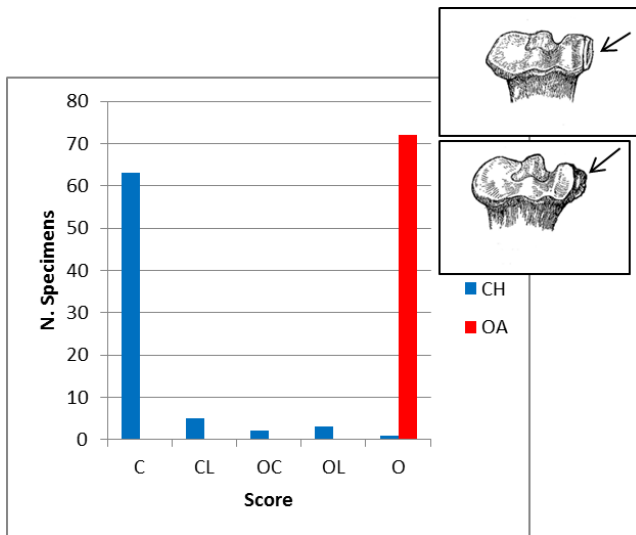


Figure 2.37 Radius, trait 1 (aspect of the lateral tuberosity): number of specimens attributed to the different categories for the two species. For details see Fig. 2.9.

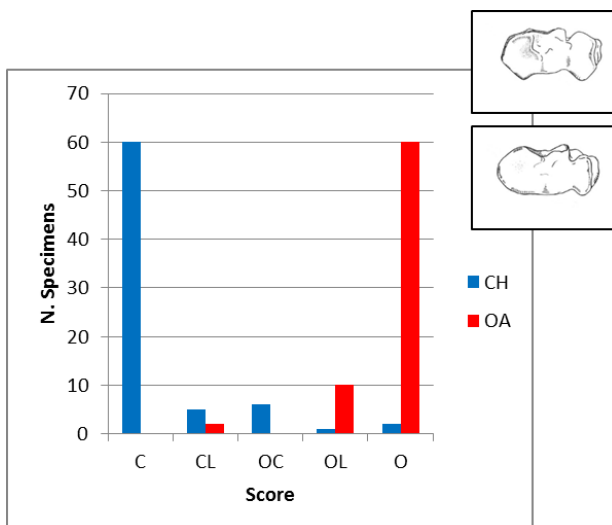


Figure 2.38 Radius, trait 2 (overall aspect of the proximal end): number of specimens attributed to the different categories for the two species. For details see Fig. 2.9.

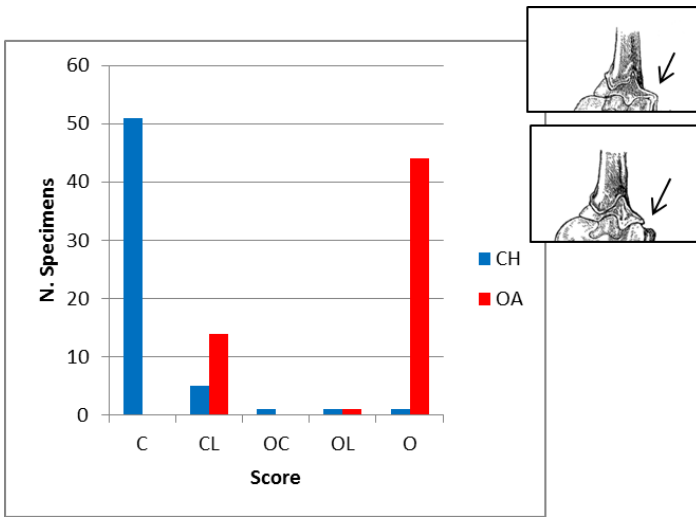


Figure 2.39 Ulna, trait 1 (projection of lateral coronoid process): number of specimens attributed to the different categories for the two species. For details see Fig. 2.9.

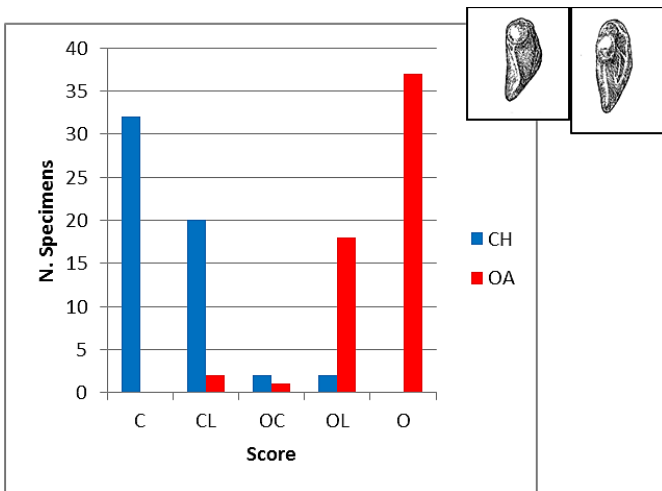


Figure 2.40 Ulna, trait 2 (shape of the *olecranon*): number of specimens attributed to the different categories for the two species. For details see Fig. 2.9.

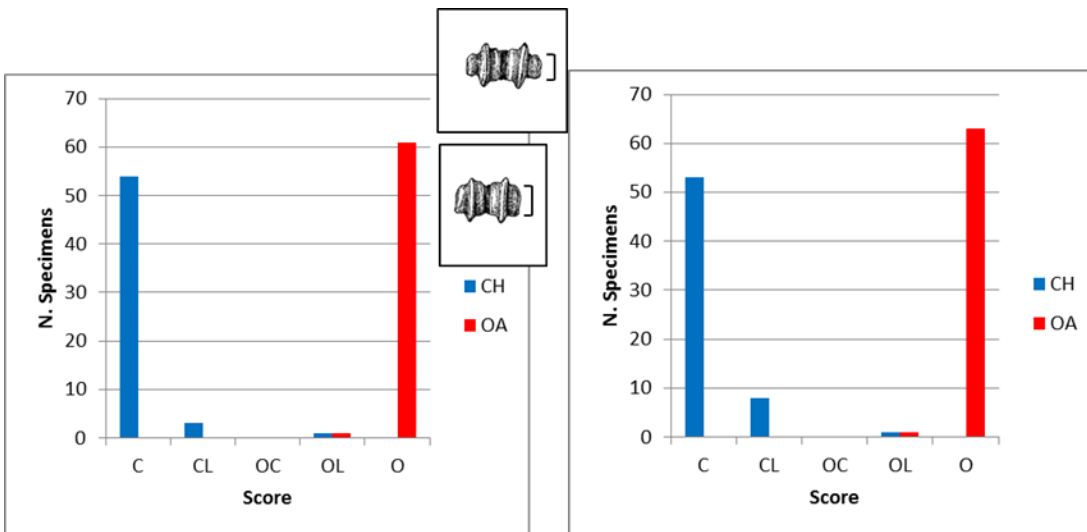


Figure 2.41 Metacarpal and metatarsal, trait 1 (dimension of the peripheral part of the trochlear condyles) number of specimens attributed to the different categories for the two species. For details see Fig. 2.9.

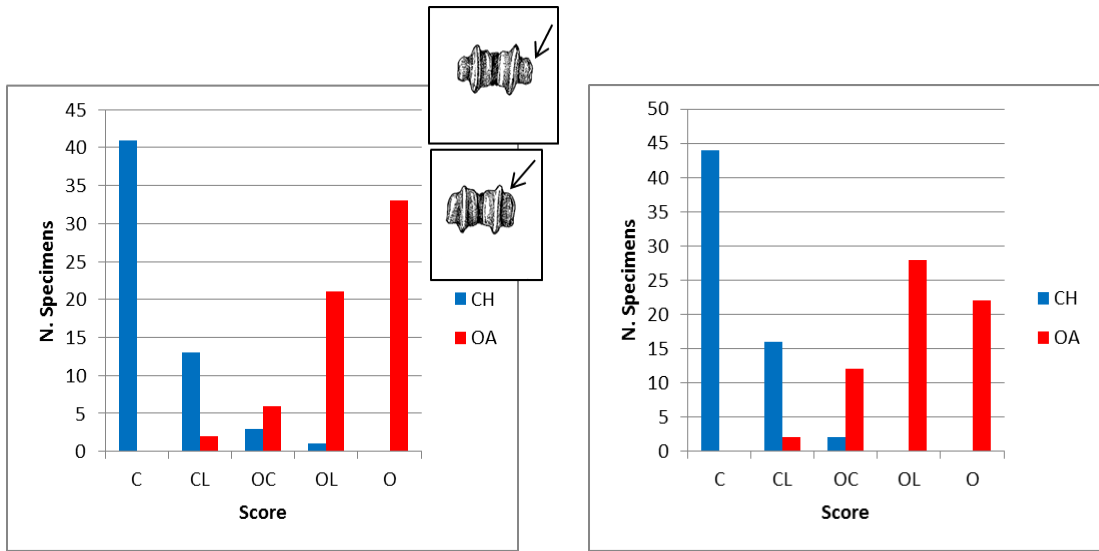


Figure 2.42 Metacarpal and metatarsal, trait 2 (definition of the peripheral part of the trochlear condyles) numbers of specimens attributed to the different categories for the two species. For details see Fig. 2.9.

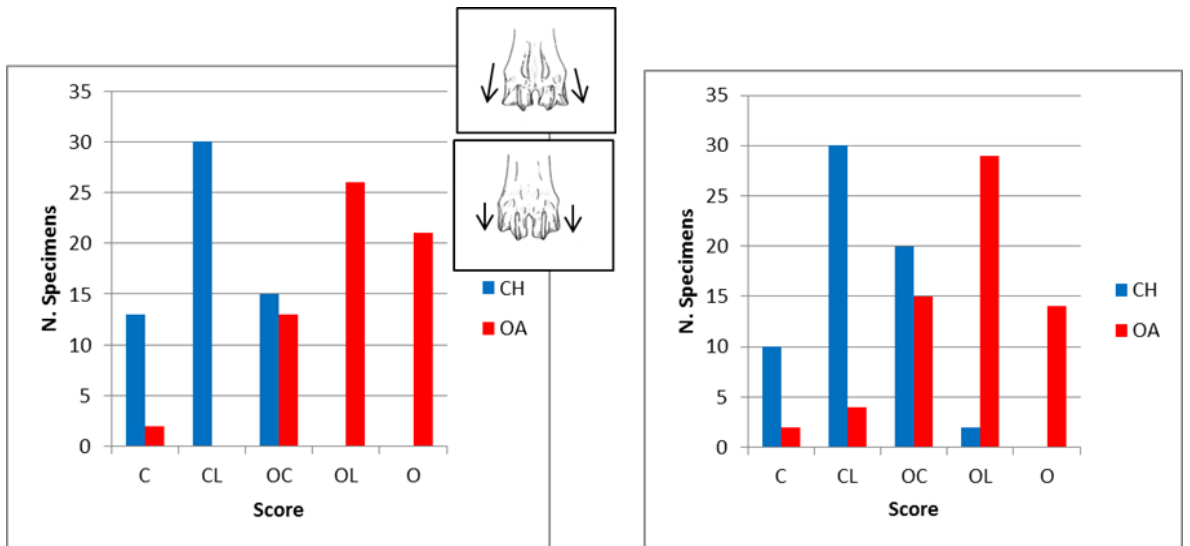


Figure 2.43 Metacarpal and metatarsal, trait 3 (aspect of the peripheral part of the trochlear condyles) number of specimens attributed to the different categories for the two species. For details see Fig. 2.9.

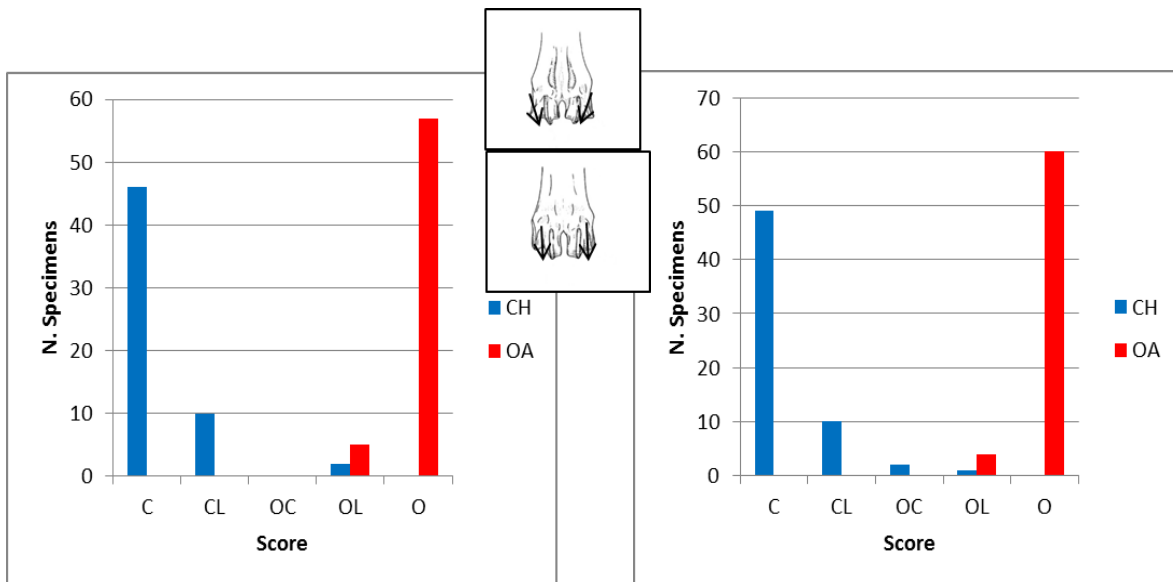


Figure 2.44 Metacarpal and metatarsal, trait 4 (direction of *verticilli*) number of specimens attributed to the different categories for the two species. For details see Fig. 2.9.

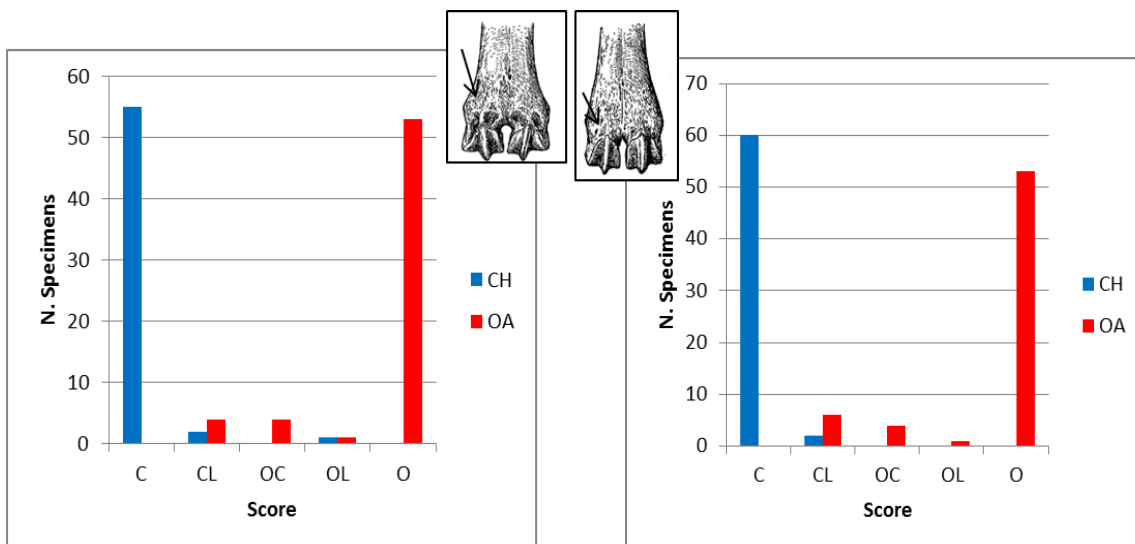


Figure 2.45 Metacarpal and metatarsal, trait 5 (development of the fossae on the proximal part of the distal trochlear condyles) number of specimens attributed to the different categories for the two species. For details see Fig. 2.9.

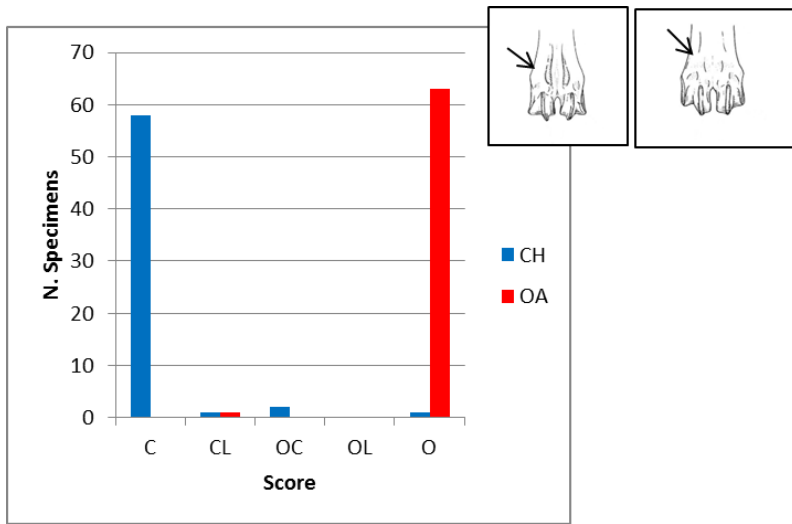


Figure 2.46 Metatarsal, trait 6 (aspect of the junction on the anterior aspect of the distal diaphysis above the distal epiphysis) number of specimens attributed to the different categories for the two species. For details see Fig. 2.9.

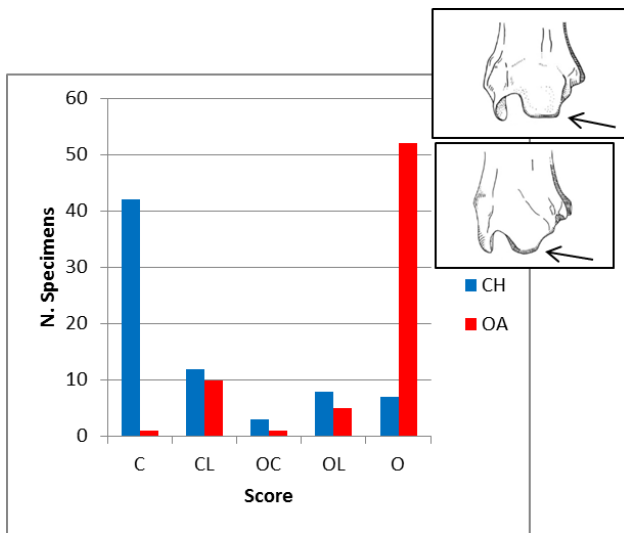


Figure 2.47 Tibia, trait 1 (dorsal prominence) number of specimens attributed to the different categories for the two species. For details see Fig. 2.9.

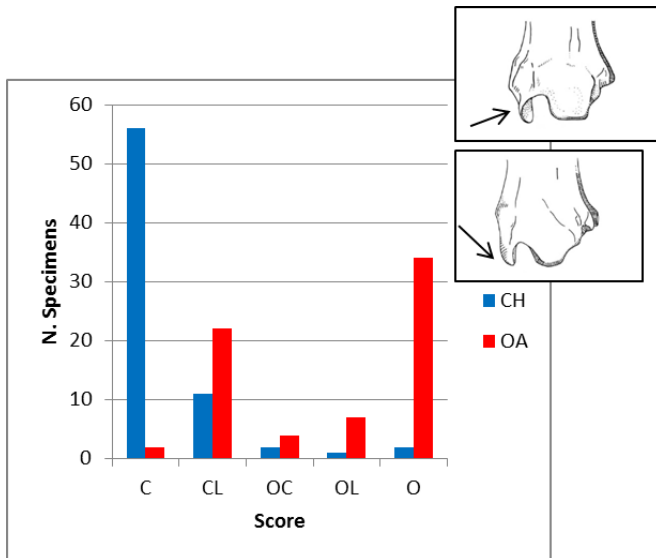


Figure 2.48 Tibia, trait 2 (medial malleolus) number of specimens attributed to the different categories for the two species. For details see Fig. 2.9.

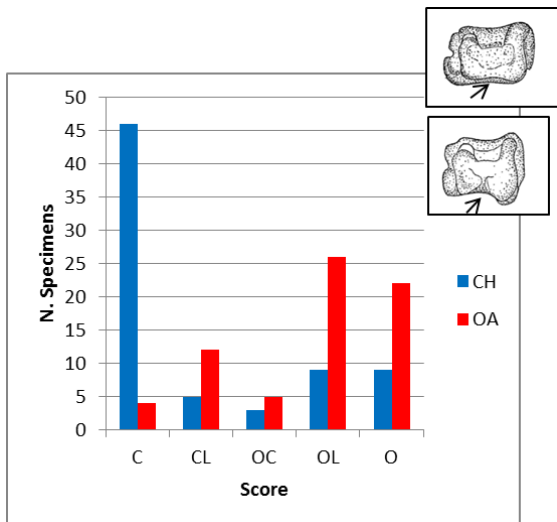


Figure 2.49 Tibia, trait 3 (presence/absence of the interruption on the plantar limbus) number of specimens attributed to the different categories for the two species. For details see Fig. 2.9.

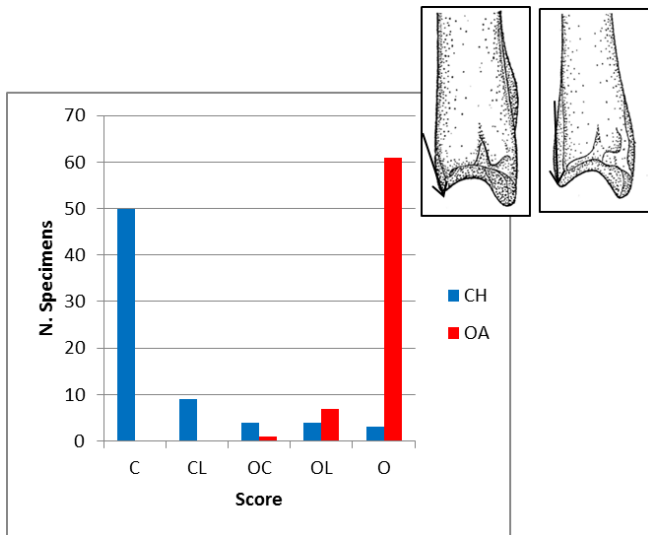


Figure 2.50 Tibia, trait 4 (lateral profile) number of specimens attributed to the different categories for the two species. For details see Fig. 2.9.

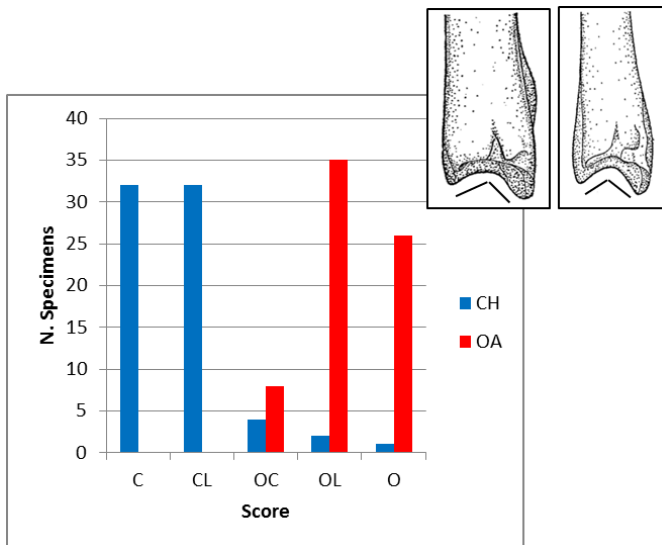


Figure 2.51 Tibia, trait 5 (shape of the anterior side of the malleolus) number of specimens attributed to the different categories for the two species. For details see Fig. 2.9.

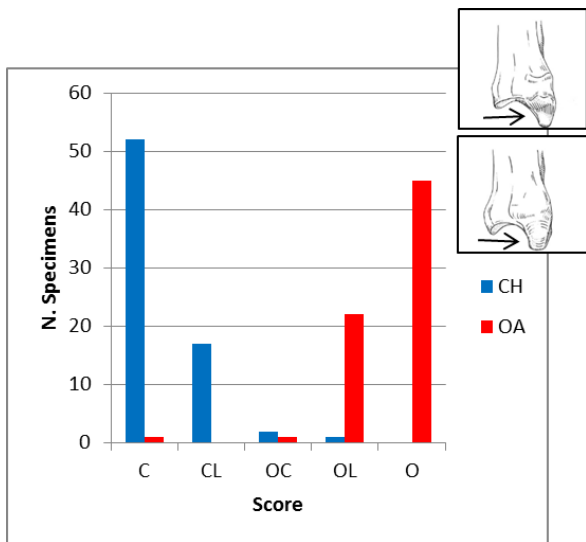


Figure 2.52 Tibia, trait 6 (aspect of the medial malleolus) number of specimens attributed to the different categories for the two species. For details see Fig. 2.9.

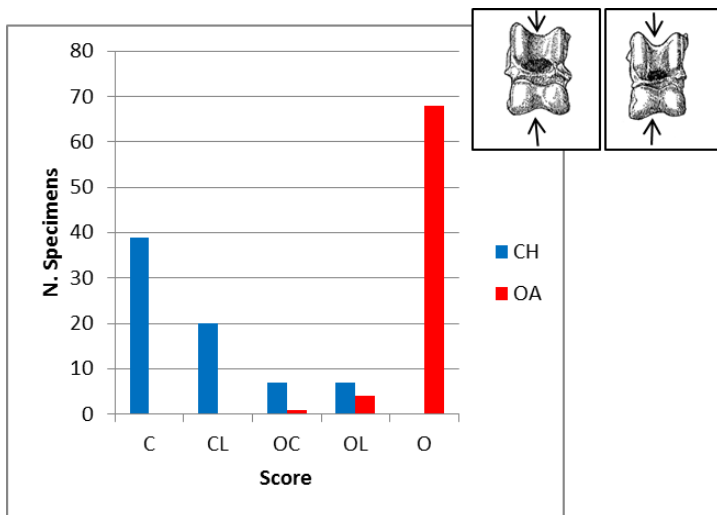


Figure 2.53 Astragalus, trait 1 (depth of the sulcus of the trochlea) number of specimens attributed to the different categories for the two species. For details see Fig. 2.9.

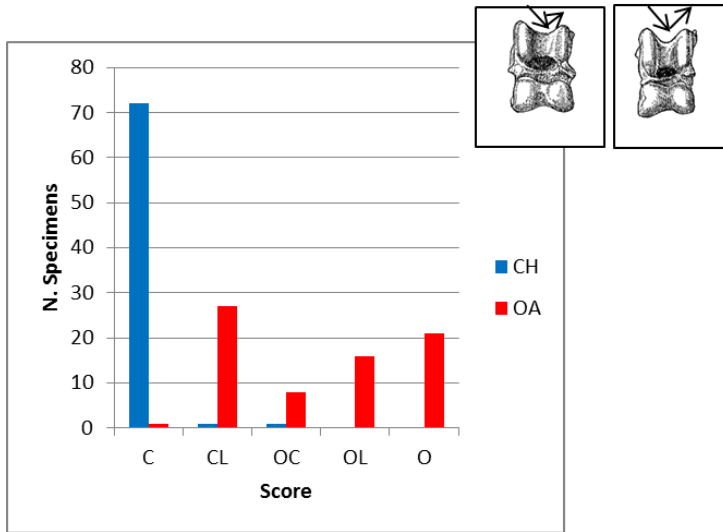


Figure 2.54 Astragalus, trait 2 (inclination of the lateral part of the trochlea) number of specimens attributed to the different categories for the two species. For details see Fig. 2.9.

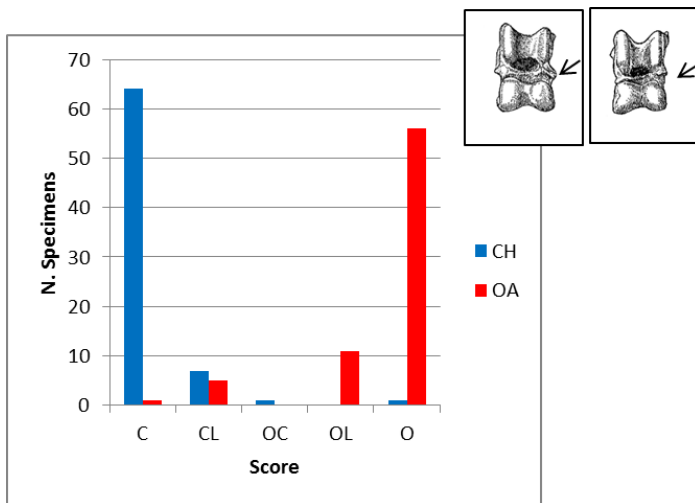


Figure 2.55 Astragalus, trait 3 (shape of the medial ridge) number of specimens attributed to the different categories for the two species. For details see Fig. 2.9.

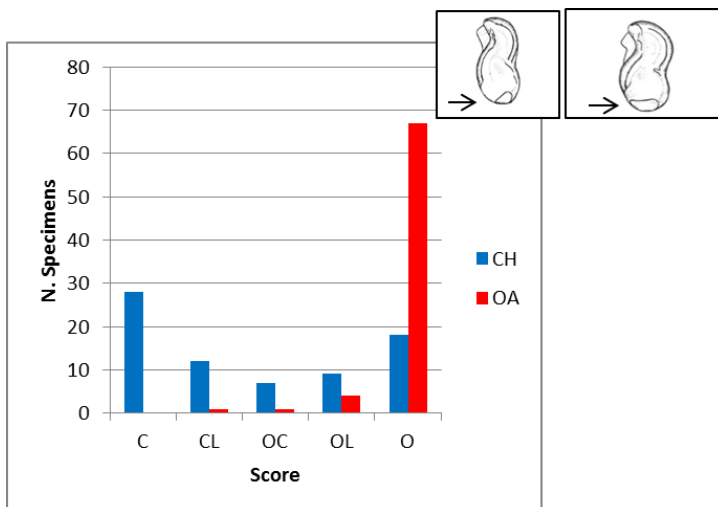


Figure 2.56 Astragalus, trait 4 (shape of the distal articular surface on the lateral aspect) number of specimens attributed to the different categories for the two species. For details see Fig. 2.9.

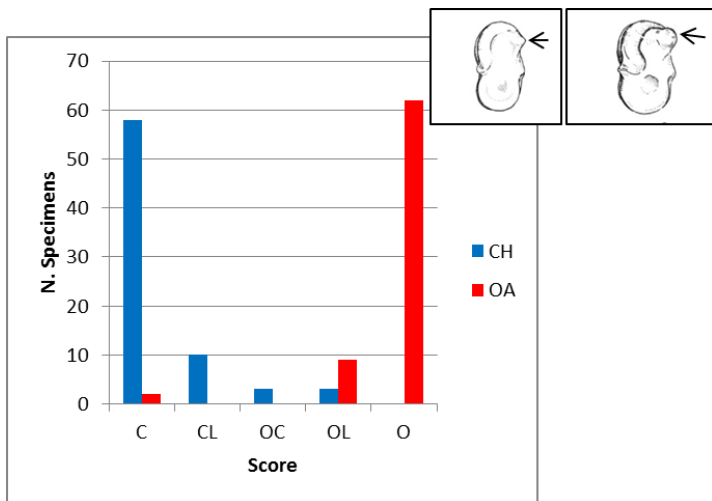


Figure 2.57 Astragalus, trait 5 (aspect of the proximo-plantar projection on the medial articular ridge of the trochlea) number of specimens attributed to the different categories for the two species. For details see Fig. 2.9.

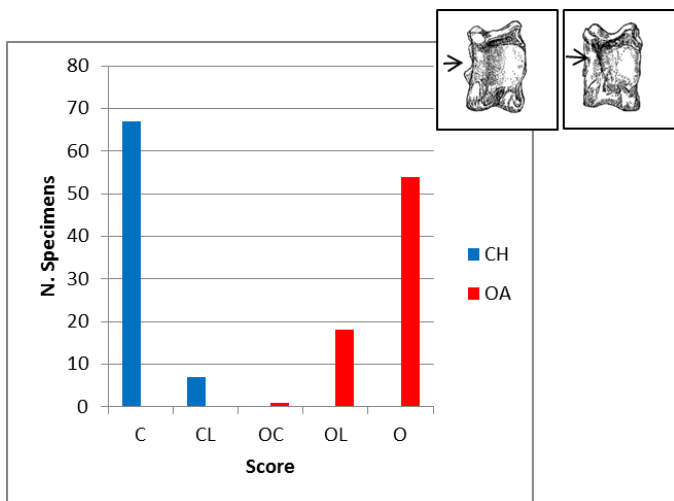


Figure 2.58 Astragalus, trait 6 (aspect and direction of the articular surface on the plantar side) number of specimens attributed to the different categories for the two species. For details see Fig. 2.9.

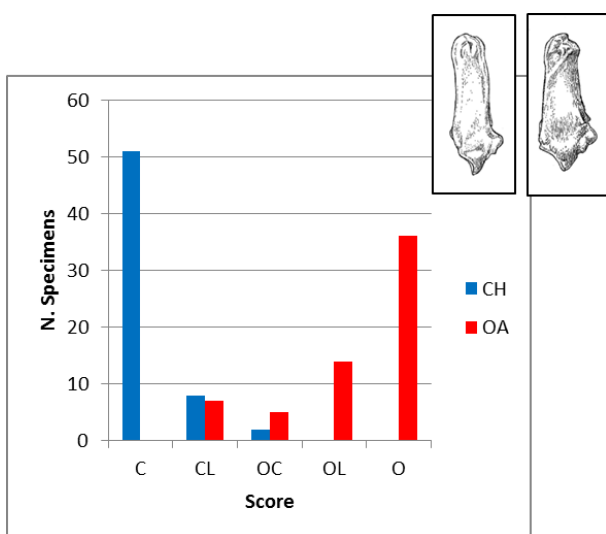


Figure 2.59 Calcaneum, trait 1 (overall aspect) number of specimens attributed to the different categories for the two species. For details see Fig. 2.9.

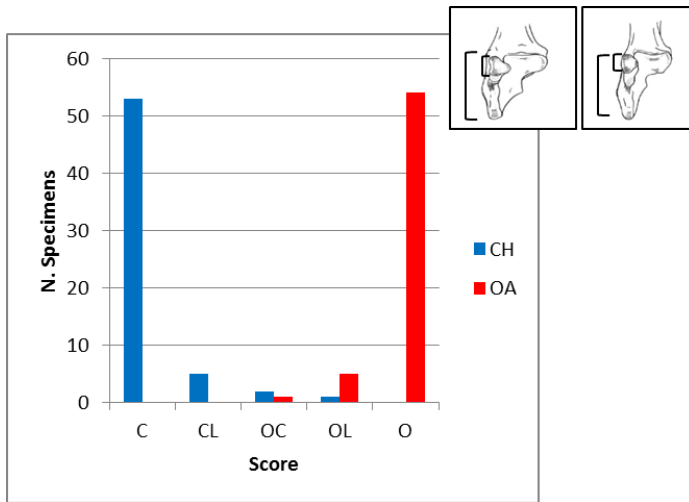


Figure 2.60 Calcaneum, trait 2 (length of the *os malleolare* vs length of the entire process) number of specimens attributed to the different categories for the two species. For details see Fig. 2.9.

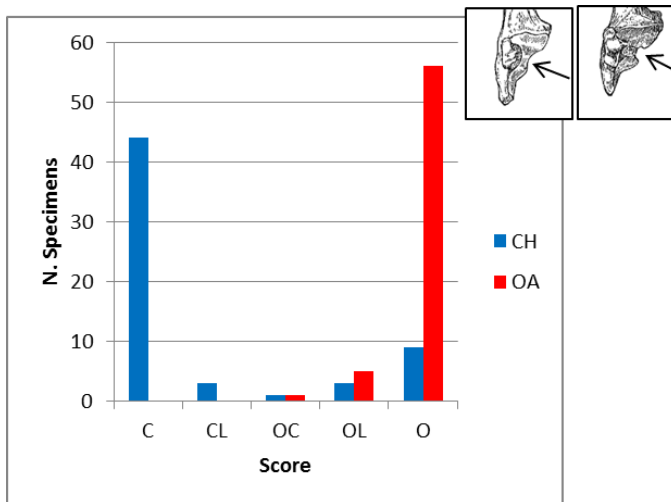


Figure 2.61 Calcaneum, trait 3 (presence/absence of the junction between the two internal articular surfaces) number of specimens attributed to the different categories for the two species. For details see Fig. 2.9.

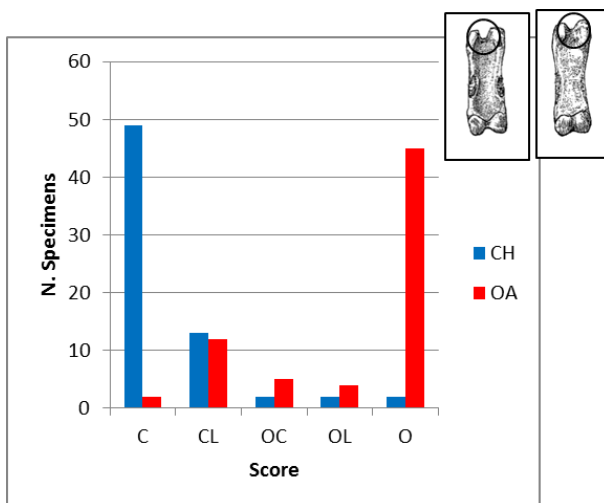


Figure 2.62 1st phalanx, trait 1 (shape of the groove in the proximal end) number of specimens attributed to the different categories for the two species. For details see Fig. 2.9.

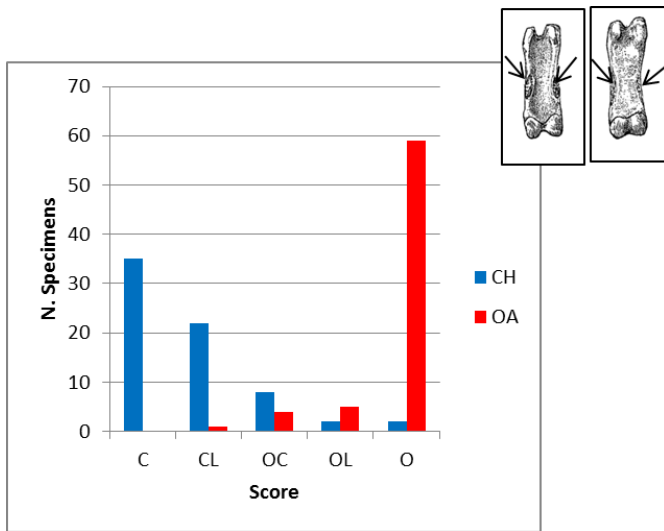


Figure 2.63 1st phalanx, trait 2 (presence of the scars for the muscular ligaments on the posterior side) number of specimens attributed to the different categories for the two species. For details see Fig. 2.9.

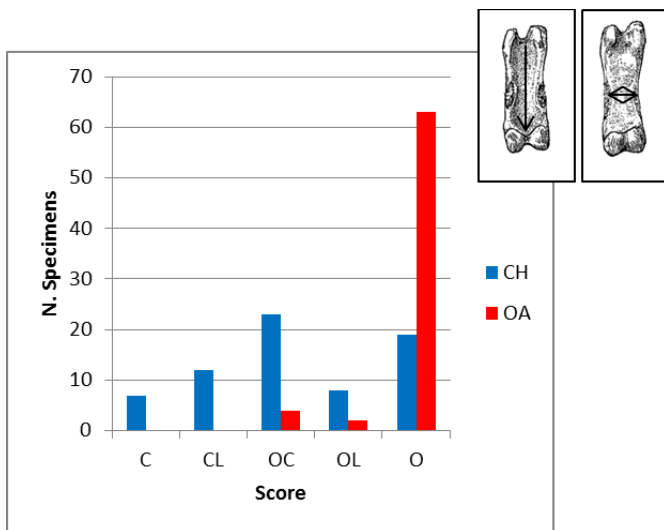


Figure 2.64 1st phalanx, trait 3 (aspect of the posterior side) number of specimens attributed to the different categories for the two species. For details see Fig. 2.9.

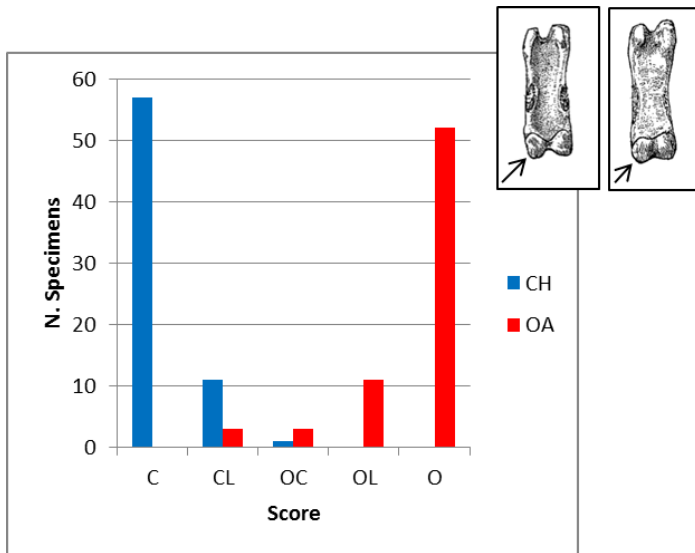


Figure 2.65 1st phalanx, trait 4 (shape of the distal articulation) number of specimens attributed to the different categories for the two species. For details see Fig. 2.9.

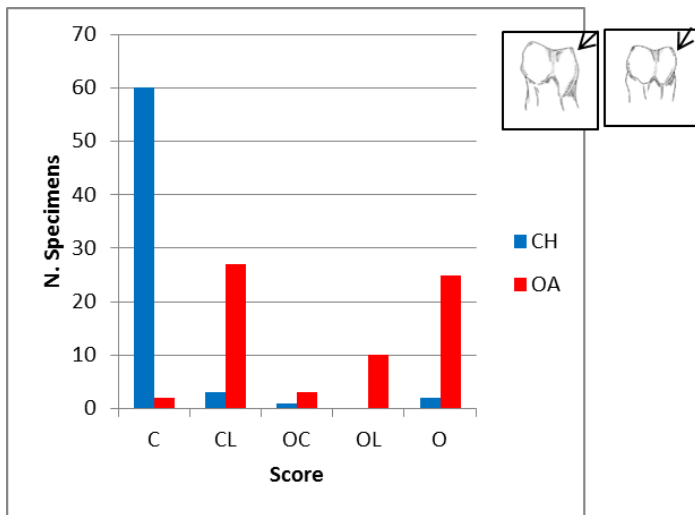


Figure 2.66 2nd phalanx, trait 1 (aspect of the axial part of the posterior side of the distal articulation) number of specimens attributed to the different categories for the two species. For details see Fig. 2.9.

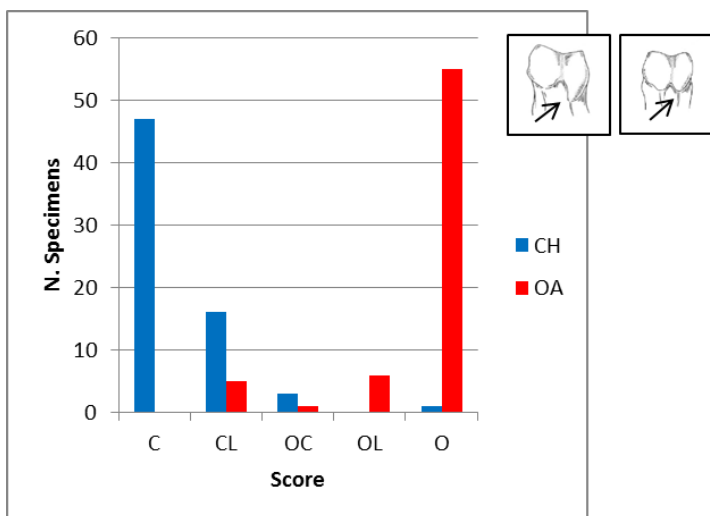


Figure 2.67 2nd phalanx, trait 2 (aspect of the ridge of the posterior side of the distal articulation) number of specimens attributed to the different categories for the two species. For details see Fig. 2.9.

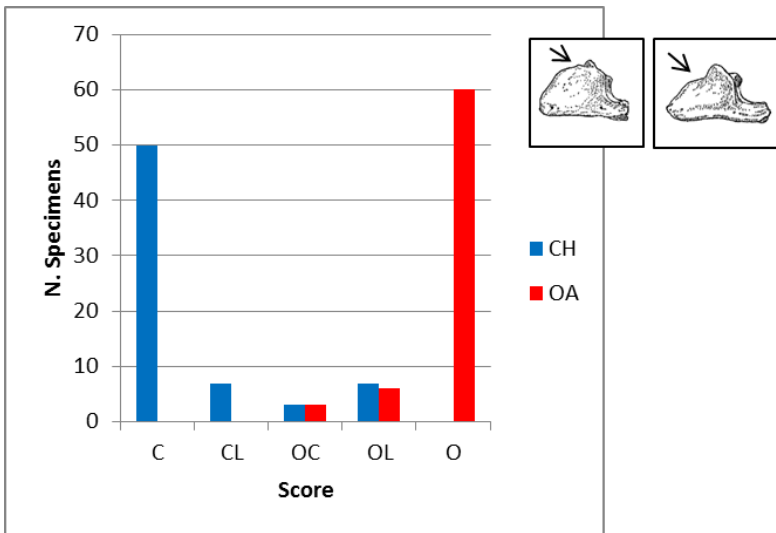


Figure 2.68 3rd phalanx, trait 1 (presence/absence of a saddle on the dorsal edge) number of specimens attributed to the different categories for the two species. For details see Fig. 2.9.

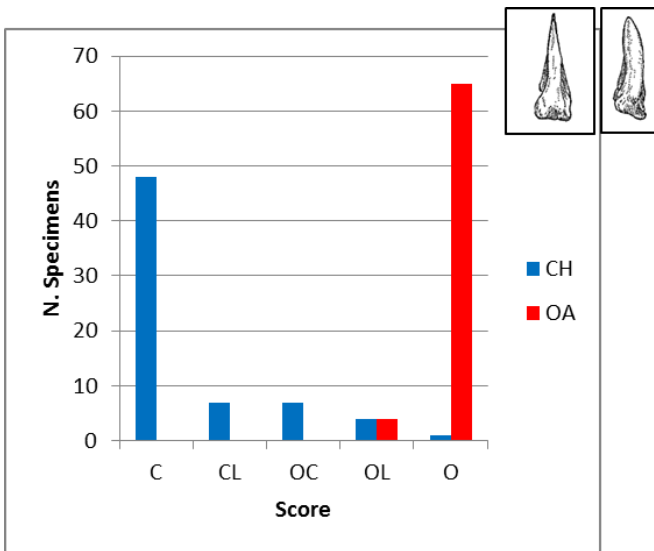


Figure 2.69 3rd phalanx, trait 2 (shape of the sole) number of specimens attributed to the different categories for the two species. For details see Fig. 2.9.

2.4.2 Influence of sex

Goats are known to be more sexually dimorphic than sheep, with males, particularly of the wild form, usually larger and more robust (Davis 1981, 2000).

This section focuses on trying to understand if the reliability of the morphological traits could be influenced by the sex of the animal. Table 2.47 summarizes the number of specimens for each species according to sex. The animals with unknown sex, as well as the one hermaphrodite, were excluded from the analysis. Tables 2.48 and 2.49 provide the percentages of correct species attributions for each morphological trait, according to sex. A series of graph displaying the results follows (Figs. 2.70 to 2.130).

Table 2.48 Number of modern specimens according to their sex for each *taxon*.

<i>Capra hircus</i>				
♂	♀	Unknown		
23	31	25		
<i>Ovis aries</i>				
♂	♀	♂♀	Hermaphrodite	Unknown
14	29	17	1	18

Table 2.49 Goat. Scores expressed in percentages given to different morphological characteristics of different cranial and post-cranial bones according to the sex of the animals.

Anatomical Elements	Traits	N. of Specimens		<i>Capra hircus</i> ♂			<i>Capra hircus</i> ♀			
		♂	♀	% of matching			% of matching			
				C	C + CL	C+CL+OC	C	C+CL	C+CL+OC	
Cranial bones	Horncore	1	10	15	100	100	100	100	100	100
		2	10	15	100	100	100	100	100	100
	Mandible	1	15	32	6.3	6.3	81.3	36.4	36.4	100
		2	12	23	92.3	100	100	59.1	90.9	100
	dP ₃	1	3	2	100	100	100	50	100	100
		2	3	1	33.3	66.6	100	0	0	100
	dP ₄	1	1	1	0	0	100	0	0	100
		2	1	2	0	100	100	0	50	50
		3	3	2	100	100	100	50	100	100
		4	1	2	100	100	100	50	50	100
	P ₃	1	13	19	84.6	100	100	52.6	68.4	73.7
		2	13	19	76.9	92.3	100	68.4	78.9	94.7
		3	13	19	84.6	92.3	92.3	73.7	84.2	94.7
	P ₄	1	12	20	50	75	91.7	35	50	85
		2	12	20	50	75	83.3	25	45	80
		3	12	20	41.7	91.7	91.7	50	85	95
	M ₃	1	11	19	9.1	45.5	100	47.4	73.7	100
		2	11	19	9.1	45.5	72.7	15.8	42.1	89.5
		3	12	19	33.3	83.3	100	68.4	89.5	100
		4	12	19	0	66.7	100	31.6	78.9	100
5		11	19	90.9	90.9	100	94.7	94.7	94.7	
Scapula	1	21	28	57.1	85.7	90.5	60.7	85.7	92.9	
	2	21	28	85.7	85.7	95.2	78.6	89.3	92.9	
Humerus	1	22	29	50	100	100	82.8	100	100	
	2	22	29	59.1	81.8	90.9	48.3	82.8	100	
	3	22	29	81.8	86.4	90.9	65.5	86.2	100	
	4	22	29	59.1	77.3	81.8	86.2	86.2	89.7	
	5	22	29	77.3	86.4	95.5	89.7	100	100	
Radius	1	21	29	71.4	85.7	90.5	91.3	91.3	96.6	
	2	21	29	66.7	76.2	90.5	82.8	89.7	96.6	
Ulna	1	18	26	88.9	94.4	94.4	96.2	100	100	
	2	18	24	61.1	88.9	94.4	45.8	95.8	100	
Metacarpal	1	16	25	93.8	100	100	92	96	96	
	2	16	25	75	100	100	64	88	96	
	3	16	25	12.5	68.8	100	20	72	100	
	4	16	25	81.3	100	100	80	92	92	
	5	16	25	93.8	100	100	92	96	96	
Metatarsal	1	17	26	82.4	94.1	94.1	84.6	100	100	
	2	17	26	58.8	100	100	76.9	92.3	100	
	3	17	26	76.5	94.1	100	15.4	65.4	100	
	4	17	26	76.5	94.1	100	88.5	96.2	96.2	
	5	17	26	94.1	100	100	96.2	100	100	
	6	17	26	94.1	94.1	94.1	88.5	92.3	100	
Tibia	1	21	27	81	85.7	85.7	55.6	74.1	74.1	
	2	21	27	81	95.2	100	74.1	88.9	92.6	
	3	21	27	61.9	71.4	71.4	59.3	70.4	74.1	
	4	21	25	81	90.5	90.5	76	80	84	
	5	21	26	52.4	81	90.5	50	88.5	96.2	
	6	21	27	52.4	95.2	100	77.8	96.3	100	
Astragalus	1	22	29	45.5	68.2	81.8	48.3	82.8	89.7	
	2	23	29	95.7	95.7	100	96.6	100	100	
Post Cranial bones										

Anatomical Elements	Traits	N. of Specimens			<i>Capra hircus</i> ♂			<i>Capra hircus</i> ♀		
					% of matching			% of matching		
		♂	♀	♂♀	C	C + CL	C+CL+OC	C	C+CL	C+CL+OC
		3	22	29	81.8	95.5	95.5	93.1	96.6	100
		4	23	29	56.5	69.6	73.9	27.6	55.2	65.5
		5	23	29	82.6	95.7	95.7	69	82.8	93.1
		6	23	29	87	100	100	89.7	100	100
	Calcaneum	1	19	27	84.2	89.5	100	85.2	100	100
		2	19	27	73.7	89.5	94.7	88.9	96.3	100
		3	19	26	63.2	68.4	68.4	88.5	88.5	92.3
	1 st Phalanx	1	18	29	83.3	94.4	94.4	72.4	89.7	96.6
		2	19	29	63.2	84.2	94.7	44.8	89.7	96.6
		3	19	29	10.5	31.6	63.2	10.3	37.9	79.3
		4	19	29	84.2	94.7	100	82.8	100	100
	2 nd Phalanx	1	18	27	88.9	94.4	94.4	88.9	96.3	96.3
		2	19	27	73.7	94.7	100	63	92.6	96.3
	3 rd Phalanx	1	19	29	68.4	73.7	78.9	82.8	93.1	96.6
		2	19	29	57.9	68.4	84.2	86.2	89.7	96.6

Table 2.50 Sheep. Scores expressed in percentages, given to different morphological characteristics of different cranial and post-cranial bones, according to the sex of the animal.

Anatomical Elements	Traits	N. of Specimens			<i>Ovis aries</i> ♂			<i>Ovis aries</i> ♀			<i>Ovis aries</i> ♂♀			
					% of matching			% of matching			% matching			
		♂	♀	♂♀	O	O + OL	O+OL+ OC	O	O+ OL	O+OL+ OC	O	O+ OL	O+OL+ OC	
Cranial bones	Horncore	1	9	15	3	100	100	100	100	100	100	100	100	
		2	9	15	3	100	100	100	100	100	100	0	100	100
	Mandible	1	14	29	17	28.6	28.6	71.4	34.5	34.5	86.2	52.9	52.9	70.6
		2	13	29	16	84.6	100	100	93.1	96.6	100	93.8	100	100
	dP ₃	1	3	3	2	0	66.7	66.7	66.7	100	100	100	100	100
		2	1	2	2	0	0	100	0	50	100	0	0	100
	dP ₄	1	1	1	2	0	0	100	0	0	100	0	0	100
		2	2	2	2	100	100	100	100	100	100	100	100	100
		3	2	3	2	100	100	100	100	100	100	100	100	100
		4	1	1	2	0	0	100	100	100	100	50	50	100
	P ₃	1	10	20	11	40	70	90	45	70	85	18.2	63.3	72.7
		2	10	20	11	70	90	90	60	85	95	54.5	72.7	81.8
		3	10	20	11	60	80	90	50	70	85	54.5	54.5	72.7
	P ₄	1	10	23	14	50	90	90	65.2	95.7	100	50	92.9	100
		2	10	23	14	80	100	100	56.5	78.3	100	92.9	92.9	100
		3	10	23	14	90	100	100	60.9	87	95.7	71.4	100	100
	M ₃	1	10	25	14	70	100	100	56	76	96	71.4	92.9	100
		2	10	25	14	60	70	100	16	36	100	71.4	78.6	100
		3	10	25	14	90	90	90	60	84	92	71.4	78.6	100
		4	10	25	14	10	10	90	8	52	92	0	14.3	78.6
5		10	25	14	44.4	77.8	77.8	37.5	45.8	70.8	61.5	76.9	76.9	
Scapula	1	14	26	17	100	100	100	88.5	100	100	94.1	100	100	
	2	14	26	17	57.1	64.3	71.4	69.2	80.8	84.6	35.3	47.1	47.1	
Humerus	1	13	26	17	100	100	100	92.3	100	100	88.2	100	100	
	2	13	26	17	53.8	100	100	73.1	88.5	100	47.1	88.2	100	
	3	13	26	17	92.3	100	100	88.5	100	100	100	100	100	
	4	13	26	17	76.9	84.6	84.6	80.8	84.6	88.5	82.4	100	100	
	5	13	26	17	100	100	100	96.2	100	100	100	100	100	
Radius	1	14	26	17	100	100	100	100	100	100	100	100	100	
	2	14	26	17	100	100	100	76.9	100	100	100	100	100	
Ulna	1	11	24	13	63.6	72.7	72.7	70.8	70.8	70.8	84.6	84.6	84.6	
	2	10	25	13	50	90	100	80	100	100	53.8	100	100	
Metacarpal	1	13	25	13	100	100	100	100	100	100	92.3	100	100	
	2	13	25	13	53.8	84.6	100	68	100	100	23.1	61.5	84.6	
	3	13	25	13	38.5	61.5	92.3	24	80	96	53.8	84.6	100	
	4	13	25	13	100	100	100	96	100	100	92.3	100	100	
	5	13	25	13	61.5	69.2	84.6	96	96	100	76.9	76.9	84.6	
Metatarsal	1	13	25	13	100	100	100	100	100	100	92.3	100	100	
	2	13	25	13	100	100	100	48	80	96	15.4	61.5	100	
	3	13	25	13	23.1	61.5	76.9	12	68	88	30.8	61.5	100	
	4	13	25	13	100	100	100	100	100	100	92.3	100	100	
	5	13	25	13	61.5	69.2	76.9	72	80	96	61.5	69.2	84.6	

Anatomical Elements	Traits	N. of Specimens			<i>Ovis aries</i> ♂			<i>Ovis aries</i> ♀			<i>Ovis aries</i> ♂♀			
		♂	♀	♂♀	% of matching			% of matching			% matching			
					O	O + OL	O+OL+ OC	O	O+ OL	O+OL+ OC	O	O+ OL	O+OL+ OC	
		6	13	25	13	100	100	100	96	96	96	100	100	100
Tibia	1	13	27	15	15	76.9	76.9	76.9	81.5	92.6	96.3	53.3	53.3	53.3
	2	13	27	15	15	38.5	61.5	61.5	70.4	81.5	85.2	13.3	13.3	13.3
	3	13	27	15	15	23.1	84.6	84.6	37	59.3	70.4	33.3	86.7	100
	4	13	27	15	15	76.9	92.3	100	88.9	100	100	100	100	100
	5	13	27	15	15	69.2	100	100	55.6	92.6	96.3	66.7	100	100
	6	13	27	15	15	69.2	100	100	59.3	92.6	96.3	66.7	100	100
Astragalus	1	14	28	17	17	85.7	100	100	96.4	100	100	100	100	100
	2	14	28	17	17	35.7	42.9	42.9	33.3	59.3	66.7	29.4	64.7	82.4
	3	14	28	17	17	92.9	92.9	92.9	88.3	92.9	92.9	88.2	100	100
	4	14	28	17	17	100	100	100	92.9	96.4	100	88.2	94.1	94.1
	5	14	28	17	17	100	100	100	82.1	100	100	82.4	94.1	94.1
	6	14	28	17	17	78.6	100	100	77.9	96.4	100	70.6	100	100
Calcaneum	1	12	26	13	13	41.7	75	83.3	65.4	84.6	92.3	30.8	61.5	76.9
	2	12	26	13	13	91.7	100	100	88.5	100	100	92.3	100	100
	3	12	26	13	13	91.7	91.7	91.7	96.2	96.2	96.2	92.3	92.3	92.3
1 st Phalanges	1	14	26	16	16	78.6	85.7	85.7	61.5	61.5	69.2	68.8	75	87.5
	2	14	26	17	17	100	100	100	76.9	88.5	96.2	88.2	94.1	100
	3	14	26	17	17	100	100	100	86.4	88.5	100	94.1	100	100
	4	14	26	17	17	85.7	100	100	80.8	92.3	100	70.6	88.2	88.2
2 nd Phalanges	1	14	26	17	17	35.7	64.3	64.3	26.9	42.3	42.3	58.8	64.7	76.5
	2	14	26	17	17	85.7	100	100	84.6	84.6	88.5	100	100	100
3 rd Phalanges	1	14	26	17	17	92.9	100	100	92.3	92.3	100	76.5	94.1	100
	2	14	26	17	17	100	100	100	88.5	100	100	100	100	100

Table 2.51 Goat. List of morphological traits per element per sex, which have provided a high initial percentage (>90%) of species attributions (C) and a high percentage (>95%) when the intermediate category (CL) was added.

Anatomical Element	♂	♀	♂	♀
	C > 90%	C > 90%	C and CL > 95%	C and CL > 95%
Horncore	1	1	1	1
	2	2	2	2
Mandible	2	-	2	-
dP ₃	1	-	1	1
dP ₄	-	-	2	3
	3	-	3	-
	4	-	4	-
P ₃	-	-	1	-
P ₄	-	-	-	1
M ₃	5	5	-	-
Humerus	-	-	1	1
	-	-	-	5
Radius	-	1	1	-
	-	-	2	-
Ulna	-	1	-	1
	-	-	-	2
Metacarpal	1	1	1	1
	-	-	2	-
	-	-	4	-
	5	5	5	5
Metatarsal	-	-	-	1
	-	-	2	-
	-	-	-	4
	5	5	5	5
Tibia	-	-	-	-
	-	-	6	6
Astragalus	-	-	-	1
	2	2	2	2
	-	3	3	3
	-	-	5	-
	-	-	6	6

Anatomical Element	♂	♀	♂	♀
	C > 90%	C > 90%	C and CL > 95%	C and CL > 95%
Calcaneum	-	-	-	1 2
1 st Phalanx	-	-	-	4
2 nd Phalanx	-	-	-	1

Table 2.52 Sheep. List of morphological traits per element per sex, which have provided a high initial percentage (>90%) of species attributions (O) and a high percentage (>95%) when the intermediate category (OL) was added.

Anatomical Elements	♂	♀	♂♀	♂	♀	♂♀
	O > 90%	O > 90%	O > 90%	O and OL > 95%	O and OL > 95%	O and OL > 95%
Horncore	1 2	1 2	1 -	1 2	1 2	1 2
Mandible	-	-	-	2	2	2
dP ₃	-	-	1	-	1	1
dP ₄	2 3 -	2 3 4	2 3 -	2 3 -	2 3 4	2 3 -
P ₄	- - 3	- - -	- 2 -	- 2 3	1 - -	- - 3
M ₃	3	-	-	1	-	-
Scapula	1	-	1	1	1	1
Humerus	1 - 3 - 5	1 - - - 5	- - 3 - 5	1 2 3 - 5	1 - 3 - 5	1 - 3 4 5
Radius	1 2	1 -	1 2	1 2	1 2	1 2
Ulna	- -	1 -	- -	- -	- 2	- 2
Metacarpal	1 - 4 -	1 - 4 5	1 - 4 -	1 - 4 -	1 2 4 5	1 - 4 -
Metatarsal	1 2 4 6	1 - 4 6	1 - 4 6	1 2 4 6	1 - 4 6	1 - 4 6
Tibia	- - -	- - -	4 - -	- 5 6	4 - -	4 5 6
Astragalus	- 3 4 5 -	1 - 4 - -	1 - - - -	1 - 4 5 6	1 - 4 5 6	1 3 - - 6
Calcaneum	2 3	- 3	2 3	2 -	2 3	2 -
1 st Phalanx	2 3 -	- - -	- 3 -	2 3 4	- - -	- 3 -
2 nd Phalanx	-	-	2	2	-	2
3 rd Phalanx	1 2	1 -	- 2	1 2	- 2	- 2

Tables 2.50 and 2.51 show that most of the element and morphological traits have provided high levels of taxonomic identification irrespective of the sex of the animal.

The horncore has given the highest percentages of correct attributions in both species and both sexes. This confirms that, despite the shape and size of this element changes according to the sex of the animal (Boessneck *et al.* 1967) it still retains such a distinctive morphology in both

species that it is very unlikely to be misidentified. The presence of a number of castrates, whose horncores have ‘intermediate’ morphological characteristics (Hatting 1974), does not seem to have particularly influenced the reliability of the traits (this concerns only sheep as there were no castrates in the goat sample).

Other elements that are known to be sexually dimorphic are the metapodials (Davis 1992). This study shows that in goat, and especially sheep, the majority of traits (excluding trait 3) has provided consistently high results in all sexes despite some variability. Sexual dimorphism does not affect the reliability of the morphological features.

The traits on teeth and mandible seem to have provided generally higher results in the male (and castrate for sheep) category in both species. Nevertheless, considering the small size of the tooth sample, these results have to be taken with caution.

As concerns other anatomical elements, no clear pattern links sex to the visibility of the diagnostic traits - a result that is in agreement with Zeder and Lapham’s study (2010).

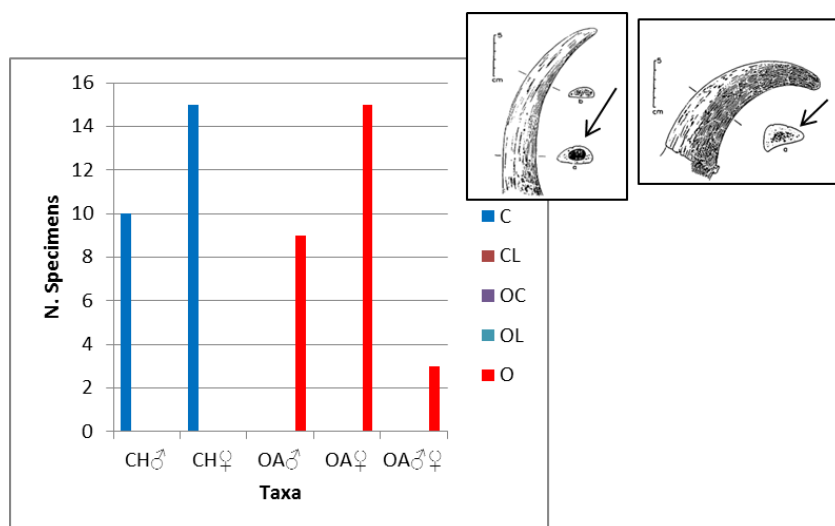


Figure 2.70 Horncore, trait 1 (section) number of specimens attributed to the different categories for the different genders for the two species (C= *Capra*; CL= *Capra-like*; OC= *Ovis/Capra*; OL= *Ovis-like*; O= *Ovis*. On the horizontal axis: CH= *Capra hircus*; OA= *Ovis aries*; ♂= male; ♀= female; ♂♀= castrate).

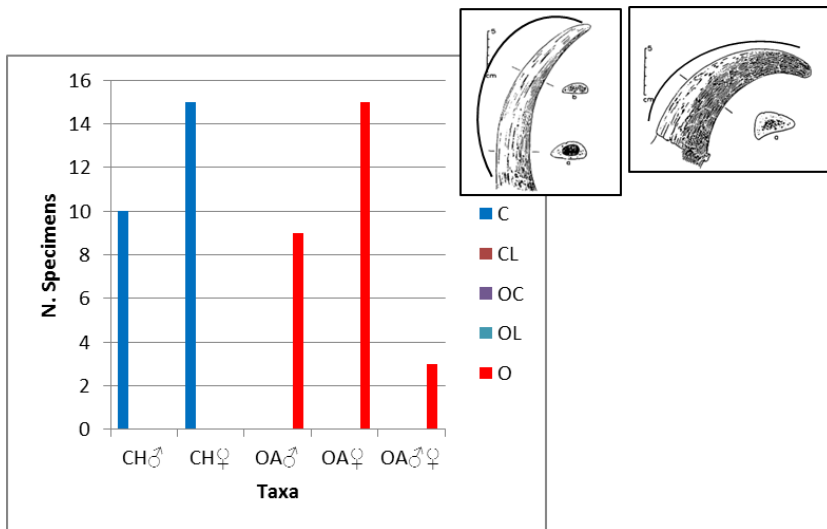


Figure 2.71 Horncore, trait 2 (curvature) number of specimens attributed to the different categories for the different genders for the two species. For details see Fig. 2.70.

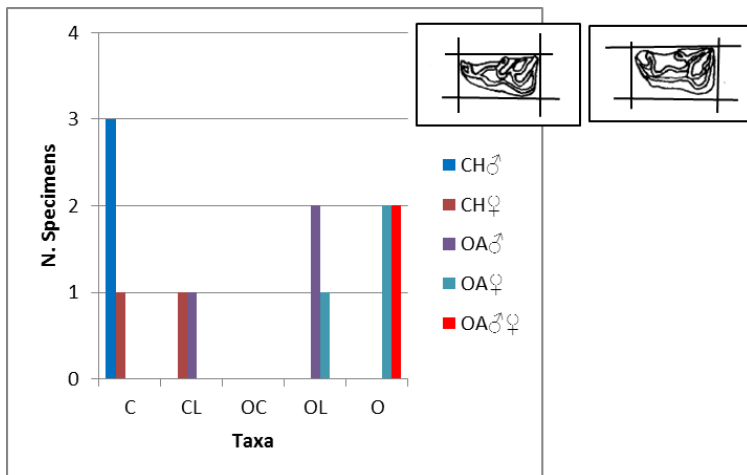


Figure 2.72 Third deciduous lower premolar dP₃, trait 1 (overall shape) number of specimens attributed to the different categories for the different genders for the two species. For details see Fig. 2.70.

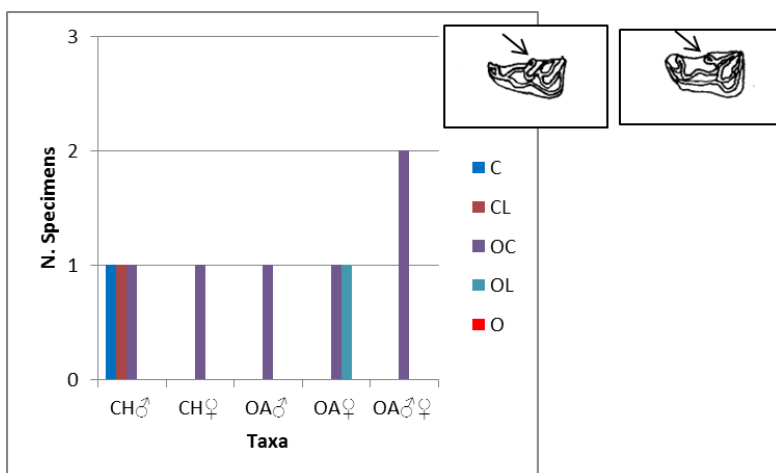


Figure 2.73 Third deciduous lower premolar dP₃, trait 2 (appearance of the metaconoid) number of specimens attributed to the different categories for the different genders for the two species. For details see Fig. 2.70.

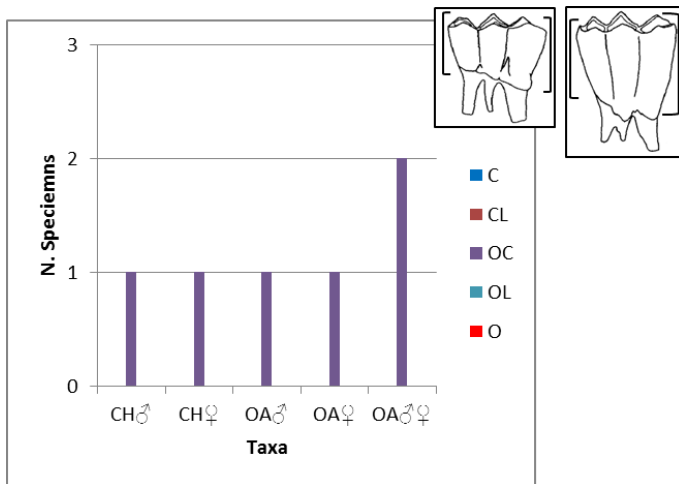


Figure 2.74 Fourth lower deciduous premolar dP_4 , trait 1 (crown aspect) number of specimens attributed to the different categories for the different genders for the two species. For details see Fig. 2.70.

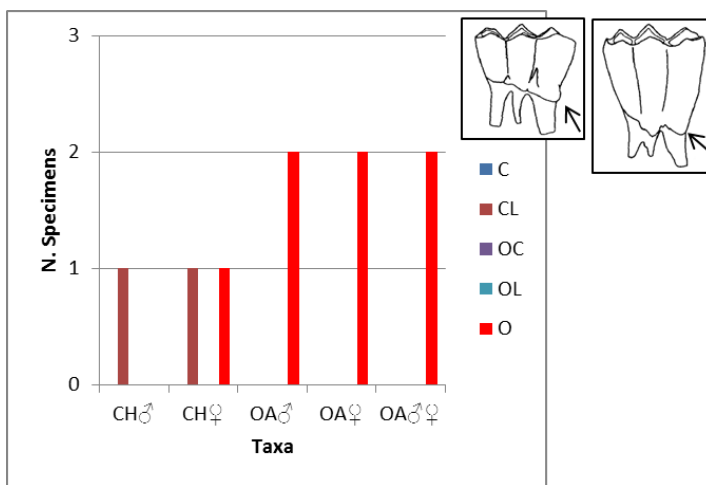


Figure 2.75 Fourth lower deciduous premolar dP_4 , trait 2 (presence/absence basal swelling) number of specimens attributed to the different categories for the different genders for the two species. For details see Fig. 2.70.

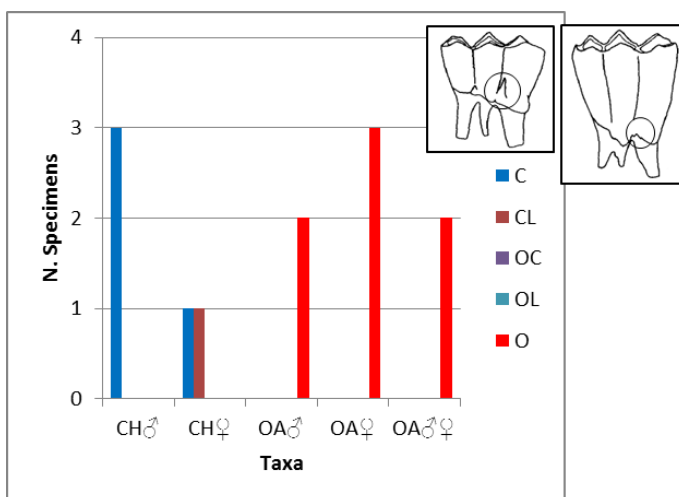


Figure 2.76 Fourth lower deciduous premolar dP_4 , trait 3 (presence/absence inter-lobar pillar) number of specimens attributed to the different categories for the different genders for the two species. For details see Fig. 2.70.

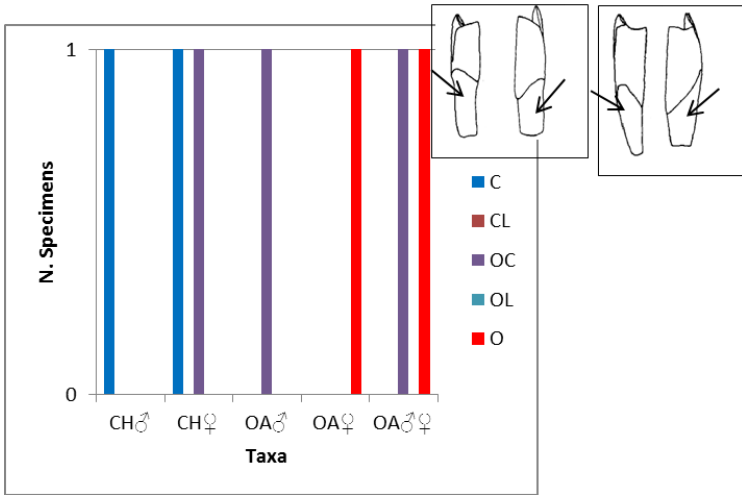


Figure 2.77 Fourth lower deciduous premolar dP₄, trait 4 (enamel development in medial and distal face) number of specimens attributed to the different categories for the different genders for the two species. For details see Fig. 2.70.

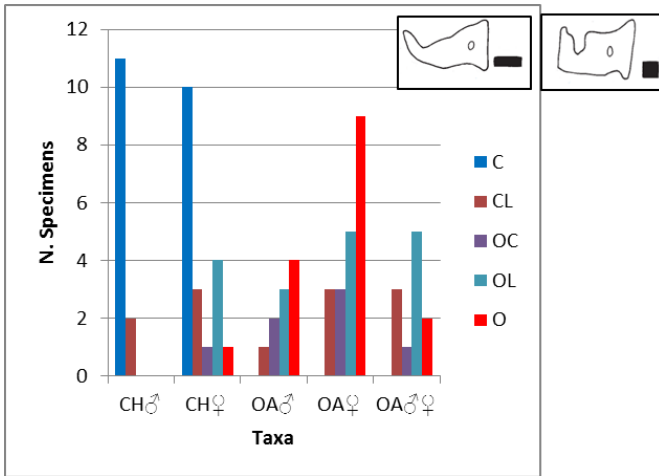


Figure 2.78 Third lower premolar P₃, trait 1 (overall shape) number of specimens attributed to the different categories for the different genders for the two species. For details see Fig. 2.70.

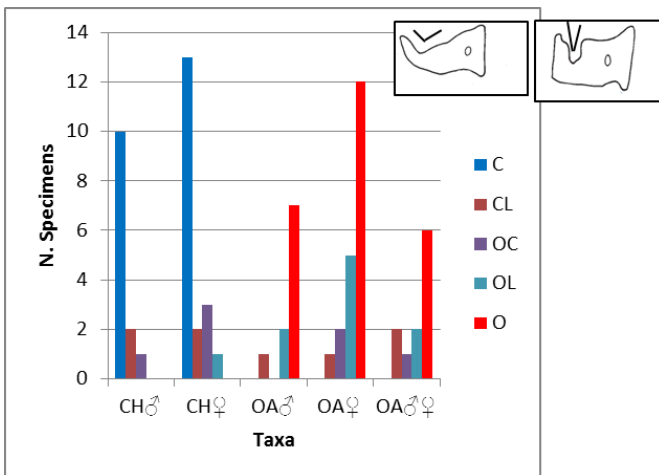


Figure 2.79 Third lower premolar P₃, trait 2 (aspect middle vertical ridge) number of specimens attributed to the different categories for the different genders for the two species. For details see Fig. 2.70.

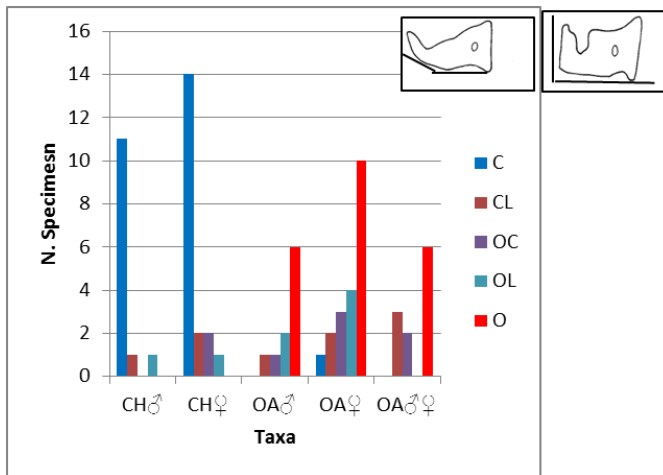


Figure 2.80 Third lower premolar P₃, trait 3 (aspect mesial-buccal angle) number of specimens attributed to the different categories for the different genders for the two species. For details see Fig. 2.70.

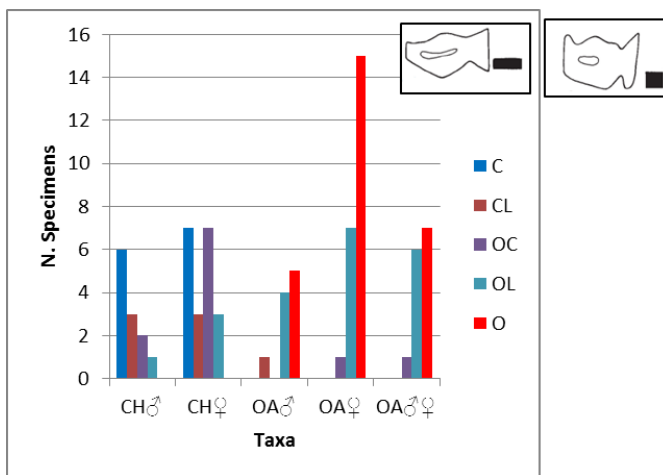


Figure 2.81 Fourth lower premolar P₄, trait 1 (overall shape) number of specimens attributed to the different categories for the different genders for the two species. For details see Fig. 2.70.

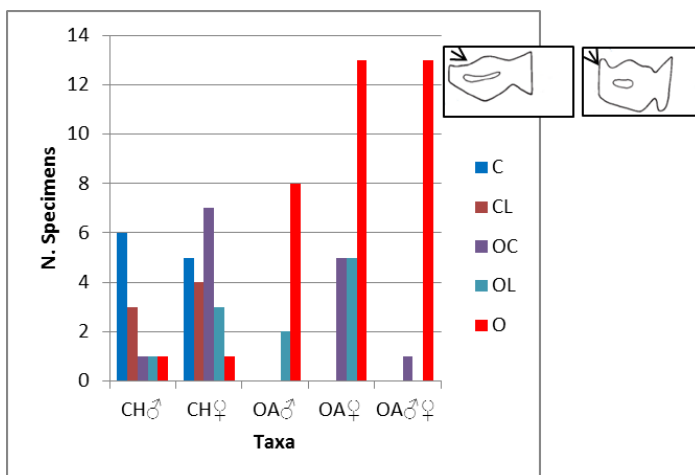


Figure 2.82 Fourth lower premolar P₄, trait 2 (aspect of the mesio-lingual rib) number of specimens attributed to the different categories for the different genders for the two species. For details see Fig. 2.70.

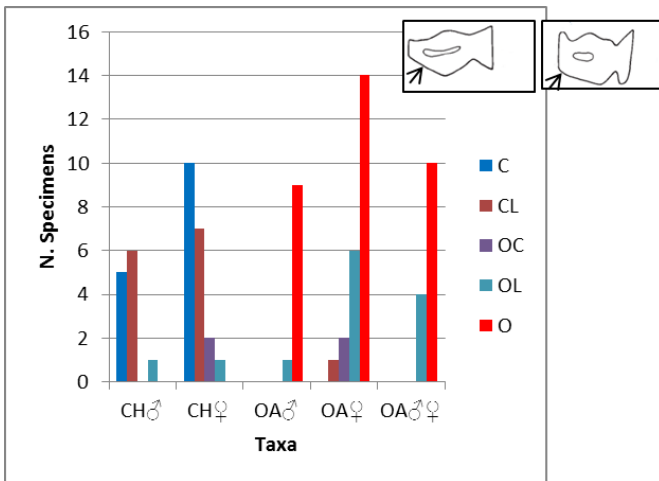


Figure 2.83 Fourth lower premolar P_4 , trait 3 (aspect of the mesio-buccal angle) number of specimens attributed to the different categories for the different genders for the two species. For details see Fig. 2.70.

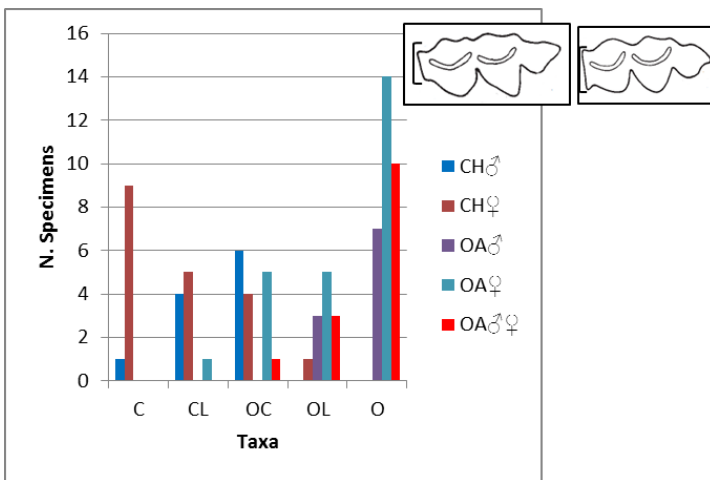


Figure 2.84 Third lower molar M_3 , trait 1 (aspect mesial face) number of specimens attributed to the different categories for the different genders for the two species. For details see Fig. 2.70.

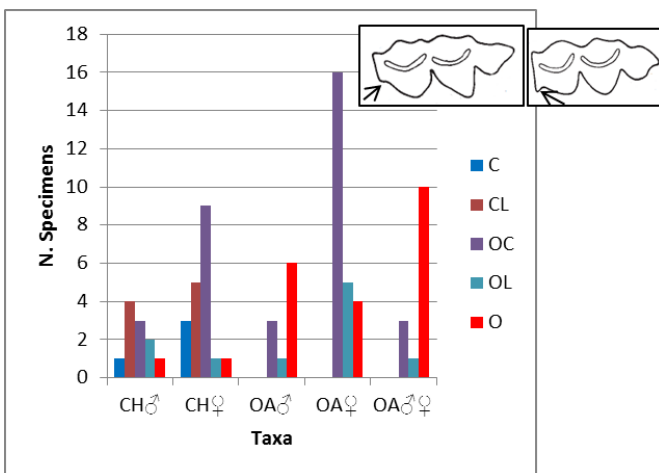


Figure 2.85 Third lower molar M_3 , trait 2 (aspect buccal edge angle) number of specimens attributed to the different categories for the different genders for the two species. For details see Fig. 2.70.

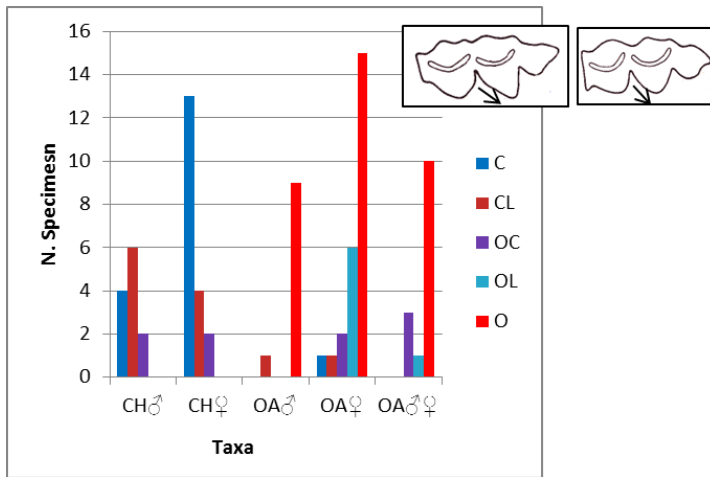


Figure 2.86 Third lower molar M_3 , trait 3 (direction of central cusp) number of specimens attributed to the different categories for the different genders for the two species. For details see Fig. 2.70.

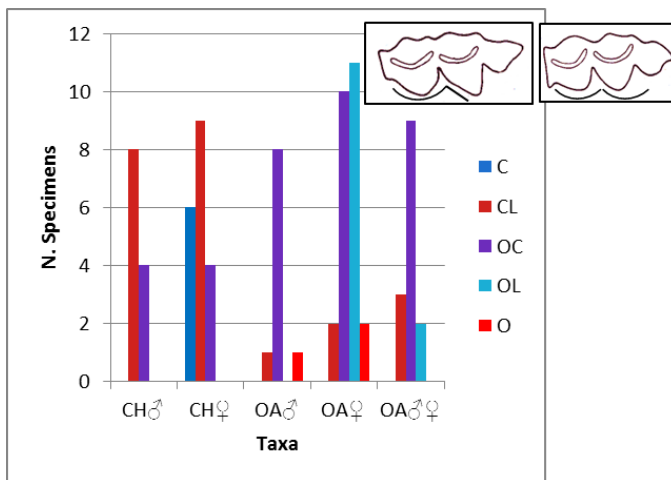


Figure 2.87 Third lower molar M_3 , trait 4 (symmetry and shape of cusps) number of specimens attributed to the different categories for the different genders for the two species. For details see Fig. 2.70.

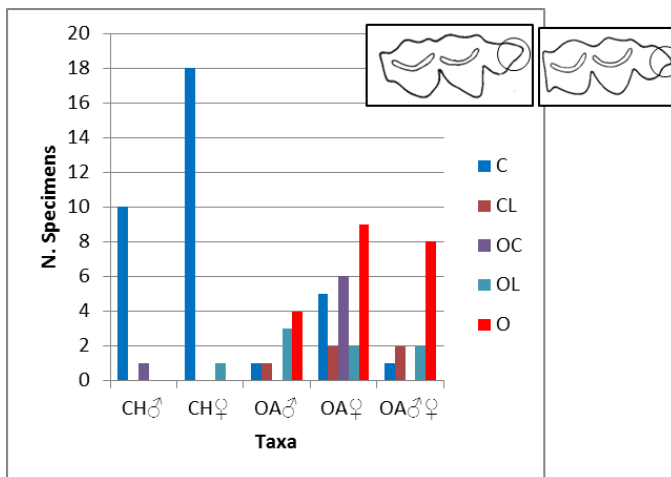


Figure 2.88 Third lower molar M_3 , trait 4 (aspect of the distal flute) number of specimens attributed to the different categories for the different genders for the two species. For details see Fig. 2.70.

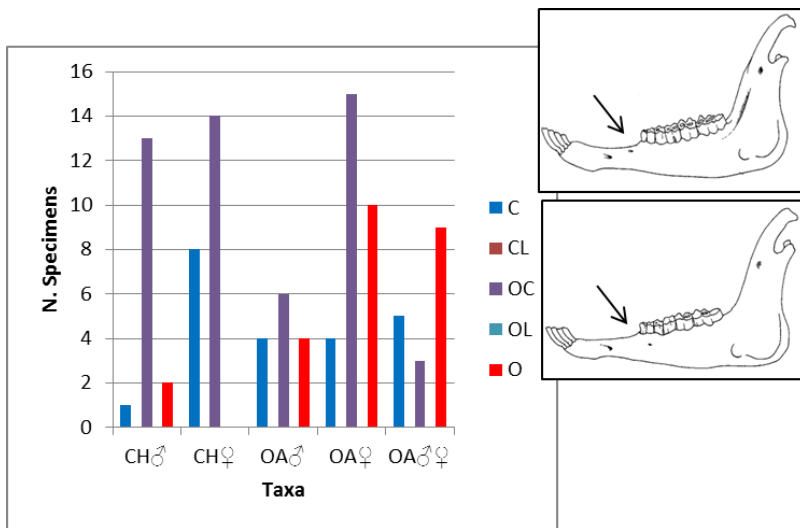


Figure 2.89 Mandible, trait 1 (presence/absence of the foramen) number of specimens attributed to the different categories for the different genders for the two species. For details see Fig. 2.70.

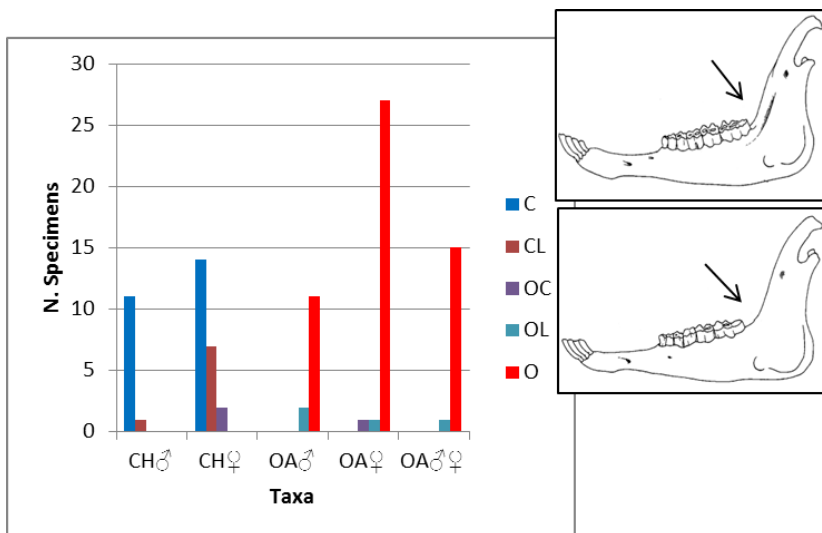


Figure 2.90 Mandible, trait 2 (posterior groove) number of specimens attributed to the different categories for the different genders for the two species. For details see Fig. 2.70.

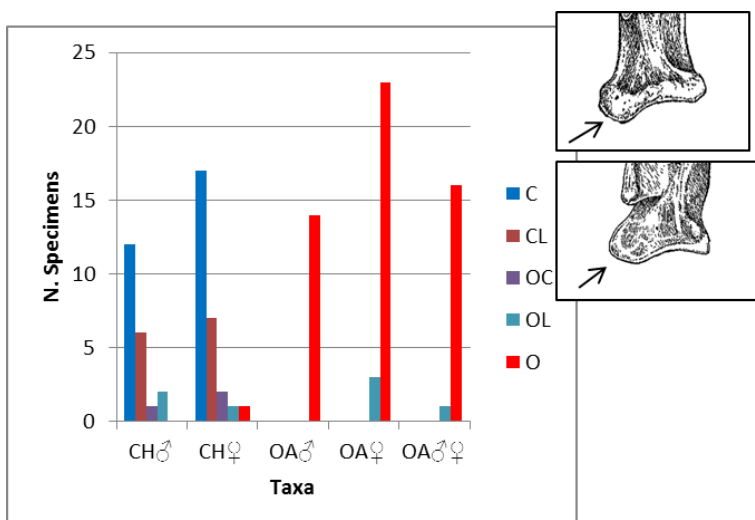


Figure 2.91 Scapula, trait 1 (shape of the glenoid tubercle) number of specimens attributed to the different categories for the different genders for the two species. For details see Fig. 2.70.

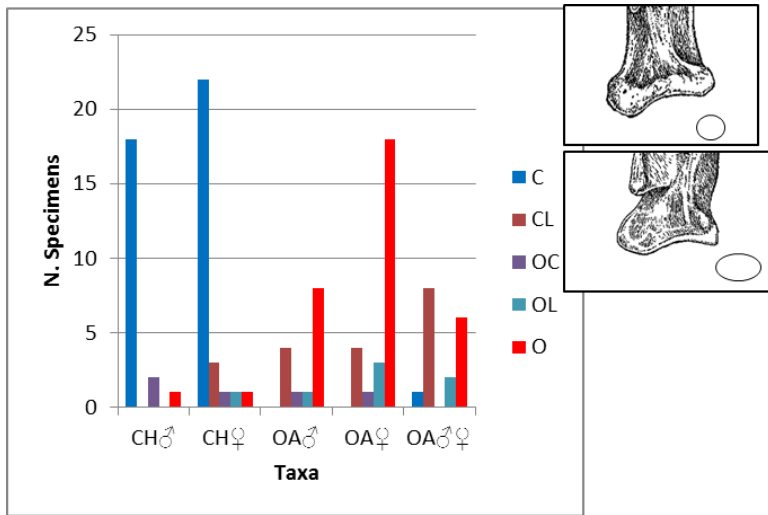


Figure 2.92 Scapula, trait 2 (shape of the glenoid cavity) number of specimens attributed to the different categories for the different genders for the two species. For details see Fig. 2.70.

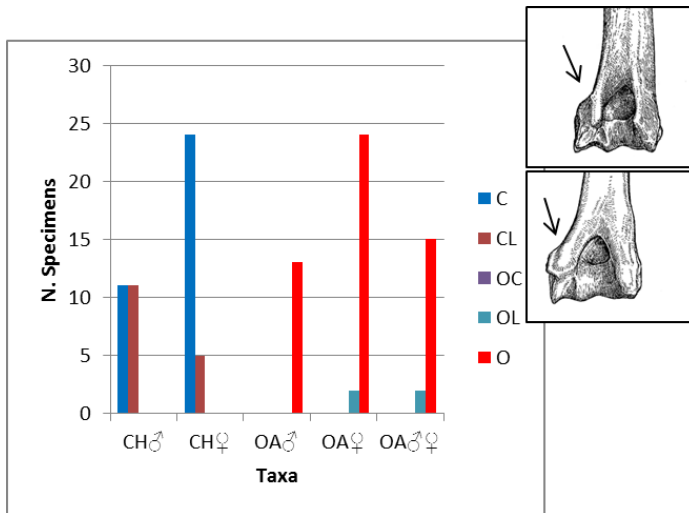


Figure 2.93 Humerus, trait 1 (shape of the lateral epicondyle) number of specimens attributed to the different categories for the different genders for the two species. For details see Fig. 2.70.

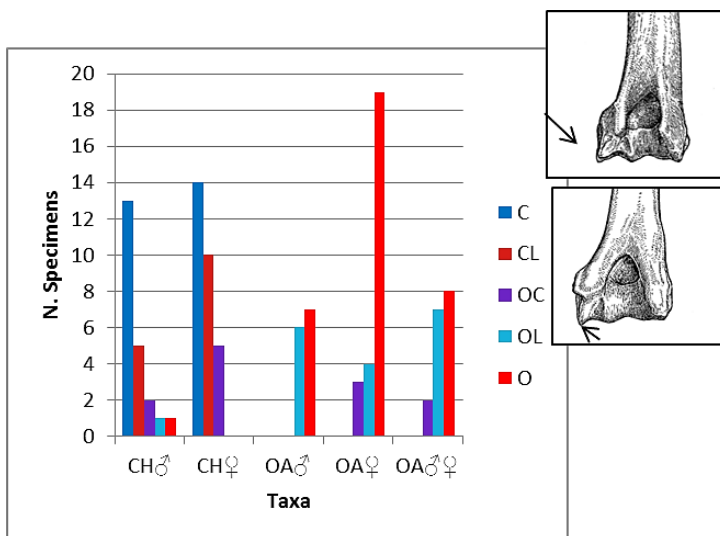


Figure 2.94 Humerus, trait 2 (aspect of the groove on the posterior side of the lateral epicondyle) number of specimens attributed to the different categories for the different genders for the two species. For details see Fig. 2.70.

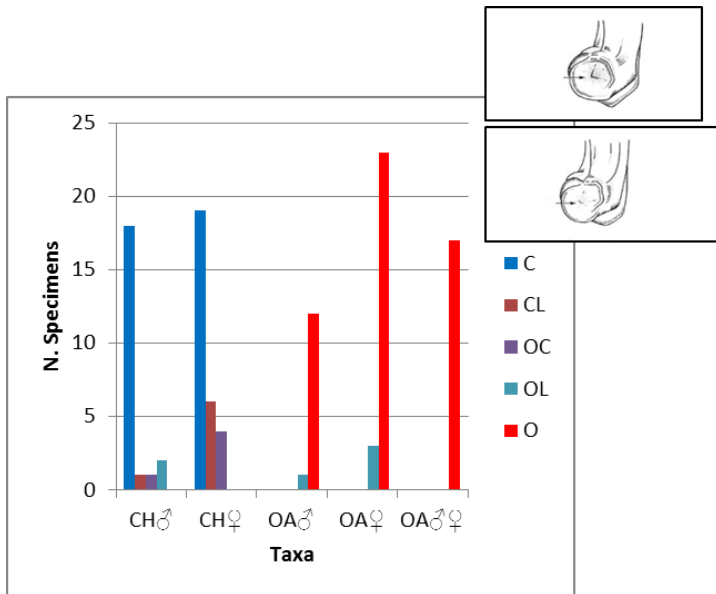


Figure 2.95 Humerus, trait 3 (aspect of the pit on the lateral epicondyle surface) number of specimens attributed to the different categories for the different genders for the two species. For details see Fig. 2.70.

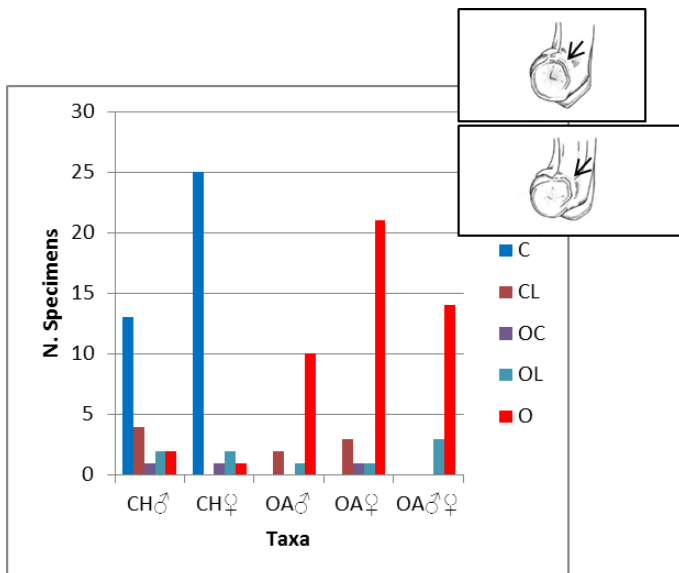


Figure 2.96 Humerus, trait 4 (presence/absence of a lateral thickening on the lateral border of epicondylar surface) number of specimens attributed to the different categories for the different genders for the two species. For details see Fig. 2.70.

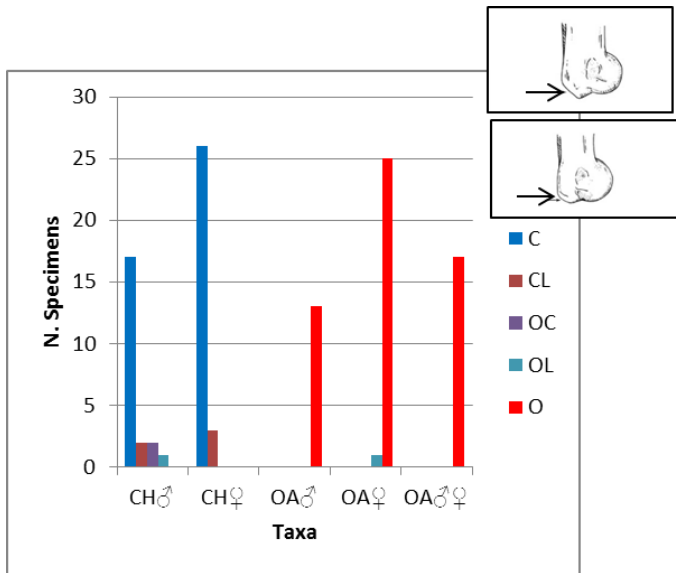


Figure 2.97 Humerus, trait 5 (aspect of the angle of the distal part of the medial epicondyle) number of specimens attributed to the different categories for the different genders for the two species. For details see Fig. 2.70.

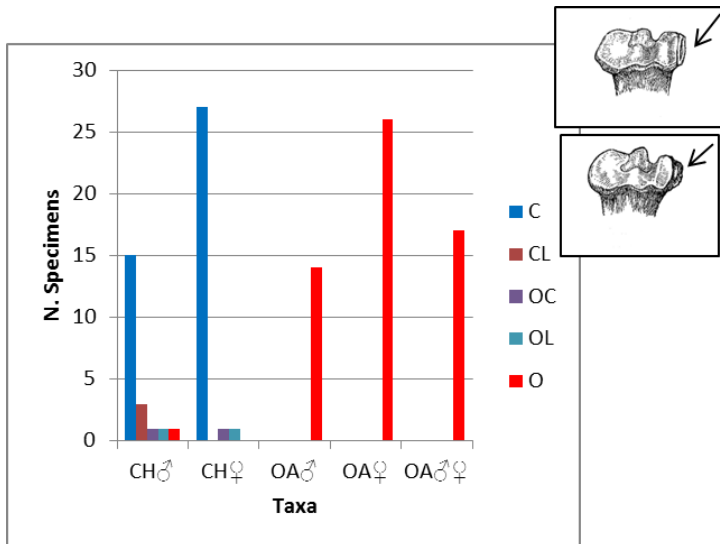


Figure 2.98 Radius, trait 1 (aspect of the lateral tuberosity) number of specimens attributed to the different categories for the different genders for the two species. For details see Fig. 2.70.

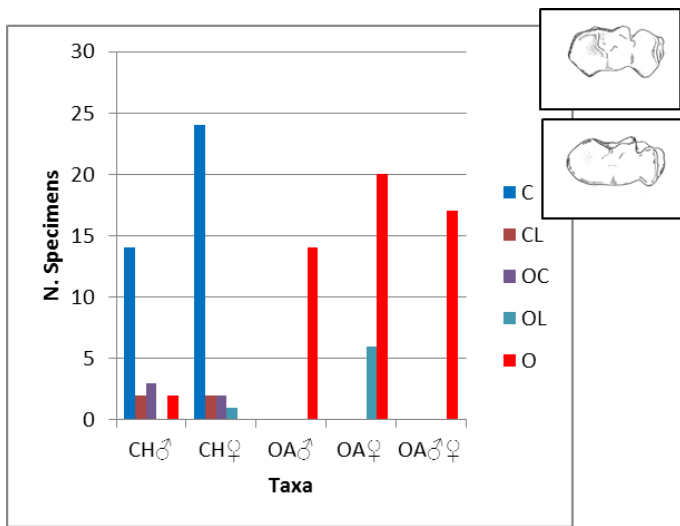


Figure 2.99 Radius, trait 2 (overall aspect of the proximal articular surface) number of specimens attributed to the different categories for the different genders for the two species. For details see Fig. 2.70.

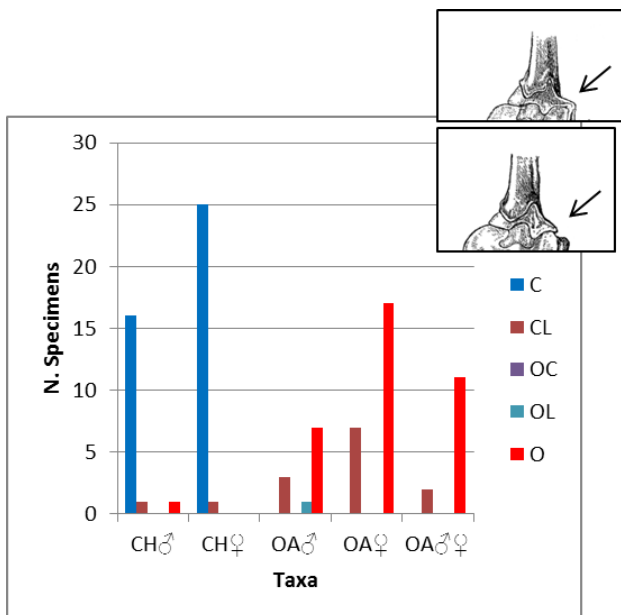


Figure 2.100 Ulna, trait 1 (projection of the lateral coronoid process) number of specimens attributed to the different categories for the different genders for the two species. For details see Fig. 2.70.

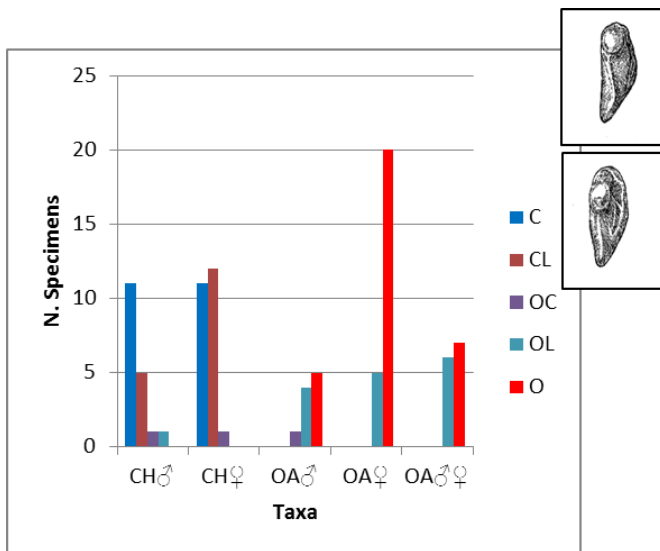


Figure 2.101 Ulna, trait 2 (overall shape of the *olecranon*) number of specimens attributed to the different categories for the different genders for the two species. For details see Fig. 2.70.

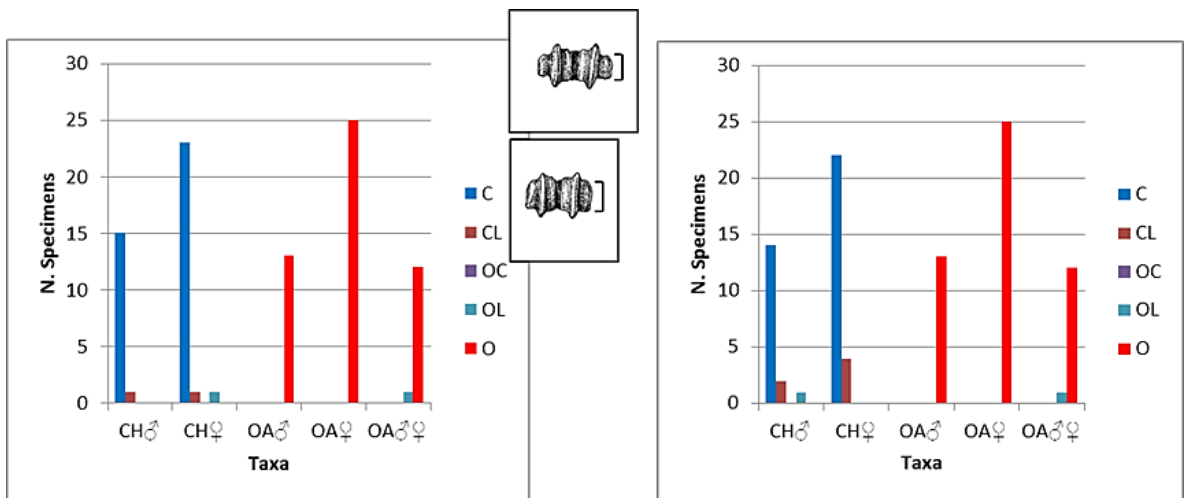


Figure 2.102 Metacarpal and metatarsal, trait 1 (dimension of the peripheral part of the trochlear condyles) number of specimens attributed to the different categories for the different genders for the two species. For details see Fig. 2.70.

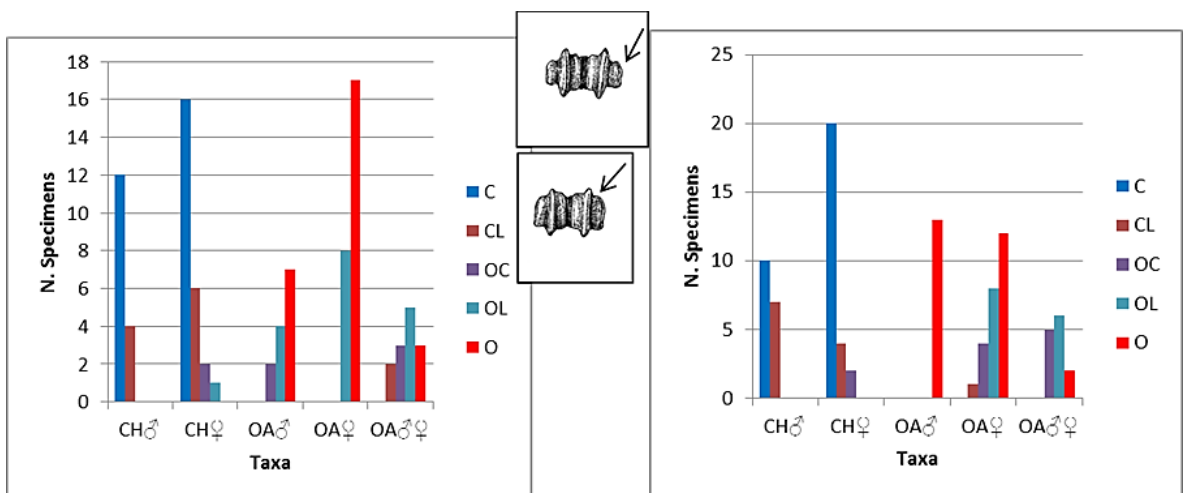


Figure 2.103 Metacarpal and metatarsal, trait 2 (definition of the peripheral part of the trochlear condyles) number of specimens attributed to the different categories for the different genders for the two species. For details see Fig. 2.70.

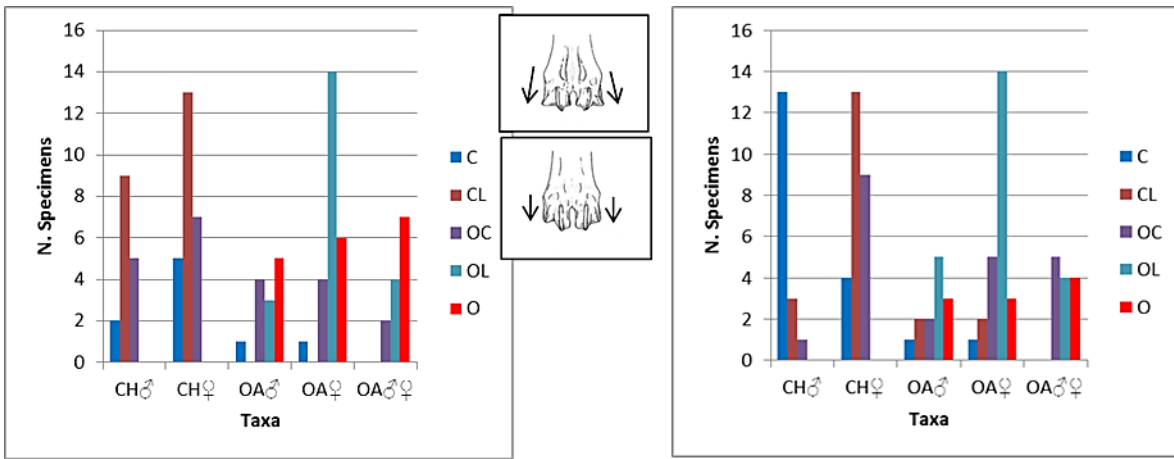


Figure 2.104 Metacarpal and metatarsal, trait 3 (aspect of the peripheral part of the trochlear condyles) number of specimens attributed to the different categories for the different genders for the two species. For details see Fig. 2.70.

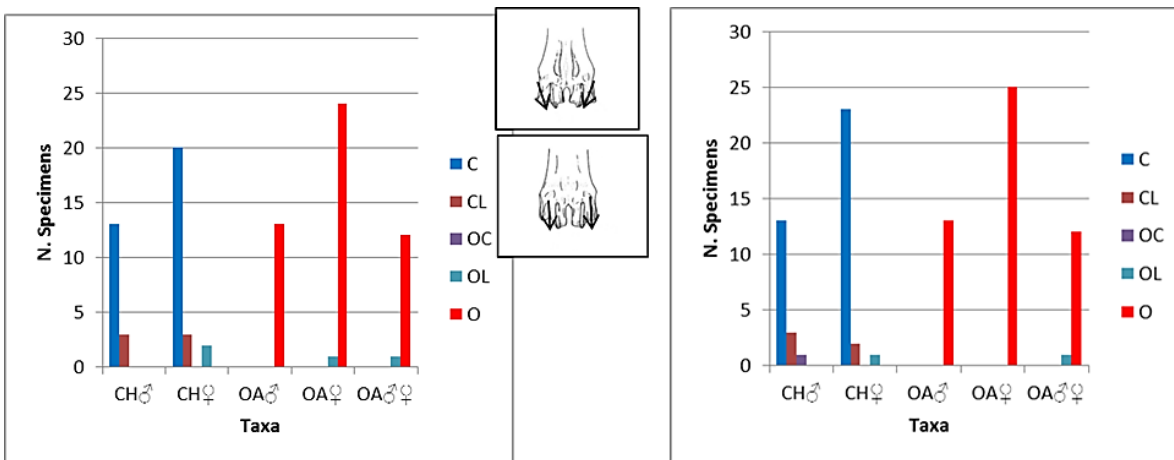


Figure 2.105 Metacarpal and metatarsal, trait 4 (direction of the *verticilli*) number of specimens attributed to the different categories for the different genders for the two species. For details see Fig. 2.70.

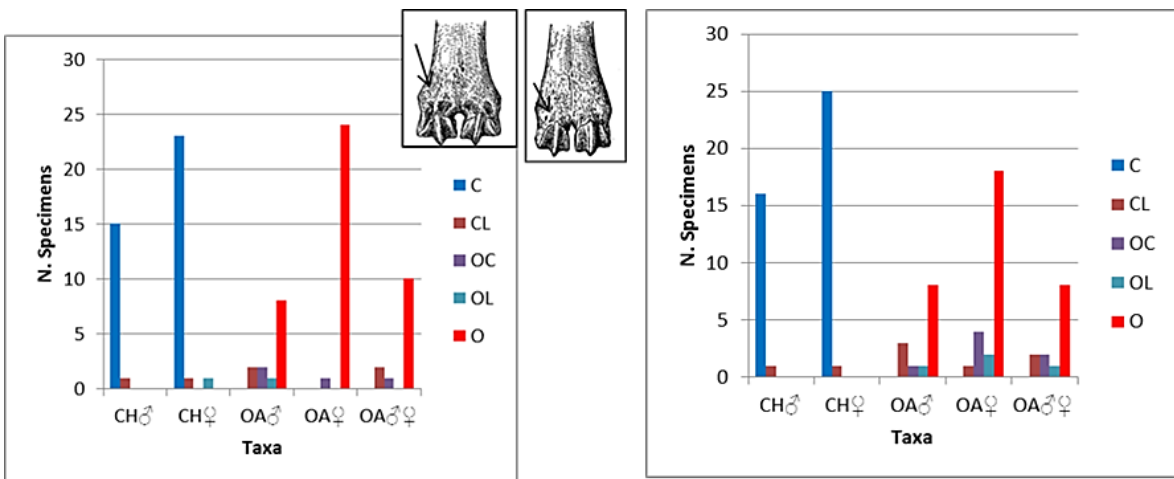


Figure 2.106 Metacarpal and metatarsal, trait 5 (development of the *fossae* on the proximal part of the distal trochlear condyles) number of specimens attributed to the different categories for the different genders for the two species. For details see Fig. 2.70.

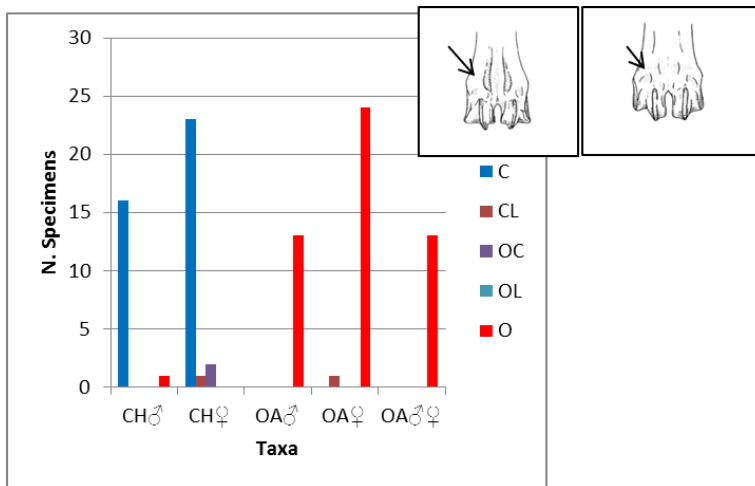


Figure 2.107 Metatarsal, trait 6 (development of the fossae on the proximal part of the distal diaphysis above the distal epiphysis) number of specimens attributed to the different categories for the different genders for the two species. For details see Fig. 2.70.

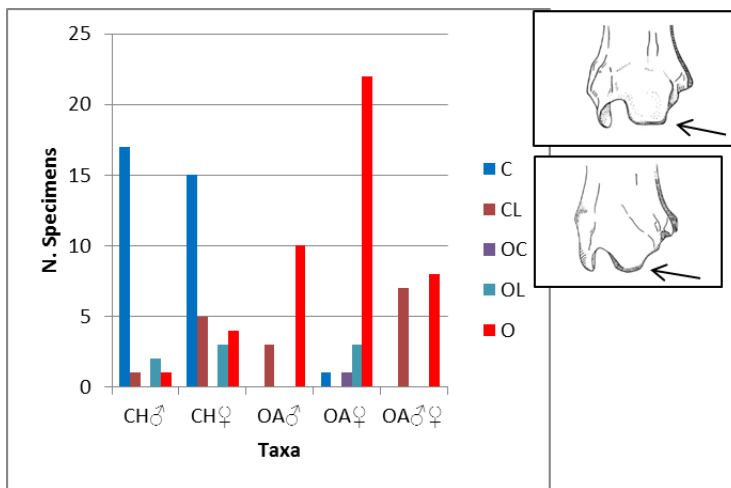


Figure 2.108 Tibia, trait 1 (dorsal prominence) number of specimens attributed to the different categories for the different genders for the two species. For details see Fig. 2.70.

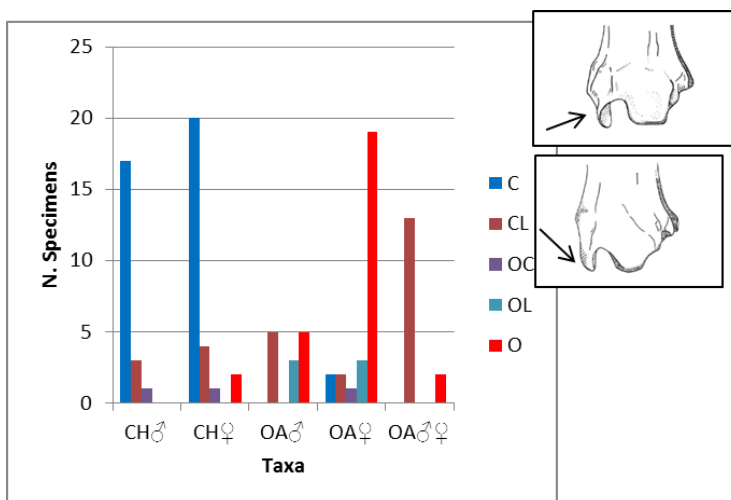


Figure 2.109 Tibia, trait 2 (medial malleolus) number of specimens attributed to the different categories for the different genders for the two species. For details see Fig. 2.70.

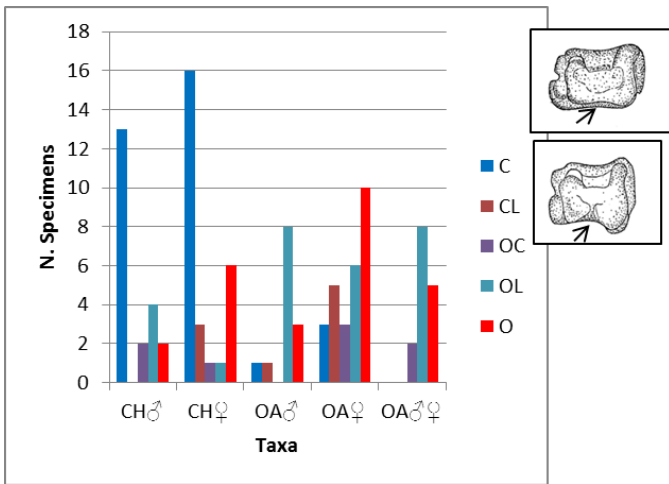


Figure 2.110 Tibia, trait 3 (presence/absence interruption on plantar limbus) number of specimens attributed to the different categories for the different genders for the two species. For details see Fig. 2.70.

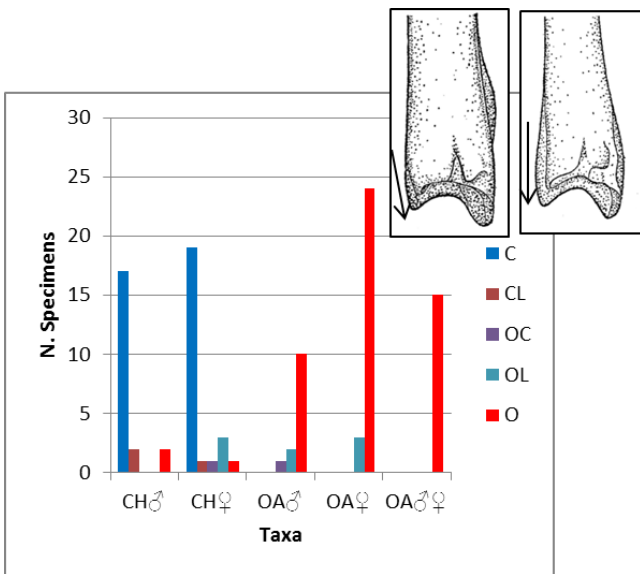


Figure 2.111 Tibia, trait 4 (lateral profile) number of specimens attributed to the different categories for the different genders for the two species. For details see Fig. 2.70.

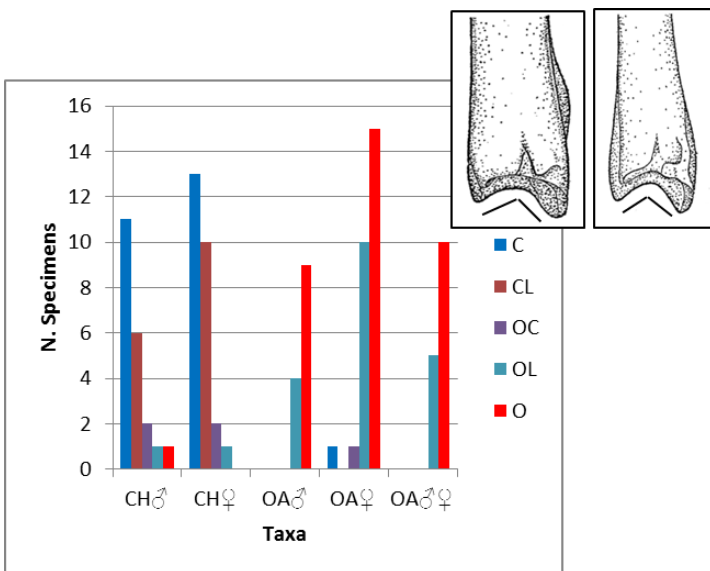


Figure 2.112 Tibia, trait 5 (shape of the anterior side of the *malleolus*) number of specimens attributed to the different categories for the different genders for the two species. For details see Fig. 2.70.

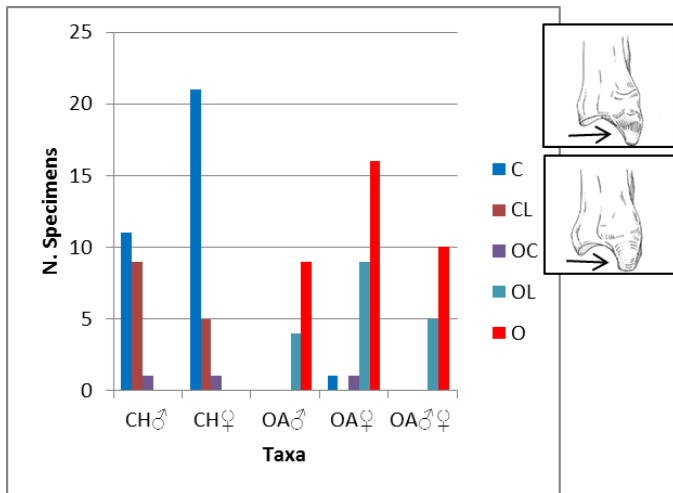


Figure 2.113 Tibia, trait 6 (aspect of the medial *malleolus*) number of specimens attributed to the different categories for the different genders for the two species. For details see Fig. 2.70.

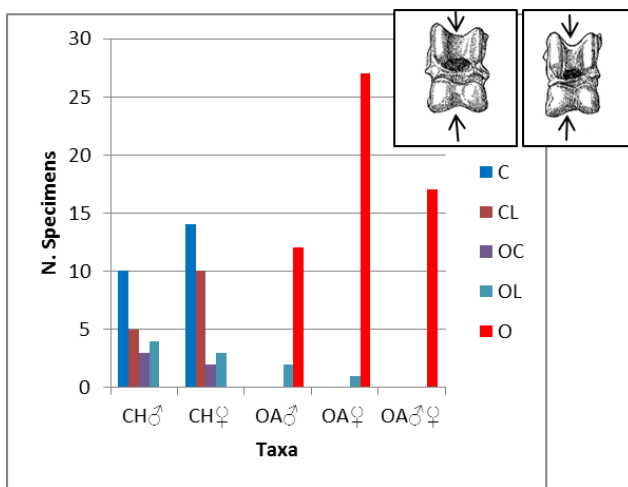


Figure 2.114 Astragalus, trait 1 (depth of the sulcus of the trochlea) number of specimens attributed to the different categories for the different genders for the two species. For details see Fig. 2.70.

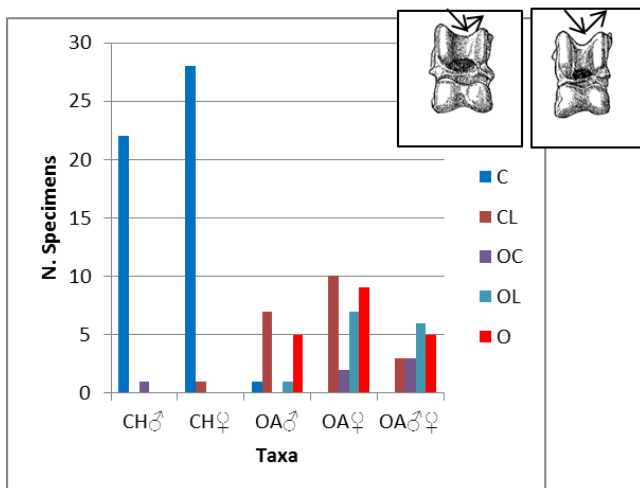


Figure 2.115 Astragalus, trait 2 (inclination of the lateral part of the trochlea) number of specimens attributed to the different categories for the different genders for the two species. For details see Fig. 2.70.

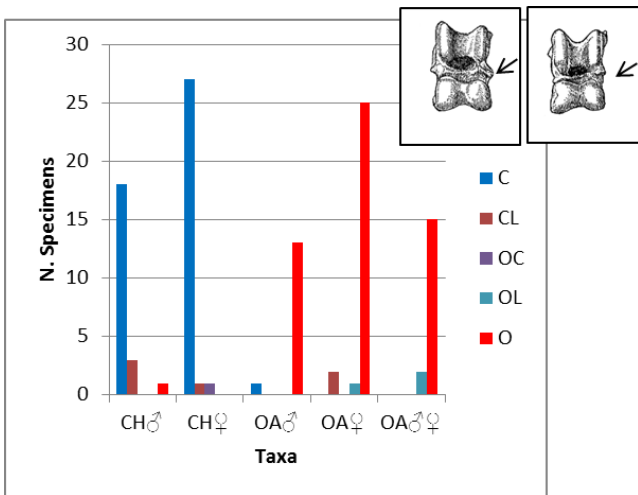


Figure 2.116 Astragalus, trait 3 (shape of the medial ridge) number of specimens attributed to the different categories for the different genders for the two species. For details see Fig. 2.70.

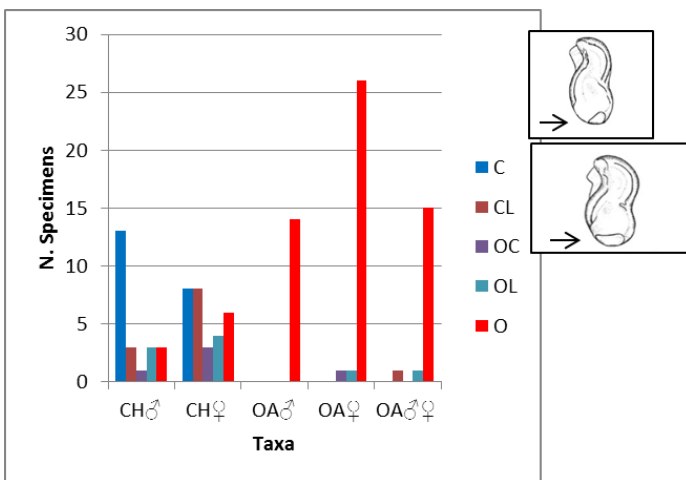


Figure 2.117 Astragalus, trait 4 (shape on the distal articular surface on the lateral aspect) number of specimens attributed to the different categories for the different genders for the two species. For details see Fig. 2.70.

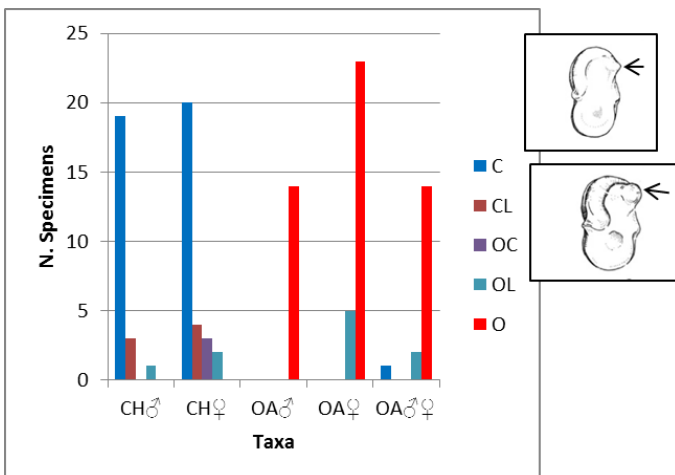


Figure 2.118 Astragalus, trait 5 (aspect of the proximo-plantar projection on the medial articular ridge of the trochlea) number of specimens attributed to the different categories for the different genders for the two species. For details see Fig. 2.70.

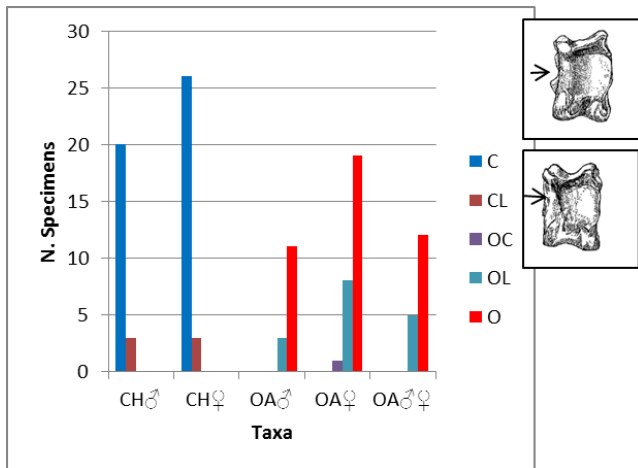


Figure 2.119 Astragalus, trait 6 (aspect of the direction of the articular surface on the plantar side) number of specimens attributed to the different categories for the different genders for the two species. For details see Fig. 2.70.

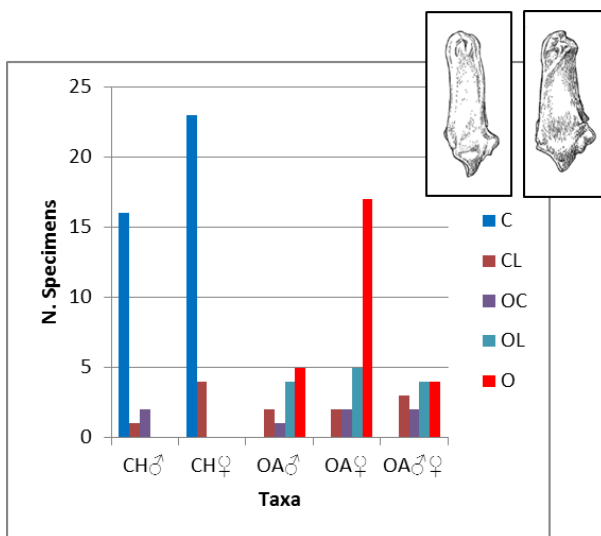


Figure 2.120 Calcaneus, trait 1 (overall aspect) number of specimens attributed to the different categories for the different genders for the two species. For details see Fig. 2.70.

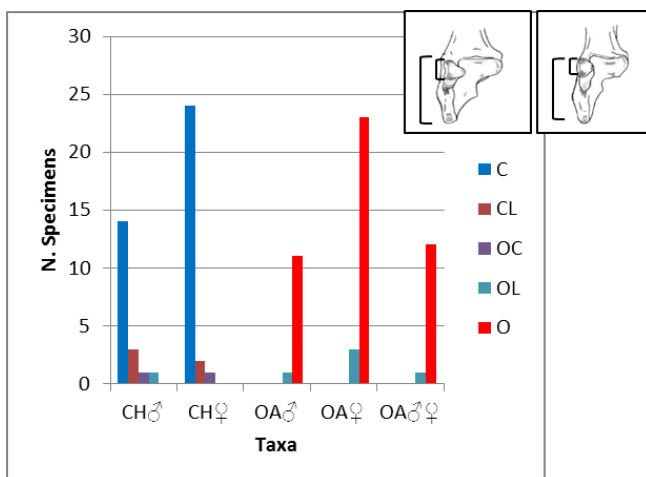


Figure 2.121 Calcaneus, trait 2 (length of the *os malleolare* vs length of the entire process) number of specimens attributed to the different categories for the different genders for the two species. For details see Fig. 2.70.

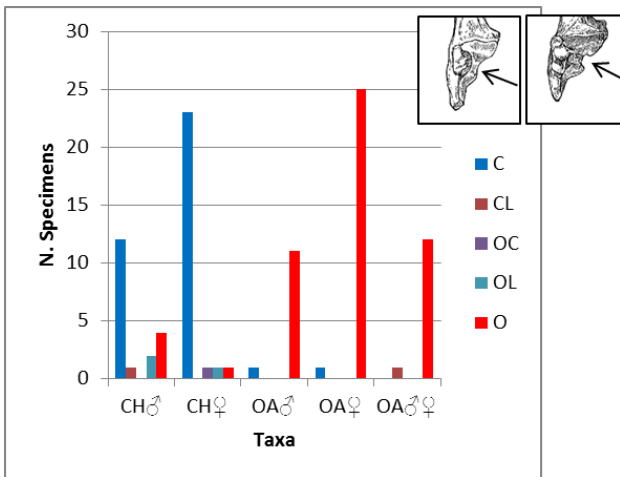


Figure 2.122 Calcaneus, trait 3 (presence/absence of the junction between the two internal articular surfaces) number of specimens attributed to the different categories for the different genders for the two species. For details see Fig. 2.70.

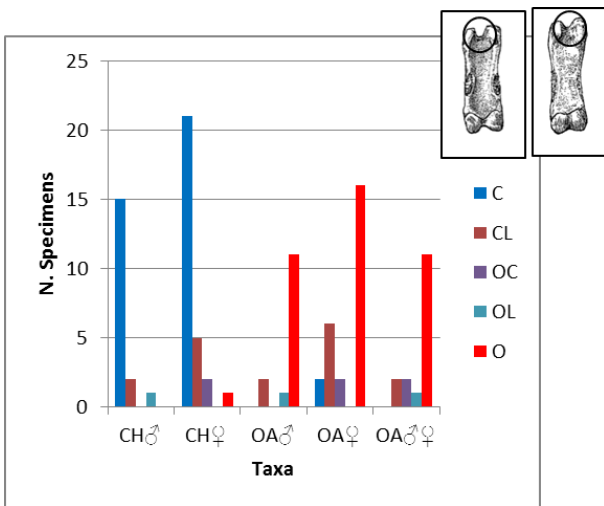


Figure 2.123 1st phalanx, trait 1 (shape of the groove on the proximal end) number of specimens attributed to the different categories for the different genders for the two species. For details see Fig. 2.70.

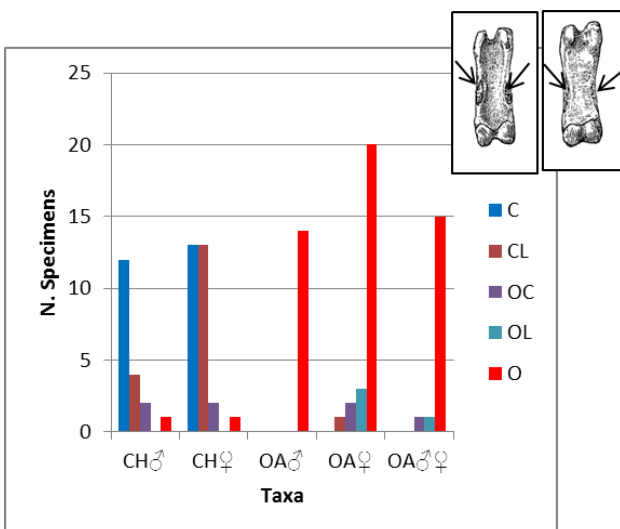


Figure 2.124 1st phalanx, trait 2 (presence of the scars of the muscular ligaments on the posterior side) number of specimens attributed to the different categories for the different genders for the two species. For details see Fig. 2.70.

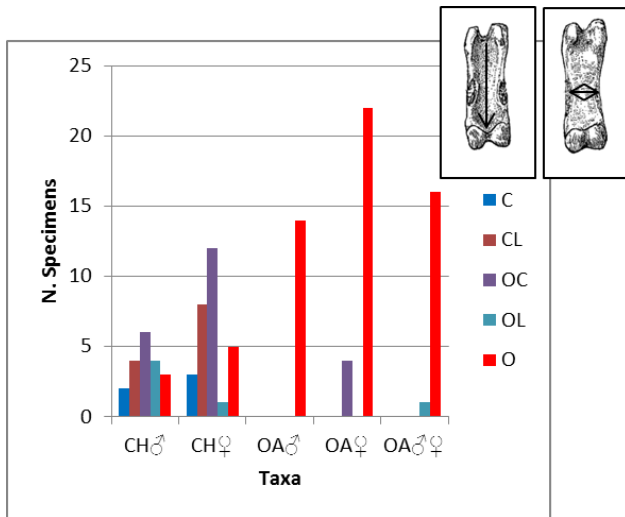


Figure 2.125 1st phalanx, trait 3 (aspect of the posterior side) number of specimens attributed to the different categories for the different genders for the two species. For details see Fig. 2.70.

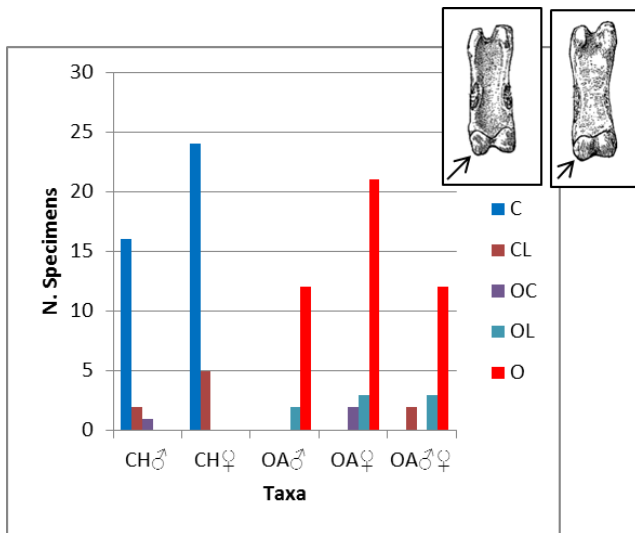


Figure 2.126 1st phalanx, trait 4 (shape of the distal articulation) number of specimens attributed to the different categories for the different genders for the two species. For details see Fig. 2.70.

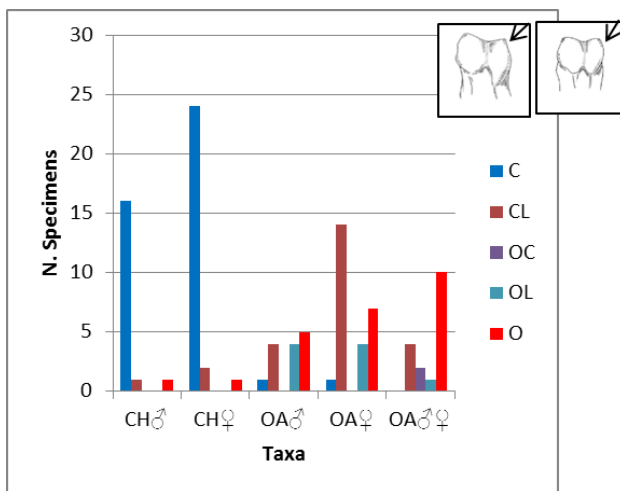


Figure 2.127 2nd phalanx, trait 1 (aspect of the axial part of the posterior side of the distal articulation) number of specimens attributed to the different categories for the different genders for the two species. For details see Fig. 2.70.

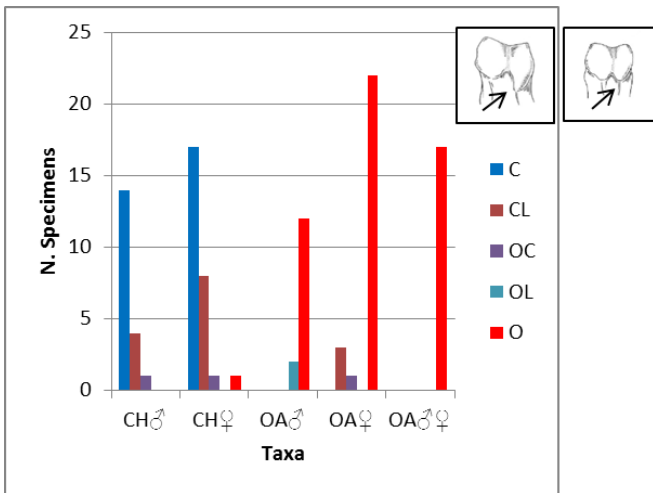


Figure 2.128 2nd phalanx, trait 2 (aspect of the ridge on the posterior edge of the distal articulation) number of specimens attributed to the different categories for the different genders for the two species. For details see Fig. 2.70.

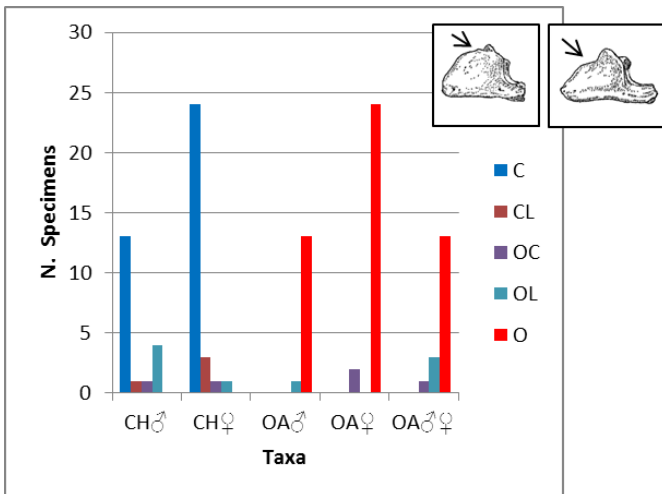


Figure 2.129 3rd phalanx, trait 1 (presence/absence of a saddle on the dorsal edge) number of specimens attributed to the different categories for the different genders for the two species. For details see Fig. 2.70.

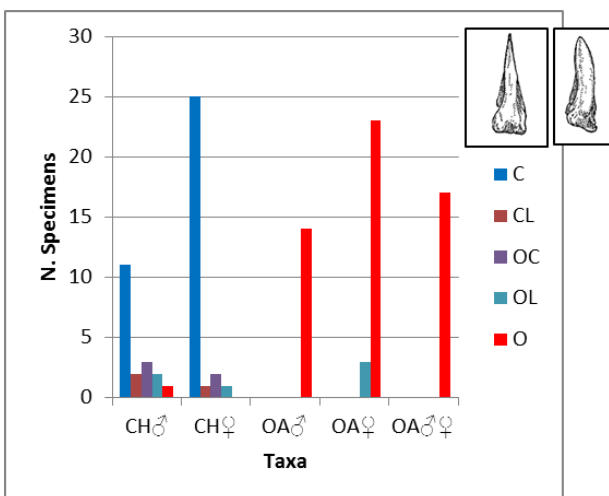


Figure 2.130 3rd phalanx, trait 2 (shape of the sole) number of specimens attributed to the different categories for the different genders for the two species. For details see Fig. 2.70.

2.4.3 Influence of age

A further analysis was carried out in order to see if the age of the animals could influence the reliability of the morphological criteria. In order to undertake this analysis, the known age at death of the animals was considered. When this information was not available, the age of the animal was established from the tooth wear, recorded following Payne's method (1973, 1987). All aged specimens were eventually combined, so that they could all be attributed to the nine age categories outlined by Payne (Tab. 2.52). For the specimens with known age at death, the final attribution to one of the categories (Tab. 2.53) was reached through a combination of the known information and the tooth wear stages, especially useful when the known age of the animal could be attributed to more than one category.

Table 2.53 Summary of the age categories established by Payne (1973; 1987) and used for this analysis.

Payne's categories	Age	Wear stages
A	0-2 months	dP ₄ still unworn
B	2-6 months	dP ₄ in wear, M ₁ unworn
C	6-12 months	M ₁ in wear, M ₂ unworn
D	1-2 years	M ₂ in wear, M ₃ unworn
E	2-3 years	M ₃ in wear, posterior cusp unworn
F	3-4 years	Posterior cup of M ₃ in wear, M ₃ pre stage 11G
G	4-6 years	M ₃ in 11G, M ₂ in stage 9A
H	6-8 years	M ₃ in 11G, M ₂ post 9A
I	8-10 years	M ₃ post stage 11G

Table 2.54 New age groups combining different Payne's age categories. The specimens present are both those for which the age was established through Payne's method and those for which the age at death was known.

Group	Stages included	<i>N. Capra hircus</i>	<i>N. Ovis aries</i>	Total number of specimens
G1 (0-12 months)	A	-	-	-
	B	1	-	1
	C	4	2	6
TOTAL				7
G2 (1-3 years)	D	4	11	15
	E	11	16	28
TOTAL				43
G3 (3-6 years)	F	12	17	29
	G	6	11	17
TOTAL				46
G4 (6-10 years)	H	19	6	25
	I	9	6	16
TOTAL				41

Final age groups, which combined several of the Payne's age categories, have been employed in order to facilitate comparisons. As shown by Table 2.53, age Groups 1 is underrepresented as the sample size is small. As a consequence the results for the very young animal group have to be considered indicative.

Table 2.55 Goat. Scores expressed in percentages given to different morphological characteristics of different cranial and post-cranial bones according to age groups.

<i>Capra hircus</i>														
Anatomical Elements	Morph. Trait.	Group 1			Group 2			Group 3			Group 4			
		% of matching			% of matching			% matching			% matching			
		C	C + CL	C+CL +OC	C	C+ CL	C+CL +OC	C	C+ CL	C+CL +OC	C	C+ CL	C+CL +OC	
Cranial bones	Hc	HC1	100	100	100	100	100	100	100	100	100	100	100	100
		HC2	100	100	100	100	100	100	100	100	100	100	100	100
	M	M1	100	100	100	13.3	13.3	86.7	20	20	100	28	28	100
		M2	25	75	50	69.2	92.3	100	73.3	93.3	100	79.2	100	100
	dP ₃	dP3/1	75	100	100	100	100	100	100	100	100	-	-	-
		dP3/2	50	50	100	0	50	100	-	-	-	-	-	-
	dP ₄	dP4/1	0	0	100	0	0	100	0	0	100	-	-	-
		dP4/2	0	0	0	0	100	0	0	0	0	-	-	-
		dP4/3	75	100	100	100	100	100	100	100	100	-	-	-
		dP4/4	66.7	66.7	100	100	100	100	100	100	100	-	-	-
	P ₃	P3/1	-	-	-	81.8	100	100	73.3	86.7	86.7	43.5	65.2	65.2
		P3/2	-	-	-	90.9	90.9	100	86.7	86.7	93.3	60.9	73.9	100
		P3/3	-	-	-	100	100	100	80	80	93.3	69.9	91.3	95.7
	P ₄	P4/1	-	-	-	66.7	91.7	91.7	66.7	86.7	100	0	36.4	77.3
		P4/2	-	-	-	50	75	75	40	66.7	80	31.8	45.5	95.5
		P4/3	-	-	-	83.3	100	100	86.7	100	100	36.4	72.7	86.4
	M ₃	M3/1	-	-	-	60	80	100	66.7	93.3	100	12.5	33.3	95.8
		M3/2	-	-	-	20	60	60	33.3	60	86.7	24	40	96
		M3/3	-	-	-	50	66.7	66.7	53.3	73.3	100	68	96	100
		M3/4	-	-	-	33.3	66.7	66.7	33.3	60	100	28	84	100
M3/5		-	-	-	75	75	100	100	100	100	92	100	100	
Post Cranial bones	Sc	Sc1	66.7	66.7	66.7	56.3	93.8	93.8	70.6	82.4	100	55.6	85.2	88.9
		Sc2	66.7	100	100	68.8	81.3	100	94.1	100	100	81.5	88.9	92.6
	Hu	Hu1	80	100	100	62.5	100	100	94.1	100	100	81.5	100	100
		Hu2	40	100	100	31.3	68.8	93.8	64.7	82.4	100	48.1	81.5	88.9
		Hu3	100	100	100	81.3	87.5	93.8	82.4	94.1	100	66.7	81.5	96.3
		Hu4	80	80	80	93.3	100	100	64.7	76.5	88.2	70.4	77.8	81.5
		Hu5	60	100	100	75	87.5	93.8	88.2	94.1	100	92.6	100	100
	Ra	Ra1	80	100	100	68.8	87.5	93.8	88.2	88.2	94.1	96	96	96
		Ra2	40	40	80	75	87.5	100	88.2	88.2	100	88	100	100
	Ul	Ul1	50	100	100	66.7	83.3	83.3	81.3	93.8	93.8	95.8	95.8	100
		Ul2	50	100	100	33.3	83.3	83.3	66.7	93.3	93.3	75	100	100
	Mc	Mc1	100	100	100	85.7	100	100	94.1	100	100	95.8	100	100
		Mc2	100	100	100	83.3	100	100	82.4	100	100	70.8	91.7	100
		Mc3	0	50	100	28.6	71.4	100	17.6	58.8	100	29.2	79.2	100
		Mc4	50	100	100	85.7	100	100	94.1	100	100	75	100	100
		Mc5	100	100	100	85.7	100	100	100	100	100	100	100	100
	Mt	Mt1	100	100	100	55.6	88.9	88.9	82.4	100	100	92.3	100	100
		Mt2	50	100	100	55.6	88.9	100	64.7	100	100	80.8	100	100
		Mt3	0	50	100	11.1	66.7	100	5.9	52.9	100	23.1	65.4	96.2
		Mt4	50	100	100	66.7	88.9	100	88.2	100	100	76.9	96.2	100
		Mt5	100	100	100	88.9	100	100	100	100	100	100	100	100
		Mt6	100	100	100	77.8	77.8	88.9	100	100	100	96.2	100	100
	Ti	Ti1	100	100	100	40	53.3	60	76.5	94.2	100	55.6	81.5	81.5
		Ti2	50	100	100	80	93.3	100	82.4	94.1	100	77.8	88.9	88.9
		Ti3	50	50	50	46.7	46.7	53.3	52.9	64.7	70.6	70.4	81.5	85.2
		Ti4	100	100	100	60	73.3	80	81.3	87.5	93.8	70.4	81.5	88.9
		Ti5	50	100	100	20	80	86.7	62.5	100	100	51.9	96.3	96.3
		Ti6	50	50	50	73.3	100	100	58.8	94.1	94.1	88.9	96.3	100
	As	Ta1	100	100	100	53.3	80	86.7	56.3	87.5	93.8	48.1	81.5	88.9
		Ta2	100	100	100	87.5	93.8	100	100	100	100	100	100	100
Ta3		100	100	100	87.5	93.8	93.8	100	100	100	88.9	100	100	
Ta4		50	50	50	37.5	43.8	56.3	37.5	62.5	68.8	33.3	55.6	66.7	
Ta5		75	75	75	75	93.8	93.8	93.8	100	100	77.8	92.6	96.3	
Ta6		100	100	100	100	100	100	100	100	100	77.8	100	100	
Cc	Cc1	100	100	100	71.4	71.4	100	87.5	100	100	81.5	100	100	
	Cc2	100	100	100	85.7	85.7	85.7	100	100	100	88.9	96.3	100	
	Cc3	100	100	100	71.4	85.7	85.7	68.8	81.3	81.3	73.1	73.1	76.9	
1 st Ph	Ph1/1	100	100	100	64.3	100	100	81.3	93.8	93.8	71.4	85.7	92.9	
	Ph1/2	66.7	66.7	100	35.7	71.4	92.9	62.5	93.8	93.8	64.3	96.4	100	
	Ph1/3	33.3	33.3	66.7	0	14.3	57.1	0	25	62.5	17.9	37.5	57.1	

<i>Capra hircus</i>														
Anatomical Elements	Morph. Trait.	Group 1			Group 2			Group 3			Group 4			
		% of matching			% of matching			% matching			% matching			
		C	C + CL	C+CL +OC	C	C+ CL	C+CL +OC	C	C+ CL	C+CL +OC	C	C+ CL	C+CL +OC	
	2 nd Ph	Ph1/4	100	100	100	64.3	100	100	81.3	100	100	89.3	96.4	100
		Ph2/1	100	100	100	92.9	92.9	92.9	93.8	100	100	92.6	96.3	100
		Ph2/2	66.7	100	100	71.4	85.7	100	68.8	100	100	74.1	96.3	100
	3 rd Ph	Ph3/1	75	75	75	53.8	61.5	69.2	66.7	80	86.7	81.5	96.3	100
		Ph3/2	50	75	100	69.2	69.2	84.6	62.5	93.8	93.8	77.8	85.2	96.3

Table 2.56 Sheep. Scores expressed in percentages given to different morphological characteristics of different cranial and post-cranial bones according to age groups.

<i>Ovis aries</i>														
Anatomical Elements	Morph. Trait.	Group 1			Group 2			Group 3			Group 4			
		% of matching			% of matching			% matching			% matching			
		O	O + OL	O+OL +OC	O	O + OL	O+OL +OC	O	O + OL	O+OL +OC	O	O + OL	O+OL +OC	
Cranial bones	Hc	HC1	-	-	-	100	100	100	100	100	100	100	100	100
		HC2	-	-	-	100	100	100	100	100	100	100	100	100
	M	M1	100	100	100	40.7	40.7	74.1	50	50	85.7	25	25	83.3
		M2	100	100	100	92	100	100	92.9	96.4	100	83.3	100	100
	dP ₃	dP3/1	100	100	100	33.3	83.3	83.3	-	-	-	-	-	-
		dP3/2	0	0	0	0	25	100	-	-	-	-	-	-
	dP ₄	dP4/1	100	100	100	0	0	100	-	-	-	-	-	-
		dP4/2	100	100	100	100	100	100	-	-	-	-	-	-
		dP4/3	100	100	100	100	100	100	-	-	-	-	-	-
		dP4/4	100	100	100	50	50	100	-	-	-	-	-	-
	P ₃	P3/1	-	-	-	33.3	66.7	100	40	68	88	66.7	100	100
		P3/2	-	-	-	66.7	83.3	88.9	60	84	92	66.7	83.3	100
		P3/3	-	-	-	55.6	72.2	83.3	52	68	84	83.3	83.3	100
	P ₄	P4/1	-	-	-	57.9	89.5	94.7	60.7	96.4	100	87.5	100	100
		P4/2	-	-	-	84.2	100	100	75	92.9	100	0	37.5	100
		P4/3	-	-	-	73.7	94.7	94.7	71.4	96.4	100	62.5	87.5	100
	M ₃	M3/1	-	-	-	68.4	94.7	100	51.9	77.8	96.3	83.3	91.7	100
		M3/2	-	-	-	84.2	94.7	100	25.9	51.9	100	0	8.3	100
		M3/3	-	-	-	89.5	94.7	94.7	70.4	81.5	84.8	58.3	83.3	100
		M3/4	-	-	-	10.5	31.6	89.5	3.7	29.6	85.2	0	41.7	100
		M3/5	-	-	-	50	81.3	93.8	55.6	63	70.4	41.7	50	75
Post Cranial bones	Sc	Sc1	100	100	100	96.3	100	100	92	100	100	75	100	100
		Sc2	100	100	100	70.4	77.8	81.5	40	52	54	58.3	66.7	66.7
	Hu	Hu1	100	100	100	84	100	100	100	100	100	100	100	100
		Hu2	0	0	100	60	100	100	69.2	88.5	100	63.6	90.9	100
		Hu3	100	100	100	92	100	100	88.5	100	100	100	100	100
		Hu4	0	0	0	68	80	84	80.8	100	100	100	100	100
		Hu5	100	100	100	96	100	100	100	100	100	100	100	100
	Ra	Ra1	100	100	100	100	100	100	100	100	100	100	100	100
		Ra2	100	100	100	84.6	96.2	96.2	80.8	96.2	96.2	72.7	100	100
	Ul	Ul1	100	100	100	88.9	88.9	88.9	76.9	76.9	76.9	45.5	45.5	45.5
		Ul2	100	100	100	52.9	94.1	100	64	100	100	75	100	100
	Mc	Mc1	100	100	100	100	100	100	100	100	100	91.7	100	100
		Mc2	100	100	100	36.8	73.7	94.7	63	92.6	96.3	66.7	100	100
		Mc3	0	100	100	47.4	73.7	89.5	25.9	66.7	100	33.3	91.7	100
		Mc4	0	100	100	100	100	100	85.2	100	100	100	100	100
		Mc5	0	0	100	63.2	68.4	84.2	96.3	100	100	100	100	100
	Mt	Mt1	100	100	100	100	100	100	96.3	100	100	100	100	100
		Mt2	100	100	100	28.6	66.7	95.2	40.7	88.9	100	33.3	75	91.7
		Mt3	0	0	100	23.8	61.9	81	22.2	63	96.3	16.7	83.3	91.7
		Mt4	100	100	100	100	100	100	88.9	100	100	100	100	100
		Mt5	0	0	100	38.1	61.9	81	88.9	88.9	96.3	75	83.3	91.7
		Mt6	100	100	100	100	100	100	100	100	100	91.7	91.7	91.7
	Ti	Ti1	100	100	100	66.7	75	75	74.1	77.8	81.5	83.3	100	100
		Ti2	100	100	100	29.2	45.8	50	51.9	63	66.7	83.3	83.3	83.3
		Ti3	50	50	100	25	79.2	79.2	37	66.7	77.8	41.7	75	83.3
		Ti4	50	100	100	83.3	95.8	100	88.9	100	100	100	100	100
		Ti5	50	50	100	29.2	75	100	37	96.3	100	33.3	100	100
		Ti6	0	50	50	66.7	100	100	74.1	100	100	50	91.7	100
	As	Ta1	100	100	100	92.3	100	100	96.3	100	100	90.9	100	100

<i>Ovis aries</i>														
Anatomical Elements	Morph. Trait	Group 1			Group 2			Group 3			Group 4			
		% of matching			% of matching			% matching			% matching			
		O	O + OL	O+OL +OC	O	O + OL	O+OL +OC	O	O + OL	O+OL +OC	O	O + OL	O+OL +OC	
	Ta	Ta2	0	0	0	23.1	46.2	53.8	33.3	55.6	63	45.5	72.7	72.7
		Ta3	0	0	0	84.6	96.2	96.2	85.2	92.6	92.6	90.9	100	100
		Ta4	100	100	100	92.3	96.2	96.2	92.6	96.3	100	90.9	100	100
		Ta5	0	100	100	84.6	92.3	92.3	81.5	100	100	90.9	100	100
		Ta6	0	100	100	76.9	100	100	66.7	96.3	100	90.9	100	100
	Cc	Cc1	100	100	100	47.4	78.9	89.5	63	77.8	88.9	45.5	81.8	81.8
		Cc2	100	100	100	94.7	100	100	92.6	96.3	100	72.7	100	100
		Cc3	100	100	100	89.5	89.5	89.5	92.6	100	100	100	100	100
	1 st Ph	Ph1/1	0	0	0	68	76	84	76.9	84.6	100	54.5	54.5	63.6
		Ph1/2	100	100	100	92.3	96.2	100	88.5	96.2	100	72.7	81.8	90.9
		Ph1/3	100	100	100	88.5	88.5	100	100	100	100	81.8	90.9	100
		Ph1/4	100	100	100	76.9	88.5	92.3	80.8	92.6	100	63.6	90.9	100
	2 nd Ph	Ph2/1	100	100	100	42.3	53.8	61.5	30.8	53.8	57.7	27.3	36.4	36.4
		Ph2/2	100	100	100	80.8	88.5	88.5	76.9	92.3	96.2	100	100	100
	3 rd Ph	Ph3/1	100	100	100	80.8	88.5	88.5	88.5	92.3	100	100	100	100
		Ph3/2	100	100	100	80.9	100	100	92.3	100	100	90.9	100	100

Tables 2.54 and 2.55 show the percentages of correct species attributions for each morphological trait for each species and age group. The same data are visually presented with the use of charts (Figs. 2.131 to 2.196).

Trait 1 on the mandible seems to have performed better in young animals (100% of correct initial attributions) than in old animals, in both taxa. The reason may be that in young animals the foramen, when present, looks relatively larger and, as such, it is more visible than in mandibles from older animals.

As far as deciduous teeth are concerned, good performances were provided by groups 1 and 2. This result is due to the fact that, as they are deciduous teeth, the traits could only be evaluated in these ‘young’ animals. It also confirms that the morphological traits are more visible when teeth are in earlier stages of wear than in advanced stages (for example Group 4).

Age also affects permanent teeth. Traits on permanent teeth were, generally, more visible in the age Groups 2 and 3 than in Group 1, in both species. This is also due to the fact that some characteristics are located in areas that are completely visible only when the tooth is completely erupted (for instance trait 3 on the P₃ and on the P₄, traits 2 and 5 on the M₃); as such, these traits are less assessable on very young mandibles. Data regarding Group 4 (older animals) show that, with a heavy degree of wear, the assessment of morphological traits becomes more difficult as the characteristics can be hidden (by calculus deposits for example) or completely worn. Despite the small sample size, the conclusions reached from this study on teeth are consistent with Zeder and Pilaar’s study (2010): morphological characteristics on teeth are highly affected by age.

The sample size increases when the other anatomical elements are considered. The traits on the horncores do not seem to be influenced by age, showing high percentages of correct

identifications for both goat and sheep at any age-group (Group 1 in sheep is simply not represented in the sample).

It has already mentioned that the articulation of the scapula is age related, as with time it tends to lose its well-defined shape (elliptical in sheep and circular in goat). This phenomenon is more visible in sheep than in goats (trait 2 has been more successful in Group 3 and 4 for goats, while in sheep it has provided high results only in Group 1). On the goat humerus, trait 3 and 4 can acquire intermediate aspects with age as the lateral crest and the pits tend to develop further (trait 4 has been defined as less consistent by Clutton-Brock *et al.* 1990 as well). Consequently, the distinction between sheep and goat becomes more difficult and the reliability of the criteria may be affected.

Trait 1 and 2 on the goat radius seems to be affected by age but in opposite ways. While the lateral bump on the proximal articulation seems to develop further with age, making the distinction with sheep more complicated in older animals, the sharpening of the shape of the proximal end (Trait 2) happens later in the development of the animal, so that this feature seems to be more reliable in juvenile and adult individuals than in young individuals (as also noticed by Zeder and Lapham 2010).

Among the goat group, the traits on the ulna were less efficient in young and juvenile animals (especially Group 1, but also marginally, for Group 2). Trait 2 has also been considered less reliable in young animals also by Clutton-Brock *et al.* (1990). This might be due to the fact that both traits tend to be fully developed when the animal is adult, while in younger individuals they can acquire an intermediate appearance. For the other anatomical elements no pattern could be clearly recognised.

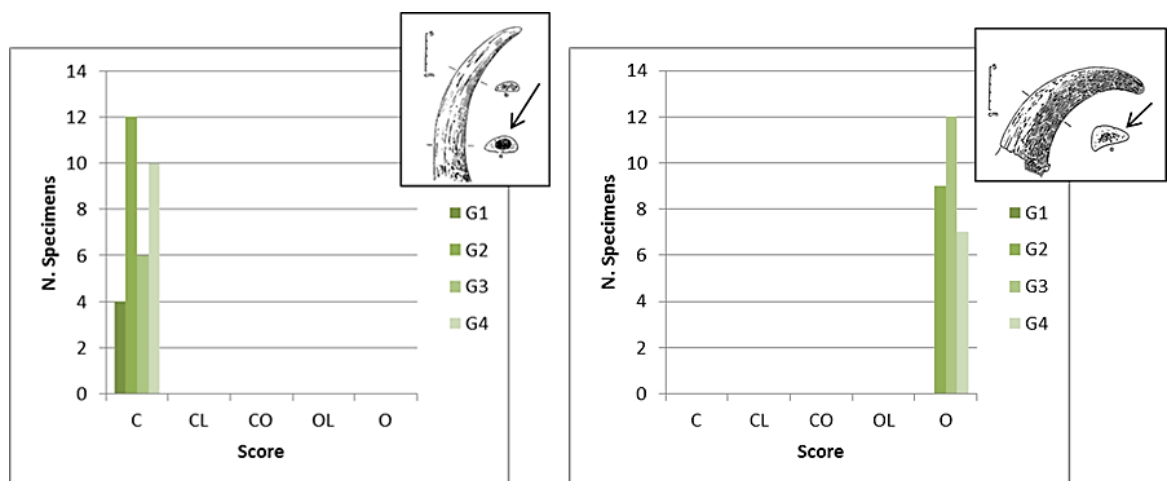


Figure 2.131 Horncore, trait 1 (section) number of specimens attributed to the different categories for the different age-groups for the goat (left) and the sheep (right). Legend: G1= age group 1; G2= age group 2; G3= age group 3; G4= age group 4. On the horizontal axis: C= *Capra*; CL= *Capra-like*; CO= *Capra/Ovis*; OL= *Ovis-like*; O=*Ovis*.

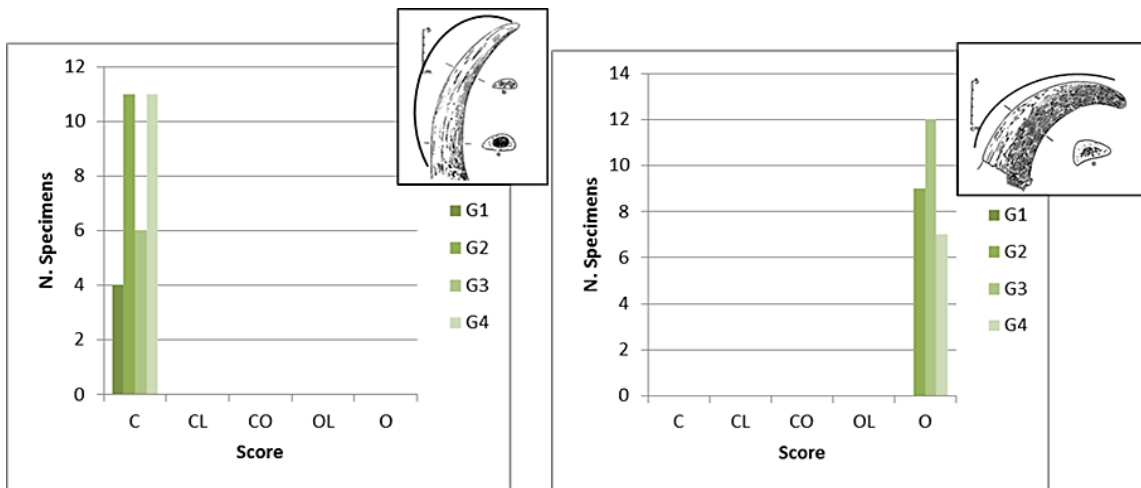


Figure 2.132 Horncore, trait 2 (curvature) number of specimens attributed to the different categories for the different age-groups for the goat (left) and the sheep (right). For details see Fig. 2.131.

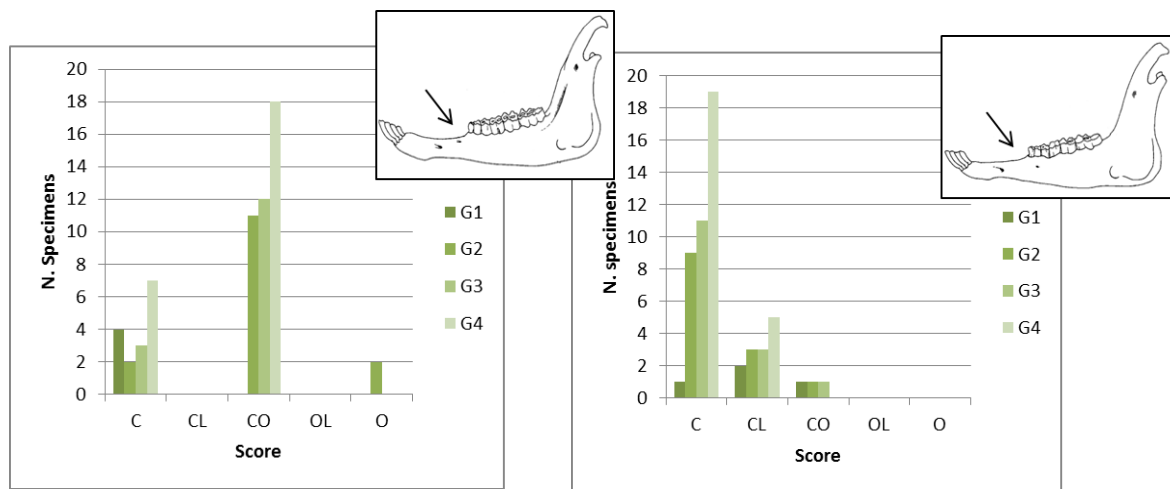


Figure 2.133 Mandible, trait 1 (presence/absence of the foramen) number of specimens attributed to the different categories for the different age-groups for the goat (left) and the sheep (right). For details see Fig. 2.131.

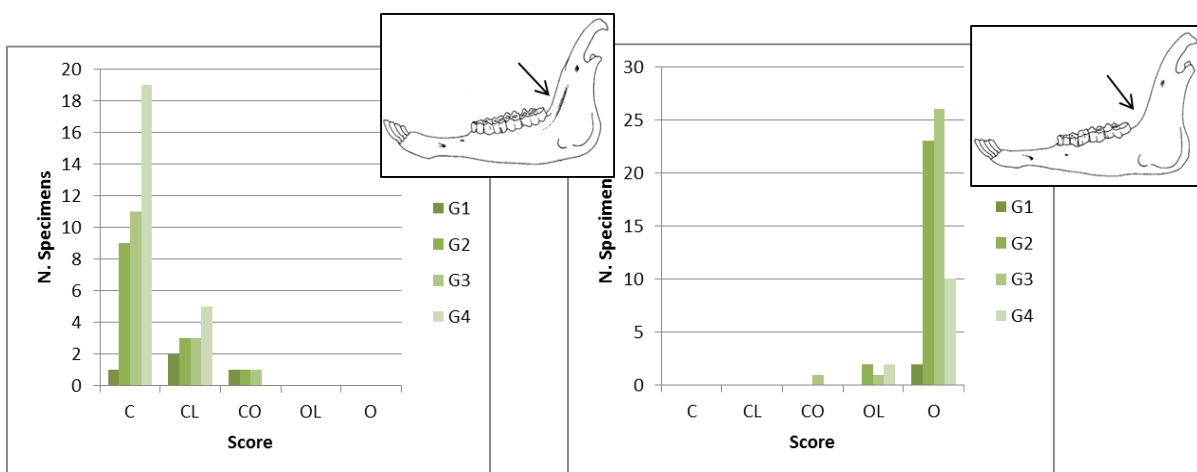


Figure 2.134 Mandible, trait 2 (aspect of the hollow) number of specimens attributed to the different categories for the different age-groups for the goat (left) and the sheep (right). For details see Fig. 2.131.

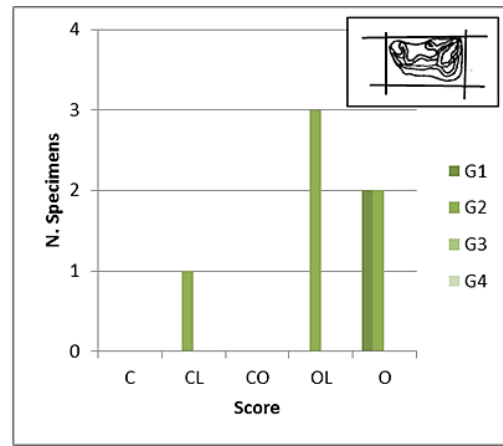
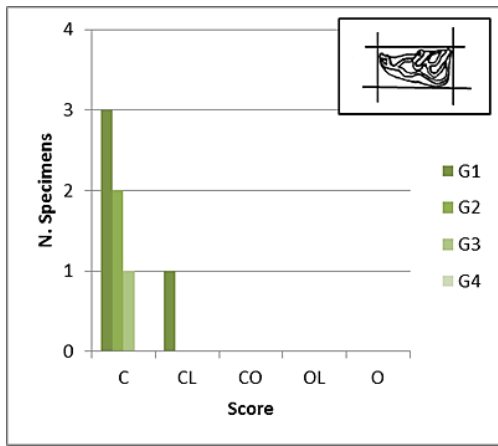


Figure 2.135 Third deciduous lower premolar dP₃, trait 1 (overall aspect) number of specimens attributed to the different categories for the different age-groups for the goat (left) and the sheep (right). For details see Fig. 2.131.

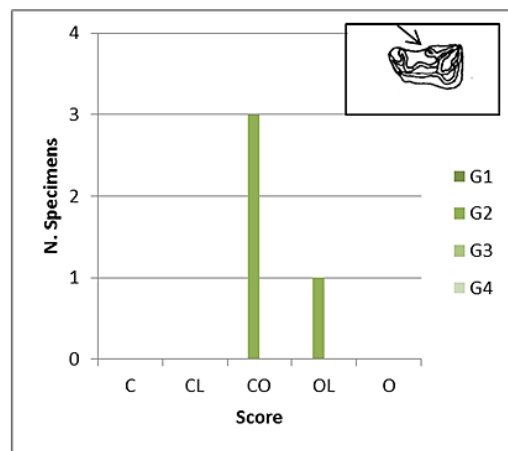
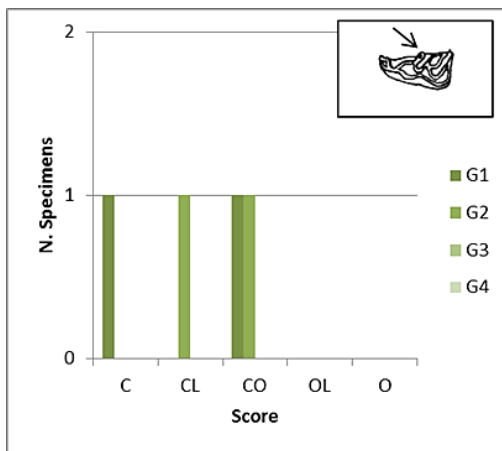


Figure 2.136 Third deciduous lower premolar dP₃, trait 2 (appearance of the metaconoid) number of specimens attributed to the different categories for the different age-groups for the goat (left) and the sheep (right). For details see Fig. 2.131.

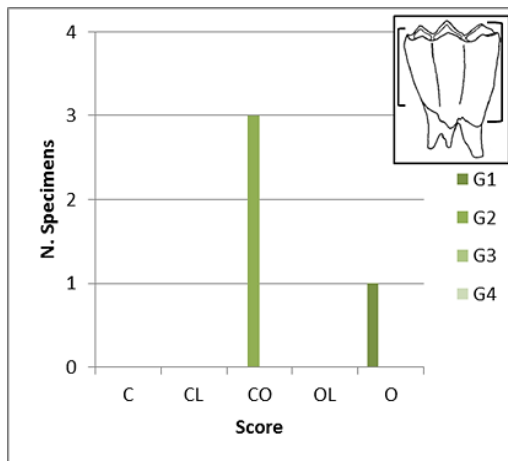
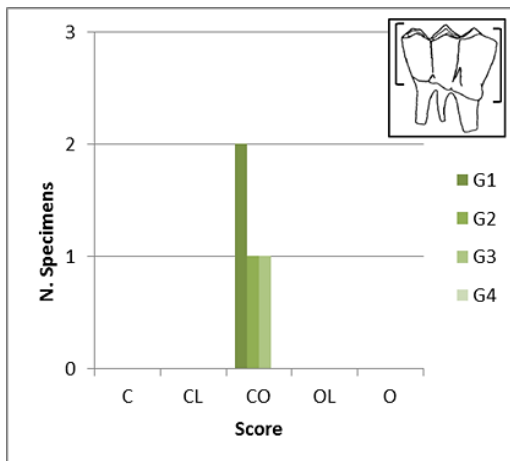


Figure 2.137 Fourth deciduous lower premolar dP₄, trait 1 (crown aspect) number of specimens attributed to the different categories for the different age-groups for the goat (left) and the sheep (right). For details see Fig. 2.131.

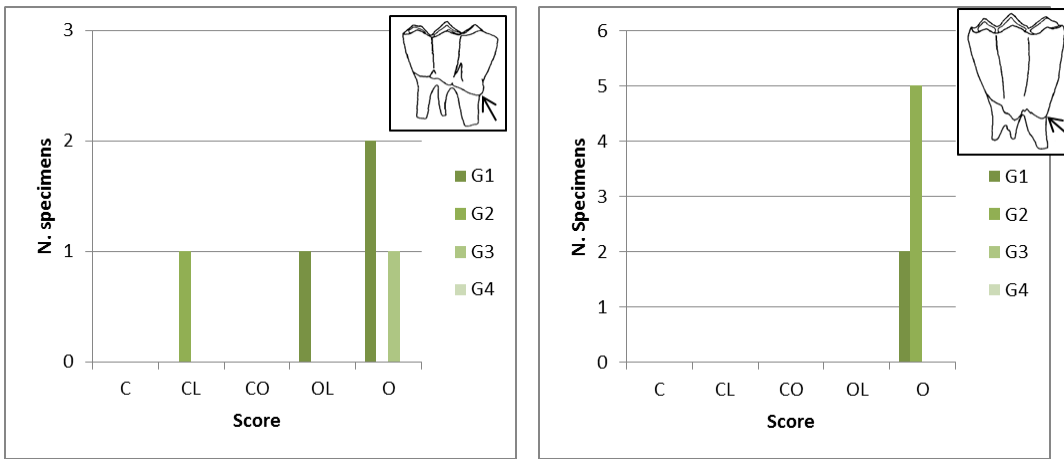


Figure 2.138 Fourth deciduous lower premolar dP_4 , trait 2 (presence/absence basal swelling) number of specimens attributed to the different categories for the different age-groups for the goat (left) and the sheep (right). For details see Fig. 2.131.

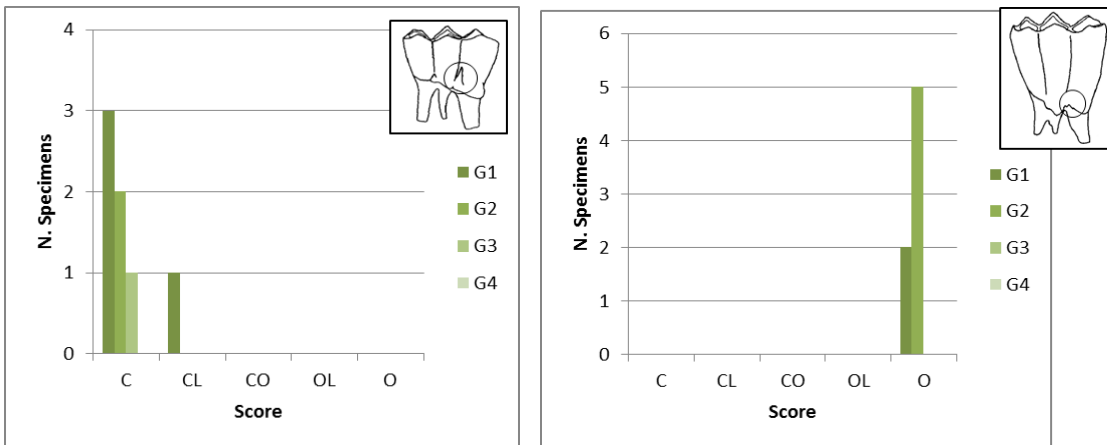


Figure 2.139 Fourth deciduous lower premolar dP_4 , trait 3 (presence/absence inter-lobar pillar) number of specimens attributed to the different categories for the different age-groups for the goat (left) and the sheep (right). For details see Fig. 2.131.

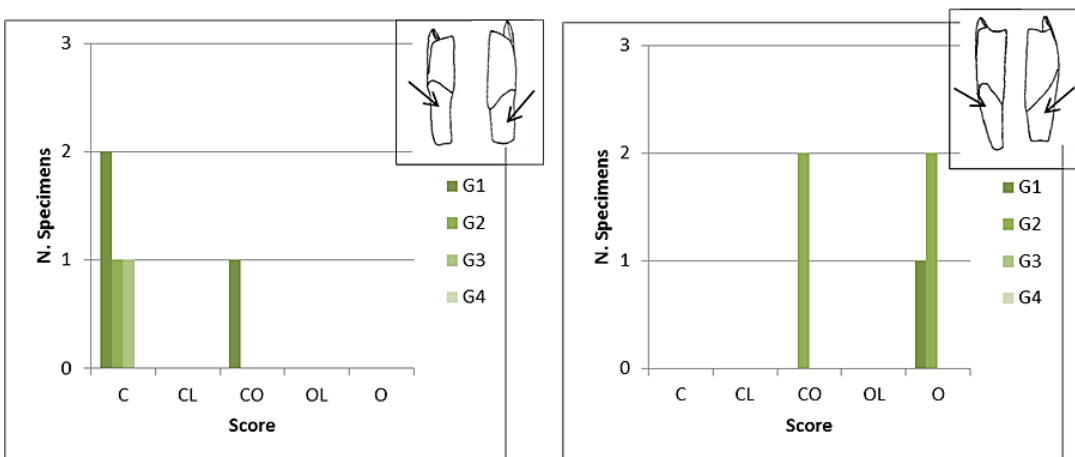


Figure 2.140 Fourth deciduous lower premolar dP_4 , trait 4 (enamel development on medial and distal face) number of specimens attributed to the different categories for the different age-groups for the goat (left) and the sheep (right). For details see Fig. 2.131.

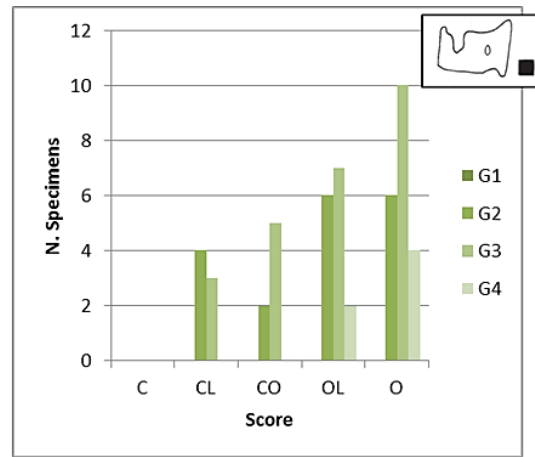
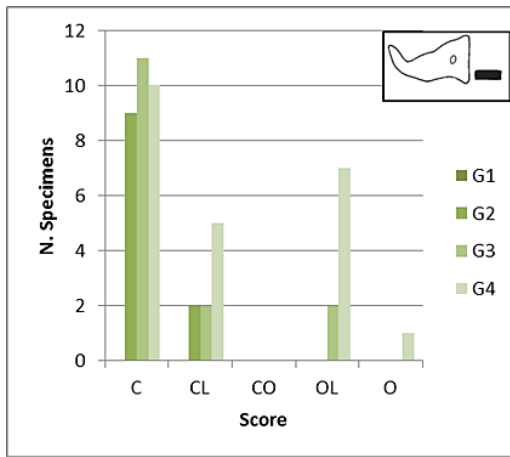


Figure 2.141 Third lower premolar P₃, trait 1 (overall aspect) number of specimens attributed to the different categories for the different age-groups for the goat (left) and the sheep (right). For details see Fig. 2.131.

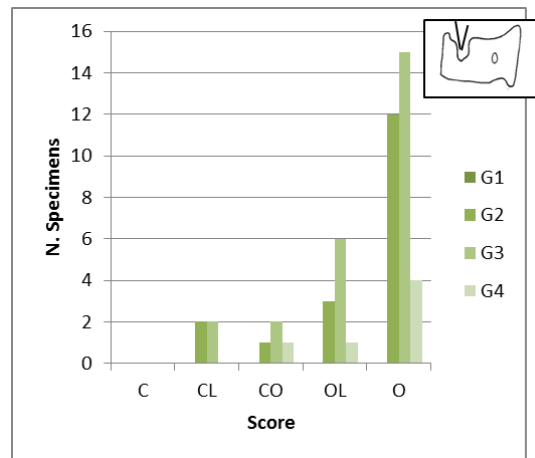
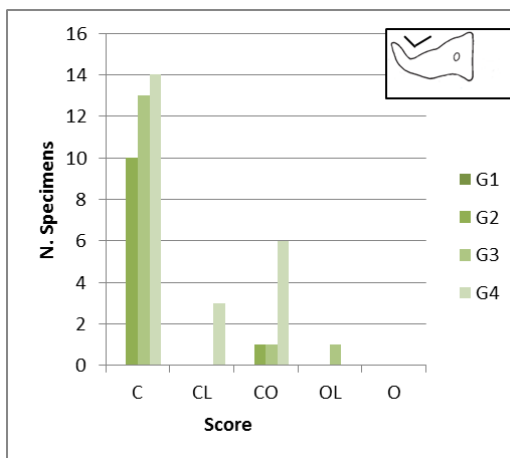


Figure 2.142 Third lower premolar P₃, trait 2 (aspect middle vertical ridge) number of specimens attributed to the different categories for the different age-groups for the goat (left) and the sheep (right). For details see Fig. 2.131.

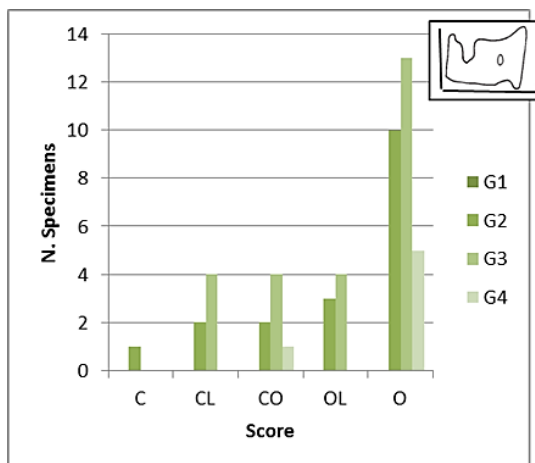
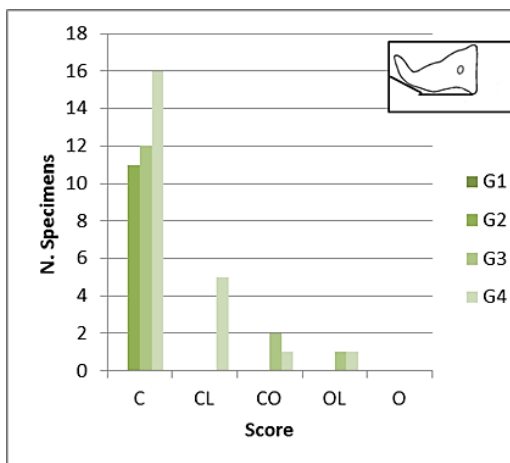


Figure 2.143 Third lower premolar P₃, trait 3 (aspect mesial-buccal angle) number of specimens attributed to the different categories for the different age-groups for the goat (left) and the sheep (right). For details see Fig. 2.131.

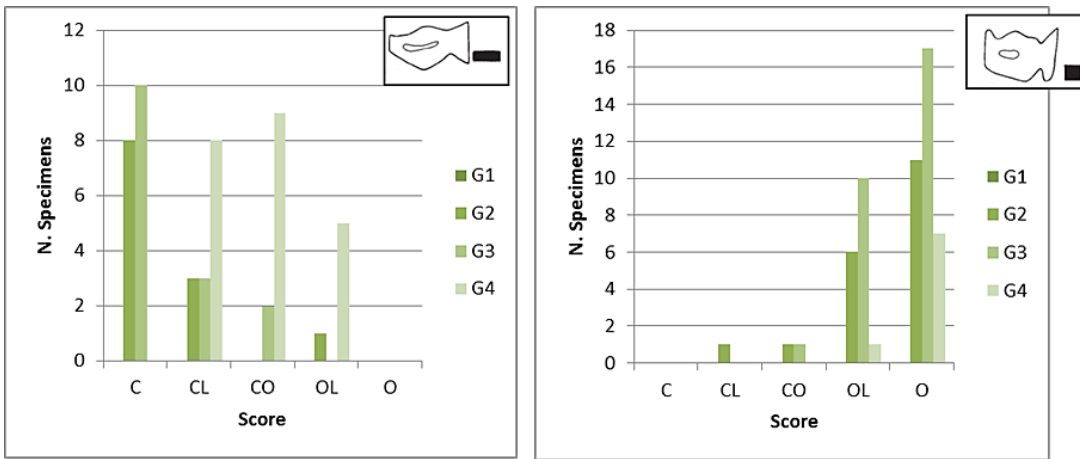


Figure 2.144 Fourth lower premolar P₄, trait 1 (overall shape) number of specimens attributed to the different categories for the different age-groups for the goat (left) and the sheep (right). For details see Fig. 2.131.

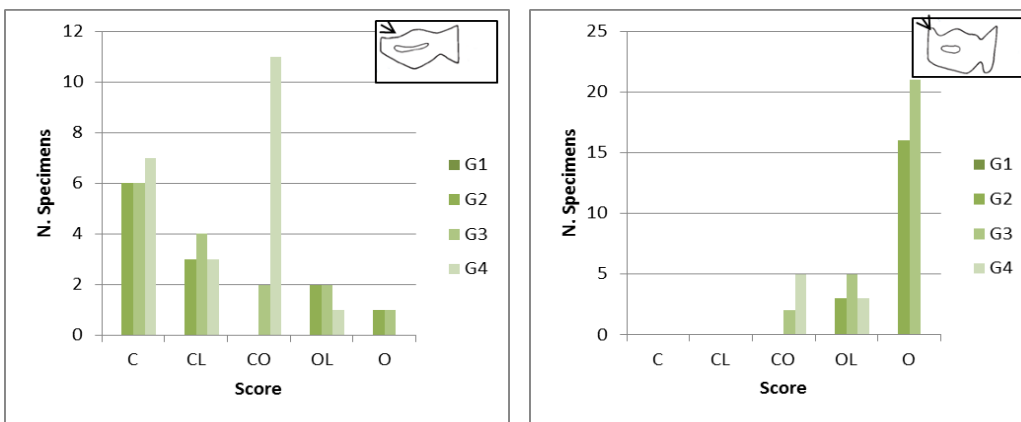


Figure 2.145 Fourth lower premolar P₄, trait 2 (aspect of the mesio-lingual rib) number of specimens attributed to the different categories for the different age-groups for the goat (left) and the sheep (right). For details see Fig. 2.131.

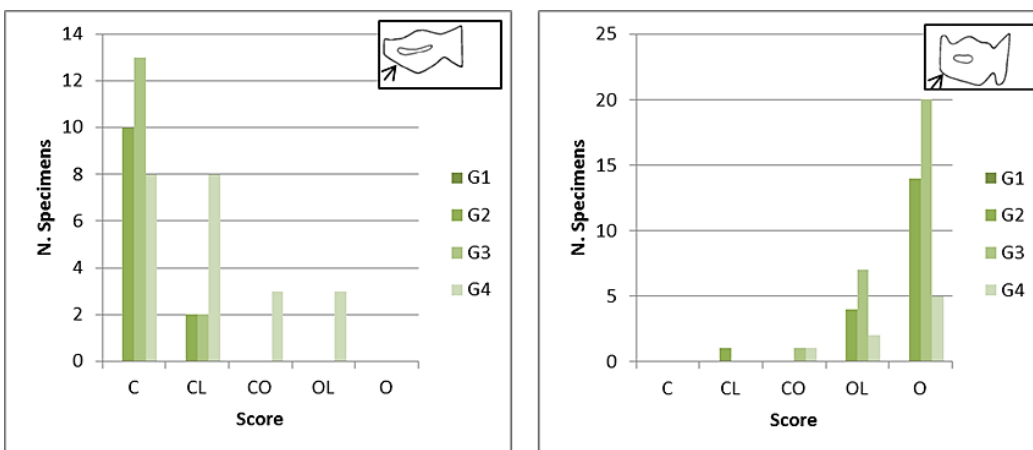


Figure 2.146 Fourth lower premolar P₄, trait 3 (aspect of the mesio-buccal angle) number of specimens attributed to the different categories for the different age-groups for the goat (left) and the sheep (right). For details see Fig. 2.131.

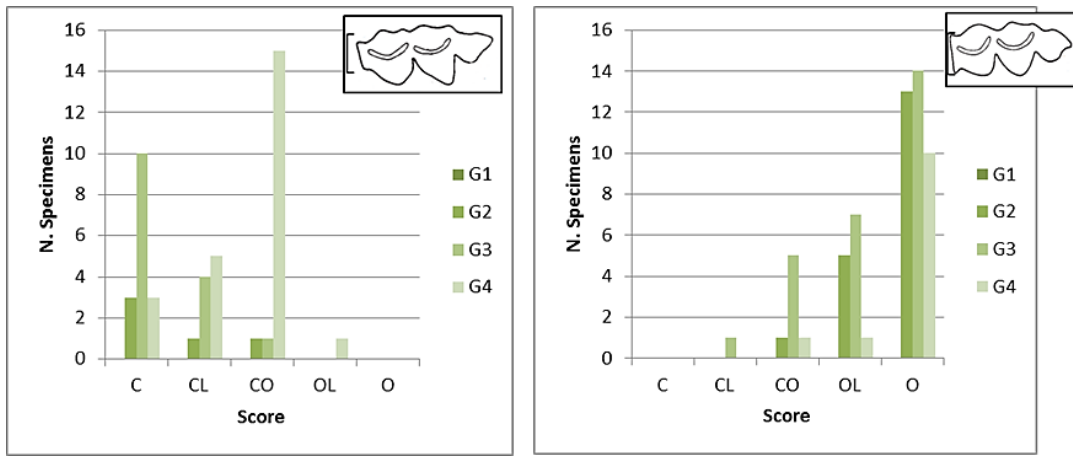


Figure 2.147 Third lower molar M_3 , trait 1 (aspect mesial face) number of specimens attributed to the different categories for the different age-groups for the goat (left) and the sheep (right). For details see Fig. 2.131.

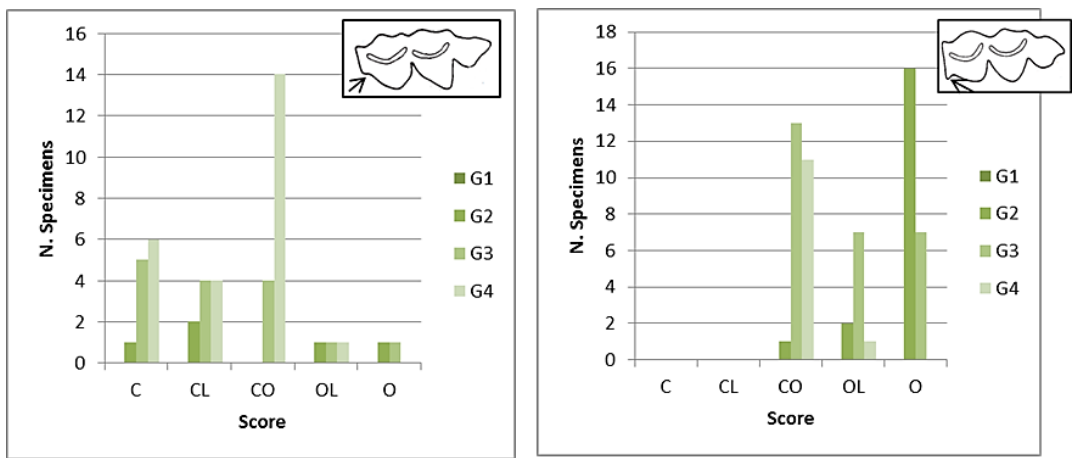


Figure 2.148 Third lower molar M_3 , trait 2 (aspect buccal edge angle) number of specimens attributed to the different categories for the different age-groups for the goat (left) and the sheep (right). For details see Fig. 2.131.

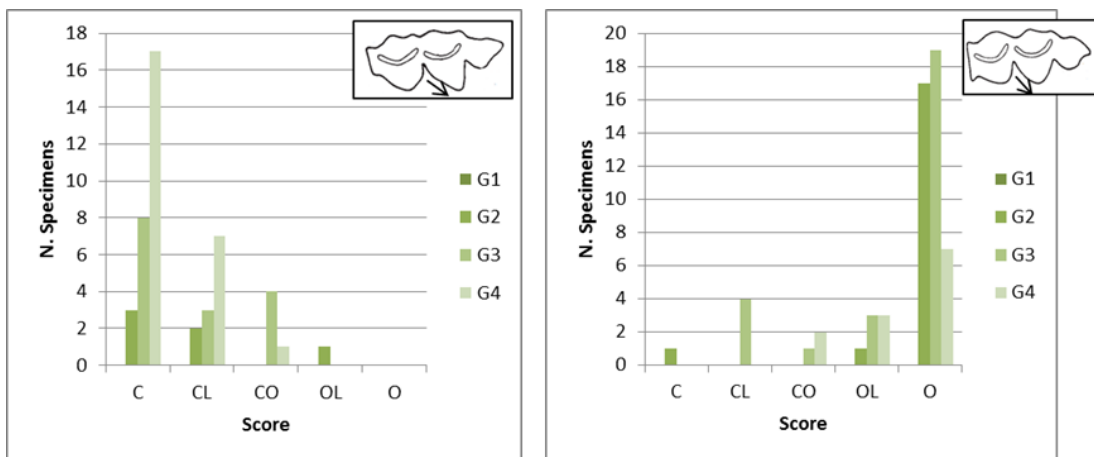


Figure 2.149 Third lower molar M_3 , trait 3 (direction of central cusp) number of specimens attributed to the different categories for the different age-groups for the goat (left) and the sheep (right). For details see Fig. 2.131.

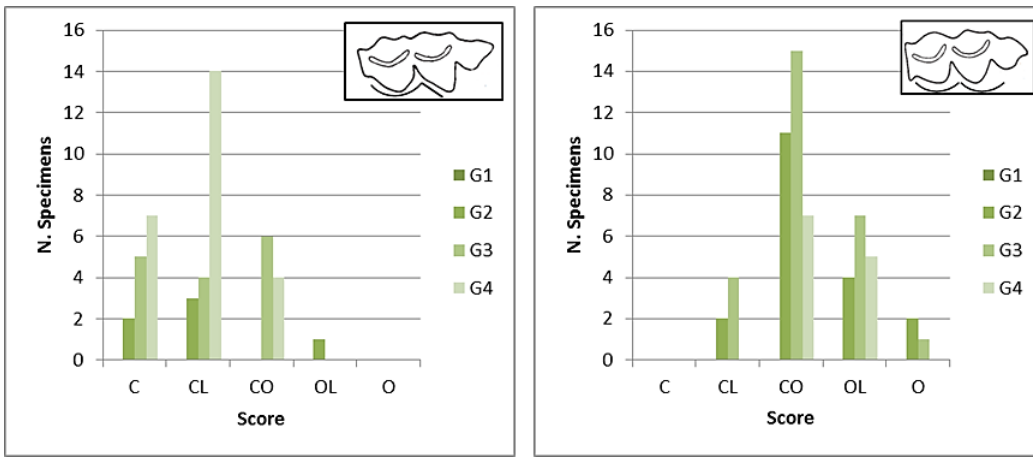


Figure 2.150 Third lower molar M_3 , trait 4 (symmetry and shape of the cusps) number of specimens attributed to the different categories for the different age-groups for the goat (left) and the sheep (right). For details see Fig. 2.131.

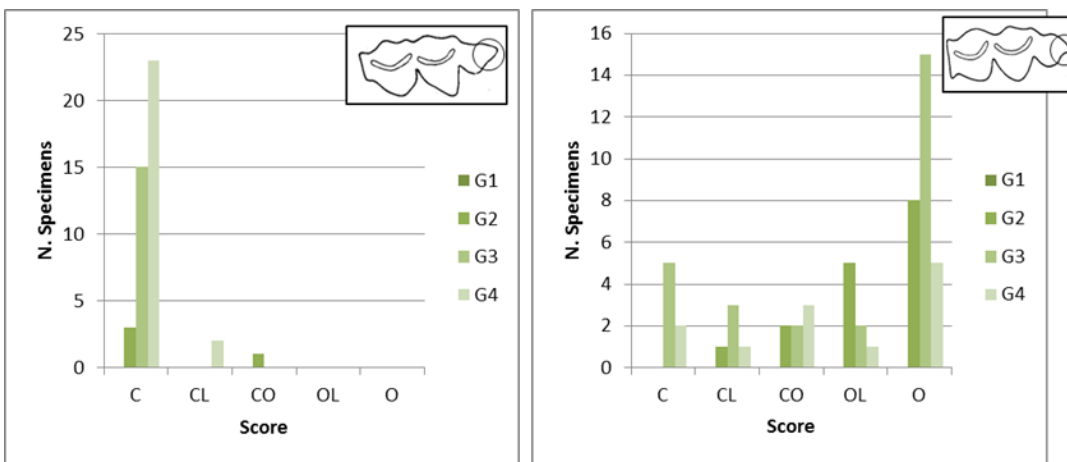


Figure 2.151 Third lower molar M_3 , trait 5 (aspect of the distal flute) number of specimens attributed to the different categories for the different age-groups for the goat (left) and the sheep (right). For details see Fig. 2.131.

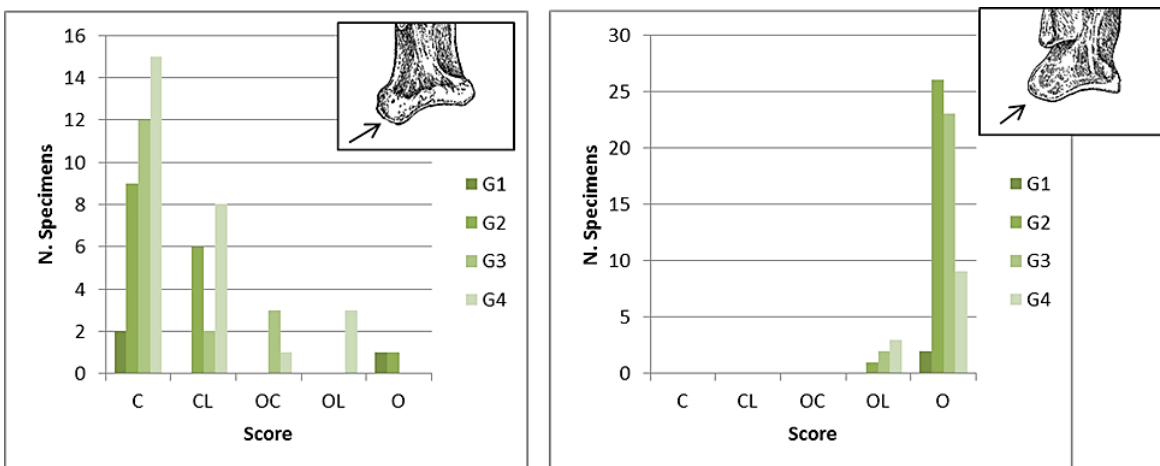


Figure 2.152 Scapula, trait 1 (shape of the glenoid tubercle) number of specimens attributed to the different categories for the different age-groups for the goat (left) and the sheep (right). For details see Fig. 2.131.

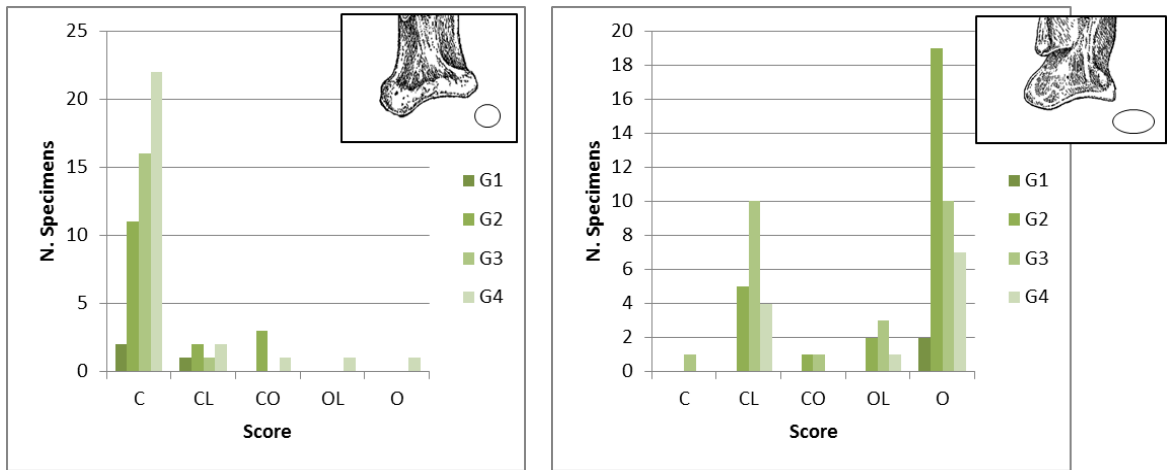


Figure 2.153 Scapula, trait 2 (shape of the glenoid cavity) number of specimens attributed to the different categories for the different age-groups for the goat (left) and the sheep (right). For details see Fig. 2.131.

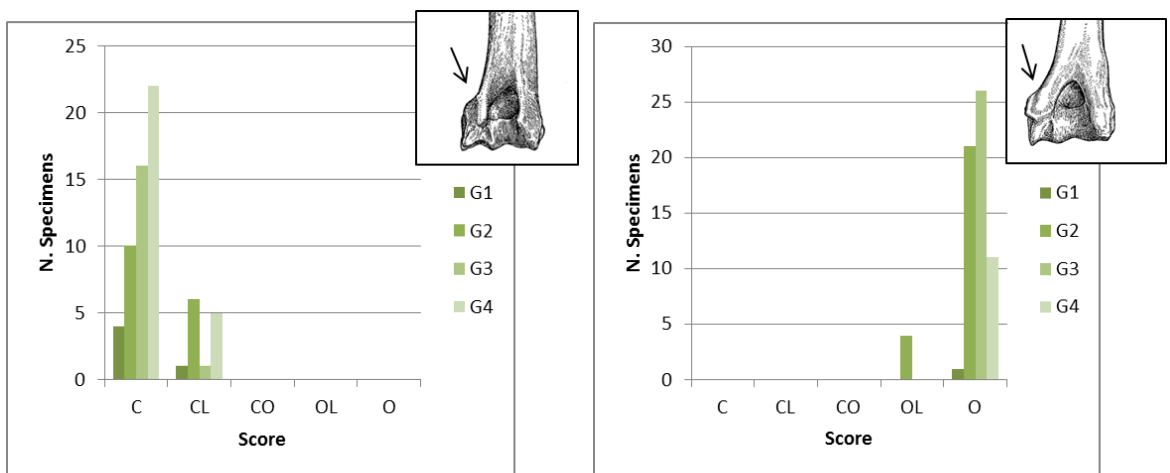


Figure 2.154 Humerus, trait 1 (shape of the lateral epicondyle) number of specimens attributed to the different categories for the different age-groups for the goat (left) and the sheep (right). For details see Fig. 2.131.

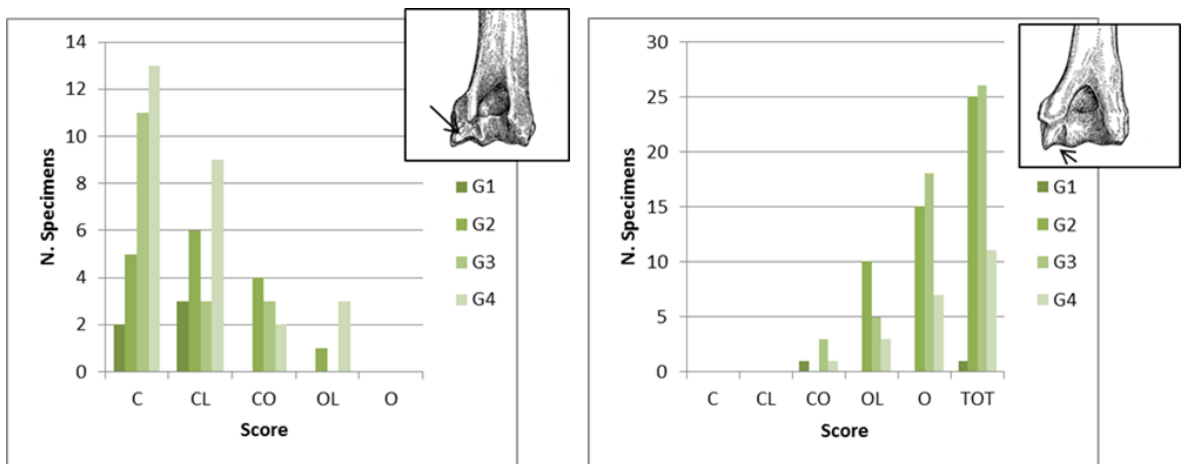


Figure 2.155 Humerus, trait 2 (aspect of the groove on the posterior side of the lateral condyle) number of specimens attributed to the different categories for the different age-groups for the goat (left) and the sheep (right). For details see Fig. 2.131.

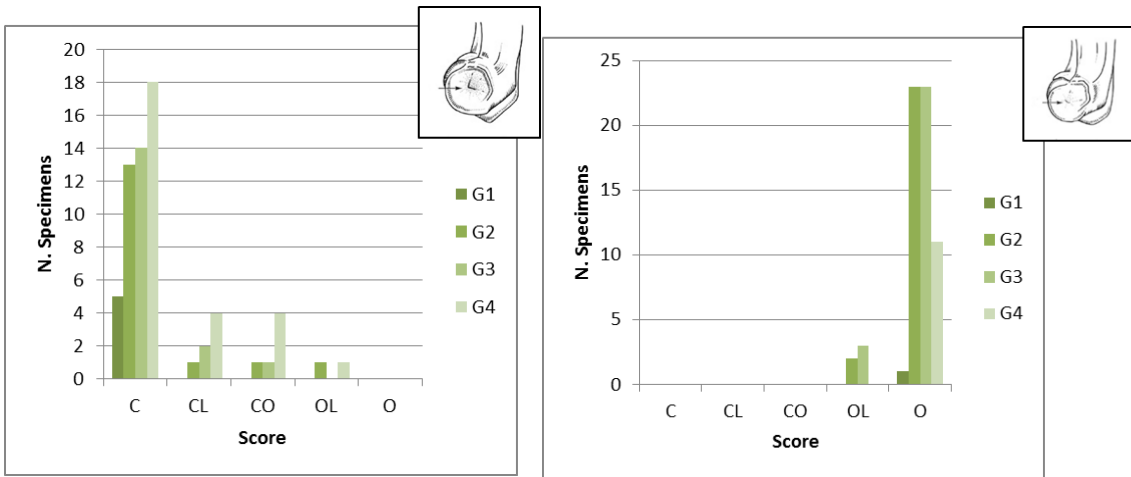


Figure 2.156 Humerus, trait 3 (aspect of the pit on the lateral epicondilar surface) number of specimens attributed to the different categories for the different age-groups for the goat (left) and the sheep (right). For details see Fig. 2.131.

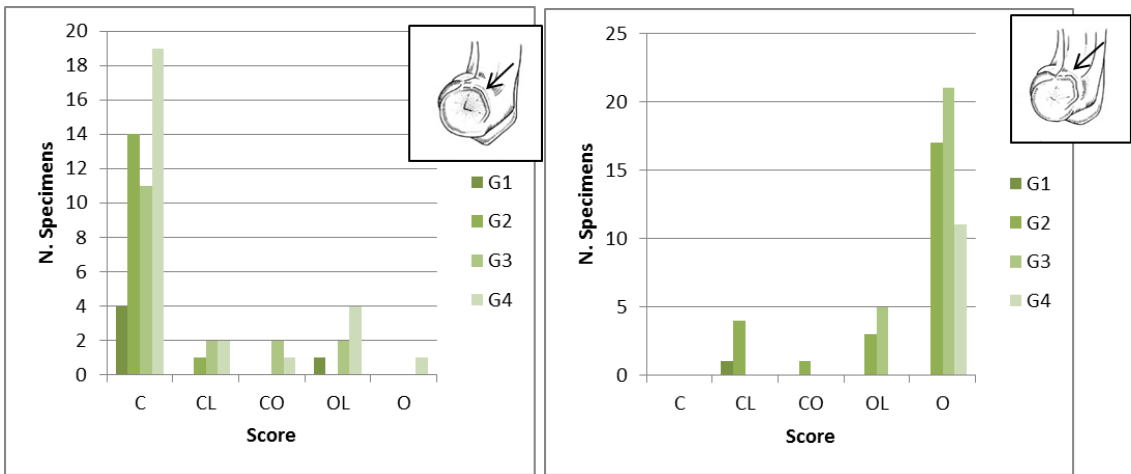


Figure 2.157 Humerus, trait 4 (absence/presence of the thickening on the lateral border of the epicondilar surface) number of specimens attributed to the different categories for the different age-groups for the goat (left) and the sheep (right). For details see Fig. 2.131.

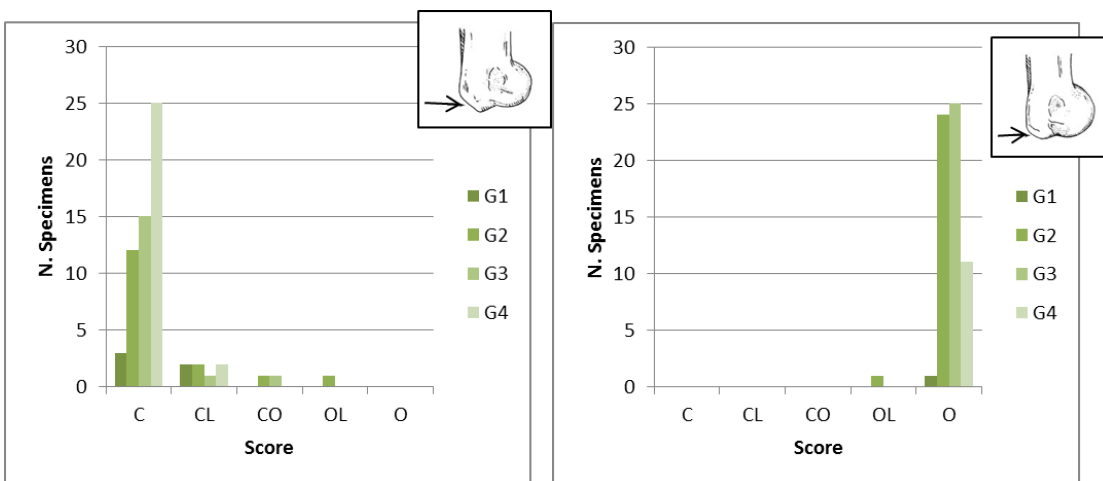


Figure 2.158 Humerus, trait 5 (aspect on the angle of the distal part of the medial epicondyle) number of specimens attributed to the different categories for the different age-groups for the goat (left) and the sheep (right). For details see Fig. 2.131.

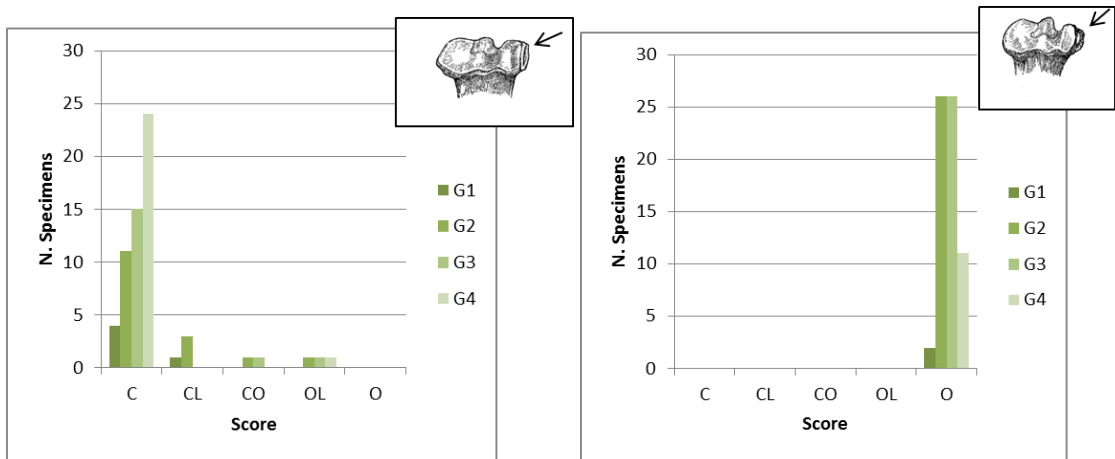


Figure 2.159 Radius, trait 1 (aspect of the lateral tuberosity) number of specimens attributed to the different categories for the different age-groups for the goat (left) and the sheep (right). For details see Fig. 2.131.

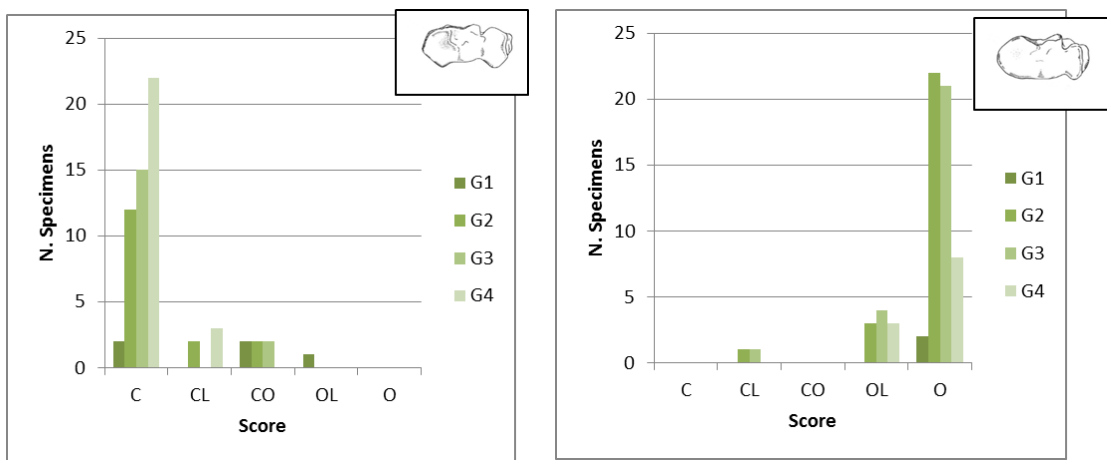


Figure 2.160 Radius, trait 2 (overall aspect of the proximal articular surface) number of specimens attributed to the different categories for the different age-groups for the goat (left) and the sheep (right). For details see Fig. 2.131.

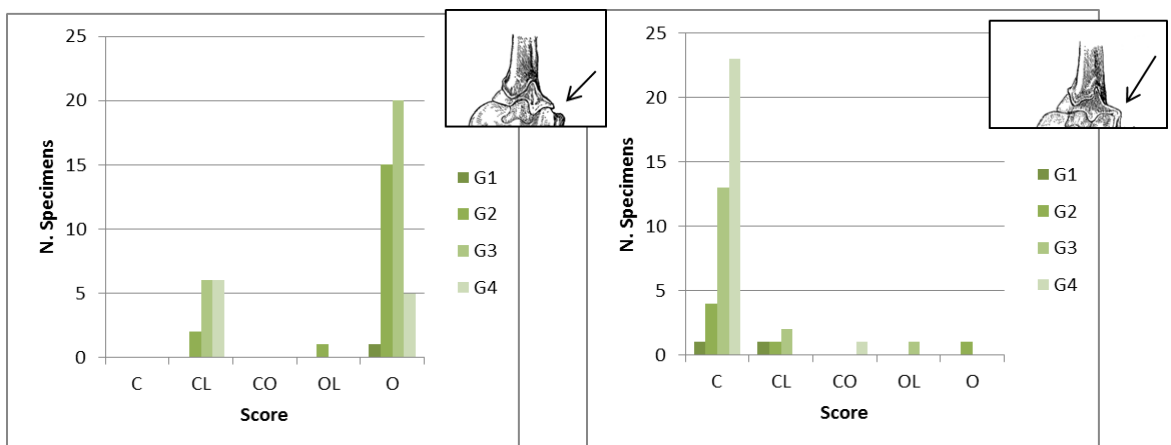


Figure 2.161 Ulna, trait 1 (projection of the lateral coronoid process) number of specimens attributed to the different categories for the different age-groups for the goat (left) and the sheep (right). For details see Fig. 2.131.

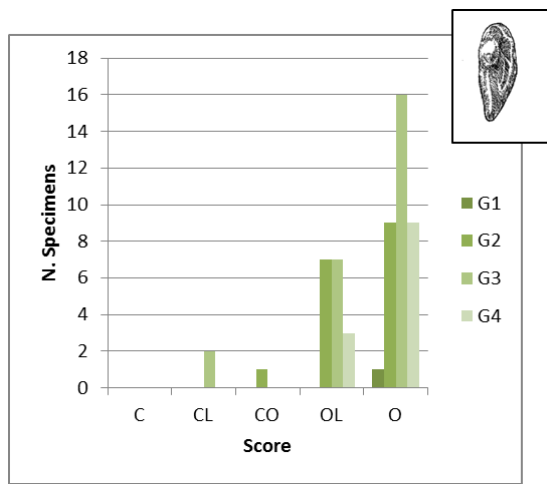
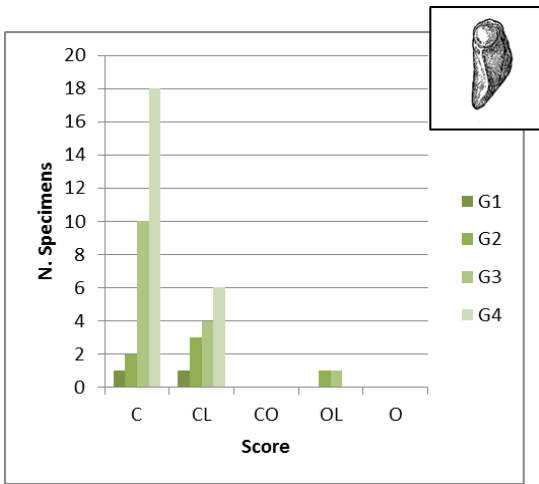


Figure 2.162 Ulna, trait 2 (overall shape of the *olecranon*) number of specimens attributed to the different categories for the different age-groups for the goat (left) and the sheep (right). For details see Fig. 2.131.

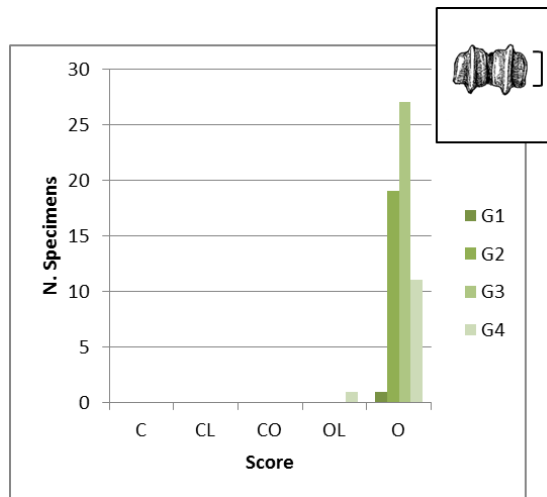
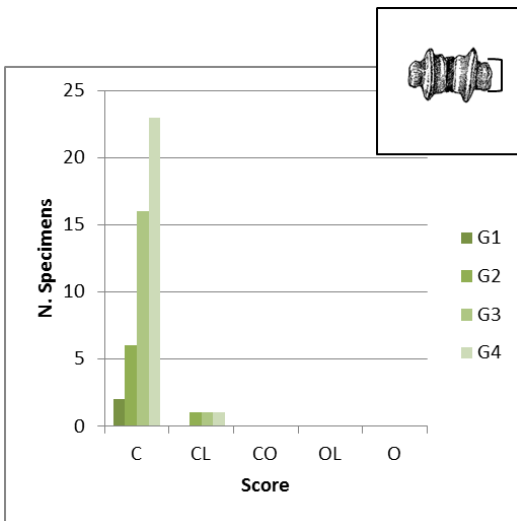


Figure 2.163 Metacarpal, trait 1 (dimension of the peripheral part of the trochlear condyles) number of specimens attributed to the different categories for the different age-groups for the goat (left) and the sheep (right). For details see Fig. 2.131.

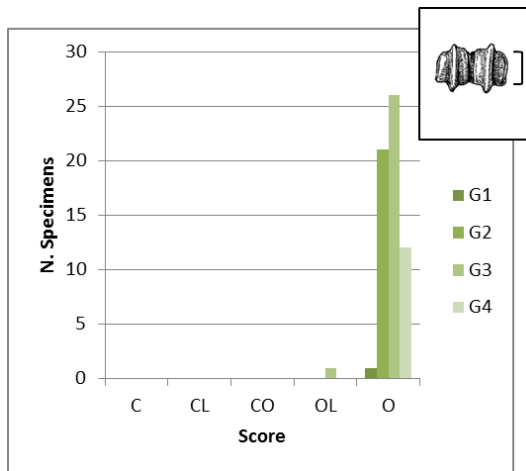
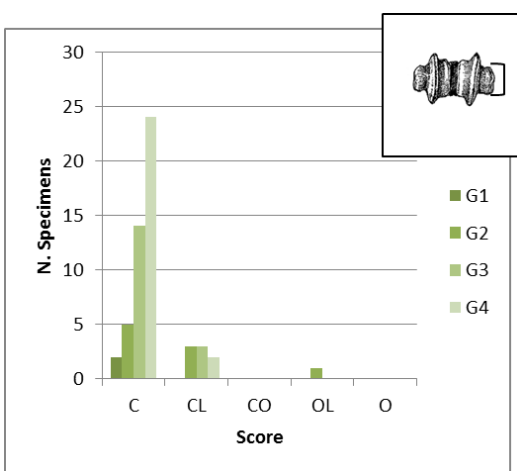


Figure 2.164 Metatarsal, trait 1 (dimension of the peripheral part of the trochlear condyles) number of specimens attributed to the different categories for the different age-groups for the goat (left) and the sheep (right). For details see Fig. 2.131.

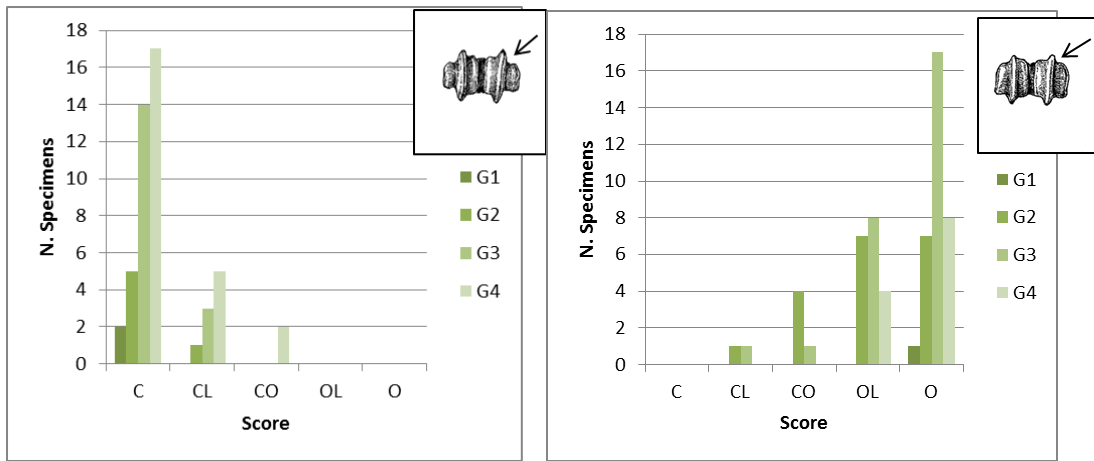


Figure 2.165 Metacarpal, trait 2 (definition of the peripheral part of the trochlear condyles) number of specimens attributed to the different categories for the different age-groups for the goat (left) and the sheep (right). For details see Fig. 2.131.

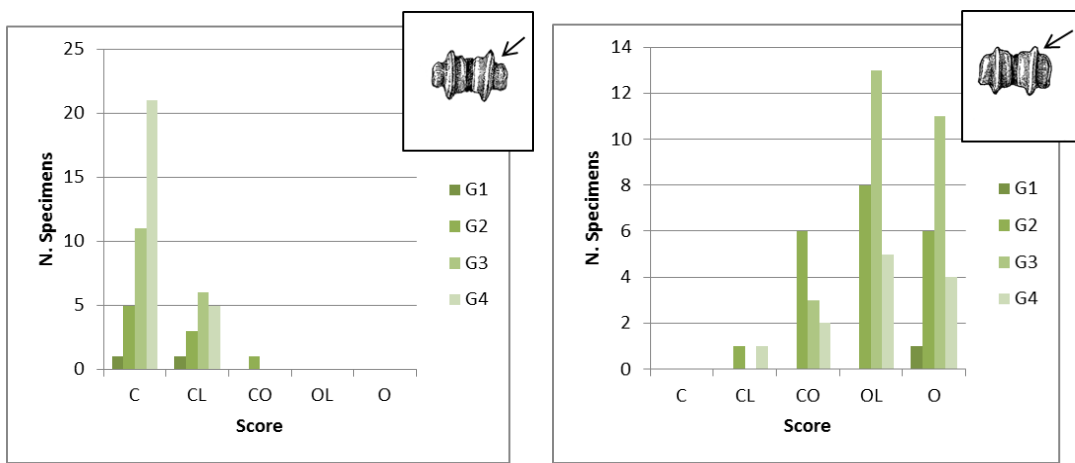


Figure 2.166 Metatarsal, trait 2 (definition of the peripheral part of the trochlear condyles) number of specimens attributed to the different categories for the different age-groups for the goat (left) and the sheep (right). For details see Fig. 2.131.

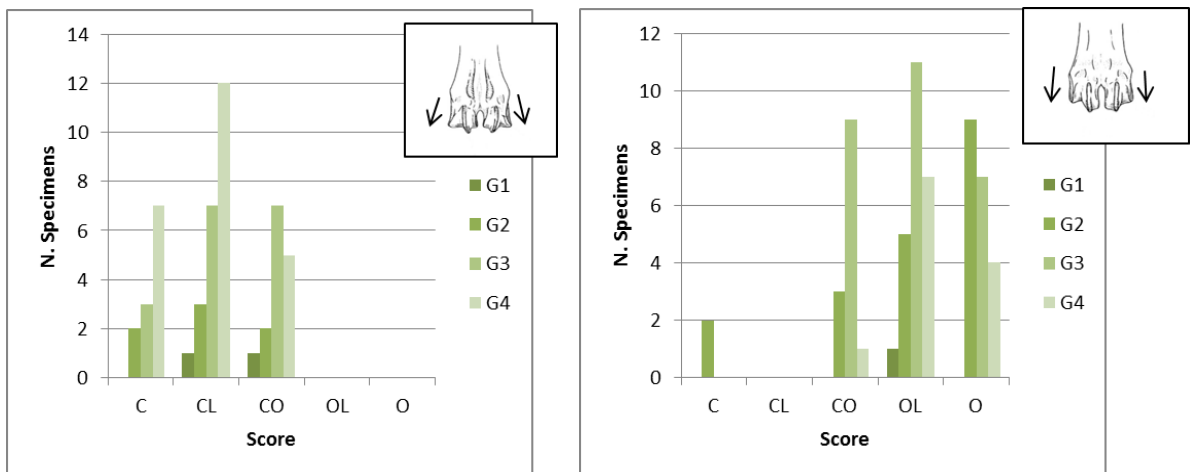


Figure 2.167 Metacarpal, trait 3 (aspect of the peripheral part of the trochlear condyles) number of specimens attributed to the different categories for the different age-groups for the goat (left) and the sheep (right). For details see Fig. 2.131.

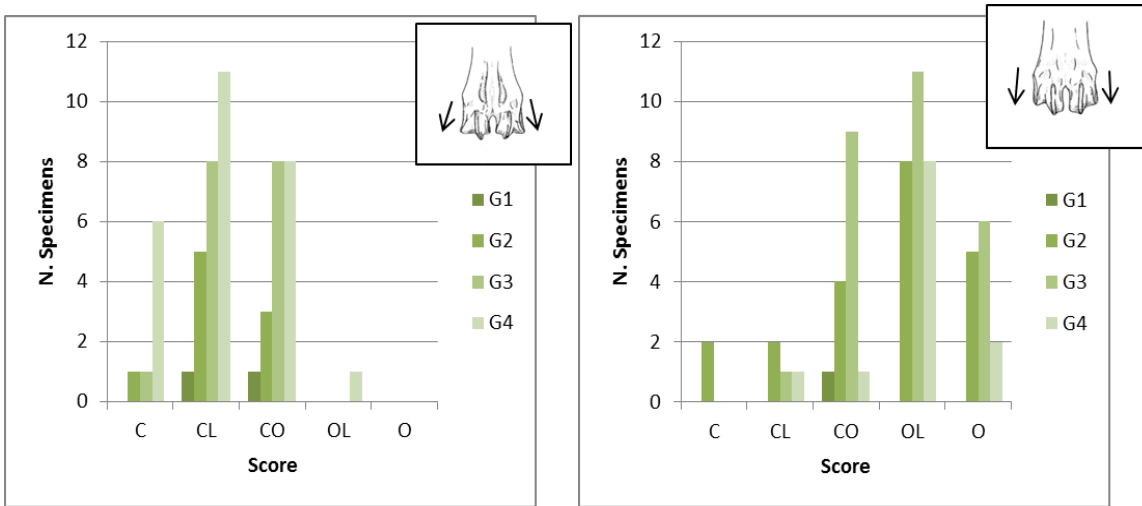


Figure 2.168 Metatarsal, trait 3 (aspect of the peripheral part of the trochlear condyles) number of specimens attributed to the different categories for the different age-groups for the goat (left) and the sheep (right). For details see Fig. 2.131.

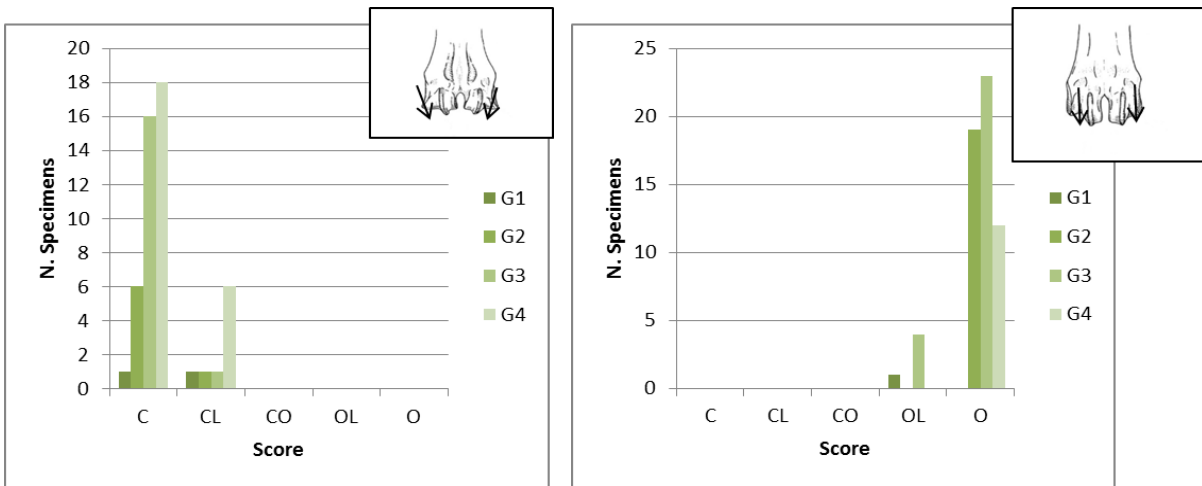


Figure 2.169 Metacarpal, trait 4 (direction of the *verticilli*) number of specimens attributed to the different categories for the different age-groups for the goat (left) and the sheep (right). For details see Fig. 2.131.

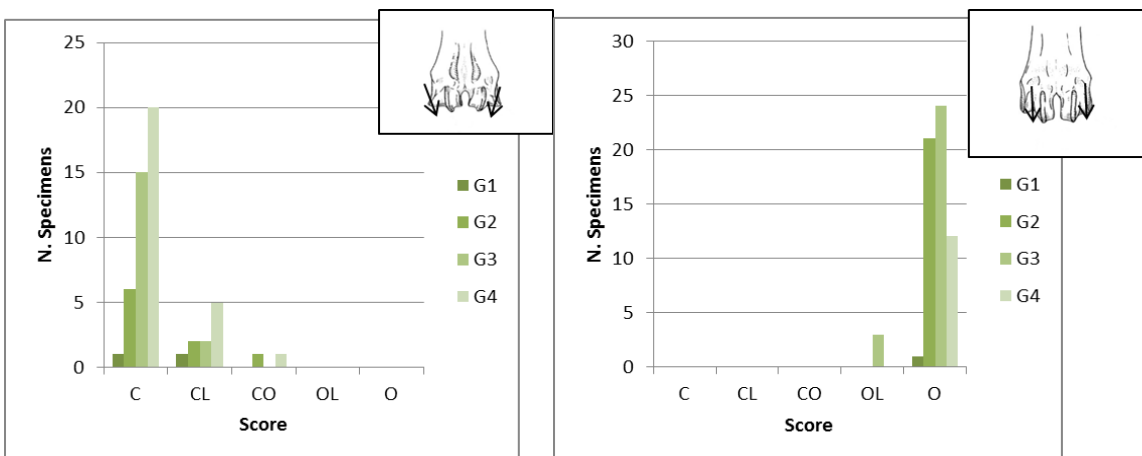


Figure 2.170 Metatarsal, trait 4 (direction of the *verticilli*) number of specimens attributed to the different categories for the different age-groups for the goat (left) and the sheep (right). For details see Fig. 2.131.

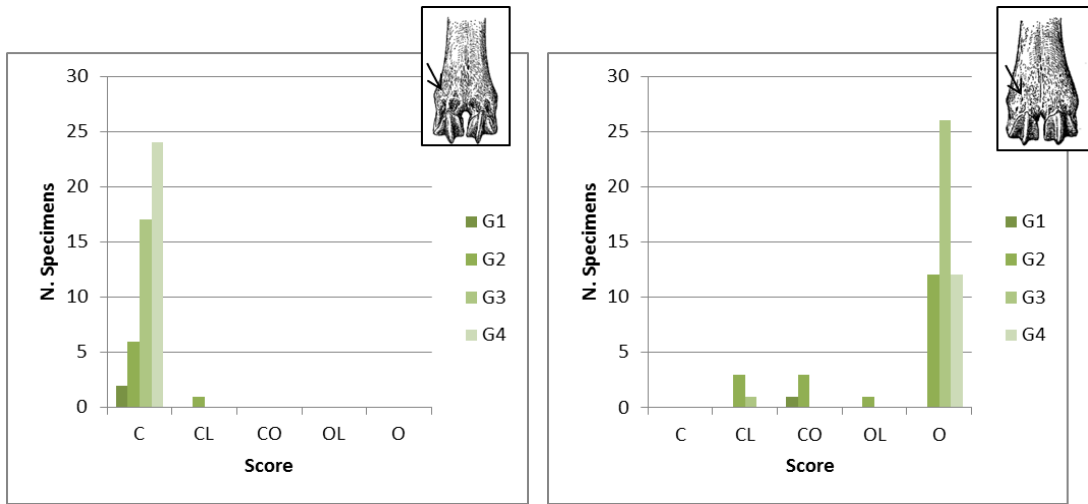


Figure 2.171 Metacarpal, trait 5 (development of the *fossae* on the proximal part of the distal trochlear condyles) number of specimens attributed to the different categories for the different age-groups for the goat (left) and the sheep (right). For details see Fig. 2.131.

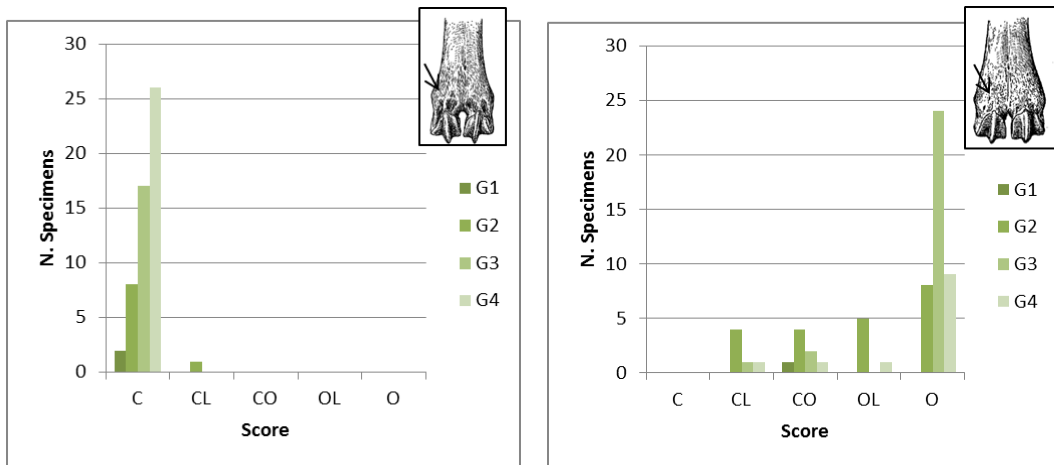


Figure 2.172 Metatarsal, trait 5 (development of the *fossae* on the proximal part of the distal trochlear condyles) number of specimens attributed to the different categories for the different age-groups for the goat (left) and the sheep (right). For details see Fig. 2.131.

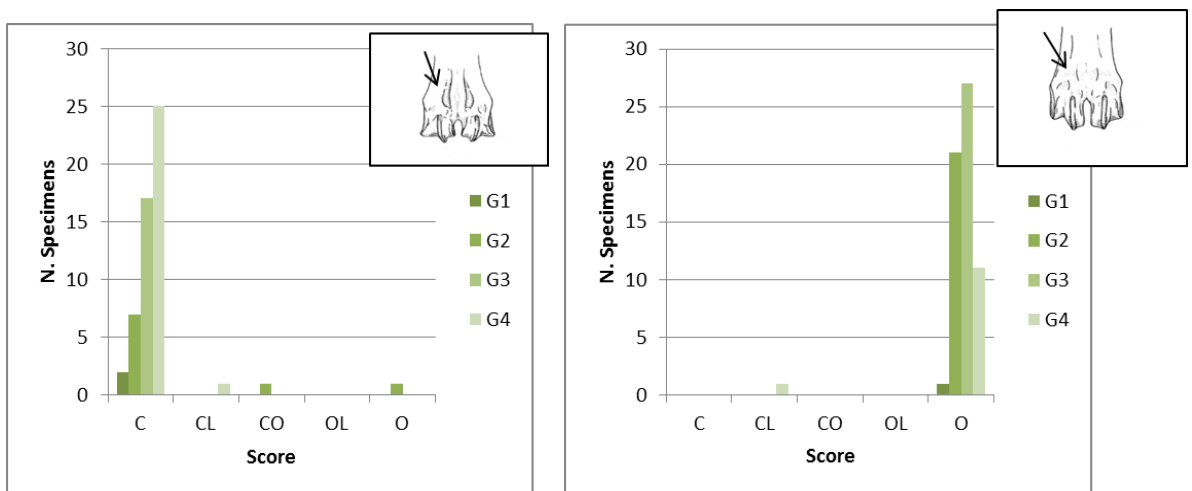


Figure 2.173 Metatarsal, trait 6 (aspect of the junction on the anterior aspect of the distal diaphysis above the distal epiphysis) number of specimens attributed to the different categories for the different age-groups for the goat (left) and the sheep (right). For details see Fig. 2.131.

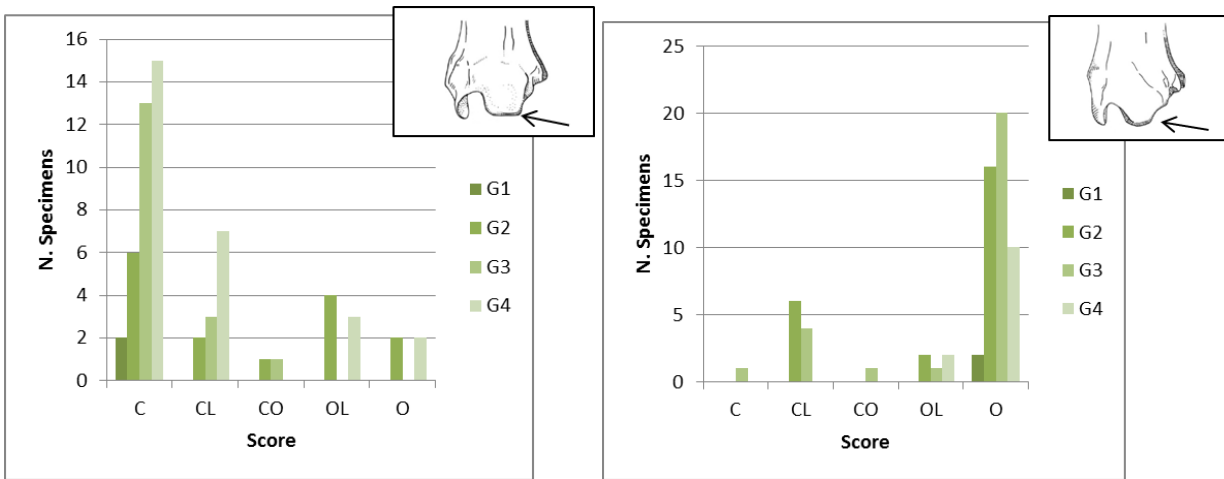


Figure 2.174 Tibia, trait 1 (dorsal prominence) number of specimens attributed to the different categories for the different age-groups for the goat (left) and the sheep (right). For details see Fig. 2.131.

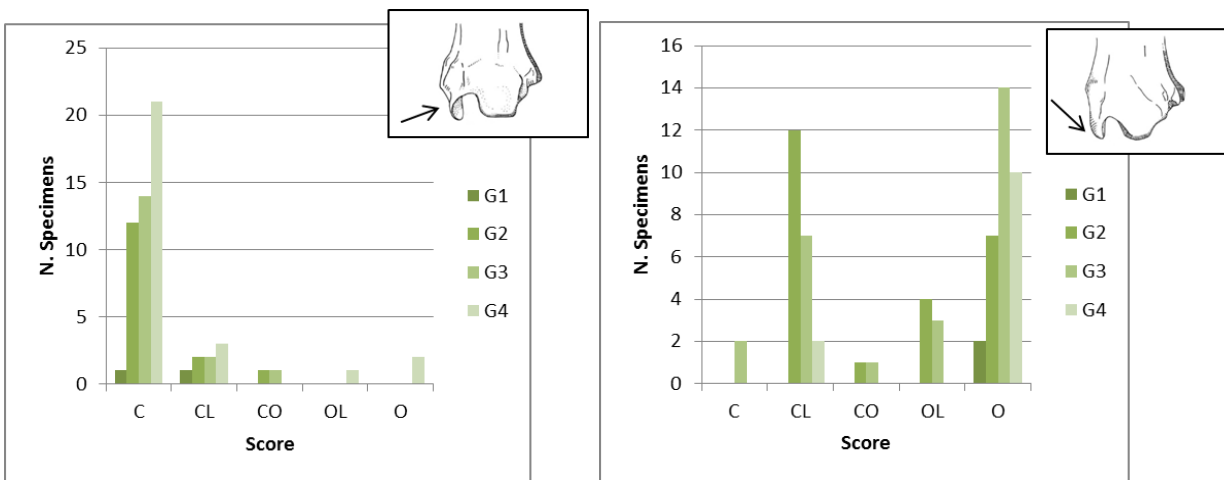


Figure 2.175 Tibia, trait 2 (medial malleolus) number of specimens attributed to the different categories for the different age-groups for the goat (left) and the sheep (right). For details see Fig. 2.131.

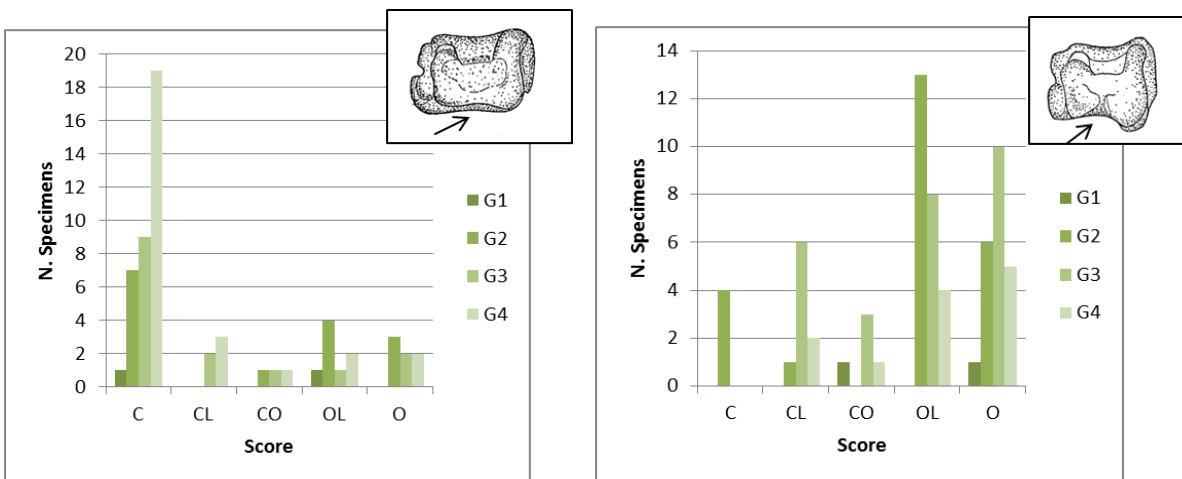


Figure 2.176 Tibia, trait 3 (presence/absence of the interruption on the plantar limbus) number of specimens attributed to the different categories for the different age-groups for the goat (left) and the sheep (right). For details see Fig. 2.131.

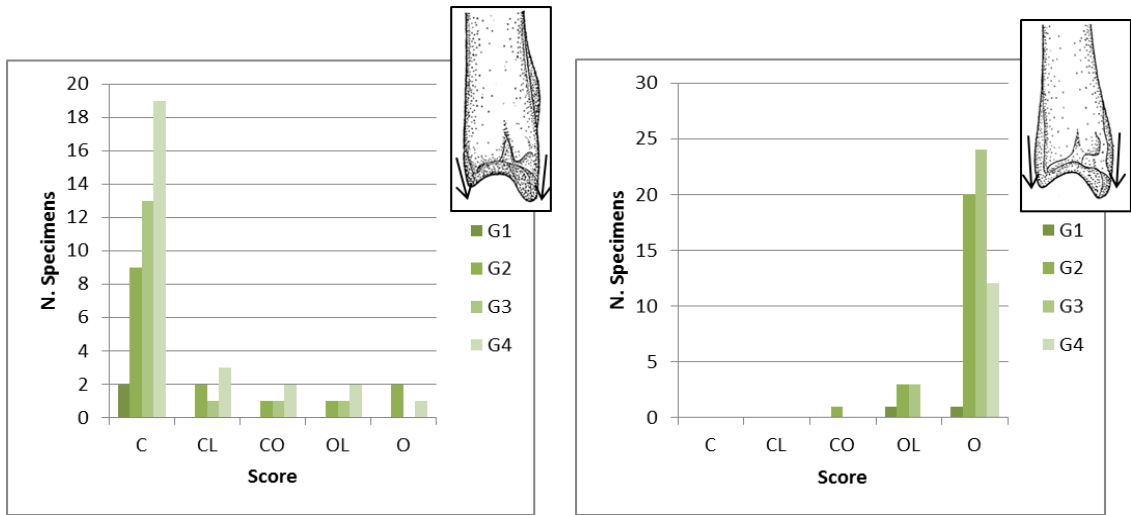


Figure 2.177 Tibia, trait 4 (lateral profile) number of specimens attributed to the different categories for the different age-groups for the goat (left) and the sheep (right). For details see Fig. 2.131.

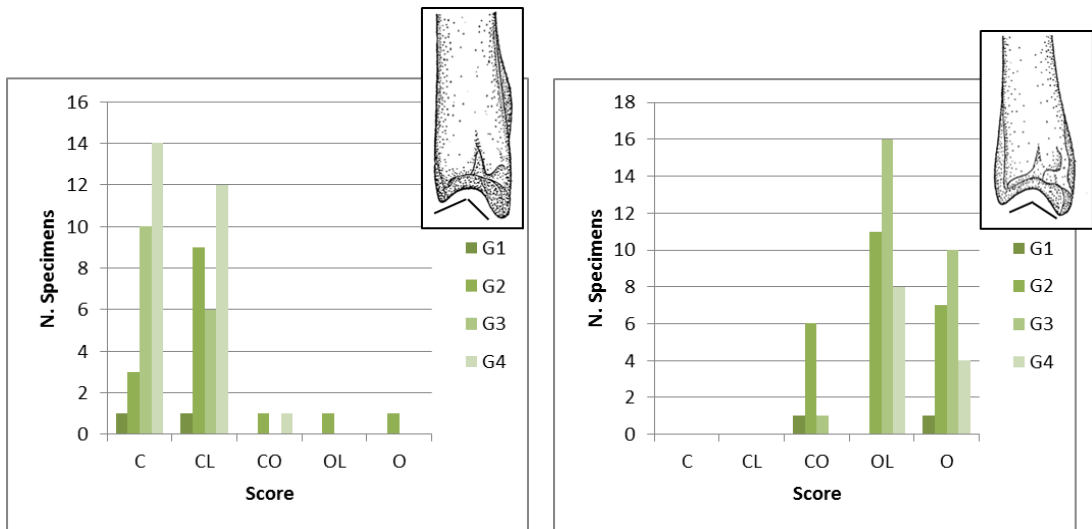


Figure 2.178 Tibia, trait 5 (shape of the anterior side of the *malleolus*) number of specimens attributed to the different categories for the different age-groups for the goat (left) and the sheep (right). For details see Fig. 2.131.

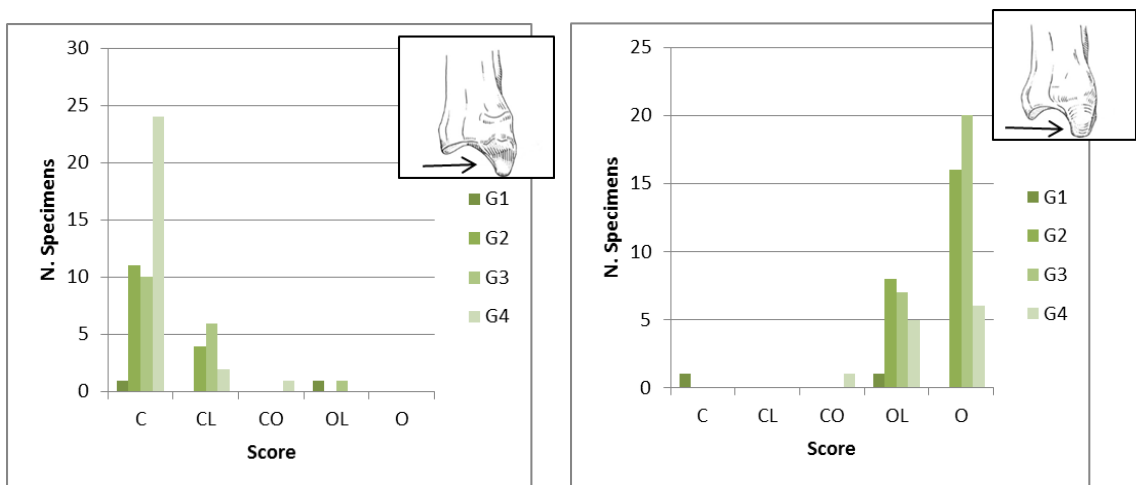


Figure 2.179 Tibia, trait 6 (aspect of the medial *malleolus*) number of specimens attributed to the different categories for the different age-groups for the goat (left) and the sheep (right). For details see Fig. 2.131.

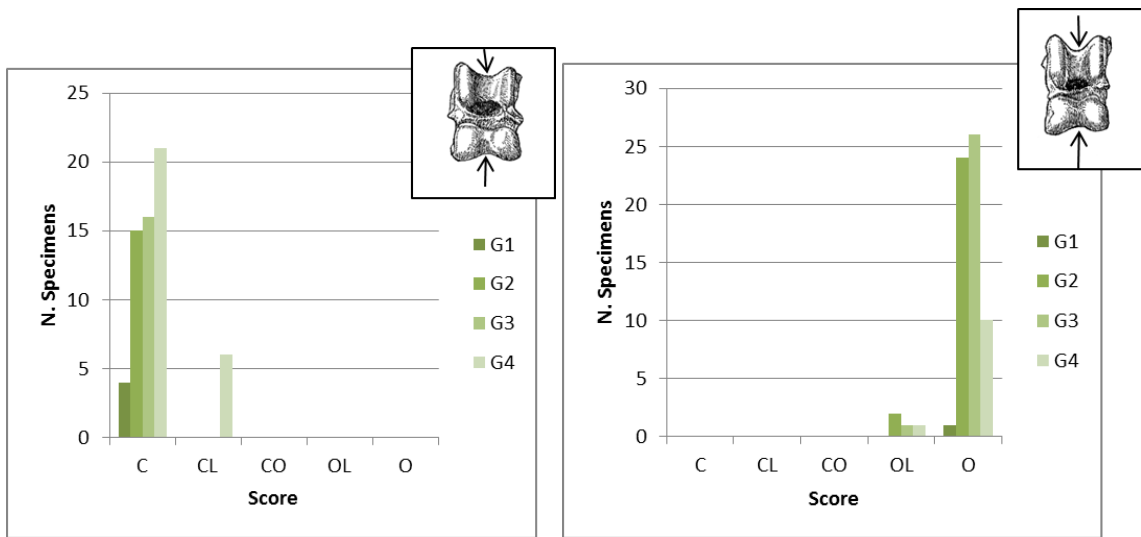


Figure 2.180 Astragalus, trait 1 (depth of the sulcus of the trochlea) number of specimens attributed to the different categories for the different age-groups for the goat (left) and the sheep (right). For details see Fig. 2.131.

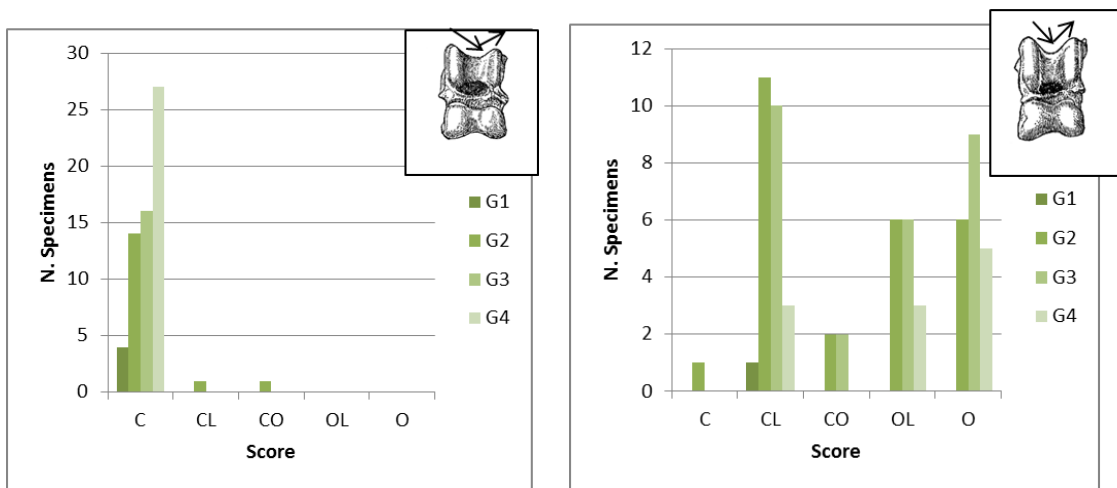


Figure 2.181 Astragalus, trait 2 (inclination of the lateral part of the trochlea) number of specimens attributed to the different categories for the different age-groups for the goat (left) and the sheep (right). For details see Fig. 2.131.

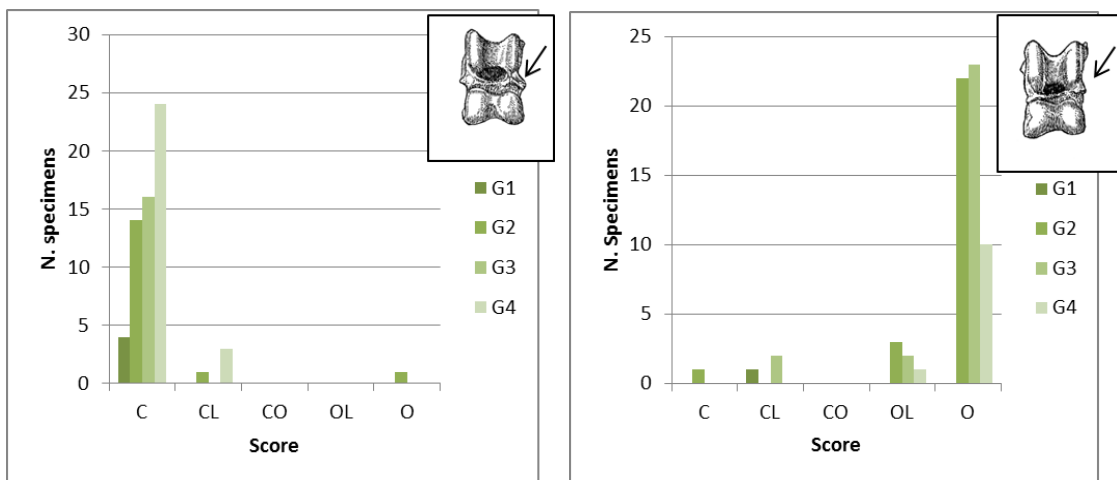


Figure 2.182 Astragalus, trait 3 (shape of the medial ridge) number of specimens attributed to the different categories for the different age-groups for the goat (left) and the sheep (right). For details see Fig. 2.131.

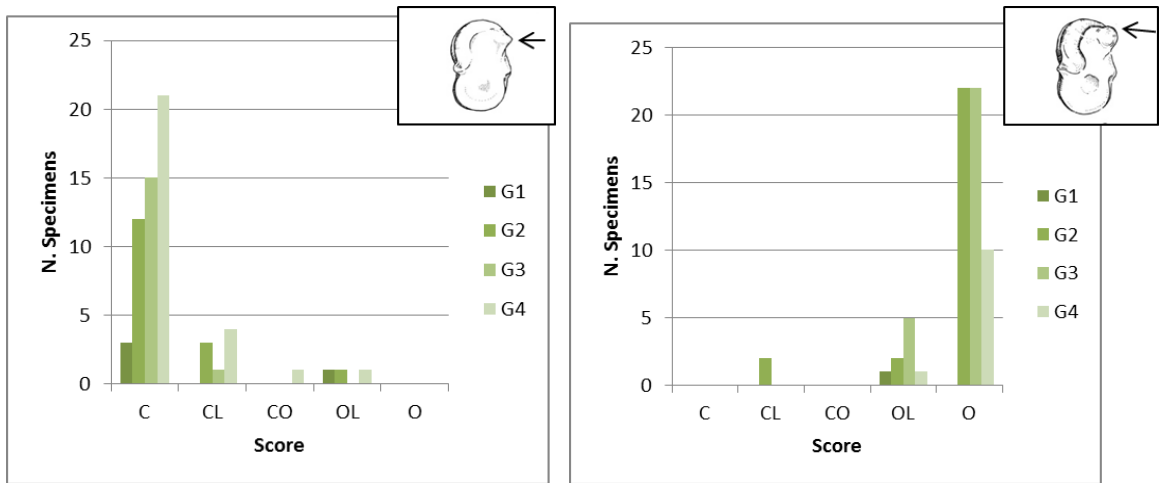


Figure 2.183 Astragalus, trait 4 (shape of the distal articular surface of the lateral aspect) number of specimens attributed to the different categories for the different age-groups for the goat (left) and the sheep (right). For details see Fig. 2.131.

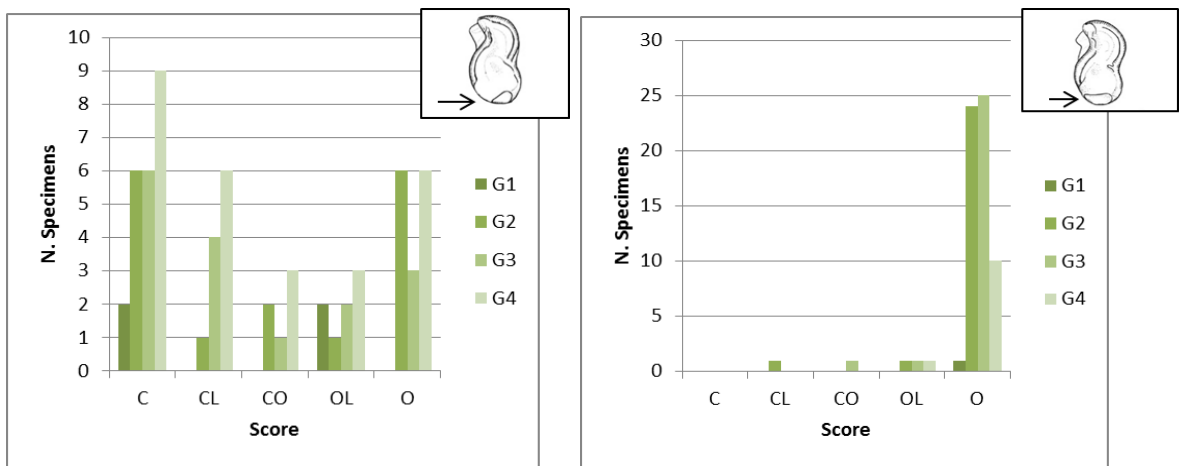


Figure 2.184 Astragalus, trait 5 (articular ridge of the trochlea) number of specimens attributed to the different categories for the different age-groups for the goat (left) and the sheep (right). For details see Fig. 2.131.

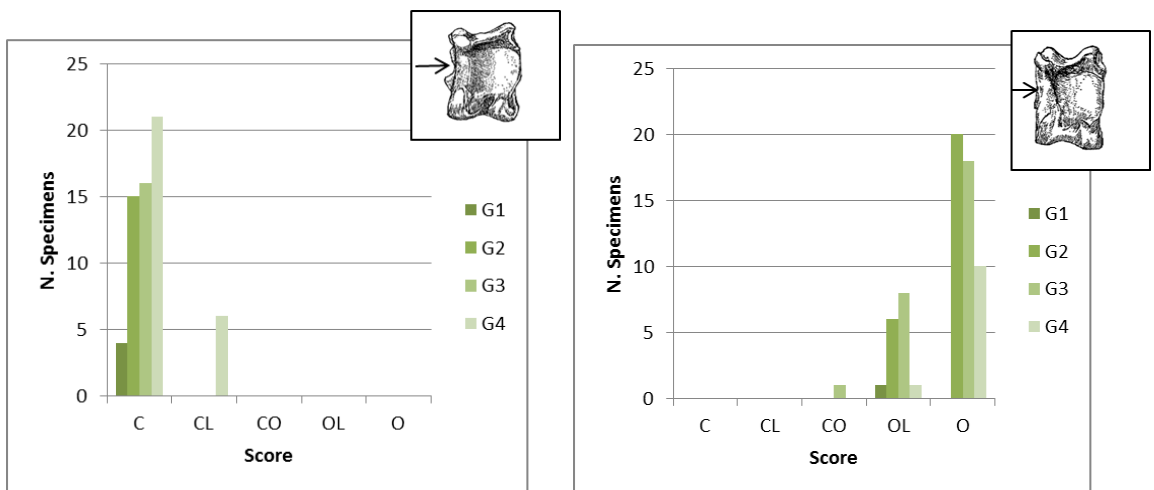


Figure 2.185 Astragalus, trait 6 (aspect and direction of the articular surface on the plantar side) number of specimens attributed to the different categories for the different age-groups for the goat (left) and the sheep (right). For details see Fig. 2.131.

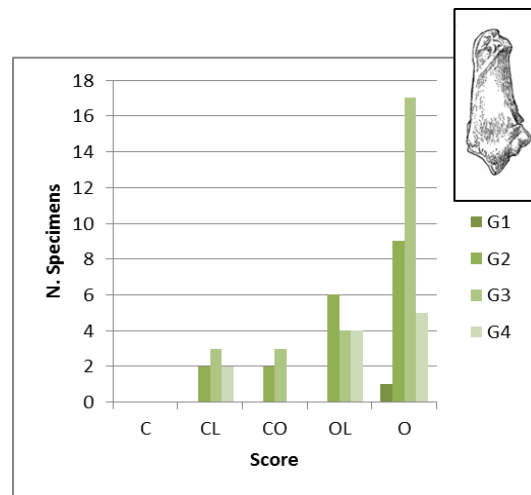
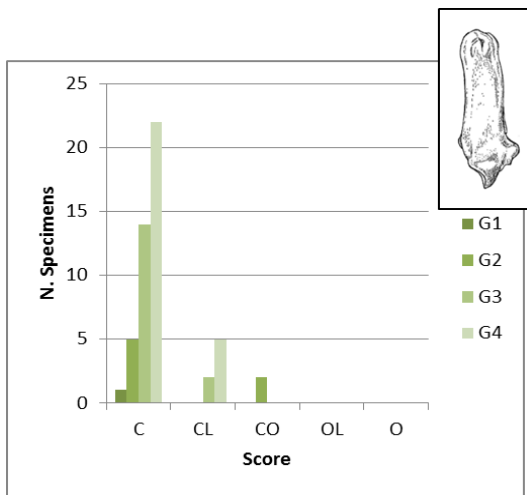


Figure 2.186 Calcaneus, trait 1 (overall aspect) number of specimens attributed to the different categories for the different age-groups for the goat (left) and the sheep (right). For details see Fig. 2.131.

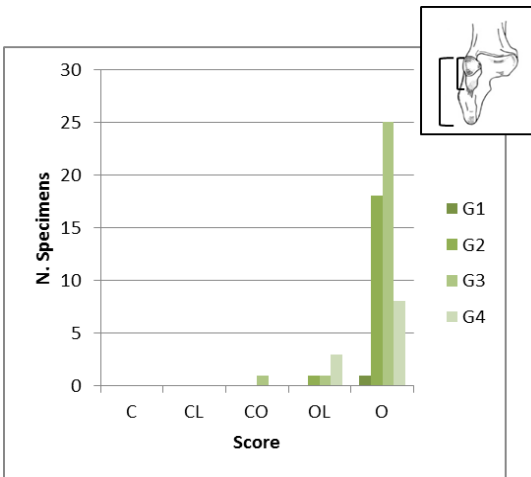
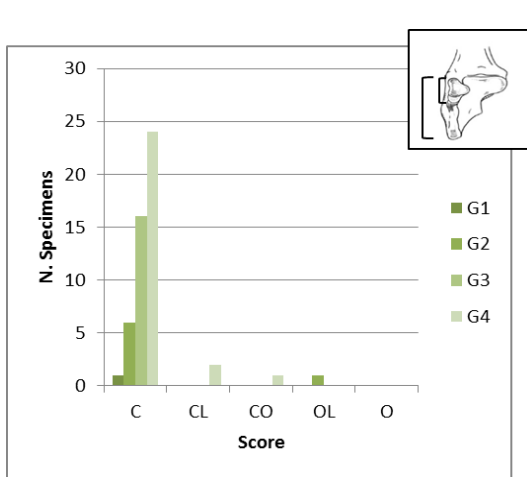


Figure 2.187 Calcaneus, trait 2 (length of the *os malleolare* vs length of the entire process) number of specimens attributed to the different categories for the different age-groups for the goat (left) and the sheep (right). For details see Fig. 2.131.

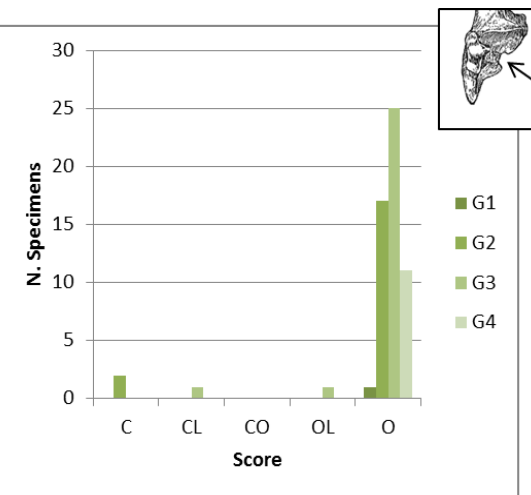
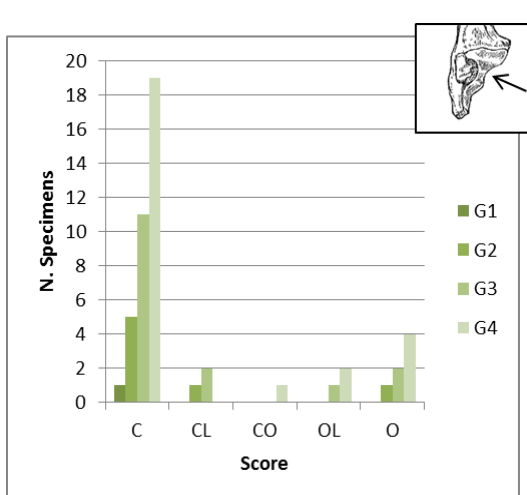


Figure 2.188 Calcaneus, trait 3 (presence/absence of the junction between the two internal articular surfaces) number of specimens attributed to the different categories for the different age-groups for the goat (left) and the sheep (right). For details see Fig. 2.131.

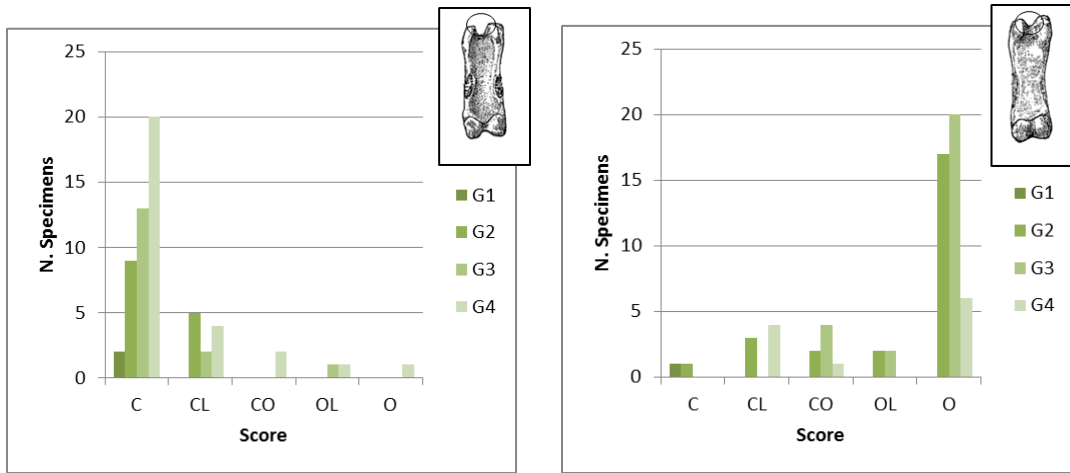


Figure 2.189 1st phalanx, trait 1 (shape of the groove on the proximal end) number of specimens attributed to the different categories for the different age-groups for the goat (left) and the sheep (right). For details see Fig. 2.131.

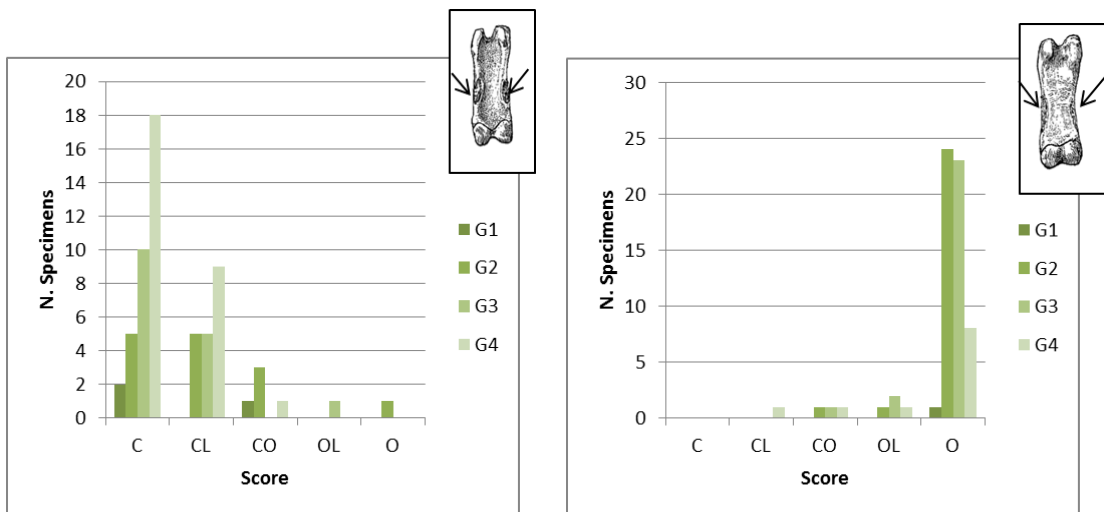


Figure 2.190 1st phalanx, trait 2 (presence of the scars for the muscular ligaments on the posterior side) number of specimens attributed to the different categories for the different age-groups for the goat (left) and the sheep (right). For details see Fig. 2.131.

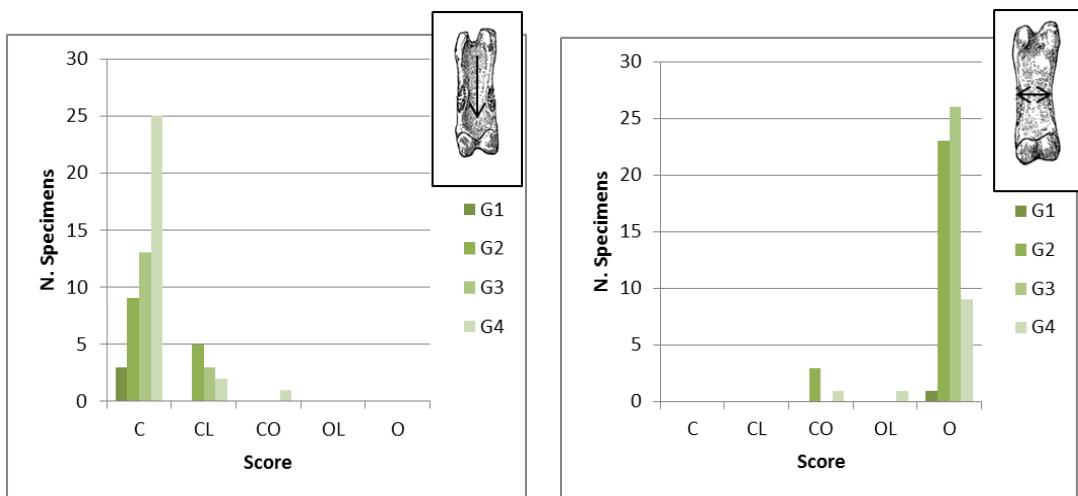


Figure 2.191 1st phalanx, trait 3 (aspect of the posterior side) number of specimens attributed to the different categories for the different age-groups for the goat (left) and the sheep (right). For details see Fig. 2.131.

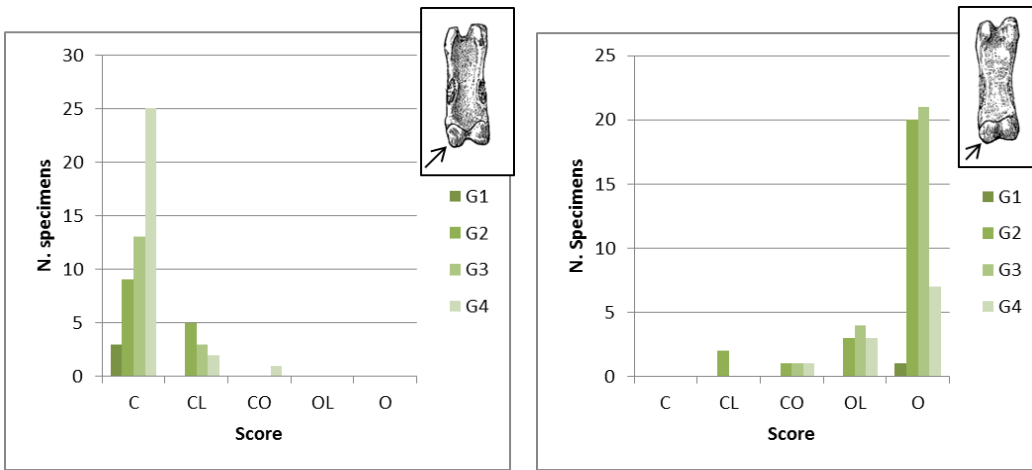


Figure 2.192 1st phalanx, trait 4 (shape of the distal articulation) number of specimens attributed to the different categories for the different age-groups for the goat (left) and the sheep (right). For details see Fig. 2.131.

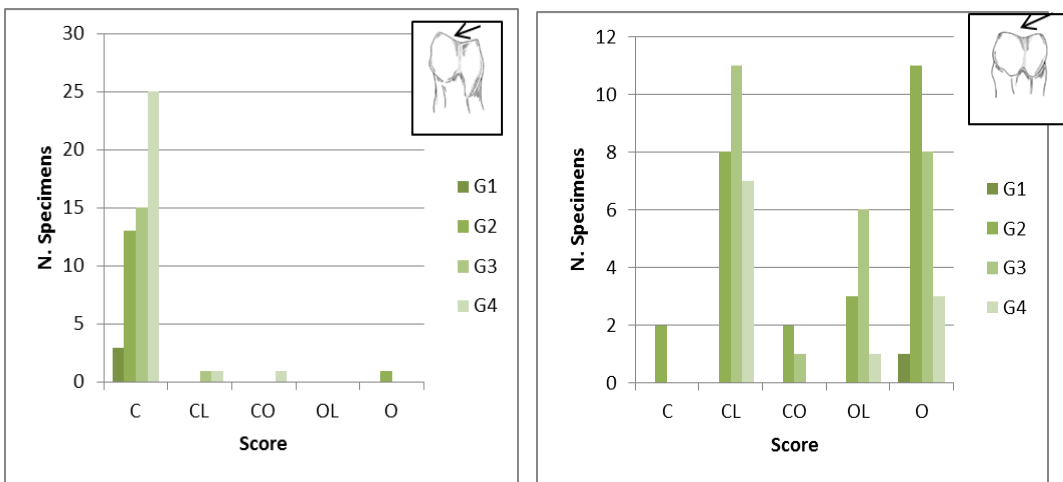


Figure 2.193 2nd phalanx, trait 1 (aspect of the axial part of the posterior side of the distal articulation) number of specimens attributed to the different categories for the different age-groups for the goat (left) and the sheep (right). For details see Fig. 2.131.

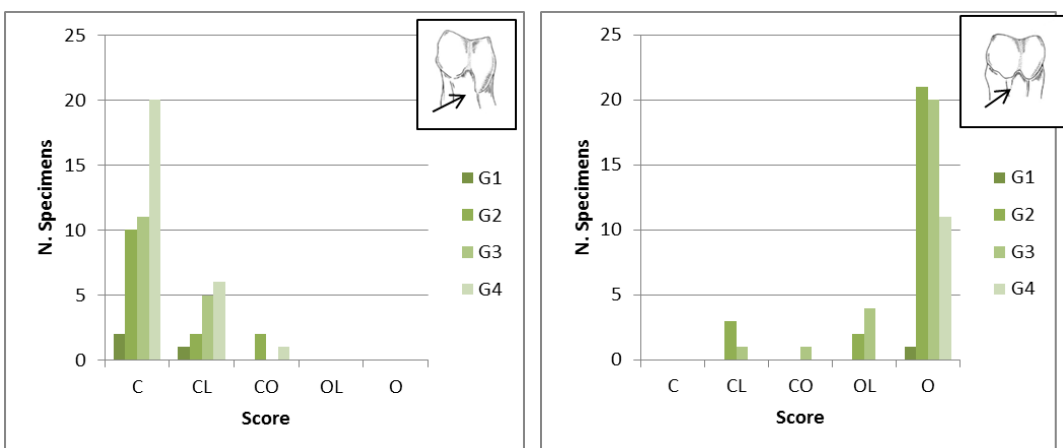


Figure 2.194 2nd phalanx, trait 2 (aspect of the ridge on the posterior side of the distal articulation) number of specimens attributed to the different categories for the different age-groups for the goat (left) and the sheep (right). For details see Fig. 2.131.

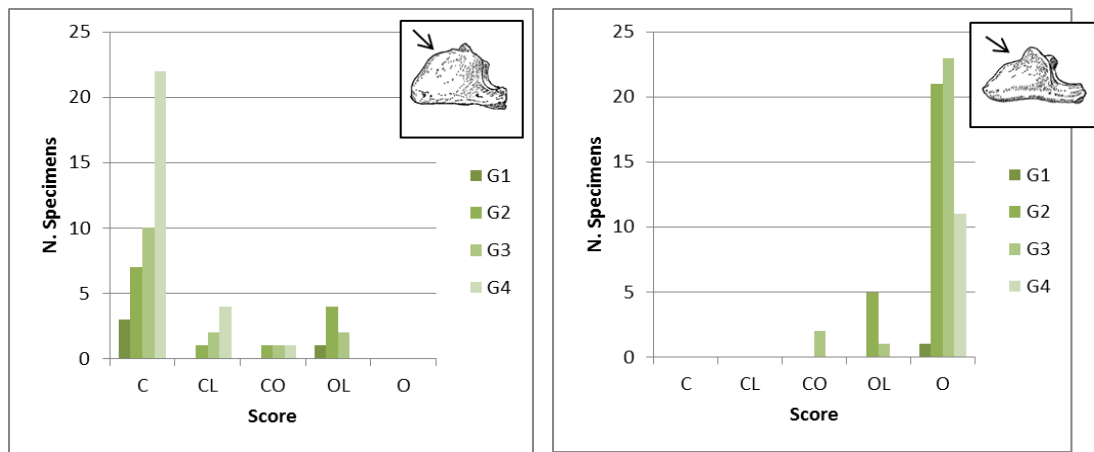


Figure 2.195 3rd phalanx, trait 1 (presence/absence of a saddle on the dorsal edge) number of specimens attributed to the different categories for the different age-groups for the goat (left) and the sheep (right). For details see Fig. 2.131.

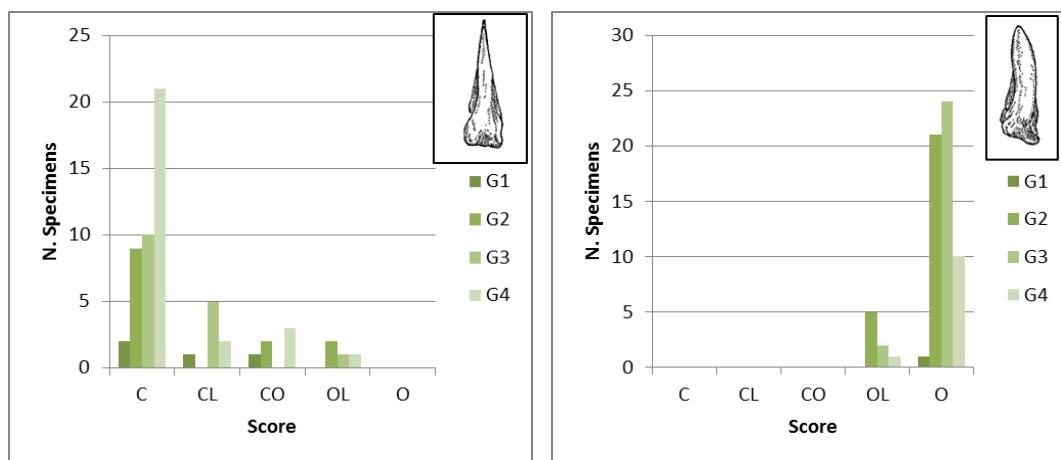


Figure 2.196 3rd phalanx, trait 2 (shape of the sole) number of specimens attributed to the different categories for the different age-groups for the goat (left) and the sheep (right). For details see Fig. 2.131.

2.4.4 Conclusions

The evidence discussed in this chapter has shown that most morphological traits have a certain degree of reliability, which mainly depends on their variability. These results are largely in line with previous scholarship (Boessneck *et al.* 1964; Helmer and Rochetau 1994; Fernández 2001; Zeder and Lapham 2010; Zeder and Pilaar 2010). Although some characteristics appear to be highly reliable on their own, others provide more tentative results, and it is therefore good practice to provide identifications based on a combination of traits.

The characteristics that make a trait reliable are the exclusivity of the trait (namely the fact that it appears in that form only on one of the two species) and the high frequency in which it appears in that specific species and in that specific form. This scenario has been noticed for a few elements and traits, which vary from one species to the other (Tabs. 2.43 and 2.44). The only elements and traits that have consistently given accurate species attributions in both species are the horncores, trait 1 in the metacarpal and trait 6 in the metatarsal. These morphological

features are those which could theoretically lead to a reliable identification even when evaluated individually. Nonetheless, even when those traits are recordable, an assessment based on the combination of traits is the most prudent procedure.

Other traits are visible and reliable only when strongly expressed but this does not always occur (Tabs. 2.45 and 2.46). These traits are very useful but, aside from those cases in which they are very clearly expressed, they should only lead to confident identifications when evaluated together with others.

Finally, traits which have given high percentages of species identifications only when the category *Ovis/Capra* was added, have to be evaluated with caution. They appear to have a high degree of variability and in no case should be used on their own.

Factors, such as sex and age, have been taken into consideration in order to assess their influence on the reliability of the morphological traits. Table 2.56 shows a summary of the traits and the different factors they may be affected by, for both species. An overall evaluation of their reliability is also provided.

No evident pattern was noticed in relation to the sex of the animals. On the contrary, age has shown to have influenced the visibility of some traits. On teeth, for instance, the heavy abrasion present in older animals obscures some traits making identification more difficult. Conversely, in young animals if the teeth are not fully erupted, traits might not be visible and as such, not assessable. Age influences also the visibility of traits on some postcranial bones: trait 2 on the scapula, trait 3 and 4 on the humerus, trait 1 and 2 on the radius and trait 1 on the ulna tend to change through time and acquire intermediate forms, making them no longer easily attributable to one species or the other.

To conclude, considering that the modern sample analysed is biased toward some age and sex categories, the outcomes from this study have to be considered as indicative of patterns and not representative of all possible variations. As most traits probably have an age stage at which it is most visible, the results that may be obtained are strictly related to the nature and composition of the assemblage itself. For example, if this sample was made up of a higher number of very young animals, a different outcome would be expected from those traits which are more visible in this age category (for example traits on deciduous teeth).

It has also to be acknowledged that it was not possible to carry out the identification 'blind' and the knowledge of the actual status of the animal (i.e. sheep or goat) may have influenced the objectivity of the attributions. Undertaking a blind test on a large sample of domestic sheep and goat, with an even spread of age stages and sexes, would provide a more objective evaluation.

Table 2.57 Summary of the reliability of the morphological traits for the two species with information regarding the factors can influence them. Reliability is expressed in scores: *= > 90%percentage of species identification (C or O), **= >/= 60% of species identification; *= <60% of species attribution. The overall reliability is, by and large, the mean between the reliability scores of the two species.**

Element	Trait	Reliability in goat	Reliability in sheep	Overall Reliability	Affected by:	Other observations:
Horncore	1	***	***	***	Dependent on the sex and age of the animal. Despite these factors have an influence on the shape and size of the horncore in both species, this element has shown to be highly reliable.	
	2	***	***	***		
Mandible	1	*	*	*	Dependant on the age of the animal. It is not exclusive of a species and presents a degree of individual variability .	
	2	**	***	**	It can present a degree of individual variability .	
dP ₃	1	**	*	*	Dependent on the age of the animal. If the tooth is too worn the trait cannot be seen. In addition individual variability is present.	All the traits on teeth are heavily influenced by the age factor (wear and stage of eruption) which limits heavily their visibility and reliability in this specific modern sample.
	2	*	*	*	Dependent on the age of the animal. If the tooth is too worn the trait cannot be seen. In addition individual variability is present.	
dP ₄	1	*	*	*	Dependent on the age of the animal. It is not easy to be seen as it would require a constant comparison between the two species. In addition individual variability is present.	Considering the limits the modern sample has, the traits are likely to give different results in a sample made out of different age classes where wear stage and eruption affect less their visibility and reliability.
	2	*	***	**	Dependent on the age of the animal. It is not an exclusive of one species. Its location does not permit to be always assessed especially when the tooth is embedded in mandible. In addition individual variability is present.	
	3	**	***	**	Dependent on the age of the animal. It is not exclusive of one of the two species. In addition individual variability is present.	
	4	**	**	**	Dependent on the age of the animal. The location of the trait does not permit it to be always assessed when embedded in mandible. In addition individual variability is present.	
P ₃	1	**	*	*	Dependent on the age of the animal. In addition individual variability is present.	
	2	**	**	**		
	3	**	*	*		
P ₄	1	*	**	*	Dependent on the age of the animal. In addition individual variability is present.	
	2	*	**	*		
	3	*	**	*		
M ₃	1	*	*	*	Dependent on the age of the animal. In addition individual variability is present.	
	2	*	*	*	Dependent on the age of the animal. In addition individual variability is present.	
	3	**	*	*	Dependent on the age of the animal. They are not	
	4	*	*	*		

Element	Trait	Reliability in goat	Reliability in sheep	Overall Reliability	Affected by:	Other observations:
					exclusive of one species. In addition individual variability is present.	
	5	***	*	**	Dependent on the age of the animal. In addition individual variability is present.	
Scapula	1	*	**	*	A degree of individual variation is present.	
	2	**	**	**	Dependent on the age of the animal.	Considering the limits the modern sample has, the trait is likely to give different results in a sample made out of different age classes where the trait would result more visible.
Humerus	1	**	***	**	A degree of individual variation is present but the reliability of the criteria is not heavily affected.	
	2	*	**	*	It is a not so easy to see trait as it would require a constant comparison between the two species. Individual variation can occur.	
	3	**	**	**	Dependent on the age of the animal. A degree of individual variation is present.	Considering the limits the modern sample has, the trait is likely to give different results in a sample made out of different age classes where the trait would result more visible.
	4	**	**	**		
	5	**	***	**	A degree of individual variation is present but the reliability of the criteria is rarely affected.	
Radius	1	**	***	**	Dependent on the age of the animal. A degree of individual variation is present.	Considering the limits the modern sample has, the trait is likely to give different results in a sample made out of different age classes where the trait would result more visible.
	2	**	**	**		
Ulna	1	**	***	**	Dependent on the age of the animal. A degree of individual variation is present.	Considering the limits the modern sample has, the trait is likely to give different results in a sample made out of different age classes where the trait would result more visible.
	2	**	**	**		
Metacarpal	1	***	***	***	All traits on this element have a degree of variation but it does not heavily affect their reliability. Age can modify the aspect of the trait 3, 4 and 5 but does not heavily compromise their reliability.	Considering the limits the modern sample has, the trait is likely to give different results in a sample made out of different age classes where the trait would result more visible.
	2	**	*	*		
	3	*	*	*		
	4	**	***	**		
	5	***	**	**		
Metatarsal	1	**	***	**	All traits on this element have a degree of variation but it does not heavily affect their reliability. Age can modify the aspect of the trait 3, 4 and 5 but does not heavily compromise their reliability.	Considering the limits the modern sample has, the trait is likely to give different results in a sample made out of different age classes where the trait would result more visible.
	2	**	*	*		
	3	*	*	*		
	4	**	***	**		
	5	***	**	**		
	6	***	***	***		
Tibia	1	*	**	*	A degree of individual variation is present. Some traits can be quite difficult to be seen.	
	2	**	*	*		
	3	**	*	*		
	4	**	**	**		
	5	**	*	*		
	6	**	**	**		
Astragalus	1	*	***	**	A degree of individual variation is present. It can affect the reliability of some traits more than	
	2	***	*	**		
	3	**	**	**		
	4	*	***	**		

Element	Trait	Reliability in goat	Reliability in sheep	Overall Reliability	Affected by:	Other observations:
	5	**	**	**	others.	
	6	***	**	**		
Calcaneus	1	**	*	*	It is not so easy to see trait as it would require a constant comparison between the two species. Individual variation can occur.	
	2	**	***	**		
	3	**	***	**		
1 st Phalanx	1	**	**	**	They are not exclusive traits.	The traits on the phalanges are also affected by the difficulty in distinguishing the anterior (morphologically more diagnostic) from the posterior . Individual variation is also present.
	2	*	**	*		
	3	*	***	**		
	4	**	**	**		
2 nd Phalanx	1	***	*	**		
	2	**	**	**		
3 rd Phalanx	1	**	**	**		
	2	**	***	**		

2.5 Biometric results

In the previous sections, the principles behind the applied methods (Section 2.1.2 and 2.1.3) have been outlined. The results of the study of the morphological data analysis have been presented in Section 2.4, with an evaluation of the effect that variables such as sex and age could have on the diagnostic power of the morphological traits that have been considered.

In the following sections the results from the biometrical study are presented. The first part will show the descriptive statistics, such as mean and Coefficient of Variation of each measurement of each element of both species (Section 2.5.1). A study utilising the observation and analysis of bivariate plots (Section 2.5.2) and ratio technique (Section 2.5.3), in order to better highlight morphological differences among the two groups, follows. The last section is dedicated to the multivariate statistical analysis which includes the Mann Whitney U test (Section 2.5.5), Linear Discriminant Analysis (Section 2.5.6) and Principal Component Analysis (Section 2.5.7). Finally a summary of the results of the biometric study is provided (Section 2.5.8).

2.5.1 Descriptive Statistics

The first step for exploring the modern data was to generate Means and Coefficients of Variation of each measurement (see also Appendix II).

Table 2.57 gives the Coefficient of Variation for individual measurements of the different anatomical parts considered, separately for sheep and goat. It can be seen that the number of the examined specimens varies by element. This may be due to the fact that the skeletal part was missing, or that it was unfused or affected by pathologies, in which case it was excluded from the analysis.

Table 2.58 Coefficients of Variation and standard values in tenths of millimeter for each measurement.

Anatomical element	Measurement	N. Specimens	CV	Mean	N. Specimens	CV	Mean
		<i>Capra hircus</i>			<i>Ovis aries</i>		
Horncore	A	39	33.6	35.5	30	28.4	35.3
	B	39	30.8	24	30	38.9	25.1
	C	36	30.8	26.4	29	26.5	30.1
	D	36	24.8	15.7	29	36.3	19.1
	E	36	41.0	149.6	28	42.9	99.6
	F	35	44.1	166.6	28	52.9	127.8
Scapula	BG	73	11.4	24.3	73	11.8	21.1
	LG	73	11.6	28.5	73	11.2	25.8
	GLP	73	11.0	35.1	73	11.5	32.9
	SLC	73	13.7	22.2	73	11.2	19.8
	ASG	73	12.9	26.1	73	10.2	21.1
Humerus	BT	75	9.5	32.0	71	10.1	28.2
	Bd	75	10.6	33.5	71	10.5	29.5
	HT	75	10.6	19.9	71	11.2	18.3
	HTC	75	10.2	15.3	71	11.6	14.3
	BE	75	12.9	10.2	71	12.4	8.5
	Dd	75	10.4	27.8	70	11.7	24.4

Anatomical element	Measurement	N. Specimens	CV	Mean	N. Specimens	CV	Mean
		<i>Capra hircus</i>			<i>Ovis aries</i>		
	BEI	75	17.4	6.2	71	16.7	6.6
Radius	Bp	73	9.9	33.1	72	10.6	31.2
	BFp	73	9.4	31.7	72	10	28.6
	Dp	73	10.7	17.1	72	10.8	15.9
	GL	55	8.9	172.9	53	9.5	150.6
	SD	72	13.9	19.3	72	12.8	16.8
Ulna	B	55	11.1	12.2	58	13.1	10.2
	L	55	13.5	27.3	58	12.4	24.1
	BPC	56	11.6	25.4	58	12	19.0
	DPA	56	11.6	28.8	57	10.2	26.6
	SDO	56	11.9	24.8	58	11.9	22.0
Metacarpal	GL	58	8.4	120.1	61	8.0	123.5
	SD	58	13.1	17.0	62	10.9	14.0
	BatF	58	9.9	29.6	62	11.2	25.9
	BFd	58	8.8	29.0	62	9.7	24.8
	a	58	8.8	13.4	62	9.9	11.5
	b	58	9.1	13	62	10	11.1
	1	58	9.5	11.1	62	11.1	11.2
	2	58	8.8	18	62	10.0	15.5
	3	58	9.5	10.5	62	10.3	10.3
	4	58	9.1	17.7	62	9.9	15.4
Metatarsal	GL	62	8.4	128.0	63	8.0	133.0
	SD	62	12.8	13.7	64	10.3	12.1
	BatF	61	9.4	26.3	64	10.8	23.9
	BFd	62	8.3	25.8	64	9.7	23.4
	a	62	8.5	12.0	64	10.5	11.1
	b	62	8.4	11.3	64	9.9	10.1
	1	62	9.5	10.7	64	11.1	10.4
	2	62	9.2	17.3	64	10.3	15.9
	3	62	9.3	10.4	64	11.1	9.6
	4	62	9.4	16.8	64	10.2	15.0
Tibia	Bd	71	9.4	27.9	69	10.7	26.3
	Dd(a)	71	9.2	21.1	69	10.4	20.9
	Dd(b)	71	9.2	18.5	69	10.8	17.4
	GL	58	8	231.1	52	10.1	203.1
	SD	71	13	15.9	68	12.2	14.9
Astragalus	Bd	72	9.4	19.6	73	10.5	18.6
	GLm	72	9.2	29.3	73	10.2	26.6
	GLl	72	9	31.4	73	10.7	28.0
	Dm	72	9.5	18.0	73	11.1	17.0
	Dl	72	9.5	16.4	73	10.6	15.6
	H	72	9.2	25.6	73	10.5	22.6
	BpT	72	8.4	14.1	73	11	12.8
Calcaneum	GB	60	9.7	17.7	62	10.5	16.2
	GL	60	9.0	63.7	62	10.4	56.2
	c	60	10	12.4	62	11.9	13.0
	d	60	8.7	24.2	62	11	22.3
	B	60	10.7	6.8	62	13.4	6.2
	DS	60	9.9	19.7	62	11.4	18.5
	Gd	60	8.3	24.4	62	11.1	22.2
3 rd Phalanx	DLS	64	11.8	33.1	69	9.2	27.2
	MBS	65	14.6	6.0	69	11.9	6.1

Table 2.59 CV values for the goat group rearranged from the highest to the lowest.

Anatomical Element	Measurements	CV <i>Capra hircus</i>
Horncore	F	44.1
	E	41
	A	33.6
	B	30.8
	C	30.8
	D	24.8
Humerus	BEI	17.4
3 rd Phalanx	MBS	14.6
Radius	SD	13.9
Scapula	SLC	13.7
Ulna	L	13.5
Metacarpal	SD	13.1
Tibia	SD	13
Scapula	ASG	12.9
Humerus	BE	12.9
Metatarsal	SD	12.8
Ulna	SDO	11.9
Ulna	DLS	11.8
Scapula	LG	11.6
Ulna	BPC	11.6
Ulna	DPA	11.6
Scapula	BG	11.4
Ulna	B	11.1
Scapula	GLP	11
Radius	Dp	10.7
Calcaneum	B	10.7
Humerus	Bd	10.6
Humerus	HT	10.6
Humerus	Dd	10.4
Humerus	HTC	10.2
Calcaneum	c	10
Radius	Bp	9.9
Calcaneum	DS	9.9
Metacarpal	BatF	9.9
Calcaneum	GB	9.7
Humerus	BT	9.5
Astragalus	Dm	9.5
Astragalus	Dl	9.5
Metacarpal	1	9.5
Metacarpal	3	9.5
Metatarsal	1	9.5
Radius	BFp	9.4
Tibia	Bd	9.4
Astragalus	Bd	9.4
Metatarsal	BatF	9.4
Metatarsal	4	9.4
Metatarsal	3	9.3
Tibia	Dd(a)	9.2
Tibia	Dd(b)	9.2
Astragalus	GLm	9.2
Astragalus	H	9.2
Metatarsal	2	9.2
Metacarpal	b	9.1
Metacarpal	4	9.1
Astragalus	GLl	9
Calcaneum	GL	9
Radius	GL	8.9
Radius	BFd	8.8
Metacarpal	a	8.8
Metacarpal	2	8.8
Calcaneum	d	8.7
Metatarsal	6	8.7

Anatomical Element	Measurements	CV <i>Capra hircus</i>
Metatarsal	5	8.6
Metacarpal	6	8.6
Metacarpal	5	8.6
Metatarsal	a	8.5
Astragalus	BpT	8.4
Metacarpal	GL	8.4
Metatarsal	GL	8.4
Metatarsal	b	8.4
Astragalus	Gd	8.3
Metatarsal	BFd	8.3
Tibia	GL	8

Table 2.60 CV values for the sheep group rearranged from the highest to the lowest.

Anatomical Element	Measurements	CV <i>Ovis aries</i>
Horncore	F	52.9
	E	42.9
	B	38.9
	D	36.3
	A	28.4
	C	26.5
Humerus	BEI	16.7
Calcaneum	B	13.4
Ulna	B	13.1
Radius	SD	12.8
Humerus	BE	12.4
Ulna	L	12.4
Tibia	SD	12.2
Ulna	BPC	12
Ulna	SDO	11.9
Calcaneum	c	11.9
3 rd Phalanx	MBS	11.9
Scapula	BG	11.8
Humerus	Dd	11.7
Humerus	HTC	11.6
Scapula	GLP	11.5
Calcaneum	DS	11.4
Scapula	LG	11.2
Scapula	SLC	11.2
Humerus	HT	11.2
Metacarpal	BatF	11.2
Astragalus	Dm	11.1
Calcaneum	Gd	11.1
Metacarpal	1	11.1
Metatarsal	1	11.1
Metatarsal	3	11.1
Astragalus	BpT	11
Calcaneum	d	11
Metacarpal	SD	10.9
Radius	Dp	10.8
Tibia	Dd(b)	10.8
Metatarsal	BatF	10.8
Tibia	Bd	10.7
Astragalus	GLI	10.7
Radius	Bp	10.6
Astragalus	DI	10.6
Astragalus	Bd	10.5
Humerus	Bd	10.5
Astragalus	H	10.5
Calcaneum	GB	10.5
Metatarsal	a	10.5

Anatomical Element	Measurements	CV <i>Ovis aries</i>
Tibia	Dd(a)	10.4
Calcaneum	GL	10.4
Metacarpal	3	10.3
Metatarsal	SD	10.3
Metatarsal	2	10.3
Scapula	ASG	10.2
Ulna	DPA	10.2
Astragalus	GLm	10.2
Metatarsal	4	10.2
Humerus	BT	10.1
Tibia	GL	10.1
Metacarpal	6	10.1
Radius	BFp	10
Metacarpal	b	10
Metacarpal	2	10
Metacarpal	a	9.9
Metacarpal	4	9.9
Metatarsal	b	9.9
Metatarsal	5	9.9
Metatarsal	6	9.9
Metacarpal	BFd	9.7
Metacarpal	5	9.7
Metatarsal	BFd	9.7
Radius	GL	9.5
Ulna	DLS	9.2
Metacarpal	GL	8

The Pearson's Coefficient of Variation, namely the Standard Deviation expressed as a percentage of the Mean, has the advantage of showing the degree of variation between the two groups and, as it is a dimensionless index, it permits a direct comparison of the variability of measured traits (Davis 1996; Yablokov 1974:8).

The CV values given by the sheep sample are often higher than the values related to the goat sample. A greater CV is synonymous of greater variability within the group. As previously mentioned, the size of the two samples in this study is basically the same (79 goats and 78 sheep). There is a variation in the number of elements measured due to several factors as previously mentioned, but this difference is never sufficiently large to produce a sample size bias (Field 2009: 34). As such, the difference in CV among the groups has to be explained in different terms.

The sheep group is mainly represented by Shetland and Soay animals, while the goat group is much more heterogeneous including German, English, Alpine and Near East specimens. The data suggest therefore that breed factor does not influence the variability as much as sex and age.

Although females predominate in both samples, in sheep castrates are also present (14 male, 29 female, 17 castrated), while only males and females make up the goat sample (23 and 31 respectively). In addition, all age groups are included in both samples but to a different degree. While in the goat group there is a prevalence of individuals belonging to Payne's stage H, in the

sheep group there are more individuals falling into Payne's stages E and F. As a consequence, it is reasonable to presume that the higher CVs reflect the sex and age heterogeneity in the sheep group.

It is interesting to note also that in both goat and sheep samples, the measurements of the limb-bone shafts (SD) always have a very high CV value (Ra, Ti, Mc and Mt) thus confirming Davis' results from his study of Shetland sheep (Davis 1996: 599). Davis interpreted this phenomenon as a peculiarity of those parts of the bone which are included in a joint (Davis 1996: 600). Shafts are not restrained by an articulation and, as a consequence, continue to grow after fusion and therefore tend to be more variable.

The relatively large CV of some small measurements in both species is also consistent with Davis' previous study. In particular, the small measurements that seem to vary the most are:

- HT and HTC in the Humerus;
- DI, Dm, Bd in the Astragalus;
- c and B in the Calcaneum;
- BatF, 1, 3 in the Metapodials.

The reasons behind this phenomenon are not well known. Davis considered the possibility of Intra-Observer Error which may determine variation of measurements taken by the same researcher in a dataset. This kind of bias could be linked to different factors: geographical area, laboratory conditions, but also experience of the researcher and the technique used to measure specimens as well as the accuracy in the way they are documented (Lymann and VanPool 2009: 487). The poor definition of measurements is also a potential case of variation. A measurement should be precisely defined so that by using easily recognized criteria comparability is allowed, namely measurements can be taken in the same way by different people. In addition, measurements should be also standardized so that the dimension measured is precisely defined allowing investigators to understand what that measurement label means (Lymann and VanPool 2009: 488).

In Davis's study, as well as in this, almost all the small measurements are well defined and standardized (Davis 1996: 601) and are therefore unlikely to be measured inconsistently. As a consequence, the issue may be due to the fact that the approximation to one tenth of millimeter, may represent a much greater approximation for smaller measurements than for the larger ones. Consequently, variation of 1 or 2 tenths of a millimeter may provide a greater index of variability in smaller measurements.

With a more accurate, element by element examination of Tables 2.57, 2.58 and 2.59 it is possible to identify which appear to be the most variable elements and which are the most variable measurements.

It is apparent that all measurements taken on horncores are highly variable. These are the skeletal elements which gave the highest CV values in both species. This is not surprising as horncores are extremely variable according to sex and age (Boessneck *et al.* 1964: 22-23). Additionally, some of the measurements taken are not very well defined. In particular it is difficult to take E and F consistently, as the points of reference of the measurements cannot be defined precisely.

High CV values in both species were also provided by the measurements taken on the scapula. In fact, considering the fact that the coracoid nucleus fuses early (Silver 1969), a low CV for the measurements taken on the glenoid cavity (BG, LG and GLP) would be expected because the bone has less time to respond to stresses and changes. Nevertheless, since evidence of some post-fusion growth in GLP of pigs has been found by Payne and Bull (1988: 30) the high CV obtained from the measurements taken on the glenoid cavity of the scapula may be related to this phenomenon which has, unfortunately, not yet been investigated in depth. In addition, this articular part is not so tightly trapped in the joint with the proximal humerus, so the possibilities for it to vary are more, compared to a body part which is restrained in a joint.

According to Payne and Bull (1988: 32), SLC in pigs and wild boars is a highly age-related measurement. This can also be seen clearly in the goat sample, where SLC measurement has the highest CV value. A high CV score for SLC is given also by the sheep group, even though it is not as high as for goat. The difference between the two species is probably related to differences in age distributions between the two samples.

Another element which gave significant CV scores in both groups is the humerus. In this anatomical element the measurements with the highest variability are BE and BEI, which is not unexpected since those new measurements are, as in the case of the horncore, not so well defined. The difficulties in defining these measurements precisely, has likely led to some inconsistency.

It is interesting to note that HTC, regarded to be relatively age independent by Payne and Bull (1988: 32) in their biometrical study of *Sus*, did indeed provide a low CV score in humerus measurements from our caprine samples too.

The measurements taken on the ulna also provided high CV scores in both groups. In particular, the breadth and the length of the *olecranon* provide high CV scores, but also the measurements taken of the articulation. B and L are measurements devised by the author in order to highlight the different shapes of the *olecranon*, but they are not easy to take consistently.

A certain degree of agreement between the CV values of the two groups has been noted and outlined above. Nevertheless, two elements have provided high variability scores but not to the same degree in both species. These are the 3rd phalanx and the calcaneum.

All the measurements taken on the 3rd phalanx have given very high variability values in the goat group, but much less so in sheep. Perhaps, in the case of the 3rd phalanges breed is indeed the main factor leading to variability.

2.5.2 Bivariate plots

In order to visualise which measurements were better at distinguishing sheep and goat, singular linear measurements were plotted against one another. The choice of which measurements to plot together was made by taking into consideration the morphological differences they could potentially highlight if displayed together, a technique that has been adopted previously (Fernández 2001; Payne 1969. For a critical review of these studies see Chapter 1, Section 1.3.3).

It is important to consider that these diagrams broadly represent size, a variable which is regarded in this work to be of no value in discriminating between sheep and goat. Therefore if the diagrams provide distinction between the two species that occurs consistently in the two measurements (basically one group is larger than the other) this is of no interest for the purpose of this work. Conversely, if the two measurements vary differently from each other, that indicates shape variation, and represents a valuable result.

Horncores

As mentioned in the previous section some standard as well as new measurements devised by the author (i.e. C, D, E and F) were taken for this element. Concerning the new measurements, the intention of defining and taking them in the most consistent way has always been a priority. Nevertheless, some of them were difficult to take accurately, partially because of the shape of the element (e.g. F is quite complicated to take because it requires the use of a semi rigid wire that has to be put on the external edge of the horncore. In addition, sometimes there is not a clear point where the horncore starts on the base of the skull, so it is not easy to establish where to place the wire) and partially because of the tool used (the measure on the wire is then transferred on a meter to be read and this practice is, despite the attention paid during the process, far from precise). Despite these limitations, it can be seen from Figures 2.197 to 2.200 that this element produced good results, confirming what had already been noted in the previous literature (Boessneck *et al.* 1964; Clutton-Brock *et al.* 1990; Schmid 1972); namely that, even though highly variable, horncores are useful indicators for sheep/goat identification.

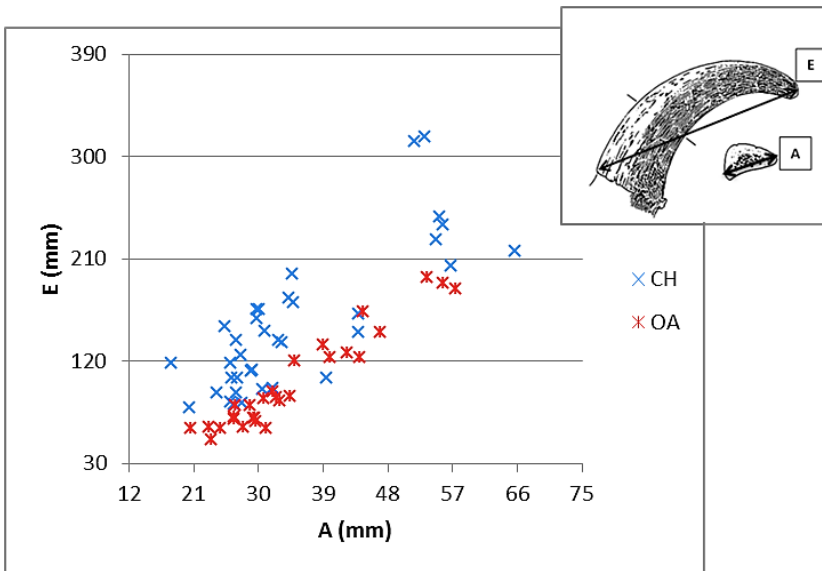


Figure 2.197 Maximum diameter at the base of the horncore plotted against the length.

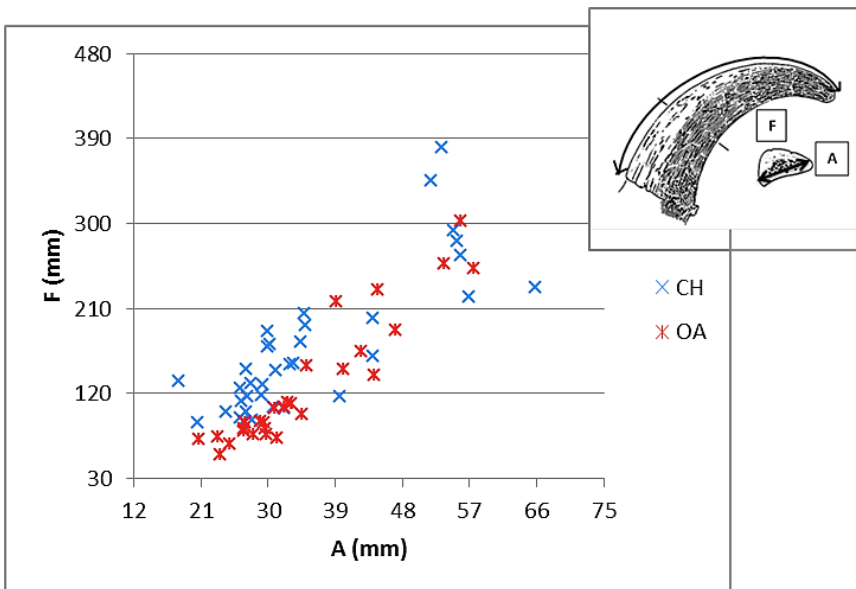


Figure 2.198 Maximum diameter at the base of the horncore plotted against the length of the outer curvature.

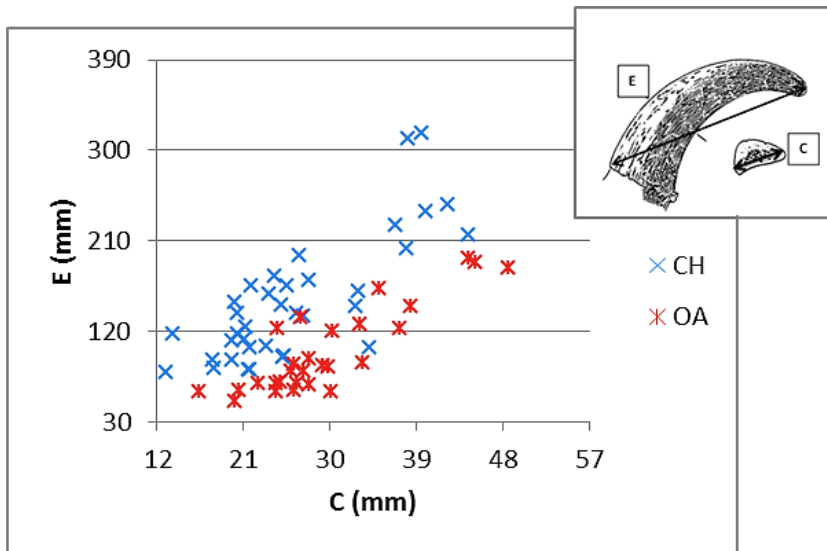


Figure 2.199 Maximum diameter of the horncore taken at the middle plotted against the length.

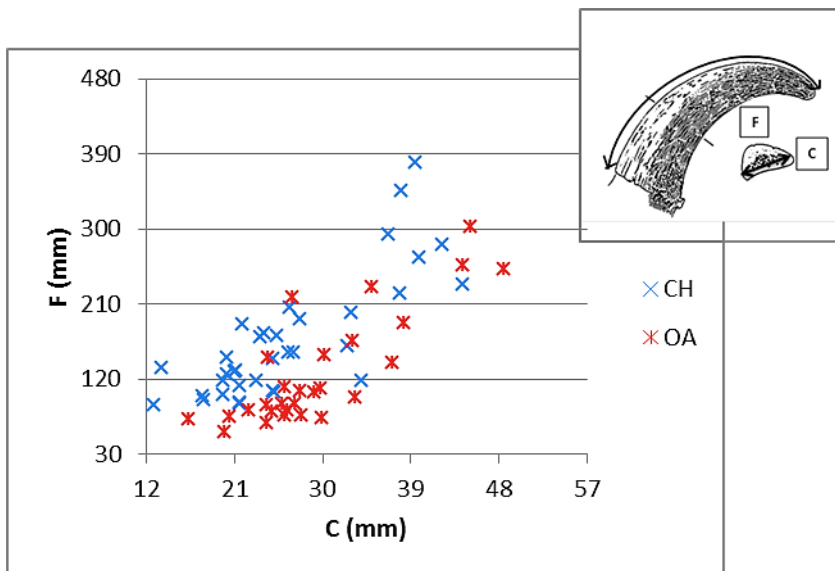


Figure 2.200 Maximum diameter of the horncore taken at the middle plotted against the length of the outer curvature.

A good distinction between the two groups can be seen by plotting the maximum diameter either at the base (measurement A) or at the middle (measurement C) with the length of the horncore (measurement E, Figs. 2.197 and 2.199) and the length of the curvature (measurement F, Figs. 2.198 and 2.200). All the scatterplots above attest that the horncore of the goat has a similar maximum diameter but a higher length and a less pronounced curvature than in sheep, characteristics that are described previously (Boessneck *et al.* 1964; Clutton-Brock *et al.* 1990; Schmid 1972).

More specifically, if individual measurements are taken into account, it can be seen that A, B and C, D were used because they could translate the difference in the section of the horncore between sheep and goat. In general, while sheep has a more or less triangular section, goat has a plano-convex section giving the horn a pronounced sharp frontal edge (Boessneck *et al.* 1964; Clutton-Brock *et al.* 1990; Schmid 1972).

Both maximum and minimum diameter at the base and at the middle of the horncore were plotted against each other in order to see if the difference between sheep and goat in the section of this anatomical element was visible. Unfortunately, the two groups do not discriminate clearly (Figs. 2.201 and 2.202). In Figure 2.201 it can be seen that the shape of the horncore base changes when size increases. In small horncores the minimum diameter appears to be larger in goats than sheep, while the opposite is the case in larger horncores.

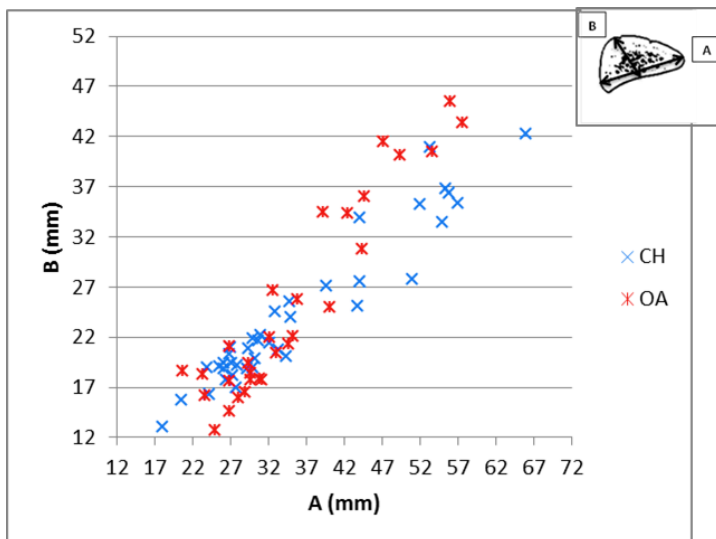


Figure 2.201 Maximum diameter plotted against the minimum diameter taken at the base of the horncore.

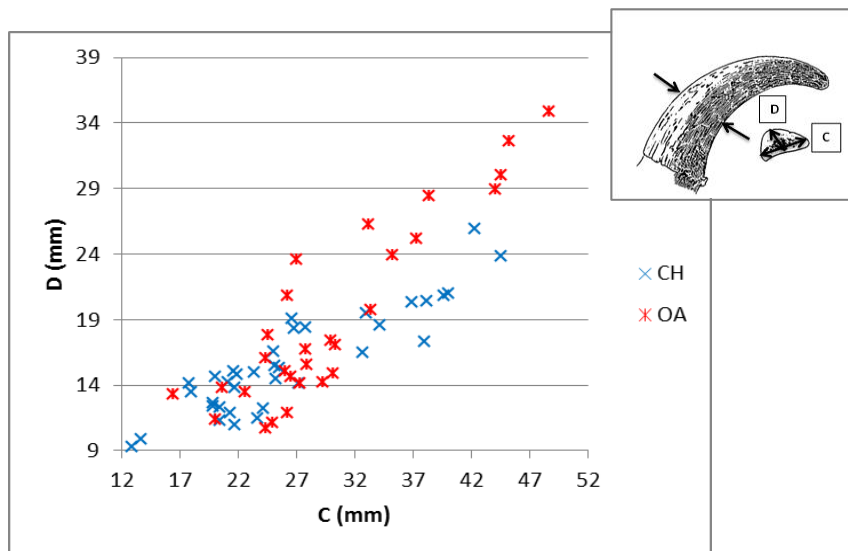


Figure 2.202 Maximum diameter plotted against the minimum diameter taken at the middle of the horncore.

The horncores are highly sexually dimorphic, especially in sheep. Ewes' horns have a sharp keel-shape anterior and posterior edges, are generally flattened medio-laterally, shorter than those of rams, and they curve below the dorsal level of the skull at a lower degree than in rams. Rams have a very pronounced D section, with an anterior edge more rounded and broader than the posterior one. In general males have more robust horns than females; they curve tightly outward and backward, assuming the typical spiralling shape around the ears. In goats, the sexual dimorphism is manifested mainly through the size of the horns as the section of this element is similar in females and males. In general, males have more robust and longer horns than females. However, in both sexes the horns rise vertically from the top of the head and do not curve as tightly as in sheep (Boessneck *et al.* 1964; Clutton-Brock *et al.* 1990; Schmid 1972). The next few scatterplots present the same biometrical indices presented above, but the modern specimens are divided according to their sex (Figs. 2.203 to 2.208).

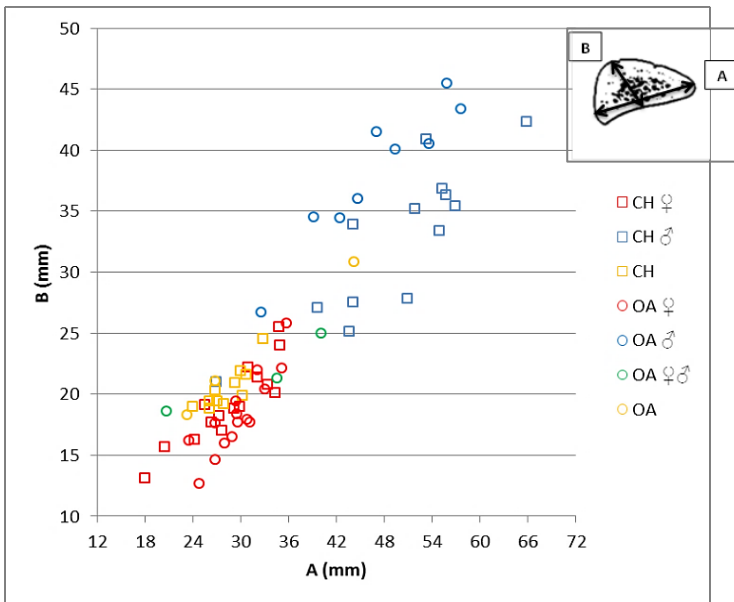


Figure 2.203 Maximum diameter of the horncore plotted against the minimum diameter at the base. Animals are divided by sex.

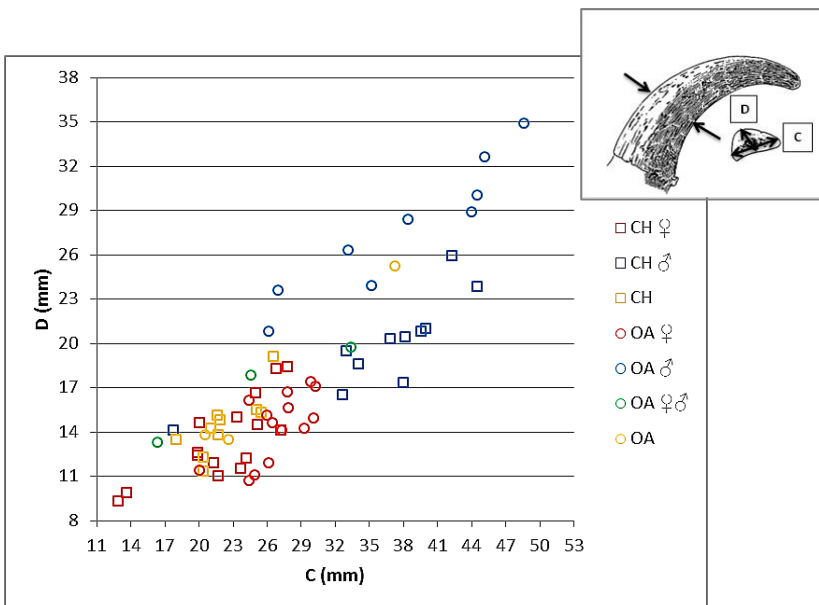


Figure 2.204 Maximum diameter plotted against the minimum diameter at the base of the horncore. Animals are divided by sex.

Figures 2.203 and 2.204 show that in both species, the maximum and minimum diameter - either taken at the base or at the middle of the horncores - can separate females from males, particularly when plotted together. Male sheep and goat have similar maximum diameter values but the male goats have a lower minimum diameter, mirroring the plano-convex section at the base of the male goat and the pronounced D section of the male sheep horncore (Boessneck *et al.* 1964; Clutton-Brock *et al.* 1990; Schmid 1972).

If the greatest length of the horncore and the outer curvature are considered, patterns become clearer (Figs. 2.205 to 2.208). The male goat has higher greatest length than the ram, mirroring the fact that the horns rise vertically and do not curve as heavily as in rams; thus, the distance from the base to the tip of the horncore is lower in rams than in male goats. In females, the same pattern can be recognised even though to a different degree. Female goats have higher E values than ewes and similar A and C values (Figs. 2.205 and 2.207).

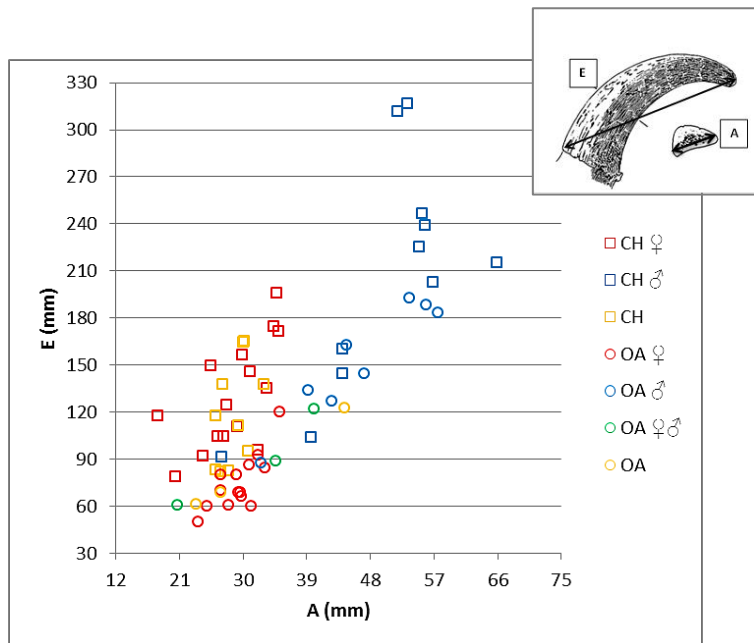


Figure 2.205 Maximum diameter at the base plotted against the greatest length of the horncore. Animals are divided by sex.

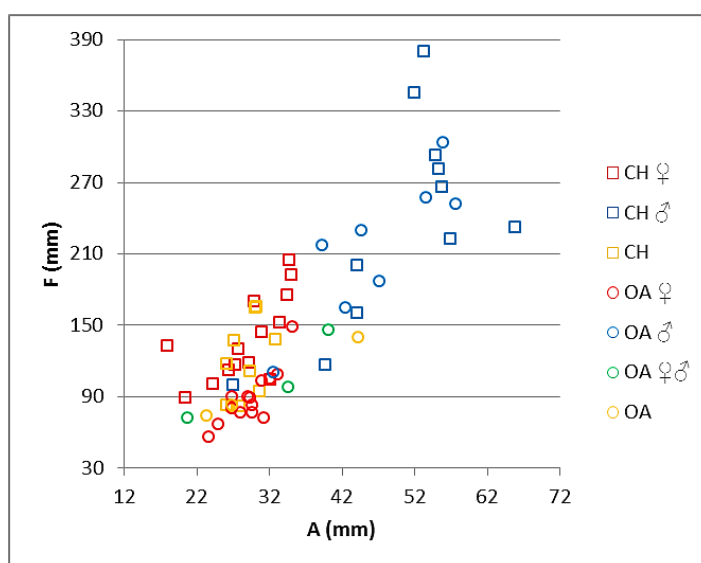


Figure 2.206 Maximum diameter at the base plotted against the length of the outer curvature of the horncore. Animals are divided by sex.

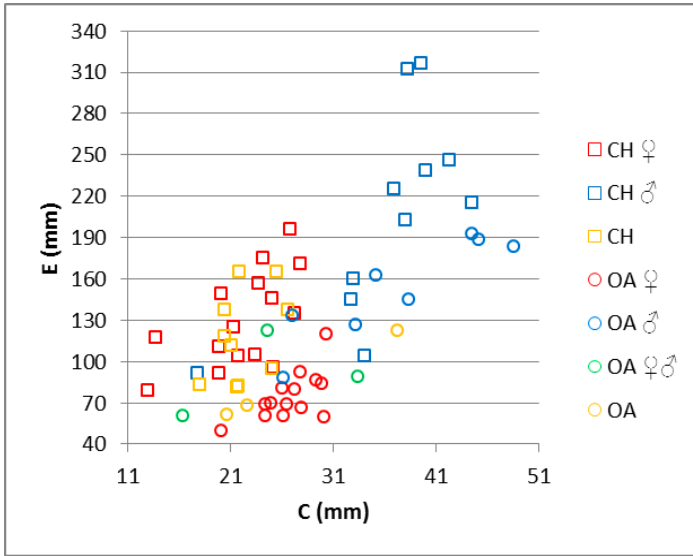


Figure 2.207 Maximum diameter at the middle of the horncore plotted against the greatest length. Animals are divided by sex.

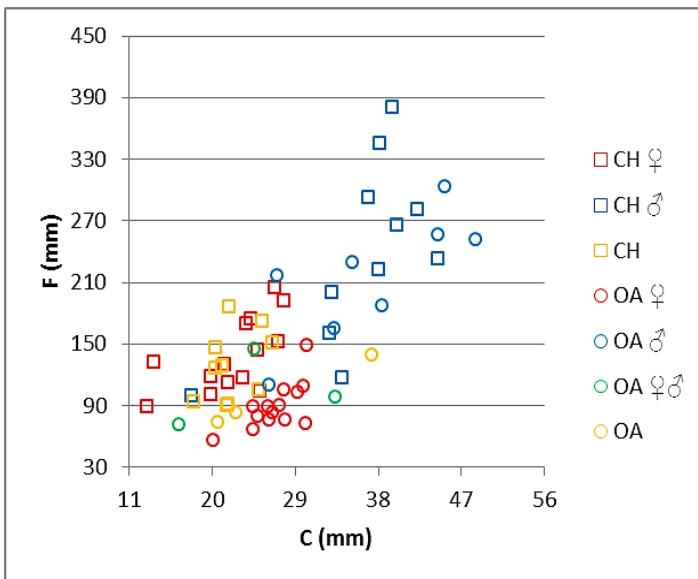


Figure 2.208 Maximum diameter at the middle of the horncores plotted against the length of the outer curvature. Animals are divided by sex.

Figures 2.206 and 2.208 show the difference in the outer curvature. Female sheep and goat have similar A and C values but female goats show higher F values, mirroring the fact that their horncores are usually thinner and very pointed giving it a very slender form, while horncores of ewes have an elliptical section with a flatted medio-lateral side and a rounded tip. The same pattern is visible for males to a greater degree: rams have similar A and C values to male goats but generally male goats have a higher F measurement as they have longer horncores.

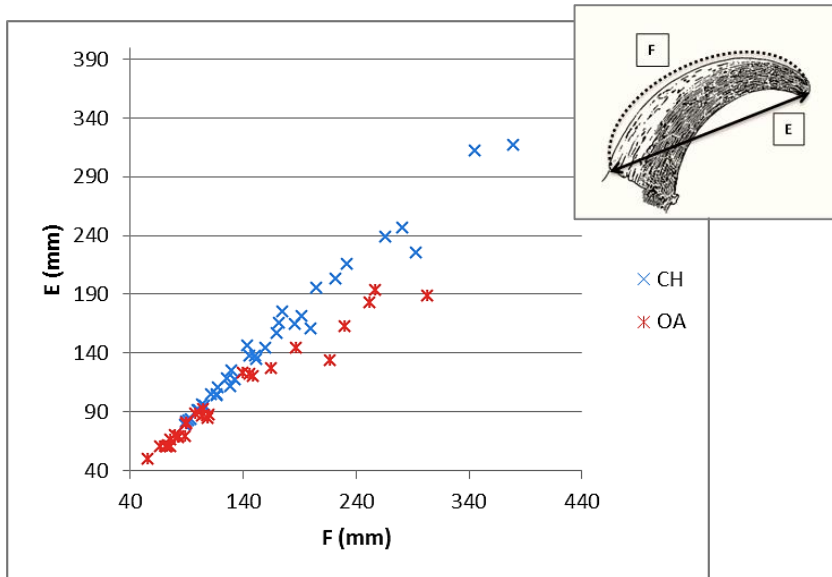


Figure 2.209 Length of the outer curvature plotted against the maximum length of the horncore.

Figure 2.209 shows that, when F and E are plotted together, a better separation between the groups can be noticed. This is not surprising as these measurements describe one of the clearest morphological differences in sheep and goat. Figure 2.210, which shows the same measurements but plotted according to the sex of the animals, highlights how with the increase in size, in rams E values tend to decrease as the horns become more spiral in shape; thus the distance from the base to the tip is shorter than in the longer and less curved male goat horncores. Clearly if the horncores are short, the sheep and goat metrical distinction based on the horncore length and its curvature is unclear. This problem affects the female groups more. Conversely, in longer male horncores, the greater curvature of the sheep elements is obvious (lower E values).

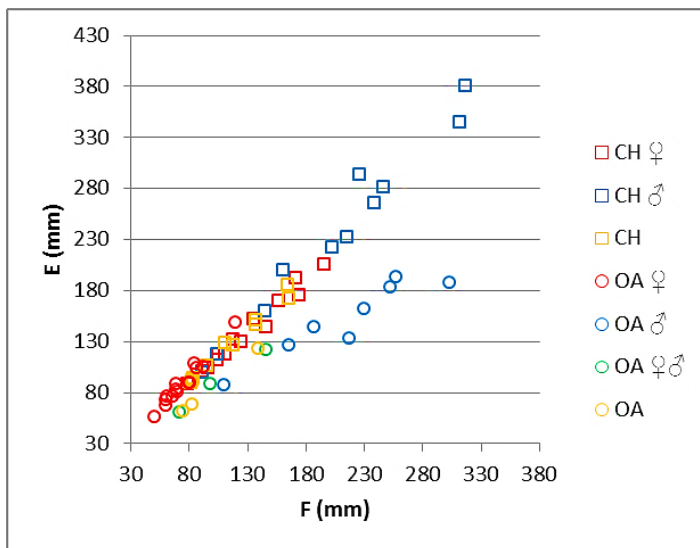


Figure 2.210 Length of the outer curvature plotted against the maximum length of the horncore. Specimens are divided by sex.

Scapula

For the scapula some new as well as already published measurements were used. BG, LG and GPL were chosen because they have the potential to describe the shape of the glenoid articulation which is elliptical in sheep and more circular in goat (Boessneck 1969; Boessneck *et al.* 1964). SLC and ASG were also taken to describe the *collum scapulae*, which is slender in goat and more robust in sheep, and the shortest distance from the spine of the scapula to the edge of the glenoid cavity, since in sheep this distance is shorter than goat, as pointed out by Boessneck *et al.* (1964: 56-59). When plotted together, these measurements gave promising results showing two fairly distinct groups despite some overlap (Figs. 2.211-2.215). In particular, the combinations BG and ASG, ASG and SLC and ASG with GLP provided the best discrimination, even though to different degrees. When BG and GLP, as well as LG and GLP are plotted together, the two groups are less clearly separated (Figs. 2.211 and 2.213) as they are in other scatterplots. This confirms partially what Helena Fernández had noted in her osteometric study on domestic and wild small Eurasian ruminants. Fernández (2001) found that the combination of BG and GLP has limited potential in modern material and is of no use for archaeological material. Nevertheless, in the present study the use of these combinations revealed some patterns; for example in goat, BG (Fig. 2.211) is constantly higher, pointing at the differences in shape of the glenoid cavity mentioned above. Less useful is the combination GLP and LG (Fig. 2.213): the measurements seem to discriminate the sheep when the bone is smaller and the goat when the bone is larger, but the difference is blurred.

Figure 2.212 (BG vs ASG) presents another morphological trait suggested in the literature as useful for discriminating the two species. This scatterplot shows the difference in the shape of

the glenoid cavity, but also how the shortest distance from the spine to the glenoid cavity is greater in goat than sheep, confirming what Boessneck *et al.* had identified (1964).

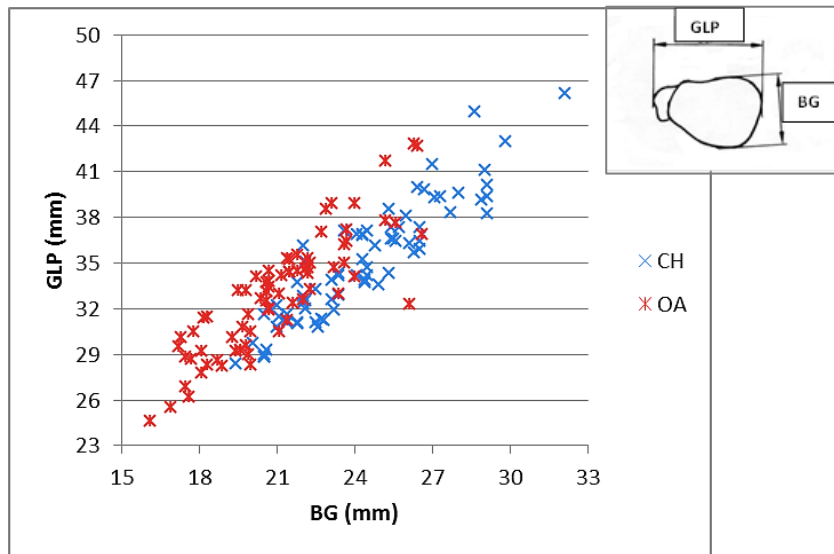


Figure 2.211 Greatest breadth of the glenoid cavity plotted against the greatest length of the *processus articularis* (image of scapula (Fig. 31b): reprinted from von den Driesch, A. *A guide to the measurement of animal bones from archaeological sites*. Peabody Museum Bulletins, vol. 1, copyright 1976 with permission from the President and Fellows of Harvard College).

Figure 2.214 shows ASG plotted against SLC. This set of measurements has previously been suggested by Boessneck *et al.* (1964) and further applied by Buitenhuis (1995) and Fernàndez (2001); it has been shown to be of limited use especially because of the high individual variation (Fernàndez 2001: 354). In this study, it can be noticed that the discrimination between groups is fairly successful and in particular, the separation of goats is clearer in larger specimens.

The same pattern can be identified in Figure 2.215, where ASG is plotted against GLP. This combination has also previously been used by Fernàndez who obtained a fairly good separation (Fernàndez 2001: 356), even though the author suggests caution because of the small sample size.

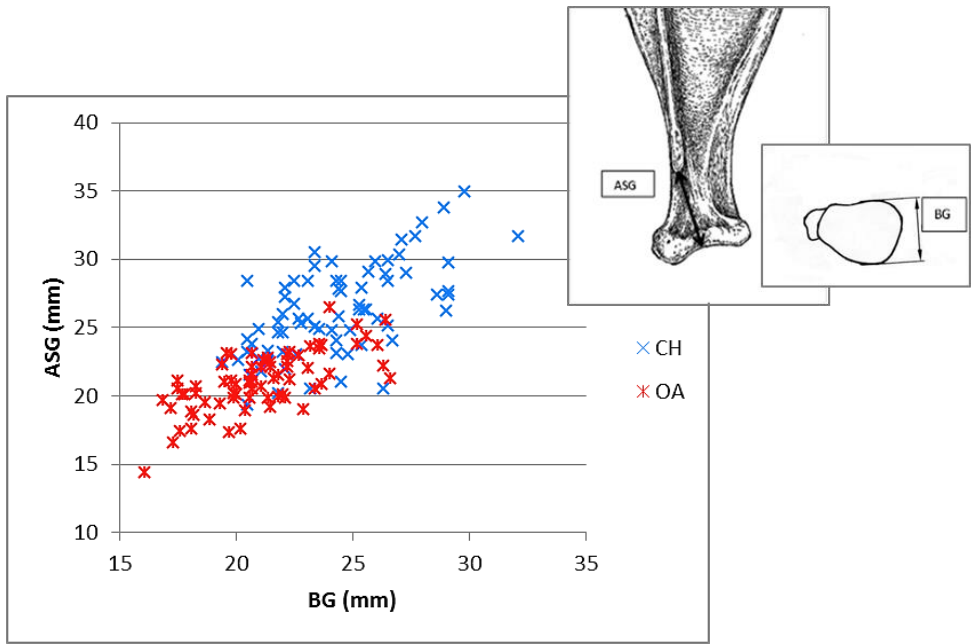


Figure 2.212 Greatest breadth of the glenoid cavity plotted against the shortest distance from the spine to the edge of the glenoid cavity.

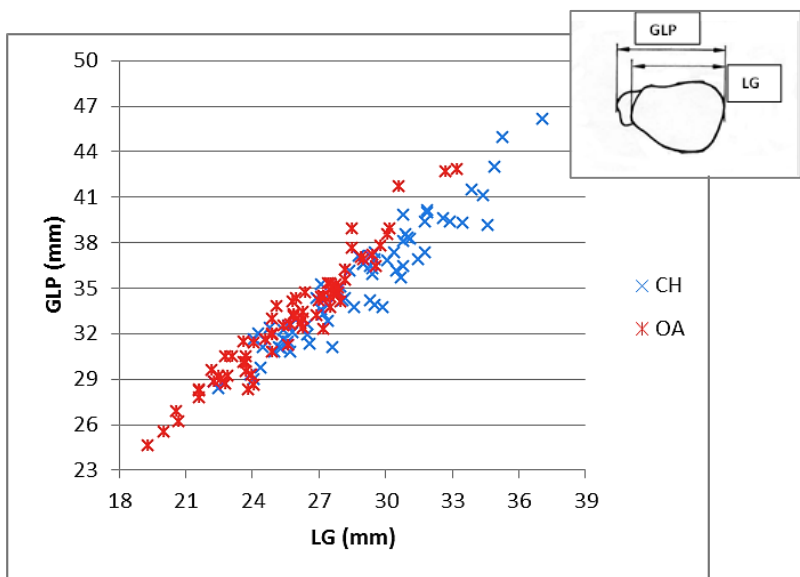


Figure 2.213 Greatest length of the glenoid cavity plotted against the greatest length of the *processus articularis*.

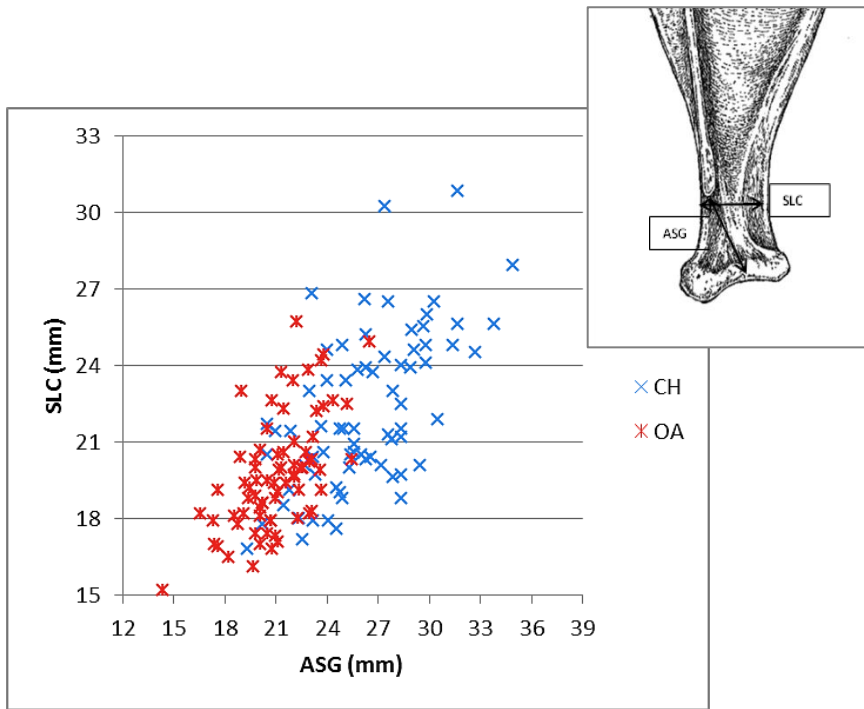


Figure 2.214 Shortest distance from the spine to the edge of the glenoid cavity plotted against the smallest length of the *collum scapulae*.

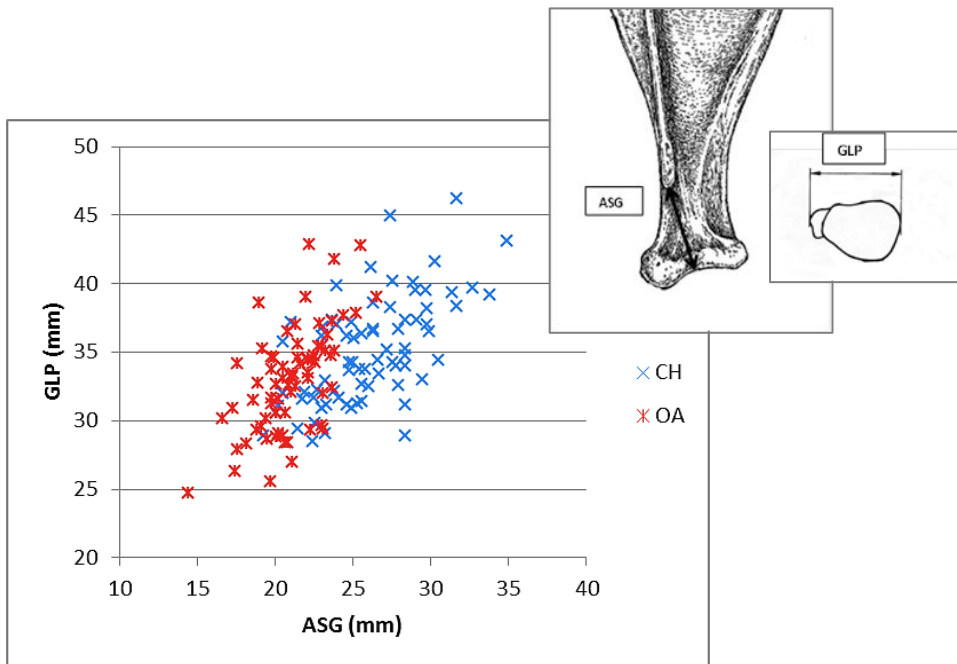


Figure 2.215 Shortest distance from the spine to the edge of the glenoid cavity plotted against the greatest length of the *processus articularis*.

Humerus

Good results have been obtained from the measurements taken on the distal articulation of the humerus. BT, Bd and Dd were taken because they can describe the shape of the distal articulation with the potential of discriminating the more elongated goat trochlea in comparison to the stouter trochlea of sheep (Boessneck 1969: 339; Boessneck *et al.* 1964:62). Following the overall difference in shape of the distal trochlea BE was created in order to describe the elongated aspect of the lateral crest of the *capitulum*. Finally, BEI was designed for describing the difference of the *epicondylus lateralis*, which is broad and arched in sheep and narrow and straighter in goat (Boessneck 1969: 340-341; Boessneck *et al.* 1964:62-65).

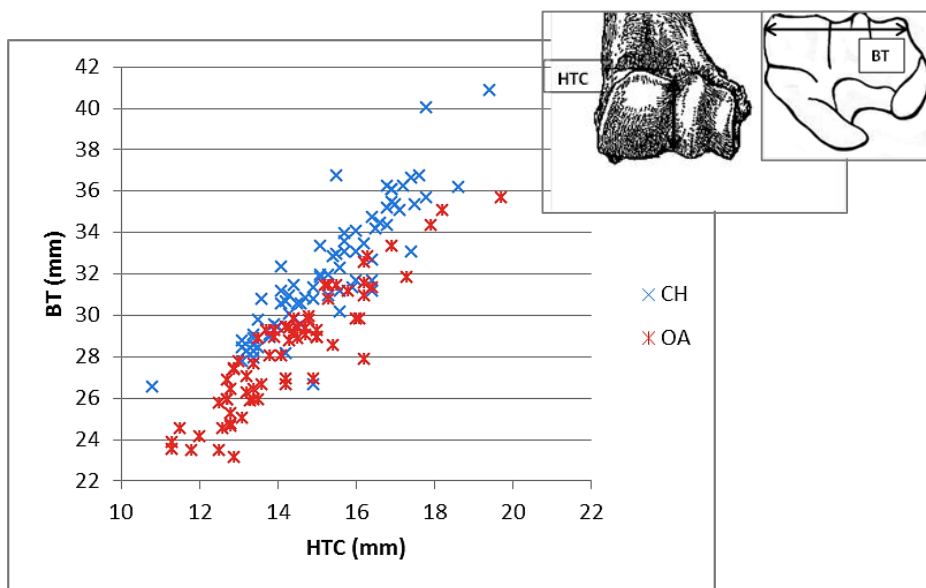


Figure 2.216 Diameter of the trochlear constriction plotted against the medio lateral width of the trochlea.

The scatterplots from 2.216 to 2.219 try to reflect such morphological differences of the humerus trochlea. Figure 2.216, shows HTC plotted against BT, a combination that Boessneck *et al.* (1964) suggested and was further applied by Fernández (2001) with good results. It can be seen that, on this sample, the sheep are clearly separated from the goats when the bone is small, in the other cases more overlap is present. Nevertheless, two different groups can still be recognised: this pattern clearly reflect the fact that goats have a more elongated trochlea than sheep (Boessneck 1969: 339; Boessneck *et al.* 1964:62). Figure 2.217 displays the combination HT-BT. Once again, this was suggested by Boessneck *et al.* (1964) and further applied by Helmer and Rocheteau (1994). Fernández applied them on wild and domestic animals belonging to *Capra* and *Ovis* with good results; similar success has been obtained in this study. From the above scatterplots it can be said that both combinations BT/HTC and BT/HT have some potential in discriminating the two domestic species.

In Figure 2.218 BE is plotted against BT. In goats, the greater breadth from the lateral crest to the *capitulum* results in an overall more elongated shape of the distal trochlea, and this is reflected in the combination of these two measurements. Overlap occurs, but some areas are exclusively occupied by sheep (bottom-left) or goats (up-right).

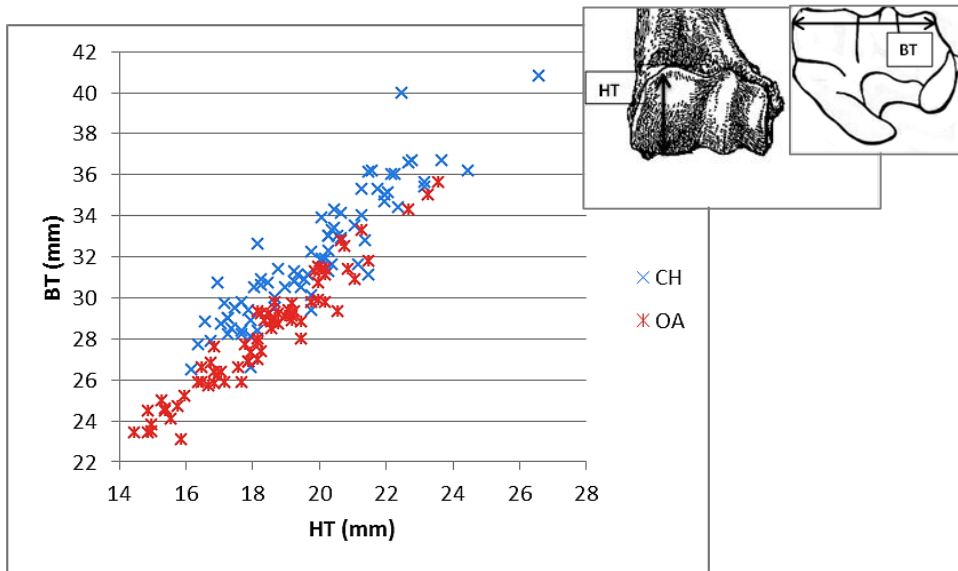


Figure 2.217 Height of the trochlea plotted against its medio lateral width.

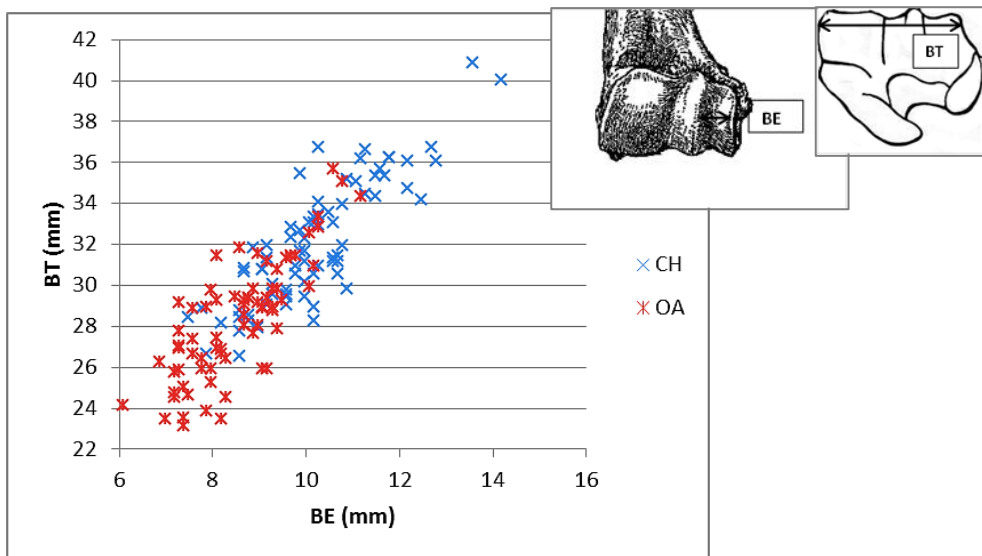


Figure 2.218 Breadth from the lateral crest to the capitulum plotted against the medio lateral width of the trochlea.

Figures 2.219 and 2.222 show that if either HT and BE or HTC and BE are considered, a fairly good discrimination among the sample can be reached, as these measurements are those that reflect the morphological differences of the distal trochlea.

Figures 2.220, 2.221 and 2.223 illustrate another morphological feature, namely the greater breadth of the *epicondylus lateralis* in sheep (Boessneck 1969: 340-341; Boessneck *et al.* 1964:62-65). This aspect is particularly visible when BEI is used in combination with Bd, Dd and BT.

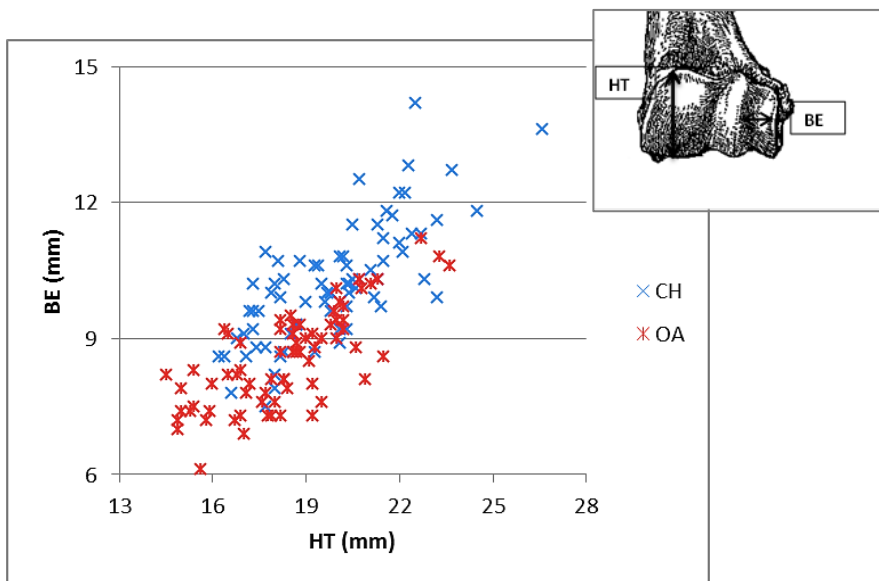


Figure 2.219 Height of the trochlea plotted against the breadth from the lateral crest to the *capitulum*.

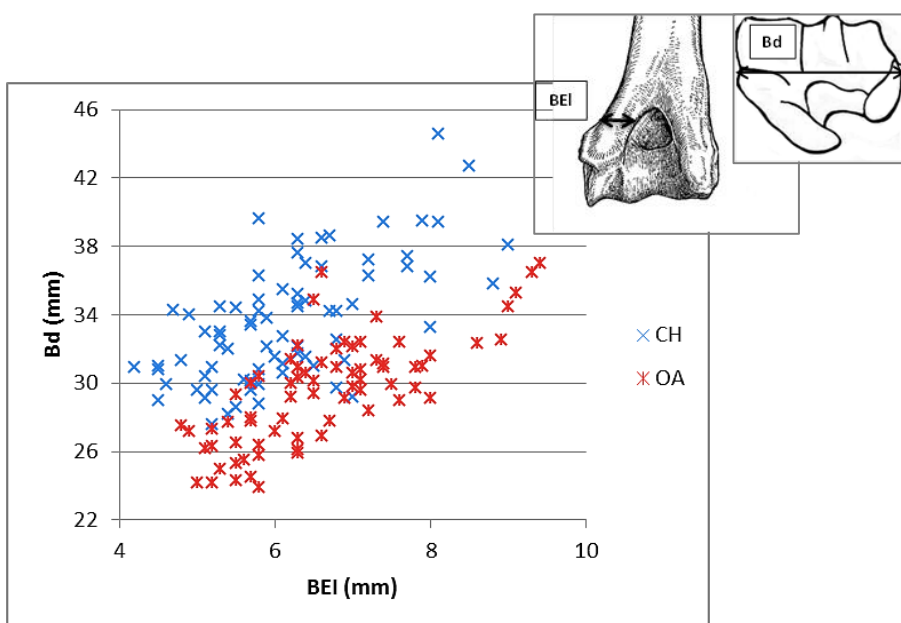


Figure 2.220 Breadth of the *epicondylus lateralis* plotted against the distal width.

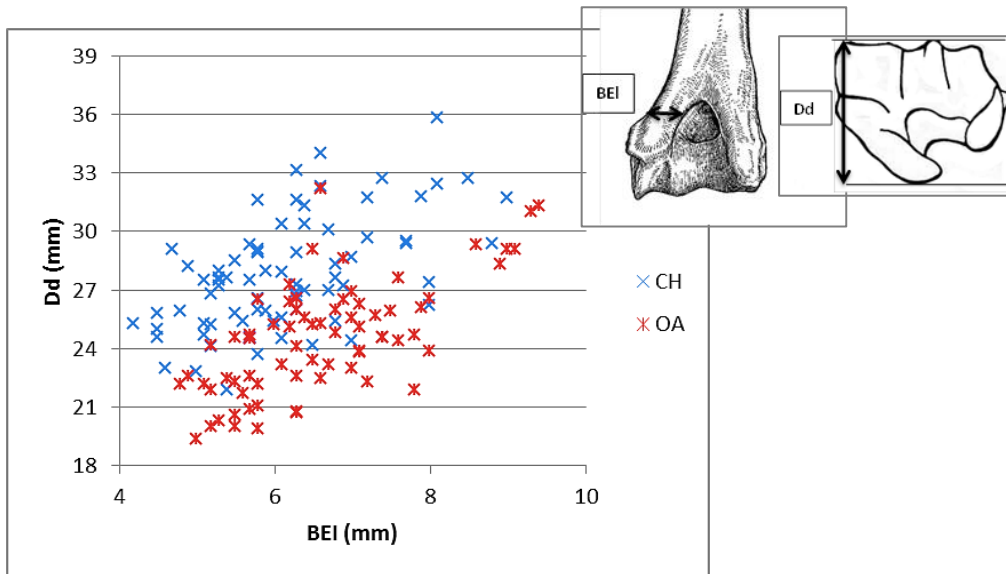


Figure 2.221 Breadth of the *epicondylus lateralis* plotted against the depth of the distal end.

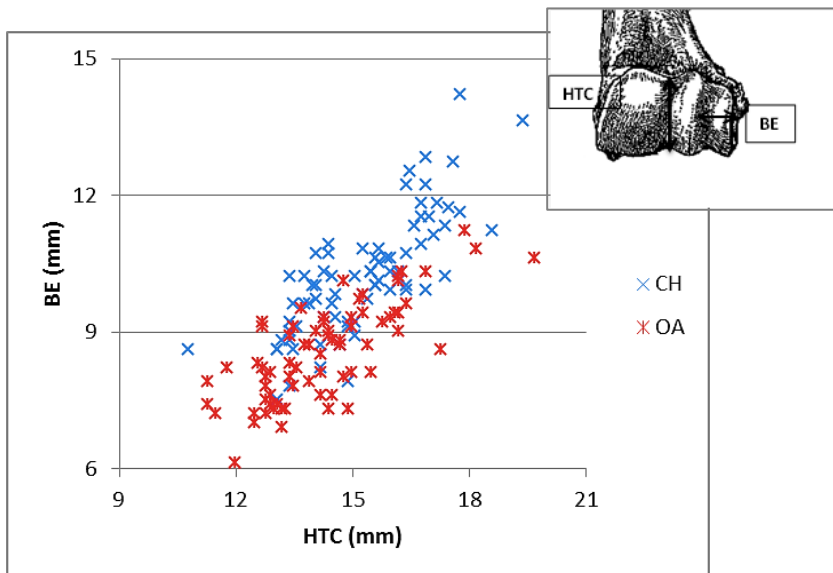


Figure 2.222 Diameter of the trochlear constriction plotted against the breadth from the lateral crest to the *capitulum*.

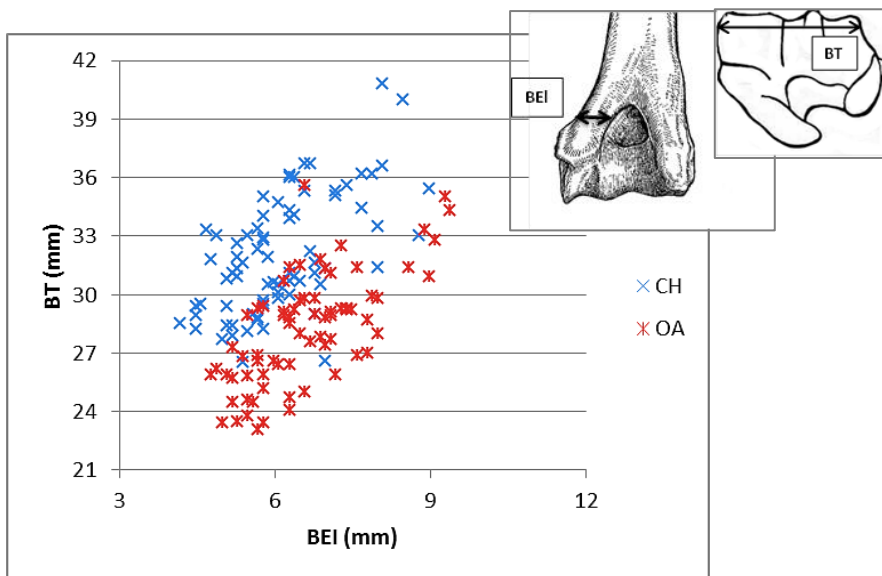


Figure 2.223 Breadth of the *epicondylus lateralis* plotted against the medio lateral width of the trochlea.

Radius

By plotting the measurements taken on the proximal articulation of the radius, promising results were obtained. Five measurements were taken on this anatomical part and, unsurprisingly, Bp and especially Bfp, which describe the most striking morphological differences between sheep and goat on the proximal end of the radius, were the most fruitful as can be seen from Figure 2.224. This set of measurements was applied by Fernández (2001) but her sample of goat was so small that no observation could be made on the potential of these measurements in discriminating the two domestic species. Figure 2.224 shows that, despite some overlap, two groups are clearly identifiable. This separation reflects the fact that while in sheep there is usually a well-developed bump on the lateral side of the proximal articular surface, the same feature is much less pronounced in goat (Boessneck 1969: 342; Boessneck *et al.* 1964:70).

Figure 2.225 displays GL plotted against SD and it can be seen a higher degree of overlap compared to the previous scatterplot but areas of differentiation are identifiable. In particular it can be noticed that the greatest length in combination with the depth of the shaft illustrate the slenderness of the goat bone compared to the more robust sheep (same or lower SD than sheep but greater GL) as mentioned in previous studies (Boessneck 1969; Boessneck *et al.* 1964).

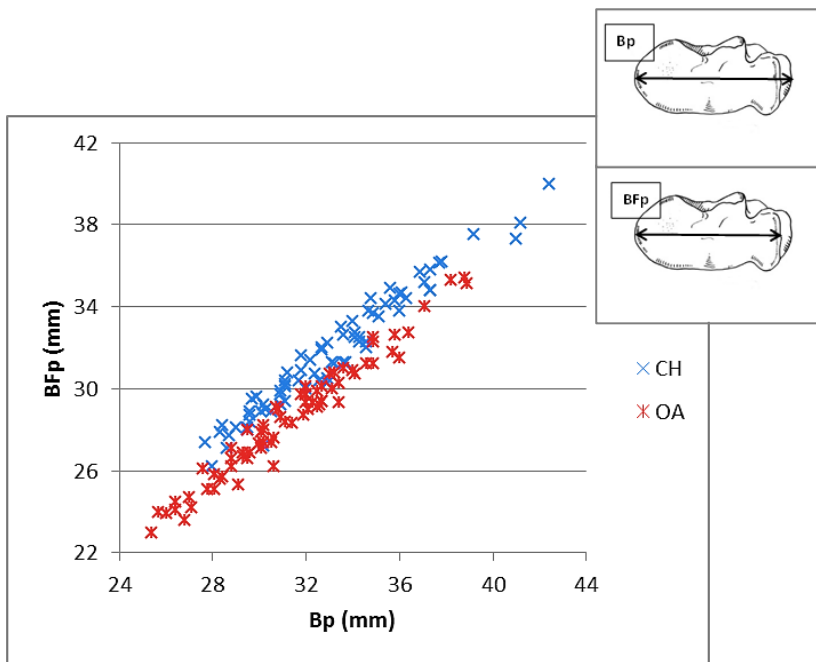


Figure 2.224 Breadth of the proximal articulation plotted against the breadth of the *facies articularis proximalis*.

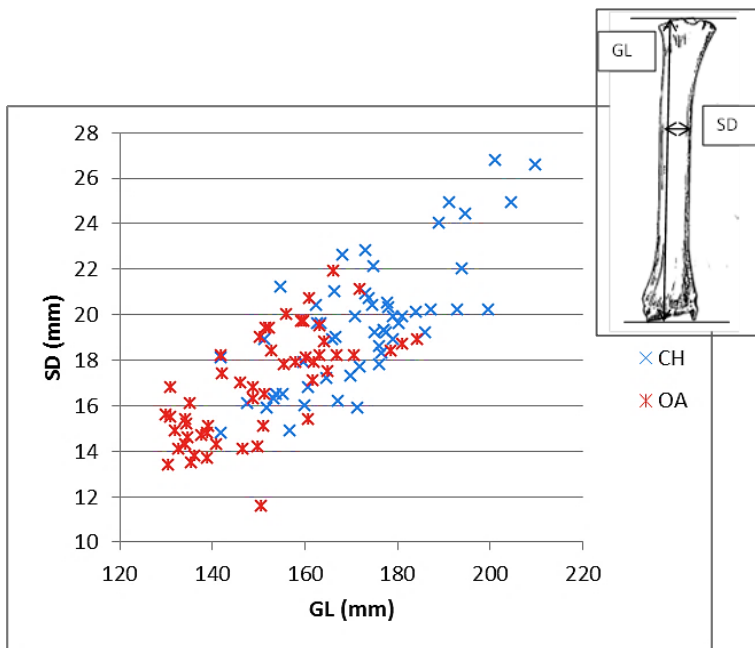


Figure 2.225 Greatest length plotted against the smallest width of the shaft (image of radius: reprinted from SCHMID, E. *Atlas of animal bones: for prehistorians, archaeologists and quaternary geologists*. Amsterdam: Elsevier, copyright 1972, with permission from Joerg Schibler).

Ulna

BPC and DPA, taken on the proximal articulation of the ulna, have provided useful results for the discrimination of sheep and goat (Figs. 2.226 and 2.227). B and L, new measurements introduced by the author in order to translate the different shape of the *olecranon*, were unfortunately less successful. Figure 2.228 does not show such a clear separation as other scatterplots do. The combination of B and L does attest to the fact that goats have a longer and thicker *olecranon* than sheep, morphological difference already noticed by Boessneck *et al.* (1964: 74; Boessneck 1969: 343), but, when translated metrically, these features are not so useful for discriminating the two species.

BPC combined with DPA and SDO represent the combinations with the highest potential in describing morphological differences of the ulna lateral coronoid process. In Figures 2.226 and 2.227 highly distinct clusters can be observed, with only a few outliers denying the opportunity for a complete distinction of the two species. It can be observed that BPC in goats is almost always higher than in sheep, echoing the fact that the lateral coronoid process projects more laterally than in sheep (morphological characteristic which has already been noticed in the past (in Boessneck 1969: 342; Boessneck *et al.* 1964: 70). These successful measurements had previously been adopted by Helena Fernández (2001) but, as seen with the radius, the goat was so poorly represented in her sample that no comments were made on their contribution to the sheep/goat distinction.

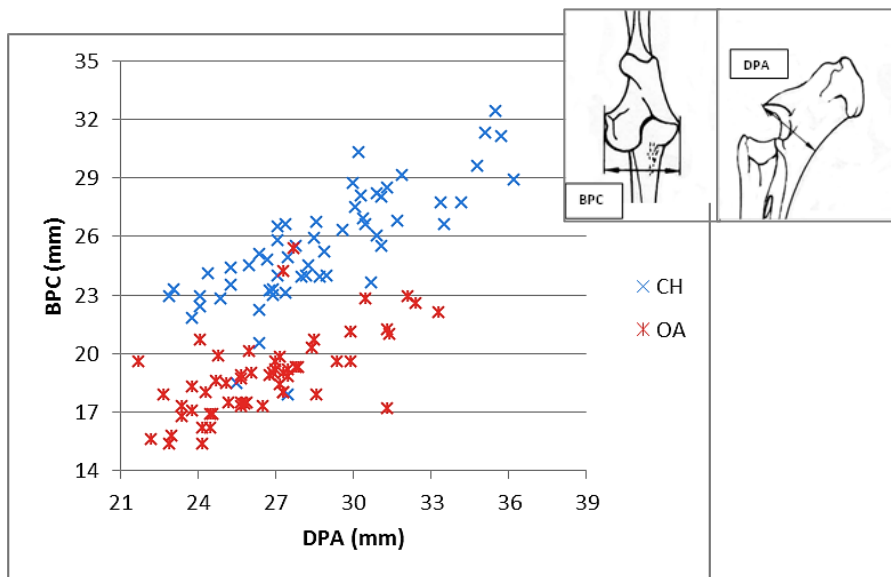


Figure 2.226 Depth across the *processus anconaeus* to the caudal border plotted against the greatest breadth across the coronoid process.

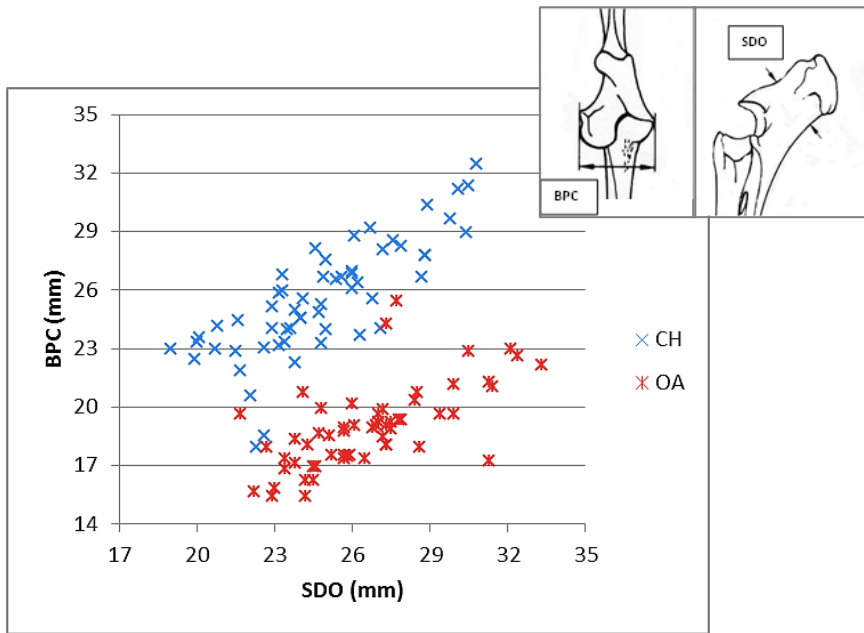


Figure 2.227 Smallest depth of the *olecranon* plotted against greatest breadth across the coronoid process.

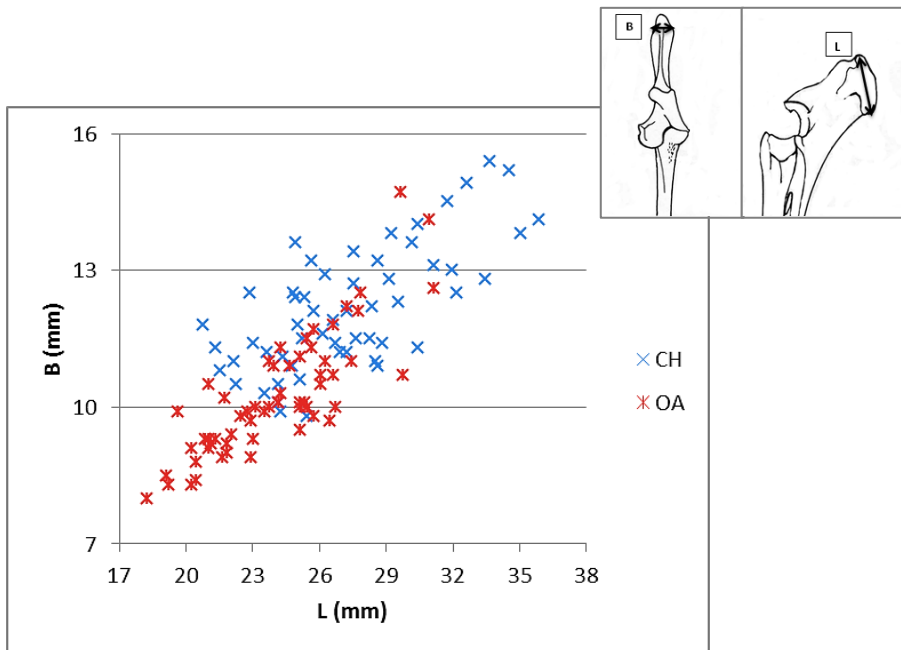


Figure 2.228 Length of the *olecranon* plotted against its breadth.

Metacarpal

The diagnostic value of metacarpals has been previously pointed out (Boessneck 1969; Boessneck *et al.* 1964; Payne 1969; Rowley-Conwy 1998). Pairs of measurements that proved to be particularly powerful in discriminating sheep from goats were 1 and a, 4 and b, 2 and 1, 5 and 4 as shown by the plots below (from 2.229 to 2.235).

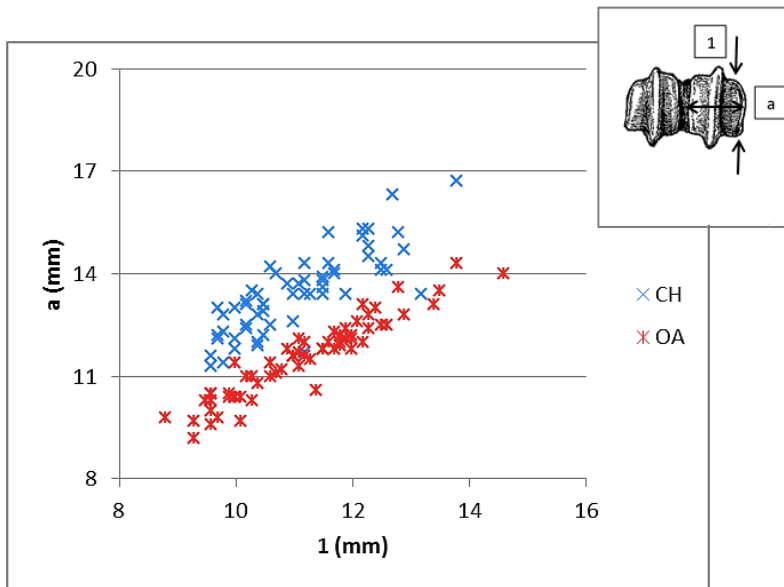


Figure 2.229 Diameter of the medial trochlea plotted against the width of the medial condyle.

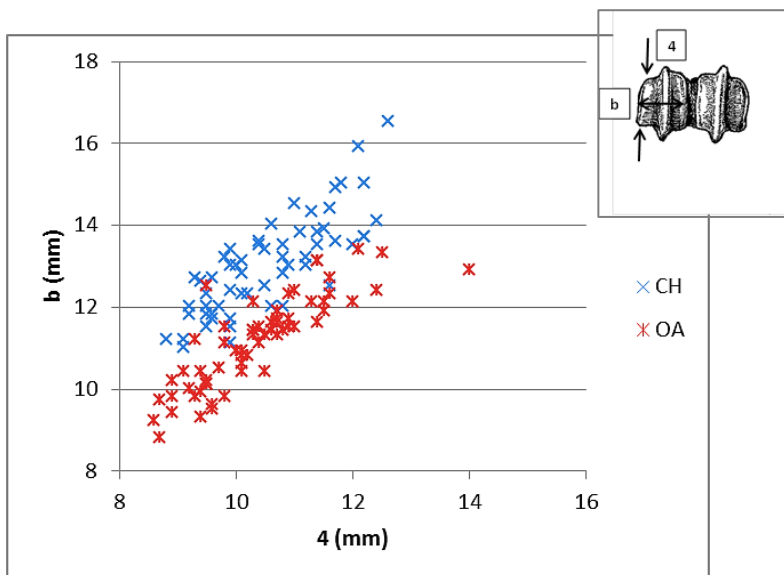


Figure 2.230 Diameter of the lateral trochlea plotted against the width of the lateral condyle.

By looking at Figures 2.229 to 2.232, which display different combinations of these measurements, some considerations can be made. First of all, it can be noticed that the separation between sheep and goat is slightly more evident on the medial (measurement a) rather than the lateral (measurement b) condyle (see also Davis 1996; Fernández 2001; Rowley-Conwy 1998). Secondly, the separation of the two clusters determined by a and b, and 1 and 2 in their different combinations, translate effectively (as just very few specimens overlap) one of the most important morphological features in this area of the metacarpal, namely that, while in goat the peripheral parts of the trochlear condyles are relatively small, in sheep they are larger. The same results were obtained by Fernández despite her sample of goat was very small (4 specimens).

If Figures 2.233 to 2.235 are considered, it can be noticed that GL combined with SD, BatF and Bdf show, despite some overlapping, how metacarpals of sheep are more slender than those of goat, as previously noted by Boessneck *et al.* (1964: 107; Boessneck 1969: 354).

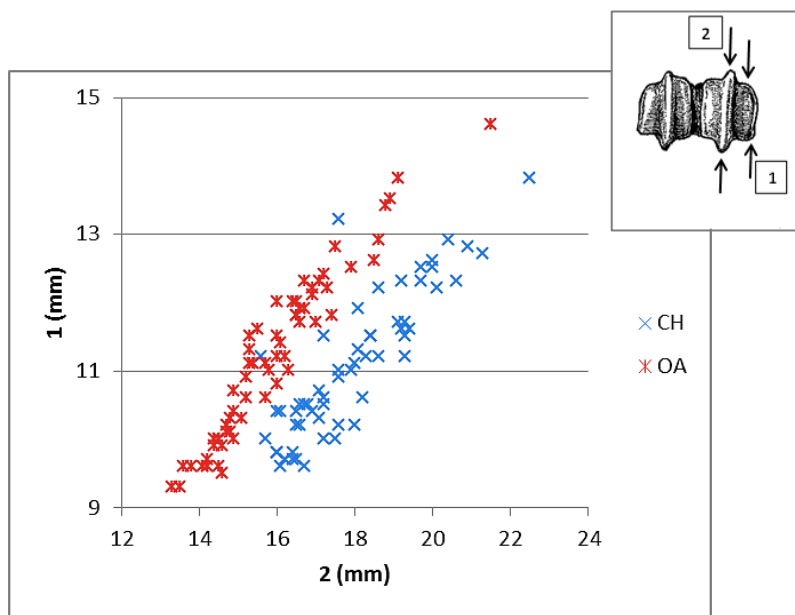


Figure 2.231 Diameter of the *verticillus* at the medial condyle plotted against the diameter of the medial trochlea.

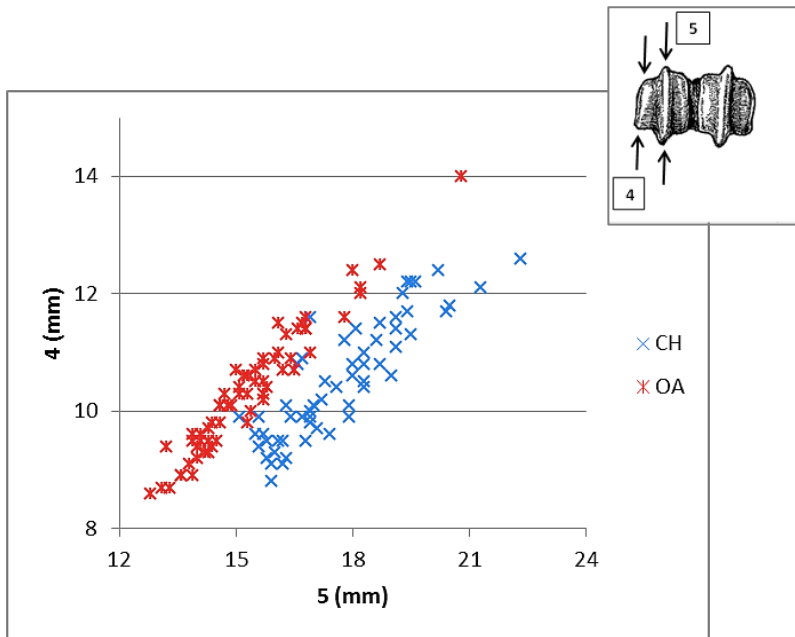


Figure 2.232 Diameter of the *verticillus* at the lateral condyle plotted against the diameter of the lateral trochlea.

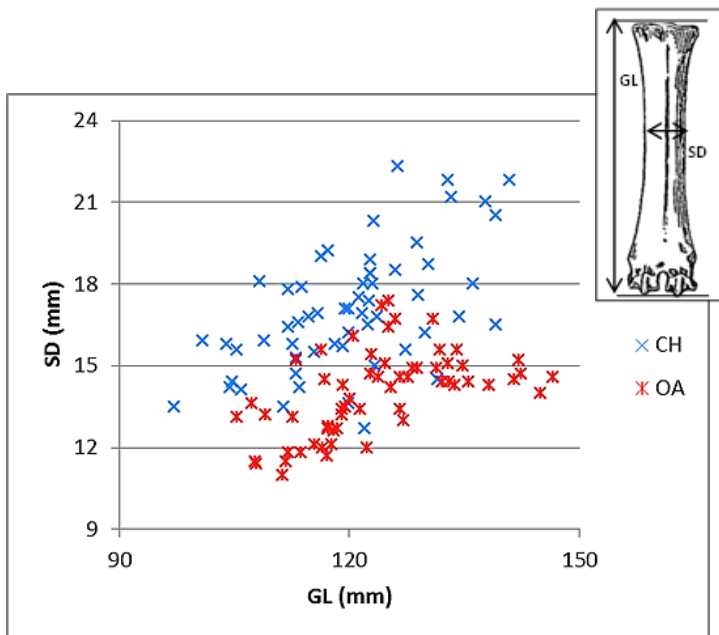


Figure 2.233 Greatest length plotted against the smallest width of the shaft (image of metacarpal: reprinted from SCHMID, E. *Atlas of animal bones: for prehistorians, archaeologists and quaternary geologists*. Amsterdam: Elsevier, copyright 1972, with permission from Joerg Schibler).

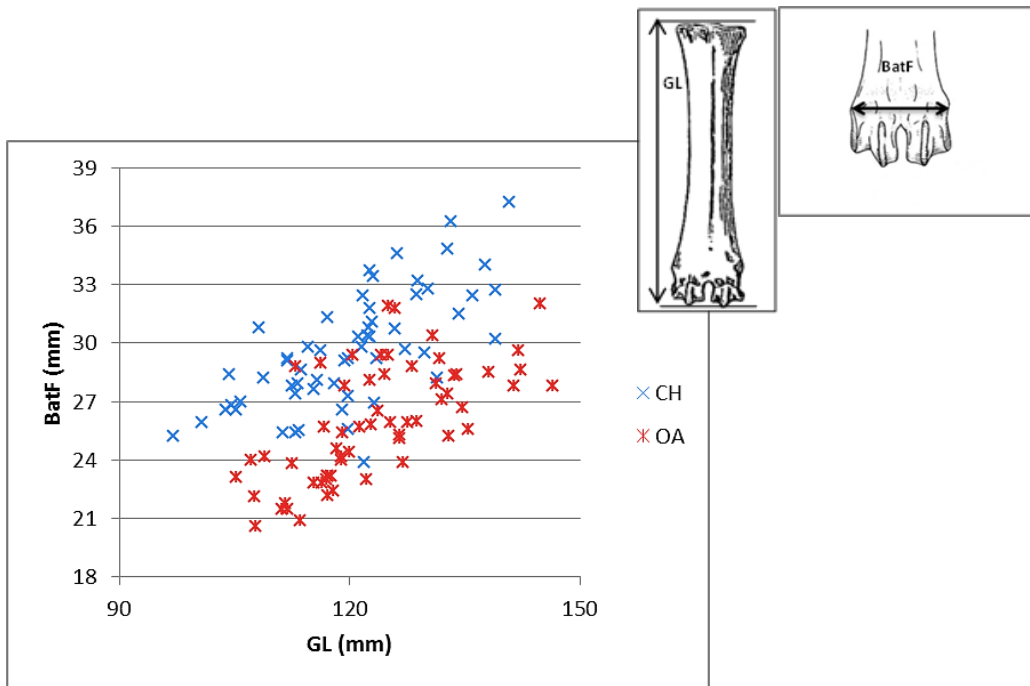


Figure 2.234 Greatest length plotted against the breadth at the fusion point of the distal end.

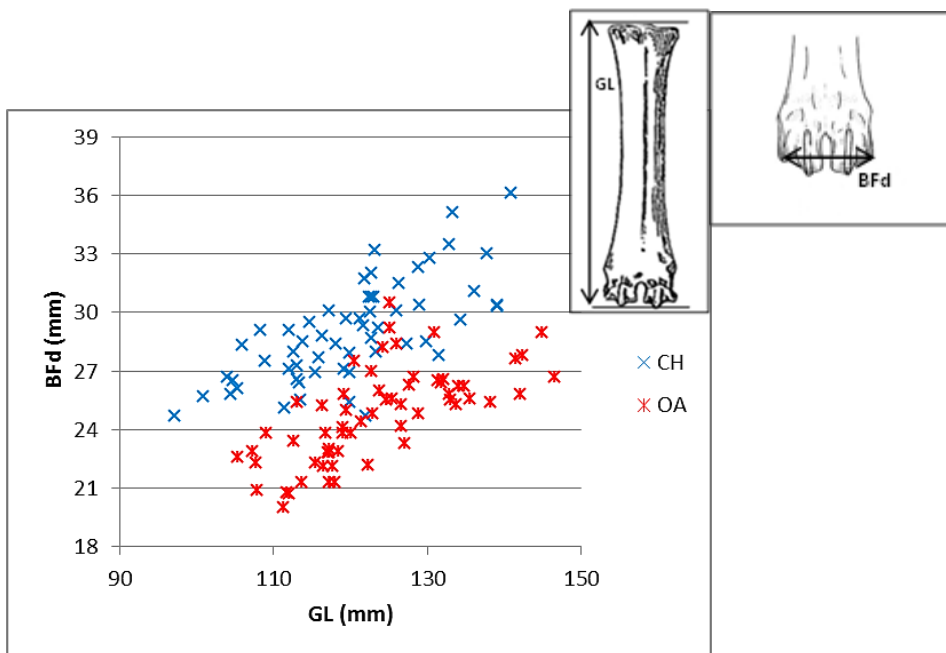


Figure 2.235 Greatest length plotted against the breadth of the distal end.

Since this anatomical element is highly sexually dimorphic (Davis 1981), plotting the data according to the sex of the animals can be useful. It is expected that females will be smaller. This is mainly noticeable for sheep (Fig. 2.237) while in goats there is more overlap (Fig. 2.236). Figure 2.237 shows also that castrates fall in between the ewes and the rams, as

previously suggested by Davis (2000: 374-385); thus it is difficult to separate the castrates from the males and the females as they tend to have intermediate characteristics.

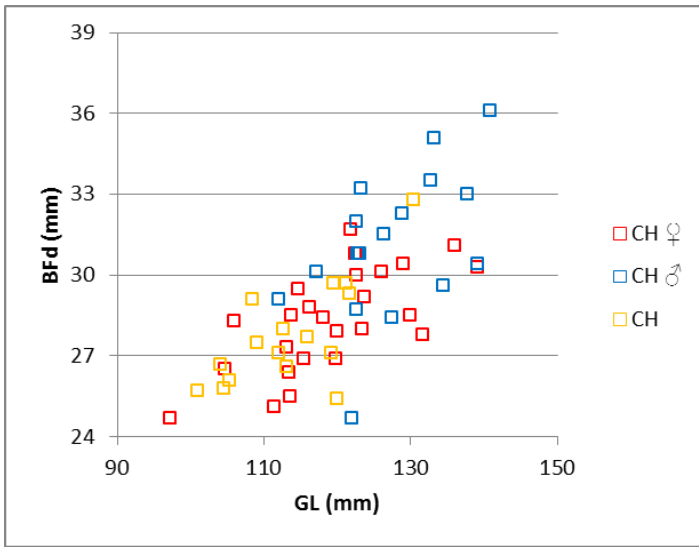


Figure 2.236 Goat. Greatest length plotted against the breadth of the distal end. Specimens divided by sex.

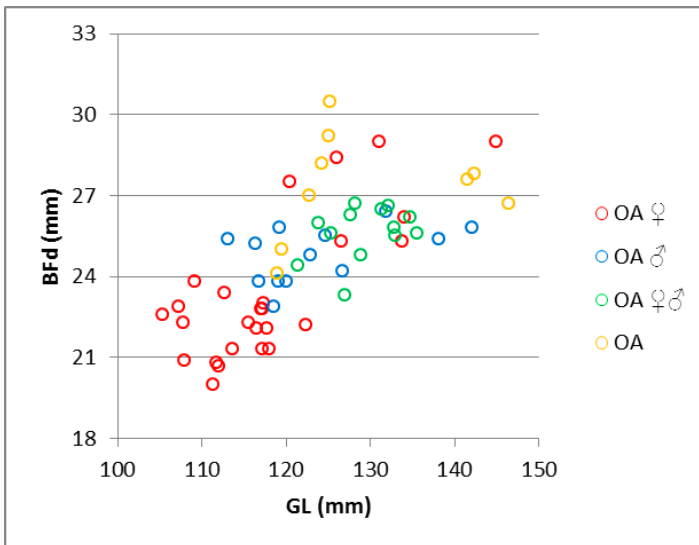


Figure 2.237 Sheep. Greatest length plotted against the breadth of the distal end. Specimens divided by sex.

Metatarsal

The same combination of measurements that proved to be effective on the metacarpal (mainly 1 and 2, 5 and 4) is also effective for the metatarsal (Figs. 2.238 and 2.239). GL combined with SD, BatF and BFp show, as in metacarpals, a certain degree of overlying but the metatarsal of sheep are more slender (Figs. 2.240 to 2.242). If the measurements are plotted by sex, despite some overlap, separate clusters can be identified (Figs. 2.243 and 2.244).

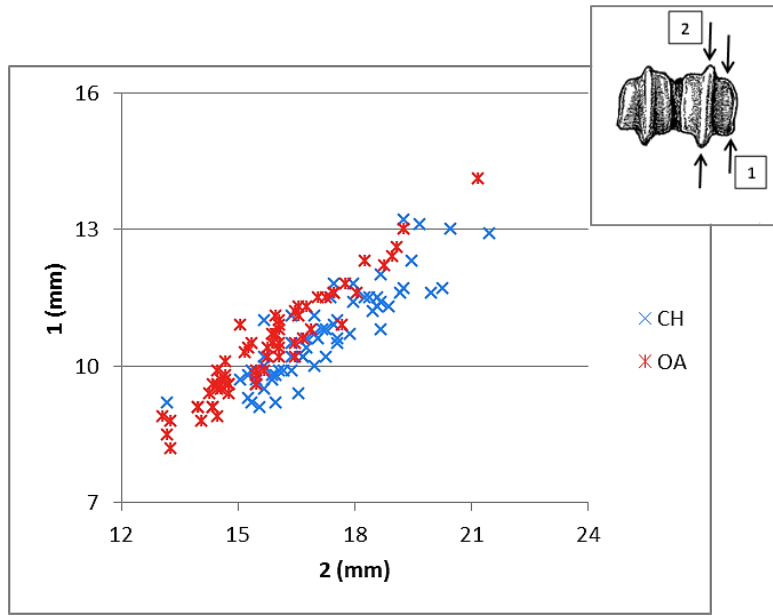


Figure 2.238 Diameter of the *verticillus* at the medial condyle plotted against the diameter of the medial trochlea.

By comparing the results obtained from the metacarpal and the metatarsal it can be seen that, while in the metacarpal plots two well defined groups can usually be recognised, the separation displayed by the metatarsal results is less clear, confirming what Boessneck (1969), Fernández (2001), Payne (1969) and Rowley-Conwy (1998) have noted previously: among the metapodials, the metacarpal is the one which retains more distinctive characteristics.

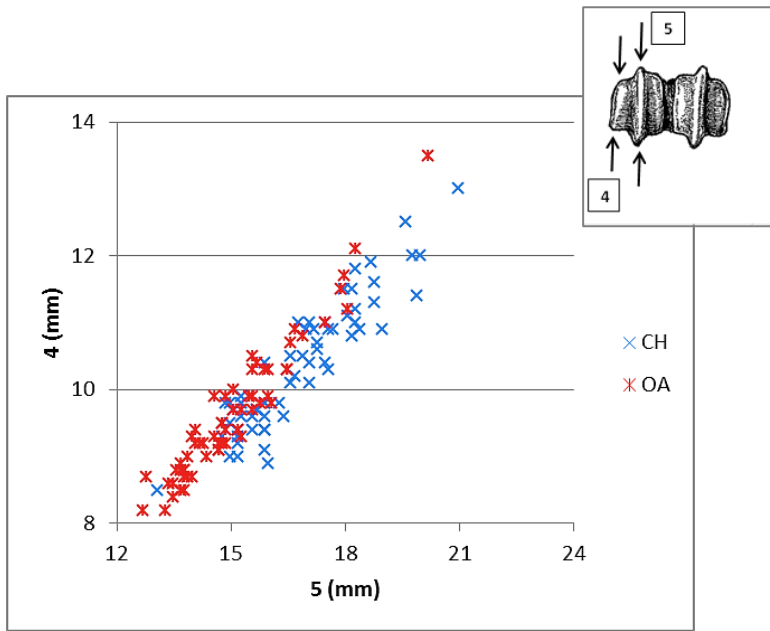


Figure 2.239 Diameter of the *verticillus* at the lateral condyle plotted against the diameter of the lateral trochlea.

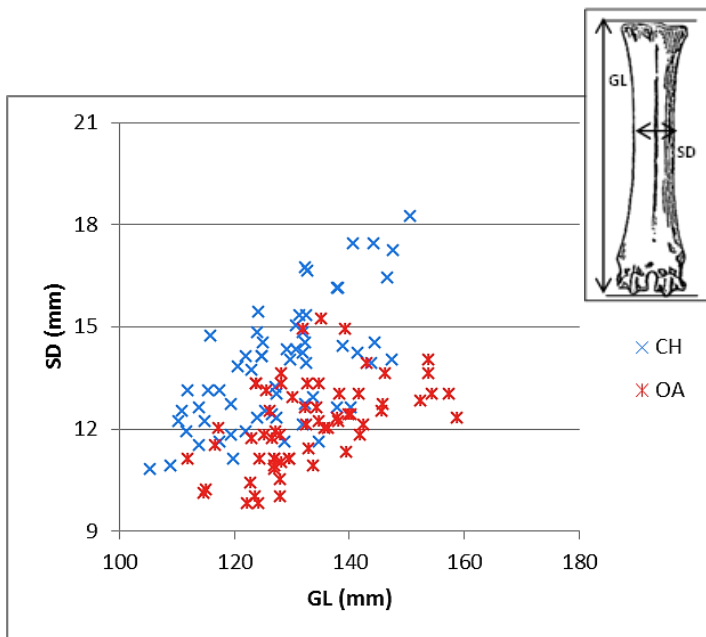


Figure 2.240 Greatest length plotted against the smallest width of the shaft.

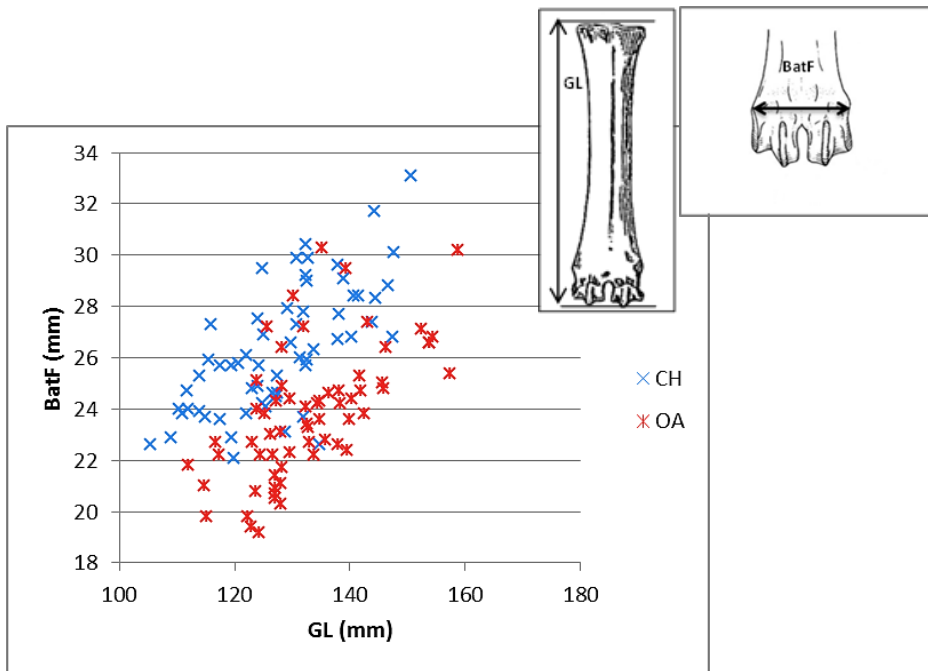


Figure 2.241 Greatest length plotted against the breadth at the fusion point of the distal end.

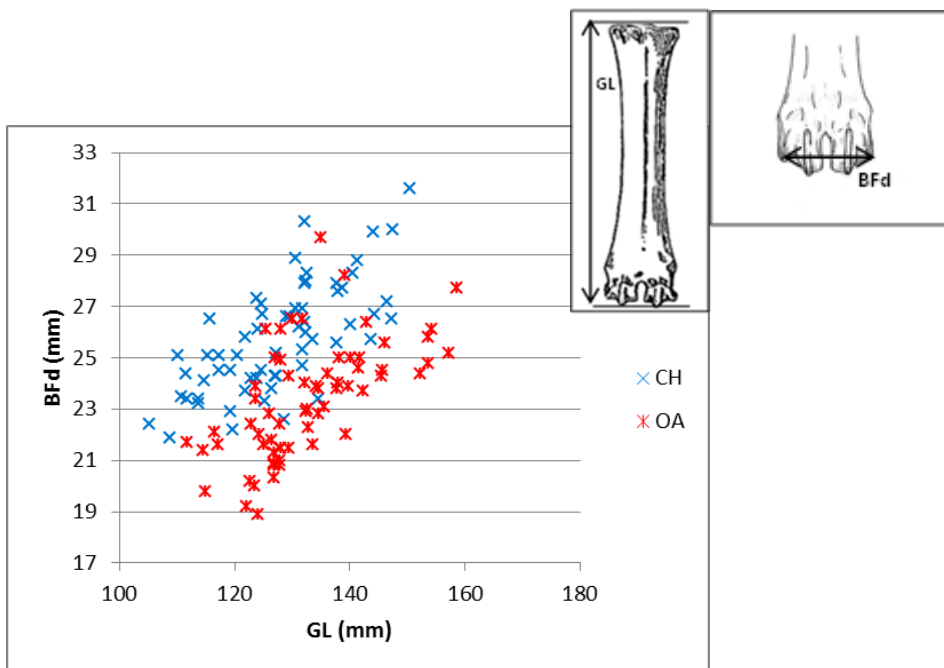


Figure 2.242 Greatest length plotted against the breadth of the distal end.

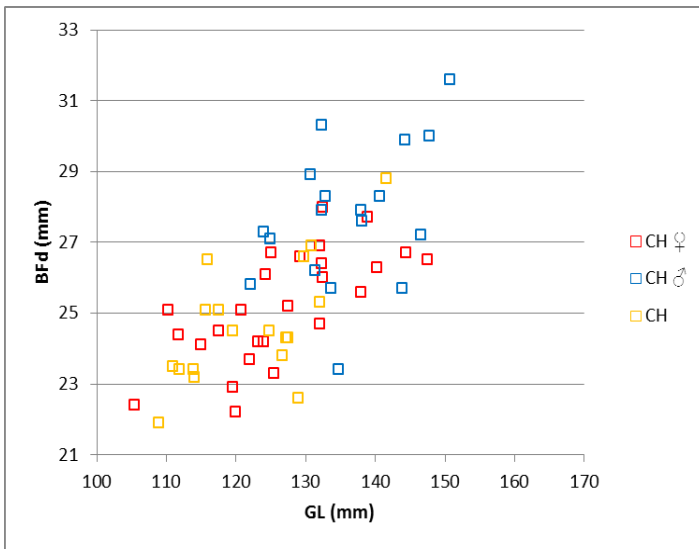


Figure 2.243 Goat. Greatest length plotted against the breadth of the distal end. Specimens are divided by sex.

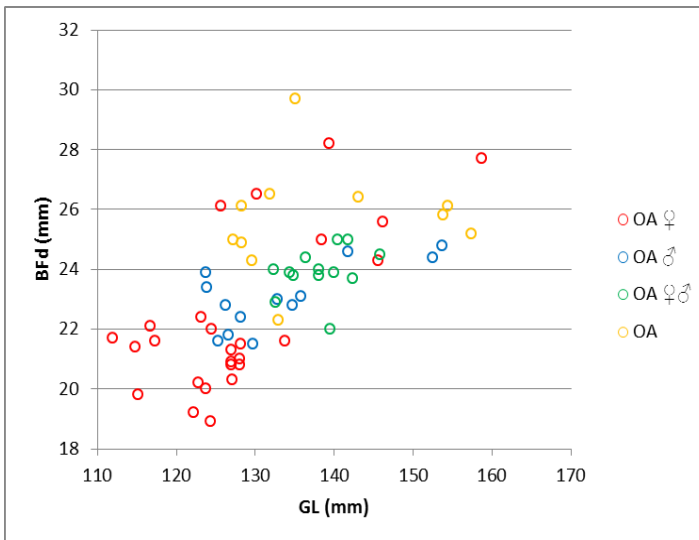


Figure 2.244 Sheep. Greatest length plotted against the breadth of the distal end. Specimens are divided by sex.

Tibia

This element has been regarded by some as difficult to discriminate between sheep and goat (Boessneck 1969; Boessneck *et al.* 1964; Zeder and Lapham 2010), but Kratochvíl (1969) did point out some useful characteristics for differentiation of the two species. Despite a certain degree of overlap, biometrical plots confirm Kratochvíl's view that the tibia can be identified to species. Among the various combinations of measurements, GL and SD are those which provided a better separation between the two groups attesting that goats are more slender than sheep (Fig. 2.247). Two clusters can also be recognised when the measurements taken on the distal articulation are considered, mirroring the morphological difference in the shape of the distal articulation; in fact, sheep have a more trapezoidal distal articulation, while in goat this is more rectangular (Kratochvíl 1969), as demonstrated by Figures 2.245 and 2.246. The combination Dd(a) and Bd was previously tried by Helena Fernández (2001) but, as her sample of goat was represented by only eight specimens, the author suggested to test these measurements on a larger sample. Figure 2.246 confirms the existence of some separation of goats and sheep based on the tibia distal articular measurements.

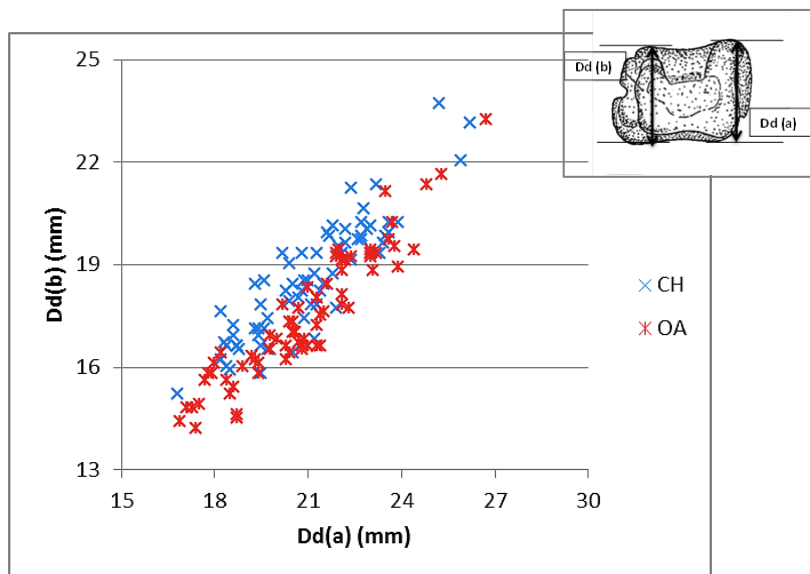


Figure 2.245 Depth of the medial side plotted against the depth of the lateral side of the distal end.

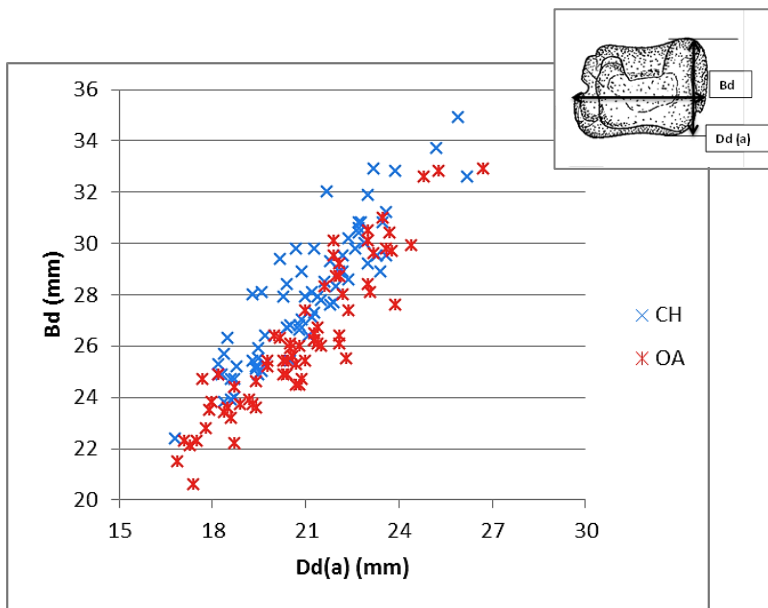


Figure 2.246 Depth of the lateral side plotted against the breadth of the distal end.

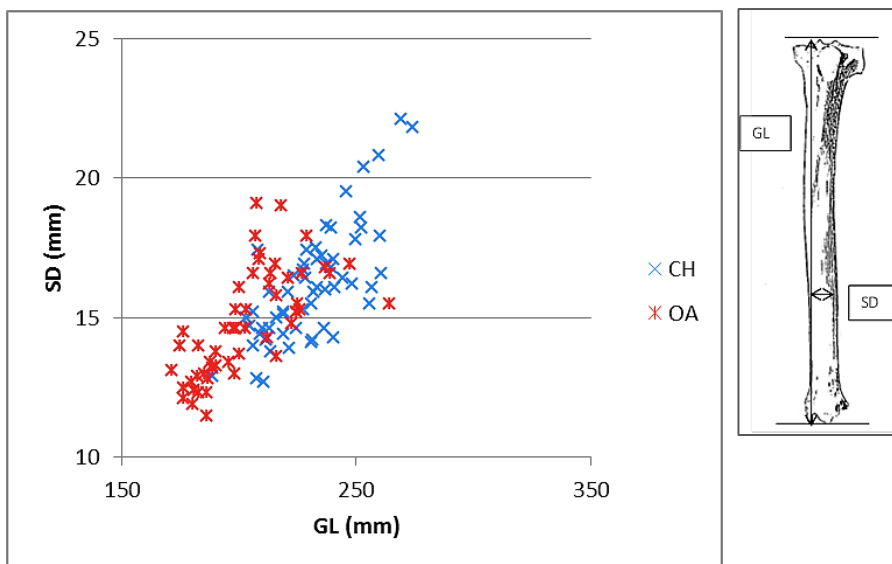


Figure 2.247 Greatest length plotted against the smallest width of the shaft (image of tibia: reprinted from SCHMID, E. *Atlas of animal bones: for prehistorians, archaeologists and quaternary geologists*. Amsterdam: Elsevier, copyright 1972, with permission from Joerg Schibler).

Astragalus

As in the case of the metacarpal, good results were, to a certain extent, expected from the study of this bone, particularly in view of Davis' recent work (in press). Figures 2.248, 2.249 and 2.250, show that Bd/GLI, H/DI and H/Bd pairings provide some degree of separation. These are new combinations, apart from Bd/GLI, which has unsuccessfully been tested by Fernández (2001). The diagrams below (Figs. 2.248 to 2.250) show that the goat is usually more slender than the sheep, but also that there are morphological differences as measurements reflect the

fact that the sulcus between the two ridges of the trochlea is less deep in goat than in sheep. When BpT and DI are plotted (Fig. 2.251) some discrimination is still obtained but the overlap is greater.

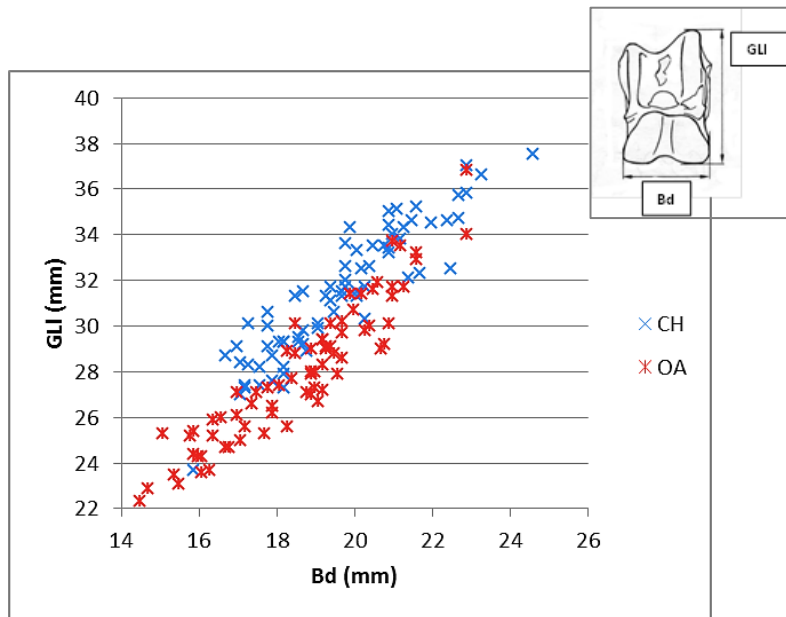


Figure 2.248 Breadth of the distal end plotted against the greatest length of the lateral part (image of astragalus (Fig. 41d): reprinted from von den Driesch, A. *A guide to the measurement of animal bones from archaeological sites*. Peabody Museum Bulletins, vol. 1, copyright 1976 with permission from the President and Fellows of Harvard College).

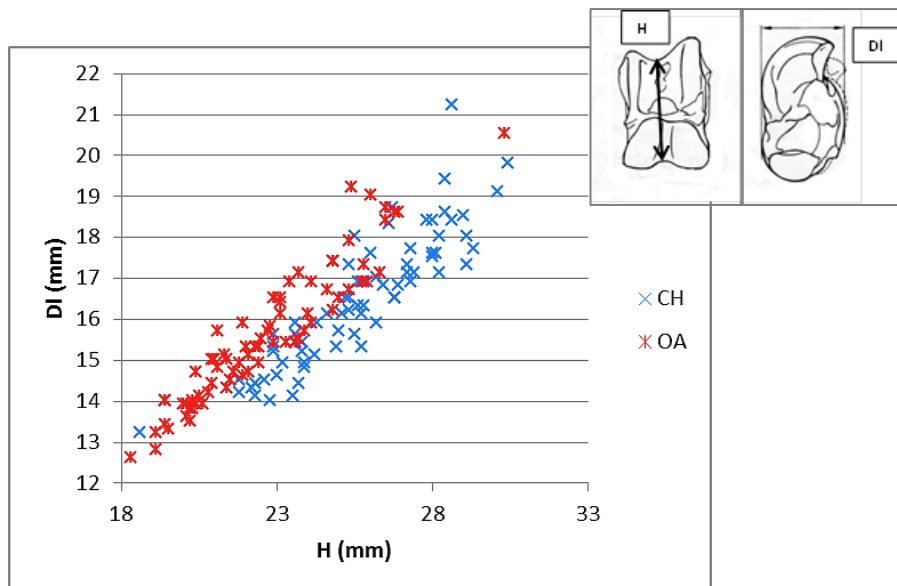


Figure 2.249 Height at the central constriction plotted against the greatest depth of the lateral half (image of lateral astragalus (Fig. 41e): reprinted from von den Driesch, A. *A guide to the measurement of animal bones from archaeological sites*. Peabody Museum Bulletins, vol. 1. Copyright 1976 with permission from the President and Fellows of Harvard College).

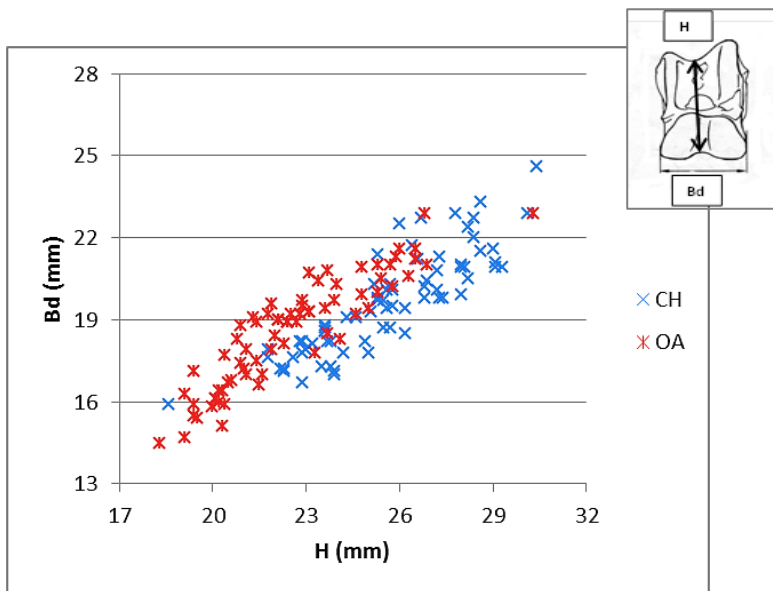


Figure 2.250 Height at the central constriction plotted against the breadth of the distal end.

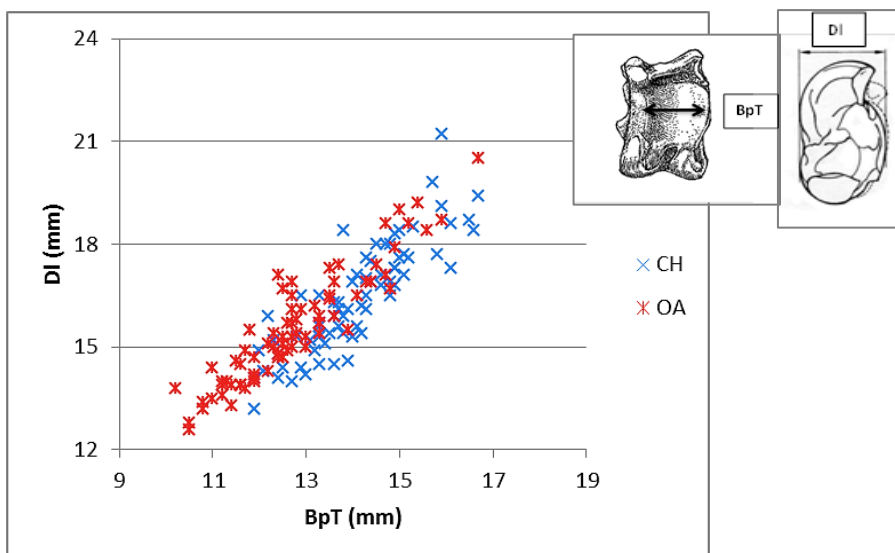


Figure 2.251 Maximum breadth of the plantar trochlea plotted against the greatest depth of the lateral half.

Calcaneum

The measurements taken on the calcaneum provided useful biometrical backing to Boessneck *et al.* (1964) claims of the morphological distinctiveness of this element. Figures 2.252 to 2.255 show that all pairings provided fairly clear distinctions, though less so for the GL/DS ratio (Fig. 2.254). In Figures 2.252 the goat's shorter length of the articular facet of the *os malleolare* on the lateral process is clearly evident, confirming what Fernández (2001) had observed in her study. Figure 2.253 shows measurements which succeed in translating the shape of the articular facet for the *os malleolare* in measurements. This faces it more triangular in sheep than goat.

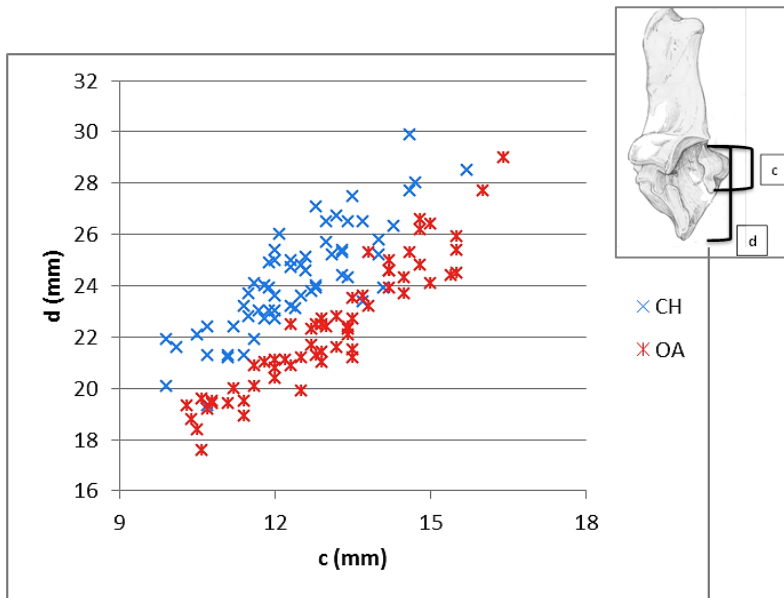


Figure 2.252 Length of the articular facet of the *os malleolare* plotted against length taken from the articular facet of the *os malleolare* to the end of the articulation-free part of the process (image of calcaneum: reprinted from ZEDER, M.A. and H.A. LAPHAM. Assessing the reliability of criteria used to identify postcranial bones in sheep, *Ovis*, and goats, *Capra*. *Journal of Archaeological Science* 37: 2887-2905, copyright 2010, with permission from Elsevier).

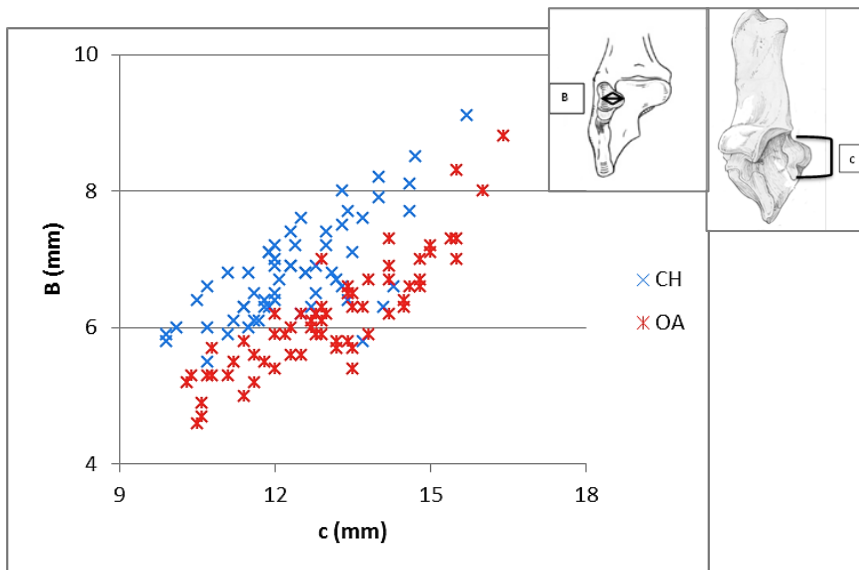


Figure 2.253 Length of the articular facet of the *os malleolare* plotted against the breadth of its articular surface.

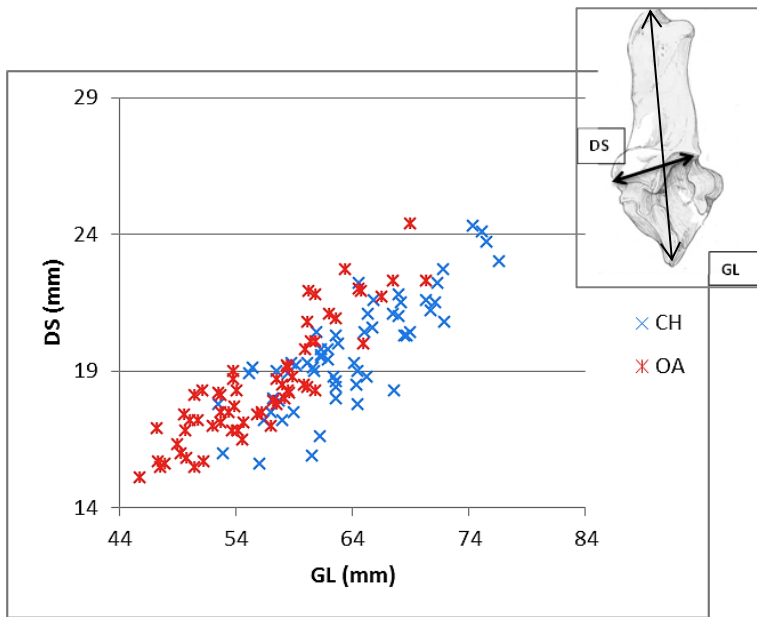


Figure 2.254 Greatest length plotted against the depth of the *sustentaculum tali*.

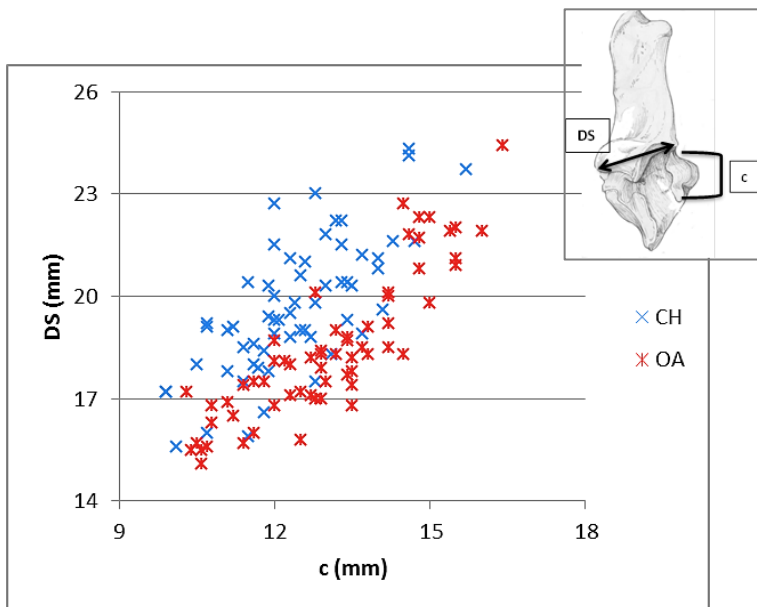


Figure 2.255 Length of the articular facet of the *os malleolare* plotted against the depth of the *sustentaculum tali*.

3rd Phalanx

On the 3rd phalanx only two measurements were taken. The pairing of DLS and MBS is quite diagnostic, and it was thought to be useful in translating the difference in the shape of the sole biometrically. In goats the sole stands almost vertically, is narrow and forms an isosceles triangle with a very short base, while in sheep the sole is thicker and curved. Figure 2.256

proves the extent to which DLS is consistently longer in goat specimens that have a similar MBS to sheep.

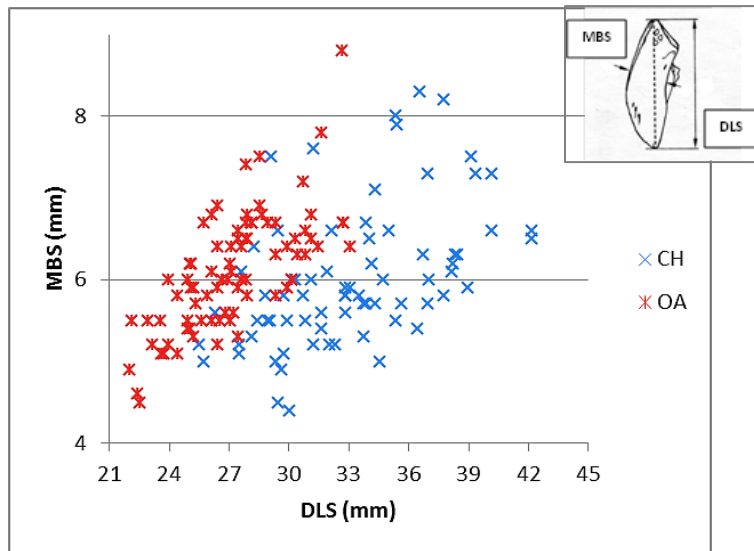


Figure 2.256 Diagonal length of the sole plotted against the middle breadth of the sole (image of 3rd phalanx (Fig. 48c): reprinted from von den Driesch, A. *A guide to the measurement of animal bones from archaeological sites*. Peabody Museum Bulletins, vol. 1, copyright 1976 with permission from the President and Fellows of Harvard College).

This exploratory analysis has especially been useful in providing an initial sense of the diagnostic values of some metric characteristics and in focusing further work particularly on those which were shown to be more fruitful for the proposed discrimination.

Deciduous teeth were recorded and measured as part of this project but eventually produced a too small sample size to provide useful results and are therefore excluded from subsequent biometrical analysis. The morphological usefulness of these elements (cf. Payne 1985) is not questioned however, and they will be still used in the archaeological applications for discriminating between sheep and goat. For a critique of the diagnostic value of caprine teeth see Zeder and Pilaar (2010).

2.5.3 Allometric shape analysis as expressed by Biometrical Indices

After this first insight into the linear measurements, in this chapter measurement ratios are plotted to emphasise potential shape differences between sheep and goats. Actual size, which is of limited interest for this analysis, will therefore mostly be removed as a factor affecting distributions. In a few cases, however, a linear measurements (as opposed to a ratio) has been retained on one of the two axes, which means that along that axis the distribution will still be

affected by size. The main purpose is to evaluate which combination of measurements has the best potential to discriminate between these two closely related species.

Horncore

Figures 2.257 and 2.258 show how, in the case of the horncores, by using ratios of measurements (in this case E/F or A/F), the separation between the two groups is better defined, with a limited overlap. From Figure 2.257, it is clear that the length of the horncore (E) and the length of its outer curvature (F), which are much more pronounced in sheep than goat, are more useful characteristics to discriminate between the two groups than the maximum diameter at the base (A). In fact, sheep and goat on the scatterplot have the same maximum diameter but a very different E/F ratio.

Figure 2.258 shows that, by plotting the ratio E/F in relation to the ratio E/A, it provides almost complete separation between the two species. This is because a better description of the bone is provided: the shape of the bone is shown from the base to the tip thanks to the use of these ratios. Sheep have a higher A/F value compared to goats, while goats have a higher E/F value than sheep. These results reflect the more curved and shorter horncores of sheep compared to the longer, sharper and less curved horncores of goats.

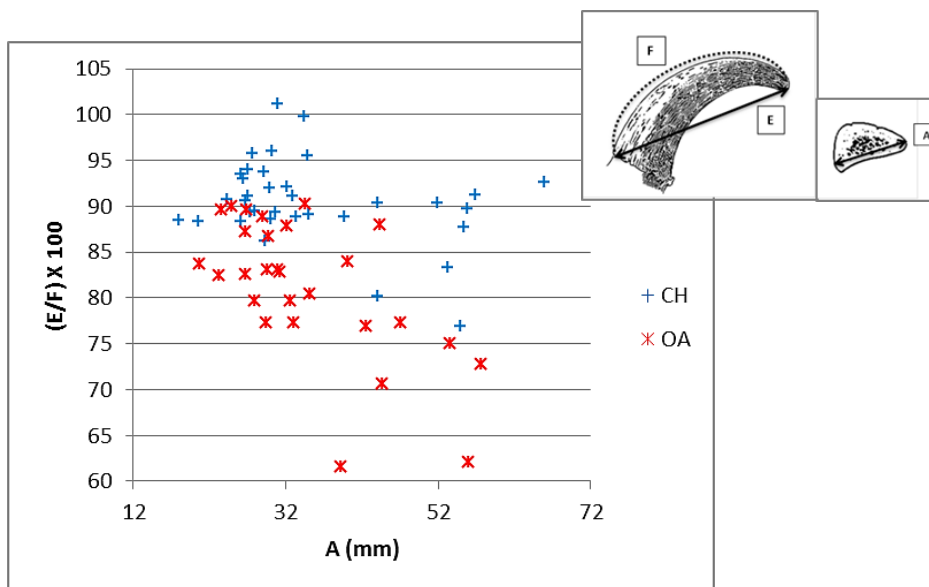


Figure 2.257 Maximum diameter taken at the base plotted against a ratio between the length and the length of the outer curvature of the horncore.

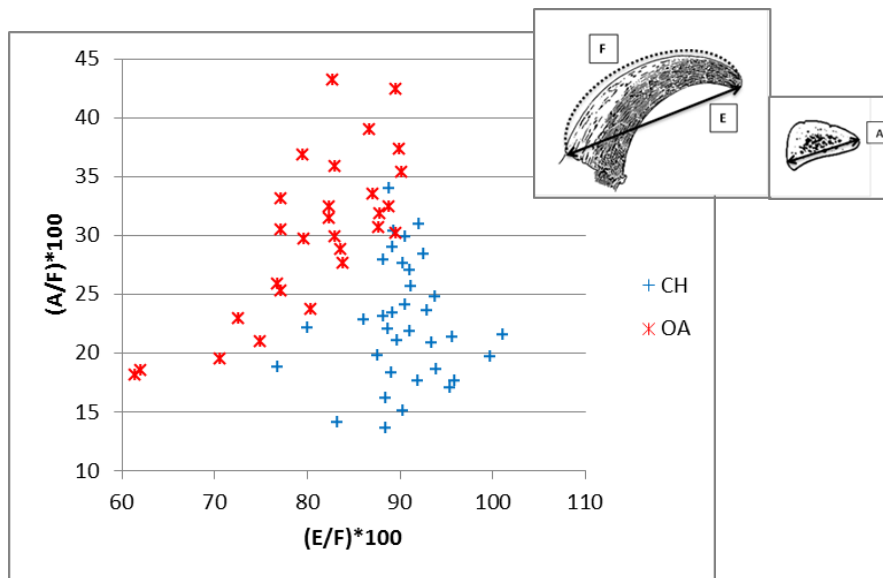


Figure 2.258 Ratio between the length and the length of the outer curvature plotted against the ratio between the maximum diameter taken at the base and the length of the outer curvature of the horncore.

Scapula

Figures 2.259 to 2.261 show ratios of measurements taken on the glenoid cavity, the neck and the spine of the scapula. The first diagram (Fig. 2.259) plots the ratio between ASG, namely the shortest distance from the base of the spine to the edge of the glenoid cavity and the breadth (BG) and length (LG) of the glenoid cavity. These ratios describe how these areas relate. It can be seen that there is significant overlap between the two groups, with a general tendency for the goat group to plot in the upper part of the diagram. This tendency is probably determined by the fact that the distance from the spine to the edge of the glenoid cavity is greater in goat than in sheep (Boessneck 1969; Boessneck *et al.* 1964; Helmer and Rocheteau 1994).

Figure 2.260 describes the area of the *processus articularis* and the articulation of the scapula, by plotting GLP (the greatest length of the *processus*) in relation to the length and breadth of the glenoid cavity. By examining the plot, it can be seen that goats plot at the bottom left of the graph showing lower values on both ratios, while sheep predominate in the upper right area having higher values in the horizontal and vertical axis. The graph clearly shows a separation despite some overlap in the middle area, especially on the horizontal axis.

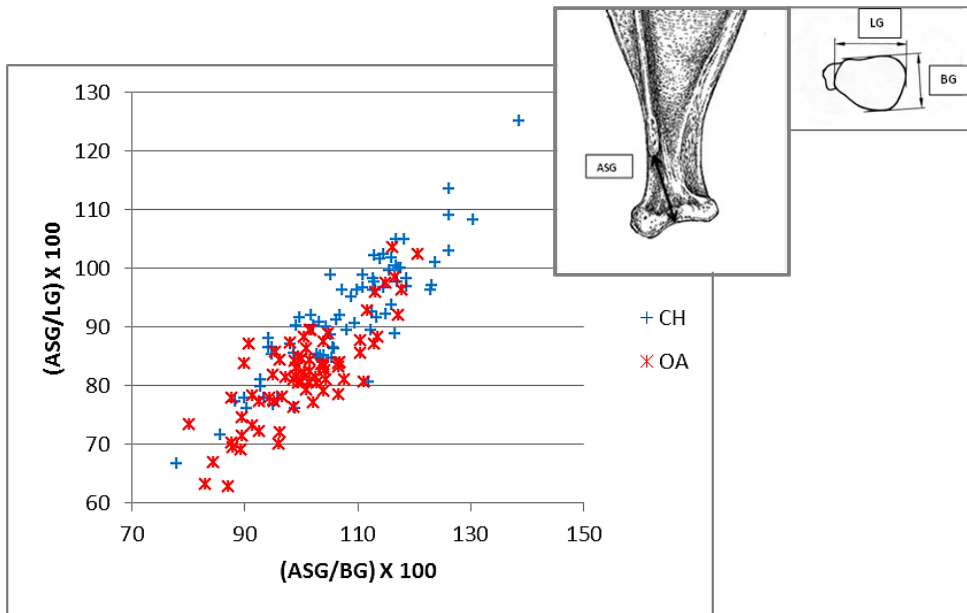


Figure 2.259 Ratio between the shortest distance from the base of spine to the edge of the glenoid cavity and the breadth of the glenoid cavity plotted against the ratio between the shortest distance from the base of the spine to the edge of the glenoid cavity and the length of the glenoid cavity.

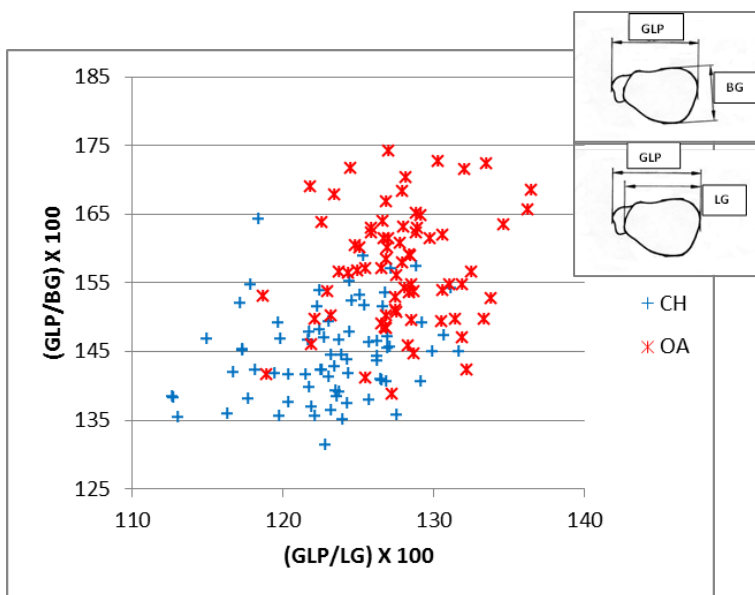


Figure 2.260 Ratio between the greatest length of the *processus articularis* and the length of the glenoid cavity plotted against the ratio between the greatest length of the *processus articularis* and the breadth of the glenoid cavity.

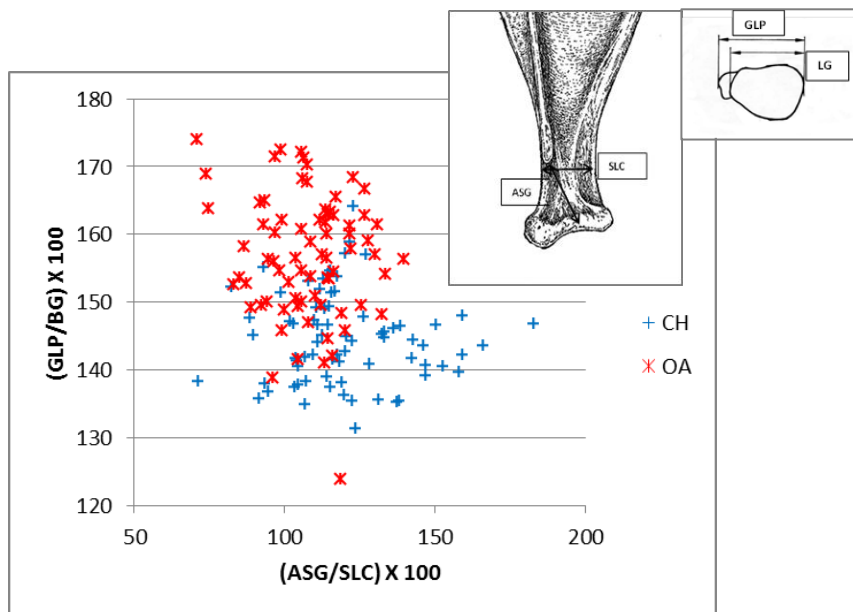


Figure 2.261 Ratio between the shortest distance from the base of the spine to the edge of the glenoid cavity (ASG) and the smallest length of the *collum scapulae* (SLC) plotted against the ratio between greatest length of the *processus articularis* (GLP) and the breadth of the glenoid cavity (BG).

Figure 2.261 presents the ratio between ASG and SLC (smallest length of the *collum scapulae*) on the horizontal axis and the ratio between GLP and BG on the vertical axis. This combination of measurements should reveal not just the difference in the shape of the glenoid cavity (Boessneck 1969; Boessneck *et al.* 1964) but also a difference in the *collum* of the scapula, as in sheep it is usually more robust and larger while in goat it is usually more slender and thin (Boessneck 1969; Boessneck *et al.* 1964; Helmer and Rocheteau 1994). On the graph, the goat cluster tends to fall in the lower area showing lower GLP/BG values but higher ASG/SLC values than sheep. These data mirror the thinner and slender *collum scapulae* of the goat, with a greater distance between the glenoid cavity and the base of the spine, compared to sheep for which the distance from the base of the spine to the glenoid cavity is lower and the *collum scapulae* is thicker.

Humerus

Figure 2.262 compares BT and HT to BT and HTC, all measurements taken on the distal trochlea in order to describe its shape. In sheep the trochlea is usually stouter. In both species the medial part is higher, but in sheep more so than in goat, giving the goat trochlea a more cylindrical shape (Boessneck 1969; Boessneck *et al.* 1964; Helmer and Rocheteau 1994). This general trend can be read on the graph as the goat specimens cluster mainly towards the top right of the diagram, indicating a greater length of the trochlea in relation to the height.

Figure 2.263 shows indices built with BE/Bd on one axis and BE/BT on the other. These combinations were thought to describe the difference in the trochlea with a focus on the relationship between BT, the distal articulation as a whole (Bd) and, the breadth of the *capitulum* (BE). This latter area of the bone is usually medio-laterally longer in goat as a consequence of the overall more elongated shape of the trochlea. Although goat specimens tend to produce higher values, there is considerable overlap and these ratios do not appear to be very diagnostic therefore.

If Figure 2.264 is considered, it can be seen that the ratio BE/HTC against the ratio BE/BT provides a slightly better separation based on the description of the area investigated before (Fig. 2.263). This is because new information is added by HTC, which seems to work somewhat better than Bd, and has been demonstrated to be an age dependent measurement in pigs (Payne and Bull 1988). Again, there is significant overlap but a trend can be seen more clearly than before.

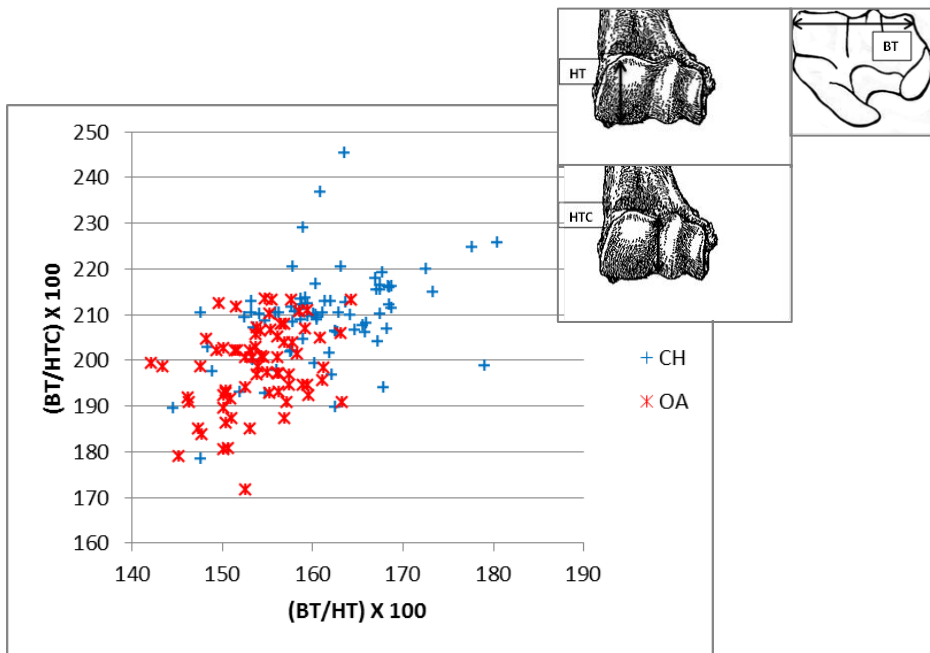


Figure 2.262 Ratio between the medio lateral width of the trochlea and its height plotted against the medio lateral width of the trochlea and the diameter of the trochlear constriction.

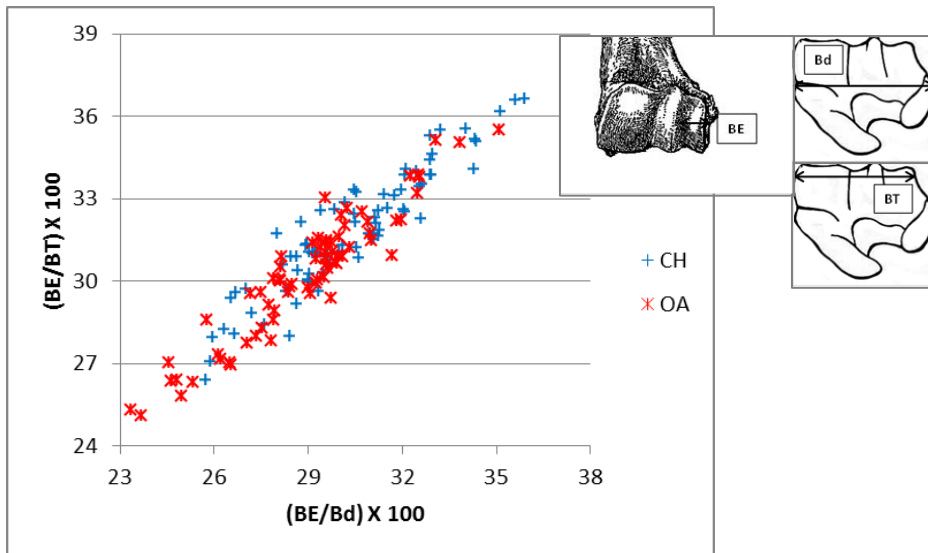


Figure 2.263 Ratio between the breadth of the capitulum and the distal width plotted against the ratio between the breadth of the capitulum and the medio lateral width of the trochlea.

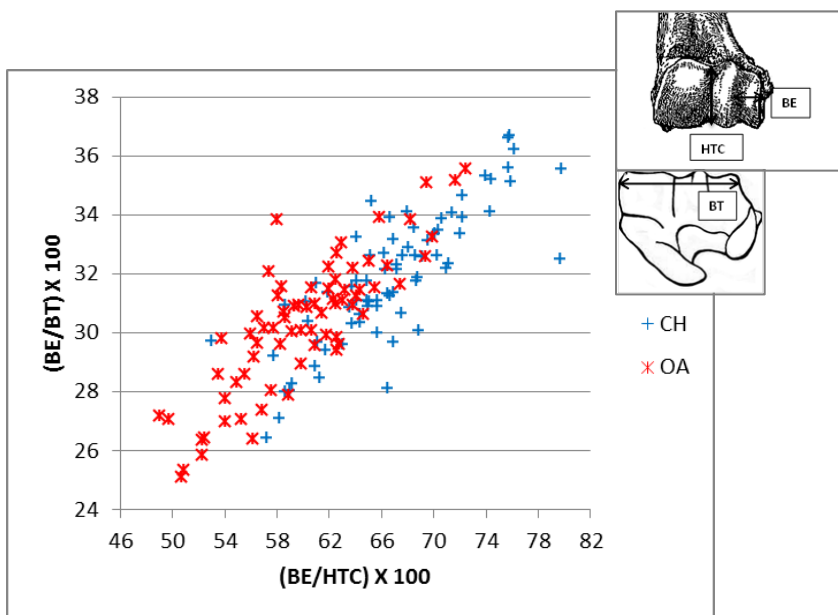


Figure 2.264 Ratio between the breadth of the *capitulum* and the diameter of the trochlea constriction plotted against the ratio between the breadth of the *capitulum* and the medio lateral width of the trochlea.

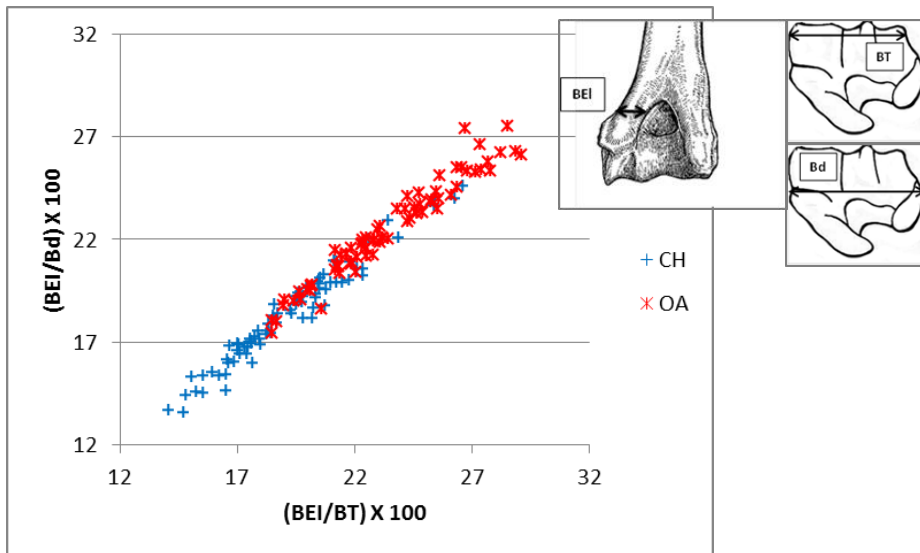


Figure 2.265 Ratio between the breadth of the *epicondyle lateralis* and the medio lateral width of the trochlea plotted against the ratio between the breadth of the *epicondyle lateralis* and the width of the distal end.

Finally, Figure 2.265 shows on the horizontal axis the ratio between BEI and BT and on the vertical axis the ratio between BEI and Bd. BEI describes the breadth of the *epicondyle lateralis* which is usually a good morphological characteristic used for discriminating sheep and goat: the transition between the shaft and the *epicondyle lateralis* in goat takes the form of narrow high ridge, while in sheep this part is broader and only slightly arched (Boessneck 1969; Boessneck *et al.* 1964; Helmer and Rocheteau 1994; Prummel and Frisch 1986; Zeder and Lapham 2010). Despite a fair amount of overlap, it can be seen in Figure 2.265 that, as a consequence of their relatively larger BEI, sheep specimens tend to plot towards the top end of the range.

It is interesting to notice that in Figure 2.263 and 2.265 the specimens plot on the same regression line (i.e. a line on a graph which represents the regression model of the relationship between the variables plotted; Field 2009:792). This is due to the fact that, as Davis has shown in his study of Shetland sheep (1996), measurements taken on the same anatomical planes (breadth, length) are highly correlated.

Radius

The ratio between BFp and Bp in the radius works well for discriminating between sheep and goat (Fig. 2.266). The measurements describe efficiently an important morphological difference, namely the presence of a well developed (in sheep) or less developed (sometime even absent in goat) lateral bicipital tuberosity at the lateral side of the proximal articular surface (Boessneck 1969; Boessneck *et al.* 1964; Prummel and Frisch 1986; Zeder and Lapham 2010).

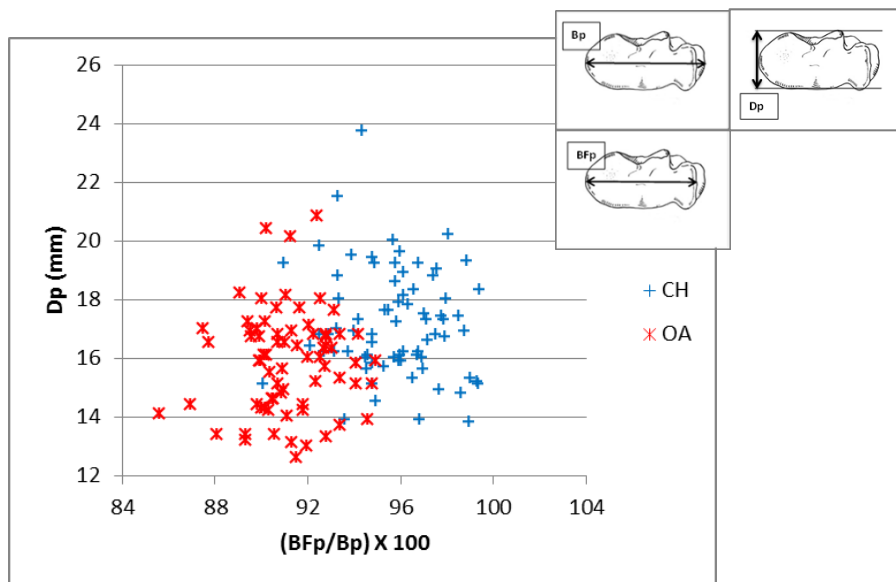


Figure 2.266 Ratio between the greatest length of the *facies articularis proximalis* and the greatest breadth of the proximal end plotted against the depth of the proximal end.

Ulna

Equally good results were obtained from the measurements taken on the *processus anconaeus* of the ulna. Since the proximal end of the radius and the *processus anconaeus* of the ulna articulate together, the measurements taken on the latter are closely related to those taken of the former. The BPC/DPA ratio in particular seems to be useful for discriminating between the two species by describing the shape of the anconaeus process. Figure 2.267 shows two distinct groups falling in two different areas of the graph with a minor degree of overlap. Goats fall on the upper right part showing higher values in both indices reflecting how the lateral coronoid process of the ulna projects more laterally than in sheep (Boessneck 1969; Boessneck *et al.* 1964). Some sheep outliers plot in the middle of the goat distribution; although these are a minority they represent a reminder of the fact that identifications based on these plots must be made cautiously and by looking at the spread of the distribution rather than individual points.

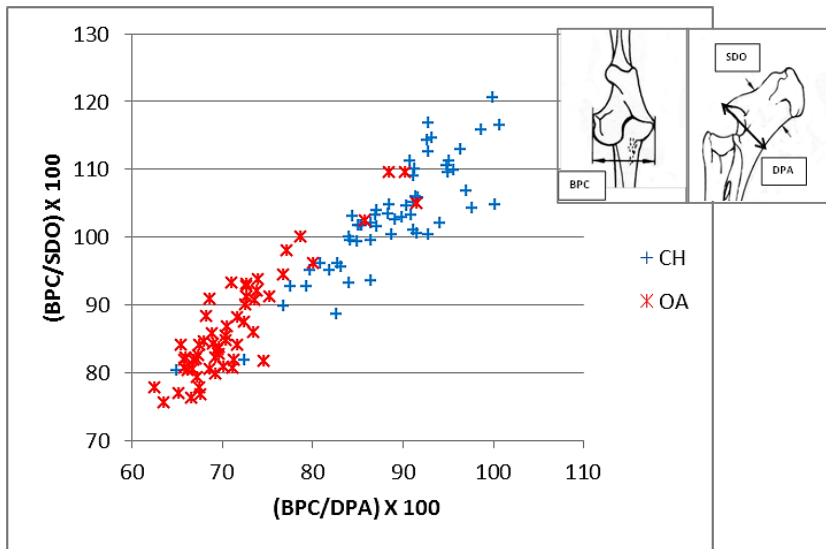


Figure 2.267 Ratio between the breadth across the coronoid process and the depth across the *processus anconaeus* to the caudal border plotted against the breadth across the coronoid process and the smallest depth of the olecranon.

Metacarpal

As previously said, the good results obtained from the measurements taken on the metacarpal were foreseeable, as Payne's biometrical study on this anatomical element (1969) showed the extent to which this skeletal part is useful for the proposed identification.

Figures 2.268 and 2.269 show that the measurements taken on the condyles and the verticilli of the distal articulation of the metacarpal, are the most effective in order to distinguish between the two species.

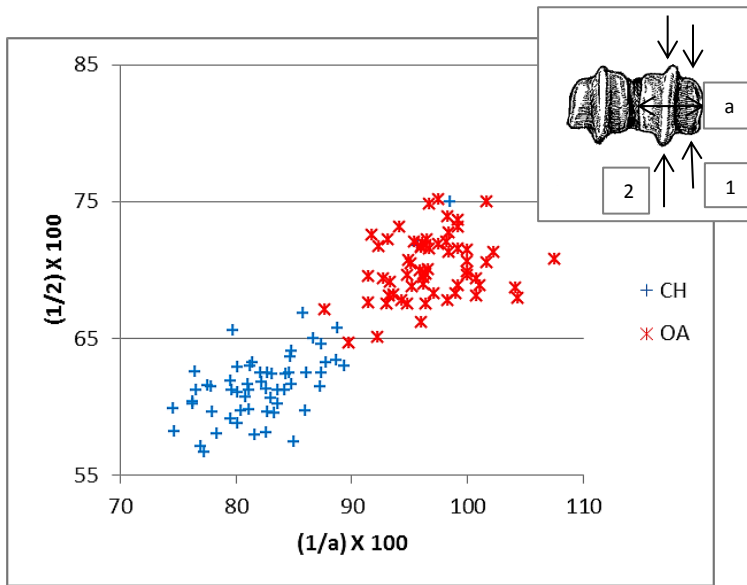


Figure 2.268 Ratio between the diameter of the medial trochlea and the width of the medial condyle plotted against the ratio between the diameter of the medial trochlea and the diameter of the *verticillus* at the medial condyle.

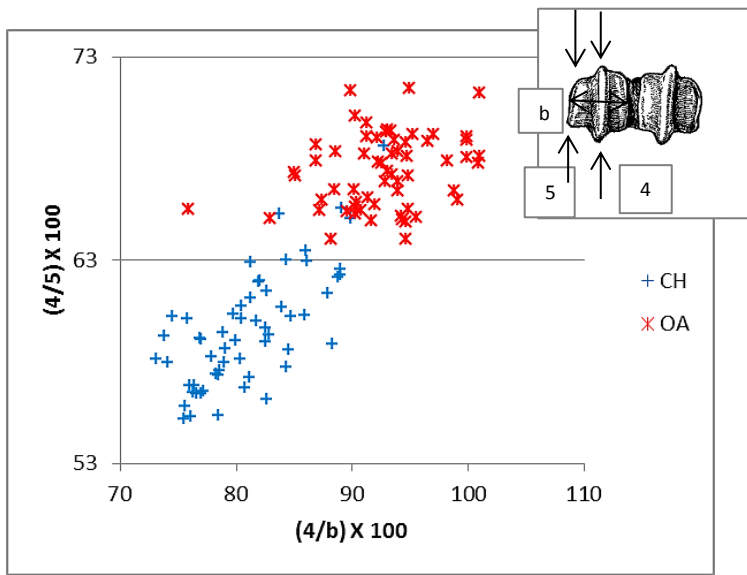


Figure 2.269 Ratio between the width of the lateral condyle and the diameter of the lateral trochlea plotted against the ratio between the diameter of the lateral condyle and the diameter of the *verticillus* on the lateral condyle.

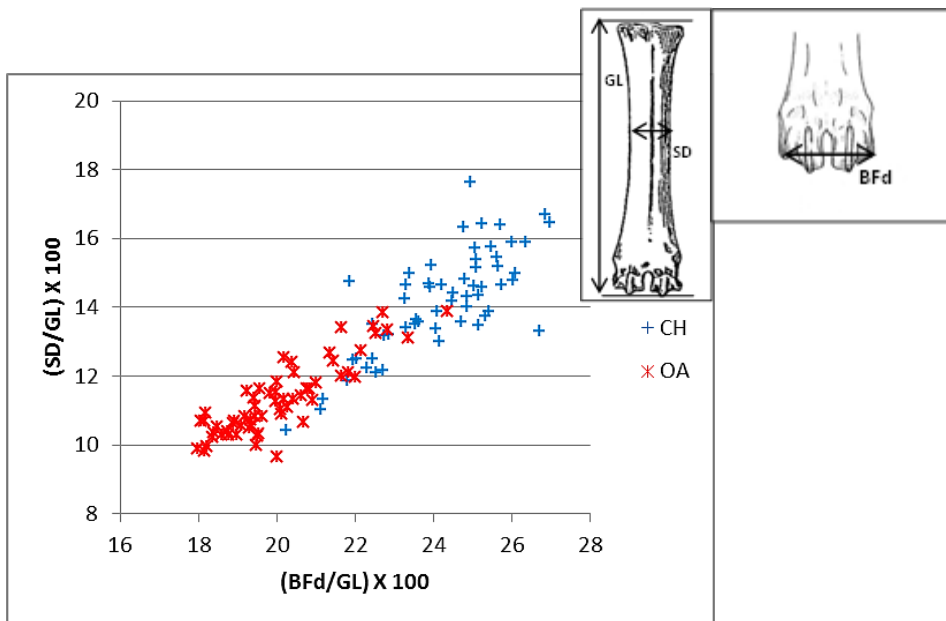


Figure 2.270 Ratio between the greatest breadth of the distal end with the greatest length plotted against the ratio between the smallest width of the shaft and the greatest length.

In Figures 2.268 and 2.269, ratios between 1/a and 4/b on the horizontal axis and 1/2 and 4/5 on the vertical axis are displayed. Consistently with previous studies (Boessneck 1969; Boessneck *et al.* 1964; Payne 1969; Rowley-Conwy 1998) the medial condyle is slightly more diagnostic than the lateral part of this element. When measurements such as a and b, which measure respectively the width of the medial and lateral condyles, are plotted against 1 and 2 on one side and 4 and 5 on the other (which respectively relate to the diameter of the medial and lateral condyle and the diameter of the *verticillus* on the medial and lateral condyle (2 and 5)), two very distinct groups can be recognized, with a minimal degree of overlap. The goat cluster plots at the bottom left area, showing lower scores on both axes, while the sheep group falls in the upper right part, having higher values on both axes. This pattern reflects the well-known morphological difference between the peripheral part of the trochlear condyles which is larger in sheep than goat (Boessneck 1969; Boessneck *et al.* 1964; Payne 1969; Zeder and Lapham 2010). The presence of a goat outlier in both Figures 2.268 and 2.269 must be noted as the ratios plotted refer to the dwarf goat specimen present in the sample. In this case, breed clearly influences the morphology of this anatomical element.

Figure 2.270 presents the ratio between BFd and GL and SD and GL. These combinations were thought to highlight the overall shape of the metacarpal as it is known that sheep are longer and thinner than goats (Boessneck 1969; Boessneck *et al.* 1964; Prummel and Frisch 1986). Again, two groups are visible, this time with a less clear separation between them. The goat group falls on the upper right part of the graph while the sheep group is located on the bottom right, though there is some overlap. The trend observed on the plot can be explained through the

morphological differences already noted (Figs. 2.233 to 2.235) in the overall shape of this element.

Metatarsal

Successful results were also obtained from the analysis of the metatarsal measurements although not quite as clearly as for metacarpals. As previously established for the metacarpal, the measurements shown to be more diagnostic are those taken on the distal articulation. However, while in the metacarpal the separation between the two groups was well-defined, for the metatarsal, the number of overlapping cases is higher (Figs. 2.271 to 2.273).

Ratios between 1/a and 4/b on the horizontal axis and 1/2 and 4/5 on the vertical axis are shown in Figures 2.271 and 2.272. The goat cluster plots on the bottom left area, showing lower scores on both axes, while the sheep group falls in the upper right part, showing higher values on both axes. This pattern reflects the same morphological difference discussed above for the metacarpal (Boessneck 1969; Boessneck *et al.* 1964; Payne 1969; Zeder and Lapham 2010).

Figure 2.273 presents the ratio between BFd and GL on one axis and SD and GL on the other, which provides some idea about the overall shape of the bone. Like the metacarpal, the metatarsal has a longer and thinner overall shape in sheep than in goat (Boessneck 1969; Boessneck *et al.* 1964; Prummel and Frisch 1986). Again, this difference can be observed in the diagram: the goat group tends to plot in the upper right part of the graph while the sheep group in the bottom left. Evidently, the same trend observed for the metacarpal is found with the metatarsal and the pattern can be linked to the morphological differences previously noted (Figs. 2.240 to 2.242) in the overall shape of the metapodial bones.

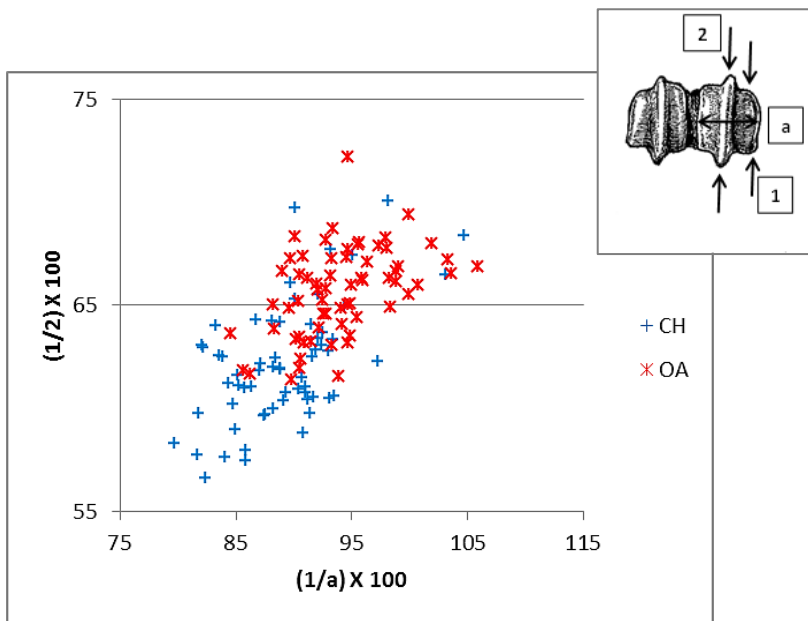


Figure 2.271 Ratio between the diameter of the medial trochlea and the width of the medial condyle plotted against the ratio between the diameter of the medial trochlea and the diameter of the *verticillus* at the medial condyle.

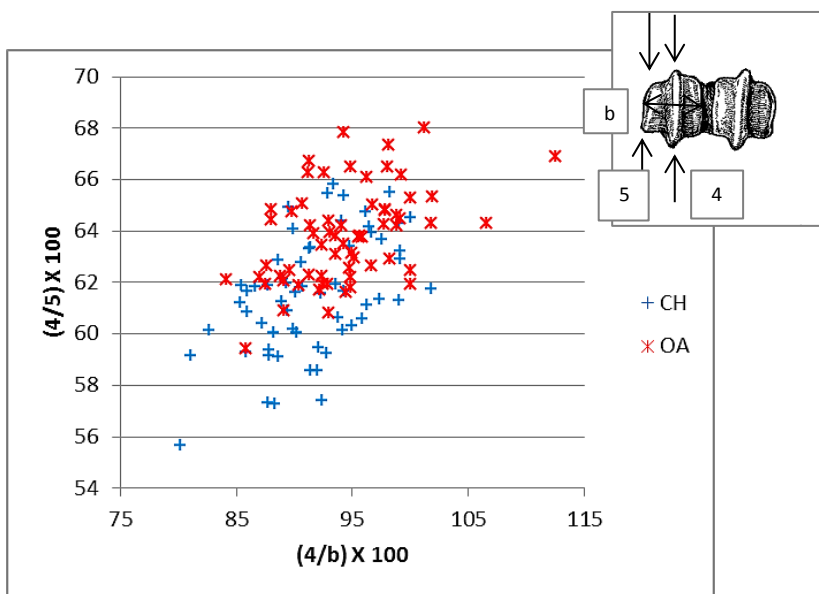


Figure 2.272 Ratio between the width of the lateral condyle and the diameter of the lateral trochlea plotted against the ratio between the diameter of the lateral condyle and the diameter of the *verticillus* on the lateral condyle.

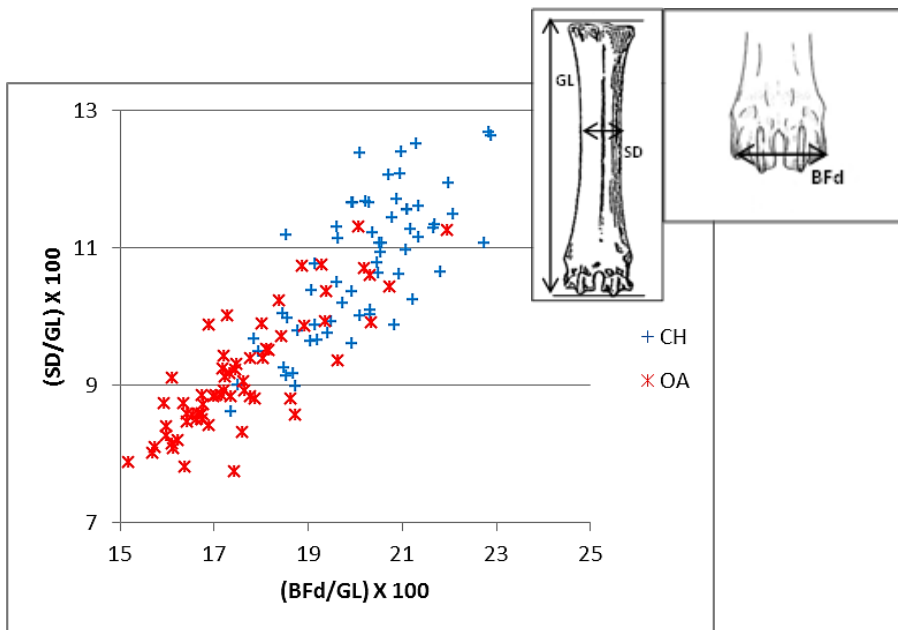


Figure 2.273 Ratio between the greatest breadth of the distal end with the greatest length plotted against the ratio between the smallest width of the shaft and the greatest length.

Tibia

As previously mentioned, the tibia is inconsistently identified as a useful element for the distinction of sheep and goat, though Kratochvil's (1969) suggested morphological criteria have been rather widely and successfully used. To confirm the solidity of Kratochvil's observations, a fairly good separation has been obtained biometrically.

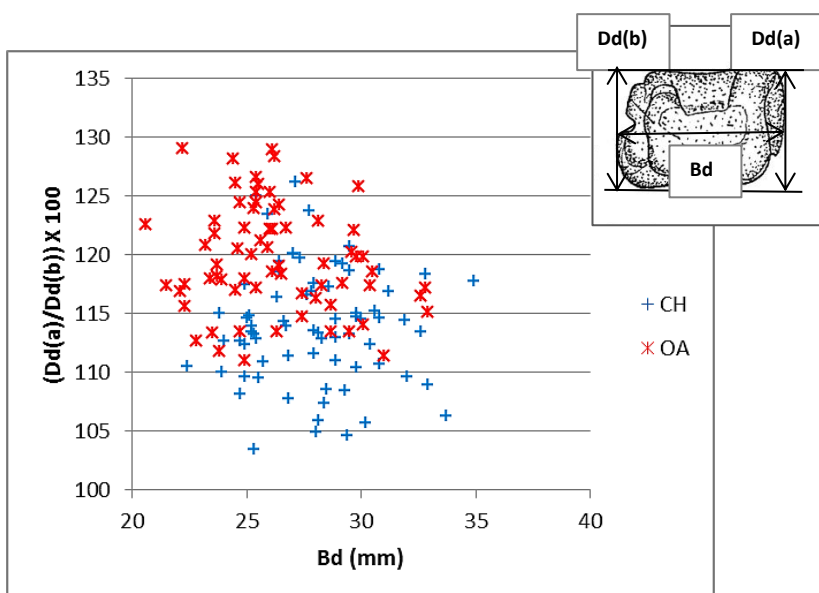


Figure 2.274 Breadth of the distal end plotted against the ratio between the depth of the medial (a) and lateral (b) side.

Figure 2.274 describes the shape of the distal articulation of the tibia (though the horizontal axis only expresses size). Although a certain degree of overlay can be seen, sheep tend to plot towards the top of the diagram and goats the bottom. This difference reflects the fact that the shape of the distal articulation can be described as a trapezium in sheep and rectangular in goat (Kratochvíl 1969; Prummel and Frisch 1986), and therefore the difference between the two measurements is more marked in sheep, providing a higher ratio value.

Astragalus

Among the measurements taken on the astragalus, most useful were those adopted by Davis (in press): GLI, DI and Bd. In addition, H, a new measurement defined here to measure the height at the central constriction of the bones, proved to have some diagnostic value (Figs. 2.275 to 2.278).

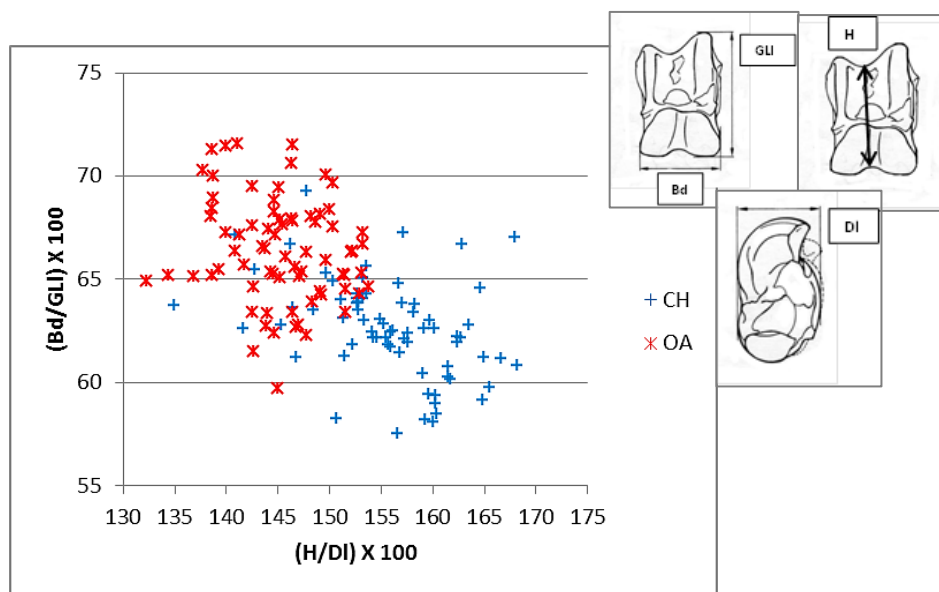


Figure 2.275 Ratio between height at the central constriction and the greatest depth of the lateral half plotted against a ratio between the breadth of the distal end and the greatest length of the lateral half.

Figure 2.275 shows the ratio between H and DI on the horizontal axis and between Bd and GLI on the vertical axis. It can be seen that the separation is determined by both axes but a major influence is exercised by H/DI. This can be explained by the fact that there are two morphological differences described by the measurements. The first is located on the sulcus at the middle of the trochlea. This is usually deeper in sheep than in goat (as a consequence goats fall in the bottom right part of the plot showing higher value on H/DI than sheep) (Boessneck

1969; Boessneck *et al.* 1964). The other morphological difference is expressed by DI, the measure of the depth of the lateral half is, in goat, influenced by the presence of an articular ridge which projects more and is shaped obliquely in a distal direction while in sheep it is less expressed and more horizontally oriented (Boessneck 1969; Boessneck *et al.* 1964; Zeder and Lapham 2010). On the other hand, sheep which fall on the upper part of the plot, show higher scores on Bd/GLI which reflects the more robust shape of the astragalus in sheep (Boessneck 1969; Boessneck *et al.* 1964).

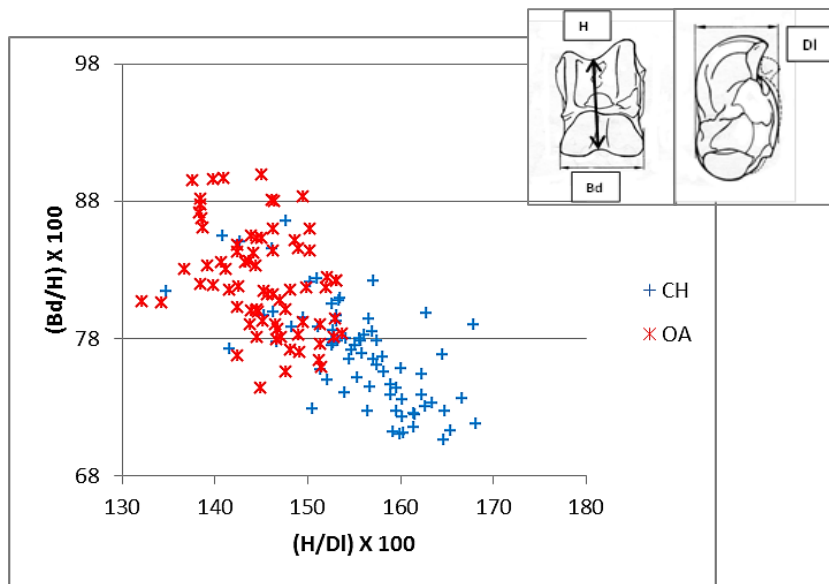


Figure 2.276 Ratio between height at the central constriction and the greatest depth of the lateral half plotted against the ratio between the breadth of the distal end and the height at the central constriction.

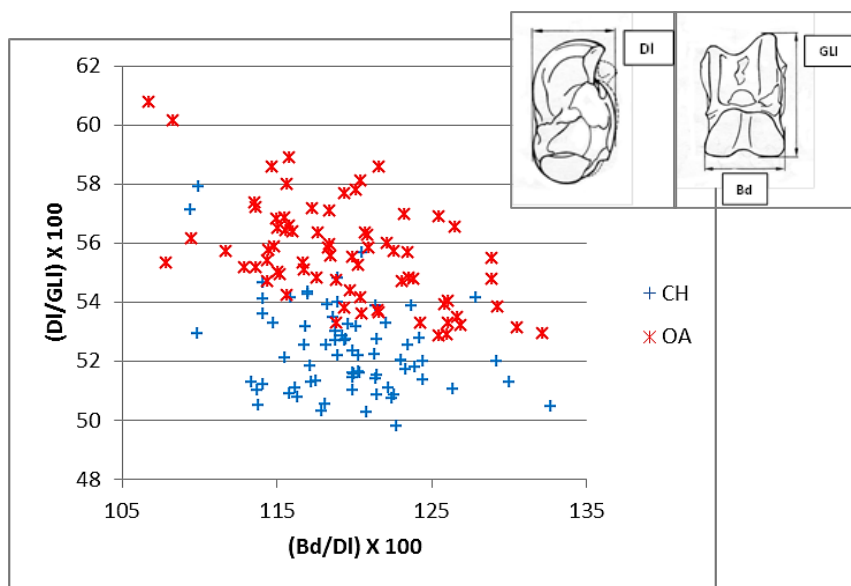


Figure 2.277 Ratio between breadth of the distal end and the greatest depth of the lateral half plotted against the ratio between the breadth of the distal end and the greatest length of the lateral half.

Figure 2.276 represents a modified version of Figure 2.275 with H replacing GLI. The pattern is similar, with the greater separation occurring on the horizontal axis (H/DI ratio).

By using the ratios Bd/DI and DI/GLI it is possible to gain an overview of the complete shape of the astragalus as all the three main dimensions of the bone are included (breadth, depth and length). Figure 2.277 shows two groups falling in two different areas of the plot with only a few specimens overlapping. The distinction is entirely due to DI/GLI , with the more robust astragali of sheep plotting in the upper part of the graph. There is no separation at all along the horizontal axis, which means that the ratio between width and depth is not diagnostic.

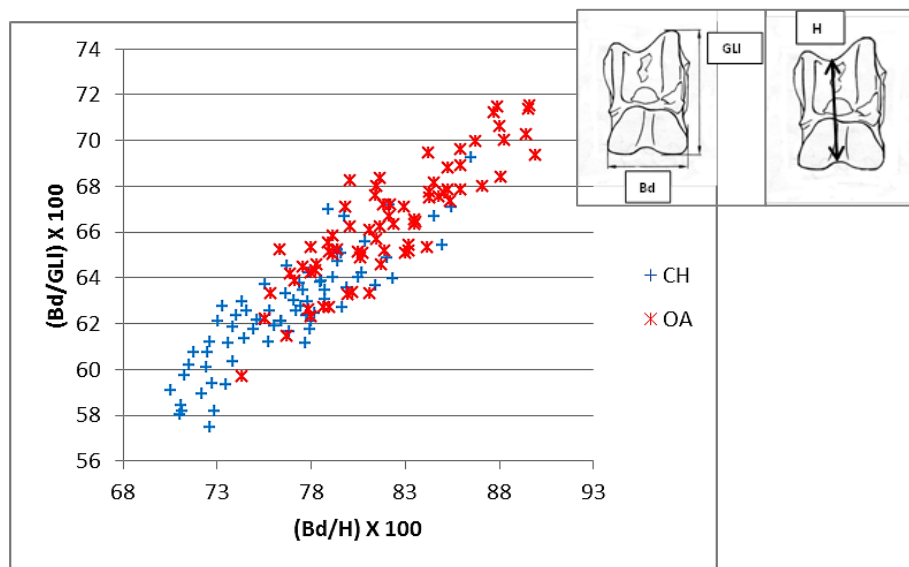


Figure 2.278 Ratio between the breadth of the distal end and the height at the central constriction and the ratio between height at the central constriction and the greatest depth of the lateral half.

The last graph (Fig. 2.278) presents substantial overlap between the two groups, but, once again, sheep tend to plot towards the top and goats the bottom.

Calcaneum

Good separation was obtained from the analysis of the measurements taken on the calcaneum. Two clearly different groups can be pinpointed on the graphs without a significant amount of overlap. Figure 2.279 demonstrates how the measurements suggested by Boessneck *et al.* (1964) (in this study c and d) can be useful and, when plotted against B, which is a new measurement describing the breadth of the articular surface of the *os malleolare*. This clear separation reflects a very clear morphological trait: the length of the articular facet for the *os malleolare* on the lateral process is greater than half of the entire process in sheep while in goat

it is smaller (Boessneck 1969; Boessneck *et al.* 1964; Zeder and Lapham 2010). In addition, B describes the difference between the articular facet of the *os malleolare* in sheep which is larger than wide, whereas the same articular facet in goat is wider than long (Boessneck 1969; Boessneck *et al.* 1964; Zeder and Lapham 2010).

A good degree of separation was also obtained when c and d were plotted against DS/c where DS is the depth of the *substantaculum tali* (Figs 2.280 and 2.281).

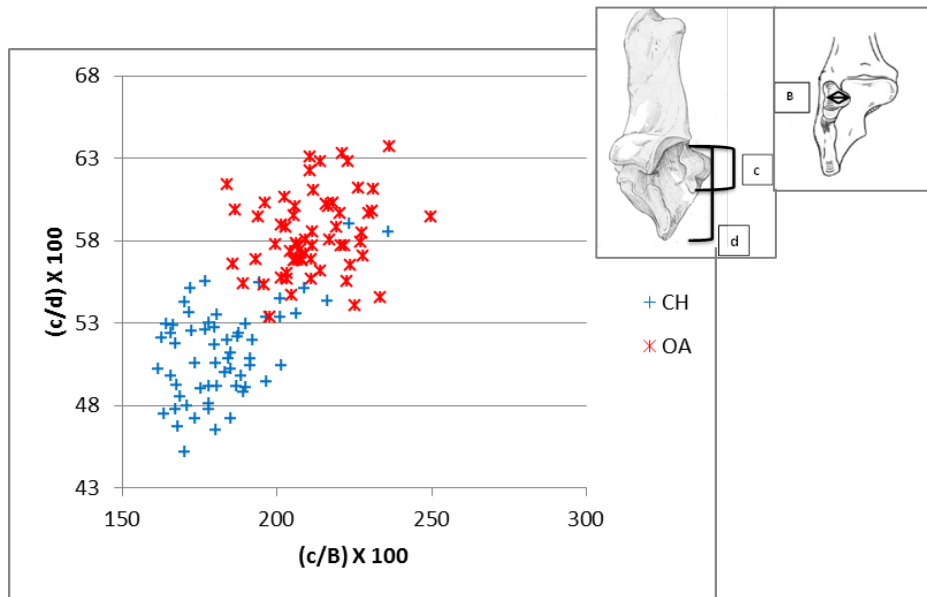


Figure 2.279 Ratio between the length and the breadth of the articular facet of the *os malleolare* plotted against the ratio between the length of the articular facet of the *os malleolare* and the length taken from the articular facet of the *os malleolare* to the end of the articulation-free part of the process.

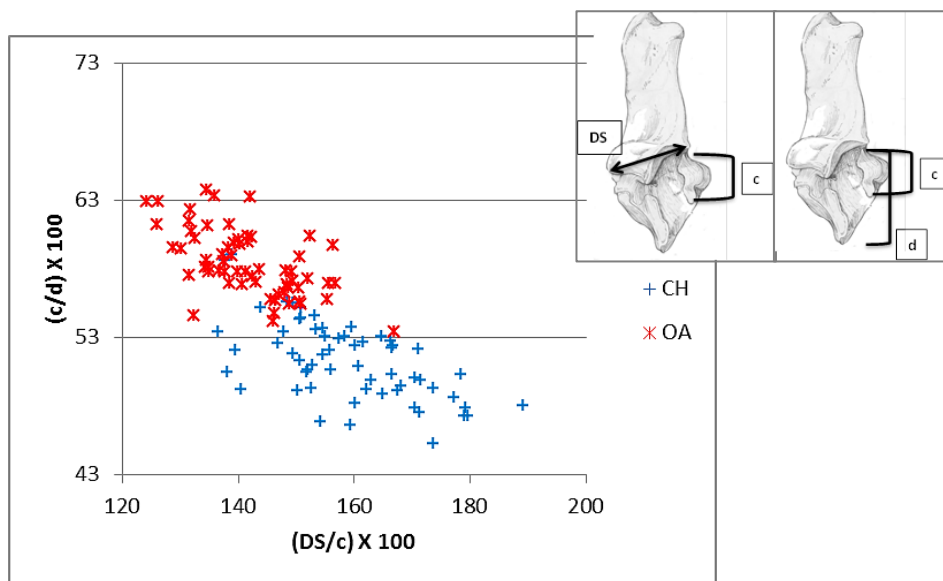


Figure 2.280 Ratio between the depth of the *substantaculum tali* and the length of the articular facet of the *os malleolare* plotted against the ratio between the length and the breadth of the articular facet of the *os malleolare*.

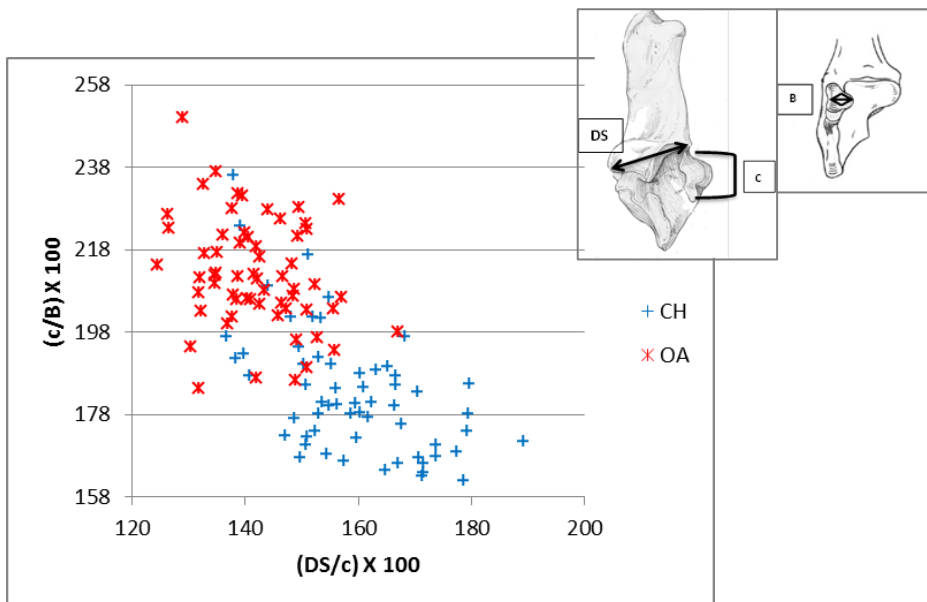


Figure 2.281 Ratio between the depth of the *substantaculum tali* and the length of the articular facet of the *os malleolare* plotted against the ratio between the length and the breadth of the articular facet of the *os malleolare*.

3rd Phalanx

Finally the 3rd phalanx was examined. Figure 2.282 shows how data behave if MBS and DLS are compared. Since one of the main morphological differences between sheep and goat for this skeletal element is represented by the shape of the sole (in sheep it is more curved and less triangular in shape than the almost isosceles shaped third phalanx of goat), DLS and MBS have been shown to be effective in describing this morphological characteristic and providing sufficient separation between the two species.

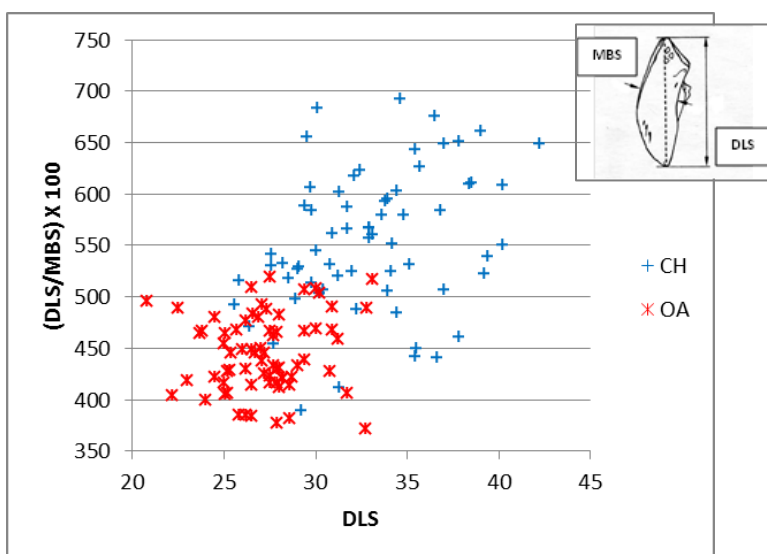


Figure 2.282 Diagonal length of the sole plotted against the ratio between the diagonal length of the sole and the middle breadth.

2.5.4 Statistical Analyses: Mann Whitney U test and Multivariate Approaches

Statistical analyses such as the Mann Whitney test of significance along with the Bonferroni adjustment and, multivariate statistical techniques such as Discriminant Analysis and Principal Component Analysis, were applied to complement the results given by the study of measurement pairs (and their ratios). In this chapter the following questions will be addressed:

- Are the biometrical differences found between the two groups due to chance or are they statistically significant?
- Can Discriminant Analysis emphasize differences among the two taxa by using all measurements at the same time?
- Can we establish, through the use of Discriminant Analysis, which variables best discriminate between the two taxa?
- Can we assign, through the use of the discriminant equation obtained from the Discriminant Analysis, into which group (sheep or goat) new cases (i.e. archaeological material) could be attributed on the basis of their measurements?
- Can the Principal Component Analysis, by compressing the information contained in a large number of variables into a smaller number of new variables (Shennan 1997: 267), highlight patterns underlying the data that could better explain and clarify the variance between samples?

Before moving to the discussion of the results provided by the statistical analysis, it has to be mentioned that, in this study, prior to the running of any statistical analyses, all the assumptions these techniques require have been checked and evaluated. A brief description of the assumptions is given in Appendix III. For a more in depth description of the assumptions, see Field (2009) and Tabachnick and Fidell (2007).

During the preliminary analysis of the modern data, in some cases, a few of the above requirements were not met. For example, in the Discriminant Analysis, the Box's M test, which is a test for assessing the presence of homogeneity of variance-covariance matrices, gave significant results. Significant results attest the presence of heterogeneity, so the null hypothesis could not be retained. However, when the sample is large, a significant result is not regarded as cause for concern, as the Box's M test is considered to be an over-sensitive test (Tabachnick and Fidell 2007: 383). Similarly, the Kaiser-Meyer-Olkin (KMO) measure of sample adequacy (which represents the ratio of the squared correlations between variables to the squared partial correlation between variables; Field 2009: 647) in the Principal Component Analysis, gave in some cases results which suggested that Factor Analysis may have been inappropriate (value >0.5 are defined as barely acceptable, values between 0.5 and 0.7 as mediocre, values between 0.7 and 0.8 as good, values between 0.8 and 0.9 as great and values above 0.9 as superb. Hutcheson and Sofroniou 1999; Field 2009). Despite these difficulties, the choice to proceed

with the analyses was made because the statistical analyses was considered, since the beginning, an additional (and not the only) tool with the potential of providing a further insight on sheep and goat identification.

2.5.5 Mann Whitney U-test and Manova

The Mann Whitney test of significance was run on the indices adopted for the ratio analysis, using the taxa as a grouping variable. The choice of adopting this test was made in order to see if the differences noticed between the two groups were statistically significant.

The results of the Mann Whitney U test are provided in Table 2.60. Information such as Sample Size and the Median (middle score of a set of ordered observations; this value is more appropriate than the mean for non-parametric tests; Field 2009: 789) of each ratio are given. In addition, Effect Size values (objective and standardized measure of the magnitude of an observed effect; Field 2009: 785), which have been calculated manually by using the equation z (z -score obtained from the Wilcoxon statistic procedure that SPSS produces)/ \sqrt{n} . of specimens, are presented. Finally, the Bonferroni adjustment was applied in order to avoid Type I Error. The threshold value adopted is 0.05 which, divided by the number of groups, gives a new value. This newly obtained value is the new threshold, so that, to be significant, the value for each ratio must be lower than the Bonferroni adjusted value (Field 2009: 372-373).

Table 2.61 Median, Effect Size, Mann-Whitney U test and Bonferroni adjustment results, calculated for each ratio index on each skeletal element included in the study. The probability level was determined as significant when $p < 0.05$ (*) and highly significant when $p < 0.01$ ().**

Skeletal part	Index	N. Specimens	Median	r Effect size	Mann-Whitney U; z approximation	Probability level (p)		Bonferroni adjustment	
Horncore	A:F	35 CH 28 OA	25.2	-0.53	U=182.0 z= -4.261	0.000	**	0.02	**
	E:F		88.5	-0.65	U= 114.0 z= -5.202	0.000	**		**
Scapula	ASG:BG	74 CH 73 OA	103.9	-0.34	U= 1609.5 z= -4.229	0.000	**	0.01	**
	ASG:LG		86.2	-0.49	U= 1139.0 z= -6.052	0.000	**		**
	GLP:BG		149.5	-0.63	U= 721.0 z= -7.671	0.000	**		**
	GLP:LG		125.9	-0.56	U= 1081.5 z= -6.275	0.000	**		**
Humerus	BT:HT	76 CH 71 OA	157.7	-0.53	U= 1012.5 z= -6.534	0.000	**	0.00	**
	BT:HTC		206	-0.57	U= 1030.5 z= -6.464	0.000	**		**
	BE:BT		31.1	-0.37	U= 1679.5 z= -3.949	0.003	**		n.s.
	BE:Bd		29.6	-0.30	U= 1853.5 z= -3.274	0.001	**		n.s.
	BE:HTC		63.7	-0.54	U= 990.5 z= -6.619	0.000	**		**
	BEI:Bd		20	-0.65	U= 652.0 z= -7.932	0.000	**		**
	BEI:BT		21.2	-0.67	U= 748.0 z= -7.560	0.000	**		**

Skeletal part	Index	N. Specimens	Median	<i>r</i> Effect size	Mann-Whitney U; <i>z</i> approximation	Probability level (<i>p</i>)		Bonferroni adjustment	
Radius	BFp:Bp	74 CH 71 OA	93.3	-0.77	U= 266.5 <i>z</i> = -9.337	0.000	**	0.05	**
Ulna	BPC:DPA	57 CH 57 OA	79.6	-0.76	U= 187.5 <i>z</i> = -8.144	0.000	**	0.02	**
	BPC:SDO		94	-0.77	U= 298.0 <i>z</i> = -7.518	0.000	**		**
Metacarpal	1:a	58 CH 62 OA	91.5	-0.82	U= 69.0 <i>z</i> = -9.081	0.000	**	0.01	**
	1:2		67.3	-0.80	U= 115.0 <i>z</i> = -8.839	0.000	**		**
	4:b		88.3	-0.85	U= 159.5 <i>z</i> = -8.605	0.000	**		**
	4:5		65	-0.82	U= 73.5 <i>z</i> = -9.057	0.000	**		**
	SD:GL	58 CH 61OA	12.5	-0.72	U= 236.5 <i>z</i> = -8.150	0.000	**		**
	BFd:GL		22	-0.84	U= 129.5 <i>z</i> = -8.718	0.000	**		**
Metatarsal	1:a	62 CH 64 OA	91.6	-0.50	U= 834.5 <i>z</i> = -5.610	0.000	**	0.01	**
	1:2		63.9	-0.58	U= 649.0 <i>z</i> = -6.515	0.000	**		**
	4:b		92.9	-0.25	U= 1402.0 <i>z</i> = -2.840	0.005	*		**
	4:5		62.9	-0.48	U= 876.5 <i>z</i> = -5.406	0.000	**		**
	SD:GL	62 CH 63 OA	9.9	-0.66	U= 450.0 <i>z</i> = -7.426	0.000	**		**
	BFd:GL		18.8	-0.69	U= 378.0 <i>z</i> = -7.779	0.000	**		**
Tibia	Dd(a):Dd(b)	71 CH 69 OA	116.8	-0.53	U= 938.5 <i>z</i> = -6.298	0.000	**	0.05	**
Astragalus	H:Dl	72 CH 73 OA	150.3	-0.69	U= 516.5 <i>z</i> = -8.350	0.000	**	0.01	**
	Bd:GLl		64.2	-0.63	U= 708.0 <i>z</i> = -7.594	0.000	**		**
	Bd:H		79.2	-0.59	U= 827.5 <i>z</i> = -7.120	0.000	**		**
	Bd:Dl		119.4	-0.01	U= 2582.0 <i>z</i> = -0.170	0.865	n.s.		n.s.
	Dl:GL		53.9	-0.73	U= 399.0 <i>z</i> = -8.816	0.000	**		**
Calcaneus	c:d	60 CH 62 OA	55.3	-0.81	U= 104.5 <i>z</i> = -8.991	0.000	**	0.02	**
	c:B		199	-0.72	U= 290.5 <i>z</i> = -8.038	0.000	**		**
	DS:c		149.5	-0.62	U= 518.0 <i>z</i> = -6.873	0.000	**		**
3 rd Phalanx	MBS:DLS	72 CH 81 OA	484.5	-0.70	U= 532.0 <i>z</i> = -8.714	0.000	**	0.05	**

The Mann Whitney test (Mann and Whitney 1947) is a non-parametric test which is used to establish if two group means are different and if this difference is large enough to rule out a chance result (Field 2009: 331). It was chosen in place of the independent t-test (parametric test) because the U test is its equivalent but requires fewer assumptions about the type of data used (Field 2009: 540). In fact, the Mann Whitney U test can be carried out on non-normally distributed data, the best choice for a sample such as this in which two different populations

were compared.

By looking at Table 2.60, it can be seen that almost all the metrical indices show highly significant scores. With a p value <0.001 , they confirm that the two groups are significantly different to one another, supporting what had already been noted during the previous analysis.

Only the ratios 4/b on the metatarsal and Bd/Dl in the astragalus gave results that indicate less than highly significant differences between the two taxa. While the difference in 4/b is still significant, the complete lack of any significant difference in the Bd/Dl ratio is not surprising as limited difference had been noticed in the scatterplot diagrams and the relationship between the two measurements does not describe any known morphological difference between sheep and goat. The greater slenderness of the goat astragali can be better described by other measurements, such as the ratio between Bd and GLI.

Since the running of many consecutive paired tests can lead to a Type I Error, namely to find more significant differences than actually exist, a Bonferroni adjustment was adopted. This correction is used in these cases even though it is known to be too conservative, leading to a Type Error II, thus opening the possibility of missing genuine differences in the data (Field 2009: 372-373). Nevertheless, it was applied because it is one of the easiest *post hoc* tests (namely tests based on pairwise comparisons designed to compare all different combinations of the treatment groups; Field 2009: 372) and, for the purpose of this research, the lesser evil would be under-claiming rather than over-claiming the existence of genuine differences between the groups. The Bonferroni test is calculated by dividing the Type I Error rate (also called $\alpha=0.05$) by the number of comparisons used (Field 2009: 372-373). The resulting value is the new threshold we should use to interpret the probability level value (p).

When the Bonferroni correction was applied, it confirmed the significant difference of almost all ratios, apart from the afore mentioned combination Bd/Dl on the astragalus, but also BE/BT and BE/Bd on the humerus, which had been considered significantly different by the Mann Whitney U Test. Despite the risk of Type Error II, the Bonferroni test thus confirms the presence of genuine differences between the two groups for most of the identified ratios.

As suggested by Field (2009: 551) when the results from a Mann-Whitney test are discussed, the Effect Size must be reported as well. The Effect Size value r (calculated from z value as suggested by Rosenthal 1991: 91) indicates the size of associations or the sizes of differences observed in a sample and it is important to report it for many reasons. First of all, because it represents a standardized measure of the size of the effect observed and as so, useful information that other researchers can use for comparisons (Field 2009: 550). Secondly, as the Effect Size increases, the null hypothesis that the observed differences between the two groups are due to chance decreases, so that the Effect Size does not only test the null hypothesis but it

also expresses precisely how large the effects observed in the data really are (Walker 2007-2008). A small Effect Size is one in which there is a real effect but it is not large enough to be observed with the naked eye. On the other hand, a large Effect Size measures an effect which is substantial and can be seen without an in-depth study (Walker 2007-2008). The threshold for defining the degree of effect is small if the value is between 0.1 and 0.3, medium if the value is between 0.3 and 0.5, large if the value is between 0.5 and 0.7, and finally very large when higher than 0.7 (Cohen 1988; Rosenthal 1996).

In this study, the r values (Table 2.60), which express the Effect Size, have all, apart from the two indices identified above (metatarsal b/4 and the astragalus Bd/Dl), large values (according to Cohen 1988). In addition, high r values are associated with high U values, reinforcing the idea that the differences between the two species are strong and not due to chance.

The Mann-Whitney test could detect the presence of statistical significant differences in the two samples only for individual ratios. In order to test if such statistical significant differences were present also when two biometrical ratios were compared simultaneously, Manova was carried out. The test was run for every combination of ratios used and Table 2.61 shows the results. The values which are important are the F value and the related p value. These tell us if the two population means are equal or not; for the test to be significant, the F value has to be greater than one, and the p value be significant at $p < 0.001$, so that the null hypothesis of equality of group means can be rejected (Field 2009: 354).

As Table 2.61 shows, all the F values are greater than 1 and the related p values are all significant confirming that the differences between the modern sheep and goat samples, even when multiple ratios are combined, are statistically significant. This outcome mirrors what the graphs in Section 2.5.3 present visually (Figs. 2.257 to 2.282).

Table 2.62 Results from Manova for each combination of ratios used in the allometric shape analysis (Section 2.5.3). *p* value significant a $p < 0.001 = *$.**

Skeletal Part	Ratios	F	Wilk's lambda	<i>p</i>	Significance
Horncore	A/E:F	23.41	0.5617	0.001 (3.059E-08)	***
	E:F/A:F	60.44	0.3317	0.001 (4201E-15)	***
Scapula	ASG:BG/ASG:LG	24.78	0.744	0.001 (5.639E-10)	***
	GLP:LG/GLP:BG	54.02	0.5713	0.001 (3.135E-18)	***
	ASG:SLC/GLP:BG	47.92	0.6004	0.001 (1.116E-16)	***
Humerus	BT:HT/BT:HTC	37.58	0.6571	0.001 (7.383E-14)	***
	BE:Bd/BE:BT	8.991	0.889	0.001 (0.0002091)	***
	BE:HTC/BE:BT	36.13	0.6659	0.001 (1.928E-13)	***
	BEI:BT/BEI:Bd	55.44	0.5649	0.001 (1.395E-18)	***
Radius	BFp:Bp/Dp	111.3	0.3895	0.001 (8.366E-30)	***
Ulna	BPC:DPA/BPC:SDO	102.4	0.3515	0.001 (6.266E-26)	***
Metacarpal	1:a/1:2	206.3	0.2209	0.001 (4.319E-39)	***
	4:b/4:5	171.8	0.254	0.001 (1.524E-35)	***
	BFd:GL/SD:GL	110.8	0.3436	0.001 (1.229E-27)	***
Metatarsal	1:a/1:2	31.38	0.6621	0.001 (9.733E-12)	***
	4:b/4:5	18.15	0.7721	0.001 (1.237E-07)	***
	BFd:GL/SD:GL	58.51	0.5104	0.001 (1.523E-18)	***
Tibia	Bd/Dd(a):Dd(b)	31.33	0.6861	0.001 (6.226E-12)	***
Astragalus	H:DI/Bd:GLI	79.79	0.4709	0.001 (5.969E-24)	***
	H:DI/Bd:H	65.11	0.5216	0.001 (8.58E-21)	***
	Bd:DI/DI:GLI	90.36	0.44	0.001 (4.848E-26)	***
	Bd:H/Bd:GLI	42.48	0.6257	0.001 (3.472E-15)	***
Calcaneum	c:B/c:d	128.7	0.3162	0.001 (1.757E-30)	***
	DS:c/c:d	152.1	0.2813	0.001 (1.666E-33)	***
	DS:c/c:B	103.4	0.3653	0.001 (9.519E-27)	***
3 rd Phalanx	DLS/DLS:MBS	95.53	0.4086	0.001 (2.215E-26)	***

2.5.6 Discriminant Analysis

Discriminant Analysis was chosen among other multivariate analyses because it uses different variables to find a means of maximising the separation between groups of data. It also identifies which variables best discriminate the groups. In addition, the analysis runs a reclassification of the known cases to test the validity of the discriminating criteria. Finally, the discriminant equation calculated can be used as a tool for predicting group membership (Baxter 2003: 105).

As the main aim of the project is to look at the morphology of the bones without taking into consideration size, which can sometimes cloud the results, a method of standardisation was applied to the raw data.

This method was previously applied on animal bones material by Davis (1983) in a study focused on detecting morphological differences among different populations of house mice (*Mus musculus*) from Britain and the Faroe Islands. Davis, aware of the effect of size on his mandibular measurements, introduced a method of standardizing the data in order to eliminate the possibility that it was included as a variable in the discriminant analysis. This technique consists of expressing each measurement of each bone as a fraction of the whole (Davis 1983: 523). The same standardisation method has been applied to the modern data of this study.

The Standard or Direct option (Tabachnick and Fidell 2007: 395) was preferred to the Stepwise or Statistical method (Tabachnick and Fidell 2007: 396) because all the variables are included together at once during the analysis; with the Stepwise method they are inserted by the program which chooses, according to different statistical criteria, which variables are the most effective (Tabachnick and Fidell 2007: 395-396). The problem with this kind of approach is that the order of entry of the variables may be dependent on differences in the relationship among predictors that are irrelevant, so that they do not reflect population differences (Tabachnick and Fidell 2007: 395). In addition, there is no control over the variable selection process.

As the methodology used in this study has been designed for the analysis of archaeological material, there are some measurements that are chosen because they are more likely to be taken on fragmented specimens than others (i.e. GL is rarely taken unless you have a complete bone). For these reasons, a 'manual' control of the variables has been preferred (Standard Discriminant Analysis).

Standard Discriminant Analysis was undertaken for each element individually, using species as the grouping variable and the chosen measurements as the independent variables. Output options were set to give case-by-case discriminant data, so that the identification result for each individual specimen was obtained as well as a summary table. A plot of all cases was also produced using the canonical discriminant individual scores as the vertical axis.

The results obtained for the two species are presented in the following pages on an element-by-element basis. Comments on the results for each element are also included so that the limitations can be understood.

Table 2.63 Percentage of correct classifications by element and species from Linear Discriminant Analysis.

Anatomical Element	% CH correctly identified	% OA correctly identified	Overall % of correct identifications	Overall % of correct identifications with cross-validation (leave one out)	Measurements kept by the analysis
Horncore	94.3%	96.4%	95.2%	95.2%	A, B, C, D, E
Scapula	86.5%	86.3%	86.4%	83%	ASG, LG, BG, GLP, SLC
Humerus	89.5%	87.1%	88.4%	86.3%	HT, Bd, HTC, BE, BEI
Radius	85.1%	90.1%	93.5%	93.5%	BFp, Bp, Dp, GL, SD
Ulna	94.6%	91.2%	92.9%	92.0%	B, L, SDO, DPA, BPC
Metacarpal	96.6%	100%	98.3%	97.5%	GL, SD, BFd, BatF, a, b, 1, 2, 3, 4, 5, 6
Metatarsal	91.8%	93.7%	92.7%	91.1%	GL, SD, BFd, BatF, a, b, 1, 2, 3, 4, 5, 6
Tibia	93.1%	78.8%	89.1%	86.4%	GL, SD, Dd(a), Dd(b), Bd
Astragalus	90.3%	87.7%	89.0%	86.9%	H, Dl, Dm, GLI, GLm, Bd, BpT
Calcaneum	91.7%	98.4%	95.1%	95.1%	c, d, B, DS, SB, GL, Gd
3 rd Phalanx	83.1%	89.9%	85.8%	85.8%	DLS, MBS

Table 2.62 displays the percentage of correct attributions gained by running Linear Discriminant Analysis on each skeletal element. According to the score (in descending order), the elements are listed as follows:

- Metacarpal
- Horncore
- Calcaneum
- Radius
- Ulna
- Metatarsal
- Tibia
- Astragalus
- Humerus
- Scapula
- 3rd Phalanx

Remarkably, no element provided an identification score that is lower than 85.8%. Although the diagnostic power of biometry had been previously shown, for example on the metapodials (Boessneck 1969; Payne 1969), astragali (Davis in press), and other postcranial elements (Fernández 2001), this is the first time that it is demonstrated by using statistical analysis. Even after having applied cross-validation (in this study the ‘Leave-one-out’, one of the possible methods used to assess the accuracy of a model in different samples. Field 2009), the identification scores are still successful, with no elements providing scores lower than 83%.

The lower values that resulted from some elements are not totally unexpected reflecting the low reliability of some measurements for translating morphological differences. In addition, some morphological traits were visible, but only marginally so, and therefore they did not show up clearly in the biometrical analysis.

Horncore

All measurements taken on the horncore were included in the analysis. The percentage of variance explained by the model can be calculated by squaring the canonical correlation coefficient. In this case, the model explains 75% of the variance within the sample (Tab. 2.63).

Table 2.64 Canonical correlation coefficient for the horncore.

Eigenvalues				
Function	Eigenvalue	% of Variance	Cumulative %	Canonical Correlation
1	3.046 ^a	100.0	100.0	.868
a. First 1 canonical discriminant functions were used in the analysis.				

Table 2.65 Wilks' Lambda test for the horncore.

Wilks' Lambda				
Test of Function(s)	Wilks' Lambda	Chi-square	df	Sig.
1	.247	81.771	5	.000

An additional important value given is the Wilks' Lambda (Tab. 2.64). This score shows that the model fits very well with the data, being $p < .05$ (namely significant); the smaller the Wilks' Lambda value, the better the function discriminates between the groups (Field 2009: 621).

Table 2.66 Structure matrix for the horncore showing the canonical variate correlation coefficients.

Structure Matrix	
	Function
	1
E	.840
D	-.604
C	-.510
A	-.422
B	-.407
F ^a	.220
Pooled within-groups correlations between discriminating variables and standardized canonical discriminant functions.	
Variables ordered by absolute size of correlation within function.	
a. This variable not used in the analysis.	

Table 2.65 shows the canonical variate correlation coefficients (the term variate is used to refer to the outcome of a variable (as defined by Stack exchange inc. 2015). They are similar to factor loadings and indicate the nature of the variate so that the dependent variables (in this case measurements) with high correlation scores are those that contribute the most to the group separation (Bargman 1970; Field 2009: 619). As a consequence, the coefficients express the relative contribution of each variable to the variate (Field 2009: 620). By looking at the scores for each variable, some considerations can be made.

Firstly, the coefficients for each variable are different in magnitude and have a different relationship with the variate (positive or negative). The coefficients with higher values are those which are more important for the discrimination, in this case E and D, but also C, A and B. The positive or negative coefficients present on the structure matrix Table attest that variables/measurements have the opposite effect on the function. In this case it can be seen that, while E and F have positive scores, the other measurements have negative scores. This difference indicates that two different contributions are made to the differentiation process. It is not surprising that the negative values measure the maximum and minimum diameter of the horncore while the positive values refer to the length and the length of the curvature of the horncore, as they measure two different dimensions of the same element.

It must be observed that F has been excluded from the analysis by the program. This variable has been left out because it correlates too highly with other variables, causing multicollinearity or singularity problems, as attested by the tolerance test executed by SPSS (Tab. 2.66).

Table 2.67 Tolerance test for the horncore.

Variables Failing Tolerance Test^a			
	Within-Groups Variance	Tolerance	Minimum Tolerance
F	9.346	.000	.000
All variables passing the tolerance criteria are entered simultaneously.			
a. Minimum tolerance level is .001.			

Having made these considerations, from Table 2.65 it can be seen that E is shown to be the most important variable (length taken from the base to the tip of the horn) contributing to the discrimination, followed by D and C (minimum and maximum diameter taken at the middle). Clearly the function is highly determined by the length of the horncore (E) and the shape of the base (taken either at the middle (C and D) or at the base of the bone (A and B)).

Table 2.68 Classification results for the horncore.

Classification Results^{a,c}					
		TAXA	Predicted Group Membership		Total
			CH	OA	
Original	Count	CH	33	2	35
		OA	1	27	28
	%	CH	94.3	5.7	100.0
		OA	3.6	96.4	100.0
Cross-validated ^b	Count	CH	33	2	35
		OA	1	27	28
	%	CH	94.3	5.7	100.0
		OA	3.6	96.4	100.0
a. 95.2% of original grouped cases correctly classified.					
b. Cross validation is done only for those cases in the analysis. In cross validation, each case is classified by the functions derived from all cases other than that case.					
c. 95.2% of cross-validated grouped cases correctly classified.					

Table 2.67 shows the percentage of original grouped specimens that were correctly classified during the Discriminant Analysis. The percentage is 95.2% which means that 95 out of 100 unknown cases would be correctly identified. Of 35 goat specimens, 33 were classified correctly while two were classified as sheep. On the other hand, of the 28 sheep specimens, 27 were correctly attributed to the right taxon while just one was wrongly identified.

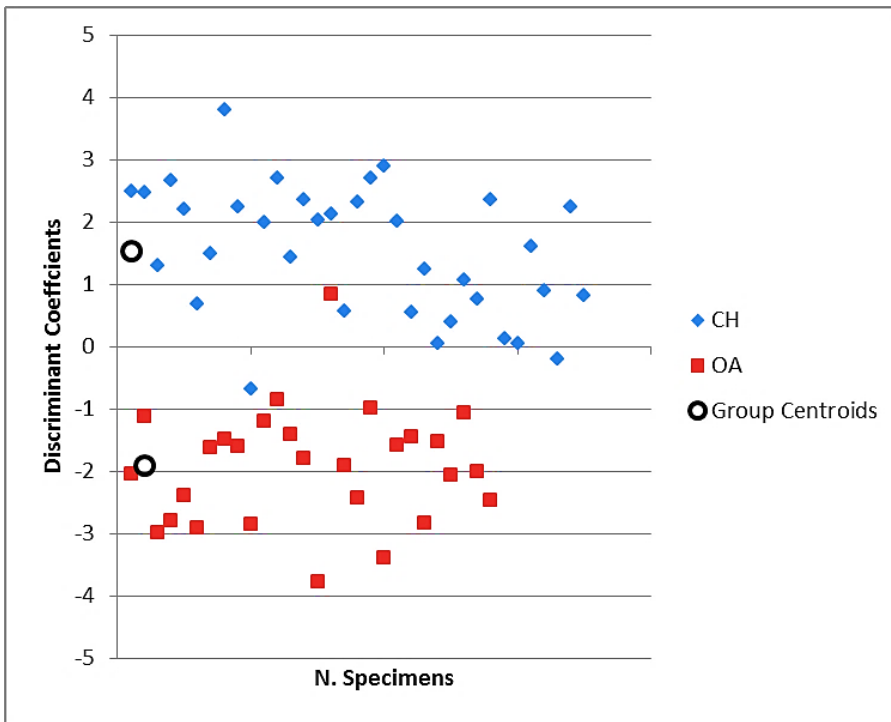


Figure 2.283 Horncore: scatterplot of the individual discriminant scores.

Figure 2.283 shows the individual scores given by the function to each specimens making up the modern sample. It can be seen that the specimens are relatively scattered around the group centroids (i.e. group means of the predictor variables). Nevertheless, two almost completely distinct groups can be identified confirming the fact that horncores can be assigned with a high degree of success to one of the two species.

A method for refining the discrimination is to check if, by dropping a pair of measurements, it is possible to reach a better separation between the two groups. The presence of too many variables may, in fact, cloud the issue.

Table 2.69 List of the set of measurements of the horncore dropped from the analysis along with their percentage of correct attributions.

Dropped Pair of Measurements	% of correct attributions
A and B	96.8%
C and D	95.2%
E and F	85.7%
A and C	96.8%
B and D	96.8%

As can be seen from Table 2.68, the variables that most influence the results are E and F. If one or the other is dropped, the reattribution score does not decrease but, if both of them are left out, the degree of correct identification is substantially reduced from 95.2% to 85.7%. All the other variables on the other hand, seem to participate to the same degree to the group separation and,

as such, the percentage of right attributions does not significantly change if a pair of these variables is dropped.

To sum up, Discriminant Analysis applied to the horncore has shown that the measurements taken on this anatomical element have a high potential in discriminating between the two species. As a consequence, the length of the horncore (E) along with the maximum and minimum diameter at the middle/base (A, B and C, D) should be taken whenever possible when analysing archaeological material. These measurements can in fact be used as confirmation of the identification already reached by looking at the morphological characteristics, or as a valid aid to discrimination, if the morphology is unconvincing.

While F has been excluded from the statistical analysis, it is highly recommended to record it if possible, as its contribution in separating the two species has been prove during the precious stages of analysis (linear and paired measurements).

Scapula

For this element the function elaborated by SPSS explains 50% of the variance in the sample, which is not a very high percentage (Tab. 2.69). Nevertheless, Wilks' Lambda test confirms that the function fits with the data and the differences detected in the sample are not due to chance, being $p < 0.05$ (Tab. 2.70).

Table 2.70 Canonical correlation coefficient for the scapula.

Eigenvalues				
Function	Eigenvalue	% of Variance	Cumulative %	Canonical Correlation
1	1.026 ^a	100.0	100.0	.712
a. First 1 canonical discriminant functions were used in the analysis.				

Table 2.71 Wilks' Lambda test for the scapula.

Wilks' Lambda				
Test of Function(s)	Wilks' Lambda	Chi-square	df	Sig.
1	.494	100.614	5	.000

Table 2.71 reveals the presence of both positive and negative values of very different magnitude. The variables which mostly contribute to the separation are GLP and ASG, which present high scores even though GLP has a positive coefficient while ASG has a negative one.

As explained previously, this difference attests to the fact that the variables contribute to the function but in different directions. The other variables such as LG, BG and SLC have all very small coefficients, attesting the low contribution they give to the function.

Table 2.72 Structure matrix for the scapula showing the canonical variate correlation coefficients.

Structure Matrix	
	Function
	1
GLP	.953
ASG	-.589
LG	.298
BG	-.271
SLC	.097
Pooled within-groups correlations between discriminating variables and standardized canonical discriminant functions	
Variables ordered by absolute size of correlation within function.	

Table 2.73 Classification results for the scapula.

Classification Results^{a,c}					
		TAXA	Predicted Group Membership		Total
			CH	OA	
Original	Count	CH	64	10	74
		OA	10	63	73
	%	CH	86.5	13.5	100.0
		OA	13.7	86.3	100.0
Cross-validated ^b	Count	CH	61	13	74
		OA	12	61	73
	%	CH	82.4	17.6	100.0
		OA	16.4	83.6	100.0
a. 86.4% of original grouped cases correctly classified.					
b. Cross validation is done only for those cases in the analysis. In cross validation, each case is classified by the functions derived from all cases other than that case.					
c. 83.0% of cross-validated grouped cases correctly classified.					

If Table 2.72, which presents the classification results, is considered, it can be observed that the percentage of correct identification is 86.4% which means that, in a sample of 100 specimens, 86 would be attributed to the correct species while 14 would be wrongly attributed. This

percentage is relatively high, but it must still be considered a useful result as the potential of this anatomical element in discriminating the two species has been acknowledged only by few researchers (Boessneck 1969; Boessneck *et al.* 1964; Buitenhuis 1995; Helmer and Rocheteau 1994; Prummel and Fisch 1986). Among the goat group, 10 specimens have been wrongly attributed; among the sheep group, 10 specimens were wrongly identified as goats. The relative success of the discriminant function becomes clear when the individual discriminating scores are plotted.

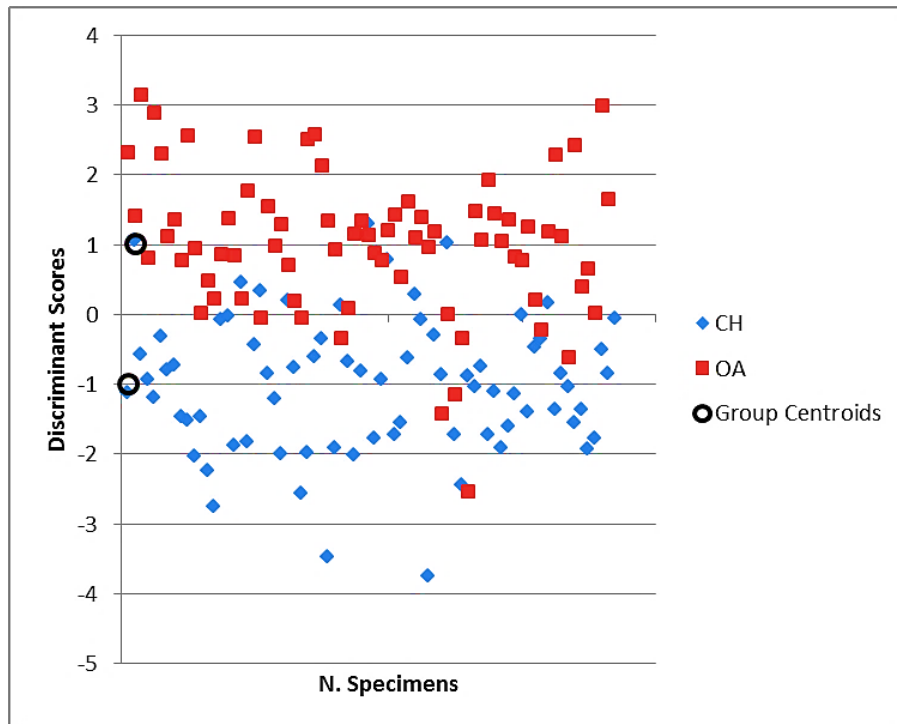


Figure 2.284 Scapula: scatterplot of the individual discriminant scores.

Figure 2.284 shows that the specimens are scattered around the group centroids. There is an area of overlap where specimens of both species fall but, at the same time, there are areas of the graph where mainly only sheep (at the top of the graph) or goats (at the bottom) lie.

It is interesting to observe that, if pairs of measurements are left out from the analysis, the reclassification rate changes (Tab. 2.73).

Table 2.74 List of the set of measurements on the scapula dropped from the analysis along with their percentage of correct attributions.

Dropped pair of measurements	% of correct attributions
GLP and SLC	82.3%
BG and LG	84.4%
SLC and BG	83%
ASG and BG	85.7%
GLP and ASG	69.3%

Table 2.73 shows the extent to which the reclassification rate varies according to which set of variables is dropped and, it can be observed that the set GLP and ASG is the one which influences the results most, causing a relevant diminution of the identification rate (from 86.4% to 69.3%). The combination GLP and SLC then follows determining a slight decrease of the identification rate (82.3%), while the other pairs of variables affect the separation to the same degree.

What can be suggested from the results with the scapula is that ASG (shortest distance from the spine to the edge of the glenoid cavity) and GLP (greatest length of the glenoid process) are most useful for separating the two species. These measurements fortunately can be frequently taken on archaeological material as the glenoid cavity, the *collum*, and the attachment of the spine (the spine is rarely preserved but if the attachment of it is visible on the *collum*, then the measurement can be taken) are the parts of this anatomical element that are most likely to survive.

Humerus

The function used for the humerus accounts for 57% of the variance in the sample. As seen for the scapula above, it is not a very high value (Tab. 2.74).

Table 2.75 Canonical correlation coefficient for the humerus.

Eigenvalues				
Function	Eigenvalue	% of Variance	Cumulative %	Canonical Correlation
1	1.362 ^a	100.0	100.0	.759
a. First 1 canonical discriminant functions were used in the analysis.				

Nevertheless, the Wilks' Lambda value reveals that the difference within the sample is not due to chance and it is statistically significant (Tab. 2.75).

Table 2.76 Wilks' Lambda test for the humerus.

Wilks' Lambda				
Test of Function(s)	Wilks' Lambda	Chi-square	df	Sig.
1	.423	120.736	7	.000

Table 2.76 shows the presence of some high positive scores, such as the coefficient given by BEI (breadth of the lateral epicondyle) and, to a lesser degree, HTC (diameter of the trochlear constriction) and HT (height of the trochlea). On the other hand, negative coefficients are given by all the other variables. BE (breadth of the *Capitulum*) and BT (breadth of the trochlea) have given the highest negative values, while Bd and Dd (breadth and depth of the distal end) the lowest. Evidently these latter variables give only a small contribution to the separation.

Table 2.77 Structure matrix for the humerus showing the canonical variate correlation coefficients.

Structure Matrix	
	Function
	1
BEI	.627
BE	-.409
HTC	.406
HT	.362
BT	-.316
Bd	-.285
Dd	-.103
Pooled within-groups correlations between discriminating variables and standardized canonical discriminant functions Variables ordered by absolute size of correlation within function.	

Table 2.78 Classification results for the humerus.

Classification Results^{a,c}					
		TAXA	Predicted Group Membership		Total
			CH	OA	
Original	Count	CH	67	9	76
		OA	8	62	70
	%	CH	88.2	11.8	100.0
		OA	11.4	88.6	100.0
Cross-validated ^b	Count	CH	66	10	76
		OA	10	60	70
	%	CH	86.8	13.2	100.0
		OA	14.3	85.7	100.0
a. 88.4% of original grouped cases correctly classified.					
b. Cross validation is done only for those cases in the analysis. In cross validation, each case is classified by the functions derived from all cases other than that case.					
c. 86.3% of cross-validated grouped cases correctly classified.					

Table 2.77 attests that the percentage of cases correctly classified is 88.4%. This score can be considered a good result considering that measurements taken on the distal humerus have never been considered useful for sheep and goat discrimination before the study conducted by Fernández (2001). The percentage of correct classifications attests that in a sample of 100 specimens, 88 would be correctly assigned to the right species. Among the goat group, nine specimens out of 76 were wrongly identified as sheep, while among the sheep group, eight out of 70 were assigned to the goat. If a pair of measurements is dropped, the reattribution score changes as follow:

Table 2.79 List of the set of measurements of the humerus dropped from the analysis along with their percentage of correct attributions.

Dropped pair of measurements	% of correct attributions
HT and HTC	89.0%
BEI and BE	79.5%
BEI and Bd	81.5%
BEI and HT	87.7%
BEI and HTC	88.4%
BEI and BT	82.9%
BE and HTC	88.4%

It is clear from Table 2.78 that the pair BEI and BE is the combination that has a major impact on the function as, if they are left out, the attribution rate decreases from 88.4% to 79.5%. Notably, all the combinations in which BEI is included show a decrease in the identification rate, attesting the importance of this variable. On the other hand, if the combination HT and HTC is dropped, the attribution score increases slightly from 88.4% to 89.0%.

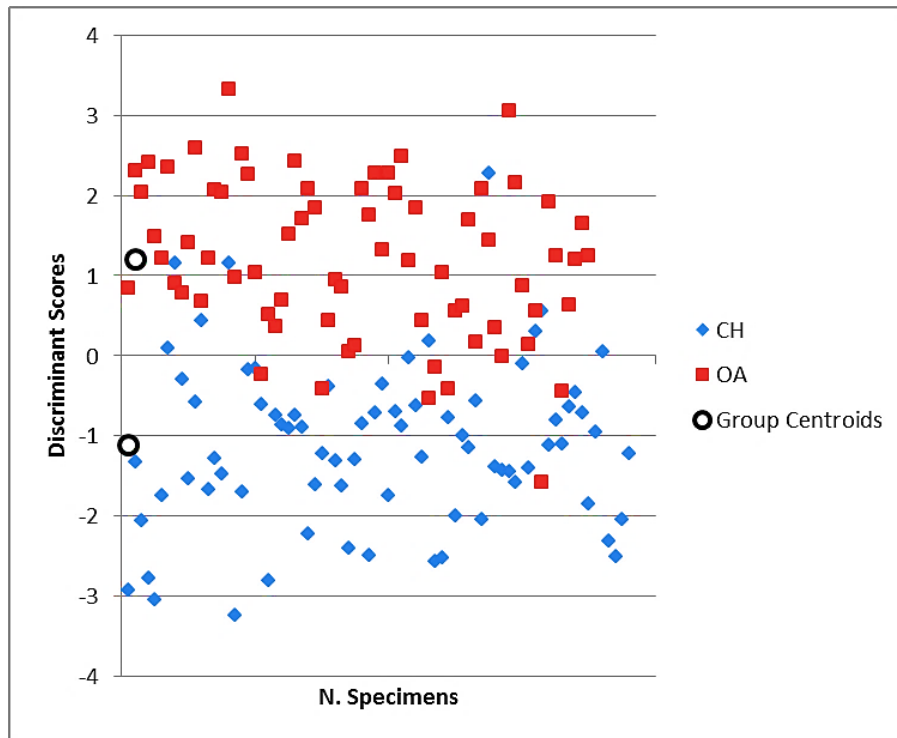


Figure 2.285 Humerus: scatterplot of the individual discriminant scores.

As the scatterplot of the individual discriminant coefficients demonstrates (Fig. 2.285), the specimens spread around the group centroids. The goat sample seems to be slightly more variable than the sheep sample, as the values from the former are more scattered on the graph than the values for the latter. There is a discrete area of the graph in which specimens from both groups fall but, at the same time, as seen before in the case of the scapula, there are parts of the graph in which, by and large, only one *taxon* can be found.

In conclusion, on the basis of the Discriminant Analysis results, it can be said that the measurements of the distal end of the humerus have some potential in discriminating between sheep and goat. For this reason, BEI and BE are especially recommended as measurements to be taken on archaeological material, along with HTC and BT and/or Bd. These are all measurements that can frequently be taken, as this part of the bone tends to survive well archaeologically.

Radius

For the proximal end of the radius the function elaborated by SPSS accounts for 68% of the variance within the sample (Tab. 2.79).

Table 2.80 Canonical correlation coefficient for the radius.

Eigenvalues				
Function	Eigenvalue	% of Variance	Cumulative %	Canonical Correlation
1	2.218 ^a	100.0	100.0	.830

a. First 1 canonical discriminant functions were used in the analysis.

Table 2.81 Wilks' Lambda test for the radius.

Wilks' Lambda				
Test of Function(s)	Wilks' Lambda	Chi-square	df	Sig.
1	.311	119.810	5	.000

Wilks' Lambda appears to be statistically significant attesting that the model fits well with the data and that the differences in the sample are due to a reason different than contingency (Tab. 2.80).

Table 2.82 Structure matrix for the radius showing the canonical variate correlation coefficients.

Structure Matrix	
	Function
	1
Bp	-.520
GL	.222
Dp	-.178
SD	.087
BFp	-.067

Pooled within-groups correlations between discriminating variables and standardized canonical discriminant functions
Variables ordered by absolute size of correlation within function.

By looking at Table 2.81, it can be seen that Bp has the highest negative coefficient, followed by GL which has the highest positive score. Clearly these variables contribute to the separation in an opposite way. All the other variables such as Dp (depth of the proximal end), SD and BFp

have very low coefficients attesting their low contribution to the separation.

Table 2.83 Classification results for the radius.

Classification Results^{a,c}					
		TAXA	Predicted Group Membership		Total
			CH	OA	
Original	Count	CH	53	3	56
		OA	4	47	51
	%	CH	94.6	5.4	100.0
		OA	7.8	92.2	100.0
Cross-validated ^b	Count	CH	53	3	56
		OA	4	47	51
	%	CH	94.6	5.4	100.0
		OA	7.8	92.2	100.0
a. 93.5% of original grouped cases correctly classified.					
b. Cross validation is done only for those cases in the analysis. In cross validation, each case is classified by the functions derived from all cases other than that case.					
c. 93.5% of cross-validated grouped cases correctly classified.					

The classification rate calculated for the proximal radius, as shown by Table 2.82, is 93.5%, a high promising value. In a hypothetical sample of 100 specimens, 93 would be correctly attributed. Among the group of 56 goats, only three were wrongly interpreted as sheep, while, in the sheep group, four specimens out of 51 were misidentified as goats.

If sets of measurements are dropped, the reclassification score changes (Tab. 2.83). If Bp and GL are left out from the analysis, the attribution rate decreases drastically from 93.5% to 59.8% confirming that these measurements are the most important. The next most significant combination is BFp and Bp which, if dropped, gives a percentage of correct attribution of 70.1%. The other pairs of variables affect the separation to a lesser degree.

Table 2.84 List of the set of measurements of the radius dropped from the analysis along with their percentage of correct attributions.

Dropped pair of measurements	% of correct attributions
GL and SD	92.5%
Bp and GL	59.8%
BFp and Bp	70.1%
BFp and Dp	88.8%
Bp and Dp	90.7%
Dp and GL	92.5%

The scatterplot of the individual discriminant scores (Fig. 2.286) shows the variability of this skeletal element among the two species; in fact the sheep as well as the goat specimens are more scattered than clustered around the group centroids. The scatterplot shows clearly that there is a zone in which a few specimens overlap, but there are also areas in which only goats or sheep fall. In fact, while the upper part of the graph gathers mainly goat specimens, the lower area is principally occupied by the sheep group.

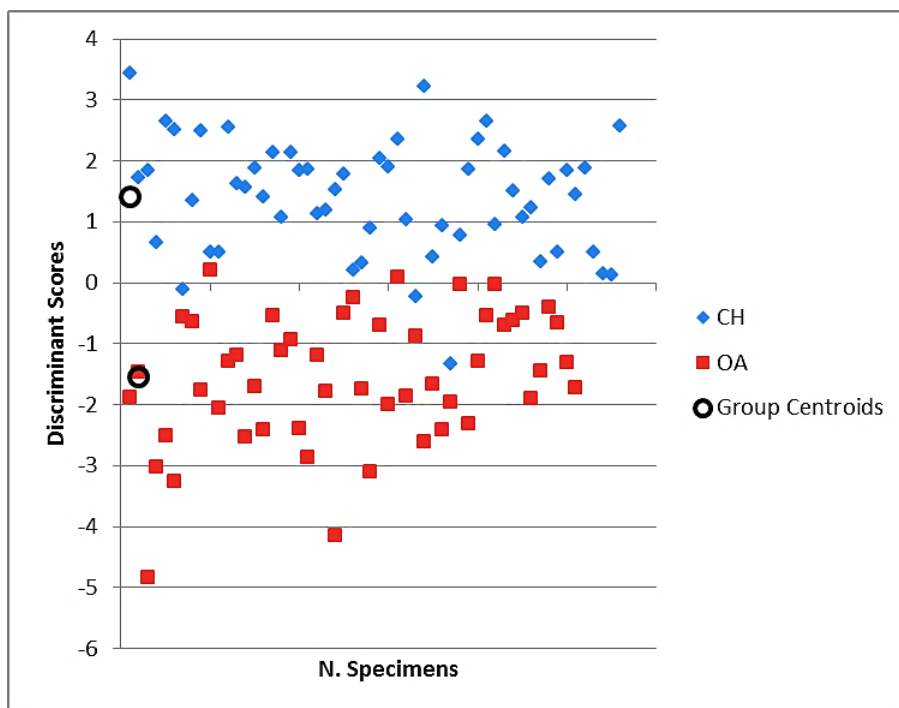


Figure 2.286 Radius: scatterplot of the individual discriminant scores.

Summing up, it can be said that the Discriminant Analysis applied to the radius has given a very good result. As a consequence, using Bp and GL is highly recommended. Unfortunately, it is rare to find complete *radia* among archaeological material but, as the other measurements taken of the proximal articulation such as Dp, Bp and BFP have been shown to have potential (see Biometrical Indices), they can partially compensate for the loss of information. As such, all the measurements suggested should be taken routinely.

Ulna

When the proximal articulation of the ulna is considered, the discriminant function accounts for 67% of the variance within the sample (Tab. 2.84).

Once again the Wilks' Lambda score is significant, confirming the presence of a difference not due to chance between the two groups (Tab. 2.85).

Table 2.85 Canonical correlation coefficient for the ulna.

Eigenvalues				
Function	Eigenvalue	% of Variance	Cumulative %	Canonical Correlation
1	2.051 ^a	100.0	100.0	.820
a. First 1 canonical discriminant functions were used in the analysis.				

Table 2.86 Wilks' Lambda test for the ulna.

Wilks' Lambda				
Test of Function(s)	Wilks' Lambda	Chi-square	df	Sig.
1	.328	121.037	5	.000

Table 2.87 Structure matrix for the ulna showing the canonical variate correlation coefficients.

Structure Matrix	
	Function
	1
DPA	.883
BPC	-.739
SDO	.432
L	.187
B	-.137

Structure Matrix
Pooled within-groups correlations between discriminating variables and standardized canonical discriminant functions
Variables ordered by absolute size of correlation within function.

By looking at Table 2.86, it can be seen that DPA and SDO have the highest positive values, while BPC has the highest negative value. These variables, as said before for other elements with positive and negative coefficients, all contribute heavily to the separation but with different directions. L (length of the *olecranon*) and B (breadth of the *olecranon*) on the other hand have very low coefficients, which means that they do not participate heavily to the separation of the two groups.

Table 2.88 Classification results for the ulna.

Classification Results^{a,c}					
		TAXA	Predicted Group Membership		Total
			CH	OA	
Original	Count	CH	53	3	56
		OA	5	52	57
	%	CH	94.6	5.4	100.0
		OA	8.8	91.2	100.0
Cross-validated ^b	Count	CH	52	4	56
		OA	5	52	57
	%	CH	92.9	7.1	100.0
		OA	8.8	91.2	100.0
a. 92.9% of original grouped cases correctly classified.					
b. Cross validation is done only for those cases in the analysis. In cross validation, each case is classified by the functions derived from all cases other than that case.					
c. 92.0% of cross-validated grouped cases correctly classified.					

The classification rate for the ulna is 92.9% which is another very high percentage, as shown by Table 2.87. Of the goat sample which was composed of 56 specimens, only three were attributed to the wrong species. On the other hand, for the sheep group five specimens out of 57 were wrongly identified.

Table 2.89 List of the set of measurements of the ulna dropped from the analysis along with their percentage of correct attributions.

Dropped pair of measurements	% of correct attributions
L and B	92.9%
DPA and BPC	73.5%
SDO and BPC	92.9%
SDO and DPA	92%

Table 2.88 confirms that the combination of variables with a major influence on the function is DPA and BPC. If these are left out, the attribution rate drops from 92.9% to 73.5%. Also the combinations SDO and BPC or SDO and DPA seem to have a certain degree of influence, but not as much as the pair DPA and BPC.

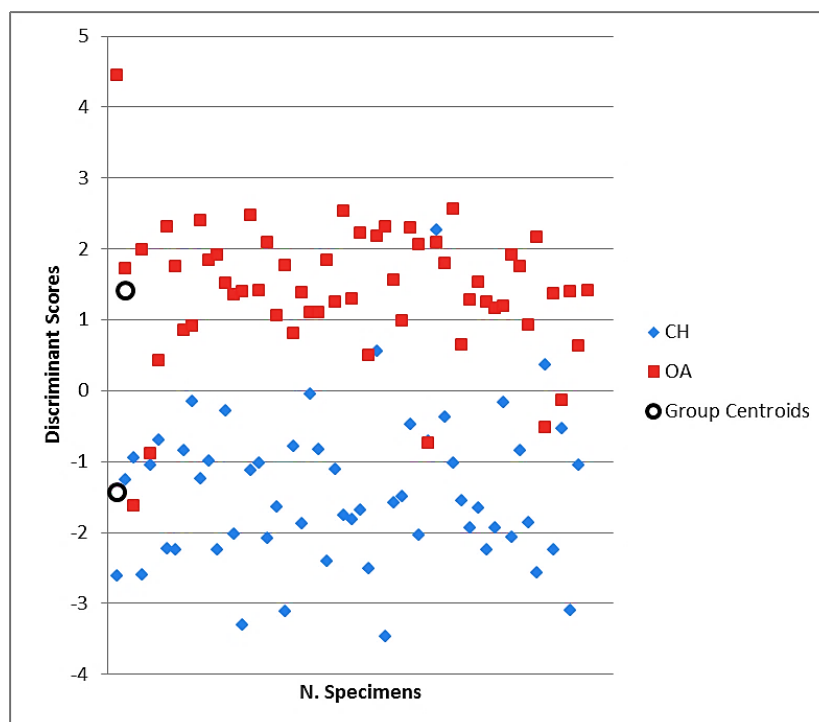


Figure 2.287 Ulna: scatterplot of the individual discriminant scores.

From Figure 2.287 it can be seen that there is a high degree of variation in both groups. In fact, sheep as well as goat specimens are widely spread in the graph area and not clustered around the group centroids. Despite the presence of few goat specimens in the sheep area and some sheep specimens in the goat area, the existence of two clear groups can be seen.

What emerges from this analysis is that BPC, DPA and SDO are the most effective variables in

discriminating between the two groups therefore, it is highly recommended to take these measurements. In addition, their location on an area of this anatomical element, which can be found relatively well preserved in an archaeological assemblage, makes them likely to be recorded, representing a useful aid for the sheep and goat discrimination.

Metacarpal

Good results from the analysis of the metacarpal were expected. SPSS found a function which accounts for 86% of the variability of the sample (Tab. 2.89).

Table 2.90 Canonical correlation coefficient for the metacarpal.

Eigenvalues				
Function	Eigenvalue	% of Variance	Cumulative %	Canonical Correlation
1	6.489 ^a	100.0	100.0	.931
a. First 1 canonical discriminant functions were used in the analysis.				

As seen for other skeletal elements, Wilks' Lambda *p* value confirms that the function elaborated by the program has a very good fit with the data, and it can discriminate very well between the two groups (Tab. 2.90).

Table 2.91 Wilks' Lambda test for the metacarpal.

Wilks' Lambda				
Test of Function(s)	Wilks' Lambda	Chi-square	df	Sig.
1	.134	223.486	12	.000

Table 2.92 Structure matrix for the metacarpal showing the canonical variate correlation coefficients.

Structure Matrix	
	Function
	1
BFd	-.528
a	-.509
GL	.488
5	-.481
b	-.454
2	-.372
SD	-.369
1	.307
BatF	-.301
6	-.271
3	-.253
4	.212
Pooled within-groups correlations between discriminating variables and standardized canonical discriminant functions	
Variables ordered by absolute size of correlation within function.	

From Table 2.91 it can be seen that GL, 1 (diameter of the medial trochlea) and 4 (diameter of the lateral trochlea) have positive values, while all the other measurements are negative. Amongst the variables with positive coefficients, GL and 1 have the highest, showing that they contribute to the discrimination more than 4. Among the negative coefficients, BFd (greatest breadth of the distal end) has the highest, followed by a (width of the medial condyle), 5 (diameter of the *verticillus* of the lateral condyle), b (width of the lateral condyle) and 2 (diameter of the *verticillus* of the medial condyle). SD, BatF (breadth at the fusion point on the distal end), 6 (diameter of the lateral part of the lateral condyle), and 3 (diameter of the lateral part of the medial condyle) all have negative and low coefficients, attesting to the fact that they contribute to the discrimination to a lesser degree than the other variables with negative coefficients.

Table 2.93 Classification results for the metacarpal.

Classification Results^{a,c}					
		TAXA	Predicted Group Membership		Total
			CH	OA	
Original	Count	CH	56	2	58
		OA	0	61	61
	%	CH	96.6	3.4	100.0
		OA	.0	100.0	100.0
Cross-validated ^b	Count	CH	55	3	58
		OA	0	61	61
	%	CH	94.8	5.2	100.0
		OA	.0	100.0	100.0
a. 98.3% of original grouped cases correctly classified.					
b. Cross validation is done only for those cases in the analysis. In cross validation, each case is classified by the functions derived from all cases other than that case.					
c. 97.5% of cross-validated grouped cases correctly classified.					

The overall percentage of grouped cases correctly classified for the metacarpal is 98.3% as displayed by Table 2.92. 98.3% is the highest score obtained, and it leaves a very low probability of wrong attributions at about 2% in a sample of 100 specimens. In this sample, all the specimens of sheep have been correctly identified while just two specimens out of 58 among the goat group, have been wrongly attributed.

In order to find out which variables most affect the discriminating power of the function, sets of measurements were dropped from the analysis with the following results:

Table 2.94 List of the set of measurements on the metacarpal dropped from the analysis along with their percentage of correct attributions.

Dropped pair of measurements	% of correct attributions
GL and SD	98.3%
BatF and BFd	98.3%
a and b	98.3%
1, 2 and 3	98.3%
4, 5 and 6	98.3%
1 and 4	98.3%

The results shown by Table 2.93 indicate that all the measurements contribute to the same degree to the strong discriminant power of the function. In fact, despite various sets of measurements being dropped from the analysis, the losses did not undermine the reattribution rate, which remained constant. This phenomenon is also partially reflected by the structure matrix; while with other elements the difference in magnitude between the coefficients given by

the different variables are significant, the metacarpal variables have coefficients that are of a relatively similar magnitude, attesting to a similar degree of participation to the function.

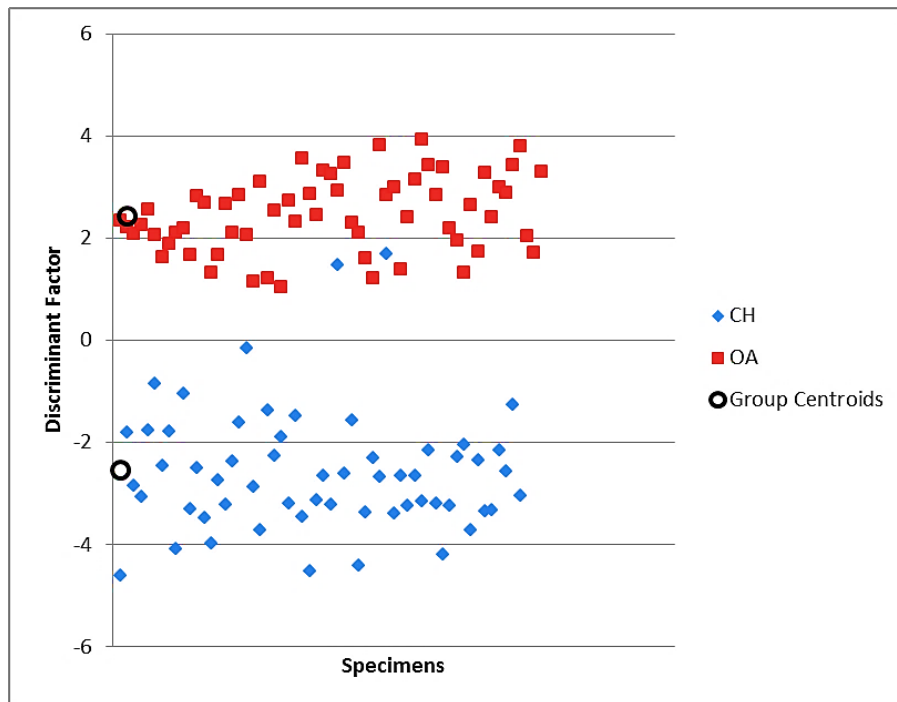


Figure 2.288 Metacarpal: scatterplot of the individual discriminant scores

If the scatterplot of the individual discriminant scores (Fig. 2.288) is observed, two clearly distinct groups, with just two specimens of goat plotting in the sheep area, can be identified. The variability in this case is clearly lower than for other elements. Nevertheless, the goat group seems to be more affected by variability than the sheep group; in fact sheep are more concentrated around their group centroid than the goat group. This could be due to the fact that the goat group is more heterogeneous than the sheep group: different breeds are present within it, while only two breeds form the sheep group. Other factors can also affect the variability of the groups, such as age and sex. However, while in both groups there are, as seen previously, more females than males, in the goat group there are older individuals than in the sheep group, a factor which could contribute to the higher variability recorded in the goat group.

To sum up, the high potential of this element in discriminating between sheep and goat have been confirmed. It is highly recommended to take all the measurements on the metacarpal used in this project, paying particular attention to a and b, BFd, GL and SD. Measurements 1 to 6 are also important, as demonstrated by the analysis or measurement ratios, even though they appear to be less effective on the discriminant function. As a consequence all measurements can usefully be recorded on both the medial and lateral condyles.

The measurements taken on the metacarpal (apart from GL that can be taken only if the whole bone is preserved) can commonly be taken as, most of the time, complete or almost complete distal articulations of this element are recovered from archaeological sites.

Metatarsal

For the metatarsal the results were satisfactory but less accurate than the metacarpal. The function elaborated by SPSS explains 74% of the variance within the sample (Tab. 2.94) and it is shown that the model fits well with the data as the Wilks' Lambda value is once again, significant (Tab. 2.95).

Table 2.95 Canonical correlation coefficient for the metatarsal.

Eigenvalues				
Function	Eigenvalue	% of Variance	Cumulative %	Canonical Correlation
1	2.964 ^a	100.0	100.0	.865
a. First 1 canonical discriminant functions were used in the analysis.				

Table 2.96 Wilks' Lambda test for the metatarsal.

Wilks' Lambda				
Test of Function(s)	Wilks' Lambda	Chi-square	df	Sig.
1	.252	159.764	12	.000

Table 2.97 Structure matrix for the metatarsal showing the canonical variate correlation coefficients.

Structure Matrix	
	Function
	1
5	.690
6	.678
GL	-.622
3	.521
b	.484
BFd	.466
2	.434
BatF	.406

Structure Matrix	
SD	.369
a	.339
4	.292
1	-.028
Pooled within-groups correlations between discriminating variables and standardized canonical discriminant functions	
Variables ordered by absolute size of correlation within function.	

Table 2.96 shows positive and negative values with different magnitudes. GL has the highest negative coefficient, followed by 1 (diameter of the medial trochlea) whose coefficient is so low that its participation to the separation can be regarded as minimal. Among the variables with positive values, 5 (diameter of the *verticillus* at the lateral condyle), 6 (diameter of the medial part of the lateral condyle) and 3 (diameter of the medial part of the medial condyle) have the highest. b (width of the lateral condyle), BFd (greatest breadth of the distal end), 2 (diameter of the *verticillus* at the medial condyle), BatF (breadth at the fusion point of the distal end), SD, a (width of the medial condyle) and 4 (diameter of the lateral trochlea) follow. It appears that the greatest length (GL), along with the diameter of the *verticillus* of the lateral condyle (5), the diameter of the medial part of the lateral (6) and medial (3) condyles play a major role in discriminating between the two groups.

Table 2.98 Classification results for the metatarsal.

Classification Results ^{a,c}					
		TAXA	Predicted Group Membership		Total
			CH	OA	
Original	Count	CH	56	5	61
		OA	4	59	63
	%	CH	91.8	8.2	100.0
		OA	6.3	93.7	100.0
Cross-validated ^b	Count	CH	54	7	61
		OA	4	59	63
	%	CH	88.5	11.5	100.0
		OA	6.3	93.7	100.0
a. 92.7% of original grouped cases correctly classified.					
b. Cross validation is done only for those cases in the analysis. In cross validation, each case is classified by the functions derived from all cases other than that case.					
c. 91.1% of cross-validated grouped cases correctly classified.					

The percentage of correct attribution, as shown by Table 2.97, is 92.7%. It is a very high percentage, attesting that on a theoretical sample of 100 specimens, 92 would have been correctly attributed to the right species. Five specimens out of 61 among the goat group were wrongly attributed to sheep while four specimens out of 63 were mistakenly considered goat.

If sets of variables are dropped from the analysis the results are as follows:

Table 2.99 List of the set of measurements on the metatarsal dropped from the analysis along with their percentage of correct attributions.

Dropped pair of measurements	% of correct attributions
GL and SD	93.5%
BatF and BFd	91.9%
a and b	93.5%
1, 2 and 3	95.2%
4, 5 and 6	89.5%
1 and 4	92.7%
1, 2, 3, a and b	93.5%

It seems that the combination of 4, 5 and 6 affects the reattribution rate more than any other combination, causing a decrease of the percentage of correct identifications from 92.7% to 89.5%. If the measurements of the medial condyle are left out from the analysis, the attribution rate increases to 95.2%. The measurements of the lateral condyle on the metatarsal seem to contribute more than those of the metacarpal to define the two groups (Tab. 2.98).

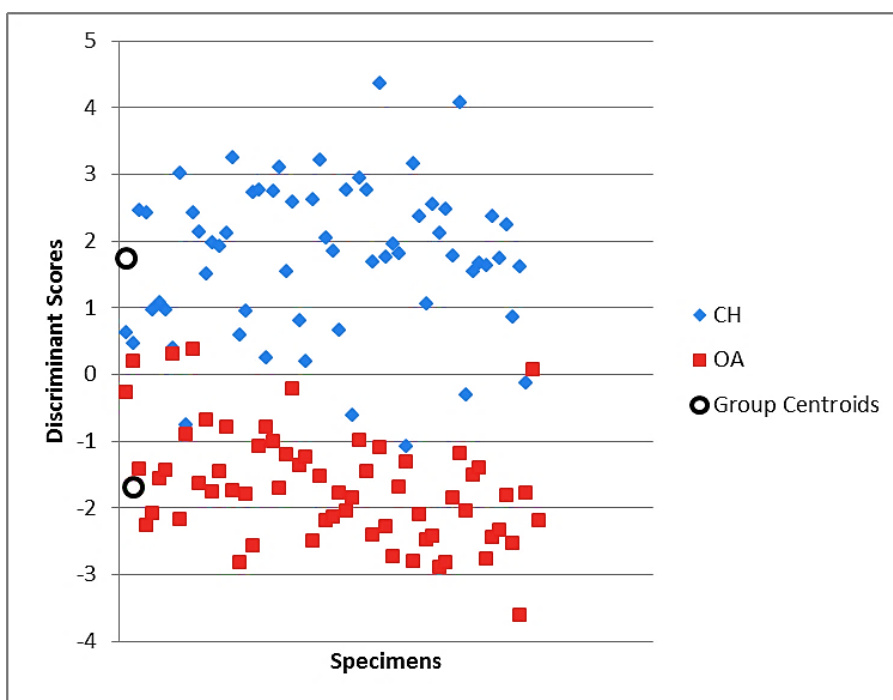


Figure 2.289 Metatarsal: scatterplot of the individual discriminant scores.

Figure 2.289 displays clearly the presence of two almost completely distinct groups. The separation between them is not as sharp as it was in the case of the metacarpal, but the overlap is not particularly significant, attesting to the fact that the metatarsal can also be a useful skeletal element for discriminating sheep from goat.

As seen before, the goat group presents the higher variability. In fact, the discriminant scores for this cluster are more widely spread on the graph area than the sheep group, which is, on the contrary, more clustered around its group centroid.

In conclusion, it is strongly suggested that metatarsal measurements GL, 3, 5 and 6, along with b and BFd are taken routinely. With the exception of GL, these measurements can be commonly taken as the distal articulation is frequently found in archaeological assemblages. In the case of the metatarsal, the Discriminant Analysis attests that the lateral condyle plays a more important role than the medial in discriminating between the two groups. Nevertheless, as previously seen in the case of the metacarpal, the measurements have demonstrable potential in discriminating sheep from goat (ratios).

Tibia

For the tibia, the model obtained by SPSS with the Standard Discriminant Analysis explains 56% of the total variance within the sample (Tab. 2.99). The model fits again very well with the modern sample as demonstrated by Wilk's Lambda value which is highly significant (Tab. 2.100).

Table 2.100 Canonical correlation coefficient for the tibia.

Eigenvalues				
Function	Eigenvalue	% of Variance	Cumulative %	Canonical Correlation
1	1.309 ^a	100.0	100.0	.753
a. First 1 canonical discriminant functions were used in the analysis.				

Table 2.101 Wilks' Lambda test for the tibia.

Wilks' Lambda				
Test of Function(s)	Wilks' Lambda	Chi-square	df	Sig.
1	.433	88.285	5	.000

Table 2.101 shows the most important variable contributing to the separation is Dd(a) (depth of the medial side of the distal end) which has provided the highest negative value. There are also two positive scores, even though of a lower magnitude than Dd(a); these coefficients are given by GL and SD. Finally, Dd(b) (depth of the lateral side of the distal end) and Bd have provided negative values as well but they are the lowest, attesting the lesser role that these variables play for the discriminant power of the function.

Table 2.102 Structure matrix for the tibia showing the canonical variate correlation coefficients.

Structure Matrix	
	Function
	1
Dd(a)	-.682
GL	.393
SD	.322
Dd(b)	-.286
Bd	-.250
Pooled within-groups correlations between discriminating variables and standardized canonical discriminant functions	
Variables ordered by absolute size of correlation within function.	

Table 2.103 Classification results for the tibia.

Classification Results^{a,c}					
		TAXA	Predicted Group Membership		Total
			CH	OA	
Original	Count	CH	55	3	58
		OA	9	43	52
	%	CH	94.8	5.2	100.0
		OA	17.3	82.7	100.0
Cross-validated ^b	Count	CH	54	4	58
		OA	11	41	52
	%	CH	93.1	6.9	100.0
		OA	21.2	78.8	100.0
a. 89.1% of original grouped cases correctly classified.					
b. Cross validation is done only for those cases in the analysis. In cross validation, each case is classified by the functions derived from all cases other than that case.					
c. 86.4% of cross-validated grouped cases correctly classified.					

Table 2.102 reveals that 89.1% of the specimens have been correctly attributed. This is a successful percentage confirming the potential in discriminating between the two species, already noted during the previous analysis, which this element has. Among the goat group, only three specimens have been wrongly attributed to sheep, while in the case of sheep, nine specimens were considered goats.

Table 2.104 List of the set of measurements on the tibia dropped from the analysis along with their percentage of correct attributions.

Dropped pair of measurements	% of correct attributions
GL and SD	80.9%
Bd and Dd(a)	82.7%
Bd and Dd(b)	84.5%
Dd(a) and Dd(b)	85.5%
Dd(a) and GL	76.4%

Table 2.103 clearly attests that Dd(a) and GL provide the most important combination of measurements, as the rate of attribution falls from 89.1% to 76.4%. Along with this, the pair GL and SD determines, if left out, a decrease of the rate to 80.9%. Less influential but still important to the success of the function are also the combinations Bd/Dd(a) and Bd/Dd(b).

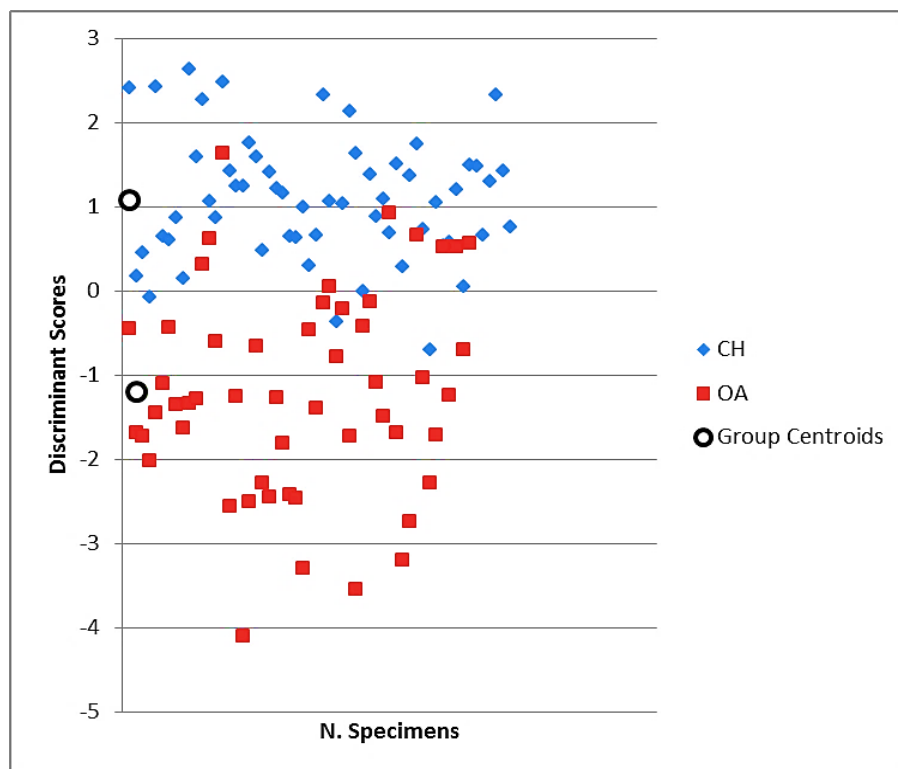


Figure 2.290 Tibia: scatterplot of the individual discriminant scores.

In the case of this anatomical element, the sheep group is the one which presents more variability, having the specimens more scattered around the graph than the goats. Figure 2.290 shows also that there is an area on the graph where overlap is recorded but, at the same time, most of the specimens fall into different areas with just a few exceptions.

Considering that this element has been considered less important for sheep and goat identification in previous studies (Boessneck *et al.* 1964; Clutton-Brock *et al.* 1990; Zeder and Lapham 2010), the results obtained with this analysis can be considered extremely encouraging. It is highly recommended to take Dd(a), GL and SD, even though these latter imply the presence of a complete bone. It is highly recommended to take also Bd and Dd(b) because, despite the fact that, they contribute less to the function according to Discriminant Analysis, they define better the shape of the articulation (as showed by the Biometrical Indices analysis) in combination with other measurements and consequently, they can be useful for the proposed discrimination.

Astragalus

The results obtained from the study of the measurements taken on the astragalus are presented in Tables 2.104 to 2.108.

Table 2.105 Canonical correlation coefficient for the astragalus.

Eigenvalues				
Function	Eigenvalue	% of Variance	Cumulative %	Canonical Correlation
1	1.605 ^a	100.0	100.0	.785
a. First 1 canonical discriminant functions were used in the analysis.				

SPSS found a canonical discriminant function which explains 61% of the variance among the two groups (Tab. 2.104). The function elaborated fits, once again, very well with the data, *p* being significant (< 0.05) (Tab. 2.105).

Table 2.106 Wilks' Lambda test for the astragalus.

Wilks' Lambda				
Test of Function(s)	Wilks' Lambda	Chi-square	df	Sig.
1	.384	133.547	7	.000

Table 2.107 Structure matrix for the astragalus showing the canonical variate correlation coefficients.

Structure Matrix	
	Function
	1
DI	-.281
H	.276
Bd	-.244
GLI	.204
Dm	-.167
BpT	.047
GLm	.031
Pooled within-groups correlations between discriminating variables and standardized canonical discriminant functions	
Variables ordered by absolute size of correlation within function.	

Table 2.106 attests that H (height at the central constriction) and GLI are the measurements with the highest positive values, while DI and Bd are those with higher negative scores. As a consequence, these are the variables which have a major impact on the discriminating power of the function, even though they contribute in different directions. Dm, BpT (maximum breadth of the plantar trochlea) and GLm has a minor influence on the discrimination as demonstrated by their very low coefficients.

Table 2.108 Classification results for the astragalus.

Classification Results^{a,c}					
		TAXA	Predicted Group Membership		Total
			CH	OA	
Original	Count	CH	65	7	72
		OA	9	64	73
	%	CH	90.3	9.7	100.0
		OA	12.3	87.7	100.0
Cross-validated ^b	Count	CH	64	8	72
		OA	11	62	73
	%	CH	88.9	11.1	100.0
		OA	15.1	84.9	100.0
a. 89.0% of original grouped cases correctly classified.					
b. Cross validation is done only for those cases in the analysis. In cross validation, each case is classified by the functions derived from all cases other than that case.					
c. 86.9% of cross-validated grouped cases correctly classified.					

Table 2.107 indicates a reattribution score of 89.0%, which means that, in a hypothetical sample of 100 specimens, 89 would have been correctly classified. The percentage is high, although not among the highest found so far. The specimens misclassified are seven out of 72 within the goat group, and nine out of 73 within the sheep group.

Table 2.109 List of the set of measurements on the astragalus dropped from the analysis along with their percentage of correct attributions.

Dropped pair of variables	% of correct attributions
Glm and Dm	90.3%
GLI and DI	82.8%
GLI and Bd	86.2%
GLI and H	89.7%
DI and H	85.5%
Bd and H	91.7%
GLm, BpT and H	91.0%

If different combinations as GLI and DI, along with DI with H and, GLI and Bd are dropped, the percentages of right attributions decrease significantly (respectively 82.8%, 86.2% and 85.5%) (Tab. 2.108). This clearly confirms that these measurements are particularly important for the discrimination of sheep and goat. On the other hand, Bd and H, GLm, BpT and H, along with GLI and H are, among the combinations used, those which influence the least the attribution rate, as shown by Table 2.108.

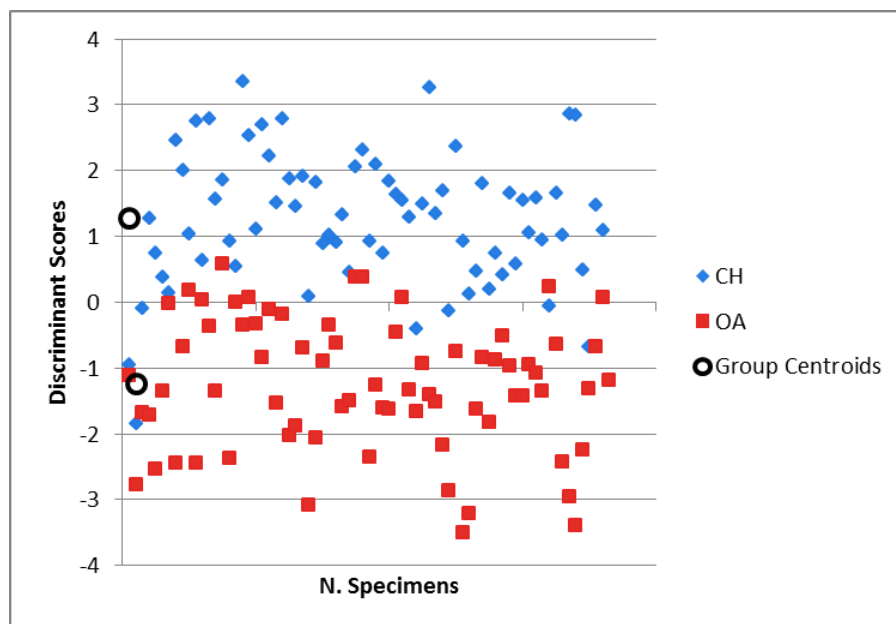


Figure 2.2.291 Astragalus: scatterplot of the individual discriminant scores.

Figure 2.291 shows that, an area of overlap is present. Nevertheless, the upper part of the graph is occupied just by goat specimens and the lower part by sheep specimens. This distribution attests to the fact that this element has potential in separating sheep and goat specimens.

To sum up, it is highly recommended to record measurements such as H, DI and Bd along with GLI on the astragalus, because these can help in the discrimination process. As the astragalus survives very well (Binford and Betram 1977; Lyman 1984), it should be possible to take these measurements on a regular basis on archaeological material.

Calcaneum

For the calcaneum, the Standard Discriminant analysis found a function which explains 73% of the variability in the groups (Tab. 2.109).

Table 2.110 Canonical correlation coefficient for the calcaneum.

Eigenvalues				
Function	Eigenvalue	% of Variance	Cumulative %	Canonical Correlation
1	2.751 ^a	100.0	100.0	.856
a. First 1 canonical discriminant functions were used in the analysis.				

The Wilk's Lambda test confirms that the function fits very efficiently with the data as the *p* value is highly significant (Tab. 2.110).

Table 2.111 Wilks' Lambda test for the calcaneum.

Wilks' Lambda				
Test of Function(s)	Wilks' Lambda	Chi-square	df	Sig.
1	.267	154.008	7	.000

Table 2.112 Structure matrix for the calcaneum showing the canonical variate correlation coefficients.

Structure Matrix	
	Function
	1
c	.450
GL	-.214
DS	.092
B	-.031
Gd	-.030
d	.028
SB	-.012
Pooled within-groups correlations between discriminating variables and standardized canonical discriminant functions	
Variables ordered by absolute size of correlation within function.	

Table 2.111 shows the importance of c (length of the articular facet of the *os malleolare*) which has the highest positive coefficient and GL, which as the highest negative score, leaving out the other measurements such as DS (depth of the *substantaculum tali*), B (breadth of the articular facet of the *os malleolare*), Gd (greatest depth), d (length taken from the articular facet of the *os malleolare* to the end of the articulation-free part of the process), and SB (greatest breadth) which contribute far less to the separating power of the function, as attested by their low scores.

Table 2.113 Classification results for the calcaneum.

Classification Results ^{a,c}					
		TAXA	Predicted Group Membership		Total
			CH	OA	
Original	Count	CH	55	5	60
		OA	1	61	62
	%	CH	91.7	8.3	100.0
		OA	1.6	98.4	100.0
Cross-validated ^b	Count	CH	55	5	60
		OA	1	61	62
	%	CH	91.7	8.3	100.0
		OA	1.6	98.4	100.0
a. 95.1% of original grouped cases correctly classified.					
b. Cross validation is done only for those cases in the analysis. In cross validation, each case is classified by the functions derived from all cases other than that case.					
c. 95.1% of cross-validated grouped cases correctly classified.					

Standard Discriminant Analysis calculated a reattribution rate of 95.1% which is a significantly high value. On a sample of 60 goats, only five were wrongly identified as sheep while, on a sample of 62 sheep, just one specimen was attributed to the wrong taxon (Tab. 2.112).

In order to understand which sets of variables influence the function most, some were dropped from the analysis with the following results:

Table 2.114 List of the set of measurements on the calcaneus dropped from the analysis along with their percentage of correct attributions.

Dropped pair of measurements	% of correct attributions
c, d and B	69.7%
c and GL	62.3%
c and B	86.1%
GL and SB	95.1%
GL and Gd	95.1%
DS and Gd	95.1%

A significant drop in the percentage of the reattribution value can be observed (Tab. 2.113). In particular, when c and GL are dropped, the rate decreases from 95.1% to 62.3%. There is a substantial drop also when c, d and B are removed. This output suggests that these are the measurements to be focused on if the aim of the study is distinguishing the two species. The combination of c and B also seems to have some influence (86.1%) while the reattribution rate does not change if GL/Gd and DS/Gd are excluded from the analysis.

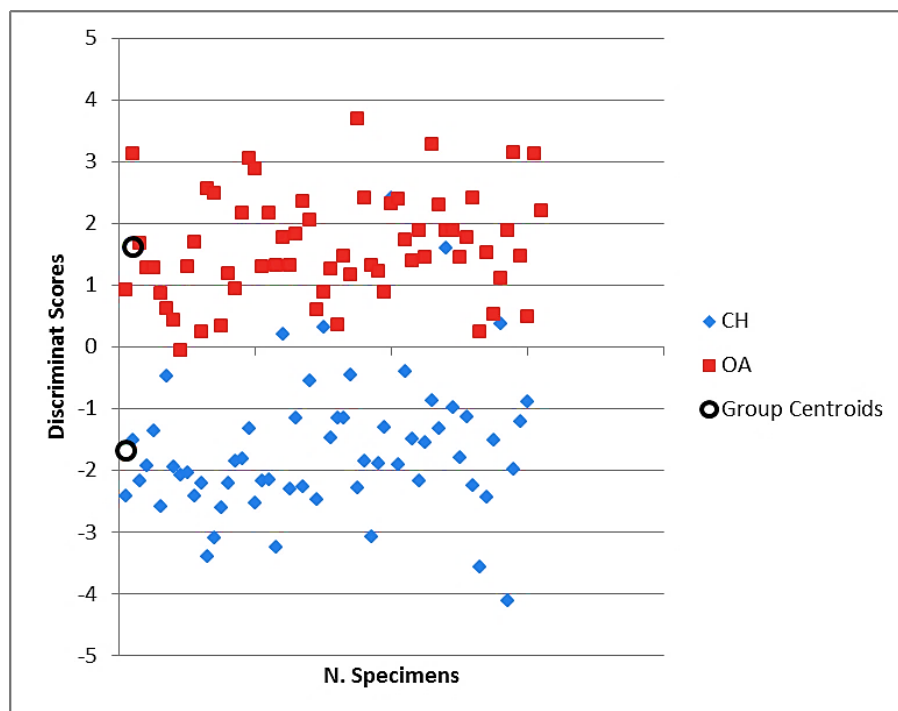


Figure 2.292 Calcaneum: scatterplot of the individual discriminant scores.

Figure 2.292 shows a good separation between the two groups with just some goat specimens present in the sheep area of the graph. Specimens are scattered around the group centroids attesting the presence of some variation which is affecting more the goat group than the sheep one.

In conclusion, the calcaneum seems to be a useful element for discriminating between sheep and goat. Important measurements such as c, d and B must be taken routinely on archaeological material if preservation allows.

3rd Phalanx

For the 3rd phalanx, just two measurements were taken so only two variables could be input into SPSS. The results show that the function could explain 51% of the variance within the sample (Tab. 2.114).

Table 2.115 Canonical correlation coefficient for the 3rd phalanx.

Eigenvalues				
Function	Eigenvalue	% of Variance	Cumulative %	Canonical Correlation
1	1.056 ^a	100.0	100.0	.717
a. First 1 canonical discriminant functions were used in the analysis.				

The function, according to the tests, fits well with the data as Wilks' Lambda test shows (Tab. 2.115).

Table 2.116 Wilks' Lambda test for the 3rd phalanx.

Wilks' Lambda				
Test of Function(s)	Wilks' Lambda	Chi-square	df	Sig.
1	.486	94.807	1	.000

When taking into account the structure matrix Table (Tab. 2.116), it is clear that a case of multicollinearity (a situation in which two or more variables are very closely linearly related; Field 2009: 790) is present. That is why Table 2.116 suggests that only one of the two variables should be retained for discriminating between the two groups.

Table 2.117 Structure matrix for the 3rd phalanx showing the canonical variate correlation coefficients.

Structure Matrix	
	Function
	1
MBS ^a	-1.000
DLS	1.000
Pooled within-groups correlations between discriminating variables and standardized canonical discriminant functions	
Variables ordered by absolute size of correlation within function.	
a. This variable not used in the analysis.	

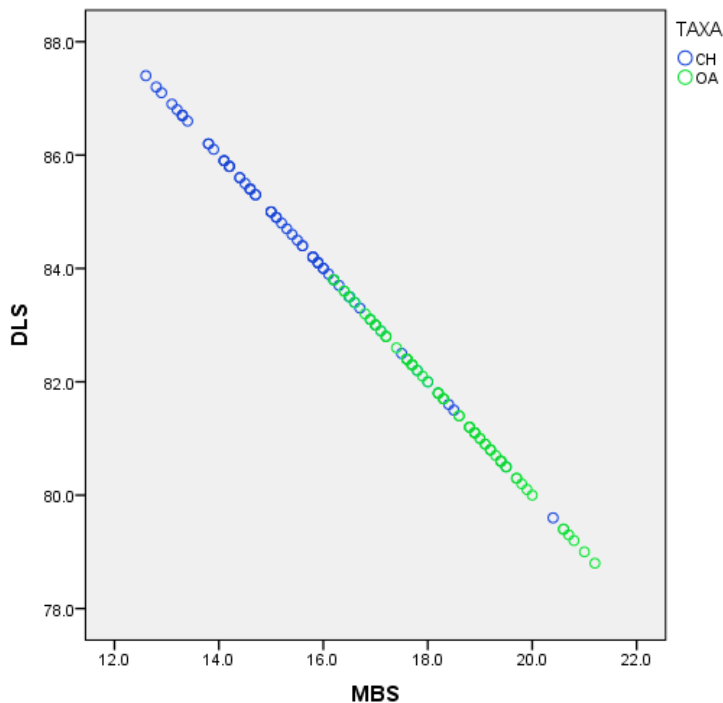


Figure 2.293 3rd phalanx: MBS plotted against DLS shows the presence of multicollinearity.

The closely linear relationship between the two variables is confirmed when the two variables are plotted against each other (Fig. 2.293). It must be noted that both the axes (namely the measurements) can clearly discriminate between the two groups, with just a few specimens falling in the wrong area of the graph. As the absence of multicollinearity is one of the assumptions Discriminant Analysis requires, the following results have to be taken with caution.

Table 2.118 Classification results for the 3rd phalanx.

Classification Results ^{a,c}					
		TAXA	Predicted Group Membership		Total
			CH	OA	
Original	Count	CH	55	10	65
		OA	9	60	69
	%	CH	84.6	15.4	100.0
		OA	13.0	87.0	100.0
Cross-validated ^b	Count	CH	55	10	65
		OA	9	60	69
	%	CH	84.6	15.4	100.0
		OA	13.0	87.0	100.0
a. 85.8% of original grouped cases correctly classified.					
b. Cross validation is done only for those cases in the analysis. In cross validation, each case is classified by the functions derived from all cases other than that case.					
c. 85.8% of cross-validated grouped cases correctly classified.					

From Table 2.117 it can be seen that a score of 85.8% of original grouped cases classified has been reached. This value is not very high but it still has some importance. Of the goat group, 10 specimens out of 65 have been wrongly attributed to sheep while nine specimens out of 69 were considered goat incorrectly.

If the scatterplot with the individual discriminant scores is analysed (Fig. 2.294), it can be seen that a significant area of the graph gathers sheep and goat specimens showing a relative high overlap but, as said before for other elements, some areas of the graph, especially the upper part for goat specimens and the lower part for sheep specimens, are only occupied by one species.

A high variability can be seen in both groups, this is the reason why the specimens are spread on the graph, with the goat group providing more variability than the sheep. This may be due to different factors such as differences in age and breed between the two groups but also, due to the fact that phalanges from the anterior and posterior leg are different. Unfortunately it is extremely difficult, if not impossible, to distinguish between phalanges from the fore limb and hind limb.

In the case of the 3rd phalanx, I suggest that both measurements should be taken routinely as they have clearly shown to be useful in distinguishing the two closely related species.

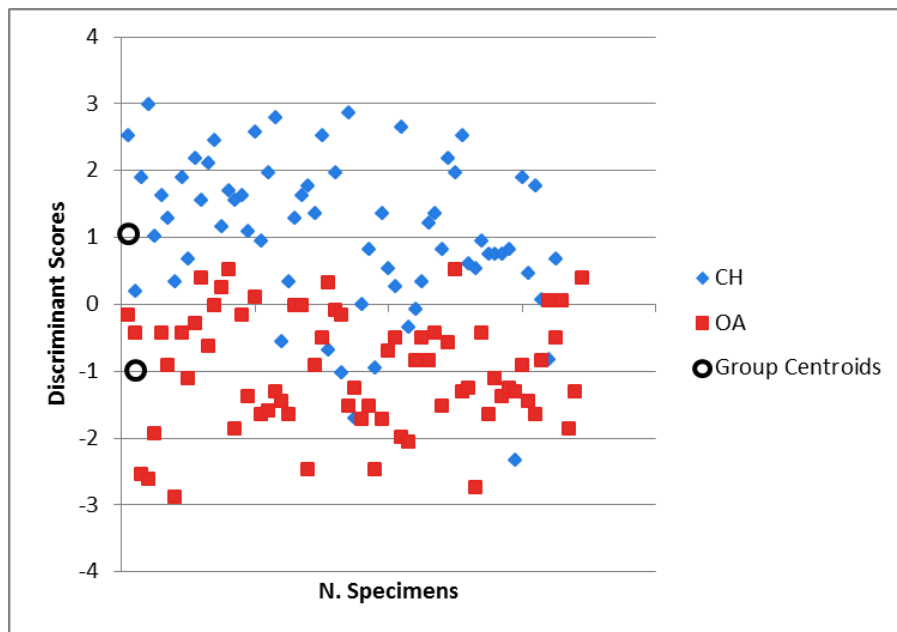


Figure 2.294 3rd phalanx: scatterplot of the individual discriminant scores.

2.5.7 Principal Component Analysis

Principal Component analysis was run for different purposes:

- to analyse the relationships between the variables in order to see if some were more important than others for the sheep/goat distinction;
- to see if hidden major trends could be identified within the data.

Principal Component Analysis is a technique of data reduction: it compresses a very large percentage of the variation into a smaller number of variables by transformation. This transformation implies the elaboration of new variables which are independent from one another (Baxter 2003:73; Field 2009: 627; Shennan 1997: 297; Tabachnick and Fidell 2007: 607).

PCA was undertaken for each element individually, using the chosen measurements as variables. Output options were set to give case-by-case function coefficients, so that the function result for each individual specimen was obtained as well as a summary table. Varimax rotation (namely orthogonal rotation for unrelated/independent factors), one of the most commonly used method of rotation, was selected in order to see if the loadings of a variable into a single factor could be maximized (Tabachnick and Fidell 2007: 620). Finally, plots of all cases were also produced using the function individual scores for each function identified.

The results obtained for the two species are presented on the following pages on an element-by-element basis; these are also commented on, so that the limitations can be understood. Some necessary concepts, in order to understand better Principal Component Analysis, are given in

Horncore

Table 2.118 presents KMO and Bartlett’s Test values. It can be seen that the KMO value does not meet the requirement, as an acceptable sample should give a minimum value of 0.5 (Field 2009: 647); this is not worrying, as KMO is more relevant in factor analysis than in Principal Component Analysis (Stack exchange inc. 2015b). In addition, as the solution for low KMO would have been to gather more data, an unfeasible task for the state of the research, KMO will be ignored.

On the other hand, the value for the Bartlett’s Test is highly significant ($p < .001$) attesting the existence of relationships between the variables studied, which is an encouraging result. Nevertheless, the fact that there are correlations does not mean that they are large enough to make the analysis meaningful (Field 2009: 648). Another method for checking the relationships between variables is adopted, which is to consider the correlation matrix and look for the presence of too low or too high correlations between the variables, as they must be avoided. If low correlations (below 0.3) are present, all variables are perfectly independent from one another and finding clusters (which is the reason for PCA) would be impossible as variables do not correlate (Field 2009: 648). On the other hand, if variables correlate too highly there would be the risk of extreme multicollinearity and singularity (values above 0.9), namely when variables are highly or perfectly correlated, so that the single contribution of a variable to the function cannot be determined. A solution in both cases could be dropping the variables that correlate, either too lowly or too highly, from the factor analysis. As multicollinearity (value > 0.9) does not represent a serious problem for Principal Component Analysis (Tabachnick and Fidell 2007: 614), and low correlations (values lower than 0.3) cannot be detected in the Correlation matrix related to the analysis of the horncore (Tab. 2.119), it was not necessary to eliminate variables.

Table 2.119 KMO and Bartlett's Test for measurements taken on the horncores.

KMO and Bartlett's Test		
Kaiser-Meyer-Olkin Measure of Sampling Adequacy.		.390
Bartlett's Test of Sphericity	Approx. Chi-Square	862.636
	df	15
	Sig.	.000

Table 2.120 Correlation matrix for the horncore.

Correlation Matrix ^a							
		A	B	C	D	E	F
Correlation	A	1.000	.759	.928	.794	-.802	-.878
	B	.759	1.000	.625	.870	-.830	-.638
	C	.928	.625	1.000	.792	-.781	-.856
	D	.794	.870	.792	1.000	-.872	-.719
	E	-.802	-.830	-.781	-.872	1.000	.515
	F	-.878	-.638	-.856	-.719	.515	1.000
Sig. (1-tailed)	A		.000	.000	.000	.000	.000
	B	.000		.000	.000	.000	.000
	C	.000	.000		.000	.000	.000
	D	.000	.000	.000		.000	.000
	E	.000	.000	.000	.000		.000
	F	.000	.000	.000	.000	.000	
a. Determinant = 4.66E-007							

Table 2.119 shows that low correlations are completely absent while high correlations can be identified, especially between A and C. This is hardly surprising as A and C both measure the maximum diameter respectively at the base and at the middle of the horncore.

Moving to the Table 2.120, it can be seen that six components have been found but, the first one is the most important as it accounts for 81.5% of the variance within the sample.

Table 2.121 Total Variance explained for the horncore.

Total Variance Explained						
Component	Initial Eigenvalues			Extraction Sums of Squared Loadings		
	Total	% of Variance	Cumulative %	Total	% of Variance	Cumulative %
1	4.894	81.565	81.565	4.894	81.565	81.565
2	.646	10.759	92.324			
3	.294	4.896	97.220			
4	.140	2.334	99.555			
5	.027	.443	99.998			
6	.000	.002	100.000			
Extraction Method: Principal Component Analysis.						

Table 2.122 Component matrix for the horncore.

Component Matrix^a	
	Component
	1
A	.954
D	.932
C	.921
E	-.888
B	.870
F	-.849
Extraction Method: Principal Component Analysis.	
a. 1 component extracted.	

The Component matrix (Tab. 2.121) suggests that shape rather than size is involved in the component and this is suggested by the presence of loadings with different signs (positive and negative) and magnitudes (Baxton 2003; Davis 1996; Shennan 1997).

If we look at the single loadings for each variable, it can be seen that A has the highest positive score followed by D and C. The measurements taken at the base and at the middle of the horncore have the same sign and almost the same magnitude, except for B which presents a slightly lower value. E and F measure the straight length and the length of the outer curvature of the horncore; they have high negative values, which means that they go in the opposite direction compared to the variables which have a positive loading.

These data suggest that, on the one hand, the component found is dominated by the measurements taken at the base and the middle of the horncore. As these variables are described with values of the same sign and similar magnitude, they all contribute to the function relatively to the same degree (among the variables mentioned, A and D are of particular importance). The length of the horncore taken from the base to the tip (measure E) influences as well the function. As a consequence, it can be said that the diameter measurements, along with the length of the horncores, are the measurements that better explain the function and the variance within the sample.

By plotting the factor scores given to each individual (Fig. 2.295), it can be seen that the goat group occupies mainly the lower part of the graph, while the upper part of the scatterplot shows mainly sheep specimens so that a division line could be drawn corresponding to the 0.5 value on the vertical axis. A certain degree of overlap is apparent: several specimens of sheep can be seen in the predominantly goat areas, just as goat specimens are present in the mainly sheep area. Nevertheless a discrete separation is present.

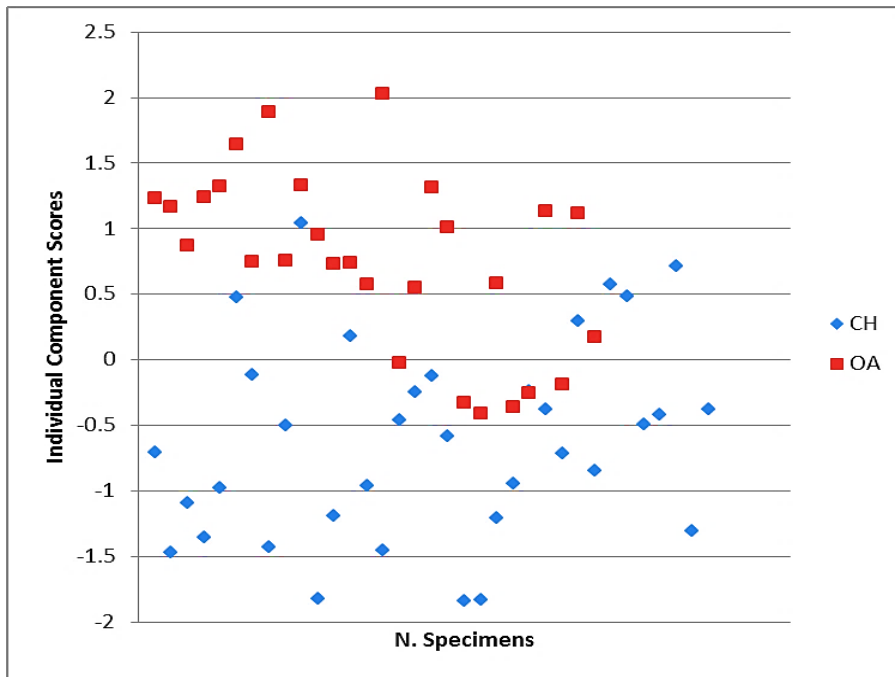


Figure 2.295 Horncore: scatterplot of the individual component scores.

As the program has found only one component, Varimax rotation could not be applied.

Scapula

As previously observed, the KMO value does not meet the requirement but the Bartlett's Test of Sphericity is highly significant ($p < .001$), thus attesting the existence of relationships between the analysed variables (Tab. 2.122).

If the Correlation matrix Table is taken into account (Tab. 2.123), it can be seen that BG has some low correlation values, as does SLC. Nevertheless they were not dropped from the analysis as it would have meant a great loss of information for this anatomical element.

Table 2.123 KMO and Bartlett's Test for the measurements taken on the scapula.

KMO and Bartlett's Test		
Kaiser-Meyer-Olkin Measure of Sampling Adequacy.		.142
Bartlett's Test of Sphericity	Approx. Chi-Square	991.431
	df	10
	Sig.	.000

Table 2.124 Correlation matrix for the scapula.

Correlation Matrix ^a						
		ASG	LG	BG	GLP	SLC
Correlation	ASG	1.000	-.676	-.083	-.777	-.322
	LG	-.676	1.000	-.147	.549	-.123
	BG	-.083	-.147	1.000	-.261	-.241
	GLP	-.777	.549	-.261	1.000	-.007
	SLC	-.322	-.123	-.241	-.007	1.000
Sig. (1-tailed)	ASG		.000	.159	.000	.000
	LG	.000		.038	.000	.069
	BG	.159	.038		.001	.002
	GLP	.000	.000	.001		.466
	SLC	.000	.069	.002	.466	
a. Determinant = .001						

From Table 2.124 it can be seen that two components have been found. The first, which is the most significant, accounts for 47.6% of the variance in the sample. The second component identified, accounts for 24.4% of the variance. Both components explain in total 72.0% of the variance in the sample.

Table 2.125 Total Variance Explained for the scapula.

Total Variance Explained									
Component	Initial Eigenvalues			Extraction Sums of Squared Loadings			Rotation Sums of Squared Loadings		
	Total	% of Variance	Cumulative %	Total	% of Variance	Cumulative %	Total	% of Variance	Cumulative %
1	2.381	47.627	47.627	2.381	47.627	47.627	2.333	46.659	46.659
2	1.221	24.420	72.048	1.221	24.420	72.048	1.269	25.389	72.048
3	.959	19.176	91.224						
4	.438	8.760	99.984						
5	.001	.016	100.000						
Extraction Method: Principal Component Analysis.									

Table 2.126 Component matrix for the scapula.

Component Matrix ^a		
	Component	
	1	2
ASG	-.924	-.045
GLP	.885	.049
LG	.812	.268
SLC	.178	-.826
BG	-.229	.680
Extraction Method: Principal Component Analysis.		
a. 2 components extracted.		

Table 2.125 enables us to examine the components singularly. Once again, shape is shown to be important as both components have positive and negative values with different magnitude.

The first component seems to be influenced mainly by ASG, GLP and, to a lesser extent, LG. All these measurements are related to length (of the articulation, of the glenoid cavity and the distance from the base of the spine to the edge of the glenoid cavity) which means that the first component is determined by length.

The second component is mainly determined by SLC and, to a lesser extent, by BG, which measure respectively the length of the *collum* and the breadth of the glenoid cavity. The difference in sign is due to the fact that they measure different dimensions of the bone.

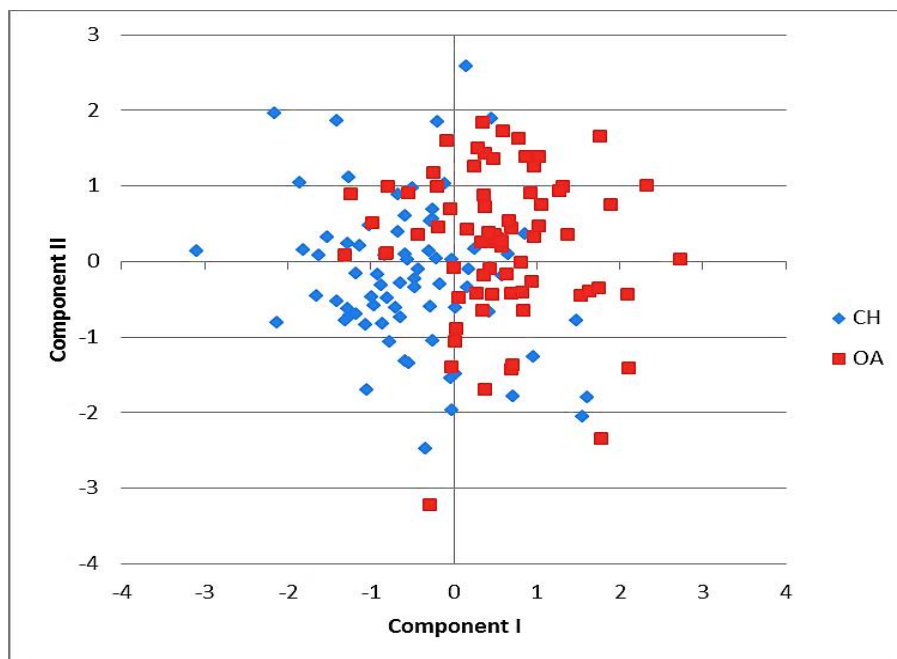


Figure 2.296 Scapula: scatterplot of the individual discriminant score for component I and component II.

If the factor scores for the two components are plotted (Fig. 2.296), it can be seen that goat specimens fall mainly in the centre-left part of the graph, while the sheep specimens occupy mainly the right area. Clearly there is a considerable amount of overlap: the area between 1 and -1 on the horizontal axis as well as on the vertical axis includes most of the overlap. Nevertheless, the specimens seem to be better separated by component I (Fig. 2.297) which is evidently the most important function as also testified by the percentage of total variance that this variable explains (Tab. 2.124). As a consequence, it can be said that length measurements like ASG, GLP and LG are the variables that best explain the variation within the sample.

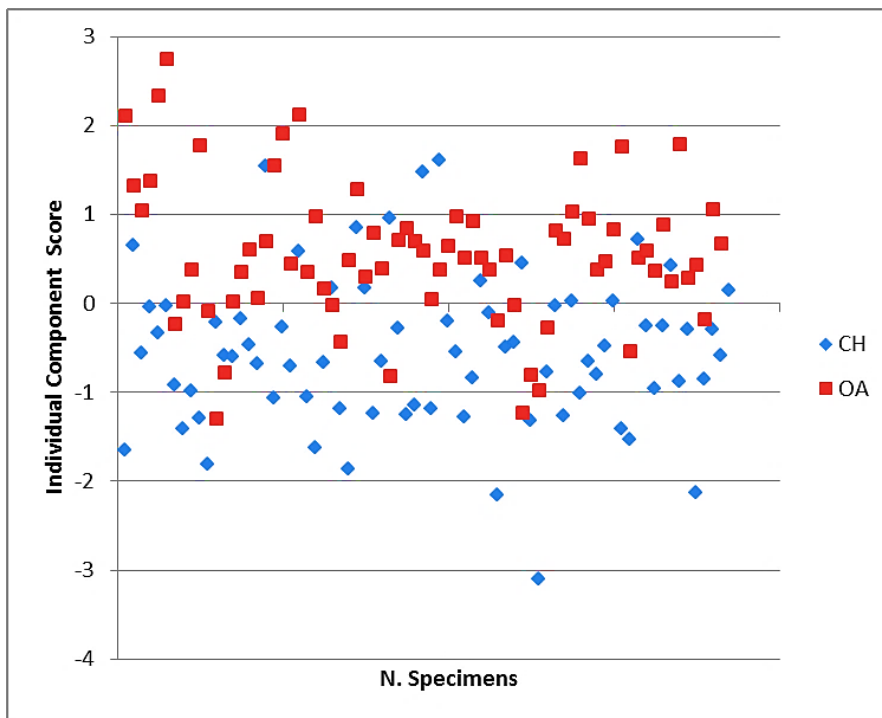


Figure 2.297 Scapula: scatterplot of the individual component scores for Component I.

The importance of the above mentioned variables for each component is confirmed by the results gained from the Varimax rotation applied (Tab. 2.126).

Table 2.127 Rotated Component matrix for the scapula.

Rotated Component Matrix ^a		
	Component	
	1	2
ASG	-.914	-.144
GLP	.876	.133
LG	.850	-.097
SLC	.006	.845
BG	-.085	-.713
Extraction Method: Principal Component Analysis.		
Rotation Method: Varimax with Kaiser Normalization.		
a. Rotation converged in 3 iterations.		

For component I, the important measures are ASG, GLP and LG, while for component II, SLC and BG are the most valid as shown by Figure 2.298.

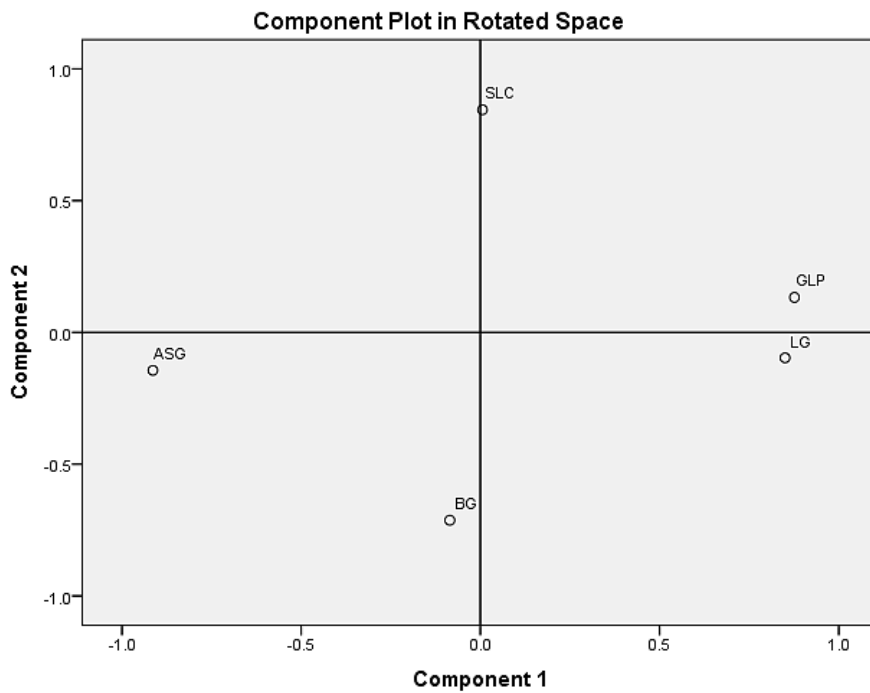


Figure 2.298 Scapula: rotated variable loading for Component I and II.

Humerus

For the humerus, the KMO value does not meet the requirement but Bartlett's Test is, once again, highly significant (Tab. 2.127).

Table 2.128 KMO and Bartlett's Test for the measurements taken on the humerus.

KMO and Bartlett's Test		
Kaiser-Meyer-Olkin Measure of Sampling Adequacy.	.098	
Bartlett's Test of Sphericity	Approx. Chi-Square	999.981
	df	21
	Sig.	.000

Table 2.129 Correlation matrix for the humerus.

Correlation Matrix^a								
		BT	HT	Bd	HTC	BE	BEI	Dd
Correlation	BT	1.000	.035	.529	-.179	.182	-.285	-.507
	HT	.035	1.000	.111	.311	-.353	.275	-.516
	Bd	.529	.111	1.000	-.224	.052	-.009	-.666
	HTC	-.179	.311	-.224	1.000	-.248	.174	-.255
	BE	.182	-.353	.052	-.248	1.000	-.335	-.085
	BEI	-.285	.275	-.009	.174	-.335	1.000	-.403
	Dd	-.507	-.516	-.666	-.255	-.085	-.403	1.000
Sig. (1-tailed)	BT		.336	.000	.015	.014	.000	.000
	HT	.336		.091	.000	.000	.000	.000
	Bd	.000	.091		.003	.266	.456	.000
	HTC	.015	.000	.003		.001	.018	.001
	BE	.014	.000	.266	.001		.000	.153
	BEI	.000	.000	.456	.018	.000		.000
	Dd	.000	.000	.000	.001	.153	.000	

a. Determinant = .001

The Correlation matrix Table (Tab. 2.128), shows some low correlation values. HT, HTC, BE and BEI gave low values but they were retained for two reasons. Firstly, because dropping them would have represented a loss of information. Secondly, because the exclusion of such variables would have affected the possibility to see possible hidden trends. As a consequence, all the measurements were retained.

The analysis found two components. The first explains 33.0% of the variance of the sample while the second component accounts for 28.9% of the total variance. Combined they describe a total of 62% of the variance (Tab. 2.129).

Table 2.130 Total Variance Explained for the humerus.

Total Variance Explained									
Component	Initial Eigenvalues			Extraction Sums of Squared Loadings			Rotation Sums of Squared Loadings		
	Total	% of Variance	Cumulative %	Total	% of Variance	Cumulative %	Total	% of Variance	Cumulative %
1	2.313	33.042	33.042	2.313	33.042	33.042	2.250	32.148	32.148
2	2.027	28.962	62.005	2.027	28.962	62.005	2.090	29.857	62.005
3	.903	12.901	74.906						
4	.812	11.595	86.500						
5	.551	7.870	94.371						
6	.393	5.613	99.983						
7	.001	.017	100.000						

Extraction Method: Principal Component Analysis.

Table 2.131 Component matrix for the humerus.

Component Matrix^a		
	Component	
	1	2
Dd	-.962	-.033
Bd	.722	.466
HT	.611	-.485
BE	-.125	.652
BT	.557	.632
BEI	.356	-.612
HTC	.203	-.612

Extraction Method: Principal Component Analysis.
a. 2 components extracted.

By looking at the Component matrix Table (Tab. 2.130), an initial consideration can be made regarding the sign and the magnitude of the values. Different signs and different magnitudes in both component can be seen, indicating that shape is the main factor rather than size.

It can also be observed that component one is mainly dominated by Dd (depth of the trochlea) on the one hand and Bd and HT (its breadth and height) on the other.

The second component is mainly defined by BE and BT and, with negative scores, by BEI and HTC. The individual component scores for both components are can be seen in Figure 2.299.

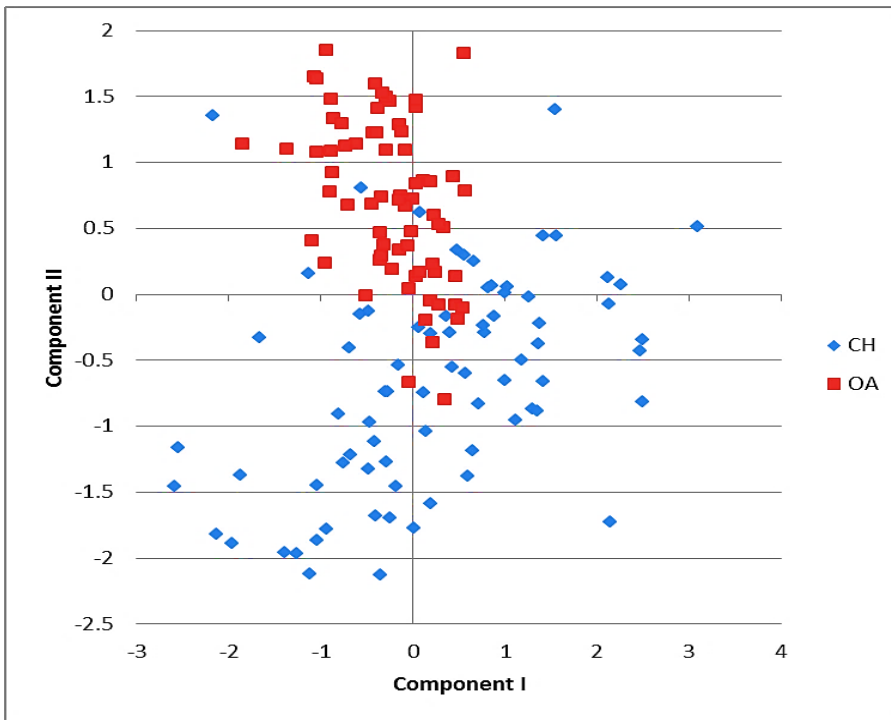


Figure 2.299 Humerus: individual component scores for component I and II.

This shows that, while the goat group lies mainly in the lower part of the graph, the sheep group occupies mainly the central-left upper part. A certain degree of overlap is present especially in the area included between -0.5 and 0.5 on the vertical axis and -1.0 and 1.0 on the horizontal axis.

From the way the clusters are gathered, it is clear that both components have potential in discriminating between the two groups but, the most powerful seems to be the second component as a line separating the sheep from the goats could be drawn between -0.5 and 0 on the vertical axis. As a consequence, measurements such as BEI, HTC, BE and BT contribute to a greater degree to the definition of the clusters than the others.

What must also be noted from Figure 2.299 is that, while the sheep group is more tightly clustered, the goat group is more widely scattered, indicating the greater variability of the latter. Interestingly, slightly different results are given by the rotated Component matrix (Tab. 2.131). The first component is mainly defined by Dd, Bd and BT while the second is mainly determined by HT, BEI, HTC and BE.

Table 2.132 Rotated Component matrix for the humerus.

Rotated Component Matrix ^a		
	Component	
	1	2
Dd	-.865	-.422
Bd	.856	-.074
BT	.788	-.298
HT	.313	.714
BEI	.028	.708
HTC	-.107	.636
BE	.195	-.635

Extraction Method: Principal Component Analysis.
Rotation Method: Varimax with Kaiser Normalization.

a. Rotation converged in 3 iterations.

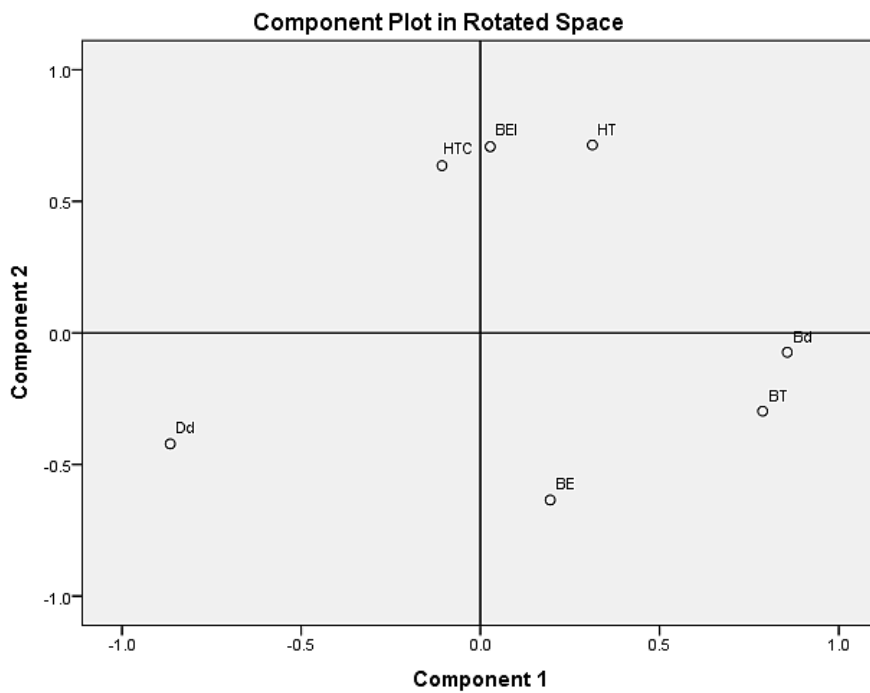


Figure 2.300 Humerus: rotated variable loadings for each component.

As the measurements BEI, HTC and BE seem to be the variables which load on component II before and after the rotation, they have to be considered important for the function (Fig. 2.300).

Radius

Table 2.132 shows, once again, that the KMO requirement is not met but the presence of a relationship between the variables is confirmed by Bartlett's Test.

Table 2.133 KMO and Bartlett's Test for the measurements taken on the radius.

KMO and Bartlett's Test		
Kaiser-Meyer-Olkin Measure of Sampling Adequacy.		.278
Bartlett's Test of Sphericity	Approx. Chi-Square	810.437
	df	10
	Sig.	.000

If a closer look is given to the Correlation matrix Table (Tab. 2.133), it can be seen that some high and low scores are present but, for the reasons previously explained for other elements, all the variables have been retained in the analysis.

Table 2.134 Correlation matrix for the radius.

Correlation Matrix^a						
		GL	SD	BFp	Bp	Dp
Correlation	GL	1.000	-.483	-.819	-.854	-.768
	SD	-.483	1.000	.080	.116	.094
	BFp	-.819	.080	1.000	.732	.675
	Bp	-.854	.116	.732	1.000	.623
	Dp	-.768	.094	.675	.623	1.000
Sig. (1-tailed)	GL		.000	.000	.000	.000
	SD	.000		.206	.117	.169
	BFp	.000	.206		.000	.000
	Bp	.000	.117	.000		.000
	Dp	.000	.169	.000	.000	

a. Determinant = .000

SPSS initially found just one component. Nevertheless, two other components which account for less variability than component I have been forced into the analysis, this in order to see if, with more comparisons, clearer results could be obtained (Tab. 2.134).

The first component accounts for 62.3% of the variance while the second accounts for 21.3% and the third accounts for 7.7%. If all of them are considered, a high score of 94.7% of explained variance is reached.

Table 2.135 Total Variance Explained for the radius.

Total Variance Explained

Component	Initial Eigenvalues			Extraction Sums of Squared Loadings			Rotation Sums of Squared Loadings		
	Total	% of Variance	Cumulative %	Total	% of Variance	Cumulative %	Total	% of Variance	Cumulative %
1	3.312	66.237	66.237	3.312	66.237	66.237	2.296	45.928	45.928
2	1.040	20.798	87.035	1.040	20.798	87.035	1.271	25.412	71.340
3	.387	7.744	94.779	.387	7.744	94.779	1.172	23.439	94.779
4	.260	5.198	99.977						
5	.001	.023	100.000						

Extraction Method: Principal Component Analysis.

Table 2.136 Component matrix for the radius.

Component Matrix^a			
	Component		
	1	2	3
GL	-.981	-.187	.033
Bp	.882	-.151	-.339
BFp	.881	-.216	-.114
Dp	.834	-.189	.507
SD	.314	.949	.028

Extraction Method: Principal Component Analysis.

a. 3 components extracted.

If the single loadings for each variable on each component are taken into account (Tab. 2.135), then some considerations can be made: the first component is affected mainly by Bp and BFp in one direction, and by GL in the other direction. The second component has a very high negative loading on SD. Component III has high loadings on Dp and Bp. Clearly the length and the breadth of the proximal end determine the component I, while component II is primarily linked to the depth of the shaft and component III to the shape of the proximal end.

Figure 2.301 plots components I and II together. It can be seen that the area of overlap is extensive, despite the left part of the graph shows a preponderance of goats and the right part of sheep. However, component I appears to be the most effective for separating the clusters, as there is much less overlap along the horizontal axis.

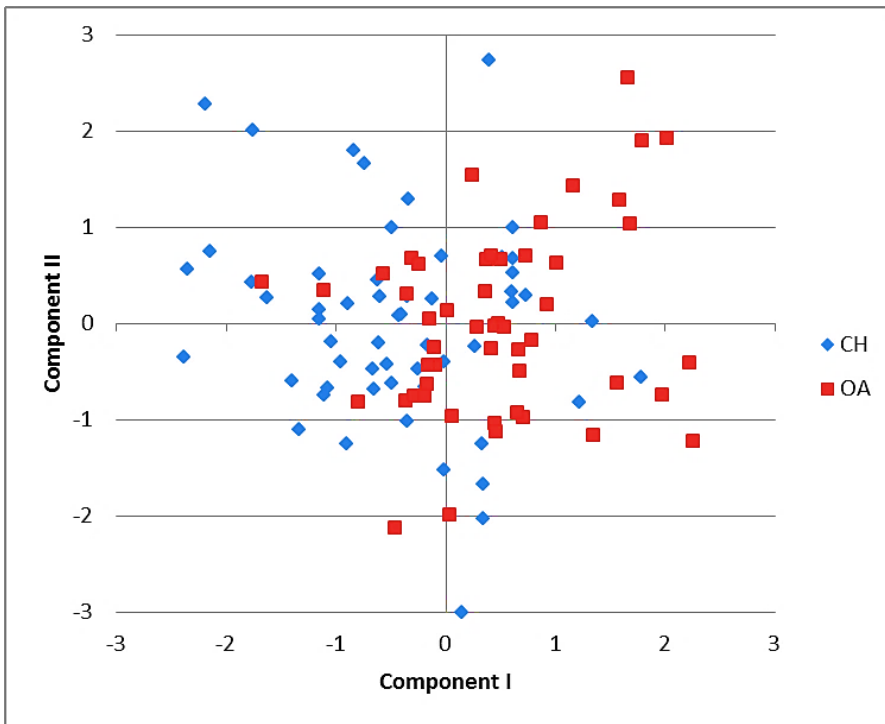


Figure 2.301 Radius: scatterplot of the individual component scores for component I and II.

If component II is plotted against III (Fig. 2.302), the results are not improved, showing more overlap than the previous graph. Now all specimens cluster in the same area of the graph, making the separation impossible.

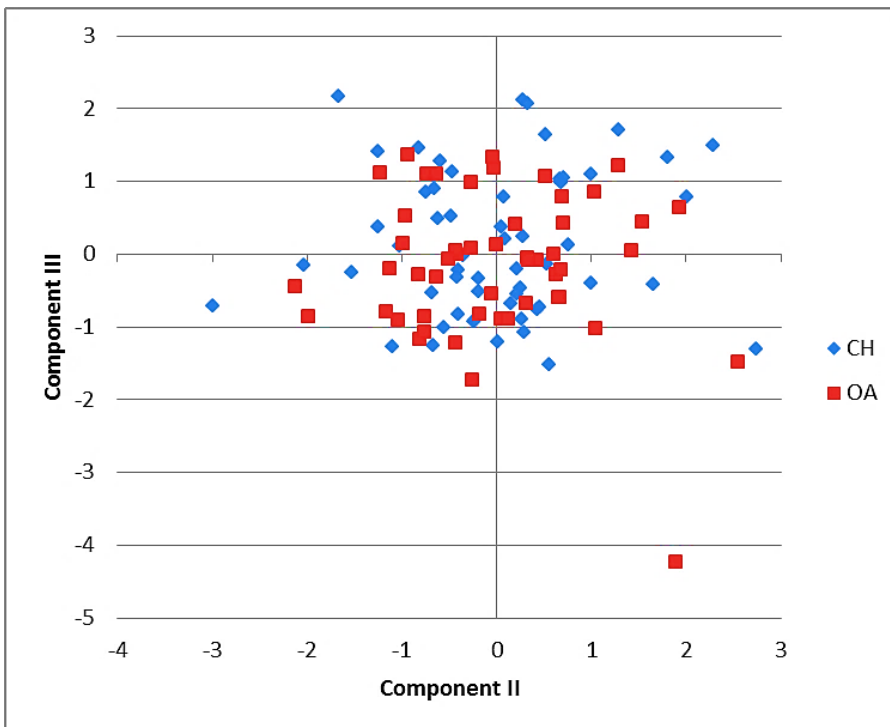


Figure 2.302 Radius: individual component scores of component II and III.

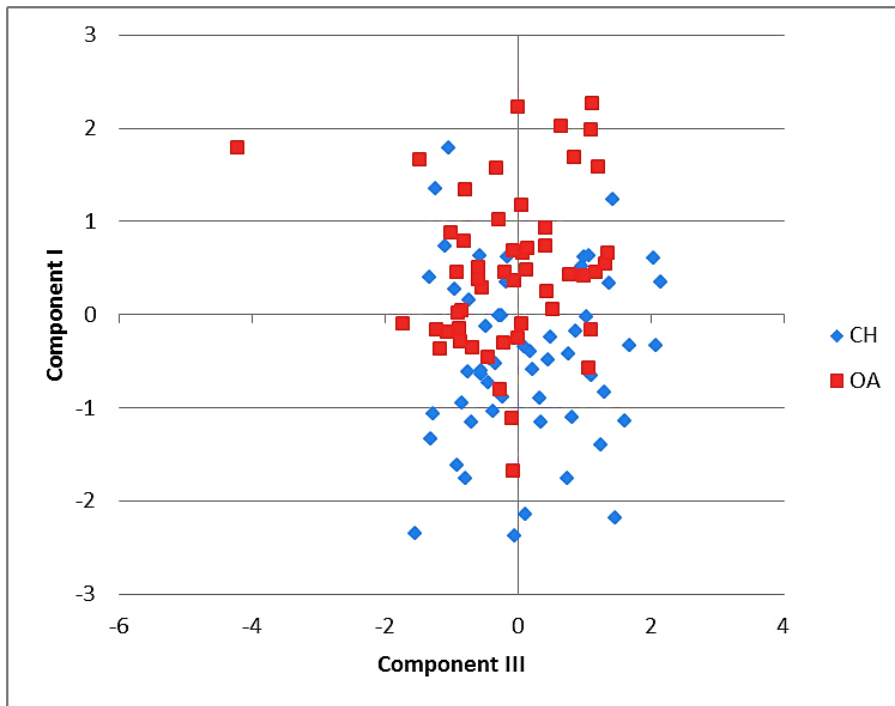


Figure 2.303 Radius: individual component scores for component III and I.

Finally, if component III is plotted against component I (Fig. 2.303), an improvement on Figure 2.302 can be observed, with goats mainly plotting at the bottom of the graph and sheep at the top. Once again, the amount of overlap is significant, but component I is clearly the one which has the most potential of separating the groups, while the other components are less effective.

If the rotated Component matrix is taken into account (Tab. 2.136), component I is still mainly determined by Bp, BFp and GL. Different results are given for component II which is influenced by Dp and GL and component III, which is linked to SD and GL. Despite some difference, component I has given the same results in both matrices, confirming its importance. A visual representation of the different loadings for each variable and for each component is given by Figure 2.304.

Table 2.137 Rotated Component matrix for the radius.

Rotated Component Matrix^a			
	Component		
	1	2	3
Bp	.928	.227	.054
BFp	.812	.422	-.001
GL	-.774	-.475	-.417
Dp	.415	.903	.039
SD	.069	.032	.997

Extraction Method: Principal Component Analysis.
 Rotation Method: Varimax with Kaiser Normalization.

a. Rotation converged in 4 iterations.

Component Plot in Rotated Space

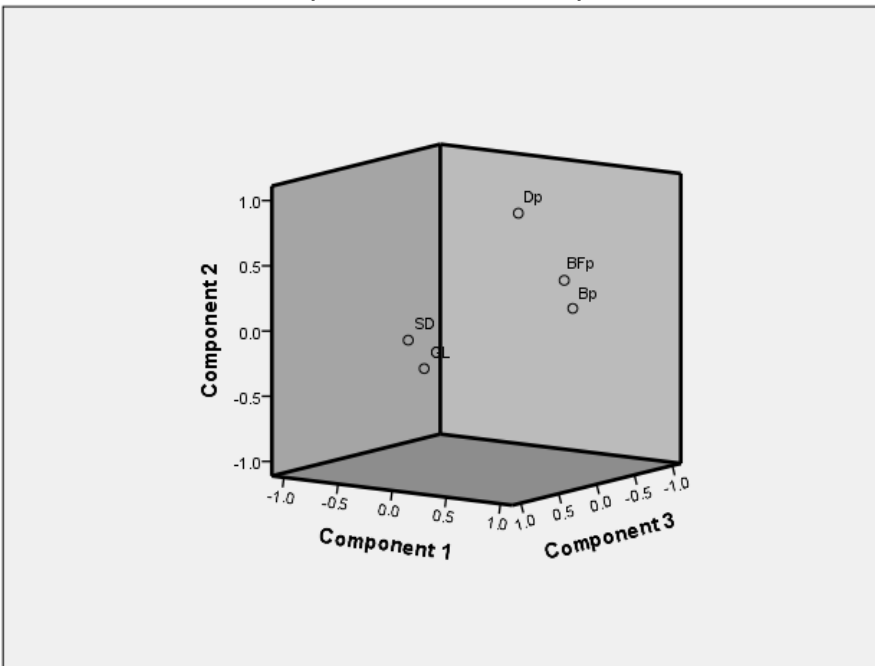


Figure 2.304 Radius: rotated variable loadings for each component.

Table 2.137 shows, once again, that the KMO value is too low. On the other hand, the Bartlett's Test of Sphericity confirms the presence of relationships between the variables.

Table 2.138 KMO and Bartlett's Test for measurements taken on the ulna.

KMO and Bartlett's Test		
Kaiser-Meyer-Olkin Measure of Sampling Adequacy.		.167
Bartlett's Test of Sphericity	Approx. Chi-Square	832.932
	df	10
	Sig.	.000

Table 2.138 shows, as in previous cases, high and low correlation values. Nevertheless all the variables were retained for the analysis.

Table 2.139 Correlation matrix for the ulna.

Correlation Matrix^a						
		B	L	SDO	DPA	BPC
Correlation	B	1.000	-.300	-.099	-.312	.038
	L	-.300	1.000	.341	.124	-.610
	SDO	-.099	.341	1.000	.444	-.751
	DPA	-.312	.124	.444	1.000	-.721
	BPC	.038	-.610	-.751	-.721	1.000
Sig. (1-tailed)	B		.001	.149	.000	.344
	L	.001		.000	.096	.000
	SDO	.149	.000		.000	.000
	DPA	.000	.096	.000		.000
	BPC	.344	.000	.000	.000	

a. Determinant = .000

Two components have been identified. The first one describes 52.5% of the total variance in the sample while the component II accounts for 20.9%. Both components together explain 73.5% of the total variance (Tab. 2.139).

Table 2.140 Total Variance Explained for the ulna.

Total Variance Explained			
Component	Initial Eigenvalues	Extraction Sums of Squared Loadings	Rotation Sums of Squared Loadings

	Total	% of	Cumulative	Total	% of	Cumulative	Total	% of	Cumulative
		Variance	%		Variance	%		Variance	%
1	2.627	52.536	52.536	2.627	52.536	52.536	2.453	49.066	49.066
2	1.049	20.984	73.521	1.049	20.984	73.521	1.223	24.455	73.521
3	.871	17.428	90.948						
4	.452	9.043	99.991						
5	.000	.009	100.000						

Extraction Method: Principal Component Analysis.

Table 2.141 Component matrix for the ulna.

Component Matrix^a		
	Component	
	1	2
BPC	-.950	-.263
SDO	.798	.287
DPA	.751	.002
L	.642	-.278
B	-.333	.906
Extraction Method: Principal Component Analysis.		
a. 2 components extracted.		

It can be seen that, by reference to the loadings for each variable on the Component matrix Table (Tab. 2.140), the first component has high loadings for BPC, SDO and DPA, namely measurements which describe the coronoid process. The second component is mainly influenced by B, SDO and L, measurements which are linked to the proximal articulation, the *olecranon*.

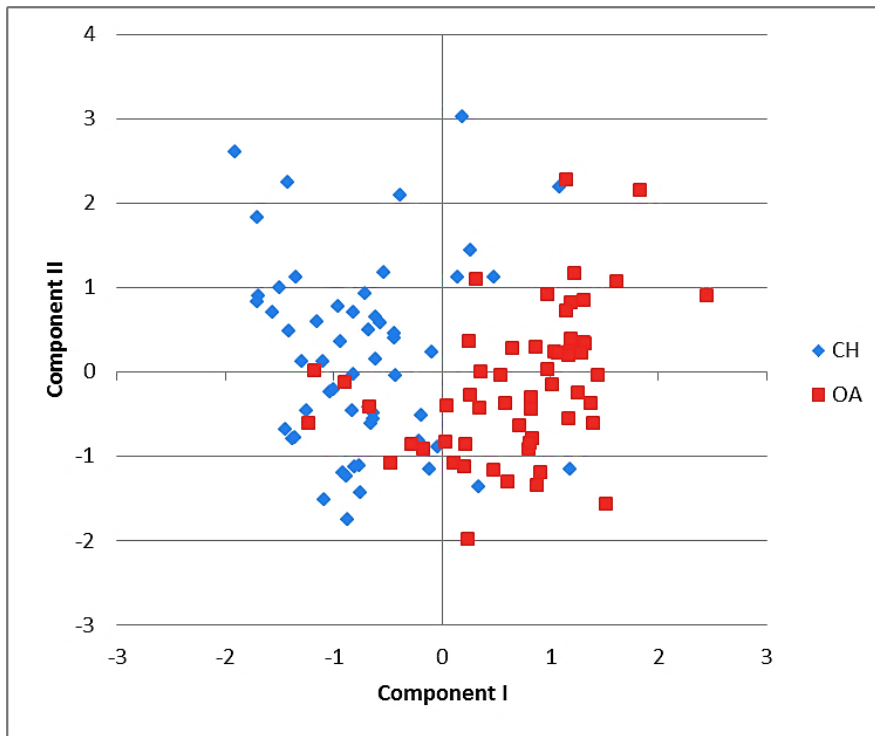


Figure 2.305 Ulna: scatterplot of the individual discriminant scores for Component I and II.

If the individual scores for the first and second components are plotted together, a relatively clear division between the two groups can be observed (Fig. 2.305). The goat group lies mainly on the left area of the graph, while sheep specimens are mainly clustered on the right. Some specimens of sheep lie in the goat area and vice versa but these are few. Clearly, in the case of this skeletal element, component I better discriminates between the two species than component II, as 0 on the horizontal axis could represent a good division line for separating the clusters. As a consequence, the shape of the *anconaeus* process is very important in determining the separation between the two groups.

Table 2.142 Rotated Component matrix for the ulna.

Rotated Component Matrix ^a		
	Component	
	1	2
BPC	-.983	.067
SDO	.848	.006
DPA	.710	-.247
L	.513	-.475
B	-.014	.965
Extraction Method: Principal Component Analysis.		
Rotation Method: Varimax with Kaiser Normalization.		
a. Rotation converged in 3 iterations.		

If the rotated Component matrix (Tab. 2.141) and the relative scatterplot (Fig. 2.306) are taken into consideration, it can be seen that they confirm what has already been noted: component I is determined by BPC, SDO and DPA while component II is defined by B and L.

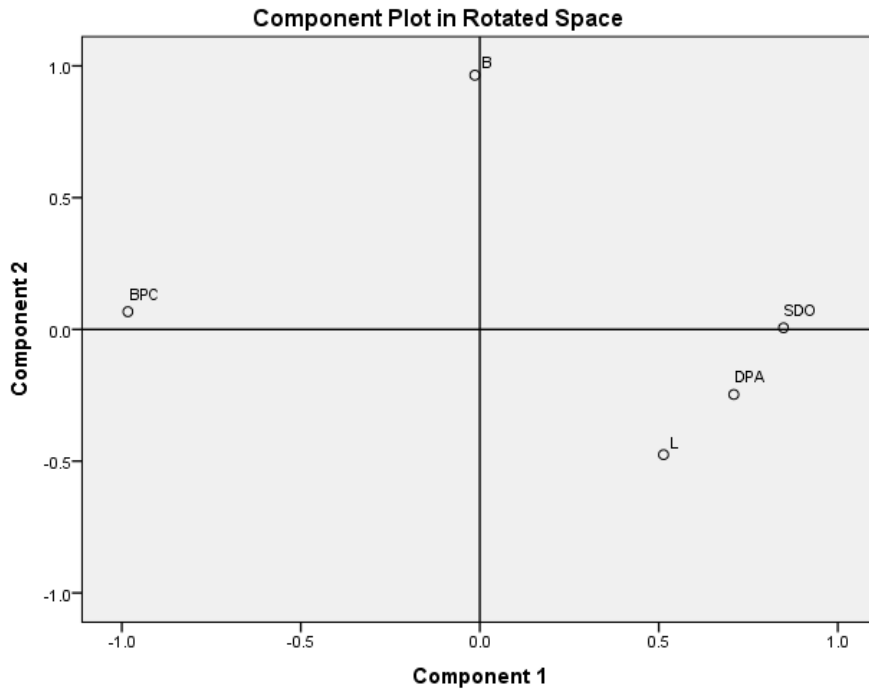


Figure 2.306 Ulna: rotated variable scores for each component.

Metacarpal

In the case of the metacarpal, the KMO value is acceptable so the sample size can be considered adequate. Bartlett's Test of Sphericity is once again significant (Tab. 2.142).

Table 2.143 KMO and Bartlett's Test for the measurements taken on the metacarpal.

KMO and Bartlett's Test		
Kaiser-Meyer-Olkin Measure of Sampling Adequacy.		.635
Bartlett's Test of Sphericity	Approx. Chi-Square	2378.256
	df	66
	Sig.	.000

If the Correlation matrix Table is observed (Tab. 2.143), it can be seen that high values as well as low values are present. Nevertheless, because of the reasons previously explained, the analysis was carried out including all the variables.

Table 2.144 Correlation matrix for the metacarpal.

Correlation Matrix ^a													
		GL	SD	BFd	BatF	a	b	1	2	4	5	3	6
Correlation	GL	1.000	-.834	-.916	-.844	-.891	-.877	.219	-.789	.125	-.817	-.677	-.689
	SD	-.834	1.000	.788	.784	.735	.763	-.370	.504	-.272	.564	.344	.348
	BFd	-.916	.788	1.000	.783	.948	.948	-.376	.619	-.363	.688	.461	.477
	BatF	-.844	.784	.783	1.000	.727	.786	-.270	.493	-.254	.525	.363	.405
	a	-.891	.735	.948	.727	1.000	.910	-.330	.637	-.333	.688	.479	.496
	b	-.877	.763	.948	.786	.910	1.000	-.375	.550	-.374	.630	.417	.434
	1	.219	-.370	-.376	-.270	-.330	-.375	1.000	-.182	.758	-.336	-.003	-.034
	2	-.789	.504	.619	.493	.637	.550	-.182	1.000	-.031	.945	.824	.814
	4	.125	-.272	-.363	-.254	-.333	-.374	.758	-.031	1.000	-.112	.233	.140
	5	-.817	.564	.688	.525	.688	.630	-.336	.945	-.112	1.000	.791	.801
	3	-.677	.344	.461	.363	.479	.417	-.003	.824	.233	.791	1.000	.916
6	-.689	.348	.477	.405	.496	.434	-.034	.814	.140	.801	.916	1.000	
Sig. (1-tailed)	GL		.000	.000	.000	.000	.000	.008	.000	.089	.000	.000	.000
	SD	.000		.000	.000	.000	.000	.000	.000	.001	.000	.000	.000
	BFd	.000	.000		.000	.000	.000	.000	.000	.000	.000	.000	.000
	BatF	.000	.000	.000		.000	.000	.002	.000	.003	.000	.000	.000
	a	.000	.000	.000	.000		.000	.000	.000	.000	.000	.000	.000
	b	.000	.000	.000	.000	.000		.000	.000	.000	.000	.000	.000
	1	.008	.000	.000	.002	.000	.000		.024	.000	.000	.487	.355
	2	.000	.000	.000	.000	.000	.000	.024		.368	.000	.000	.000
	4	.089	.001	.000	.003	.000	.000	.000	.368		.112	.005	.064
	5	.000	.000	.000	.000	.000	.000	.000	.000	.112		.000	.000
	3	.000	.000	.000	.000	.000	.000	.487	.000	.005	.000		.000
6	.000	.000	.000	.000	.000	.000	.355	.000	.064	.000	.000		

a. Determinant = 7.47E-010

Three components have been found through the Principal Component Analysis. The first component accounts for 61.3% of the total variance. The second component explains 19.0% and the third accounts for 9.1% of the variance within the sample. In total, all three components account for 89.4% of the variance (Tab. 2.144).

Table 2.145 Total Variance Explained for the metacarpal.

Total Variance Explained

Component	Initial Eigenvalues			Extraction Sums of Squared Loadings			Rotation Sums of Squared Loadings		
	Total	% of Variance	Cumulative %	Total	% of Variance	Cumulative %	Total	% of Variance	Cumulative %
1	7.361	61.341	61.341	7.361	61.341	61.341	4.936	41.135	41.135
2	2.284	19.034	80.375	2.284	19.034	80.375	3.876	32.303	73.438
3	1.093	9.111	89.486	1.093	9.111	89.486	1.926	16.047	89.486
4	.393	3.279	92.765						
5	.268	2.233	94.998						
6	.219	1.825	96.823						
7	.160	1.331	98.153						
8	.078	.647	98.800						
9	.076	.636	99.436						
10	.037	.311	99.747						
11	.029	.239	99.985						
12	.002	.015	100.000						

Extraction Method: Principal Component Analysis.

Table 2.146 Component matrix for the metacarpal.

Component Matrix^a			
	Component		
	1	2	3
GL	-.979	-.064	-.186
BFd	.923	-.234	.169
a	.905	-.181	.151
b	.888	-.275	.202
5	.873	.267	-.312
2	.828	.384	-.267
SD	.805	-.264	.261
BatF	.804	-.213	.339
6	.714	.573	-.240
3	.696	.626	-.210
4	-.260	.807	.410
1	-.373	.641	.587
Extraction Method: Principal Component Analysis.			
a. 3 components extracted.			

Table 2.145 shows that both positive and negative values with different magnitude are present in both the components, meaning that the shape factor is influencing the sample. It can be also seen that the first component is mainly determined by GL and BFd. The second component is defined by 4 and 1 on the one side, and b and SD on the other. Finally, the third component is

defined by 5 and 2 on the one side, and 4 and 1 on the other. In order to understand how the different variables contribute to the components, the rotated Component matrix should also be evaluated (Fig. 2.307 and Tab. 2.146).

Table 2.147 Rotated matrix for the metacarpal.

Rotated Component Matrix^a			
	Component		
	1	2	3
b	.883	.266	-.231
BFd	.879	.329	-.232
BatF	.874	.189	-.077
SD	.849	.195	-.167
a	.839	.360	-.204
GL	-.836	-.545	.023
3	.220	.921	.155
6	.234	.912	.093
2	.368	.874	-.080
5	.415	.847	-.202
1	-.170	-.096	.926
4	-.234	.163	.898
Extraction Method: Principal Component Analysis.			
Rotation Method: Varimax with Kaiser Normalization.			
a. Rotation converged in 5 iterations.			

By comparing the two matrix Tables (Tab. 2.145 and 2.146) it can be seen that the first component is mainly affected by BFd with a high positive value and GL with the highest negative one. It can be said then that this component is determined by the greatest length and the measurements taken at the distal breadth; as such, it is linked to the slenderness of the specimen.

For the second and third components, the two matrices agree to a lesser extent. In fact, component II appears to be mainly determined by 4 and 1 followed by 3 and 6. GL has a high negative value for the second component. The rotated value Table (Tab. 2.146 and Fig. 2.307) attests that 3 and 6 along with GL have an influence on component II. Despite some differences, it can be said that this component depends on the measurements of the *verticilli* along with the greatest length.

The third component is mainly affected by 5 and 2 and 4 and 1 according to the normal Component matrix, while, for the rotated version, 1 and 4 influence it more, along with b and BFd. Clearly this last component is determined by the diameter of the external trochlea.

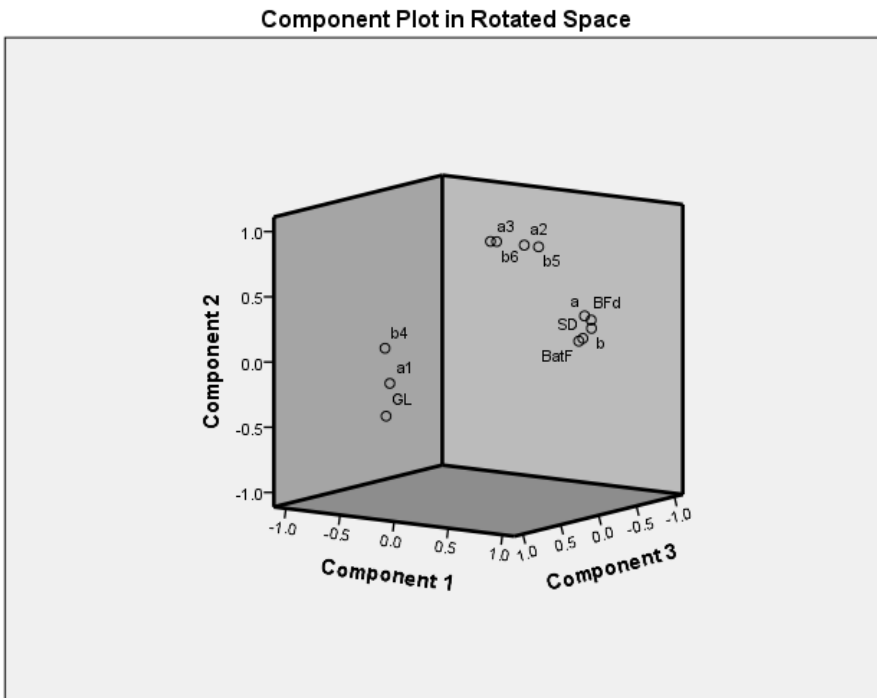


Figure 2.307 Metacarpal: rotated variable scores for each component.

Scatterplots 2.308 to 2.310 show the individual scores for each component. Figure 2.308 displays a good separation determined by the combination of the first and second component. The goat group is mainly scattered on the top-right area of the graph, while the sheep are at the bottom-left. Some overlap is present but it is not extensive. A separating line can be drawn diagonally from top left to bottom right, separating most specimens into taxa.

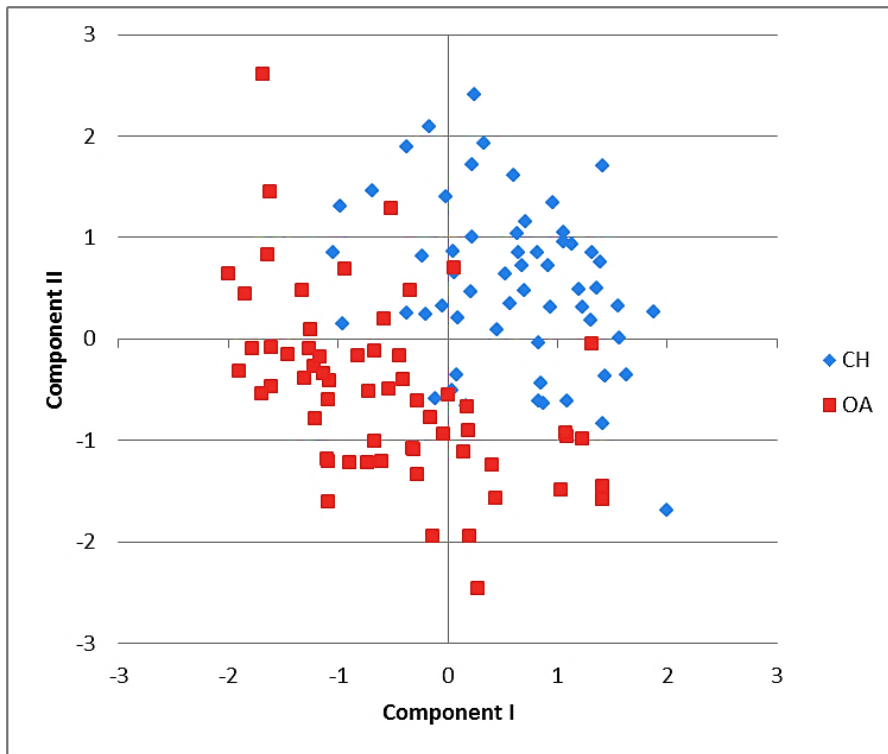


Figure 2.308 Metacarpal: scatterplot of the individual component scores for components I and II.

Figure 2.309 shows the individual loadings for component II and component III. As seen in the previous case, both components contribute to the separation of the clusters but component II seems to be slightly more efficient. Sheep specimens are mainly on the left side of the plot while goat specimens are mainly on the right. An area of overlap is present in the central part of the graph. In this case as well, a dividing line could be drawn from the upper right part to the right lower corner.

Finally Figure 2.310 shows the same scores but for component I and III. Sheep still occupy the left part of the graph while goats fall on the right. Both components contribute to the separation but component I works slightly better.

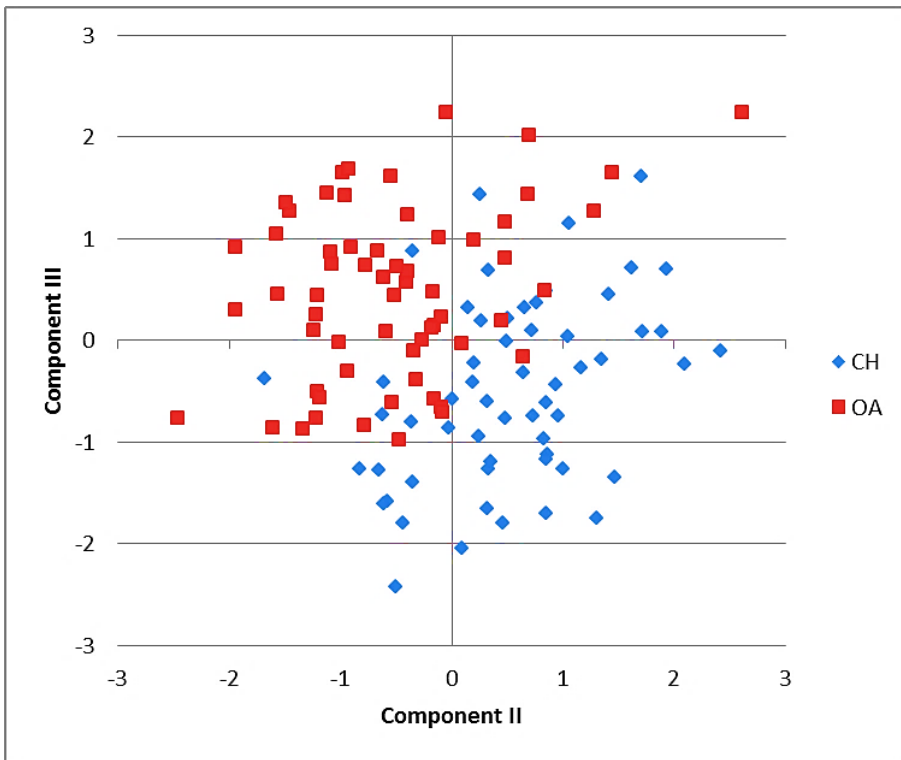


Figure 2.309 Metacarpal: scatterplot of the individual component scores for components II and III.

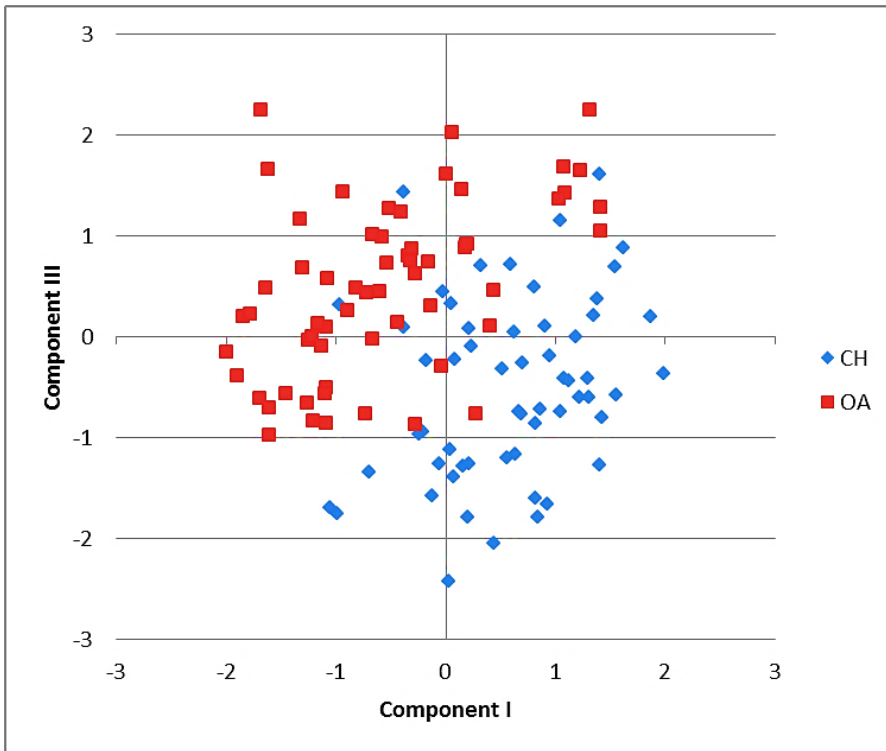


Figure 2.310 Metacarpal: scatterplot of the individual component scores for components I and III.

Metatarsal

The KMO value for the metatarsal is sufficient for factor analysis. The results of Bartlett's test of sphericity are once again significant as shown by Table 2.147.

Table 2.148 KMO and Bartlett's Test for measurements taken on the metatarsal.

KMO and Bartlett's Test		
Kaiser-Meyer-Olkin Measure of Sampling Adequacy.		.572
Bartlett's Test of Sphericity	Approx. Chi-Square	2286.474
	df	66
	Sig.	.000

Table 2.149 Correlation matrix for the metatarsal.

Correlation Matrix ^a													
		GL	SD	BFd	BatF	a	b	1	2	4	5	3	6
Correlation	GL	1.000	-.728	-.887	-.872	-.823	-.837	-.310	-.799	-.641	-.846	-.786	-.827
	SD	-.728	1.000	.677	.671	.593	.610	.097	.444	.271	.500	.356	.463
	BFd	-.887	.677	1.000	.849	.904	.902	.145	.547	.362	.602	.566	.578
	BatF	-.872	.671	.849	1.000	.782	.769	.166	.507	.445	.591	.550	.600
	a	-.823	.593	.904	.782	1.000	.859	.233	.518	.338	.518	.481	.493
	b	-.837	.610	.902	.769	.859	1.000	.072	.521	.377	.598	.527	.582
	1	-.310	.097	.145	.166	.233	.072	1.000	.349	.475	.194	.259	.254
	2	-.799	.444	.547	.507	.518	.521	.349	1.000	.659	.914	.833	.814
	4	-.641	.271	.362	.445	.338	.377	.475	.659	1.000	.709	.649	.661
	5	-.846	.500	.602	.591	.518	.598	.194	.914	.709	1.000	.843	.889
3	-.786	.356	.566	.550	.481	.527	.259	.833	.649	.843	1.000	.891	
6	-.827	.463	.578	.600	.493	.582	.254	.814	.661	.889	.891	1.000	
Sig. (1-tailed)	GL		.000	.000	.000	.000	.000	.000	.000	.000	.000	.000	.000
	SD	.000		.000	.000	.000	.000	.142	.000	.001	.000	.000	.000
	BFd	.000	.000		.000	.000	.000	.054	.000	.000	.000	.000	.000
	BatF	.000	.000	.000		.000	.000	.032	.000	.000	.000	.000	.000
	a	.000	.000	.000	.000		.000	.005	.000	.000	.000	.000	.000
	b	.000	.000	.000	.000	.000		.212	.000	.000	.000	.000	.000
	1	.000	.142	.054	.032	.005	.212		.000	.000	.015	.002	.002
	2	.000	.000	.000	.000	.000	.000	.000		.000	.000	.000	.000
	4	.000	.001	.000	.000	.000	.000	.000	.000		.000	.000	.000
	5	.000	.000	.000	.000	.000	.000	.015	.000	.000		.000	.000
3	.000	.000	.000	.000	.000	.000	.002	.000	.000	.000		.000	
6	.000	.000	.000	.000	.000	.000	.002	.000	.000	.000	.000		

a. Determinant = 3.95E-009

The Correlation matrix Table (Tab. 2.148) shows once again that high and low values are present. Despite this all the measurements have been retained for the analysis.

Table 2.149 shows that two components have been found for the metatarsal. The first component accounts for 64.0% of the total variance within the sample while the second component accounts for 14.4%. Both of them taken together explain 78.5% of the total variance.

Table 2.150 Total Variance Explained for the metatarsal.

Total Variance Explained									
Component	Initial Eigenvalues			Extraction Sums of Squared Loadings			Rotation Sums of Squared Loadings		
	Total	% of Variance	Cumulative %	Total	% of Variance	Cumulative %	Total	% of Variance	Cumulative %
1	7.684	64.037	64.037	7.684	64.037	64.037	5.161	43.005	43.005
2	1.738	14.481	78.518	1.738	14.481	78.518	4.262	35.513	78.518
3	.946	7.880	86.399						
4	.507	4.224	90.623						
5	.371	3.091	93.714						
6	.265	2.211	95.925						
7	.176	1.469	97.393						
8	.122	1.019	98.412						
9	.090	.747	99.159						
10	.064	.536	99.695						
11	.035	.293	99.988						
12	.001	.012	100.000						

Extraction Method: Principal Component Analysis.

Table 2.151 Component matrix for the metatarsal.

Component Matrix^a		
	Component	
	1	2
GL	-.995	.069
5	.879	.312
BFd	.863	-.429
6	.859	.324
BatF	.836	-.338
2	.836	.385
b	.828	-.412
3	.826	.374
a	.805	-.426
SD	.683	-.380
4	.676	.517
1	.314	.425
Extraction Method: Principal Component Analysis.		
a. 2 components extracted.		

If the loadings for each variable are considered, the Component matrix Table (Tab. 2.150) shows that the first component is mainly determined by GL on the one side, and BFd on the other. The second component is influenced by 4 and 1 on the one side and b and a on the other. If the rotated Component matrix is taken into consideration (Tab. 2.151 and Fig. 2.311), component I is determined mainly by GL and BFd confirming what was observed previously, while the second component is determined by 2 and 4 and 3 and 5.

Table 2.152 Rotated Component matrix for the metatarsal.

Rotated Component Matrix ^a		
	Component	
	1	2
BFd	.935	.237
b	.897	.227
a	.888	.201
BatF	.855	.288
GL	-.800	-.596
SD	.766	.157
2	.384	.837
4	.176	.832
3	.383	.822
5	.464	.809
6	.440	.806
1	-.038	.527
Extraction Method: Principal Component Analysis.		
Rotation Method: Varimax with Kaiser Normalization.		
a. Rotation converged in 3 iterations.		

In conclusion, it can be said that, while the first component seems to be affected mainly by BFd and GL, namely by the overall shape of the bone, component II is mainly affected by measurements taken on the *verticilli* and the condyles.

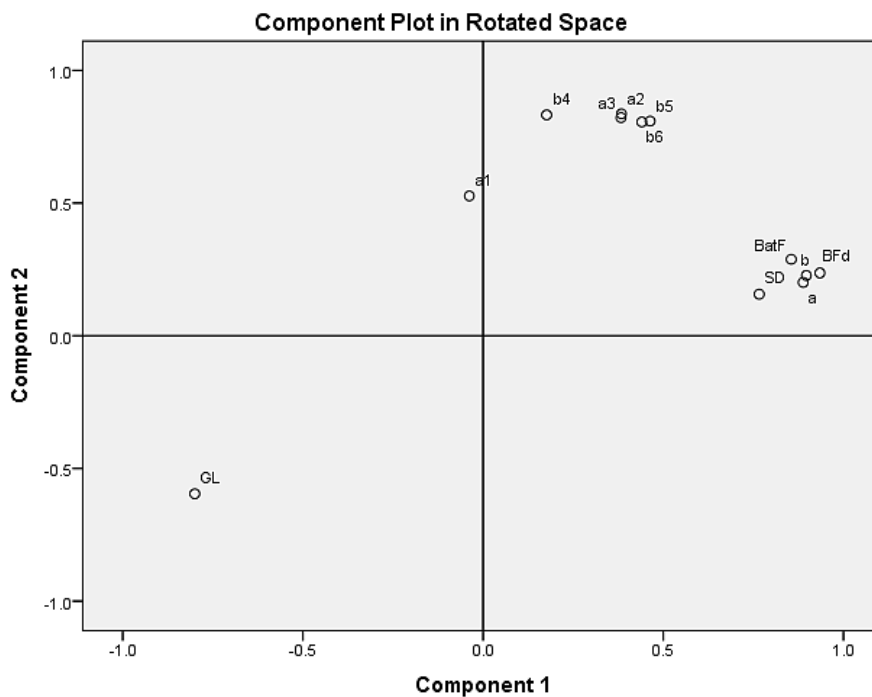


Figure 2.311 Metatarsal: rotated variable scores for each component.

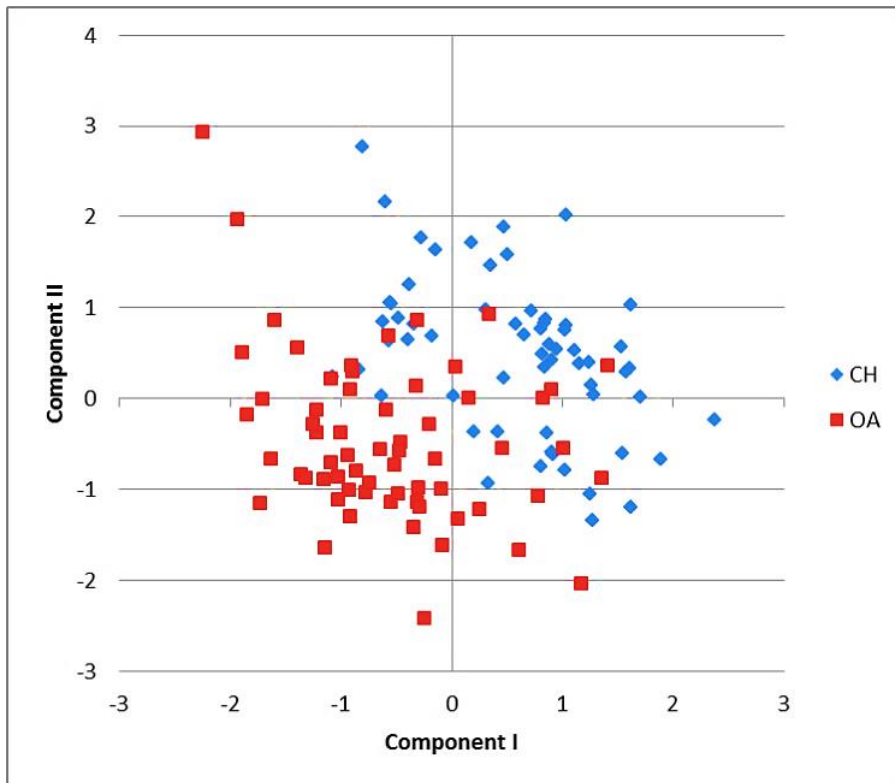


Figure 2.312 Metatarsal: scatterplot of the individual component scores for components I and II.

The scatterplot 2.312 shows individual loadings for component I plotted against component II. Two groups can be seen but the area of overlap is larger than for the metacarpal, showing that the metatarsal has less potential than the metacarpal for discriminating between the two species. Nevertheless, the upper-right part of the graph is mainly occupied by goats while the bottom-left mainly by sheep. Both components seem to affect the separation of the clusters, yet component I has much fewer cases of overlap than component II, making it more effective.

Tibia

In the case of the tibia, the KMO value requirements are met. Once more, Bartlett's Test attest to the existence of a relationship between the variables considered (Tab. 2.152).

Table 2.153 KMO and Bartlett's Test for the measurement taken on the tibia.

KMO and Bartlett's Test		
Kaiser-Meyer-Olkin Measure of Sampling Adequacy.		.593
Bartlett's Test of Sphericity	Approx. Chi-Square	601.542
	df	10
	Sig.	.000

By looking at the Correlation matrix Table (Tab. 2.153), it can be seen that high and low values are present. Nevertheless all the variables have been included in the analysis.

Table 2.154 Correlation matrix for the tibia.

Correlation Matrix^a						
		GL	SD	Dd(a)	Dd(b)	Bd
Correlation	GL	1.000	-.254	-.851	-.909	-.921
	SD	-.254	1.000	-.039	.164	.180
	Dd(a)	-.851	-.039	1.000	.740	.722
	Dd(b)	-.909	.164	.740	1.000	.838
	Bd	-.921	.180	.722	.838	1.000
Sig. (1-tailed)	GL		.004	.000	.000	.000
	SD	.004		.341	.044	.030
	Dd(a)	.000	.341		.000	.000
	Dd(b)	.000	.044	.000		.000
	Bd	.000	.030	.000	.000	

a. Determinant = .004

Table 2.154 shows the percentage of total variance explained by the components the program has identified. The first component accounts for 70.5% of the variance while the second explains 20.4%. The first and second components combined describe 91% of the total variance in the sample which is one of the highest percentages seen.

Table 2.155 Total Variance Explained for the tibia.

Total Variance Explained									
Component	Initial Eigenvalues			Extraction Sums of Squared Loadings			Rotation Sums of Squared Loadings		
	Total	% of Variance	Cumulative %	Total	% of Variance	Cumulative %	Total	% of Variance	Cumulative %
1	3.528	70.563	70.563	3.528	70.563	70.563	3.478	69.552	69.552
2	1.022	20.439	91.002	1.022	20.439	91.002	1.073	21.450	91.002
3	.265	5.304	96.306						
4	.162	3.238	99.545						
5	.023	.455	100.000						

Extraction Method: Principal Component Analysis.

Table 2.156 Component matrix for the tibia.

Component Matrix^a		
	Component	
	1	2
GL	-.990	-.045
Bd	.934	.008
Dd(b)	.934	-.016
Dd(a)	.870	-.280
SD	.213	.970
Extraction Method: Principal Component Analysis.		
a. 2 components extracted.		

Table 2.155 displays the scores for every variable for each component and it can be seen that the first component is dominated by GL and, to the same degrees, Bd and Dd(b). The second component is influenced by SD. These observations are confirmed by the rotated Component matrix (Tab. 2.156). Component I results are influenced by GL, Dd(b) and Bd, while component II is determined by mainly SD. A visual representation of the loading for each variable for each component is given by Figure 2.313.

Table 2.157 Rotated Component matrix for the tibia.

Rotated Component Matrix^a		
	Component	
	1	2
GL	-.974	-.186
Dd(b)	.927	.116
Bd	.924	.141
Dd(a)	.901	-.153
SD	.073	.991
Extraction Method: Principal Component Analysis.		
Rotation Method: Varimax with Kaiser Normalization.		
a. Rotation converged in 3 iterations.		

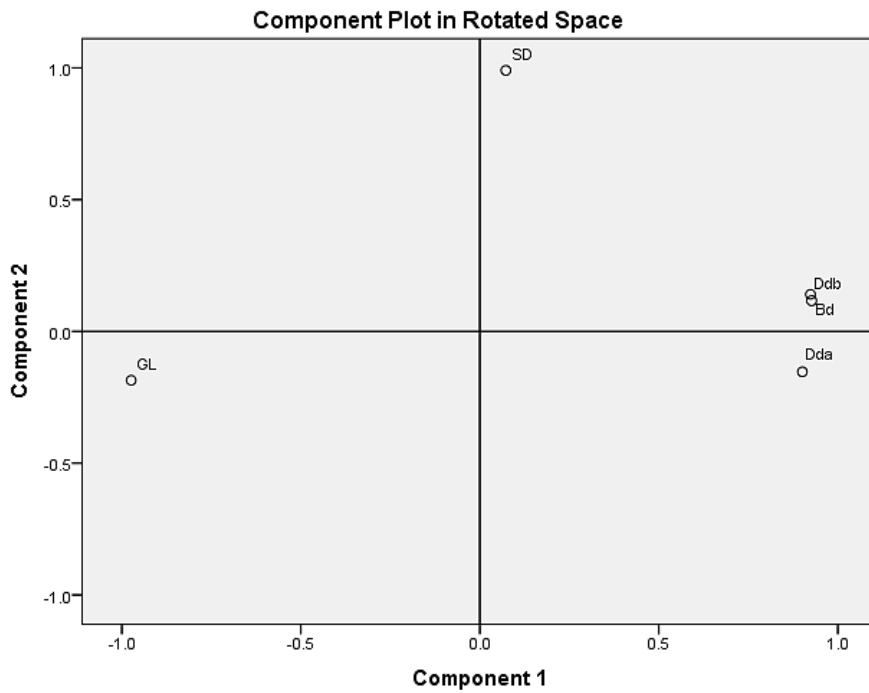


Figure 2.313 Tibia: rotated variable loadings for each component.

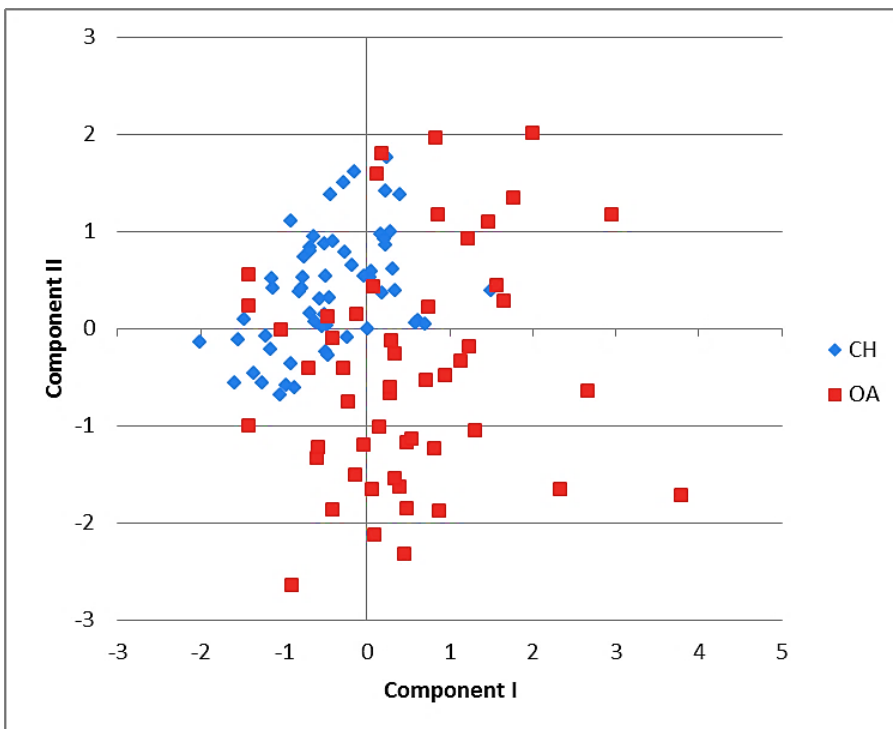


Figure 2.314 Tibia: scatterplot of the individual component scores for components I and II.

The individual component scores for each component are plotted in Figure 2.314. The sheep values are highly scattered, while the goat ones are much more compact. This means that goats have less variability than sheep.

Most goat specimens plot in the left-upper part of the graph, while most sheep are at the bottom-right part but, as this group is more widely spread, a number of sheep specimens lie among the goat group, clouding the separation. Better separation can be obtained along the horizontal axis (i.e. component I).

Astragalus

The KMO value does not have a high value when the data from the astragalus are considered. Despite this, the significance of Bartlett's Test attests to the existence of relationships between the variables (Tab. 2.157).

Table 2.158 KMO and Bartlett's Test for the measurements taken on the astragalus.

KMO and Bartlett's Test		
Kaiser-Meyer-Olkin Measure of Sampling Adequacy.		.363
Bartlett's Test of Sphericity	Approx. Chi-Square	1687.935
	df	21
	Sig.	.000

Table 2.159 Correlation matrix for the astragalus.

Correlation Matrix^a								
		H	Dl	Dm	Bd	GLl	GLm	BpT
Correlation	H	1.000	.503	-.822	.441	.886	-.807	-.680
	Dl	.503	1.000	-.672	.724	.659	-.804	-.699
	Dm	-.822	-.672	1.000	-.667	-.882	.790	.649
	Bd	.441	.724	-.667	1.000	.607	-.761	-.710
	GLl	.886	.659	-.882	.607	1.000	-.893	-.772
	GLm	-.807	-.804	.790	-.761	-.893	1.000	.726
	BpT	-.680	-.699	.649	-.710	-.772	.726	1.000
Sig. (1-tailed)	H		.000	.000	.000	.000	.000	.000
	Dl	.000		.000	.000	.000	.000	.000
	Dm	.000	.000		.000	.000	.000	.000
	Bd	.000	.000	.000		.000	.000	.000
	GLl	.000	.000	.000	.000		.000	.000
	GLm	.000	.000	.000	.000	.000		.000
	BpT	.000	.000	.000	.000	.000	.000	
a. Determinant = 6.235E-006								

If the Correlation matrix is examined (Tab. 2.158), only high or very high values can be recognised which eliminates the risk of low correlations between the variables. Initially, SPSS found only one component but, as the individual scores were plotted and the results were not clear, a second component was forced into the analysis. Table 2.159 shows the two principal

components for this anatomical element. The first explains 76.4% of the total variance while the second component accounts for 10.8%. Both components explain a total of 87.2% of the variance within the sample.

Table 2.160 Total Variance Explained for the astragalus.

Total Variance Explained									
Component	Initial Eigenvalues			Extraction Sums of Squared Loadings			Rotation Sums of Squared Loadings		
	Total	% of Variance	Cumulative %	Total	% of Variance	Cumulative %	Total	% of Variance	Cumulative %
1	5.349	76.408	76.408	5.349	76.408	76.408	3.236	46.233	46.233
2	.757	10.812	87.219	.757	10.812	87.219	2.869	40.987	87.219
3	.342	4.885	92.105						
4	.281	4.015	96.120						
5	.184	2.631	98.750						
6	.086	1.235	99.986						
7	.001	.014	100.000						

Extraction Method: Principal Component Analysis.

Table 2.160 displays the variables that contribute most to the components. In this case, the first component is determined by GLm, Dm on one side and GLl and H on the other. Component II has high loadings on H and Bd. Clearly component I is linked to length and the depth of the bone, while component II is linked to the breadth and the height at the central constriction.

Table 2.161 Component matrix for the astragalus.

Component Matrix^a		
	Component	
	1	2
GLm	-.948	-.014
GLl	.938	-.267
Dm	-.899	.190
BpT	-.854	-.128
H	.847	-.490
Dl	.824	.392
Bd	.797	.489
Extraction Method: Principal Component Analysis.		
a. 2 components extracted.		

If the rotated Component matrix is investigated (Tab. 2.161), component I results are linked to H and GLl on one side, and Dm and GLm on the other. Component II is determined by Bd and Dl on one hand, and BpT and GLm on the other (see also Fig. 2.315). As such, these results confirm partially the pattern previously observed where the first component, the most important one, is determined by length and depth of the astragalus, while the second component is related to the breadth and height of the bone.

Table 2.162 Rotated Component matrix for the astragalus.

Rotated Component Matrix^a		
	Component	
	1	2
H	.955	.214
GLl	.870	.440
Dm	-.790	-.471
GLm	-.687	-.653
Bd	.254	.900
Dl	.340	.847
BpT	-.541	-.673
Extraction Method: Principal Component Analysis.		
Rotation Method: Varimax with Kaiser Normalization.		
a. Rotation converged in 3 iterations.		

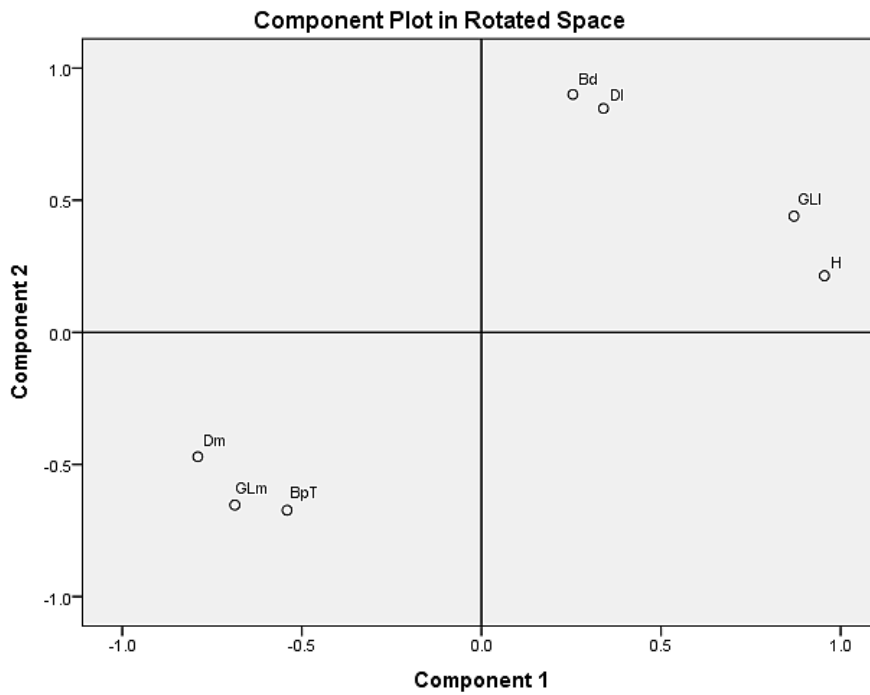


Figure 2.315 Astragalus: rotated variable loadings for each component.

Figure 2.316 shows that two groups can be identified: sheep on the left upper part of the graph while goats are mainly scattered in the lower right part of the plot area. As for other skeletal elements, there is an area of overlap but in the astragalus is not very extensive. If the effectiveness of the two components are considered and compared, it is clear by looking at the scatterplot that component I more effectively discriminates the clusters.

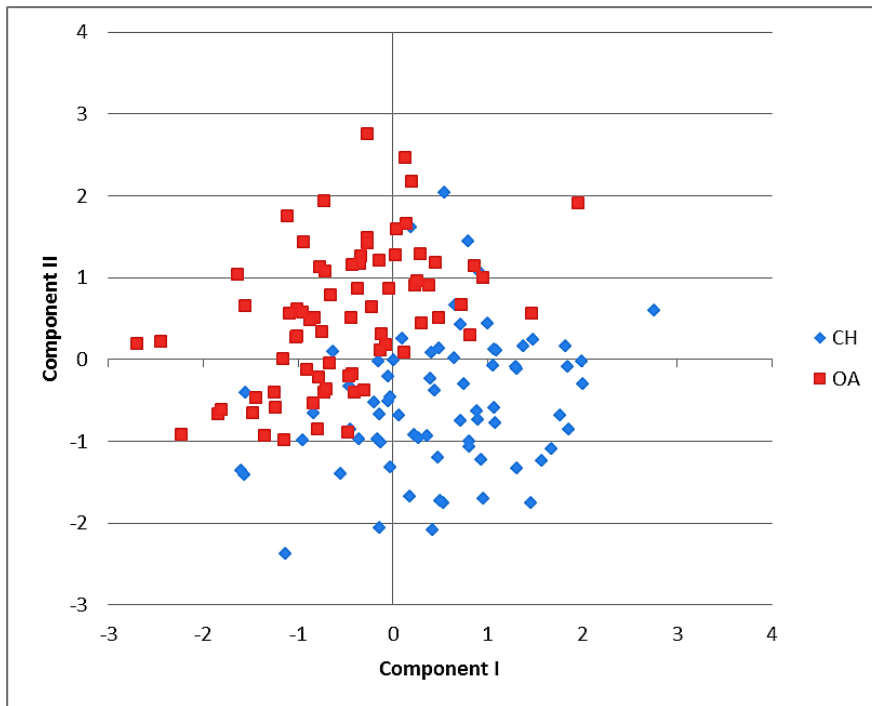


Figure 2.316 Astragalus: scatterplot of the individual component scores for components I and II.

Calcaneum

The KMO value is low for the calcaneum too, but the Bartlett's test of sphericity is highly significant (Tab. 2.162).

Table 2.163 KMO and Bartlett's Test for the measurements taken on the calcaneum.

KMO and Bartlett's Test		
Kaiser-Meyer-Olkin Measure of Sampling Adequacy.		.359
Bartlett's Test of Sphericity	Approx. Chi-Square	1309.141
	df	21
	Sig.	.000

The Correlation matrix (Tab. 2.163) shows that low correlations are completely absent, making the sample highly suitable for running the Principal Component Analysis.

The first component accounts for 75.9% of the total variance while the second component explains 7.2%, for a total of 83.2% of total variance within the sample explained (Tab. 2.164).

Table 2.164 Correlation matrix for the calcaneum.

Correlation Matrix ^a								
		c	d	B	DS	GB	GL	Gd
Correlation	c	1.000	.714	.562	.649	-.605	-.843	-.685
	d	.714	1.000	.732	.769	-.753	-.875	-.811
	B	.562	.732	1.000	.696	-.632	-.748	-.710
	DS	.649	.769	.696	1.000	-.720	-.850	-.739
	BS	-.605	-.753	-.632	-.720	1.000	.608	.697
	GL	-.843	-.875	-.748	-.850	.608	1.000	.679
	Gd	-.685	-.811	-.710	-.739	.697	.679	1.000

a. Determinant = 1.496E-005

Table 2.165 Total Variance Explained for the calcaneum.

Total Variance Explained									
Component	Initial Eigenvalues			Extraction Sums of Squared Loadings			Rotation Sums of Squared Loadings		
	Total	% of Variance	Cumulative %	Total	% of Variance	Cumulative %	Total	% of Variance	Cumulative %
1	5.320	75.997	75.997	5.320	75.997	75.997	3.207	45.808	45.808
2	.510	7.280	83.277	.510	7.280	83.277	2.623	37.469	83.277
3	.403	5.752	89.029						
4	.313	4.478	93.507						
5	.254	3.635	97.142						
6	.199	2.846	99.988						
7	.001	.012	100.000						

Extraction Method: Principal Component Analysis.

By looking at the loadings for each variable on each component (Tab. 2.165), some observations can be drawn.

Table 2.166 Component matrix for the calcaneum.

Component Matrix^a		
	Component	
	1	2
D	.930	-.017
GL	-.922	-.315
DS	.891	-.036
Gd	-.872	.168
B	.832	-.204
C	.829	.451
BS	-.819	.368
Extraction Method: Principal Component Analysis.		
a. 2 components extracted.		

First of all, component I is chiefly determined by GL and Gd on one side, and d and DS on the other. Component II is mainly determined by c and BS in one direction, and GL in the other. The rotated Component matrix below (Tab. 2.166) can help in better focusing the variables which contribute to the components.

Table 2.167 Rotated Component matrix for the calcaneum.

Rotated Component Matrix^a		
	Component	
	1	2
BS	-.857	-.268
Gd	-.765	-.452
B	.758	.399
d	.707	.604
DS	.691	.564
c	.321	.887
GL	-.481	-.847
Extraction Method: Principal Component Analysis.		
Rotation Method: Varimax with Kaiser Normalization.		
a. Rotation converged in 3 iterations.		

Table 2.166 shows that component I is linked to BS and Gd in addition to B, while component II is determined by c, d and GL. Clearly, component I depends on the length and depth measurements of the bone, while component II is determined by the shape of the articular facet of the *os malleolare* and the articulation-free part of the process (see also Fig. 2.317).

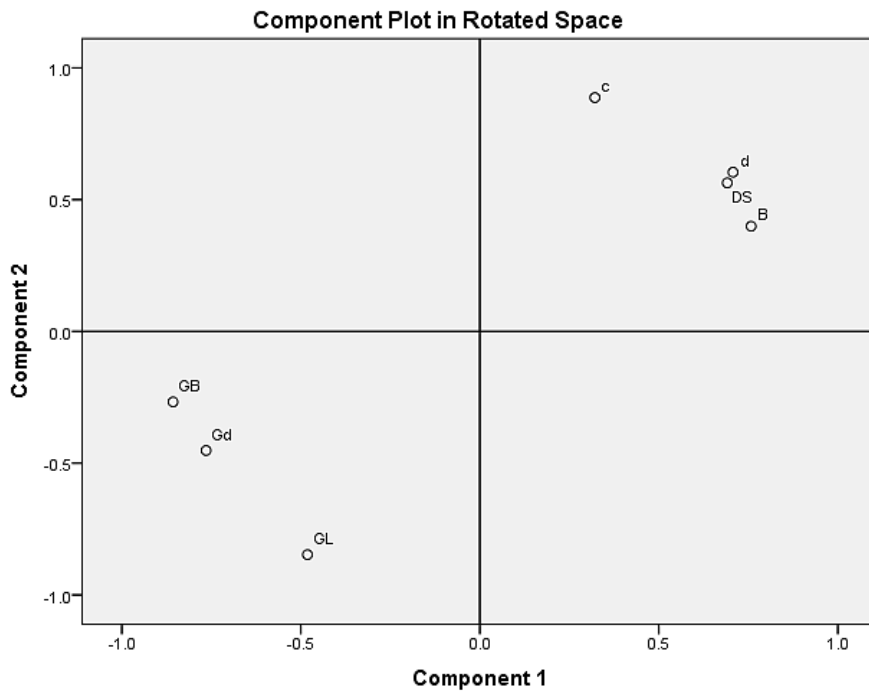


Figure 2.317 Calcaneum: rotated variable loadings for each component.

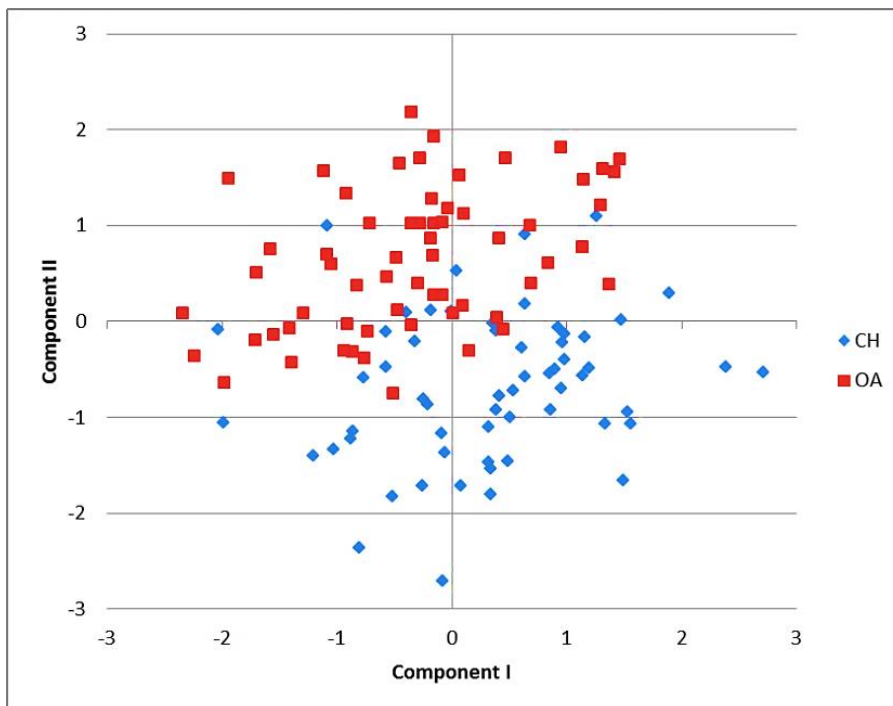


Figure 2.318 Calcaneum: scatterplot of the individual component scores for components I and II.

Figure 2.318 shows a blurred separation between the two groups. Overlap is present but, once again, the lower right part shows mainly goat specimens, while the upper left shows, even with some overlap, mainly sheep samples. The separation is better determined in this case by the

second component rather than the first making c, d and GL the most important variables for discrimination.

3rd Phalanx

Principal Component Analysis was also run on this anatomical element but the result was a not positive definite matrix. In this case it is probably due to the presence of too highly correlated variables in the matrix (Field 2009:656).

2.5.8 Conclusions

Some biometric methods for separating the bones of sheep and goat have been proposed in the past and have, in some cases, shown to be promising (Boessneck 1969; Boessneck *et al.* 1964; Fernández 2001), and in others to be definitively effective (Payne 1969).

In this project new measurements are suggested, as well as the use of new Biometrical Indices for the discrimination of sheep and goat. By testing this new approach on modern material of known taxonomic origin, valuable results have been obtained. The process of analysis of the results from a more “superficial” level (linear measurements) to a more in depth level (BI and multivariate statistical analyses), revealed that agreement is present between the different tools used: the measurements which translate the more consistent and well defined morphological differences, are those which have shown to be most successful in discriminating the two species using Biometrical Indices (BI), Discriminant Analysis (DA) and Principal Component Analysis (PCA).

The application of different Biometrical Indices, has shown that some measurements when plotted against each other, describe better the shape of the anatomical element targeted, as a consequence they have the potential to separate *Ovis* from *Capra*. The most successful BI are shown by Table 2.167.

All the BI have been verified through a statistical approach and have, by and large, been proven to be significant. Mann Whitney U test was carried out (along with Bonferroni adjustment) in order to see if the difference for each ratio between the two groups was statistically significant and the results confirmed that almost all the ratios applied (apart from BE/BT and BE/Bd on the distal humerus and Bd/Dl on the astragalus) are highly statistically significant, confirming that the nature of the difference is not to chance.

Further analyses such as Linear Discriminant Analysis and Principal Component Analysis were conducted for different purposes. DA was run in order to see if using all measurements at once could maximize the separation between the two groups while PCA was used in order to see the

extent to which the individual measurements contributed to explain the variation among the sample with the ultimate result of, if necessary, eliminating redundant measurements. DA was definitely very successful as it indeed boosts the separation between the groups. In terms of understanding how and the extent to which the different measurements relate to each other and contribute to the variation of the sample, PCA gave a more in depth insight.

When Linear Discriminant Analysis was carried out, remarkably no anatomical elements were found providing an identification score lower than 85.8%. The most useful elements for discriminating between the two closely related species the metacarpal (98.3%), the horncore (95.2%), the calcaneum (95.1%), the radius (93.5%), the ulna (92.9%), the metatarsal (92.7%), the tibia (89.1%) and the astragalus (89.0%). The measurements which resulted to be the most effective for the discrimination between sheep and goat were essentially those which proved effective when the ratio analysis were conducted.

If the results from the PCA are taken into account, the same pattern can be recognised: the measurements which resulted to be effective in the previous analyses are found to be those which mostly determine the variation among the sample when PCA was run.

Table 2.167 summarises the results obtained from BI, DA and PCA, showing the common outcomes.

Table 2.168 List of the most important measurements per anatomical element according to the different analyses adopted.

Anatomical elements	Ratios analysis	DA	PCA
Horncore	E/F vs A/F	D and E	1 component: it is influenced by the minimum and maximum diameter taken either at the base or at the middle (A and D particularly) and the length of the horncore (E)
Scapula	ASG/SLC vs GLP/BG; GLP/LG vs GLP/BG.	ASG, GLP and to a lesser degree LG	2 components: 1 st is determined by length measurements (ASG, GLP and, to a lesser extent LG); 2 nd is influenced by SLC and, to a lesser extent, by BG, describing the region of the <i>collum</i> and the glenoid cavity.
Humerus	BE/HTC vs BE/BT; BEI/BT vs BEI/Bd.	BE, BEI and to a lesser degree HTC	2 components: 1 st is determined by Dd on the one hand and Bd and HT on the other. 2 nd is mainly defined by BE and BT and by BEI and HTC.
Radius	BFp/Bp vs Dp.	Bp and GL	3 components: 1 st dominated by length and breadth of the proximal end (Bp and BFp in one direction, and by GL in the other). 2 nd is primarily linked to the depth of the shaft

Anatomical elements	Ratios analysis	DA	PCA
			(SD). 3 rd is connected to the shape of the proximal end (Dp and Bp)
Ulna	BPC/DPA vs BPC/SDO.	DPA, BPC and to a lesser degree SDO	2 components: 1 st is influenced by the shape of the coronoid process (BPC, SDO and DPA). 2 nd is mainly influenced the shape of the <i>olecranon</i> (B, SDO and L).
Tibia	Bd vs Dd(a)/Dd(b).	Dd(a), GL and to a lesser extent SD	2 components: 1 st is dominated by GL, Bd and Dd(b)). 2 nd is influenced by SD.
Metacarpal	1/a vs 1/2; 4/b vs 4/5; BFd/GL vs SD/GL.	a, b, 5, BFd and GL	3 components: 1 st is linked to the slenderness of the specimen (BFd and GL). 2 nd depends on the measurements taken of the <i>verticilli</i> along with the greatest length (4 and 1, 3, 6 and GL). 3 rd is determined by the diameter of the external trochlea (5, 2, 4 and 1)
Metatarsal	1/a vs 1/2; 4/b vs 4/5; BFd/GL vs SD/GL.	b, 3, 5, 6, BFd, GL	2 components: 1 st first is affected by the overall shape of the bone (BFd and GL). 2 nd is mainly affected by measurements taken on the <i>verticilli</i> and the condyles (4, 1 and b, a).
Astragalus	H/Dl vs Bd/GLl; Bd/Dl vs GLl/Dl; Bd/H vs Bd/GLl.	H, Dl, GLl and Bd	2 components: 1 st is determined by length and the depth of the bone (GLm, Dm on one side and GLl and H on the other). 2 nd is linked to the breadth and the height at the central constriction (H and Bd).
Calcaneum	c/B vs c/d; DS/c vs c/d; DS/c vs c/B.	c and GL	2 components: 1 st is linked to the length and depth measurements of the bone (GB, Gd and B). 2 nd is determined by the shape of the articular facet of the <i>os malleolare</i> and the articulation-free part of the process. (c,d and GL).
3 rd Phalanx	DLS vs MBS/DLS.	DLS and MBS	N.A.

The successful results obtained with the BI, successively confirmed by the Multivariate Statistical Analyses validate the fact that the new methodology represents a powerful tool; therefore it is highly suggested to adopt it routinely when dealing with sheep and goat identification. This new morphometrical approach has in fact the potential of:

1. filling the gaps left behind by previous biometrical studies conducted on this subject;
2. representing an additional means for supporting/questioning identifications made through the use of morphological criteria;

3. representing a tool that allows taxonomic identifications to be based on more objective and verifiable criteria.

It is, however, also important that the morphometric criteria suggested here are used in combination with the morphological approach, which has been adopted for many decades and that has still an important value.

2.6 Discussion of the study of the modern material: morphological and biometrical approach

The results obtained from the analysis of the modern material have confirmed what other researchers (Boessneck *et al.* 1964; Fernández 2001; Helmer and Rochetau 1994; Zeder and Lapham 2010; Zeder and Pilaar 2010) had previously observed, namely that morphological identifications need to be assessed by using a combination of traits rather than individual features.

Although some traits appear to be fairly reliable on their own - as they were consistently recorded in a specific form only on one of the two species - an assessment based on a combination of traits represents the most prudent and recommended procedure. Some traits can very clearly point towards sheep or goat but are not always expressed in a very distinct way, which means that caution needs to be applied. Some other traits, though useful, appear to be highly variable, and they can help identification only in combination with other, more defined characteristics.

Despite such caution many traits provided relatively high percentages of correct identifications, which emphasises that the morphological approach remains effective tool for the distinction of *Ovis* and *Capra* specimens. Nevertheless, this approach clearly has some limitations. To those mentioned above we should add the consideration that analysed modern sample, though large, cannot comprehensively cover all the possible variations that one may encounter in sheep and goat populations. We still do not know if the same traits that have performed well in this study, would perform as successfully on sheep and goat from different geographic areas or on different age groups.

Another issue that needs considering is the level of experience of the researcher as a well-trained eye will be able to recognise a diagnostic trait more easily. Furthermore, some researchers will be more prepared than others to 'push' identifications. As a consequence, the 'subjectivity' of the researcher has to be considered, alongside the variability of the

morphological traits, a factor that makes the morphological approach more subjective than is desirable.

In order to overcome the limits of the morphological approach, following the successful path paved by some pioneering biometric studies (Boessneck *et al.* 1964; Davis in press; Fernández 2001; Payne 1969; Rowley-Conwy 1998), a new method based on biometry has been developed and tested as part of this research project.

Whereas most previous studies were restricted only to a few elements and areas of the bones, this new method proposes a more extensive biometrical approach: a variety of measurements has been taken on several cranial and post cranial elements of the modern reference material with the aim of translating diagnostic morphological traits into Biometrical Indices.

In order to verify whether the measurements contributing to the new protocol could easily be taken by anyone and to test whether the instructions concerning how to take the measurements, especially for the newly introduced ones, were clear to whoever was using the protocol for the first time, a Coefficient of Variation (CV) analysis, an Inter-Observer Error and Intra-Observer Error (Inter Correlation Coefficient) analyses were conducted. The results of the CV revealed a fairly high level of consistency in the way most measurements were taken, as many CV values were lower than 5%. When the more appropriate ICC was run, the results revealed that most of the measurements in this study can be taken rather consistently. The measurements that were taken less consistent when the Inter-Observer Error was run, were mainly those described by previous literature as problematic (and a few additional ones), namely: B and L on P₃, L on P₄; H and B on the mandible; ASG in scapula; BEI in humerus; DI and Dm in the astragalus; c in the calcaneum. A similar pattern was noted when the Intra-Observer Error test was conducted, notably the results from this test were more successful than those obtained from the Inter-Observer Error, reinforcing the idea that the measurements in the recording protocol are highly repeatable.

The application of Biometrical Indices (BI) (i.e. metric ratios) has produced encouraging results. In many cases morphological traits could successfully be described through BI. The most diagnostic indices have proven to be:

- Horncore: E:F/E:A.
- Scapula: ASG:SLC/ GLP:BG; GLP:LG/GLP:BG.
- Humerus: BE:HTC/BE:BT; BEI:BT/BEI:Bd.
- Radius: BFp:Bp/Dp.
- Ulna: BPC:DPA/BPC:SDO.
- Tibia: Bd/Dd(a):Dd(b).
- Metacarpal: 1:a/1:2; 4:b/4:5; BFd:GL/SD:GL.

- Metatarsal: 1:a/1:2; 4:b/4:5; BFd:GL/SD:GL.
- Astragalus: H:DI/Bd:GLI; Bd:DI/GLI:DI; Bd:H/Bd:GLI.
- Calcaneum: c:B/c:d; DS:c/c:d; DS:c/c:B.
- 3rd Phalanx: DLS/MBS:DLS.

Despite measurements ASG on the Scapula and DI on the Astragalus gave the lowest reliability results when the Inter-Observer Error test was run, they were kept among the list of diagnostic measurements. This was because the Intra-Observer Error gave significant results, inconsistently with the Inter-Observer results. In addition, the ratio analysis showed that, when combined with other measurements, ASG and DI are useful for discriminating the two species (the combination ASG/SLC for the scapula and H/DI for the Astragalus were particularly useful).

The Mann Whitney U test and Manova have been applied to the Biometrical Indices respectively individually and simultaneously, to verify the statistical significance of the difference among the two modern samples. The results confirmed that almost all the ratios were significantly different between the two species.

Multivariate analysis, i.e. Linear Discriminant Analysis (DA) and Principal Component Analysis (PCA), has also been conducted. DA was run in order to see if the use of all measurements at once could maximize the separation between the two samples, while with PCA we wanted to understand the extent to which the individual measurements contributed to explain the variance within the sample.

The results from the DA have shown that separation between the groups is boosted, producing, in few cases, an almost complete separation between species (horncores and metacarpals). No anatomical elements among those evaluated provided an identification score lower than 85.8%. The most successful elements have proven to be: metacarpal (96.6%), horncore (95.2%), calcaneum (95.1%), radius (93.5%), ulna (92.9%), metatarsal (92.7%), tibia (89.1%) and astragalus (89.0%). These elements are by and large also those that had provided the best results when the ratio analysis was conducted.

In terms of understanding how different measurements relate to each other and which contribute most to the variation of the sample, the results from the PCA provided a more in-depth insight than DA. The results obtained were consistent with those from the previous analyses: the measurements which resulted to be effective with BI and DA are also those that mostly determine the variation among the sample when PCA was applied. According to the PCA analysis the most important measurements were:

- Horncore: A, D and E.
- Scapula: ASG, GLP and LG.
- Humerus: Dd, Bd and HT.
- Radius: Bp, BFp and GL.
- Ulna: BPC, SDO and DPA.
- Tibia: GL, Bd and Dd(b).
- Metacarpal: BFd and GL.
- Metatarsal: BFd and GL.
- Astragalus: GLm, Dm, GLl and H.
- Calcaneum: GB, Gd and B.

The results indicate that the new methodology represents a powerful tool, which reduces and overcomes some of the limits of the morphological approach. As previously mentioned, these limits are the biological variability of the species and the subjectivity of the method.

The biological variability of animals, which inevitably influences the reliability of the morphological traits, is something that cannot be completely controlled or avoided (especially with domestic species, the variability of which is even higher than among their wild counterparts). Variability is something that is intrinsic to species and populations, and is what allows adaptation and evolution. It is also valuable for archaeologists as, through an analysis of variability in time and space, we can understand patterns of change in the relationship between humans and animals. It is therefore important that any approach to the identification of closely related species, such as sheep and goat, does not try to remove variability as a factor – an impossible task – but rather acknowledges the existence of such variability and analyses it for the information that it can provide. It is for this reason that biometric thresholds are rarely useful and it is much more productive to look at patterns of distributions and relative similarities and differences between taxonomic groups.

The Oxford English dictionary (Oxford University Press 2015) defines the word objective as *“of a person or his or her judgement: not influenced by personal feelings or opinions in considering and representing facts; impartial, detached”*. Since the new methodology is based on measurements, which can be consistently taken by anyone - as shown by the positive results obtained from the reliability tests - and are prone to verification, it represents a tool that allows taxonomic identifications to be based on more objective criteria. As such it overcomes the subjectivity bias.

Finally, it is important to highlight that this research is not suggesting the use of the biometrical method as the only reliable approach. The morphometric criteria suggested here are thought to

be used in combination with the morphological approach, which has been adopted for a long time and has still an important role to play. The new approach intends to represent an additional means for supporting/questioning identifications proposed through the use of morphological criteria

Chapter 3 Reevaluation of the role of the goat in medieval England

Chapter 3 presents the results of the application of the new methodology to a number of English medieval sheep and goat archaeological assemblages. In Section 3.1 the medieval sites selected for this study are briefly presented along with the reasons why they were chosen. Section 3.2, 3.3 and 3.4 present respectively the results for each of the case studies: the historical and zooarchaeological background is provided for each case study, followed by a quantification of body parts, a ratio analysis and then a Discriminant Analysis. Chapter 3 also includes a discussion of the application of the new methodology on archaeological material (Section 3.5), a reassessment of the role that the goat had in medieval husbandry and economy in England (Section 3.6) and a section dedicated to future developments (Section 3.7).

3.1 The archaeological sites

Three case studies were selected as most suitable for testing the new methodology. These sites were respectively the medieval port of King's Lynn in Norfolk (1050-1800 AD), the medieval urban town of Lincoln in Lincolnshire (Flaxengate) (Late 11th century; late 14th-middle 16th century AD), and the medieval town of Northampton in Northamptonshire (Woolmonger and Kingswell street) (1000-1550 AD).

These sites were selected for several reasons. In the case of King's Lynn the zooarchaeological investigation carried out in 1977 by Noddle revealed an unusual number of goat bones; an anomaly - compared to the trend identified elsewhere - which called for verification.

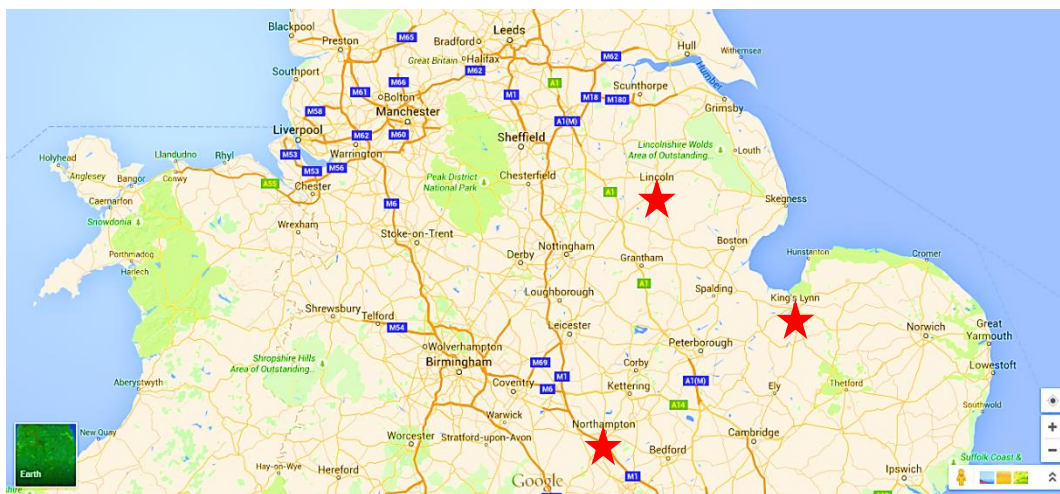


Figure 3.1 Map of central England. The red stars represent the position on the map of the archaeological sites analysed (map from <https://www.google.com/maps/@53.043617,-1.3465121,8z>).

The other two sites are also urban but they are located inland and in different regions; thus they represent different geographic scenarios (Figure 3.1), which are worth comparing with King's Lynn. They also provided substantial assemblages of reasonably refined chronologies, for which the status of the goat had not been fully clarified.

3.2 King's Lynn (1050-1800 AD)

3.2.1 Introduction

King's Lynn is situated in the county of Norfolk in the east of England. Located on a triangular bay in the south-eastern area of the great estuary called the Wash, King's Lynn's is located in an important area of convergence of roads, rivers and sea routes. A web of rivers, along with several important land routes to which the site was close, represented important factors influencing the development of the town as a centre of trade: a role that King's Lynn would embrace from the 13th century onwards, maintaining trade contacts with France, the Low Countries and Scandinavia along with lively inland commerce (Parker 1971).

Information on the town in the early stages of its life comes from the written resources. The first written documents in which the town is mentioned are the Domesday Book (AD 1086) and the Bishop's register of Norwich (AD 1101), a document in which King's Lynn is described as a salt-producing agricultural community, close to salt marshes and an estuarine lake. This record is an important document also because it attests not only to the late 11th century foundation of a priory and a market, but also, probably, to an already existing small settlement in the area, suggesting the presence of human occupation prior to the 11th century.

In the early 12th century, a series of improvements and expansions point to the development of the town. According to calculations based on ranges of tenement sizes for the period *c.* 1150, King's Lynn must have had from 200 to 300 tenements. A further and later expansion, evidenced also by written resources (William of Newburgh in 1180 defines King's Lynn as "*urbs commeatu et commerciis nobilis*"; King John's charter in which the status and privileges of the borough were confirmed, 1204), suggest both an increase in size of the settlement and an expansion of the population during the first half of the 12th century.

The importance of King's Lynn as a trade centre continued through the 13th century and was reinforced in the mid-13th century when the diversion of the River Great Ouse extended King's Lynn's inland communications by water. Tax documents, such as the 1377 Poll Tax, refer to King's Lynn as the seventh wealthiest town in England, attesting to the success of the town. The 15th century marks a change in the character of King's Lynn along with a decrease in trade, although trade with northern Europe and the Baltic was maintained (Clarke and Carter 1977).

3.2.2 Archaeological Investigations

In April 1962, following the post-war rebuilding movement and the development which occurred in King's Lynn, archaeological excavations along with a survey of architectural heritage and research into documentary evidence were carried out in order to gather as much information as possible about the medieval borough. A particular focus was placed on finding

evidence and information about the early medieval settlement, as very little was known at the time of the excavation about the early history of the town (Clarke and Carter 1977).

The archaeological excavations at King's Lynn took place from 1963 to 1970 under the direction of Helen Clarke (1963 to 1967), E.J. Talbot (1967 to 1968) and Alan Carter (1968 to 1971). The investigations were mainly restricted to the waterfront area as it was identified as the part of the town which would have contained the most productive sites. Different sites were excavated in order to cover the area between Millfleet and Purfleet and the New Land north of the Purfleet (Fig. 3.2). These major sites were:

- Courtyard of Thoresby College: the site, located close to the east bank of the River Great Ouse, released some interesting findings, such as a piece of woollen cloth called "wadmal" probably of Norwegian origin and three complete leather soles.
- Baker Lane: located between Baker Lane and Purfleet. Remarkable is the quantity of old shoes and scrap leather found in this area along with needles and a knife for leather working; evidence interpreted as linked to the presence of a yard behind a cobbler's workshop.
- Sedgeford Lane: located between Sedgeford Lane and New Conduit Street. Leather was found in great abundance, most of the specimens consisted of off-cuts and patches from cobbling; a number of complete soles and parts of uppers, scarps of fine leather with frilled edges caused by over-sewing, seem to come from a sort of clothing. Different types of scabbards were found as well. The worked bone objects discovered along with an accumulation of metapodials are of a different nature: slices of bones perforated for the making of buttons, others prepared for the perforation process, rings formed by transverse slices of long bones and unfinished objects, such as an ivory handle and a gaming piece. Such a concentration, which indicates that some sort of bone-working was probably carried out, was found only at this site. Horn-working is also evidenced here more than anywhere else at King's Lynn, by the presence of several goat horncores.
- Marks and Spencer site: located between Surrey Street and Norfolk Street. Interesting is the finding in this area of the town of a bench (wattle phase III) interpreted, as it was surrounded by shoe leather soles and off-cuts, as a cobbler's work-bench. Unfortunately, no comparable medieval benches have been found so a more domestic use cannot be ruled out. A small accumulation of horn cores, mainly belonging to goat, was also found.
- Junction of All Saints Street and Bridge Street: a small accumulation of horncores, mainly of goat, was found in this area.

Some minor sites were also investigated (50 King Street, rear of 10 Norfolk Street, Broad Street, 4-1 High Street- where an accumulation of goat and cattle horncore was found- 19 Purfleet Street, 21-7 South Clough Lane, Sedgeford Lane south side and 21 High Street, Barker Lane, Windsor Terrace, Hillington Square and Crooked Lane).

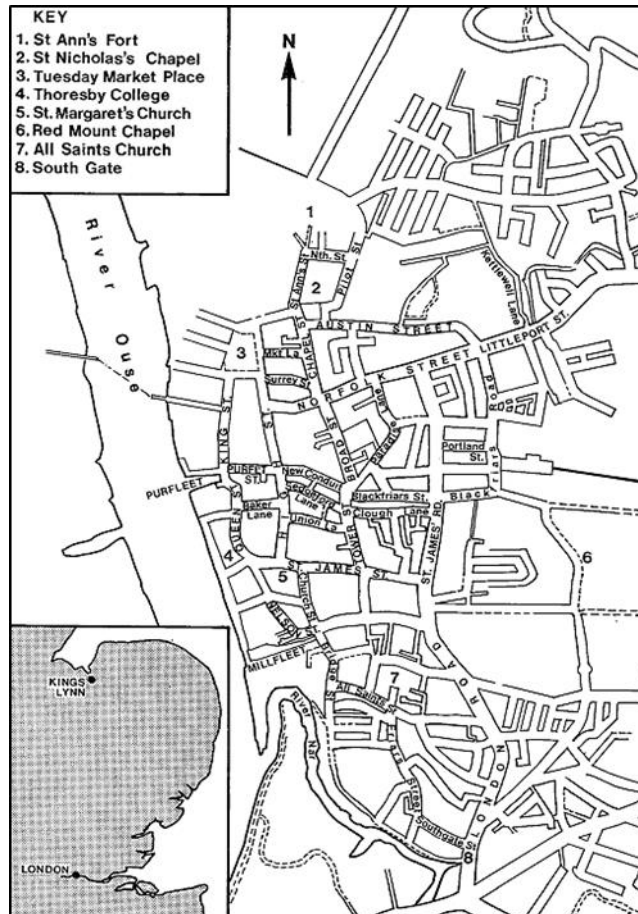


Figure 3.2 Map of the location of King's Lynn and the investigated areas (image reprinted from CLARKE, H. and A. CARTER, eds. *Excavation in King's Lynn 1963-1970*. Medieval Archaeology Monograph Series 7, copyright 1977. London: Society for Medieval Archaeology with permission from Helen Clarke).

The chronology, which includes four periods (Table 3.1), was elaborated according to the analysis of the material culture (pottery) and in order to allow correlations it is common to all the sites.

Table 3.1 Division into chronological periods for the sites excavated at King's Lynn (Clarke and Carter 1977).

PERIOD	Date
I	c. 1050-1250
II	c. 1250-1350
III	c. 1350-1500
IV	c. 1500-1800

3.2.3 Activities at King's Lynn

The archaeological evidence for industry at King's Lynn is poor compared to the documentary evidence, which suggests the presence in the town of crafts and industries. The exceptional waterlogged conditions allowed perishable material such as leather to be preserved and found. These related to two different forms of leather working. The first is shoe-mending, which is evidenced by irregular coarse off-cuts, found at every site in the town and interpreted as refuse from cobbling - probably a domestic activity which has to be separated from the specialist craft of shoe-making. The latter is indicated by the presence of a knife, found at the Baker Lane site, which may have been used in the shoe-making process. Leather was also probably used for the production of other objects but no archaeological evidence can support this hypothesis (Clarke and Carter 1977).

Goat skins and cow hides seem to have been the main raw materials used, as suggested not only by the residue of skins recovered, but also by the large deposits of goat and cattle horncores found at the sites of High Street, Sedgeford Lane, Marks and Spencer and All Saints Street. These deposits, interpreted as by-products of the tanning activity, fit with the documentary evidence that horns and foot bones were still attached when the hides were removed (Serjeantson 1989: 136). At King's Lynn, apart from a deposit of sheep/goat metapodials found at Sedgeford Lane, all the other deposits were composed exclusively of horncores. A tool which might have been associated with tanning, a "sleaker", probably used to remove dirt from the hide, was also found but the tannery site itself has still, unfortunately, not been located. Bone and horn-working were also activities carried out at King's Lynn, as shown by evidence related to button-making. In addition, the presence of horncores showing cut marks and chop marks in the region of the bone where the outer sheath is attached, confirms that some form of horn-working took place.

Because of its location (3 miles upstream from the Wash on a channel with sufficient water to allow cargo ships to anchor), King's Lynn was ideal for sea communications and its importance as a trade centre is attested to by a series of documents which demonstrate the establishment and development of inland trade as well as thriving trade between King's Lynn and mainland Europe by the early 13th century which increased until the beginning of the 14th century (Clarke and Carter 1977) (Fig. 3.3).

It seems that the town did not have good inland communications until the 13th century diversion of the river; nevertheless, documentary evidence suggests that significant trade was already passing through King's Lynn by the beginning of the 13th century. The importance of King's Lynn for the inland trade is confirmed by the fact that the town was chosen as a staple port in

the later 14th century by virtue of the various rivers running through different counties and bringing wool and other goods, easily and cheaply, to the town.

King's Lynn's influence on sea trade was not affected by the underdeveloped nature of its inland trade networks. In fact, many documents mention extensive commerce between England and other Countries as early as the beginning of the 13th century. Some archaeological evidence as well demonstrates the existence of such fertile commercial exchanges (i.e. foreign pottery and woollen clothes woven in Iceland). Contact with the Low Countries continued throughout the Middle Ages, although, unfortunately, archaeological evidence does not throw much light on the contacts the town maintained with the Baltic and Scandinavia.

The early 14th century is definitely the period in when King's Lynn reached the height of its trading importance. By the end of the century, as happened to other ports in England, trade began to decline due to the general reduction of the wool trade and also because of the effect of the Hundred Years War on the wine trade. Nevertheless, several historical resources show that trade between King's Lynn's and the Hanseatic ports as well as the Baltic continued, although on a different scale, from the 14th century onwards.



Figure 3.3 Map of the international trade (in pottery and other goods) between King's Lynn and several inland and foreign cities on the left. On the right is a map showing the source attribution of the medieval pottery found at King's Lynn (images reprinted from CLARKE, H. and A. CARTER, eds. *Excavation in King's Lynn 1963-1970*, Medieval Archaeology Monograph Series 7, copyright 1977. London: Society for Medieval Archaeology, with permission from Helen Clarke).

3.2.4 What does the zooarchaeological evidence say?

The animal bones excavated at King's Lynn were originally studied by Barbara Noddle and represent an unusual assemblage. Noddle suggested that goat was common at the site (Fig. 3.4)

and added that “the considerable population of goats in King’s Lynn is by no means unique” (Noddle 1977: 397). This is a surprising claim as evidence from many other sites indicates that the goat is far from abundant in medieval sites and decreases even further in numbers in the Post-medieval period (Albarella 1999).

It is also true that goat horncores are far more commonly found (Albarella 1999), but unfortunately, Noddle’s report provides no details of which goat body parts she identified. There are, however, hints in the report, such as the provision of goat ageing details, that she was not only referring to horncores, and that other elements had also been identified.

The analysis of the age at death allowed Noddle to establish that 80% of goats survived to maturity but no information was given up on which type of element the age classes were established (i.e. epiphyseal fusion or tooth wear). She also suggests, through the study of horncore shape and size, that females were predominant in almost all the periods. This, combined with the kill-off pattern, led her to conclude that goats at King’s Lynn were mainly exploited for milk and dairy products. Along with the females she also identified some males and castrates. Noddle argues that, while castrate goats were probably kept alive long enough to allow the skin to grow large enough to be used in the shoe-making process, 50% of the male specimens were represented by young animals, which may have been used for their meat and horns as well as their skins. The ‘goat-economy’ that Noddle presents is based on dairy and leather production so that meat and horn are seen as by-products of these more important activities (Noddle 1977).

However, while distinguishing between male and female horncores in sheep is relatively straightforward, as not only the size but also the shape of the horncores is very sexually dimorphic (Boessneck *et al.* 1964), in the case of goat, such distinction is less evident as it is mainly the size and not the shape, which is the factor most useful in distinguishing the two sexes. In fact, in adult animals, male horns are more developed and larger than female horns but, while the distinction is easy in extreme cases (very large horncores), it becomes more complicated in moderate cases in which such a development has not yet taken place (young and sub-adult animals). The fact that Noddle identified so many females is yet another anomaly as most goat horncores found in medieval towns have been attributed to males (Albarella 2003).

Because of the similarity between sheep and goat bones, Noddle says that “it is possible that several goat bones have been described as sheep” (Noddle 1977: 391) though it seems obvious that, if such uncertainty about the identifications existed, the reverse could also have happened.

ANIMAL AND PLANT REMAINS															
TABLE I. TOTAL NUMBER OF FRAGMENTS OF MAMMAL BONE															
	PERIOD I				PERIOD II					PERIOD III POST-M.					
	BL/C	BL/D	AS	TOTAL	BL/B	BL/C	BL/D	BL/D-E	AS	OTHER	TOTAL	AS	OTHER	TOTAL	TOTAL
CATTLE															
Total fragments	43	167	393	603	563	66	318	280	459	807	2493	134	540	674	75 25 52 743 895
1st-class joints	37	126	259	422	363	41	229	191	294	444	1562	66	369	435	50 18 31 466 565
2nd-class joints	6	38	117	161	153	16	74	86	141	332	802	48	157	205	21 7 15 249 292
Loose teeth	0	3	17	20	34	4	14	4	22	31	109	20	14	34	8 0 1 38 47
No. individuals	15	34	64	113	93	28	84	27	99	48	379	11	23	34	22 10 8 60 100
Age range	N	0	3	3	6	1	0	4	3	5	4	17	1	2	3 0 0 0 7 7
	A	0	4	8	12	20	2	12	6	13	5	58	1	3	4 7 1 1 12 21
	B	10	9	20	39	20	5	15	10	27	7	84	3	7	10 2 3 3 15 23
	C	2	10	19	31	31	9	25	9	30	12	116	4	9	13 5 2 2 20 29
SHEEP															
Total fragments	36	152	527	715	374	44	307	156	398	582	1861	111	300	411	44 15 19 435 513
1st-class joints	37	131	426	594	283	35	247	126	262	341	1294	58	221	279	29 13 16 265 323
2nd-class joints	3	17	89	109	84	6	61	23	126	221	521	31	72	103	11 2 3 131 147
Loose teeth	0	5	8	13	15	3	4	7	15	20	64	22	7	29	4 0 0 39 43
No. individuals	14	27	91	132	76	20	75	20	101	50	342	16	25	41	12 4 7 53 76
Age range	N	0	1	2	3	0	0	3	1	1	6	11	0	4	4 0 0 0 3 3
	A	1	2	12	15	6	1	8	4	19	3	41	2	6	8 1 1 0 10 12
	B	4	6	32	42	16	4	18	6	22	2	68	5	5	10 1 1 3 13 18
	C	7	9	35	51	34	7	17	8	48	6	120	8	11	19 6 1 1 24 32
PIG															
Total fragments	16	58	276	350	173	31	89	99	141	231	764	49	160	209	8 9 14 164 195
1st-class joints	11	31	161	203	131	25	58	62	87	146	509	29	95	124	5 6 9 111 131
2nd-class joints	5	20	92	117	42	6	29	33	43	72	225	14	59	73	1 3 5 45 54
Loose teeth	0	7	23	30	16	0	4	4	9	13	46	6	6	12	1 0 0 8 9
No. individuals	6	19	55	80	56	15	28	12	47	24	182	8	18	26	5 2 5 30 42
Age range	N	0	1	0	1	0	0	0	3	0	3	0	1	1	0 0 0 2 2
	A	1	2	9	12	20	1	2	1	10	4	38	3	3	6 1 1 0 8 10
	B	3	7	23	33	20	3	12	9	23	8	75	4	7	11 3 1 2 15 21
	C	1	5	14	20	12	4	5	2	6	12	41	1	7	8 1 0 2 5 8
GOAT															
Total fragments	7	32	57	96	29	9	30	29	40	42	179	2	60	62	9 2 4 23 38
No. individuals	5	11	19	35	20	5	14	6	23	18	86	2	12	14	9 2 1 11 23
Age range	A	0	0	0	0	0	1	0	0	1	2	0	2	2	0 0 0 0 0
	B	2	2	5	9	6	0	3	0	3	13	0	1	1	1 0 0 3 4
	C	2	6	6	14	10	2	4	5	7	9	37	0	4	4 7 2 1 7 17

Figure 3.4 Table of NISP (number of identified specimens), MNI (minimum number of individuals) and age classes for the domestic species for each chronological period at King's Lynn, as identified by Noddle (image reprinted from NODDLE, B.A. Mammal bone. In *Excavation in King's Lynn 1963-1970*, H. CLARKE and A. CARTER, 378-399, copyright 1977. The Society for Medieval Archaeology Monograph Series 7. London: Society for Medieval Archaeology, with permission from Helen Clarke).

Relying mainly on the material from the Baker Street site, Noddle also suggested that, in Period II (1250-1350), a decline in the presence of goat could be seen, followed by an increase in the Post-medieval period (1550-1880), which would go against the trend identified at other sites (Albarella 1999).

The claimed abundance of goat bones, as well as the lack of detail in Noddle's report, made this site ideal for an application of the new methodological approach developed as part of this dissertation. The following objectives were identified:

1. To verify the apparently unusual nature of the sheep/goat assemblage from the site: was the relatively high number of goat bones genuine?
2. To evaluate the body part distributions of the sheep/goat assemblage, with the main aim to assess whether goats were mainly represented by horncores or also other anatomical elements.
3. Review the role of the goat in King's Lynn.

4. To test the new recording protocol in order to see whether the traditional morphological approach in combination with the new biometrical approach could help to enhance the identification process.
5. To test the extent to which the new methodology was effective on fragmented archaeological material.

3.2.5 Reevaluation of King's Lynn sheep/goat bone material: methodology

For the reanalysis of the sheep/goat assemblage of King's Lynn the same methodology previously applied on the modern material was used: selected morphological traits as well as a list of measurements were recorded on the archaeological material (see Chapter 2, Section 2.1). Initial identification was assessed by using the selected morphological traits. The categories used were:

Ovis - if all the morphological traits pointed toward sheep, or the majority of the traits pointed toward sheep and a minority had mixed features, i.e. could only be assigned to 'sheep/goat';

Capra - if all the morphological traits pointed toward goat, or the majority of the traits pointed toward goat and a minority had mixed features, i.e. could only be assigned to 'sheep/goat';

Ovis/Capra - if only a minority of traits could be attributed to a single species, or a mix of traits was attributed to 'sheep' and 'goat'.

A database composed of four different sections was created: two sections were dedicated to the recording of morphological traits and biometrical data for postcranial bones, while the other two recorded the same data for loose teeth and mandibles. For each element, information such as the chronological phase it belonged to (following the same chronological subdivision used by Noddle 1977; see also Tab. 3.1) and the presence of anomalies (pathologies and human modifications such as butchery) were noted and recorded.

The results are presented on a phase by phase basis. The first type of analysis carried out is a simple quantification according to body parts, so that the number of identified specimens and body parts representation can be better evaluated. An analysis of Biometric Indices and a Discriminant Analysis then follow; this is in order to:

- a) check whether the identifications carried out through the use of the morphological traits are supported by the biometrical analysis;
- b) assess the extent to which measurements could help in attributing those specimens that were unidentifiable using the morphological approach;
- c) to evaluate whether the new methodology could work successfully on fragmented archaeological material.

3.2.6 Morphological Approach: Results

Phase I

For phase I, 219 fragments were identified: 191 were definitively attributed to sheep (*Ovis*), 10 to goat (*Capra*) and 18 to sheep/goat (*Ovis/Capra*) (Tab. 3.2). Only two of the goat specimens are not represented by horncores.

SHEEP				GOAT					
Total fragments	36	152	527	715	Total fragments	7	32	57	96
1st-class joints	37	131	426	594	No. individuals	5	11	19	35
2nd-class joints	3	17	89	109	Age range	A	0	0	0
Loose teeth	0	5	8	13	B	2	2	5	9
No. individuals	14	27	91	132	C	2	6	6	14
Age range	N	0	1	2	3				
	A	1	2	12	15				
	B	4	6	32	42				
	C	7	9	35	51				

Figure 3.5 NISP and MNI for sheep and goat in phase I according to Noddle 1977 (image reprinted from NODDLE, B.A. Mammal bone. In *Excavation in King's Lynn 1963-1970*, H. CLARKE and A. CARTER, 378-399, copyright 1977. The Society for Medieval Archaeology Monograph Series 7. London: Society for Medieval Archaeology, with permission from Helen Clarke).

Table 3.2 NISP for the three categories identified for phase I (1050-1250).

	<i>Ovis aries</i>	<i>Capra hircus</i>	<i>Ovis/ Capra</i>
Horncore	13	8	-
Jaw	22	-	6
Teeth	3	-	-
Scapula	24	2	5
Humerus	30	-	1
Radius	24	-	
Ulna	10	-	1
Metacarpal	3	-	1
Metatarsal	2	-	-
Tibia	39	-	3
Astragalus	6	-	-
Calcaneum	8	-	-
1st Phalanx	7	-	1
Total Identified Specimens	191	10	18

The NISP values recorded by Noddle (1977) are much higher (Fig. 3.5), but this is because she did not use a selective recording system but counted every identifiable specimen. Moreover, it is also likely that some of the bones Noddle recorded as part of stratified phases have been included in the unstratified category in this study, as a consequence of stricter criteria of

attribution to phase, as well as loss of contextual information through the decades. It must also be considered that Noddle did not use an *Ovis/Capra* category, attributing every bone to one or the other species.

Despite the inconsistency of the recording systems it is worth pointing out that in my study the sheep/goat ratio is 19:1, while in Noddle's study this is represented by the much lower 7:1, which means that, proportionally, Noddle identified many more goats. Perhaps more significantly, once horncores are excluded, the ratio in my study increases to as much as 89:1. Since Noddle did not provide separate values for horncores and other elements, we do not know to what extent her goat proportion was affected by horncore abundance.

Phase II

Figures for this phase can be found in Table 3.3, while Noddle's calculations are provided in Figure 3.6. For phase II a total of 294 bones were recorded: 258 were attributed to sheep (*Ovis*), 23 to goat (*Capra*) and 13 to the category sheep/goat (*Ovis/Capra*). Goat is only represented by horncores. The sheep/goat ratio for phase II is 14:1 in Noddle and 11:1 in this study. The proportion of the two species of the two studies is more similar in this phase but, as said for the previous phase, we do not know the extent to which the Noddle sheep/goat ratio is affected by horncore occurrence.

SHEEP							GOAT							
Total fragments	374	44	307	156	398	582	Total fragments	29	9	30	29	40	42	
1st-class joints	283	35	247	126	262	341	No. individuals	20	5	14	6	23	18	
2nd-class joints	84	6	61	23	126	221		A	0	0	1	0	0	1
Loose teeth	15	3	4	7	15	20	Age range	B	6	0	3	0	3	1
No. individuals	76	20	75	20	101	50		C	10	2	4	5	7	9
	N	0	0	3	1	1	6							
Age range	A	6	1	8	4	19	3							
	B	16	4	18	6	22	2							
	C	34	7	17	8	48	6							

Figure 3.6 NISP and MNI for sheep and goat in phase II according to Noddle (image reprinted from NODDLE, B.A. Mammal bone. In *Excavation in King's Lynn 1963-1970*, H. CLARKE and A. CARTER, 378-399, copyright 1977. The Society for Medieval Archaeology Monograph Series 7. London: Society for Medieval Archaeology, with permission from Helen Clarke).

The NISP values recorded by Noddle (1977) are once again much higher (Fig. 3.6) than the values recorded in this study, the reasons for this have been previously pointed out.

Table 3.3 NISP for the three categories identified for phase II (1250-1350).

	<i>Ovis aries</i>	<i>Capra hircus</i>	<i>Ovis/ Capra</i>
Horncore	6	23	-
Jaw	32	-	4
Teeth	1	-	1
Scapula	26	-	1
Humerus	29	-	2
Radius	29	-	-
Ulna	17	-	2
Metacarpal	14	-	-
Metatarsal	19	-	-
Tibia	28	-	2
Astragalus	16	-	-
Calcaneum	20	-	-
1st Phalanx	19	-	-
2nd Phalanx	2	-	1
Total Identified Specimens	258	23	13

Phase III

A total of 189 bones have been identified: 134 were attributed to sheep (*Ovis*), 27 to goat (*Capra*) and 28 to the sheep/goat group (*Ovis/Capra*). Table 3.4 shows that goat is represented mainly by horncores and just two postcranial bones. The sheep/goat ratio is for this study 5:1 and for Noddle 7:1; the higher value given by Noddle attests that, proportionally she identified fewer goats (Fig. 3.7). If the horncores are excluded, the ratio in my study increases to 65:1, highlighting the overwhelming presence of sheep.

SHEEP					GOAT				
Total fragments	1861	111	300	411	Total fragments	179	2	60	62
1st-class joints	1294	58	221	279	No. individuals	86	2	12	14
2nd-class joints	521	31	72	103	Age range	A	2	0	2
Loose teeth	64	22	7	29	B	13	0	1	1
No. individuals	342	16	25	41	C	37	0	4	4
Age range	N	11	0	4					
	A	41	2	6					
	B	68	5	5					
	C	120	8	11					

Figure 3.7 NISP and MNI for sheep and goat in phase III according to Noddle (image reprinted from NODDLE, B.A. Mammal bone. In *Excavation in King's Lynn 1963-1970*, H. CLARKE and A. CARTER, 378-399, copyright 1977. The Society for Medieval Archaeology Monograph Series 7. London: Society for Medieval Archaeology, with permission from Helen Clarke).

Table 3.4 NISP for the three categories identified for phase III (1350-1550).

	<i>Ovis aries</i>	<i>Capra hircus</i>	<i>Ovis/ Capra</i>
Horncore	4	25	-
Jaw	25	-	20
Teeth	1	-	2
Scapula	7	-	2
Humerus	20	-	2
Radius	18	1	-
Ulna	11	-	-
Metacarpal	4	-	-
Tibia	27	-	-
Astragalus	5	-	-
Calcaneum	2	-	-
1 st Phalanx	9	1	1
2 nd Phalanx	1	-	1
Total Identified Specimens	134	27	28

Phase IV

A total of 118 bones were recorded for this phase: 104 have been assigned to sheep (*Ovis*), six to goat (*Capra*) and eight to sheep/goat (*Ovis/ Capra*). Table 3.5 shows that goat, in this phase too, is exclusively represented by horncores.

SHEEP				GOAT						
Total fragments	15	19	435	513	9	2	4	23	38	
1st-class joints	13	16	265	323	9	2	1	11	23	
2nd-class joints	2	3	131	147	A	0	0	0	0	
Loose teeth	0	0	39	43	B	1	0	0	3	4
No. individuals	4	7	53	76	C	7	2	1	7	17
Age range	N	0	0	3	3					
	A	1	0	10	12					
	B	1	3	13	18					
	C	1	1	24	32					

Figure 3.8 NISP and MNI for sheep and goat in phase IV according to Noddle (image reprinted from NODDLE, B.A. Mammal bone. In *Excavation in King's Lynn 1963-1970*, H. CLARKE and A. CARTER, 378-399, copyright 1977. The Society for Medieval Archaeology Monograph Series 7. London: Society for Medieval Archaeology, with permission from Helen Clarke).

The sheep/goat ratio is of 13:1 in Noddle's study (see also Fig. 3.8) and 17:1 in this study.

Table 3.5 NISP for the three categories identified for phase IV (1550-1880).

	<i>Ovis aries</i>	<i>Capra hircus</i>	<i>Ovis/ Capra</i>
Horncore	5	6	-
Jaw	12	-	2
Teeth	6	-	-
Scapula	13	-	3
Humerus	12	-	-
Radius	9	-	-
Ulna	8	-	1
Metacarpal	3	-	-
Metatarsal	18	-	-
Tibia	8	-	2
Astragalus	3	-	-
Calcaneum	3	-	-
1st Phalanx	3	-	-
2nd Phalanx	1	-	-
Total Identified Specimens	104	6	8

Unstratified

Despite a careful analysis of archival information, many contexts could not be clearly attributed to a specific chronological phase. Nevertheless, the material was recorded, as it was probably included in Noddle's paper and, to ignore it, would have limited comparability between the two studies.

Table 3.6 NISP for the three categories identified among the unstratified bones.

	<i>Ovis aries</i>	<i>Capra hircus</i>	<i>Ovis vel Capra</i>
Horncore	2	10	-
Jaw	26	-	8
Teeth	4	-	-
Scapula	6	-	1
Humerus	16	1	3
Radius	19	-	-
Ulna	9	-	1
Metacarpal	18	-	-
Metatarsal	7	-	-
Metapodial	-	-	1
Tibia	30	-	-
Astragalus	7	-	-
Calcaneum	8	-	-
1st Phalanx	6	-	-
2nd Phalanx	-	-	1
Total Identified Specimens	158	11	15

Of the 184 bones (Tab. 3.6), 158 were assigned to sheep (*Ovis*), 11 to goat (*Capra*) and 15 to sheep/goat (*Ovis/Capra*). In this phase too, goat is almost exclusively represented by horncores. The sheep/goat ratio is 14:1 when horncores are included, and 156:1 when they aren't. Consistently with the datable phases, sheep is overwhelmingly better represented for all body parts, except horncores for which goat predominates in all phases apart from phase I.

In general the evidence presented above points out to the fact that, apart from horncores, sheep were far more common than goats in all King's Lynn phases. This evidence is therefore in line with what is known for the rest of England and it does not support Noddle's claim of an abundance of goats at King's Lynn, e.g. "*...there are a number of towns where few goat bones have been found...and others where it has been plentiful. The latter include... King's Lynn, Norfolk*" (Noddle 1994: 120). The abundance of goat horncores is also not unusual.

3.2.7 Shape analysis as expressed by Biometrical Indices

The same biometrical approach applied to the modern data was adopted for the archaeological data. A shape analysis was carried out by using only those metric ratios that had been proven to be reasonably successful in separating the two species on the modern material. To provide a baseline of reference, the modern data are plotted together with the archaeological data.

Phase I

Horncore

Figures 3.9 and 3.10 show the results regarding the horncores related to the first chronological phase. Figure 3.9 shows that most archaeological specimens that were identified as definite sheep or goat according to the morphological characteristics, fall among the modern groups of the same species. An archaeological sheep specimen, however, falls in the area of overlap of the two modern groups.

In Figure 3.9 the cluster of archaeological goat specimens may be related to sex variation, though it is very difficult to be sure on such a small sample.

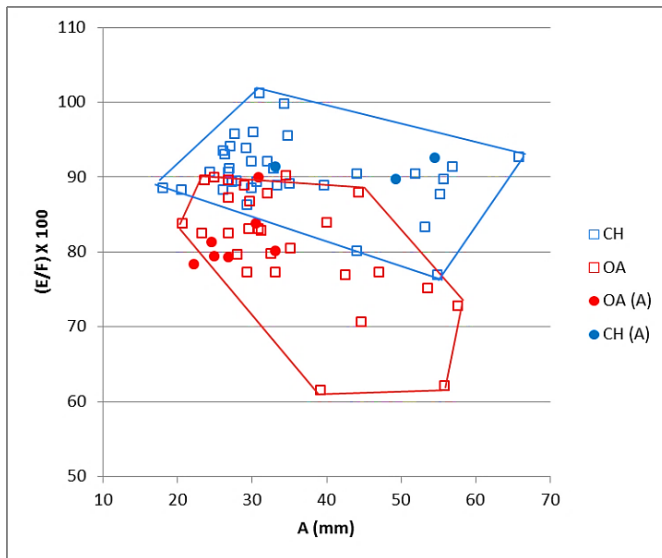


Figure 3.9 Maximum diameter taken at the base plotted against a ratio between the length and the length of the outer curvature of the horncore. The modern data are represented by the square empty symbol, blue for modern goats, red for modern sheep, while the archaeological material is represented by the filled dot symbol: blue for goats, red for sheep and green for sheep/goat.

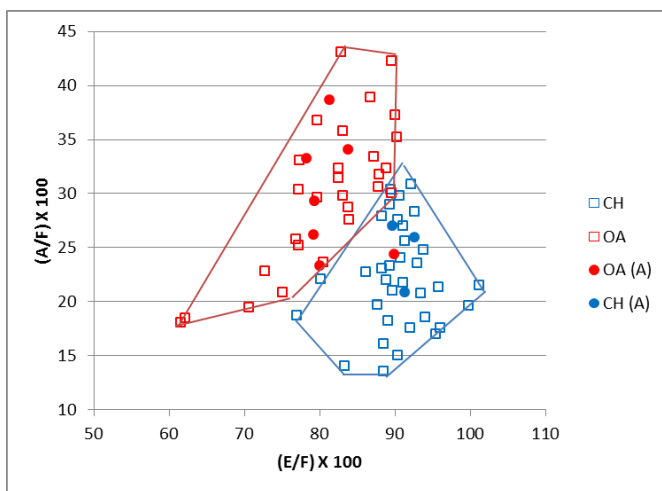


Figure 3.10 Ratio between the length and the length of the outer curvature plotted against the ratio between the maximum diameter taken at the base and the length of the outer curvature of the horncore. Symbols explained in Fig. 3.9.

Figure 3.10 shows that by and large the archaeological specimens also fall among the modern specimens of the same species, confirming identifications. One archaeological sheep specimen, however, plots in the middle of the goat modern group (this is the same specimen that was borderline in the previous diagram), raising the possibility of a misidentification. Nevertheless, the overall pattern of a slight predominance of sheep horncores in this phase is confirmed.

Scapula

Regarding the scapula, Figures 3.11 and 3.12 describe the shape of the glenoid cavity and the region of the neck, the most diagnostic areas for this element. Although some archaeological

specimens plot in the area of overlap between modern sheep and goat, they are potentially consistent with the morphological identifications. In Figure 3.11 one of the archaeological goat specimens has an unusually high GLP/LG ratio, but the other ratio is very consistent with the modern goat cluster (Fig. 3.12). The archaeological specimen that could not be identified at species level remains of uncertain attribution as it plots in the area of biometrical overlap between sheep and goat.

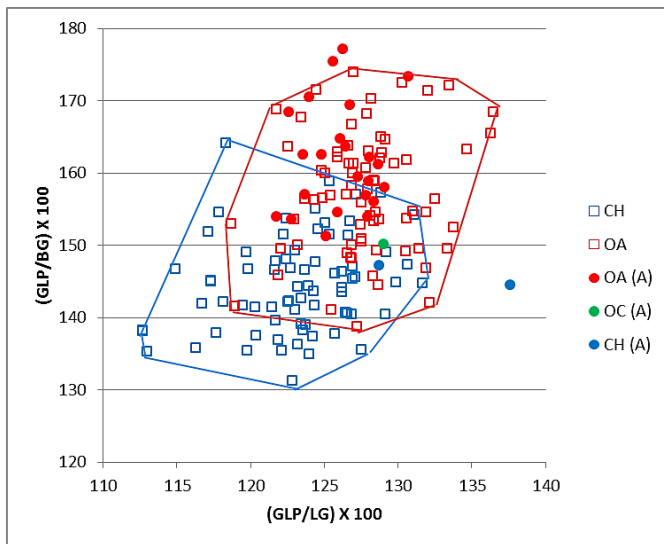


Figure 3.11 Ratio between the greatest length of the *processus articularis* and the length of the glenoid cavity plotted against the ratio between the greatest length of the *processus articularis* and the breadth of the glenoid cavity. Symbols explained in Fig. 3.9.

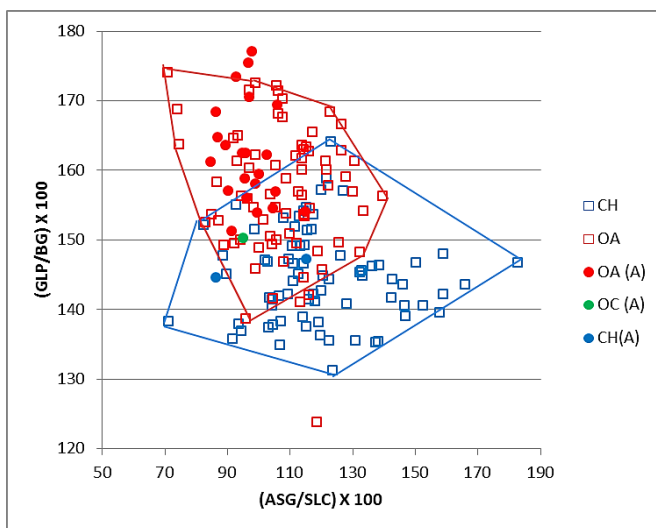


Figure 3.12 Ratio between the shortest distance from the base of the spine to the edge of the glenoid cavity and the smallest length of the *collum scapulae* plotted against the ratio between the greatest length of the *processus articularis* and the breadth of the glenoid cavity. Symbols explained in Fig. 3.9.

Humerus

Figures 3.13 to 3.16 show ratios of measurements taken on the distal articulation of the humerus. No goat archaeological humeri were identified morphologically and all sheep humeri plot within the modern sheep cluster or the area of overlap of the two species. One sheep specimen in Figure 3.13, marginally plots in the goat area, but is consistent with sheep in all other diagrams and is therefore more likely to be indeed a sheep. The uncertain specimen plots in the area of overlap and therefore cannot be identified biometrically.

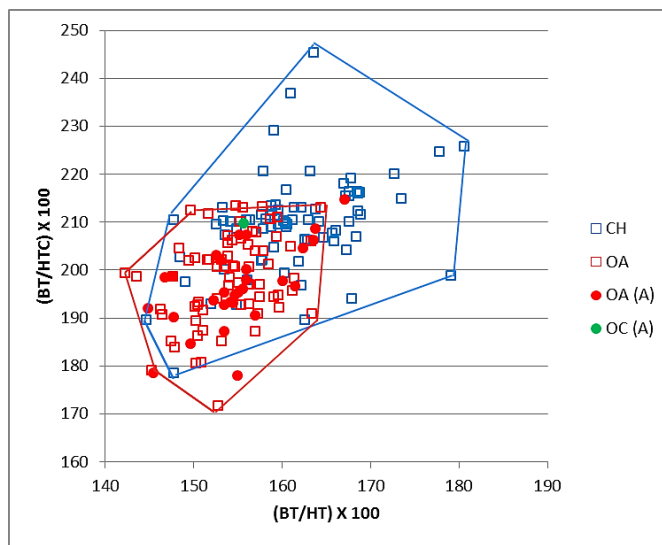


Figure 3.13 Ratio between the medio lateral width of the trochlea and its height plotted against the medio lateral width of the trochlea and the diameter of the trochlear constriction. Symbols explained in Fig. 3.9.

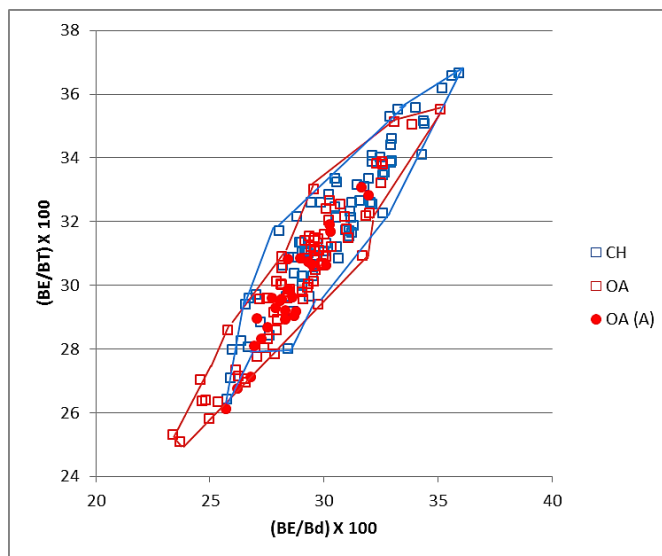


Figure 3.14 Ratio between the breadth of the *capitulum* and the distal width plotted against the ratio between the breadth of the *capitulum* and the medio lateral width of the trochlea. Symbols explained in Fig. 3.9.

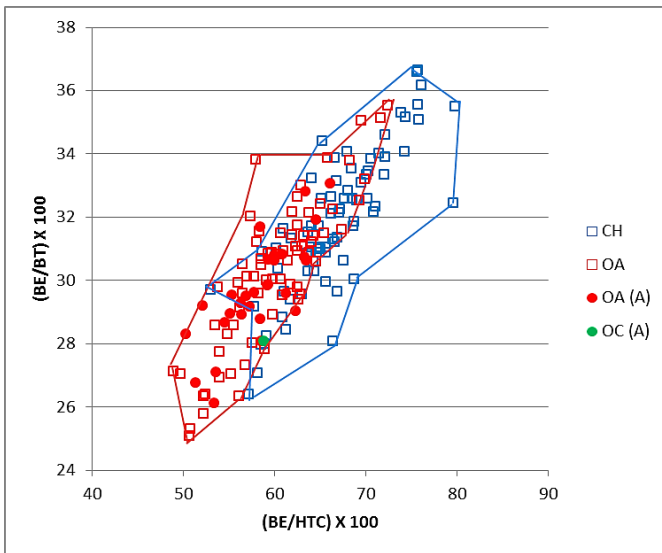


Figure 3.15 Ratio between the breadth of the *capitulum* and the diameter of the trochlea constriction plotted against the ratio between the breadth of the *capitulum* and the medio lateral width of the trochlea. Symbols explained in Fig. 3.9.

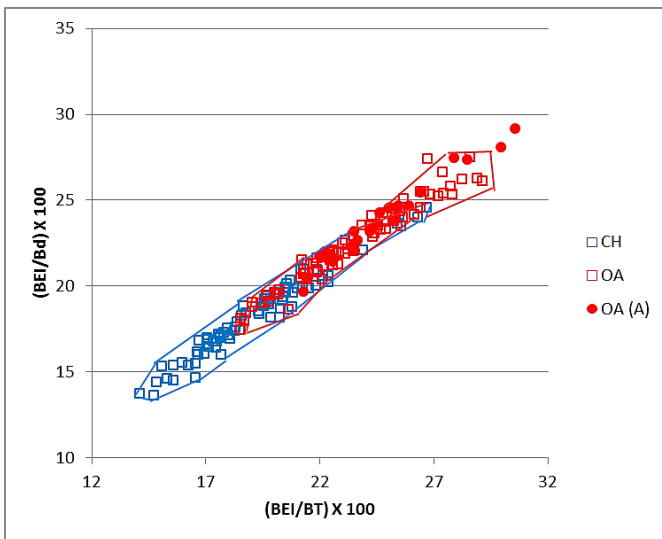


Figure 3.16 Ratio between the breadth of the epicondyle *lateralis* and the medio lateral width of the trochlea plotted against the ratio between the breadth of the epicondyle *lateralis* and the width of the distal end. Symbols explained in Fig. 3.9.

Radius

Only sheep archaeological specimens were identified. All archaeological sheep, except one, cluster with the modern sheep group (Fig. 3.17). The one exception is insufficiently distant from the sheep cluster to be confidently regarded as a misidentification.

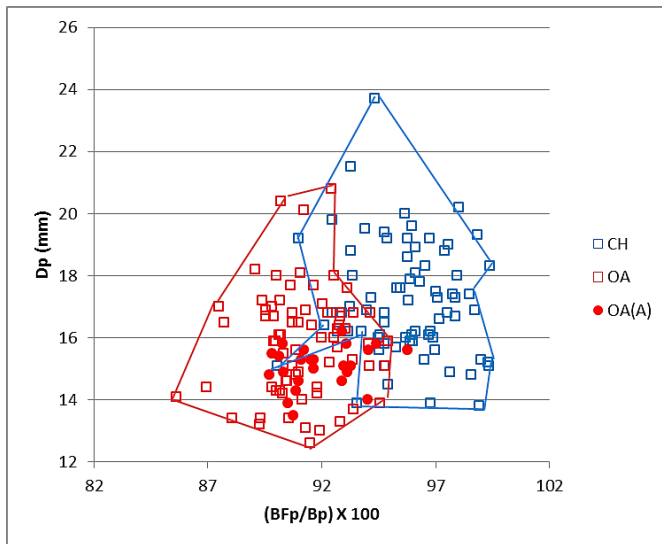


Figure 3.17 Ratio between the greatest length of the *facies articularis proximalis* and the greatest breadth of the proximal end plotted against the depth of the proximal end. Symbols explained in Fig. 3.9.

Ulna

For this element the sheep archaeological specimens are divided into two clusters (Fig. 3.18). The most numerous cluster plots clearly at the sheep end of the range. Three specimens (including one that could not be identified morphologically) plot in the middle of the overall sheep/goat range. In view of their distance from the main cluster the possibility that they could represent goats cannot be excluded.

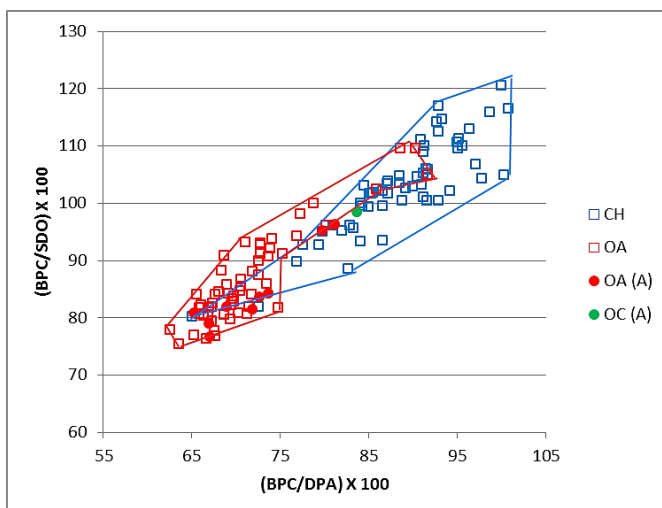


Figure 3.18 Ratio between the breadth across the coronoid process and the depth across the *processus anconaeus* to the caudal border plotted against the breadth across the coronoid process and the smallest depth of the olecranon. Symbols explained in Fig. 3.9.

Metapodials

For metapodials, the lack of complete bones prevented the use of all the diagnostic ratios. Figures 3.19 to 3.22 plot medial and lateral condyle metric ratios. No archaeological goats had been identified morphologically and the archaeological sheep all fall among the modern sheep group or in the area of overlap for the two species, thus providing support to the original identification. The pattern is much clearer for metacarpals than metatarsals. One unidentified specimen in Figure 3.20 plots among the modern goats, but insufficiently distantly from the sheep cluster to give confidence about its identification as goat.

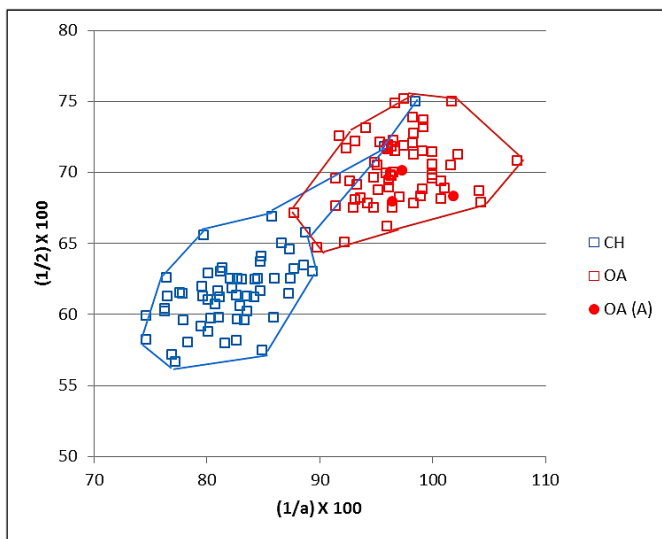


Figure 3.19 Metacarpal. Ratio between the diameter of the medial trochlea and the width of the medial condyle plotted against the ratio between the diameter of the *verticillus* at the medial condyle and the diameter of the medial trochlea. Symbols explained in Fig. 3.9.

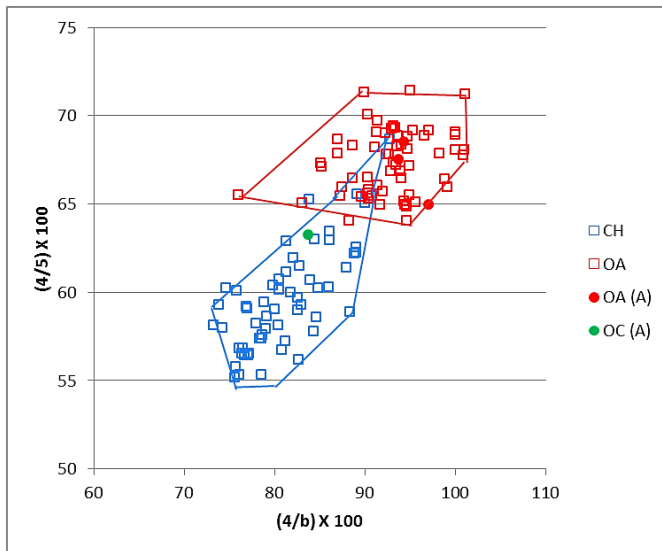


Figure 3.20 Metacarpal. Ratio between the width of the lateral condyle and the diameter of the lateral trochlea plotted against the ratio between the diameter of the lateral condyle and the diameter of the *verticillus* on the lateral condyle. Symbols explained in Fig. 3.9.

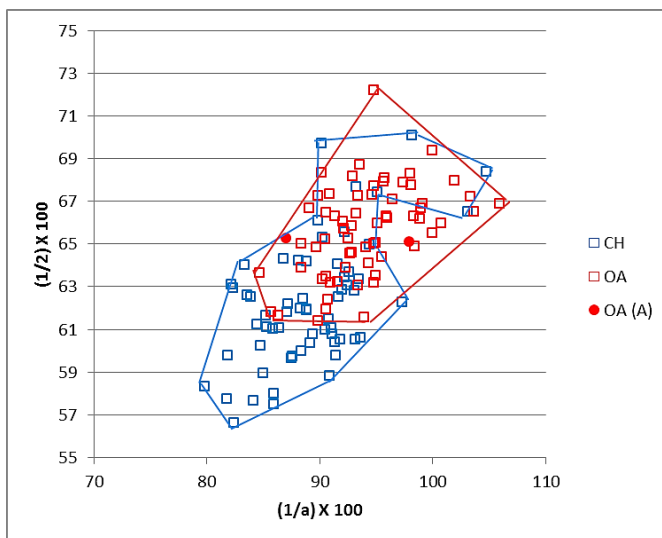


Figure 3.21 Metatarsal. Ratio between the diameter of the medial trochlea and the width of the medial condyle plotted against the ratio between the diameter of the *verticillus* at the medial condyle and the diameter of the medial trochlea. Symbols explained in Fig. 3.9.

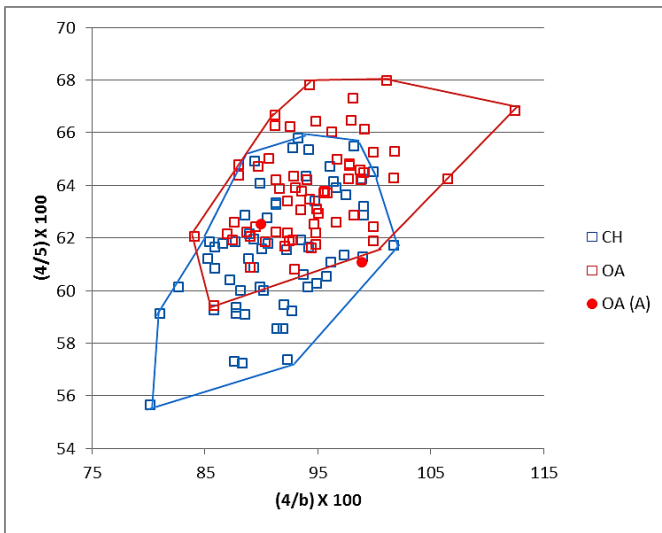


Figure 3.22 Metatarsal. Ratio between the width of the lateral condyle and the diameter of the lateral trochlea plotted against the ratio between the diameter of the *verticillus* on the lateral condyle and the diameter of the lateral condyle. Symbols explained in Fig. 3.9.

Tibia

Figure 3.23 shows ratios of the measurements taken on the distal articulation of the tibia. The likely absence of archaeological goats is confirmed by the biometrical analysis. All specimens identified morphologically as sheep fall among their modern counterparts or in the area of overlap of the two modern species; as such they are consistent with the morphological identifications. Nothing can be said regarding the unidentified specimens as they fall in the area of overlap.

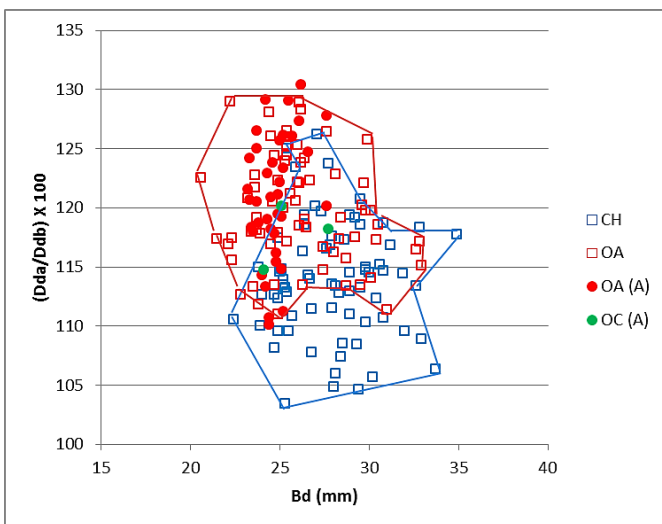


Figure 3.23 Breadth of the distal end plotted against the ratio between the depth of the medial (a) and lateral (b) side. Symbols explained in Fig. 3.9.

Astragalus

All the archaeological sheep identified as such according to the morphological traits, fall among the modern sheep group or very close to it (Figs. 3.24 to 3.27) with the ratios in Figure 3.26 providing the clearest pattern. Thus, the biometrical results clearly confirm the morphological identifications.

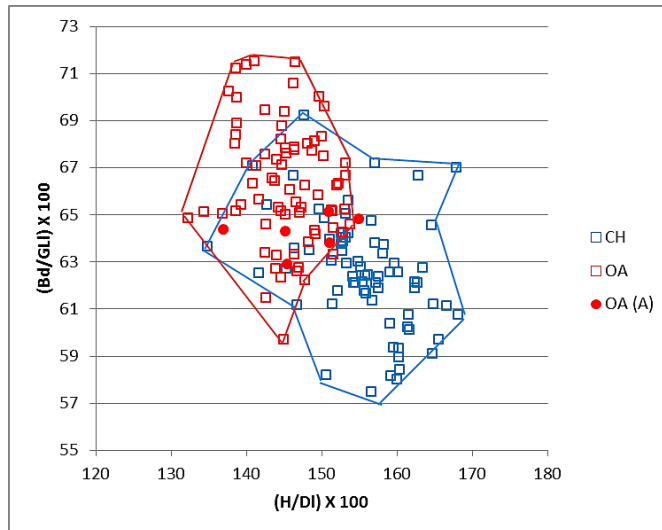


Figure 3.24 Ratio between height at the central constriction and the greatest depth of the lateral half plotted against a ratio between the breadth of the distal end and the greatest length of the lateral half. Symbols explained in Fig. 3.9.

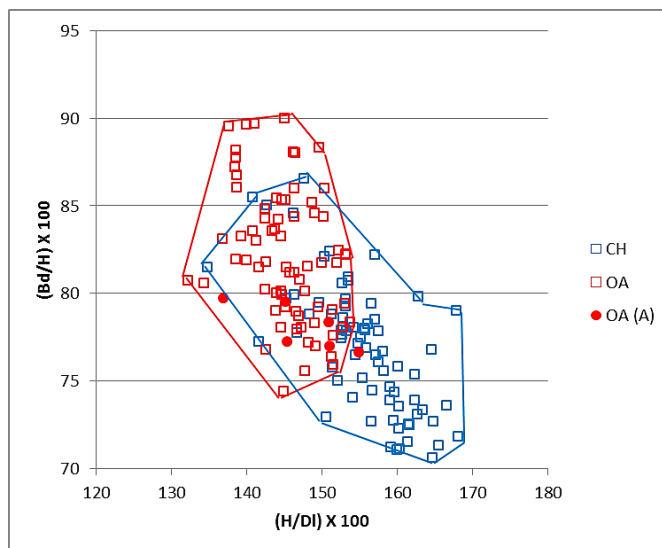


Figure 3.25 Ratio between height at the central constriction and the greatest depth of the lateral half plotted against the ratio between the breadth of the distal end and the height at the central constriction. Symbols explained in Fig. 3.9.

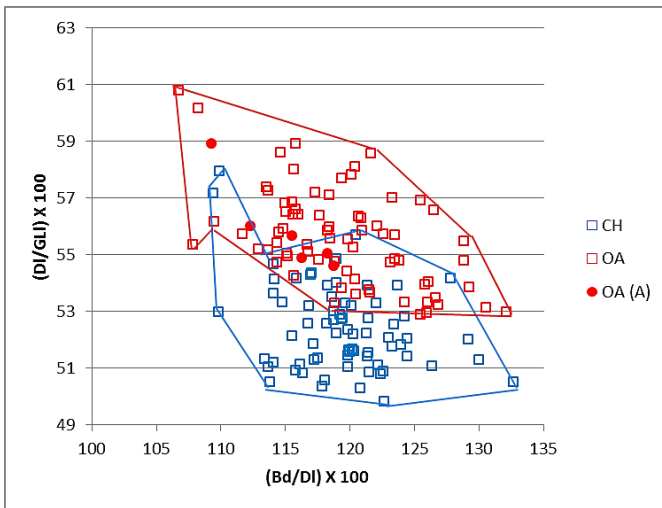


Figure 3.26 Ratio between breadth of the distal end and the greatest depth of the lateral half plotted against the ratio between the breadth of the distal end and the greatest depth of the lateral half. Symbols explained in Fig. 3.9.

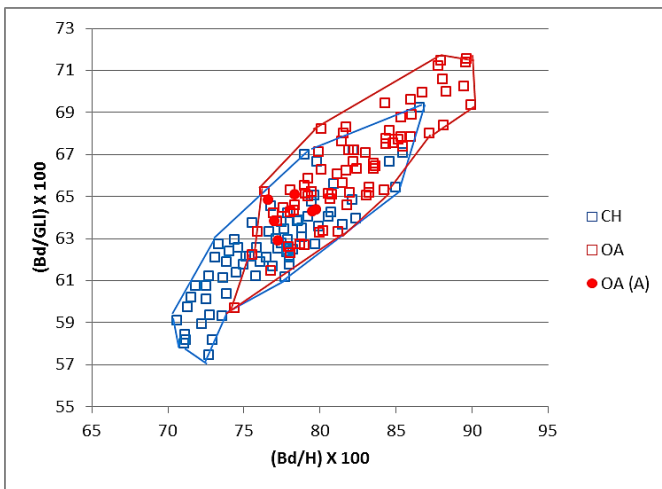


Figure 3.27 Ratio between the breadth of the distal end and the height at the central constriction and the ratio between height at the central constriction and the greatest depth of the lateral half. Symbols explained in Fig. 3.9.

Calcaneum

Figures 3.28 to 3.30 show different ratios used for the calcaneum. No archaeological goats had been identified morphologically. The biometrical outcome confirms this identification as all archaeological specimens clearly plot within the modern sheep group, in all three diagrams.

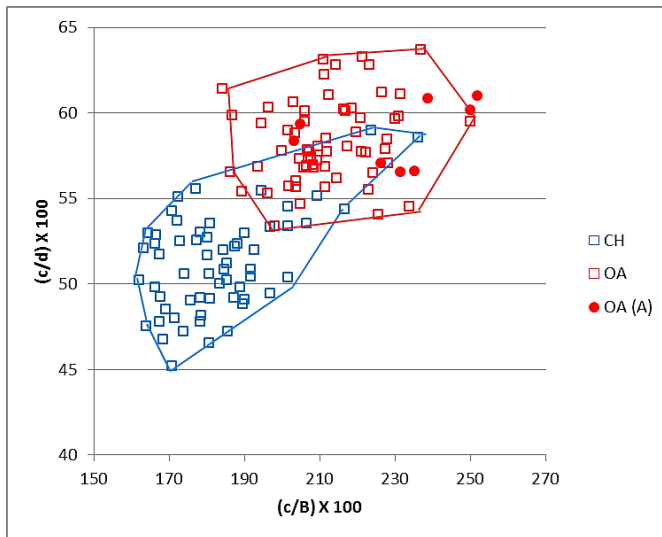


Figure 3.28 Ratio between the length and the breadth of the articular facet of the *os malleolare* plotted against the ratio between the length of the articular facet of the *os malleolare* and the length taken from the articular facet of the *os malleolare* to the end of the articulation-free part of the process. Symbols explained in Fig. 3.9.

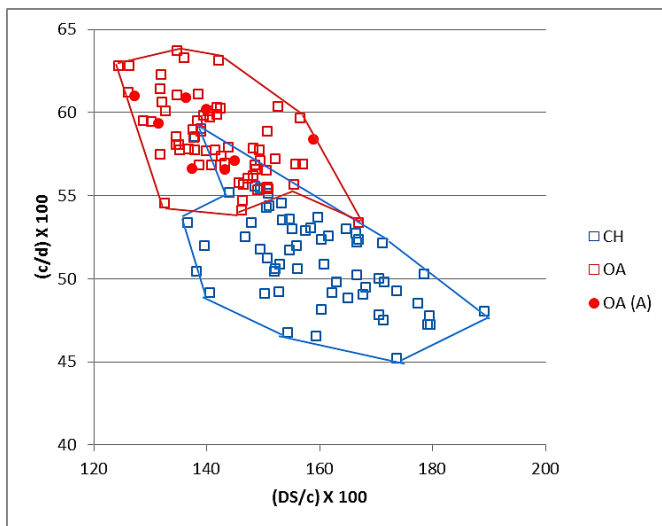


Figure 3.29 Ratio between the depth of the *substentaculum tali* and the length of the articular facet of the *os malleolare* plotted against the ratio between the length and the breadth of the articular facet of the *os malleolare*. Symbols explained in Fig. 3.9.

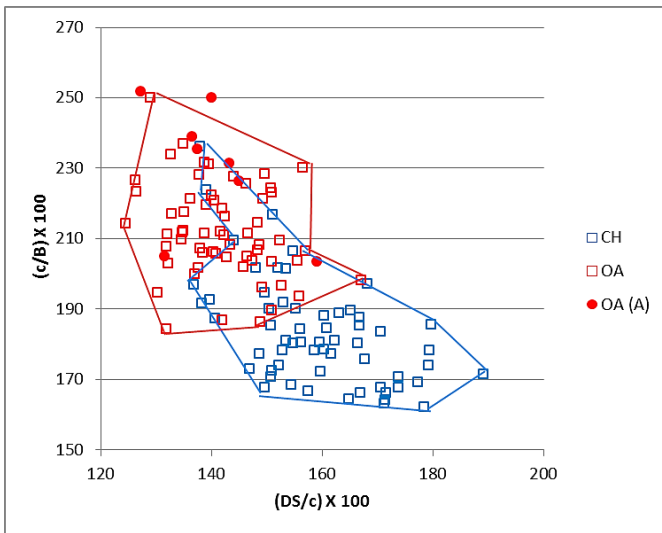


Figure 3.30 Ratio between the depth of the *substantaculum tali* and the length of the articular facet of the *os malleolare* plotted against the ratio between the length and the breadth of the articular facet of the *os malleolare*. Symbols explained in Fig. 3.9.

Phase II

Horncores

In this phase more goat than sheep horncores had been identified. The biometrical analysis confirms the morphological identifications (Figs. 3.31 and 3.32), the pattern being particularly clear when using the ratios plotted in Figure 3.32. Like in the previous phase the separation of the archaeological goats into two groups (Fig. 3.31), may be due to sexual dimorphism.

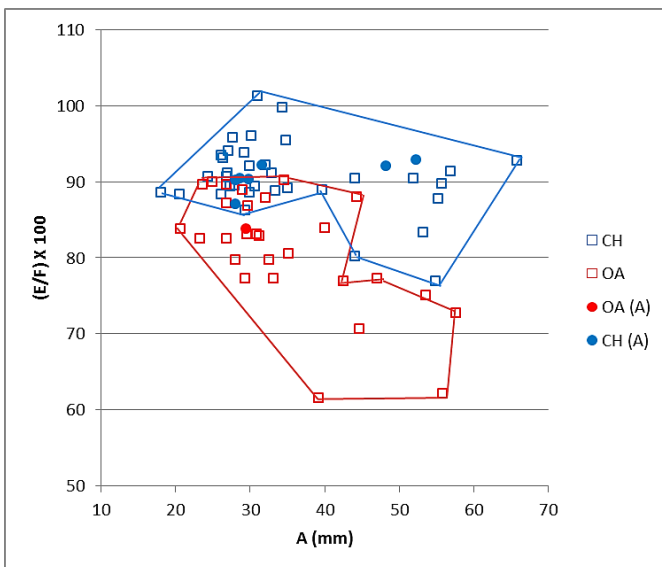


Figure 3.31 Maximum diameter taken at the base plotted against a ratio between the length and the length of the outer curvature of the horncore. Symbols explained in Fig. 3.9.

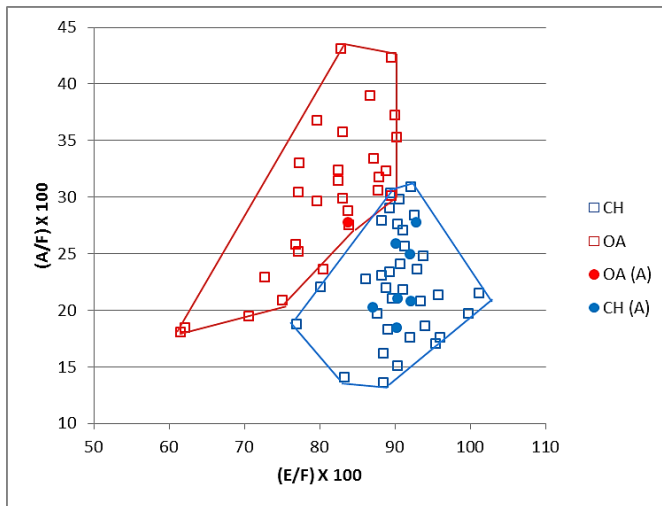


Figure 3.32 Ratio between the length and the length of the outer curvature plotted against the ratio between the maximum diameter taken at the base and the length of the outer curvature of the horncore. Symbols explained in Fig. 3.9.

Scapula

All the archaeological scapulae were attributed to sheep according to their morphology. Figures 3.33 and 3.34 show that the morphological identifications are confirmed by the biometry. One unidentified specimen appears to be consistent with sheep rather than goat (Fig. 3.34).

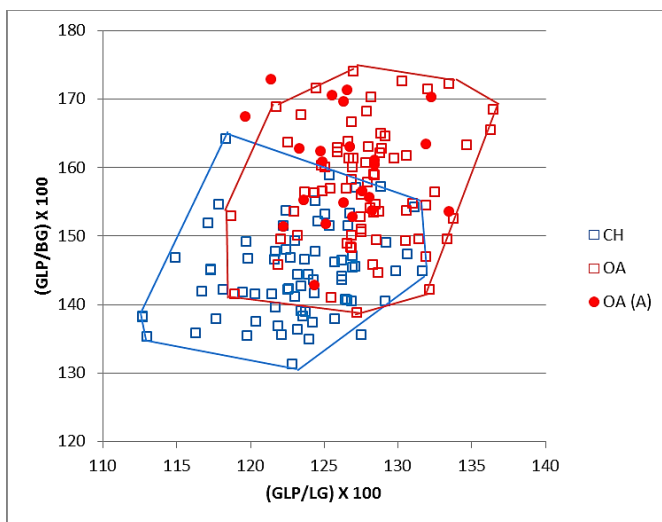


Figure 3.33 Ratio between the greatest length of the *processus articularis* and the length of the glenoid cavity plotted against the ratio between the greatest length of the *processus articularis* and the breadth of the glenoid cavity. Symbols explained in Fig. 3.9.

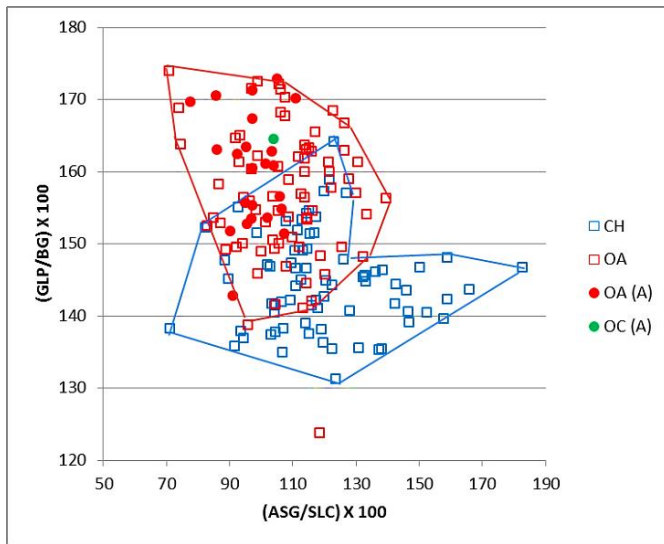


Figure 3.34 Ratio between the shortest distance from the base of the spine to the edge of the glenoid cavity and the smallest length of the *collum scapulae* plotted against a ratio between the greatest length of the *processus articularis* and the breadth of the glenoid cavity. Symbols explained in Fig. 3.9.

Humerus

Figures 3.35 to 3.38 display ratios related to the distal humerus. No archaeological goats had been identified morphologically. All archaeological sheep fall well within the modern sheep group or in the area of overlap between the two species, thus supporting the morphological identifications.

Due to the high level of overlap between the two modern groups it is difficult to be sure about the taxonomy of the unidentified specimens (Figs. 3.35 to 3.37). Nevertheless, in all diagrams they are highly consistent with sheep and are therefore more likely to belong to this species.

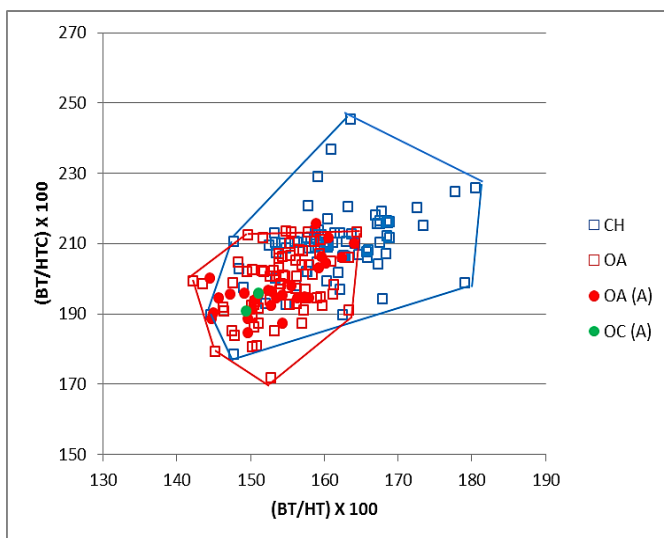


Figure 3.35 Ratio between the medio lateral width of the trochlea and its height plotted against the medio lateral width of the trochlea and the diameter of the trochlear constriction. Symbols explained in Fig. 3.9.

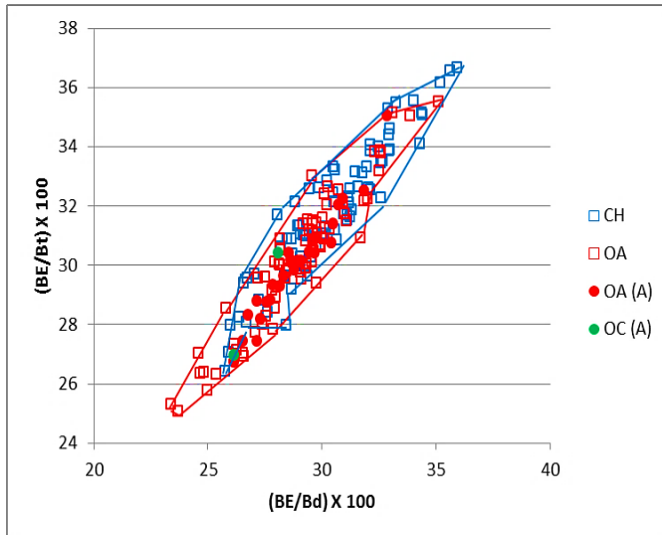


Figure 3.36 Ratio between the breadth of the *capitulum* and the distal width plotted against the ratio between the breadth of the *capitulum* and the medio lateral width of the trochlea. Symbols explained in Fig. 3.9.

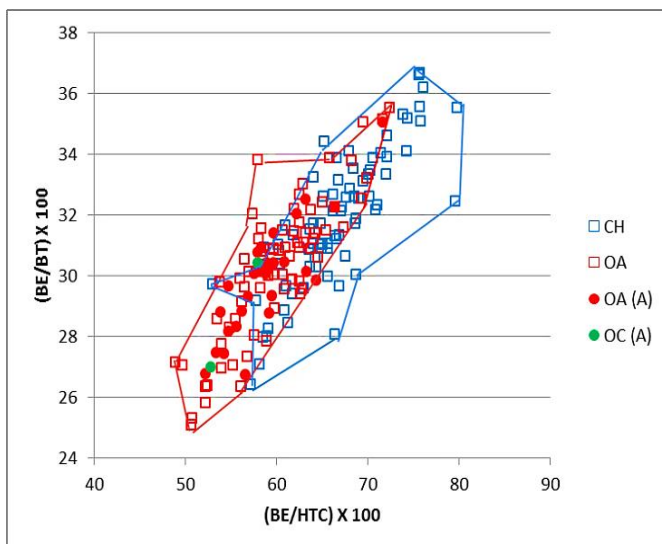


Figure 3.37 Ratio between the breadth of the *capitulum* and the diameter of the trochlear constriction plotted against the ratio between the breadth of the *capitulum* and the medio lateral width of the trochlea. Symbols explained in Fig. 3.9.

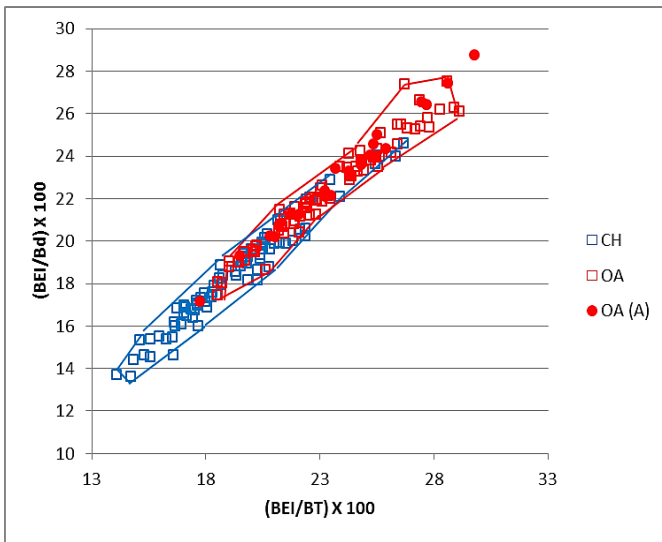


Figure 3.38 Ratio between the breadth of the epicondyle *lateralis* and the medio lateral width of the trochlea plotted against the ratio between the breadth of the epicondyle *lateralis* and the width of the distal end. Symbols explained in Fig. 3.9.

Radius

Figure 3.39 shows that, most of the archaeological sheep identified as such according to their morphology, are consistent with the sheep cluster, falling among the modern sheep or in the area of overlap. Only one specimen, plotting at the top of the graph among the modern goat, is doubtful. In this case, morphological misidentification as well as individual variation could explain the phenomenon.

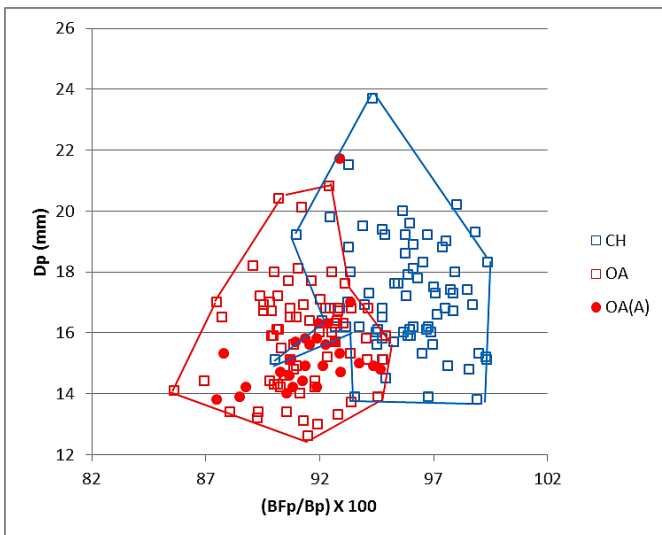


Figure 3.39 Ratio between the greatest length of the *facies articularis proximalis* and the greatest breadth of the proximal end plotted against the depth of the proximal end. Symbols explained in Fig. 3.9.

Ulna

Most of the archaeological sheep fall among the modern sheep group (Fig. 3.40), confirming the morphological identification. Two archaeological sheep are outliers at the left bottom corner of the graph: they appear to have very pronounced sheep characteristics. The unidentified specimens, as they fall in the area of overlap, cannot be confidently attributed to species.

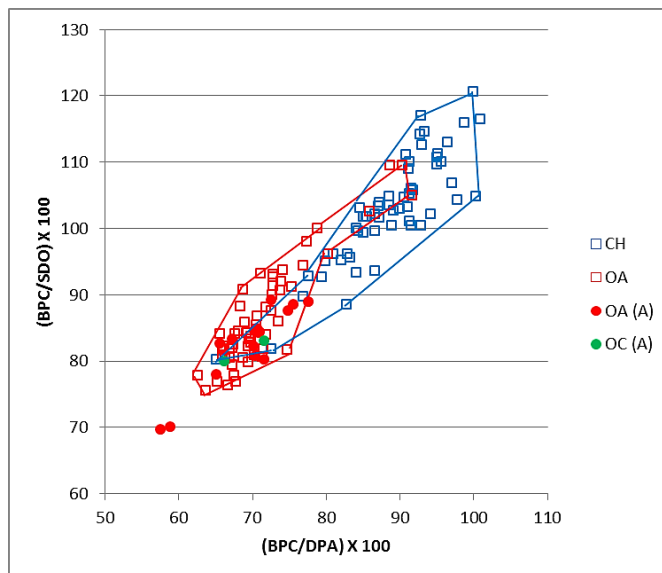


Figure 3.40 Ratio between the breadth across the coronoid process and the depth across the *processus anconaeus* to the caudal border plotted against the breadth across the coronoid process and the smallest depth of the olecranon. Symbols explained in Fig. 3.9.

Metapodials

More complete metapodials were available for this phase, so that an additional ratio could be used. As can be seen in Figures 3.41 to 3.46, no archaeological metapodials were assigned to goat. This identification is largely confirmed by the biometrical data though two ‘sheep’ specimens fall within the goat cluster in Figure 3.42. Because that the lateral condyle is less effective in separating the two species (Payne 1969; Rowley-Conwy 1998) and specimens do not plot far from the archaeological sheep cluster, the evidence is not strong enough for them to be considered misidentified. Their correct attribution to the sheep is also supported by the diagrams that use the overall bone length as one of the variables (Figures 3.43 and 3.46).

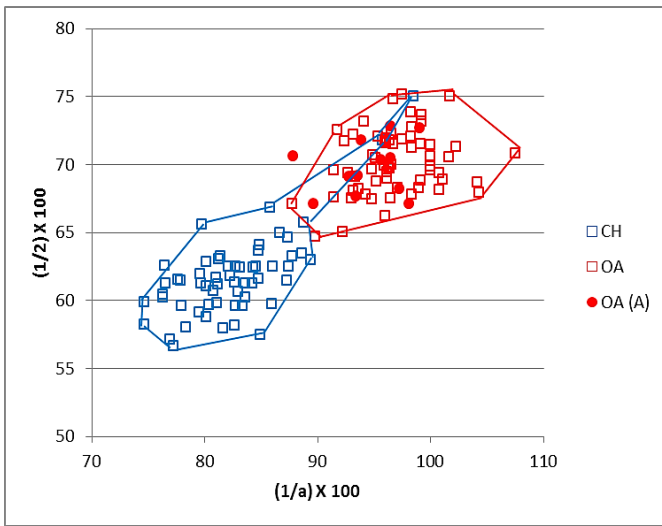


Figure 3.41 Metacarpal. Ratio between the diameter of the medial trochlea and the width of the medial condyle plotted against the ratio between the diameter of the *verticillus* at the medial condyle and the diameter of the medial trochlea. Symbols explained in Fig. 3.9.

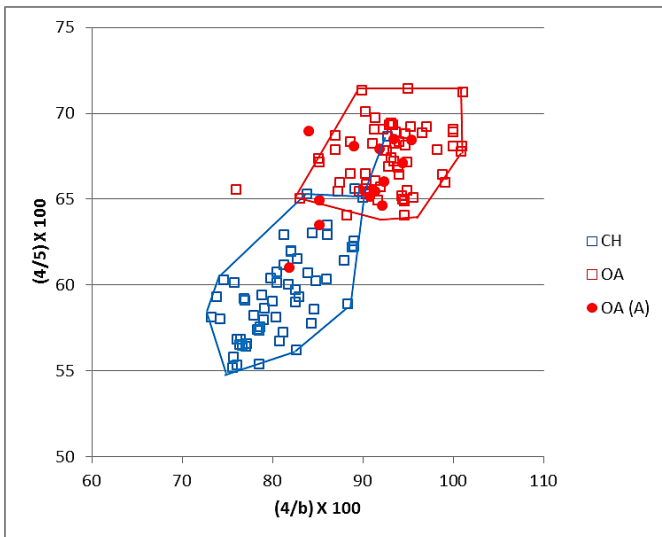


Figure 3.42 Metacarpal. Ratio between the width of the lateral condyle and the diameter of the lateral trochlea plotted against the ratio between the diameter of the *verticillus* the lateral condyle and the diameter of the lateral condyle. Symbols explained in Fig. 3.9.

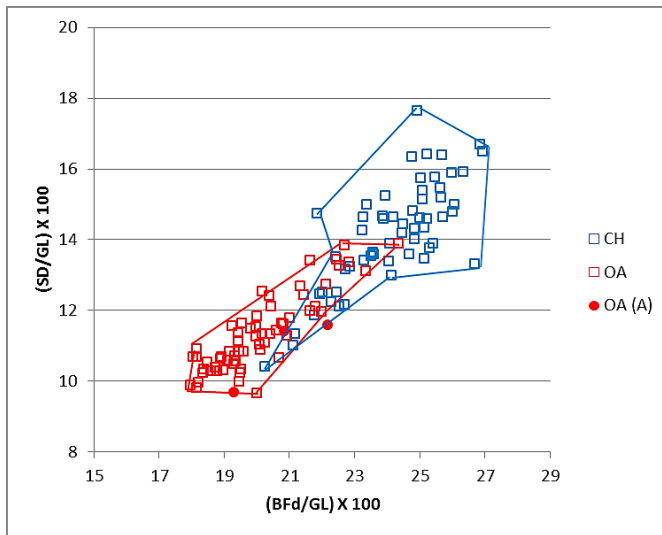


Figure 3.43 Metacarpal. Ratio between the greatest breadth of the distal end with the greatest length plotted against the ratio between the smallest width of the shaft and the greatest length. Symbols explained in Fig. 3.9.

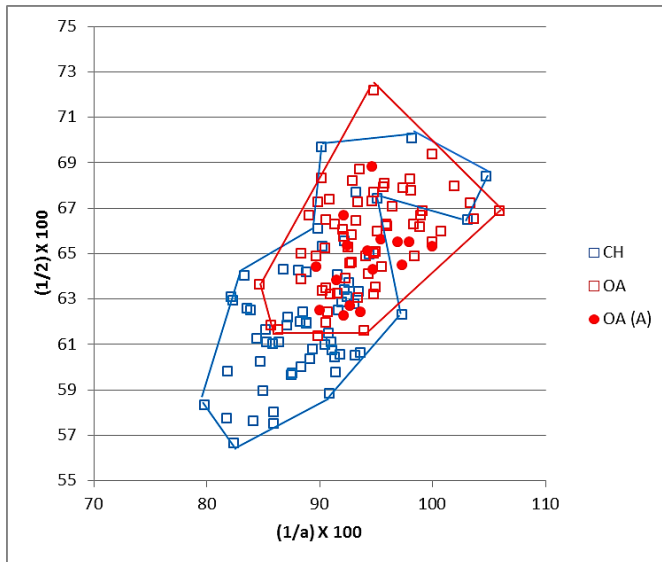


Figure 3.44 Metatarsal. Ratio between the diameter of the medial trochlea and the width of the medial condyle plotted against the ratio between the diameter of the *verticillus* at the medial condyle and the diameter of the medial trochlea. Symbols explained in Fig. 3.9.

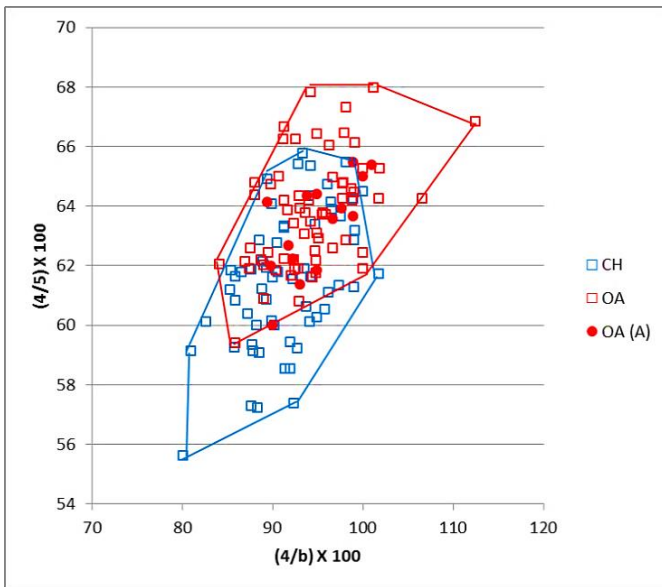


Figure 3.45 Metatarsal. Ratio between the width of the lateral condyle and the diameter of the lateral trochlea plotted against the ratio between the diameter of the *verticillus* on the lateral condyle and the diameter of the lateral condyle. Symbols explained in Fig. 3.9.

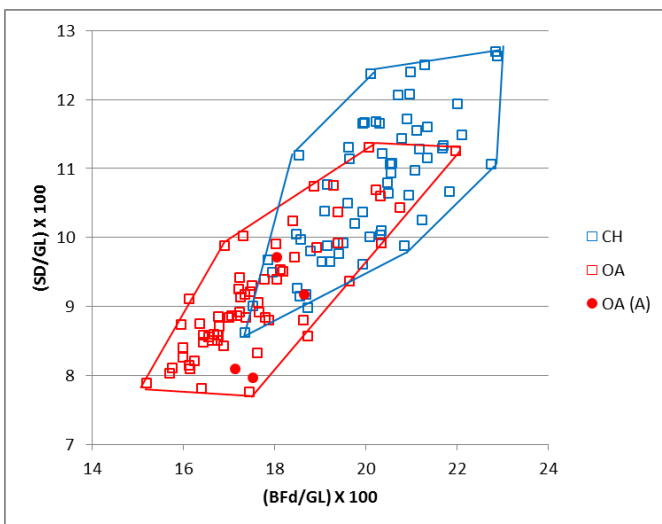


Figure 3.46 Metatarsal. Ratio between the greatest breadth of the distal end with the greatest length plotted against the ratio between the smallest width of the shaft and the greatest length. Symbols explained in Fig. 3.9.

Tibia

No goat archaeological tibiae have been identified according to their morphology. Figure 3.47 shows that the majority of the archaeological sheep fall among the modern counterparts or in the area of overlap, as such they are consistent with the morphological identification. The unidentified specimens, even though they seem to be more consistent with the sheep pattern, cannot be confidently attributed to species level as they fall in the area of overlap. One archaeological sheep plots among the modern goat group; it lies sufficiently distant from the archaeological sheep cluster for the morphological identification to be questioned.

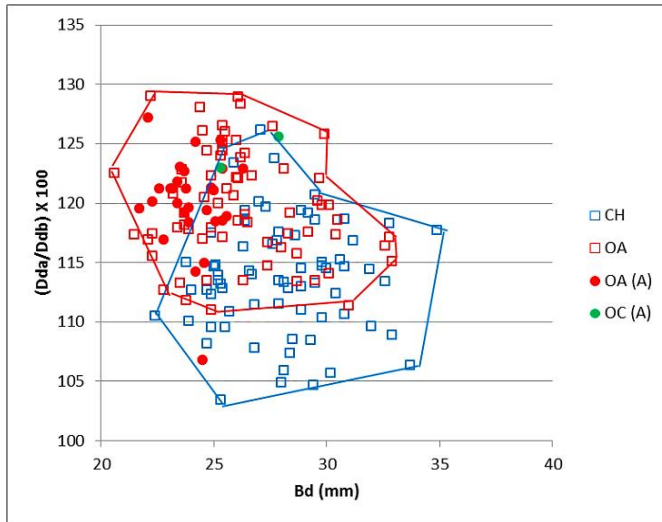


Figure 3.47 Breadth of the distal end plotted against the ratio between the depth of the medial (a) and lateral (b) side. Symbols explained in Fig. 3.9.

Astragalus

Figures 3.48 to 3.51 show the astragalus biometric ratios. No archaeological goats had been identified. Although most of the archaeological sheep specimens fall among the modern sheep group or in the area of overlap, two archaeological sheep specimens plot in the modern goat area (as in Figs. 3.48, 3.49 and 3.50). While they are not far from the sheep cluster, the fact that in all three diagrams they consistently plot with the goat group raises serious doubts on the morphologically-based identifications.

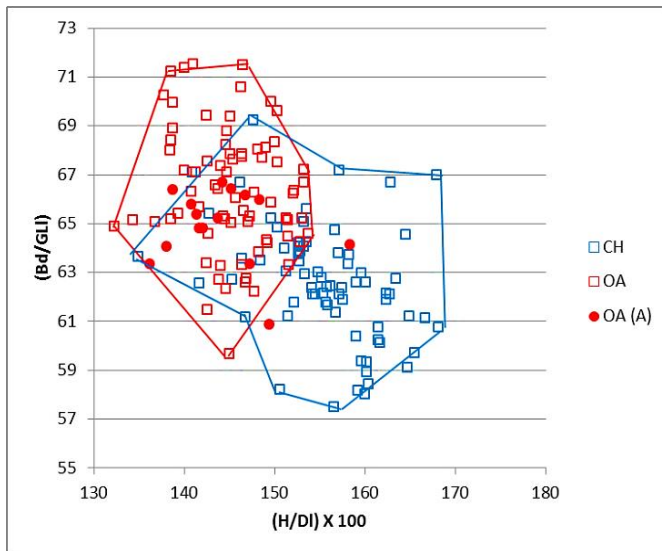


Figure 3.48 Ratio between height at the central constriction and the greatest depth of the lateral half plotted against a ratio between the breadth of the distal end and the greatest length of the lateral half. Symbols explained in Fig. 3.9.

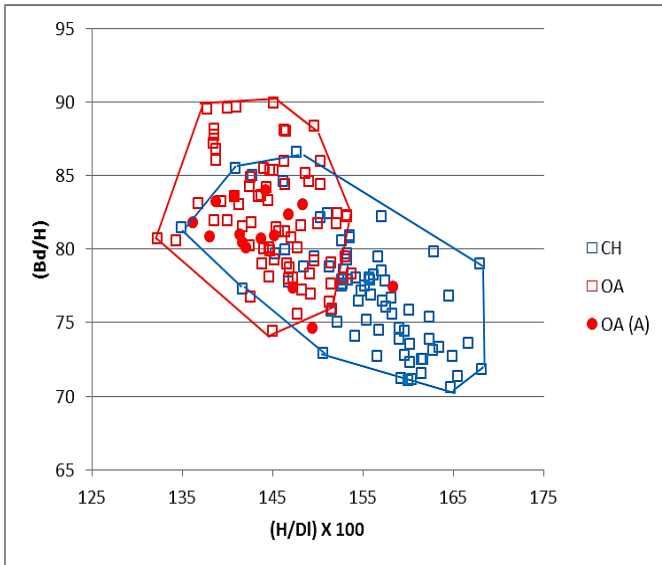


Figure 3.49 Ratio between height at the central constriction and the greatest depth of the lateral half plotted against the ratio between the breadth of the distal end and the height at the central constriction. Symbols explained in Fig. 3.9.

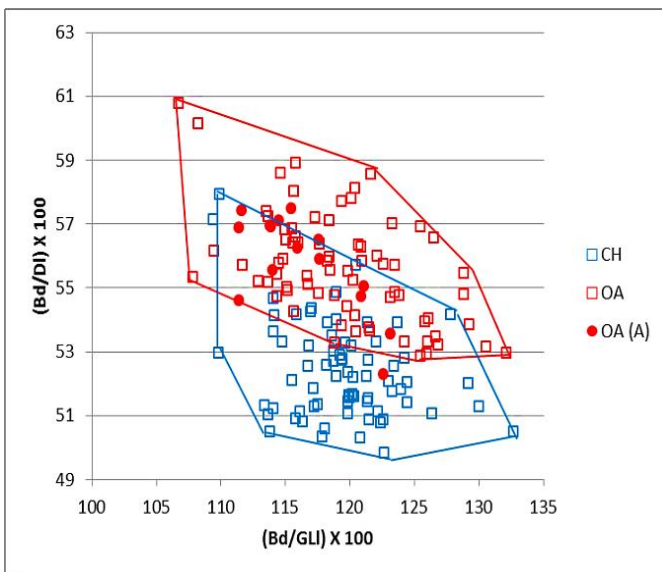


Figure 3.50 Ratio between breadth of the distal end and the greatest depth of the lateral half plotted against the ratio between the breadth of the distal end and the greatest depth of the lateral half. Symbols explained in Fig. 3.9.

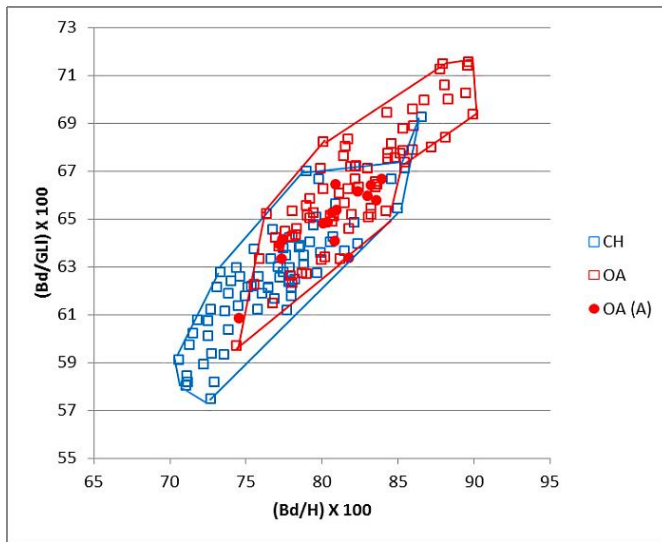


Figure 3.51 Ratio between the breadth of the distal end and the height at the central constriction and the ratio between height at the central constriction and the greatest depth of the lateral half. Symbols explained in Fig. 3.9.

Calcaneum

Figures 3.52 to 3.54 show different biometric ratios applied to the calcaneum. The biometry confirms the morphological identifications as the archaeological group consistently plots together with the modern sheep. In all diagrams one of the archaeological specimens plots as a rather extreme outlier. It has highly marked sheep characteristics; therefore its taxonomic identification is not in doubt.

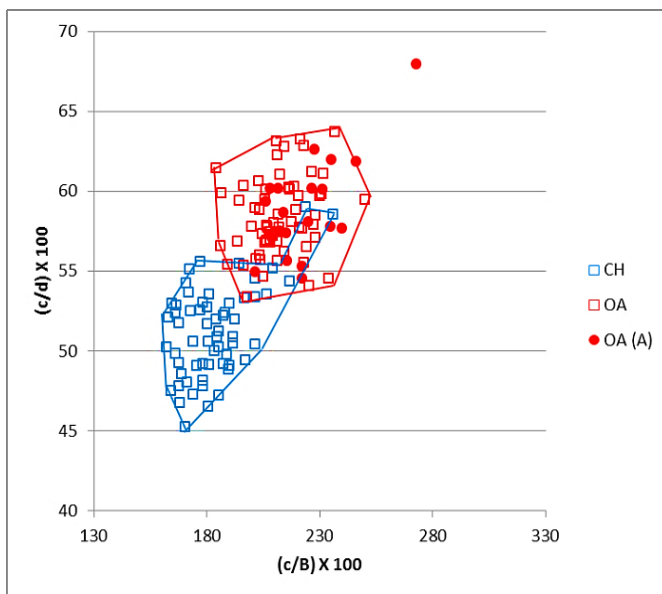


Figure 3.52 Ratio between the length and the breadth of the articular facet of the *os malleolare* plotted against the ratio between the length of the articular facet of the *os malleolare* and the length taken from the articular facet of the *os malleolare* to the end of the articulation-free part of the process. Symbols explained in Fig. 3.9.

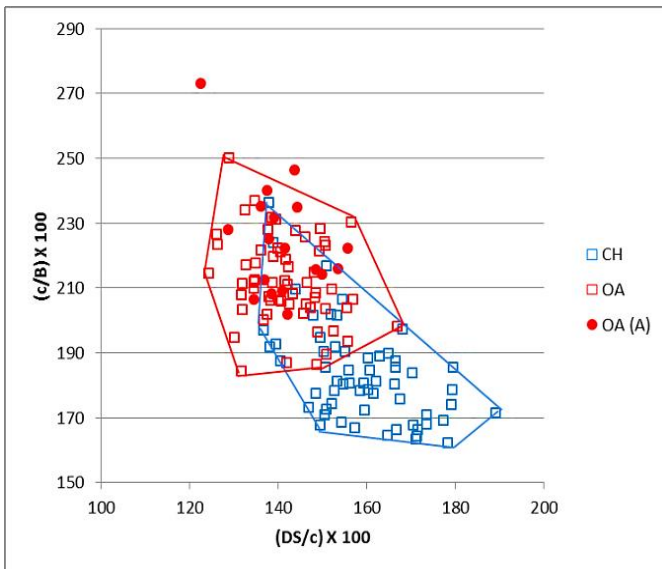


Figure 3.53 Ratio between the depth of the *subtentaculum tali* and the length of the articular facet of the *os malleolare* plotted against the ratio between the length and the breadth of the articular facet of the *os malleolare*. Symbols explained in Fig. 3.9.

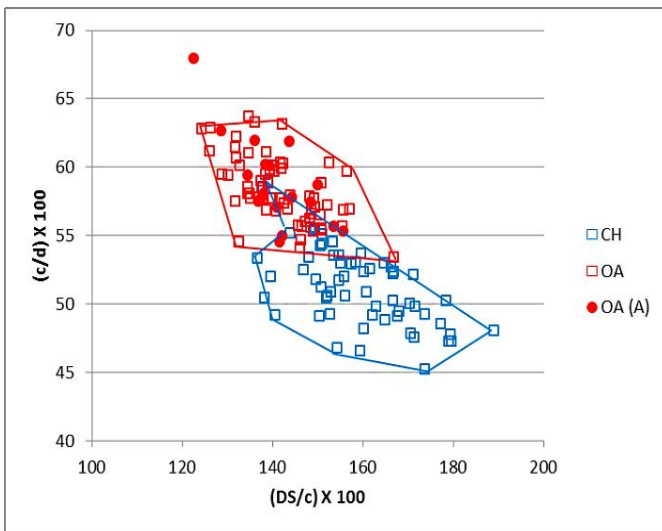


Figure 3.54 Ratio between the depth of the *subtentaculum tali* and the length of the articular facet of the *os malleolare* plotted against the ratio between the length and the breadth of the articular facet of the *os malleolare*. Symbols explained in Fig. 3.9.

Phase III

Horncore

Biometry confirms the morphological identifications when the ratios for the horncores are considered. The archaeological goats fall among the modern counterparts or in the area of overlap between the two species, while the archaeological sheep fall among the sheep modern group (Figs. 3.55 and 3.56). The separation of the archaeological goats into two clusters is less clear than in previous phases (Figure 3.55), but it is still possible that the five specimens on the

left are females and the five on the right hand side are males/castrates. Figure 3.56 shows a few archaeological border-line goats but, as they follow clearly the goat pattern in Figure 3.55 the identification is probably save.

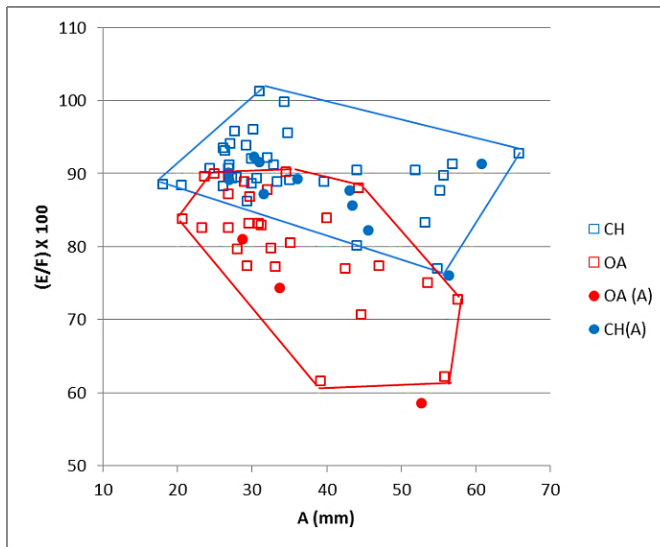


Figure 3.55 Maximum diameter taken at the base plotted against a ratio between the length and the length of the outer curvature of the horncore. Symbols explained in Fig. 3.9.

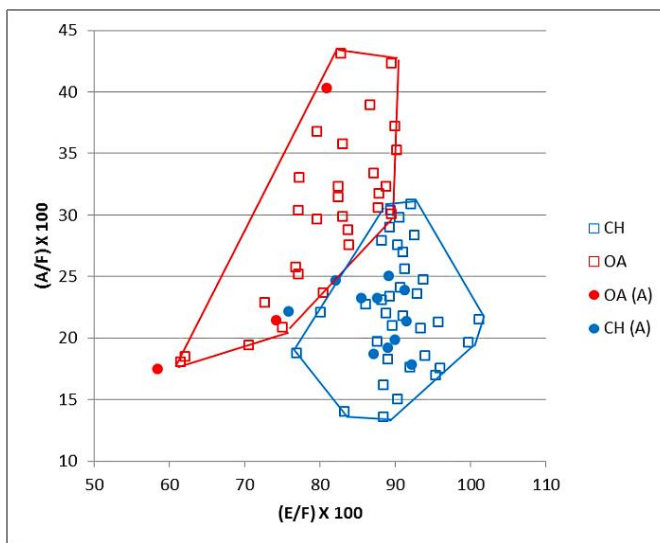


Figure 3.56 Ratio between the length and the length of the outer curvature plotted against the ratio between the maximum diameter taken at the base and the length of the outer curvature of the horncore. Symbols explained in Fig. 3.9.

Scapula

No goat scapulae were identified morphologically. Figures 3.57 and 3.58 show that all the archaeological sheep fall among the modern sheep cluster or in the overlap area between the two species; therefore, they are consistent with the morphological identifications.

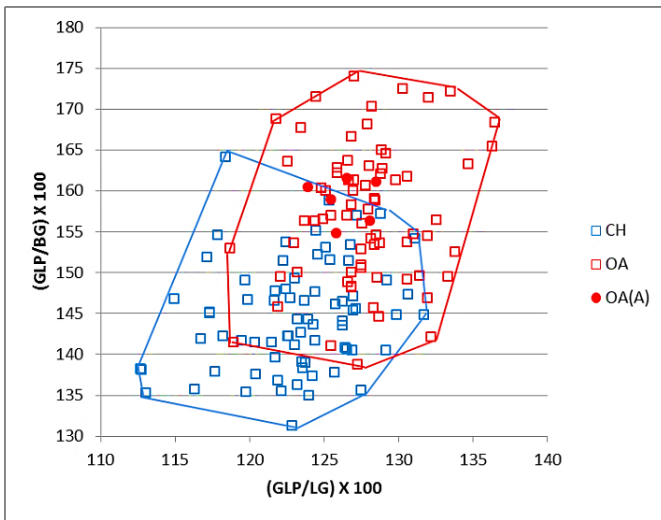


Figure 3.57 Ratio between the greatest length of the *processus articularis* and the length of the glenoid cavity plotted against the ratio between the greatest length of the *processus articularis* and the breadth of the glenoid cavity. Symbols explained in Fig. 3.9.

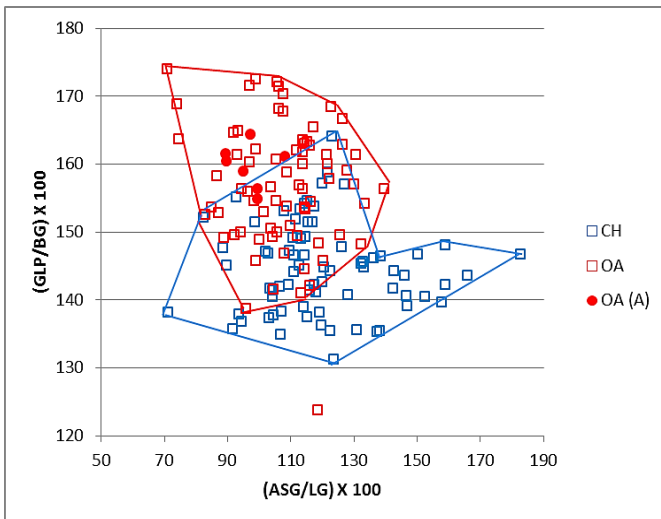


Figure 3.58 Ratio between the shortest distance from the base of the spine to the edge of the glenoid cavity and the smallest length of the *collum scapulae* plotted against the ratio between the greatest length of the *processus articularis* and the breadth of the glenoid cavity. Symbols explained in Fig. 3.9.

Humerus

No archaeological humeri were attributed to goat. Figures 3.59 to 3.62 show that all the archaeological sheep fall among the modern sheep group or in the area of overlap between the two species, confirming the morphological identifications. One specimen that could not be identified morphologically, plots in the area of overlap in Figures 3.60 and 3.61, but in the goat area in Figure 3.62, therefore it probably represents a goat.

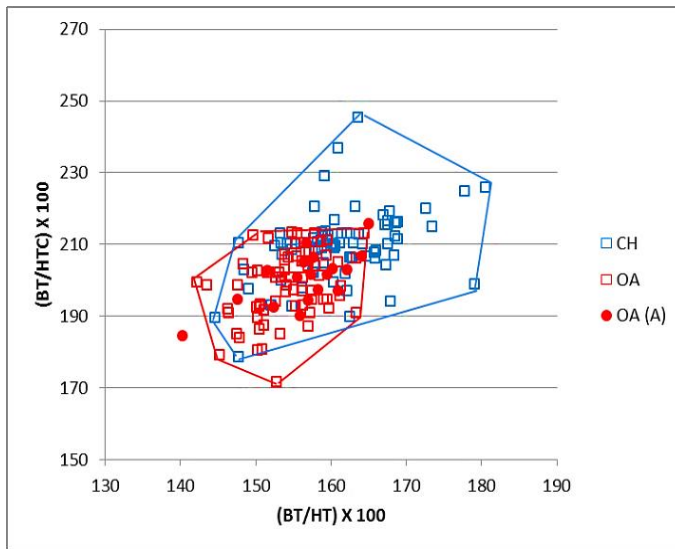


Figure 3.59 Ratio between the medio lateral width of the trochlea and its height plotted against the medio lateral width of the trochlea and the diameter of the trochlear constriction. Symbols explained in Fig. 3.9.

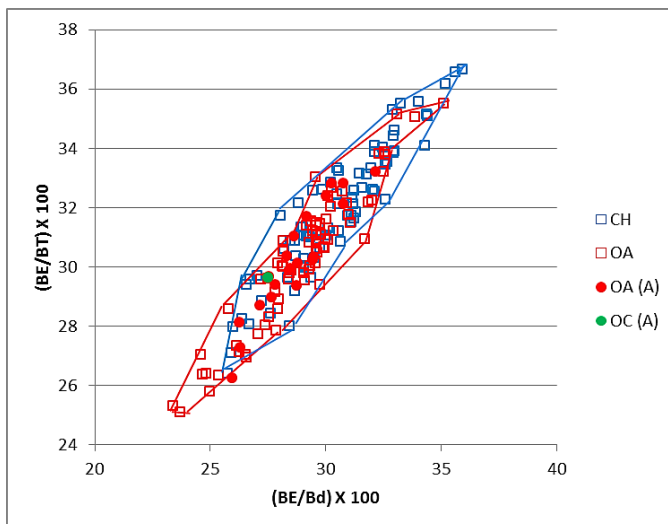


Figure 3.60 Ratio between the breadth of the *capitulum* and the distal width plotted against the ratio between the breadth of the *capitulum* and the medio lateral width of the trochlea. Symbols explained in Fig. 3.9.

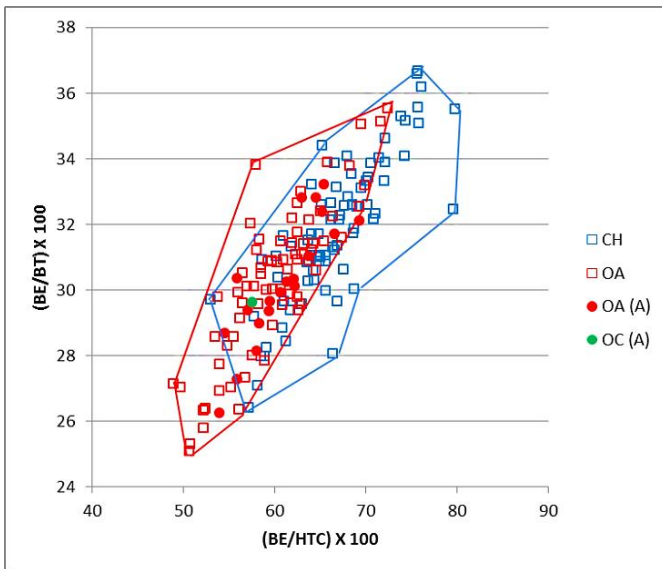


Figure 3.61 Ratio between the breadth of the *capitulum* and the diameter of the trochlear constriction plotted against the ratio between the breadth of the *capitulum* and the medio lateral width of the trochlea. Symbols explained in Fig. 3.9.

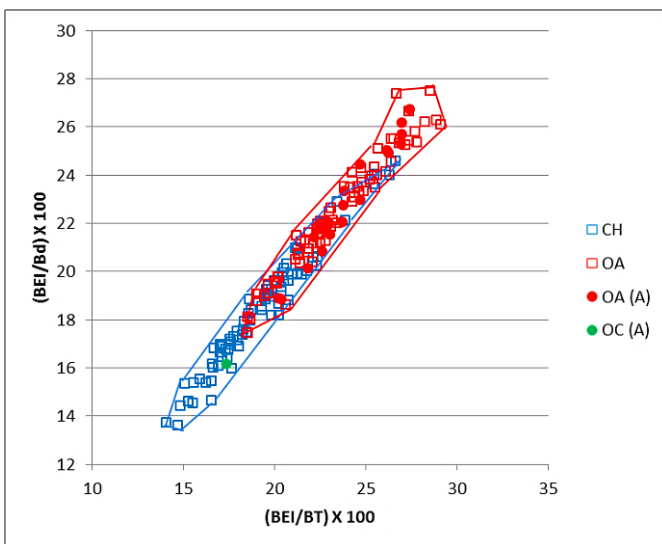


Figure 3.62 Ratio between the breadth of the *epicondyle lateralis* and the medio lateral width of the trochlea plotted against the ratio between the breadth of the *epicondyle lateralis* and the width of the distal end. Symbols explained in Fig. 3.9.

Radius

Only one radius was attributed to goat on the basis of its morphology while all the other specimens were identified as sheep. Figure 3.63 shows that biometry confirms the morphological identifications as the archaeological goat falls amongst the modern goat group and the archaeological sheep amongst the modern sheep or in the area of overlap.

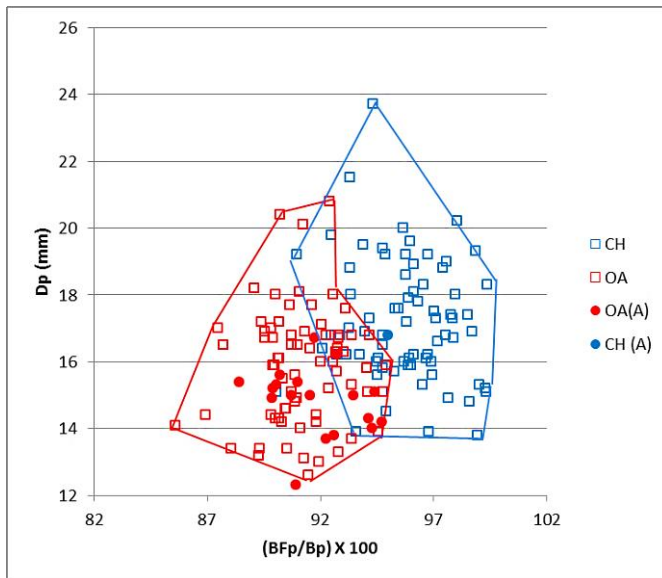


Figure 3.63 Ratio between the greatest length of the *facies articularis proximalis* and the greatest breadth of the proximal end plotted against the depth of the proximal end. Symbols explained in Fig. 3.9.

Ulna

Only sheep archaeological species were identified. The agreement between biometrical and morphological identification is shown by Figure 3.64: all the archaeological sheep fall among the modern sheep or in the area of overlap, therefore they are consistent with the morphological identifications.

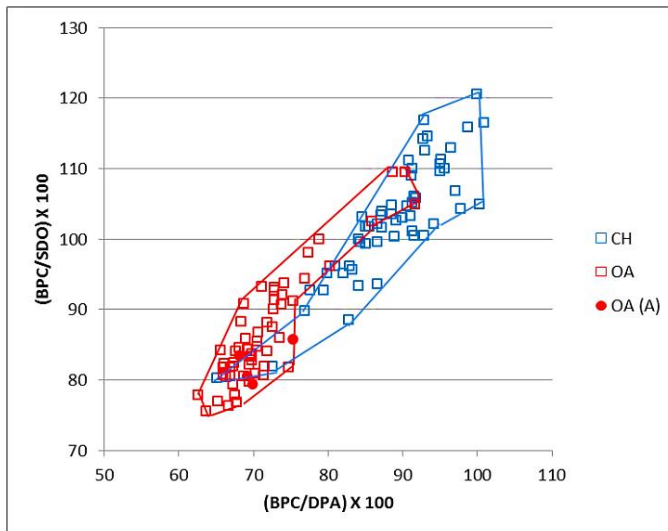


Figure 3.64 Ratio between the breadth across the coronoid process and the depth across the *processus anconaeus* to the caudal border plotted against the breadth across the coronoid process and the smallest depth of the olecranon. Symbols explained in Fig. 3.9.

Metapodials

No metatarsals but only metacarpals were found in phase III. Clear agreement is present once again, between the biometrical and the morphological identifications. Figures 3.65 to 3.67 show that in all biometric ratios the King's Lynn specimens consistently plot together with the modern sheep.

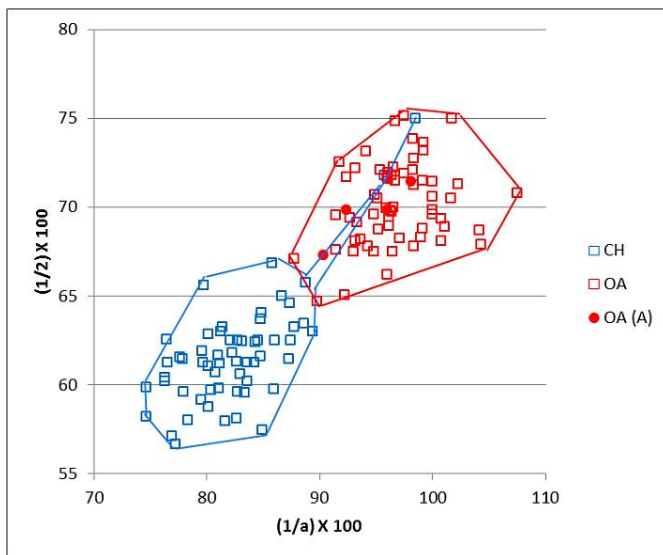


Figure 3.65 Metacarpal. Ratio between the diameter of the medial trochlea and the width of the medial condyle plotted against the ratio between the diameter of the *verticillus* at the medial condyle and the diameter of the medial trochlea. Symbols explained in Fig. 3.9.

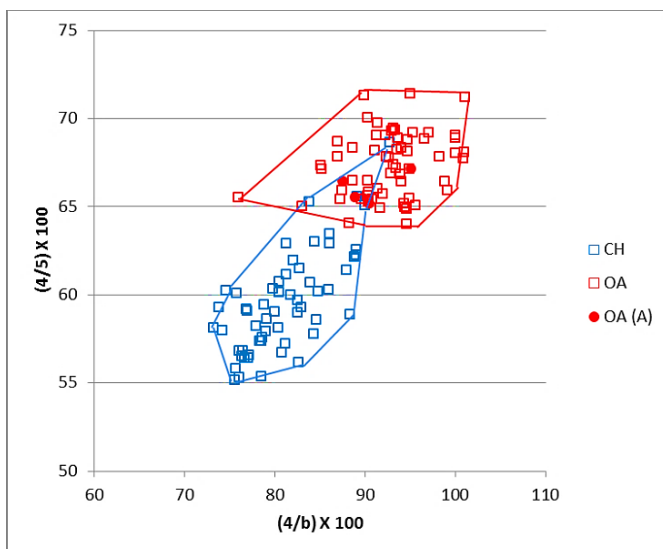


Figure 3.66 Metacarpal. Ratio between the width of the lateral condyle and the diameter of the lateral trochlea plotted against the ratio between the diameter of the *verticillus* on the lateral condyle and the diameter of the lateral condyle. Symbols explained in Fig. 3.9.

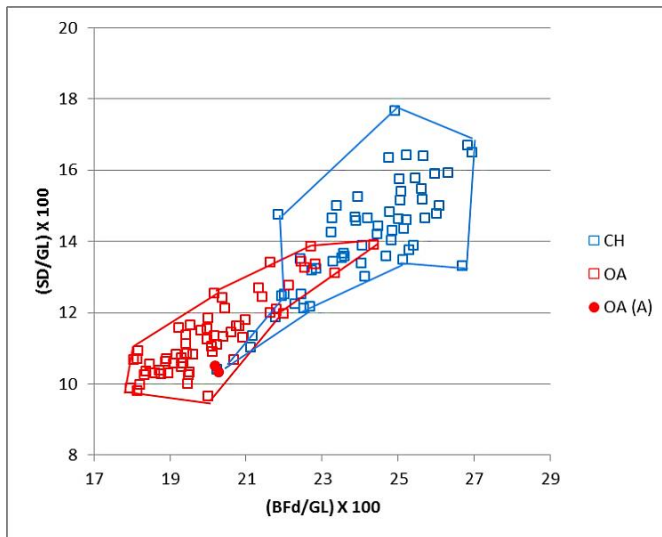


Figure 3.67 Metacarpal. Ratio between the greatest breadth of the distal end with the greatest length plotted against the ratio between the smallest width of the shaft and the greatest length. Symbols explained in Fig. 3.9.

Tibia

Only archaeological sheep tibiae have been identified and, as shown by Figure 3.68, they all fall among the modern sheep group and, only marginally, in the overlapping area of the two modern groups. As such, they are perfectly consistent with their morphological identifications.

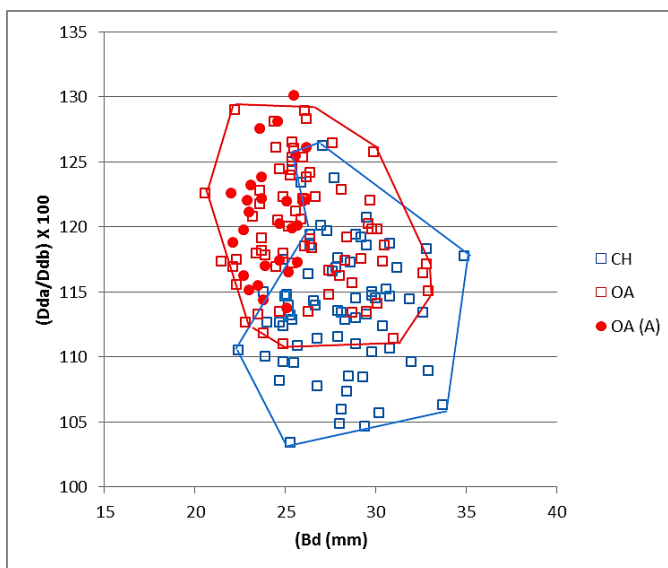


Figure 3.68 Breadth of the distal end plotted against the ratio between the depth of the medial (a) and lateral (b) side. Symbols explained in Fig. 3.9.

Astragalus

No archaeological goats have been morphologically identified, but only sheep. Figures 3.69 to 3.72 confirm, with the use of different ratios, the identification of the archaeological specimens as sheep, since they all fall among the modern sheep cluster or in the area of overlap between the two species.

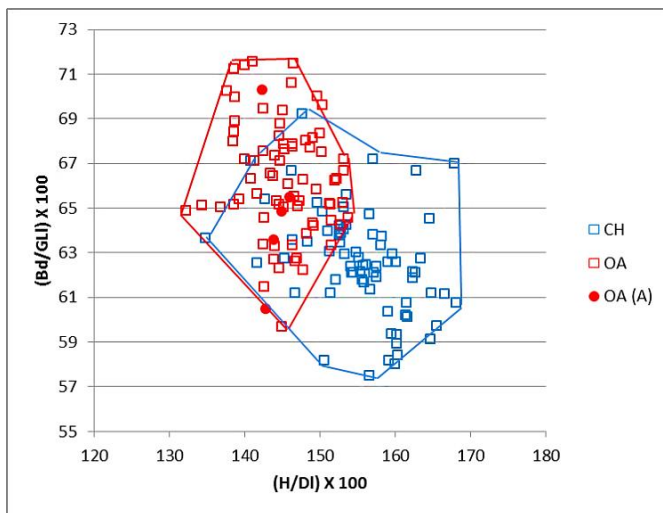


Figure 3.69 Ratio between height at the central constriction and the greatest depth of the lateral half plotted against a ratio between the breadth of the distal end and the greatest length of the lateral half. Symbols explained in Fig. 3.9.

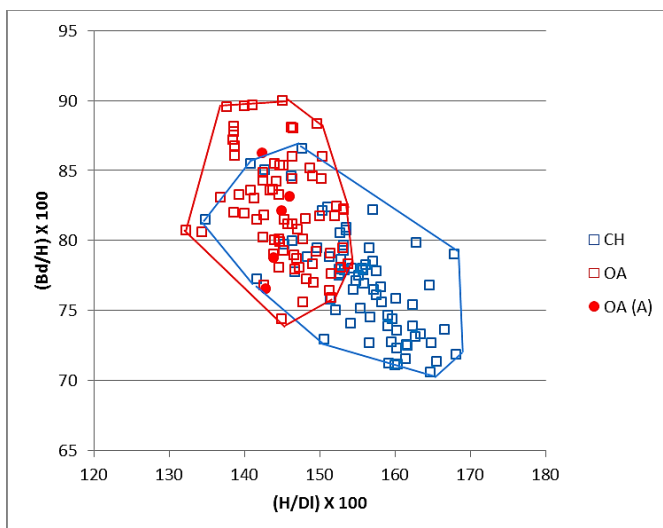


Figure 3.70 Ratio between height at the central constriction and the greatest depth of the lateral half plotted against the ratio between the breadth of the distal end and the height at the central constriction. Symbols explained in Fig. 3.9.

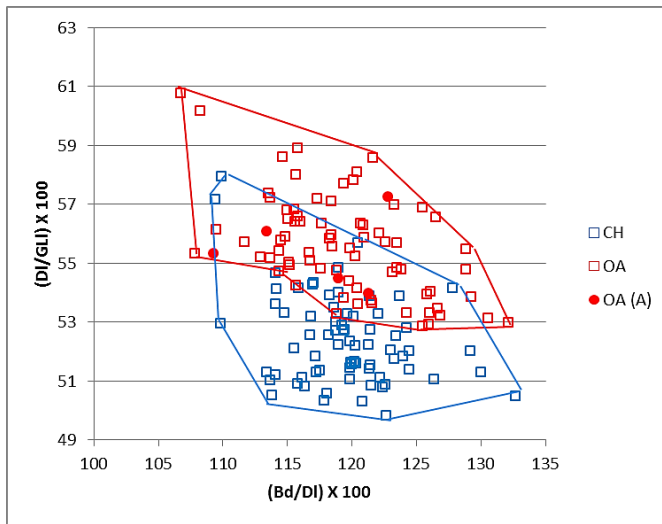


Figure 3.71 Ratio between breadth of the distal end and the greatest depth of the lateral half plotted against the ratio between the breadth of the distal end and the greatest depth of the lateral half. Symbols explained in Fig. 3.9.

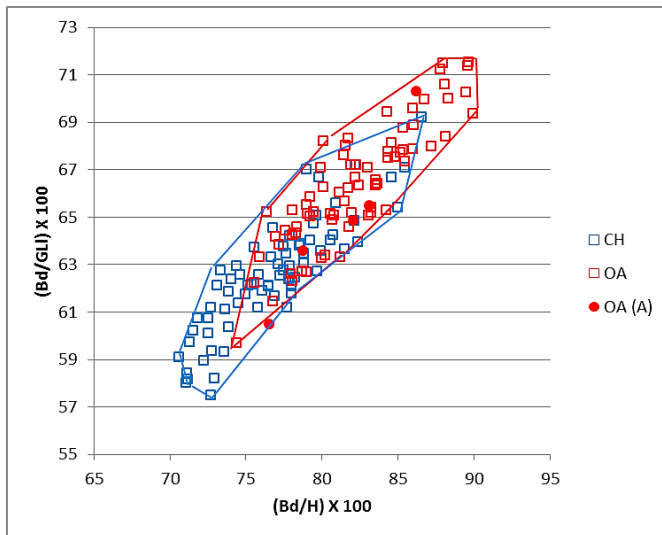


Figure 3.72 Ratio between the breadth of the distal end and the height at the central constriction and the ratio between height at the central constriction and the greatest depth of the lateral half. Symbols explained in Fig. 3.9.

Calcaneum

No goat calcanea were identified morphologically. Figures 3.73 to 3.75 show that this identification is confirmed by the biometrical data: all the archaeological sheep lie amongst the modern sheep or in the area of overlap between the two modern groups.

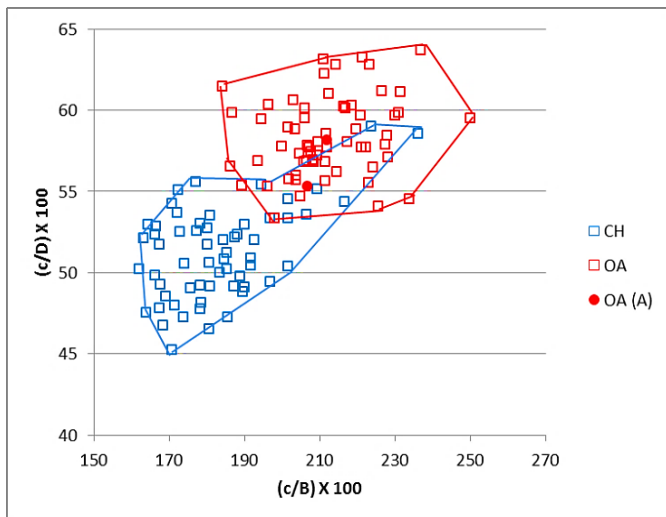


Figure 3.73 Ratio between the length and the breadth of the articular facet of the *os malleolare* plotted against the ratio between the length of the articular facet of the *os malleolare* and the length taken from the articular facet of the *os malleolare* to the end of the articulation-free part of the process. Symbols explained in Fig. 3.9.

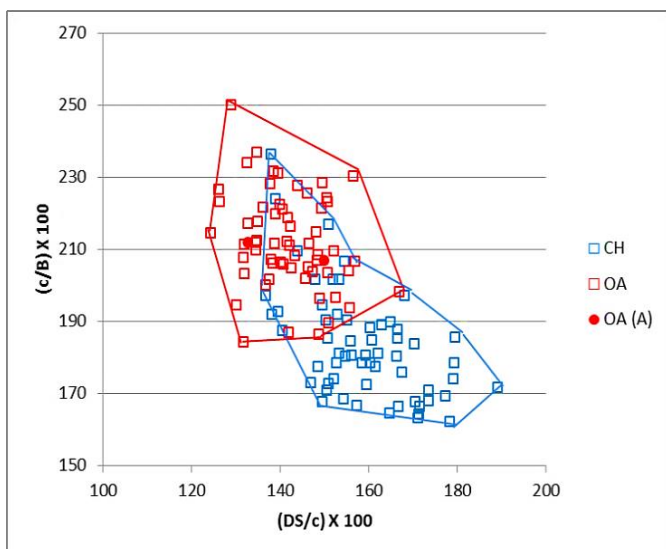


Figure 3.74 Ratio between the depth of the *substantaculum tali* and the length of the articular facet of the *os malleolare* plotted against the ratio between the length and the breadth of the articular facet of the *os malleolare*. Symbols explained in Fig. 3.9.

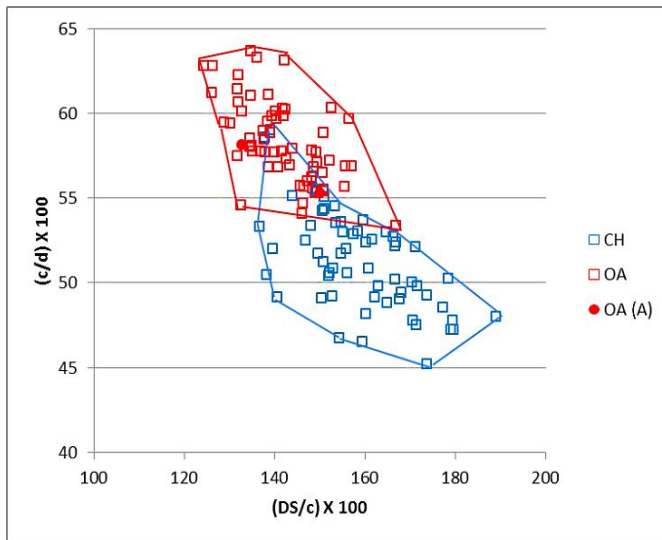


Figure 3.75 Ratio between the depth of the *subtentaculum tali* and the length of the articular facet of the *os malleolare* plotted against the ratio between the length and the breadth of the articular facet of the *os malleolare*. Symbols explained in Fig. 3.9.

Phase IV

Horncore

Figures 3.76 and 3.77 attest very clearly that biometry confirms the identification assessed through the morphology: two archaeological groups, sheep and goats, can be identified and they both fall in the areas where the modern counterparts are, without any overlap.

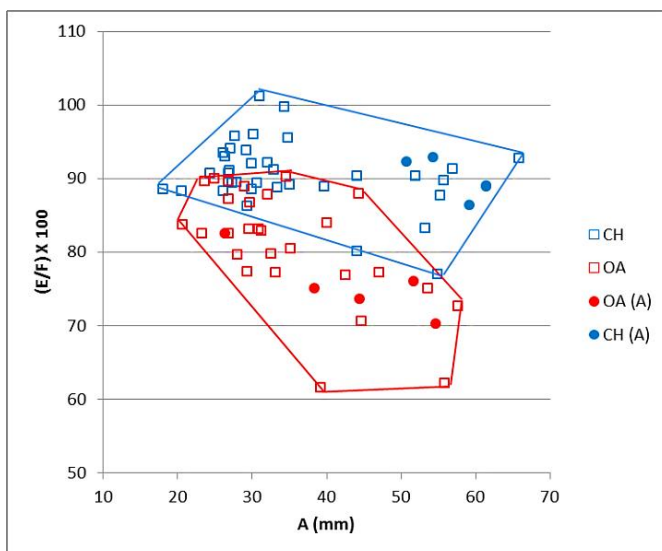


Figure 3.76 Maximum diameter taken at the base plotted against a ratio between the length and the length of the outer curvature of the horncore. Symbols explained in Fig. 3.9.

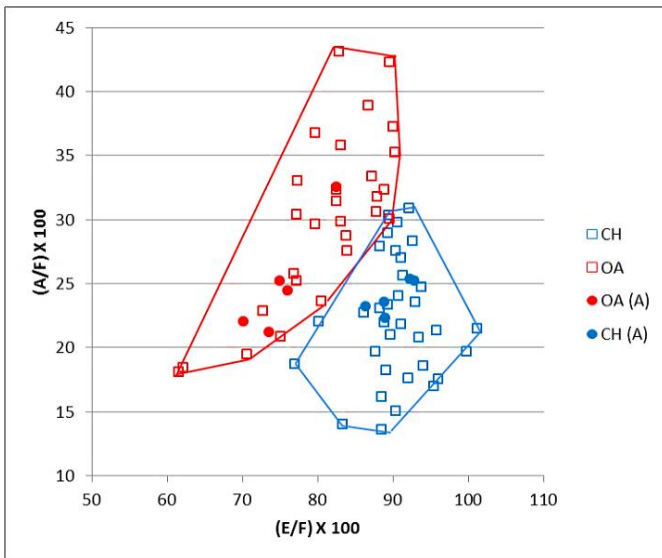


Figure 3.77 Ratio between the length and the length of the outer curvature plotted against the ratio between the maximum diameter taken at the base and the length of the outer curvature of the horncore. Symbols explained in Fig. 3.9.

Scapula

No archaeological goats were identified morphologically. Figures 3.78 and 3.79 show that most archaeological specimens fall among the modern sheep or in the area of overlap. A marginal outlier is present in both diagrams, having strongly marked sheep characteristics.

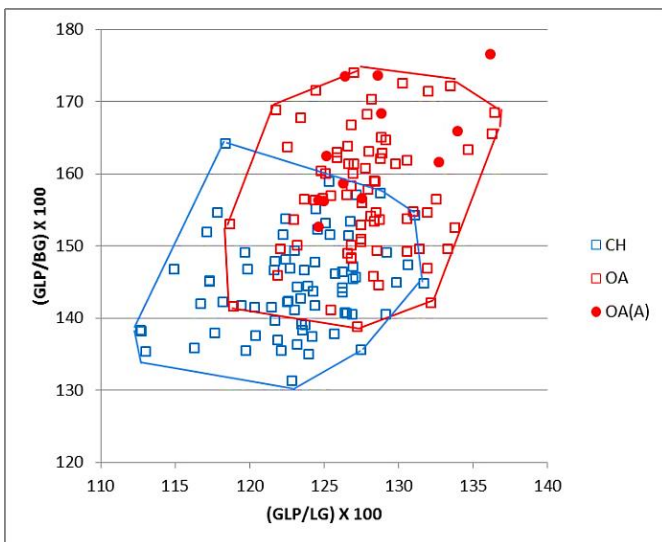


Figure 3.78 Ratio between the greatest length of the *processus articularis* and the length of the glenoid cavity plotted against the ratio between the greatest length of the *processus articularis* and the breadth of the glenoid cavity. Symbols explained in Fig. 3.9.

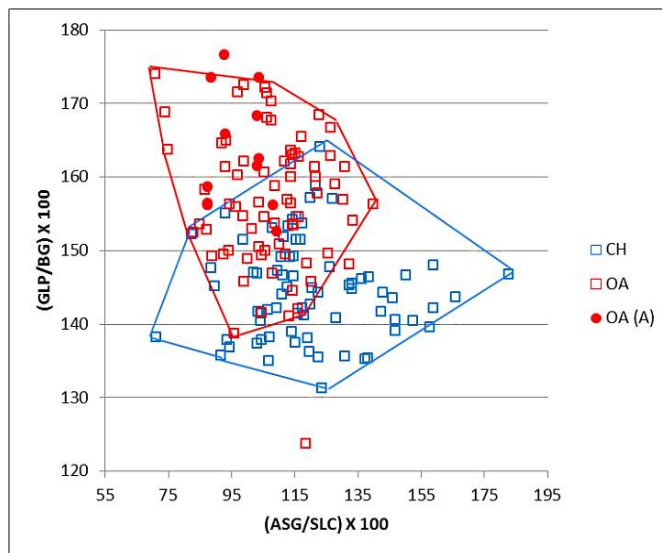


Figure 3.79 Ratio between the shortest distance from the base of the spine to the edge of the glenoid cavity and the smallest length of the *collum scapulae* plotted against a ratio between the greatest length of the *processus articularis* and the breadth of the glenoid cavity plotted against the ratio between. Symbols explained in Fig. 3.9.

Humerus

All humeri were assigned, on the basis of their morphology, to sheep. Figures 3.80 to 3.83 show that the archaeological sheep specimens fall in the area of the graph where the modern sheep specimens lie, or in the overlap area. As such, they are consistent with their identifications. One archaeological specimen, however, plots away from the main cluster in Figures 3.81 and 3.82. It would therefore appear to be more consistent with a goat, but the fact that the other ratios (Figs. 3.80 and 3.83) do not follow the same trend and the similarity of some modern sheep to this particular specimen, do not give sufficient confidence for its re-identification. It is safer to regard it as an uncertain ‘sheep/goat’.

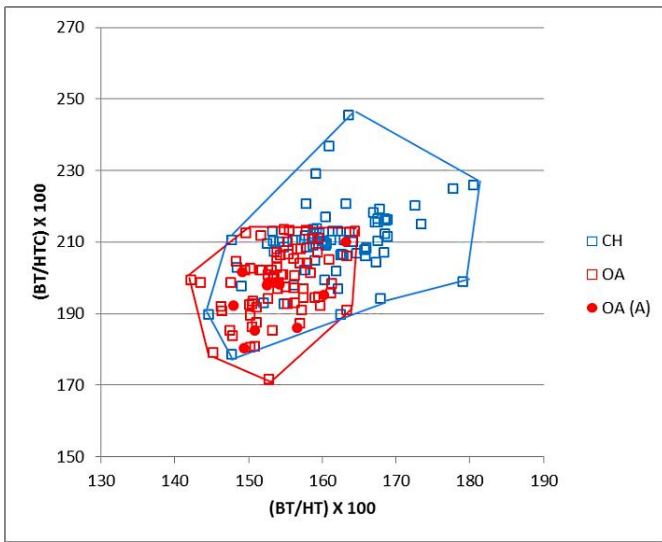


Figure 3.80 Ratio between the medio lateral width of the trochlea and its height plotted against the medio lateral width of the trochlea and the diameter of the trochlear constriction. Symbols explained in Fig. 3.9.

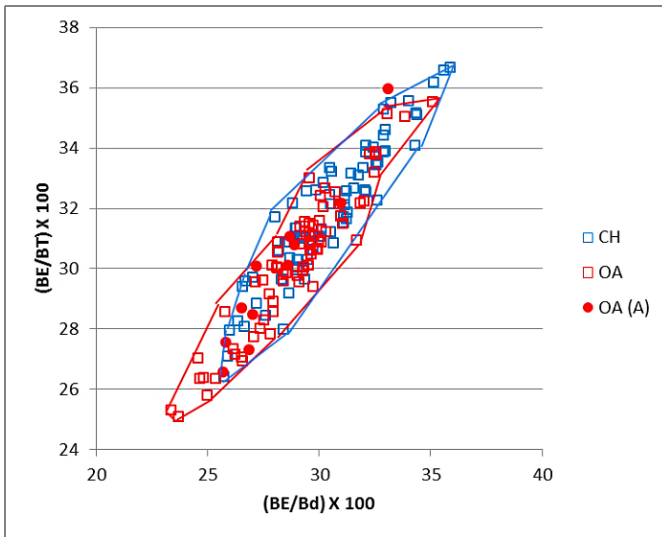


Figure 3.81 Ratio between the breadth of the *capitulum* and the distal width plotted against the ratio between the breadth of the *capitulum* and the medio lateral width of the trochlea. Symbols explained in Fig. 3.9.

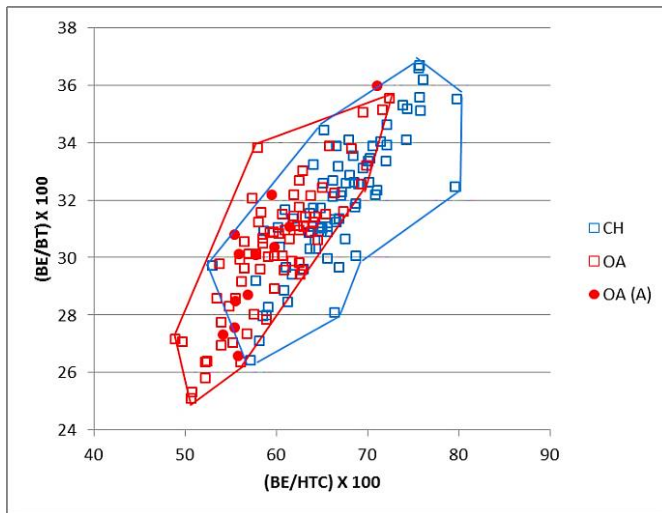


Figure 3.82 Ratio between the breadth of the *capitulum* and the diameter of the trochlear constriction plotted against the ratio between the breadth of the *capitulum* and the medio lateral width of the trochlea. Symbols explained in Fig. 3.9.

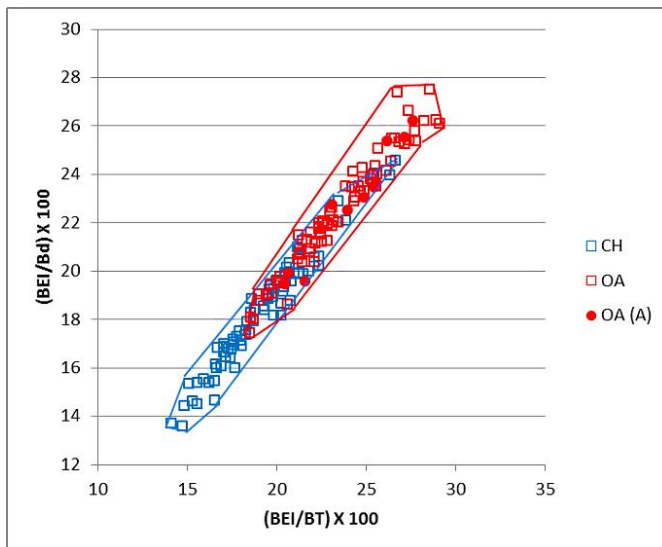


Figure 3.83 Ratio between the breadth of the *epicondyle lateralis* and the medio lateral width of the trochlea plotted against the ratio between the breadth of the *epicondyle lateralis* and the width of the distal end. Symbols explained in Fig. 3.9.

Radius

Figure 3.84 shows a phenomenon which has been noticed for the radius: no archaeological goats have been morphologically identified, nevertheless the biometry seems to suggest something different. Some archaeological sheep fall among the modern sheep group or in the area of overlap, as such their identification as sheep cannot be argued. However, a few other specimens plot rather closer to the goat group, raising doubts about their identification. While misidentification cannot be excluded, measurements of the proximal radius are known to be heavily age-related (in pigs, Bull and Payne 1988). The modern material represents a controlled

sample in terms of age (with only a very few old specimens); it may therefore be that the archaeological specimens come from older animals than those making up the modern sample; as such, they plot in a different area of the graph.

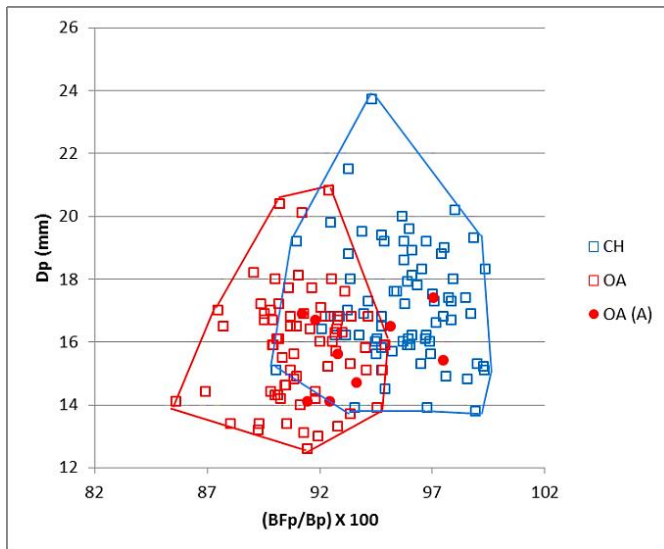


Figure 3.84 Ratio between the greatest length of the *facies articularis proximalis* and the greatest breadth of the proximal end plotted against the depth of the proximal end. Symbols explained in Fig. 3.9.

Ulna

Figure 3.85 shows that all the archaeological specimens plot in the same cluster at the ‘sheep end’ of the diagram, confirming the morphological interpretations. Two specimens in particular appear to have extreme sheep-like traits. Thus, biometry confirms the morphological identification. The only morphologically unidentified specimen is border-line but closer to the sheep cluster and therefore more likely to belong to this species.

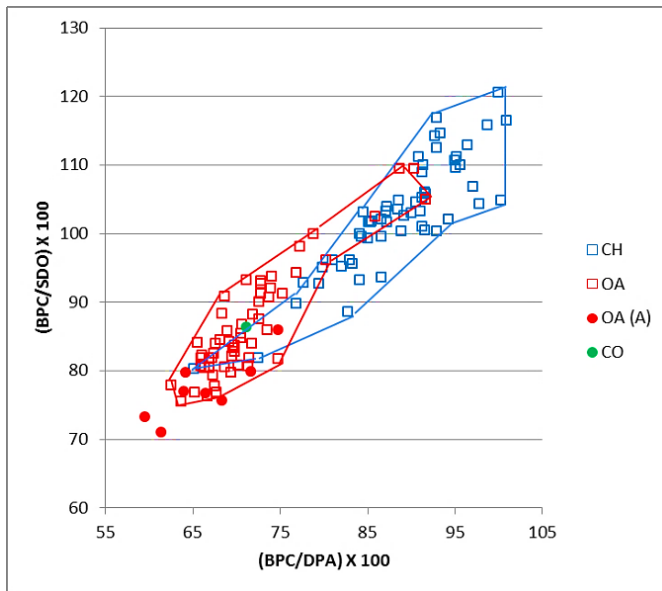


Figure 3.85 Ratio between the breadth across the coronoid process and the depth across the *processus anconaeus* to the caudal border plotted against the breadth across the coronoid process and the smallest depth of the olecranon. Symbols explained in Fig. 3.9.

Metapodials

No metapodials belonging to goat were identified morphologically. The biometry, as Figures 3.86 to 3.91 show, confirms such identification: almost all archaeological sheep fall among the modern sheep or in the area of overlap between the two species. In Figure 3.91 an archaeological sheep clearly plots among the modern goats, but in all other diagrams the specimen does not appear as an outlier. Given the inconsistency of the evidence it is safer to regard that specimen of uncertain attribution.

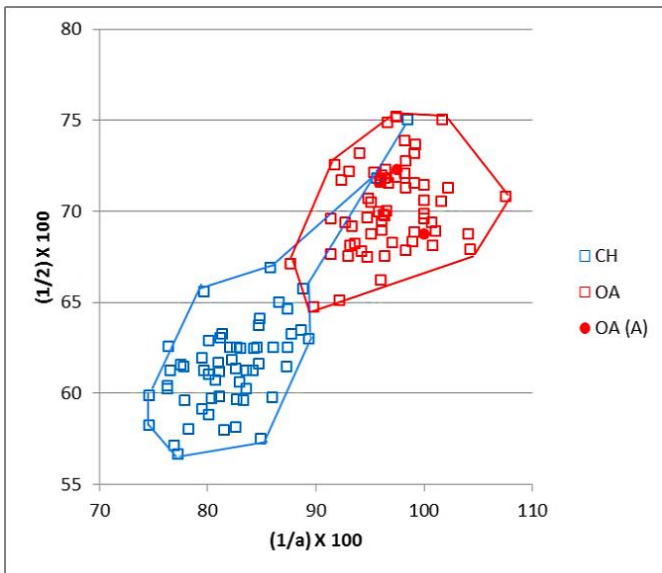


Figure 3.86 Metacarpal. Ratio between the diameter of the medial trochlea and the width of the medial condyle plotted against the ratio between the diameter of the *verticillus* at the medial condyle and the diameter of the medial trochlea. Symbols explained in Fig. 3.9.

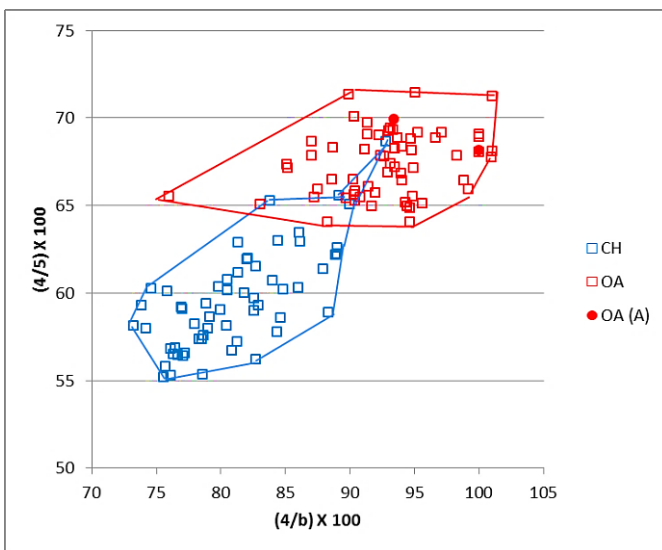


Figure 3.87 Metacarpal. Ratio between the width of the lateral condyle and the diameter of the lateral trochlea plotted against the ratio between the diameter of the *verticillus* on the lateral condyle and the diameter of the lateral condyle. Symbols explained in Fig. 3.9.

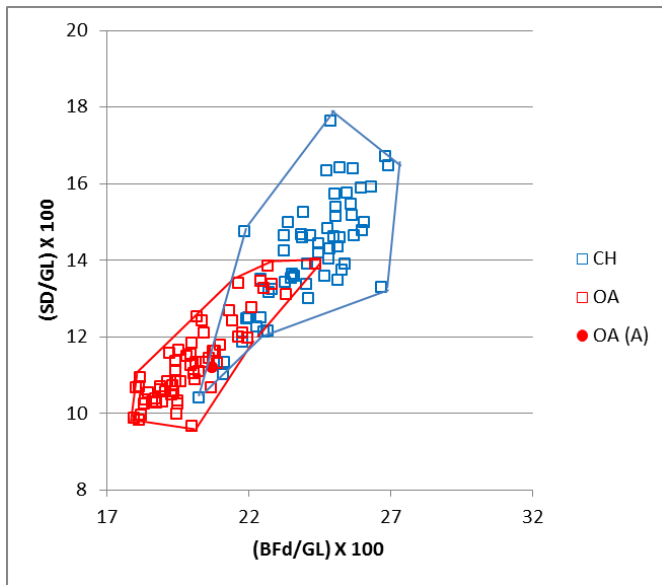


Figure 3.88 Metacarpal. Ratio between the greatest breadth of the distal end with the greatest length plotted against the ratio between the smallest width of the shaft and the greatest length. Symbols explained in Fig. 3.9.

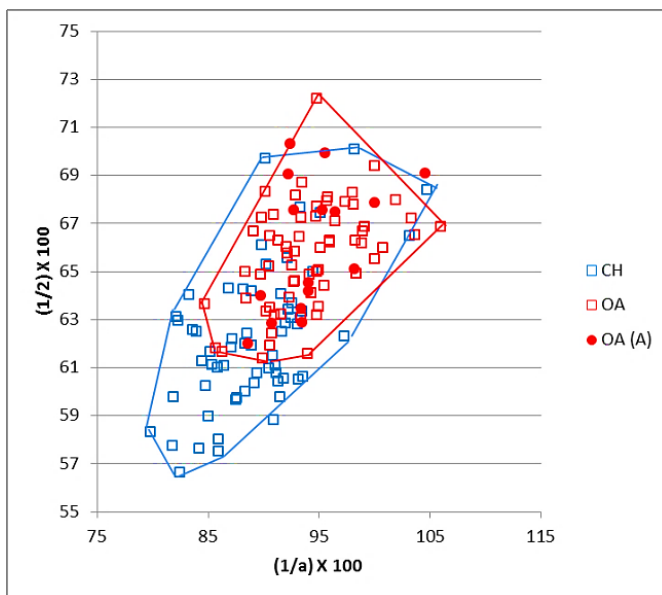


Figure 3.89 Metatarsal. Ratio between the diameter of the medial trochlea and the width of the medial condyle plotted against the ratio between the diameter of the *verticillus* at the medial condyle and the diameter of the medial trochlea. Symbols explained in Fig. 3.9.

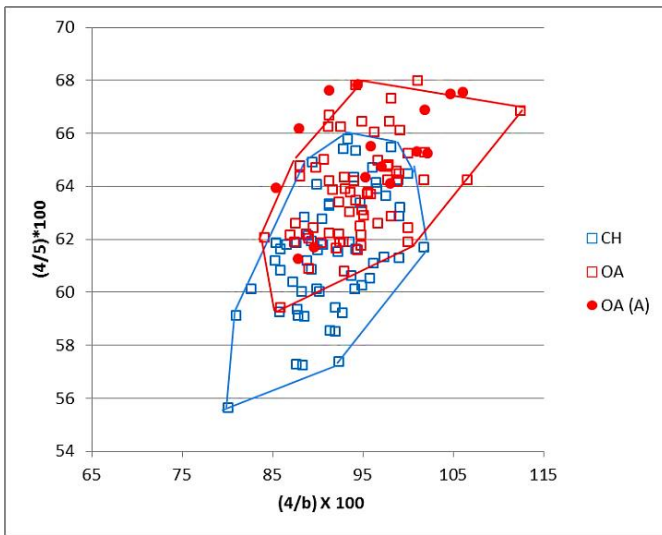


Figure 3.90 Metatarsal. Ratio between the width of the lateral condyle and the diameter of the lateral trochlea plotted against the ratio between the diameter of the *verticillus* on the lateral condyle and the diameter of the lateral condyle. Symbols explained in Fig. 3.9.

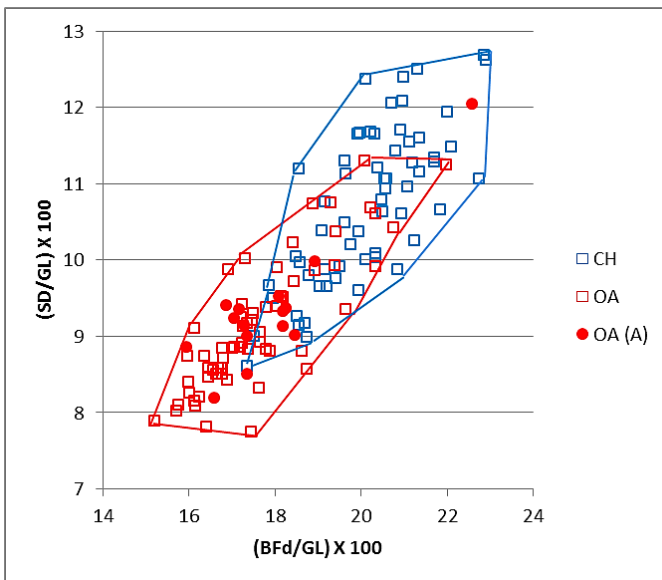


Figure 3.91 Metatarsal. Ratio between the greatest breadth of the distal end with the greatest length plotted against the ratio between the smallest width of the shaft and the greatest length. Symbols explained in Fig. 3.9.

Tibia

Figure 3.92 shows the ratios applied for the distal tibia. No archaeological goats were identified morphologically. The archaeological sheep fall among the modern sheep group or in the area of overlap between the modern specimens, as such their identification is confirmed by the biometry. Nothing can be said of the unidentified specimens, as they lie in the area of overlap between the two species. One archaeological sheep, despite following the sheep pattern, falls outside the modern group area, perhaps indicating a case of individual variation.

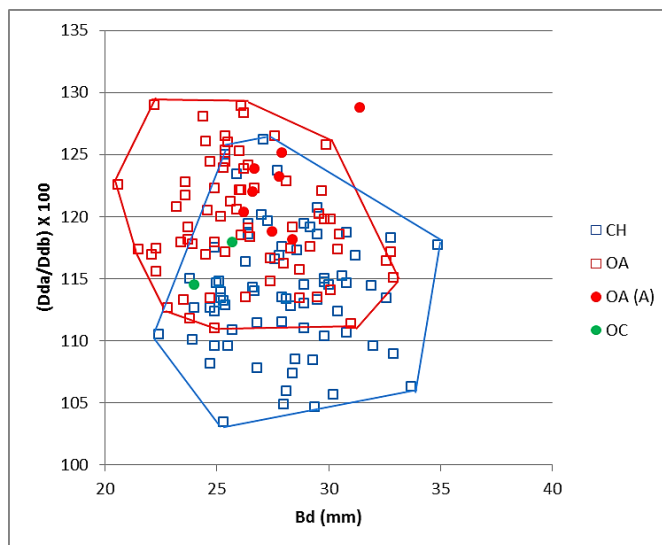


Figure 3.92 Breadth of the distal end plotted against the ratio between the depth of the medial (a) and lateral (b) side. Symbols explained in Fig. 3.9.

Astragalus

Three astragali were identified as sheep in this phase. Figures 3.93 to 3.96 show the agreement between the biometrical data and the morphological identification: the archaeological sheep fall among the modern sheep group or in the area of intersection between the two modern groups. In Figure 3.95 one archaeological specimen appears to be border-line but, given its consistency with the sheep cluster in the other diagrams, it remains highly likely that it belonged to a sheep.

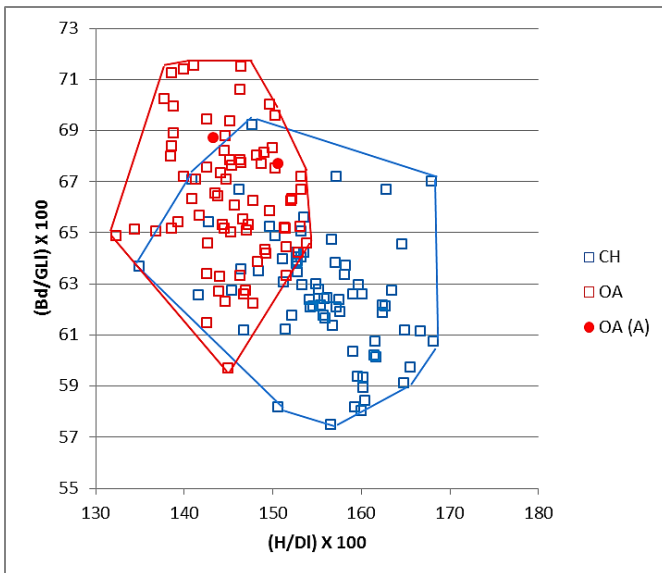


Figure 3.93 Ratio between height at the central constriction and the greatest depth of the lateral half plotted against a ratio between the breadth of the distal end and the greatest length of the lateral half. Symbols explained in Fig. 3.9.

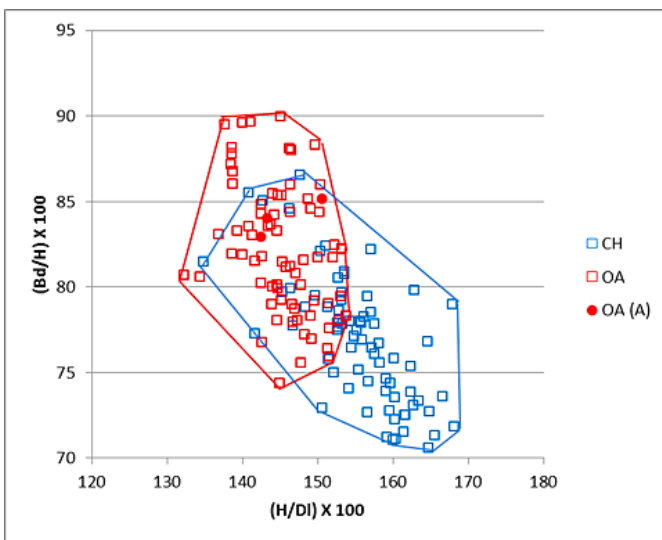


Figure 3.94 Ratio between height at the central constriction and the greatest depth of the lateral half plotted against the ratio between the breadth of the distal end and the height at the central constriction. Symbols explained in Fig. 3.9.

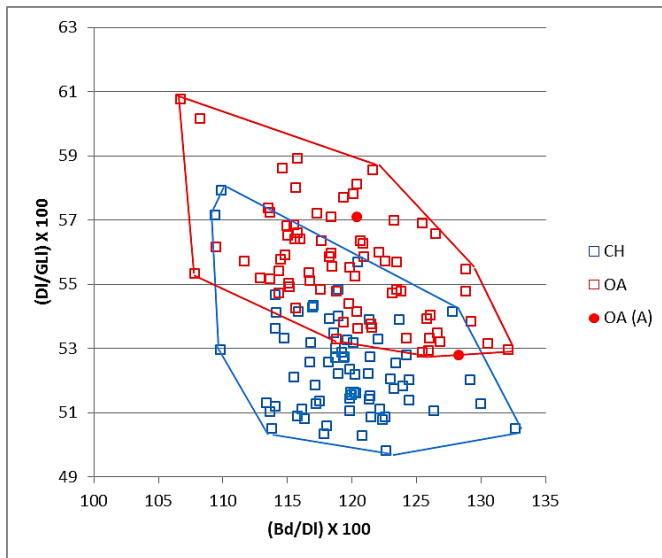


Figure 3.95 Ratio between breadth of the distal end and the greatest depth of the lateral half plotted against the ratio between the breadth of the distal end and the greatest depth of the lateral half. Symbols explained in Fig. 3.9.

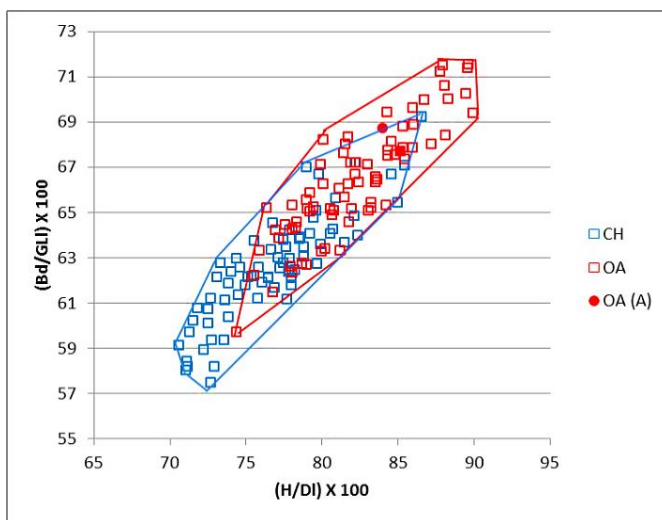


Figure 3.96 Ratio between the breadth of the distal end and the height at the central constriction and the ratio between height at the central constriction and the greatest depth of the lateral half. Symbols explained in Fig. 3.9.

Calcaneum

No goat calcanea were identified morphologically. These results are confirmed by the biometry. Figures 3.97 to 3.99 show that the three archaeological sheep lie among the modern sheep group or in the area of overlap; as a consequence their identification is confirmed.

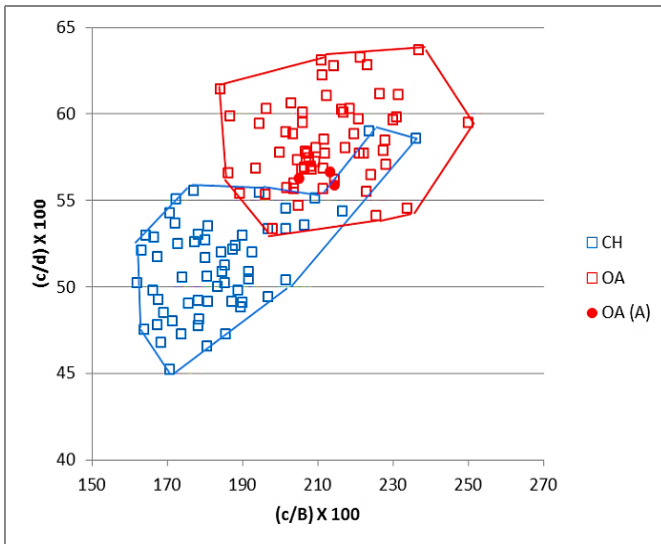


Figure 3.97 Ratio between the length and the breadth of the articular facet of the *os malleolare* plotted against the ratio between the length of the articular facet of the *os malleolare* and the length taken from the articular facet of the *os malleolare* to the end of the articulation-free part of the process. Symbols explained in Fig. 3.9.

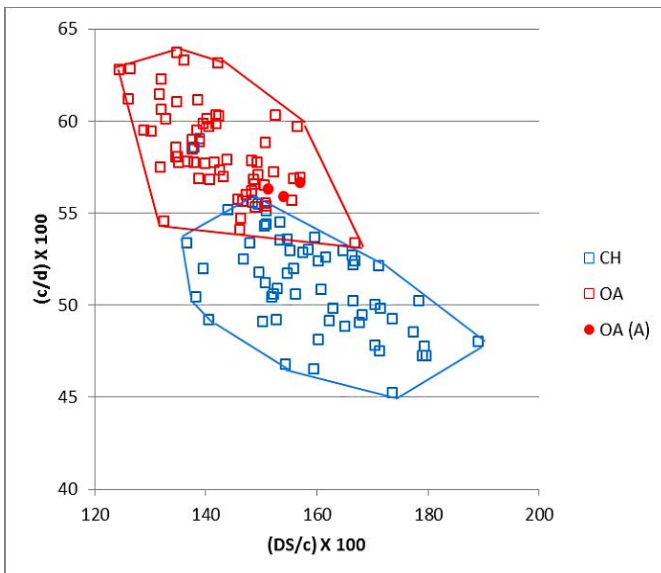


Figure 3.98 Ratio between the depth of the *substantaculum tali* and the length of the articular facet of the *os malleolare* plotted against the ratio between the length and the breadth of the articular facet of the *os malleolare*. Symbols explained in Fig. 3.9.

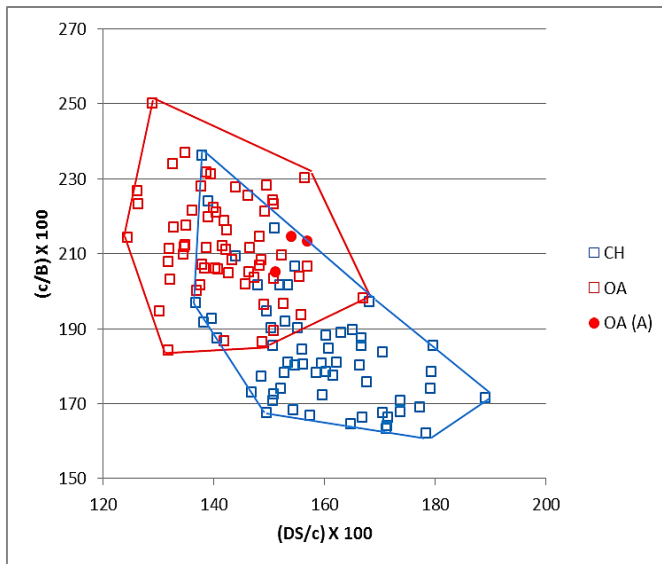


Figure 3.99 Ratio between the depth of the *subtentaculum tali* and the length of the articular facet of the *os malleolare* plotted against the ratio between the length and the breadth of the articular facet of the *os malleolare*. Symbols explained in Fig. 3.9.

Unstratified specimens

Horncore

As for the stratified phases, in this group too the biometry supports the morphological identifications of the sheep and goat horncores (Figs. 3.100 and 3.101).

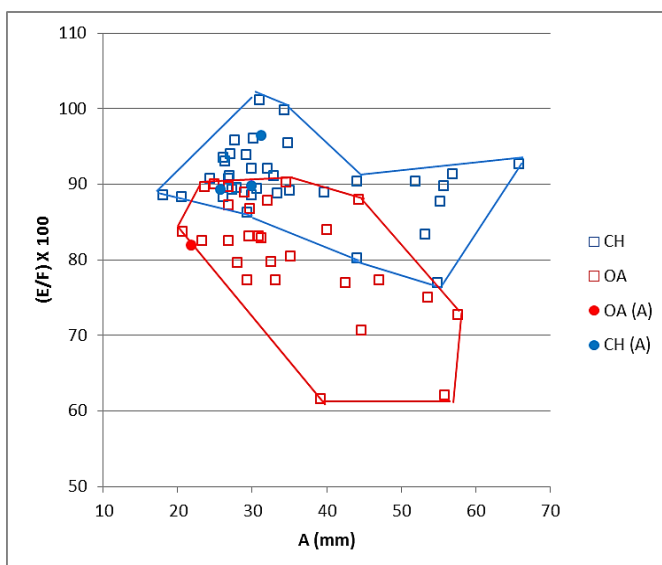


Figure 3.100 Maximum diameter taken at the base plotted against a ratio between the length and the length of the outer curvature of the horncore. Symbols explained in Fig. 3.9.

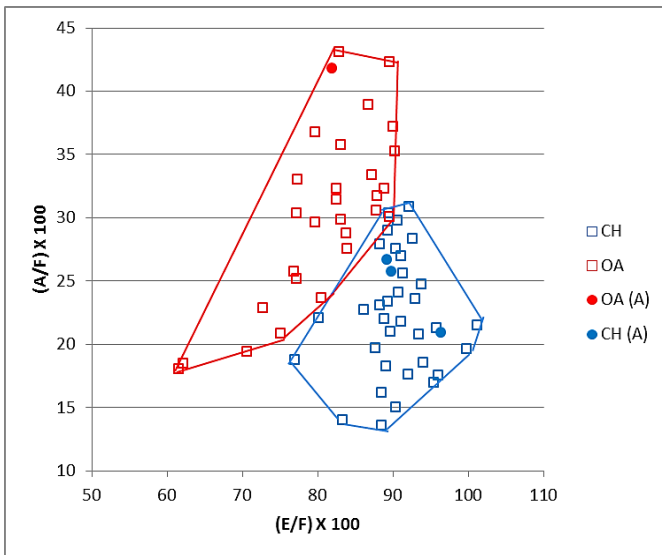


Figure 3.101 Ratio between the length and the length of the outer curvature plotted against the ratio between the maximum diameter taken at the base and the length of the outer curvature of the horncore. Symbols explained in Fig. 3.9.

Scapula

No scapulae were assigned morphologically to the goat. These results are broadly supported by Figures 3.102 and 3.103. The archaeological sheep all fall among the modern sheep group or in the area of overlap between the two species, though one specimen in particular is very much borderline.

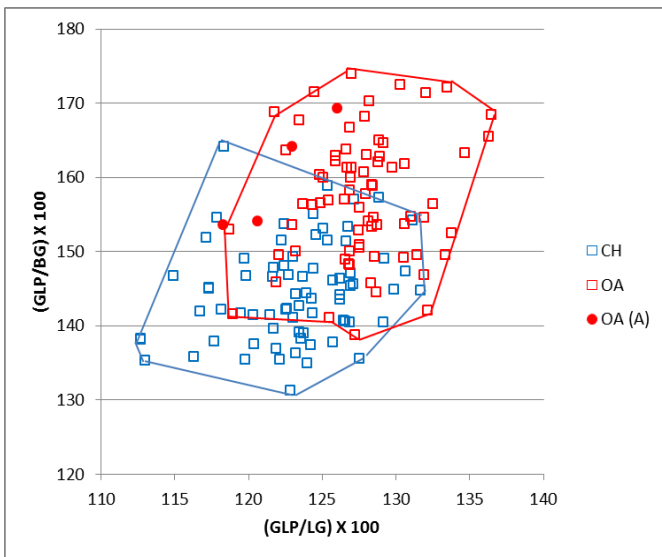


Figure 3.102 Ratio between the greatest length of the *processus articularis* and the length of the glenoid cavity plotted against the ratio between the greatest length of the *processus articularis* and the breadth of the glenoid cavity. Symbols explained in Fig. 3.9.

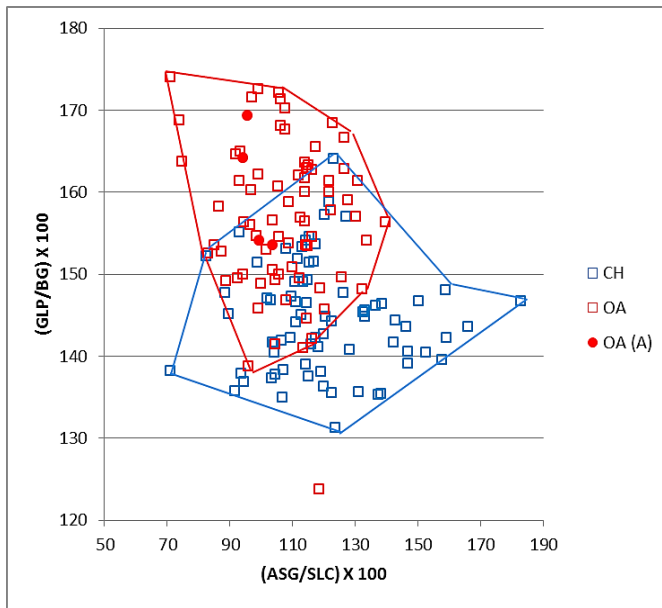


Figure 3.103 Ratio between the shortest distance from the base of the spine to the edge of the glenoid cavity and the smallest length of the *collum scapulae* plotted against a ratio between the greatest length of the *processus articularis* and the breadth of the glenoid cavity. Symbols explained in Fig. 3.9.

Humerus

Only one humerus was assigned to *Capra* according to the morphological traits. Figures 3.104 to 3.107 show that most archaeological specimens fall within the sheep cluster. The single goat specimen is in the area of overlap in Figures 3.105 and 3.106 but clearly in the goat group in Fig. 3.107, therefore confirming identification. The morphologically unidentified specimens all fall within the ample area of overlap, and thus biometry cannot assist in attributing them to species level.

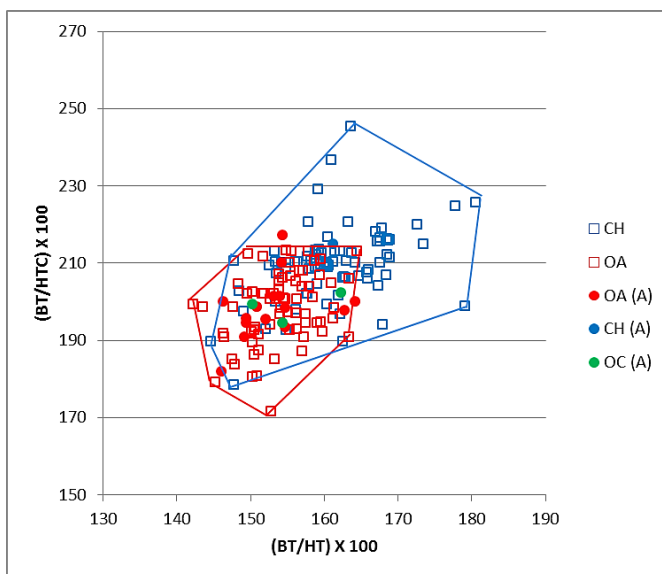


Figure 3.104 Ratio between the medio lateral width of the trochlea and its height plotted against the medio lateral width of the trochlea and the diameter of the trochlear constriction. Symbols explained in Fig. 3.9.

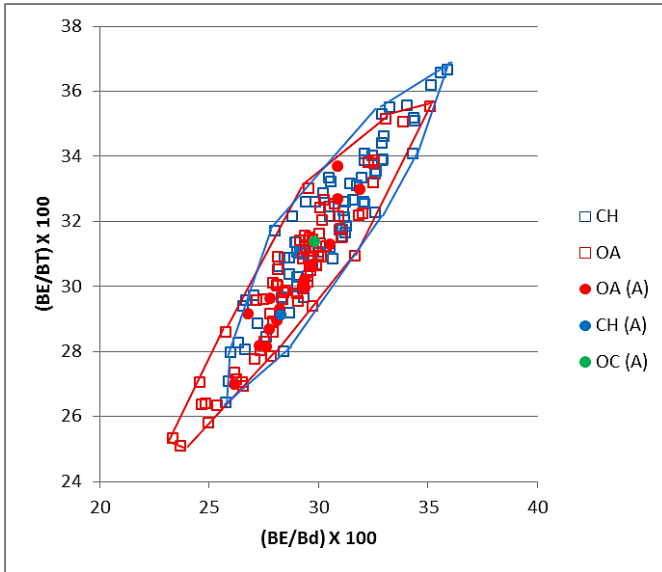


Figure 3.105 Ratio between the breadth of the *capitulum* and the distal width plotted against the ratio between the breadth of the *capitulum* and the medio lateral width of the trochlea. Symbols explained in Fig. 3.9.

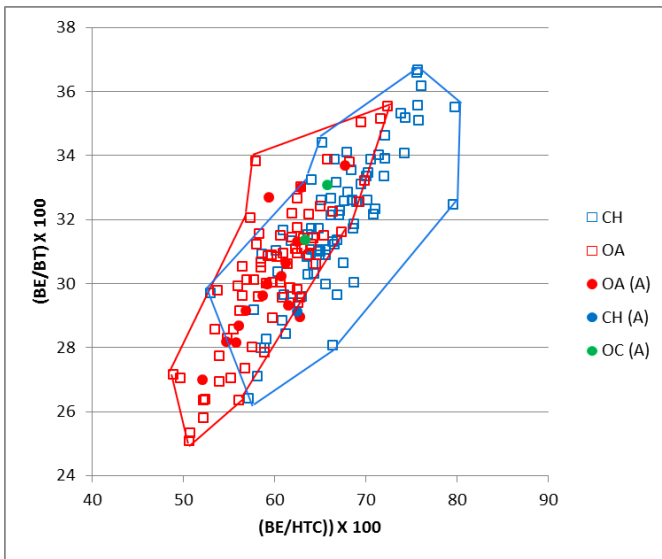


Figure 3.106 Ratio between the breadth of the *capitulum* and the diameter of the trochlear constriction plotted against the ratio between the breadth of the *capitulum* and the medio lateral width of the trochlea. Symbols explained in Fig. 3.9.

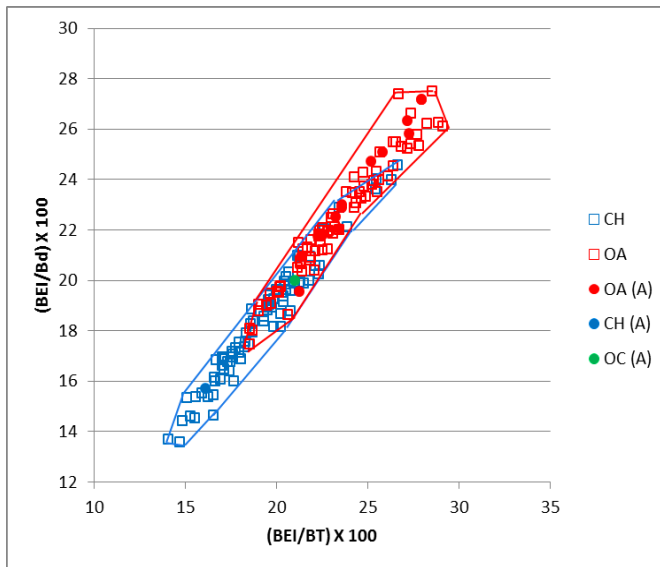


Figure 3.107 Ratio between the breadth of the *epicondyle lateralis* and the medio lateral width of the trochlea plotted against the ratio between the breadth of the *epicondyle lateralis* and the width of the distal end. Symbols explained in Fig. 3.9.

Radius

No archaeological goats were identified on the basis of the morphology. The archaeological sheep mostly fall among the modern sheep group or in the area of overlap; as such they are consistent with the morphological identifications. One archaeological sheep lies among the modern goats but, as previously seen, this phenomenon can be due to different factors (such as the age of the animal). Considering the fact that the specimen does not fall far from the archaeological sheep cluster, it more likely represents an example of individual variation (Fig. 3.108).

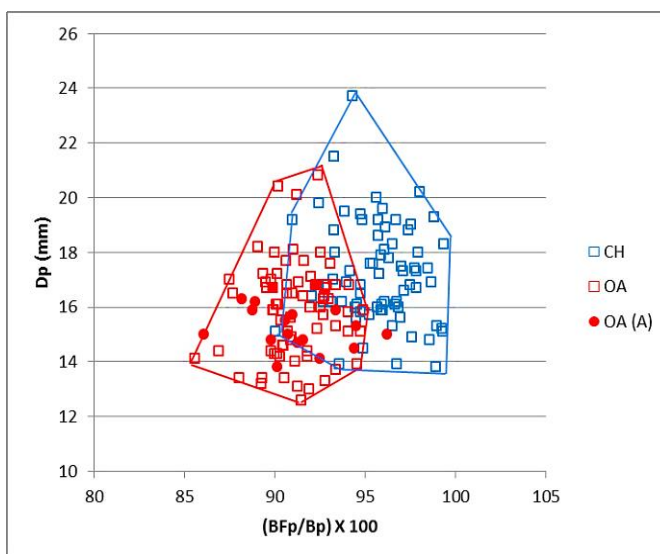


Figure 3.108 Ratio between the greatest length of the *facies articularis proximalis* and the greatest breadth of the proximal end plotted against the depth of the proximal end. Symbols explained in Fig. 3.9.

Ulna

No archaeological ulnae were morphologically attributed to the goat. Figure 3.109 shows that the archaeological specimens are indeed consistent with the modern sheep cluster, with one specimen bearing particularly strong sheep traits. The only morphologically unidentified specimen falls in the overlap area, though much closer to the sheep cluster. It must remain as unidentified, though it is more likely to belong to a sheep.

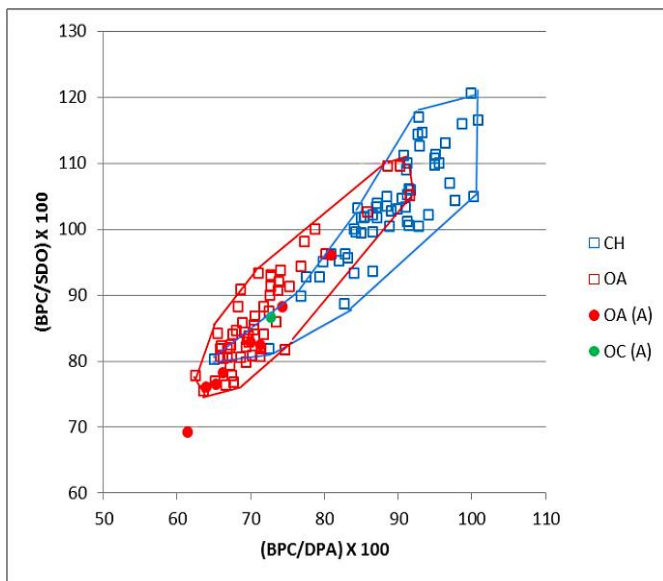


Figure 3.109 Ratio between the breadth across the coronoid process and the depth across the *processus anconaeus* to the caudal border plotted against the breadth across the coronoid process and the smallest depth of the olecranon. Symbols explained in Fig. 3.9.

Metapodials

No *Capra* metapodials were identified on the basis of the morphological traits. Figures 3.110 to 3.115 show that almost all archaeological sheep fall in the area occupied by the modern sheep (mainly metacarpals) or in the area of overlap between the modern groups (mainly metatarsals), attesting their consistency with the morphological identifications. Figures 3.111 and 3.113 provide a couple of examples of specimens marginally plotting in the goat cluster, but those same specimens are consistent with sheep in the other diagrams and therefore the evidence is not strong enough to revise the identifications.

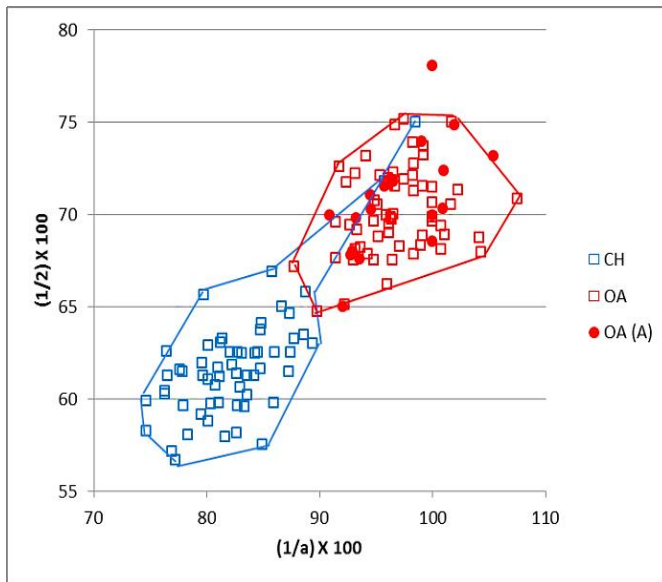


Figure 3.110 Metacarpal. Ratio between the diameter of the medial trochlea and the width of the medial condyle plotted against the ratio between the diameter of the *verticillus* at the medial condyle and the diameter of the medial trochlea. Symbols explained in Fig. 3.9.

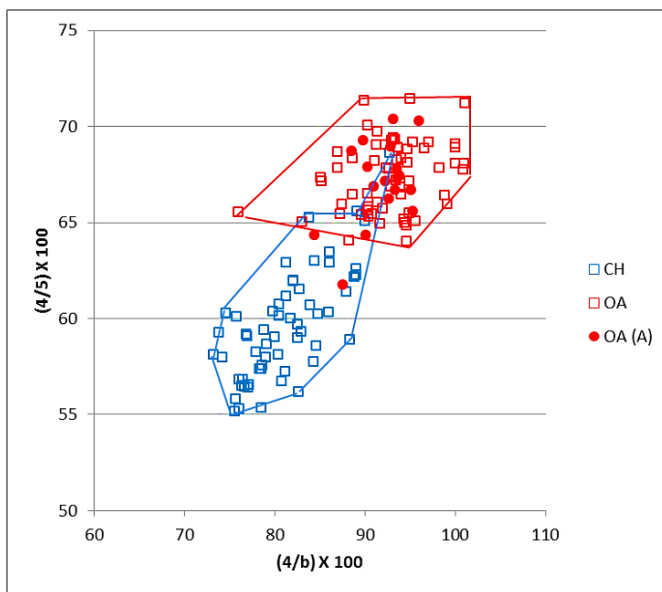


Figure 3.111 Metacarpal. Ratio between the width of the lateral condyle and the diameter of the lateral trochlea plotted against the ratio between the diameter of the *verticillus* on the lateral condyle and the diameter of the lateral condyle. Symbols explained in Fig. 3.9.

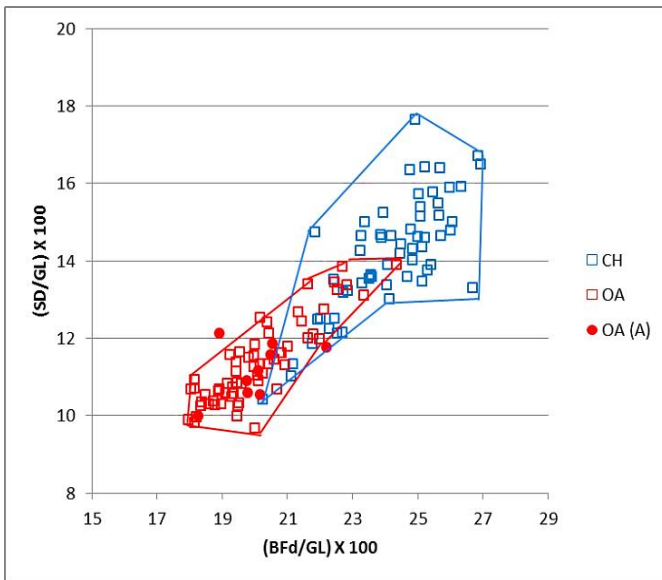


Figure 3.112 Metacarpal. Ratio between the greatest breadth of the distal end with the greatest length plotted against the ratio between the smallest width of the shaft and the greatest length. Symbols explained in Fig. 3.9.

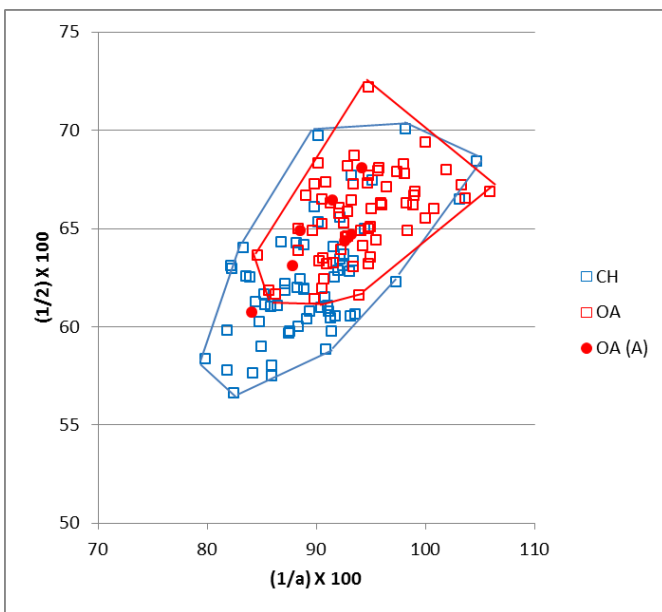


Figure 3.113 Metatarsal. Ratio between the diameter of the medial trochlea and the width of the medial condyle plotted against the ratio between the diameter of the *verticillus* at the medial condyle and the diameter of the medial trochlea. Symbols explained in Fig. 3.9.

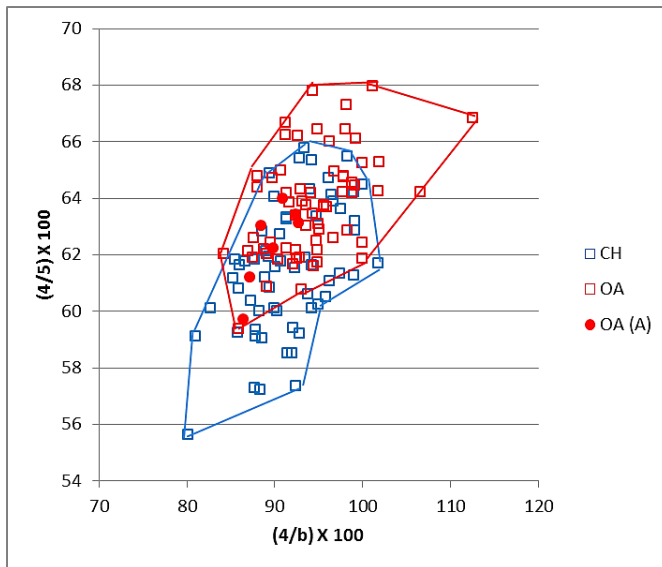


Figure 3.114 Metatarsal. Ratio between the width of the lateral condyle and the diameter of the lateral trochlea plotted against the ratio between the diameter of the *verticillus* on the lateral condyle and the diameter of the lateral condyle. Symbols explained in Fig. 3.9.

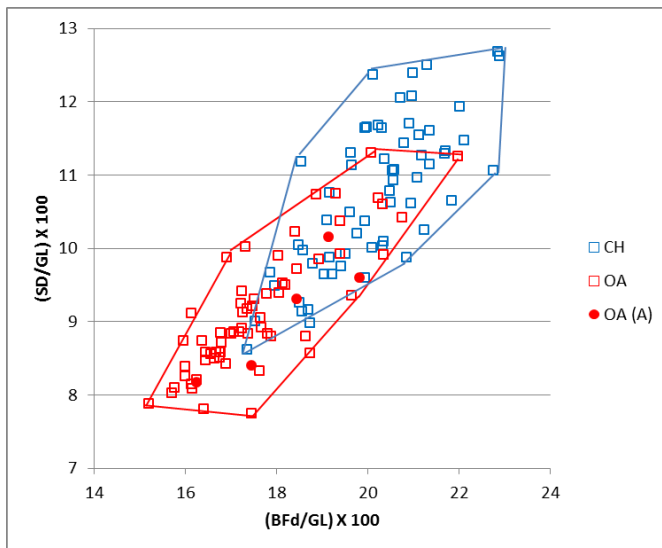


Figure 3.115 Metatarsal. Ratio between the greatest breadth of the distal end with the greatest length plotted against the ratio between the smallest width of the shaft and the greatest length. Symbols explained in Fig. 3.9.

Tibia

All the archaeological tibiae were attributed to *Ovis*. Figure 3.116 shows that this is supported by the biometry.

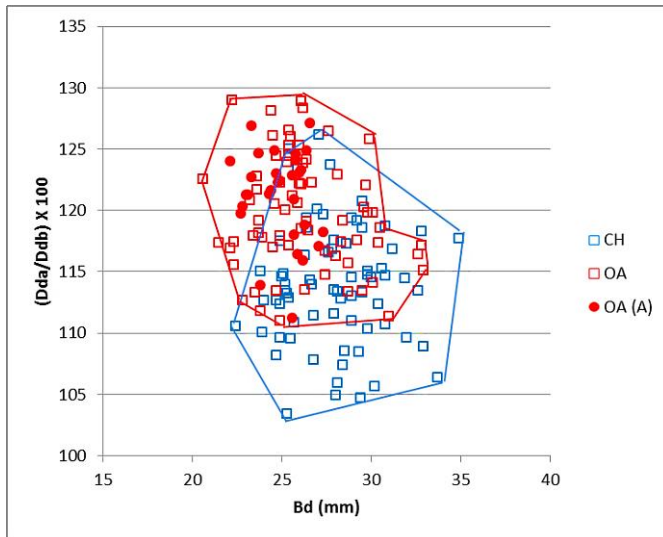


Figure 3.116 Breadth of the distal end plotted against the ratio between the depth of the medial (a) and lateral (b) side. Symbols explained in Fig. 3.9.

Astragalus

No archaeological *Capra* astragali were identified according to their morphology. Figures 3.117 to 3.120 show that the biometrical data support the morphological identifications: all the archaeological sheep lie in the same area as the modern sheep or in the area of overlap between the two groups. Only one archaeological sheep, despite following the sheep general pattern, plots separately from the others, but it has strongly pronounced sheep characteristics which distances itself heavily from the goat group.

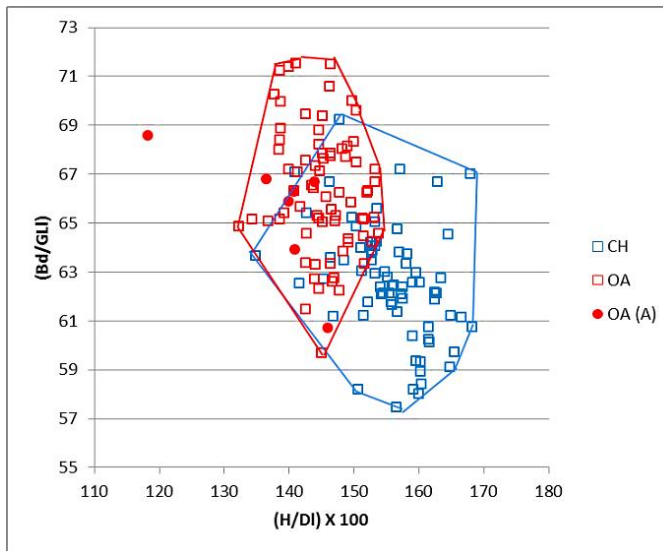


Figure 3.117 Ratio between height at the central constriction and the greatest depth of the lateral half plotted against a ratio between the breadth of the distal end and the greatest length of the lateral half. Symbols explained in Fig. 3.9.

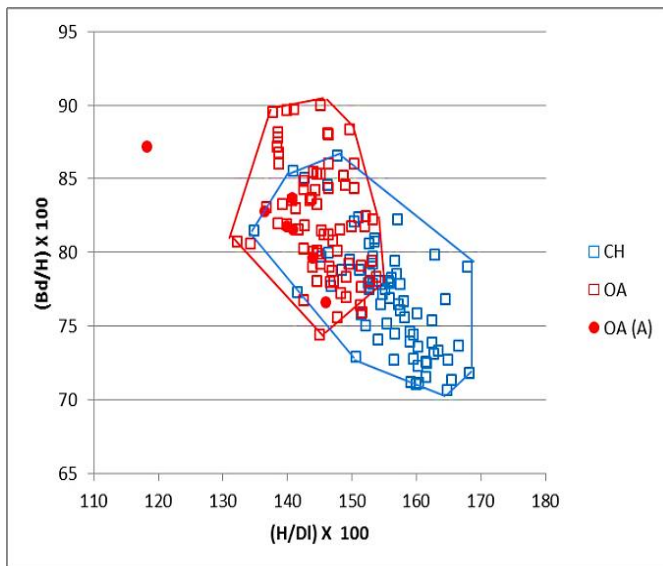


Figure 3.118 Ratio between height at the central constriction and the greatest depth of the lateral half plotted against the ratio between the breadth of the distal end and the height at the central constriction. Symbols explained in Fig. 3.9.

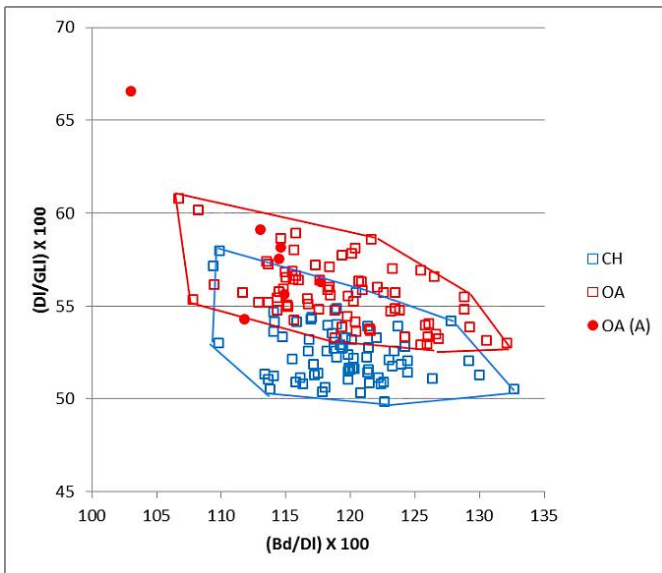


Figure 3.119 Ratio between breadth of the distal end and the greatest depth of the lateral half plotted against the ratio between the breadth of the distal end and the greatest depth of the lateral half. Symbols explained in Fig. 3.9.

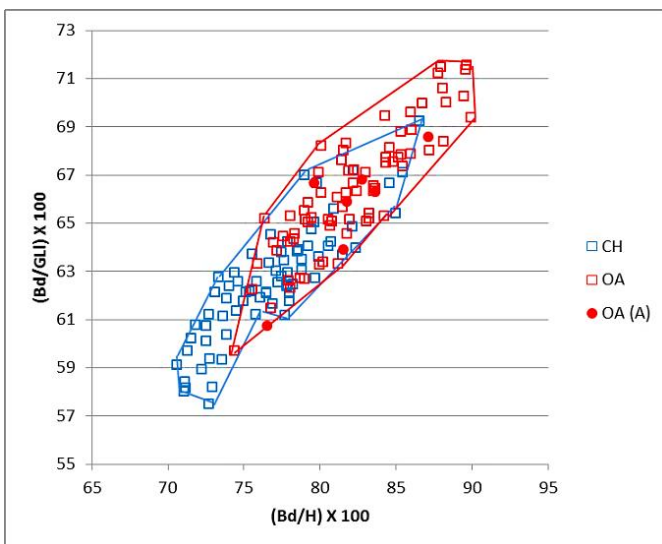


Figure 3.120 Ratio between the breadth of the distal end and the height at the central constriction and the ratio between height at the central constriction and the greatest depth of the lateral half. Symbols explained in Fig. 3.9.

Calcaneum

Figures 3.121 to 3.123 show that all the archaeological specimens identified as sheep occupy the same area of the graphs where the modern sheep are, or the area of overlap between the two modern groups. Thus, the biometrical data support the morphological identifications. One archaeological sheep has particularly pronounced sheep characteristics (Figs. 3.121 and 3.123).

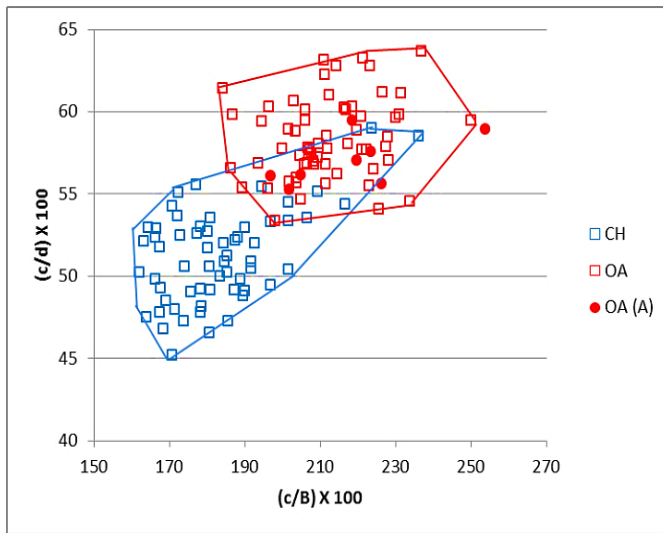


Figure 3.121 Ratio between the length and the breadth of the articular facet of the *os malleolare* plotted against the ratio between the length of the articular facet of the *os malleolare* and the length taken from the articular facet of the *os malleolare* to the end of the articulation-free part of the process. Symbols explained in Fig. 3.9.

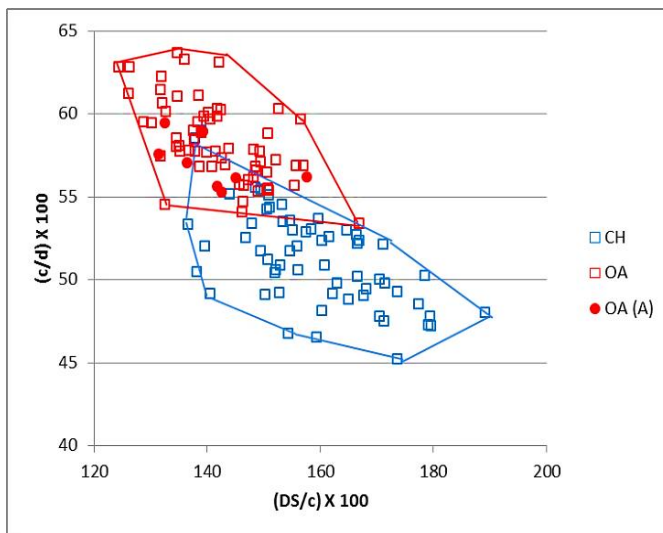


Figure 3.122 Ratio between the depth of the *substentaculum tali* and the length of the articular facet of the *os malleolare* plotted against the ratio between the length and the breadth of the articular facet of the *os malleolare*. Symbols explained in Fig. 3.9.

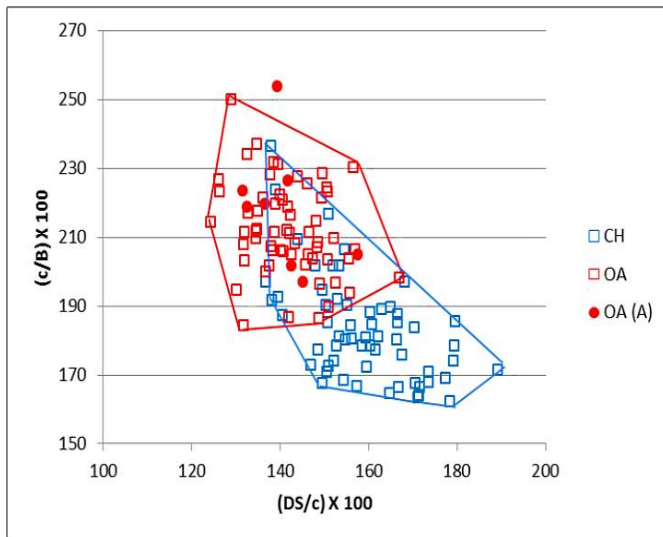


Figure 3.123 Ratio between the depth of the *subtentaculum tali* and the length of the articular facet of the *os malleolare* plotted against the ratio between the length and the breadth of the articular facet of the *os malleolare*. Symbols explained in Fig. 3.9.

Having completed the bones shape analysis with the use of different ratios for each chronological phase, some conclusions can be drawn. Firstly, the modern material has shown to be a very good model for comparison with the archaeological material: the archaeological specimens by and large follow the same pattern of distribution with only few outliers. Interestingly, the archaeological specimens seem to be more tightly clustered than the modern specimens; this is probably due to their greater morphotype homogeneity. Secondly, it is clear that the combination of morphology and biometry increases the amount of information that a researcher can derive from the analysed assemblage, as it allows a mutual verification of the identifications.

In the case of King's Lynn, when the comparison between the two approaches, morphological and biometrical is made, it emerges that the biometry often supports and reinforces what has already been observed through the morphological analysis. Sheep specimens are far more numerous than goats in all chronological phases and for all the anatomical elements apart from horncores. The biometry has pointed out some additional cases of potential goat specimens, but these are few in number and do not change the overall pattern.

Overall, the biometrical analysis contributed greatly to:

1. support (when an archaeological specimen assigned to a group species fell among the modern specimens of the same species or in an area of intersection between the two modern groups) or reject (when an archaeological specimen assigned to a group species fell among the modern group of the opposite species) the identification based on morphological traits;
2. attribute to species level a few specimens that could not be identified morphologically;

3. identify morphometric variation within a species;
4. provide a more objective system to present identifications, which can be scrutinised by other scholars.

3.2.8 DA predictions of the sheep/goat assemblage from King's Lynn

DA was run on the sheep/goat material for each chronological phase at the site. In order to include specimens for which not all the measurements could be taken, which were otherwise excluded from the analysis, DA was rerun with the exclusion of some of the unavailable variables/measurements.

To increase the archaeological sample size and to better understand the extent to which the new methodology was effective on the archaeological material, DA was additionally run on the whole King's Lynn sheep/goat assemblage without any regards to chronological phase; the results of this study are presented in Section 3.2.9.

Discriminant Analysis: Phase I

Horncore

Table 3.7 shows the results obtained when DA was run on the horncores. For the modern material the total reattribution rate is 95.2%, a very high value. If the archaeological material is considered, all three goat horncores were correctly reattributed, while only one specimen among the sheep was misattributed. The total percentage of correct reattributions for King's Lynn material is 90%. This value has slightly decreased (which is not surprising since the archaeological sample is much smaller than the modern) compared to the reattribution value of the modern material but it is still a very high value. As such, Discriminant Analysis has shown to be successful.

Table 3.7 Results from the Discriminant Analysis when applied on the archaeological horncores of phase I. a = percentage of correct attributions related to the modern material (selected original grouped cases); b = percentage of correct attributions related to the archaeological material (unselected original grouped cases); d = percentage of correct attributions when cross-validation was applied. Same terminology is adopted in all the following tables.

Classification Results ^{a,b,d}						
			TAXA	Predicted Group Membership		Total
				CH	OA	
Modern Material	Original	Count	CH	33	2	35
			OA	1	27	28
		%	CH	94.3	5.7	100.0
			OA	3.6	96.4	100.0
King's Lynn	Original	Count	CH	3	0	3
			OA	1	6	7
		%	CH	100.0	.0	100.0
			OA	14.3	85.7	100.0
a. 95.2% of selected original grouped cases correctly classified.						
b. 90.0% of unselected original grouped cases correctly classified.						
d. 95.2% of selected cross-validated grouped cases correctly classified. Cross validation is done only for those cases in the analysis. In cross validation, each case is classified by the functions derived from all cases other than that case.						

Scapula

The reattribution rate when DA was applied to modern scapulae was 86.4%, a high result but not one of the highest. Surprisingly, a better reattribution rate was obtained from the archaeological material (Tab. 3.8). Although the sample is smaller than the modern, all the archaeological goats were identified as such by the program. The total percentage of correct reattribution for the archaeological material is a very satisfactory 91.7%.

Table 3.8 Results from the Discriminant Analysis when applied on the archaeological scapulae of phase I.

Classification Results ^{a,b,d}						
			TAXA	Predicted Group Membership		Total
				CH	OA	
Modern Material	Original	Count	CH	64	10	74
			OA	10	63	73
		%	CH	86.5	13.5	100.0
			OA	13.7	86.3	100.0
King's Lynn	Original	Count	CH	1	1	2
			OA	1	21	22
			O/C	0	1	1
		%	CH	50.0	50.0	100.0
			OA	4.5	95.5	100.0
			O/C	.0	100.0	100.0
a. 86.4% of selected original grouped cases correctly classified.						
b. 91.7% of unselected original grouped cases correctly classified.						
d. 83.0% of selected cross-validated grouped cases correctly classified. Cross validation is done only for those cases in the analysis. In cross validation, each case is classified by the functions derived from all cases other than that case.						

Humerus

The DA run on the humerus for the modern material gave a reattribution rate of 88.4%. On the archaeological material, the analysis gave an even higher result as shown in Table 3.9. In fact, the final reattribution percentage for this element is 92.6%, a very high value.

Table 3.9 Results from the Discriminant Analysis when applied on the archaeological humeri of phase I.

Classification Results ^{a,b,d}						
			TAXA	Predicted Group Membership		Total
				CH	OA	
Modern Material	Original	Count	CH	67	9	76
			OA	8	62	70
		%	CH	88.2	11.8	100.0
			OA	11.4	88.6	100.0
King's Lynn	Original	Count	CH	0	0	0
			OA	2	25	27
		%	CH	.0	.0	100.0
			OA	7.4	92.6	100.0
a. 88.4% of selected original grouped cases correctly classified.						
b. 92.6% of unselected original grouped cases correctly classified.						
d. 86.3% of selected cross-validated grouped cases correctly classified. Cross validation is done only for those cases in the analysis. In cross validation, each case is classified by the functions derived from all cases other than that case.						

Radius

The interesting pattern already noticed during the ratio analysis for this element is mirrored by the results of the DA. It must be noted that the variables GL and SD were not included in the analysis because of the lack of complete radii; as such, the reattribution rate on the modern material decreases from 93.5% (when all measurements are included) to 89.7%, which is still a good result. On the archaeological material, unfortunately, the reattribution rate is lower, at 79.2% (Tab. 3.10) as some of the archaeological sheep were identified as goat. This relatively high level of disagreement of attributions between the morphological and the biometrical data could be due to the same reasons previously mentioned (the occurrence of misidentification or the age ratio of the archaeological material which do not find a good fit with the age-ratio of the modern material) but also to the fact that with the exclusion of GL and SD some of the discriminating power of the function is lost and this may have a larger impact on the small archaeological sample than on the large modern sample.

Table 3.10 Results from the Discriminant Analysis when applied on the archaeological radii of phase I, excluding variables GL and SD.

Classification Results ^{a,b,d}						
			TAXA	Predicted Group Membership		Total
				CH	OA	
Modern Material	Original	Count	CH	64	10	74
			OA	5	66	71
		%	CH	86.5	13.5	100.0
			OA	7.0	93.0	100.0
King's Lynn	Original	Count	CH	0	0	0
			OA	5	19	24
		%	CH	.0	.0	100.0
			OA	20.8	79.2	100.0
a. 89.7% of selected original grouped cases correctly classified.						
b. 79.2% of unselected original grouped cases correctly classified.						
d. 88.3% of selected cross-validated grouped cases correctly classified. Cross validation is done only for those cases in the analysis. In cross validation, each case is classified by the functions derived from all cases other than that case.						

Ulna

For the ulnae, two different DA analyses were run: one including all the variables (Tab. 3.11) and one including only some (Tab. 3.12). Table 3.11 shows that, on the modern material, when all the measurements were included, the reattribution rate was 92.9%, a very high value. On the archaeological material, the reattribution rate is even higher, namely 100%: all the archaeological sheep were correctly attributed.

Table 3.11 Results from the Discriminant Analysis when applied on the archaeological ulnae of phase I.

Classification Results ^{a,b,d}						
			TAXA	Predicted Group Membership		Total
				CH	OA	
Modern Material	Original	Count	CH	53	3	56
			OA	5	52	57
		%	CH	94.6	5.4	100.0
			OA	8.8	91.2	100.0
King's Lynn	Original	Count	CH	0	0	0
			OA	0	6	6
		%	CH	.0	.0	100.0
			OA	.0	100.0	100.0
a. 92.9% of selected original grouped cases correctly classified.						
b. 100.0% of unselected original grouped cases correctly classified.						
d. 92.0% of selected cross-validated grouped cases correctly classified. Cross validation is done only for those cases in the analysis. In cross validation, each case is classified by the functions derived from all cases other than that case.						

Table 3.12 shows that, with the exclusion of B and L, on the modern material the reattribution rate remained almost identical (92.0% compared to from 92.2%). On the archaeological material, the impact of the exclusion of B and L is bigger as the reattribution score decreases from 100% to 77.8%, which is still a relatively high result although not as high as when all the variables were considered. Clearly, B and L have an impact on the predictive equation power. The only unidentified specimen present was classified as goat by DA.

Table 3.12 Results from the Discriminant Analysis when applied on the archaeological ulnae of phase I, excluding the variables B and L.

Classification Results ^{a,b,d}						
			TAXA	Predicted Group Membership		Total
				CH	OA	
Modern Material	Original	Count	CH	52	4	56
			OA	5	52	57
		%	CH	92.9	7.1	100.0
			OA	8.8	91.2	100.0
King's Lynn	Original	Count	CH	0	0	0
			OA	2	7	9
			O/C	1	0	1
		%	CH	.0	.0	100.0
			OA	22.2	77.8	100.0
			O/C	100.0	.0	100.0
a. 92.0% of selected original grouped cases correctly classified.						
b. 77.8% of unselected original grouped cases correctly classified.						
d. 91.2% of selected cross-validated grouped cases correctly classified. Cross validation is done only for those cases in the analysis. In cross validation, each case is classified by the functions derived from all cases other than that case.						

Metacarpal

For the metacarpal, two different Discriminant Analyses were also carried out, one including all the variables (Tab. 3.13) and one including the specimens for which the variables GL and SD could not be taken (Tab. 1.14). Table 3.13 shows that, on the modern material, the reattribution rate for the metacarpal was 98.3%, the highest result obtained. For the archaeological material, only one complete specimen was available for phase I and it was correctly attributed to the sheep group.

Table 3.13 Results from the Discriminant Analysis when applied on the archaeological metacarpals of phase I.

Classification Results ^{a,b,d}						
			TAXA	Predicted Group Membership		Total
				CH	OA	
Modern Material	Original	Count	CH	56	2	58
			OA	0	61	61
		%	CH	96.6	3.4	100.0
			OA	.0	100.0	100.0
King's Lynn	Original	Count	CH	0	0	0
			OA	0	1	1
		%	CH	.0	.0	100.0
			OA	.0	100.0	100.0
a. 98.3% of selected original grouped cases correctly classified.						
b. 100.0% of unselected original grouped cases correctly classified.						
d. 97.5% of selected cross-validated grouped cases correctly classified. Cross validation is done only for those cases in the analysis. In cross validation, each case is classified by the functions derived from all cases other than that case.						

In Table 3.14 it can be seen that the reattribution rate for the modern material, if GL and SD were not included, decreases only very slightly from 98.3% to 97.5%. For the small sample of archaeological material as well, the result is very successful: all archaeological sheep were classified correctly leading to a final percentage of 100% of correct reattributions.

Table 3.14 Results from the Discriminant Analysis when applied on the archaeological metacarpals of phase I, excluding the variables GL and SD.

Classification Results ^{a,b,d}						
			TAXA	Predicted Group Membership		Total
				CH	OA	
Modern Material	Original	Count	CH	56	2	58
			OA	1	60	61
		%	CH	96.6	3.4	100.0
			OA	1.6	98.4	100.0
	Cross-validated ^c	Count	CH	55	3	58
			OA	1	60	61
		%	CH	94.8	5.2	100.0
			OA	1.6	98.4	100.0
King's Lynn	Original	Count	CH	0	0	0
			OA	0	3	3
		%	CH	.0	.0	100.0
			OA	.0	100.0	100.0
a. 97.5% of selected original grouped cases correctly classified.						

Classification Results ^{a,b,d}	
b.	100.0% of unselected original grouped cases correctly classified.
d.	96.6% of selected cross-validated grouped cases correctly classified. Cross validation is done only for those cases in the analysis. In cross validation, each case is classified by the functions derived from all cases other than that case.

Metatarsal

Two different DA analyses were carried out for the metatarsals as well. Table 3.15 shows the results when all the variables were included. On the modern material, the final reattribution score was 92.7%. Only one archaeological specimen was available and DA confirmed the morphological identification.

Table 3.15 Results from the Discriminant Analysis when applied on the archaeological metatarsals of phase I.

Classification Results ^{a,b,d}						
			TAXA	Predicted Group Membership		Total
				CH	OA	
Modern Material	Original	Count	CH	56	5	61
			OA	4	59	63
		%	CH	91.8	8.2	100.0
			OA	6.3	93.7	100.0
King's Lynn	Original	Count	CH	0	0	0
			OA	0	1	1
		%	CH	.0	.0	100.0
			OA	.0	100.0	100.0
a. 92.7% of selected original grouped cases correctly classified.						
b. 100.0% of unselected original grouped cases correctly classified.						
d. 91.1% of selected cross-validated grouped cases correctly classified. Cross validation is done only for those cases in the analysis. In cross validation, each case is classified by the functions derived from all cases other than that case.						

Table 3.16 shows the results when the variables GL and SD were excluded from the analysis. The modern material reattribution rate decreases from 92.7% to 88.7%, showing the effect of the exclusion of the two variables. Two archaeological specimens were available and only in one case the morphological identification was supported by DA. Clearly in this case, the small sample and the excluded variables had an impact on the results. Misidentification is, however, unlikely as it is not supported by the BI results.

Table 3.16 Results from the Discriminant Analysis when applied on the archaeological metatarsals of phase I, excluding variables GL and SD.

Classification Results ^{a,b,d}						
			TAXA	Predicted Group Membership		Total
				CH	OA	
Modern Material	Original	Count	CH	51	10	61
			OA	4	59	63
		%	CH	83.6	16.4	100.0
			OA	6.3	93.7	100.0
King's Lynn	Original	Count	CH	0	0	0
			OA	1	1	2
		%	CH	.0	.0	100.0
			OA	50.0	50.0	100.0
a. 88.7% of selected original grouped cases correctly classified.						
b. 50.0% of unselected original grouped cases correctly classified.						
d. 85.5% of selected cross-validated grouped cases correctly classified. Cross validation is done only for those cases in the analysis. In cross validation, each case is classified by the functions derived from all cases other than that case.						

Tibia

Only one complete archaeological tibia was recorded as sheep according to its morphological characteristics. Table 3.17 shows that this identification is confirmed by DA. As the archaeological sample of complete tibiae was very small, additional Discriminant Analyses were run (Tab. 3.18 and 3.19) excluding variables, such as SD and GL, which could not be recorded on the fragmented bones.

Table 3.17 Results from the Discriminant Analysis when applied on the archaeological tibiae of phase I.

Classification Results ^{a,b,d}						
			TAXA	Predicted Group Membership		Total
				CH	OA	
Modern Material	Original	Count	CH	55	3	58
			OA	9	43	52
		%	CH	94.8	5.2	100.0
			OA	17.3	82.7	100.0
King's Lynn	Original	Count	CH	0	0	0
			OA	0	1	1
		%	CH	.0	.0	100.0
			OA	.0	100.0	100.0
a. 89.1% of selected original grouped cases correctly classified.						
b. 100.0% of unselected original grouped cases correctly classified.						
d. 86.4% of selected cross-validated grouped cases correctly classified. Cross validation is done only for those cases in the analysis. In cross validation, each case is classified by the functions derived from all cases other than that case.						

Table 3.18 shows the results when only variable GL was excluded. The reattribution rate of the modern material drops from 89.1% to 74.5%, clearly this variable has an impact on the discriminant power of the analysis. On the archaeological material, the same pattern is visible: despite an increase in sample size, the percentage of correct reattribution decreases from 100% to 75.9%. Of two unidentified specimens, one was attributed to sheep and one to goat.

Table 3.18 Results from the Discriminant Analysis when applied on the archaeological tibiae of phase I, excluding the variable GL.

Classification Results ^{a,b,d}						
			TAXA	Predicted Group Membership		Total
				CH	OA	
Modern Material	Original	Count	CH	45	13	58
			OA	15	37	52
		%	CH	77.6	22.4	100.0
			OA	28.8	71.2	100.0
King's Lynn	Original	Count	CH	0	0	0
			OA	7	22	29
			O/C	1	1	2
		%	CH	.0	.0	100.0
			OA	24.1	75.9	100.0
			O/C	50.0	50.0	100.0
a. 74.5% of selected original grouped cases correctly classified.						
b. 75.9% of unselected original grouped cases correctly classified.						

Classification Results ^{a,b,d}	
d. 72.7% of selected cross-validated grouped cases correctly classified. Cross validation is done only for those cases in the analysis. In cross validation, each case is classified by the functions derived from all cases other than that case.	

Finally, Table 3.19 presents the results when both variables GL and SD were excluded. The reattribution rate for the modern material decreases further: from 74.5% when only GL was excluded, to 71.8% when both GL and SD are excluded. For the archaeological material, the attribution rate increases slightly with the increase of the sample size (from 75.9% to 76.3%). The three unidentified specimens were all attributed to the goat.

Table 3.19 Results from the Discriminant Analysis when applied on the archaeological tibiae of phase I, excluding the variables GL and SD.

Classification Results ^{a,b,d}						
			TAXA	Predicted Group Membership		Total
				CH	OA	
Modern Material	Original	Count	CH	42	16	58
			OA	15	37	52
		%	CH	72.4	27.6	100.0
			OA	28.8	71.2	100.0
King's Lynn	Original	Count	CH	0	0	0
			OA	9	29	38
			O/C	3	0	3
		%	CH	.0	.0	100.0
			OA	23.7	76.3	100.0
			O/C	100.0	.0	100.0

a. 71.8% of selected original grouped cases correctly classified.
b. 76.3% of unselected original grouped cases correctly classified.
d. 70.0% of selected cross-validated grouped cases correctly classified. Cross validation is done only for those cases in the analysis. In cross validation, each case is classified by the functions derived from all cases other than that case.

Astragalus

The DA reattribution rate for the astragali on the modern material was as high as 89.9%. For the archaeological material, despite the small sample size, the attribution rate is very successful as well: all of the six sheep astragali were assigned to sheep group, leading to a final score of 100% (Tab. 3.20).

Table 3.20 Results from the Discriminant Analysis when applied on the archaeological astragali of phase I.

Classification Results ^{a,b,d}						
			TAXA	Predicted Group Membership		Total
				CH	OA	
Modern Material	Original	Count	CH	65	7	72
			OA	9	64	73
		%	CH	90.3	9.7	100.0
			OA	12.3	87.7	100.0
King's Lynn	Original	Count	CH	0	0	0
			OA	0	6	6
		%	CH	.0	.0	100.0
			OA	.0	100.0	100.0
a. 89.0% of selected original grouped cases correctly classified.						
b. 100.0% of unselected original grouped cases correctly classified.						
d. 86.9% of selected cross-validated grouped cases correctly classified. Cross validation is done only for those cases in the analysis. In cross validation, each case is classified by the functions derived from all cases other than that case.						

Calcaneum

Very good results were also obtained when DA was run on the calcaneum. On the modern material, the analysis gave a very high reattribution score of 95.1%. A very high 100% correct reattribution score is also given by the archaeological material: all seven sheep archaeological calcanei were reattributed to the right group (Tab. 3.21).

Table 3.21 Results from the Discriminant Analysis when applied on the archaeological calcanea of phase I.

Classification Results ^{a,b,d}						
			TAXA	Predicted Group Membership		Total
				CH	OA	
Modern Material	Original	Count	CH	55	5	60
			OA	1	61	62
		%	CH	91.7	8.3	100.0
			OA	1.6	98.4	100.0
King's Lynn	Original	Count	CH	0	0	0
			OA	0	7	7
		%	CH	.0	.0	100.0
			OA	.0	100.0	100.0
a. 95.1% of selected original grouped cases correctly classified.						
b. 100.0% of unselected original grouped cases correctly classified.						

Classification Results ^{a,b,d}	
d. 95.1% of selected cross-validated grouped cases correctly classified. Cross validation is done only for those cases in the analysis. In cross validation, each case is classified by the functions derived from all cases other than that case.	

Discriminant Analysis: Phase II

Horncores

When all the variables were included, the final reattribution rate for the archaeological horncores from phase II is very successful (100% for the archaeological). This value confirms the agreement between the morphological and the biometrical results (Tab. 3.22).

Table 3.22 Results from the Discriminant Analysis when applied on the archaeological horncores of phase II.

Classification Results ^{a,b,d}						
			TAXA	Predicted Group Membership		Total
				CH	OA	
Modern Material	Original	Count	CH	33	2	35
			OA	1	27	28
		%	CH	94.3	5.7	100.0
			OA	3.6	96.4	100.0
King's Lynn	Original	Count	CH	7	0	7
			OA	0	1	1
		%	CH	100.0	.0	100.0
			OA	.0	100.0	100.0
a. 95.2% of selected original grouped cases correctly classified.						
b. 100.0% of unselected original grouped cases correctly classified.						
d. 95.2% of selected cross-validated grouped cases correctly classified. Cross validation is done only for those cases in the analysis. In cross validation, each case is classified by the functions derived from all cases other than that case.						

When variables E and F are excluded (Tab. 3.23), the reattribution rate decreases (from 100% to 90.5% for the archaeological) showing the influence that variables E and F have on the discriminating power of the analysis.

Table 3.23 Results from the Discriminant Analysis when applied on the archaeological horncores of phase II, excluding E and F variables.

Classification Results ^{a,b,d}						
			TAXA	Predicted Group Membership		Total
				CH	OA	
Modern Material	Original	Count	CH	25	10	35
			OA	2	26	28
		%	CH	71.4	28.6	100.0
			OA	7.1	92.9	100.0
King's Lynn	Original	Count	CH	17	2	19
			OA	0	2	2
		%	CH	89.5	10.5	100.0
			OA	.0	100.0	100.0
a. 81.0% of selected original grouped cases correctly classified.						
b. 90.5% of unselected original grouped cases correctly classified.						
d. 79.4% of selected cross-validated grouped cases correctly classified. Cross validation is done only for those cases in the analysis. In cross validation, each case is classified by the functions derived from all cases other than that case.						

Scapula

The reattribution rate for the archaeological scapulae is more successful (95.7%) than for the modern material (86.5%), confirming the pattern seen for the previous phase. Table 3.24 shows that only one originally classified sheep has been reclassified as goat.

Table 3.24 Results from the Discriminant Analysis when applied on the archaeological scapulae of phase II.

Classification Results ^{a,b,d}						
			TAXA	Predicted Group Membership		Total
				CH	OA	
Modern Material	Original	Count	CH	64	10	74
			OA	10	63	73
		%	CH	86.5	13.5	100.0
			OA	13.7	86.3	100.0
King's Lynn	Original	Count	CH	0	0	0
			OA	1	22	23
		%	CH	.0	.0	100.0
			OA	4.3	95.7	100.0
a. 86.4% of selected original grouped cases correctly classified.						
b. 95.7% of unselected original grouped cases correctly classified.						

Classification Results ^{a,b,d}	
d. 83.0% of selected cross-validated grouped cases correctly classified. Cross validation is done only for those cases in the analysis. In cross validation, each case is classified by the functions derived from all cases other than that case.	

Humerus

The percentage of correct reattribution for the humerus is also successful (92%). As shown by Table 3.25, of the 25 archaeological humeri originally assigned to sheep, two were misclassified as goat.

Table 3.25 Results from the Discriminant Analysis when applied on the archaeological humeri of phase II.

Classification Results ^{a,b,d}						
			TAXA	Predicted Group Membership		Total
				CH	OA	
Modern Material	Original	Count	CH	67	9	76
			OA	8	62	70
		%	CH	88.2	11.8	100.0
			OA	11.4	88.6	100.0
King's Lynn	Original	Count	CH	0	0	0
			OA	2	23	25
		%	CH	.0	.0	100.0
			OA	8.0	92.0	100.0

a. 88.4% of selected original grouped cases correctly classified.
 b. 92.0% of unselected original grouped cases correctly classified.
 d. 86.3% of selected cross-validated grouped cases correctly classified. Cross validation is done only for those cases in the analysis. In cross validation, each case is classified by the functions derived from all cases other than that case.

Radius

Table 3.26 shows that all the complete archaeological radii (only five) originally classified as sheep were attributed correctly, resulting in a 100% correct reattribution rate.

Table 3.26 Results from the Discriminant Analysis when applied on the archaeological radii of phase II.

Classification Results ^{a,b,d}						
			TAXA	Predicted Group Membership		Total
				CH	OA	
Modern Material	Original	Count	CH	53	3	56
			OA	4	47	51
		%	CH	94.6	5.4	100.0
			OA	7.8	92.2	100.0
King's Lynn	Original	Count	CH	0	0	0
			OA	0	5	5
		%	CH	.0	.0	100.0
			OA	.0	100.0	100.0
a. 93.5% of selected original grouped cases correctly classified.						
b. 100.0% of unselected original grouped cases correctly classified.						
d. 93.5% of selected cross-validated grouped cases correctly classified. Cross validation is done only for those cases in the analysis. In cross validation, each case is classified by the functions derived from all cases other than that case.						

When GL and SD are excluded, the results from both the modern and archaeological sample decrease significantly (Tab. 3.27). Despite the fact that the archaeological sample size has increased significantly, a higher number of misclassifications occurred, highlighting the influence of the two excluded variables. Nevertheless, the final correct reattribution rate is still a satisfactory 89.3%.

Table 3.27 Results from the Discriminant Analysis when applied on the archaeological radii of phase II, excluding variables GL and SD.

Classification Results ^{a,b,d}						
			TAXA	Predicted Group Membership		Total
				CH	OA	
Modern Material	Original	Count	CH	64	10	74
			OA	5	66	71
		%	CH	86.5	13.5	100.0
			OA	7.0	93.0	100.0
King's Lynn	Original	Count	CH	0	0	0
			OA	3	25	28
		%	CH	.0	.0	100.0
			OA	10.7	89.3	100.0
a. 89.7% of selected original grouped cases correctly classified.						
b. 89.3% of unselected original grouped cases correctly classified.						
d. 88.3% of selected cross-validated grouped cases correctly classified. Cross validation is done only for those cases in the analysis. In cross validation, each case is classified by the functions derived from all cases other than that case.						

Ulna

Table 3.28 shows that, when all measurements are included, complete agreement exists between the morphological and the biometrical results (100% or correct reattributions). The unidentified specimen present has been identified as sheep.

Table 3.28 Results from the Discriminant Analysis when applied on the archaeological ulnae of phase II.

Classification Results ^{a,b,d}						
			TAXA	Predicted Group Membership		Total
				CH	OA	
Modern Material	Original	Count	CH	53	3	56
			OA	5	52	57
		%	CH	94.6	5.4	100.0
			OA	8.8	91.2	100.0
King's Lynn	Original	Count	CH	0	0	0
			OA	0	4	4
			O/C	0	1	1
		%	CH	.0	.0	100.0
			OA	.0	100.0	100.0
			O/C	.0	100.0	100.0
a. 92.9% of selected original grouped cases correctly classified.						
b. 100.0% of unselected original grouped cases correctly classified.						
d. 92.0% of selected cross-validated grouped cases correctly classified. Cross validation is done only for those cases in the analysis. In cross validation, each case is classified by the functions derived from all cases other than that case.						

The correct reattribution rate decreases only slightly for both the archaeological (93.8%) and the modern sample (92%) when B and L are excluded (Tab. 3.29). Clearly these variables concur to a lesser degree to the discrimination. Both the unidentified specimens were assigned to the sheep group.

Table 3.29 Results from the Discriminant Analysis when applied on the archaeological ulnae of phase II, excluding variables B and L.

Classification Results ^{a,b,d}						
			TAXA	Predicted Group Membership		Total
				CH	OA	
Modern Material	Original	Count	CH	52	4	56
			OA	5	52	57
		%	CH	92.9	7.1	100.0
			OA	8.8	91.2	100.0
King's Lynn	Original	Count	CH	0	0	0
			OA	1	15	16
			O/C	0	2	2
		%	CH	.0	.0	100.0
			OA	6.3	93.8	100.0
			O/C	.0	100.0	100.0
a. 92.0% of selected original grouped cases correctly classified.						
b. 93.8% of unselected original grouped cases correctly classified.						
d. 91.2% of selected cross-validated grouped cases correctly classified. Cross validation is done only for those cases in the analysis. In cross validation, each case is classified by the functions derived from all cases other than that case.						

Metacarpal

Table 3.30 shows that, despite the small archaeological sample size, when all the variables for the metacarpal are included, a very high reattribution rate was reached (100%).

Table 3.30 Results from the Discriminant Analysis when applied on the archaeological metacarpals of phase II.

Classification Results ^{a,b,d}						
			TAXA	Predicted Group Membership		Total
				CH	OA	
Modern Material	Original	Count	CH	56	2	58
			OA	0	61	61
		%	CH	96.6	3.4	100.0
			OA	.0	100.0	100.0
King's Lynn	Original	Count	CH	0	0	0
			OA	0	3	3
		%	CH	.0	.0	100.0
			OA	.0	100.0	100.0
a. 98.3% of selected original grouped cases correctly classified.						
b. 100.0% of unselected original grouped cases correctly classified.						

Classification Results ^{a,b,d}	
d. 97.5% of selected cross-validated grouped cases correctly classified. Cross validation is done only for those cases in the analysis. In cross validation, each case is classified by the functions derived from all cases other than that case.	

When GL and SD are excluded (Tab. 3.31), a drop in the percentage of correct reattributions, both in the modern (97.5%) and in the archaeological sample (83.3%), can be seen. This decrease is more significant for the archaeological sample due to its small size.

Table 3.31 Results from the Discriminant Analysis when applied on the archaeological metacarpals of phase II, excluding variables GL and SD.

Classification Results ^{a,b,d}						
			TAXA	Predicted Group Membership		Total
				CH	OA	
Modern Material	Original	Count	CH	56	2	58
			OA	1	60	61
		%	CH	96.6	3.4	100.0
			OA	1.6	98.4	100.0
King's Lynn	Original	Count	CH	0	0	0
			OA	2	10	12
		%	CH	.0	.0	100.0
			OA	16.7	83.3	100.0
a. 97.5% of selected original grouped cases correctly classified.						
b. 83.3% of unselected original grouped cases correctly classified.						
d. 96.6% of selected cross-validated grouped cases correctly classified. Cross validation is done only for those cases in the analysis. In cross validation, each case is classified by the functions derived from all cases other than that case.						

Metatarsal

When all the variables for the metatarsal are included, complete agreement between the morphological identifications and the DA results is present (100% of correct reattributions. Tab. 3.32).

Table 3.32 Results from the Discriminant Analysis when applied on the archaeological metatarsals of phase II.

Classification Results ^{a,b,d}						
			TAXA	Predicted Group Membership		Total
				CH	OA	
Modern Material	Original	Count	CH	56	5	61
			OA	4	59	63
		%	CH	91.8	8.2	100.0
			OA	6.3	93.7	100.0
King's Lynn	Original	Count	CH	0	0	0
			OA	0	2	2
		%	CH	.0	.0	100.0
			OA	.0	100.0	100.0

a. 92.7% of selected original grouped cases correctly classified.

b. 100.0% of unselected original grouped cases correctly classified.

d. 91.1% of selected cross-validated grouped cases correctly classified. Cross validation is done only for those cases in the analysis. In cross validation, each case is classified by the functions derived from all cases other than that case.

The exclusion of GL and SD (Tab. 3.33) increases the archaeological sample size but does not influence the results which stay stable at 100% of correct reattributions.

Table 3.33 Results from the Discriminant Analysis when applied on the archaeological metatarsals of phase II, excluding variables GL and SD.

Classification Results ^{a,b,d}						
			TAXA	Predicted Group Membership		Total
				CH	OA	
Modern Material	Original	Count	CH	51	10	61
			OA	4	59	63
		%	CH	83.6	16.4	100.0
			OA	6.3	93.7	100.0
King's Lynn	Original	Count	CH	0	0	0
			OA	0	11	11
		%	CH	.0	.0	100.0
			OA	.0	100.0	100.0

a. 88.7% of selected original grouped cases correctly classified.

b. 100.0% of unselected original grouped cases correctly classified.

d. 85.5% of selected cross-validated grouped cases correctly classified. Cross validation is done only for those cases in the analysis. In cross validation, each case is classified by the functions derived from all cases other than that case.

Tibia

No complete archaeological tibiae were recorded; as such, variable GL was excluded from the beginning. The results (Tab. 3.34) show that three of the 18 originally classified sheep were misclassified as goat. Despite some disagreement between morphological and biometrical identifications, the total percentage of correct reattributions is 83.3%, a higher value than the results from the modern material (74.5%). The unidentified specimen has been attributed to the sheep species.

Table 3.34 Results from the Discriminant Analysis when applied on the archaeological tibiae of phase II, excluding variable GL.

Classification Results ^{a,b,d}						
			TAXA	Predicted Group Membership		Total
				CH	OA	
Modern Material	Original	Count	CH	45	13	58
			OA	15	37	52
		%	CH	77.6	22.4	100.0
			OA	28.8	71.2	100.0
King's Lynn	Original	Count	CH	0	0	0
			OA	3	15	18
			O/C	0	1	1
		%	CH	.0	.0	100.0
			OA	16.7	83.3	100.0
			O/C	.0	100.0	100.0
a. 74.5% of selected original grouped cases correctly classified.						
b. 83.3% of unselected original grouped cases correctly classified.						
d. 72.7% of selected cross-validated grouped cases correctly classified. Cross validation is done only for those cases in the analysis. In cross validation, each case is classified by the functions derived from all cases other than that case.						

When both GL and SD are excluded (Tab. 3.35), both the modern (71.8%) and the archaeological (71.4%) reattribution rates decrease. A higher number of misclassifications occurred in both samples, showing the influence GL and SD have on the discriminant power of DA.

Table 3.35 Results from the Discriminant Analysis when applied on the archaeological tibiae of phase II, excluding variables GL and SD.

Classification Results ^{a,b,d}						
			TAXA	Predicted Group Membership		Total
				CH	OA	
Modern Material	Original	Count	CH	42	16	58
			OA	15	37	52
		%	CH	72.4	27.6	100.0
			OA	28.8	71.2	100.0
King's Lynn	Original	Count	CH	0	0	0
			OA	8	20	28
			OC	0	2	2
		%	CH	.0	.0	100.0
			OA	28.6	71.4	100.0
			OC	.0	100.0	100.0
a. 71.8% of selected original grouped cases correctly classified.						
b. 71.4% of unselected original grouped cases correctly classified.						
d. 70.0% of selected cross-validated grouped cases correctly classified. Cross validation is done only for those cases in the analysis. In cross validation, each case is classified by the functions derived from all cases other than that case.						

Astragalus

The percentage of correct attributions for the astragalus is 76.9% (Tab. 3.36) as two archaeological sheep were misclassified as goat. The low percentage given by this element is perhaps influenced by the reduced archaeological sample size.

Table 3.36 Results from the Discriminant Analysis when applied on the archaeological astragali of phase II.

Classification Results ^{a,b,d}						
			TAXA	Predicted Group Membership		Total
				CH	OA	
Modern Material	Original	Count	CH	65	7	72
			OA	9	64	73
		%	CH	90.3	9.7	100.0
			OA	12.3	87.7	100.0
King's Lynn	Original	Count	CH	0	0	0
			OA	3	10	13
		%	CH	.0	.0	100.0
			OA	23.1	76.9	100.0
a. 89.0% of selected original grouped cases correctly classified.						

Classification Results ^{a,b,d}	
b. 76.9% of unselected original grouped cases correctly classified.	
d. 86.9% of selected cross-validated grouped cases correctly classified. Cross validation is done only for those cases in the analysis. In cross validation, each case is classified by the functions derived from all cases other than that case.	

Calcaneum

Complete agreement between the morphological and the biometrical identifications (Tab. 3.37) is attested by the outcomes from the analysis of the archaeological calcanea (100% of correct reattributions).

Table 3.37 Results from the Discriminant Analysis when applied on the archaeological calcanea of phase II.

Classification Results ^{a,b,d}						
			TAXA	Predicted Group Membership		Total
				CH	OA	
Modern Material	Original	Count	CH	55	5	60
			OA	1	61	62
		%	CH	91.7	8.3	100.0
			OA	1.6	98.4	100.0
King's Lynn	Original	Count	CH	0	0	0
			OA	0	13	13
		%	CH	.0	.0	100.0
			OA	.0	100.0	100.0
a. 95.1% of selected original grouped cases correctly classified.						
b. 100.0% of unselected original grouped cases correctly classified.						
d. 95.1% of selected cross-validated grouped cases correctly classified. Cross validation is done only for those cases in the analysis. In cross validation, each case is classified by the functions derived from all cases other than that case.						

Table 3.38 demonstrates that, when the variables SB and GL are excluded, the correct reattribution rate does not change for the archaeological material (100%).

Table 3.38 Results from the Discriminant Analysis when applied on the archaeological calcanea of phase II, excluding variables SB and GL.

Classification Results ^{a,b,d}						
			TAXA	Predicted Group Membership		Total
				CH	OA	
Modern Material	Original	Count	CH	53	7	60
			OA	2	60	62
		%	CH	88.3	11.7	100.0
			OA	3.2	96.8	100.0
King's Lynn	Original	Count	CH	0	0	0
			OA	0	18	18
		%	CH	.0	.0	100.0
			OA	.0	100.0	100.0
a. 92.6% of selected original grouped cases correctly classified.						
b. 100.0% of unselected original grouped cases correctly classified.						
d. 92.6% of selected cross-validated grouped cases correctly classified. Cross validation is done only for those cases in the analysis. In cross validation, each case is classified by the functions derived from all cases other than that case.						

Discriminant Analysis: Phase III

Horncores

Very high agreement between the morphological and biometrical identifications is confirmed once again for the horncores. The percentage of correct reattribution is, in fact, 92.9% (Tab. 3.39).

Table 3.39 Results from the Discriminant Analysis when applied on the archaeological horncores of phase III.

Classification Results ^{a,b,d}						
			TAXA	Predicted Group Membership		Total
				CH	OA	
Modern Material	Original	Count	CH	33	2	35
			OA	1	27	28
		%	CH	94.3	5.7	100.0
			OA	3.6	96.4	100.0
King's Lynn	Original	Count	CH	10	1	11
			OA	0	3	3
		%	CH	90.9	9.1	100.0
			OA	.0	100.0	100.0
a. 95.2% of selected original grouped cases correctly classified.						

Classification Results ^{a,b,d}	
b. 92.9% of unselected original grouped cases correctly classified.	
d. 95.2% of selected cross-validated grouped cases correctly classified. Cross validation is done only for those cases in the analysis. In cross validation, each case is classified by the functions derived from all cases other than that case.	

The archaeological reattribution rate decreases when E and F are excluded (84.6%), confirming the same pattern observed for the previous phases (Fig. 3.40).

Table 3.40 Results from the Discriminant Analysis when applied on the archaeological horncores of phase III, excluding variables E and F.

Classification Results ^{a,b,d}						
			TAXA	Predicted Group Membership		Total
				CH	OA	
Modern Material	Original	Count	CH	25	10	35
			OA	2	26	28
		%	CH	71.4	28.6	100.0
			OA	7.1	92.9	100.0
King's Lynn	Original	Count	CH	19	4	23
			OA	0	3	3
		%	CH	82.6	17.4	100.0
			OA	.0	100.0	100.0
a. 81.0% of selected original grouped cases correctly classified.						
b. 84.6% of unselected original grouped cases correctly classified.						
d. 79.4% of selected cross-validated grouped cases correctly classified. Cross validation is done only for those cases in the analysis. In cross validation, each case is classified by the functions derived from all cases other than that case.						

Scapula

Table 3.41 shows that the archaeological sample provided higher results (100% of correct reattribution) compared to the outcomes of the modern sample. Thus complete agreement between morphology and biometry is confirmed.

Table 3.41 Results from the Discriminant Analysis when applied on the archaeological scapulae of phase III.

Classification Results ^{a,b,d}						
			TAXA	Predicted Group Membership		Total
				CH	OA	
Modern Material	Original	Count	CH	64	10	74
			OA	10	63	73
		%	CH	86.5	13.5	100.0
			OA	13.7	86.3	100.0
King's Lynn	Original	Count	CH	0	0	0
			OA	0	6	6
		%	CH	.0	.0	100.0
			OA	.0	100.0	100.0
a. 86.4% of selected original grouped cases correctly classified.						
b. 100.0% of unselected original grouped cases correctly classified.						
d. 83.0% of selected cross-validated grouped cases correctly classified. Cross validation is done only for those cases in the analysis. In cross validation, each case is classified by the functions derived from all cases other than that case.						

Humerus

The percentage of correct reattributions for the humerus in phase III is slightly lower than the previous phases (Tab. 3.42). Nevertheless, the result is still a satisfactory 83.3%.

Table 3.42 Results from the Discriminant Analysis when applied on the archaeological humeri of phase III.

Classification Results ^{a,b,d}						
			TAXA	Predicted Group Membership		Total
				CH	OA	
Modern Material	Original	Count	CH	67	9	76
			OA	8	62	70
		%	CH	88.2	11.8	100.0
			OA	11.4	88.6	100.0
King's Lynn	Original	Count	CH	0	0	0
			OA	3	15	18
			OC	1	0	1
		%	CH	.0	.0	100.0
			OA	16.7	83.3	100.0
			OC	100.0	.0	100.0
a. 88.4% of selected original grouped cases correctly classified.						
b. 83.3% of unselected original grouped cases correctly classified.						

Classification Results ^{a,b,d}	
d. 86.3% of selected cross-validated grouped cases correctly classified. Cross validation is done only for those cases in the analysis. In cross validation, each case is classified by the functions derived from all cases other than that case.	

Radius

When all variables are included, the result for the radius is a disappointing 40% (Tab. 3.43). This low result cannot only be due to a misidentification of the morphological criteria as, if this were the case, the same pattern would also have emerged from the analysis of the BI. The results might have been biased by it the very small sample size.

Table 3.43 Results from the Discriminant Analysis when applied on the archaeological radii of phase III.

Classification Results ^{a,b,d}						
			TAXA	Predicted Group Membership		Total
				CH	OA	
Modern Material	Original	Count	CH	53	3	56
			OA	4	47	51
		%	CH	94.6	5.4	100.0
			OA	7.8	92.2	100.0
King's Lynn	Original	Count	CH	0	0	0
			OA	3	2	5
		%	CH	.0	.0	100.0
			OA	60.0	40.0	100.0
a. 93.5% of selected original grouped cases correctly classified.						
b. 40.0% of unselected original grouped cases correctly classified.						
d. 93.5% of selected cross-validated grouped cases correctly classified. Cross validation is done only for those cases in the analysis. In cross validation, each case is classified by the functions derived from all cases other than that case.						

Table 3.44 shows that, with the exclusion of GL and SD, the archaeological sample size increases as does the percentage of correct reattribution (78.9%), confirming the influence of the sample size. The only radius morphologically classified as goat was also recognised as such by SPSS.

Table 3.44 Results from the Discriminant Analysis when applied on the archaeological radii of phase III, excluding variables GL and SD.

Classification Results ^{a,b,d}						
			TAXA	Predicted Group Membership		Total
				CH	OA	
Modern Material	Original	Count	CH	64	10	74
			OA	5	66	71
		%	CH	86.5	13.5	100.0
			OA	7.0	93.0	100.0
King's Lynn	Original	Count	CH	1	0	1
			OA	4	14	18
		%	CH	100.0	.0	100.0
			OA	22.2	77.8	100.0
a. 89.7% of selected original grouped cases correctly classified.						
b. 78.9% of unselected original grouped cases correctly classified.						
d. 88.3% of selected cross-validated grouped cases correctly classified. Cross validation is done only for those cases in the analysis. In cross validation, each case is classified by the functions derived from all cases other than that case.						

Ulna

Table 3.45 shows that the only complete ulna present was also attributed to sheep by DA.

Table 3.45 Results from the Discriminant Analysis when applied on the archaeological ulnae of phase III.

Classification Results ^{a,b,d}						
			TAXA	Predicted Group Membership		Total
				CH	OA	
Modern Material	Original	Count	CH	53	3	56
			OA	5	52	57
		%	CH	94.6	5.4	100.0
			OA	8.8	91.2	100.0
King's Lynn	Original	Count	CH	0	0	0
			OA	0	1	1
		%	CH	.0	.0	100.0
			OA	.0	100.0	100.0
a. 92.9% of selected original grouped cases correctly classified.						
b. 100.0% of unselected original grouped cases correctly classified.						
d. 92.0% of selected cross-validated grouped cases correctly classified. Cross validation is done only for those cases in the analysis. In cross validation, each case is classified by the functions derived from all cases other than that case.						

When the variables B and L are excluded, results remain stable at 80%. Only one sheep specimen reclassified as goat is present (Tab. 3.46).

Table 3.46 Results from the Discriminant Analysis when applied on the archaeological ulnae of phase III, excluding variables B and L.

Classification Results ^{a,b,d}						
			TAXA	Predicted Group Membership		Total
				CH	OA	
Modern Material	Original	Count	CH	52	4	56
			OA	5	52	57
		%	CH	92.9	7.1	100.0
			OA	8.8	91.2	100.0
King's Lynn	Original	Count	CH	0	0	0
			OA	1	4	5
		%	CH	.0	.0	100.0
			OA	20.0	80.0	100.0
a. 92.0% of selected original grouped cases correctly classified.						
b. 80.0% of unselected original grouped cases correctly classified.						
d. 91.2% of selected cross-validated grouped cases correctly classified. Cross validation is done only for those cases in the analysis. In cross validation, each case is classified by the functions derived from all cases other than that case.						

Metacarpal

Only two complete sheep metacarpals were recorded and results from DA agree with this identification (Tab. 3.47).

The percentage of correct reattributions also stays stable when GL and SD are excluded and the archaeological sample slightly increases (Tab. 3.48).

Table 3.47 Results from the Discriminant Analysis when applied on the archaeological metacarpals of phase III.

Classification Results ^{a,b,d}						
			TAXA	Predicted Group Membership		Total
				CH	OA	
Modern Material	Original	Count	CH	56	2	58
			OA	0	61	61
		%	CH	96.6	3.4	100.0
			OA	.0	100.0	100.0
	Cross-validated ^c	Count	CH	55	3	58
			OA	0	61	61
		%	CH	94.8	5.2	100.0
			OA	.0	100.0	100.0
King's Lynn	Original	Count	CH	0	0	0
			OA	0	2	2
		%	CH	.0	.0	100.0
			OA	.0	100.0	100.0
a. 98.3% of selected original grouped cases correctly classified.						
b. 100.0% of unselected original grouped cases correctly classified.						
d. 97.5% of selected cross-validated grouped cases correctly classified. Cross validation is done only for those cases in the analysis. In cross validation, each case is classified by the functions derived from all cases other than that case.						

Table 3.48 Results from the Discriminant Analysis when applied on the archaeological metacarpals of phase III, excluding variables GL and SD.

Classification Results ^{a,b,d}						
			TAXA	Predicted Group Membership		Total
				CH	OA	
Modern Material	Original	Count	CH	56	2	58
			OA	1	60	61
		%	CH	96.6	3.4	100.0
			OA	1.6	98.4	100.0
King's Lynn	Original	Count	CH	0	0	0
			OA	0	4	4
		%	CH	.0	.0	100.0
			OA	.0	100.0	100.0
a. 97.5% of selected original grouped cases correctly classified.						
b. 100.0% of unselected original grouped cases correctly classified.						
d. 96.6% of selected cross-validated grouped cases correctly classified. Cross validation is done only for those cases in the analysis. In cross validation, each case is classified by the functions derived from all cases other than that case.						

Tibia

The reattribution rate for the tibia in this phase (78.9%), if compared to the results obtained in the previous phases, is slightly lower. A certain degree of agreement can nevertheless be seen between the morphological and biometrical identifications (Tab. 3.49).

Table 3.49 Results from the Discriminant Analysis when applied on the archaeological tibiae of phase III, excluding variable GL.

Classification Results ^{a,b,d}						
			TAXA	Predicted Group Membership		Total
				CH	OA	
Modern Material	Original	Count	CH	45	13	58
			OA	15	37	52
		%	CH	77.6	22.4	100.0
			OA	28.8	71.2	100.0
King's Lynn	Original	Count	CH	0	0	0
			OA	4	15	19
		%	CH	.0	.0	100.0
			OA	21.1	78.9	100.0
a. 74.5% of selected original grouped cases correctly classified.						
b. 78.9% of unselected original grouped cases correctly classified.						
d. 72.7% of selected cross-validated grouped cases correctly classified. Cross validation is done only for those cases in the analysis. In cross validation, each case is classified by the functions derived from all cases other than that case.						

Table 3.50 shows that, with the exclusion of GL and SD, the results for both samples decrease (from 78.9% to 74.1% for the archaeological material). This highlights, once again, the impact of the exclusion on the discriminant power of the DA.

Table 3.50 Results from the Discriminant Analysis when applied on the archaeological tibiae of phase III, excluding variables GL and SD.

Classification Results ^{a,b,d}						
			TAXA	Predicted Group Membership		Total
				CH	OA	
Modern Material	Original	Count	CH	42	16	58
			OA	15	37	52
		%	CH	72.4	27.6	100.0
			OA	28.8	71.2	100.0
King's Lynn	Original	Count	CH	0	0	0
			OA	7	20	27
		%	CH	.0	.0	100.0
			OA	25.9	74.1	100.0
a. 71.8% of selected original grouped cases correctly classified.						
b. 74.1% of unselected original grouped cases correctly classified.						
d. 70.0% of selected cross-validated grouped cases correctly classified. Cross validation is done only for those cases in the analysis. In cross validation, each case is classified by the functions derived from all cases other than that case.						

Astragalus

The results for the astragalus are satisfactory (80%) even though the sample size is extremely small. One sheep was reclassified as goat but a certain degree of agreement between morphological and biometrical identifications is attested (Tab. 3.51).

Table 3.51 Results from the Discriminant Analysis when applied on the archaeological astragali of phase III.

Classification Results ^{a,b,d}						
			TAXA	Predicted Group Membership		Total
				CH	OA	
Modern Material	Original	Count	CH	65	7	72
			OA	9	64	73
		%	CH	90.3	9.7	100.0
			OA	12.3	87.7	100.0
King's Lynn	Original	Count	CH	0	0	0
			OA	1	4	5
		%	CH	.0	.0	100.0
			OA	20.0	80.0	100.0
a. 89.0% of selected original grouped cases correctly classified.						
b. 80.0% of unselected original grouped cases correctly classified.						
d. 86.9% of selected cross-validated grouped cases correctly classified. Cross validation is done only for those cases in the analysis. In cross validation, each case is classified by the functions derived from all cases other than that case.						

Calcaneum

Table 3.52 shows that, for the calcaneum, the DA did not give high results (50%). The archaeological sample size is extremely small and, of the two originally identified sheep, one was attributed to goat by the DA. As this disagreement has not been noticed when the BI were applied, it is likely to be due to the small archaeological sample size.

Table 3.52 Results from the Discriminant Analysis when applied on the archaeological calcanea of phase III.

Classification Results ^{a,b,d}						
			TAXA	Predicted Group Membership		Total
				CH	OA	
Modern Material	Original	Count	CH	55	5	60
			OA	1	61	62
		%	CH	91.7	8.3	100.0
			OA	1.6	98.4	100.0
King's Lynn	Original	Count	CH	0	0	0
			OA	1	1	2
		%	CH	.0	.0	100.0
			OA	50.0	50.0	100.0
a. 95.1% of selected original grouped cases correctly classified.						
b. 50.0% of unselected original grouped cases correctly classified.						
d. 95.1% of selected cross-validated grouped cases correctly classified. Cross validation is done only for those cases in the analysis. In cross validation, each case is classified by the functions derived from all cases other than that case.						

Discriminant Analysis: Phase IV

Horncores

Complete agreement (100%) is, once again, present between biometrical and morphological attributions for the horncores from Phase IV (Tab. 3.53).

The percentage of correct reattributions decreases in both samples, but is still a very high value (90.9% for the archaeological material) when E and F are excluded (Tab. 3.54).

Table 3.53 Results from the Discriminant Analysis when applied on the archaeological horncores of phase IV.

Classification Results ^{a,b,d}						
			TAXA	Predicted Group Membership		Total
				CH	OA	
Modern Material	Original	Count	CH	33	2	35
			OA	1	27	28
		%	CH	94.3	5.7	100.0
			OA	3.6	96.4	100.0
King's Lynn	Original	Count	CH	5	0	5
			OA	0	5	5
		%	CH	100.0	.0	100.0
			OA	.0	100.0	100.0
a. 95.2% of selected original grouped cases correctly classified.						
b. 100.0% of unselected original grouped cases correctly classified.						
d. 95.2% of selected cross-validated grouped cases correctly classified. Cross validation is done only for those cases in the analysis. In cross validation, each case is classified by the functions derived from all cases other than that case.						

Table 3.54 Results from the Discriminant Analysis when applied on the archaeological calcanei of phase IV, excluding E and F variables.

Classification Results ^{a,b,d}						
			TAXA	Predicted Group Membership		Total
				CH	OA	
Modern Material	Original	Count	CH	25	10	35
			OA	2	26	28
		%	CH	71.4	28.6	100.0
			OA	7.1	92.9	100.0
King's Lynn	Original	Count	CH	6	0	6
			OA	1	4	5
		%	CH	100.0	.0	100.0
			OA	20.0	80.0	100.0
a. 81.0% of selected original grouped cases correctly classified.						

Classification Results ^{a,b,d}	
b. 90.9% of unselected original grouped cases correctly classified.	
d. 79.4% of selected cross-validated grouped cases correctly classified. Cross validation is done only for those cases in the analysis. In cross validation, each case is classified by the functions derived from all cases other than that case.	

Scapula

Table 3.55 shows that all the 12 sheep scapulae were correctly attributed to sheep by the DA, leading to a total percentage of correct reattributions of 100%.

Table 3.55 Results from the Discriminant Analysis when applied on the archaeological scapulae of phase IV.

Classification Results ^{a,b,d}						
			TAXA	Predicted Group Membership		Total
				CH	OA	
Modern Material	Original	Count	CH	64	10	74
			OA	10	63	73
		%	CH	86.5	13.5	100.0
			OA	13.7	86.3	100.0
King's Lynn	Original	Count	CH	0	0	0
			OA	0	12	12
		%	CH	.0	.0	100.0
			OA	.0	100.0	100.0
a. 86.4% of selected original grouped cases correctly classified.						
b. 100.0% of unselected original grouped cases correctly classified.						
d. 83.0% of selected cross-validated grouped cases correctly classified. Cross validation is done only for those cases in the analysis. In cross validation, each case is classified by the functions derived from all cases other than that case.						

Humerus

All ten morphologically identified sheep humeri were classified as such by DA (Tab. 3.56). Complete agreement is thus present between biometry and morphology.

Table 3.56 Results from the Discriminant Analysis when applied on the archaeological humeri of phase IV.

Classification Results ^{a,b,d}						
			TAXA	Predicted Group Membership		Total
				CH	OA	
Modern Material	Original	Count	CH	67	9	76
			OA	8	62	70
		%	CH	88.2	11.8	100.0
			OA	11.4	88.6	100.0
King's Lynn	Original	Count	CH	0	0	0
			OA	0	10	10
		%	CH	.0	.0	100.0
			OA	.0	100.0	100.0
a. 88.4% of selected original grouped cases correctly classified.						
b. 100.0% of unselected original grouped cases correctly classified.						
d. 86.3% of selected cross-validated grouped cases correctly classified. Cross validation is done only for those cases in the analysis. In cross validation, each case is classified by the functions derived from all cases other than that case.						

Radius

Despite the very small archaeological sample size, complete agreement is present when the radii are considered (Tab. 3.57).

Table 3.57 Results from the Discriminant Analysis when applied on the archaeological radii of phase IV.

Classification Results ^{a,b,d}						
			TAXA	Predicted Group Membership		Total
				CH	OA	
Modern Material	Original	Count	CH	53	3	56
			OA	4	47	51
		%	CH	94.6	5.4	100.0
			OA	7.8	92.2	100.0
King's Lynn	Original	Count	CH	0	0	0
			OA	0	2	2
		%	CH	.0	.0	100.0
			OA	.0	100.0	100.0
a. 93.5% of selected original grouped cases correctly classified.						
b. 100.0% of unselected original grouped cases correctly classified.						
d. 93.5% of selected cross-validated grouped cases correctly classified. Cross validation is done only for those cases in the analysis. In cross validation, each case is classified by the functions derived from all cases other than that case.						

With the exclusion of GL and DS and a slight increase of the sample size, the percentage of correct reattributions decreases (55.6%). Table 3.58 shows that more misclassified specimens are present, revealing the impact of the exclusions on the discriminant power of DA.

Table 3.58 Results from the Discriminant Analysis when applied on the archaeological radii of phase IV, excluding variables GL and SD.

Classification Results ^{a,b,d}						
			TAXA	Predicted Group Membership		Total
				CH	OA	
Modern Material	Original	Count	CH	64	10	74
			OA	5	66	71
		%	CH	86.5	13.5	100.0
			OA	7.0	93.0	100.0
King's Lynn	Original	Count	CH	0	0	0
			OA	4	5	9
		%	CH	.0	.0	100.0
			OA	44.4	55.6	100.0
a. 89.7% of selected original grouped cases correctly classified.						
b. 55.6% of unselected original grouped cases correctly classified.						
d. 88.3% of selected cross-validated grouped cases correctly classified. Cross validation is done only for those cases in the analysis. In cross validation, each case is classified by the functions derived from all cases other than that case.						

Ulna

All the archaeological ulnae morphologically identified as sheep were assigned to the same species by DA, confirming complete agreement between the morphological and the biometrical identifications (Tab. 3.59).

Table 3.59 Results from the Discriminant Analysis when applied on the archaeological ulnae of phase IV.

Classification Results ^{a,b,d}						
			TAXA	Predicted Group Membership		Total
				CH	OA	
Modern Material	Original	Count	CH	53	3	56
			OA	5	52	57
		%	CH	94.6	5.4	100.0
			OA	8.8	91.2	100.0
King's Lynn	Original	Count	CH	0	0	0
			OA	0	5	5
		%	CH	.0	.0	100.0
			OA	.0	100.0	100.0
a. 92.9% of selected original grouped cases correctly classified.						
b. 100.0% of unselected original grouped cases correctly classified.						
d. 92.0% of selected cross-validated grouped cases correctly classified. Cross validation is done only for those cases in the analysis. In cross validation, each case is classified by the functions derived from all cases other than that case.						

Table 3.60 shows that the exclusion of B and L does not have an impact on the discriminant power of DA. In fact, the percentage of total correct reattributions is still very high (100%).

Table 3.60 Results from the Discriminant Analysis when applied on the archaeological ulnae of phase IV, excluding B and L variables.

Classification Results ^{a,b,d}						
			TAXA	Predicted Group Membership		Total
				CH	OA	
Modern Material	Original	Count	CH	52	4	56
			OA	5	52	57
		%	CH	92.9	7.1	100.0
			OA	8.8	91.2	100.0
King's Lynn	Original	Count	CH	0	0	0
			OA	0	8	8
			OC	0	1	1
		%	CH	.0	.0	100.0
			OA	.0	100.0	100.0
			OC	.0	100.0	100.0
a. 92.0% of selected original grouped cases correctly classified.						
b. 100.0% of unselected original grouped cases correctly classified.						
d. 91.2% of selected cross-validated grouped cases correctly classified. Cross validation is done only for those cases in the analysis. In cross validation, each case is classified by the functions derived from all cases other than that case.						

Metacarpal

The only complete archaeological metacarpal morphologically attributed to the sheep was also considered as such by DA (Tab. 3.61).

Table 3.61 Results from the Discriminant Analysis when applied on the archaeological metacarpals of phase IV.

Classification Results ^{a,b,d}						
			TAXA	Predicted Group Membership		Total
				CH	OA	
Modern Material	Original	Count	CH	56	2	58
			OA	0	61	61
		%	CH	96.6	3.4	100.0
			OA	.0	100.0	100.0
King's Lynn	Original	Count	CH	0	0	0
			OA	0	1	1
		%	CH	.0	.0	100.0
			OA	.0	100.0	100.0
a. 98.3% of selected original grouped cases correctly classified.						
b. 100.0% of unselected original grouped cases correctly classified.						
d. 97.5% of selected cross-validated grouped cases correctly classified. Cross validation is done only for those cases in the analysis. In cross validation, each case is classified by the functions derived from all cases other than that case.						

When GL and SD are left out (Tab. 3.62), the archaeological sample size increases slightly and the percentage of correct reattributions remains stable (100%).

Table 3.62 Results from the Discriminant Analysis when applied on the archaeological metacarpals of phase IV, excluding variables GL and SD.

Classification Results ^{a,b,d}						
			TAXA	Predicted Group Membership		Total
				CH	OA	
Modern Material	Original	Count	CH	56	2	58
			OA	1	60	61
		%	CH	96.6	3.4	100.0
			OA	1.6	98.4	100.0
King's Lynn	Original	Count	CH	0	0	0
			OA	0	2	2
		%	CH	.0	.0	100.0
			OA	.0	100.0	100.0
a. 97.5% of selected original grouped cases correctly classified.						
b. 100.0% of unselected original grouped cases correctly classified.						

Classification Results ^{a,b,d}
d. 96.6% of selected cross-validated grouped cases correctly classified. Cross validation is done only for those cases in the analysis. In cross validation, each case is classified by the functions derived from all cases other than that case.

Metatarsal

Less successful results, although still high, are provided by the archaeological metatarsals. When all the variables are included, the percentage of correct reattributions is 83.3% (Tab. 3.63). Two of the 12 sheep metatarsals were attributed to the goat species by DA.

Table 3.63 Results from the Discriminant Analysis when applied on the archaeological metatarsals of phase IV.

Classification Results ^{a,b,d}						
			TAXA	Predicted Group Membership		Total
				CH	OA	
Modern Material	Original	Count	CH	56	5	61
			OA	4	59	63
		%	CH	91.8	8.2	100.0
			OA	6.3	93.7	100.0
King's Lynn	Original	Count	CH	0	0	0
			OA	2	10	12
		%	CH	.0	.0	100.0
			OA	16.7	83.3	100.0
a. 92.7% of selected original grouped cases correctly classified.						
b. 83.3% of unselected original grouped cases correctly classified.						
d. 91.1% of selected cross-validated grouped cases correctly classified. Cross validation is done only for those cases in the analysis. In cross validation, each case is classified by the functions derived from all cases other than that case.						

With the exclusion of GL and SD, despite the sample size increasing slightly, the percentage of correct attribution drops to 78.6% (Tab. 3.64).

Table 3.64 Results from the Discriminant Analysis when applied on the archaeological metatarsals of phase IV, excluding variables GL and SD.

Classification Results ^{a,b,d}						
			TAXA	Predicted Group Membership		Total
				CH	OA	
Modern Material	Original	Count	CH	51	10	61
			OA	4	59	63
		%	CH	83.6	16.4	100.0
			OA	6.3	93.7	100.0
King's Lynn	Original	Count	CH	0	0	0
			OA	3	11	14
		%	CH	.0	.0	100.0
			OA	21.4	78.6	100.0
a. 88.7% of selected original grouped cases correctly classified.						
b. 78.6% of unselected original grouped cases correctly classified.						
d. 85.5% of selected cross-validated grouped cases correctly classified. Cross validation is done only for those cases in the analysis. In cross validation, each case is classified by the functions derived from all cases other than that case.						

Tibia

Due to the mixture of morphological traits, the only complete tibia present was not attributed to one species or the other. According to SPSS, this specimen is a sheep (Tab. 3.65).

Table 3.65 Results from the Discriminant Analysis when applied on the archaeological tibiae of phase IV.

Classification Results ^{a,b,d}						
			TAXA	Predicted Group Membership		Total
				CH	OA	
Modern Material	Original	Count	CH	55	3	58
			OA	9	43	52
		%	CH	94.8	5.2	100.0
			OA	17.3	82.7	100.0
King's Lynn	Original	Count	CH	0	0	0
			OA	0	0	0
			O/C	0	1	1
		%	CH	.0	.0	100.0
			OA	.0	.0	100.0
			O/C	.0	100.0	100.0
a. 89.1% of selected original grouped cases correctly classified.						
b. .0% of unselected original grouped cases correctly classified.						

Classification Results ^{a,b,d}	
d. 86.4% of selected cross-validated grouped cases correctly classified. Cross validation is done only for those cases in the analysis. In cross validation, each case is classified by the functions derived from all cases other than that case.	

When only GL is excluded (Tab. 3.66), complete agreement is present between morphological and biometrical identifications (100%). One specimen that could not be attributed to species level has been assigned to the sheep species by the DA.

Table 3.66 Results from the Discriminant Analysis when applied on the archaeological tibiae of phase IV, excluding variable GL.

Classification Results ^{a,b,d}						
			TAXA	Predicted Group Membership		Total
				CH	OA	
Modern Material	Original	Count	CH	45	13	58
			OA	15	37	52
		%	CH	77.6	22.4	100.0
			OA	28.8	71.2	100.0
King's Lynn	Original	Count	CH	0	0	0
			OA	0	7	7
			O/C	0	1	1
		%	CH	.0	.0	100.0
			OA	.0	100.0	100.0
			O/C	.0	100.0	100.0
a. 74.5% of selected original grouped cases correctly classified.						
b. 100.0% of unselected original grouped cases correctly classified.						
d. 72.7% of selected cross-validated grouped cases correctly classified. Cross validation is done only for those cases in the analysis. In cross validation, each case is classified by the functions derived from all cases other than that case.						

When both SD and GL are excluded (Tab. 3.67), the final percentage of reattributions does not change, remaining stable at 100%. Both the two unidentified specimens have been attributed to the sheep group by SPSS.

Table 3.67 Results from the Discriminant Analysis when applied on the archaeological tibiae of phase IV, excluding variables GL and SD.

Classification Results ^{a,b,d}						
			TAXA	Predicted Group Membership		Total
				CH	OA	
Modern Material	Original	Count	CH	42	16	58
			OA	15	37	52
		%	CH	72.4	27.6	100.0
			OA	28.8	71.2	100.0
King's Lynn	Original	Count	CH	0	0	0
			OA	0	8	8
			O/C	0	2	2
		%	CH	.0	.0	100.0
			OA	.0	100.0	100.0
			O/C	.0	100.0	100.0
a. 71.8% of selected original grouped cases correctly classified.						
b. 100.0% of unselected original grouped cases correctly classified.						
d. 70.0% of selected cross-validated grouped cases correctly classified. Cross validation is done only for those cases in the analysis. In cross validation, each case is classified by the functions derived from all cases other than that case.						

Astragalus

The percentage of correct reattributions for the astragalus is low (Tab. 3.68); a result probably influenced by the very small archaeological sample size.

Table 3.68 Results from the Discriminant Analysis when applied on the archaeological astragali of phase IV.

Classification Results ^{a,b,d}						
			TAXA	Predicted Group Membership		Total
				CH	OA	
Modern Material	Original	Count	CH	65	7	72
			OA	9	64	73
		%	CH	90.3	9.7	100.0
			OA	12.3	87.7	100.0
King's Lynn	Original	Count	CH	0	0	0
			OA	1	1	2
		%	CH	.0	.0	100.0
			OA	50.0	50.0	100.0
a. 89.0% of selected original grouped cases correctly classified.						
b. 50.0% of unselected original grouped cases correctly classified.						

Classification Results ^{a,b,d}	
d. 86.9% of selected cross-validated grouped cases correctly classified. Cross validation is done only for those cases in the analysis. In cross validation, each case is classified by the functions derived from all cases other than that case.	

Calcaneum

Complete agreement between biometrical and morphological identifications is shown by Table 3.69 for the calcanea.

Table 3.69 Results from the Discriminant Analysis when applied on the archaeological calcanea of phase IV.

Classification Results ^{a,b,d}						
			TAXA	Predicted Group Membership		Total
				CH	OA	
Modern Material	Original	Count	CH	55	5	60
			OA	1	61	62
		%	CH	91.7	8.3	100.0
			OA	1.6	98.4	100.0
King's Lynn	Original	Count	CH	0	0	0
			OA	0	3	3
		%	CH	.0	.0	100.0
			OA	.0	100.0	100.0
a. 95.1% of selected original grouped cases correctly classified.						
b. 100.0% of unselected original grouped cases correctly classified.						
d. 95.1% of selected cross-validated grouped cases correctly classified. Cross validation is done only for those cases in the analysis. In cross validation, each case is classified by the functions derived from all cases other than that case.						

Discriminant Analysis: Unstratified specimens

Horncores

The morphological identification of the horncores is totally confirmed by the biometrical data. No misclassified specimens are present leading to 100% correct reattribution (Tab. 3.70).

Less satisfactory results are obtained with the exclusion of E and F, as the percentage of correct reattributions decreases to 57.1% (Tab. 3.71). Once again, the influence of the exclusion of E and F is evident.

Table 3.70 Results from the Discriminant Analysis when applied on the unstratified archaeological horncores.

Classification Results ^{a,b,d}						
			TAXA	Predicted Group Membership		Total
				CH	OA	
Modern Material	Original	Count	CH	33	2	35
			OA	1	27	28
		%	CH	94.3	5.7	100.0
			OA	3.6	96.4	100.0
King's Lynn	Original	Count	CH	3	0	3
			OA	0	1	1
		%	CH	100.0	.0	100.0
			OA	.0	100.0	100.0
a. 95.2% of selected original grouped cases correctly classified.						
b. 100.0% of unselected original grouped cases correctly classified.						
d. 95.2% of selected cross-validated grouped cases correctly classified. Cross validation is done only for those cases in the analysis. In cross validation, each case is classified by the functions derived from all cases other than that case.						

Table 3.71 Results from the Discriminant Analysis when applied on the archaeological unstratified horncores, excluding variables E and F.

Classification Results ^{a,b,d}						
			TAXA	Predicted Group Membership		Total
				CH	OA	
Modern Material	Original	Count	CH	25	10	35
			OA	2	26	28
		%	CH	71.4	28.6	100.0
			OA	7.1	92.9	100.0
Kyng's Lynn	Original	Count	CH	3	3	6
			OA	0	1	1
		%	CH	50.0	50.0	100.0
			OA	.0	100.0	100.0
a. 81.0% of selected original grouped cases correctly classified.						
b. 57.1% of unselected original grouped cases correctly classified.						
d. 79.4% of selected cross-validated grouped cases correctly classified. Cross validation is done only for those cases in the analysis. In cross validation, each case is classified by the functions derived from all cases other than that case.						

Scapula

Some disagreement between biometrical and morphological identifications is present regarding the scapulae, as DA detected a goat which was not identified morphologically. The percentage of correct reclassifications for this element is 75% (Tab. 3.72).

Table 3.72 Results from the Discriminant Analysis when applied on the unstratified archaeological scapulae.

Classification Results ^{a,b,d}						
			TAXA	Predicted Group Membership		Total
				CH	OA	
Modern Material	Original	Count	CH	64	10	74
			OA	10	63	73
		%	CH	86.5	13.5	100.0
			OA	13.7	86.3	100.0
King's Lynn	Original	Count	CH	0	0	0
			OA	1	3	4
		%	CH	.0	.0	100.0
			OA	25.0	75.0	100.0
a. 86.4% of selected original grouped cases correctly classified.						
b. 75.0% of unselected original grouped cases correctly classified.						
d. 83.0% of selected cross-validated grouped cases correctly classified. Cross validation is done only for those cases in the analysis. In cross validation, each case is classified by the functions derived from all cases other than that case.						

Humerus

Complete agreement is present between morphological and biometrical identifications for the humeri. Table 3.73 shows that the percentage of correct reclassified specimens is 100%. The only unidentified specimen has been assigned to the goat group by the DA.

Table 3.73 Results from the Discriminant Analysis when applied on the unstratified archaeological humeri.

Classification Results ^{a,b,d}						
			TAXA	Predicted Group Membership		Total
				CH	OA	
Modern Material	Original	Count	CH	67	9	76
			OA	8	62	70
		%	CH	88.2	11.8	100.0
			OA	11.4	88.6	100.0
King's Lynn	Original	Count	CH	1	0	1
			OA	0	10	10
			O/C	1	0	1
		%	CH	100.0	.0	100.0
			OA	.0	100.0	100.0
			O/C	100.0	.0	100.0
a. 88.4% of selected original grouped cases correctly classified.						
b. 100.0% of unselected original grouped cases correctly classified.						
d. 86.3% of selected cross-validated grouped cases correctly classified. Cross validation is done only for those cases in the analysis. In cross validation, each case is classified by the functions derived from all cases other than that case.						

Radius

Some disagreement between the morphological and the biometrical results is present for the radii, as one goat, not identified morphologically, was detected among the sheep (Tab. 3.74) by DA.

Table 3.74 Results from the Discriminant Analysis when applied on the unstratified archaeological radii.

Classification Results ^{a,b,d}						
			TAXA	Predicted Group Membership		Total
				CH	OA	
Modern Material	Original	Count	CH	53	3	56
			OA	4	47	51
		%	CH	94.6	5.4	100.0
			OA	7.8	92.2	100.0
King's Lynn	Original	Count	CH	0	0	0
			OA	1	4	5
		%	CH	.0	.0	100.0
			OA	20.0	80.0	100.0
a. 93.5% of selected original grouped cases correctly classified.						
b. 80.0% of unselected original grouped cases correctly classified.						

Classification Results^{a,b,d}
d. 93.5% of selected cross-validated grouped cases correctly classified. Cross validation is done only for those cases in the analysis. In cross validation, each case is classified by the functions derived from all cases other than that case.

With the exclusion of GL and SD and the increase of the sample size, the percentage of correct reattributions rises slightly (83.3%. Tab. 3.75).

Table 3.75 Results from the Discriminant Analysis when applied on the unstratified archaeological radii, excluding variables GL and SD.

Classification Results^{a,b,d}						
			TAXA	Predicted Group Membership		Total
				CH	OA	
Modern Material	Original	Count	CH	64	10	74
			OA	5	66	71
		%	CH	86.5	13.5	100.0
			OA	7.0	93.0	100.0
King's Lynn	Original	Count	CH	0	0	0
			OA	3	15	18
		%	CH	.0	.0	100.0
			OA	16.7	83.3	100.0
a. 89.7% of selected original grouped cases correctly classified.						
b. 83.3% of unselected original grouped cases correctly classified.						
d. 88.3% of selected cross-validated grouped cases correctly classified. Cross validation is done only for those cases in the analysis. In cross validation, each case is classified by the functions derived from all cases other than that case.						

Ulna

The results for the complete unstratified ulnae are unimpressive. The low percentage of correct reattributions (50%) is probably influenced by the small sample size (Tab. 3.76). In fact, when the sample size increases and B and L variables are excluded (Tab. 3.77), the percentage of correct reattributions increases notably from 50% to 87.5%. The only unidentified specimen was identified as a sheep by SPSS.

Table 3.76 Results from the Discriminant Analysis when applied on the unstratified archaeological ulnae.

Classification Results ^{a,b,d}						
			TAXA	Predicted Group Membership		Total
				CH	OA	
Modern Material	Original	Count	CH	53	3	56
			OA	5	52	57
		%	CH	94.6	5.4	100.0
			OA	8.8	91.2	100.0
King's Lynn	Original	Count	CH	0	0	0
			OA	1	1	2
		%	CH	.0	.0	100.0
			OA	50.0	50.0	100.0
a. 92.9% of selected original grouped cases correctly classified.						
b. 50.0% of unselected original grouped cases correctly classified.						
d. 92.0% of selected cross-validated grouped cases correctly classified. Cross validation is done only for those cases in the analysis. In cross validation, each case is classified by the functions derived from all cases other than that case.						

Table 3.77 Results from the Discriminant Analysis when applied on the unstratified archaeological ulnae, excluding variables B and L.

Classification Results ^{a,b,d}						
			TAXA	Predicted Group Membership		Total
				CH	OA	
Modern Material	Original	Count	CH	52	4	56
			OA	5	52	57
		%	CH	92.9	7.1	100.0
			OA	8.8	91.2	100.0
King's Lynn	Original	Count	CH	0	0	0
			OA	1	7	8
			O/C	0	1	1
		%	CH	.0	.0	100.0
			OA	12.5	87.5	100.0
			O/C	.0	100.0	100.0
a. 92.0% of selected original grouped cases correctly classified.						
b. 87.5% of unselected original grouped cases correctly classified.						
d. 91.2% of selected cross-validated grouped cases correctly classified. Cross validation is done only for those cases in the analysis. In cross validation, each case is classified by the functions derived from all cases other than that case.						

Metacarpal

Total agreement between biometrical and morphological results is present for the complete archaeological metacarpals (100% of correct attributions. Tab. 3.78).

The percentage of correct reattributions remains stable (100%) when GL and SD variables are excluded from the analysis and the sample size increases slightly (Tab. 3.79).

Table 3.78 Results from the Discriminant Analysis when applied on the unstratified archaeological metacarpals.

Classification Results ^{a,b,d}						
			TAXA	Predicted Group Membership		Total
				CH	OA	
Modern Material	Original	Count	CH	56	2	58
			OA	0	61	61
		%	CH	96.6	3.4	100.0
			OA	.0	100.0	100.0
King's Lynn	Original	Count	CH	0	0	0
			OA	0	9	9
		%	CH	.0	.0	100.0
			OA	.0	100.0	100.0
a. 98.3% of selected original grouped cases correctly classified.						
b. 100.0% of unselected original grouped cases correctly classified.						
d. 97.5% of selected cross-validated grouped cases correctly classified. Cross validation is done only for those cases in the analysis. In cross validation, each case is classified by the functions derived from all cases other than that case.						

Table 3.79 Results from the Discriminant Analysis when applied on the unstratified archaeological metacarpals, excluding variables GL and SD.

Classification Results ^{a,b,d}						
			TAXA	Predicted Group Membership		Total
				CH	OA	
Modern Material	Original	Count	CH	56	2	58
			OA	1	60	61
		%	CH	96.6	3.4	100.0
			OA	1.6	98.4	100.0
King's Lynn	Original	Count	CH	0	0	0
			OA	0	17	17
		%	CH	.0	.0	100.0
			OA	.0	100.0	100.0
a. 97.5% of selected original grouped cases correctly classified.						
b. 100.0% of unselected original grouped cases correctly classified.						

Classification Results ^{a,b,d}	
d. 96.6% of selected cross-validated grouped cases correctly classified. Cross validation is done only for those cases in the analysis. In cross validation, each case is classified by the functions derived from all cases other than that case.	

Metatarsal

The results from the metatarsals are not as high as the metacarpals but can be considered good. Table 3.80 shows that the percentage of correct reattributions when all variables are included is 80%.

Table 3.80 Results from the Discriminant Analysis when applied on the unstratified archaeological metatarsals.

Classification Results ^{a,b,d}						
			TAXA	Predicted Group Membership		Total
				CH	OA	
Modern Material	Original	Count	CH	56	5	61
			OA	4	59	63
		%	CH	91.8	8.2	100.0
			OA	6.3	93.7	100.0
King's Lynn	Original	Count	CH	0	0	0
			OA	1	4	5
		%	CH	.0	.0	100.0
			OA	20.0	80.0	100.0
a. 92.7% of selected original grouped cases correctly classified.						
b. 80.0% of unselected original grouped cases correctly classified.						
d. 91.1% of selected cross-validated grouped cases correctly classified. Cross validation is done only for those cases in the analysis. In cross validation, each case is classified by the functions derived from all cases other than that case.						

When GL and SD are excluded, despite the sample size increasing slightly, the percentage of correct reattributions decreases to 71.4% (Tab. 3.81).

Table 3.81 Results from the Discriminant Analysis when applied on the unstratified archaeological metatarsals, excluding GL and SD variables.

Classification Results ^{a,b,d}						
			TAXA	Predicted Group Membership		Total
				CH	OA	
Modern Material	Original	Count	CH	51	10	61
			OA	4	59	63
		%	CH	83.6	16.4	100.0
			OA	6.3	93.7	100.0
King's Lynn	Original	Count	CH	0	0	0
			OA	2	5	7
		%	CH	.0	.0	100.0
			OA	28.6	71.4	100.0
a. 88.7% of selected original grouped cases correctly classified.						
b. 71.4% of unselected original grouped cases correctly classified.						
d. 85.5% of selected cross-validated grouped cases correctly classified. Cross validation is done only for those cases in the analysis. In cross validation, each case is classified by the functions derived from all cases other than that case.						

Tibia

Some agreement is present between the morphological and biometrical identifications for the two complete tibiae recorded (Tab. 3.82). The results are higher when GL is excluded from the analysis and the sample size increased notably (100%, Tab. 3.83).

When both variables GL and SD are excluded (Tab. 3.84), the loss of the two variables makes the percentage of correct reattributions drop. Nevertheless, the outcome is still significant (90%).

Table 3.82 Results from the Discriminant Analysis when applied on the unstratified archaeological tibiae.

Classification Results ^{a,b,d}						
			TAXA	Predicted Group Membership		Total
				CH	OA	
Modern Material	Original	Count	CH	55	3	58
			OA	9	43	52
		%	CH	94.8	5.2	100.0
			OA	17.3	82.7	100.0
	Cross-validated ^c	Count	CH	54	4	58
			OA	11	41	52
		%	CH	93.1	6.9	100.0
			OA	21.2	78.8	100.0
King's Lynn	Original	Count	CH	0	0	0
			OA	1	1	2
		%	CH	.0	.0	100.0
			OA	50.0	50.0	100.0

a. 89.1% of selected original grouped cases correctly classified.

b. 50.0% of unselected original grouped cases correctly classified.

d. 86.4% of selected cross-validated grouped cases correctly classified. Cross validation is done only for those cases in the analysis. In cross validation, each case is classified by the functions derived from all cases other than that case.

Table 3.83 Results from the Discriminant Analysis when applied on the unstratified archaeological tibiae, excluding variable GL.

Classification Results ^{a,b,d}						
			TAXA	Predicted Group Membership		Total
				CH	OA	
Modern Material	Original	Count	CH	45	13	58
			OA	15	37	52
		%	CH	77.6	22.4	100.0
			OA	28.8	71.2	100.0
King's Lynn	Original	Count	CH	0	0	0
			OA	0	21	21
		%	CH	.0	.0	100.0
			OA	.0	100.0	100.0

a. 74.5% of selected original grouped cases correctly classified.

b. 100.0% of unselected original grouped cases correctly classified.

d. 72.7% of selected cross-validated grouped cases correctly classified. Cross validation is done only for those cases in the analysis. In cross validation, each case is classified by the functions derived from all cases other than that case.

Table 3.84 Results from the Discriminant Analysis when applied on the unstratified archaeological tibiae, excluding variables GL and SD.

Classification Results ^{a,b,d}						
			TAXA	Predicted Group Membership		Total
				CH	OA	
Modern Material	Original	Count	CH	42	16	58
			OA	15	37	52
		%	CH	72.4	27.6	100.0
			OA	28.8	71.2	100.0
King's Lynn	Original	Count	CH	0	0	0
			OA	3	27	30
		%	CH	.0	.0	100.0
			OA	10.0	90.0	100.0
a. 71.8% of selected original grouped cases correctly classified.						
b. 90.0% of unselected original grouped cases correctly classified.						
d. 70.0% of selected cross-validated grouped cases correctly classified. Cross validation is done only for those cases in the analysis. In cross validation, each case is classified by the functions derived from all cases other than that case.						

Astragalus

Complete agreement between biometrical and morphological identifications is also present for the astragali (100% of correct reclassified specimens. Tab. 3.85).

Table 3.85 Results from the Discriminant Analysis when applied on the unstratified archaeological astragali.

Classification Results ^{a,b,d}						
			TAXA	Predicted Group Membership		Total
				CH	OA	
Modern Material	Original	Count	CH	65	7	72
			OA	9	64	73
		%	CH	90.3	9.7	100.0
			OA	12.3	87.7	100.0
King's Lynn	Original	Count	CH	0	0	0
			OA	0	5	5
		%	CH	.0	.0	100.0
			OA	.0	100.0	100.0
a. 89.0% of selected original grouped cases correctly classified.						
b. 100.0% of unselected original grouped cases correctly classified.						
d. 86.9% of selected cross-validated grouped cases correctly classified. Cross validation is done only for those cases in the analysis. In cross validation, each case is classified by the functions derived from all cases other than that case.						

Calcaneum

Table 3.86 shows that no misclassified specimens are present for the calcaneum, attesting to the complete agreement between biometrical and morphological identifications.

Table 3.86 Results from the Discriminant Analysis when applied on the unstratified archaeological calcanea.

Classification Results ^{a,b,d}						
			TAXA	Predicted Group Membership		Total
				CH	OA	
Modern Material	Original	Count	CH	55	5	60
			OA	1	61	62
		%	CH	91.7	8.3	100.0
			OA	1.6	98.4	100.0
King's Lynn	Original	Count	CH	0	0	0
			OA	0	4	4
		%	CH	.0	.0	100.0
			OA	.0	100.0	100.0
a. 95.1% of selected original grouped cases correctly classified.						
b. 100.0% of unselected original grouped cases correctly classified.						
d. 95.1% of selected cross-validated grouped cases correctly classified. Cross validation is done only for those cases in the analysis. In cross validation, each case is classified by the functions derived from all cases other than that case.						

If variables such as GL and SB are left out of the analysis, the results are equally satisfactory (Tab. 3.87).

Table 3.87 Results from the Discriminant Analysis when applied on the unstratified archaeological calcanea, excluding variables GL and SB.

Classification Results ^{a,b,d}						
			TAXA	Predicted Group Membership		Total
				CH	OA	
Modern Material	Original	Count	CH	53	7	60
			OA	2	60	62
		%	CH	88.3	11.7	100.0
			OA	3.2	96.8	100.0
King's Lynn	Original	Count	CH	0	0	0
			OA	0	8	8
		%	CH	.0	.0	100.0
			OA	.0	100.0	100.0
a. 92.6% of selected original grouped cases correctly classified.						
b. 100.0% of unselected original grouped cases correctly classified.						
d. 92.6% of selected cross-validated grouped cases correctly classified. Cross validation is done only for those cases in the analysis. In cross validation, each case is classified by the functions derived from all cases other than that case.						

3.2.9 Discriminant Analysis on the King's Lynn material *in toto*

In order to be able to better assess the potential of the new methodology on archaeological material, and gain a better idea of the extent of the agreement between biometry and morphology, DA was applied on the material from King's Lynn *in toto*. This has increased the sample size and, thus permits better assessment of the effectiveness of the various combinations of measurements.

Results on an element by element basis follow, accompanied by a series of diagrams. The diagrams show, on the horizontal axis, the Individual Discriminant Score attributed by the DA to each case of the archaeological specimens and, on the vertical axis, the species attributions assigned by the program. The only possible attributions were goat, identified by the number 1, and sheep, identified by the number 2 (vertical axis). The vertical lines on the graph represents the group centroids (i.e. group means) for each species.

Horncore

Table 3.88 shows that the percentage of consistent identifications of the archaeological material is 95.7%, a very high result, even higher than the results obtained from the modern material (95.2%). With the exclusion of measurements E and F, the degree of consistency decreases to 81% in the modern material and 84.6% in the archaeological material, which therefore makes the effectiveness of DA on the horncores much more questionable (Tab. 3.89).

Table 3.88 Results from the Discriminant Analysis when applied on all the archaeological horncores.

Classification Results ^{a,b,d}						
			TAXA	Predicted Group Membership		Total
				CH	OA	
Modern Material	Original	Count	CH	33	2	35
			OA	1	27	28
		%	CH	94.3	5.7	100.0
			OA	3.6	96.4	100.0
King's Lynn	Original	Count	CH	28	1	29
			OA	1	16	17
		%	CH	96.6	3.4	100.0
			OA	5.9	94.1	100.0
a. 95.2% of selected original grouped cases correctly classified.						
b. 95.7% of unselected original grouped cases correctly classified.						
d. 95.2% of selected cross-validated grouped cases correctly classified. Cross validation is done only for those cases in the analysis. In cross validation, each case is classified by the functions derived from all cases other than that case.						

Table 3.89 Results from the Discriminant Analysis when applied on all the archaeological horncores, excluding variables E and F.

Classification Results ^{a,b,d}						
			TAXA	Predicted Group Membership		Total
				CH	OA	
Modern Material	Original	Count	CH	25	10	35
			OA	2	26	28
		%	CH	71.4	28.6	100.0
			OA	7.1	92.9	100.0
King's Lynn	Original	Count	CH	45	9	54
			OA	1	10	11
		%	CH	83.3	16.7	100.0
			OA	9.1	90.9	100.0
a. 81.0% of selected original grouped cases correctly classified.						
b. 84.6% of unselected original grouped cases correctly classified.						
d. 79.4% of selected cross-validated grouped cases correctly classified. Cross validation is done only for those cases in the analysis. In cross validation, each case is classified by the functions derived from all cases other than that case.						

Figure 3.124 shows that, when all measurements are included, only two specimens are re-attributed by the DA. Most morphologically identified sheep and goat specimens tend to gather around the group centroid lines of the correct taxa. The 'goat' reclassified as sheep by the DA is

approximately equidistant from the two centroid lines and is marginally an outlier in the sheep range, whereas the reclassified 'sheep' plots well within the goat range and is slightly closer to the goat centroid. The scatterplots with the BI (Figs.3.9-3.10) show that, in phase I, there is indeed a sheep specimen plotting consistently in the goat area.

Considering that the percentage of consistent reattributions obtained from the archaeological material has exceeded the expectations - namely the results from the modern material - and that DA bears a bias itself, there is limited argument for reclassification of the morphologically identified specimens, though the possibility that one of the horncores attributed to the sheep is indeed a goat must be considered.

More misidentified specimens are present when E and F are excluded (Fig. 3.125), which is not surprising as less information are available to the DA. Clearly the exclusion of E and F has an impact on the discrimination power of the function. The fact that expectations are exceeded in the archaeological material means, however, that the reclassifications carried out by the DA are within the expected range of error (i.e. according to the results of the modern material) for this method.

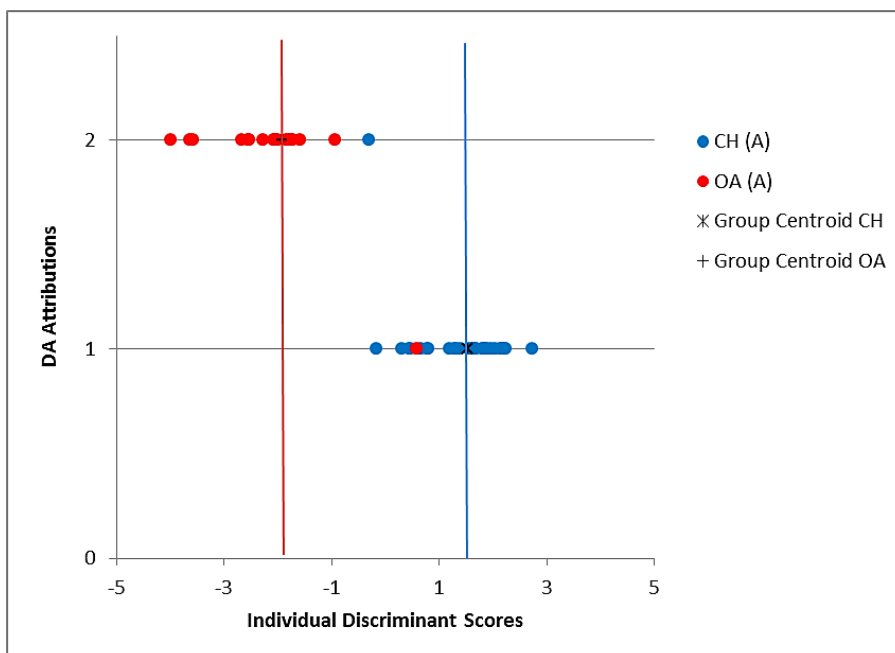


Figure 3.124 Diagram of the individual discriminant scores attributed to the archaeological material by DA for the horncore.

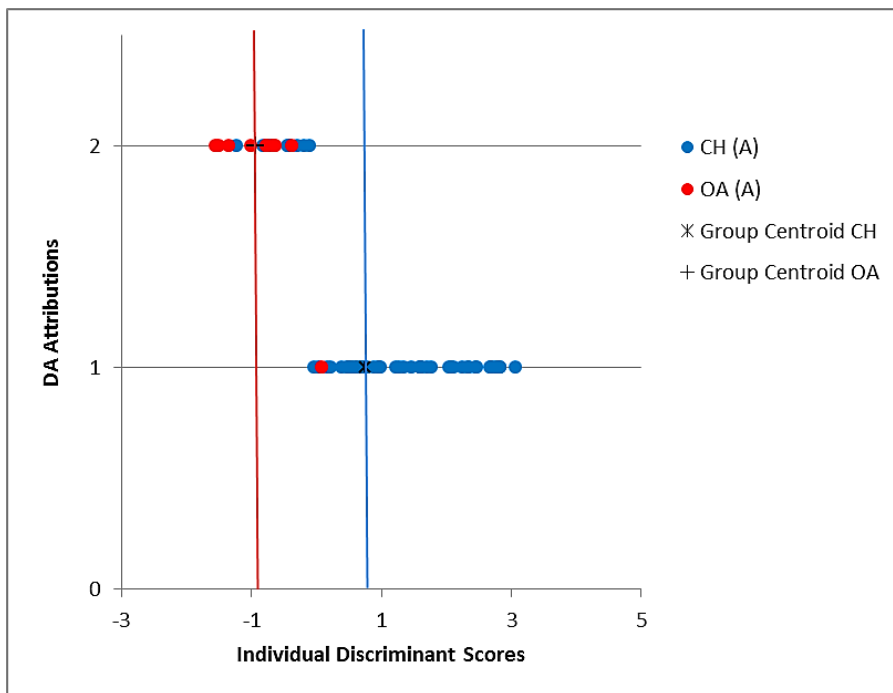


Figure 3.125 Diagram of the individual discriminant scores attributed to the archaeological material by DA for the horncore when variables E and F were excluded.

Scapula

For this element, the degree of consistency (94.2%) is higher than that provided by the modern material (86.4%). A scapula identified morphologically as goat belongs to a sheep (Tab. 3.90), while three morphologically identified sheep scapulae have been attributed to goat. The morphologically unidentified specimen has been attributed to the sheep by DA.

Figure 3.126 shows the position on the diagram of the specimens that were reclassified by the DA. Of these, the three sheep reattributed to goat are equidistant from the two centroids and, as such, their reclassification cannot be relied on, especially considering the error that is inherent to the method. Conversely, the goat scapula reattributed to sheep plots far away from the goat centroid and in the midst of the sheep distribution - it may indeed represent mistaken identification.

Table 3.90 Results from the Discriminant Analysis when applied on all the archaeological scapulae.

Classification Results ^{a,b,d}						
			TAXA	Predicted Group Membership		Total
				CH	OA	
Modern Material	Original	Count	CH	64	10	74
			OA	10	63	73
		%	CH	86.5	13.5	100.0
			OA	13.7	86.3	100.0
King's Lynn	Original	Count	CH	1	1	2
			OA	3	64	67
			O/C	0	1	1
		%	CH	50.0	50.0	100.0
			OA	4.5	95.5	100.0
			O/C	.0	100.0	100.0

a. 86.4% of selected original grouped cases correctly classified.

b. 94.2% of unselected original grouped cases correctly classified.

d. 83.0% of selected cross-validated grouped cases correctly classified. Cross validation is done only for those cases in the analysis. In cross validation, each case is classified by the functions derived from all cases other than that case.

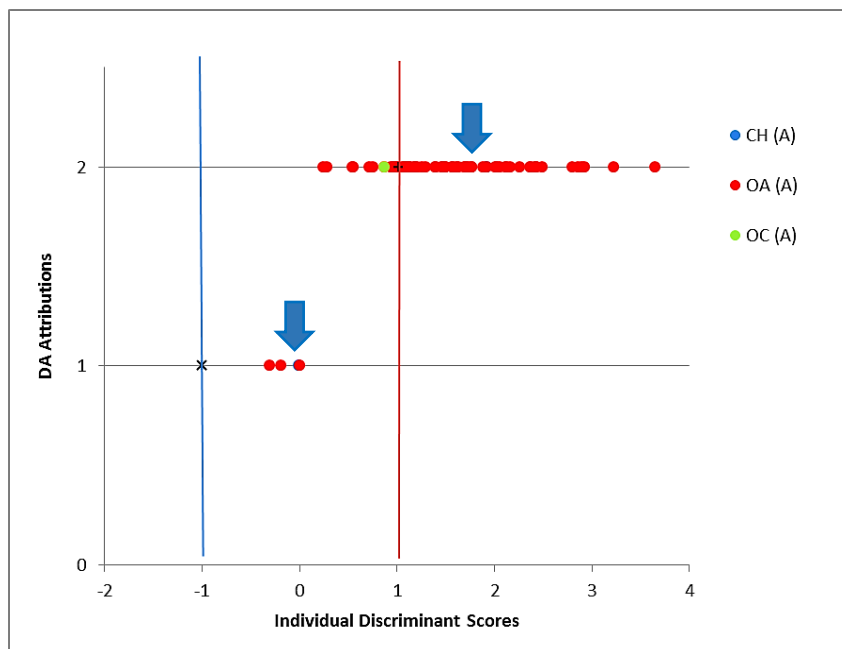


Figure 3.126 Diagram of the individual discriminant scores attributed to the archaeological material by DA for the scapula. Blue arrows indicate the position of the two archaeological goats.

Humerus

The percentage of consistent reattributions for the archaeological humeri is 93.3%, a higher value than the percentage obtained from modern material (88.4%) (Tab. 3.91).

Table 3.91 Results from the Discriminant Analysis when applied on all the archaeological humeri.

Classification Results ^{a,b,d}						
			TAXA	Predicted Group Membership		Total
				CH	OA	
Modern Material	Original	Count	CH	67	9	76
			OA	8	62	70
		%	CH	88.2	11.8	100.0
			OA	11.4	88.6	100.0
King's Lynn	Original	Count	CH	1	0	1
			OA	6	83	89
			O/C	2	0	2
		%	CH	100.0	.0	100.0
			OA	6.7	93.3	100.0
			O/C	100.0	.0	100.0
a. 88.4% of selected original grouped cases correctly classified.						
b. 93.3% of unselected original grouped cases correctly classified.						
d. 86.3% of selected cross-validated grouped cases correctly classified. Cross validation is done only for those cases in the analysis. In cross validation, each case is classified by the functions derived from all cases other than that case.						

Consequently, all the reclassifications proposed by the DA may be regarded as due to the inherent error of the method. However, some of the 'sheep' and 'sheep/goat' specimens reattributed to the 'goat', which plot very close to the goat centroid (Fig. 3.127), may indeed belong to *Capra hircus*.

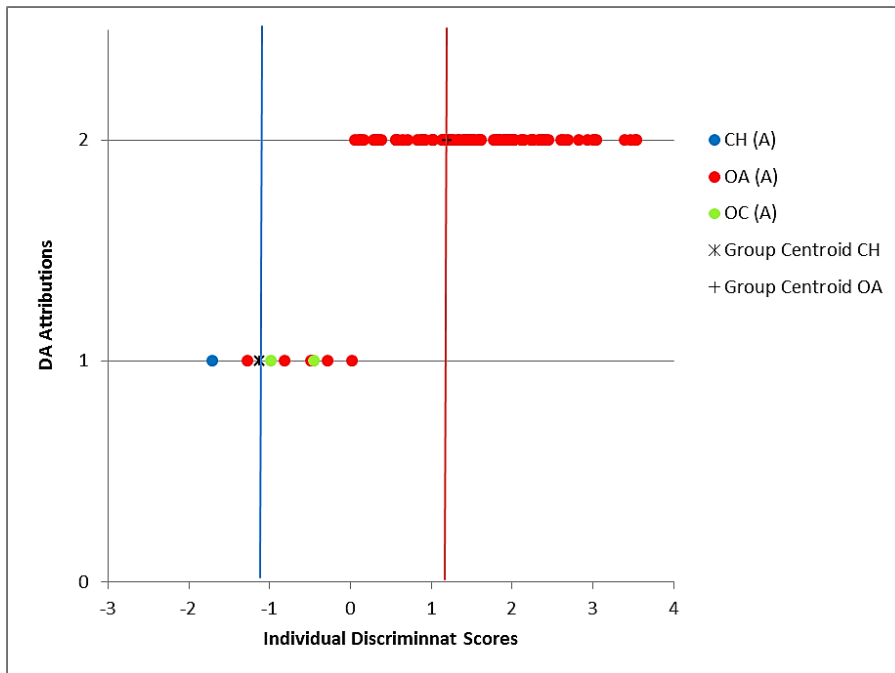


Figure 3.127 Diagram of the individual discriminant scores attributed to the archaeological material by DA for the humerus.

Radius

The percentage of consistent reclassifications for the archaeological radii is 77.8% when all variables are included. This percentage is significantly lower than the results obtained from the modern material (Tab. 3.92), which means that the identification error is higher than what one can reasonably expect from this application. The relative inconsistency between the morphological analysis and the DA may also have partly been caused by the small sample size (n=18). When variables such as GL and SD are excluded from the analysis and the sample size increases significantly (n=80), the percentage of correct reattributions decreases further, though marginally so (76.3%) (Tab. 3.93).

Table 3.92 Results from the Discriminant Analysis when applied on all the archaeological radii.

Classification Results ^{a,b,d}						
			TAXA	Predicted Group Membership		Total
				CH	OA	
Modern Material	Original	Count	CH	53	3	56
			OA	4	47	51
		%	CH	94.6	5.4	100.0
			OA	7.8	92.2	100.0
	Cross-validated ^c	Count	CH	53	3	56
			OA	4	47	51
		%	CH	94.6	5.4	100.0
			OA	7.8	92.2	100.0
King's Lynn	Original	Count	CH	0	0	0
			OA	4	14	18
		%	CH	.0	.0	100.0
			OA	22.2	77.8	100.0
a. 93.5% of selected original grouped cases correctly classified.						
b. 77.8% of unselected original grouped cases correctly classified.						
d. 93.5% of selected cross-validated grouped cases correctly classified. Cross validation is done only for those cases in the analysis. In cross validation, each case is classified by the functions derived from all cases other than that case.						

Table 3.93 Results from the Discriminant Analysis when applied on all the archaeological radii, excluding variables GL and SD.

Classification Results ^{a,b,d}						
			TAXA	Predicted Group Membership		Total
				CH	OA	
Modern Material	Original	Count	CH	64	10	74
			OA	5	66	71
		%	CH	86.5	13.5	100.0
			OA	7.0	93.0	100.0
	Cross-validated ^c	Count	CH	63	11	74
			OA	6	65	71
		%	CH	85.1	14.9	100.0
			OA	8.5	91.5	100.0
King's Lynn	Original	Count	CH	1	0	1
			OA	19	60	79
		%	CH	100.0	.0	100.0
			OA	24.1	75.9	100.0
a. 89.7% of selected original grouped cases correctly classified.						
b. 76.3% of unselected original grouped cases correctly classified.						

Classification Results^{a,b,d}

d. 88.3% of selected cross-validated grouped cases correctly classified. Cross validation is done only for those cases in the analysis. In cross validation, each case is classified by the functions derived from all cases other than that case.

Figure 3.128 shows that the archaeological sheep identified as goat by DA fall in the area between the two group centroid lines. There are no archaeological sheep falling clearly on the goat group centroid or beyond that line; as such there is not very strong evidence to support the idea that these specimens are goats. The same pattern is visible if the scatterplots of the BI are considered: there are border-line specimens (Figs. 3.17; 3.39; 3.63) and others (four) which fall clearly among the goat modern group (Figs. 3.84 and 3.108).

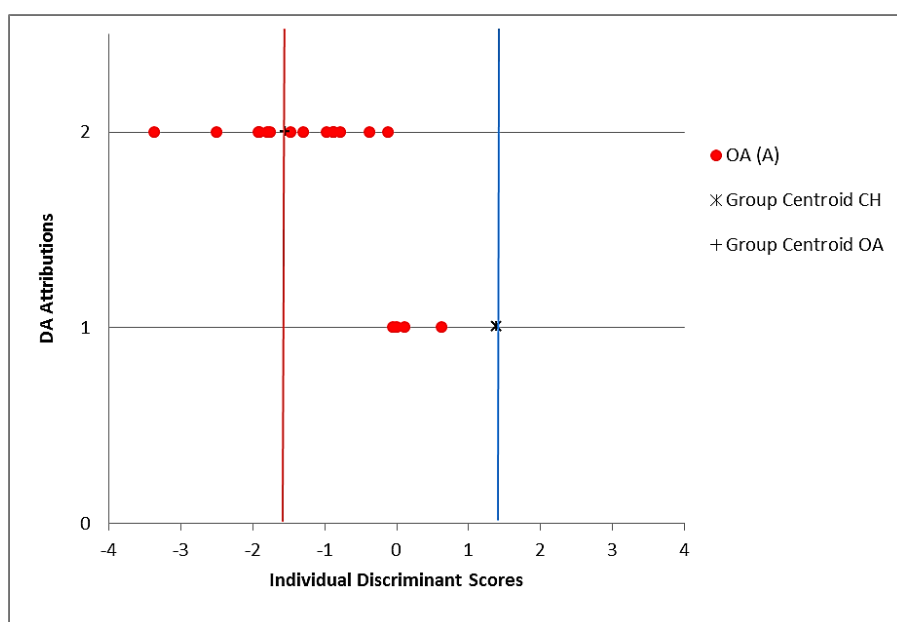


Figure 3.128 Diagram of the individual discriminant scores attributed to the archaeological material by DA for the radius.

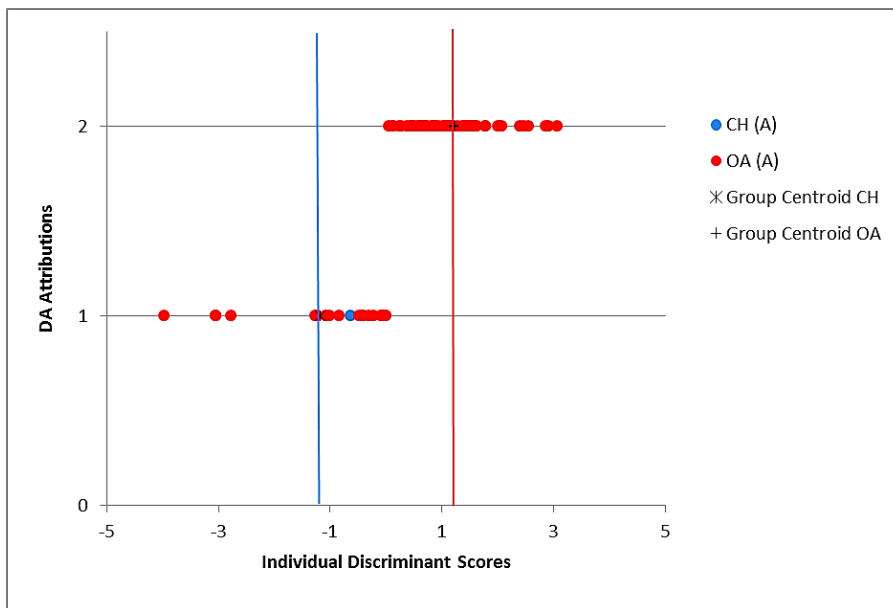


Figure 3.129 Diagram of the individual discriminant scores attributed to the archaeological material by DA for the radius when variables GL and SD were excluded.

In Figure 3.129 the GL and SD measurements are dropped. This shows that a greater number of sheep specimens are regarded to be misidentified by the DA. Several archaeological sheep fall in the area between the two group centroid lines, but a few others fall beyond the goat centroid line showing values that are more consistent with the goat group. These three specimens could have indeed been misclassified but we must be cautious, as the dropping of the measurements GL and SD means that this analysis mainly relies on the proximal radius. This articular end has an early fusing epiphysis and may be subject to substantial post-fusion increase (see Payne and Bull 1988 for a parallel case in pigs), which may confuse morphometric patterns.

Ulna

For the ulna the percentage of correct matches with the morphological identifications (94.4%) is higher than the results obtained from the modern material (Tab. 3.94). This means that any reclassification (of which there is only one) is likely to be due to the method's normal margin of error.

When the variables B and L are excluded from the analysis, the percentage of correct reattributions is still a high 91.1% (Tab. 3.95). Consequently the exclusion of B and L does not heavily influence the diagnostic power of the DA.

Table 3.94 Results from the Discriminant Analysis when applied on all the archaeological ulnae.

Classification Results ^{a,b,d}						
			TAXA	Predicted Group Membership		Total
				CH	OA	
Modern Material	Original	Count	CH	53	3	56
			OA	5	52	57
		%	CH	94.6	5.4	100.0
			OA	8.8	91.2	100.0
King's Lynn	Original	Count	CH	0	0	0
			OA	1	17	18
			O/C	0	1	1
		%	CH	.0	.0	100.0
			OA	5.6	94.4	100.0
			O/C	.0	100.0	100.0
a. 92.9% of selected original grouped cases correctly classified.						
b. 94.4% of unselected original grouped cases correctly classified.						
d. 92.0% of selected cross-validated grouped cases correctly classified. Cross validation is done only for those cases in the analysis. In cross validation, each case is classified by the functions derived from all cases other than that case.						

Table 3.95 Results from the Discriminant Analysis when applied on all the archaeological ulnae, excluding variables B and L.

Classification Results ^{a,b,d}						
			TAXA	Predicted Group Membership		Total
				CH	OA	
Modern Material	Original	Count	CH	52	4	56
			OA	5	52	57
		%	CH	92.9	7.1	100.0
			OA	8.8	91.2	100.0
	Cross-validated ^c	Count	CH	52	4	56
			OA	6	51	57
		%	CH	92.9	7.1	100.0
			OA	10.5	89.5	100.0
King's Lynn	Original	Count	CH	0	0	0
			OA	4	41	45
			O/C	1	4	5
		%	CH	.0	.0	100.0
			OA	8.9	91.1	100.0
			O/C	20.0	80.0	100.0
a. 92.0% of selected original grouped cases correctly classified.						
b. 91.1% of unselected original grouped cases correctly classified.						

Classification Results^{a,b,d}

d. 91.2% of selected cross-validated grouped cases correctly classified. Cross validation is done only for those cases in the analysis. In cross validation, each case is classified by the functions derived from all cases other than that case.

Figure 3.130 shows that only one archaeological ‘sheep’ has been identified as goat by the DA. This specimen falls among the two group centroid lines and, as such, it cannot be confidently considered to belong to a goat. The one uncertain specimen clearly plots with the sheep group.

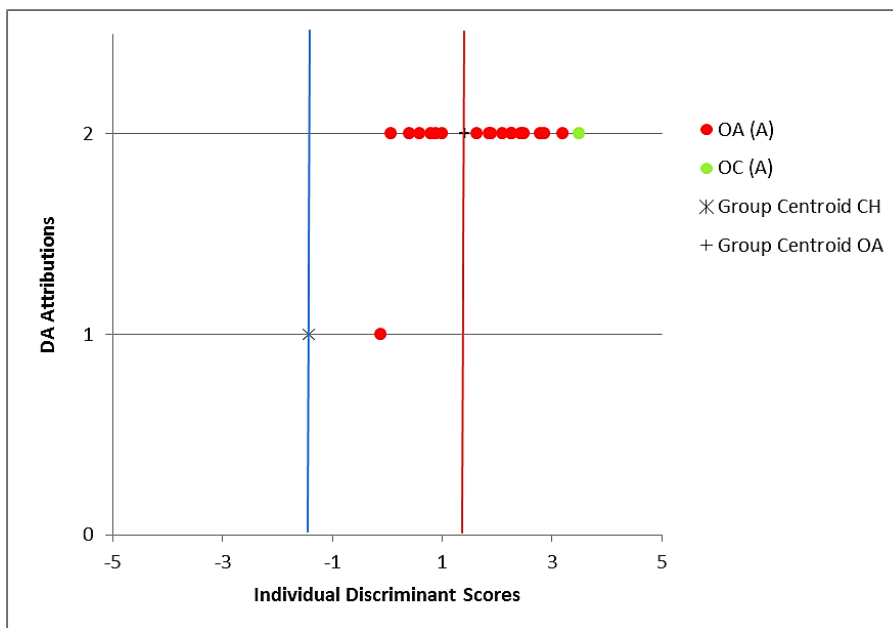


Figure 3.130 Diagram of the individual discriminant scores attributed to the archaeological material by DA for the ulna.

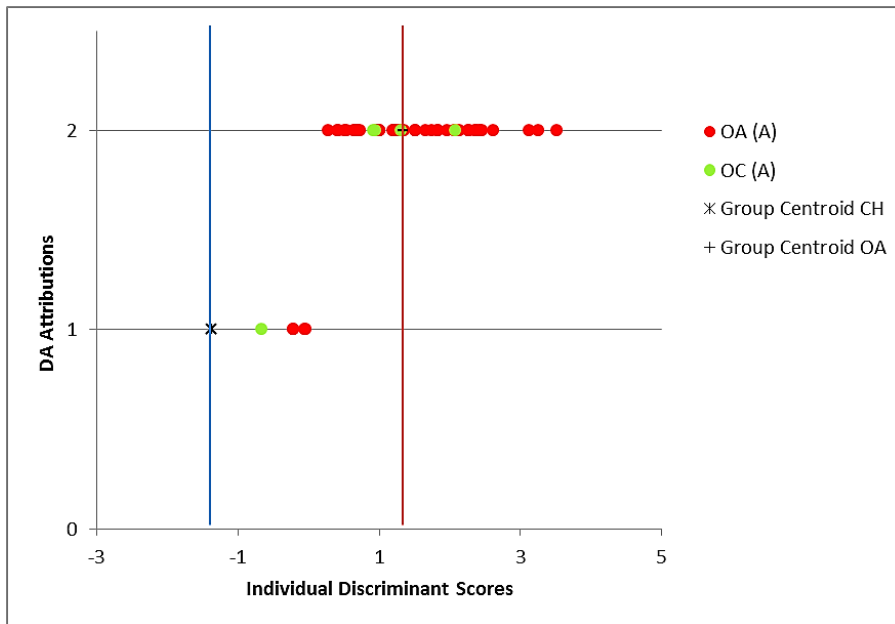


Figure 3.131 Diagram of the individual discriminant scores attributed to the archaeological material by DA for the ulna when variables B and L were excluded.

When variables B and L were not included, the disagreement between morphology and biometry increased slightly (Fig. 3.131). A few archaeological sheep fall in the area between the two group centroids but none of them plot on or beyond the goat group centroid. The combined result is that the DA reclassification cannot be relied on and the original morphological evaluation must stand.

Metacarpal

When all the measurements were included in the analysis, the morphological attribution to sheep of the 16 metacarpals was 100% confirmed by the DA (Tab. 3.96 and Fig. 3.132). When the variables GL and SD were excluded from the analysis, the value of correct reattributions decreased to 94.3%, with two of the 35 metacarpals reclassified as goat (Tab. 3.97). Since the percentage of correct identifications of the modern material was slightly higher (97.5%) than the consistency of the archaeological material obtained by the DA, it is worth looking at the position of these uncertain specimens on the diagram (Fig. 3.133).

Table 3.96 Results from the Discriminant Analysis when applied on all the archaeological metacarpals.

Classification Results ^{a,b,d}						
			TAXA	Predicted Group Membership		Total
				CH	OA	
Modern Material	Original	Count	CH	56	2	58
			OA	0	61	61
		%	CH	96.6	3.4	100.0
			OA	.0	100.0	100.0
	Cross-validated ^c	Count	CH	55	3	58
			OA	0	61	61
		%	CH	94.8	5.2	100.0
			OA	.0	100.0	100.0
King's Lynn	Original	Count	CH	0	0	0
			OA	0	16	16
		%	CH	.0	.0	100.0
			OA	.0	100.0	100.0
a. 98.3% of selected original grouped cases correctly classified.						
b. 100.0% of unselected original grouped cases correctly classified.						
d. 97.5% of selected cross-validated grouped cases correctly classified. Cross validation is done only for those cases in the analysis. In cross validation, each case is classified by the functions derived from all cases other than that case.						

Table 3.97 Results from the Discriminant Analysis when applied on all the archaeological metacarpals, excluding variables GL and SD.

Classification Results ^{a,b,d}						
			TAXA	Predicted Group Membership		Total
				CH	OA	
Modern Material	Original	Count	CH	56	2	58
			OA	1	60	61
		%	CH	96.6	3.4	100.0
			OA	1.6	98.4	100.0
	Cross-validated ^c	Count	CH	55	3	58
			OA	1	60	61
		%	CH	94.8	5.2	100.0
			OA	1.6	98.4	100.0
King's Lynn	Original	Count	CH	0	0	0
			OA	2	33	35
		%	CH	.0	.0	100.0
			OA	5.7	94.3	100.0
a. 97.5% of selected original grouped cases correctly classified.						

Classification Results^{a,b,d}
b. 94.3% of unselected original grouped cases correctly classified.
d. 96.6% of selected cross-validated grouped cases correctly classified. Cross validation is done only for those cases in the analysis. In cross validation, each case is classified by the functions derived from all cases other than that case.

Figure 3.133 shows that these two sheep specimens fall in the area between the two group centroids and therefore that there is insufficient evidence for the DA reclassification to overrule the original morphological identification.

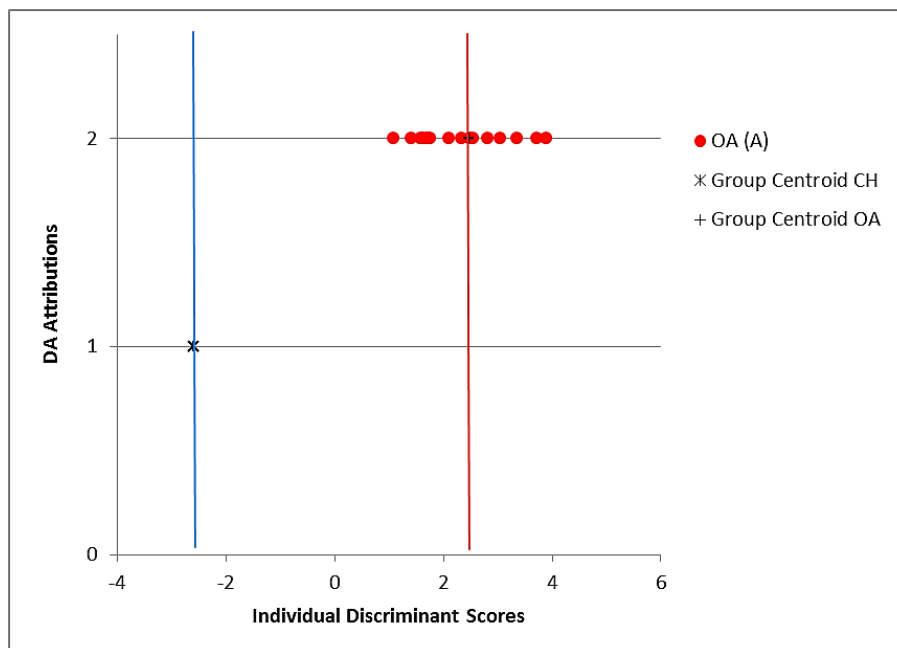


Figure 3.132 Diagram of the individual discriminant scores attributed to the archaeological material by DA for the metacarpal.

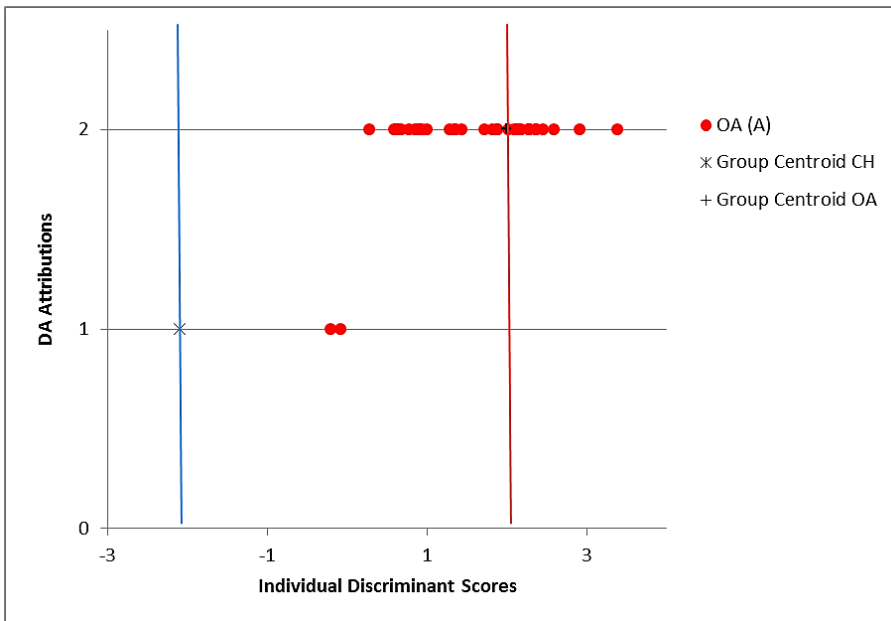


Figure 3.133 Diagram of the individual discriminant scores attributed to the archaeological material by DA for the metacarpal when variables GL and SD were excluded.

Metatarsal

When all the measurements were included, in 85% of cases the classification was consistent with the morphological identifications (Tab. 3.98). When the variables GL and SD were excluded from the analysis, the percentage of consistent attributions decreased slightly (81.8%) (Tab. 3.99). In both cases these percentages are lower than the proportion of correct identifications as expected on the basis of the modern material, therefore the possibility of morphological misidentification of the archaeological material must be considered.

Table 3.98 Results from the Discriminant Analysis when applied on all the archaeological metatarsals.

Classification Results ^{a,b,d}						
			TAXA	Predicted Group Membership		Total
				CH	OA	
Modern Material	Original	Count	CH	56	5	61
			OA	4	59	63
		%	CH	91.8	8.2	100.0
			OA	6.3	93.7	100.0
King's Lynn	Original	Count	CH	0	0	0
			OA	3	17	20
		%	CH	.0	.0	100.0
			OA	15.0	85.0	100.0

a. 92.7% of selected original grouped cases correctly classified.

b. 85.0% of unselected original grouped cases correctly classified.

Classification Results ^{a,b,d}	
d. 91.1% of selected cross-validated grouped cases correctly classified. Cross validation is done only for those cases in the analysis. In cross validation, each case is classified by the functions derived from all cases other than that case.	

Table 3.99 Results from the Discriminant Analysis when applied on all the archaeological metatarsals, excluding variables GL and SD.

Classification Results ^{a,b,d}						
			TAXA	Predicted Group Membership		Total
				CH	OA	
Modern Material	Original	Count	CH	51	10	61
			OA	4	59	63
		%	CH	83.6	16.4	100.0
			OA	6.3	93.7	100.0
King's Lynn	Original	Count	CH	0	0	0
			OA	6	27	33
		%	CH	.0	.0	100.0
			OA	18.2	81.8	100.0
a. 88.7% of selected original grouped cases correctly classified.						
b. 81.8% of unselected original grouped cases correctly classified.						
d. 85.5% of selected cross-validated grouped cases correctly classified. Cross validation is done only for those cases in the analysis. In cross validation, each case is classified by the functions derived from all cases other than that case.						

Figure 3.134 displays the results when all the variables were included. Three of the 20 specimens morphologically attributed to the sheep are reclassified as goat by the DA. Of these, two plot between the two centroids and therefore cannot be confidently reattributed to the goat, while another clearly plots in the goat area of the diagram and is therefore likely to have been misidentified at the morphological level. This assumption is also confirmed by the analysis of the Biometric Indices (Fig. 3.91).

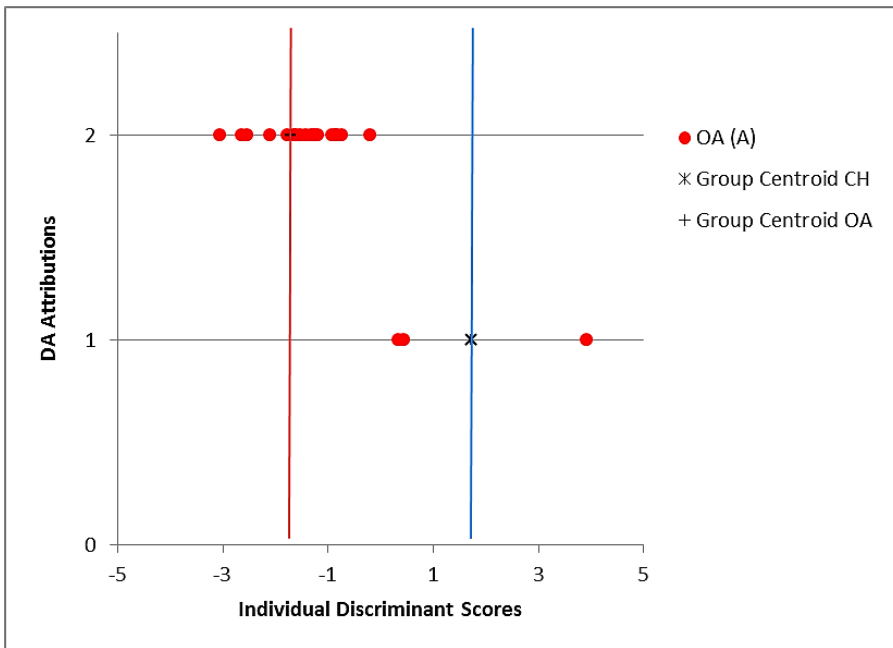


Figure 3.134 Diagram of the individual discriminant scores attributed to archaeological material by DA for the metatarsal.

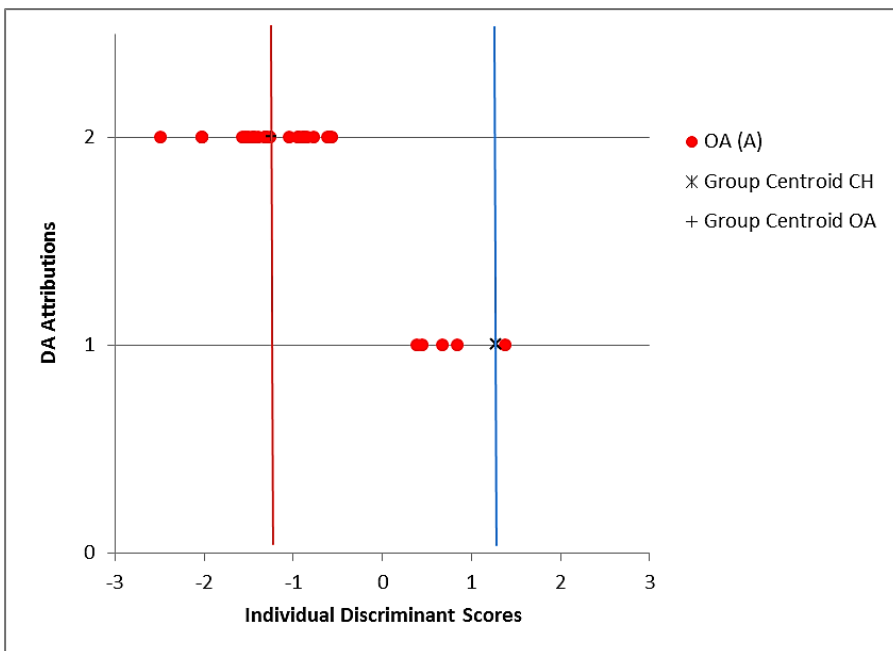


Figure 3.135 Diagram of the individual discriminant scores attributed to the archaeological material by DA for the metatarsal when variables GL and SD were excluded.

In Figure 3.135 (which excludes SD and GL), we can see that most of the reclassified sheep fall in the area between the two group centroids and, although some lean more towards the goat centroid, the evidence is insufficiently strong to be confident about a reidentification. The one specimen plotting on the right of the goat centroid is the same that plots as an outlier in Figure 3.134, therefore confirming the validity of its reidentification as a goat.

Tibia

For the tibia, the percentage of consistent attributions is much lower than for the modern material (Tab. 3.100) but this is not a meaningful proportion, due to the very small sample size. When measurements are dropped the sample size increases and the degree of consistency is very similar to that achieved on modern material (Tabs. 3.101 and 3.102), indicating that any reclassification may be a consequence of the method's inherent error.

Table 3.100 Results from the Discriminant Analysis when applied on all the archaeological tibiae.

Classification Results ^{a,b,d}						
			TAXA	Predicted Group Membership		Total
				CH	OA	
Modern Material	Original	Count	CH	55	3	58
			OA	9	43	52
		%	CH	94.8	5.2	100.0
			OA	17.3	82.7	100.0
	Cross-validated ^c	Count	CH	54	4	58
			OA	11	41	52
		%	CH	93.1	6.9	100.0
			OA	21.2	78.8	100.0
King's Lynn	Original	Count	CH	0	0	0
			OA	1	2	3
			O/C	0	1	1
		%	CH	.0	.0	100.0
			OA	33.3	66.7	100.0
			O/C	.0	100.0	100.0
a. 89.1% of selected original grouped cases correctly classified.						
b. 66.7% of unselected original grouped cases correctly classified.						
d. 86.4% of selected cross-validated grouped cases correctly classified. Cross validation is done only for those cases in the analysis. In cross validation, each case is classified by the functions derived from all cases other than that case.						

Table 3.101 Results from the Discriminant Analysis when applied on all the archaeological tibiae, excluding variable GL.

Classification Results ^{a,b,d}						
			TAXA	Predicted Group Membership		Total
				CH	OA	
Modern Material	Original	Count	CH	45	13	58
			OA	15	37	52
		%	CH	77.6	22.4	100.0
			OA	28.8	71.2	100.0
King's Lynn	Original	Count	CH	0	0	0
			OA	15	79	94
			O/C	0	4	4
		%	CH	.0	.0	100.0
			OA	16.0	84.0	100.0
			O/C	.0	100.0	100.0
a. 74.5% of selected original grouped cases correctly classified.						
b. 84.0% of unselected original grouped cases correctly classified.						
d. 72.7% of selected cross-validated grouped cases correctly classified. Cross validation is done only for those cases in the analysis. In cross validation, each case is classified by the functions derived from all cases other than that case.						

Table 3.102 Results from the Discriminant Analysis when applied on all the archaeological tibiae, excluding variables GL and SD.

Classification Results ^{a,b,d}						
			TAXA	Predicted Group Membership		Total
				CH	OA	
Modern Material	Original	Count	CH	42	16	58
			OA	15	37	52
		%	CH	72.4	27.6	100.0
			OA	28.8	71.2	100.0
King's Lynn	Original	Count	CH	0	0	0
			OA	27	104	131
			O/C	3	4	7
		%	CH	.0	.0	100.0
			OA	20.6	79.4	100.0
			O/C	42.9	57.1	100.0
a. 71.8% of selected original grouped cases correctly classified.						
b. 79.4% of unselected original grouped cases correctly classified.						
d. 70.0% of selected cross-validated grouped cases correctly classified. Cross validation is done only for those cases in the analysis. In cross validation, each case is classified by the functions derived from all cases other than that case.						

Figure 3.136 displays visually the results when all the variables are included. The complete specimens are just a few. Three out of four plot around the sheep group centroid while one is definitely more in the goat area, to the extent that the original morphological identification must be questioned.

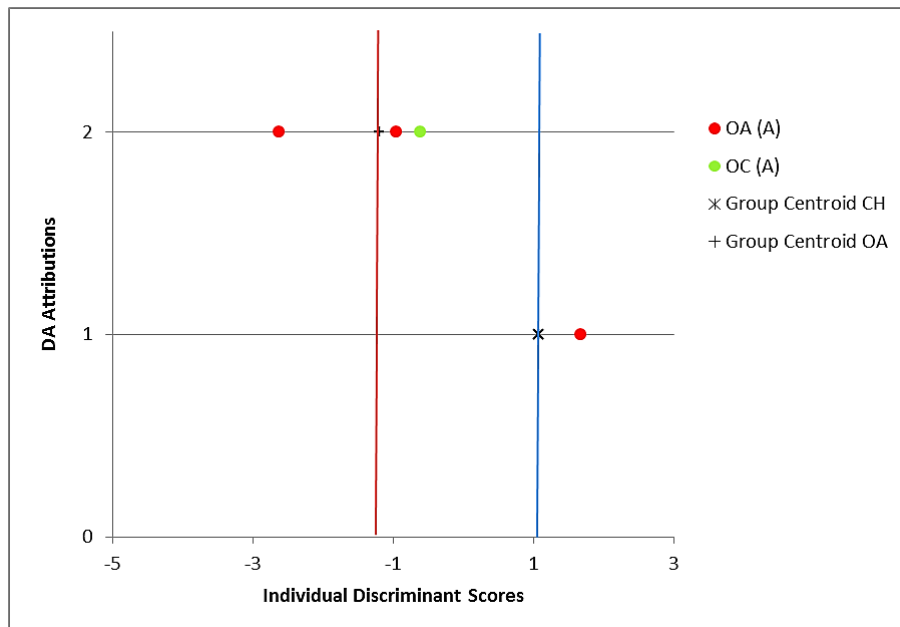


Figure 3.136 Diagram of the individual discriminant scores attributed to the archaeological material by DA for the tibia.

Figures 3.137 and 3.138 display respectively the results from the DA run without the variable GL, and then by excluding GL and SD. As mentioned, the relatively high number of inconsistencies with the morphological identifications is expected and it is probably due to the method's error. However, the outlier in Figure 3.138 is likely to be another goat (this specimen is different from the one in Fig. 3.136).

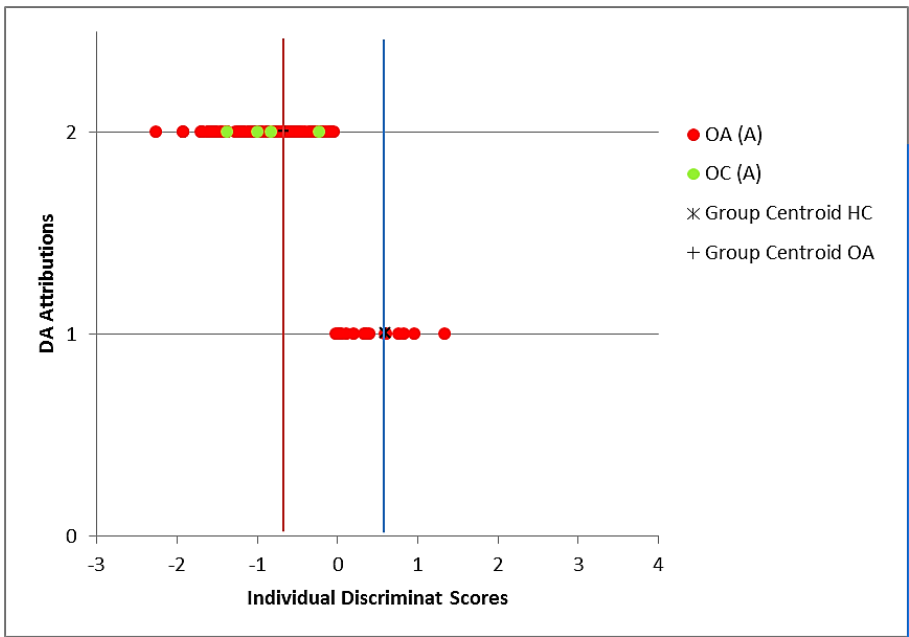


Figure 3.137 Diagram of the individual discriminant scores attributed to the archaeological material by DA for the tibia when variable GL was excluded.

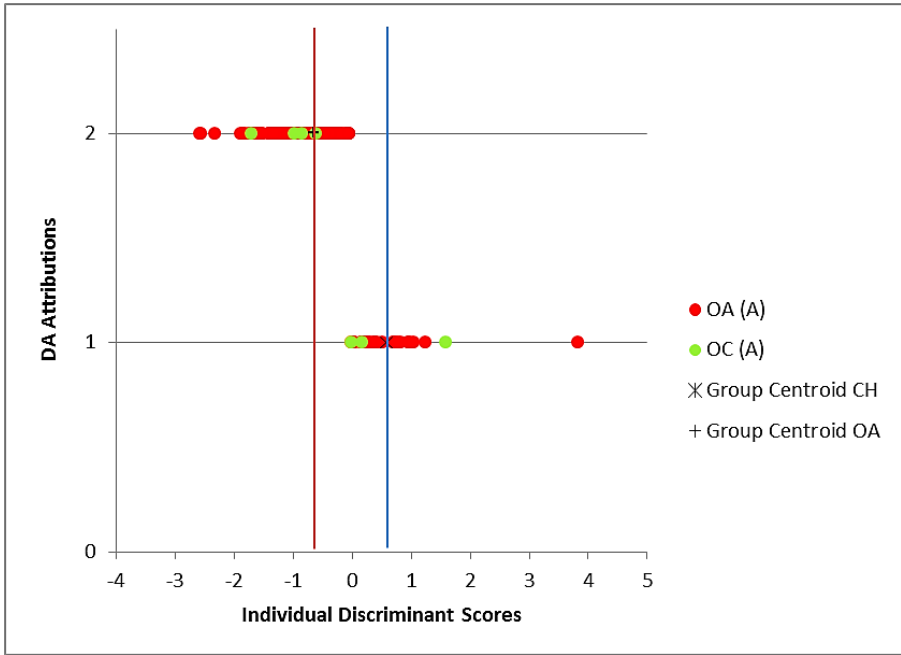


Figure 3.138 Diagram of the individual discriminant scores attributed to the archaeological material by DA for the tibia when variables GL and SD were excluded.

Astragalus

The percentage of consistent reattributions obtained for the astragalus is 83.9%, which is slightly lower than the one obtained on the modern material (89%) (Tab. 3.103), therefore raising the question of possible morphological misidentifications.

Table 3.103 Results from the Discriminant Analysis when applied on all the archaeological astragali.

Classification Results ^{a,b,d}						
			TAXA	Predicted Group Membership		Total
				CH	OA	
Modern Material	Original	Count	CH	65	7	72
			OA	9	64	73
		%	CH	90.3	9.7	100.0
			OA	12.3	87.7	100.0
King's Lynn	Original	Count	CH	0	0	0
			OA	5	26	31
		%	CH	.0	.0	100.0
			OA	16.1	83.9	100.0
a. 89.0% of selected original grouped cases correctly classified.						
b. 83.9% of unselected original grouped cases correctly classified.						
d. 86.9% of selected cross-validated grouped cases correctly classified. Cross validation is done only for those cases in the analysis. In cross validation, each case is classified by the functions derived from all cases other than that case.						

Figure 3.139 shows visually the results. Four of the five 'sheep' reclassified as goat by the DA fall in between the two group centroids. Their status as border-line specimens is consistent with what we had seen in the analysis of the BI (Figs. 3.24 and 3.25; 3.48-3.50). The most dubious specimen is the one falling slightly on the right of the goat centroid value. For this specimen a morphological misidentification is possible.

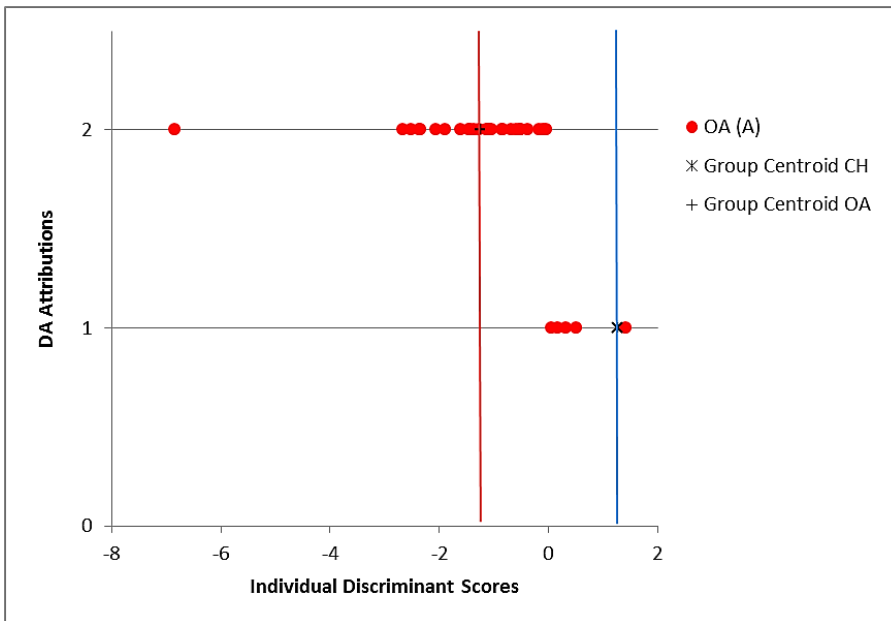


Figure 3.139 Diagram of the individual discriminant scores attributed to the archaeological material by DA for the astragalus.

Calcaneum

Table 3.104 shows that the percentage of consistent reattributions for this element is a very high 96.6%, which is higher than the results obtained from the modern material (95.1%). When variables GL and SB are excluded (Tab. 3.105), the degree of consistency does not decrease, indicating that even in incomplete specimens this element can be generally successfully classified.

Table 3.104 Results from the Discriminant Analysis when applied on all the archaeological calcanea.

Classification Results ^{a,b,d}						
			TAXA	Predicted Group Membership		Total
				CH	OA	
Modern Material	Original	Count	CH	55	5	60
			OA	1	61	62
		%	CH	91.7	8.3	100.0
			OA	1.6	98.4	100.0
King's Lynn	Original	Count	CH	0	0	0
			OA	1	28	29
		%	CH	.0	.0	100.0
			OA	3.4	96.6	100.0

a. 95.1% of selected original grouped cases correctly classified.

b. 96.6% of unselected original grouped cases correctly classified.

d. 95.1% of selected cross-validated grouped cases correctly classified. Cross validation is done only for those cases in the analysis. In cross validation, each case is classified by the functions derived from all cases other than that case.

Table 3.105 Results from the Discriminant Analysis when applied on all the archaeological calcanea, excluding GL and SB variables.

Classification Results ^{a,b,d}						
			TAXA	Predicted Group Membership		Total
				CH	OA	
Modern Material	Original	Count	CH	53	7	60
			OA	2	60	62
		%	CH	88.3	11.7	100.0
			OA	3.2	96.8	100.0
	Cross-validated ^c	Count	CH	53	7	60
			OA	2	60	62
		%	CH	88.3	11.7	100.0
			OA	3.2	96.8	100.0
King's Lynn	Original	Count	CH	0	0	0
			OA	0	39	39
		%	CH	.0	.0	100.0
			OA	.0	100.0	100.0

a. 92.6% of selected original grouped cases correctly classified.

b. 100.0% of unselected original grouped cases correctly classified.

d. 92.6% of selected cross-validated grouped cases correctly classified. Cross validation is done only for those cases in the analysis. In cross validation, each case is classified by the functions derived from all cases other than that case.

Figure 3.140 shows that the only sheep specimen that was reclassified as goat by the DA plots between the two centroids, and therefore cannot be confidently reclassified (as also confirmed by the fact that this same specimen is classified as 'sheep' by the DA in Fig. 3.141).

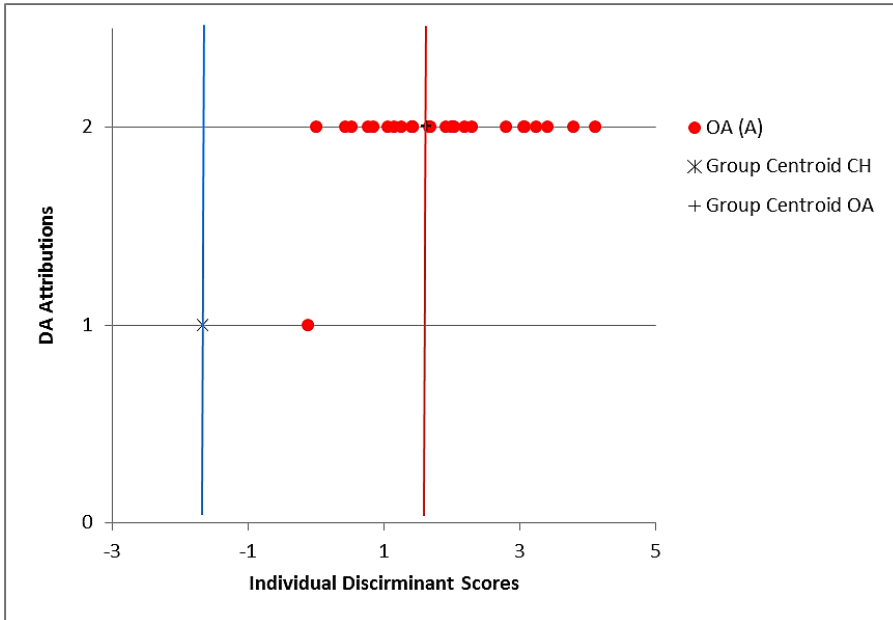


Figure 3.140 Diagram of the individual discriminant scores attributed to the archaeological material by DA for the calcaneum.

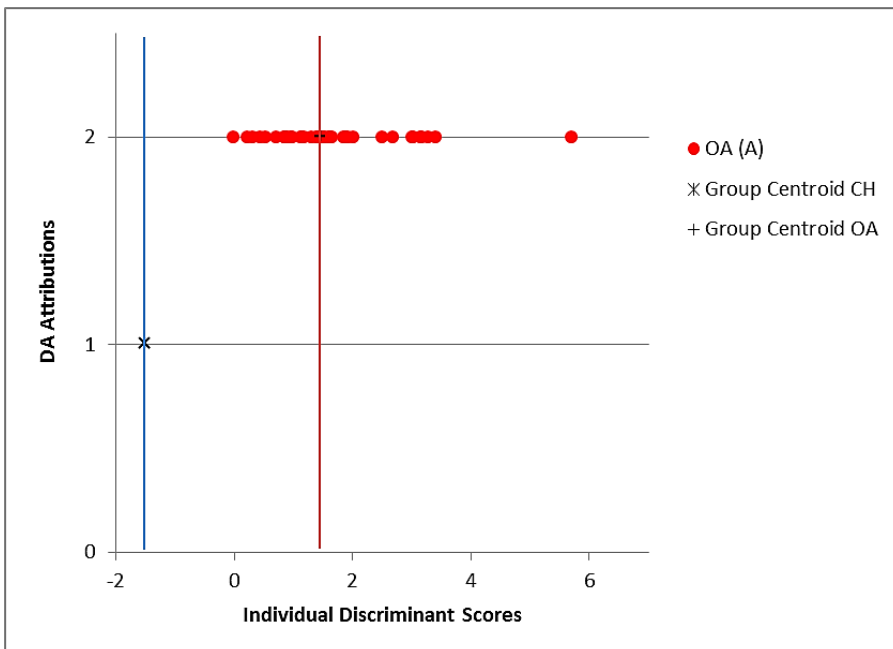


Figure 3.141 Diagram of the individual discriminant scores attributed to the archaeological material by DA for the calcaneum when variables GL and SB were excluded.

3.2.10 Discussion

The application of the Discriminant Analysis on the whole sheep/goat material from King's Lynn, allows some considerations to be made regarding the new methodology itself.

Table 3.106 Percentages of correct reattributions for the modern material and for the archaeological material (whole assemblage) provided by the DA. An asterisk mark small sample sizes (less than 10 specimens).

Anatomical Element	DA % of total correct reattributions modern material	DA % of total correct attributions on the archaeological material as a whole
Hc	95.2%	95.6%
Hc (excluding E and F)	81%	84.6%
Sc	86.4%	94.2%
Hu	88.4%	93.3%
Ra	93.5%	77.8%
Ra (excluding GL and SD)	89.7%	76.3%
Ul	92.2%	94.4%
Ul (excluding B and L)	92%	91.1%
Mc	98.3%	100%
Mc (excluding GL and SD)	97.5%	94.3%
Mt	92.7%	85%
Mt (excluding GL and SD)	88.7%	81.8%
Ti	89.1%	66.7%*
Ti (excluding GL)	74.5%	84%
Ti (excluding GL and SD)	71.8%	79.4%
Astragalus	89%	83.9%
Calcaneum	95.1%	96.6%
Calcaneum (excluding SB and GL)	92.6%	100%

Most of the anatomical elements considered provided high percentages of consistent reattributions, largely following the pattern of the modern material (Tab. 3.106). Most elements exceeded expectations in terms of consistency with the morphological identifications, and on the basis of the terms of reference provided by the modern material (this perhaps indicates the greater morphotype homogeneity of the archaeological material). The only two elements for which the percentage of consistent reattributions did not meet the expectations were the tibia and the radius but, for the tibia the outcomes are clearly heavily influenced by the very small sample size. Different is the case of the radius, which has proven to be a rather problematic element, with lower reattribution rates. This is probably due to the fact that the proximal end (on which the analysis is based) is very variable with age (Payne and Bull 1988) and this may lead to confusion in taxonomic identification.

In evaluating these results, it is essential that we consider that the DA bears an intrinsic error. Evidence of this is the fact that, in the modern material, the percentages of correct reattributions are never 100%, which, in other words, means that modern specimens, whose taxonomic origin is known, were occasionally misclassified. Consequently, it is likely that some misidentified archaeological specimens occurred because of this bias. In addition, as DA works following very rigid rules, all the new archaeological cases could be exclusively assigned to *Ovis* or *Capra*. These are the only two categories allowed by DA, which does not have an *Ovis/Capra* category. Therefore, as all elements are identified, the probability that errors will occur increases.

The outcomes obtained have brought to light different scenarios for which the following guidelines have been adopted:

1. When the percentage of correct reattributions of the archaeological material is as high as, or higher, than the percentage provided by the modern material, the expectations of correct reattributions are exceeded. As such, the possibility that archaeological specimens were misidentified morphologically is reduced, though the identification of specimens that plot much closer to the centroid of the other species must still be questioned.
2. When the modern material has provided a higher percentage of correct reattributions compared to the archaeological, the misattributed specimens must be scrutinised closely as the probability of genuinely incorrect identifications is higher. A crosscheck between the different approaches is highly desirable, as this will allow the opportunity to make a more detailed and more reliable assessment of the actual relative frequency of sheep and goat.

3.2.10.1 An assessment of the new methodology

The results from the DA have been compared and integrated with the results from the other approaches. Table 3.107 shows the degree of agreement between the different approaches adopted. The morphological identifications are frequently confirmed by the results from the BI and also by the outcomes of the DA. Only a few specimens that had been morphologically identified as sheep have been found to be biometrically consistent with the goat group (i.e. horncore and metatarsal). Among the morphologically unidentified specimens, only one could be identified biometrically (a likely goat humerus). The high degree of agreement between the biometry-based methods (BI and DA) is testified by the fact that the specimens genuinely 'misattributed' by the DA can be identified as such, also with the aid of the BI. The comparison between the different approaches has highlighted the potential of the biometry-based methods (BI and DA) as tools for:

1. confirming or rejecting the identifications assessed through the morphological study

2. assigning to species level the morphologically unidentified specimens
3. providing a visual and more objective way to assess identifications, allowing for them to be scrutinised.

Table 3.107 Summary table of the results obtained from the morphological approach and the biometrical approach in the form of both Biometrical Indices (BI) and Discriminant Analysis (DA), when the sheep/goat assemblage from King’s Lynn was considered *in toto*. The specimens considered as ‘misclassified’ are those which, as they fall on or beyond the group centroid line of the opposite species, are more likely to represent a morphological misclassification. The expectations are based on the results provided by the modern material; if the archaeological material has given a higher percentage of consistent attributions than the modern, the expectations are exceeded.

		Biometrical Approach							
		Morphological Approach			Biometrical Indices (BI)		Discriminant Analysis (DA)		
Anatomical element	<i>Ovis aries</i>	<i>Capra hircus</i>	<i>Ovis/ Capra</i>		Modern material DA%	King’s Lynn DA%	Identified <i>Ovis/ Capra</i>	‘Misclassified’	Comments
Horncore	30	72	-	All goats plot among the goat group. One sheep plots more toward the goat group (phase I), and may represent a possible misidentification. No other specimens plotting clearly among the goat group are present.	95.2%	95.7%	-	One goat might have been ‘misidentified’ as sheep. No strong evidence to argue against the morphological id. of other specimens.	Expectations exceeded. The exclusion of E and F reduces the diagnostic power of the DA
Jaw	117	-	40	-	-	-	-	-	N.A.
Teeth	15	-	3	-	-	-	-	-	N.A.
Scapula	76	2	12	All goats plot among the goat group or in the area of overlap. One unidentified specimen is consistent with the sheep group; the other unidentified specimens fall in the area of overlap. No other specimens plotting clearly among the goat group are present.	86.4%	94.2%	-	One sheep might have been ‘misidentified’ as goat. No strong evidence to argue against the morphological id. of other specimens	Expectations exceeded.
Humerus	107	1	8	The only morphologically identified goat is consistent with the goat group. One unidentified specimen plots among the goats; the other unidentified specimens plot in the area of overlap. No other specimens plotting clearly	88.4%	93.3%	One possible goat.	Two goats might have been ‘misidentified’ as sheep.	Expectations exceeded.

		Biometrical Approach							
		Morphological Approach			Biometrical Indices (BI)	Discriminant Analysis (DA)			
Anatomical element	<i>Ovis aries</i>	<i>Capra hircus</i>	<i>Ovis/ Capra</i>		Modern material DA%	King's Lynn DA%	Identified <i>Ovis/ Capra</i>	'Misclassified'	Comments
				among the goat group are present.				No strong evidence to argue against the morphological id. of other the specimens.	
Radius	99	1	-	The only morphologically identified goat plots among the goat group. Four sheep plot more toward the goat group than the sheep group but they are still compatible with the range of variation of the sheep group. No other specimens plotting clearly among the goat group are present.	93.5%	76.3%	-	No strong evidence to argue against the morphological id.	The exclusion of GL and SD influences the diagnostic power of the DA.
Ulna	55	-	5	Two unidentified specimens plot among the sheep group, the other unidentified specimens plot in the area of overlap. No other specimens plotting clearly among the goat group are present.	92.9%	94.4%	One specimen identified as sheep	No strong evidence to argue against the morphological id.	Expectations exceeded. Discriminant power of DA not affected by the exclusion of B and L
Metacarpal	42	-	1	One unidentified specimen plot more toward the goat group but it is still compatible with the range of variation of the sheep group. No other specimens plotting clearly among the goat group are present.	98.3%	100%	-	-	Expectations exceeded. The exclusion of GL and SD influences the diagnostic power of DA.

		Biometrical Approach							
		Morphological Approach			Biometrical Indices (BI)	Discriminant Analysis (DA)			
Anatomical element	<i>Ovis aries</i>	<i>Capra hircus</i>	<i>Ovis/ Capra</i>		Modern material DA%	King's Lynn DA%	Identified <i>Ovis/ Capra</i>	'Misclassified'	Comments
Metatarsal	46	-	-	One sheep plots clearly among the goat group; it represents a possible misidentification. No other specimens plotting clearly among the goat group are present.	92.7%	85%	-	One goat might have been 'misidentified' as sheep. No strong evidence to argue against the morphological id. of the other specimens.	The exclusion of GL and SD influences the diagnostic power of the DA.
Metapodials	-	-	1	-	-	-	-	N.A.	-
Tibia	132	-	7	The unidentified specimens fall in the area of overlap or among the sheep group. One sheep plot more toward the goat group but it is still compatible with the range of variation of the sheep group. No other specimens plotting clearly among the goat group are present.	89.1%	66.7%	-	One goat might have been misidentified as sheep. No strong evidence to argue against the morphological id. of the other specimens.	The exclusion of GL and SD influence the diagnostic power of the DA.
Astragalus	37	-	-	Two sheep plot more toward the goat group but they are still compatible with the range of variation of the sheep group. No other specimens plotting clearly among the goat group are present.	89%	83.9%	-	One goat might have been 'misidentified' as sheep. No strong evidence to argue against the morphological id. of the other specimens.	-
Calcaneum	41	-	-	No specimens plotting clearly among the goat group are present.	95.1%	96.6%		No strong evidence to argue against the morphological id.	Expectations exceeded. Discriminant power of DA not affected by

		Biometrical Approach								
		Morphological Approach			Biometrical Indices (BI)		Discriminant Analysis (DA)			
Anatomical element	<i>Ovis aries</i>	<i>Capra hircus</i>	<i>Ovis/ Capra</i>			Modern material DA%	King's Lynn DA%	Identified <i>Ovis/ Capra</i>	'Misclassified'	Comments
										the exclusion of GL and SB.
1st Phalanx	44	1	2					-	N.A.	
2nd Phalanx	4	-	3					-	-	N.A.
3rd Phalanx	-	-	-					-	-	N.A.
Total Identified Specimens	845	77	82					-	-	N.A.

3.2.10.2 The King's Lynn case study

The results from the reanalysis of the sheep/goat archaeological material from King's Lynn has revealed that no evidence exists to support the claim for a "considerable population of goat" mentioned by Noddle (1976: 397). King's Lynn does not represent an exception to the general trend which sees the presence of goat, when attested, almost exclusively represented by horncores, while postcranial bones are uncommon (Albarella 2003: 81). In all phases (apart from phase I) goat horncores are more numerous than sheep horncores, but when postcranial bones are considered sheep by far outnumbers goat in all phases. This means that very few goats, or even parts of the goat carcass, were introduced to the site, to be butchered and consumed.

This evidence generated two possible scenarios. One is based on the possibility of the existence of a trade in goat horns, a useful raw material for the production of a variety of objects. Since post-cranial goat bones are rare on in English sites of many different types (Albarella 2003), this trade must have occurred with other countries, which is not inconceivable considering the reputation of King's Lynn as an important inland and international trade centre in the Middle Ages.

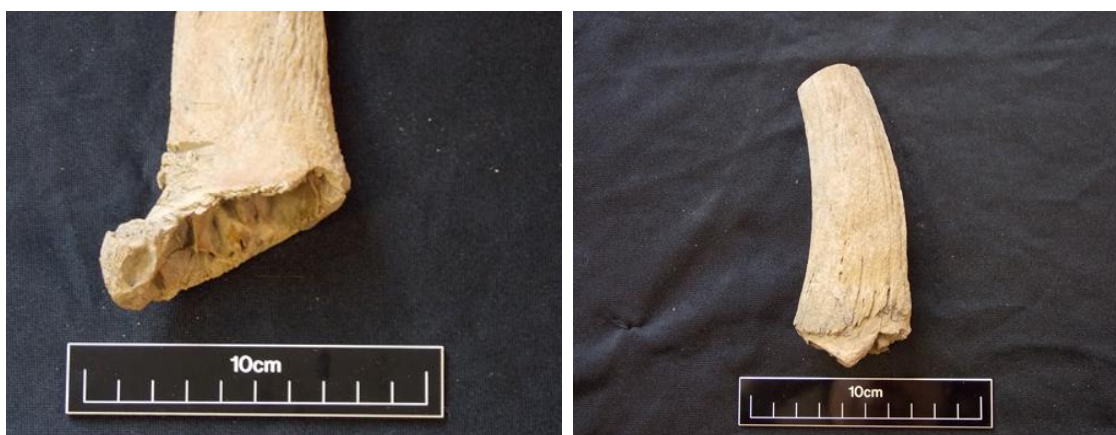


Figure 3.142 Goat horncores from King's Lynn. On the left: cut and chop marks at the base of the horncore, evidence for the removal of the keratinous sheath which covered the bony core. On the right: example of goat horncore with tip sawn.

The archaeological evidence suggests that the horns were indeed considered a useful raw material at the site (Fig. 3.142). The kind of cut and chop marks recorded on the majority of goat horncores at King's Lynn attests to the removal of the keratinous sheath - material which could be used for the production of a variety of objects. Nevertheless, as both the zooarchaeological and the historical record confirm that in this period the horn-working industry was already in decline (Albarella *et al.* unpublished), the scale of this business at King's Lynn must have not been large, perhaps confined to a few individual workshops. In

addition, if the historical records are considered, references to a trade in goat horns are completely absent (Albarella 2003:81). In the port books of Lynn (Metters 2009), which refer only to the Post-medieval period (1610-1614), no mention is made whatsoever about commerce in goat horns, while other types of trade are mentioned extensively. The trade in skins of different animals such as sheep, lamb and cat (goat are unfortunately not mentioned at all), for example, is frequently mentioned in considerable detail (it is often specified from which animal, the condition of the skins, if they have been treated or not, and their origin) (Metters 2009).

Since no written references to a horn trade can be found and considering the fact that during the Middle Ages horn-working decreases, it is more likely that the horns were imported attached to the skins. In this regard, both historical (Albarella 2003; Blair and Ramsay 1991; Reed 1972) and archaeological evidence (Albarella 2003; Albarella *et al.* unpublished) confirm the increased importance of leather production.

At King's Lynn, the relevance of the goat skins as a raw material for the production of a variety of items is evidenced by different archaeological finds, among which is the exceptional recovery of a fragment of goat skin. Goat skins in the town were used for the production of shoes, boots, laces, clothing (Carter and Clarke 1977: 349-365), clearly the qualities of the material were known at the time. Goat skin was considered as superior in toughness and tightness to the sheep skin allowing for hard-wearing soft and flexible products (Reed 1972: 43); not surprisingly it was used at the site for the production of objects, which were designed to be durable.

Historical records suggest that horns and the footbones were usually left attached to the skins (Cherry 1991: 295; Schmid 1972: 45; Serjeantson 1989: 139), as such, we would expect to find a higher number of postcranial bones along with the horncores. This is not the case at King's Lynn where only very few footbones have been found. This evidence can be perhaps explained by the fact that, for long distance trade, excessive weight was discarded, while anything with an economic value (such as the horns) was retained (Albarella 2003: 81). In addition, the horns may also have been used as an indicator of the age of the skin for the buyers (as suggested by Schmid 1974) and as such, useful to keep.

In conclusion, the hypothesis of the existence of an international trade in goat skins (with the horns still attached) seems to be the most likely. The skins were probably (as the archaeological evidence of a tannery has not been yet found at the site) worked at the site and processed into leather. The bony waste material resulting from this process, most likely only represented by horns, was sold or ceded to horn-workers so that the keratinous sheath could be used as raw material, while the internal bony core, being of little use, was discarded.

3.3 Medieval and Post-medieval Flaxengate (c. late 11th century; late 14th - middle 16th century AD)

3.3.1 Introduction

The city of Lincoln is located in the county of Lincolnshire and has a very long history. The first evidence of human occupation dates back to the Iron Age, and is followed by a Romano-British settlement, whose infrastructure was maintained until the 5th century. The foundation of a nucleated village, dated to the end of the 9th century, paved the way for the development of the city. The foundation of a Castle and a Cathedral in the Upper City and the fact that Lincoln became one of the largest urban centres in the East Midlands, sealed the change of status from town to city (by the middle 12th century) (Hill 1965; Jones 2003).

The archaeological site in Lincoln this section is focused is Flaxengate, located between Grantham Street, which delimits the southern part, and Danes Terrace, which defines the northern edge within the lower walled town (O'Connor 1982) (Fig. 3.143).

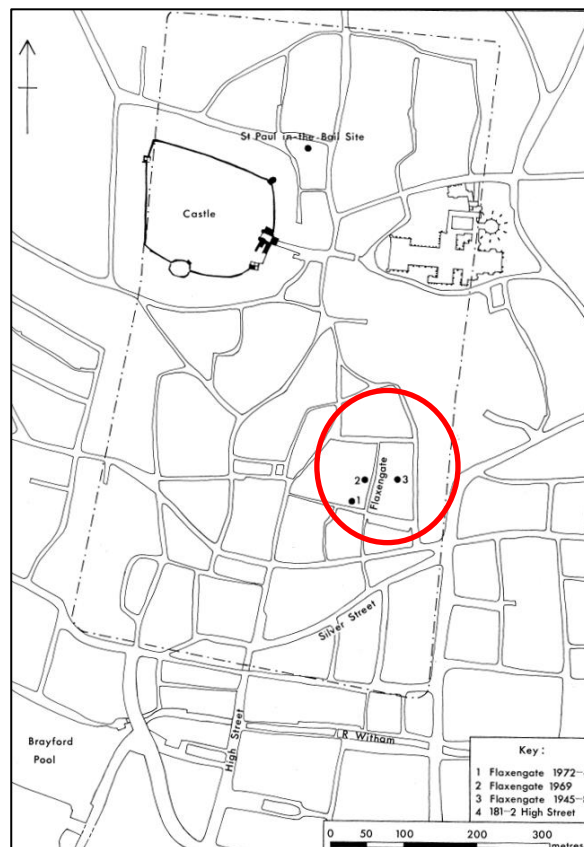


Figure 3.143 Location map of the site in relation to modern streets (image reprinted from PERRING, D. *Early medieval occupation at Flaxengate Lincoln*. The archaeology of Lincoln, IX-1. London: Council for British Archaeology for the Lincoln Archaeological Trust, copyright 1981, with permission from City of Lincoln Council).

The earliest structures discovered at the site belong to the Roman period, after which, a gap in occupation is recorded. A new occupation is then attested around the end of the 9th century, a period in which timber buildings and streets are constructed, probably after the arrival and settling of the Vikings in eastern England. At Flaxengate, the earliest discovered buildings were aligned along Flaxengate street and, according to the archaeological evidence, were of domestic nature (O'Connor 1982; Perring 1981).

The middle-late 10th century witnesses a process of re-organisation, with the occupation of the near Grantham Street and the creation of mainly glass and copper-alloy workshops. The industries declined around the middle 11th century, period in which a further re-organisation is recorded. The end of the timber buildings of the successive phase is marked by the construction of stone or stone-footed buildings dated to the late 12th and early 13th century.

From the 13th century onwards Flaxengate and the adjacent area seem to be exclusively occupied by domestic buildings, probably a single property, which was divided into smaller properties in the 16th century (Jones 1980; O'Connor 1982).

3.3.2 Archaeological Investigations

The site of Flaxengate was considered by the archaeologists of great potential for its location, as it was initially thought that Grantham Street and Flaxengate had Roman foundations, and could therefore provide information about the intra-mural Roman settlement in the lower city. In addition, since it faced two streets documented from the late 12th century and the first quarter of the 13th century and laid close to the commercial centre of the medieval city (Jones 1980: 6), the excavation had the potential to provide further insight on the medieval occupation of Lincoln.

Two initial excavations were carried out under the supervision of the Lincoln Archaeological Research Committee. The first campaign, conducted from 1945 to 1948, focused on the area east of Flaxengate. The other campaign, in 1969, dealt with the west side of Flaxengate and consisted of a trial trench to investigate the nature of the underlying material (Jones 1980: 6).

Major excavations, carried out as a result of a planned redevelopment of the area, started in July 1972 and were continued seasonally until 1976. The first two years and part of the third, were spent in the examination of the medieval and Post-medieval buildings. Then, the attention was focused on the structure placed beneath, belonging to the Anglo-Scandinavian and Saxo-Norman periods, and to the excavation of the Roman levels (Perring 1981: 3).

A series of coins and archaeomagnetic dates provided a very accurate (margin of error of 10-15 years) sequence of chronological phases for the timber buildings (Periods T) while for the

following stone building period, the chronological phases could not be so precisely defined (Periods S) (O'Connor 1982). Overall, the chronology identified covers a long time span from c 870/80-900 (Late Saxon period) to the late 17th/early 18th to 19th century.

3.3.3 What does the zooarchaeological evidence say?

The animal bone assemblage from Flaxegate was examined by O'Connor and the results were published in 1982. The greater part of the animal bones come from the Late Saxon period to c.1180, while the period 1200-1500 yielded less than 10% of the total bone recovered; thus, the report was mainly concerned with the 10th, 11th and 12th century material (O'Connor 1982).

When explaining the methodology used for studying the assemblage, O'Connor (1982) states that the distinction between sheep and goat was attempted but no details on adopted morphological or biometrical criteria are provided. The methodology section is the only part of the report where goats are mentioned, with no other references to the species found in the text. Only 'sheep' is mentioned in the rest of the report presumably meaning that the author regarded all recorded caprine specimens to belong to this species (Fig. 3.144).

		900					1000					1100		
		Pre T	TI	III	III-VI	III	TIV	TV	TVI	TVII	TVII-VIII	TVIII	TIX	
Cattle	n fragments	2314	791	2856	1669	1094	215	276	2086	3786	1188	1266	430	
	n/∑ mammals %	62.9	53.5	58.7	49.3	59.3	51.8	46.3	45.8	45.4	44.5	48.2	55.4	
Sheep	n	645	425	1338	914	489	161	237	1897	3489	1213	1024	230	
	%	17.5	28.7	27.5	27.0	26.5	38.8	39.8	41.7	41.8	45.5	39.0	29.6	
Pig	n	373	145	528	357	229	33	74	435	878	243	253	100	
	%	10.1	9.8	10.9	10.6	12.4	8.0	12.4	9.6	10.5	9.1	9.6	12.9	
Dog	n	313	104	88	390	17	3	6	55	101	8	50	3	
	%	8.5	7.0	1.8	11.5	0.9	0.7	1.0	1.2	1.2	0.3	1.9	0.4	
Cat	n	5	1	7	34	3	2	2	55	55	14	22	6	
	%	0.1	0.1	0.1	1.0	0.2	0.5	0.3	1.2	0.7	0.5	0.8	0.8	
Other mammals	n	29	13	45	20	13	1	1	15	39	2	14	7	
	%	0.8	0.9	0.9	0.6	0.7	0.2	0.2	0.3	0.5	0.1	0.5	0.9	
∑ mammals		3679	1479	4862	3384	1845	415	596	4552	8348	2668	2629	776	
∑ mammals/ TOTAL		%	77.2	79.6	80.2	80.6	76.1	71.8	79.5	75.9	76.2	76.1	78.0	73.3

		1200			1300				1400		1500		c1550		1850	
TXI	TXI-XIII	TXII	TXIII	SI	SII	SIH	SIV	SV	SVI	SVII	SVIII	SIX	SX	SXI	SXII	
764	444	478	100	125	55	205	476	58	178	338	259	103	81	69	17	
42.3	48.5	45.4	51.3	46.1	57.9	47.8	40	42	45.1	42.4	40.9	59.2	43.8	43.9	40.5	
713	352	394	67	106	32	168	490	60	185	374	290	58	63	70	17	
39.5	38.4	37.5	34.4	39.1	33.7	39.2	41.1	43.5	46.8	46.9	45.7	33.3	34.1	44.6	40.5	
164	91	126	23	32	6	34	90	15	20	76	64	9	39	12	7	
9.1	9.9	12.0	11.8	11.8	6.3	7.9	7.6	10.9	5.1	9.5	10.1	5.2	21.1	7.6	16.7	
102	13	11	2	0	0	6	1	4	2	1	0	0	0	5	1	
5.6	1.4	1.0	1.0	0	0	1.4	0.1	2.9	0.5	0.1	0	0	0	3.2	2.4	
59	11	31	3	5	0	4	68	1	3	6	12	2	1	1	0	
3.3	1.2	2.9	1.5	1.8	0	0.9	5.7	0.7	0.8	0.8	1.9	1.1	0.5	0.6	0	
5	5	12	0	3	2	12	66	0	7	2	9	2	1	0	0	
0.3	0.5	1.1	0	1.1	2.1	2.8	5.5	0	1.8	0.3	1.4	1.1	0.5	0	0	
1807	916	1052	195	271	95	429	1191	138	395	797	634	174	185	157	42	
77.9	83.5	85.1	83.7	83.9	77.2	84.8	77.3	72.3	77.6	80.7	79.9	90.2	90.2	90.2	93.3	

Figure 3.144 Number of fragments by phases identified by O'Connor (image reprinted from O'CONNOR, T. *Animal Bones from Flaxegate, Lincoln c. 870-1500*. The archaeology of Lincoln, XVIII-1. London: Council for British Archaeology for the Lincoln Archaeological Trust, copyright 1982, with permission from Terry O'Connor).

Two peaks in the frequency of sheep were identified for the 10th and 13th centuries, although it is only by the 14th and early 15th century that sheep specimens outnumber those of cattle (O'Connor 1982: 11). The 13th century peak probably coincides with the expansion of the wool economy while, for the 10th century, O'Connor (1982) finds the explanation in the social and economic pressure that affected the city around that period. In the 10th century, Lincoln arose as a major settlement, so the relative increase in the sheep presence parallels an increase in human population at the site. The increasing population brought an increase in the demand for food and, as a consequence, an expansion of the resource catchment areas; thus an increase in the number of sheep brought to town (O'Connor 1982: 48).

For the 11th century (phase T VI to T VIII), the kill-off pattern indicates that some sheep were reared for meat (the younger group) and others for secondary products (mainly wool) (O'Connor 1982: 24). In the period *c* 1150-1550, as suggested by the killing peak, the sheep were instead mainly kept for the production of wool and/or milk. However, the low proportions of young lambs (0-6 months) and very old individuals indicate that this was not a specialised economy.

The Flaxengate site was considered to be a good case study for this research for the following reasons:

1. the town represented an important urban centre and, therefore, its results could be significant for the understanding for the wider economy and society;
2. the site is located in a different geographic area from the other two case studies and has a long and well-dated chronological sequence;
3. the sample is large and therefore suitable for the application of my newly developed methodology. The lack of any goat identification and the cursory nature of the methodological explanation concerning the approach to sheep/goat distinction made this an ideal case study for testing whether goat occurrence had missed.

3.3.4 Reevaluation of Flaxengate sheep/goat bone material: methodology

For the reanalysis of the sheep/goat assemblage of Flaxengate the same methodology previously applied on the modern material and the archaeological material from King's Lynn was used (see Chapter 2, Section 2.1 and 3 Section 3.2.5).

As the sample size of the whole assemblage was extensive and time did not permit a full analysis, only two chronological phases were chosen:

- phase T VII (c 1060/70-1080/90) as representative of the Late-Saxon Norman/Early medieval period;
- phase S VII (late 14th century/early to late 15th century/early 16th century);
- phase SVIII (late 15th to early-middle 16th century) as representative of the Late medieval period.

3.3.5 Morphological Approach: Results

Phase T VII

All the sheep/goat bones attributed to this chronological phase have been re-examined and the results are shown by Table 3.108. This phase also includes the bones which were attributed to two or more different phases that included T VII (i.e. T IV-VII; T V-VII; T VI-VII; T VII-VIII).

Table 3.108 NISP for phase T VII of the three identified categories.

	<i>Ovis aries</i>	<i>Capra hircus</i>	<i>Ovis/ Capra</i>
Horncore	30	3	-
Jaw	88	-	34
Teeth	23	-	24
Scapula	44	-	20
Humerus	97	-	6
Radius	82	-	1
Ulna	27	-	3
Metacarpal	34	-	2
Metatarsal	38	-	2
Metapodial	8	-	2
Tibia	103	-	26
Astragalus	44	-	2
Calcaneum	31	-	2
1st Phalanx	68	-	7
2nd Phalanx	13	-	-
3rd Phalanx	3	-	-
Total Identified Specimens	733	3	131

Only three specimens out of 867 recorded were morphologically identified as goat: all horncores. 733 fragments were attributed to sheep and, as Table 3.108 shows, for this species all the anatomical elements included in the recording protocol were represented. 131 fragments were attributed to the category sheep/goat as they could not be identified with confidence to species level. Clearly, sheep far outnumber goats (ratio 244:1).

Phase S VII

Table 3.109 shows the results from the analysis of the sheep/goat assemblage related to the late medieval period phases (S VII and S V-VII).

Table 3.109 NISP for phase S VII of the three identified categories.

	<i>Ovis aries</i>	<i>Capra hircus</i>	<i>Ovis/ Capra</i>
Horncore	-	-	-
Jaw	5	-	2
Teeth	3	-	1
Scapula	4	-	-
Humerus	5	-	-
Radius	3	-	1
Ulna	1	-	-
Metacarpal	7	-	1
Metatarsal	10	-	1
Metapodial	-	-	-
Tibia	7	-	3
Astragalus	1	-	-
Calcaneum	4	-	-
1st Phalanx	12	-	2
2nd Phalanx	1	-	-
3rd Phalanx	-	-	-
Total Identified Specimens	63	-	11

No goat bones have been identified for this chronological phase. Of the 74 bones recorded, 63 were certainly attributed to sheep, while 11 were attributed to the sheep/goat category.

Phase S VIII

Table 3.110 presents the result for the chronological phase S VIII which also belongs to the Late medieval period, although it includes a wider time span than the previous phase (S VII).

Table 3.110 NISP for phase S VIII of the three identified categories.

	<i>Ovis aries</i>	<i>Capra hircus</i>	<i>Ovis/ Capra</i>
Horncore	1	-	-
Jaw	2	-	-
Teeth	3	-	3
Scapula	1	-	1
Humerus	9	-	-
Radius	4	-	-
Ulna	3	-	1
Metacarpal	3	-	-
Metatarsal	5	-	-
Metapodial	2	-	-
Tibia	2	-	1
Astragalus	4	-	-
Calcaneum	1	-	1
1st Phalanx	10	-	-
2nd Phalanx	-	-	-
3rd Phalanx	-	-	-
Total Identified Specimens	54	-	7

No goat bones were recorded. 54 specimens were attributed to sheep and seven to the sheep/goat category.

These morphological results are consistent with O'Connor's evaluation that sheep is overwhelmingly more common than goat at the site. Goat is only found only in phase T VII and just with three horncores.

3.3.6 Shape analysis as expressed by Biometrical Indices

Phase T VII

Horncores

Figures 3.145 to 3.148 show the extent to which the morphological identification agrees with the biometrical results. Two distinct archaeological groups can be seen in all figures: the archaeological sheep plot clearly among the sheep modern group while the goat specimens are consistent within the modern goat pattern.

In Figure 3.146 a few morphologically identified sheep fall in the area of overlap of the two modern groups but, as they are still compatible with the range of variability of the sheep group, their morphological identification can be confirmed.

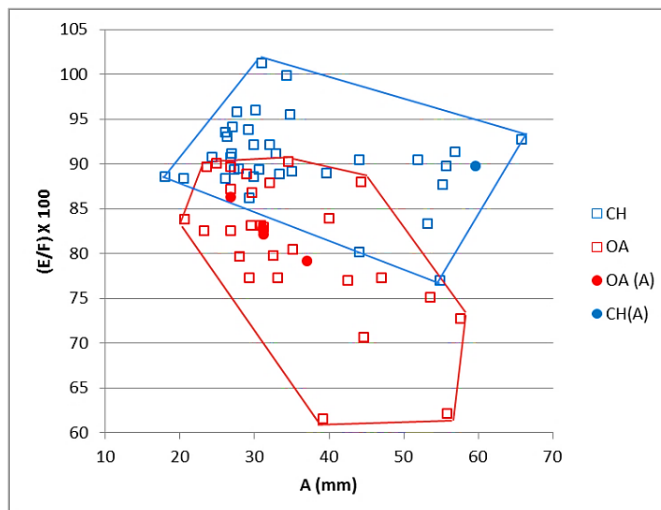


Figure 3.145 Maximum diameter taken at the base plotted against a ratio between the length and the length of the outer curvature of the horncore. The modern data are represented by the square empty symbol, blue for modern goats, red for modern sheep, while the archaeological material is represented by the filled dot symbol: blue for goats, red for sheep and green for sheep/goat.

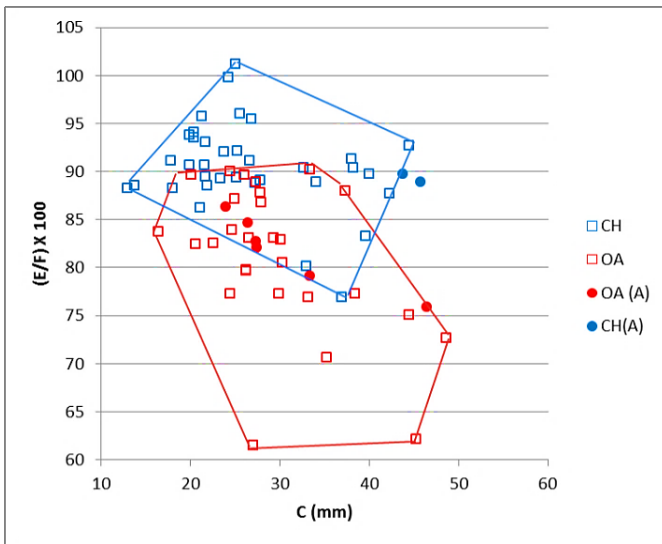


Figure 3.146 Maximum diameter taken at the middle plotted against a ratio between the length and the length of the outer curvature of the horncore. Symbols explained in Fig. 3.145.

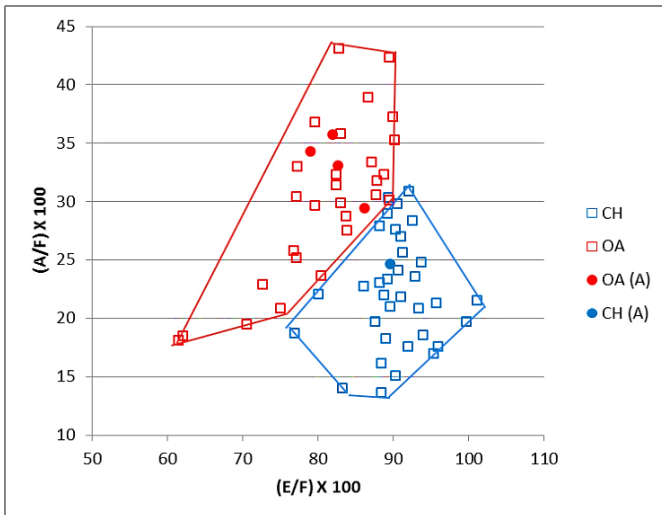


Figure 3.147 Ratio between the length and the length of the outer curvature plotted against the ratio between the maximum diameter taken at the base and the length of the outer curvature of the horncore. Symbols explained in Fig. 3.145.

As measurement C was taken more frequently than A (the base of the horncores was often fractured impeding the recording of measurement A), its inclusion would have increased the sample size for this element, as such, a ratio between E and F *versus* C and F (Fig. 3.148) was also performed. Once again the archaeological specimens plot into two distinct groups: the archaeological sheep fall among the modern sheep while the archaeological goat follows the modern goat group pattern.

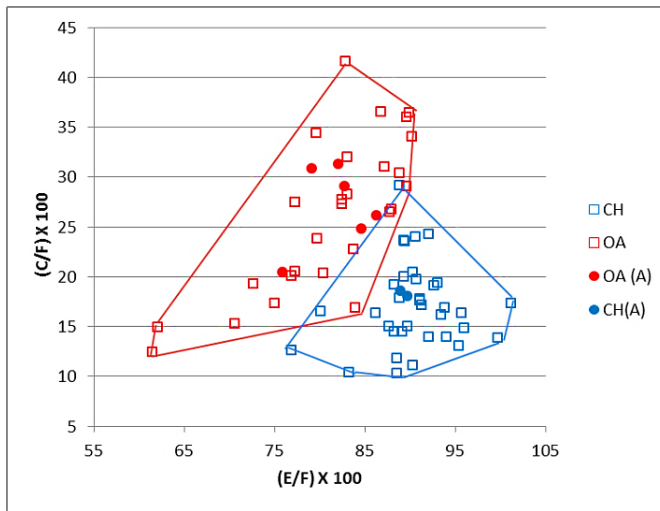


Figure 3.148 Ratio between the length and the length of the outer curvature plotted against the ratio between the maximum diameter taken at the middle and the length of the outer curvature of the horncore. Symbols explained in Fig. 3.145.

Scapula

No goats have been identified morphologically (Figs. 3.149 and 3.150). The specimens assigned to sheep fall, by and large, among the modern group, confirming their morphological identification. Only a couple of sheep specimens (Fig. 3.149) fall more toward the goat group. Nevertheless, as they are still consistent with the range of variation of the sheep group, they cannot be considered as having been misattributed. A few unidentified specimens fall either among the sheep group or in the areas of overlap between the two modern samples. In these cases biometry cannot help to assess their species. In Figure 3.149 (and to a lesser extent in Fig. 3.150) an unidentified specimen lies among the goat group but it cannot be considered to be a goat as it is within the range of variation of the sheep group.

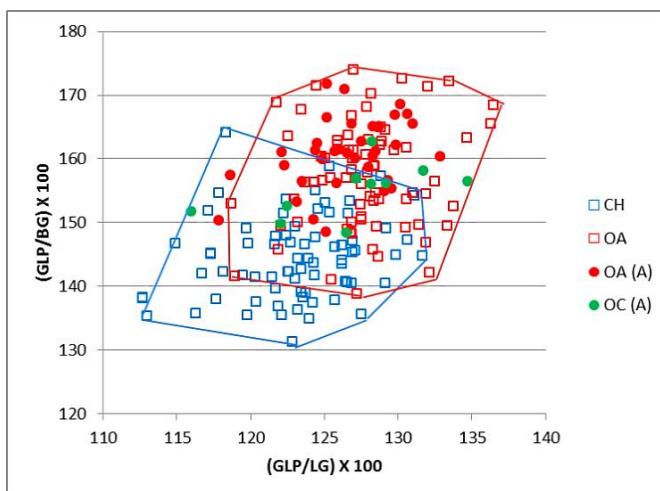


Figure 3.149 Ratio between the greatest length of the *processus articularis* and the length of the glenoid cavity plotted against the ratio between the greatest length of the *processus articularis* and the breadth of the glenoid cavity. Symbols explained in Fig. 3.145.

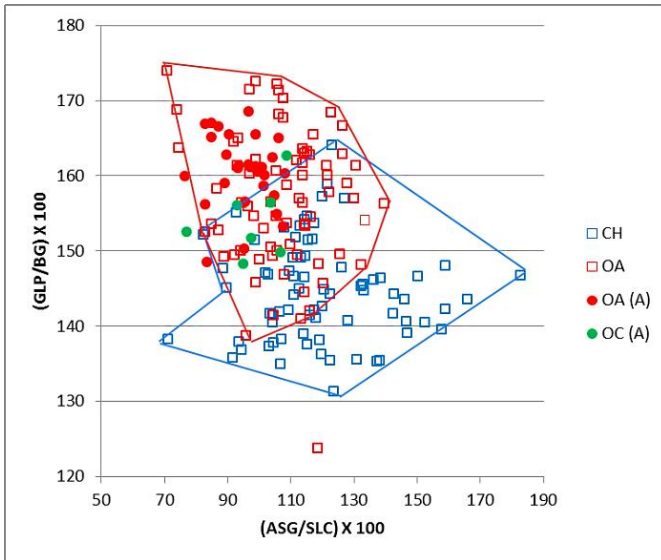


Figure 3.150 Ratio the shortest distance from the base of the spine to the edge of the glenoid cavity and the smallest length of the *collum scapulae* plotted against a ration between the greatest length of the *processus articularis* and the breadth of the glenoid cavity. Symbols explained in Fig. 3.145.

Humerus

Figures 3.151 to 3.154 show that the morphological identifications are, by and large, confirmed by biometry. Despite the considerable amount of overlap present, the archaeological sheep follow (especially in Figs. 3.152, 3.153 and 3.154) the modern sheep pattern. A few archaeological sheep plot more toward the goat group in Figure 3.151, but as they are still consistent with the variation of the sheep group, and follow the sheep pattern in the other graphs, they cannot be considered as having been misidentified. All the unidentified specimens fall in the area of overlap.

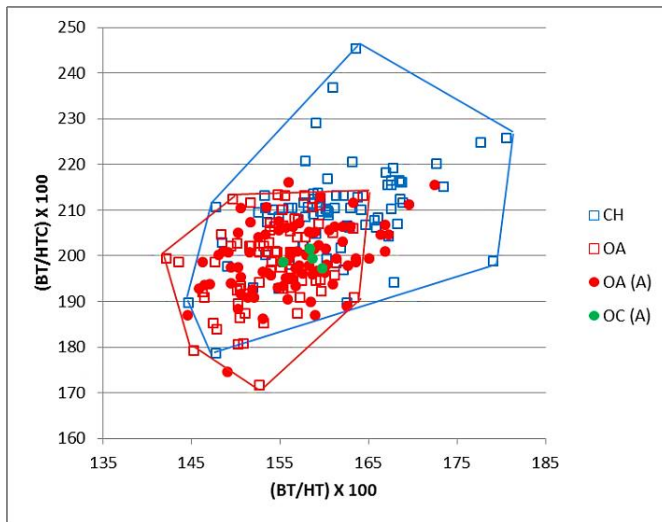


Figure 3.151 Ratio between the medio lateral width of the trochlea and its height plotted against the medio lateral width of the trochlea and the diameter of the trochlear constriction. Symbols explained in Fig. 3.145.

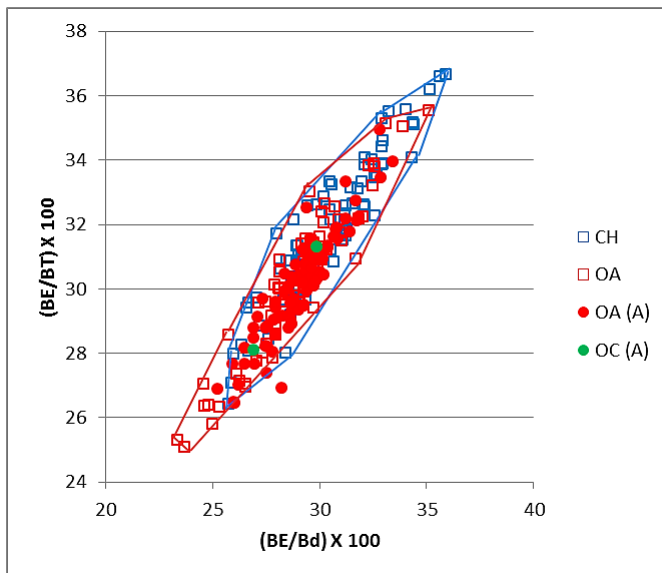


Figure 3.152 Ratio between the breadth of the *capitulum* and the distal width plotted against the ratio between the breadth of the *capitulum* and the medio lateral width of the trochlea. Symbols explained in Fig. 3.145.

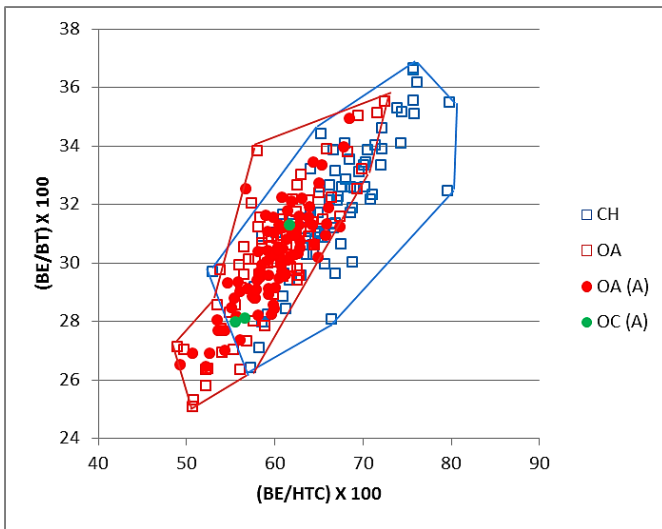


Figure 3.153 Ratio between the breadth of the *capitulum* and the diameter of the trochlea constriction plotted against the ratio between the breadth of the *capitulum* and the medio lateral width of the trochlea. Symbols explained in Fig. 3.145.

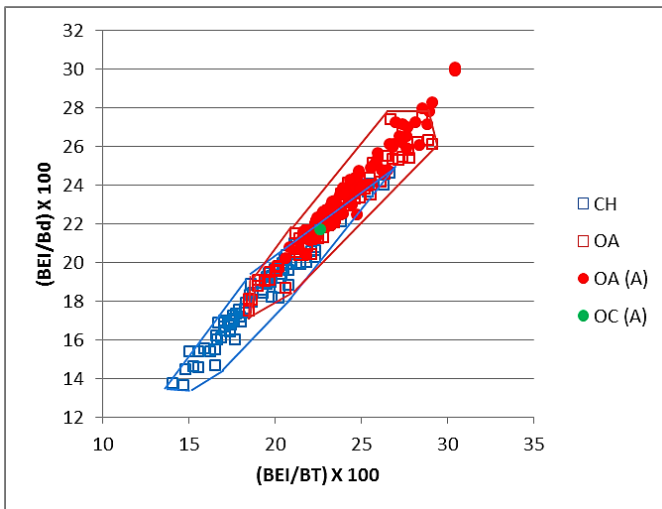


Figure 3.154 Ratio between the breadth of the epicondyle *lateralis* and the medio lateral width of the trochlea plotted against the ratio between the breadth of the epicondyle *lateralis* and the width of the distal end. Symbols explained in Fig. 3.145.

Radius

The biometrical and the morphological identification agree on the absence of archaeological goat radii (Fig. 3.155). All the morphologically identified sheep fall among the modern sheep group or in the area of overlap, as such their identification is confirmed. The only unidentified specimen falls in the area of overlap, thus cannot be identified to species.

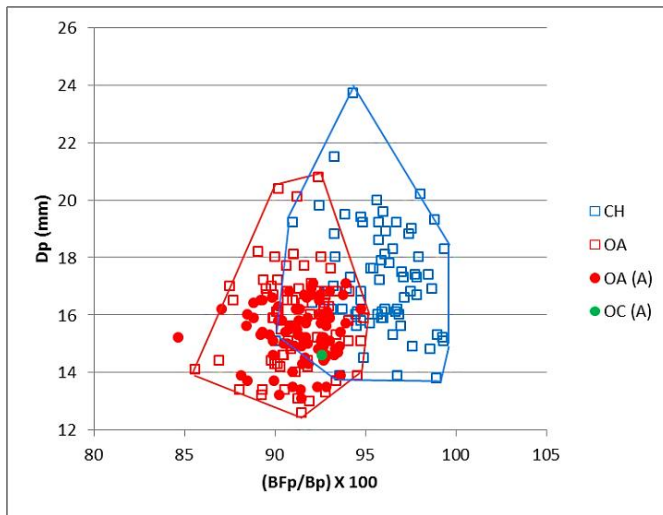


Figure 3.155 Ratio between the greatest length of the *facies articularis proximalis* and the greatest breadth of the proximal end plotted against the depth of the proximal end. Symbols explained in Fig. 3.145.

Ulna

Figure 3.156 shows the results for the ulna. The complete absence of archaeological goats is confirmed by the biometry. Only one archaeological group can be seen, it follows the sheep pattern confirming the morphological identification. Among the archaeological sheep some have very strong sheep traits, plotting at the left corner of the graph. The unidentified specimen appears to have strong *Ovis* traits.

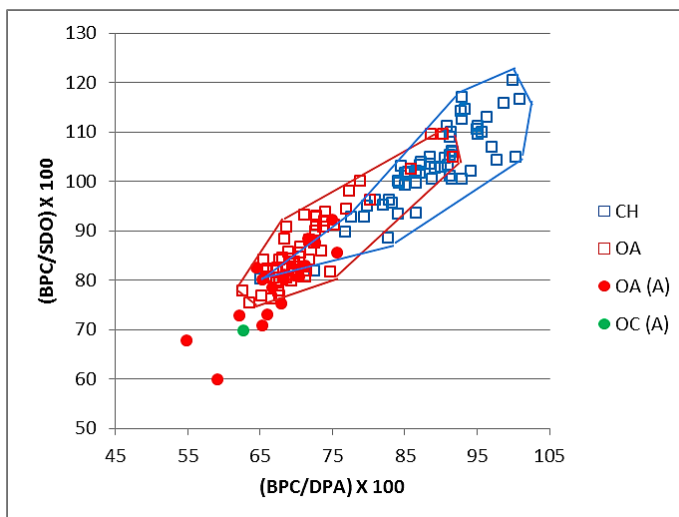


Figure 3.156 Ratio between the breadth across the coronoid process and the depth across the *processus anconaeus* to the caudal border plotted against the breadth across the coronoid process and the smallest depth of the olecranon. Symbols explained in Fig. 3.145.

Metapodials

No goats have been identified morphologically. Figures 3.157 to 3.159 show that when the metacarpals are considered, only one archaeological group can be seen. The archaeological sheep gather exactly where the modern sheep are. A few archaeological sheep could be considered border line specimens but are still compatible with the range of variation for this species.

Figures 3.157 and 3.158 shows that two unidentified specimens plot more toward the goat group but, as they do not fall far from the other archaeological sheep, there is not strong enough evidence for them to be considered as goats. Some archaeological sheep plot at the right top angle of the scatterplot (Fig. 3.158); these specimens have very marked sheep features.

Figures 3.160 to 3.162 show the results for the metatarsals. The agreement between biometry and morphology is once again confirmed. No specimens have been identified morphologically as goats. The amount of overlap is greater than with the metacarpals and many archaeological sheep fall in this area of overlap. Nevertheless, they are not inconsistent with the sheep pattern. The unidentified metatarsal specimen remains so, as it falls in the overlapping area. Some archaeological sheep show, in Figure 3.160 and 3.161, to have very strong sheep features, as they fall in the upper right part of the scatterplot.

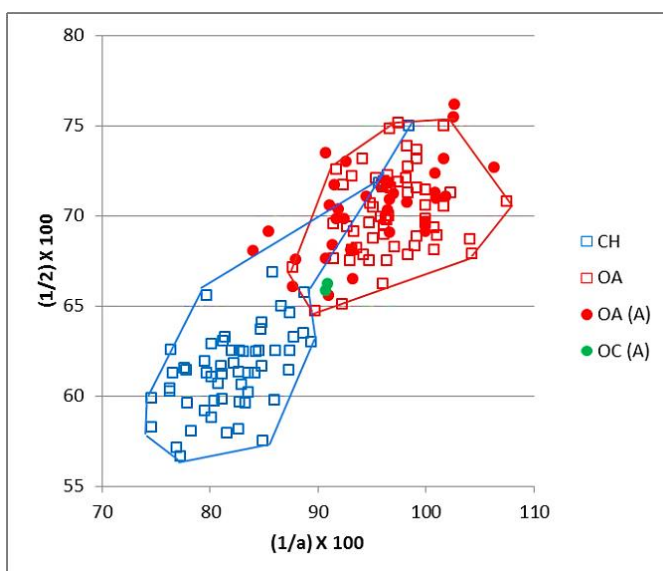


Figure 3.157 Metacarpal. Ratio between the diameter of the medial trochlea and the width of the medial condyle plotted against the ratio between the diameter of the *verticillus* at the medial condyle and the diameter of the medial trochlea. Symbols explained in Fig. 3.145.

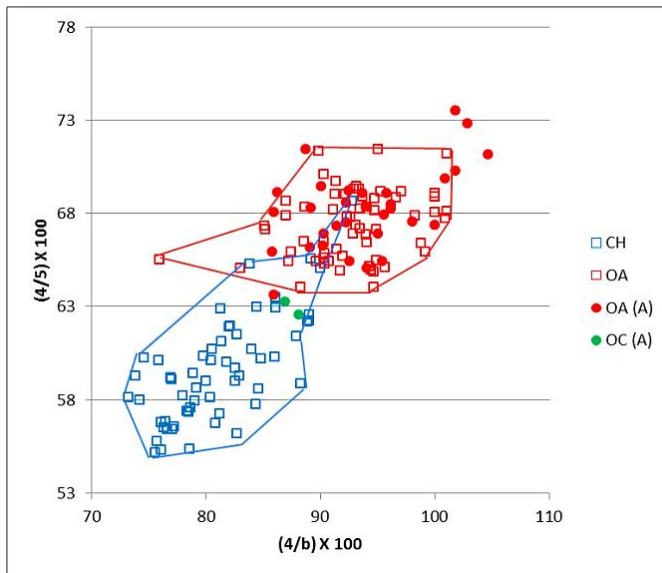


Figure 3.158 Metacarpal. Ratio between the width of the lateral condyle and the diameter of the lateral trochlea plotted against the ratio between the diameter of the lateral condyle and the diameter of the *verticillus* on the lateral condyle. Symbols explained in Fig. 3.145.

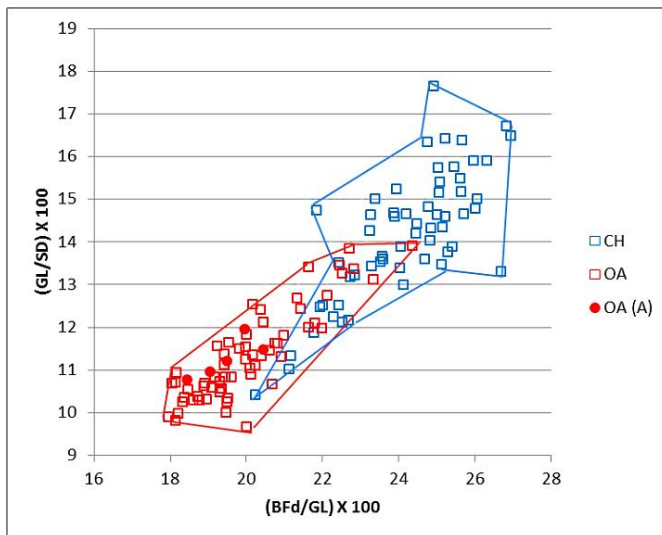


Figure 3.159 Metacarpal. Ratio between the greatest breadth of the distal end with the greatest length plotted against the ratio between the smallest width of the shaft and the greatest length. Symbols explained in Fig. 3.145.

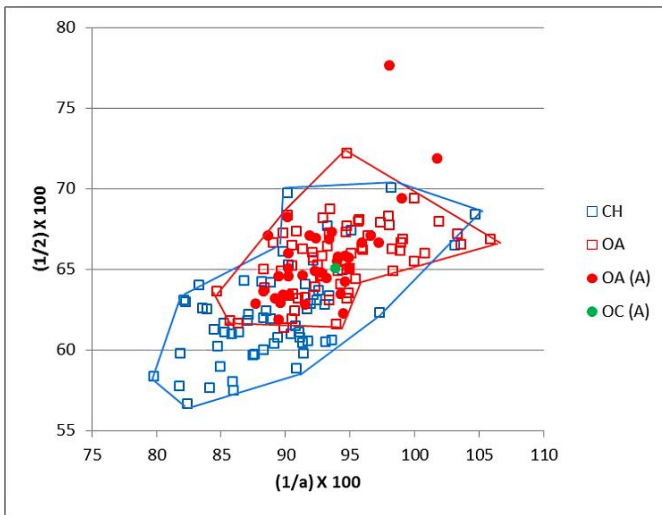


Figure 3.160 Metatarsal. Ratio between the diameter of the medial trochlea and the width of the medial condyle plotted against the ratio between the diameter of the *verticillus* at the medial condyle and the diameter of the medial trochlea. Symbols explained in Fig. 3.145.

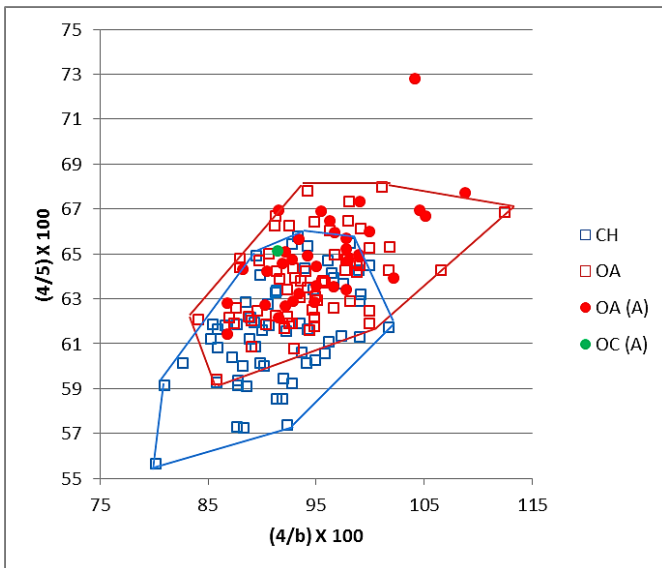


Figure 3.161 Metatarsal. Ratio between the width of the lateral condyle and the diameter of the lateral trochlea plotted against the ratio between the diameter of the *verticillus* on the lateral condyle and the diameter of the lateral condyle. Symbols explained in Fig. 3.145.

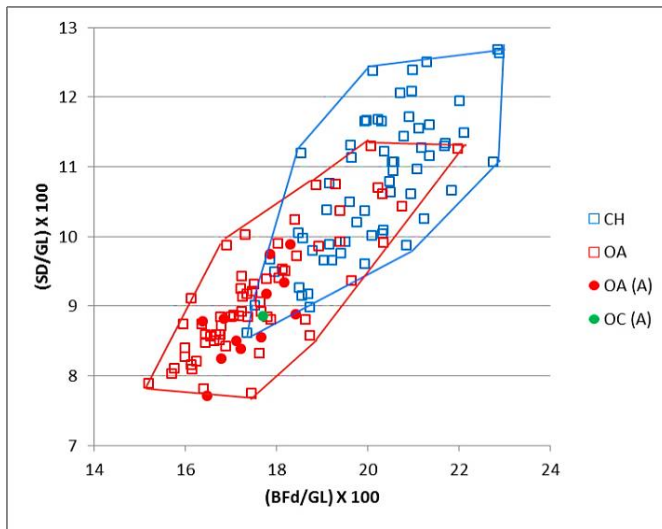


Figure 3.162 Metatarsal. Ratio between the greatest breadth of the distal end with the greatest length plotted against the ratio between the smallest width of the shaft and the greatest length. Symbols explained in Fig. 3.145.

Tibia

Biometrical results for the tibia are also consistent with the morphological analysis. No goats have been either morphologically or biometrically identified. All the archaeological sheep gather where the modern sheep are or in the area of overlap; as such their identification is confirmed. Of the several unidentified specimens, those that fall in the area where only sheep are can be assigned confidently to sheep (Fig. 3.163).

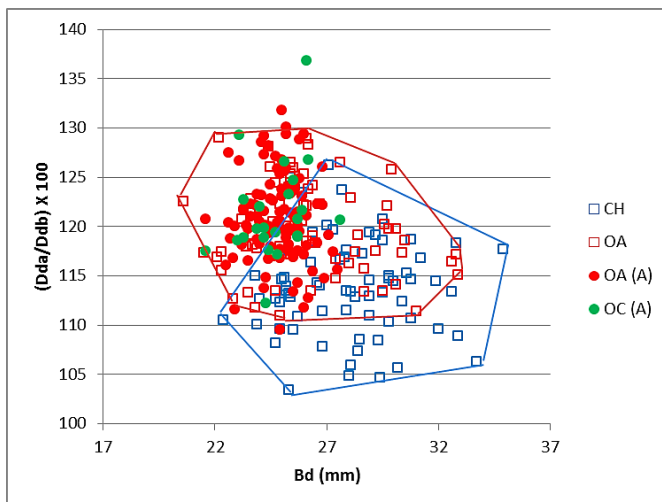


Figure 3.163 Breadth of the distal end plotted against the ratio between the depth of the medial (a) and lateral (b) side. Symbols explained in Fig. 3.145.

Astragalus

Figures 3.164 to 3.167 provide a similar pattern for astragali. The archaeological sheep fall among the modern sheep group or in the area of overlap between the two species, thus they are consistent with the morphological identification. Two archaeological sheep fall relatively distant from the other, but they can still be included in the range of variation of the sheep group. The two unidentified specimens fall consistently in the area of overlap, therefore the biometry does not allow a definite identification to be made.

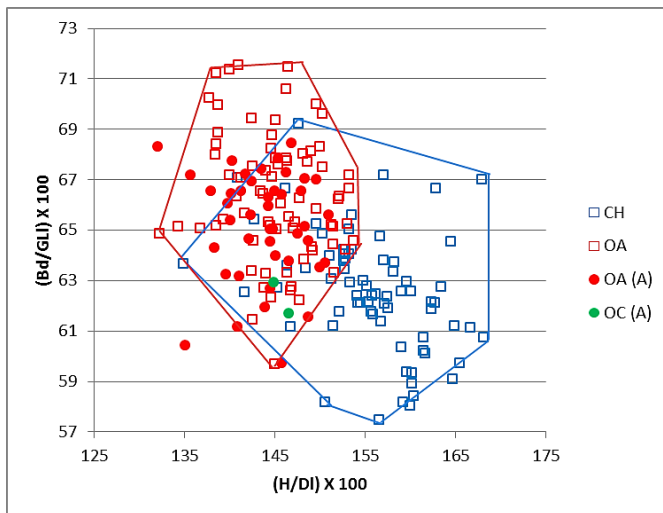


Figure 3.164 Ratio between height at the central constriction and the greatest depth of the lateral half plotted against a ratio between the breadth of the distal end and the greatest length of the lateral half. Symbols explained in Fig. 3.145.

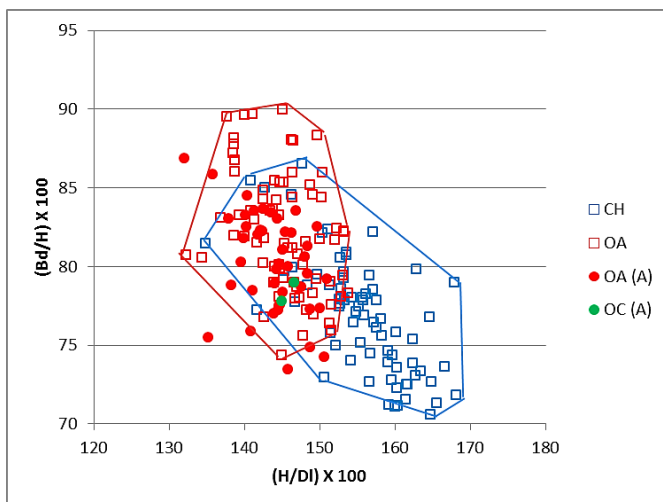


Figure 3.165 Ratio between height at the central constriction and the greatest depth of the lateral half plotted against the ratio between the breadth of the distal end and the height at the central constriction. Symbols explained in Fig. 3.145.

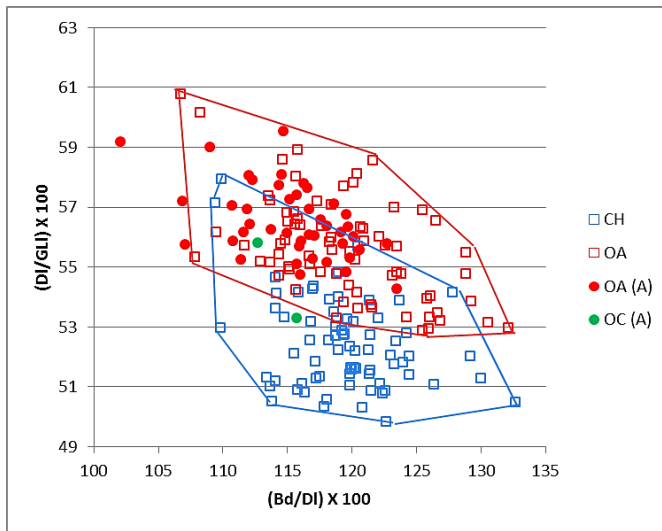


Figure 3.166 Ratio between breadth of the distal end and the greatest depth of the lateral half plotted against the ratio between the breadth of the distal end and the greatest depth of the lateral half. Symbols explained in Fig. 3.145.

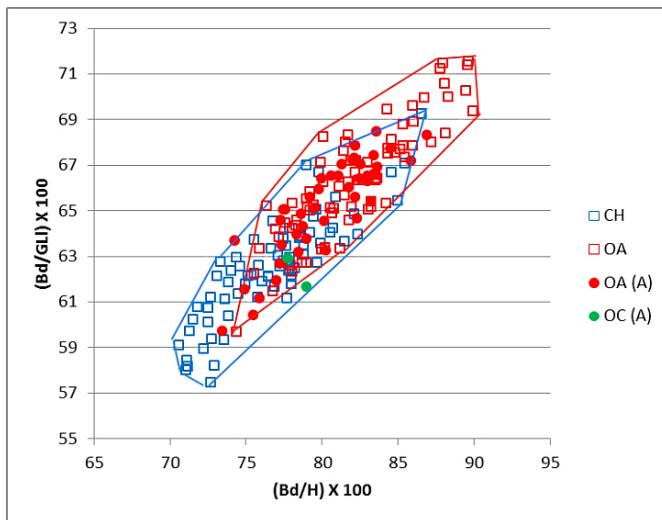


Figure 3.167 Ratio between the breadth of the distal end and the height at the central constriction and the ratio between height at the central constriction and the greatest depth of the lateral half. Symbols explained in Fig. 3.145.

Calcaneum

The likely absence of goat is supported by Figures 3.168 to 3.170. Only one archaeological group is visible; all the archaeological sheep fall among the modern sheep, following the same pattern. A few archaeological sheep appear to have very strong sheep traits. The only unidentified specimen present seems to plot more toward the goat group but, as it is not so distant from the sheep group, it cannot be confidently considered to be a goat.

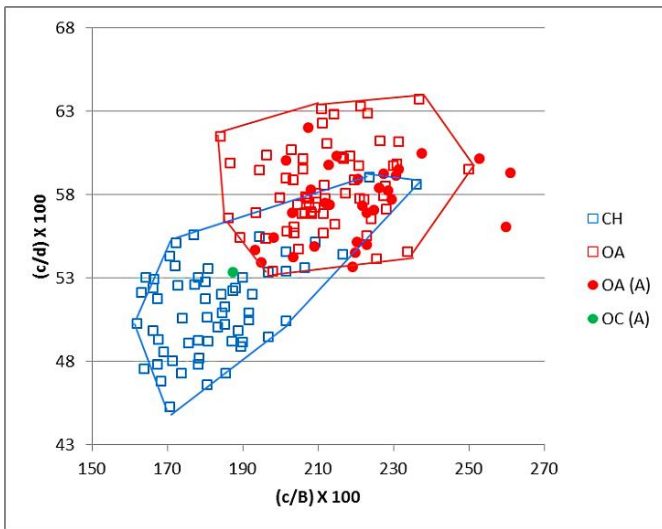


Figure 3.168 Ratio between the length and the breadth of the articular facet of the *os malleolare* plotted against the ratio between the length of the articular facet of the *os malleolare* and the length taken from the articular facet of the *os malleolare* to the end of the articulation-free part of the process. Symbols explained in Fig. 3.145.

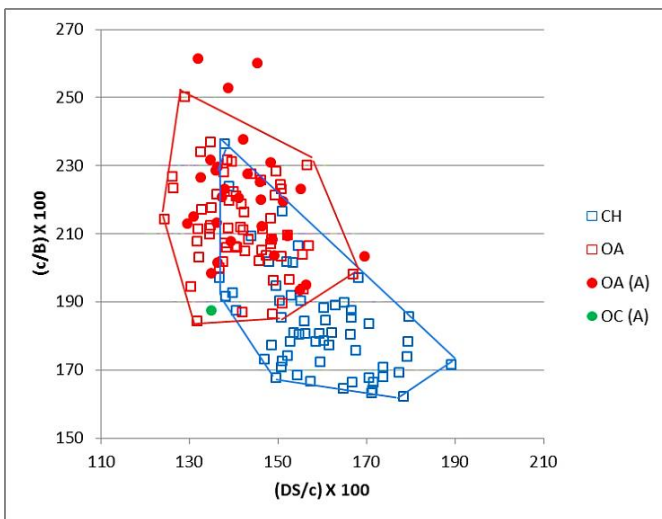


Figure 3.169 Ratio between the depth of the *substentaculum tali* and the length of the articular facet of the *os malleolare* plotted against the ratio between the length and the breadth of the articular facet of the *os malleolare*. Symbols explained in Fig. 3.145.

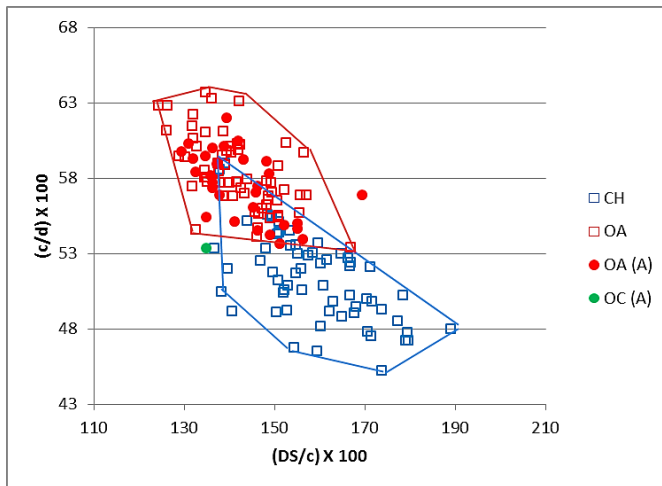


Figure 3.170 Ratio between the depth of the *substantaculum tali* and the length of the articular facet of the *os malleolare* plotted against the ratio between the length and the breadth of the articular facet of the *os malleolare*. Symbols explained in Fig. 3.145.

3rd Phalanx

Only two archaeological 3rd phalanges had been found and attributed morphologically to sheep. In Figure 3.171 they plot in the area of overlap between the two groups and are therefore consistent with a sheep identification.

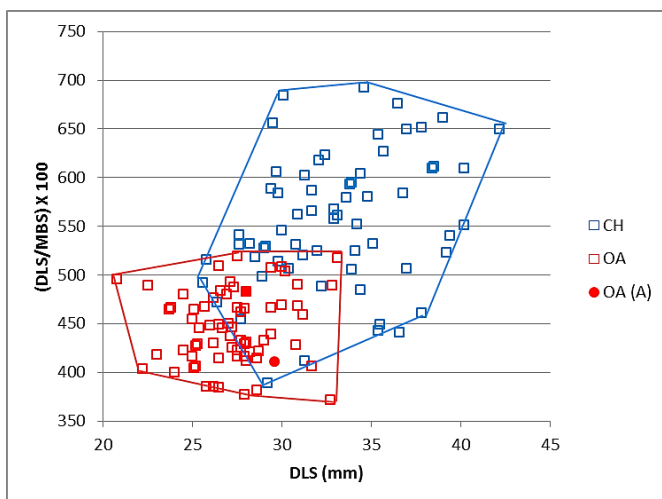


Figure 3.171 Greatest diagonal length of the sole plotted against a ratio between the greatest diagonal length of the sole and the middle breadth of the sole. Symbols explained in Fig. 3.145.

Phase S VII

Horncores

No horncores were recorded for this phase.

Scapula

Only sheep scapulae have been identified morphologically. Figures 3.172 and 3.173 confirm these identifications.

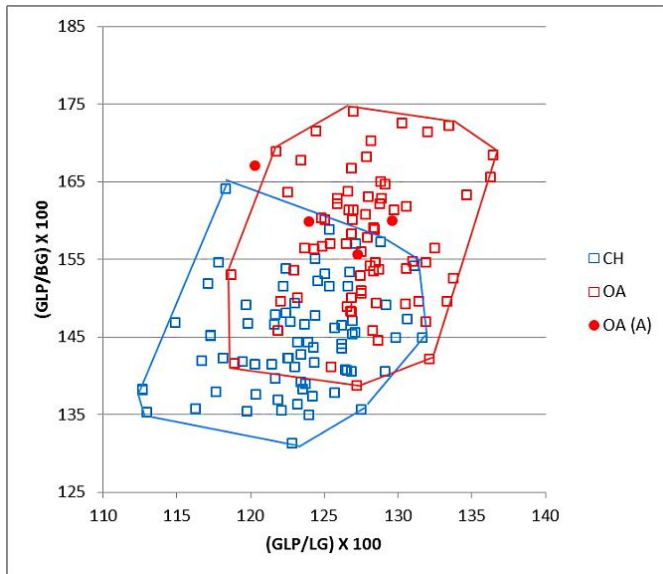


Figure 3.172 Ratio between the greatest length of the *processus articularis* and the length of the glenoid cavity plotted against the ratio between the greatest length of the *processus articularis* and the breadth of the glenoid cavity. Symbols explained in Fig. 3.145.

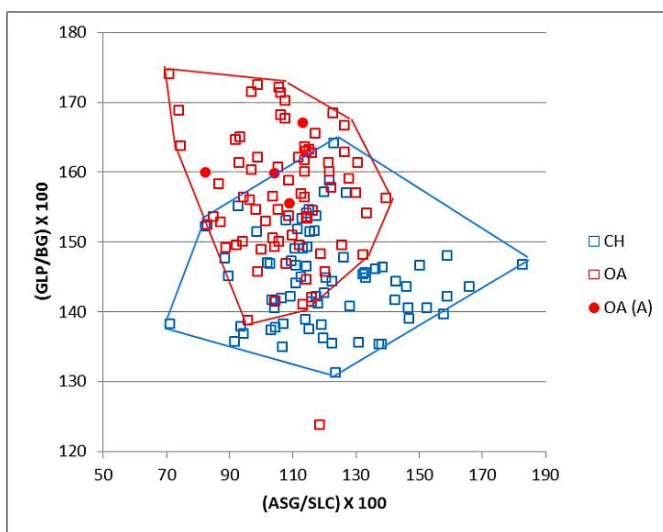


Figure 3.173 Ratio between the shortest distance from the base of the spine to the edge of the glenoid cavity and the minimum length of the *collum scapulae* plotted against a ratio the greatest length of the *processus articularis* and the breadth of the glenoid cavity. Symbols explained in Fig. 3.145.

Humerus

No humeri were attributed morphologically to goat. Such result is confirmed by the biometrical analysis as shown by Figures 3.174 to 3.177. All the morphologically identified sheep fall among the modern sheep group or in the area of overlap, confirming their identification.

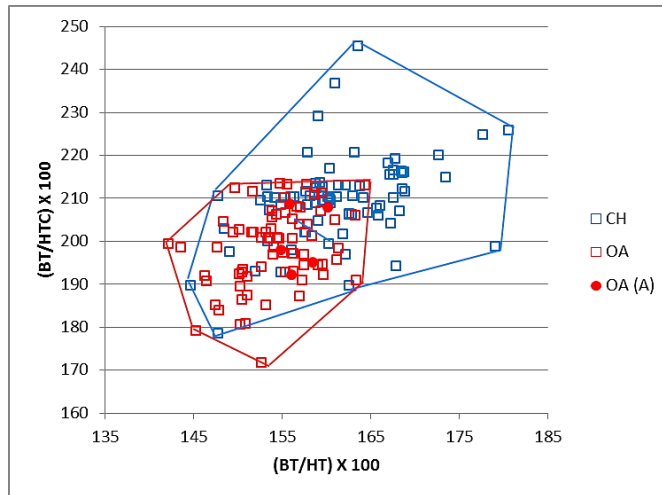


Figure 3.174 Ratio between the medio lateral width of the trochlea and its height plotted against the medio lateral width of the trochlea and the diameter of the trochlear constriction. Symbols explained in Fig. 3.145.

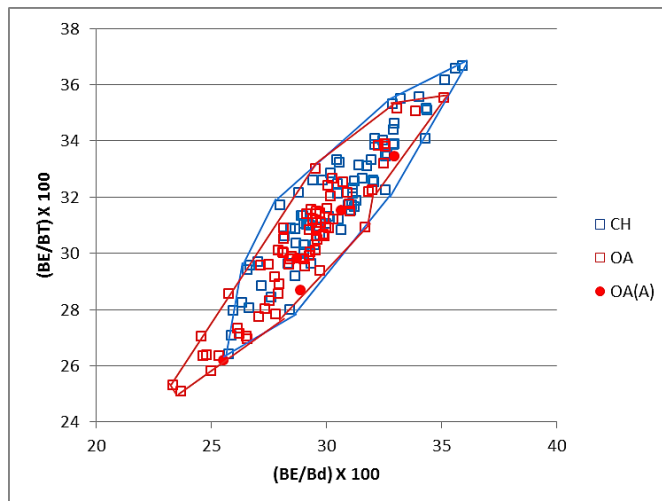


Figure 3.175 Ratio between the breadth of the *capitulum* and the distal width plotted against the ratio between the breadth of the *capitulum* and the medio lateral width of the trochlea. Symbols explained in Fig. 3.145.

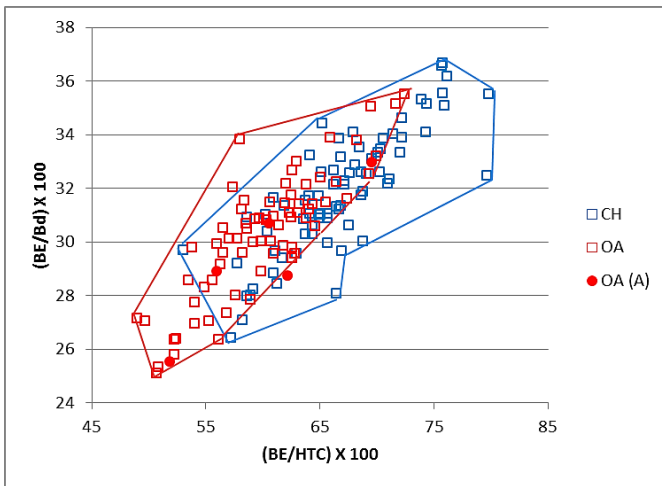


Figure 3.176 Ratio between the breadth of the *capitulum* and the diameter of the trochlea constriction plotted against the ratio between the breadth of the *capitulum* and the medio lateral width of the trochlea. Symbols explained in Fig. 3.145.

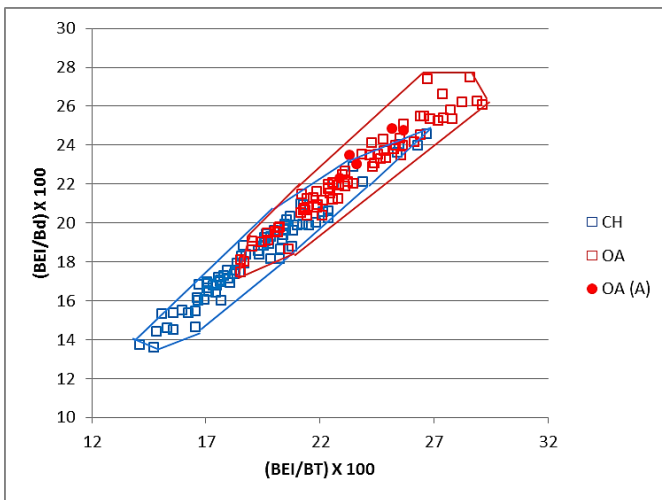


Figure 3.177 Ratio between the breadth of the epicondyle *lateralis* and the medio lateral width of the trochlea plotted against the ratio between the breadth of the epicondyle *lateralis* and the width of the distal end. Symbols explained in Fig. 3.145.

Radius

No goat radii had been morphologically identified. Figure 3.178 shows that all the archaeological sheep plot in the area of overlap and are, therefore, not inconsistent with their original identification. The only unidentified specimen plots far from the other archaeological specimens, clearly among the goat cluster. It is likely to represent a rare case of a *Capra* specimen at this site.

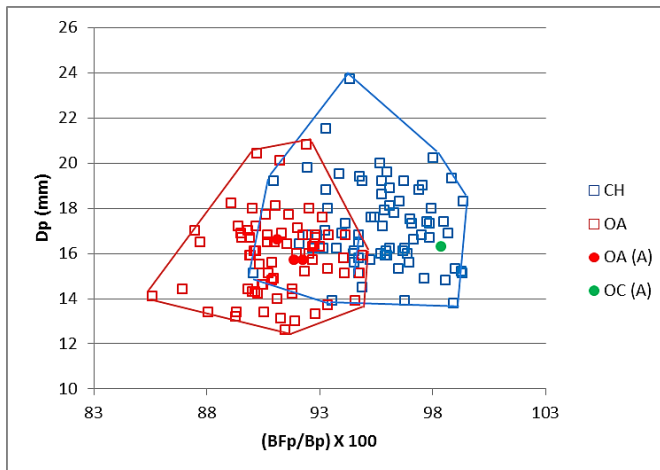


Figure 3.178 Ratio between the greatest length of the *facies articularis proximalis* and the greatest breadth of the proximal end plotted against the depth of the proximal end. Symbols explained in Fig. 3.145.

Ulna

Figure 3.179 shows that the only recorded archaeological sheep plots rather distantly from the modern specimens, but much more closely to the sheep group and it is therefore likely to constitute a specimen with strong *Ovis* traits.

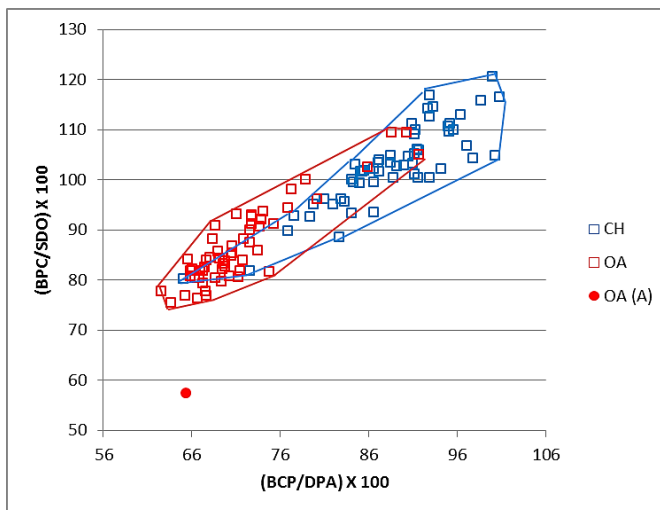


Figure 3.179 Ratio between the breadth across the coronoid process and the depth across the *processus anconaeus* to the caudal border plotted against the breadth across the coronoid process and the smallest depth of the olecranon. Symbols explained in Fig. 3.145.

Metapodials

No archaeological goats were found when the metapodials were analysed. Figures from 3.180 to 3.182 present the results for the metacarpals: all the archaeological sheep fall among the modern

sheep group or in the area of overlap, thus their morphological identification is confirmed. Only one sheep specimen is Figure 3.181 can be considered border line but, as it follows the sheep pattern in the other figures, it cannot be considered to have been misclassified.

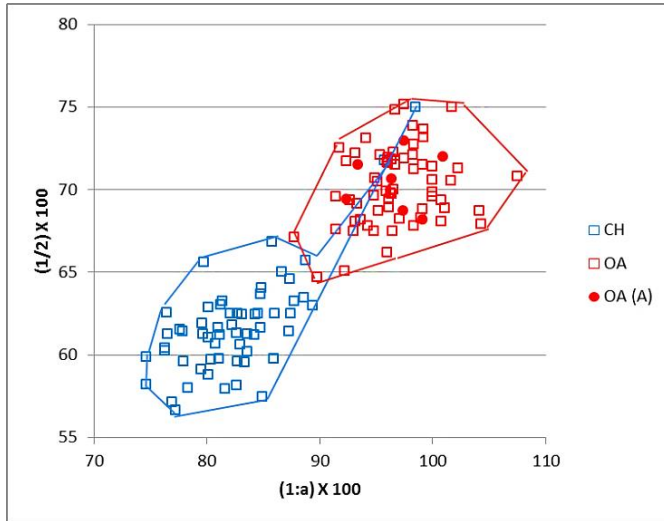


Figure 3.180 Metacarpal. Ratio between the diameter of the medial trochlea and the width of the medial condyle plotted against the ratio between the diameter of the *verticillus* at the medial condyle and the diameter of the medial trochlea. Symbols explained in Fig. 3.145.

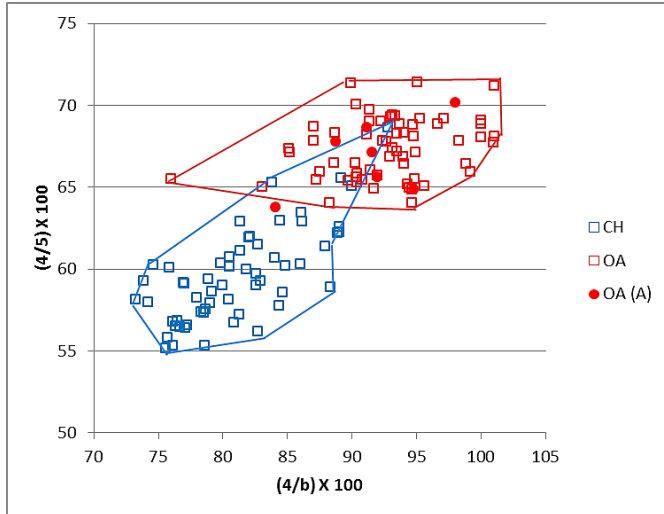


Figure 3.181 Metacarpal. Ratio between the width of the lateral condyle and the diameter of the lateral trochlea plotted against the ratio between the diameter of the lateral condyle and the diameter of the *verticillus* on the lateral condyle. Symbols explained in Fig. 3.145.

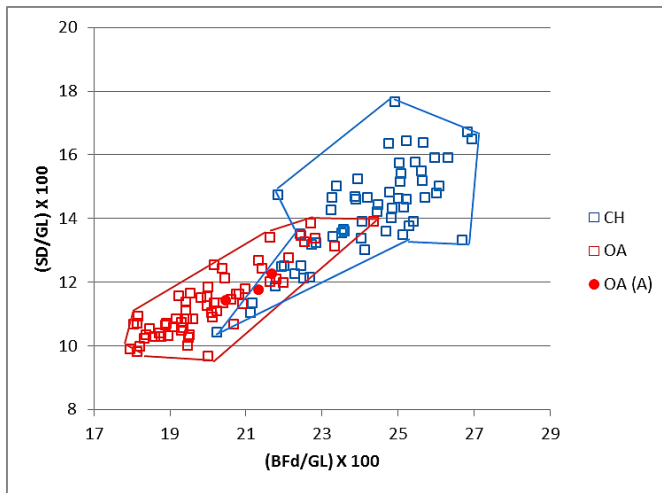


Figure 3.182 Metacarpal. Ratio between the greatest breadth of the distal end with the greatest length plotted against the ratio between the smallest width of the shaft and the greatest length. Symbols explained in Fig. 3.145.

Less clear is the separation when the metatarsals are considered (Figs. 3.183 to 3.185): more overlap is present blurring the results. Most of the archaeological sheep are consistent with the modern sheep group, falling among the modern sheep or in the area of overlap. Only one archaeological sheep seems suspicious as it plots more toward the goat group (Fig. 3.183). Nevertheless, as with the other ratios the same specimen is consistent with the sheep group, its identification cannot be doubted. The only unidentified specimen seems to follow the sheep group pattern but as it falls relatively distant from the other archaeological sheep and quite close to some of the modern goats, it cannot be attributed to species.

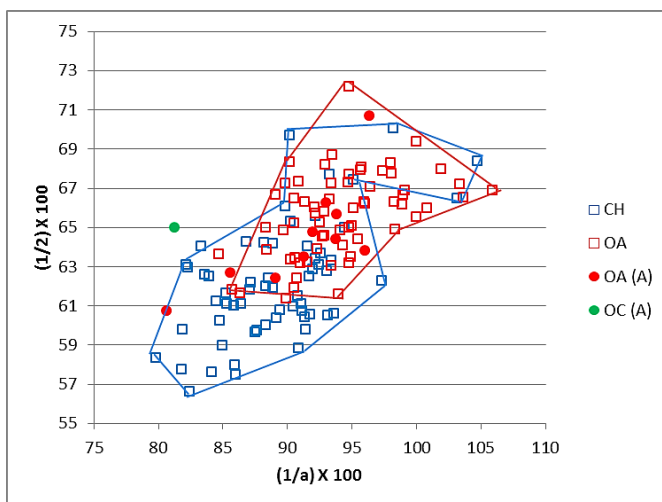


Figure 3.183 Metatarsal. Ratio between the diameter of the medial trochlea and the width of the medial condyle plotted against the ratio between the diameter of the *verticillus* at the medial condyle and the diameter of the medial trochlea. Symbols explained in Fig. 3.145.

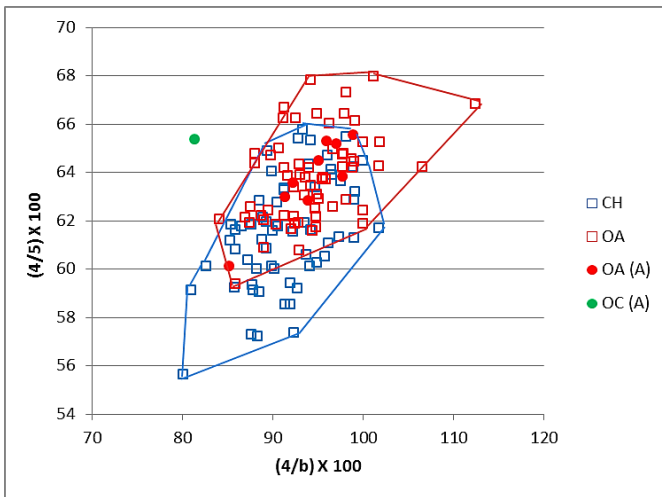


Figure 3.184 Metatarsal. Ratio between the width of the lateral condyle and the diameter of the lateral trochlea plotted against the ratio between the diameter of the *verticillus* on the lateral condyle and the diameter of the lateral condyle. Symbols explained in Fig. 3.145.

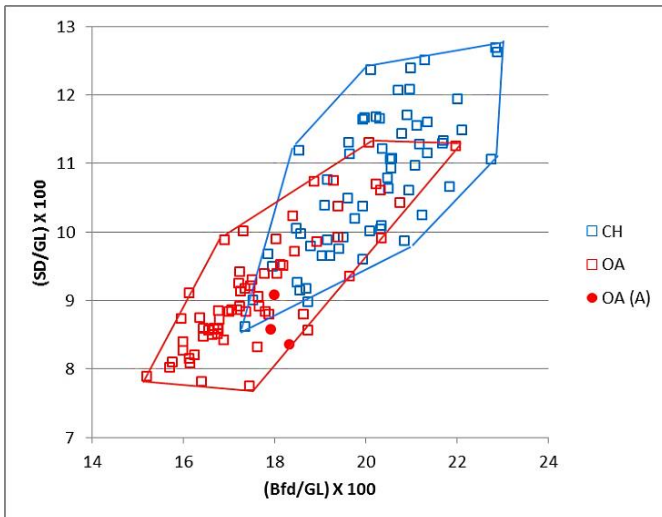


Figure 3.185 Metatarsal. Ratio between the greatest breadth of the distal end with the greatest length plotted against the ratio between the smallest width of the shaft and the greatest length. Symbols explained in Fig. 3.145.

Tibia

No goat tibiae had been morphologically identified. Such identification is confirmed by biometry. All archaeological sheep plot among the modern sheep group or in the area of overlap, confirming their morphological identification (Fig. 3.186). The unidentified specimens cannot be attributed to species level as they fall in the area of overlap.

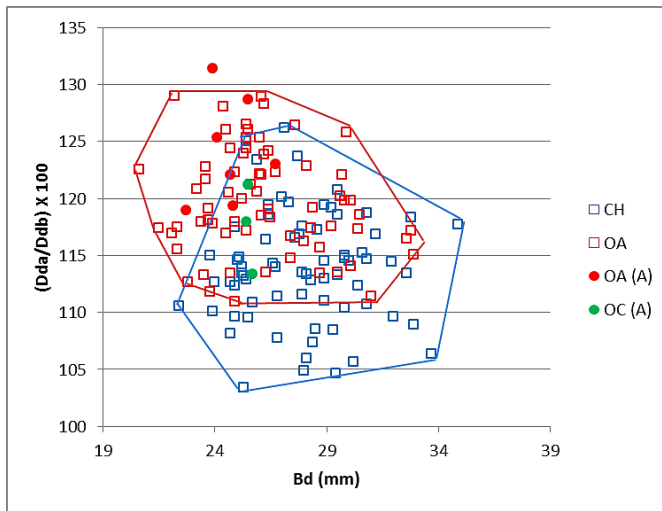


Figure 3.186 Breadth of the distal end plotted against the ratio between the depth of the medial (a) and lateral (b) side. Symbols explained in Fig. 3.145.

Astragalus

Only one and partially broken astragalus was recorded for this phase. As shown by Figure 3.187, the morphologically identified sheep falls among the modern sheep group, confirming its identification.

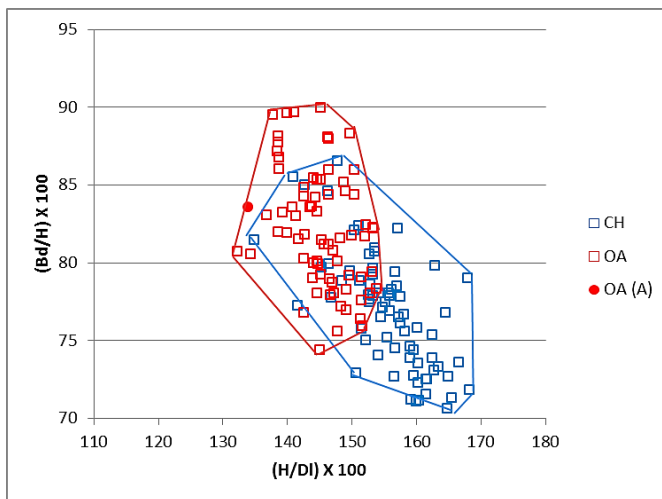


Figure 3.187 Ratio between height at the central constriction and the greatest depth of the lateral half plotted against the ratio between the breadth of the distal end and the height at the central constriction. Symbols explained in Fig. 3.145.

Calcaneum

Figures from 3.188 to 3.190 show that all the archaeological sheep calcanea are consistent with the sheep pattern, falling among the modern sheep group or in the area of overlap. The absence of goats is confirmed by the morphological as well as the biometrical data.

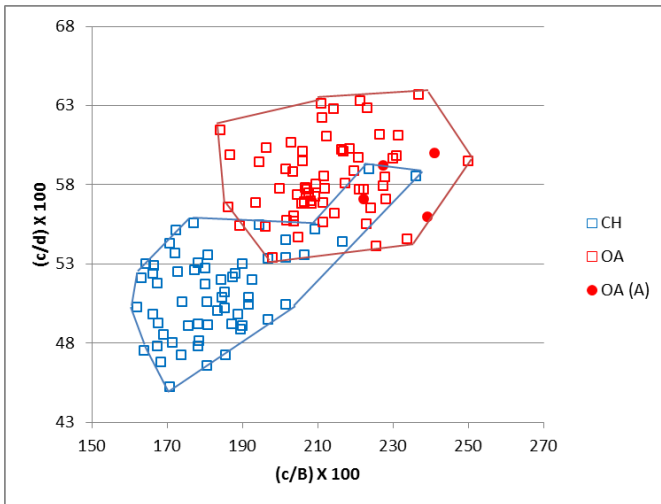


Figure 3.188 Ratio between the length and the breadth of the articular facet of the *os malleolare* plotted against the ratio between the length of the articular facet of the *os malleolare* and the length taken from the articular facet of the *os malleolare* to the end of the articulation-free part of the process. Symbols explained in Fig. 3.145.

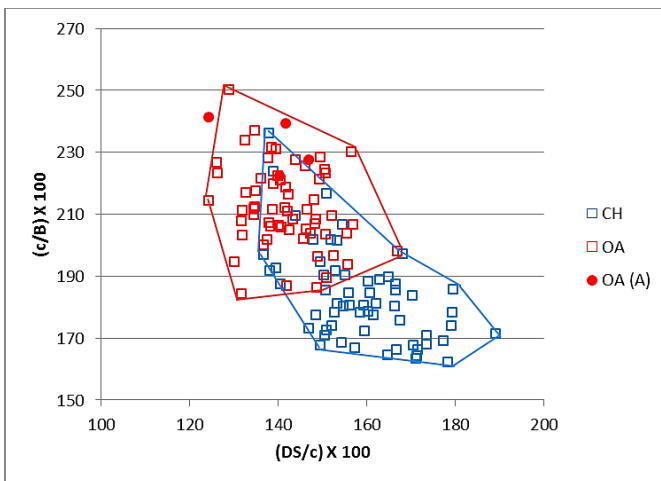


Figure 3.189 Ratio between the depth of the *substantaculum tali* and the length of the articular facet of the *os malleolare* plotted against the ratio between the length and the breadth of the articular facet of the *os malleolare*. Symbols explained in Fig. 3.145.

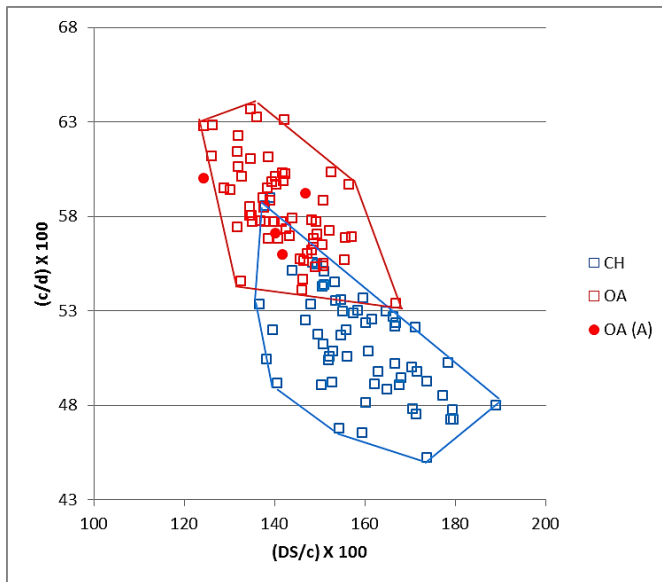


Figure 3.190 Ratio between the depth of the *subtentaculum tali* and the length of the articular facet of the *os malleolare* plotted against the ratio between the length and the breadth of the articular facet of the *os malleolare*. Symbols explained in Fig. 3.145.

Phase S VIII

Horncores

No horncores could be measured for this phase.

Scapula

Only two scapulae had been recorded; one could not be assigned to species level, the other was morphologically attributed to sheep. Figures 3.191 and 3.192 suggest that both specimens belong to sheep, as they are consistent with the modern sheep pattern.

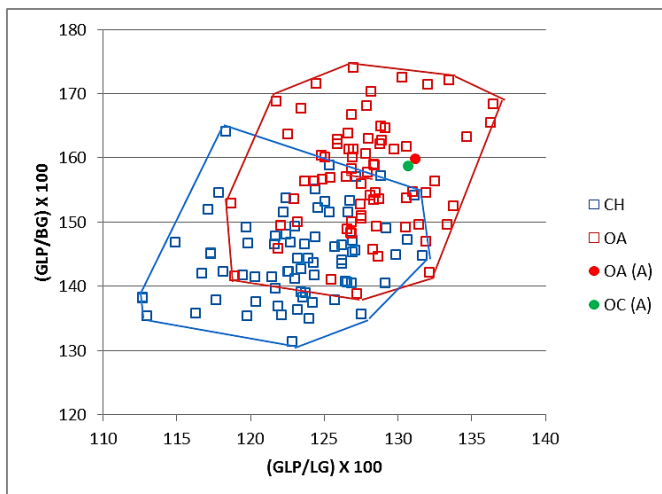


Figure 3.191 Ratio between the greatest length of the *processus articularis* and the length of the glenoid cavity plotted against the ratio between the greatest length of the *processus articularis* and the breadth of the glenoid cavity. Symbols explained in Fig. 3.145.

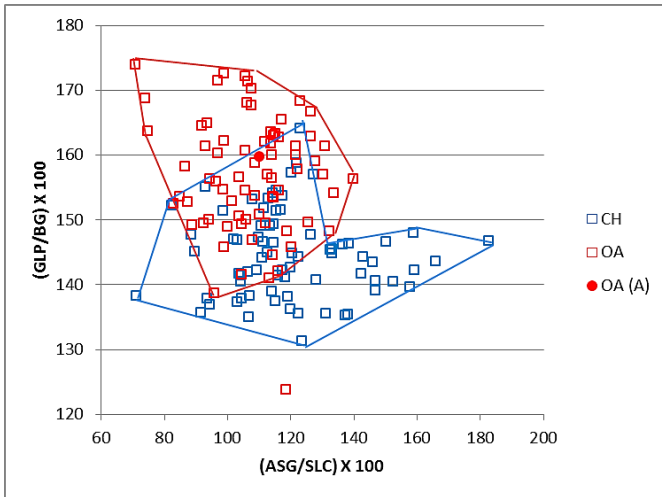


Figure 3.192 Ratio between the shortest distance from the base of the spine to the edge of the glenoid cavity and the smallest length of the *collum scapulae* plotted against the greatest length of the *processus articularis* and the breadth of the glenoid cavity. Symbols explained in Fig. 3.145.

Humerus

All the humeri were identified morphologically as *Ovis*. Figures from 3.193 to 3.196 all show that the biometry confirms the morphological identification: all the archaeological sheep fall among the sheep modern group or in the area of overlap.

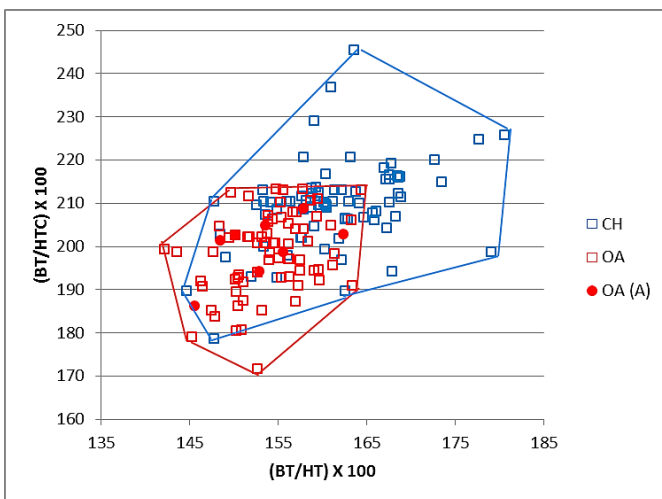


Figure 3.193 Ratio between the medio lateral width of the trochlea and its height plotted against the medio lateral width of the trochlea and the diameter of the trochlear constriction. Symbols explained in Fig. 3.145.

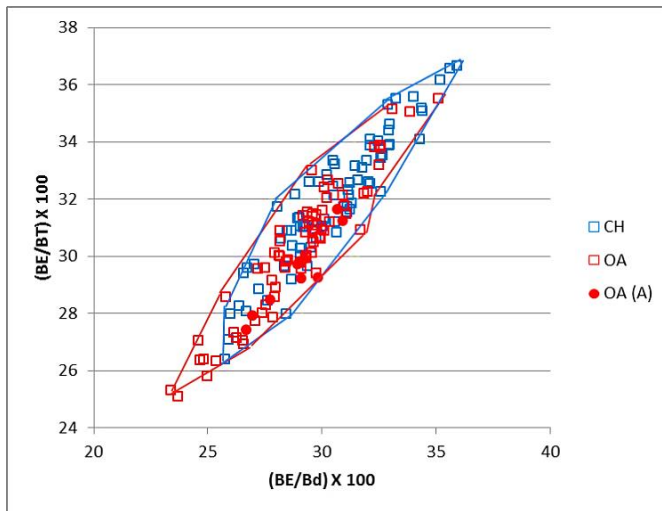


Figure 3.194 Ratio between the breadth of the *capitulum* and the distal width plotted against the ratio between the breadth of the *capitulum* and the medio lateral width of the trochlea. Symbols explained in Fig. 3.145.

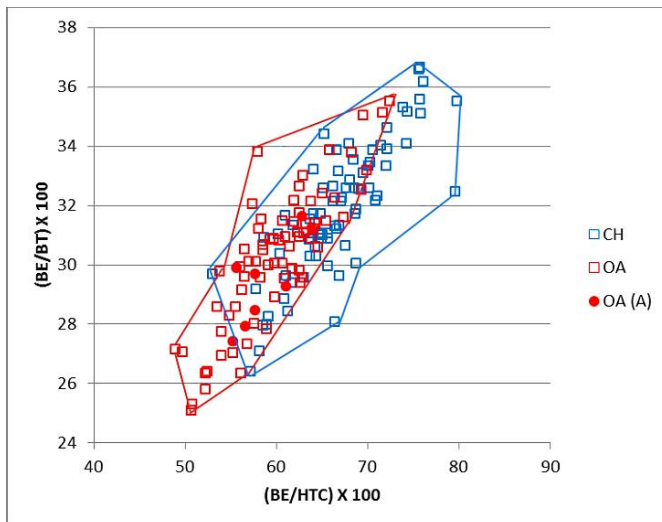


Figure 3.195 Ratio between the breadth of the *capitulum* and the diameter of the trochlear constriction plotted against the ratio between the breadth of the *capitulum* and the medio lateral width of the trochlea. Symbols explained in Fig. 3.145.

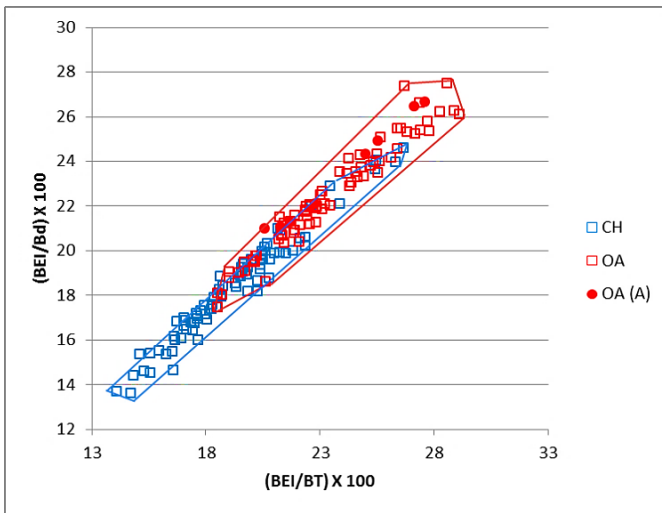


Figure 3.196 Ratio between the breadth of the epicondyle *lateralis* and the medio lateral width of the trochlea plotted against the ratio between the breadth of the epicondyle *lateralis* and the width of the distal end. Symbols explained in Fig. 3.145.

Radius

All the radii were morphologically identified as sheep and, as shown by Figure 3.197, biometrically they are consistent with the sheep pattern. The absence of goat radii is confirmed by the biometrical results.

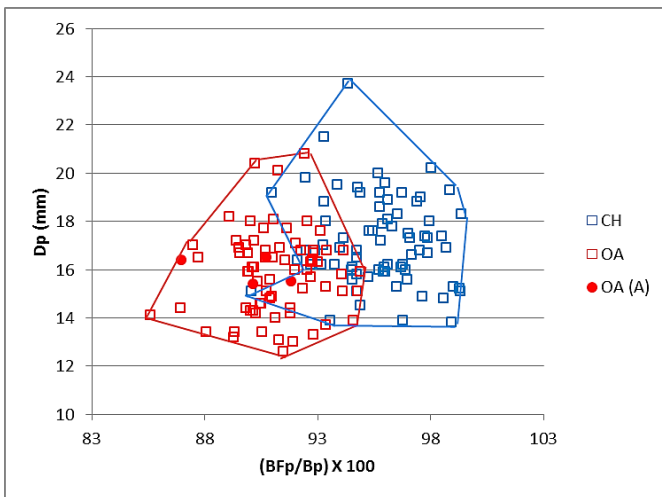


Figure 3.197 Ratio between the greatest length of the *facies articularis proximalis* and the greatest breadth of the proximal end plotted against the depth of the proximal end. Symbols explained in Fig. 3.145.

Ulna

All ulnae were morphologically attributed to *Ovis*, apart from one specimen that could not be assigned to a species. Figure 3.198 shows that the archaeological sheep fall among the sheep modern counterparts confirming their identification. The unidentified specimen remains as such, since it plots in the area of overlap between the two modern species.

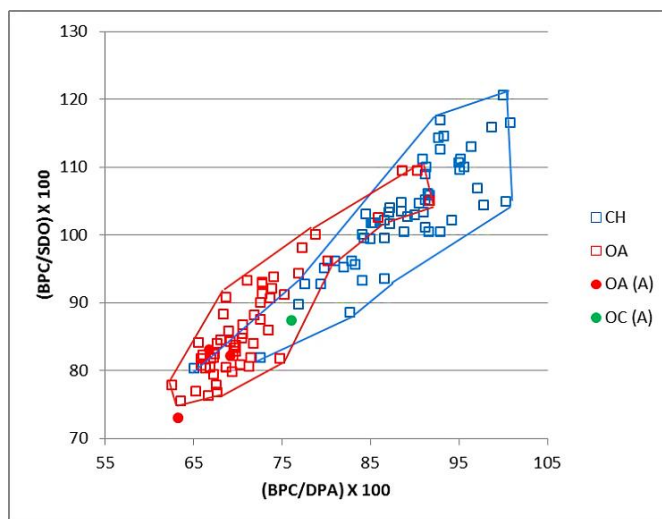


Figure 3.198 Ratio between the breadth across the coronoid process and the depth across the *processus anconaeus* to the caudal border plotted against the breadth across the coronoid process and the smallest depth of the olecranon. Symbols explained in Fig. 3.145.

Metapodials

Figures 3.199 to 3.201 show the results for the metacarpal. No archaeological specimens had been morphologically attributed to the goat species and such identification is confirmed by the biometry. All the archaeological sheep specimens are consistent with the modern sheep pattern.

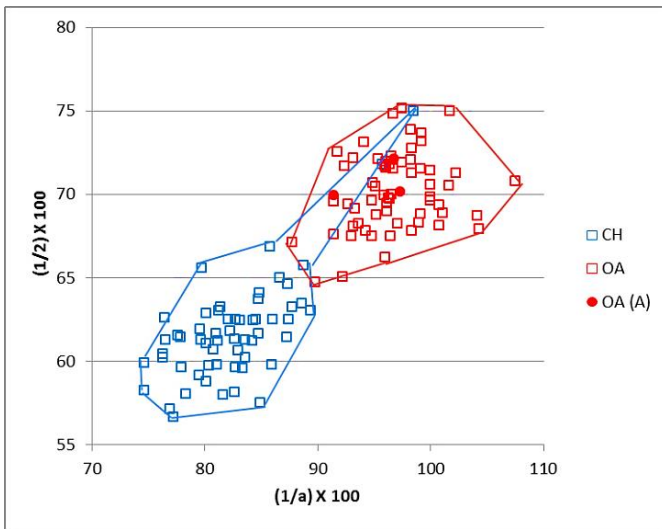


Figure 3.199 Metacarpal. Ratio between the diameter of the medial trochlea and the width of the medial condyle plotted against the ratio between the diameter of the *verticillus* at the medial condyle and the diameter of the medial trochlea. Symbols explained in Fig. 3.145.

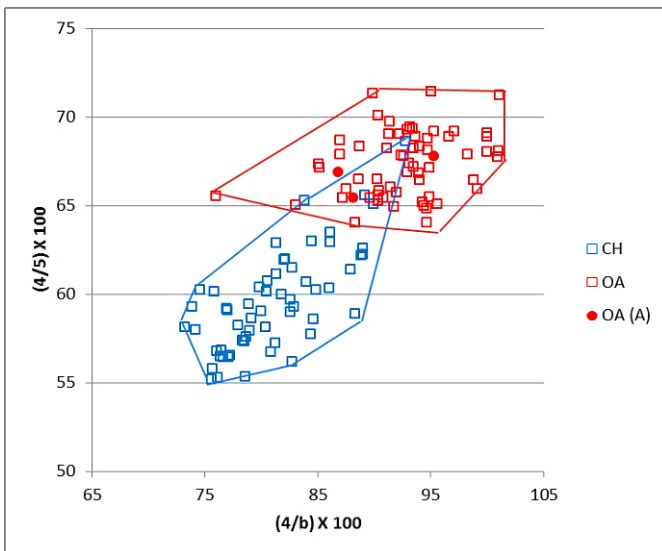


Figure 3.200 Metacarpal. Ratio between the width of the lateral condyle and the diameter of the lateral trochlea plotted against the ratio between the diameter of the *verticillus* the lateral condyle and the diameter of the lateral condyle. Symbols explained in Fig. 3.145.

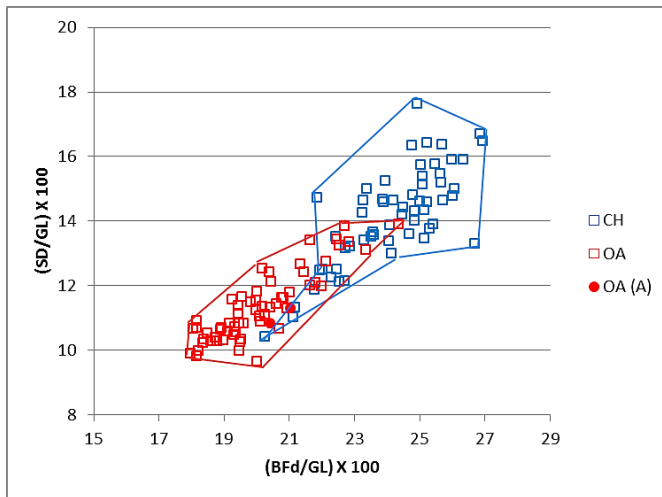


Figure 3.201 Metacarpal. Ratio between the greatest breadth of the distal end with the greatest length plotted against the ratio between the smallest width of the shaft and the greatest length. Symbols explained in Fig. 3.145.

Figures 3.202 to 3.204 attest to the consistency between morphology and biometry when the metatarsal is considered. All the morphologically identified sheep in fact, are consistent with the biometrical sheep pattern.

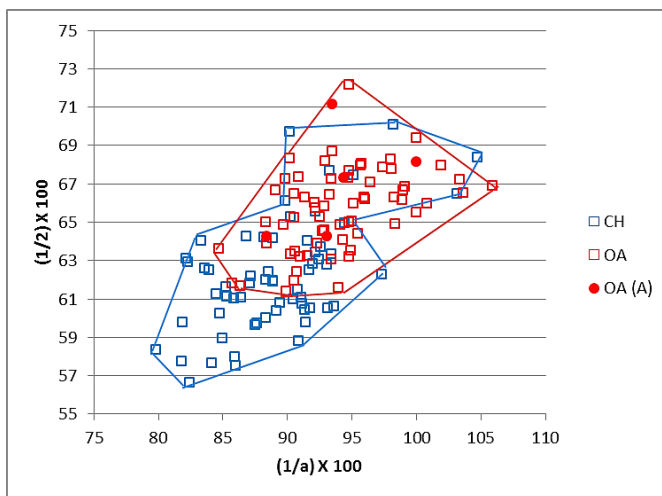


Figure 3.202 Metatarsal. Ratio between the diameter of the medial trochlea and the width of the medial condyle plotted against the ratio between the diameter of the *verticillus* at the medial condyle and the diameter of the medial trochlea. Symbols explained in Fig. 3.145.

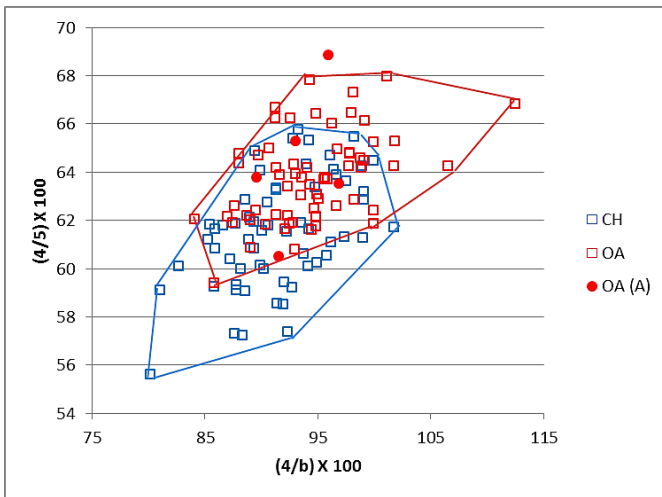


Figure 3.203 Metatarsal. Ratio between the width of the lateral condyle and the diameter of the lateral trochlea plotted against the ratio between the diameter of the *verticillus* on the lateral condyle and the diameter of the lateral condyle. Symbols explained in Fig. 3.145.

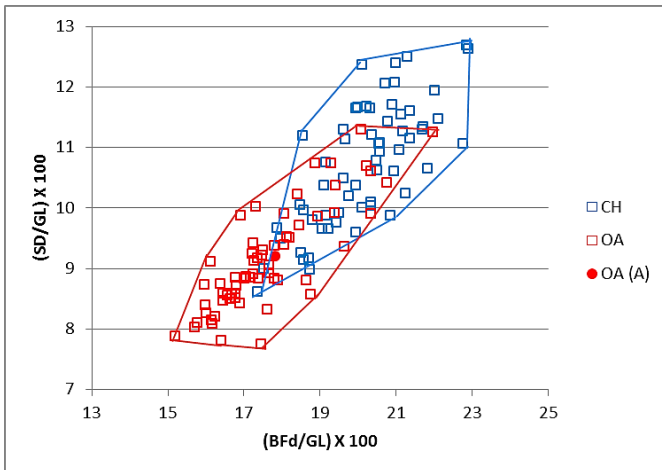


Figure 3.204 Metatarsal. Ratio between the greatest breadth of the distal end with the greatest length plotted against the ratio between the smallest width of the shaft and the greatest length. Symbols explained in Fig. 3.145.

Tibia

Two archaeological tibiae had been identified as sheep. This identification is not inconsistent with the biometrical analysis, as they fall in the area of the graph where the two groups overlap. The unidentified specimen plots in the area of overlap but is more consistent with the sheep pattern (Fig. 3.205).

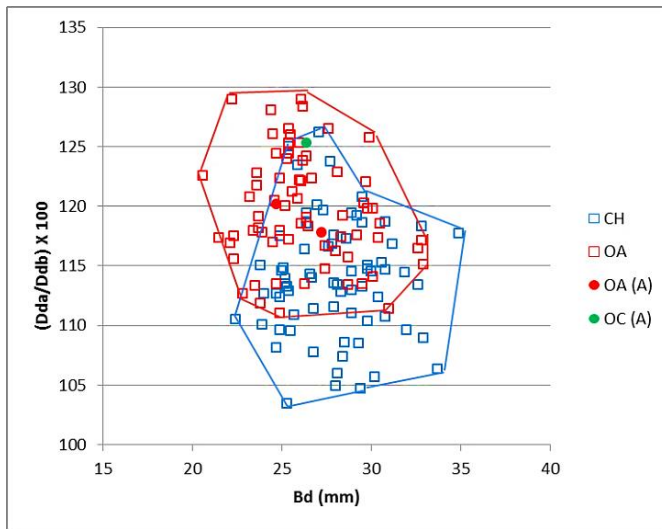


Figure 3.205 Breadth of the distal end plotted against the ratio between the depth of the medial (a) and lateral (b) side. Symbols explained in Fig. 3.145.

Astragalus

No archaeological astragali have been morphologically attributed to goat. This is mirrored in Figures 3.206 to 3.209. The morphologically identified sheep fall among the modern sheep group or in the area of overlap, confirming their identification.

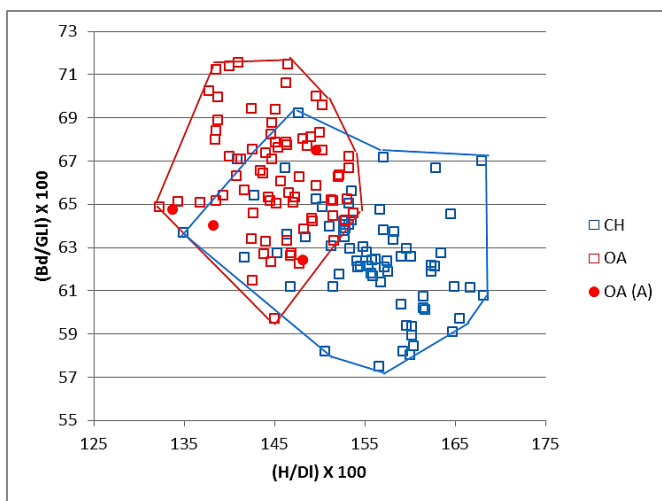


Figure 3.206 Ratio between height at the central constriction and the greatest depth of the lateral half plotted against a ratio between the breadth of the distal end and the greatest length of the lateral half. Symbols explained in Fig. 3.145.

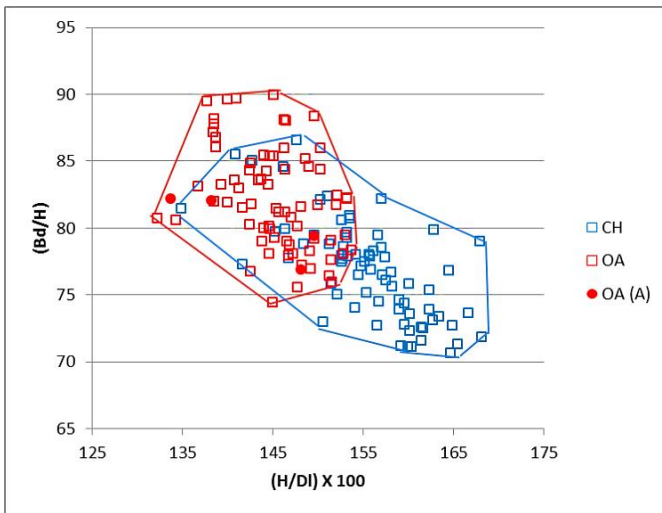


Figure 3.207 Ratio between height at the central constriction and the greatest depth of the lateral half plotted against the ratio between the breadth of the distal end and the height at the central constriction. Symbols explained in Fig. 3.145.

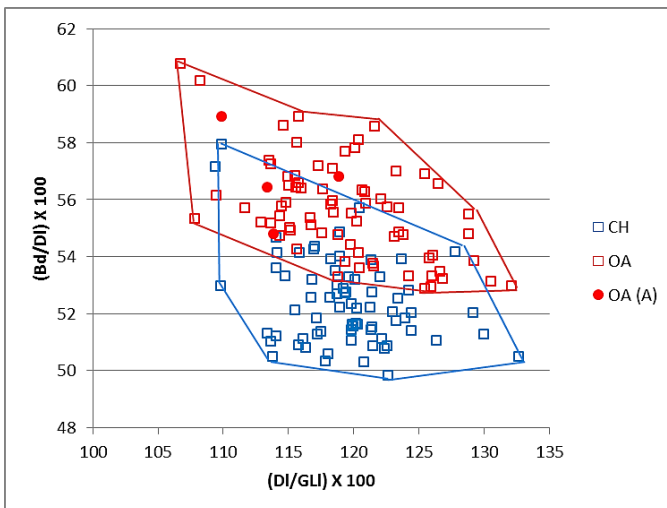


Figure 3.208 Ratio between breadth of the distal end and the greatest depth of the lateral half plotted against the ratio between the breadth of the distal end and the greatest depth of the lateral half. Symbols explained in Fig. 3.145.

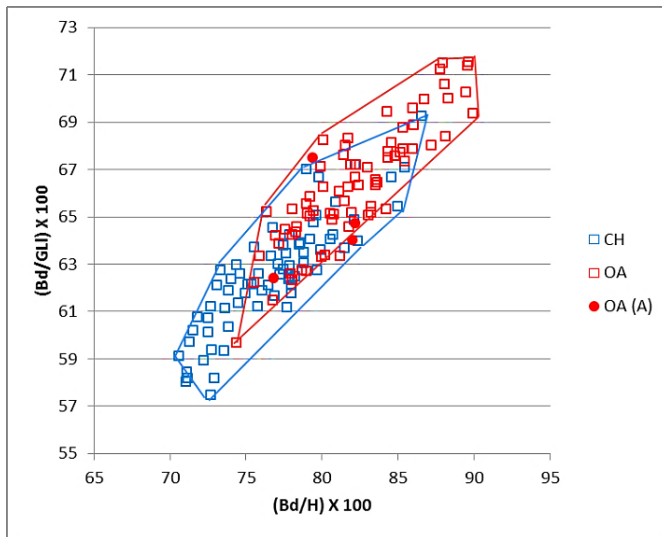


Figure 3.209 Ratio between the breadth of the distal end and the height at the central constriction and the ratio between height at the central constriction and the greatest depth of the lateral half. Symbols explained in Fig. 3.145.

Calcaneum

One of the two calcanea has been attributed morphologically to sheep and the other one to the sheep/goat category. Figures 3.210 to 3.212 show that both specimens fall in the area of overlap between the two modern groups but, while the morphological identification for the archaeological sheep is confirmed, an attribution to species level for the unidentified specimen cannot be established.

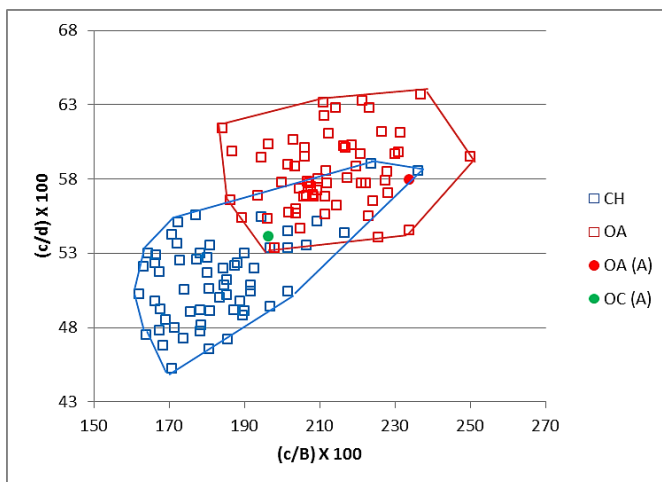


Figure 3.210 Ratio between the length and the breadth of the articular facet of the *os malleolare* plotted against the ratio between the length of the articular facet of the *os malleolare* and the length taken from the articular facet of the *os malleolare* to the end of the articulation-free part of the process. Symbols explained in Fig. 3.145.

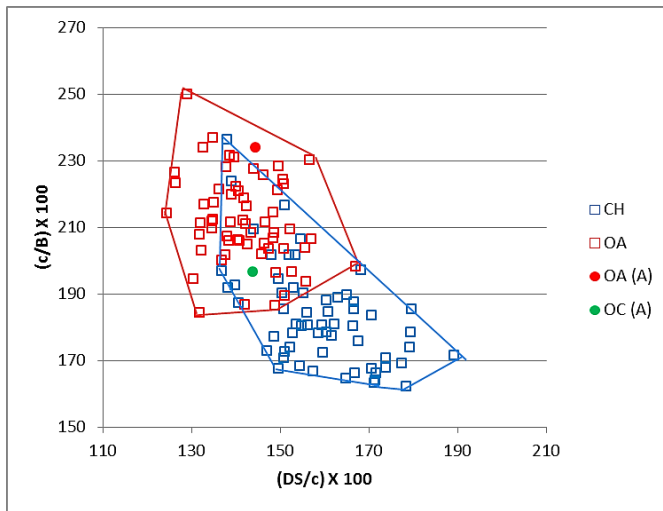


Figure 3.211 Ratio between the depth of the *sustentaculum tali* and the length of the articular facet of the *os malleolare* plotted against the ratio between the length and the breadth of the articular facet of the *os malleolare*. Symbols explained in Fig. 3.145.

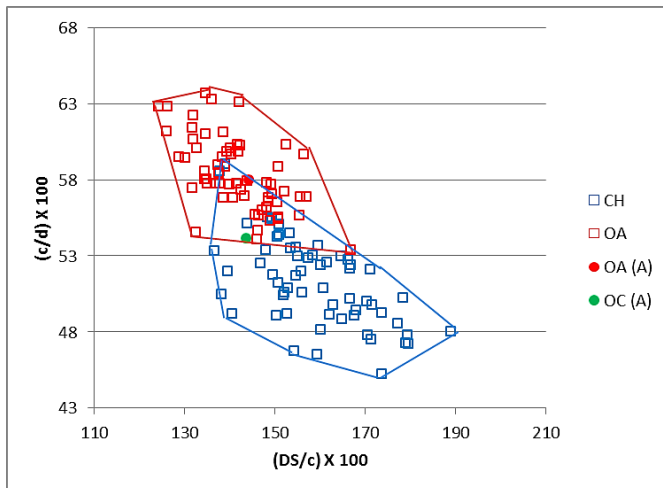


Figure 3.212 Ratio between the depth of the *sustentaculum tali* and the length of the articular facet of the *os malleolare* plotted against the ratio between the length and the breadth of the articular facet of the *os malleolare*. Symbols explained in Fig. 3.145.

The results from the shape analysis through the use of BI allow us to make some preliminary considerations. Firstly, as previously seen with the case of King's Lynn, the modern sample has confirmed to fit very well with the archaeological material. Secondly, the results confirm that the combination of morphology and biometry increases the amount of information acquired, as such it allows a mutual verification of the identifications. Thirdly, in the case of Flaxengate, when the two approaches were compared, the biometry often supported and reinforced what had already been observed through the morphological analysis: sheep specimens far outnumber goat specimens in all chronological phases and for all the anatomical elements. In addition, the biometry has pointed out an additional case of a potential goat specimen (a radius in phase S VII). Nevertheless, as it represents a single case, it does not affect the overall pattern.

O'Connor's view that the Flaxengate caprine assemblage is almost exclusively represented by sheep is confirmed by the current analysis, though slightly better qualified – the goat is present but is definitely rare.

3.3.7 Discriminant Analysis

Discriminant Analysis (DA) was carried out on the Flaxengate sheep/goat assemblage *in toto* following the procedure explained in Section 3.2.8. In order to increase the sample size and include in the study the specimens for which not all the measurements could be taken, DA was in some cases rerun with the exclusion of some measurements/variables.

Results on an element by element basis follow, coupled with a series of diagrams. For an explanation of how the diagrams should be read see Section 3.2.9.

Horncores

Table 3.111 shows the reattribution rate when all the measurements are included. Total agreement is present between morphological and biometrical identifications (100%). When measurements A and B are excluded from the analysis the percentage of correct reattributions stays the same (Tab. 3.112), suggesting that C and D can substitute A and B in case the specimen is broken.

The degree of consistency is still very high (100%) also when the measurements E and F are excluded, despite the less successful level of correct classification in the modern material (Tab. 3.113).

Table 3.111 Results from the Discriminant Analysis when applied on the archaeological horncores. a = percentage of correct attributions related to the modern material (selected original grouped cases); b = percentage of correct attributions related to the archaeological material (unselected original grouped cases); d = percentage of correct attributions when cross-validation was applied. Same terminology is adopted in all the following tables.

Classification Results ^{a,b,d}						
			TAXA	Predicted Group Membership		Total
				CH	OA	
Modern Material	Original	Count	CH	33	2	35
			OA	1	27	28
		%	CH	94.3	5.7	100.0
			OA	3.6	96.4	100.0
	Cross-validated ^c	Count	CH	33	2	35
			OA	1	27	28
		%	CH	94.3	5.7	100.0
			OA	3.6	96.4	100.0
Flaxengate Material	Original	Count	CH	1	0	1
			OA	0	4	4
		%	CH	100.0	.0	100.0
			OA	.0	100.0	100.0
a. 95.2% of selected original grouped cases correctly classified.						
b. 100.0% of unselected original grouped cases correctly classified.						
d. 95.2% of selected cross-validated grouped cases correctly classified. Cross validation is done only for those cases in the analysis. In cross validation, each case is classified by the functions derived from all cases other than that case.						

Table 3.112 Results from the Discriminant Analysis when applied on the archaeological horncores excluding measurements A and B.

Classification Results ^{a,b,d}						
			TAXA	Predicted Group Membership		Total
				CH	OA	
Modern Material	Original	Count	CH	33	2	35
			OA	1	27	28
		%	CH	94.3	5.7	100.0
			OA	3.6	96.4	100.0
	Cross-validated ^c	Count	CH	33	2	35
			OA	1	27	28
		%	CH	94.3	5.7	100.0
			OA	3.6	96.4	100.0
Flaxengate Material	Original	Count	CH	2	0	2
			OA	0	6	6
		%	CH	100.0	.0	100.0
			OA	.0	100.0	100.0
a. 95.2% of selected original grouped cases correctly classified.						

Classification Results ^{a,b,d}	
b. 100.0% of unselected original grouped cases correctly classified.	
d. 95.2% of selected cross-validated grouped cases correctly classified. Cross validation is done only for those cases in the analysis. In cross validation, each case is classified by the functions derived from all cases other than that case.	

Table 3.113 Results from the Discriminant Analysis when applied on the archaeological horncores (excluding measurements E and F).

Classification Results ^{a,b,d}						
			TAXA	Predicted Group Membership		Total
				CH	OA	
Modern Material	Original	Count	CH	25	10	35
			OA	2	26	28
		%	CH	71.4	28.6	100.0
			OA	7.1	92.9	100.0
	Cross-validated ^c	Count	CH	25	10	35
			OA	3	25	28
		%	CH	71.4	28.6	100.0
			OA	10.7	89.3	100.0
Flaxengate Material	Original	Count	CH	1	0	1
			OA	0	8	8
		%	CH	100.0	.0	100.0
			OA	.0	100.0	100.0
a. 81.0% of selected original grouped cases correctly classified.						
b. 100.0% of unselected original grouped cases correctly classified.						
d. 79.4% of selected cross-validated grouped cases correctly classified. Cross validation is done only for those cases in the analysis. In cross validation, each case is classified by the functions derived from all cases other than that case.						

Figure 3.213 shows the result when all variable are included. All archaeological specimens fall beyond the group centroid line of the attributed species, showing consistency with the morphological identifications. Figure 3.214 shows the results when measurements A and B were excluded. Despite the exclusion, the morphological identifications are confirmed by the DA: all goats fall close to the goat's group centroid line. Even when measurements E and F are excluded, no 'misattributions' are present, as attested by Figure 3.215.

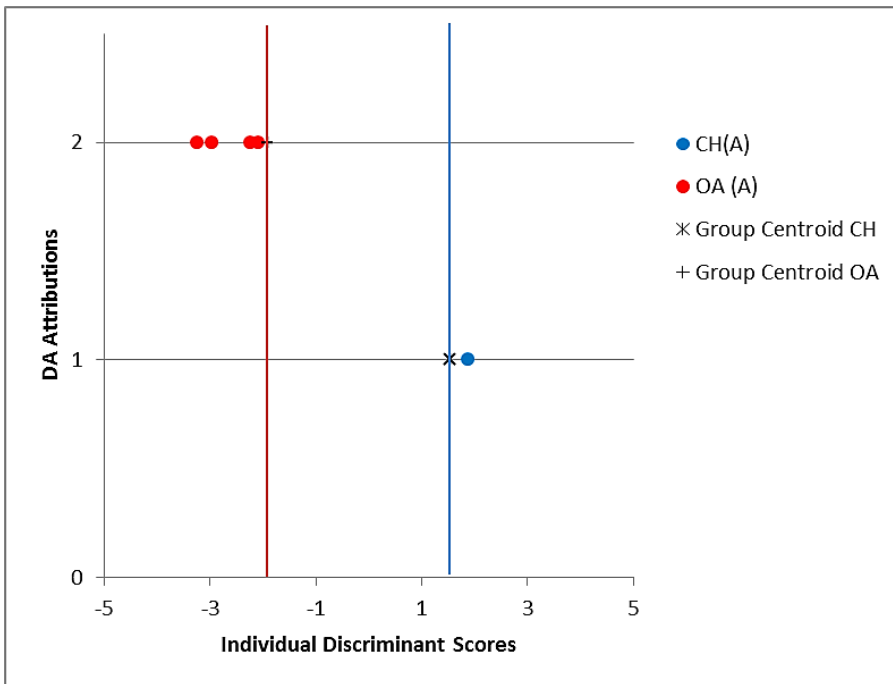


Figure 3.213 Diagram of the individual discriminant scores attributed to the modern and archaeological material by DA for the horncores.

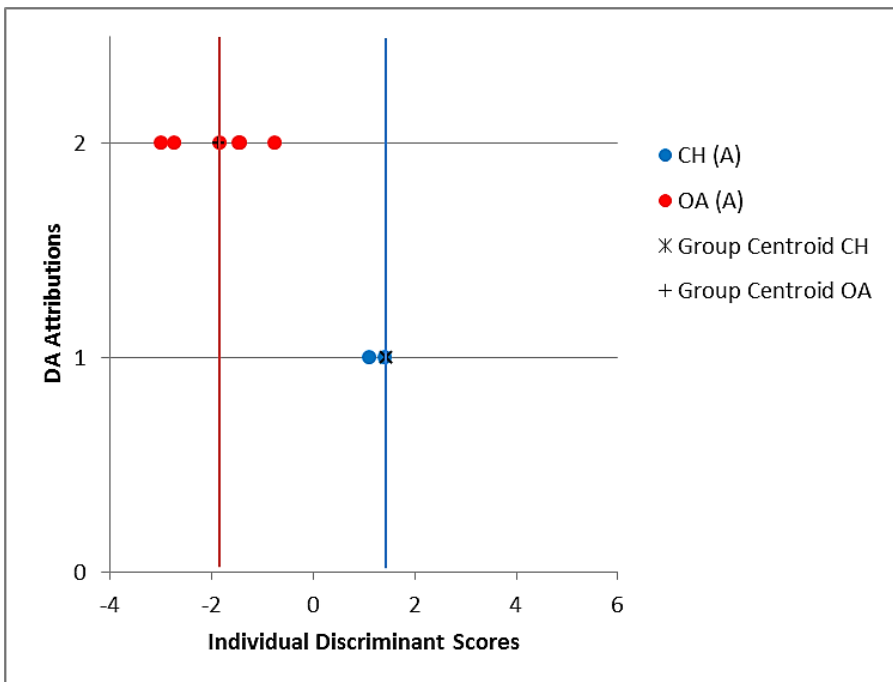


Figure 3.214 Diagram of the individual discriminant scores attributed to the modern and archaeological material by DA for the horncores (measurements A and B excluded).

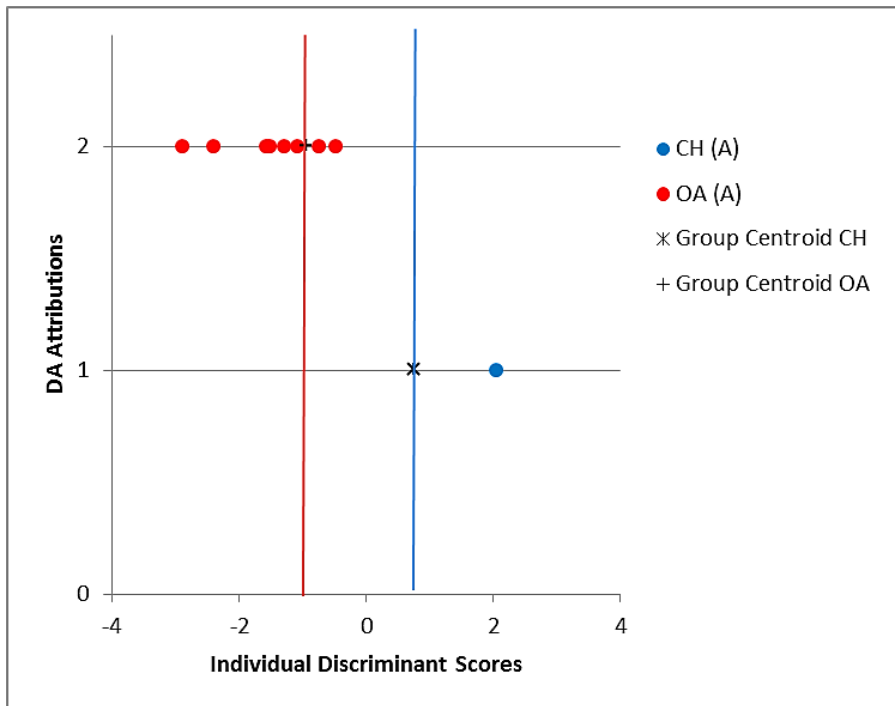


Figure 3.215 Diagram of the individual discriminant scores attributed to the modern and archaeological material by DA for the horncores (measurements E and F excluded).

Scapula

The percentage of correct reattributions is, for the scapula, 94.1%, a value which is higher than the results given by the modern material (86.4%). Two of the 34 originally identified archaeological sheep have been attributed to the goat species by DA. Of the unidentified specimens, one has been attributed to the goat species while the other six to sheep (Tab. 3.114).

Table 3.114 Results from the Discriminant Analysis when applied on the archaeological scapulae.

Classification Results ^{a,b,d}						
			TAXA	Predicted Group Membership		Total
				CH	OA	
Modern Material	Original	Count	CH	64	10	74
			OA	10	63	73
		%	CH	86.5	13.5	100.0
			OA	13.7	86.3	100.0
	Cross-validated ^c	Count	CH	61	13	74
			OA	12	61	73
		%	CH	82.4	17.6	100.0
			OA	16.4	83.6	100.0
Flaxengate Material	Original	Count	CH	0	0	0
			OA	2	32	34
			OC	1	6	7
		%	CH	.0	.0	100.0
			OA	5.9	94.1	100.0
			OC	14.3	85.7	100.0
a. 86.4% of selected original grouped cases correctly classified.						
b. 94.1% of unselected original grouped cases correctly classified.						
d. 83.0% of selected cross-validated grouped cases correctly classified. Cross validation is done only for those cases in the analysis. In cross validation, each case is classified by the functions derived from all cases other than that case.						

Figure 3.216 shows the position on the diagram of the specimens which have been reattributed. One of the two sheep, reattributed to goat, is equidistant from the two centroids and, as such, its reclassification cannot be trusted, especially considering the error that is inherent to the method. Conversely, the other sheep reattributed as goat and the unidentified specimen, fall very close to the goat group centroid line. Considering the intrinsic error of this method (higher than in the archaeological material) a reclassification of these specimens is doubtful. Of the two, however, the more likely goat is represented by the morphologically unidentified specimen, which plotted close to the goat range in Figures 3.149 and 3.150.

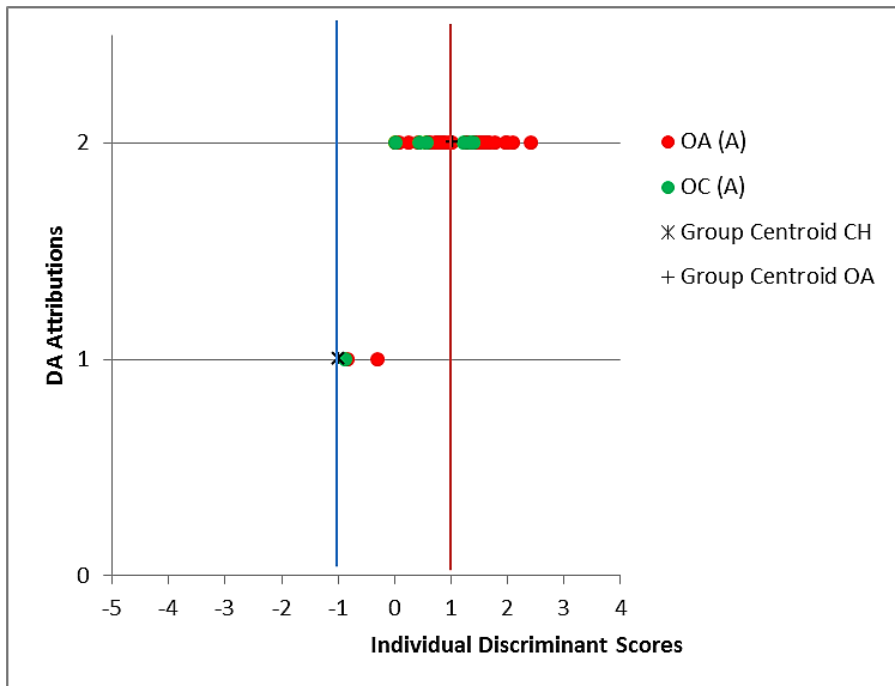


Figure 3.216 Diagram of the individual discriminant scores attributed to the modern and archaeological material by DA for the scapula.

Humerus

Table 3.115 shows the reattribution percentage for the humerus. The value obtained is higher (100%) than the results given by the modern material (88.4%). No goats have been identified morphologically and biometrically. The only unidentified specimen has been attributed to the *Ovis* group by DA.

Table 3.115 Results from the Discriminant Analysis when applied on the archaeological humeri.

Classification Results ^{a,b,d}						
			TAXA	Predicted Group Membership		Total
				CH	OA	
Modern Material	Original	Count	CH	67	9	76
			OA	8	62	70
		%	CH	88.2	11.8	100.0
			OA	11.4	88.6	100.0
	Cross-validated ^c	Count	CH	66	10	76
			OA	10	60	70
		%	CH	86.8	13.2	100.0
			OA	14.3	85.7	100.0
Flaxengate Material	Original	Count	CH	0	0	0
			OA	0	78	78
			OC	0	1	1
		%	CH	.0	.0	100.0
			OA	.0	100.0	100.0
			OC	.0	100.0	100.0

a. 88.4% of selected original grouped cases correctly classified.

b. 100.0% of unselected original grouped cases correctly classified.

d. 86.3% of selected cross-validated grouped cases correctly classified. Cross validation is done only for those cases in the analysis. In cross validation, each case is classified by the functions derived from all cases other than that case.

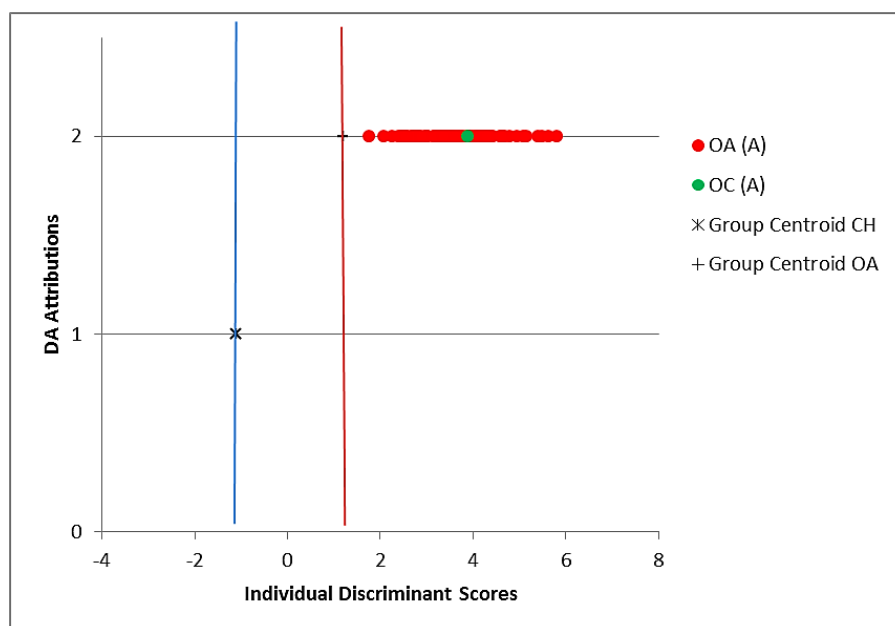


Figure 3.217 Diagram of the individual discriminant scores attributed to the modern and archaeological material by DA for humeri.

Figure 3.217 shows that all the archaeological sheep fall beyond the sheep group centroid line, following a very clear pattern. Undoubtedly, the unidentified specimen can be considered to belong to a sheep as it falls among the other sheep, well beyond the sheep group centroid line.

Radius

Table 3.116 shows the degree of consistency between the morphological and the biometrical identifications for the radius when all the measurements were included in the analysis. The percentage of correct reattributions is 100%, a value that is higher than the results provided by the modern material (93.5%). All the 12 specimens morphologically identified as sheep have been attributed to the sheep species by the DA.

Table 3.116 Results from the Discriminant Analysis when applied on the archaeological radii.

Classification Results ^{a,b,d}						
			TAXA	Predicted Group Membership		Total
				CH	OA	
Modern Material	Original	Count	CH	53	3	56
			OA	4	47	51
		%	CH	94.6	5.4	100.0
			OA	7.8	92.2	100.0
	Cross-validated ^c	Count	CH	53	3	56
			OA	4	47	51
		%	CH	94.6	5.4	100.0
			OA	7.8	92.2	100.0
Flaxengate Material	Original	Count	CH	0	0	0
			OA	0	12	12
		%	CH	.0	.0	100.0
			OA	.0	100.0	100.0
a. 93.5% of selected original grouped cases correctly classified.						
b. 100.0% of unselected original grouped cases correctly classified.						
d. 93.5% of selected cross-validated grouped cases correctly classified. Cross validation is done only for those cases in the analysis. In cross validation, each case is classified by the functions derived from all cases other than that case.						

Table 3.117 Results from the Discriminant Analysis when applied on the archaeological radii (measurements GL and SD excluded).

Classification Results ^{a,b,d}						
			TAXA	Predicted Group Membership		Total
				CH	OA	
Modern Material	Original	Count	CH	64	10	74
			OA	5	66	71
		%	CH	86.5	13.5	100.0
			OA	7.0	93.0	100.0
	Cross-validated ^c	Count	CH	63	11	74
			OA	6	65	71
		%	CH	85.1	14.9	100.0
			OA	8.5	91.5	100.0
Flaxengate Material	Original	Count	CH	0	0	0
			OA	7	82	89
			OC	1	1	2
		%	CH	.0	.0	100.0
			OA	7.9	92.1	100.0
			OC	50.0	50.0	100.0
a. 89.7% of selected original grouped cases correctly classified.						
b. 92.1% of unselected original grouped cases correctly classified.						
d. 88.3% of selected cross-validated grouped cases correctly classified. Cross validation is done only for those cases in the analysis. In cross validation, each case is classified by the functions derived from all cases other than that case.						

The percentage of correct reattributions decreases (92.1%) despite the increase of the sample size when variables SD and GL are excluded from the analysis (Tab. 3.117). Clearly the loss of information affects the diagnostic power of the DA. Seven of the 89 morphologically identified sheep have been considered goats from the DA. Of the two unidentified specimens, one has been attributed to the goat and the other one to the sheep group.

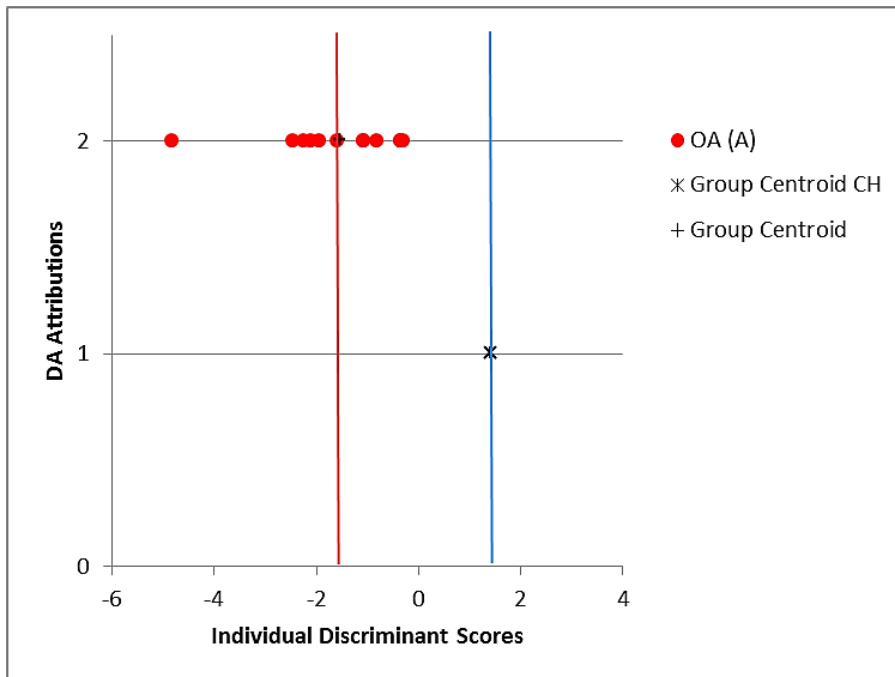


Figure 3.218 Diagram of the individual discriminant scores attributed to the modern and archaeological material by DA for the radius.

Figure 3.218 shows that when all the variables are included, the archaeological sheep fall beyond or very close to the sheep group centroid line, confirming their morphological identification.

Figure 3.219 shows where the DA ‘misidentified’ specimens fall on the graph. The seven sheep attributed to goat by the DA, fall, approximately, in line with other archaeological and biometrically identified sheep; considering the bias the method itself bears there is limited argument for their reclassification. One unidentified specimen is very consistent with the sheep group and can be considered as such, while the other unidentified specimen, which falls well beyond the goat group centroid line, may belong to a goat. This identification is confirmed by the BI (Fig. 3.178).

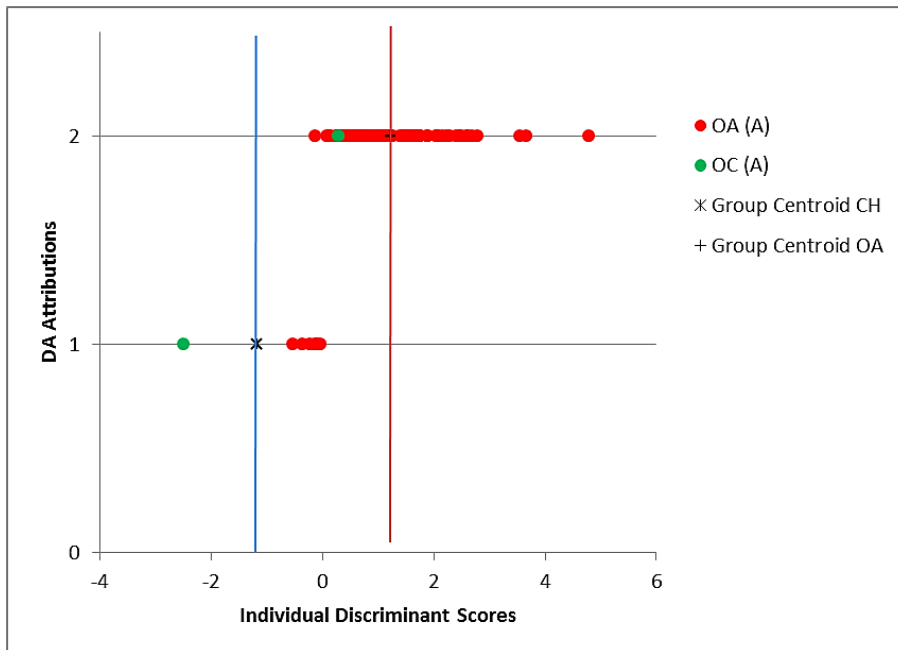


Figure 3.219 Diagram of the individual discriminant scores attributed to the modern and archaeological material by DA for the radius (measurements GL and SD excluded).

Ulna

Table 3.118 shows the percentage of reattributions when all the measurements taken on the ulna are included. The value given by the archaeological material is higher (100%) than the results provided by the modern material. All the morphological identifications have been confirmed by the DA. The only unidentified specimen present has been identified as sheep.

The exclusion of the variables B and L seems not to affect the discriminant power of the function as total agreement is present between morphological and biometrical identifications (Tab. 3.119). Both unidentified specimens have been attributed to sheep by the DA.

Table 3.118 Results from the Discriminant Analysis when applied on the archaeological ulnae.

Classification Results ^{a,b,d}						
			TAXA	Predicted Group Membership		Total
				CH	OA	
Modern Material	Original	Count	CH	53	3	56
			OA	5	52	57
		%	CH	94.6	5.4	100.0
			OA	8.8	91.2	100.0
	Cross-validated ^c	Count	CH	52	4	56
			OA	5	52	57
		%	CH	92.9	7.1	100.0
			OA	8.8	91.2	100.0
Flaxengate Material	Original	Count	CH	0	0	0
			OA	0	5	5
			OC	0	1	1
		%	CH	.0	.0	100.0
			OA	.0	100.0	100.0
			OC	.0	100.0	100.0

a. 92.9% of selected original grouped cases correctly classified.

b. 100.0% of unselected original grouped cases correctly classified.

d. 92.0% of selected cross-validated grouped cases correctly classified. Cross validation is done only for those cases in the analysis. In cross validation, each case is classified by the functions derived from all cases other than that case.

Table 3.119 Results from the Discriminant Analysis when applied on the archaeological ulnae (excluding measurements B and L).

Classification Results ^{a,b,d}						
			TAXA	Predicted Group Membership		Total
				CH	OA	
Modern Material	Original	Count	CH	52	4	56
			OA	5	52	57
		%	CH	92.9	7.1	100.0
			OA	8.8	91.2	100.0
	Cross-validated ^c	Count	CH	52	4	56
			OA	6	51	57
		%	CH	92.9	7.1	100.0
			OA	10.5	89.5	100.0
Flaxengate Material	Original	Count	CH	0	0	0
			OA	0	21	21
			OC	0	2	2
		%	CH	.0	.0	100.0
			OA	.0	100.0	100.0
			OC	.0	100.0	100.0

Classification Results ^{a,b,d}
a. 92.0% of selected original grouped cases correctly classified.
b. 100.0% of unselected original grouped cases correctly classified.
d. 91.2% of selected cross-validated grouped cases correctly classified. Cross validation is done only for those cases in the analysis. In cross validation, each case is classified by the functions derived from all cases other than that case.

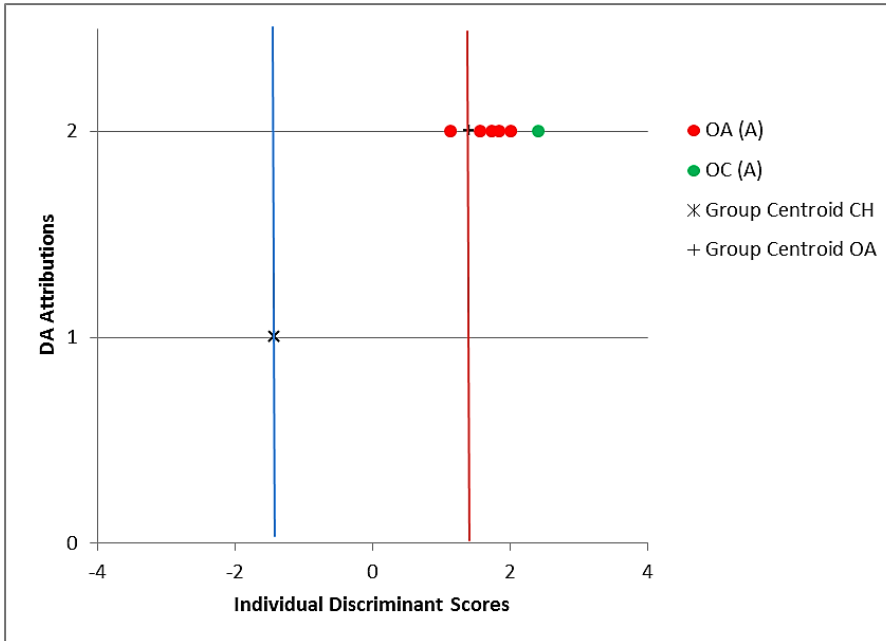


Figure 3.220 Diagram of the individual discriminant scores attributed to the modern and archaeological material by DA for the ulna.

Figure 3.220 shows that, when all measurements were included, all the morphologically identified sheep have been considered as such by the DA: they all fall very close or beyond the sheep group centroid. The unidentified specimen clearly follows the sheep pattern and as such has to be considered a sheep.

Figure 3.221 shows that with the increase of the sample size and the exclusion of some variables, the degree of consistency between the morphological and biometrical identification stays stable. All the morphologically identified sheep gather around the sheep group centroid line. The two unidentified specimens by and large follow the same pattern, though the specimen plotting at the far the left is more uncertain.

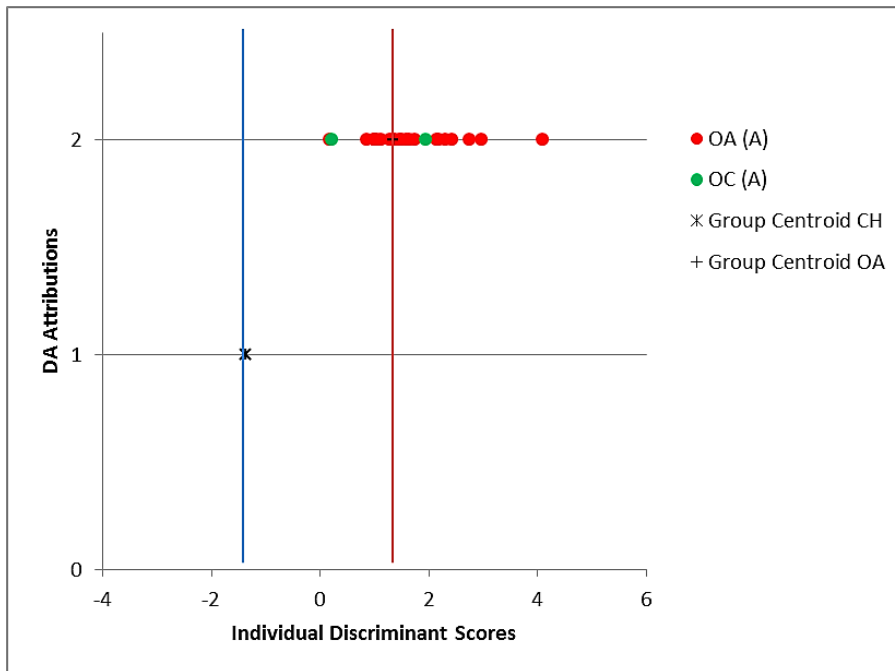


Figure 3.221 Scatterplot of the individual discriminant scores attributed to the modern and archaeological material by DA for the ulna (excluding measurements B and L).

Metacarpal

When all the measurements taken on the metacarpal could be used for the DA, the degree of consistency between the morphological and the biometrical identifications was total (100%). The value provided by the archaeological material is higher than the results provided by the modern (98.3%). Biometry and morphology agree on the absence of goat metacarpals (Tab. 3.120).

The percentage of correct reattributions decreases when measurements GL and SD are excluded from the DA (Tab. 3.121). The number of ‘misidentified’ cases increases: two of the 41 originally identified sheep were assigned to *Capra* by the DA. Both unidentified specimens were attributed to the sheep group.

Table 3.120 Results from the Discriminant Analysis when applied on the archaeological metacarpals.

Classification Results ^{a,b,d}						
			TAXA	Predicted Group Membership		Total
				CH	OA	
Modern Material	Original	Count	CH	56	2	58
			OA	0	61	61
		%	CH	96.6	3.4	100.0
			OA	.0	100.0	100.0
	Cross-validated ^c	Count	CH	55	3	58
			OA	0	61	61
		%	CH	94.8	5.2	100.0
			OA	.0	100.0	100.0
Flaxengate Material	Original	Count	CH	0	0	0
			OA	0	9	9
		%	CH	.0	.0	100.0
			OA	.0	100.0	100.0

a. 98.3% of selected original grouped cases correctly classified.

b. 100.0% of unselected original grouped cases correctly classified.

d. 97.5% of selected cross-validated grouped cases correctly classified. Cross validation is done only for those cases in the analysis. In cross validation, each case is classified by the functions derived from all cases other than that case.

Table 3.121 Results from the Discriminant Analysis when applied on the archaeological metacarpals (excluding measurements GL and SD).

Classification Results ^{a,b,d}						
			TAXA	Predicted Group Membership		Total
				CH	OA	
Modern Material	Original	Count	CH	56	2	58
			OA	1	60	61
		%	CH	96.6	3.4	100.0
			OA	1.6	98.4	100.0
	Cross-validated ^c	Count	CH	55	3	58
			OA	1	60	61
		%	CH	94.8	5.2	100.0
			OA	1.6	98.4	100.0
Flaxengate Material	Original	Count	CH	0	0	0
			OA	2	39	41
			OC	0	2	2
		%	CH	.0	.0	100.0
			OA	4.9	95.1	100.0
			OC	.0	100.0	100.0

a. 97.5% of selected original grouped cases correctly classified.

Classification Results ^{a,b,d}
b. 95.1% of unselected original grouped cases correctly classified.
d. 96.6% of selected cross-validated grouped cases correctly classified. Cross validation is done only for those cases in the analysis. In cross validation, each case is classified by the functions derived from all cases other than that case.

Figure 3.222 shows that when all the measurements were included, all the morphologically identified sheep fall very close or beyond the sheep group centroid line, confirming their identification.

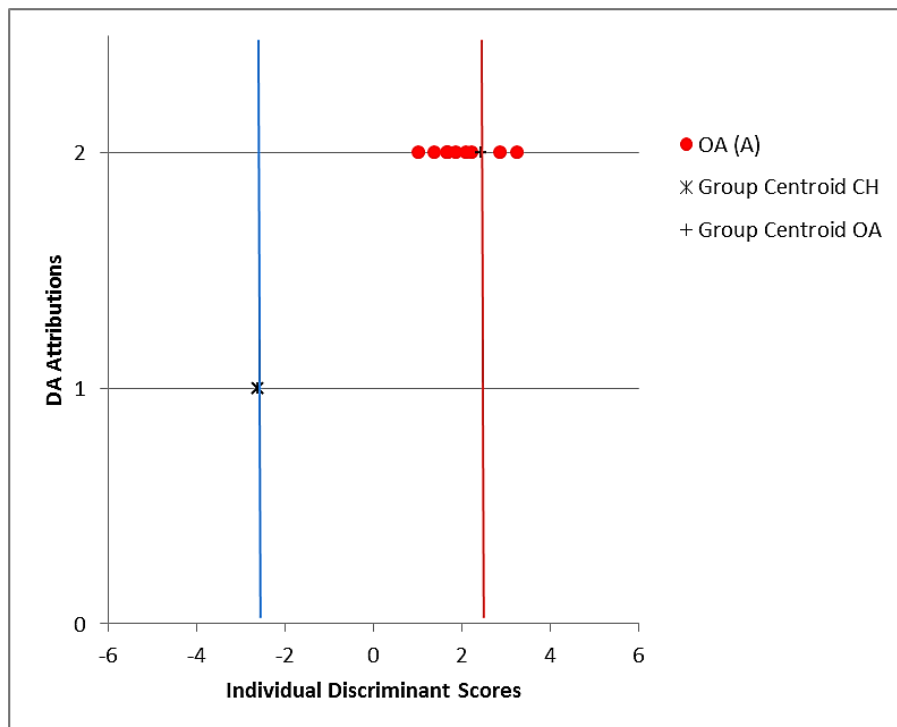


Figure 3.222 Diagram of the individual discriminant scores attributed to the modern and archaeological material by DA for the metacarpal.

Figure 3.223 shows where the DA 'misidentified' specimens fall when SD and GL were excluded from the DA. Considering that the originally identified sheep, attributed to the goat by the DA, are approximately equidistant from both the group centroid lines, that the exclusion of some variables affects the diagnostic power of DA, and that such 'misclassification' is not mirrored by the BI, there is a limited argument for their reclassification.

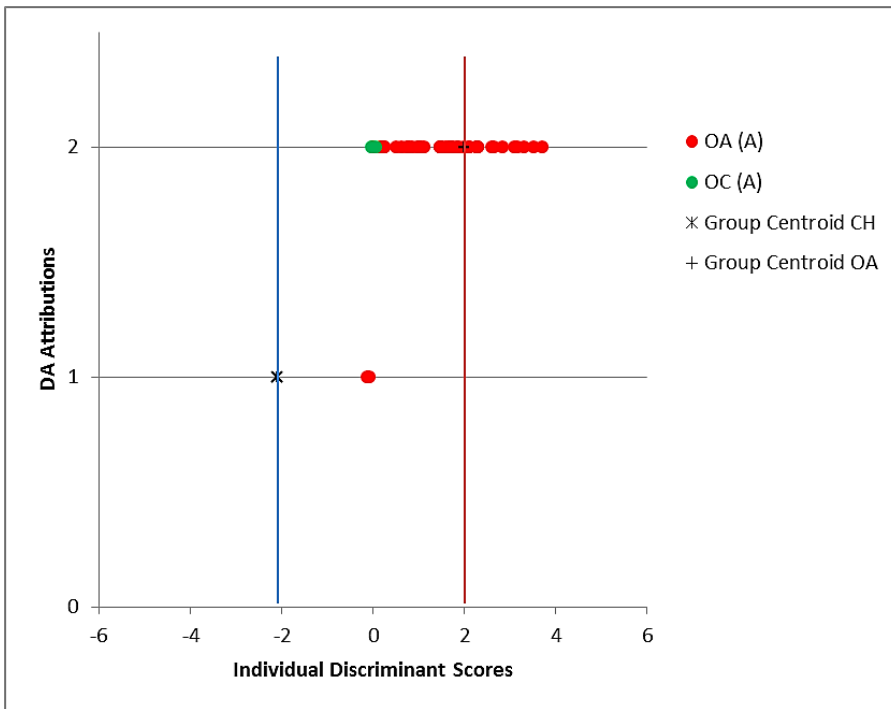


Figure 3.223 Diagram of the individual discriminant scores attributed to the modern and archaeological material by DA for the metacarpal (excluding measurements GL and SD).

Metatarsal

Complete agreement between morphological and biometrical identifications has been also achieved when all the measurements for the metatarsals were considered. Table 3.122 shows that all 15 originally identified sheep have been considered as such by the DA.

Despite the increase of the sample size, when the measurements SD and GL were excluded from the analysis the percentage of reattributions decreased significantly to 83.7% (Tab. 3.123). Clearly this exclusion had a considerable impact on the diagnostic power of the DA. Of 49 originally classified sheep, the DA has reattributed eight to the goat. The two unidentified specimens present have been identified as *Ovis*.

Table 3.122 Results from the Discriminant Analysis when applied on the archaeological metatarsals.

Classification Results ^{a,b,d}						
			TAXA	Predicted Group Membership		Total
				CH	OA	
Modern Material	Original	Count	CH	56	5	61
			OA	4	59	63
		%	CH	91.8	8.2	100.0
			OA	6.3	93.7	100.0
	Cross-validated ^c	Count	CH	54	7	61
			OA	4	59	63
		%	CH	88.5	11.5	100.0
			OA	6.3	93.7	100.0
Flaxengate Material	Original	Count	CH	0	0	0
			OA	0	15	15
		%	CH	.0	.0	100.0
			OA	.0	100.0	100.0

a. 92.7% of selected original grouped cases correctly classified.

b. 100.0% of unselected original grouped cases correctly classified.

d. 91.1% of selected cross-validated grouped cases correctly classified. Cross validation is done only for those cases in the analysis. In cross validation, each case is classified by the functions derived from all cases other than that case.

Table 3.123 Results from the Discriminant Analysis when applied on the archaeological metatarsals.

Classification Results ^{a,b,d}						
			TAXA	Predicted Group Membership		Total
				CH	OA	
Modern Material	Original	Count	CH	51	10	61
			OA	4	59	63
		%	CH	83.6	16.4	100.0
			OA	6.3	93.7	100.0
	Cross-validated ^c	Count	CH	49	12	61
			OA	6	57	63
		%	CH	80.3	19.7	100.0
			OA	9.5	90.5	100.0
Flaxengate Material	Original	Count	CH	0	0	0
			OA	8	41	49
			OC	0	2	2
		%	CH	.0	.0	100.0
			OA	16.3	83.7	100.0
			OC	.0	100.0	100.0

a. 88.7% of selected original grouped cases correctly classified.

b. 83.7% of unselected original grouped cases correctly classified.

Classification Results^{a,b,d}

d. 85.5% of selected cross-validated grouped cases correctly classified. Cross validation is done only for those cases in the analysis. In cross validation, each case is classified by the functions derived from all cases other than that case.

Figure 3.224 shows that all the morphologically identified sheep fall beyond the sheep group centroid, confirming their attribution.

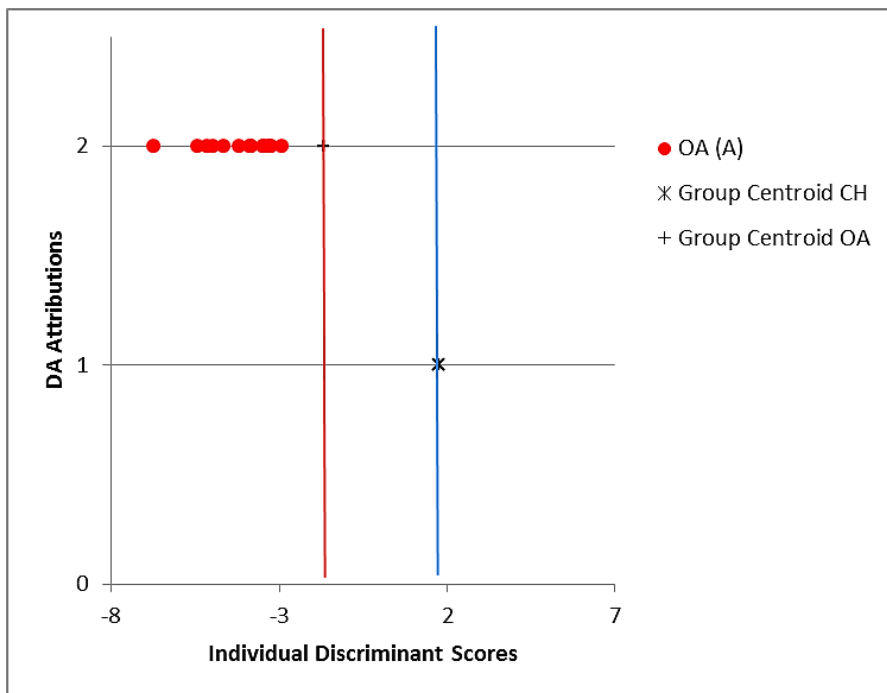


Figure 3.224 Diagram of the individual discriminant scores attributed to the modern and archaeological material by DA for the metatarsal.

Figure 3.225 shows were the 'misidentified' specimens by the DA plot. A number of sheep reidentified as 'goat' by the DA fall, by and large, equidistantly from the two group centroid lines, as such there is a limited argument for their misclassification, considering also the intrinsic bias the method has. Three sheep, reclassified as 'goat' by the DA, fall either very close or beyond the goat group centroid line; these may have been misidentified. Considering that this situation is not mirrored by the BI and that the loss of information caused by the exclusion of some variables affects heavily the DA power, there is a limited evidence for their misclassification. The two unidentified specimens clearly plot within the sheep range.

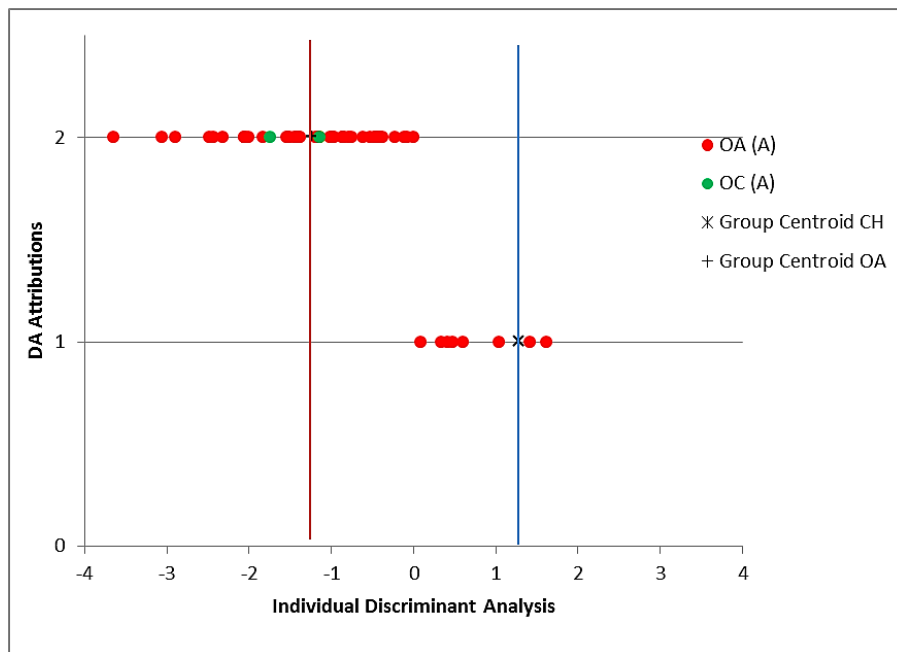


Figure 3.225 Diagram of the individual discriminant scores attributed to the modern and archaeological material by DA for the metatarsal (excluding measurements GL and SD).

Tibia

As no complete archaeological tibiae were recorded, DA was run excluding GL. The results are shown by Table 3.124. The percentage of correct reattributions is 83.8%; a higher value than the one obtained from the modern material (74.5%). 12 of the 74 morphologically identified sheep have been attributed to goat by DA. Of the 12 unidentified specimens, 10 were attributed to *Ovis* and two to *Capra*.

When GL and also SD were excluded from the analysis, the percentage of correct reattributions dropped slightly further to 82.1% (Tab. 3.125). The loss of information caused by the exclusions only marginally influenced the discriminant power of the function. A slightly higher proportion of ‘misclassified’ specimens are present: 20 of the 112 morphologically identified sheep have been considered as goat by the DA along with five of the 27 unidentified specimens. As the expectations are exceeded in the archaeological material, the reclassifications carried out by the DA are within the normal range of error for this method.

Table 3.124 Results from the Discriminant Analysis when applied on the archaeological tibiae (excluding measurement GL).

Classification Results ^{a,b,d}						
			TAXA	Predicted Group Membership		Total
				CH	OA	
Modern Material	Original	Count	CH	45	13	58
			OA	15	37	52
		%	CH	77.6	22.4	100.0
			OA	28.8	71.2	100.0
	Cross-validated ^c	Count	CH	44	14	58
			OA	16	36	52
		%	CH	75.9	24.1	100.0
			OA	30.8	69.2	100.0
Flaxengate Material	Original	Count	CH	0	0	0
			OA	12	62	74
			OC	2	10	12
		%	CH	.0	.0	100.0
			OA	16.2	83.8	100.0
			OC	16.7	83.3	100.0
a. 74.5% of selected original grouped cases correctly classified.						
b. 83.8% of unselected original grouped cases correctly classified.						
d. 72.7% of selected cross-validated grouped cases correctly classified. Cross validation is done only for those cases in the analysis. In cross validation, each case is classified by the functions derived from all cases other than that case.						

Table 3.125 Results from the Discriminant Analysis when applied on the archaeological tibiae (excluding measurement GL and SD).

Classification Results ^{a,b,d}						
			TAXA	Predicted Group Membership		Total
				CH	OA	
Modern Material	Original	Count	CH	42	16	58
			OA	15	37	52
		%	CH	72.4	27.6	100.0
			OA	28.8	71.2	100.0
	Cross-validated ^c	Count	CH	41	17	58
			OA	16	36	52
		%	CH	70.7	29.3	100.0
			OA	30.8	69.2	100.0
Flaxengate Material	Original	Count	CH	0	0	0
			OA	20	92	112
			OC	5	22	27
		%	CH	.0	.0	100.0
			OA	17.9	82.1	100.0

Classification Results ^{a,b,d}						
			OC	18.5	81.5	100.0
a. 71.8% of selected original grouped cases correctly classified.						
b. 82.1% of unselected original grouped cases correctly classified.						
d. 70.0% of selected cross-validated grouped cases correctly classified. Cross validation is done only for those cases in the analysis. In cross validation, each case is classified by the functions derived from all cases other than that case.						

Figure 3.226 shows the results obtained when all measurements, apart from GL, were used. Some of the ‘misidentified’ sheep fall equidistantly from the two group centroid lines, as such there is no strong evidence for them to be reclassified as goats. Although some specimens fall beyond the goat group centroid line, they are in continuity with the other specimens and considering the inherent error of the method, cannot be confidently reclassified. Such reclassification would also not be consistent with the results of the BI (Figs. 3.163; 3.186 and 3.205). Concerning the morphologically unidentified specimens, apart from the one plotting at the far left clearly in the sheep range, the others cannot be confidently identified due to the degree of error of the method and the area of the diagram where they plot.

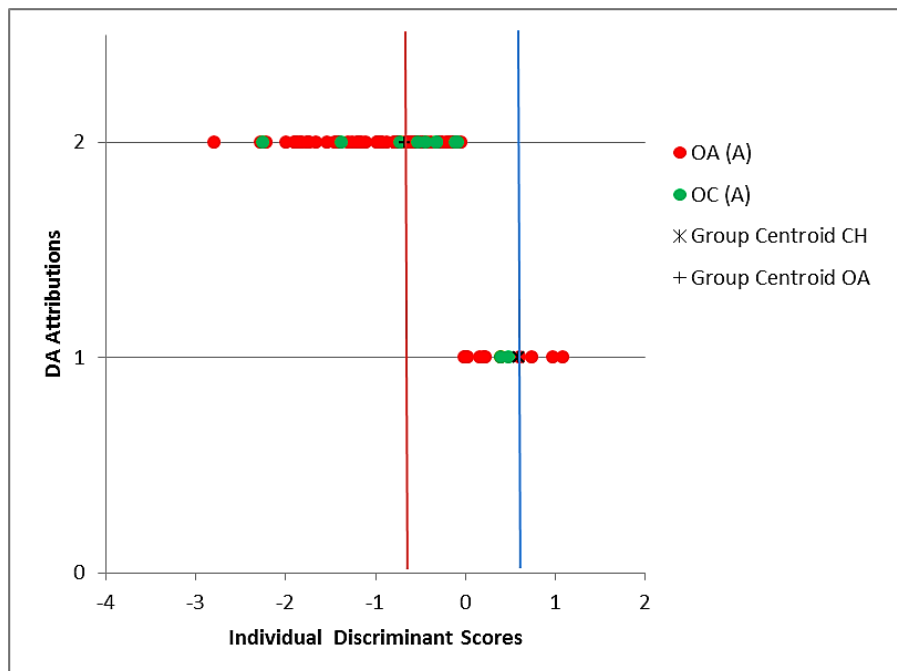


Figure 3.226 Diagram of the individual discriminant scores attributed to the modern and archaeological material by DA for the tibia (excluding measurement GL).

Figure 3.227 shows the specimens that have been ‘reclassified’ by the DA, when some measurements are dropped. For reasons similar to those discussed above, such reclassification cannot be relied on.

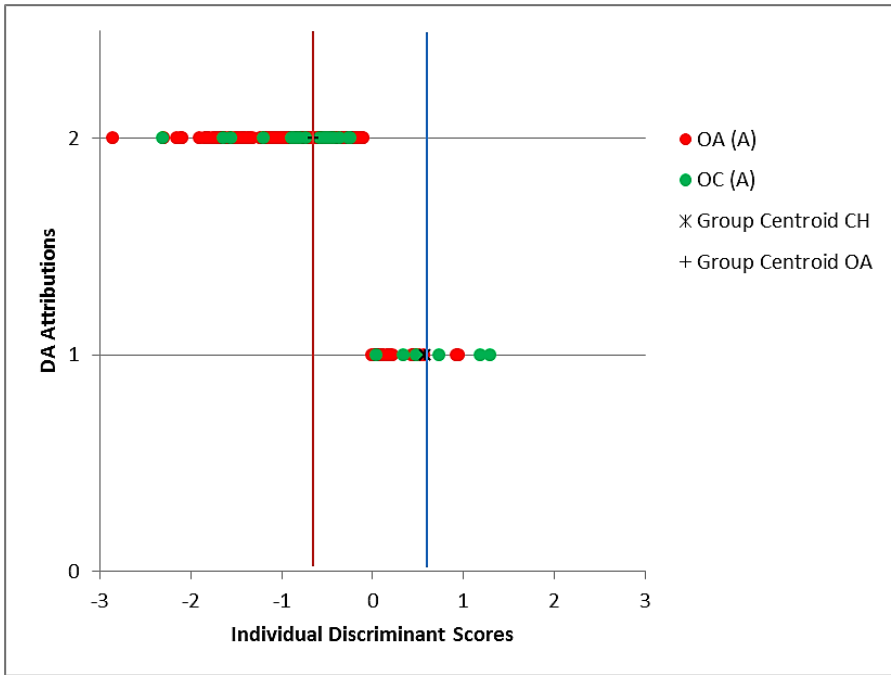


Figure 3.227 Diagram of the individual discriminant scores attributed to the modern and archaeological material by DA for the tibia (excluding measurements GL and SD).

Astragalus

Table 3.126 shows the results when DA was run on the astragalus. The percentage of correct reattributions is 90.5%, a value higher than the results provided by the modern material (89%). Of the 42 morphologically identified sheep astragali, four have been reattributed to *Capra* by DA.

Table 3.126 Results from the Discriminant Analysis when applied on the archaeological astragali.

Classification Results ^{a,b,d}						
			TAXA	Predicted Group Membership		Total
				CH	OA	
Modern Material	Original	Count	CH	65	7	72
			OA	9	64	73
		%	CH	90.3	9.7	100.0
			OA	12.3	87.7	100.0
	Cross-validated ^c	Count	CH	64	8	72
			OA	11	62	73
		%	CH	88.9	11.1	100.0
			OA	15.1	84.9	100.0
Flaxengate Material	Original	Count	CH	0	0	0
			OA	4	38	42
		%	CH	.0	.0	100.0
			OA	9.5	90.5	100.0
a. 89.0% of selected original grouped cases correctly classified.						
b. 90.5% of unselected original grouped cases correctly classified.						
d. 86.9% of selected cross-validated grouped cases correctly classified. Cross validation is done only for those cases in the analysis. In cross validation, each case is classified by the functions derived from all cases other than that case.						

Figure 3.228 shows the degree of consistency between morphological and biometrical identifications. Three sheep ‘misclassified’ as goat by the DA are by and large, equidistant from the two group centroid lines. Considering their position on the graph and that the DA bears a bias itself, there is limited argument to consider their reattribution. The sheep falling on the goat group centroid lines, on the other hand, may indeed be a *Capra*, also considering the gap existing between this specimen and the rest of the distribution. However, its reclassification is not supported by the BI (Figs. 3.164 to 3.167; 3.187; 3.206 to 3.209) and, as such, this specimen must be regarded to be on uncertain identification.

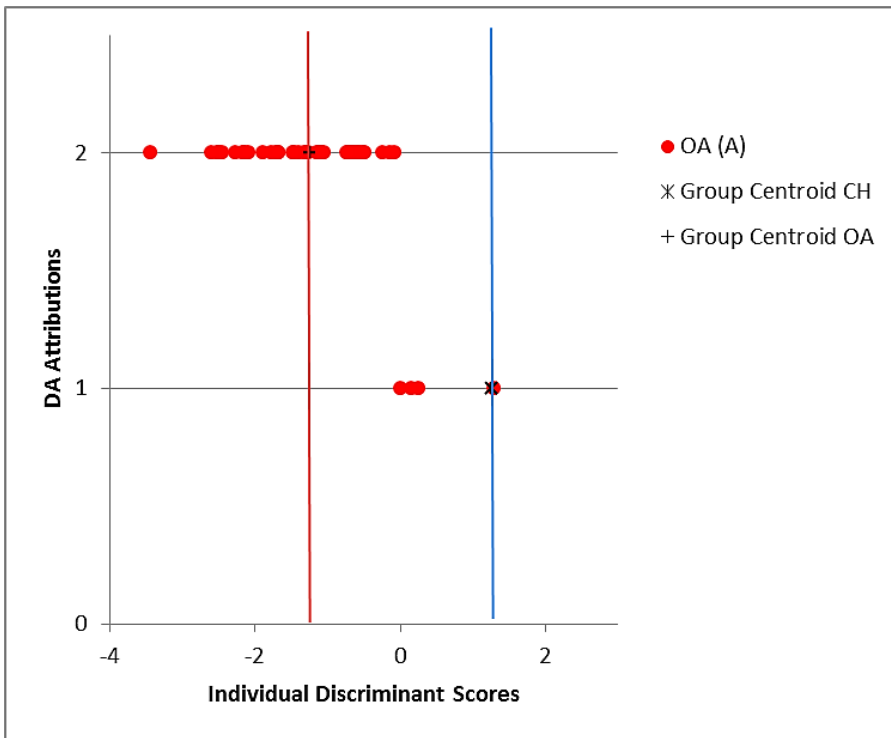


Figure 3.228 Diagram of the individual discriminant scores attributed to the modern and archaeological material by DA for the astragalus.

Calcaneum

The percentage of correct reattributions is, for the archaeological calcanea, 97.1%, a higher value than the outcome obtained from the modern material (95.1%). Only one of the 34 morphologically identified sheep has been attributed to goat by the DA. Of the two sheep/goat specimens one was classified as sheep and the other as goat (Tab. 3.127).

Table 3.127 Results from the Discriminant Analysis when applied on the archaeological calcanea.

Classification Results ^{a,b,d}						
			TAXA	Predicted Group Membership		Total
				CH	OA	
Modern Material	Original	Count	CH	55	5	60
			OA	1	61	62
		%	CH	91.7	8.3	100.0
			OA	1.6	98.4	100.0
	Cross-validated ^c	Count	CH	55	5	60
			OA	1	61	62
		%	CH	91.7	8.3	100.0
			OA	1.6	98.4	100.0
Flaxengate Material	Original	Count	CH	0	0	0
			OA	1	33	34
			OC	1	1	2
		%	CH	.0	.0	100.0
			OA	2.9	97.1	100.0
			OC	50.0	50.0	100.0
a. 95.1% of selected original grouped cases correctly classified.						
b. 97.1% of unselected original grouped cases correctly classified.						
d. 95.1% of selected cross-validated grouped cases correctly classified. Cross validation is done only for those cases in the analysis. In cross validation, each case is classified by the functions derived from all cases other than that case.						

Figure 3.229 shows that the two specimens which have been identified as ‘goat’ by the DA fall equidistantly from the two group centroid lines. Considering that the method bears an intrinsic bias, that these specimens fall equidistantly from the two group centroid lines and that no particularly suspicious specimens have been found with the study of the BI (Figs. 3.168 to 3.170; 3.188 to 3.190; 3.210 to 3.212), there is little evidence for considering their reclassification as goats.

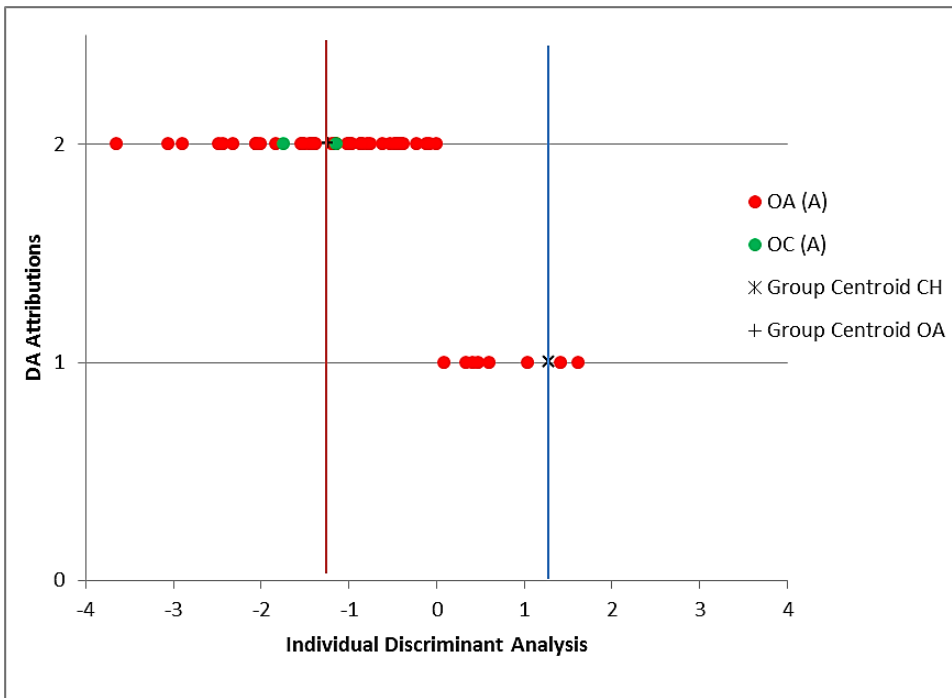


Figure 3.229 Diagram of the individual discriminant scores attributed to the modern and archaeological material by DA for the calcaneum.

3rd Phalanx

The problem of multicollinearity noticed when DA was run on the modern specimens' 3rd phalanges, prevented the use of the statistical tool on the archaeological 3rd phalanges.

3.3.8 Discussion

The analysis of the sheep/goat assemblage from Flaxengate confirms and reinforces previous observations about the new methodology. Table 3.128 shows that almost all the anatomical elements considered have provided high percentages of consistent attributions (>80%) following the pattern of the modern material. As also seen in the case of King's Lynn, most elements exceeded expectations in terms of consistency with the morphological identifications, and on the basis of the terms of reference provided by the modern material; this confirms the greater morphotype homogeneity of the archaeological material. The only two elements for which the percentage of consistent reattributions did not meet the expectations are the metapodials but only when some variables (GL and SD) were excluded from the analysis. The case study of Flaxengate confirms that the diagnostic power of the function decreases when variables are left out from DA analysis.

Unlike King's Lynn, the radius and the tibia have provided high reattribution rates at Flaxengate. This can perhaps be explained by the larger sample size. However, this may be due to the fact that the sheep/goat kill-off pattern for Flaxengate is different from King's Lynn. As the sheep/goat animal bone assemblage included in this analysis comes mainly from the period *c.*1040-1100, when, according to O'Connor (1982), the kill-off pattern included two peaks - one when the animals were 1 or 2 years old and the other when they were 3 or more years old (phase T VII) - it seems that this combination fits better the age-ratio of the modern sample compared to the older animals present at King's Lynn (Noodle 1977); thus better results have been obtained.

In evaluating the results from the DA, it is essential to bear in mind that the same guidelines, as previously outlined for King's Lynn (Section 3.2.10), have been adopted. As seen with the previous case study, the DA bears an intrinsic error: consequently, it is likely that some misidentified archaeological specimens were such because of the bias the method bears. Thus, the best results from this tool can be reached when used in combination with the morphological approach and the BI, as this combination allows having as much information as possible about the specimens.

Table 3.128 Percentages of correct reattributions for the modern material and for the archaeological material (whole assemblage) provided by the DA. An asterisk mark small sample sizes (less than 10 specimens).

Anatomical Element	DA % of total correct reattributionattributions Modern Material	DA % of total correct Attributions On the archaeological material
Hc	95.2%	100%*
Hc (no A and B)	95.2%	100%*
Hc (no E and F)	81%	100%*
Sc	86.4%	94.1%
Hu	88.4%	100%
Ra	93.5%	100%
Ra (no GL and SD)	89.7%	92.1%
Ul	92.2%	100%*
Ul (no B and L)	92%	100%
Mc	98.3%	100%*
Mc (no GL and SD)	97.5%	95.1%
Mt	92.7%	100%
Mt (no GL and SD)	88.7%	83.7%
Ti (no GL)	74.5%	83.8%
Ti (no GL and SD)	71.8%	82.3%
Astragalus	89%	90.5%
Calcaneum	95.1%	97.1%

3.3.8.1 An assessment of the new methodology

Table 3.129 shows the results when the outcome from the DA is compared and integrated with the results from the other approaches.

The degree of agreement between the different approaches adopted is even more satisfactory than for King's Lynn. The morphological identifications are very frequently confirmed by the results of the BI and also by the outcomes of the DA. No specimens that had been morphologically identified as sheep have been found to be biometrically consistent with the goat group (from both the BI and DA). Among the morphologically unidentified specimens, only one could unambiguously be identified biometrically as a goat (radius).

The already mentioned potential of the biometry-based methods (BI and DA) has been confirmed and reinforced by the case study of Flaxengate. Indeed this tool can be used to confirm or reject the identifications assessed through the morphological study, to assign to species level the morphologically unidentified specimens and finally, to provide a visual and more objective way to assess identifications. It must, however, be emphasised that, due to biological variability, a degree of uncertain will inevitably affect the classification of some specimens.

Table 3.129 Summary table of the results obtained from the morphological approach and the biometrical approach in the form of both Biometrical Indices (BI) and Discriminant Analysis (DA), when the sheep/goat assemblage from Flaxengate was considered *in toto*. The specimens considered as ‘misclassified’ are those which, as they fall on or beyond the group centroid line of the opposite species, are more likely to represent a morphological misclassification. The expectations are based on the results provided by the modern material; if the archaeological material has given a higher percentage of consistent attributions than the modern, the expectations are exceeded.

				Biometrical Approach					
Morphological Approach				Biometrical indices (BI)	Discriminant Analysis (DA)				
Anatomical element	<i>Ovis aries</i>	<i>Capra hircus</i>	<i>Ovis/ Capra</i>		Modern material DA%	Flaxengate DA%	Identified <i>Ovis/ Capra</i>	‘Misclassified’	Comments
Horncore	31	3	-	All goats plot among the goat group. No other specimens plotting clearly among the goat group are present.	95.2%	100%	-	-	Expectations are exceeded.
Jaw	95	-	36	-	-	-	-	-	N.A.
Teeth	29	-	28	-	-	-	-	-	N.A.
Scapula	49	-	21	No specimens plotting clearly among the goat group are present. The unidentified specimens fall in the area of overlap or among the sheep group.	86.4%	94.1%	One might be a goat.	No strong evidence to argue against the morphological id. of the other specimens.	Expectations are exceeded.
Humerus	111	-	6	No specimens plotting clearly among the goat group are present. The unidentified specimens fall in the area of overlap or among the sheep group.	88.4%	100%	One has been identified as sheep.	-	Expectations are exceeded.
Radius	89	-	2	One unidentified specimen falls among the goat group so has to be considered a goat. No specimens plotting	93.5%	100%	-	-	Expectations are exceeded. The exclusion of

		Biometrical Approach							
		Morphological Approach		Biometrical indices (BI)	Discriminant Analysis (DA)				
Anatomical element	<i>Ovis aries</i>	<i>Capra hircus</i>	<i>Ovis/ Capra</i>		Modern material DA%	Flaxengate DA%	Identified <i>Ovis/ Capra</i>	‘Misclassified’	Comments
				clearly among the goat group are present. The other unidentified specimen fall in the area of overlap.					measurements SD and GL has an impact on the DA power.
Ulna	31	-	4	No specimens plotting clearly among the goat group are present. The only unidentified specimen falls among other archaeological sheep.	92.9%	100%	One has been identified as sheep.		Expectations are exceeded.
Metacarpal	44	-	3	No specimens plotting clearly among the goat group are present. Two unidentified specimens plot more toward the goat group but they are still compatible with the range of variation of the sheep group. No other specimens plotting clearly among the goat group are present.	98.3%	100%	-	-	Expectations are exceeded. The exclusion of the variables SD and GL has an impact on the DA power.
Metatarsal	53	-	3	No specimens plotting clearly among the goat group are present. The unidentified specimens fall in the area of overlap or follow more the sheep pattern than the goat pattern.	92.7%	100%	-	-	Expectations are exceeded. The exclusion of the variables SD and GL has an impact on the DA power.
Metapodials	10	-	2	-	-	-	-	-	N.A.
Tibia	116	-	30	No specimens plotting clearly among the goat group are present. The unidentified specimens fall in the area of overlap or among the sheep group.	89.1%	83.8%	One has been identified as sheep.	No strong evidence to argue against the morphological id. of the other specimens.	Expectations are exceeded. The exclusion of the variables SD and GL has an impact on the DA power.

		Biometrical Approach							
		Morphological Approach			Biometrical indices (BI)	Discriminant Analysis (DA)			
Anatomical element	<i>Ovis aries</i>	<i>Capra hircus</i>	<i>Ovis/ Capra</i>		Modern material DA%	Flaxengate DA%	Identified <i>Ovis/ Capra</i>	‘Misclassified’	Comments
Astragalus	49	-	2	No specimens plotting clearly among the goat group are present. The unidentified specimens fall in the area of overlap.	89%	90.5%	-	No strong evidence to argue against the morphological id. of the other specimens.	Expectations are exceeded.
Calcaneum	36	-	3	No specimens plotting clearly among the goat group are present. The unidentified specimens fall in the area of overlap or more toward the goat group but still compatible with the range of variation of the sheep group.	95.1%	97.1%	-	No strong evidence to argue against the morphological id. of the other specimens.	Expectations are exceeded.
1st Phalanx	90	-	9	-			-	-	N.A.
2nd Phalanx	14	-	-	-			-	-	N.A.
3rd Phalanx	3	-	-	No specimens plotting clearly among the goat group are present.			-	-	N.A.
Total Identified Specimens	850	3	149				-	-	N.A.

3.3.8.2 The Flaxengate case study

The re-examination of part of the sheep/goat bone assemblage from medieval Flaxengate has confirmed what previously seen by O'Connor (1982) but it has also added some useful information.

Goat specimens, despite not being mentioned in O'Connor's report, were present in the assemblage, but in such small numbers that the choice made by O'Connor to regard the whole 'sheep-goat' group as 'sheep' is broadly justified. Unlike King's Lynn there is no concentration of goat horncores at Flaxengate, therefore indicating the absence of any specific industry or trade associated with this species. The occurrence of the three horncores may be consistent with the occurrence of a few postcranial goat bones (one certain and a few other possible), suggesting a very small contribution of this species to household provision.

3.4. Woolmonger /Kingswell Street, Northampton (c. 1000-1550 AD)

3.4.1 Introduction

Northampton lies in a central position in central-eastern England and it has always played an important strategic role. It is at the crossroad of important routes and productive agricultural areas and has had a significant role for the surrounding countryside since prehistoric times. The presence of an Iron Age village and a Roman settlement, perhaps of military nature, has been recorded in the Nene Valley. Less striking is the evidence attesting Anglo-Saxon presence at Northampton but, since pagan Saxon cemeteries and settlement sites have been discovered all around the town, an Anglo-Saxon centre may well have been present. In the area of St. Peter Church, archaeological evidence dating to the middle Saxon period (c. 650-850) has recently been found and it attests to the occurrence of a well-established settlement dated to the 8th century, perhaps an ecclesiastical/provincial administrative centre. This is considered to have been the focus for the further growth that occurred subsequently (Brown 2008; Williams 1979).

From c. 900 the number of written resources mentioning the town increases, indicating the existence of a centre under Danish administration and legislation. Unfortunately, no compelling archaeological evidence has been found to corroborate the written accounts. The position of Northampton seems to consolidate after 1066 with a series of marriages of the Earls of the city, which eventually led the city to be under royal control by the end of the 10th century/beginning of the 11th century (Brown 2008; Williams 1979). This period, which also sees the addition of a defensive circuit, is dominated by further development and general prosperity (Brown 2008).

While in the 9th century Northampton did not seem to have been intensive populated, as only a few timber buildings have been discovered, the following century was marked by the construction of cellar buildings, successively demolished and replaced by timber halls, testifying increased activity (Brown 2008). In the second half of the 12th century Northampton is mentioned as the sixth most prosperous town in the kingdom with an economy which may have been based on cloth production. The 12th and 13th centuries are characterised by a series of important events that coincide with the start of the ascent of the city (Brown 2008; Williams 1979): Northampton becomes a seat of parliament under Henry I (1100-1135), the Royal Castle is built during the reign of Henry II (middle 12th century) and an intensive reconstruction in stone of many buildings was undertaken (Brown 2008).

The 13th century is characterised by pressure for land and the emergence of Northampton as a strategic city (Brown 2008). Decline becomes evident by the 14th century, but perhaps had its origins earlier. Historical evidence suggests that the town during the 14th century was in decay, with some areas of the city experiencing poor conditions. The situation was made worse by the fire that in 1516 burnt most parts of the city: Northampton at this point had already degraded to

the level of county town (Williams 1979). Archaeological data confirm the state of decay, attesting a lack of occupation and urban regeneration until the 17th century (Brown 2008).

3.4.2 Archaeological Investigations

The first archaeological interest in Northampton occurred in the years 1972-1974, when a few trenches and a longer excavation was conducted to investigate the history of Northampton from Saxon to Late medieval period. In the years between 1981 and 1987, further investigations were conducted in different areas of Northampton in order to explore the Saxon occupation and the location of the Late Saxon town defences (Williams 1979).

In 1994, a series of new trenches (Trench 1, 2, 3 and 4) located in different areas of the site chosen according to their archaeological potential, were dug in order to better assess the condition of the surviving uncovered remains. These were followed by a second phase of trial trenches on the northern frontage of Woolmonger Street (Trench 10 and 11) and other excavations' trials. The results from these preliminary investigations, permitted the identification of three areas for full archaeological excavation: Trench 12 (extension of Trench 11, north side), Trench 13-15-16 (extension of Trench 1, north side) and Trench 14 (south part of Woolmonger Street). The investigations on the north side revealed five chronological phases dating from the Early Middle Saxon period to the Post medieval period while the investigation of the south side revealed a less precise chronology (Brown 2008; Soden 1998-1999).

In 2005, a new excavation was commissioned to Northampton Archaeology. The new fieldwork was focused on an individual area of the site identified as having the potential to throw light on the process of development of the town in the medieval period: the corner between Woolmonger Street and Kingswell Street (Fig. 3.230). The same chronological phases identified during the previous excavations were confirmed (Brown 2008).

Table 3.130 shows the chronology of the site established after the excavations conducted in 1994-1997 and 2005; from which the material of this study derives. A very brief description of the archaeological evidence unearthed is also provided.

Table 3.130 Chronology of the site with a brief description of the main features found (following Brown 2008 and Soden 1998-1999).

NORTH SIDE: EASTERN PLOTS			
Phases	Chronology	Features	
Phase 1	Early Middle Saxon period	Findings suggest a domestic occupation of 6 th century.	
Phase 2a	Late Saxon, Trenches 11 and 12	Post holes and rubbish pits	
Phase 2b	Late Saxon and Early medieval	Clustered features suggest that domestic activities as well as agricultural processes were carried out	
Phase 3	Late medieval	Timber structure is replaced by a stone building, erected during the 2 nd half of the 13 th century. The end of these structures seems to be dated to the 2 nd half of the 15 th century. The complexes have been interpreted as kitchen or malt-house. An architectural fragment found in a pit of the later phase 4 seems to point toward, if it belonged to this building, to a high status building.	
Phase 4 and 5	Post medieval	The stone building was demolished. During the late 18 th to 19 th century, warehouses were built. Nothing is known about what happened between the demolition of the late 15 th century stone building and the erection of the warehouses.	
NORTH SIDE: WESTERN PLOTS			
Phase 1	Early/Middle Saxon	no features were found	
Phase 2	sub-Phase 2a; Late Saxon	Three cellars were found, one revealed that an intense fire occurred	
	sub-Phase 2b; Late Saxon- Early medieval	New timber buildings were erected once the ground was prepared. Apparently these contained two areas of food preparation.	
Phase 3	Later medieval	In the 13 th century the timber building were replaced with stone buildings.	
Phase 4-5	Post medieval	Successively iron-stone rubble-built cellars were constructed	
SOUTH SIDE			
Phase 2a	Late Saxon		
Phase 2b	Early medieval	structural remains of a building	
Phase 3	Late medieval	retaining walls have been found	
CORNER OF KINGSWELL STREET AND WOOLMONGER STREET			
Excavation 2005	Phase 1 (LS4)	Late Saxon	Cellared building and pits
	Phase 2 (Ph0)	Saxon-Norman	Gullies and a timber building
	Phase 3 (Ph1; Ph2/0; Ph 2/2)	medieval	Stone buildings, pits, malting and bread ovens
	Phase 4 (Ph4)	Post-medieval	Late occupation of building in Kingswell Street, pits and wells
	Phase 5 (Ph5)	Late-Post medieval and Modern	Ground disturbance. Wells, cellars, walls and cess pits were found

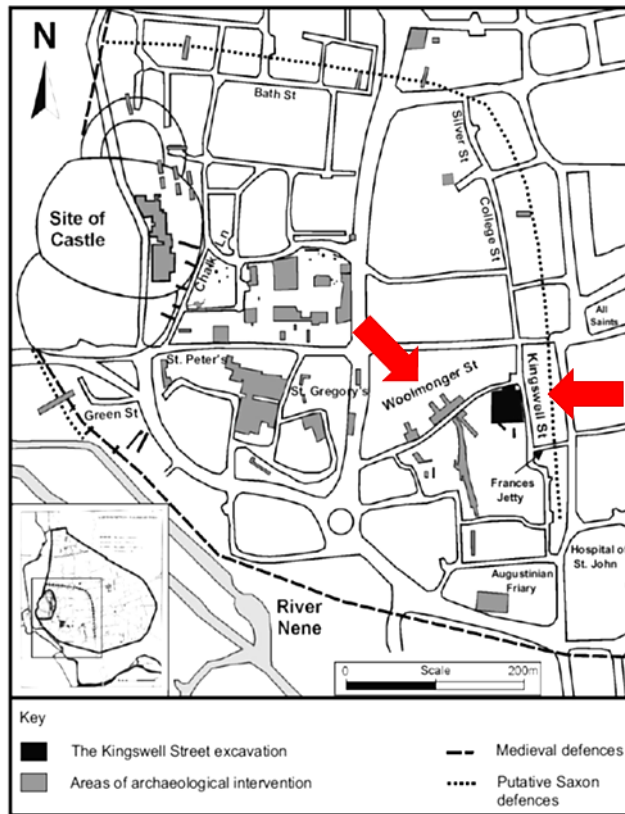


Figure 3.230 Location of the sites and of minor fieldworks (Brown 2008). Red arrows indicate the areas where 1994-1997 (left) and 2005 (right) excavations occurred (image reprinted from BROWN, J. Excavations at the corner of Kingswell Street and Woolmonger Street, Northampton. *Northamptonshire Archaeology* 35: 173-214, copyright 2008, with permission from Northamptonshire Archaeology, now MOLA Northampton).

To increase sample size the two assemblages from 1994-1997 and 2005 were combined. Again, to avoid having to deal with very small samples, the material was combined into three main phases (Tab. 3.131).

Table 3.131 Chronological phases used in this study.

New Chronological Phases	Campaign 1995	Campaign 2005	Chronology
Phase I	Sub-phase 2a	LS4	Late Saxon (AD 1000-1100)
Phase II	Sub-phase 2b	Ph0, Ph1, Ph2/0, Ph2/2	Saxon-Norman/Early and High medieval period (AD 1100-1400)
Phase III	Phase 4, Phase 5	Ph4, Ph5	Late medieval and Early Post medieval (AD 1400-1550)
Phase IV	Unstratified	Unstratified	N.A.

3.4.3 Trade activities at Northampton

Written resources attest to the presence at Northampton of different trades and crafts in all periods. Of particular interest is the name of the site ‘Woolmonger street’ also called *Vicus Lanatorum*, the street of the wool sellers, though no archaeological evidence for wool trade/industry at the site has been found. Nevertheless, the street name suggests that during the rise of sheep farming in the 12th and 13th centuries, the people of Woolmonger Street made their earnings by selling fleeces and/or woollen cloths. The pin-beaters, spindle-whorls and loom-weights found in phase 2b and 3 suggest the presence of cloth or/and tapestry-wavers in town, though a domestic- based production cannot be excluded (Soden 1998-1999).

According to the archaeological evidence, common crafts such as tanning, skinning and bone and antler working took place in the area (Fig. 3.231), though the zooarchaeological report provides little about this (Armitage 1998-1999; 2008).

Documentary evidence	Date	Archaeol. Evidence (Trench no)	Date/phase
		Flax retting (Tr5)	C10-11/2a
		Crop processing (Tr13,15,16)	C10-11/2a
		Antler working (Tr3, 13)	C11-13/2b
		Bone working (Tr12)	C11-13/2b
		Tanning (Tr5, 12, 13)	C11-13/2b
		Skinning/Tanning (Tr13)	C11-13/2b
		Metalworking (Tr10, 13)	C11-13/2b
Clerk (Clyve)	C13	Literacy (parchment prickers Tr12)	C13-14/3
		Tanning (Tr 13)	C13-15/3
Vintner (le Vyneter)	C13		
Weaver (Podder)	-1462	Weaving (?tapestry pin beaters Tr13); (spindlewhorls Tr12); (loomweight Tr10)	C11-15/2b-3
		Gardening (Tr16)	C15-16
Sadler (Willow)	c1462-1504		
Stabling (Woodward)	1545		
Draper (Spriggy)	c1389-1402		
Mercer (Edwardes, Knottynge, Bykyrston)	c1469-1504		
Fletcher (Hull, Smith)	1504	Archery (arrowhead Tr14)	C13-16
Alehouses	C16		

Figure 3.231 List of the written resources and the archaeological evidence attesting crafts at the site (image reprinted from SODEN, I. A history of urban regeneration: excavations in advance of development off St Peter’s walk, Northampton, 1994-7. *Northamptonshire Archaeology* 28: 61-127, copyright 1998-99, with permission from Iain Soden).

3.4.4 What does the zooarchaeological evidence say?

The animal bones recovered during the 1995-97 excavation, were studied by Armitage and the results were published in the form of a very concise report (1998-99). The whole assemblage constituted of 8320 fragments, of which 5428 could be identified. The chronological phases to which the fragments came from were 2a, 2b (Late Saxon and Early medieval period) and 3 (medieval period); the assemblage from phase 4 (Late medieval) was omitted from the report because of insufficient size.

Armitage attempted to distinguish between sheep and goat bones based on Boessneck *et al.* (1964) and Clutton-Brock *et al.* (1990). The methodology is the only part of the report where goats are mentioned. In the two tables included in the text, providing the list of the identified species and the percentage of the three main meat-yielding animals, only sheep numbers are mentioned. All caprine remains are reported as 'sheep', with no goat or sheep/goat categories mentioned (Fig. 3.232). The results of this study are presented in a highly summarised way, with no percentage of species or body parts provided. However, we are told that sheep, along with cattle and pig, were the main meat-provider species. The occurrence of all anatomical elements led Armitage to conclude that the animals were butchered on site. Evidence for the horn/bone working industry was scarce, only a sheep skull with some heavy axe/cleaver marks at the base of the horncores, attesting to the removal of the outer sheath. Overall, the bones were interpreted as representing domestic food waste (Armitage 1998-99).

The study of the kill-off pattern for the 1994-1997 animal bones assemblage revealed that sheep and cattle were mainly killed when adult, although lambs (calves and sucking pigs) were found occasionally. This pattern slightly changes in phase 2b: a higher number of animals killed at a young age is recorded, which indicates an appreciation of a finer meat. No clear details are given of the kill-off patterns during the later phases.

The zooarchaeological evidence points towards a rural economy able to support the slaughter of young animals (as bones of calves were found in all periods), so pressure for stock replacement must have not been heavily felt. Nevertheless, comparisons with other sites and written resources suggests that some domestic animals (pigs, chickens, geese and occasionally goats), could have also been raised at the back of houses and small holdings as home-provisioning (Armitage 1998-99).

Armitage also studied the animal bone assemblage recovered during the 2005 fieldwork. Another very concise report was published (Armitage 2008), in which he outlines the results. In this campaign 2994 fragments were recorded, of which 2112 were identified, coming from phases 1 and 2 (Late Saxon to Saxon-Norman, middle 10th to 12th century), phase 3 (medieval, 13th to 15th century) and phase 4 (Late medieval, 16th to 18th century) (Armitage 2008). No

methodology section is included to this later study so that the reader does not know if sheep and goat distinction was attempted and using which criteria. A list of identified species is provided, but, as for the earlier report, without details of their relative proportions. Consequently, it is unclear whether a separation of sheep and goat was attempted (Fig. 3.233).

		Cattle % Sheep % Pig %			
DOMESTIC:					
<i>Equus caballus</i> (domestic)	Horse				
<i>Equus asinus</i> (domestic)	Donkey				
<i>Bos</i> (domestic)	Cattle				
<i>Ovis/Capra</i> (domestic)	Sheep/goat (probably predominantly sheep)				
<i>Sus</i> (domestic)	Pig				
<i>Canis</i> (domestic)	Dog				
<i>Felis</i> (domestic)	Cat				
<i>Gallus gallus</i>	Domestic Fowl				
<i>Anser anser</i> (domestic)	Domestic Goose				
<i>Columbia livia</i>	Rock dove, probably domestic pigeon				
COMMENSAL:					
<i>Mus musculus</i> (<i>m.domesticus</i>)	House Mouse				
WILD SPECIES:					
<i>Cervus elaphus</i>	Red Deer				
<i>Dama dama</i>	Fallow Deer				
<i>Lepus</i> sp.	Probably Hare (brown or common hare)				
<i>Rana temporaria</i>	Common Frog				
<i>Vanellus vanellus</i>	Lapwing, pccwiv/green plover				
<i>Anas penelope</i>	Widgeon				
<i>Corvus corone</i>	Carriion Crow				
		Woolmonger Street			
		Phase 2a	39.2	51.5	9.3
		Phase 2b	44.8	48.5	6.7
		Phase 3	32.9	59.0	8.1

Figure 3.232 List of the species identified at the site by Armitage in 1998-1999 (right). Percentages of the main species based on NISP at the site (image reprinted from ARMITAGE, P. Faunal remains. In A history of urban regeneration: excavations in advance of development off St Peter's walk, Northampton, 1994-97, I. SODEN, 102-106, copyright 1998-99. *Northamptonshire Archaeology* 28, with permission from Philip Armitage).

The results from the study of the animal bone assemblage unearthed in 2005 mainly confirmed the trend identified in the previous analysis: the main meat-provider animals were cattle, sheep and, to a lesser degree, pig (Armitage 2008). Nothing is mentioned about kill-off patterns for sheep and goat and also we do not know about relative proportions of body parts.

In phase 3, the presence of all body parts for cattle and sheep, including head and extremities, led the author to think that the animals may have been butchered at the site or that butchers', tanners' and hornworkers' waste was left in the area, intermixed with household refuse. The presence of two detached and chopped sheep horncores, a cranium with the horncores removed and a single goat horncore seem to support this hypothesis (Armitage 2008). This horncore is the only *Capra* specimen mentioned in the report.

BIRDS
 Grey-lag/domestic goose, *Anser anser*/domestic
 Domestic fowl, *Gallus gallus* (domestic)
 cf Partridge, *Perdix perdix*
 Teal/domestic duck, *Anas platyrhynchos* (domestic)
 Carrion crow, *Corvus corone*
 Turdidae cf Songthrush, *Turdus ericetorum*

FISH
 Cod, *Gadus morhua*
 Haddock, *Melanogrammus aeglefinus*
 Herring, *Clupea harengus*
 cf Turbot, *Scophthalmus maximus*
 Thornback ray (or roker), *Raja clavatus*
 Freshwater eel, *Anguilla anguilla*
 Pike, *Esox lucius*
 Perch, *Perca fluviatilis*
 Amphibians
 Common frog, *Rana temporaria*

MAMMALS
 Horse, *Equus caballus* (domestic)
 Cattle, *Bos* (domestic)
 Sheep, *Ovis* (domestic)
 Goat, *Capra* (domestic)
 Pig, *Sus* (domestic)
 Dog, *Canis* (domestic)
 Cat, *Felis* (domestic)
 Fallow deer, *Dama dama*
 Brown hare, *Lepus* cf. *capensis*
 Rabbit, *Oryctolagus cuniculus*
 Black rat, *Rattus rattus*
 House mouse, *Mus musculus*

Figure 3.233 List of the identified species from the 2005 excavation (image reprinted from ARMITAGE, P. Mammal, bird and fish bones. In Excavations at the corner of Kingswell Street and Woolmonger Street, Northampton, J. BROWN, 206-208, copyright 2008. *Northamptonshire Archaeology* 35, with permission from Philip Armitage).

The limits of the previous zooarchaeological analysis, which have been outlined, make the re-examination of the sheep/goat assemblage from Northampton important for several reasons:

considering that the name of the site (Woolmonger) could reveal the activities carried out at the site, it was worth investigating whether the assemblage was indeed dominated by sheep;
 as town workshops have been attested by both archaeological and written sources, it would be interesting to see if there is any connection between the craft activities taking place there and the animals under study;
 the site is located in a different geographic area from the other two case studies and, as such, it is valuable for a wider geographic and cultural understanding of the wider economy and society.
 the sample is relatively large and therefore suited to the application of my newly developed methodology. The lack of goat identifications and clarity regarding the methodology used makes this as an ideal case study.

3.4.5 Reevaluation of Woolmonger/ Kingswell Street sheep/goat bone material: methodology

For the reanalysis of the sheep/goat assemblage of Northampton, the same methodology previously applied on the modern material and archaeological material from King's Lynn and Flaxengate was adopted (see Chapter 3 Section 3.2.5 and 3.3.4).

3.4.6 Morphological Approach: Results

Phase I

Only 79 specimens could be analysed, 67 of which were attributed to *Ovis* and 12 to *Ovis/Capra*. No specimen was attributed to the goat (Table 3.132).

Table 3.132 NISP for the three identified categories for phase I.

	<i>Ovis aries</i>	<i>Capra hircus</i>	<i>Ovis/ Capra</i>
Horncore	5	-	-
Jaw	14	-	5
Teeth	6	-	3
Scapula	4	-	3
Humerus	3	-	-
Radius	5	-	-
Ulna	2	-	-
Metacarpal	2	-	-
Metatarsal	2	-	-
Metapodial	1	-	-
Tibia	11	-	1
Astragalus	1	-	-
Calcaneum	2	-	-
1st Phalanx	8	-	-
3rd Phalanx	1	-	-
Total Identified Specimens	67	0	12

Phase II

For phase II a larger sample size of 358 specimens was available. 305 have been classified as sheep and 49 were attributed to sheep/goat. Four specimens were classified as goat: a horncore and three postcranial bones (Tab. 3.133).

Table 3.133 NISP for the three identified categories for phase II.

	<i>Ovis aries</i>	<i>Capra hircus</i>	<i>Ovis/ Capra</i>
Horncore	16	1	-
Jaw	27	-	13
Teeth	26	-	15
Scapula	8	-	5
Humerus	32	-	2
Radius	22	1	1
Ulna	10	-	1
Metacarpal	23	-	-
Metatarsal	17	1	1
Metapodial	6	-	-
Tibia	37	1	8
Astragalus	3	-	-
Calcaneum	14	-	-
1st Phalanx	49	-	3
2nd Phalanx	12	-	-
3rd Phalanx	3	-	-
Total Identified Specimens	305	4	49

Phase III

Phase III produced the smallest sample, with 35 specimens identified as sheep, one as goat (1st phalanx) and six unattributed to species (Tab. 3.134).

Table 3.134 NISP for the three identified categories for phase III.

	<i>Ovis aries</i>	<i>Capra hircus</i>	<i>Ovis/ Capra</i>
Horncore	-	-	-
Jaw	-	-	-
Teeth	4	-	4
Scapula	1	-	-
Humerus	2	-	1
Radius	-	-	-
Ulna	-	-	-
Metacarpal	2	-	-
Metatarsal	4	-	-
Metapodial	-	-	-
Tibia	1	-	-
Astragalus	2	-	-
Calcaneum	-	-	-
1st Phalanx	16	1	1
2nd Phalanx	2	-	-
3rd Phalanx	1	-	-
Total Identified Specimens	35	1	6

Unstratified

Despite a careful research of archival information, many contexts could not be clearly attributed to a specific chronological phase. Nevertheless, this material has been recorded and analysed. 313 specimens were identified as sheep and 57 as sheep/goat. The presence of the goat is attested by five horncores, a metatarsal and three 1st phalanges (Tab. 3.135).

Table 3.135 NISP for the three identified categories amongst the unstratified specimens.

	<i>Ovis aries</i>	<i>Capra hircus</i>	<i>Ovis/ Capra</i>
Horncore	11	5	-
Jaw	27	-	18
Teeth	25	-	14
Scapula	14	-	8
Humerus	39	-	1
Radius	21	-	-
Ulna	13	-	1
Metacarpal	20	-	-
Metatarsal	20	1	-
Metapodial	1	-	-
Tibia	44	-	7
Astragalus	3	-	-
Calcaneum	10	-	2
1st Phalanx	54	3	6
2nd Phalanx	9	-	-
3rd Phalanx	2	-	-
Total Identified Specimens	313	9	57

In all chronological phases, sheep bones predominate and are represented by a variety of anatomical elements. Goat is only attested by a few horncores, and even fewer post-cranial bones. Clearly the goat is very scarce and the predominance of horncores (mainly registered in the unstratified material) is minimal, far from the scale seen at other sites, such as Kings Lynn.

3.4.7 Shape analysis as expressed by Biometrical Indices

Phase I

Horncore

Figures 3.234 and 3.235 show the results for the horncores related to the first chronological phase. Both scatterplots show that the only archaeological specimen, identified as sheep according to the morphological traits, falls among the modern group of the same species. As such, biometry confirms the morphological identification.

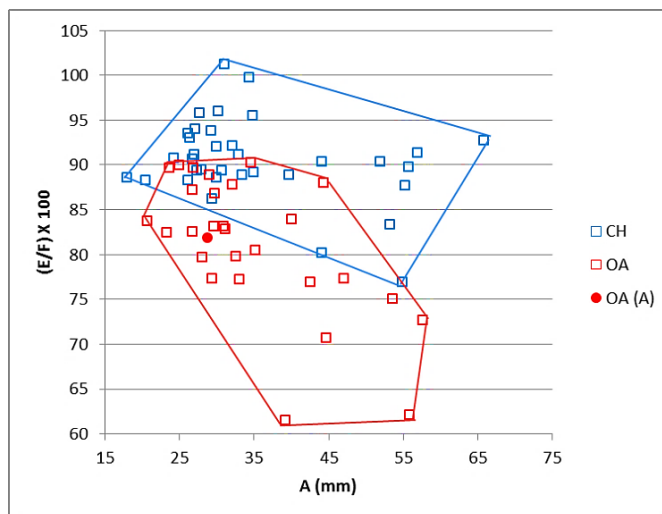


Figure 3.234 Maximum diameter taken at the base plotted against a ratio between the length and the length of the outer curvature of the horncore. The modern data are represented by the square empty symbol, blue for modern goats, red for modern sheep, while the archaeological material is represented by the filled dot symbol: blue for goats, red for sheep and green for sheep/goat.

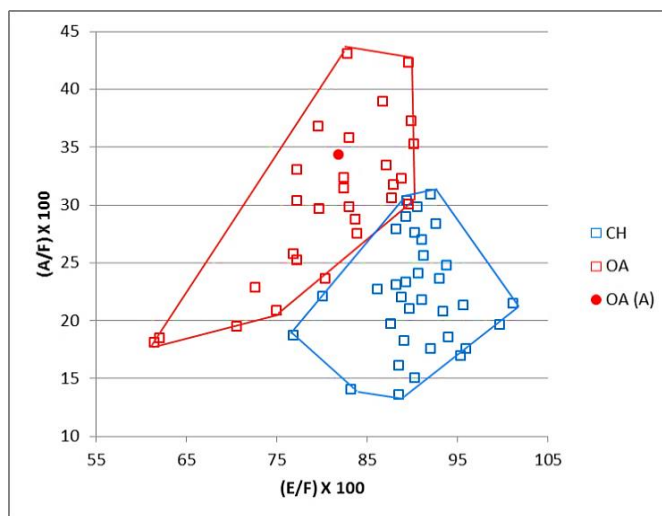


Figure 3.235 Ratio between the length and the length of the outer curvature plotted against the ratio between the maximum diameter taken at the base and the length of the outer curvature of the horncore. Symbols explained in Fig. 3.234.

Scapula

Figures 3.236 and 3.237 describe the most diagnostic areas for the scapula. No archaeological goats have been identified morphologically. Although some archaeological sheep are border-line, they are potentially consistent with the morphological identifications. One of the archaeological sheep specimens in both figures has high ratios, showing strong sheep traits. The unidentified archaeological specimen remains of uncertain attribution as it is border-line between the two groups.

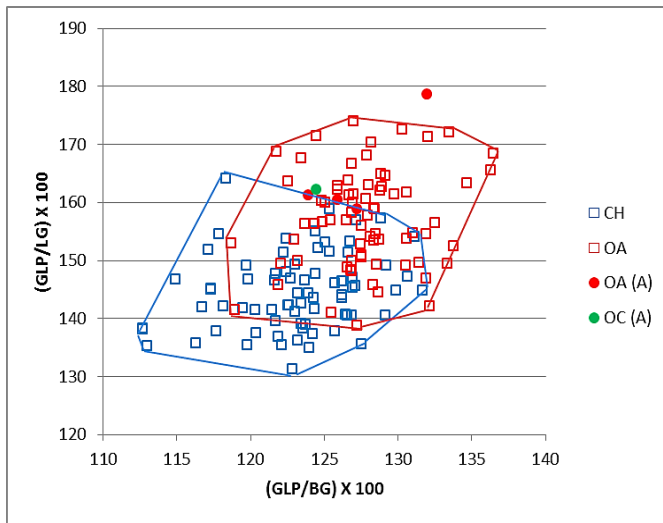


Figure 3.236 Ratio between the greatest length of the *processus articularis* and the length of the glenoid cavity plotted against the ratio between the greatest length of the *processus articularis* and the breadth of the glenoid cavity. Symbols explained in Fig. 3.234.

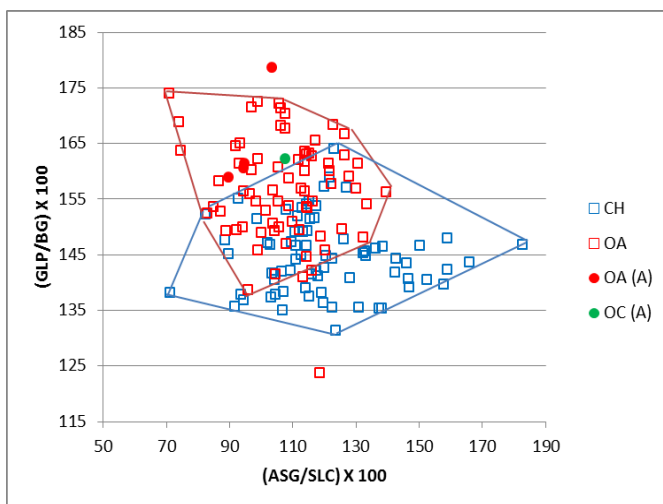


Figure 3.237 Ratio between the shortest distance from the base of the spine to the edge of the glenoid cavity and the smallest length of the *collum scapulae* plotted against the ratio between the greatest length of the *processus articularis* and the breadth of the glenoid cavity. Symbols explained in Fig. 3.234.

Humerus

Figures 3.238 to 3.241 show ratios of measurements taken on the distal articulation of the humerus. No goat archaeological humeri were identified morphologically. All sheep humeri plot within the modern sheep cluster or the area of overlap of the two species and are therefore consistent with the morphological identifications.

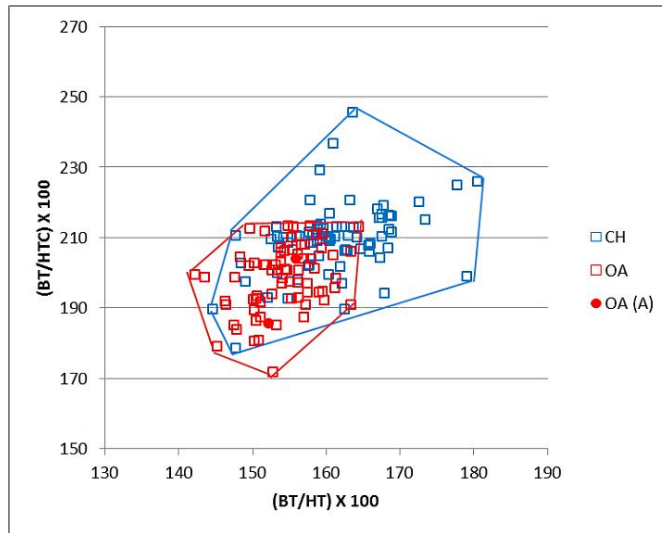


Figure 3.238 Ratio between the medio lateral width of the trochlea and its height plotted against the medio lateral width of the trochlea and the diameter of the trochlear constriction. Symbols explained in Fig. 3.234.

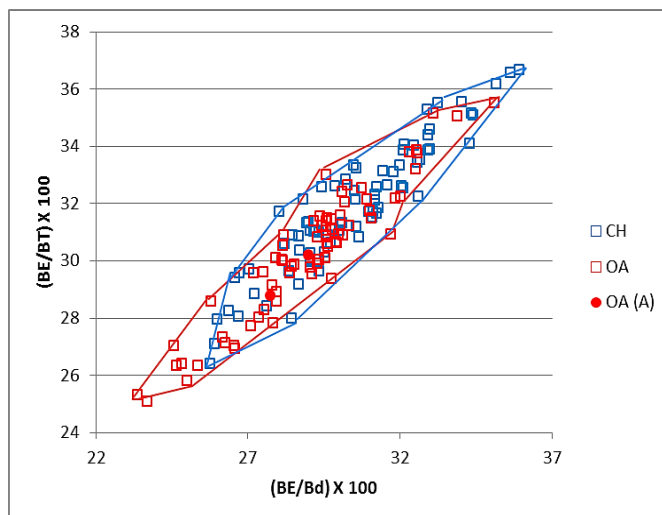


Figure 3.239 Ratio between the breadth of the *capitulum* and the distal width plotted against the ratio between the breadth of the *capitulum* and the medio lateral width of the trochlea. Symbols explained in Fig. 3.234.

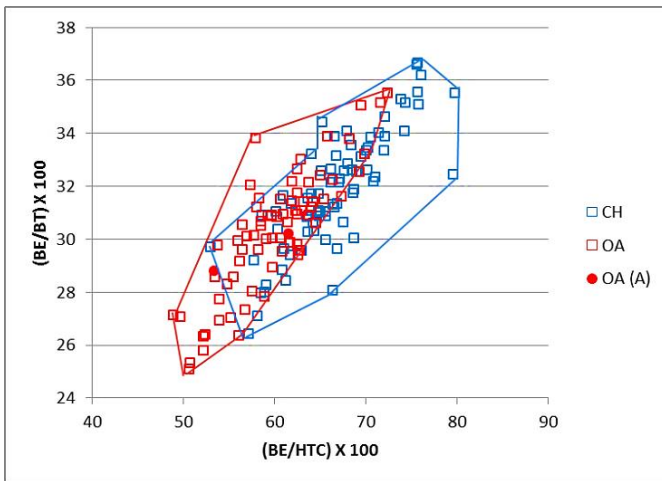


Figure 3.240 Ratio between the breadth of the *capitulum* and the diameter of the trochlea constriction plotted against the ratio between the breadth of the *capitulum* and the medio lateral width of the trochlea. Symbols explained in Fig. 3.234.

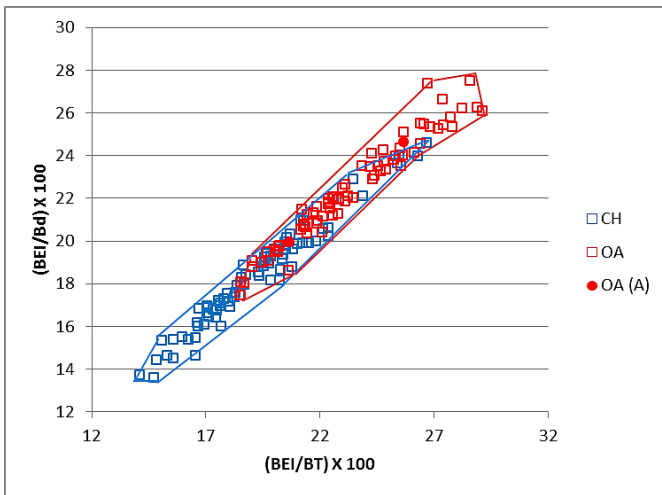


Figure 3.241 Ratio between the breadth of the epicondyle *lateralis* and the medio lateral width of the trochlea plotted against the ratio between the breadth of the epicondyle *lateralis* and the width of the distal end. Symbols explained in Fig. 3.234.

Radius

Only sheep archaeological radii were identified morphologically and all of them cluster with the modern sheep group (Fig. 3.242) or in the area of overlap between the two groups. As such, the biometrical results are consistent with the morphological identifications.

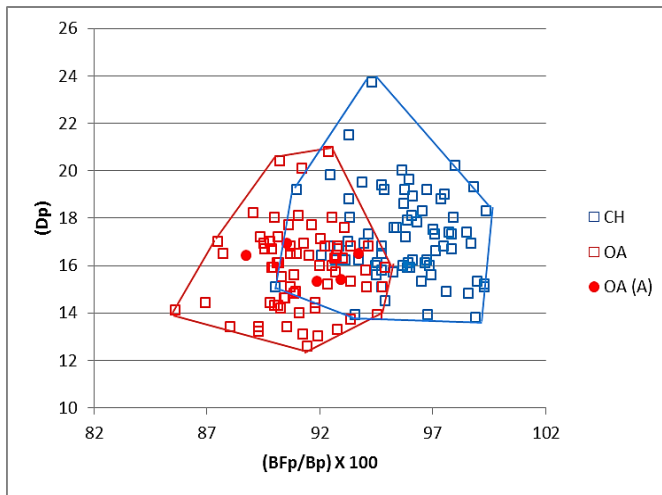


Figure 3.242 Ratio between the greatest length of the *facies articularis proximalis* and the greatest breadth of the proximal end plotted against the depth of the proximal end. Symbols explained in Fig. 3.234.

Ulna

Only two archaeological ulnae, both attributed to sheep according to their morphology, have been recorded in this phase (Fig. 3.243). Both specimens are consistent with the modern sheep group; notably one plots clearly at the sheep end of the range showing strong sheep features.

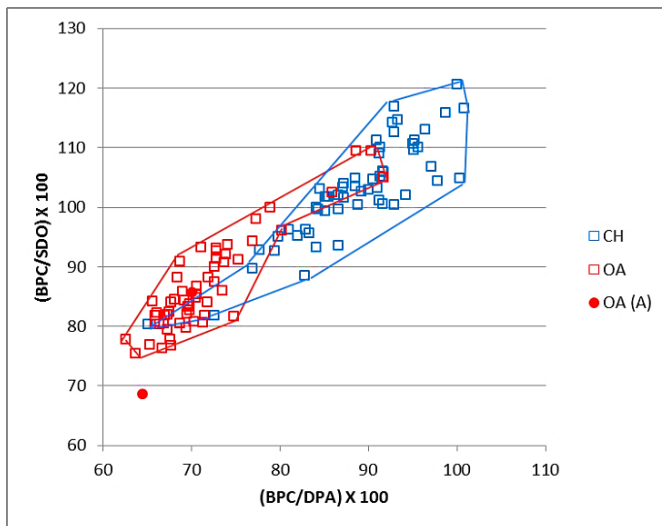


Figure 3.243 Ratio between the breadth across the coronoid process and the depth across the *processus anconaeus* to the caudal border plotted against the breadth across the coronoid process and the smallest depth of the olecranon. Symbols explained in Fig. 3.234.

Metapodials

For metapodials, the lack of complete bones prevented the use of all the diagnostic ratios. Figures 3.244 to 3.247 show medial and lateral condyle metric ratios. No archaeological goats had been identified morphologically and the use of the BI confirms this evidence. The morphologically identified sheep all fall among the modern sheep group or in the area of overlap for the two species, thus the original identification is confirmed.

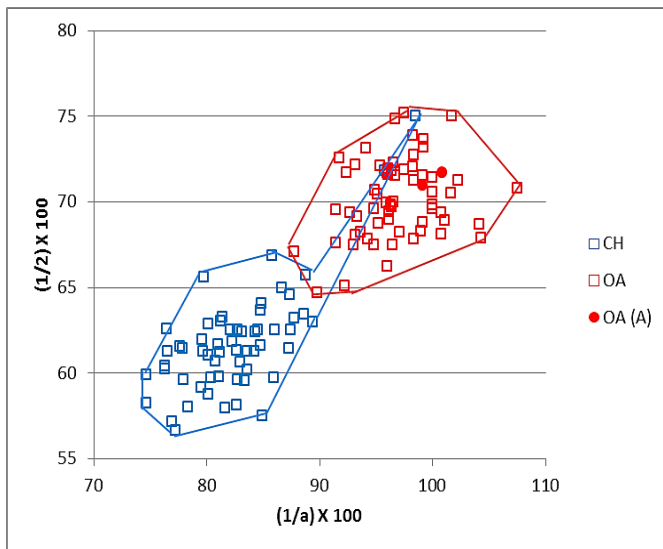


Figure 3.244 Metacarpal. Ratio between the diameter of the medial trochlea and the width of the medial condyle plotted against the ratio between the diameter of the *verticillus* at the medial condyle and the diameter of the medial trochlea. Symbols explained in Fig. 3.234.

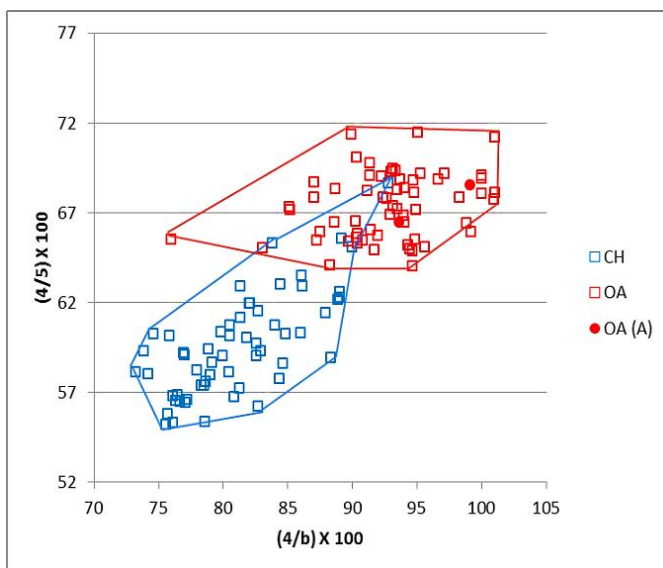


Figure 3.245 Metacarpal. Ratio between the width of the lateral condyle and the diameter of the lateral trochlea plotted against the ratio between the diameter of the lateral condyle and the diameter of the *verticillus* on the lateral condyle. Symbols explained in Fig. 3.234.

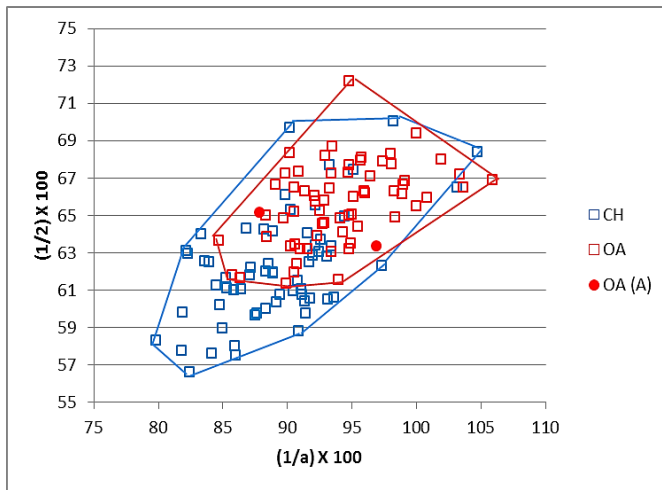


Figure 3.246 Metatarsal. Ratio between the diameter of the medial trochlea and the width of the medial condyle plotted against the ratio between the diameter of the *verticillus* at the medial condyle and the diameter of the medial trochlea. Symbols explained in Fig. 3.234.

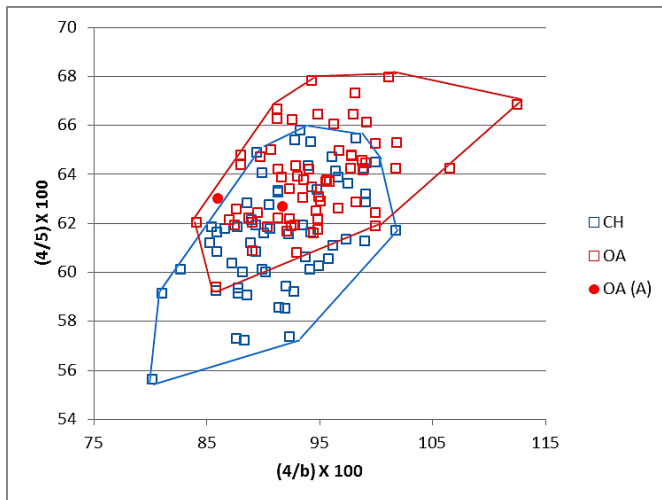


Figure 3.247 Metatarsal. Ratio between the width of the lateral condyle and the diameter of the lateral trochlea plotted against the ratio between the diameter of the *verticillus* on the lateral condyle and the diameter of the lateral condyle. Symbols explained in Fig. 3.234.

Figure 3.248 shows ratios which describe the overall shape of the metatarsal. Only one complete archaeological specimen was recorded and identified morphologically as sheep. This specimen fall in the area of overlap between the two modern groups, thus it is consistent with the range of variation of the sheep group.

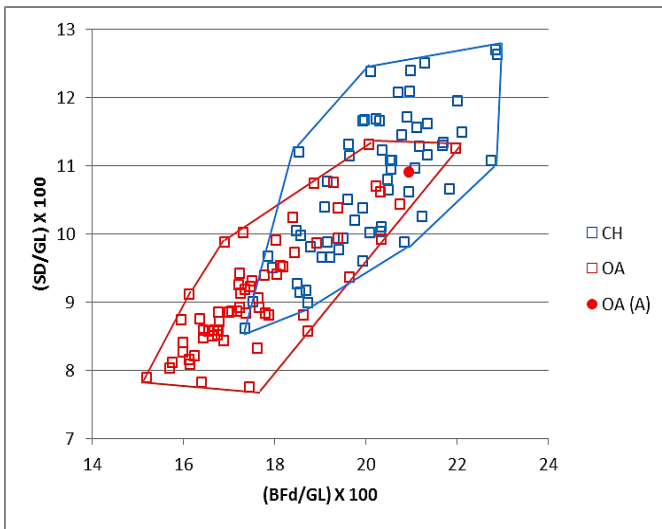


Figure 3.248 Metatarsal. Ratio between the greatest breadth of the distal end with the greatest length plotted against the ratio between the smallest width of the shaft and the greatest length. Symbols explained in Fig. 3.234.

Tibia

Figure 3.249 shows the results when metrical ratios related to the distal articulation of the tibia are plotted together. The absence of archaeological goats is confirmed by the biometrical analysis. All specimens identified morphologically as sheep fall among their modern counterparts or in the area of overlap; as such, their identification is retained.

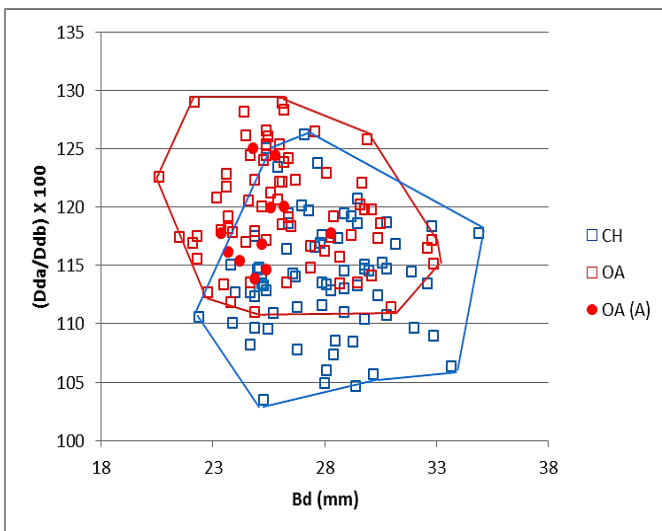


Figure 3.249 Breadth of the distal end plotted against the ratio between the depth of the medial (a) and lateral (b) side. Symbols explained in Fig. 3.234.

Astragalus

All the BI for the astragalus are presented in Figures 3.250 to 3.253. Only one archaeological specimen has been recorded for this phase and identified as sheep according to its morphological traits. As the scatterplots show, it falls in the area of overlap between the two groups, thus it is perfectly consistent with the sheep pattern.

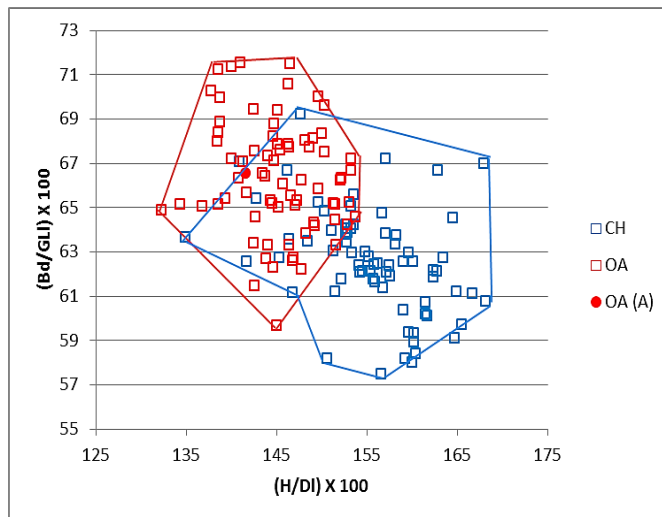


Figure 3.250 Ratio between height at the central constriction and the greatest depth of the lateral half plotted against a ratio between the breadth of the distal end and the greatest length of the lateral half. Symbols explained in Fig. 3.234.

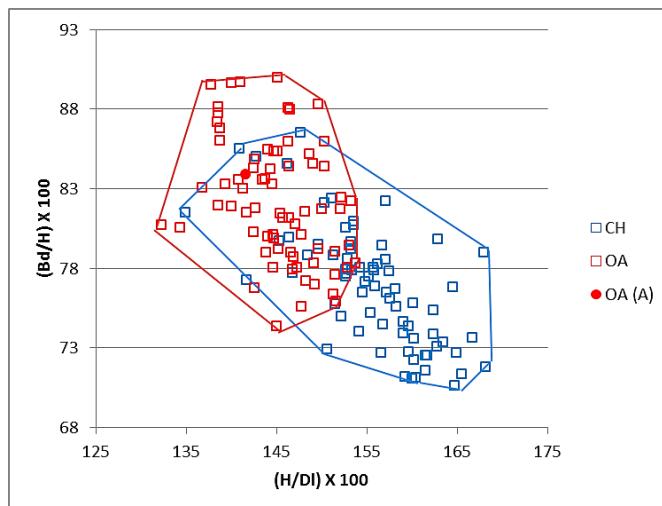


Figure 3.251 Ratio between height at the central constriction and the greatest depth of the lateral half plotted against the ratio between the breadth of the distal end and the height at the central constriction. Symbols explained in Fig. 3.234.

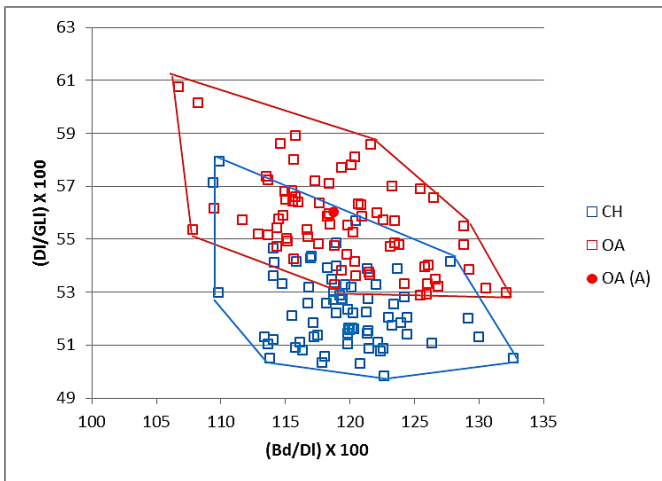


Figure 3.252 Ratio between breadth of the distal end and the greatest depth of the lateral half plotted against the ratio between the breadth of the distal end and the greatest depth of the lateral half. Symbols explained in Fig. 3.234.

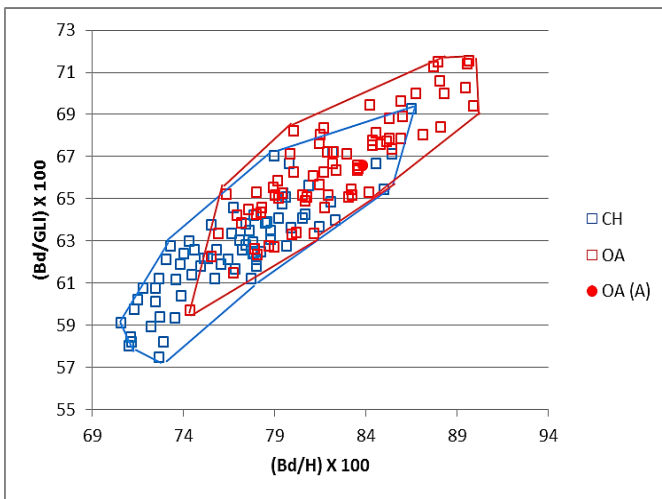


Figure 3.253 Ratio between the breadth of the distal end and the height at the central constriction and the ratio between height at the central constriction and the greatest depth of the lateral half. Symbols explained in Fig. 3.234.

Calcaneum

Figures 3.253 to 3.256 show different BI used for the calcaneum. No goats had been identified morphologically. The biometry confirms this identification as both sheep archaeological specimens clearly plot within the modern sheep group in all three diagrams.

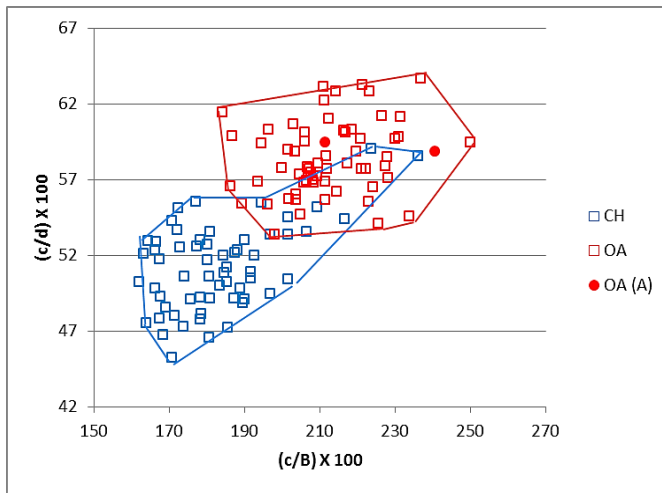


Figure 3.254 Ratio between the length and the breadth of the articular facet of the *os malleolare* plotted against the ratio between the length of the articular facet of the *os malleolare* and the length taken from the articular facet of the *os malleolare* to the end of the articulation-free part of the process. Symbols explained in Fig. 3.234.

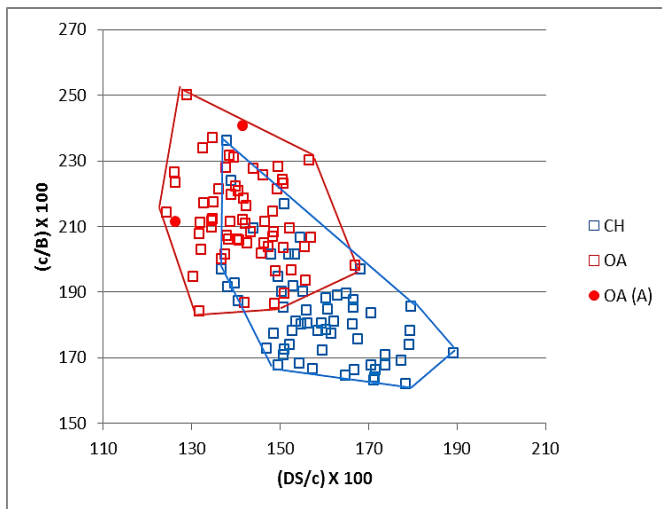


Figure 3.255 Ratio between the depth of the *sustentaculum tali* and the length of the articular facet of the *os malleolare* plotted against the ratio between the length and the breadth of the articular facet of the *os malleolare*. Symbols explained in Fig. 3.234.

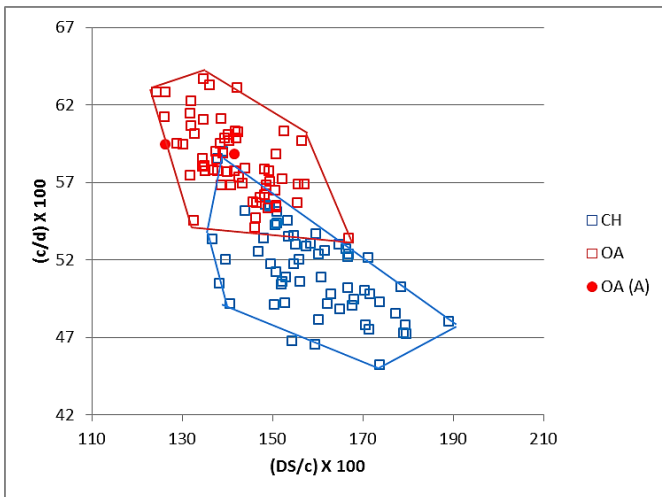


Figure 3.256 Ratio between the depth of the *sustentaculum tali* and the length of the articular facet of the *os malleolare* plotted against the ratio between the length and the breadth of the articular facet of the *os malleolare*. Symbols explained in Fig. 3.234.

3rd Phalanx

Figure 3.257 shows the results for the 3rd phalanx. Only one archaeological specimen, identified as sheep on the basis of its morphology has been recorded. This identification is consistent with the biometrical results as it falls in the area of overlap between the two modern groups.

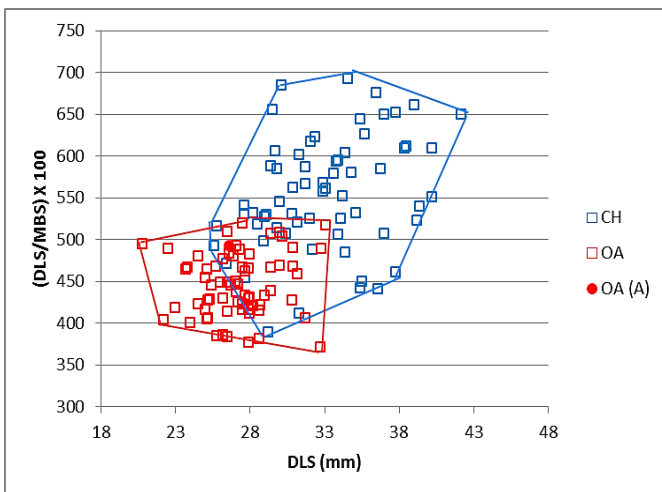


Figure 3.257 Greatest diagonal length of the sole plotted against a ratio between the greatest diagonal length of the sole and the middle breadth of the sole. Symbols explained in Fig. 3.234.

Phase II

Horncores

Because of the fragmentary state of the horncores, not many measurements could be taken, as such no BI could be applied on this anatomical element for this phase.

Scapula

No goat archaeological scapulae were identified. Figures 3.258 and 3.259 show the extent to which the biometrical results agree with the morphological outcomes. All the archaeological sheep are consistent with the sheep modern group pattern. Two of the unidentified specimens plot in the area of overlap but are much closer to the centre of the sheep distribution in both diagrams. Another is border-line between the two groups but, as shown by both figures, much more in the goat area, and may indeed represent a rare occurrence of this species at Woolmonger Street.

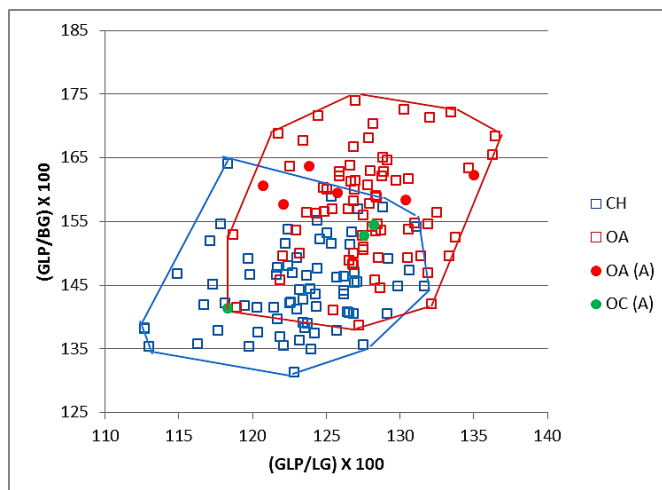


Figure 3.258 Ratio between the greatest length of the *processus articularis* and the length of the glenoid cavity plotted against the ratio between the greatest length of the *processus articularis* and the breadth of the glenoid cavity. Symbols explained in Fig. 3.234.

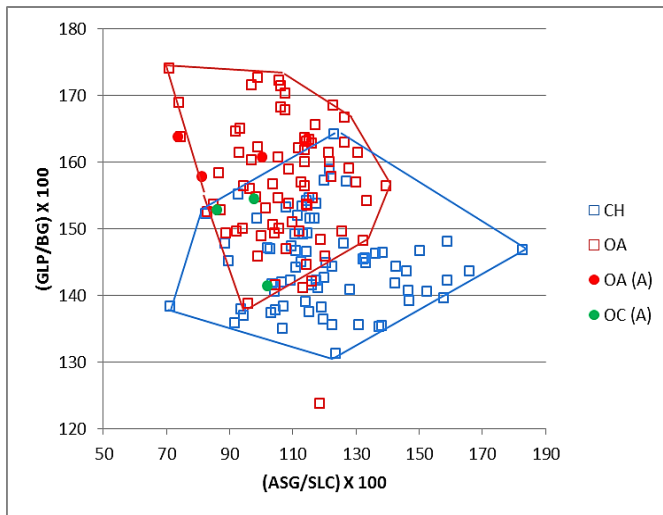


Figure 3.259 Ratio between the shortest distance from the base of the spine to the edge of the glenoid cavity and the smallest length of the *collum scapulae* plotted against a ratio between the greatest length of the *processus articularis* and the breadth of the glenoid cavity. Symbols explained in Fig. 3.234.

Humerus

No archaeological goats had been identified morphologically. The majority of the archaeological sheep fall well within the modern sheep group or in the area of overlap between the two species, thus supporting the morphological identifications (Figs. 3.260 to 3.263). A few archaeological sheep (Fig. 3.260) lean more toward the goat group but, as they do not represent outliers from the main sheep distribution, the evidence is insufficiently strong for a reclassification.

Due to the high level of overlap between the two modern groups it is difficult to be sure about the taxonomy of the unidentified specimens (Figs. 3.260 and 3.262). Nevertheless, in all diagrams they seem to be more consistent with sheep.

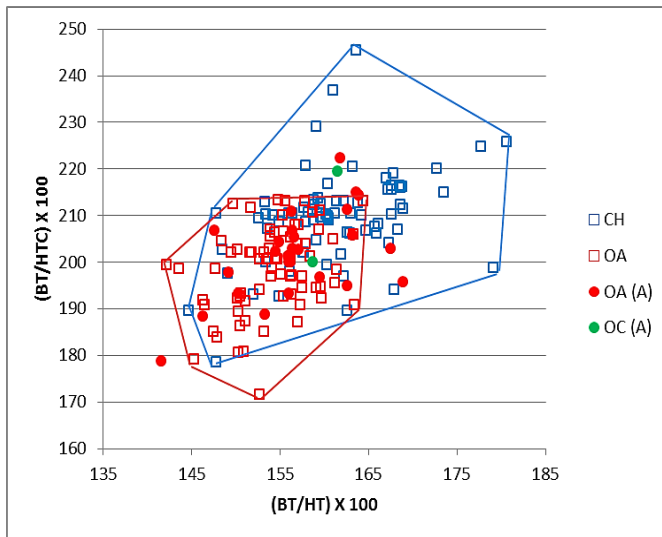


Figure 3.260 Ratio between the medio lateral width of the trochlea and its height plotted against the medio lateral width of the trochlea and the diameter of the trochlear constriction. Symbols explained in Fig. 3.234.

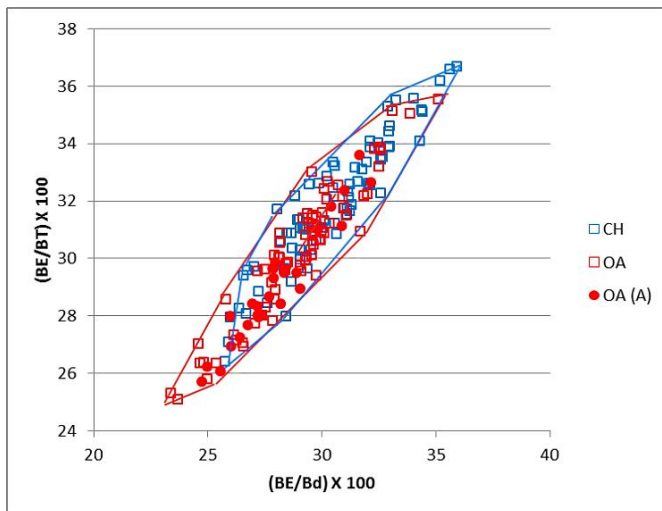


Figure 3.261 Ratio between the breadth of the *capitulum* and the distal width plotted against the ratio between the breadth of the *capitulum* and the medio lateral width of the trochlea. Symbols explained in Fig. 3.234.

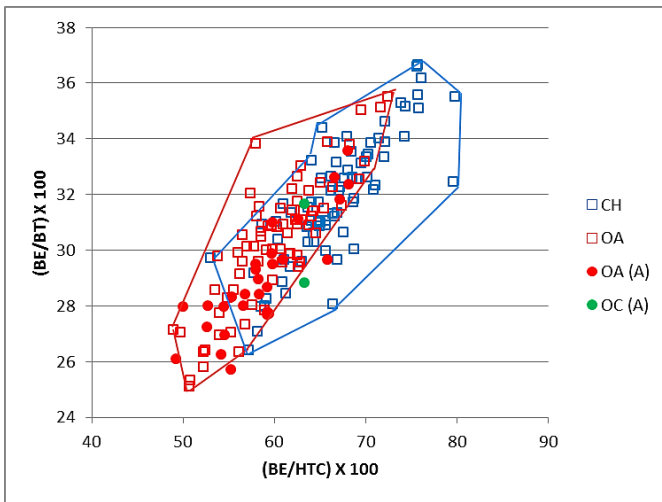


Figure 3.262 Ratio between the breadth of the *capitulum* and the diameter of the trochlear constriction plotted against the ratio between the breadth of the *capitulum* and the medio lateral width of the trochlea. Symbols explained in Fig. 3.234.

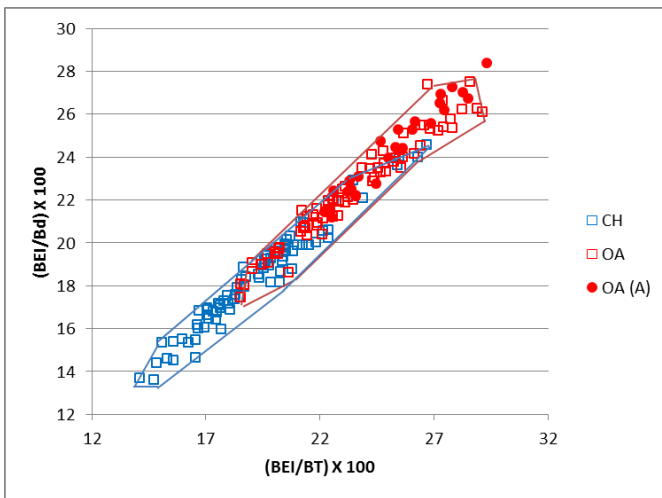


Figure 3.263 Ratio between the breadth of the epicondyle *lateralis* and the medio lateral width of the trochlea plotted against the ratio between the breadth of the epicondyle *lateralis* and the width of the distal end. Symbols explained in Fig. 3.234.

Radius

Figure 3.264 shows that most of the radii identified morphologically as belonging to sheep are consistent with the sheep modern cluster (falling among the modern sheep or in the area of overlap). The only unidentified specimen falls in the area of overlap and therefore its identity remains uncertain.

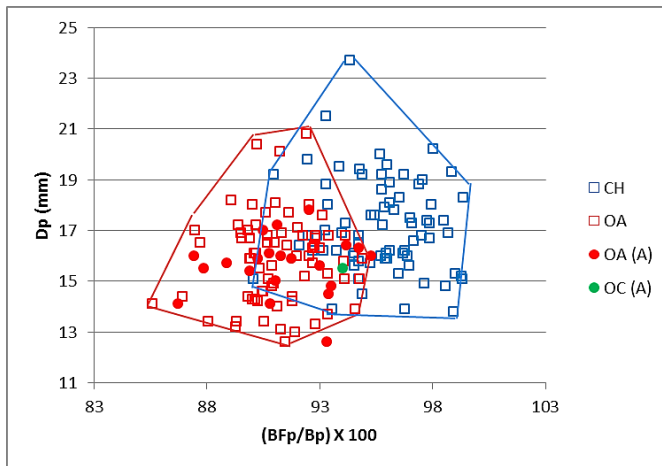


Figure 3.264 Ratio between the greatest length of the *facies articularis proximalis* and the greatest breadth of the proximal end plotted against the depth of the proximal end. Symbols explained in Fig. 3.234.

Ulna

All the ulnae identified morphologically as belonging to sheep clearly fall among the modern sheep group (Fig.3.265), indicating agreement between biometrical and morphological results. One archaeological sheep has very pronounced sheep characteristics as it falls at the lower range of the sheep group. Biometry and morphology agree about the absence of goat ulnae.

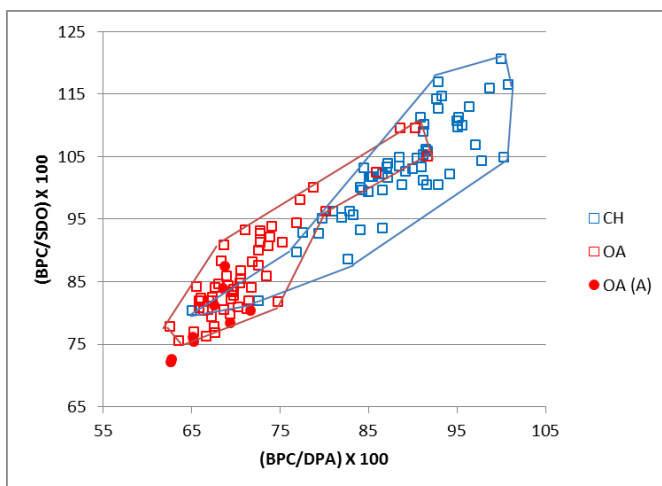


Figure 3.265 Ratio between the breadth across the coronoid process and the depth across the *processus anconaeus* to the caudal border plotted against the breadth across the coronoid process and the smallest depth of the olecranon. Symbols explained in Fig. 3.234.

Metapodials

No archaeological metacarpals were assigned to goat on the basis of their morphology. This identification is largely confirmed by the biometrical data (Figs.3.266-3.268), though two 'sheep' metacarpals plot separately from the main sheep cluster and more towards the goat in Figure 3.266. One of these plots well within the goat distribution in Figure 3.267, suggesting that it is indeed likely to represent a goat and, therefore, that the original morphological identification is incorrect. For the other specimen, as it plots within the sheep range in Figure 3.266, it cannot be confidently considered a goat (information on the overall shape of these two specimens were not available). Figure 3.268 shows that, when the overall shape of the complete metacarpals is considered, no goats are found.

Figures 3.274 and 3.275 show the results for the metatarsal. The only goat identified morphologically (Fig. 3.274 and 3.275) falls in the area of overlap, as such it can be considered to be consistent with the modern goat pattern. The archaeological sheep fall within the modern sheep group or in the area of overlap, thus biometry confirms the morphological identifications.

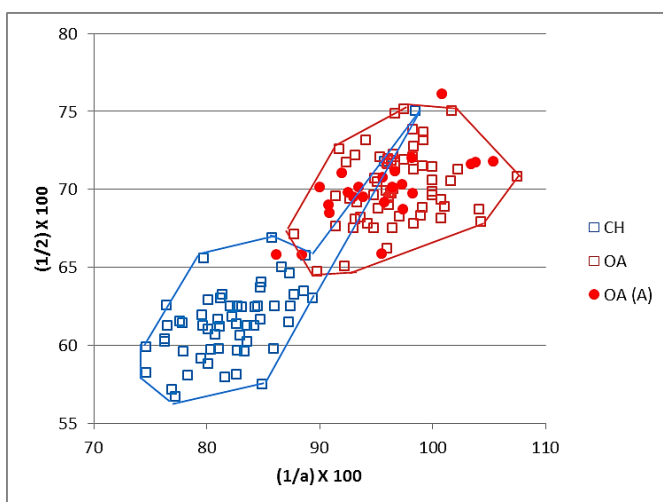


Figure 3.266 Metacarpal. Ratio between the diameter of the medial trochlea and the width of the medial condyle plotted against the ratio between the diameter of the *verticillus* at the medial condyle and the diameter of the medial trochlea. Symbols explained in Fig. 3.234.

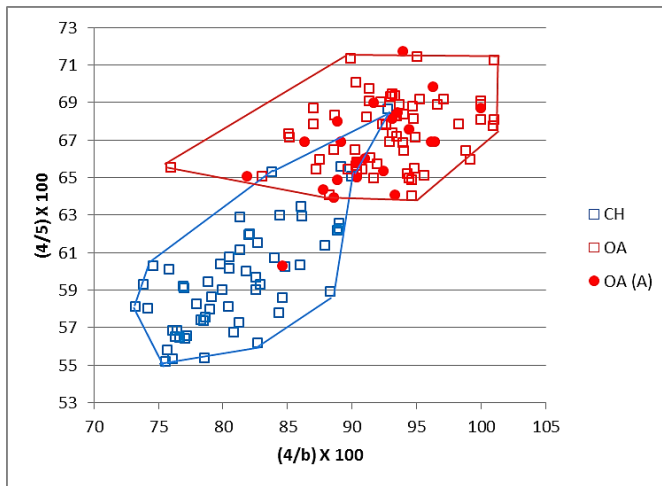


Figure 3.267 Metacarpal. Ratio between the width of the lateral condyle and the diameter of the lateral trochlea plotted against the ratio between the diameter of the *verticillus* the lateral condyle and the diameter of the lateral condyle. Symbols explained in Fig. 3.234.

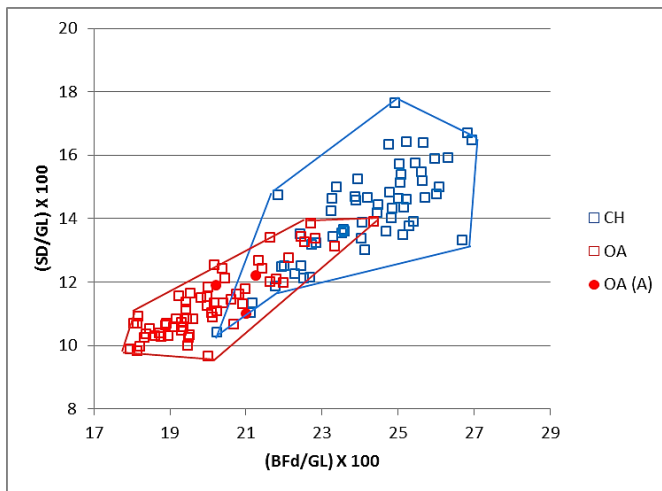


Figure 3.268 Metacarpal. Ratio between the greatest breadth of the distal end with the greatest length plotted against the ratio between the smallest width of the shaft and the greatest length. Symbols explained in Fig. 3.234.

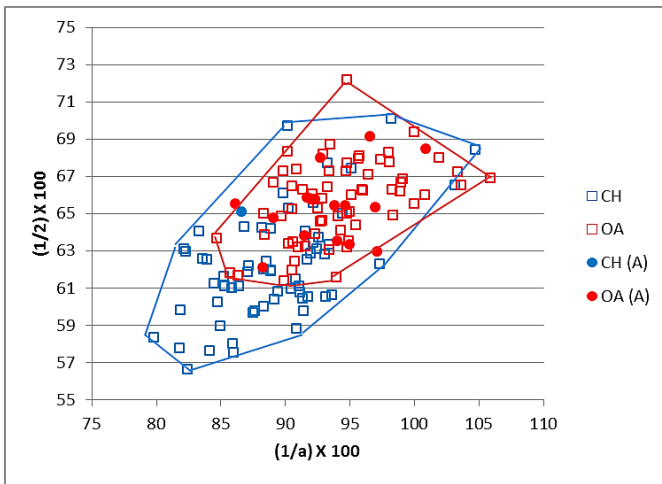


Figure 3.269 Metatarsal. Ratio between the diameter of the medial trochlea and the width of the medial condyle plotted against the ratio between the diameter of the *verticillus* at the medial condyle and the diameter of the medial trochlea. Symbols explained in Fig. 3.234.

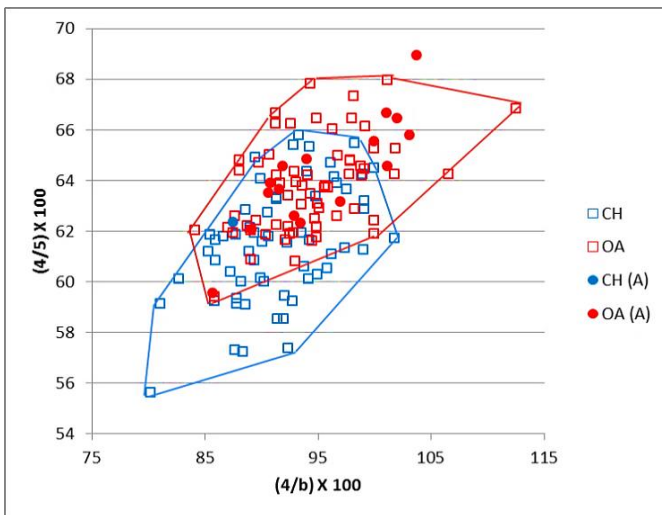


Figure 3.270 Metatarsal. Ratio between the width of the lateral condyle and the diameter of the lateral trochlea plotted against the ratio between the diameter of the *verticillus* on the lateral condyle and the diameter of the lateral condyle. Symbols explained in Fig. 3.234.

Tibia

One goat archaeological tibia was identified according to its morphology. In Figure 3.271 this specimen plots in the area of overlap between the two groups, and is therefore potentially consistent with the original identification. All archaeological sheep fall in the area of overlap, within the sheep range, or even beyond it, showing particularly strong sheep traits. The majority of the unidentified specimens fall in the area of overlap and cannot be identified with any degree of confidence. However, two unidentified specimens can be assigned to a species as one definitely plots in the sheep range, as such it can be considered a sheep. Another plots well within the goat range, and therefore can be considered a *Capra*.

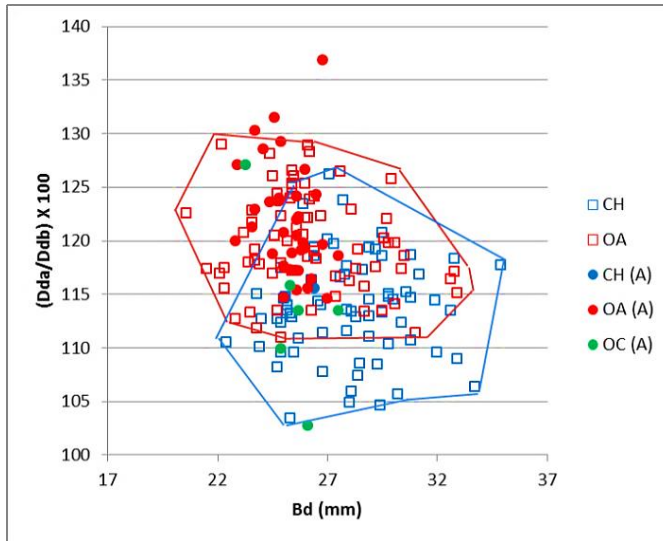


Figure 3.271 Breadth of the distal end plotted against the ratio between the depth of the medial (a) and lateral (b) side. Symbols explained in Fig. 3.234.

Astragalus

Figures 3.272 to 3.275 show the BI, which describe the shape of the astragalus. No archaeological goats had been identified morphologically. This outcome is confirmed by biometry: the two archaeological sheep specimens fall among the modern sheep group or in the area of overlap, so that their identification cannot be questioned.

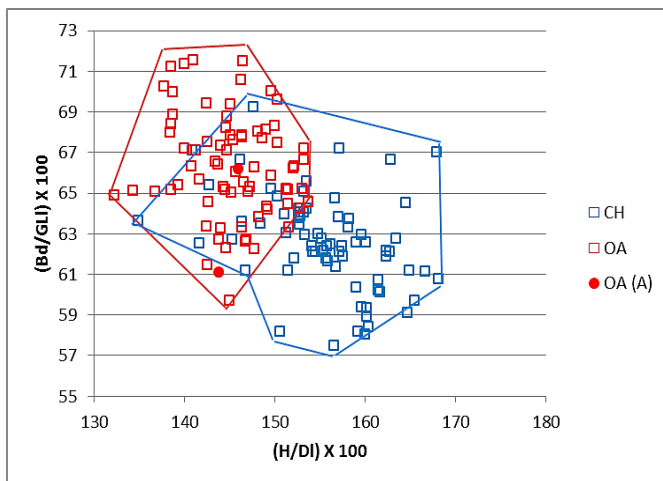


Figure 3.272 Ratio between height at the central constriction and the greatest depth of the lateral half plotted against a ratio between the breadth of the distal end and the greatest length of the lateral half. Symbols explained in Fig. 3.234.

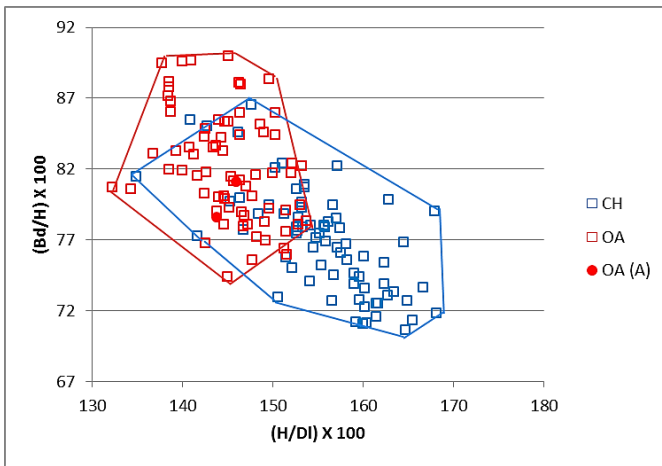


Figure 3.273 Ratio between height at the central constriction and the greatest depth of the lateral half plotted against the ratio between the breadth of the distal end and the height at the central constriction. Symbols explained in Fig. 3.234.

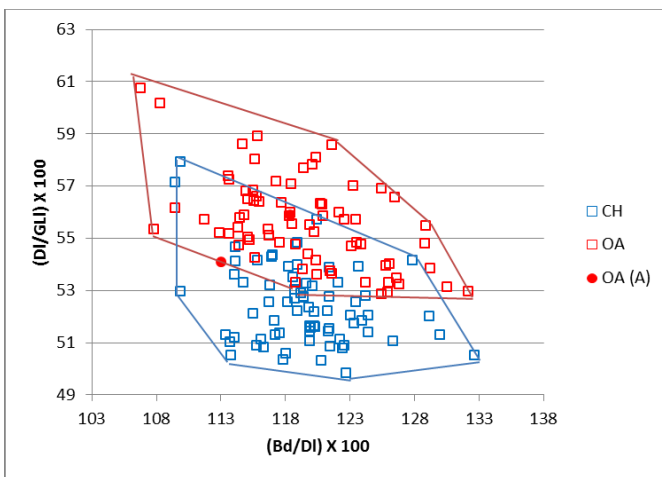


Figure 3.274 Ratio between breadth of the distal end and the greatest depth of the lateral half plotted against the ratio between the breadth of the distal end and the greatest depth of the lateral half. Symbols explained in Fig. 3.234.

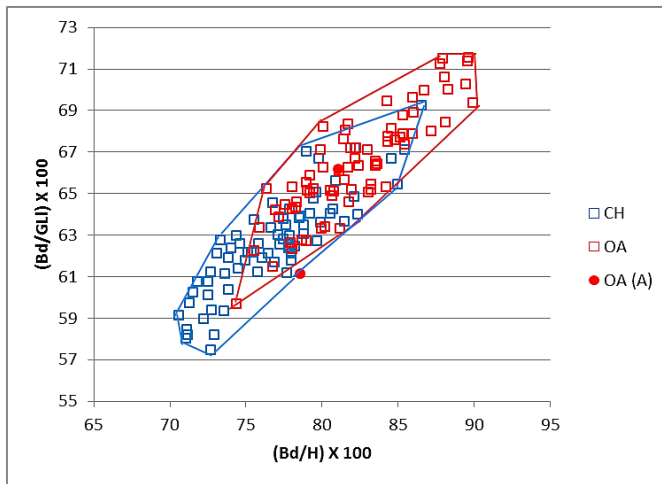


Figure 3.275 Ratio between the breadth of the distal end and the height at the central constriction and the ratio between height at the central constriction and the greatest depth of the lateral half. Symbols explained in Fig. 3.234.

Calcaneum

Figures 3.276 to 3.278 show the results for the calcaneum. The biometry, expressed through the use of different indices, confirms the morphological identifications: the archaeological sheep form a defined group which is highly consistent with the modern sheep pattern. Both the biometrical and morphological evidence confirm the lack of goat calcanea.

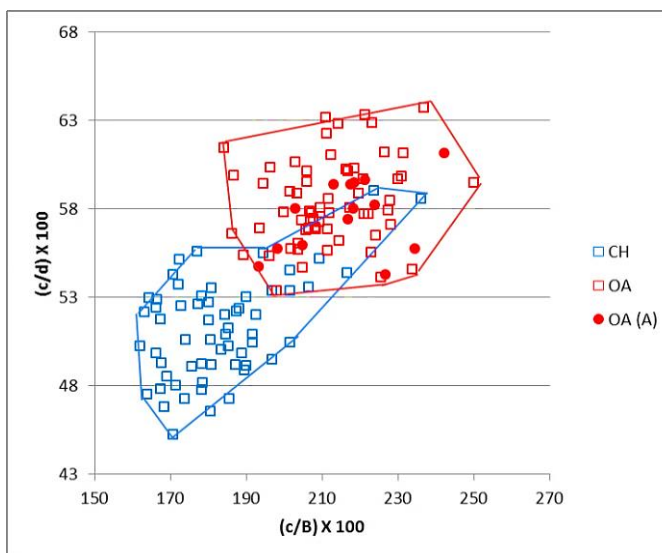


Figure 3.276 Ratio between the length and the breadth of the articular facet of the *os malleolare* plotted against the ratio between the length of the articular facet of the *os malleolare* and the length taken from the articular facet of the *os malleolare* to the end of the articulation-free part of the process. Symbols explained in Fig. 3.234.

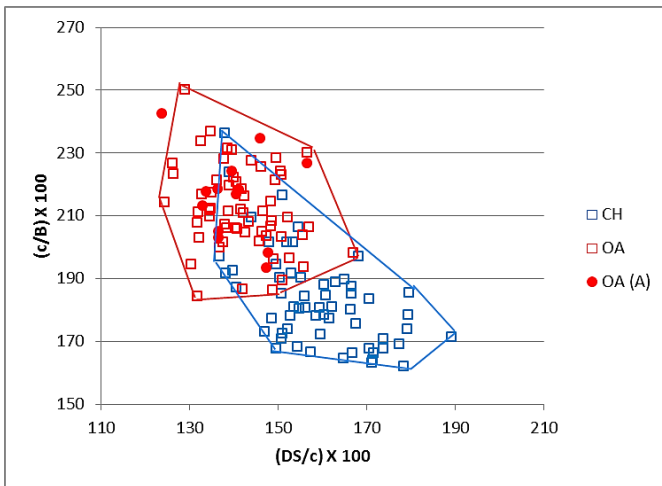


Figure 3.277 Ratio between the depth of the *subtentaculum tali* and the length of the articular facet of the *os malleolare* plotted against the ratio between the length and the breadth of the articular facet of the *os malleolare*. Symbols explained in Fig. 3.234.

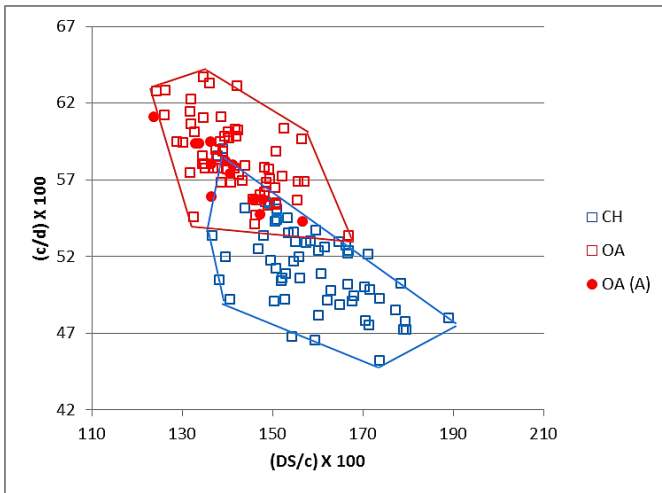


Figure 3.278 Ratio between the depth of the *subtentaculum tali* and the length of the articular facet of the *os malleolare* plotted against the ratio between the length and the breadth of the articular facet of the *os malleolare*. Symbols explained in Fig. 3.234.

3rd Phalanx

Only two archaeological 3rd phalanges had been found and attributed, on the basis of their morphology, to sheep. Such identification is supported by the biometry (Fig. 3.279). Both archaeological sheep plot clearly in the sheep area showing to be consistent with their morphological identifications.

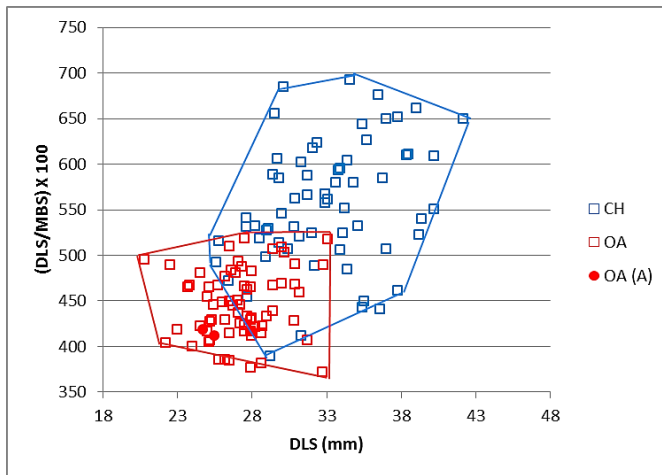


Figure 3.279 Greatest diagonal length of the sole plotted against a ratio between the greatest diagonal length of the sole and the middle breadth of the sole. Symbols explained in Fig. 3.234.

Phase III

Horncores

No horncores have been found in this phase.

Scapula

Only one scapula was recorded and identified as sheep. Figure 3.280 shows that the archaeological sheep falls among the modern goat cluster but not too far from the modern sheep specimens. As no other BI could be used, the evidence is not conclusive and the specimen cannot be confidently considered to have been misidentified.

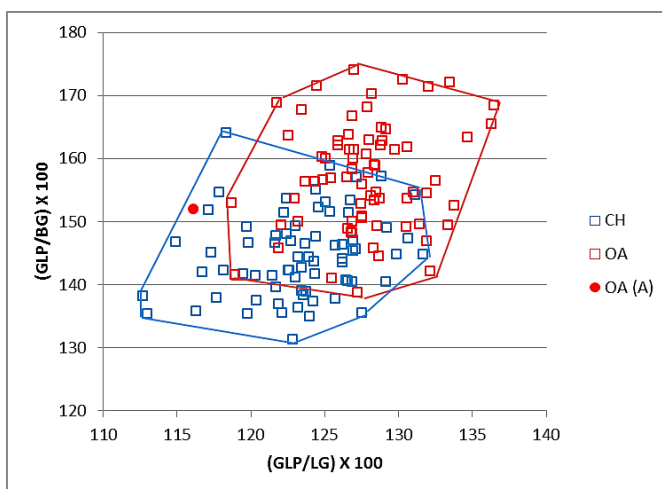


Figure 3.280 Ratio between the greatest length of the *processus articularis* and the length of the glenoid cavity plotted against the ratio between the greatest length of the *processus articularis* and the breadth of the glenoid cavity. Symbols explained in Fig. 3.234.

Humerus

No archaeological humeri have been attributed to goat. Figures 3.281 to 3.284 show that all the archaeological sheep fall among the modern sheep group or in the area of overlap between the two species, confirming the morphological identifications. The unidentified specimen plots in the area of overlap (Fig. 3.281) as such, it remains of uncertain attribution.

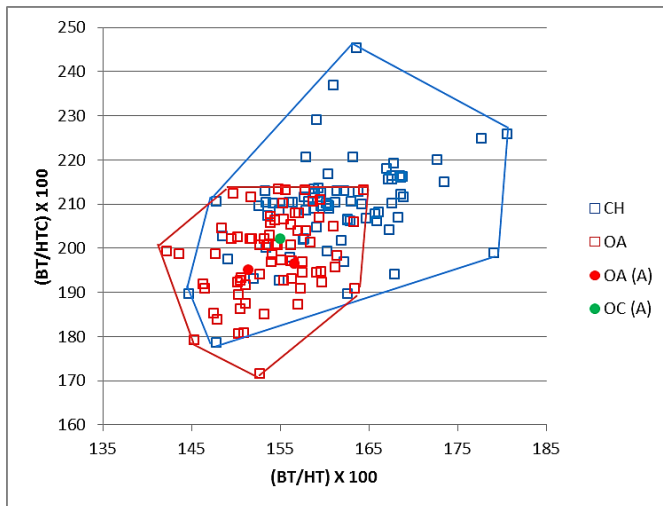


Figure 3.281 Ratio between the medio lateral width of the trochlea and its height plotted against the medio lateral width of the trochlea and the diameter of the trochlear constriction. Symbols explained in Fig. 3.234.

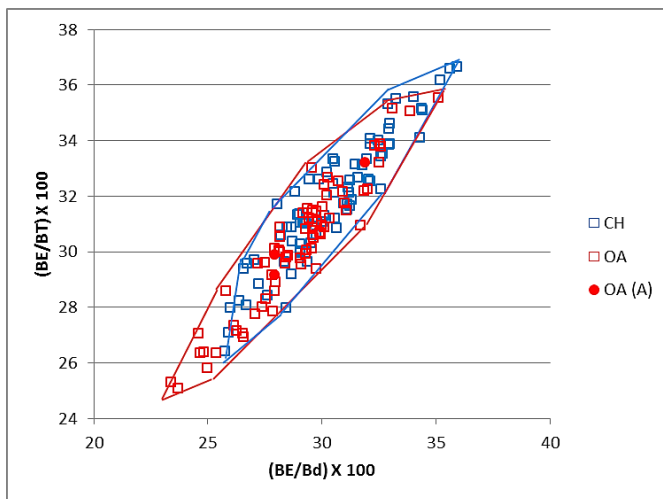


Figure 3.282 Ratio between the breadth of the *capitulum* and the distal width plotted against the ratio between the breadth of the *capitulum* and the medio lateral width of the trochlea. Symbols explained in Fig. 3.234.

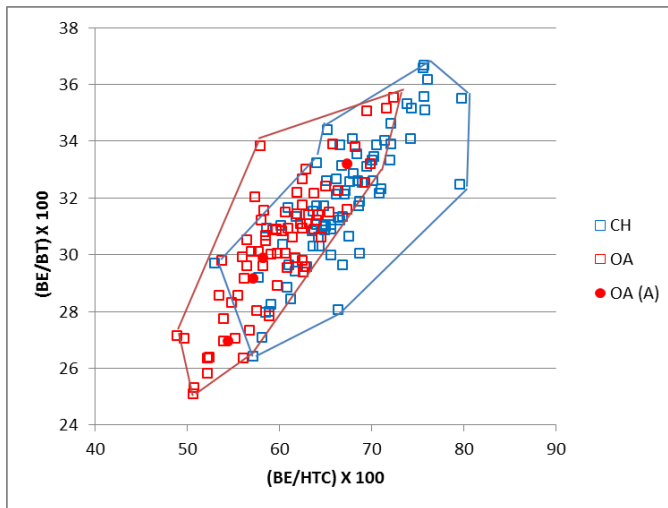


Figure 3.283 Ratio between the breadth of the *capitulum* and the diameter of the trochlear constriction plotted against the ratio between the breadth of the *capitulum* and the medio lateral width of the trochlea. Symbols explained in Fig. 3.234.

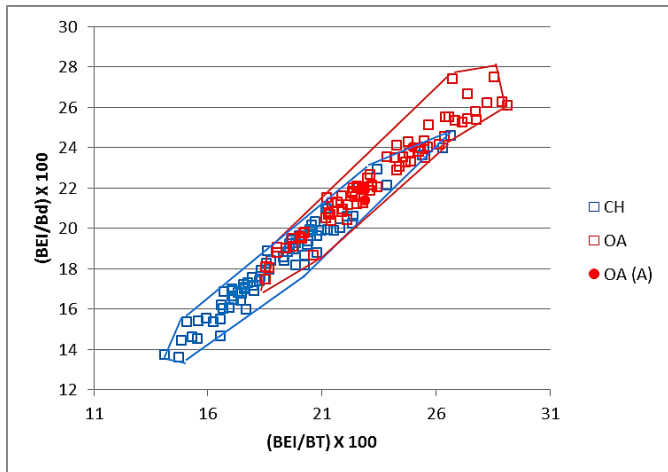


Figure 3.284 Ratio between the breadth of the *epicondyle lateralis* and the medio lateral width of the trochlea plotted against the ratio between the breadth of the *epicondyle lateralis* and the width of the distal end. Symbols explained in Fig. 3.234.

Radius

Only one radius has been recorded and attributed to the sheep on the basis of its morphology. Figure 3.285 shows that biometry confirms the morphological identification: the archaeological sheep falls in the middle of the sheep cluster and only marginally in the area of overlap of the two modern groups.

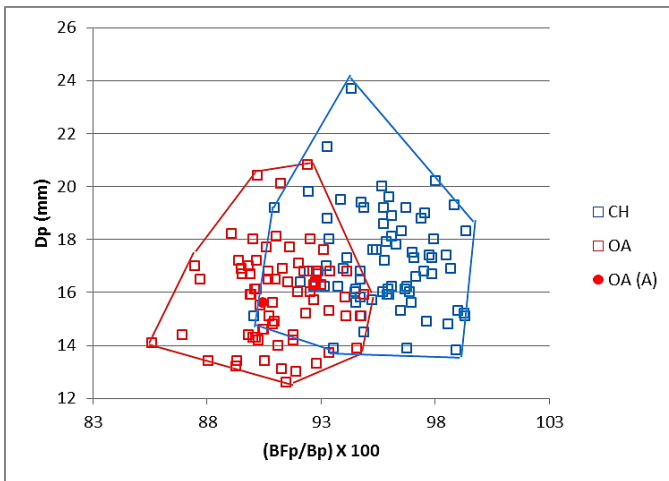


Figure 3.285 Ratio between the greatest length of the *facies articularis proximalis* and the greatest breadth of the proximal end plotted against the depth of the proximal end. Symbols explained in Fig. 3.234.

Metapodials

Clear agreement is present between the biometrical and the morphological identifications for the metapodials. Figures 3.286 to 3.290 show that in all BI the sheep metapodials consistently plot together with the modern sheep or in the area of overlap between the two groups, giving no reasons to doubt the original identifications.

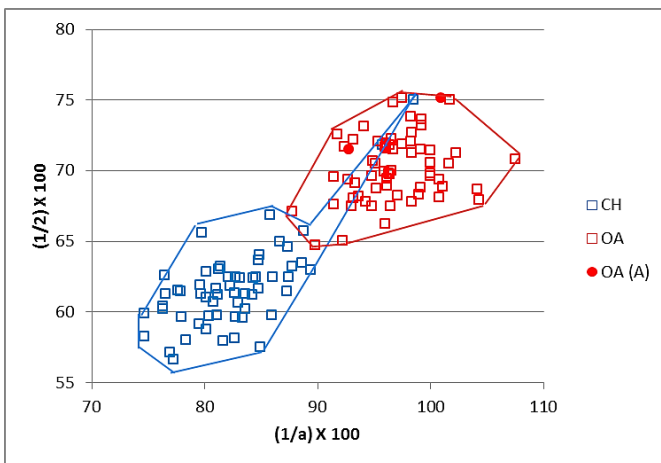


Figure 3.286 Metacarpal. Ratio between the diameter of the medial trochlea and the width of the medial condyle plotted against the ratio between the diameter of the *verticillus* at the medial condyle and the diameter of the medial trochlea. Symbols explained in Fig. 3.234.

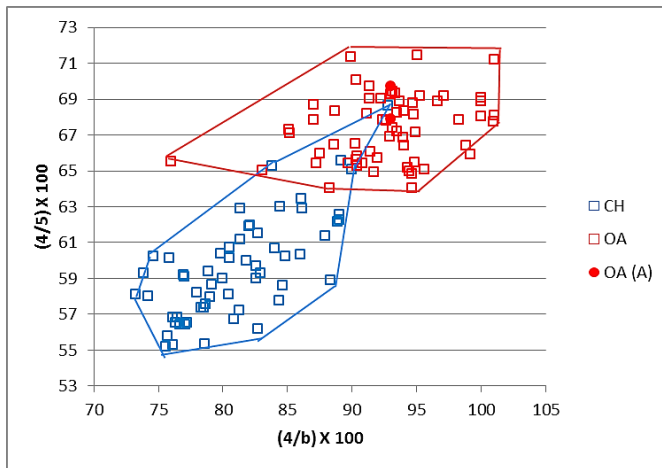


Figure 3.287 Metacarpal. Ratio between the width of the lateral condyle and the diameter of the lateral trochlea plotted against the ratio between the diameter of the *verticillus* on the lateral condyle and the diameter of the lateral condyle. Symbols explained in Fig. 3.234.

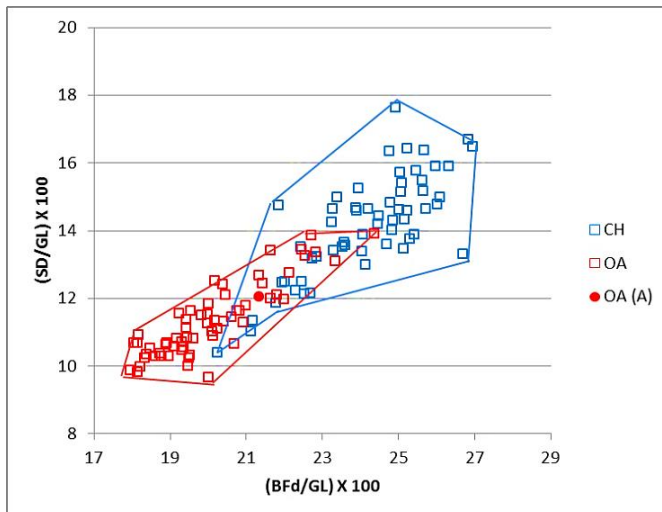


Figure 3.288 Metacarpal. Ratio between the greatest breadth of the distal end with the greatest length plotted against the ratio between the smallest width of the shaft and the greatest length. Symbols explained in Fig. 3.234.

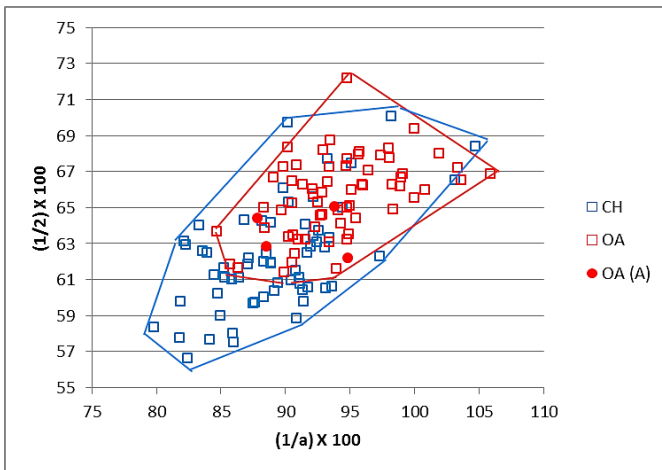


Figure 3.289 Metatarsal. Ratio between the diameter of the medial trochlea and the width of the medial condyle plotted against the ratio between the diameter of the *verticillus* at the medial condyle and the diameter of the medial trochlea. Symbols explained in Fig. 3.234.

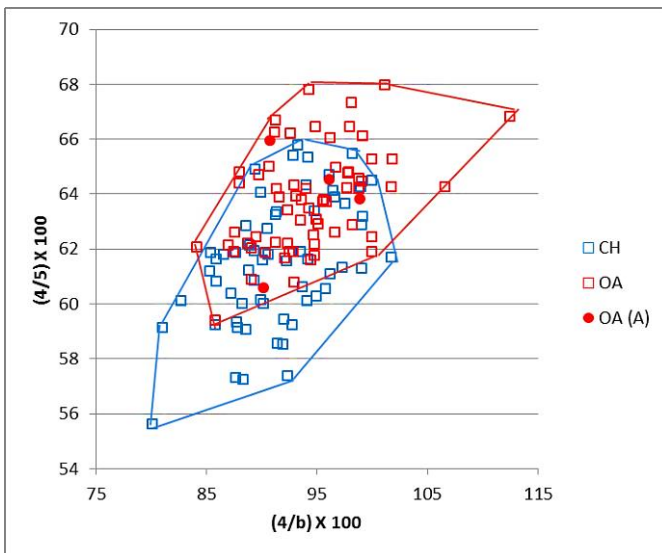


Figure 3.290 Metatarsal. Ratio between the width of the lateral condyle and the diameter of the lateral trochlea plotted against the ratio between the diameter of the *verticillus* on the lateral condyle and the diameter of the lateral condyle. Symbols explained in Fig. 3.234.

Tibia

Only two archaeological tibiae were recorded. One has been attributed morphologically to sheep and clearly follows the sheep pattern (Fig. 3.291). The other one, which is an unidentified specimen, cannot be certainly assigned as it is border-line and falls between the two groups.

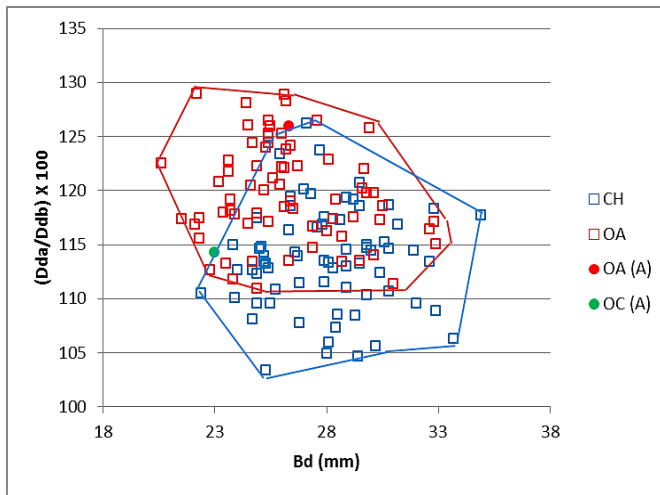


Figure 3.291 Breadth of the distal end plotted against the ratio between the depth of the medial (a) and lateral (b) side. Symbols explained in Fig. 3.234.

Astragalus

No archaeological goat astragali have been identified morphologically. Figures 3.292 to 3.295 attest to the degree to which biometrical and morphological identifications agree: both the archaeological sheep specimens lay within the modern sheep cluster or in the area of overlap, showing to be consistent with the sheep pattern.

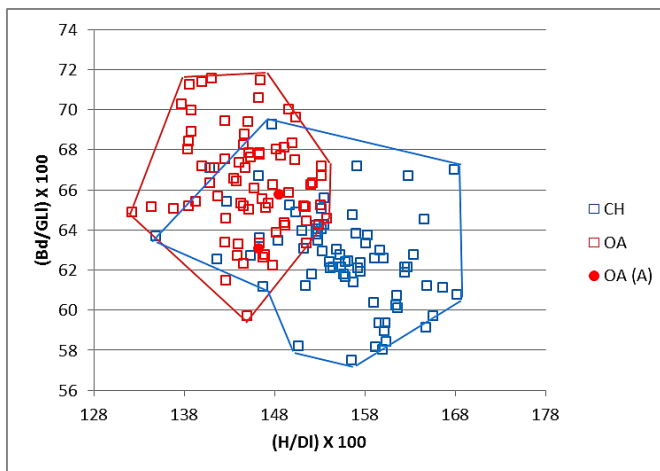


Figure 3.292 Ratio between height at the central constriction and the greatest depth of the lateral half plotted against a ratio between the breadth of the distal end and the greatest length of the lateral half. Symbols explained in Fig. 3.234.

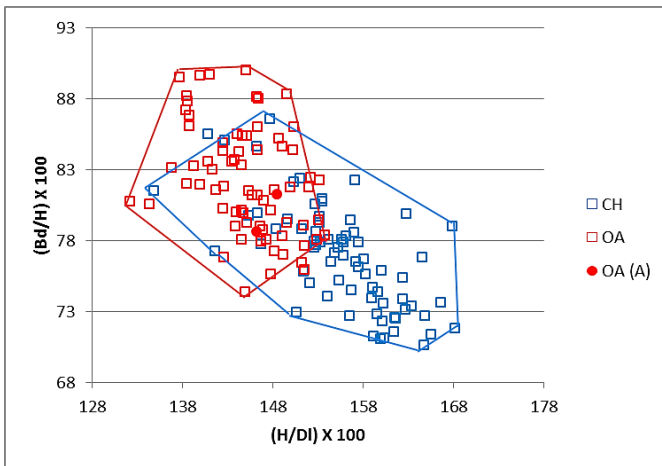


Figure 3.293 Ratio between height at the central constriction and the greatest depth of the lateral half plotted against the ratio between the breadth of the distal end and the height at the central constriction. Symbols explained in Fig. 3.234.

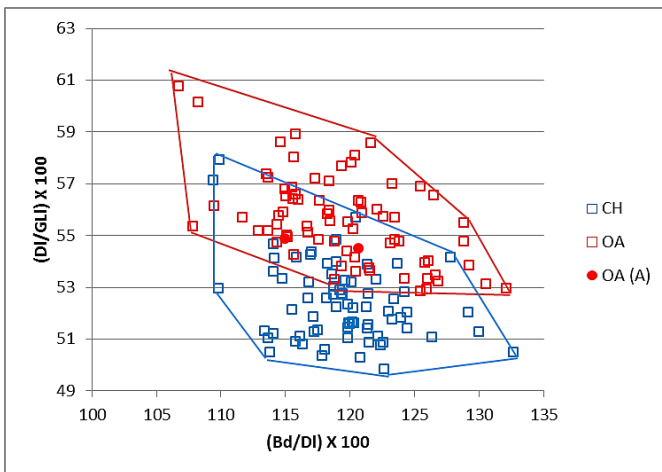


Figure 3.294 Ratio between breadth of the distal end and the greatest depth of the lateral half plotted against the ratio between the breadth of the distal end and the greatest depth of the lateral half. Symbols explained in Fig. 3.234.

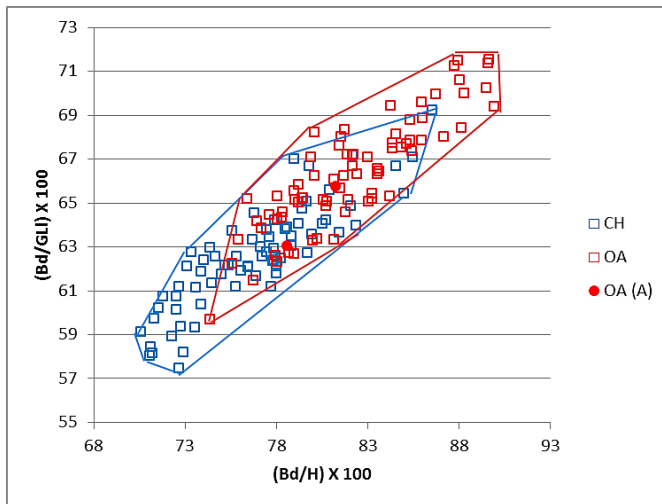


Figure 3.295 Ratio between the breadth of the distal end and the height at the central constriction and the ratio between height at the central constriction and the greatest depth of the lateral half. Symbols explained in Fig. 3.234.

3rd Phalanx

Only one 3rd phalanx has been recorded and identified as sheep, according to its morphological traits. Such a result is confirmed by biometry. Figure 3.296 shows that the sheep specimen is consistent with the sheep pattern falling in the middle of the sheep distribution and only marginally in the area of overlap between the two species.

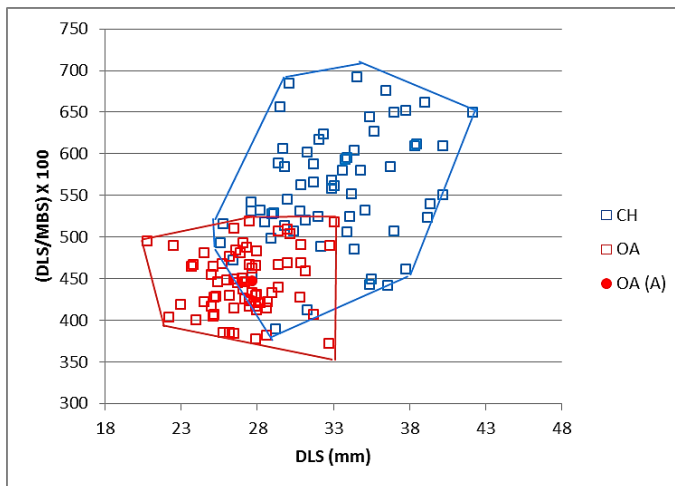


Figure 3.296 Greatest diagonal length of the sole plotted against a ratio between the greatest diagonal length of the sole and the middle breadth of the sole. Symbols explained in Fig. 3.234.

Unstratified

Horncore

In Figures 3.297 and 3.298 two groups can be seen: the archaeological goat falls in the area of overlap or amongst the modern counterparts while the archaeological sheep follow clearly the sheep pattern. Thus the morphological identifications are confirmed.

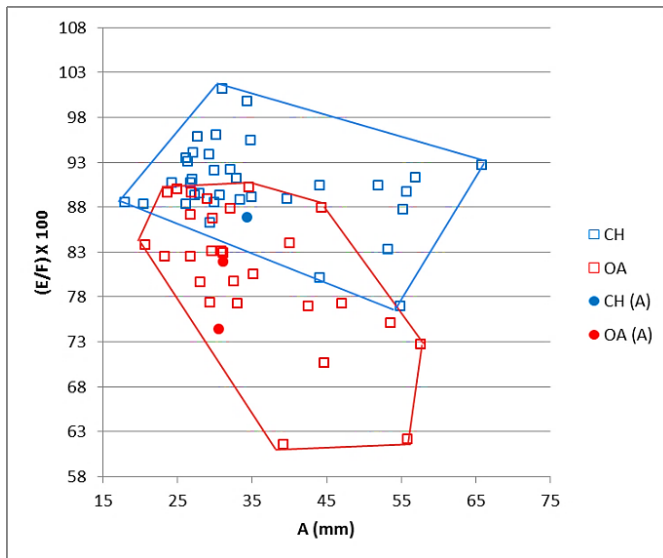


Figure 3.297 Maximum diameter taken at the base plotted against a ratio between the length and the length of the outer curvature of the horncore. Symbols explained in Fig. 3.234.

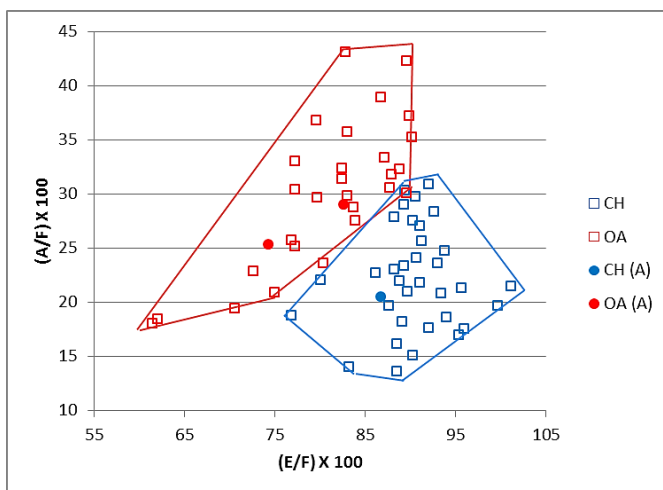


Figure 3.298 Ratio between the length and the length of the outer curvature plotted against the ratio between the maximum diameter taken at the base and the length of the outer curvature of the horncore. Symbols explained in Fig. 3.234.

Scapula

No scapulae have been assigned morphologically to the goat. These results are definitely supported by Figures 3.299 and 3.300. The archaeological sheep all fall among the modern sheep group or in the area of overlap between the two species. The unidentified specimens seem to be more consistent with the sheep pattern despite falling in the area of overlap or close to it. Two archaeological sheep plot at the top of the sheep group showing very marked sheep features.

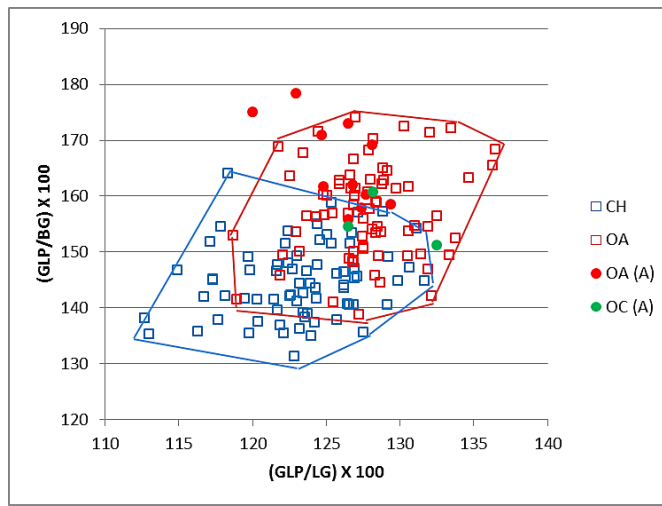


Figure 3.299 Ratio between the greatest length of the *processus articularis* and the length of the glenoid cavity plotted against the ratio between the greatest length of the *processus articularis* and the breadth of the glenoid cavity. Symbols explained in Fig. 3.234.

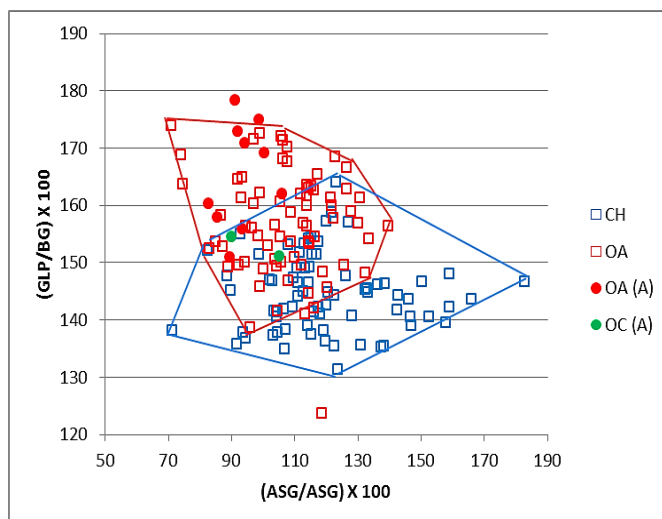


Figure 3.300 Ratio between the shortest distance from the base of the spine to the edge of the glenoid cavity and the smallest length of the *collum scapulae* plotted against a ratio between the greatest length of the *processus articularis* and the breadth of the glenoid cavity. Symbols explained in Fig. 3.234.

Humerus

No archaeological humeri were assigned to *Capra*. Figures 3.301 to 3.304 show that, by and large, all the archaeological sheep fall within the sheep cluster. In Figure 3.301, one archaeological sheep plots in the goat range, but it is not an outlier from the other sheep and therefore cannot be confidently reclassified. In Figures 3.302, 3.303 and 3.304 some archaeological sheep fall out of the sheep modern group range, clearly exhibiting sheep traits. In all Figures, but in Figure 3.301 in particular, the specimens plot in a very compact cluster, showing their morphological homogeneity despite the uncertain chronology. The only unidentified specimen falls within the ample area of overlap, and thus biometry cannot assist in attributing it to species.

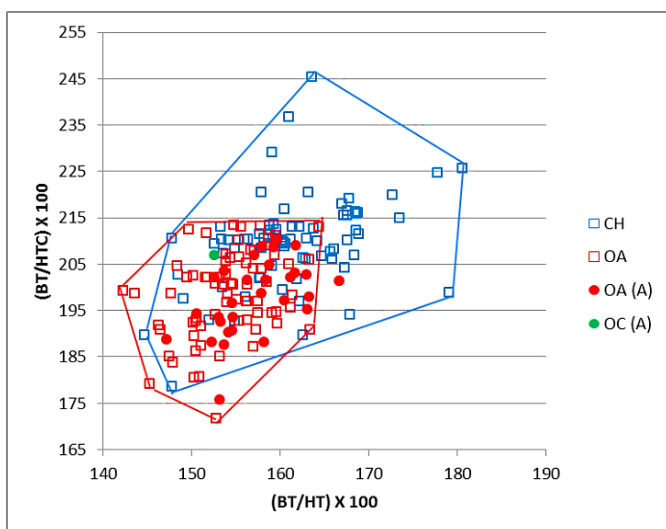


Figure 3.301 Ratio between the medio lateral width of the trochlea and its height plotted against the medio lateral width of the trochlea and the diameter of the trochlear constriction. Symbols explained in Fig. 3.234.

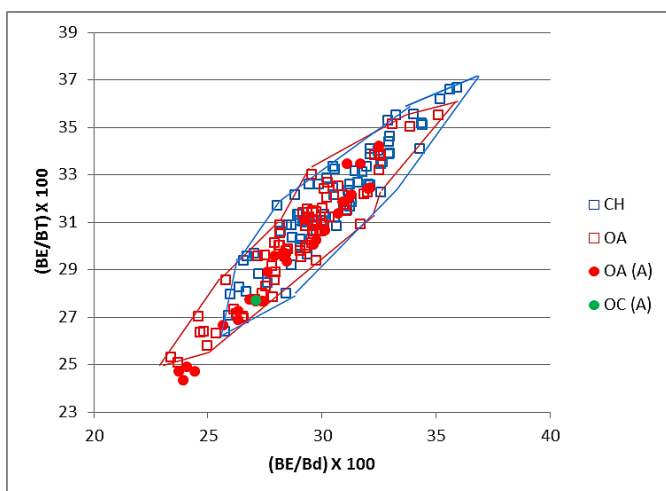


Figure 3.302 Ratio between the breadth of the *capitulum* and the distal width plotted against the ratio between the breadth of the *capitulum* and the medio lateral width of the trochlea. Symbols explained in Fig. 3.234.

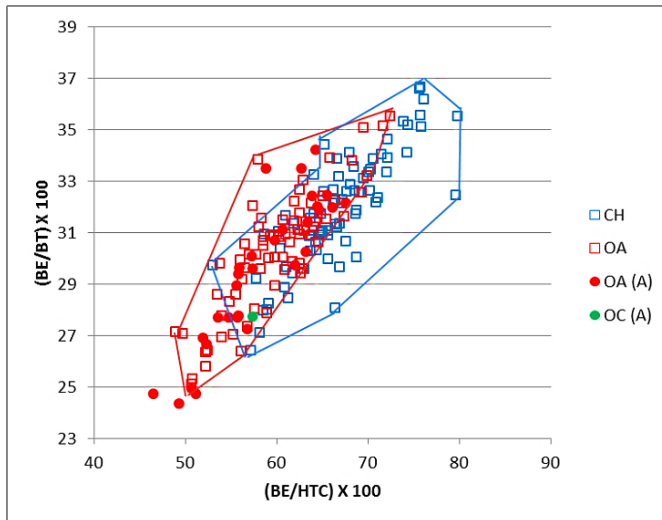


Figure 3.303 Ratio between the breadth of the *capitulum* and the diameter of the trochlear constriction plotted against the ratio between the breadth of the *capitulum* and the medio lateral width of the trochlea. Symbols explained in Fig. 3.234.

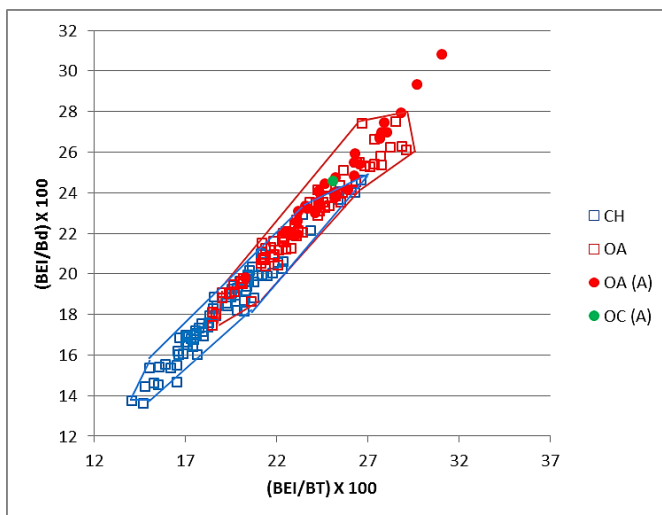


Figure 3.304 Ratio between the breadth of the *epicondyle lateralis* and the medio lateral width of the trochlea plotted against the ratio between the breadth of the *epicondyle lateralis* and the width of the distal end. Symbols explained in Fig. 3.234.

Radius

No archaeological goats were identified on the basis of the morphology. The sheep mostly fall among the modern sheep group or in the area of overlap, which supports their morphological identifications. One archaeological sheep is border-line with the goat group but, considering that the specimen does not fall far from the archaeological sheep cluster, it likely represents ordinary variation within the sheep group (Fig. 3.305).

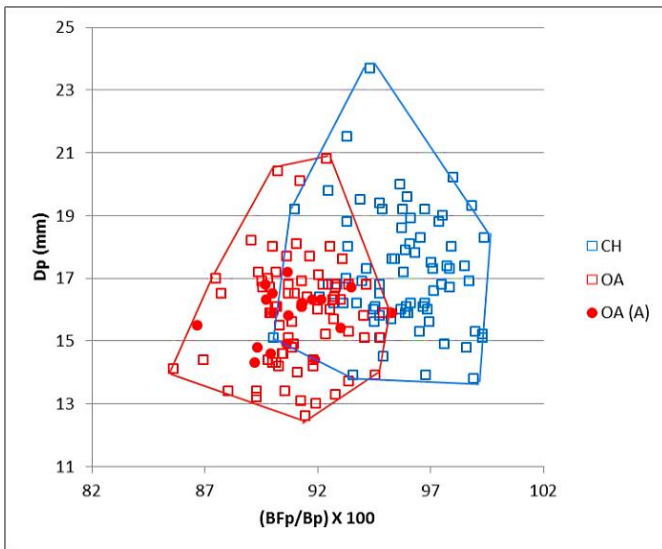


Figure 3.305 Ratio between the greatest length of the *facies articularis proximalis* and the greatest breadth of the proximal end plotted against the depth of the proximal end. Symbols explained in Fig. 3.234.

Ulna

Only archaeological sheep ulnae and one unidentified specimen have been recorded. Figure 3.306 shows that the archaeological sheep specimens are consistent with the sheep pattern, with some showing particularly strong sheep traits (bottom-left angle of the graph). The unidentified specimen falls in the overlap area as such it must remain unidentified.

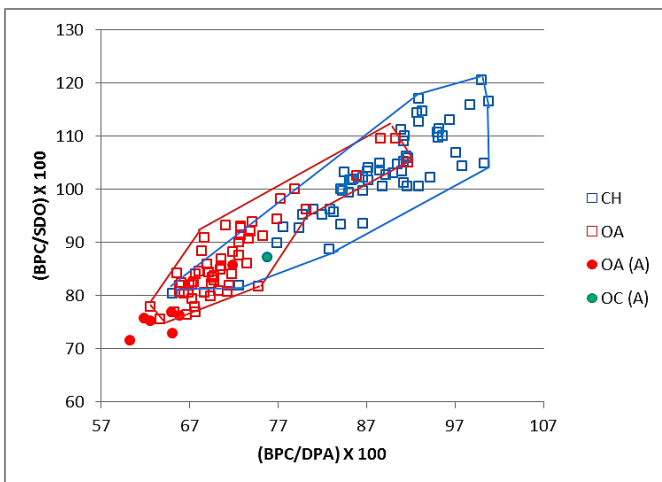


Figure 3.306 Ratio between the breadth across the coronoid process and the depth across the *processus anconaeus* to the caudal border plotted against the breadth across the coronoid process and the smallest depth of the olecranon. Symbols explained in Fig. 3.234.

Metapodials

No *Capra* metacarpals were identified on the basis of the morphological traits but one goat metatarsal was recorded. Figures 3.307 to 3.312 show that almost all the archaeological sheep fall in the area occupied by the modern sheep (mainly metacarpals) or in the area of overlap between the modern groups (mainly metatarsals), attesting their consistency with the morphological identifications.

Figures 3.307 and 3.308 (for the metacarpals) and Figures 3.310 and 3.311 (for the metatarsals) show a couple of specimens marginally plotting out of the sheep area: they show to have strongly expressed sheep traits. The identification of the goat metatarsal (Figs. 3.310 to 3.311) is confirmed by the biometry since the specimen falls in the area of overlap between the two modern groups, but also in the middle of the goat cluster.

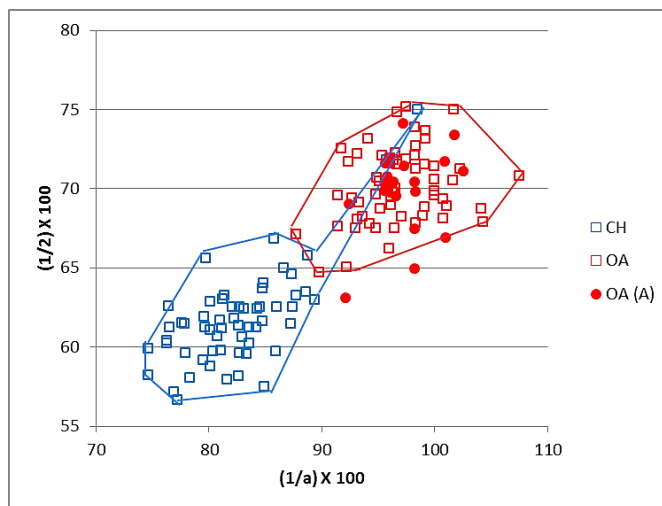


Figure 3.307 Metacarpal. Ratio between the diameter of the medial trochlea and the width of the medial condyle plotted against the ratio between the diameter of the *vericillus* at the medial condyle and the diameter of the medial trochlea. Symbols explained in Fig. 3.234.

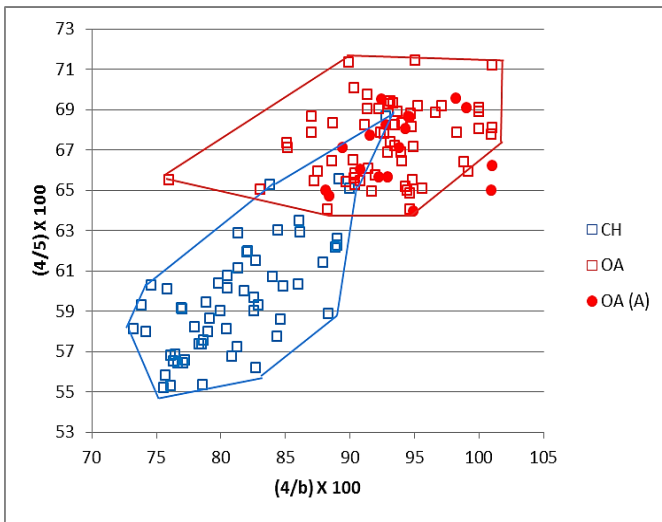


Figure 3.308 Metacarpal. Ratio between the width of the lateral condyle and the diameter of the lateral trochlea plotted against the ratio between the diameter of the *verticillus* on the lateral condyle and the diameter of the lateral condyle. Symbols explained in Fig. 3.234.

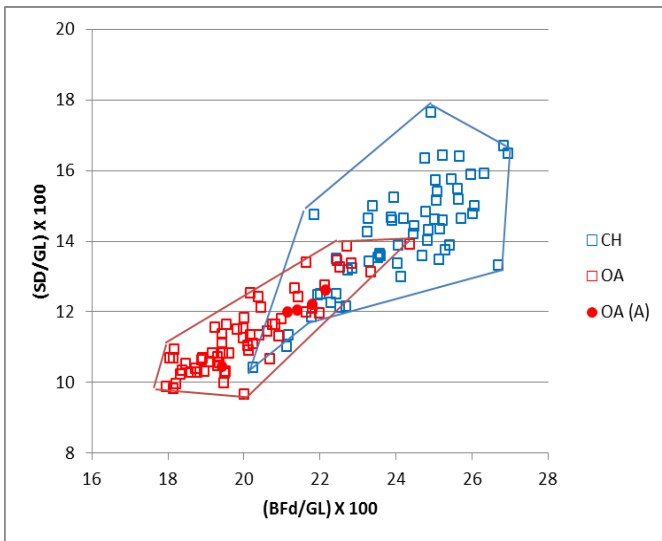


Figure 3.309 Metacarpal. Ratio between the greatest breadth of the distal end with the greatest length plotted against the ratio between the smallest width of the shaft and the greatest length. Symbols explained in Fig. 3.234.

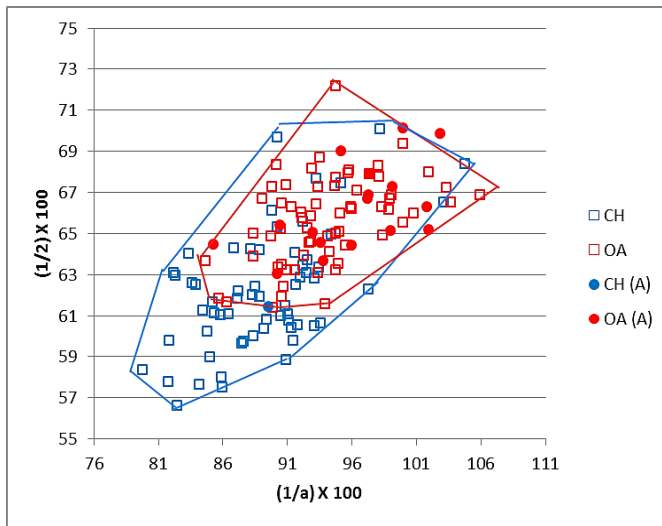


Figure 3.310 Metatarsal. Ratio between the diameter of the medial trochlea and the width of the medial condyle plotted against the ratio between the diameter of the *verticillus* at the medial condyle and the diameter of the medial trochlea. Symbols explained in Fig. 3.234.

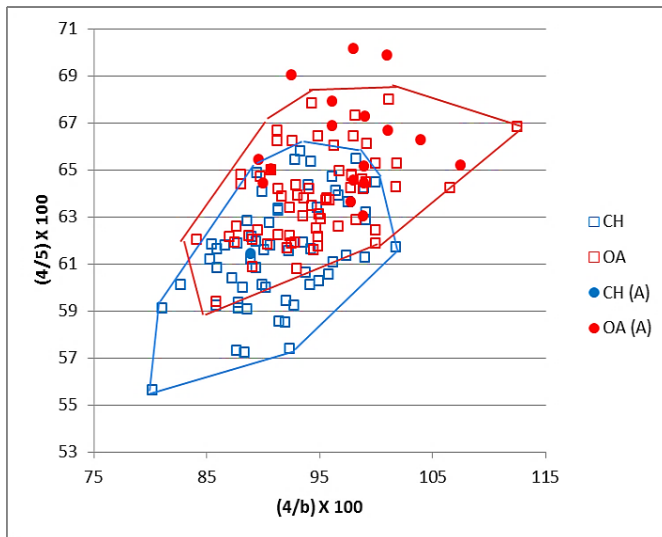


Figure 3.311 Metatarsal. Ratio between the width of the lateral condyle and the diameter of the lateral trochlea plotted against the ratio between the diameter of the *verticillus* on the lateral condyle and the diameter of the lateral condyle. Symbols explained in Fig. 3.234.

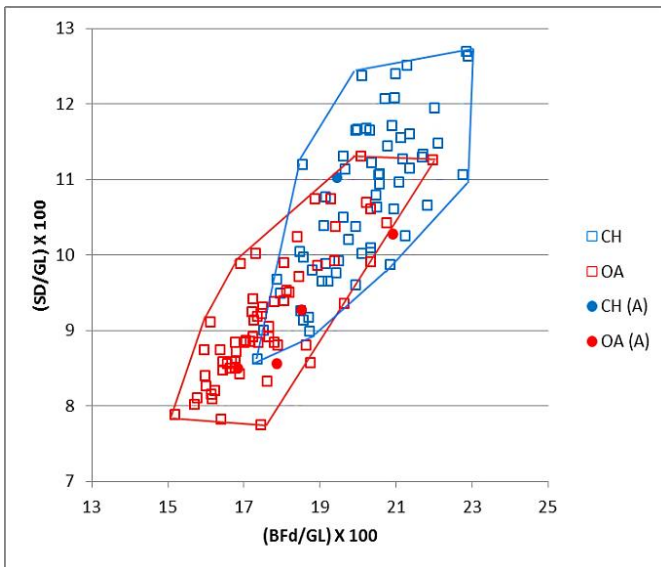


Figure 3.312 Metatarsal. Ratio between the greatest breadth of the distal end with the greatest length plotted against the ratio between the smallest width of the shaft and the greatest length. Symbols explained in Fig. 3.234.

Tibia

No tibiae have been assigned to goat. Figure 3.313 might shows that most of the archaeological sheep plot in a tight group that falls amongst the modern sheep or in the area of overlap, confirming their identification. One sheep, however, clearly falls among the goats, due to the shape (Dd(a)/Dd(b)) rather than size (Bd). Tentatively, we must consider it to be a goat. The six unidentified specimens fall in the middle of the sheep range. Since they are close or within the area of overlap it is difficult to be completely confident about their identification, but they do look much more like sheep than goat.

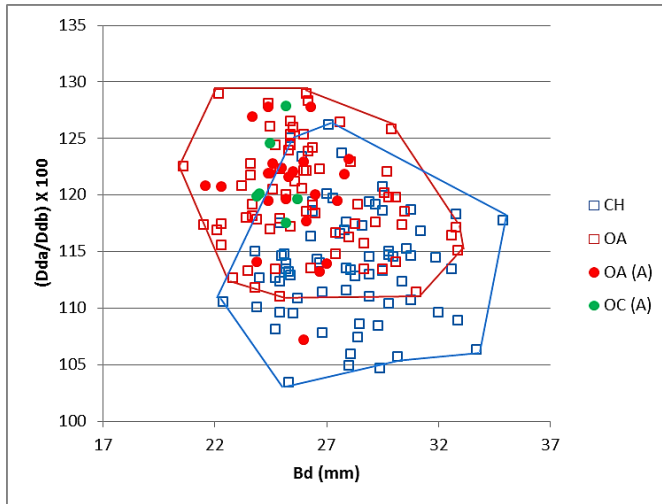


Figure 3.313 Breadth of the distal end plotted against the ratio between the depth of the medial (a) and lateral (b) side. Symbols explained in Fig. 3.234.

Astragalus

No archaeological *Capra* astragali were identified according to their morphology. Figures 3.314 to 3.317 show that the biometrical data support the morphological identifications: all the archaeological sheep occupy the area of overlap between the two groups, confirming their identifications.

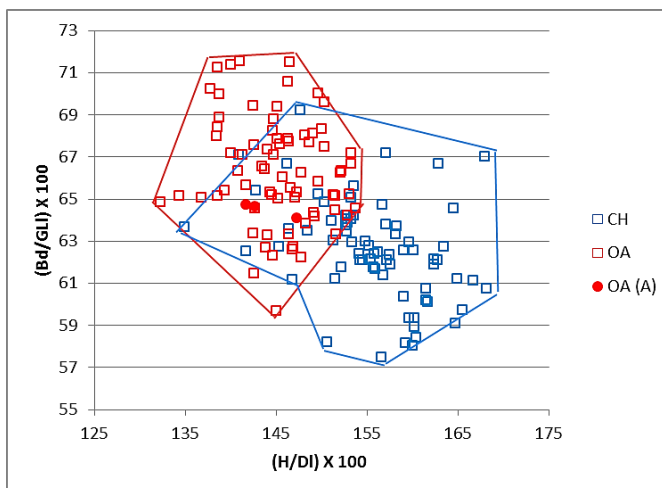


Figure 3.314 Ratio between height at the central constriction and the greatest depth of the lateral half plotted against a ratio between the breadth of the distal end and the greatest length of the lateral half. Symbols explained in Fig. 3.234.

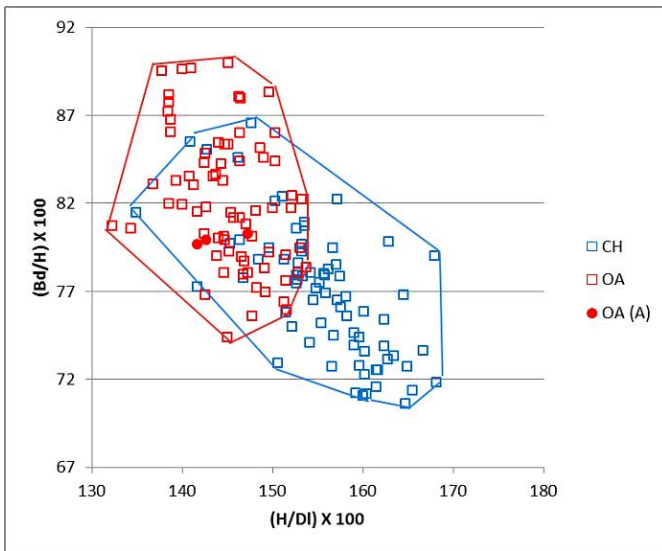


Figure 3.315 Ratio between height at the central constriction and the greatest depth of the lateral half plotted against the ratio between the breadth of the distal end and the height at the central constriction. Symbols explained in Fig. 3.234.

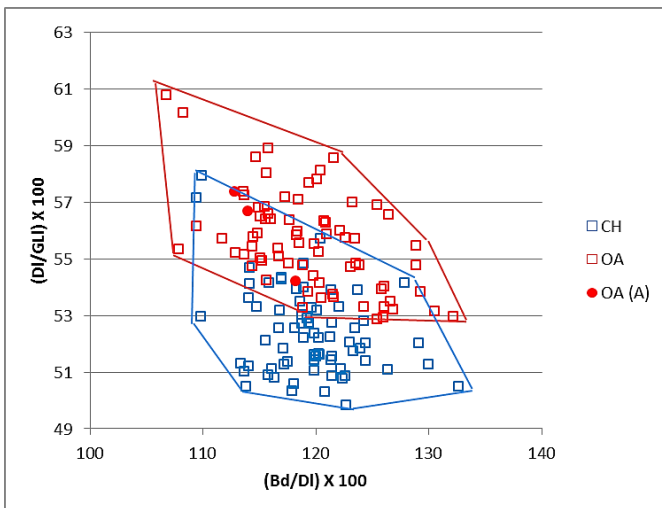


Figure 3.316 Ratio between breadth of the distal end and the greatest depth of the lateral half plotted against the ratio between the breadth of the distal end and the greatest depth of the lateral half. Symbols explained in Fig. 3.234.

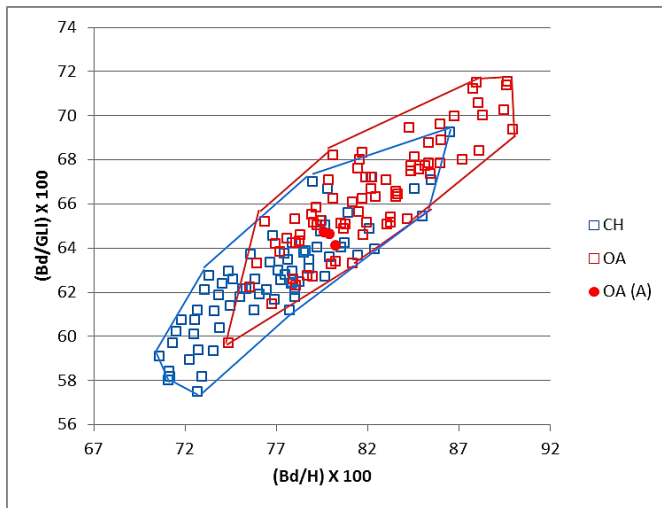


Figure 3.317 Ratio between the breadth of the distal end and the height at the central constriction and the ratio between height at the central constriction and the greatest depth of the lateral half. Symbols explained in Fig. 3.234.

Calcaneum

Figures 3.318 to 3.32 show that all the archaeological specimens identified as sheep occupy the central area of the sheep distribution though they are also close to the area of overlap between the two modern groups. All in all, the biometrical data support the morphological identifications. The only unidentified specimen plots very close to the others, but since it falls in the area of overlap between the two modern groups, it cannot be confidently classified.

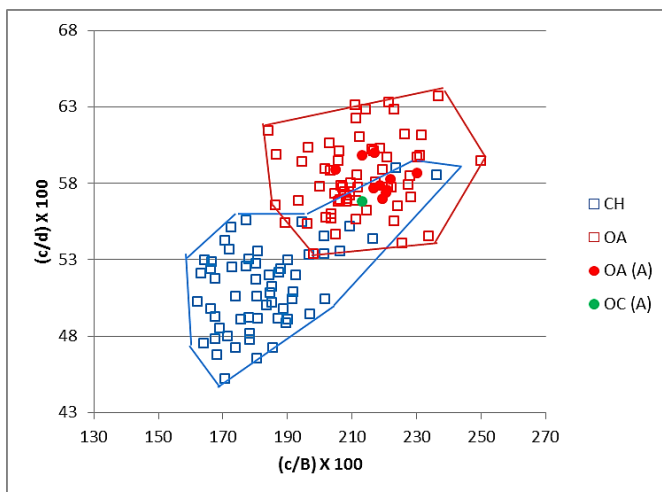


Figure 3.318 Ratio between the length and the breadth of the articular facet of the *os malleolare* plotted against the ratio between the length of the articular facet of the *os malleolare* and the length taken from the articular facet of the *os malleolare* to the end of the articulation-free part of the process. Symbols explained in Fig. 3.234.

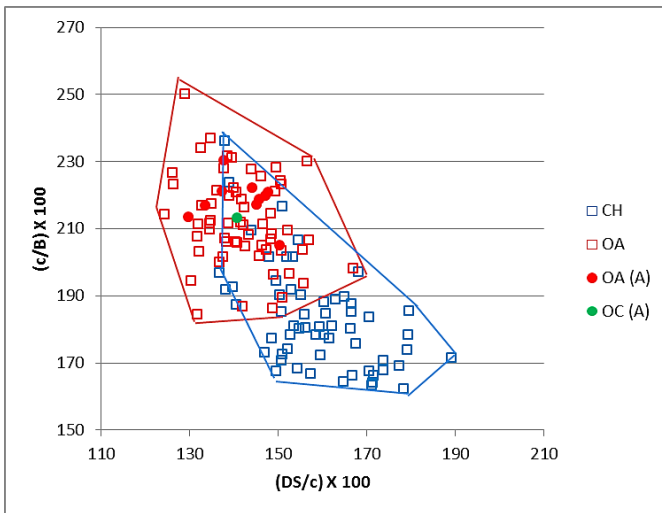


Figure 3.319 Ratio between the depth of the *substantaculum tali* and the length of the articular facet of the *os malleolare* plotted against the ratio between the length and the breadth of the articular facet of the *os malleolare*. Symbols explained in Fig. 3.234.

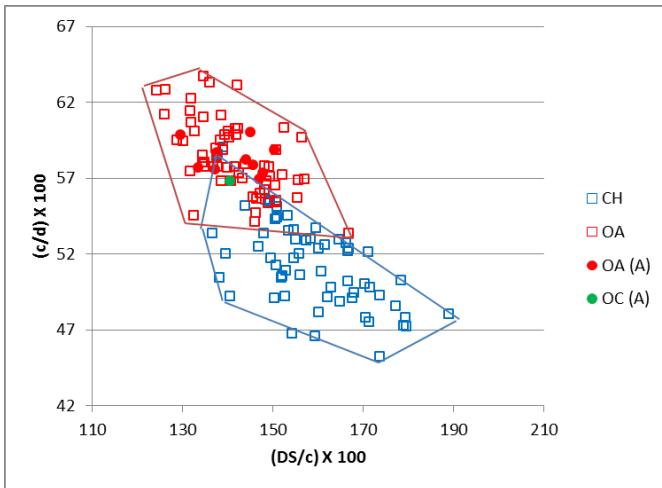


Figure 3.320 Ratio between the depth of the *substantaculum tali* and the length of the articular facet of the *os malleolare* plotted against the ratio between the length and the breadth of the articular facet of the *os malleolare*. Symbols explained in Fig. 3.234.

3rd Phalanx

The only 3rd phalanx found has been morphologically attributed to sheep and biometry, as Figure 3.321 displays, supports this identification.

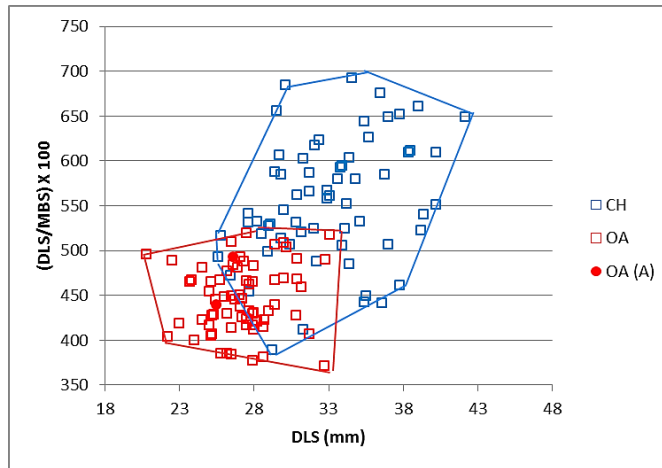


Figure 3.321 Greatest diagonal length of the sole plotted against a ratio between the greatest diagonal length of the sole and the middle breadth of the sole. Symbols explained in Fig. 3.234.

As previously seen with the other archaeological cases, the study of the Biometrical Indices reveals that the modern material is a very good model for comparison with the archaeological material. The effectiveness of the combination of morphology and biometry is once again demonstrated. At Woolmonger Street/Kingswell Street biometry generally supports and reinforces what was already observed through the morphological analysis. Sheep specimens outnumber goats' in all chronological phases and for all the anatomical elements. The biometry has also pointed to the occurrence of some additional cases of potential goat specimens, but these are very few and do not alter the overall pattern.

3.4.8 Discriminant Analysis

As for the previous archaeological cases, Discriminant Analysis (DA) was carried out on the combined phases of the Woolmonger Street/Kingswell Street sheep/goat assemblage, following the same procedures explained in Sections 3.2.5 and 3.3.4. To increase sample size, DA was in some cases rerun with the exclusion of some measurements.

Results on an element by element basis follow coupled with a series of diagrams. For an explanation of how the diagrams should be read see Section 3.2.9.

Horncores

The sample of complete horncores is unfortunately very small due to the high fragmentation of the material. As Table 3.136 shows, the results from the DA are highly consistent with the morphological identifications, reaching a value of 'correct' reattributions which is higher than the results obtained from the modern material (95.2%).

With the exclusion of measurements E and F, the degree of consistency decreases to 60% for the archaeological material, thus the effectiveness of DA on the horncores is compromised (Tab. 3.137).

Table 3.136 Results from the Discriminant Analysis when applied on all the archaeological horncores.

Classification Results ^{a,b,d}						
			TAXA	Predicted Group Membership		Total
				CH	OA	
Modern Material	Original	Count	CH	33	2	35
			OA	1	27	28
		%	CH	94.3	5.7	100.0
			OA	3.6	96.4	100.0
	Cross-validated ^c	Count	CH	33	2	35
			OA	1	27	28
		%	CH	94.3	5.7	100.0
			OA	3.6	96.4	100.0
Woolmonger Material	Original	Count	CH	1	0	1
			OA	0	2	2
		%	CH	100.0	.0	100.0
			OA	.0	100.0	100.0
a. 95.2% of selected original grouped cases correctly classified.						
b. 100.0% of unselected original grouped cases correctly classified.						
d. 95.2% of selected cross-validated grouped cases correctly classified. Cross validation is done only for those cases in the analysis. In cross validation, each case is classified by the functions derived from all cases other than that case.						

Table 3.137 Results from the Discriminant Analysis when applied on all the archaeological horncores, excluding variables E and F.

Classification Results ^{a,b,d}						
			TAXA	Predicted Group Membership		Total
				CH	OA	
Modern Material	Original	Count	CH	25	10	35
			OA	2	26	28
		%	CH	71.4	28.6	100.0
			OA	7.1	92.9	100.0
	Cross-validated ^c	Count	CH	25	10	35
			OA	3	25	28
		%	CH	71.4	28.6	100.0
			OA	10.7	89.3	100.0
Woolmonger Material	Original	Count	CH	1	0	1
			OA	2	2	4
		%	CH	100.0	.0	100.0
			OA	50.0	50.0	100.0
a. 81.0% of selected original grouped cases correctly classified.						
b. 60.0% of unselected original grouped cases correctly classified.						
d. 79.4% of selected cross-validated grouped cases correctly classified. Cross validation is done only for those cases in the analysis. In cross validation, each case is classified by the functions derived from all cases other than that case.						

Figure 3.322 shows that, when all measurements are included, no specimens are ‘wrongly’ re-attributed by the DA. All the morphologically identified sheep and goat specimens gather around the group centroid lines of the correct taxa.

Two morphologically identified sheep specimens are reclassified as ‘goat’ when E and F are excluded (Fig. 3.323), which is not surprising as less information is available to the DA. Clearly, as mentioned, the exclusion of E and F has an impact on the discrimination power of the function. Considering the small sample size and the fact that no possible misidentified specimens have been observed with the use of the BI (Figs. 3.234 to 3.235 but also 3.297 and 3.298), the reclassifications carried out by the DA are likely to be a product of the DA bias.

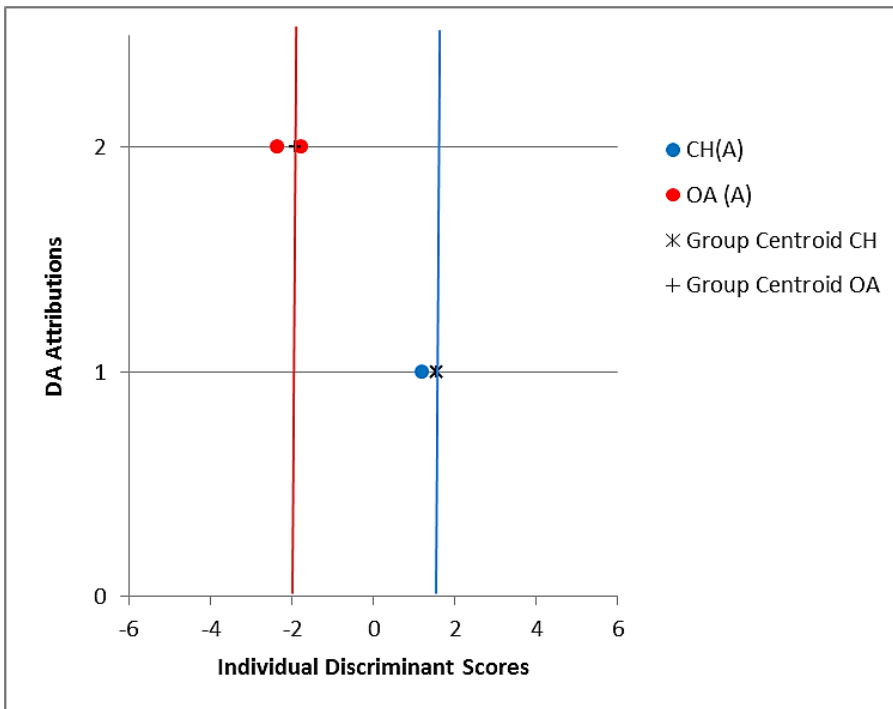


Figure 3.322 Diagram of the individual discriminant scores attributed to the archaeological material by DA for the horncore.

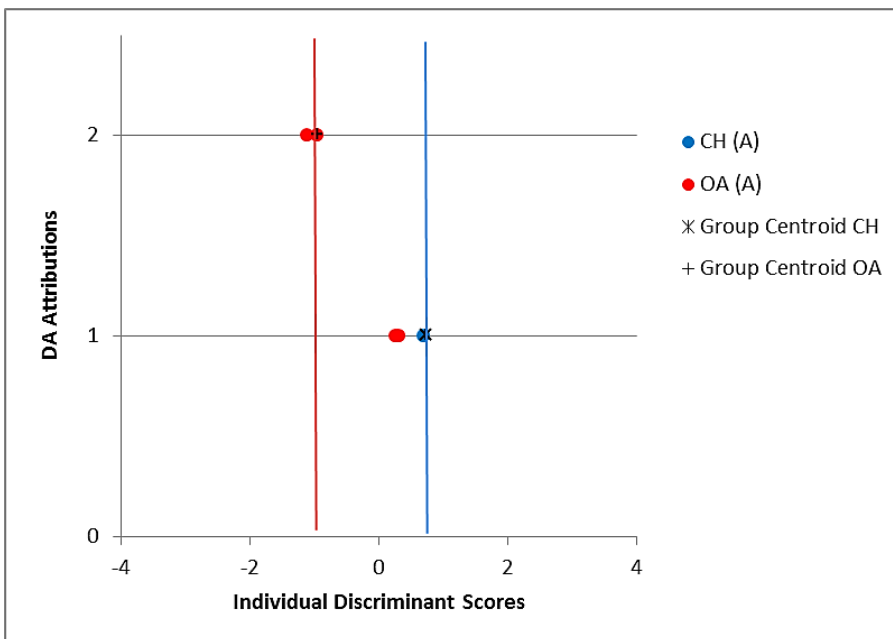


Figure 3.323 Diagram of the individual discriminant scores attributed to the archaeological material by DA for the horncore when variables E and F were excluded.

Scapula

The degree of agreement between morphological and biometrical identifications for this element is higher (100%) than that provided by the modern material (86.4%) (Tab. 3.138). No

specimens have been ‘misattributed’ by the DA. Of the six unidentified specimens, one has been identified as goat and five as sheep.

Figure 3.324 shows that all the morphologically identified sheep gather around the group centroid of the sheep group. Most morphologically unidentified specimens also plot close to the sheep group centroid, while one (from phase II) coincides almost exactly with the goat centroid. Considering the separation between this latter specimen and the sheep group, the DA identifications are likely to be genuine (see also Fig. 3.258).

Table 3.138 Results from the Discriminant Analysis when applied on all the archaeological scapulae.

Classification Results ^{a,b,d}						
			TAXA	Predicted Group Membership		Total
				CH	OA	
Modern Material	Original	Count	CH	64	10	74
			OA	10	63	73
		%	CH	86.5	13.5	100.0
			OA	13.7	86.3	100.0
	Cross-validated ^c	Count	CH	61	13	74
			OA	12	61	73
		%	CH	82.4	17.6	100.0
			OA	16.4	83.6	100.0
Woolmonger Material	Original	Count	CH	0	0	0
			OA	0	16	16
			OC	1	5	6
		%	CH	.0	.0	100.0
			OA	.0	100.0	100.0
			OC	16.7	83.3	100.0
a. 86.4% of selected original grouped cases correctly classified.						
b. 100.0% of unselected original grouped cases correctly classified.						
d. 83.0% of selected cross-validated grouped cases correctly classified. Cross validation is done only for those cases in the analysis. In cross validation, each case is classified by the functions derived from all cases other than that case.						

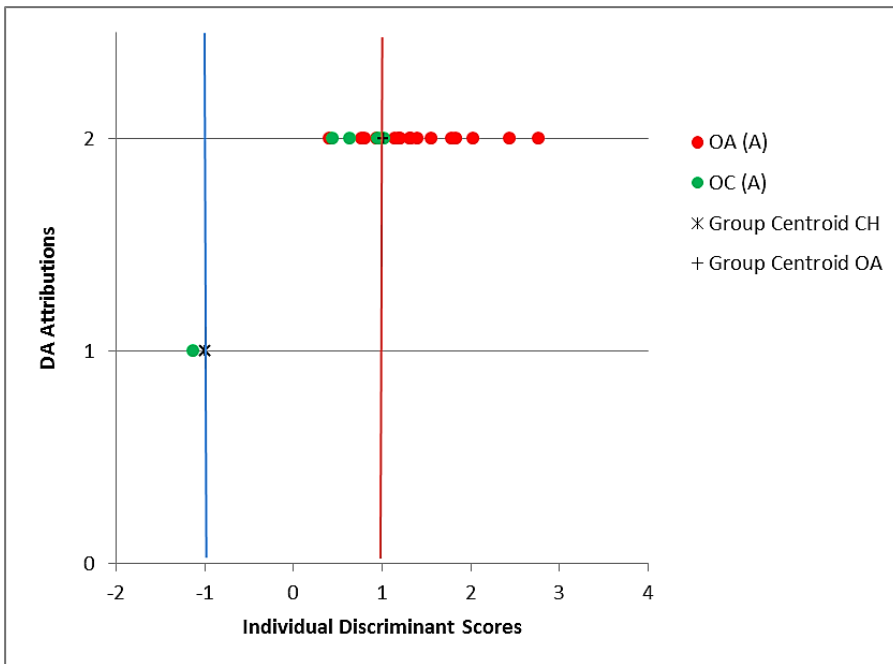


Figure 3.324 Diagram of the individual discriminant scores attributed to the archaeological material by DA for the scapula.

Humerus

The agreement between the morphological and biometrical identification is total, as attested by Table 3.139. No goat humeri have been found with any of the different methods used.

Table 3.139 Results from the Discriminant Analysis when applied on all the archaeological humeri.

Classification Results ^{a,b,d}						
			TAXA	Predicted Group Membership		Total
				CH	OA	
Modern Material	Original	Count	CH	67	9	76
			OA	8	62	70
		%	CH	88.2	11.8	100.0
			OA	11.4	88.6	100.0
	Cross-validated ^c	Count	CH	66	10	76
			OA	10	60	70
		%	CH	86.8	13.2	100.0
			OA	14.3	85.7	100.0
Woolmonger Material	Original	Count	CH	0	0	0
			OA	0	43	43
		%	CH	.0	.0	100.0
			OA	.0	100.0	100.0

a. 88.4% of selected original grouped cases correctly classified.

Classification Results ^{a,b,d}
b. 100.0% of unselected original grouped cases correctly classified.
d. 86.3% of selected cross-validated grouped cases correctly classified. Cross validation is done only for those cases in the analysis. In cross validation, each case is classified by the functions derived from all cases other than that case.

Figure 3.325 shows the position of the specimens that were reclassified by the DA. All the morphologically and biometrically identified sheep gather around (and beyond) the sheep group centroid line, showing to have strong sheep characteristics.

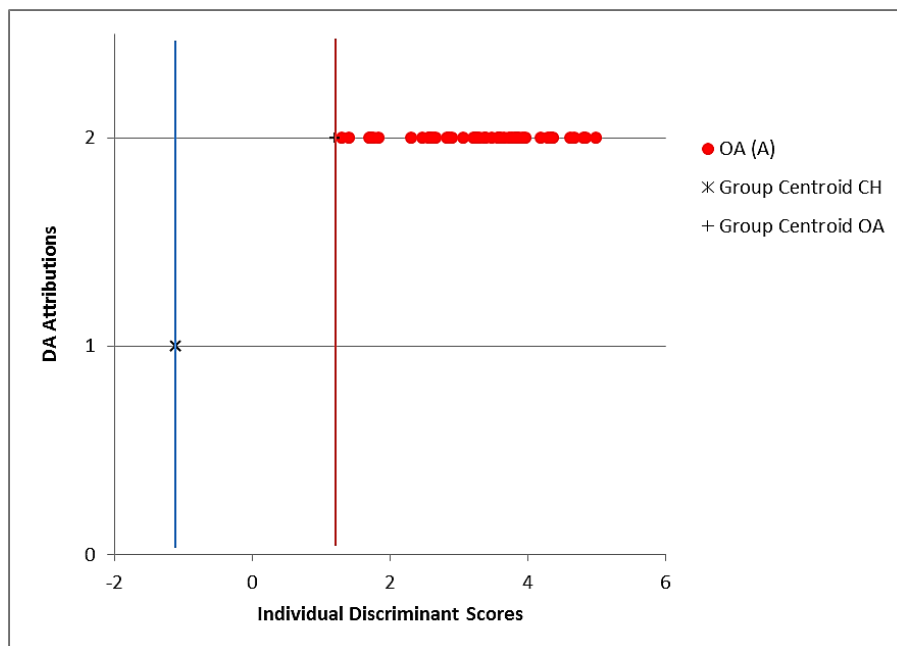


Figure 3.325 Diagram of the individual discriminant scores attributed to the archaeological material by DA for the humerus.

Radius

The percentage of consistent reclassifications for the archaeological radii is 90% when all variables are included. This percentage is slightly lower than the results obtained from the modern material (Tab. 3.140). The disagreement between the morphological analysis and the DA is related to an individual specimen identified morphologically as sheep and reidentified as 'goat' by the DA. It is important to bear in mind that the partial inconsistency between the two approaches may have been caused by the small sample size.

Nevertheless, when variables such as GL and SD are excluded from the analysis, despite the sample size increases significantly (49 specimens), the percentage of correct reattributions decreases further (83.3%) (Tab. 3.141).

Table 3.140 Results from the Discriminant Analysis when applied on all the archaeological radii.

Classification Results ^{a,b,d}						
			TAXA	Predicted Group Membership		Total
				CH	OA	
Modern Material	Original	Count	CH	53	3	56
			OA	4	47	51
		%	CH	94.6	5.4	100.0
			OA	7.8	92.2	100.0
	Cross-validated ^c	Count	CH	53	3	56
			OA	4	47	51
		%	CH	94.6	5.4	100.0
			OA	7.8	92.2	100.0
Woolmonger Material	Original	Count	CH	0	0	0
			OA	1	9	10
		%	CH	.0	.0	100.0
			OA	10.0	90.0	100.0

a. 93.5% of selected original grouped cases correctly classified.

b. 90.0% of unselected original grouped cases correctly classified.

d. 93.5% of selected cross-validated grouped cases correctly classified. Cross validation is done only for those cases in the analysis. In cross validation, each case is classified by the functions derived from all cases other than that case.

Table 3.141 Results from the Discriminant Analysis when applied on all the archaeological radii, excluding variables GL and SD.

Classification Results ^{a,b,d}						
			TAXA	Predicted Group Membership		Total
				CH	OA	
Modern Material	Original	Count	CH	64	10	74
			OA	5	66	71
		%	CH	86.5	13.5	100.0
			OA	7.0	93.0	100.0
	Cross-validated ^c	Count	CH	63	11	74
			OA	6	65	71
		%	CH	85.1	14.9	100.0
			OA	8.5	91.5	100.0
Woolmonger Material	Original	Count	CH	0	0	0
			OA	8	40	48
			OC	1	0	1
		%	CH	.0	.0	100.0
			OA	16.7	83.3	100.0
			OC	100.0	.0	100.0

a. 89.7% of selected original grouped cases correctly classified.

Classification Results ^{a,b,d}
b. 83.3% of unselected original grouped cases correctly classified.
d. 88.3% of selected cross-validated grouped cases correctly classified. Cross validation is done only for those cases in the analysis. In cross validation, each case is classified by the functions derived from all cases other than that case.

Figure 3.326 shows that the sheep specimen reclassified as ‘goat’ by the DA falls equidistantly from the two group centroid lines. If one considers the error that is inherent to the DA and the fact that the analysis of the BI had not highlighted any clear inconsistency with the morphological identifications (Figs. 3.242; 3.264; 3.285 and 3.305), the DA reclassification cannot be relied on.

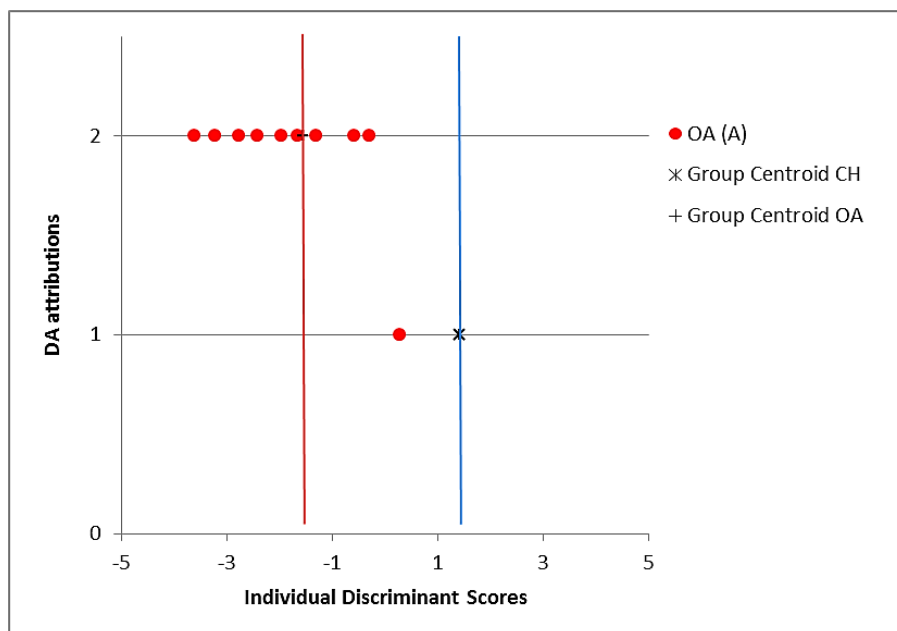


Figure 3.326 Diagram of the individual discriminant scores attributed to the archaeological material by DA for the radius.

Figure 3.327 shows the position of the specimens reclassified by the DA when the variables GL and SD were dropped. A greater number of sheep specimens have been ‘misidentified’ by the DA. None of them falls beyond the goat group centroids but all fall in the area between the two group centroid lines, with some being equidistant from both lines (for example the unidentified specimen). Considering the position of the specimens and the fact that no possible goats have been found with the BI analysis, the specimens reattributed by DA cannot be confidently considered as goats.

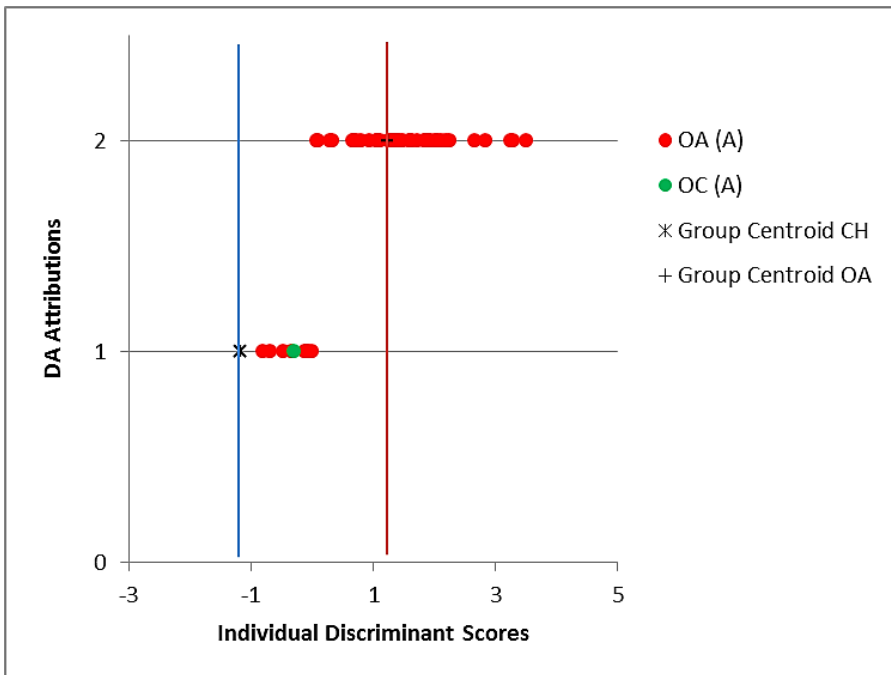


Figure 3.327 Diagram of the individual discriminant scores attributed to the archaeological material by DA for the radius when variables GL and SD were excluded.

Ulna

Perfect matching is present between the morphological and the biometrical identifications for the ulna (Tab. 3.142). When the variables B and L are excluded from the analysis, the percentage of correct reattributions stays the same (Tab. 3.143). Clearly, the exclusion of B and L does not heavily influence the diagnostic power of the DA.

Figure 3.328 shows that no archaeological ‘sheep’ has been identified as goat by the DA. All the sheep specimens fall very close or beyond the sheep centroid group. Figure 3.329 shows that the same output is also reached when a larger sample size is used and variables B and L are excluded. One morphologically unidentified specimen also plots convincingly with the sheep group.

Table 3.142 Results from the Discriminant Analysis when applied on all the archaeological ulnae.

Classification Results ^{a,b,d}						
			TAXA	Predicted Group Membership		Total
				CH	OA	
Modern Material	Original	Count	CH	53	3	56
			OA	5	52	57
		%	CH	94.6	5.4	100.0
			OA	8.8	91.2	100.0
	Cross-validated ^c	Count	CH	52	4	56
			OA	5	52	57
		%	CH	92.9	7.1	100.0
			OA	8.8	91.2	100.0
Woolmonger Material	Original	Count	CH	0	0	0
			OA	0	10	10
		%	CH	.0	.0	100.0
			OA	.0	100.0	100.0
a. 92.9% of selected original grouped cases correctly classified.						
b. 100.0% of unselected original grouped cases correctly classified.						
d. 92.0% of selected cross-validated grouped cases correctly classified. Cross validation is done only for those cases in the analysis. In cross validation, each case is classified by the functions derived from all cases other than that case.						

Table 3.143 Results from the Discriminant Analysis when applied on all the archaeological ulnae, excluding variables B and L.

Classification Results ^{a,b,d}						
			TAXA	Predicted Group Membership		Total
				CH	OA	
Modern Material	Original	Count	CH	52	4	56
			OA	5	52	57
		%	CH	92.9	7.1	100.0
			OA	8.8	91.2	100.0
	Cross-validated ^c	Count	CH	52	4	56
			OA	6	51	57
		%	CH	92.9	7.1	100.0
			OA	10.5	89.5	100.0
Woolmonger Street	Original	Count	CH	0	0	0
			OA	0	18	18
			OC	0	1	1
		%	CH	.0	.0	100.0
			OA	.0	100.0	100.0
			OC	.0	100.0	100.0
a. 92.0% of selected original grouped cases correctly classified.						
b. 100.0% of unselected original grouped cases correctly classified.						

Classification Results^{a,b,d}

d. 91.2% of selected cross-validated grouped cases correctly classified. Cross validation is done only for those cases in the analysis. In cross validation, each case is classified by the functions derived from all cases other than that case.

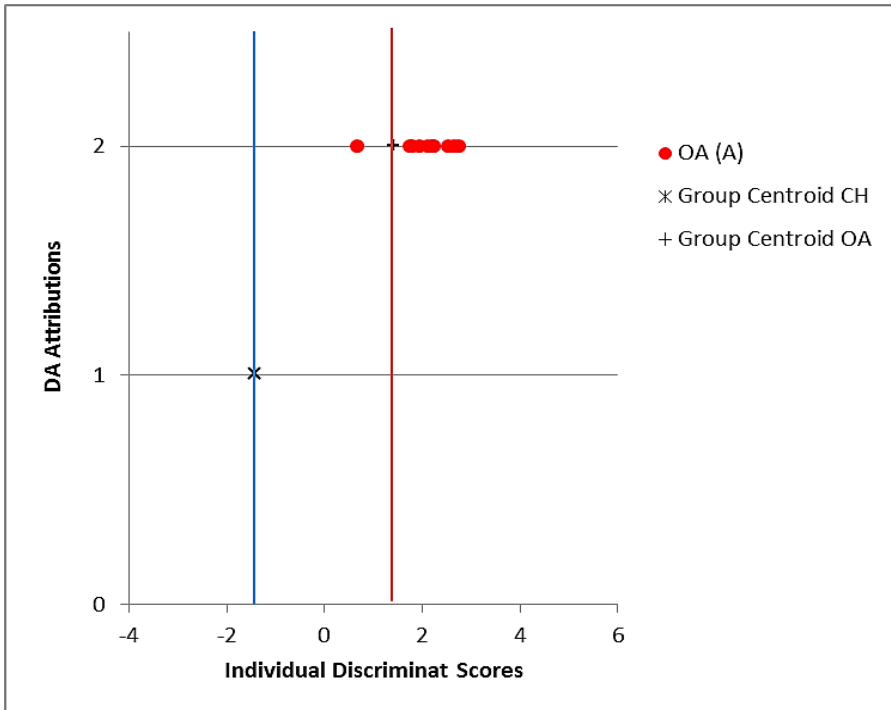


Figure 3.328 Diagram of the individual discriminant scores attributed to the archaeological material by DA for the ulna.

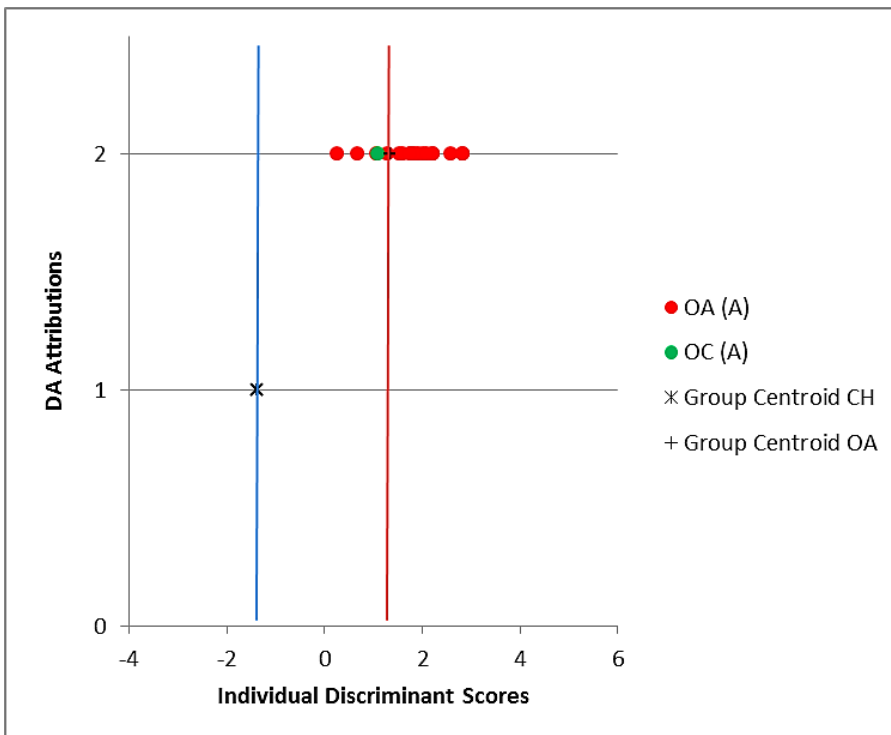


Figure 3.329 Diagram of the individual discriminant scores attributed to the archaeological material by DA for the ulna when variables B and L were excluded.

Metacarpal

When all the measurements were included in the analysis, the seven metacarpals morphological attributed to sheep, were also identified as such by the DA (100%) (Tab. 3.144 and Fig. 3.330).

When the variables GL and SD were excluded from the analysis, the value of ‘correct’ reattributions decreased to 97.6%, with one of the 42 metacarpals being reclassified as ‘goat’ by the DA (Tab. 3.145). Since the percentage of correct identifications of the modern material was almost identical (97.5%), the reclassified archaeological specimen can be considered within the method’s normal margin of error (Fig. 3.331).

Table 3.144 Results from the Discriminant Analysis when applied on all the archaeological metacarpals.

Classification Results ^{a,b,d}						
			TAXA	Predicted Group Membership		Total
				CH	OA	
Modern Material	Original	Count	CH	56	2	58
			OA	0	61	61
		%	CH	96.6	3.4	100.0
			OA	.0	100.0	100.0
	Cross-validated ^c	Count	CH	55	3	58
			OA	0	61	61
		%	CH	94.8	5.2	100.0
			OA	.0	100.0	100.0
Woolmonger Material	Original	Count	CH	0	0	0
			OA	0	7	7
		%	CH	.0	.0	100.0
			OA	.0	100.0	100.0
a. 98.3% of selected original grouped cases correctly classified.						
b. 100.0% of unselected original grouped cases correctly classified.						
d. 97.5% of selected cross-validated grouped cases correctly classified. Cross validation is done only for those cases in the analysis. In cross validation, each case is classified by the functions derived from all cases other than that case.						

Table 3.145 Results from the Discriminant Analysis when applied on all the archaeological metacarpals, excluding variables GL and SD.

Classification Results ^{a,b,d}						
			TAXA	Predicted Group Membership		Total
				CH	OA	
Modern Material	Original	Count	CH	56	2	58
			OA	1	60	61
		%	CH	96.6	3.4	100.0
			OA	1.6	98.4	100.0
	Cross-validated ^c	Count	CH	55	3	58
			OA	1	60	61
		%	CH	94.8	5.2	100.0
			OA	1.6	98.4	100.0
Woolmonger Material	Original	Count	CH	0	0	0
			OA	1	41	42
		%	CH	.0	.0	100.0
			OA	2.4	97.6	100.0
a. 97.5% of selected original grouped cases correctly classified.						
b. 97.6% of unselected original grouped cases correctly classified.						
d. 96.6% of selected cross-validated grouped cases correctly classified. Cross validation is done only for those cases in the analysis. In cross validation, each case is classified by the functions derived from all cases other than that case.						

Figure 3.330 shows the results when all variables were included in the analysis. All the archaeological sheep gather around the sheep centroid line, consistently with the morphological identification. No goat specimens have been identified by the DA.

Figure 3.331 shows the results when the variables B and L were excluded from the analysis. The morphologically identified sheep, considered as ‘goat’ by the DA falls almost equidistantly between the two group centroids line, and cannot be confidently considered to be a goat.

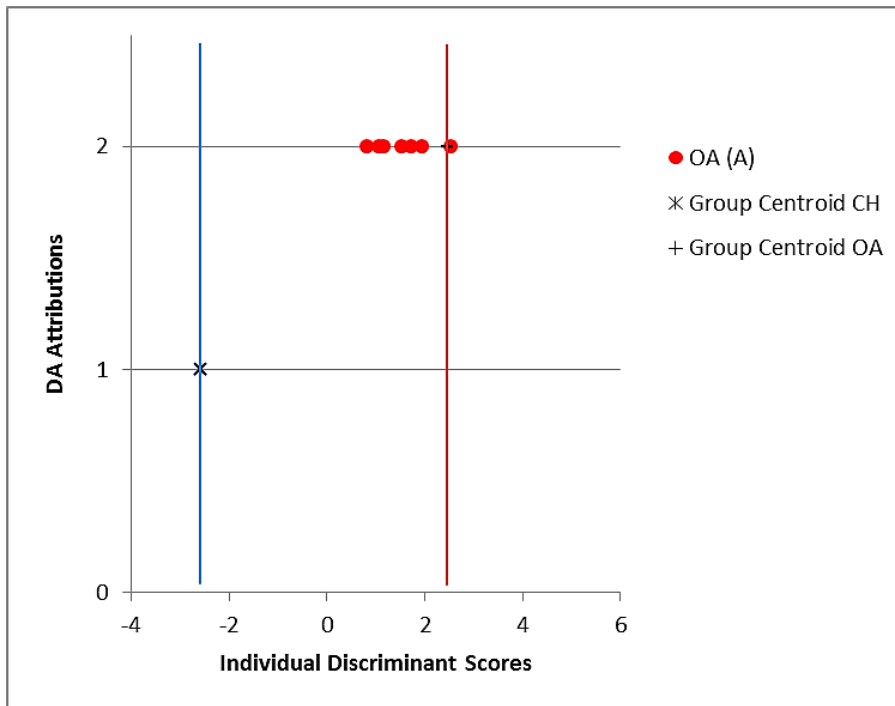


Figure 3.330 Diagram of the individual discriminant scores attributed to the archaeological material by DA for the metacarpal.

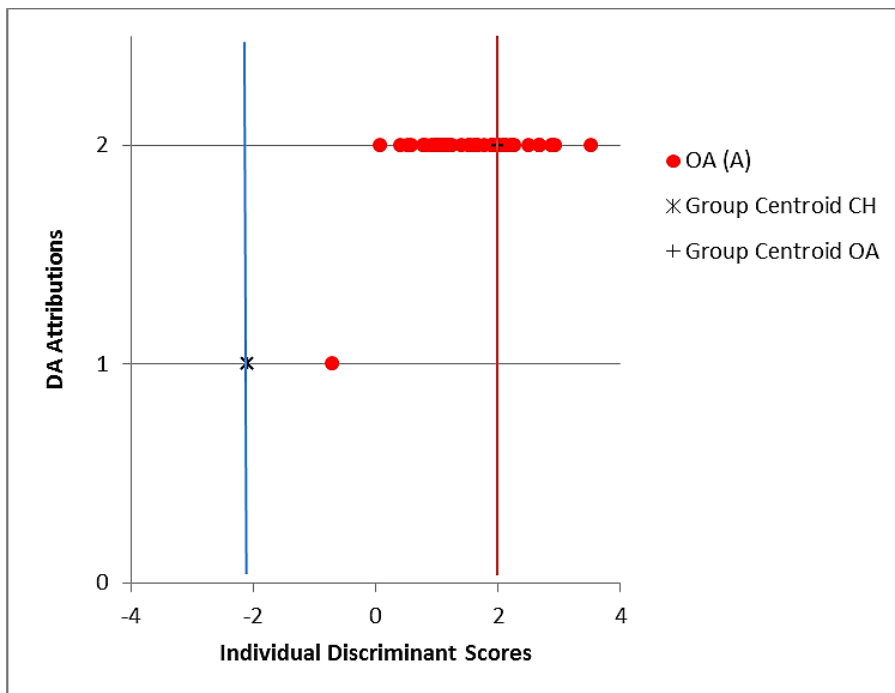


Figure 3.331 Diagram of the individual discriminant scores attributed to the archaeological material by DA for the metacarpal when variables GL and SD were excluded.

Metatarsal

When all the measurements were included, the agreement between the morphological and the biometrical identifications for the metatarsals was complete (100%) (Tab. 3.146).

When the variables GL and SD were excluded from the analysis, the percentage of consistent attributions decreased significantly (85.4%) (Tab. 3.147). In this last case the percentage of correct reattributions is lower than the proportion of correct identifications as expected on the basis of the modern material; thus the possibility that morphological misidentification occurred must be considered.

Table 3.146 Results from the Discriminant Analysis when applied on all the archaeological metatarsals.

Classification Results ^{a,b,d}						
			TAXA	Predicted Group Membership		Total
				CH	OA	
Modern Material	Original	Count	CH	56	5	61
			OA	4	59	63
		%	CH	91.8	8.2	100.0
			OA	6.3	93.7	100.0
	Cross-validated ^c	Count	CH	54	7	61
			OA	4	59	63
		%	CH	88.5	11.5	100.0
			OA	6.3	93.7	100.0
Woolmonger Material	Original	Count	CH	1	0	1
			OA	0	5	5
		%	CH	100.0	.0	100.0
			OA	.0	100.0	100.0
a. 92.7% of selected original grouped cases correctly classified.						
b. 100.0% of unselected original grouped cases correctly classified.						
d. 91.1% of selected cross-validated grouped cases correctly classified. Cross validation is done only for those cases in the analysis. In cross validation, each case is classified by the functions derived from all cases other than that case.						

Table 3.147 Results from the Discriminant Analysis when applied on all the archaeological metatarsals, excluding variables GL and SD.

Classification Results ^{a,b,d}						
			TAXA	Predicted Group Membership		Total
				CH	OA	
Modern Material	Original	Count	CH	51	10	61
			OA	4	59	63
		%	CH	83.6	16.4	100.0
			OA	6.3	93.7	100.0
	Cross-validated ^c	Count	CH	49	12	61
			OA	6	57	63
		%	CH	80.3	19.7	100.0
			OA	9.5	90.5	100.0
Woolmonger Material	Original	Count	CH	2	0	2
			OA	6	33	39
		%	CH	100.0	.0	100.0
			OA	15.4	84.6	100.0

a. 88.7% of selected original grouped cases correctly classified.

b. 85.4% of unselected original grouped cases correctly classified.

d. 85.5% of selected cross-validated grouped cases correctly classified. Cross validation is done only for those cases in the analysis. In cross validation, each case is classified by the functions derived from all cases other than that case.

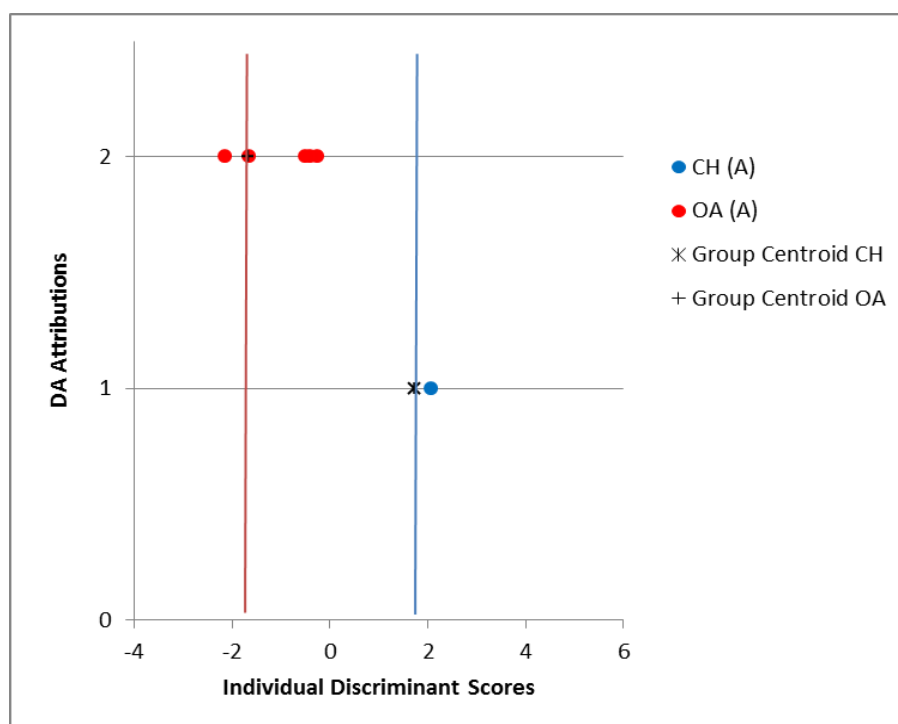


Figure 3.332 Diagram of the individual discriminant scores attributed to archaeological material by DA for the metatarsal.

Figure 3.332 shows that, when all the variables were included, despite the small sample size, all the morphologically identified sheep gather around the sheep group centroid line while the morphologically identified goat falls beyond the goat group centroid line. Thus there is no discrepancy between morphological and biometrical results.

Figure 3.333 displays the position of the specimens when variables GL and SD were excluded. Most of the reclassified sheep fall in the area between the two group centroids and, although some lean more towards the goat centroid, the evidence is insufficiently strong for a re-identification.

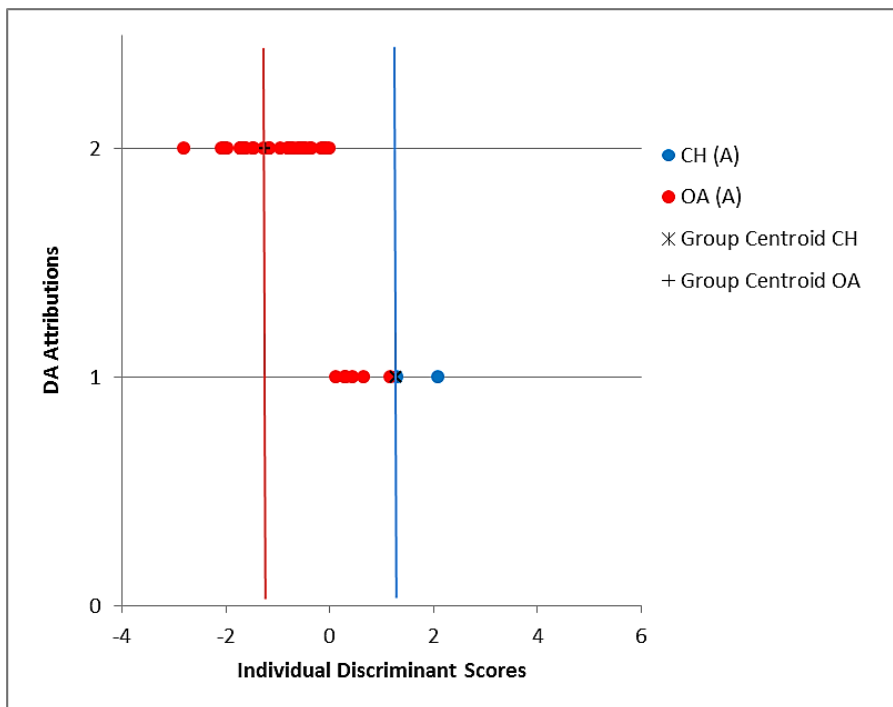


Figure 3.333 Diagram of the individual discriminant scores attributed to the archaeological material by DA for the metatarsal when variables GL and SD were excluded.

Tibia

For the tibia, the percentage of consistent attributions is, when all the measurements are included in the analysis, higher than the modern material (Tab. 3.148) but this result has to be taken with caution considering that it applies to only three specimens (all consistently classified as sheep).

Table 3.148 Results from the Discriminant Analysis when applied on all the archaeological tibiae.

Classification Results ^{a,b,d}						
			TAXA	Predicted Group Membership		Total
				CH	OA	
Modern Material	Original	Count	CH	55	3	58
			OA	9	43	52
		%	CH	94.8	5.2	100.0
			OA	17.3	82.7	100.0
	Cross-validated ^c	Count	CH	54	4	58
			OA	11	41	52
		%	CH	93.1	6.9	100.0
			OA	21.2	78.8	100.0
Woolmonger Material	Original	Count	CH	0	0	0
			OA	0	3	3
		%	CH	.0	.0	100.0
			OA	.0	100.0	100.0
<p>a. 89.1% of selected original grouped cases correctly classified.</p> <p>b. 100.0% of unselected original grouped cases correctly classified.</p> <p>d. 86.4% of selected cross-validated grouped cases correctly classified. Cross validation is done only for those cases in the analysis. In cross validation, each case is classified by the functions derived from all cases other than that case.</p>						

Table 3.149 Results from the Discriminant Analysis when applied on all the archaeological tibiae, excluding variable GL.

Classification Results ^{a,b,d}						
			TAXA	Predicted Group Membership		Total
				CH	OA	
Modern Material	Original	Count	CH	45	13	58
			OA	15	37	52
		%	CH	77.6	22.4	100.0
			OA	28.8	71.2	100.0
	Cross-validated ^c	Count	CH	44	14	58
			OA	16	36	52
		%	CH	75.9	24.1	100.0
			OA	30.8	69.2	100.0
Woolmonger Material	Original	Count	CH	1	0	1
			OA	14	24	38
			OC	5	2	7
		%	CH	100.0	.0	100.0
			OA	36.8	63.2	100.0
			OC	71.4	28.6	100.0
<p>a. 74.5% of selected original grouped cases correctly classified.</p>						

Classification Results ^{a,b,d}	
b.	64.1% of unselected original grouped cases correctly classified.
d.	72.7% of selected cross-validated grouped cases correctly classified. Cross validation is done only for those cases in the analysis. In cross validation, each case is classified by the functions derived from all cases other than that case.

Conversely to previous cases, the inclusion of measurement SD seems to create more confusion than clarity. In fact, the percentage of correct reattributions of the archaeological material decreases at 64.1%, a value that is significantly lower than the one obtained with the modern material (Tab. 3.149). When both SD and GL are excluded, the reattribution rate increases at 73.6%, which is higher than for the modern material. As a consequence any reclassification may be a consequence of the method's inherent error (Tab. 3.150).

Table 3.150 Results from the Discriminant Analysis when applied on all the archaeological tibiae, excluding variables GL and SD.

Classification Results ^{a,b,d}						
			TAXA	Predicted Group Membership		Total
				CH	OA	
Modern Material	Original	Count	CH	42	16	58
			OA	15	37	52
		%	CH	72.4	27.6	100.0
			OA	28.8	71.2	100.0
	Cross-validated ^c	Count	CH	41	17	58
			OA	16	36	52
		%	CH	70.7	29.3	100.0
			OA	30.8	69.2	100.0
Woolmonger Material	Original	Count	CH	1	0	1
			OA	19	52	71
			OC	7	7	14
		%	CH	100.0	.0	100.0
			OA	26.8	73.2	100.0
			OC	50.0	50.0	100.0
a. 71.8% of selected original grouped cases correctly classified.						
b. 73.6% of unselected original grouped cases correctly classified.						
d. 70.0% of selected cross-validated grouped cases correctly classified. Cross validation is done only for those cases in the analysis. In cross validation, each case is classified by the functions derived from all cases other than that case.						

Figures 3.334 to 3.336 display the position of the specimens reclassified by the DA (two sheep specimens plot in the same spot). Figure 3.334 shows the complete agreement between the morphological and the biometrical identifications when all variables were included.

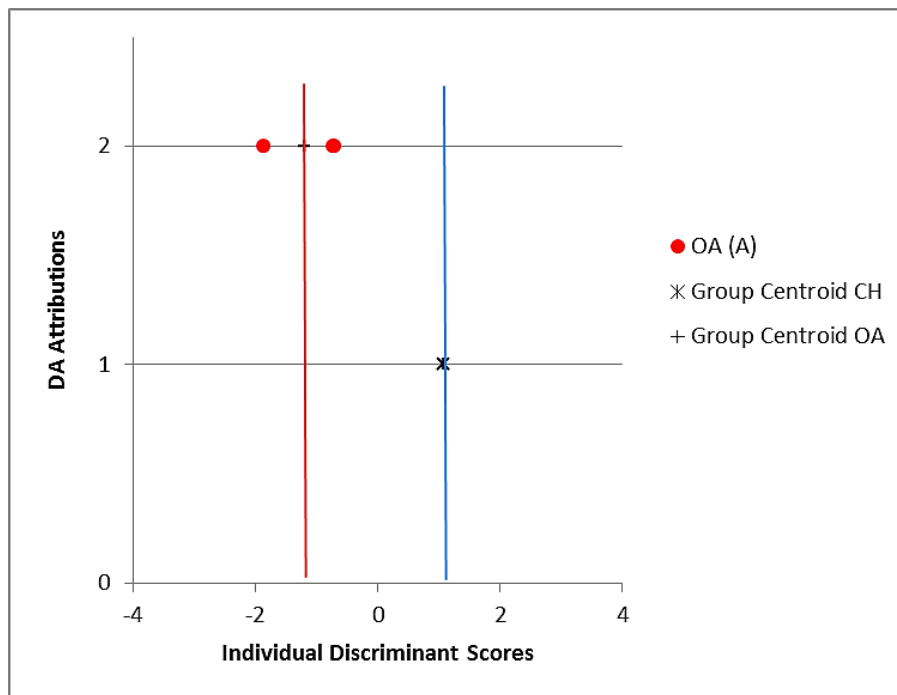


Figure 3.334 Diagram of the individual discriminant scores attributed to the archaeological material by DA for the tibia.

Figure 3.335 shows that, with the exclusion of GL, there are more specimens which have been ‘misattributed’ by the DA. Many of the specimens which have been identified morphologically as sheep and reidentified as ‘goats’ from the DA are in fact in continuity with the sheep range and cannot be confidently regarded to be goats, also considering the inherent error of the method. The two outliers on the right (a ‘sheep’ and a ‘sheep/goat’ on the basis of their morphology) look genuinely different and may indeed represent genuine goats. Such small number of possibly reclassified specimens would be consistent with the evidence of the BI (Figs. 3.271 and 3.313). In particular, the ‘sheep’ belongs to the unstratified group and it is the one placed among the goats in Figure 3.313. The unidentified specimen belongs to phase II and falls, as shown by Figure 3.271, on the lower edge of the modern goat group. Altogether the evidence suggests that these two specimens are goats.

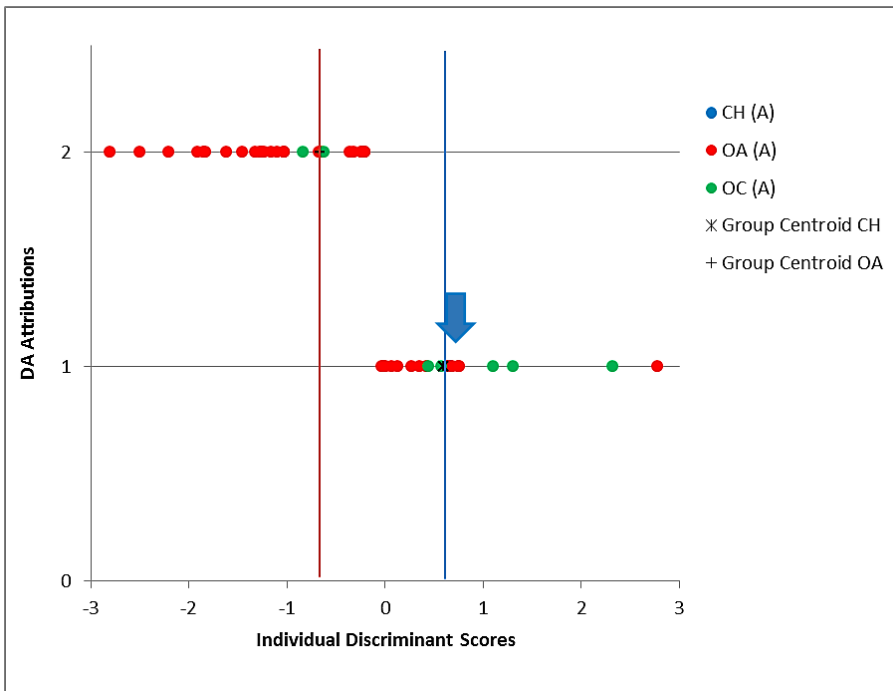


Figure 3.335 Diagram of the individual discriminant scores attributed to the archaeological material by DA for the tibia when variable GL was excluded. The blue arrow indicates the position of the archaeological goat.

A slightly better result is obtained when both SD and GL are excluded, as shown by Figure 3.336. The overall pattern is similar to that seen in the previous Figure, with the two outliers on the right again likely to represent goats.

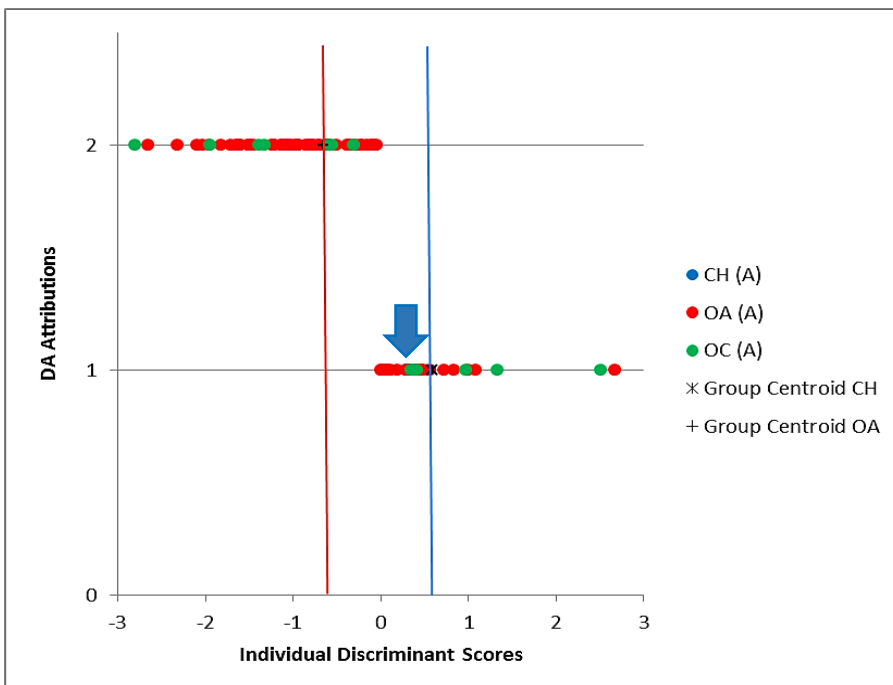


Figure 3.336 Diagram of the individual discriminant scores attributed to the archaeological material by DA for the tibia when variables GL and SD were excluded. The blue arrow indicates the position of the archaeological goat.

Astragalus

The percentage of agreement between the morphological and biometrical identifications is for the astragalus 87.5%, a result which is very similar to that obtained for the modern material (89%) (Tab. 3.151). Among the eight originally identified sheep, one was classified as ‘goat’ by the DA.

Figure 3.337 shows that the specimen which has been reclassified as ‘goat’ falls equidistantly between the two group centroid lines. Considering its position on the digram, there is not enough evidence to question the original morphological identification as ‘sheep’: reclassification is, in fact, not supported by the BI analysis (Figs. 3.250 to 3.253; 3.272 to 3.275; 3.292 to 3.295; 3.314 to 3.317).

Table 3.151 Results from the Discriminant Analysis when applied on all the archaeological astragali.

Classification Results ^{a,b,d}						
			TAXA	Predicted Group Membership		Total
				CH	OA	
Modern Material	Original	Count	CH	65	7	72
			OA	9	64	73
		%	CH	90.3	9.7	100.0
			OA	12.3	87.7	100.0
	Cross-validated ^c	Count	CH	64	8	72
			OA	11	62	73
		%	CH	88.9	11.1	100.0
			OA	15.1	84.9	100.0
Woolmonger Material	Original	Count	CH	0	0	0
			OA	1	7	8
		%	CH	.0	.0	100.0
			OA	12.5	87.5	100.0
a. 89.0% of selected original grouped cases correctly classified.						
b. 87.5% of unselected original grouped cases correctly classified.						
d. 86.9% of selected cross-validated grouped cases correctly classified. Cross validation is done only for those cases in the analysis. In cross validation, each case is classified by the functions derived from all cases other than that case.						

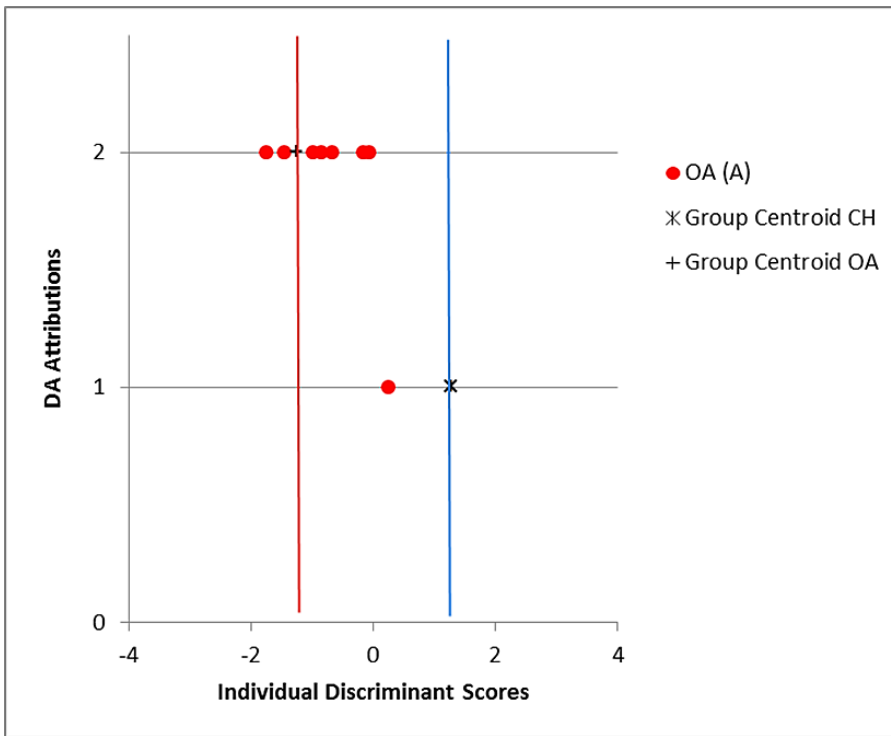


Figure 3.337 Diagram of the individual discriminant scores attributed to the archaeological material by DA for the astragalus.

Calcaneum

Table 3.152 shows that the percentage of consistent reattributions for the calcaneum is 100% when all the variables are included. When variables GL and SB are excluded (Tab. 3.153), the degree of consistency decreases but only slightly (95.8%), supporting the idea that even incomplete specimens can generally be successfully classified.

Table 3.152 Results from the Discriminant Analysis when applied on all the archaeological calcanea.

Classification Results ^{a,b,d}						
			TAXA	Predicted Group Membership		Total
				CH	OA	
Modern Material	Original	Count	CH	55	5	60
			OA	1	61	62
		%	CH	91.7	8.3	100.0
			OA	1.6	98.4	100.0
	Cross-validated ^c	Count	CH	55	5	60
			OA	1	61	62
		%	CH	91.7	8.3	100.0
			OA	1.6	98.4	100.0
Woolmonger Material	Original	Count	CH	0	0	0
			OA	0	15	15
			OC	0	1	1
		%	CH	.0	.0	100.0
			OA	.0	100.0	100.0
			OC	.0	100.0	100.0
a. 95.1% of selected original grouped cases correctly classified.						
b. 100.0% of unselected original grouped cases correctly classified.						
d. 95.1% of selected cross-validated grouped cases correctly classified. Cross validation is done only for those cases in the analysis. In cross validation, each case is classified by the functions derived from all cases other than that case.						

Table 3.153 Results from the Discriminant Analysis when applied on all the archaeological calcanea, excluding GL and SB variables.

Classification Results ^{a,b,d}						
			TAXA	Predicted Group Membership		Total
				CH	OA	
Modern Material	Original	Count	CH	53	7	60
			OA	2	60	62
		%	CH	88.3	11.7	100.0
			OA	3.2	96.8	100.0
	Cross-validated ^c	Count	CH	53	7	60
			OA	2	60	62
		%	CH	88.3	11.7	100.0
			OA	3.2	96.8	100.0
Woolmonger Material	Original	Count	CH	0	0	0
			OA	1	23	24
			OC	0	2	2
		%	CH	.0	.0	100.0
			OA	4.2	95.8	100.0

Classification Results ^{a,b,d}					
			OC	.0	100.0
a. 92.6% of selected original grouped cases correctly classified.					
b. 95.8% of unselected original grouped cases correctly classified.					
d. 92.6% of selected cross-validated grouped cases correctly classified. Cross validation is done only for those cases in the analysis. In cross validation, each case is classified by the functions derived from all cases other than that case.					

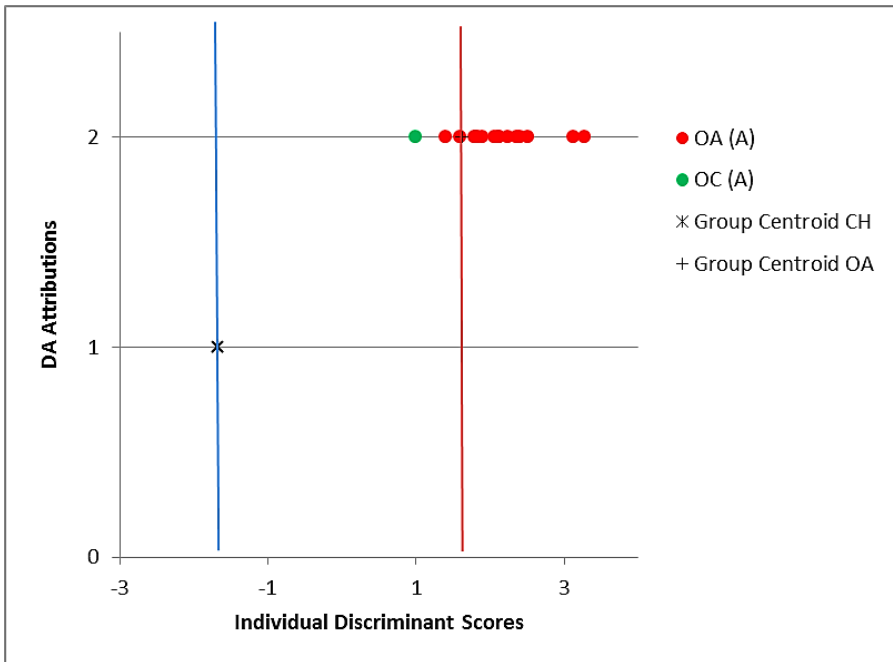


Figure 3.338 Diagram of the individual discriminant scores attributed to the archaeological material by DA for the calcaneum.

Figure 3.338 shows that the all the morphologically identified sheep were reclassified as sheep by the DA and they gather around the sheep group centroid. One unidentified specimen plot very close to the sheep group centroid line, but the evidence is not strong enough to be certainly assigned to *Ovis*.

Figure 3.339 shows the results when GL and SB are taken out of the analysis. One specimen identified morphologically as sheep has been attributed to the goat by DA but, as the expectations from the archaeological material have exceeded those of the modern, and the position of this specimen on the graph is not convincing (equidistant from both centroid lines), there is not enough evidence for its reclassification

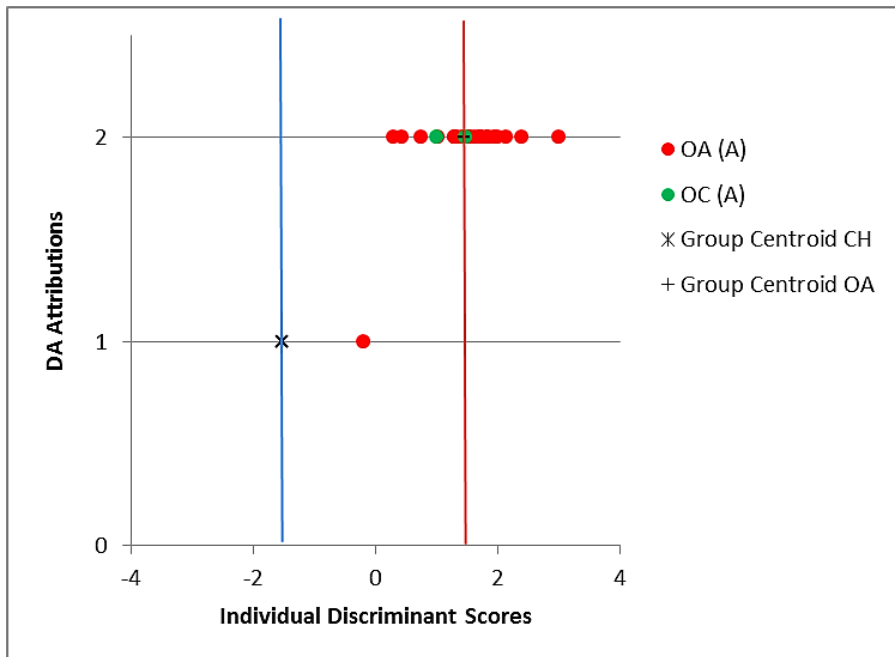


Figure 3.339 Diagram of the individual discriminant scores attributed to the archaeological material by DA for the calcaneum when variables GL and SB were excluded.

3rd phalanx

The problem of multicollinearity noticed when DA was run on the modern specimens' 3rd phalanges, prevented the use of the statistical tool on the archaeological 3rd phalanges.

3.4.9 Discussion

The application of the Discriminant Analysis on the whole sheep/goat material from Woolmonger/Kingswell Street leads to some considerations.

Table 3.154 Percentages of correct reattributions for the modern material and for the archaeological material (whole assemblage) provided by the DA. An asterisk mark small sample sizes (less than 10 specimens).

Anatomical Element	DA % of total correct reattributions modern material	DA % of total correct attributions on the archaeological material as a whole
Hc	95.2%	100%*
Hc (excluding E and F)	81%	60%*
Sc	86.4%	100%
Hu	88.4%	100%
Ra	93.5%	90%*
Ra (excluding GL and SD)	89.7%	83.3%
Ul	92.2%	100%*
Ul (excluding B and L)	92%	100%
Mc	98.3%	100%*
Mc (excluding GL and SD)	97.5%	97.6%
Mt	92.7%	100%*
Mt (excluding GL and SD)	88.7%	85.4%
Ti	89.1%	100%*
Ti (excluding GL)	74.5%	64.1%
Ti (excluding GL and SD)	71.8%	73.6%
Astragalus	89%	87.5%*
Calcaneum	95.1%	100%
Calcaneum (excluding SB and GL)	92.6%	95.8%

Most of the anatomical elements considered provided high percentages of consistent attributions (>80%) (Tab. 3.154), largely following the pattern of the modern material. Most elements exceeded expectations in terms of consistency with morphological identifications, and on the basis of the terms of reference provided by the modern material. The higher results often obtained from the archaeological material indicate a greater morphotype homogeneity of the medieval animals. The only element for which the percentage of consistent reattributions did not meet the expectations is the radius which, as previously mentioned, has proven to be a rather problematic element for its age-related changes (the astragalus has not been considered as in the previous case studies it has provided good results and in this case the low results are likely to be due to the small sample size).

In evaluating the results from the DA, it is essential to remember that the same guidelines, as previously outlined for King's Lynn and Flaxengate, have been adopted. As seen with the previous case studies, the DA bears an intrinsic error, thus, it is likely that some apparently misidentified archaeological specimens were such because of the bias the method bears. Once again it has to be reminded that the best results from this tool can be reached when used in combination with the morphological approach and the Biometrical Indices.

3.4.9.1 An assessment of the new methodology

When the results from the DA are compared and integrated with the results from the other approaches, the outcomes are as shown by Table 3.155.

The degree of agreement between the different approaches adopted is remarkable. The morphological identifications are frequently confirmed by the results from the BI and also by the outcomes of the DA. Only a few specimens that had been morphologically identified as sheep have been found to be biometrically consistent with the goat group (i.e. a scapula and a tibia). Among the morphologically unidentified specimens, only two likely goats could be identified biometrically (a tibia and a scapula).

The high degree of agreement between the biometry-based methods (BI and DA) is testified by the fact that the specimens genuinely 'misattributed' by the DA can be identified as such, also with the aid of the BI.

Table 3.155 Summary table of the results obtained from the morphological approach and the biometrical approach in the form of both Biometrical Indices (BI) and Discriminant Analysis (DA), when the sheep/goat assemblage from Woolmonger/Kingswell Street was considered *in toto*. The specimens considered as ‘misclassified’ are those which, as they fall on or beyond the group centroid line of the opposite species, are more likely to represent a morphological misclassification. The expectations are based on the results provided by the modern material; if the archaeological material has given a higher percentage of consistent attributions than the modern, the expectations are exceeded.

		Biometrical Approach							
		Morphological Approach			Biometrical Indices (BI)	Discriminant Analysis (DA)			
Anatomical element	<i>Ovis aries</i>	<i>Capra hircus</i>	<i>Ovis/ Capra</i>		Modern material DA%	Woolmonger material DA%	Identified <i>Ovis/ Capra</i>	‘Misclassified’	Comments
Horncore	32	6	-	All goats plot among the goat group. All sheep plot among the sheep group. No specimens plotting clearly among the goat group are present.	95.2%	100%	-	No strong evidence to argue against the morphological id. of the specimens.	Expectations exceeded. The exclusion of E and F reduces the diagnostic power of the DA
Jaw	68	-	36	-	-	-	-	-	N.A.
Teeth	61	-	36	-	-	-	-	-	N.A.
Scapula	27	-	16	All sheep plot among the sheep group or in the area of overlap. One sheep specimen plot among the goat group (phase III) but it is still consistent with the sheep group. One unidentified specimen is consistent with the sheep group; the other unidentified specimens fall in the area of overlap. No specimens plotting clearly among the goat group are present.	86.4%	100%	One may be a goat.	No strong evidence to argue against the morphological id. of the specimens.	Expectations exceeded.
Humerus	76	-	4	All the archaeological sheep are consistent with the sheep group. The unidentified specimens plot among the	88.4%	100%	-	No strong evidence to argue	Expectations exceeded.

				Biometrical Approach					
				Biometrical Indices (BI)	Discriminant Analysis (DA)				
Morphological Approach									
Anatomical element	<i>Ovis aries</i>	<i>Capra hircus</i>	<i>Ovis/ Capra</i>		Modern material DA%	Woolmonger material DA%	Identified <i>Ovis/ Capra</i>	‘Misclassified’	Comments
				sheep or in the area of overlap. No specimens plotting clearly among the goat group are present.				against the morphological id. of the specimens.	
Radius	48	1	1	All sheep plot among the sheep group or in the area of overlap. The only unidentified specimen falls in the area of overlap. No specimens plotting clearly among the goat group are present.	93.5%	90%	-	No strong evidence to argue against the morphological id. of the specimens.	The exclusion of GL and SD influences the diagnostic power of the DA.
Ulna	25	-	2	All sheep plot among the sheep group. The only unidentified specimen plots in the area of overlap. No specimens plotting clearly among the goat group are present.	92.9%	100%	-	No strong evidence to argue against the morphological id. of the specimens.	Expectations exceeded. Discriminant power of DA not affected by the exclusion of B and L
Metacarpal	47	-	-	All sheep plot among the sheep group or in the area of overlap. One sheep specimen plots more toward the goat group (phase II, Fig. 38) but it is still compatible with the range of variation of the sheep group. No other specimens plotting clearly among the goat group are present.	98.3%	100%	-	No strong evidence to argue against the morphological id. of the specimens.	Expectations exceeded. The exclusion of GL and SD influences the diagnostic power of DA.

				Biometrical Approach					
Morphological Approach				Biometrical Indices (BI)	Discriminant Analysis (DA)				
Anatomical element	<i>Ovis aries</i>	<i>Capra hircus</i>	<i>Ovis/ Capra</i>		Modern material DA%	Woolmonger material DA%	Identified <i>Ovis/ Capra</i>	‘Misclassified’	Comments
Metatarsal	43	2	1	The only two morphologically identified goats plot in the area of overlap. All sheep plot in the area of overlap or among the sheep group. No specimens plotting clearly among the goat group are present.	92.7%	100%	-	No strong evidence to argue against the morphological id. of the specimens.	The exclusion of GL and SD influences the diagnostic power of the DA.
Metapodials	8	-	-	-	-	-	-	N.A.	-
Tibia	93	1	16	The unidentified specimens fall in the area of overlap or among the sheep group. One nevertheless falls among the goat group (phase II, Fig. 42) and is consistent with the goat species. All sheep plot among the sheep group or in the area of overlap, apart from one (Unstrat, Fig. 3.84) which has been probably misidentified as it falls among the modern goat. No other specimens plotting clearly among the goat group are present.	89.1%	100% (73.6% with the exclusion of GL and SD)	One may be a goat (see Fig. 3.340 and 3.341)	One goat might have been misidentified as sheep (see Fig. 3.340 and 3.341). No strong evidence to argue against the morphological id. of the other specimens.	The exclusion of GL and SD influence the diagnostic power of the DA.
Astragalus	9	-	-	All sheep plot among the sheep group or in the area of overlap. No specimens plotting clearly among the goat group are present.	89%	87.5%	-	No strong evidence to argue against the morphological id. of the specimens.	-
Calcaneum	26	-	2	All sheep plot among the sheep group or in the area of overlap. No specimens plotting clearly among the goat group are present.	95.1%	100%	-	No strong evidence to argue against the morphological id. of the specimens.	Expectations exceeded. Discriminant power of DA not

		Biometrical Approach							
		Morphological Approach			Biometrical Indices (BI)	Discriminant Analysis (DA)			
Anatomical element	<i>Ovis aries</i>	<i>Capra hircus</i>	<i>Ovis/ Capra</i>		Modern material DA%	Woolmonger material DA%	Identified <i>Ovis/ Capra</i>	'Misclassified'	Comments
									affected by the exclusion of GL and SB.
1st Phalanx	127	4	10	-			-	-	N.A.
2nd Phalanx	23	-	-	-			-	-	N.A.
3rd Phalanx	7	-	-	-			-	-	N.A.
Total Identified Specimens	720	14	124						N.A.

3.4.9.2 The Woolmonger/Kingswell Street case study

The reexamination of the sheep/goat bone assemblage from Woolmonger/Kingswell Street clearly indicates that the overwhelming majority of the caprine specimens belong to the sheep. This, to some extent, justifies Armitage's use of the term 'sheep' for the whole caprine assemblage, though some qualifications would have helped. The goat, however, is rare but not absent. It is mainly represented by horncores though a few postcranial bones have also been identified.

As seen for Flaxengate, also at Woolmonger/Kingswell Street, the absence of concentrations of goat horncores suggests that this animal was not involved in a specific industry or trade but it was mainly considered as a supplementary household provision.

3.5 Discussion of the application of the new methodology on Archaeological assemblages

The application of the new methodology on three different medieval English sheep and goat assemblages has provided very good results. Overall, the positive outcome of the analysis of the modern material has been confirmed, but some new considerations can be made.

Concerning the morphological criteria, the analysis of the archaeological material has permitted a short-list of most useful diagnostic traits to be identified through the study of the modern sample. A list of these traits, with some comments about their effectiveness, is provided in Table 3.156.

Most of the morphological traits that had proven diagnostic on the modern material have also been successful on the archaeological material, but some were less clearly visible. This may in some cases be due to the greater completeness of the modern specimens, but also to the higher homogeneity of the modern sample. In addition, variable age-related factors may also explain the slight discrepancies between the modern and archaeological materials.

From the morphometric point of view, the application of Biometrical Indices (BI) on fragmented archaeological material has provided very good results. The ratios which were applied previously on modern material have all succeeded in highlighting different distributions for sheep and goat. The BI that have provided the clearest results - and as such are highly recommended - are shown in Table 3.157.

Table 3.156 List of the morphological trait per anatomical element which have resulted to be particularly useful in the identification of the archaeological material.

Anatomical Element	Trait	Notes
dP ₃	2	If the degree of wear of the tooth is heavy, this trait may no longer be visible.
dP ₄	3 and 4	If the degree of wear of the tooth is heavy, trait 3 may no longer be visible. If the tooth is not fully erupted both traits may be hidden. If the tooth is still embedded in the mandible, trait 4 is not visible.
P ₃	2 and 3	If the degree of wear of the tooth is heavy, traits may no longer be visible.
P ₄	2 and 3	If the degree of wear of the tooth is heavy, traits may no longer be visible.
M ₃	1 and 5	Both traits may be difficult to assess if the tooth is unworn. If the degree of wear of the tooth is heavy, both traits may no longer be visible.
Horncore	1 and 2	
Scapula	2	Trait 2 is less reliable when the animal is old.
Humerus	1 and 5	
Radius	1 and 2	Both traits are less useful in very young and old animals.
Ulna	1	
Tibia	1, 2 and 5	Trait 1 and 5 are rather variable.
Metapodials	1, 4, 5 and 6 (trait 6 for the Metatarsal only)	
Astragalus	3, 4 and 5	
Calcaneum	2 and 3	
1 st Phalanx	2 and 4	Trait 2 is less useful with old animals.
2 nd Phalanx	1 and 2	
3 rd Phalanx	2	

The modern material sample used as guideline for the identification of patterns in the archaeological material, has generally shown a consistent pattern of distribution with the archaeological specimens. In other words, the archaeological sheep and goats tend to plot in the same areas as their modern counterparts with some outliers. A noticeable exception to this trend regards the proximal radius which has not provided particularly clear results. This has been interpreted as a consequence of the fact that the morphology of the proximal radius is very

variable with age (Payne and Bull 1988) and this may lead to confusion in taxonomic identifications.

In general, the BI have proven to be extremely valuable as they can be used for supporting or questioning identifications made through the use of morphological criteria. An example of such potential is demonstrated by those morphologically misidentified sheep that were biometrically classified as goats. BI can also assist in speciating the specimens that could not be identified morphologically, though this only applied to a few cases. The most important feature of the BI is, however, the opportunity to provide transparency to the identification process, and therefore opening it up for re-interpretation when required.

Table 3.157 List of the BI that have proven most successful in separating archaeological sheep and goats.

Anatomical Element	BI	Notes
Horncore	A/E:F E:F/A:F	Unfortunately the tip of the horncore is often missing, as such measurements E and F can rarely be taken. Despite A works well, if the base of the horncore is not preserved, C (the maximum diameter at the middle) can be used in place of A.
Scapula	GLP:LG/GLP:BG ASG:SLC/ GLP:BG	
Humerus	BT:HT/BT:HTC; BEI:BT/BEI:Bd	
Radius	BFp:Bp/Dp	The success of this ratio depends on the age ratio of the population under analysis.
Ulna	BPC:DPA/BPC:SDO	
Tibia	Bd/Dd(a):Dd(b)	
Metapodials	1:a/1:2 BFd:GL/SD:GL	In case measurements 1, 2 and a are not available, a good separation can be obtained through the 4:b/4:5 ratio. The ratio BFd:GL/SD:GL is useful but in fragmented material the length can only rarely be taken.
Astragalus	H:DI/Bd:GLI; H:DI/Bd:H; Bd:DI/GLI:DI.	
Calcaneum	c:B/c:d; DS:c/c:d; DS:C/c:d	The first two ratios are those for which less overlap between the two groups occurs, but the DS:C/c:d ratio has also some potential.
3 rd Phalanx	DLS/MBS:DLS	

The application of the DA as a tool to predict species identification has for the first time been applied on archaeological sheep and goat assemblages. High consistency has been noticed

between the morphological approach and BI and DA results. Almost all elements have provided high reattribution rates, showing a high rate of agreement with the morphological identification. As seen with the BI, the most problematic element in DA analysis was the proximal radius. In some cases the rate of identification success obtained with DA was lower than what expected on the basis of the analysis of the modern material.

Despite its successful application it is clear that DA should not be used in isolation, as it has its own drawbacks. For example, sample size can clearly influence the results, thus the smaller the sample the less confident we can be about the reliability of the DA attributions. In addition, the exclusion of some variables/measurements from the DA, a likely scenario when dealing with fragmented archaeological material, may affect the results detrimentally, which means that the power of this method will be diminished. Finally, in evaluating the DA results, it is essential to consider that the method bears an intrinsic error. Evidence of this is the fact that some modern specimens, whose taxonomic origin was known, were occasionally misclassified. The nature of this error is strictly linked to the biological nature of the two species analysed and their variability: as they are closely related species, a certain degree of overlap between the two will always exist. DA follows rigid rules, as all specimens are assigned to one of the two categories (*Ovis* or *Capra*). With all specimens attributed to species and no room left for uncertainty (e.g. sheep/goat, sheep? goat?), it is almost inevitable that some misidentifications will occur.

Some recommendations on how to interpret the archaeological data when using the DA as a predicting tool have been provided. If used appropriately DA has the potential to:

be a further means to supporting/questioning identifications assessed with the other two approaches;
assist in establishing the identity of the *Ovis/Capra* specimens;
provide further visual aid of the distribution patterns of the caprine specimens from a given assemblage.

In conclusion, it is the combination of these techniques that can provide the best results and has the potential to increase the possibility to achieve reliable identifications. However, if there is no time for a thorough analysis, even the application of only the BI approach in addition to the more traditional morphological approach, will contribute to enhance the identifications and make them openly subject to scrutiny.

3.6 Reassessment of the role of the goat in medieval English husbandry and economy: a beginning.

The analysis of three English medieval goat and sheep assemblages with the use of the new methodological approach here proposed has permitted a reassessment of the role that the goat played in the English economy and society of the time.

Overall, the results have confirmed what many researchers had observed in the past, namely that the goat was not abundant in medieval England (Albarella 1997, 1999, 2003; Albarella *et al.* unpublished; Clutton-Brock 1976; Dyer 2004; Grant 1988; Noddle 1994). Most of these previous works had, however, cautioned about the fact that only a morphological reassessment of goat identifications could confirm this situation. The main aim of this dissertation was the development of a methodological tool that allowed for such assessment to be undertaken, rather than the assessment itself. However, a preliminary archaeological application does confirm the trend and suggests that the goat has *not* been under-estimated in medieval English animal bone assemblages.

In the archaeological record this animal is mainly represented by horncores, while post cranial bones are sporadic. In this regard, all three case studies have, by and large, shown and confirmed the pattern: goat horncores are more numerous than sheep horncores, but when postcranial bones are considered, sheep by far outnumber goat. This means that only very few goats, or parts of the goat carcass, were introduced/present at the sites to be butchered and consumed.

In the case of King's Lynn, the disproportion between goat horncores and post cranial elements was particularly evident. The abundance of horncores, the fact that many were found in discrete accumulations, and the high frequency of cut and chop-marks, suggest a specialised use for this material, beyond mere food consumption. Considering that in the course of the Middle Ages horn-working activities decreased while leather production increased notably (Albarella 2003), a tanning or a tawying process is the most likely cause behind the accumulation of horncores. Horns were likely to be still attached to the skins when they arrived at the site (Serjeantson 1989). The skins were worked and processed into leather either at the site, even though in the case of King's Lynn no tannery has been discovered yet, or they may have been sent to another place to be worked. In this latter case, which implies a movement of highly perishable material from one site to another, it is likely that the horncores, still attached to the skins, were removed and left behind at the "primary" place in order to make the goods more easily transferable and less prone to decay. In either of the two cases, the horns were the most likely waste material

resulting from this process and were discarded or sold to horn-workers so that the keratinous sheath could be used as raw material.

The evidence that goat bones are rare at all sites regardless of geographical location or status, leads us to the conclusion that a trade in goat skins may have existed with other countries as, otherwise, it is difficult to explain what happened to the many skeletons that belonged to the specimens whose horncores have so frequently been found (for a list of sites see Chapter 1, Section 1.4.2). This hypothesis fits well with the role that King's Lynn had as an important port and trade centre.

Following this hypothesis, we would expect to find a greater number of horncore deposits at coastal and port sites, i.e. places of import. The zooarchaeological evidence seems to confirm such reasoning. Beside King's Lynn in fact, there are a number of coastal medieval sites in which accumulations of horncores have been found with very little evidence for goat post cranials. Some examples for the eastern areas are the sites of Fishergate (10th century-14th century onwards) (Jones 1994), Castle Mall (Albarella *et al.* 1997) and Coslany Street (10th-14th century) (Albarella 1997) in Norwich (Norfolk) and Ipswich (mid. 7th century-12th century) (Crabtree 1994; Jones *et al.* 1983) in Suffolk. In the south-western regions, the sites of Exeter (Maltby 1981) and at Exe Brige (Levitan 1987) in Devon as well as Bristol (14th century) (Noodle 1975) and Hereford (11th century-16th century) (Baxter unpublished) provide the same pattern. A more comprehensive review is nevertheless necessary to better assess and understand such phenomenon.

Considering the effort that such trade would have required, a question arises: which was the purpose behind such movements of goat skins? Several studies have demonstrated that goat skins have particular qualities (i.e. tenacity and strength) (Reed 1972; Salehi *et al.* 2013), which make them more suitable than sheep skins for the production of durable objects such as shoes, boots and garments. However, this reason seems not to be strong enough to justify a trade in goat skins, especially considering that the more readily available sheep skins would have represented a reasonable alternative.

A recent study on parchment folios from European medieval pocket Bibles conducted by Fiddymment *et al.* (2015) opens a new perspective on the matter. The analysis, with the use of peptide fingerprints, has in fact revealed that in England during the 12th and 13th century, parchment from sheep skins was mainly destined to the production of legal documents, while folios from goat skins were used for the manufacture of pocket Bibles. This evidence is intriguing and may point toward a specialised use of goat skins.

As seen in Chapter 1 (Section 1.4.2), a similar situation to King's Lynn is common to other English medieval assemblages. Data from these sites are important to consider, as they indicate and confirm the existence of a pattern: in more industrialized centres goat was used, with other animals, for some specific industrial activities. At sites like Harrison Street in Hereford (Hertfordshire, 15th century) (Baxter unpublished), Skeldergate in York (11th-12th century) (O'Connor 1984), Hornpot Lane in York (14th century) (Wenham 1964), Empire Cinema in Bedford (Bedfordshire, 11th-12th century) (Grant 1983) and St Johns Street 29-39 in Bedford (Bedfordshire, 11th-13th century) (Grant 1979) accumulations of goat horncores (more rarely of footbones) in association with other archaeological (e.g. soaking pits, leather fragments, decomposed bark used for the tanning process) (Serjeantson 1989) and historical evidence have been found, suggesting a connection between goat and horn and leather industries.

Similar cases have also been recorded in other countries. For example, accumulations of goat horncores with rare postcranial bones have been found at the sites of Dordrecht and Dorestand in the Netherlands (Prummel 1982). At s'-Hertogenbosch-Gertru, also in the Netherlands (Prummel 1982), there is an equally impressive accumulation of goat horncores, but, unusually, there is also an abundance of goat postcranial bones. This is a situation that is unknown in England and suggests that goats, as opposed to their mere skins or horns, must have been present at the site in substantial numbers. The medieval site of Haithabu in Germany also deserves to be mentioned as, despite goat bones represented only a small percentage of the total of caprine remains, a high percentage of the leather remains were attributed to *Capra* (Reichstein and Tiessen 1974).

The situation for the other two archaeological case studies analysed here, Flaxengate and Woolmonger/Kingswell Street, is rather different. Both sites are urban in nature and, at both, goat is mainly represented by horncores but, unlike King's Lynn, these anatomical elements appear in small numbers. The absence of any concentration of goat horncores and, as such, of a strong evidence of a bias in favour of these elements, indicates the absence of any specific industry or trade associated with this species (or indeed others, as there is no evidence for craft of industrial use of sheep and cattle remains either). It is important to keep in mind that the fact that concentrations of goat horncores have not been found does not necessarily exclude the possibility that they existed. Nonetheless, the available evidence indicates that at Flaxengate and Woolmonger/Kingswells Street there is some consistency in the occurrence of goat horncores and postcranial bones. This suggests the occasional, rather than intensive, use of this species, probably for household provision rather than industrial exploitation.

This particular scenario, according to which the goat is present in different numbers according to different exploitation patterns, was identified by Noddle (1994: 120), who mentioned that "there are a number of towns where only a few goat bones have been found and others where it has been plentiful". The illustrated archaeological examples described in this study indeed

points toward a diversified picture for the medieval English goat, though the “plentiful” scenario identified by Noddle does not apply to King’s Lynn or any other site in England.

In urbanised and industrially specialised centres, where accumulations of goat horncores have been found, the goat appears to have been mainly used for its skin and horns, as in King’s Lynn case. These site types, mainly located on the east coast, are likely to have been associated with a trade in goat skins with southern Europe, where this species was more abundant. There are a number of historical resources confirming the existence of hide and skin trades. Though not affecting the east coast, there is documentary evidence attesting to the importation of skins from Ireland to towns in the west of England (Clarkson 1966). Similarly, goat skins seem to have been imported to the site of Gamlebyen in Norway (Reichstein and Tiessen 1974). It is therefore possible that a similar commerce existed between England and other European countries.

In rural sites and in urban sites outside industrialised areas, the goat may have represented an alternative, but rarely used, source of meat and dairy products, as attested at Flaxengate and Woolmonger Street/Kingswell Street. Interestingly, a higher presence of goats in hilly and wooded counties is indicated by both charters and toponymy (Dyer 2004). This pattern is also confirmed by the Domesday Book (Darby 1977). Consequently, the regions in which goats were likely to be more common were the uncultivated areas and those areas where other farm animals could not easily feed. Particularly from the 13th century, southern, eastern and midland England had a distinct market-oriented husbandry system in which the goat did not have a place (Dyer 2004).

Unfortunately, the scarcity of available archaeological data from rural and less urbanised sites prevents us from undertaking an in-depth study of this phenomenon. In particular it is difficult to compare directly the archaeological data with those from written sources, such as the Domesday book, which seems to indicate a higher occurrence of the goat in the English medieval countryside than is apparent from archaeological sites. Nevertheless, the scanty available evidence seems to suggest that the goat was rare at rural sites too. Among the few rural sites where *Capra* remains have been recorded, it is worth mentioning the 12th-early 13th century Boteler’s Castle (Oversley, Warwickshire) (Pinter-Bellows 1997) and the 12th century site of Walton (Aylesbury, Buckinghamshire) (Noddle 1976). At both sites the small number of goat bones unearthed and the absence of concentration of goat horncores seem to confirm the idea that goat was husbanded rather than used in industrial activities.

3.7 Future developments: the way is paved

A full reassessment of the role that the goat in the Middle Ages in England on the basis on three case studies is inappropriate, and the proposed methodology will need to be applied much more extensively.

The chosen case studies were selected for several reasons, already outlined in Section 3.1. Among these, one important factor concerned their locations. Despite being all located in the central and eastern part of England, they are geographically different. As such they had the potential to be representative of patterns related to the goat in different regions.

Nevertheless, it is recommended that the new methodology is applied to sheep and goat assemblages from different parts of England, so that a more comprehensive evaluation of the role played by the goat can be carried out. Of particular interest would be to analyse sheep and goat assemblages from more western English sites in order to double check whether the proportion between goat horncores and post cranial bones is indeed different than what recorded for the eastern sites. The working hypothesis would be to verify the possible greater role of goat husbandry in western regions, as supported by historical (Darby 1977; Dyer 2004) and, preliminarily, archaeological evidence (Albarella *et al.* unpublished).

Another area that needs further investigation concerns the potential decline of the goat thorough time, as also suggested by historical and archaeological literature (Albarella 1997, 1999; Albarella *et al.* unpublished; Dyer 2004). It would be useful to study more English medieval sites with a long time-span so that diachronic trends can be better evaluated. The three sites specifically analysed in this dissertation all had long chronologies, but the problem is that the goat was so sparsely represented that the numbers are simply not large enough to be able to make a proper chronological assessment. Therefore it is clear that an evaluation of this phenomenon will need to be carried out at a large, regional, scale, combining evidence from many sites.

The method proposed here has been designed in such a way that could be suitable for such a broad review to be carried out. It is fairly easy and cheap and does not require the handling of complicated laboratory techniques, though it would be useful to integrate some of those (e.g. genetics, isotopes) in specific cases. Zooarchaeology by mass spectrometry as well as DNA analysis could represent for example, a further way to confirm or reject species identifications based on other approaches. It also would have the potential to attribute to species level the archaeological specimens which could not be morphologically identified because of the lack of diagnostic traits.

If the hypothesis of a trade in goat skins with other countries is considered, isotopic analyses could have the potential to help in identifying the place of origin of the medieval goats. The lack of goat teeth does, however, represent a problem in the application of Strontium and Oxygen isotopic analyses.

Another possibility for the future concerns the integration of this method with a geometric-morphometric approach (Cheverud *et al.* 1983). Having narrowed down, as part of this project, the list of particularly useful anatomical elements and morphological traits, these could be further verified through geometric morphometrics; this could allow us to further refine our identification abilities. It has to be kept in mind though that GMM is a time consuming technique and it is therefore unlikely that it could routinely be applied to large assemblages. Perhaps, its main purpose could be as a means of verification of identifications carried out through more traditional morphometric approaches.

Chapter 4 Conclusions

1. The morphological approaches traditionally used to distinguish between sheep and goat bones and teeth have allowed to move archaeological knowledge substantially forward, but they do have limitations. The main problem is that morphological differences can only be assessed subjectively.
2. When dealing with Britain, an additional issue is that most morphological diagnostic criteria have been established through observations of caprine skeletons from many parts of the world (e.g. the Mediterranean and the Near East) and may therefore not be entirely relevant to the region.
3. In order to overcome some of these problems, a study of the reliability of selected morphological traits on modern sheep and goat specimens from central and northern European countries has been conducted. The results have shown that, while some traits appear are fairly reliable on their own, a combination of traits, rather than the use of individual characteristics, is recommended. The most successful and reliable morphological traits have been short-listed (Tab. 2.56) and form the basis of a new methodological approach.
4. As part of the study of the reliability of the diagnostic morphological criteria, the examination of the influence of factors such as sex and age on the visibility of the traits has been conducted. The results confirm what researchers have previously noticed (Zeder and Lapham 2010; Zeder and Pilaar 2010), namely that age has an impact while sex is less influential.
5. The traditional morphological approach has been complemented with the creation of a newly devised biometrical approach, with the scope of providing a more objective and verifiable tool for identification purposes. Particular attention has been put on trying to translate diagnostic morphological features into Biometrical Indices. This methodology, when tested on the modern material, has provided promising results. Biometry, in the

form of Biometrical Indices (BI), has good potential in describing morphological differences between the two closely related species. The most effective indices which are recommended to be used when dealing with archaeological sheep and goat identification are:

- Horncores: A/E:F and E:F/A:F
 - Scapula: GLP:LG/GLP:BG and ASG:SLC/GLP:BG
 - Humerus: BT:HT/BT:HTC and BEI:BT/BEI:Bd
 - Radius: BFp:Bp/Dp
 - Ulna: BPC:DPA/BPD:SDO
 - Tibia: Bd/Dd(a):Dd(b)
 - Metapodials: 1:a/1:b and BFd:GL/SD:GL
 - Astragalus: H:DI/Bd:GLI, H:DI/Bd:H, Bd:DI/GLI:DI
 - Calcaneum: c:B/c:d and DS:c/c:d
 - 3rd Phalanx: DLS/MBS:DLS
6. The measurements making up the new recording protocol have been tested with the use of a consistency test (ICC for Inter and Intra-Observer Error) and the results have shown that most of them can be taken consistently by different researchers as well as by the same researcher.
7. A Mann Whitney U test was also conducted on individual BI in order to statistically test the significance of differences observed in the diagrams. The outcome was reassuring: the differences noticed between the two groups were statistically significant for the majority of the ratios. A Manova test was also carried out with the aim of testing whether differences were still statistically significant when ratios were compared simultaneously. This was indeed the case.
8. Multivariate analysis in the form of DA was also applied on the modern material in order to see if the combined use of all measurements could provide a better separation between sheep and goat. The results have shown that the inclusion of all measurements can indeed optimise the separation between the two groups, showing, in some cases, an almost complete separation between species.
9. PCA was also applied in order to detect which measurements were the most influential

in determining the variation among sheep and goat. The results have proven to be consistent with those obtained from the other lines of investigation; the measurements which resulted to be effective with BI and DA are also those that mostly determine the variation among the samples when PCA was conducted.

10. This combination of approaches, morphological and morphometrical, has successively been applied to three English medieval sheep and goat assemblages in order to test its potential on archaeological material and to lay the basis for a re-assessment of the role of the goat in medieval England.

a. Concerning the morphological traits, the analysis of the archaeological material has permitted the development of a refined list of useful diagnostic criteria. The morphological traits which are recommended for the identification of archaeological sheep and goats are:

- dP₃: trait 2;
- dP₄: traits 3 and 4;
- P₃: traits 2 and 3;
- P₄: traits 2 and 3 ;
- M₃: traits 1 and 5;
- Horcore: traits 1 and 2;
- Scapula: trait 2;
- Humerus: traits 1 and 5;
- Radius: traits 1 and 2;
- Ulna: trait 1;
- Tibia: traits 1, 2 and 5;
- Metapodials: traits 1, 4, 5 (6 only for metatarsals);
- Astragalus: traits 3, 4 and 5;
- Calcaneus: traits 2 and 3;
- 1st Phalanx: traits 2 and 4;
- 2nd Phalanx: traits 1 and 2;
- 3rd Phalanx: trait 2.

b. From the morphometric point of view, the use of BI has given very good results.

The ratios that had previously been applied on the modern material have, by and large, also provided good results when applied to the archaeological material. A noticeable exception to this trend regards the proximal radius, which has not worked quite as well when applied to the archaeological material. This is a consequence of the fact that the morphology of the proximal radius is very variable with age (Payne and Bull 1988) and this may lead to confusion in taxonomic attributions. In general, the BI have proven to be extremely useful as they can be used for supporting or questioning identifications made through the use of morphological criteria. They can also assist in attributing to species level the specimens that could not be identified morphologically. Most importantly, the application of BI makes the identification process transparent and open to scrutiny.

- c. The application of DA on the archaeological material has, as well, demonstrated to be largely successful. Nevertheless, like all others, this approach also has some limitations. It attributes all specimens to one species or the other, not allowing for grey areas (the well known 'sheep/goat' category). This inevitably leads to some mis-identifications, but the application to modern material of known taxonomic origins has allowed an assessment of the likely rate of error so that this could be considered in the interpretation of archaeological material. Overall, if used appropriately, DA can be a valuable tool to support/question identifications based on the other two approaches. It can also aid in establishing the identity of unidentified *Ovis/Capra* specimens and provide a further insight in the distribution patterns of caprine specimens from a given assemblage. As such, the use of DA in combination with BI and morphological approach is highly recommended.
 - d. As repeatedly stated, it is the combination of the different techniques applied in this study that will provide the best results. Nevertheless, if there is no time for an in-depth analysis of an archaeological assemblage, the exclusive use of BI in combination with the morphological approach still represents a powerful tool, which can enhance identifications and make them open to scrutiny.
11. The known trend according to which the goat was scarcely present in medieval England (Albarella 1997, 1999, 2003; Albarella *et al.* unpublished; Clutton-Brock 1976; Dyer 2004; Grant 1988; Noddle 1994) has been confirmed by the results of the application of

the new methodology on three archaeological case studies. The evidence suggests that the scarcity of goat is due to reasons other than an under-estimation of this animal by zooarchaeologists.

- a. In the archaeological record, *Capra* is mainly represented by horncores while post cranial bones are sporadic. All three case studies have, by and large, shown and confirmed this pattern. This means that only very few goats, or perhaps only parts of the goat carcass, were introduced/present at the sites to be butchered and consumed.

- b. In the case of King's Lynn, the disproportion between goat horncores and post cranial elements was particularly noticeable. The abundance of horncores, the fact that many were found in accumulations, and the high frequency of cut and chop-marks noticed on them, has led to the suggestion of a specialised use for this material. Historical and archaeological evidence attests to the development of leather production (Albarella 2003) during the medieval period. As such a tanning process is the most likely factor behind the accumulation of horncores. Horns were likely to be still attached to the skins (Serjeantson 1989) when introduced to the site, the skins were worked and processed into leather while the waste material, the horns, was discarded or sold. The rarity of goat bones at all sites regardless of geographical location or status (Albarella *et al.* unpublished), leads to think that a trade in goat skins may have existed with other countries as, otherwise, we would not be able to explain the underrepresentation of the other body parts. This hypothesis fits well with the role that King's Lynn had as important port and trade centre.

- c. A similar situation to King's Lynn has been identified for other English medieval assemblages. This evidence indicates and confirms the existence of a pattern: in urbanised and industrialized centres goat was used, with other species, for some specific industrial activities. Accumulations of goat horncores (more rarely of footbones) in association with other archaeological and historical evidence have been found at a number of sites (Harrison Street in Hertford (Baxter unpublished), Skeldergate (Addyman 1984) and Hornpot Lane in York (Wenham 1964), Empire Cinema (Grant 1983) and St Johns Street 29-39 in Bedford (Grant 1979))

confirming the connection of goat with horn and leather industries. Some parallels have also been found with contemporary sites in other countries such as the Netherlands (Dordrecht, Dorestand and s'-Hertogenbosch-Gertru) (Prummel 1982) and Germany (Haithabu) (Reichstein and Tiessen 1974).

- d. The situation for the other two archaeological case studies, Flaxengate and Woolmonger/Kingswell street, is quite different. At both sites goat is mainly represented by horncores, but these elements appear in small numbers despite the urban nature of the sites. The absence of any concentration of goat horncores and, as such, of a strong evidence of a bias in favour of these elements, indicates the absence of any evidence of a specific industry or trade associated with this species. Despite the possible existence of concentrations of goat horncores at these sites cannot be totally excluded, on the basis of the available evidence at Flaxengate and Woolmonger/Kingswells street goat horncores and postcranial bones are not represented in as unequal proportions as at King's Lynn. This suggests the occasional, rather than intensive, use of this animal, probably for household provision rather than any industrial exploitation.

- e. The archaeological examples presented describe a diversified picture for the medieval English goat. On the one hand, in more urbanised and industrially specialised centers, where accumulations of goat horncores are discovered, the goat appears to have mainly been used for its skin and to a lesser degree its horns. This type of sites, mainly located on the more urbanised east coast, is likely to have been associated with a trade in goat skins with southern Europe, where this species was more abundant (Albarella 2003). On the other hand, in non (or less) industrial contexts, the goat may have represented an alternative, but rarely used, source of meat and dairy products.

It is hoped that this thesis and the new methodology proposed will provide zooarchaeologists with a more objective tool that can be used for the identification of sheep and goats from archaeological sites. The new methodology has been developed particularly in view of resolving a pending question regarding medieval England – was the goat under-represented in the medieval English record due to misidentifications? The preliminary answer to this question –

based on a limited number of case studies – is negative, but clearly more work is needed in order to carry out a comprehensive review. However, the approach proposed in this thesis can have applications well beyond medieval England and will, hopefully, contribute to clarify further the role of these two animals, which have been so fundamental to the development of human societies.

References

- ADDYMAN, P.V. 1984. The archaeology. In *Selected groups of bones from Skeldergate and Walmgate*. The archaeology of York, 15/1, T. O'Connor, 10-11. York: Council for British Archaeology.
- ALBARELLA, U. 1997. Size, power, wool and veal: zooarchaeological evidence for late medieval innovations. In *Environment and subsistence in medieval Europe*, eds. G. DE BOE and F. VERHAEGHE, 19-30. Brugge: Institute for the Archaeological Heritage of Flanders.
- ALBARELLA, U. 1999. The mystery of husbandry: medieval animals and the problem of integrating historical and archaeological evidence. *Antiquity* 73: 867-875.
- ALBARELLA, U. 2003. Tanners, tawyers, horn working and the mystery of the missing goat. In *The environmental archaeology of industry*, eds. P. MURPHY and P. WILTSHIRE, 71-86. Oxford: Oxbow Books.
- ALBARELLA, U. 2006. Pig husbandry and pork consumption in medieval England. In *Food in medieval England: diet and nutrition*, eds. C.M. WOOLGAR, D. SERJEANTSON and T. WALDRON, 72-87. Medieval History and Archaeology. Oxford: Oxford University Press.
- ALBARELLA, U. and S.J.M. DAVIS. 1996. Mammals and birds from Launceston castle, Cornwall: decline in status and the rise of agriculture. *Circaea* 12: 1-156.
- ALBARELLA, U. and S. PAYNE. 2005. Neolithic pigs from Durrington Walls, Wiltshire, England: a biometrical database. *Journal of Archaeological Science* 32: 589-599.
- ALBARELLA, U., with T. PIRNIE and S. VINER. (unpublished). *Animals of our past: a review of the zooarchaeology of Central England*.
- ANSCHUTZ, K. 1966. *Die Tierknochenfunde aus der mittelalterlichen Siedlung Ulm-Weinhof*. Stuttgart. Inaugural Dissertation. University of Munich.
- ARMITAGE, P. 1998-1999. Faunal remains. In A history of urban regeneration: excavations in advance of development off St Peter's walk, Northampton, 1994-97, I. SODEN, 102-106. *Northamptonshire Archaeology* 28.
- ARMITAGE, P. 2008. Mammal, bird and fish bones. In Excavations at the corner of Kingswell Street and Woolmonger Street, Northampton, J. BROWN, 206-208. *Northamptonshire Archaeology* 35.
- BAKER, J. and D. BROTHWELL. 1980. *Animal diseases in archaeology*. London: Academic Press.

- BALASSE, M. and S.H. AMBROSE. 2005. Distinguishing sheep and goats using dental morphology and stable carbon isotopes in C₄ grassland environments. *Journal of Archaeological Science* 32: 681-702.
- BAR-GAL, G.K, P. DUCOS and L. KOLSKA HORWITZ. 2003. The application of ancient DNA analysis to identify Neolithic caprinae: a case study from the site of Hatoula, Israel. *International Journal of Osteoarchaeology* 13: 120-131.
- BARGMAN, R.E. 1970. Interpretation and use of a generalized discriminant function. In *Essays in probability and statistics*, ed. R.C. BOSE. Chapel Hill: University of North Carolina Press.
- BAXTER, M.J. 2003. *Statistics in archaeology*. London: Arnold.
- BAXTER, I. Unpublished. The faunal remains. In *Hereford City excavations*, P.J. PIKES and H. SHERLOCK. Hereford City Excavations 5.
- BINFORD, L.R. and J.B. BETRAM. 1977. Bone frequencies and attritional processes. In *For theory building in archaeology*, ed. L.R. BINFORD, 77-153. New York: Academic Press.
- BLAIR, J. and N. RAMSAY, eds. 1991. *English medieval industries: craftsmen, techniques, products*. London: The Hambledon Press.
- BLAND, J.M and D.G. ALTMAN. 1986. Statistical methods for assessing agreement between two methods of clinical measurement. *The Lancet* 327: 307-310.
- BOESSNECK, J. 1969. Osteological differences between sheep (*Ovis aries* Linné) and goat (*Capra hircus* Linné). In *Science in archaeology: a survey of progress and research*, eds. D. BROTHWELL and E. HIGGS, 331-358. London: Thames and Hudson.
- BOESSNECK, J., H. MÜLLER and M. TEICHERT. 1964. Osteologische Unterscheidungsmerkmale zwischen Schaf (*Ovis aries* Linné) und Ziege (*Capra hircus* Linné). *Kühn-Archiv* 78: 1-129.
- BÖKÖNYI, S. 1974. History of domestic mammals in central and eastern Europe. Budapest: Akadémiai Kiadó.
- BOND, J.M. and T. O'CONNOR. 1999. *Bones from Medieval deposits at 16-22 Coppergate and other sites in York*. York archaeological Trust for Excavation and Research. The animal bones 15/5. York: Council of British Archaeology.
- BOURDILLON, J. and COY, J. 1980. The animal bone. In *Excavations at Melbourne Street, Southampton 1971-1976*, ed. P. Holdsworth, 79-121. London: Council of British Archaeology. Research Report no. 33.
- BROWN, J. 2008. Excavations at the corner of Kingswell Street and Woolmonger Street, Northampton. *Northamptonshire Archaeology* 35: 173-214.

- BRUTON, A., J.H. CONWAY and S.T. HOLGATE. 2000. Reliability: what is it, and how is it measured? *Physiotherapy* 86: 94-99.
- BUCKLEY, M., S. WHITCHER KANSA, S. HOWARD, S. CAMPBELL, J. THOMAS-OATES and M. COLLINS. 2010. Distinguishing between archaeological sheep and goat bones using a single collagen peptide. *Journal of Archaeological Science* 37: 13-20.
- BUITENHUIS, H. 1995. A quantitative approach to species determination of ovicapridae. In *Archaeology of the Near East II*, eds H. BUITENHUIS and H.P. UERPMANN, 140-55. Leiden: Backhuys publishers.
- BURKE, J. 1834. *British husbandry; exhibiting the farming practice in various parts of the United Kingdom*. London: Baldwin & Cradock.
- BURNS, R.B. and R. BURNS. 2008. Discriminant Analysis. In *Business research methods and statistics using SPSS*, R.B. BURNS, 590-608. London: Sage Publications Ltd.
- CHERRY, J. 1991. Leather. In *Medieval Industries*, eds J. BLAIR and N. RAMSAY, 295-318. London: The Hambledon Press.
- CHEVERUD, J., J. L. LEWIS, W. BACHRACH and W. D. LEW. 1983. The measurement of form and variation in form: an application of three-dimensional quantitative morphology by finite-element methods. *American Journal of Physical Anthropology* 62: 151-165.
- CLARKE, H. and A. CARTER, eds. 1977. *Excavation in King's Lynn 1963-1970*. Medieval Archaeology Monograph Series 7. London: Society for Medieval Archaeology.
- CLARKSON, L.A. 1966. The leather crafts in Tudor and Stuart England. *The Agricultural History Review* XIV part I: 25-39.
- CLUTTON-BROCK, J. 1976. The animal resources. In *The archaeology of Anglo-Saxon England*, ed. D.M. Wilson, 373-392. London: Methuen.
- CLUTTON-BROCK, J. 1999. *A natural history of domesticated mammals*. Cambridge: University Press.
- CLUTTON-BROCK J., K. DENNIS-BRYAN, P. L. ARMITAGE and P.A. JEWELL. 1990. Osteology of the Soay sheep. *Bulletin of the British Museum(Natural History) Zoology* 56: 1-56.
- COHEN, J. 1988. *Statistical power analysis for the behavioral sciences*. 2nd Edition. Hillsdale: Lawrence Erlbaum.
- CORBET, G.B. 1978. *The mammals of the Palaearctic region: a taxonomic review*. London: British Meuseum (Natural History).
- CORBET, G.B. and J.E. HILL. 1980. *A world list of mammalian species*. London: British Meuseum (Natural History).

- CORNEVIN, C. and F.-X. LESBRE. 1891. Caracteres ostéologiques différentiels de la chèvre et du mouton. *Bulletin de la Société d'Anthropologie de Lyon* 10: 47-73.
- CRABTREE, P.J. 1989. *West Stow. Suffolk: early Anglo-Saxon animal husbandry*. Ipswich: Suffolk County Planning Department. East Anglian Archaeology Report no. 47.
- DARBY, H.C. 1977. *Domesday England*. Cambridge: Cambridge University Press.
- DAVIS, S.J.M. 1981. The effects of temperature change and domestication on the body size of Late Pleistocene to Holocene mammals of Israel. *Paleobiology* 7: 101-114.
- DAVIS, S.J.M. 1983. Morphometric variation of population of house mice *Mus domesticus* in Britain and Faroe. *Journal of Zoology London* 199: 521-534.
- DAVIS, S.J.M. 1992. *A rapid method for recording information about mammal bones from archaeological sites*. London: Ancient Monument Laboratory Report no. 19.
- DAVIS, S.J.M. 1996. Measurements of a group of adult female Shetland sheep skeletons from a single flock: a baseline for zooarchaeologists. *Journal of Archaeological Science* 23: 593-612.
- DAVIS, S.J.M. 2000. The effect of castration and age on the development of the Shetland sheep skeleton and a metric comparison between bones of males, females and castrates. *Journal of Archaeological Science* 27: 373-390.
- DAVIS, S.J.M. (in press). A metrical distinction between sheep and goat astragali. In *Papers in memory of Anthony Legge*. Oxford: Oxbow books.
- DAVIS, S.J.M. and BECKETT, J.V. 1999. Animal husbandry and agricultural improvement: the archaeological evidence from animal bones and teeth. *Rural History*, 10: 1-17.
- DE VET, H.C.W., C.B. TERWEE, D. L. KNOL and L.M. BOUTER. 2006. When to use agreement versus reliability measures. *Journal of Clinical Epidemiology* 59: 1033-1039.
- DRIESCH A. VON DEN. 1976. *A guide to the measurement of animal bones from archaeological sites*. Peabody Museum Bulletin 1. Cambridge: Peabody Museum of Archaeology and Ethnology, Harvard University.
- DYER, C. 1991. The west Midlands. In *The agrarian history of England and Wales Volume III, 1348-1500*, ed. E. MILLER, 145-161. Cambridge: Cambridge University Press.
- DYER, C. 1994. *Everyday life in Medieval England*. London: The Hambledon Press.
- DYER, C. 2006. Seasonal patterns in food consumption in the later Middle Ages. In *Food in Medieval England: diet and nutrition*, eds. C.M. WOOLGAR, D. SERJEANTSON and T. WALDRON, 201-213. Medieval History and Archaeology. Oxford: Oxford University Press.
- DYER, C. 2004. Alternative agriculture: goats in medieval England. In *People, landscape and agriculture: essays for Joan Thirsk*, ed. R.W.HOYLE, 20-38. Exeter: British Agricultural

History Society.

ENGLISH HERITAGE. (forthcoming). *The sheep/goat working party (1986-1991): biometric and morphological surveys and results*. Portsmouth: English Heritage. Research Department Report.

FERNÁNDEZ, H. 2001. *Ostéologie compare des petit ruminants eurasiatiques sauvages et domestiques (genres Rupicapra, Ovis, Capra et Capreolus): diagnose différentielle du squelette appendiculaire*. PhD Thesis. University of Geneva.

FERNÁNDEZ, H. 2002. Dètermination spècifique des restes osseux de chèvre (*Capra hircus*) et de mounon (*Ovis aries*): application aux caprinès du site de Sion-Ritz. In *La faune du site nèolithique de Sion-Avenue Ritz (Valais, Suisse): histoire d'un èlevage villageois il y a 5000 ans*, I. CHENAL-VELARDE, 116-151. British Archaeological Reports International Series 1081. Oxford: Archeopress.

FERNÁNDEZ, H., P. TABERLET, M. MASHKOUR, J.-D. VIGNE and G. LUIKART. 2002. Assessing the origin and diffusion of domestic goats using ancient DNA. In *The first steps of animal domestication*, eds. J.-D.VIGNE and P. HELMER, 50-54. Oxford: Oxbow book.

FERNÁNDEZ, H., S. HUGES, J.-D. VIGNE, D. HELMER, G. HODGINS, C. MIQUEL, C. HÄNNI, G. LUIKART, and P. TABERLET. 2006. Divergent mtDNA lineages of goats in an early Neolithic site, far from the initial domestication areas. In *Proceedings of the National Academy of Sciences of the United States of America*, 103: 15375-15379.

FIDDYMENT, S., B. HOLSINGER, C. RUZZIER, A. DEVINE, A. BINOIS, U. ALBARELLA, R. FISCHER, E. NICHOLS, A. CURTIS, E. CHEESE, M.D. TEASDALE, C. CHECKLEY-SCOTT, S.J. MILNER, K.M. RUDY, E.J. JOHNSON, J.ří Vnoučekp, M. GARRISON, S. McGRORY, D.G. BRADLEY, and M.J. COLLINS. 2015. Animal origin of 13th-century uterine vellum revealed using noninvasive peptide fingerprinting. *Proceedings of the National Academy of Science*, 49: 15066-15071.

FIELD, A. 2009. *Discovering statistics using SPSS*. 3rd Edition. London: Sage publications Ltd.

FRENCH, M.H. 1970. *Observations on the goat*. Rome: Food and Agriculture Organization of the United Nations.

FUSSELL, G. 1936. English farming before 1815. In *English farming: past and present*, E. LORDE, xxi-lxxv. 6th Edition. London: Heinemann.

GABLER, K-O. 1985. *Osteologische Unterscheidungsmerkmale am postkranialen skelett zwischen Mährenspringer (Ammotragus lervia), Hausschaf (Ovis aries) und Hausziege (Capra hircus)*. Inaugural-Dissertation. University of Munich.

GEBBELS, A. 1976. The animal bones. 198-207. In: Excavations on Fuller's Hill, Great Yarmouth, A. Rogerson. *East Anglian Archaeology*, 2: 131-245.

- GILLIS, R., L. CHAIX and J.-D. VIGNE. 2011. An assessment of morphological criteria for discriminating sheep and goat mandibles on a large prehistoric archaeological assemblage (Kerma, Sudan). *Journal of Archaeological Science* 38: 2324-2339.
- GRANT, A. 1979. The animal bones. In St John's street, J. HASSAL, 97-126. In *Excavation in Bedford 1967-77*, D. BAKER, E. BAKER, J. HASSALL and A. SIMCO, 103-107. *Bedfordshire Archaeology Journal* 13.
- GRANT, A. 1983. The animal bones. In *Excavations in Bedford 1977-1978*, J. HASSALL, 51-52. *Bedfordshire archaeology Journal* 16.
- GRANT, A. 1984. Medieval animal husbandry: the zooarchaeological evidence. In *Animals and archaeology: 4, husbandry in Europe*, eds. C. GRIGSON and J. CLUTTON-BROCK, 179-186. British Archaeological Reports International Series 227. Oxford: British Archaeological Reports.
- GRANT, A. 1988. Animal resources. In *The countryside of medieval England*, eds. A. GRENVILLE and A. GRANT, 149-187. Oxford: Basil Blackwell.
- GRAY, A.P. 1972. *Mammalian hybrids: a check-list with bibliography*. Farnham Royal: Commonwealth Agricultural Bureaux.
- GRINE, F.E., G. FOSSE, D.W. KRAUSE and W.L. JUNGERS. 1986. Analysis of enamel ultrastructure in archaeology: the identification of *Ovis aries* and *Capra hircus* dental remains. *Journal of Archaeological Science* 13: 579-595.
- GROMOVA, V. 1953. Osteologicheskie otlichiiia rodov *Capra* (kozly) i *Ovis* (barany); rukovodstvo dlia opredeleniia iskopaemykh ostatkov. Akademiia Nauk SSSR. *Trudy Komissii Po Izucheniiu Chetvertichnogo Perioda* 10(1): 3-122.
- HALLAM, H. ed. 1988. *The agrarian history of England and Wales II: 1042-1350*. Cambridge: Cambridge University Press.
- HALSTEAD, P., P. COLLINS and V. ISAKKIDOU. 2002. Sorting the sheep from the goats: morphological distinctions between the mandibles and mandibular teeth of adult *Ovis* and *Capra*. *Journal of Archaeological Science* 29: 545-553.
- HAMILTON-DYER, S. 2002. Some notes on the faunal remains. 180-182. In *Barkingwich? Saxon and medieval features adjacent to Barking Abbey*, G. HULL, 157-190. *Essex Archaeology and History* 33.
- HARUDA, A. 2014. Central Asian economy and ecologies in the Late Bronze Age: geometric morphometrics of the caprid astragalus and zooarchaeological investigations of pastoralism. PhD Thesis. University of Exeter.
- HATTING, T. 1974. The influence of castration on sheep horns. In *Archaeological studies*, ed. A. CLASON, 345-351. Amsterdam: Elsevier.

- HELMER, D. 2000. Discrimination des genres *Ovis* et *Capra* à l'aide des prémolaires inférieures 3 et 4 et interprétation des âges d'abattage: l'exemple de Dikili Tash (Grèce). *Anthropozoologica* 31: 29-38.
- HELMER, D. and M. ROCHETEAU. 1994. Atlas du squelette appendiculaire des principaux genres Holocènes de petits ruminants du nord de la Méditerranée et du Proche-Orient (*Capra*, *Ovis*, *Rupicapra*, *Capreolus*, *Gazella*). *Fiches d'Ostéologie Animale pour l'Archéologie, Série B: Mammifères*. Juan les Pins, France: Centre de Recherches Archéologiques du CNRS, APDCA.
- HILDEBRAND, M. 1955. Skeletal differences between deer, sheep, and goats. *California Fish and Game* 41: 327-346.
- HILL, J.W.F. 1965. *Medieval Lincoln*. Cambridge: Cambridge at the University Press.
- HILLS, C. 1999. Early historic Britain. In *The archaeology of Britain: an introduction from the Upper Palaeolithic to the industrial revolution*, eds. J. HUNTER and I. RALSTON, 176-193. London: Routledge.
- HODGSON, G.W.I. 1980. Report on the animal remains excavated during 1975-6 from the medieval levels at the High Street site, Perth. Unpublished.
- HODGSON, G.W.I. 1983. The animal remains from medieval sites within three burghs on the eastern Scottish seaboard. In *Site, environment and economy*, ed. B. PROUDFOOT, 3-32. Symposium of the Association for Environmental Archaeology 3. British Archaeological Reports International Series 173. Oxford: British Archaeological Reports.
- HOLE, F. 1996. The context of the caprine domestication in the Zagros region. In *The origins and spread of agriculture and pastoralism in Eurasia*, ed. D.R. HARRIS, 263-281. London: University College of London press.
- HOLE, F. 1969. The animal bones. In *Prehistory and human ecology of the Deh Luran plain*, F. HOLE, K. FLANNERY and J. NEELY, 262-330. Memoir of the Museum of Anthropology 1. Ann Arbor: University of Michigan.
- HOLMES, M. (unpublished). *Souther England: a review of animal remains from Saxon, Medieval and Post Medieval archaeological sites*. Portsmouth: English Heritage.
- HUTCHESON, G.D. and N. SOFRONIOU. 1999. *The multivariate social scientist: an introduction to generalized linear models*. London: Sage Publications Ltd.
- JOHNSTONE, C.J. 2004. *A biometric study of equids in roman world*. PhD Thesis. University of York.
- JONES, J.M. 2003. *The city by the pool: assessing the archaeology of the city of Lincoln*. Lincoln Archaeological Studies 10. Oxford: Oxbow Books.

- JONES, R.H. 1980. *Medieval houses at Flaxengate Lincoln*. The archaeology of Lincoln, XI-1. London : Council for British Archaeology for the Lincoln Archaeological Trust.
- KELK, A.D., C.G. GARTLEY, B.C. BUCKRELL and W.A. KING. 1997. The interbreeding of sheep and goats. *Canadian Veterinary Journal* 38: 235-237.
- KERSHAW, I. 1973. The great famine and the agrarian crisis in England 1315-1322. *Past & Present* 59: 3-50.
- KRATOCHVÍL, Z. 1969. Species criteria on the distal section of the tibia in *Ovis ammon* F. *aries* L. and *Capra aegagrus* F. *hircus* L. *Acta Veterinaria* (Brno) 38: 483-490.
- KÜHNHOLD, B. 1971. *Die tierknochenfunde aus unterregenbach, einer mittelalterlichen siedlung Württembergs*. Inaugural-Dissertation. University of Munich.
- LANDERS, R.N. 2011. Computing Interclass Correlations (ICC) as estimates of Interrater Reliability in SPSS. <http://neoacademic.com/2011/11/16/computing-intraclass-correlations-icc-as-estimates-of-interrater-reliability-in-spss/#.VUCncyFViko> (last accessed 29 April 2015).
- LANGDON, J. 1986. *Horses, Oxen and technological innovation: the use of draught animals in the English farming from 1066 to 1500*. Cambridge: Cambridge University Press.
- LEGGE, T. 1996. The beginning of caprine domestication in Southwest Asia. In *The origins and spread of agriculture and pastoralism in Eurasia*, ed. D.R. HARRIS, 238-262. London: University College of London press.
- LEVITAN, B. 1987. Medieval animal husbandry in south west England: a selective review and suggested approach. In *Studies in palaeoeconomy and environment in south west England*. British Archaeological Series, 181: 51-80. Oxford: Archaeopress.
- LOREILLE, O., J.-D. VIGNE, C. CALLOU, F. TREINEN-CLAUSTRE, N. DENNEBOUY and M. MONNET. 1997. First distinction of sheep and goat archaeological bones by the means of their fossil mtDNA. *Journal of Archaeological Science* 24: 33-37.
- LIE, R.W. 1988. Animal bones. In *De arkeologiske utgravninger in Gamlebyen, Oslo 5*. "Mindets Tomt"- "Søndrefelt", 153-195. Øvre Ervik: Alvheim and Eide.
- LYMAN, R.L. 1984. Bone density and differential survivorship of fossil classes. *Journal of Anthropological Archaeology* 3: 259-299.
- LYMAN, R.L. and T.L. VANPOOL. 2009. Metric data in archaeology: a study of inter-analyst and intra-analyst variation. *American Antiquity* 74: 485-504.
- LUIKART, G., L. GIELLY, L. EXCOFFIER, J.-D. VIGNE, J. BOUVET and P. TABLERLET. 2001. Multiple maternal origins and weak phylogeographic structure in domestic goats. *Proceedings of the Nation Academy of Sciences of the United States of America* 98: 5927-5932.
- LUIKART, G., H. FERNÁNDEZ, M. MASHKOUR, P.R. ENGLAND and P. TABERLET.

2006. Origins and diffusion of domestic goats inferred from DNA markers. In *Documenting domestication: new genetic and archaeological paradigms*, eds. M.A. ZEDER, D.G. BRADLEY, E. EMSWILLER and B.D. SMITH, 294-305. Berkley, CA: University of California Press.
- MALTBY, M. 1979. *Faunal studies on urban sites : the animal bones from Exeter 1971-1975*. Exeter archaeological reports. Sheffield : Department of Prehistory and Archaeology, University of Sheffield.
- MANN, H.B. and D.R. WHITNEY. 1947. On a test of whether one of two random variables is stochastically larger than the other. *Annals of Mathematical Statistics* 18: 50-60.
- MASON, I. 1984. *Evolution of domesticated animals*. London: Logman.
- METTERS, A., ed. 2009. *The King's Lynn Port Books 1610-1614*. Norfolk Record Society, LXXIII. Norwich: The Norfolk Record Society.
- NODDLE, B.A. 1975. A comparison of the animal bones from 8 Medieval sites in southern Britain. In *Archaeozoological studies*, ed. A. CLASON, 248-260. Amsterdam: North Holland Publishing Company.
- NODDLE, B.A. 1976. Report on animal bones from Walton, Aylesbury. In *Saxon and Medieval Walton, Aylesbury: Excavations 1973-4*, M. FARLEY, 269-287. Records of Buckinghamshire, XX part II.
- NODDLE, B.A. 1977. Mammal bone. In *Excavation in King's Lynn 1963-1970*, H. CLARKE and A. CARTER, 378-399, The Society for Medieval Archaeology Monograph Series 7. London: Society for Medieval Archaeology.
- NODDLE, B.A. 1980. The animal bone. In *Excavations in North Elmham Park 1967-72*, ed. P. WADE-MARTINS, 375-409. Norwich: Norfolk Archaeology Unit, East Anglian Archaeology Report no.9.
- NODDLE, B.A. 1985. Some of the faunal remains from Mary-Le-Port, Bristol. In *Mary-Le-Port, Bristol: Excavations 1962/3*. Eds. L. WATTS and P. RAHTZ, 177-179. Bristol: City of Bristol Museum and Art gallery Monograph 7.
- NODDLE, B.A. 1987. Animal bones from Jarrow. 3rd Report. *Ancient Monuments Laboratory Report 80/87*. London: English Heritage.
- NODDLE, B.A. 1991. The animal bones. In *Excavations at Chepstow 1973-4*, R. SHOESMITH, 150-155. Bangor: Cambrian Archaeological Association Monographs 4.
- NODDLE, B.A. 1992. Animal bone from Wonkwearmouth. Durham: Durham University. Unpublished.
- NODDLE, B.A. 1994. The under-rated goat. In *Urban-rural connexions: perspectives from*

environmental archaeology. Symposia of the Association of Environmental Archaeology 12, eds. H. HALL and K. KENWARD, 117-128. Oxford: Oxbow books.

NOODLE, B.A. and R. HARTCOURT. 1985. The animal bones. In *Hereford city excavations* 3, ed. R. SHOESMITH, 84-94. London: Council for British Archaeology Research Report 56.

O'CONNOR, T. 1982. *Animal Bones from Flaxengate, Lincoln c. 870-1500*. The archaeology of Lincoln, XVIII-1. London: Council for British Archaeology for the Lincoln Archaeological Trust.

O'CONNOR, T. 1984. *Selected groups of bones from Skeldergate and Walmgate*. The Archaeology of York, The Animal Bones 15/1. York: Council for British Archaeology.

ONAR, V., G. PAZVANT and O. BELLI. 2008. Osteometric examination of metapodial bones in sheep (*Ovis aries* L.) and goat (*Capra hircus* L.) unearthed from the upper Anzaf Castle in eastern Anatolia. *Revue De Médecine Vétérinaire*, 159: 150-158.

OXFORD UNIVERSITY PRESS. 2015. Oxford English dictionary: the definitive record of the English language. <http://www.oed.com> (last consulted 17 September 2015).

PARKER, V. 1971. *The making of King's Lynn: secular buildings from the 11th to the 17th century*. Kings Lynn archaeological survey 1. London: Phillimore.

PAYNE, S. 1969. A metrical distinction between sheep and goat metacarpal. In *The domestication and exploitation of plants and animals*, eds. P.J. UCKO and G.W. DIMBLEBY, 295-306. London: Duckworth.

PAYNE, S. 1973. Kill-off patterns in sheep and goats: the mandibles from Aşvan Kale. *Anatolian Studies* 23: 292-303.

PAYNE, S. 1985. Morphological distinctions between the mandibular teeth of young sheep, *Ovis*, and goats, *Capra*. *Journal of Archaeological Science* 12: 139-147.

PAYNE, S. 1987. Reference codes for wear states in the mandibular check teeth of sheep and goat. *Journal of Archaeological Science* 14: 609-614.

PAYNE, S. and G. BULL. 1988. Components of variation in measurements of pig bones and teeth, and the use of measurements to distinguish wild from domestic pig remains. *ArchaeoZoologia* II: 27-66.

PERRING, D. 1981. *Early medieval occupation at Flaxengate Lincoln*. The archaeology of Lincoln, IX-1. London: Council for British Archaeology for the Lincoln Archaeological Trust.

PINTER-BELLOWS, S. 1997. Animal bones. In *Excavation in the outer enclosure of Boteler's Castle, Oversley, Alcester, 1992-93*, C. JONES, G. EYRE-MORGAN, S. PALMER and N. PALMER, 65-73. Transactions of the Birmingham and Warwickshire Archaeological Society, Vol. 101.

- POPKIN, P.R.W., P. BAKER, F. WORLEY, S. PAYNE and H. HAMMON. 2012. The sheep project: determining skeletal growth, timing of epiphyseal fusion and morphometric variation in unimproved Shetland sheep of known age, sex, castration status and nutrition. *Journal of Archaeological Science* 39: 1775-1792.
- PRUMMEL, W. 1978. Animal bones from tannery pits of s'-Hertogenbosch. *Berichten Rijksdienst voor het Oudheidkundig Bodemonderzoek* 20: 399-422.
- PRUMMEL, W. 1982. The archaeological study of medieval sites in the Netherlands. In *Environmental archaeology in the urban context*, eds. A.R. HALL and H.K. KENWARD, 117-122. London: Lonsdale Universal Printing Ltd. Council of British Archaeology Research Report 43.
- PRUMMEL, W. and H.J. FRIESCH. 1986. A guide for the distinction of species, sex and body side in bones of sheep and goat. *Journal of Archaeological Science* 13: 567-577.
- RACKHAM, D.J. 1979. Animal resources. In Three Anglo-Saxon tenements in Durham city, ed. M. O. H. CARVER, 47-54. *Medieval Archaeology Journal* 23: 1-80.
- RACKHAM, D.J. 1988. Animal bones. In Anglo-Saxon monastery at Church Close, Hartlepool, Cleveland, R. DANIELS, 197-199. *The Archaeological Journal* 145: 158-210.
- RANKIN, G. and M. STOKES. 1998. Reliability of assessment tools in rehabilitation: an illustration of appropriate statistical analyses. *Clinical Rehabilitation* 12: 187-199.
- REICHSTEIN, H. and M. TIESSEN. 1974. Ergebnisse und Probleme von Untersuchungen an Wildtieren aus Haithabu (Ausgrabung 1963-1964). In *Berichte über die Ausgrabungen in Haithabu 7: Untersuchungen an Tierknochenfunden*, eds. K. SCHIETZEL, 103-144. Neumünster: Wachholtz.
- REED, R. 1972. *Ancient skins, parchments and leathers*. London: Seminar Press Ltd.
- RIDEOUT C.B. and R.S. HOFFMAN. 1975. *Oreamnos americanus*. *Mammalian Species* 63: 1-6.
- ROSENTHAL, R. 1991. *Meta-analytic procedures for social research*. 2nd Edition. Newbury Park, CA: Sage publications Ltd.
- ROSENTHAL, J.A. 1996. Qualitative descriptors of strength of association and effect size. *Journal of Social Service Research* 21: 37-59.
- RYDER, M.L. 1983. *Sheep & man*. London: Gerald Duckworth & CO Ltd.
- ROWLEY-CONWY, P. 1998. Improved separation of Neolithic metapodials of sheep (*Ovis*) and goats (*Capra*) from Arene Candide cave, Liguria, Italy. *Journal of Archaeological Science* 25: 251-258.
- SALAMI, S.O., C.S. IBE, A.D. UMOSEN, I.E. AJAYI and S.M. MAIDAWA. 2011.

Comparative osteometric study of long bones in Yankasa and Red Sokoto goats. *International Journal of Morphology* 29: 100-104.

SALEHI, M., I. KADIM, O. MAHGOUB, Sh. NEGAHDARI and R.S. ESHRAGHI NAEENI. 2013. Effects of type, sex and age on goat skin and leather characteristics. *Animal Production Science*, 54: 638-644.

SAUNDERS, C. 1977. A sixteenth century tannery in St Albans. *Hertfordshire's Past* 3: 9-12.

SAURO, J. 2004-2015. The standard deviation and coefficient of variation. <http://www.usablestats.com/lessons/sdcv> (last accessed 29 April 2015).

SCHAFFER, W.M. and C.A. REED. 1972. The co-evolution of social behaviour and cranial morphology in sheep and goats (Bovidae, Caprini). *Fieldiana (zoology)* 61: 1-88.

SCHATZ, H. 1963. *Die Tierknochenfunde au seiner mittelalterlichen siedlung Württembergs*. Inaugural-Dissertation. University of Munich.

SCHMID, E. 1969. Knochenfunde als archäologische Quellen durch sorgfältige Ausgrabungen. In *Archäologie und Biologie. Forschungsberichte 15*, S. WIESBADEN, 100-111. Deutsche Forschungsgemeinschaft. Wiesbaden: Steiner.

SCHMID, E. 1972. *Atlas of animal bones: for prehistorians, archaeologists and quaternary geologists*. Amsterdam: Elsevier.

SCHRAMM, Z. 1967. Różnice morfologiczne niektórych kości kozy i owcy. *Rozniki Wyższej Szkoły Rolniczej ro Poznaniu XXXVI*: 107-132.

SERJEANTSON, D. 1989. Animal remains and the tanning trade. In *Diet and crafts in towns*, eds. D. Serjeantson and T. Waldron, 129-146. British Archaeological Report British Series 199. Oxford: British Archaeological Reports.

SERJEANTSON, D. and H. REES. 2009. *Food, craft and status in Medieval Winchester: the plant and animal remains from the suburbs and city defences*. Winchester: Winchester Museum.

SHENNAN, S. 1997. *Quantifying archaeology*. 2nd Edition. Edinburgh: Edinburgh University Press.

SILVER, A. 1969. The ageing of domestic animals. In *Science in archaeology, a survey of progress and research*. Revised Edition, eds. D.R. BROTHWELL and E.S. HIGGS, 283-302. London: Thames and Hudson.

SIMPSON, G.G., A. ROE and R.C. LEWONTIN. 1960. *Quantitative zoology*. Revised edition. New York :Dover Publications INC.

SODEN, I. 1998-1999. A history of urban regeneration: excavations in advance of development off St Peter's walk, Northampton, 1994-7. *Northamptonshire Archaeology* 28: 61-127.

STACK EXCHANGE 2015. Differences between variable and variate. <http://math.stackexchange.com/questions/204705/differences-between-variable-and-variate> (last consulted 30 April 2015).

STACK EXCHANGE 2015b. Skewed variables in PCA or factor analysis. <http://stats.stackexchange.com/questions/38709/skewed-variables-in-pca-or-factor-analysis> (last consulted 30 April 2015).

STALLIBRASS, S. 1995. Review of the vertebrate remains. In *Plant and vertebrate remains from archaeological sites in northern England: data reviews and future directions*, J.P. HUNTLEY and S. STALLIBRASS, 84-194. Research Report No.4. Durham: Architectural and Archaeological Society of Durham and Northumberland.

SYKES, N.J. 2006. From Cu and Scaep to Beffe and Motton. In *Food in Medieval England: diet and nutrition*, eds. C.M. WOOLGAR, D. SERJEANTSON and T. WALDRON, 56-71. Oxford: Oxford University Press.

TABACHNICK, B.G. and L.S. FIDELL, eds. 2007. *Using multivariate statistics*. 5th Edition. Boston: Pearson/Allyn and Bacon.

THIRSK, J. 1967. *The agrarian history of England and Wales*. Vol. 2. London: Cambridge University Press.

THIRSK, J. 1997. *Alternative agriculture: a history from the Black Death to the present day*. Oxford: Oxford University Press.

THOMAS, R. 2002. Animal, economy and status: the integration of historical and zooarchaeological evidence in the study of a Medieval castle. PhD Thesis. University of Birmingham.

THOMAS, R. 2005. *Animals, economy and status: integrating zooarchaeological and historical data in the study of Dudley castle, West Midlands (c.1100-1750)*, British Archaeological Report British Series 392. Oxford: Archaeopress.

THOMAS, R. 2005b. Zooarchaeology, improvement and the British Agricultural Revolution. *International Journal of Historical Archaeology*, 9/2: 71-88.

THOMAS, R., HOLMES, M. and MORRIS, J. 2013. "So bigge as bigge may be": tracking size and shape change in domestic livestock in London (AD 1220-1900). *Journal of Archaeological Science* 40: 3309-3325.

THOMPSON, D., ed. 1995. *The concise Oxford dictionary of current English*. 9th Edition, Oxford: Clarendon Press.

UERPMANN, H.-P. 1996. Animal domestication-accident or intention? In *The origins and spread of agriculture and pastoralism in Eurasia*, ed. D.R. HARRIS, 227-237. London: University College of London.

ULIJASZEK, S.J. and J.A. LOURIE. 1994. Intra- and inter-observer error in anthropometric measurement. In *Anthropometry: the individual and the population*, eds. S.J. ULIJASZEK and C.G.N. MASCIE-TAYLOR, 30-55. New York: Cambridge University Press.

UTEMOHLE, C.J. and S.L. ZEGURA. 1982. Intra- and interobserver error in craniometry: a cautionary tale. *American Journal of Physical Anthropology* 57: 303-310.

VIGNE, J.-D., D. HELMER and J. PETERS. 2005. New archaeozoological approaches for the first steps of animal domestication: general presentation, reflections and proposals. In *First steps of animal domestication: new archaeozoological approaches. Volume 9 of Proceedings of the 9th Conference of the International Council of Archaeozoology, Durham, August 2002*, International Council for Archaeozoology Conference (Durham, England), eds. J.-D. VIGNE and D. HELMER, 1-16. Oxford: Oxbow books.

WALKER, E.P. 1975. *Mammals of the world*. London: Johns Hopkins University Press.

WALKER, I. 2007-2008. Null hypothesis testing and effect sizes. <http://staff.bath.ac.uk/pssiw/stats2/page2/page14/page14.html> (last consulted 30 April 2015).

WENHAM, L.P. 1965. Hornpot Lane and the horns of York. *Annual Report of the Council of the Yorkshire Philosophical Society for 1964*: 25-26.

WESTGARD, J. 2009. Z-4: mean, standard deviation, and coefficient of variation. <http://www.westgard.com/lesson34.htm#2> (last accessed 29 April 2015).

WHITE, K.D. 1970. *Roman farming*. Great Britain: Thames and Hudson.

WILLIAMS, J.H. 1979. *St Peter's Street Northampton: excavations 1973-1976*. Archaeological monograph 2. England: Belmont Press.

WILLIAMSON, T. 2002. *The transformation of rural England: farming and landscape 1700-1870*. Exeter: University of Exeter Press.

WILLSON, D.E. and D.M. REEDER. 2005. *Mammal species of the world: a taxonomic and geographic reference*. Baltimore: Johns Hopkins University Press.

WILSON, C.A. 1973. *Food and drink in Britain: from the Stone Age to recent times*. London: Constable.

WOOLGAR, C.M. 2006. Meat and dairy products in Late Medieval England. In *Food in Medieval England: diet and nutrition*. Eds. C.M. WOOLGAR, D. SERJEANTSON and T. WALDRON, 88-101. Medieval History and Archaeology. Oxford: Oxford University Press.

WRIGHT, E. 2014. The history of the European aurochs from the Middle Pleistocene to its extinction: an archaeological investigation of its evolution, morphological variability and response to human exploitation. PhD Thesis. University of Sheffield.

WRIGLEY, E and R. SCHOFIELD. 1981. *The population history of England, 1541-1871: a*

reconstruction. London: Edward Arnold.

YABLOKOV, A.V. 1974. *Variability of mammals*. Washington, DC: Smithsonian Institution and National Science Foundation.

ZEDER, M.A. 2006. A critical assessment of markers of initial domestication in goats (*Capra hircus*). In *Documenting domestication: new genetic and archaeological paradigms*, eds. M.A. ZEDER, D.G. BRADLEY, E. EMSHWILLER and B.D. SMITH, 181-208. Berkley: University of California Press.

ZEDER, M.A. 2008. Domestication and early agriculture in Mediterranean basin: origins, diffusion, and impact. *Proceedings of the National Academy of Sciences of the United States of America* 105: 11597-11604.

ZEDER, M.A., D.G. BRADLEY, E. EMSHWILLER and B.D. SMITH, eds. 2006. *Documenting domestication: new genetic and archaeological paradigms*. Berkley: University of California Press.

ZEDER, M.A. and B. HESSE. 2000. The initial domestication of goats (*Capra hircus*) in the Zagros Mountains 10,000 years ago. *Science* 28: 2254-2257.

ZEDER, M.A. and H.A. LAPHAM. 2010. Assessing the reliability of criteria used to identify postcranial bones in sheep, *Ovis*, and goats, *Capra*. *Journal of Archaeological Science* 37: 2887-2905.

ZEDER, M.A. and S.E. PILAAR. 2010. Assessing the reliability of criteria used to identify mandibles and mandibular teeth in sheep, *Ovis*, and goats, *Capra*. *Journal of Archaeological Science* 37: 225-242.

ZEUNER, F.E. 1963. *A history of domesticated animals*. London: Hutchinson & Co.

ZOARY, D., E. TCHERNOV and L. KOLSKA HORWITZ. 1998. The role of unconscious selection in the domestication of sheep and goats. *Journal of Zoological Society of London* 245: 129-135.

Appendices

Appendix I: The importance of the goat in the human past

1.1 The domestication of the goat: background, dynamics, place and time

The goat was one of the first farm animals to be domesticated and an important component of the so-called 'Neolithic Revolution'. Its long-term interaction with humans has been demonstrated by archaeological evidence, which suggests that its domestication, along with that of the sheep, took place between 11,000 and 10,500 years BP, and perhaps even earlier (Zeder 2008). The importance of this species for human societies is also attested by its worldwide distribution, which is a consequence of its value as a source of milk and meat (French 1970; Luikart *et al.* 2001; Mason 1984; Noddle 1994).

The earliest domestication of the goat has been widely debated and the subject has also benefitted from biomolecular analytical methods of investigation (Fernández *et al.* 2002; Fernández *et al.* 2006; Luikart *et al.* 2001; Luikart *et al.* 2006; Zeder 2008; Zeder and Hesse 2000; Zeder *et al.* 2006; Zohary *et al.* 1998). All these studies agree in identifying the Middle East, and more precisely the area where Iraq, Turkey and Iran currently meet, as the primary location where the domestication of the goat began.

The domestication of sheep and goat has to be considered as a gradual, long and complex process, the basis of which are deeply rooted in a series of climatic as well as cultural changes. The period of transition between the Late Pleistocene and Early Holocene witnessed important climatic changes which may represent the background to the emergence of sedentary or semi-sedentary lifestyles in the Near East (Zeuner 1963; Mason 1984; Hole 1996; Uerpmann 1996). The alteration of warm and cold climatic phases forced human populations to adopt different survival strategies. These changes were accompanied by a shift in settlement patterns; sheltered lowland locations were chosen in preference to high elevation locations (Mason 1984).

The difficult living conditions imposed by the cold-dry phase of the Younger Dryas forced humans to intensify the use of the food already available and to organise more efficiently regimes of food production, such as harvesting, storing, food-processing, plant and livestock protection. This general situation led to the growth, about 13,000 BP, of villages (Natufian culture) which are likely to have practiced (despite the absence of demonstrable evidence) a form of control on wild animals, including sheep and goats domestication or plant cultivation. The availability of caprine herds and their attitude toward human domination may have constituted an encouraging factor for experiments in husbandry (Mason 1984; Hole 1996). The

beginning of the Holocene (c.11,500 BP), signalled by a period of warmer climate, represents the moment in when the domestication of cereals and animals started (during the Pre-Pottery Neolithic B).

Studies focused on domestication are based on the identification of bones from archaeological sites located in the Fertile Crescent, the region stretching from the east Mediterranean to the Persian Gulf (Thompson 1995). This material represents a valuable source of information about the time and the ways through which the process occurred but many questions remain open. Different factors affect the reliability of the research conducted, first of all the difficulty in distinguishing between the bones of wild ancestors and those of domesticated animals. The availability of wild goats in the region of south-western Asia, where agriculture was already present, and the physical characteristics of these animals (i.e. their hardiness and ability to adapt to extreme conditions) have led some researchers (Zeuner 1963; Bökönyi 1974; Mason 1984, Uerpmann 1996) to suggest that goats were probably more suitable animals, than sheep and other herbivores, for domestication. It is accepted that the first step toward domestication was probably the separation of some individuals from the wild population and their maintenance in reproductive isolation. Given this background, the first domesticated goats were likely to have been morphologically similar to their wild counterparts (French 1970; Uerpmann 1996; Zeder *et al.* 2006). In addition, the identification process is made more complicated by the difficulty of discriminating between the bones of sheep and goats. Sheep and goats, although genetically distinct, differ from each other morphologically only in some features that are not always easily recognisable. This difficulty is exacerbated when dealing with highly fragmented assemblages. A heavy degree of fragmentation due to butchery - the intensity of exploitation of the animal resources in such an early period of history must have been considerable so that all the possible nutritious substances were extracted from the bones (i.e. marrow and grease) - leads to a very fragmented animal bone waste assemblage, reducing the possibility of carrying out detailed taxonomic identifications (French 1970; Mason 1984; Legge 1996; Zeder *et al.* 2006).

Despite these limitations, our understanding of the domestication process has increased significantly and, as pointed out in recent studies, a variety of sources of evidence is considered (though with different degrees of reliability) to point out to domestication. By the late 1990s, the idea that the main sign of animal domestication was represented by morphological changes, in particular through decreased body size, was internationally accepted among zooarchaeologists (Zeder and Hesse 2000). Recent studies conducted on modern reference collections and archaeological assemblages, however, have highlighted the fact that factors, other than domestic status, can influence the body size of an animal (Vigne *et al.* 2005; Zeder and Hesse 2000; Zeder *et al.* 2006; Zeder 2008). As a consequence, what was previously interpreted as direct proof of the emergence of smaller domestic animals, is now thought, in some cases, to be a consequence of changed culling strategies. This hypothesis is based on the assumption that an

archaeological assemblage deriving from herders would show a kill-off pattern dominated by the culling of young males (whose excessive presence was not needed for the continuity of the herd) and the presence of females killed at an older age, after their prime reproductive years. An assemblage deriving from hunters, on the other hand, would be characterised by the presence of large adult animals, which are ideal preys if the aim was to optimize return (Luikart *et al.* 2001; Zeder 2008; Zeder *et al.* 2006). This new approach, recently applied to previously studied material from Iraq and Iran, has shown clear evidence of managed herds much earlier than the advent of the ‘domestication-induced’ morphological changes, which require several generations to become manifest (Zeder *et al.* 2006).

In light of these new discoveries, the origin of goat domestication, despite all uncertainties, can probably be assumed to have occurred in different periods and in different parts of the Fertile Crescent (Zeder 2008). At least two places have been identified, where the domestication process may have happened independently: Ganj Dareh in the highlands of Iran (9,900 BP) and Nevali Çori, in the southern Turkish region of the Euphrates valley (10,000 BP) (Zeder 2008; Zeder and Hesse 2000; Zeder *et al.* 2006). In addition to the archaeological data, recent genetic studies have identified the existence of as many as six goat haplotypes (Luikart *et al.* 2001; Fernández *et al.* 2006). Although scientists are still unsure about how to interpret this evidence, it seems that independent processes of domestication occurred at different times and in different areas (Luikart *et al.* 2000; Fernández *et al.* 2002; Fernández *et al.* 2006; Zeder 2008).

1.2 The wild progenitor of the domestic goat

The identification of the wild progenitor of the domestic goat relies on the combination of different lines of evidence. The wild Bezoar of southwest Asia (*Capra aegagrus*) has long been regarded as the most likely wild ancestor of the domestic goat (*Capra hircus*), although some researchers believe that the markhor (*Capra falconieri*) played a role during a second wave of domestication in Pakistan, and is responsible for the emergence of the cashmere breed in Southern Asia (Mason 1984; Luikart *et al.* 2000).

Capra aegagrus, as well as the wild ancestor of the domestic sheep, *Ovis orientalis*, was an endemic and widely distributed species in the Fertile Crescent, the area where goat domestication first occurred (French 1970; Mason 1984; Uerpmann 1996). Comparative morphological studies support the hypothesis of a lineage between the wild Bezoar and the domestic goat (French 1970; Mason 1984). The morphological approaches base their reasoning on the observation of how some morphological features noticed in the domestic animal (such as the anterior keel of the horns and their scimitar shape) could have only been acquired from the Bezoar. Genetic analyses (Fernández *et al.* 2006; Luikart *et al.* 2000; Luikart *et al.* 2006; Zeder 2008; Zeder *et al.* 2006; Zeder and Hesse 2000) have also confirmed that the Bezoar is the most likely progenitor of the domestic goat.

1.3 Differences and similarities with the sheep

Although they belong to the same family, subfamily and tribe, sheep and goat represent different genera, respectively *Ovis* and *Capra*. They have different chromosome numbers, consequently they are thought to be unable to interbreed naturally (French 1970; Mason 1984; Noddle 1994), though interbreeding has occurred in human-controlled environments (Kelk *et al.* 1997).

Sheep and goat have often been confused because of their skeletal resemblance, and also because they provide similar products such as meat, milk, wool (though only a few goat breeds, such as Angora and Cashmere, are suitable for wool production), skins and horns. Although they display important and clear common characteristics, physical and behavioural differences can be recognised.

From a physical standpoint, goats differ from sheep in:

- the presence of a beard (French 1970; Mason 1984)
- the presence of caudal scent glands in male individuals (Mason 1984);
- the absence of suborbital tear glands and lachrymal pits in sheep skulls (Mason 1984)
- the presence of foot glands only in the forefeet (this is not a constant trait though) while these glands are present in sheep in both hind and forefeet (Mason 1984);
- the presence of odoriferous tail-glands in male individuals (French 1970);
- the presence of constant and well defined horn characteristics. Goat horns rise vertically from the head and bend backwards in a scimitar-shape curve (French 1970: 3). In sheep, horns are much more sturdy and more closely curled than the slender vertical horns of goats (Schaffer and Reed 1972).
- the way they hold the tail. Goats hold the tail erect while sheep do not (French 1970).
- the shape of the skull. Since sheep have a tendency to butt with much greater violence than goats, they have developed a particular skull shape and thickness in order to avoid damage (Mason 1984).

In terms of behaviour and habits, it is widely known that while sheep are animals of grassy plains ('grazers'), goats are 'browsers' and they prefer mountainous habitats (French 1970; Mason 1984; Noddle 1994; Clutton-Brock 1999; Balasse and Ambrose 2005). Goats are well adapted to severe conditions such as semi-desert environments and they can survive on very scarce fodder, which means that this species can extract nutrients from areas unable to support sheep and other animals (French 1970; Mason 1984).

Goats are more inclined toward the eating of weeds, shrubs, bushes and trees, even though they do not abhor pasture herbage. They prefer to pick small portions of food and tend to move rapidly to another area. Sheep with their bifid upper lip are able to graze closer to the ground and in doing so they frequently eradicate the smaller grass species causing damage. This suggests that sheep are more likely to begin and perpetuate erosive action than goats (French 1970).

Moreover, while sheep tend to develop and follow well known paths, goats prefer generally to wander (French 1970). Goats are known as more independent animals: they do not follow each other so easily, they are less easy to drive than sheep (Noodle 1994), but their greater independence means that they require less labour (French 1970).

Appendix II: Bland and Altman plots as integration of the ICC (Inter-Observer Error)

As previously mentioned (Section 2.3.1), the ICC has some disadvantages which make it unsuitable for use in isolation. As such, the test was performed along with Bland and Altman plots in order to provide an alternative and supportive way of exploring the reliability of the measurements. The following plots, particularly useful in order to see if patterns, bias or potential outliers among the raters can be recognised, show two rows of dots. Each row represents the specimen measured while each dot represents a rater. On the horizontal axis, the Mean of the values given by the different raters is shown while, on the vertical axis, the difference of the Mean for the eight raters is displayed.

The Bland and Altman plots (Figs. A2.1 and A2.2) related to measurement on the lower 3rd premolar show that measurements on specimen 2 have been taken more consistently than those taken on specimen 1. In specimen 1 in fact, both B and L values are spread along the line (difference between the Mean of raters is higher) while in specimen 2 the dots are closer to 0.

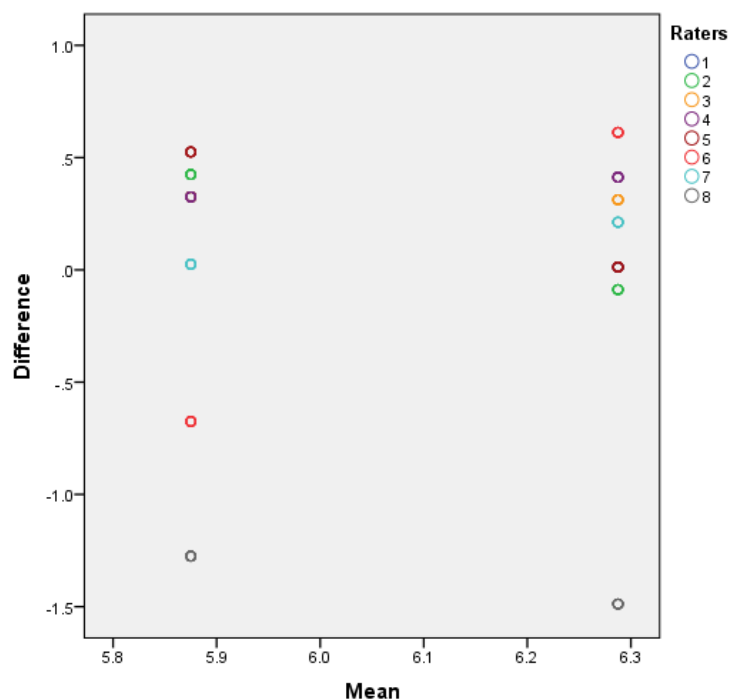


Figure A2.1 Scatterplot of the Mean versus difference of B measurement on Pm₃, for two specimens taken by 8 raters.

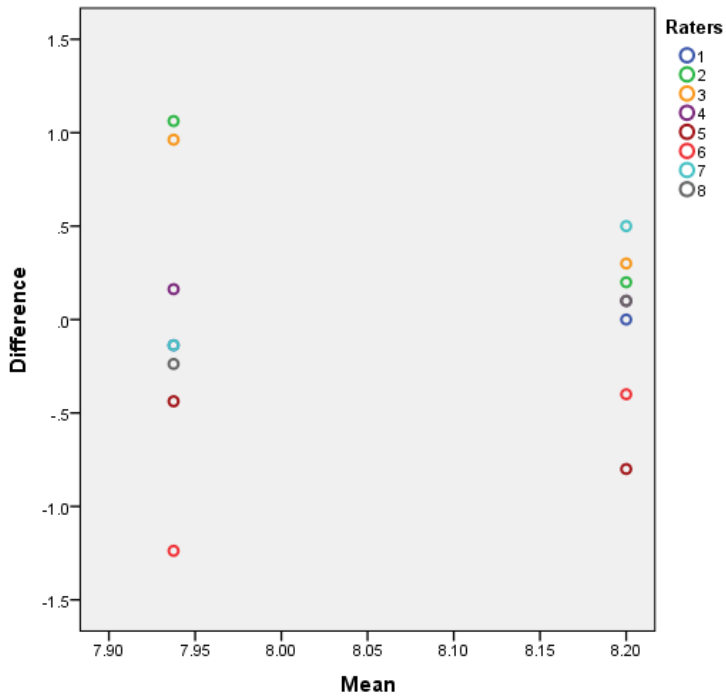


Figure A2.2 Scatterplot of the Mean versus difference of L measurement on Pm₃, for two specimens taken by 8 raters.

The plots A2.3 and A2.4 show the results for the measurements taken on the 4th lower premolar. In both measurements B and L dots are scattered along the vertical line for all the two specimens. Thus, the presence of difference in Mean between the raters is attested.

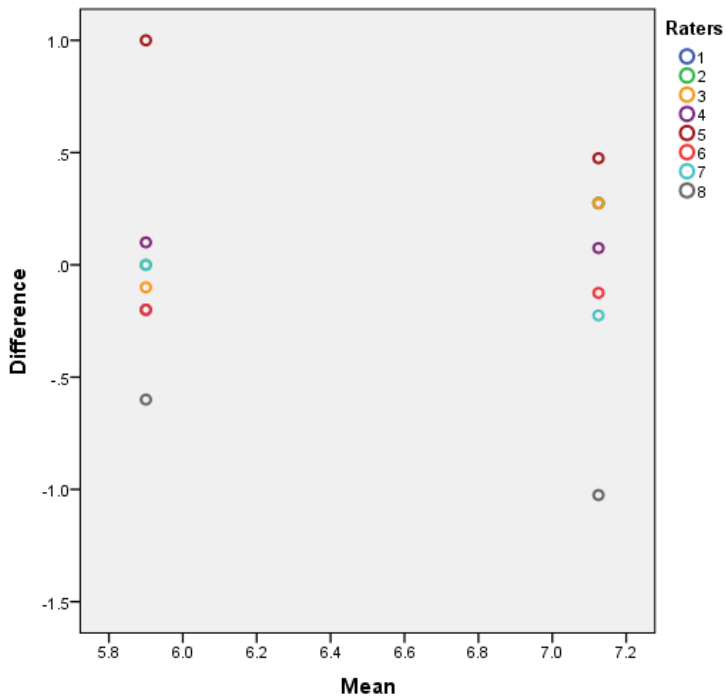


Figure A2.3 Scatterplot of the Mean versus difference of B measurement on P₄, for two specimens taken by 8 raters.

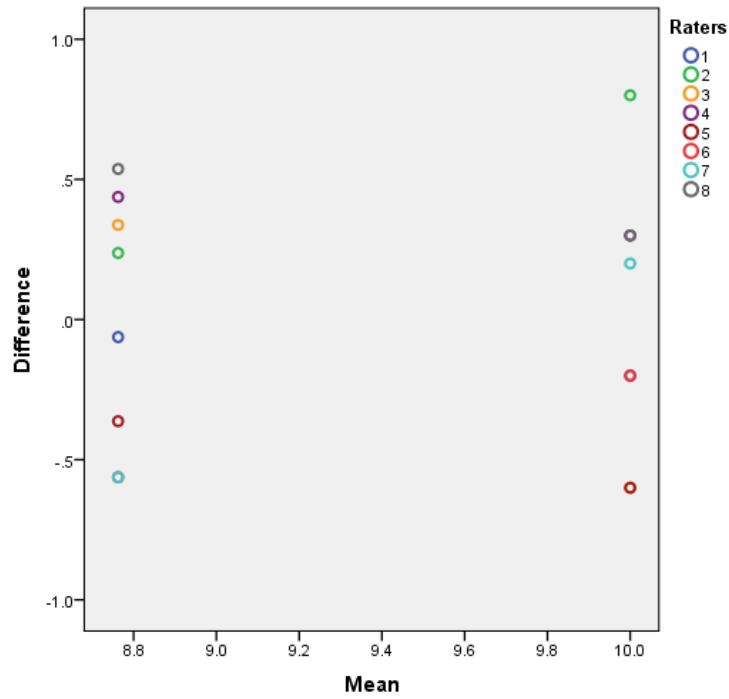


Figure A2.4 Scatterplot of the Mean versus difference of L measurement on P₄, for two specimens taken by 8 raters.

The graphs A2.5 and A2.6 are related to the measurements taken on the mandible. They show that, in taking both H and B, rater 5 is the one who has the highest difference values; this has had probably an influence on the (low) ICC value for H. Overall, the dots are spread along the vertical line in both specimens for both measurements, showing that there is some difference in Mean among the raters.

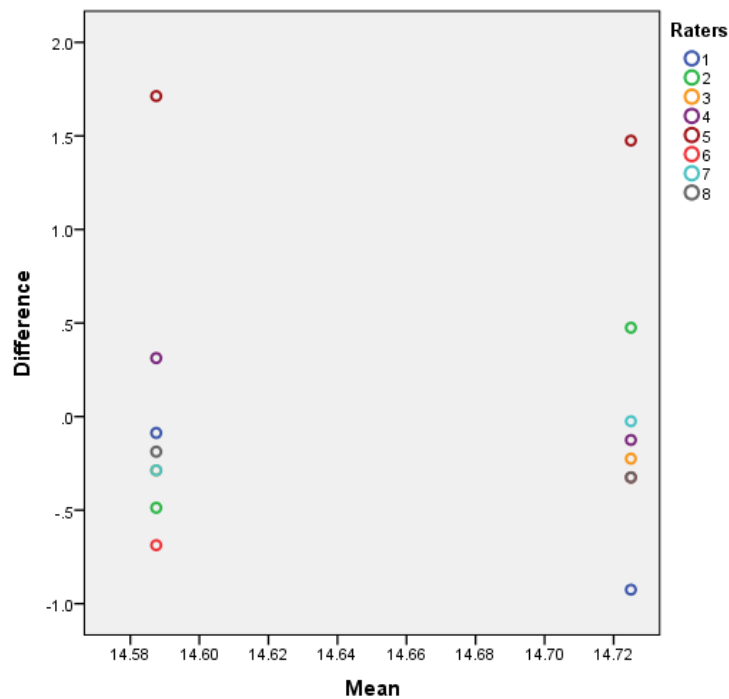


Figure A2.5 Scatterplot of the Mean versus difference of H measurement on the mandible, for two specimens taken by 8 raters.

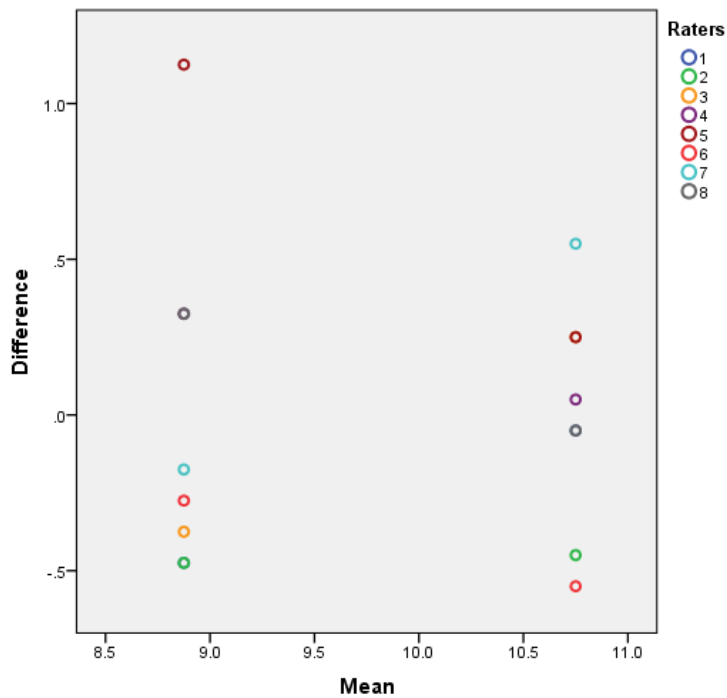


Figure A2.6 Scatterplot of the Mean versus difference of B measurement on the mandible, for two specimens taken by 8 raters.

The scatterplots (Figs. A2.7-A2.12) related to the measurements taken on the horncores reveal that, if we exclude rater 1, most dots cluster around 0, attesting that the measurements are taken consistently. This is particularly evident for measurements such as A, B, C and D (Figs. A2.7-A2.10). Dots become noticeably more scattered along the vertical line in E and F (Figs. A2.11 and A2.12); nevertheless they are still close to 0. Clearly rater 1 has repeatedly taken the measurements on the horncore in the wrong way. It is the only outlier present and clearly recognizable on the plots. Why this happened is difficult to say. It is unlikely that there was a problem in misunderstanding the protocol. More likely the problem was either due to callipers calibration or a recording error which, in the case of this trial, would have meant writing the measurements in the wrong cell.

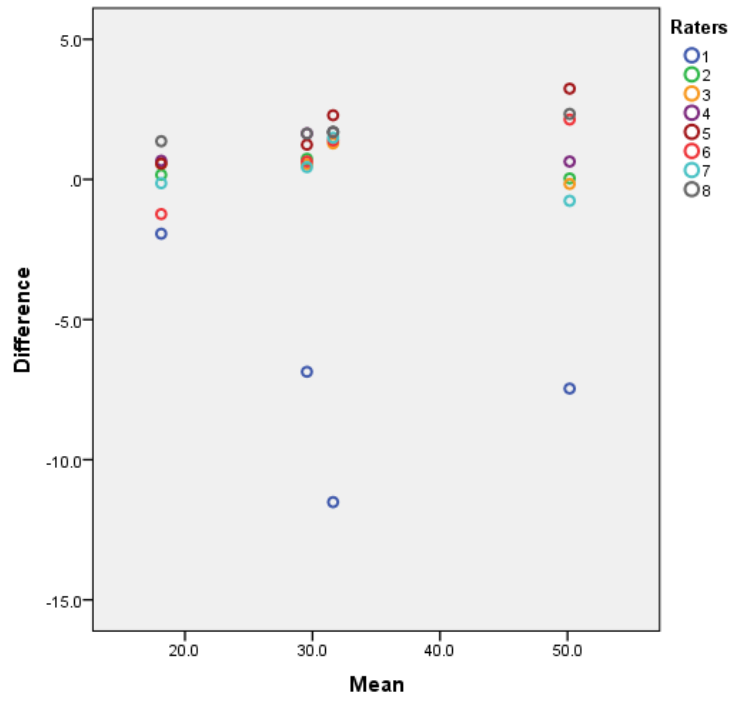


Figure A2.7 Scatterplot of the Mean versus difference of A measurement taken on the horncore, on four specimens by 8 raters.

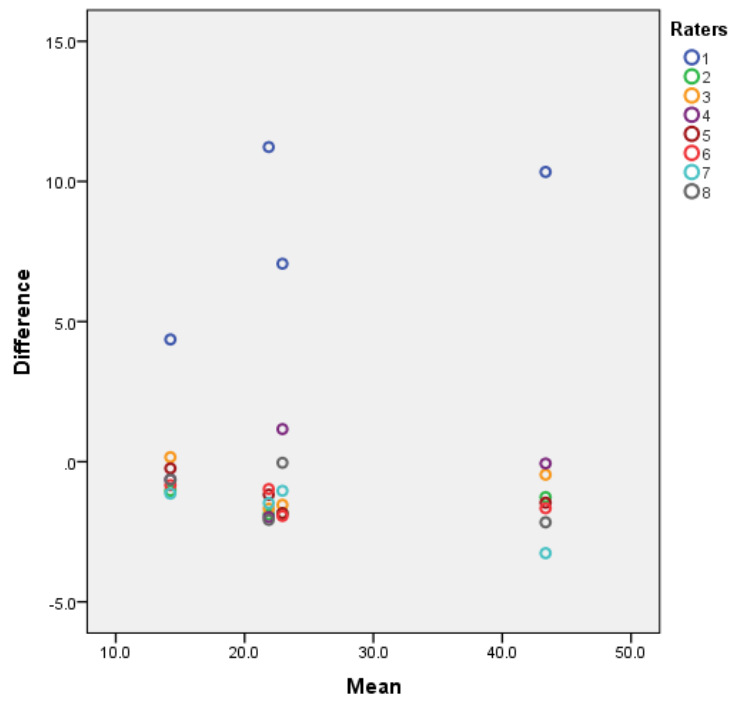


Figure A2.8 Scatterplot of the Mean versus difference of B measurement taken on the horncore, on four specimens by 8 raters.

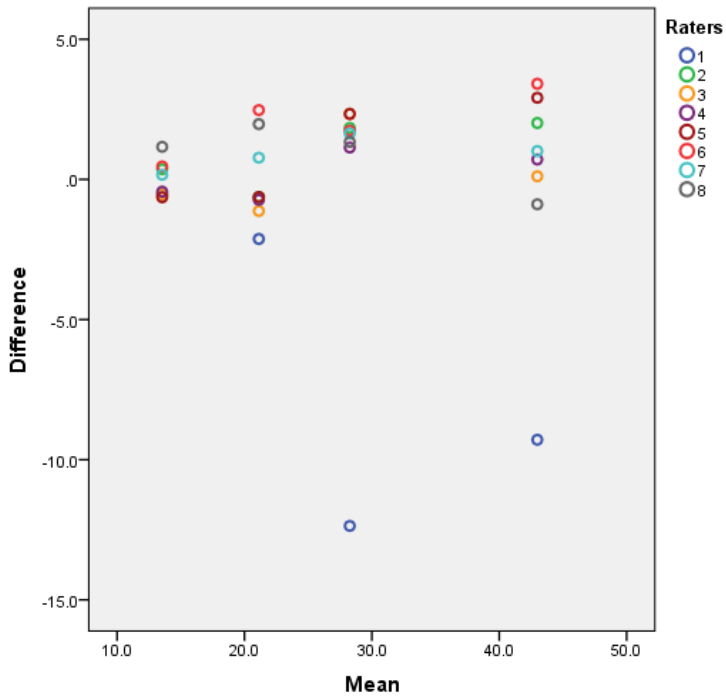


Figure A2.9 Scatterplot of the Mean versus difference of C measurement taken on the horncore, on four specimens by 8 raters.

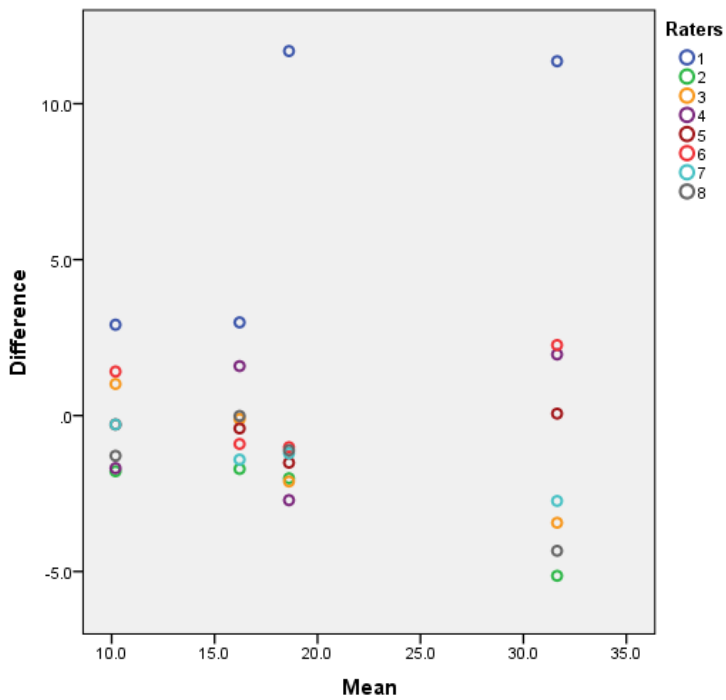


Figure A2.10 Scatterplot of the Mean versus difference of D measurement taken on the horncore, on four specimens by 8 raters.

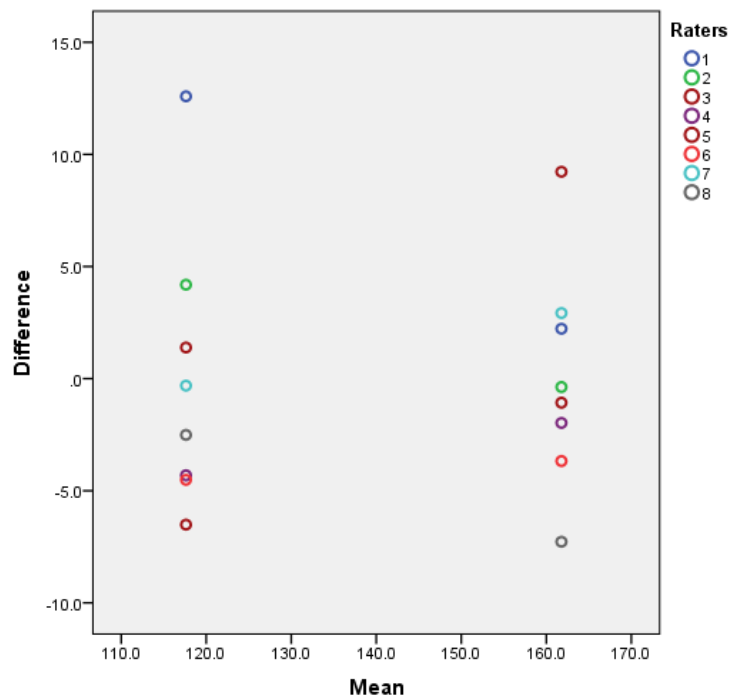


Figure A2.11 Scatterplot of the Mean versus difference of E measurement taken on the horncore, on two specimens by 8 raters.

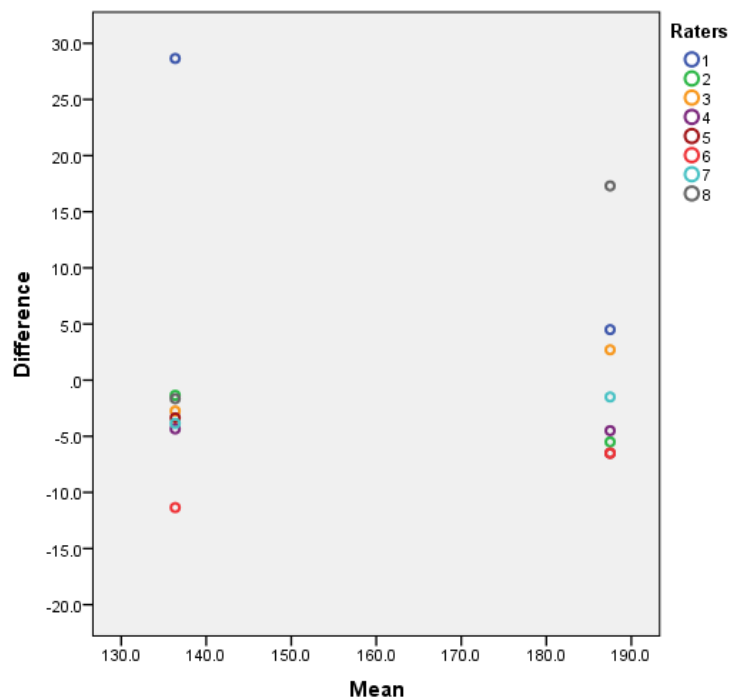


Figure A2.12 Scatterplot of the Mean versus difference of F measurement taken on the horncore, on two specimens by 8 raters.

The Bland and Altman plots for the measurements related to the scapula are presented in Figures A2.13 to A2.17. All dots related to specimen 1 in Figure A2.13 (BG), A2.14 (GLP) and A2.15 (LG) (dots on the graph seem fewer than the actual sample size because of the overlap between raters) are clustered around 0 more than for other specimens, showing consistency

between raters. On the other hand, specimen 4 is the one which shows the highest difference in Mean. For measurements SLC (Fig. A2.16) and ASG (A2.17), dots are scattered along all the lines showing less consistency among the raters' scores.

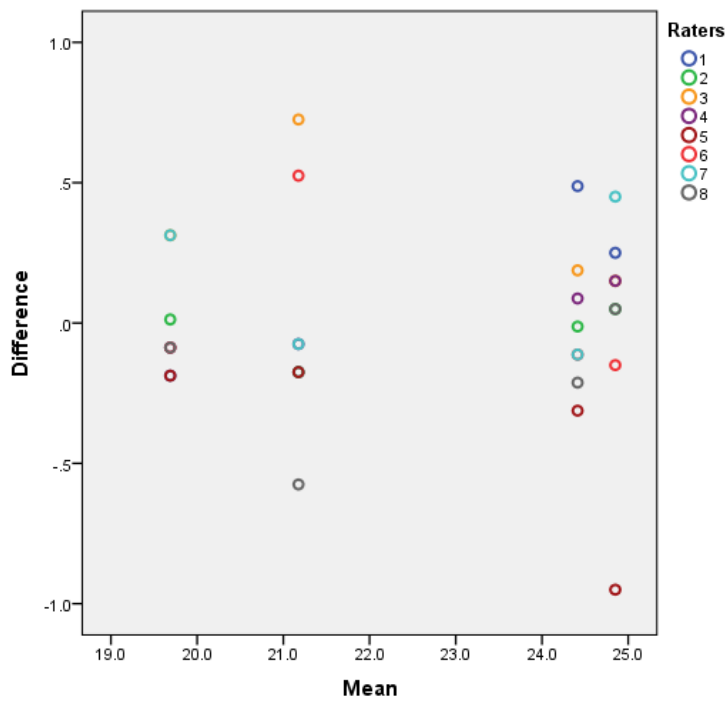


Figure A2.13 Scatterplot of the Mean versus difference of BG measurement taken on the scapula, on four specimens by 8 raters.

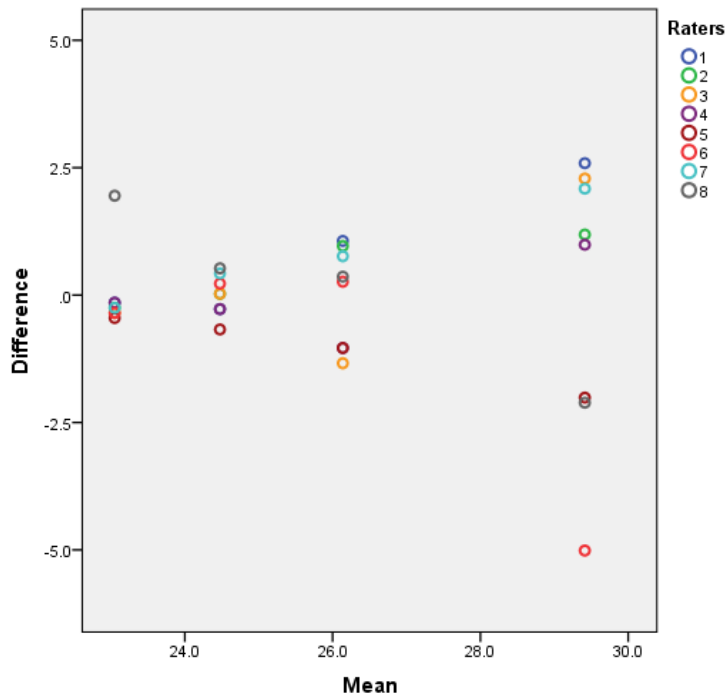


Figure A2.14 Scatterplot of the Mean versus difference of GLP measurement taken on the scapula, on four specimens by 8 raters.

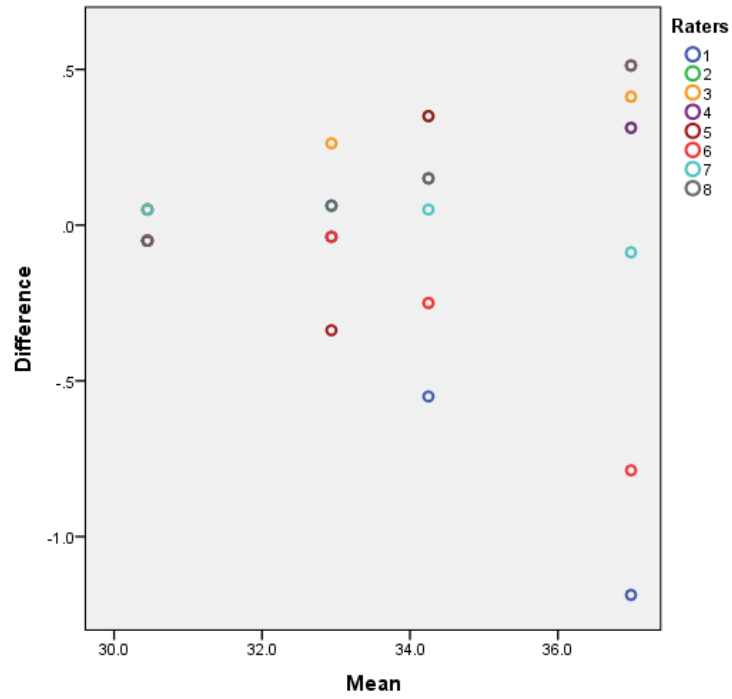


Figure A2.15 Scatterplot of the Mean versus difference of LG measurement taken on the scapula, on four specimens by 8 raters.

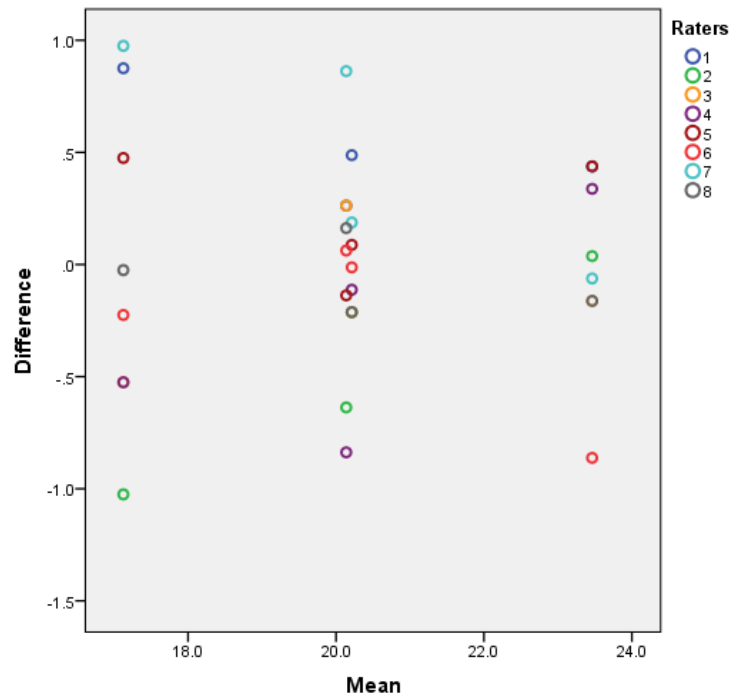


Figure A2.16 Scatterplot of the Mean versus difference of SLC measurement taken on the scapula, on four specimens by 8 raters.

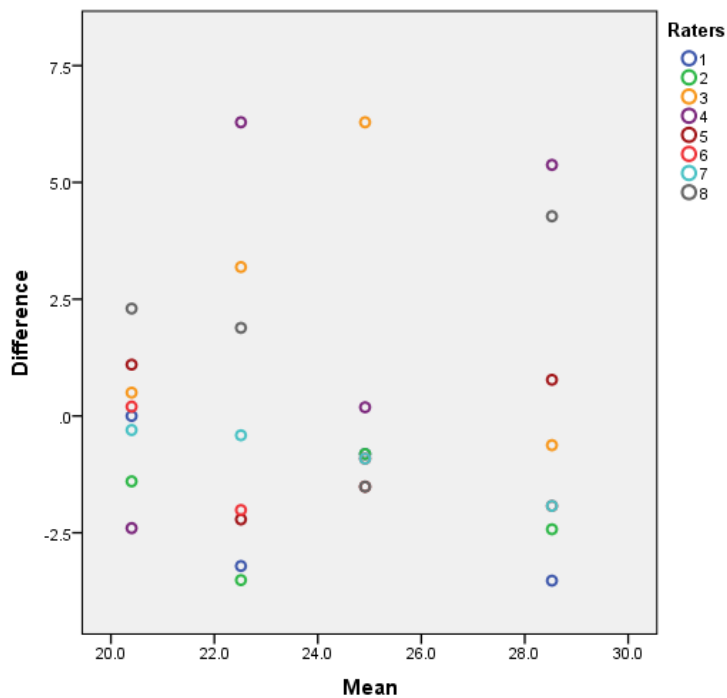


Figure A2.17 Scatterplot of the Mean versus difference of ASG measurement taken on the scapula, on four specimens by 8 raters.

The plots for measurements taken on the humerus are presented in Figures A2.18 to A2.24. Figure A2.18 related to measurement BT shows that all the dots for each specimen are spread along the vertical line, meaning that there was not a lot of agreement between the raters. For Bd (Fig. A2.19), specimens 1 (if the Mean of rater 7 is excluded as it seems to be an outlier) and 3 have dots closer to 0 than the other specimens, demonstrating that more agreement in the measurements was present among the raters. Results for measurement Dd are shown by Figure A2.20. Specimen 4 is the one which has been measured more consistently by the raters while in the case of measurement BE (Fig. A2.21) specimen 1 is the one for which dots are clustered around 0 (excluding the extreme score given by rater 5) while the dots for the other specimens are spread along the vertical line. Thus more agreement in measurement among the raters was present for specimen 1. In regard to BEI (Fig. A2.22), specimens 1 and 2 are those showing more agreement in measurements than the others while for HTC (Fig. A2.23) more consistency is present for specimens 1 and 3 (dots closer to 0) compared to the other specimens. Finally, Figure A2.24 shows the results for measurement HT for which specimens 1, 2 and 3, are those showing more agreement among the raters.

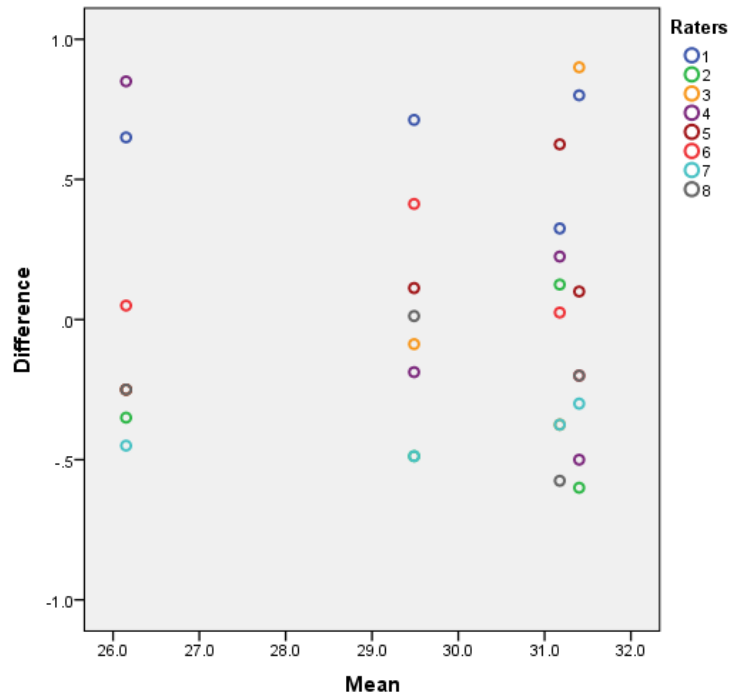


Figure A2.18 Scatterplot of the Mean versus difference of BT measurement taken on the humerus, on four specimens by 8 raters.

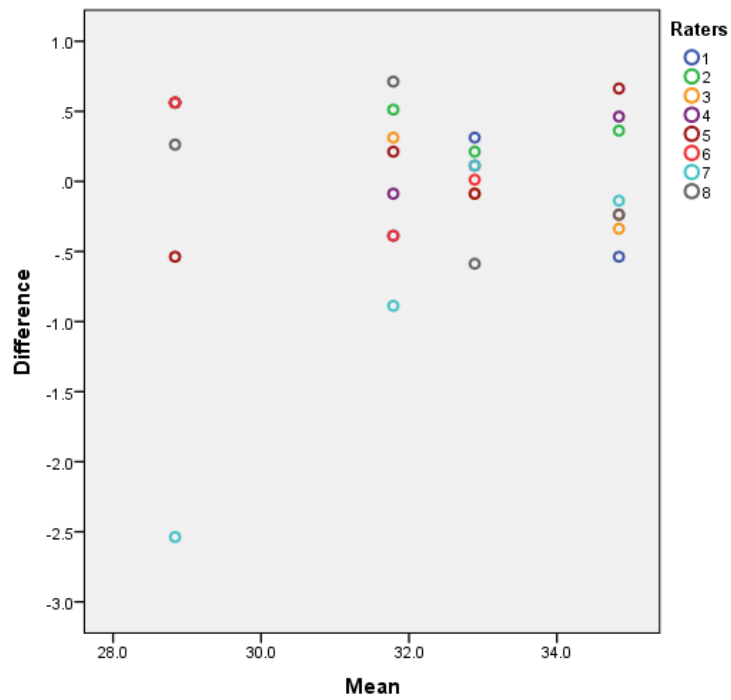


Figure A2.19 Scatterplot of the Mean versus difference of Bd measurement taken on the humerus, on four specimens by 8 raters.

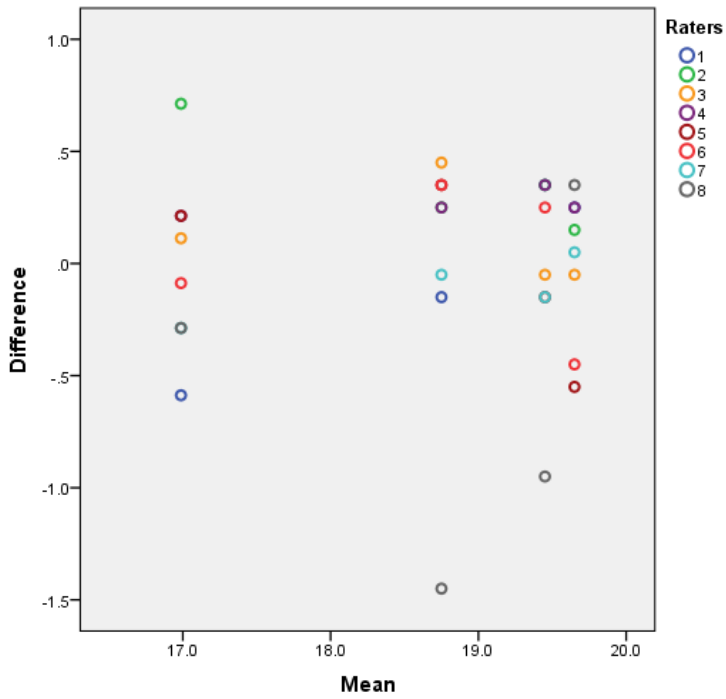


Figure A2.20 Scatterplot of the Mean versus difference of Dd measurement taken on the humerus, on four specimens by 8 raters.

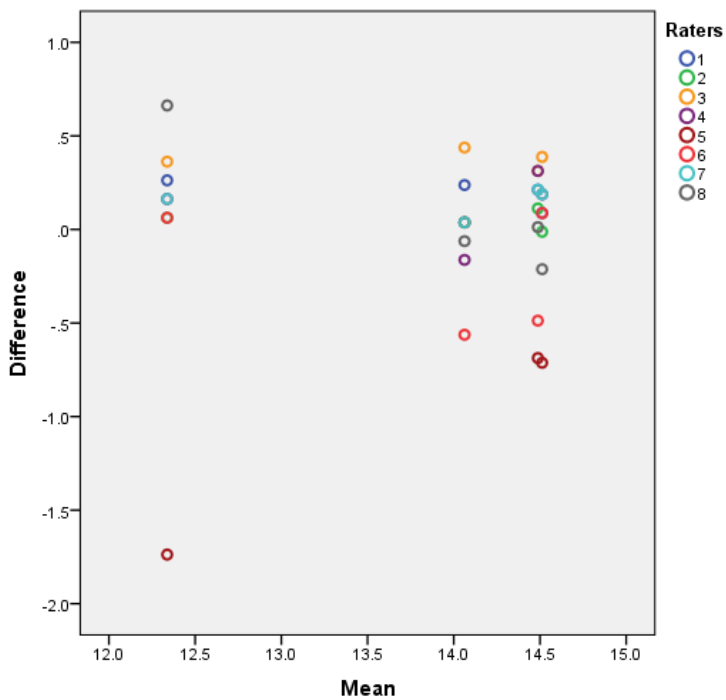


Figure A2.21 Scatterplot of the Mean versus difference of BE measurement taken on the humerus, on four specimens by 8 raters.

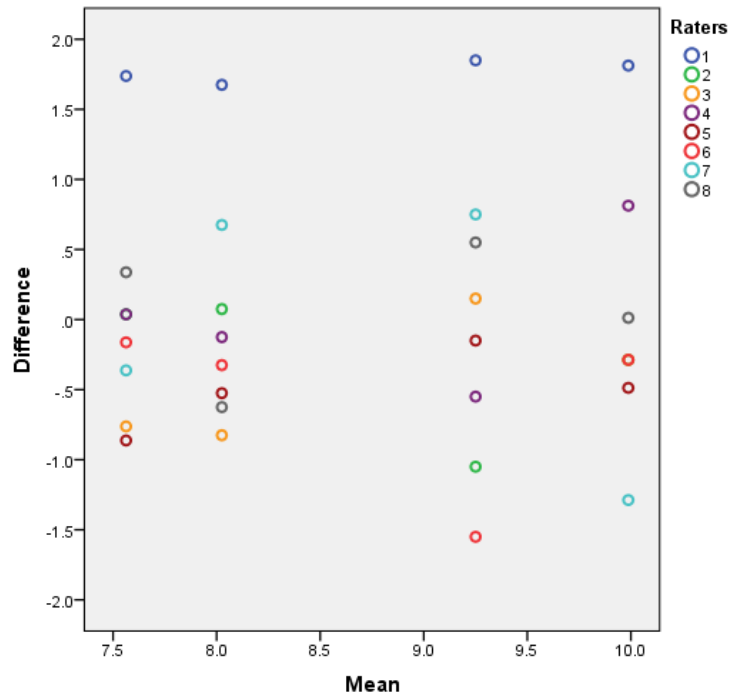


Figure A2.22 Scatterplot of the Mean versus difference of BEI measurement taken on the humerus, on four specimens by 8 raters.

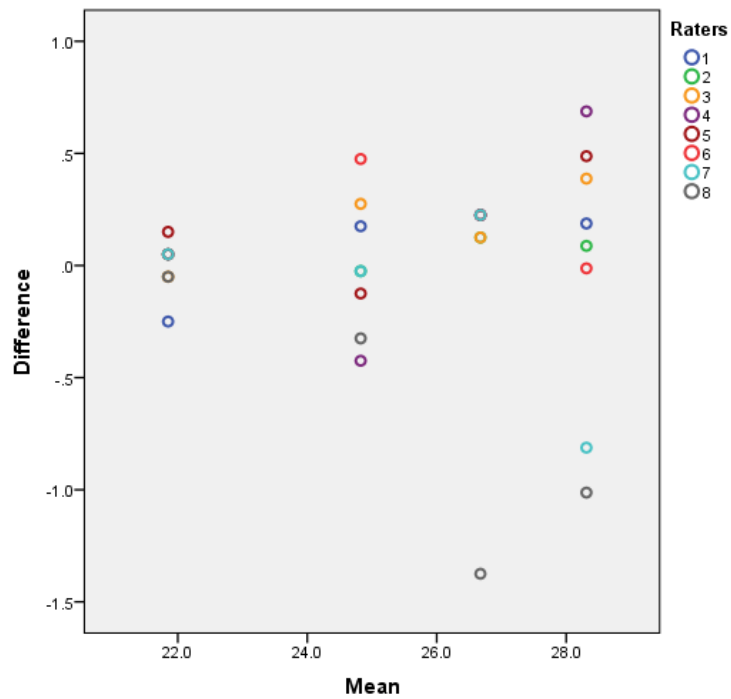


Figure A2.23 Scatterplot of the Mean versus difference of HTC measurement taken on the humerus, on four specimens by 8 raters.

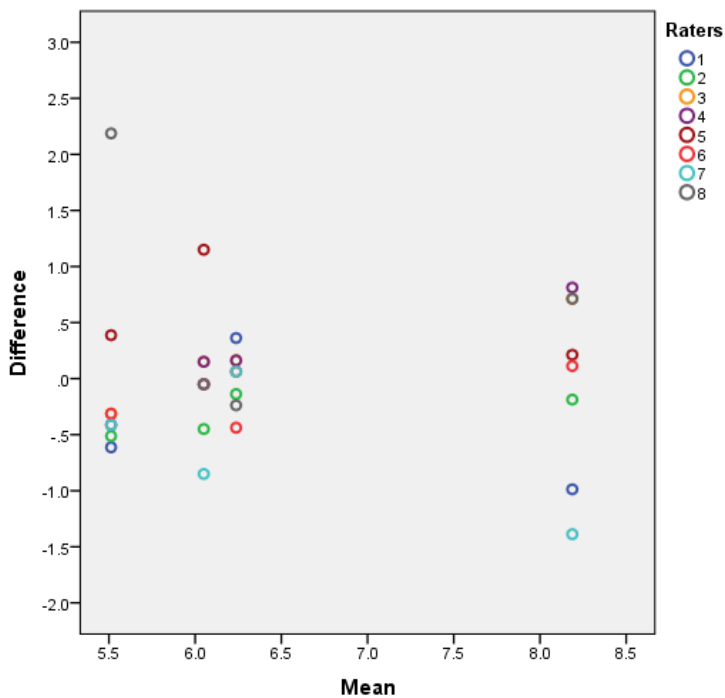


Figure A2.24 Scatterplot of the Mean versus difference of HT measurement taken on the humerus, on four specimens by 8 raters.

The scatterplots A2.25 to A2.29 are related to the measurements taken on the radius. Figure A2.25 (measurement Bp) shows that the dots for specimen 1 are more clustered around 0 than the other specimens, while for measurement BFp (Fig. A2.26), specimens 2 and 3 have been measured more consistently than the other specimens, as they have dots scattered along the vertical line. In the case of Dp (fig. A2.27), the most consistently measured specimens were 1, 2 and 3 while the scattered dots for specimen 4 attest the presence of lower agreement between the raters. Figure A2.28, related to measurement GL shows that the dots related to rater 1 are extremely distant from the dots representing the other raters which instead fall in a very similar position. Rater 1 represents clearly an outlier. Finally, Figure A2.29, which presents the values for measurement SD, shows that dots for all the specimens (if the high results from rater 8 are excluded) are close to 0, attesting agreement among the other raters.

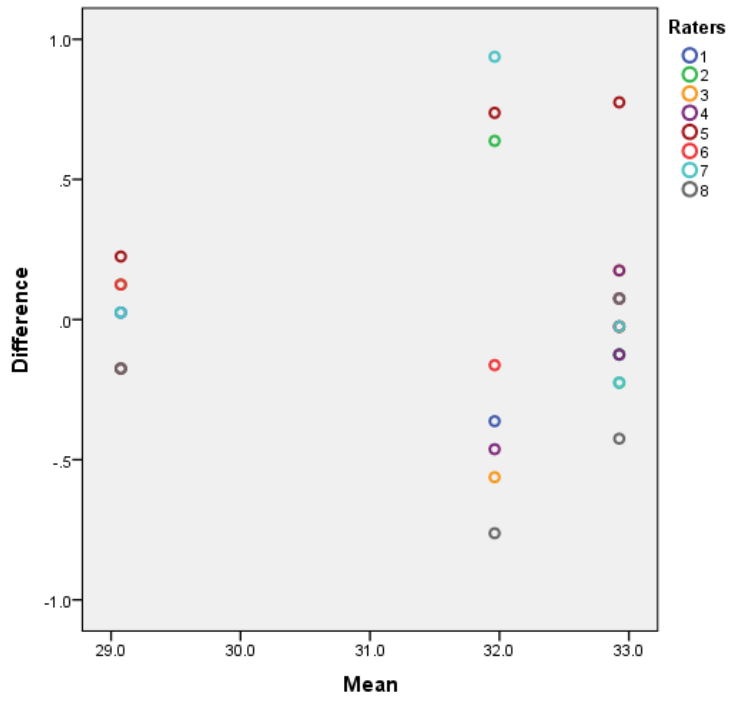


Figure A2.25 Scatterplot of the Mean versus difference of Bp measurement taken on the radius, on four specimens by 8 raters.

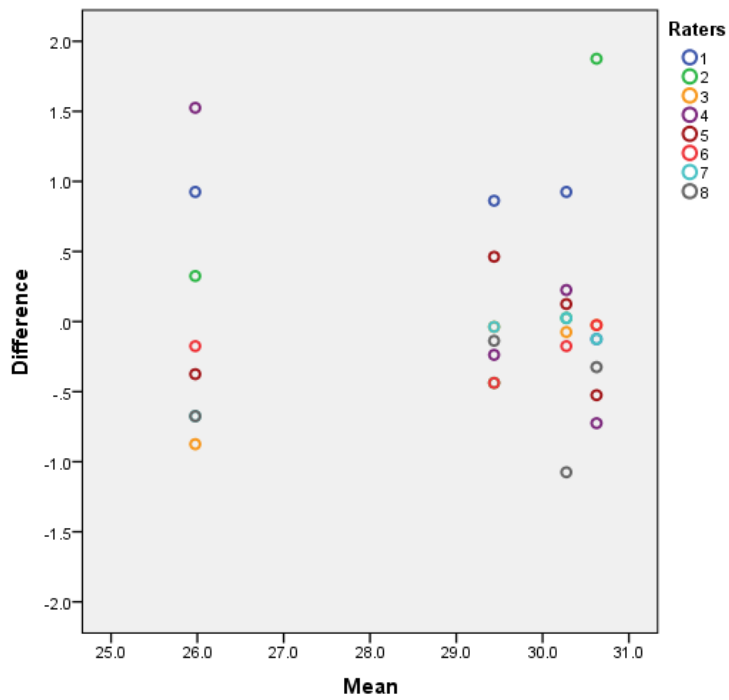


Figure A2.26 Scatterplot of the Mean versus difference of BFp measurement taken on the radius, on four specimens by 8 raters.

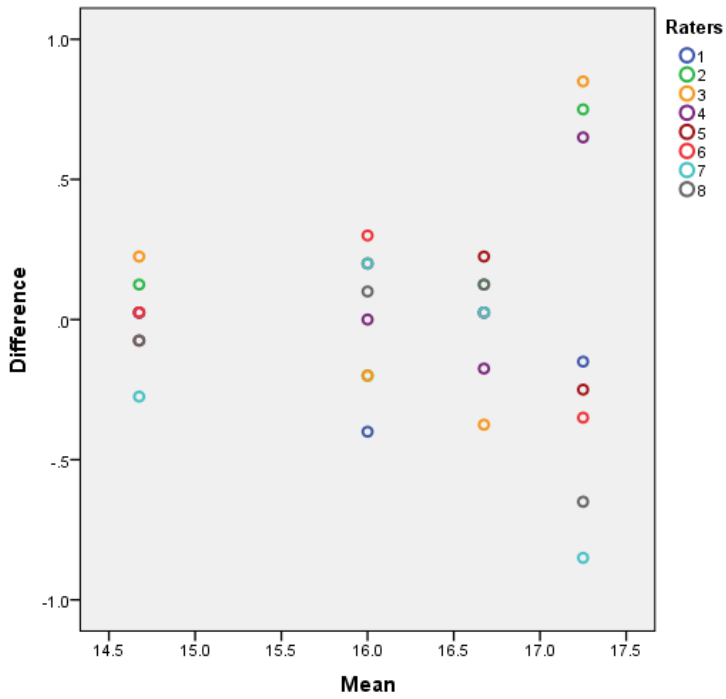


Figure A2.27 Scatterplot of the Mean versus difference of Dp measurement taken on the radius, on four specimens by 8 raters.

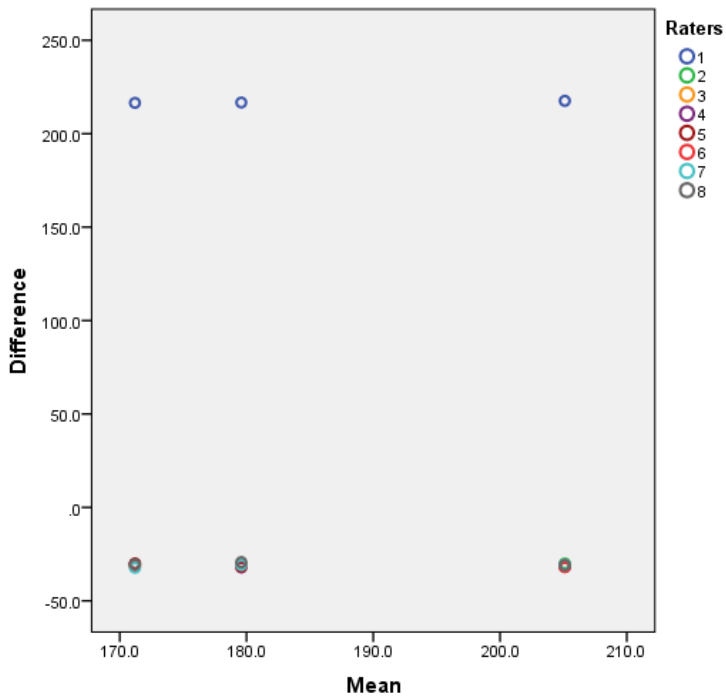


Figure A2.28 Scatterplot of the Mean versus difference of GL measurement taken on the radius, on three specimens by 8 raters.

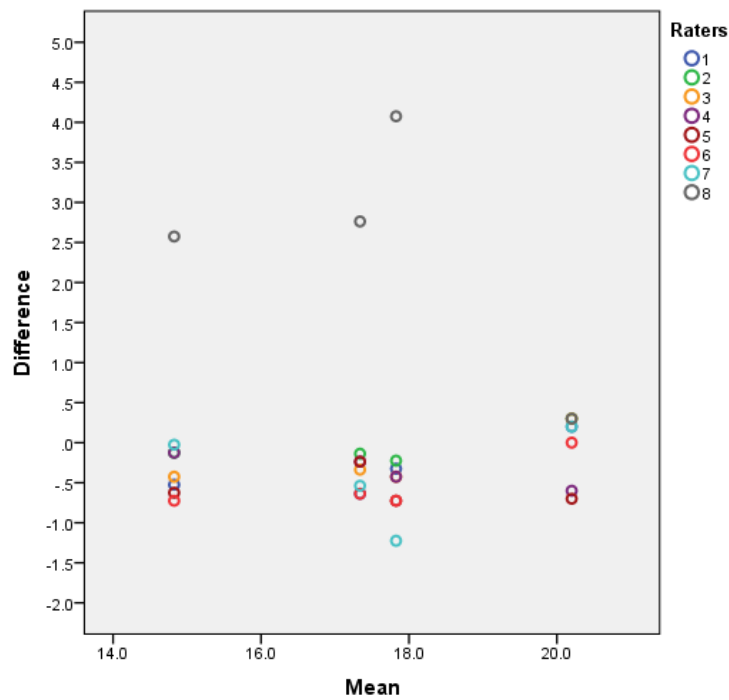


Figure A2.29 Scatterplot of the Mean versus difference of SD measurement taken on the radius, on three specimens by 8 raters.

Data from measurements taken on the ulna are shown by Figures A2.30 to A2.34. When measurement B is considered, Figure A2.30 shows that specimens 1 and 2 have been measured more consistently by the raters than specimen 3. More agreement between the raters is present for L (Fig. A2.31) and for measurement BPC (Fig. A2.33), as all specimens have dots gathered around 0. On the other hand, for measurements SDO and DPA, scatterplots (Figs. A2.32 and A2.34) show dots widely spread along the vertical line for all the specimens, attesting to the variability among raters' scores.

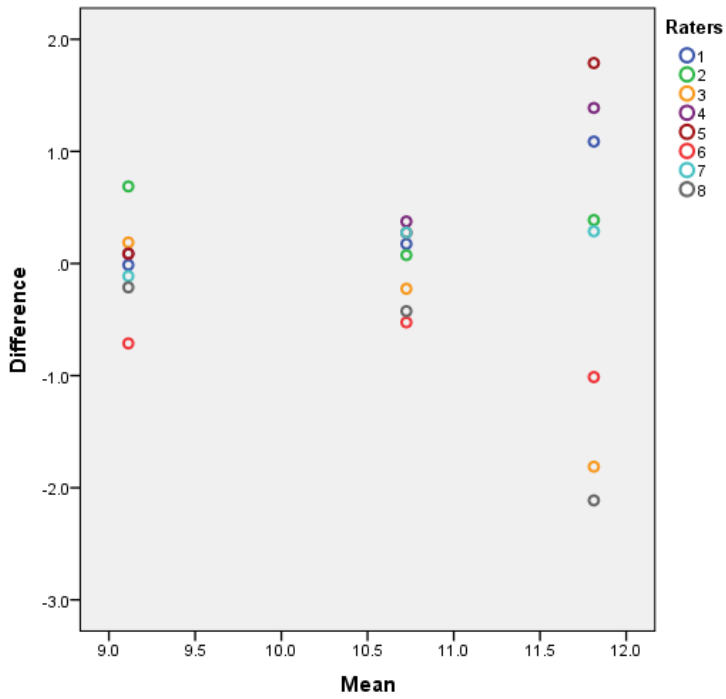


Figure A2.30 Scatterplot of the Mean versus difference of B measurement taken on the ulna, on three specimens by 8 raters.

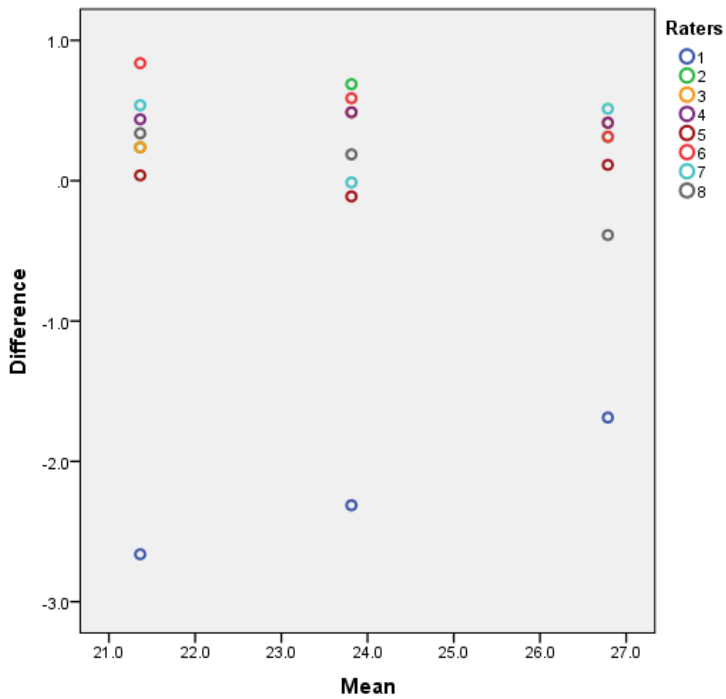


Figure A2.31 Scatterplot of the Mean versus difference of L measurement taken on the ulna, on three specimens by 8 raters.

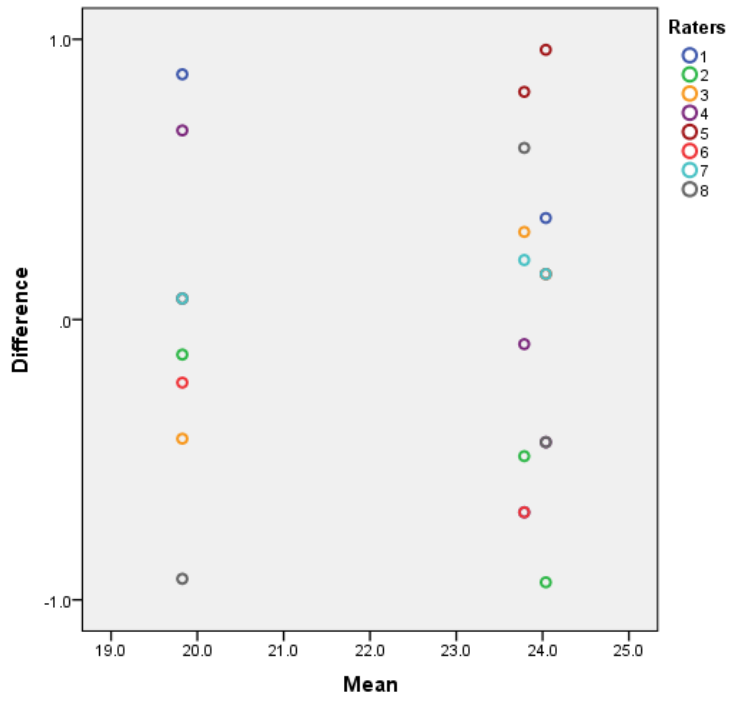


Figure A2.32 Scatterplot of the Mean versus difference of SDO measurement taken on the ulna, on three specimens by 8 raters.

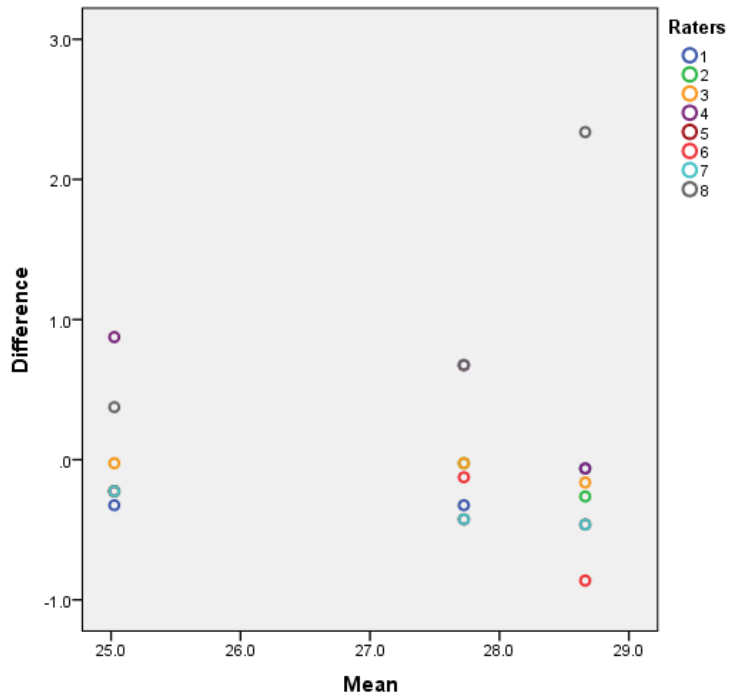


Figure A2.33 Scatterplot of the Mean versus difference of BPC measurement taken on the ulna, on three specimens by 8 raters.

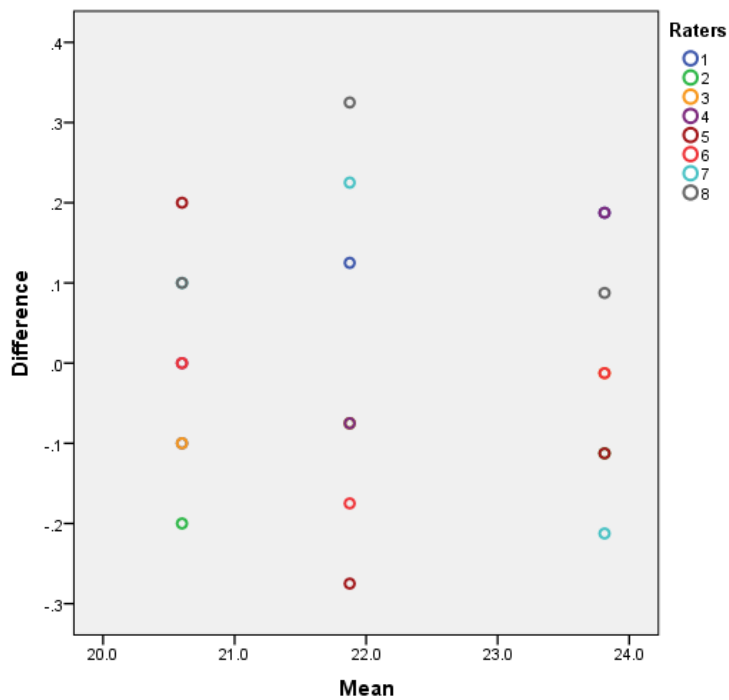


Figure A2.34 Scatterplot of the Mean versus difference of DPA measurement taken on the ulna, on three specimens by 8 raters.

Figures A2.35 to A2.46 show the results for the measurements taken on the metacarpal.

Figure A2.35 represents the results for measurement GL. Less difference among the raters is present in specimen 1 than the others, as the dots for this specimen are more gathered around 0 than the dots for the other specimens measured. Regarding SD (Fig. A2.36), specimen 2 is the one where least agreement among the raters can be observed. Figure A2.37 shows that when BatF is considered, despite a certain degree of agreement among the raters can be identified, variability still affects this measurement. Higher variability is shown by Bfd (Fig. A2.38) as all the dots for all specimens are spread on the vertical lines (if the extreme score given by rater 7 is not considered, less difference among the raters is present for specimens 2 and 4).

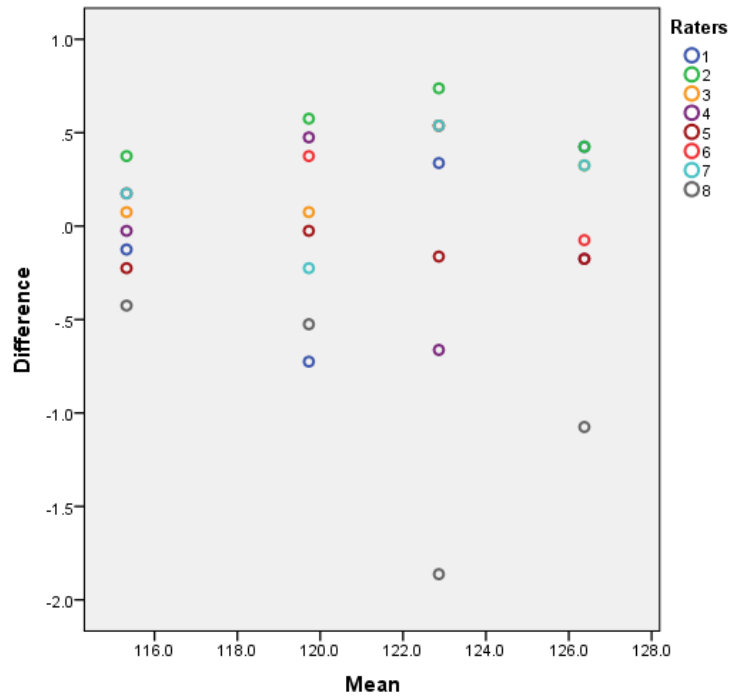


Figure A2.35 Scatterplot of the Mean versus difference of GL measurement taken on the metacarpal, on three specimens by 8 raters.

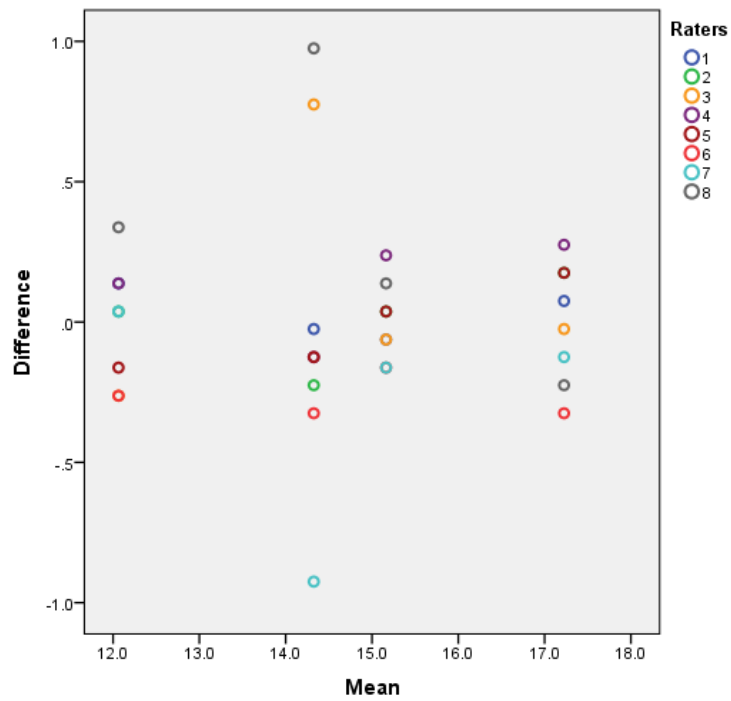


Figure A2.36 Scatterplot of the Mean versus difference of SD measurement taken on the metacarpal, on three specimens by 8 raters.

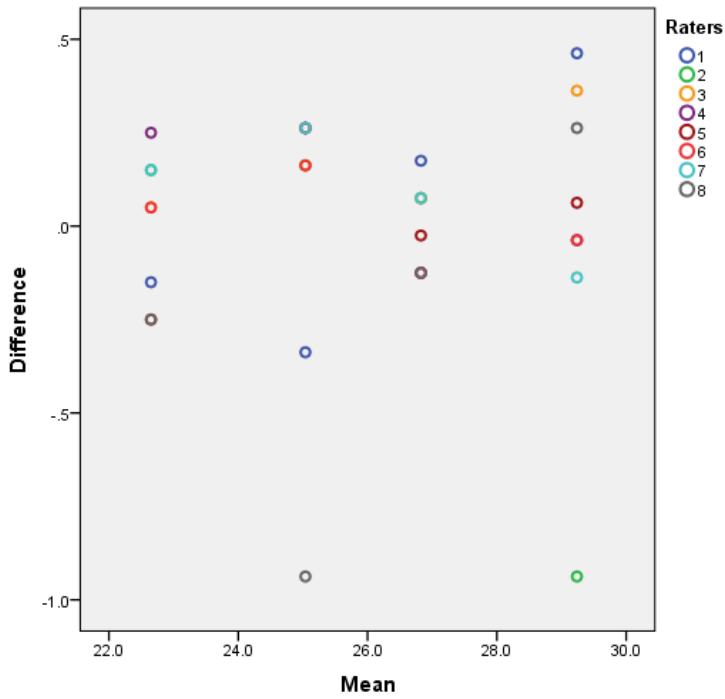


Figure A2.37 Scatterplot of the Mean versus difference of BatF measurement taken on the metacarpal, on three specimens by 8 raters.

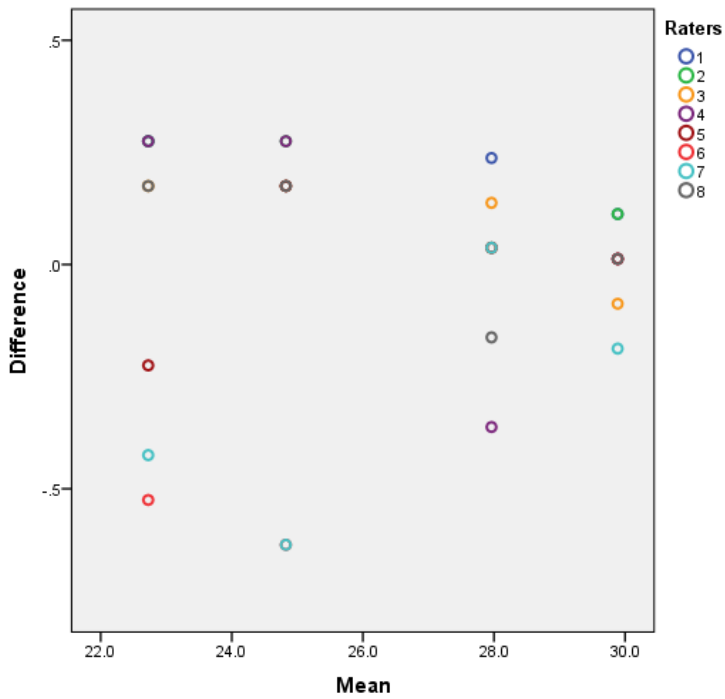


Figure A2.38 Scatterplot of the Mean versus difference of Bfd measurement taken on the metacarpal, on three specimens by 8 raters.

The results for measurement a (Figs. A2.39) show that more agreement among the raters was present for specimens 1, 2 (excluding the extreme score given by rater 8) and 3, while more difference among the raters is present for specimen 4. For measurement b (Fig. A2.40), more agreement among the raters for specimen 1 is present, while the same degree of agreement can

be recognised for the other specimens, if the some extreme scores (given by rater 8 on specimens 2 and 3; rater 2 on specimens 3 and 4 and rater 1 on specimen 4) are not taken into consideration. Measurements 1 and 3 (Figs. A2.41 and A2.43) show a higher spread of the dots for each specimen, attesting to their high variability while for measurement 2 (Fig. A2.42), more agreement is present among the raters as the dots are still spread on the vertical line but not to the same extend that they are for measurements 1 and 3 (Figs. A2.41 and A2.43). This higher consistency of measurement 2 could be due to the fact that the landmark used to position the calliper on the verticillus is the same as explained by Davies (1996). In addition, there is less possibility of variation in taking this measurement, as the way you position the calliper on this part of the bone can be limited while, on the other hand, when taking 1 and 3 (diameter of the medial trochlea and of the lateral part of the medial condyle) the calliper can be positioned in many different ways, creating the conditions for increased variability.

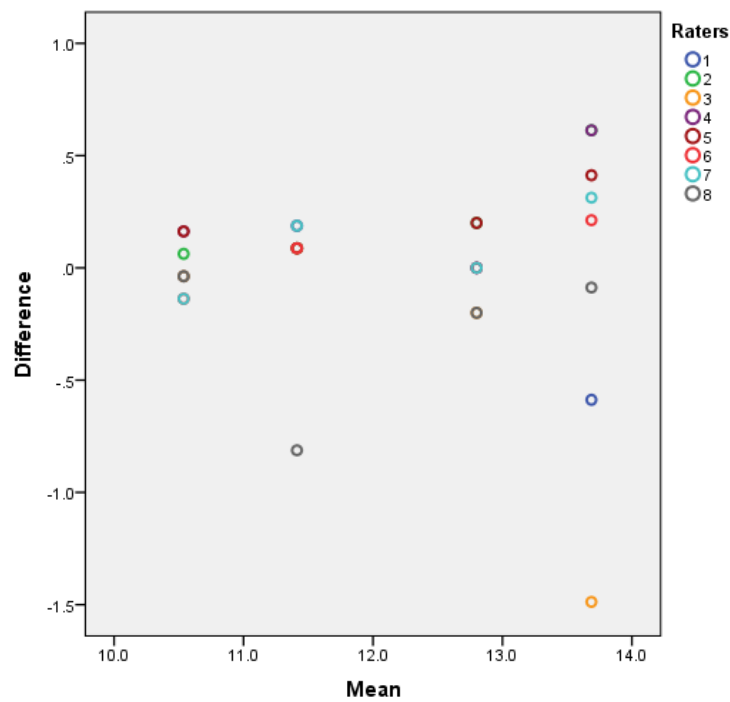


Figure A2.39 Scatterplot of the Mean versus difference of a measurement taken on the metacarpal, on three specimens by 8 raters.

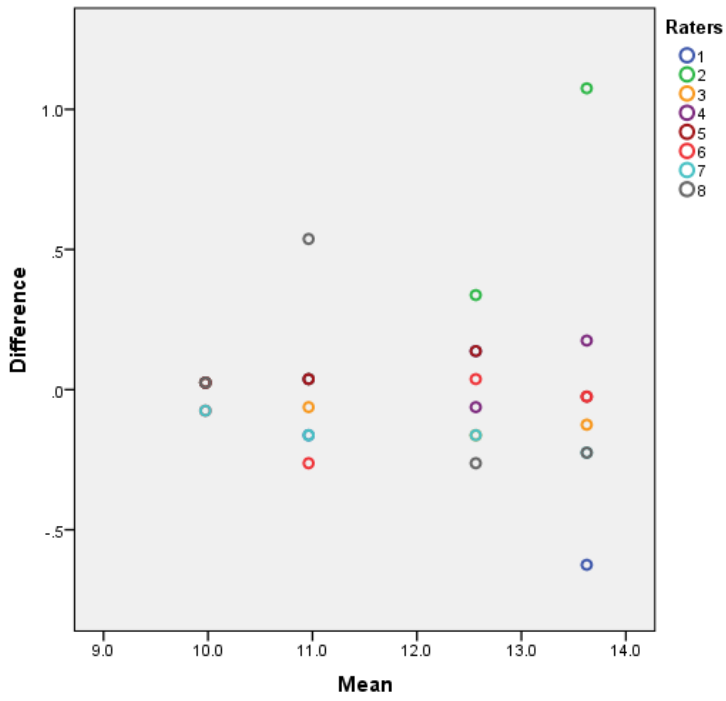


Figure A2.40 Scatterplot of the Mean versus difference of b measurement taken on the metacarpal, on three specimens by 8 raters.

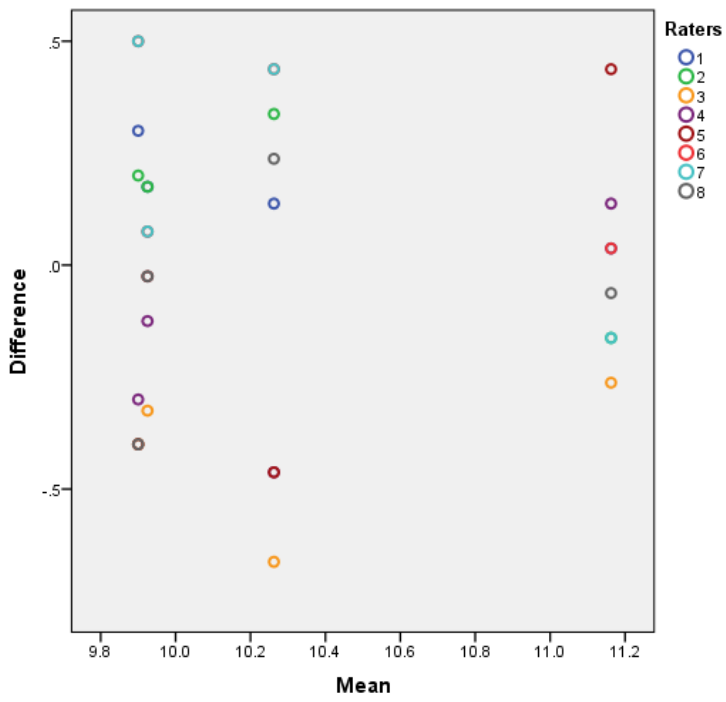


Figure A2.41 Scatterplot of the Mean versus difference of 1 measurement taken on the metacarpal, on three specimens by 8 raters.

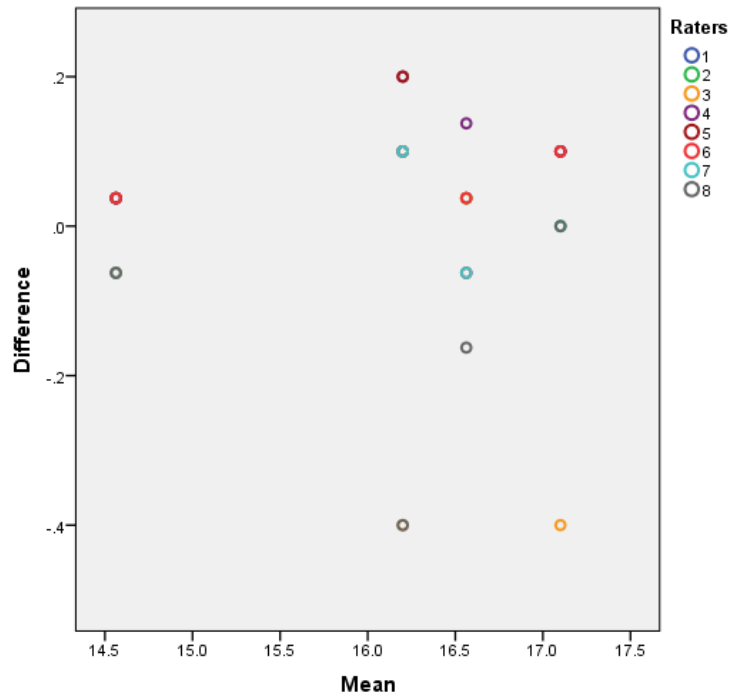


Figure A2.42 Scatterplot of the Mean versus difference of 2 measurement taken on the metacarpal, on three specimens by 8 raters.

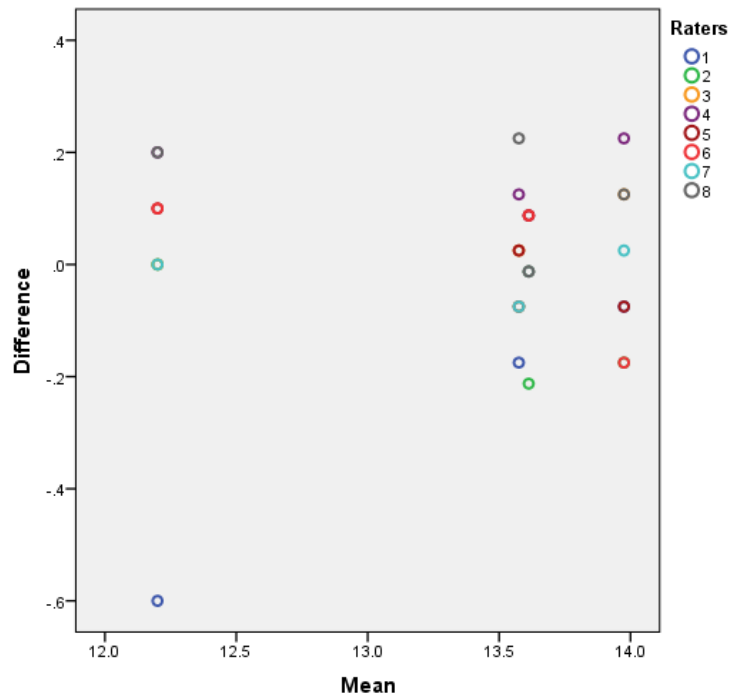


Figure A2.43 Scatterplot of the Mean versus difference of 3 measurement taken on the metacarpal, on three specimens by 8 raters.

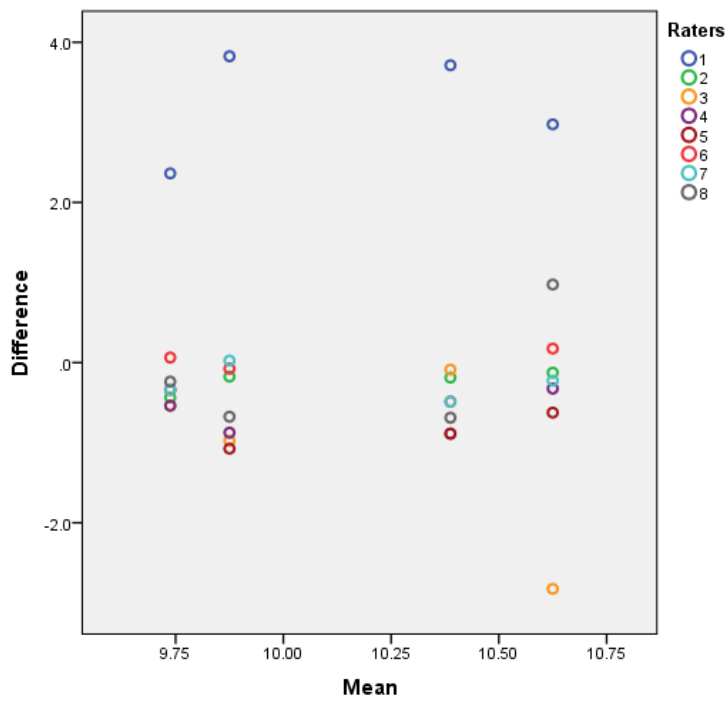


Figure A2.44 Scatterplot of the Mean versus difference of 4 measurement taken on the metacarpal, on three specimens by 8 raters.

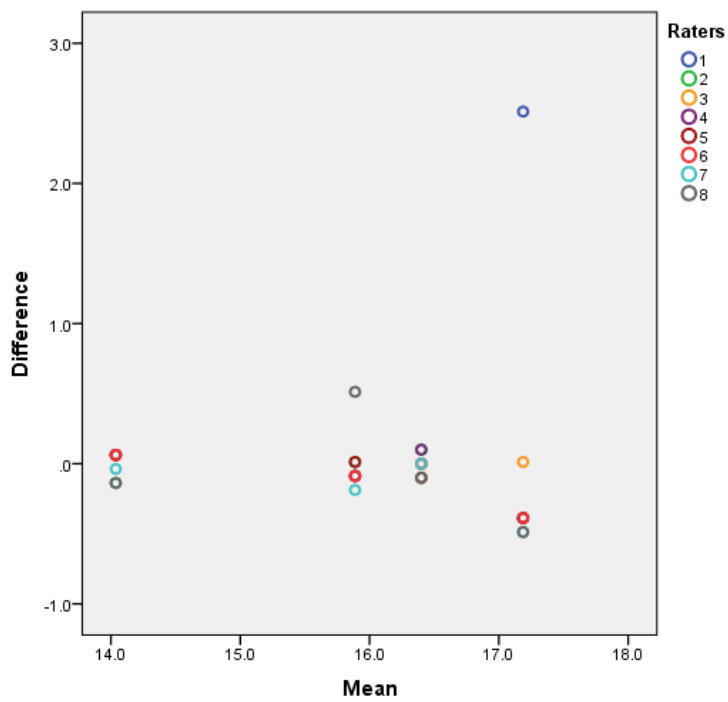


Figure A2.45 Scatterplot of the Mean versus difference of 5 measurement taken on the metacarpal, on three specimens by 8 raters.

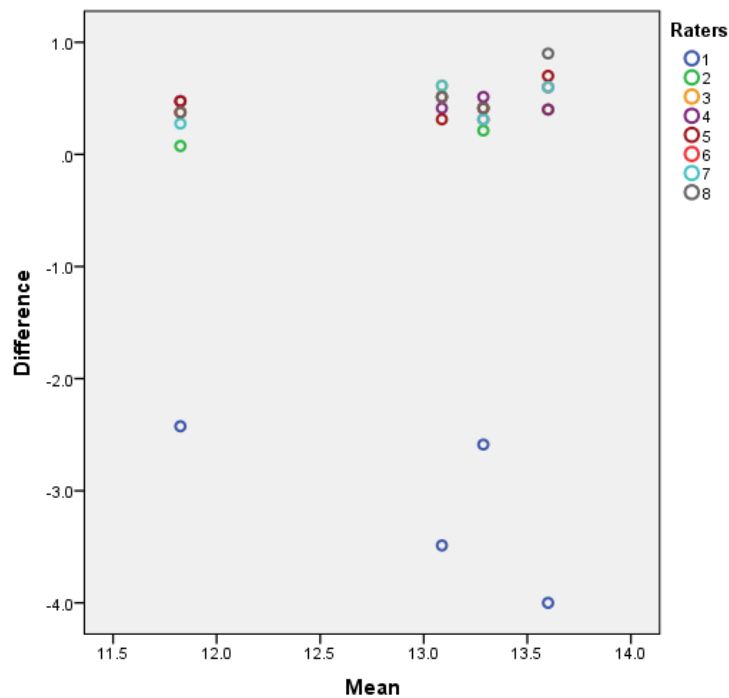


Figure A2.46 Scatterplot of the Mean versus difference of 6 measurement taken on the metacarpal, on three specimens by 8 raters.

Lower variability is shown by the measurements taken on the lateral condyle than the medial (measurements 4, 5, 6), as, in all of the three scatterplots (Figs. A2.44-A2.46), the dots are less spread on the vertical line than those seen for the measurements taken on the medial condyle (measurements 1, 2, 3). Despite this, the same pattern seen on the medial condyle can be recognised on the lateral: more agreement among the raters is present for measurement 5 (Fig. A2.45) than for 4 (Fig. A2.44) and 6 (Fig. A2.46), as the dots are more closely gathered around 0 than the dots for the other measurements. This phenomenon is probably due to the same reason given above for the medial condyle.

Figures A2.47 to A2.58 deal with measurements taken on the metatarsus.

Figure A2.47 is related to measurement GL and, if some extreme results are not considered (mainly rater 8 in specimen 2, raters 5 and 6 on specimens 3 and 4), dots gather to a certain extent around 0, confirming that some agreement was present among the raters. For SD (Fig. A2.48), BatF (Fig. A2.49) and Bfd (Fig. A2.50) on the contrary, more spread among the dots is noticeable, thus fairly high variation among the raters is present.

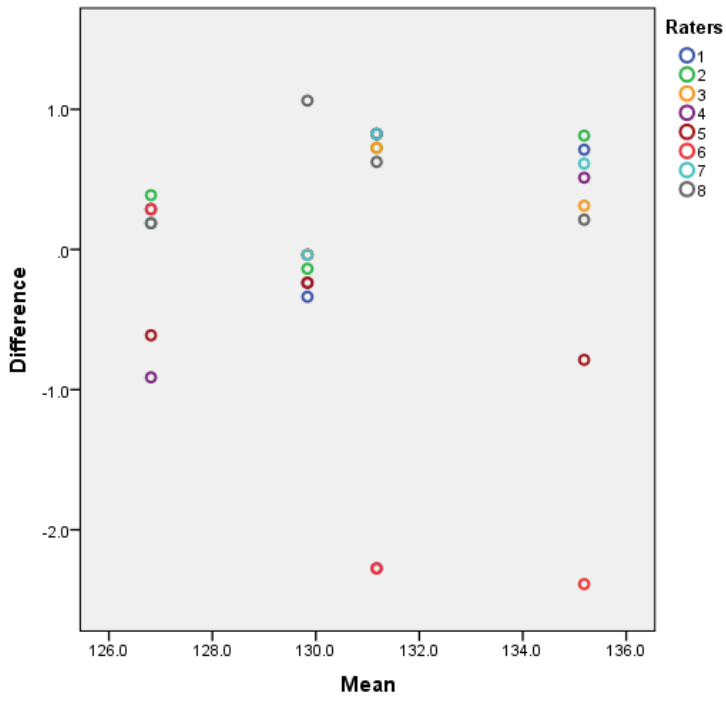


Figure A2.47 Scatterplot of the Mean versus difference of GL measurement taken on the metatarsal, on three specimens by 8 raters.

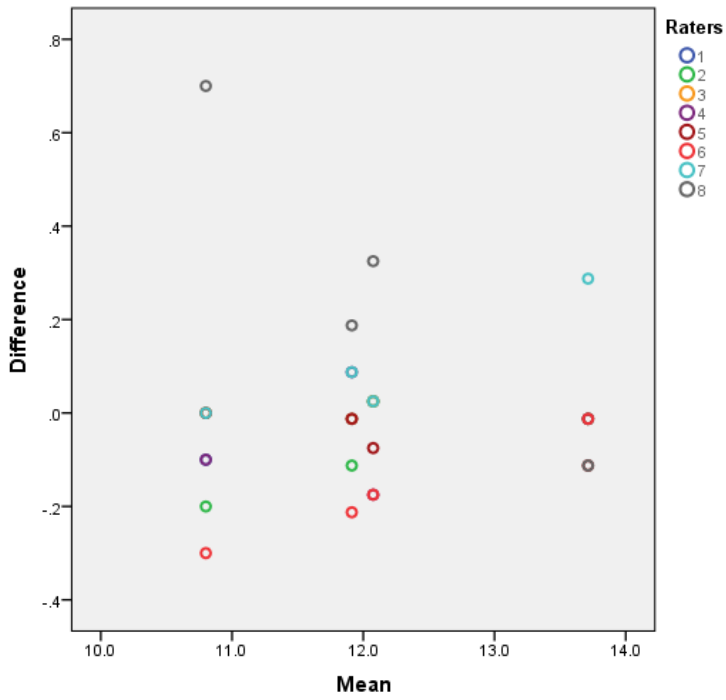


Figure A2.48 Scatterplot of the Mean versus difference of SD measurement taken on the metatarsal, on three specimens by 8 raters.

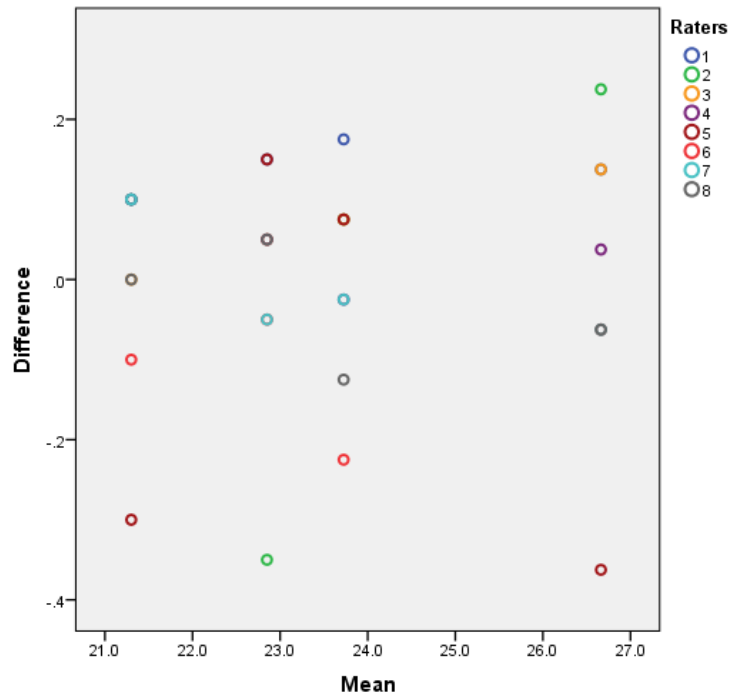


Figure A2.49 Scatterplot of the Mean versus difference of BatF measurement taken on the metatarsal, on three specimens by 8 raters.

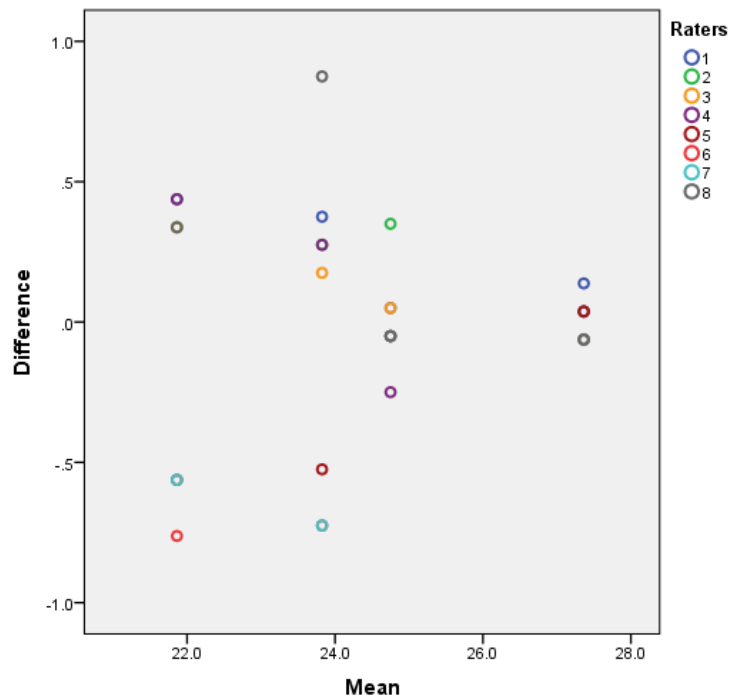
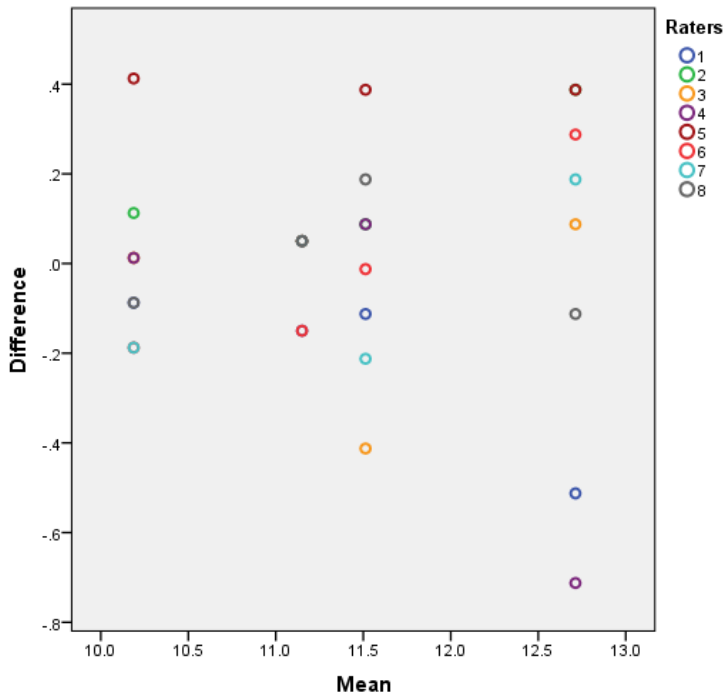


Figure A2.50 Scatterplot of the Mean versus difference of Bfd measurement taken on the metatarsal, on three specimens by 8 raters.



Figur A2.51 Scatterplot of the Mean versus difference of a measurement taken on the metatarsal, on three specimens by 8 raters.

Greater disagreement can be observed among the raters for measurement a and b: both scatterplots have the raters' dots spread all along the vertical line (Figs. A2.51 and A2.52).

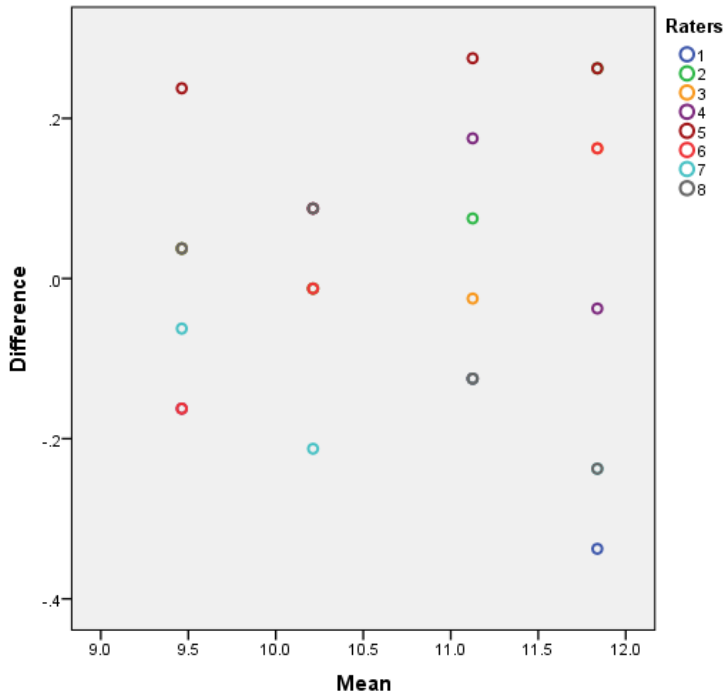


Figure A2.52 Scatterplot of the Mean versus difference of b measurement taken on the metatarsal, on three specimens by 8 raters.

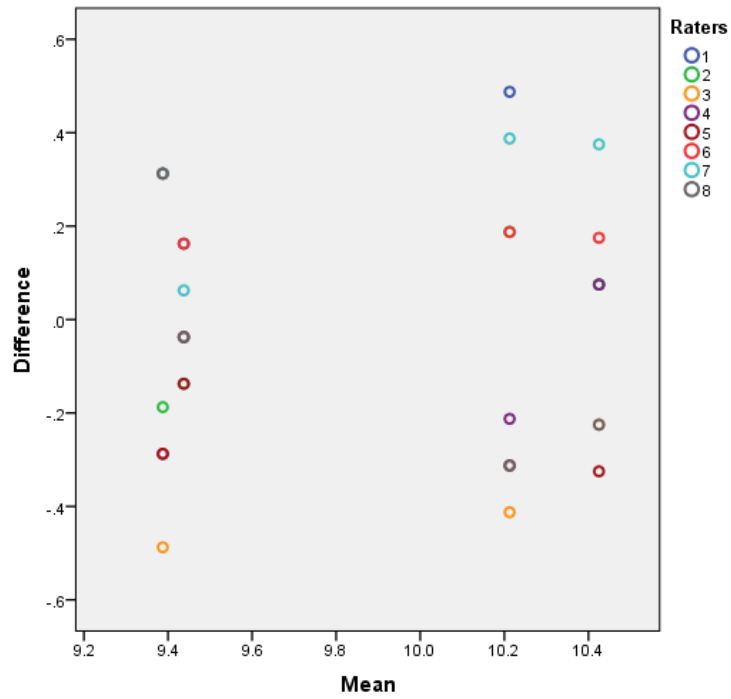


Figure A2.53 Scatterplot of the Mean versus difference of 1 measurement taken on the metatarsal, on three specimens by 8 raters.

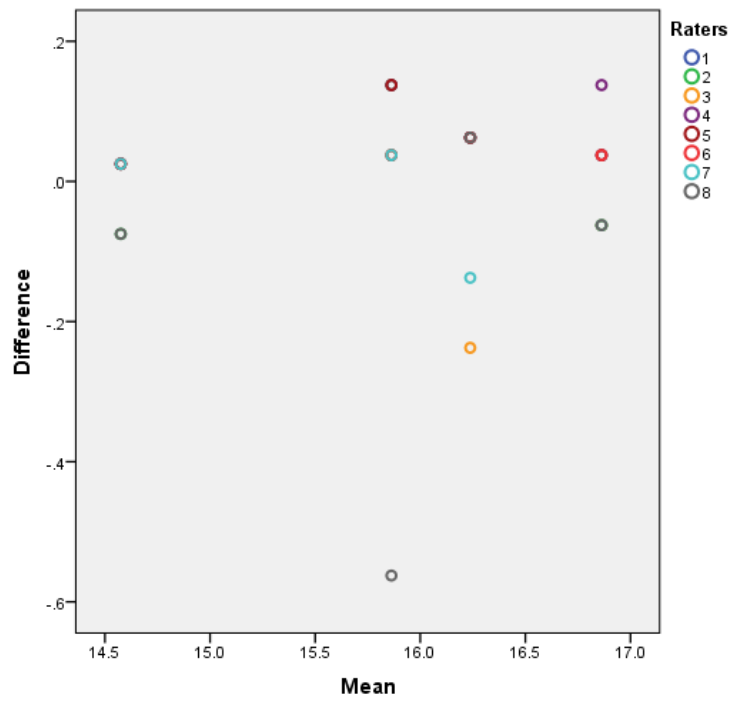


Figure A2.54 Scatterplot of the Mean versus difference of 2 measurement taken on the metatarsal, on three specimens by 8 raters.

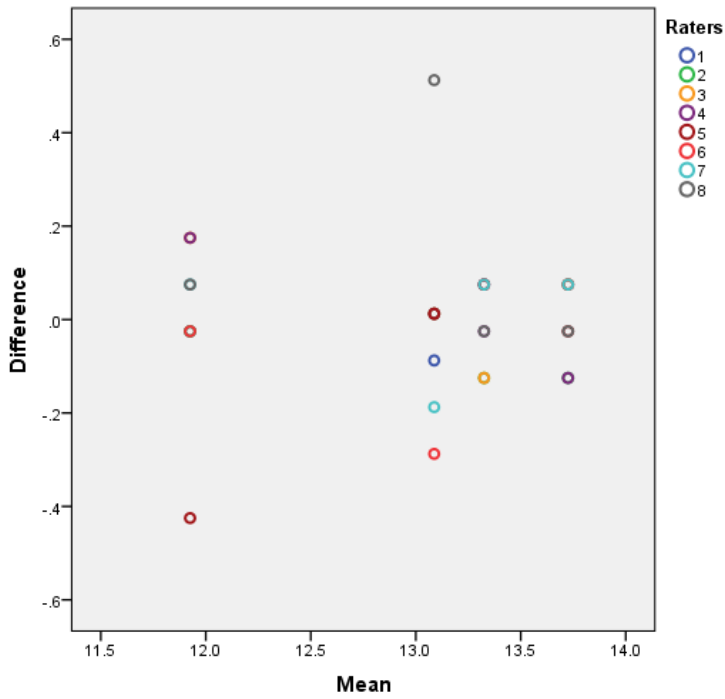


Figure A2.55 Scatterplot of the Mean versus difference of 3 measurement taken on the metatarsal, on three specimens by 8 raters.

Figures A2.53 to A2.55 display the results from the measurements taken on the medial condyle (1, 2 and 3). Measurement 1 is the one for which the raters disagreed the most (Fig. A2.53) while more agreement is shown by measurement 3 (Fig. A2.55) and, to a greater extent, by measurement 2 (Fig. A2.54).

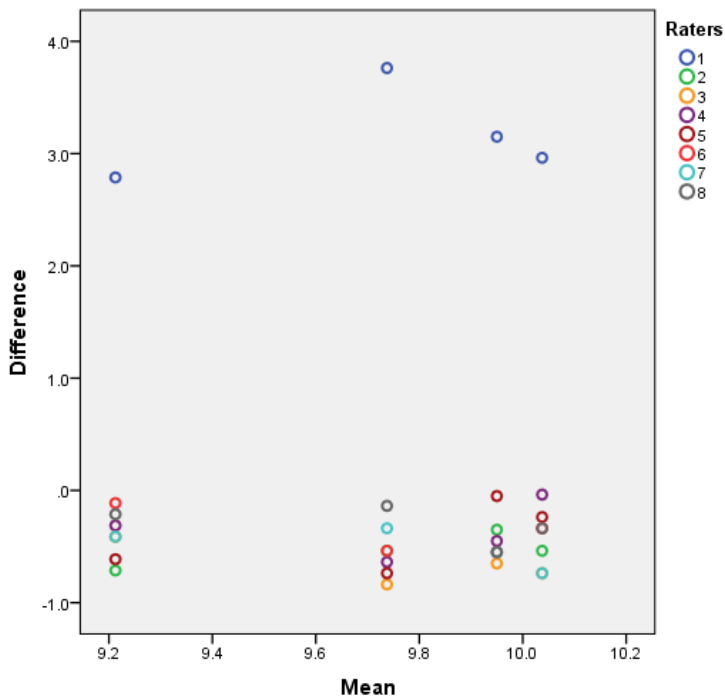


Figure A2.56 Scatterplot of the Mean versus difference of 4 measurement taken on the metatarsal, on three specimens by 8 raters.

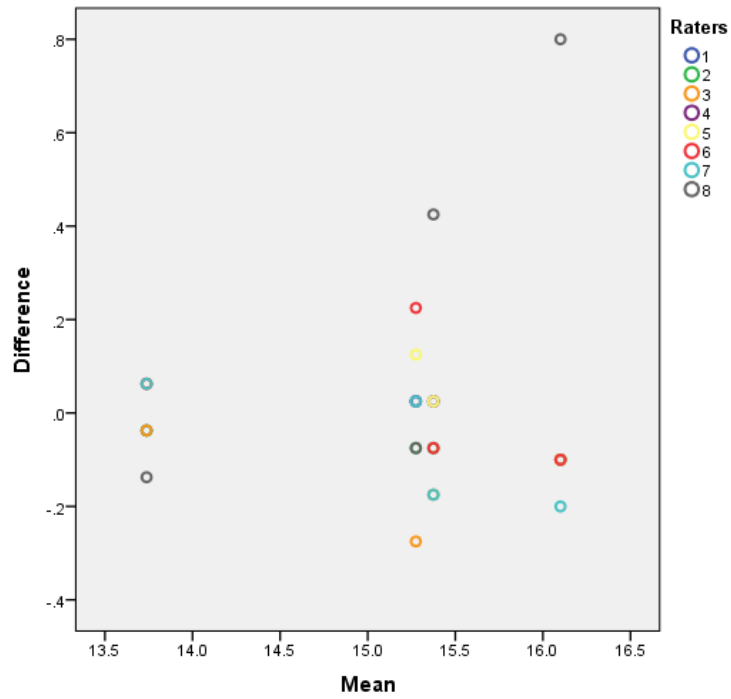


Figure A2.57 Scatterplot of the Mean versus difference of 5 measurement taken on the metatarsal, on three specimens by 8 raters.

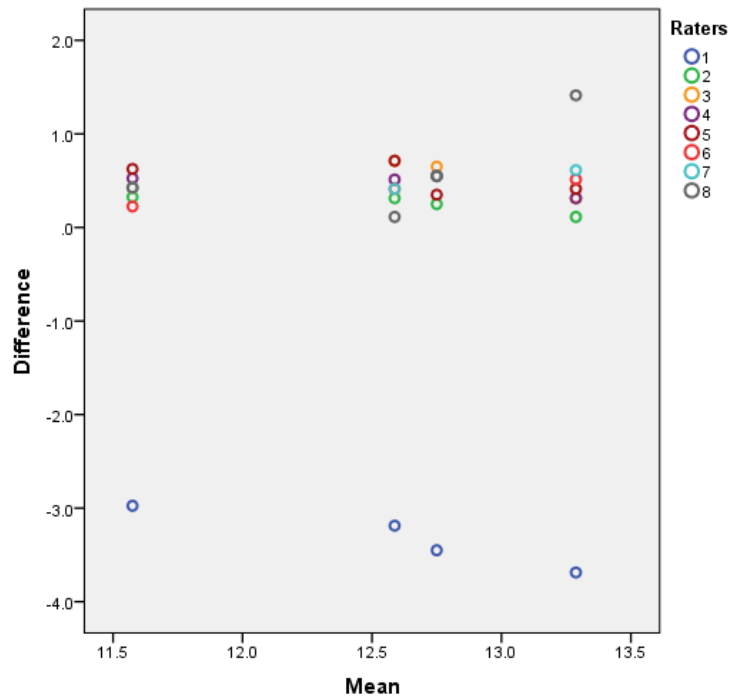


Figure A2.58 Scatterplot of the Mean versus difference of 6 measurement taken on the metatarsal, on three specimens by 8 raters.

Measurements 4 and 6 (Figs. A2.56 and A2.58) on the lateral condyle seem to show more agreement on this occasion among the raters than measurement 5 (Fig. A2.57).

Figures A2.59 to A2.61 are the scatterplots related to measurements on the tibia. Measurement Bd (Fig. A2.59) shows that, apart from the extreme low difference score given by rater 5 on

specimen 2, there is relative agreement among the raters: the dots for each line are clustered around 0, confirming the presence of consistency among raters. On the contrary, the results from Dd(a) (Fig. A2.60) shows much more disagreement among the raters: the dots for each specimen, in fact, are spread over the vertical lines. The same phenomenon can be seen for Dd(b) (Fig. A2.61). In addition, on specimen 4, an extreme value is given by rater 3, increasing the sense of spread.

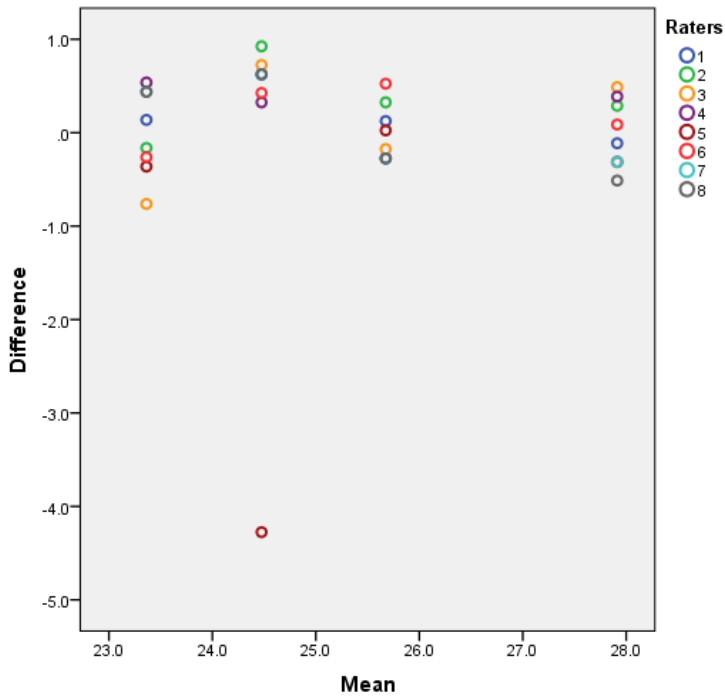


Figure A2.59 Scatterplot of the Mean versus difference of Bd measurement taken on the tibia, on four specimens by 8 raters.

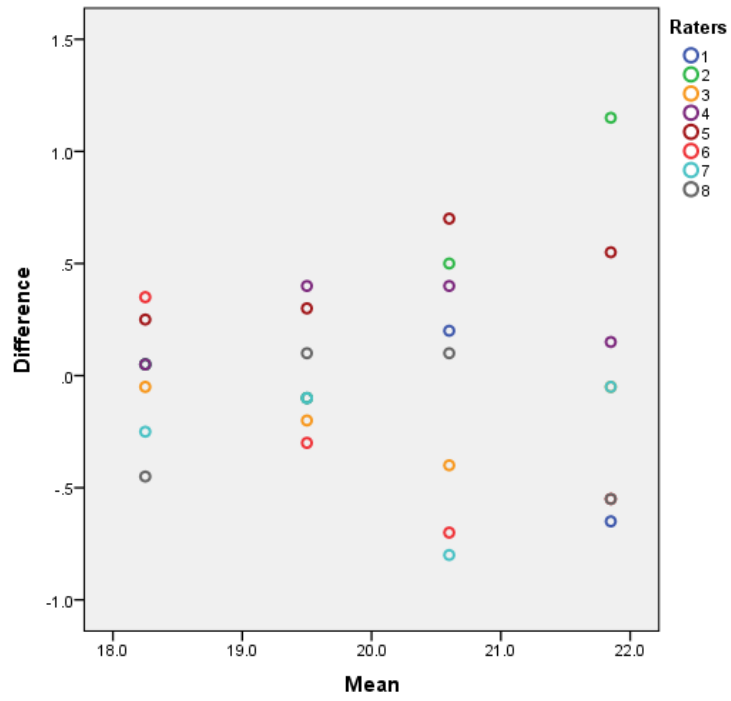


Figure A2.60 Scatterplot of the Mean versus difference of Dd(a) measurement taken on the tibia, on four specimens by 8 raters.

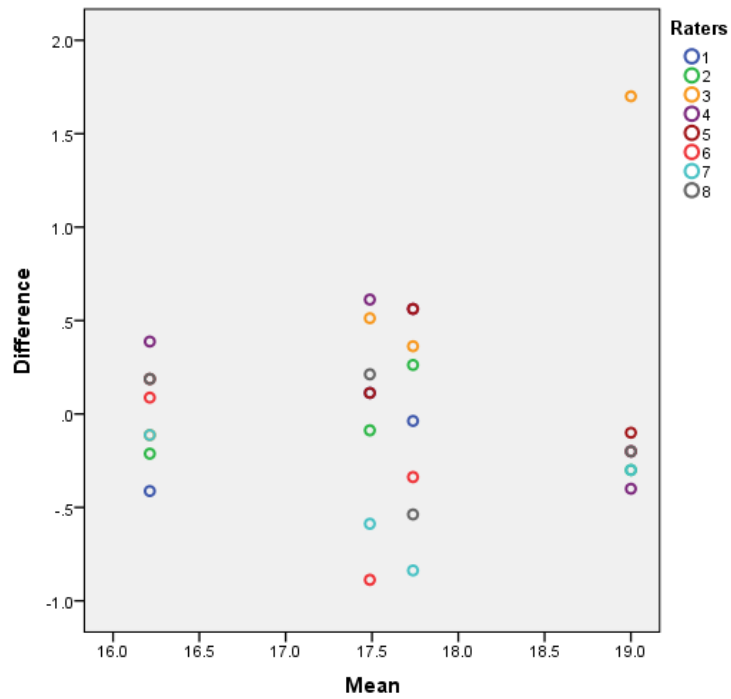


Figure A2.61 Scatterplot of the Mean versus difference of Dd(b) measurement taken on the tibia, on four specimens by 8 raters.

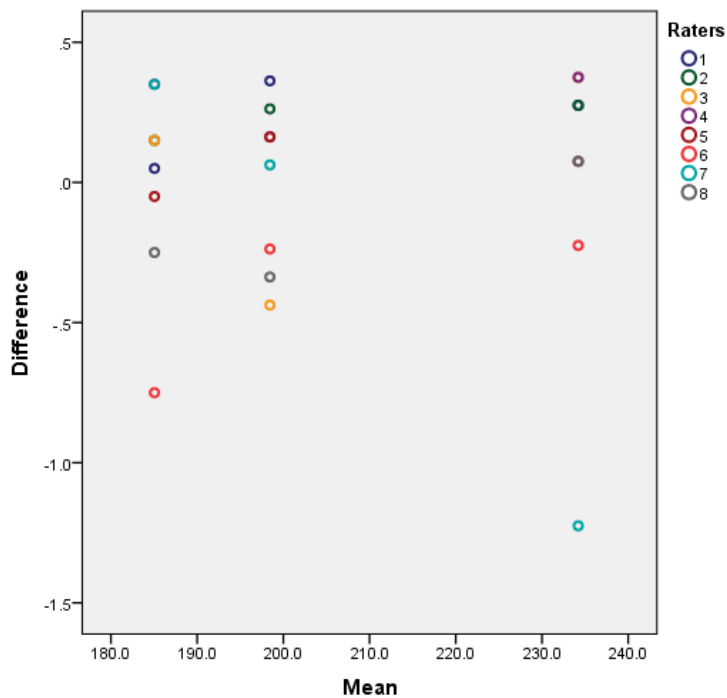


Figure A2.62 Scatterplot of the Mean versus difference of GL measurement taken on the tibia, on three specimens by 8 raters.

As the dots are partially gathered around 0, agreement was present among the raters when taking measurement GL (Fig. A2.62) while the results for measurement SD (Fig. A2.63) show more variability among the raters. In fact, the dots are more spread along the vertical line than they were for GL. Nevertheless, some agreement can be observed.

Scatterplots A2.63 to A2.70 display the results for the astragalus.

Figure A2.64 shows the presence of differences among the scores of the raters for measurement Bd: dots are spread along the vertical lines and not gathered around 0. Dots are spread on the vertical line also for measurements GLl and GLm (Figs. A2.65 and A2.66). The presence of some extreme difference scores increases the sense of spread. Differences are present among the scores the raters gave also for measurements Dl and Dm (Figs. A2.67 and A2.68). Specimen 3 on Figure A2.67 seems the one where least differences can be detected among the raters as the dots are more clustered around 0 and less spread on the vertical line than the other specimens. Despite differences can be found among the raters scores (on specimen 4, rater 5 gave an extreme value, magnifying the impression of the spread of the scores) dots for the measurement Dm are less spread out than for Dl.

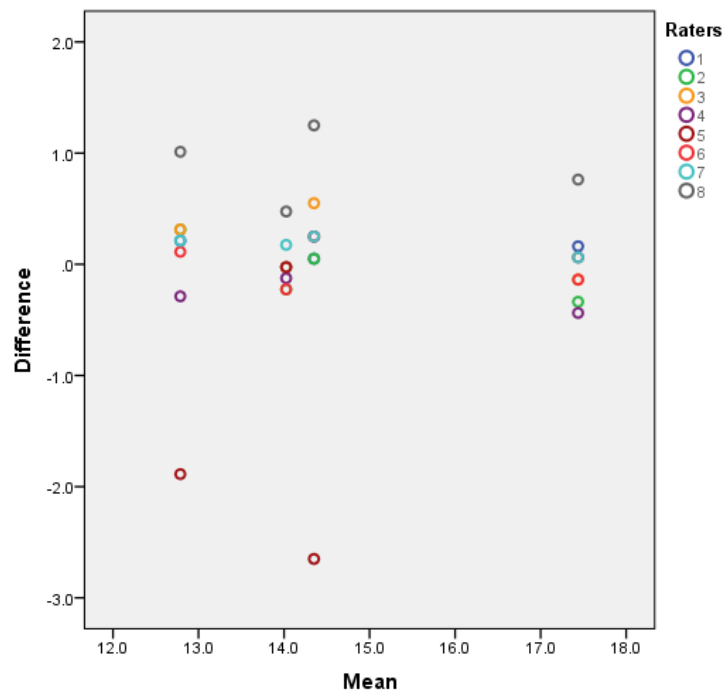


Figure A2.63 Scatterplot of the Mean versus difference of SD measurement taken on the tibia, on four specimens by 8 raters.

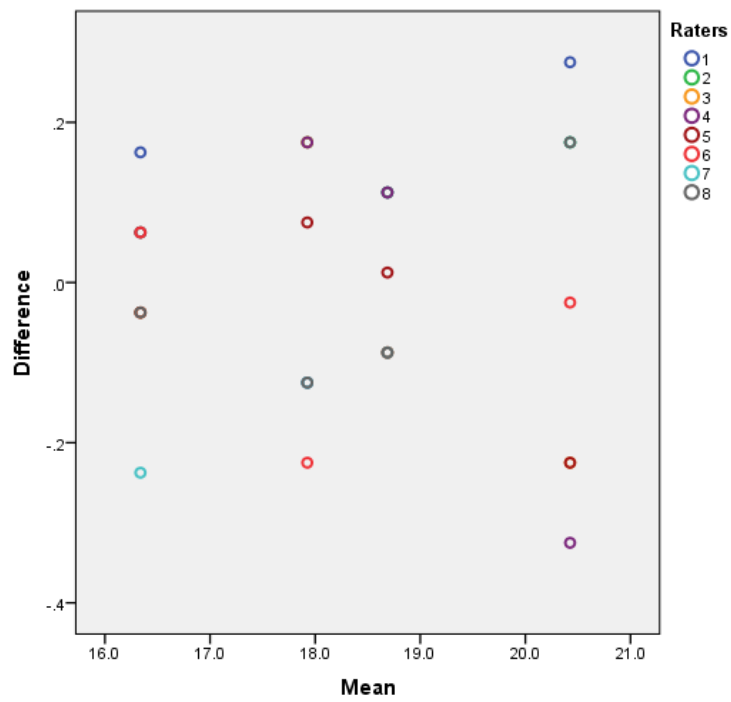


Figure A2.64 Scatterplot of the Mean versus difference of Bd measurement taken on the astragalus, on four specimens by 8 raters.

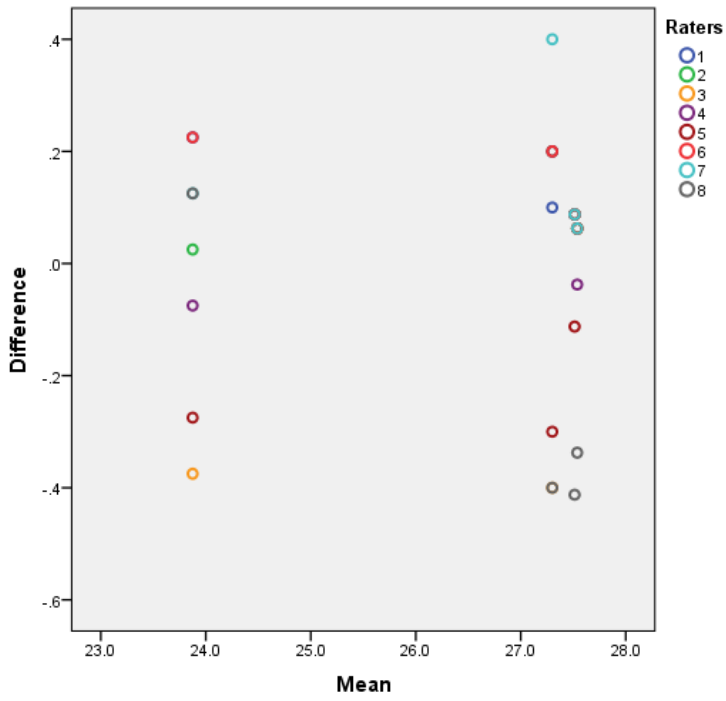


Figure A2.65 Scatterplot of the Mean versus difference of GLI measurement taken on the astragalus, on four specimens by 8 raters.

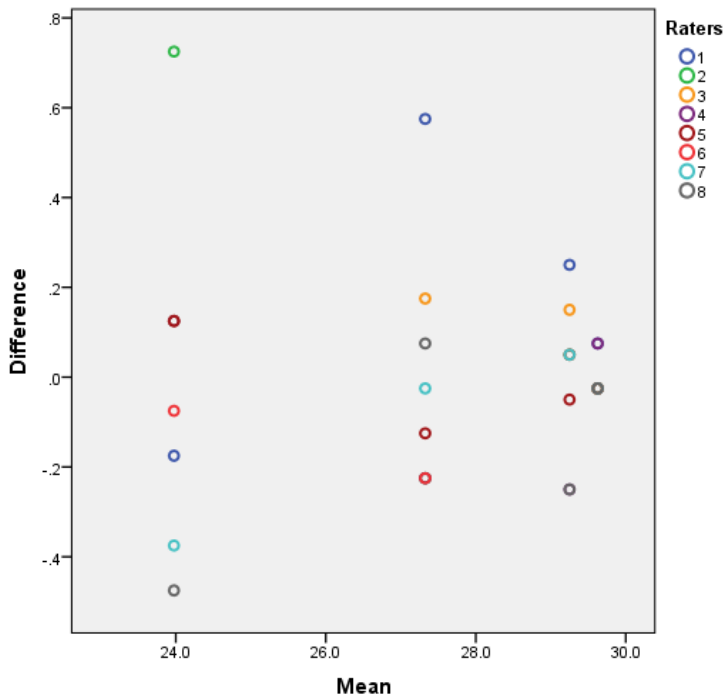


Figure A2.66 Scatterplot of the Mean versus difference of GLM measurement taken on the astragalus, on four specimens by 8 raters.

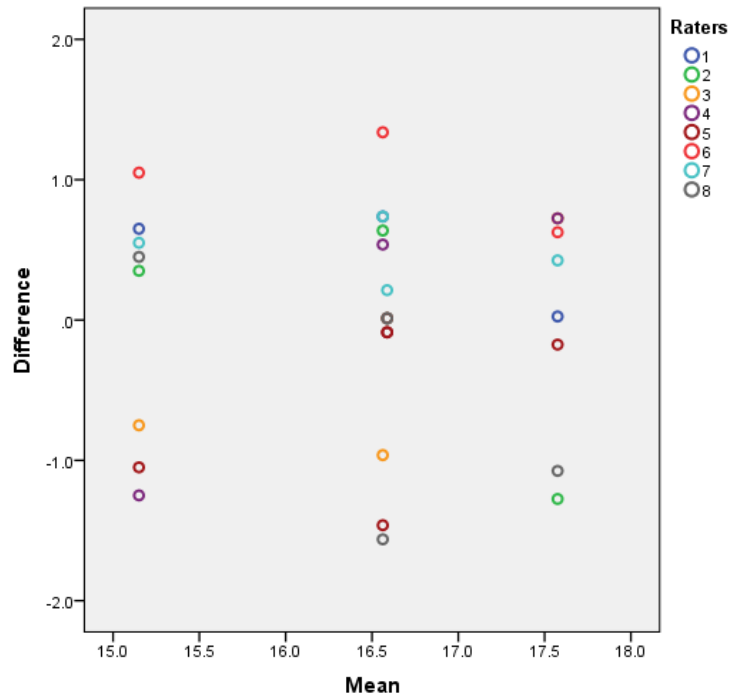


Figure A2.67 Scatterplot of the Mean versus difference of DI measurement taken on the astragalus, on four specimens by 8 raters.

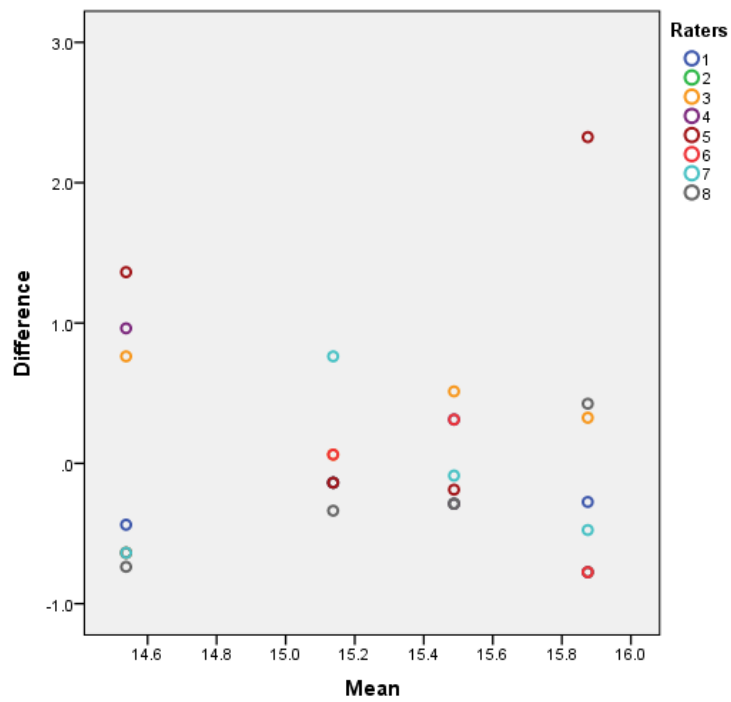


Figure A2.68 Scatterplot of the Mean versus difference of Dm measurement taken on the astragalus, on four specimens by 8 raters.

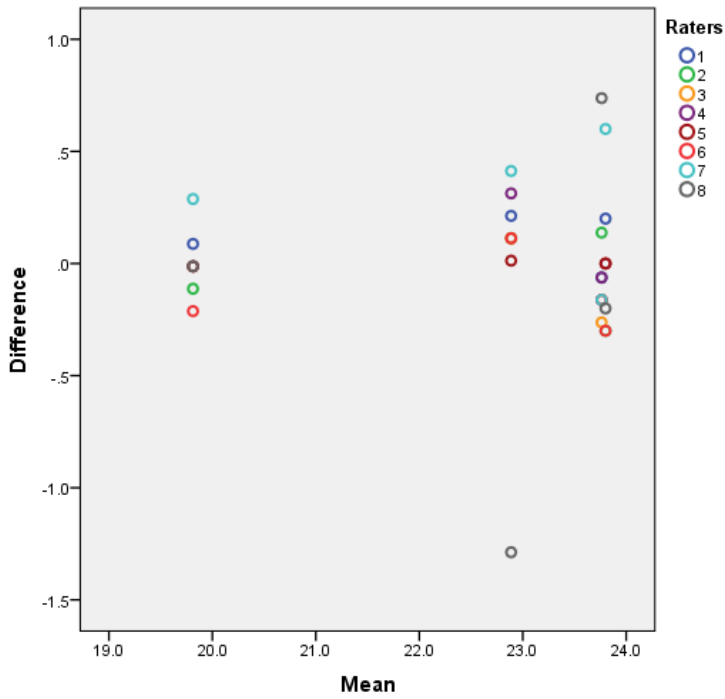


Figure A2.69 Scatterplot of the Mean versus difference of H measurement taken on the astragalus, on four specimens by 8 raters.

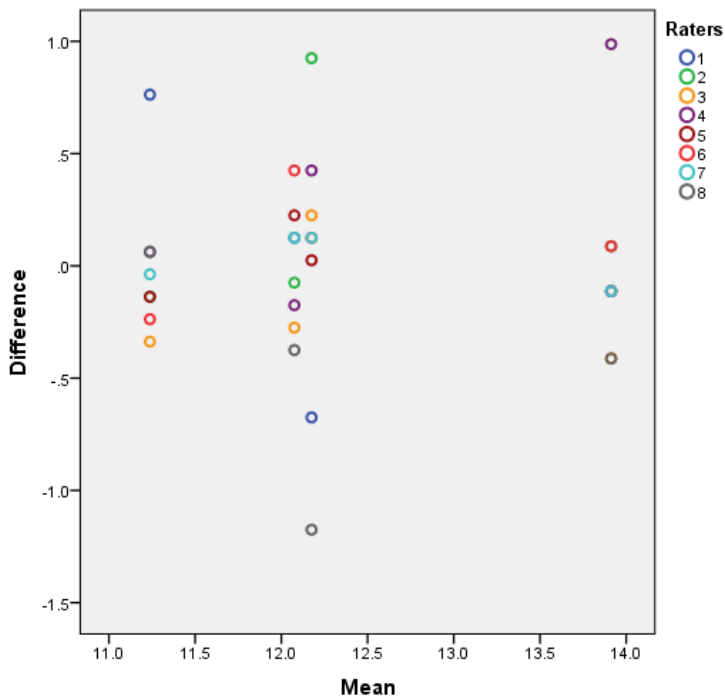


Figure A2.70 Scatterplot of the Mean versus difference of BpT measurement taken on the astragalus, on four specimens by 8 raters.

With measurement H (Fig. A2.69) there is more spread in the results for specimens 3 and 4, while specimens 1 and 2 (if the extreme score given by rater 8 is excluded) have dots gathered close to 0, attesting agreement among the raters. Finally for measurement BpT (Fig. A2.70),

specimens 1 and 3 have been measured more consistently by the raters. The presence of some extreme difference values increases the impression of scattering.

Figures A2.71 to A1.78 show the results from the measurements taken on the calcaneum.

Scatterplot A1.71, related to measurement GL, shows that the dots for each specimen are mainly gathered around 0 (apart from some outliers). Thus the raters have been taking GL consistently.

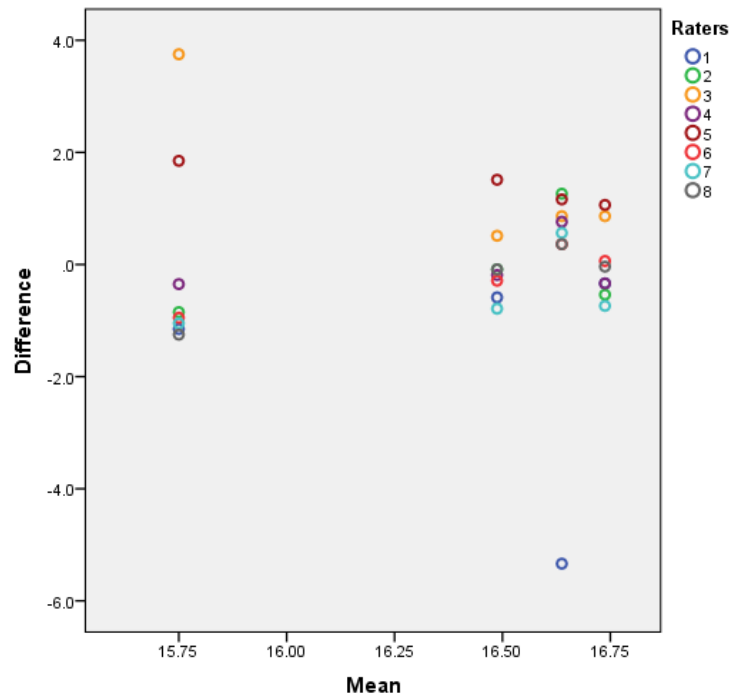


Figure A2.71 Scatterplot of the Mean versus difference of GL measurement taken on the calcaneum, on four specimens by 8 raters.

In the case of SB (Fig. A2.72), the presence of some extreme values is evident but, at the same time, the dots are more scattered on the vertical line than in the case of GL (Fig. A2.71), attesting that some differences were indeed present among the raters. This could be due to the fact that SB is very similar to the measurement suggested by Von den Driesch, GB, but taken in a slightly different way, so that confusion may have occurred among the raters (for more details see Chapter 2).

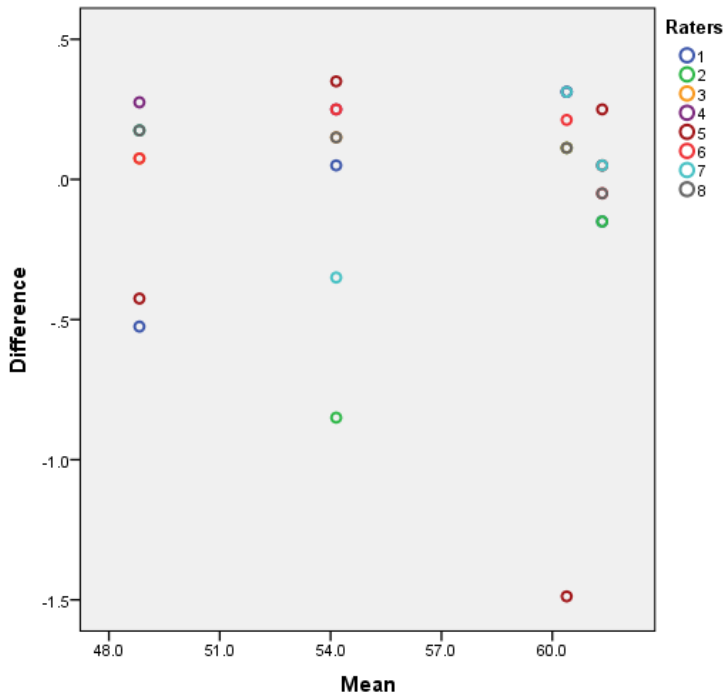


Figure A2.72 Scatterplot of the Mean versus difference of SB measurement taken on the calcaneum, on four specimens by 8 raters.

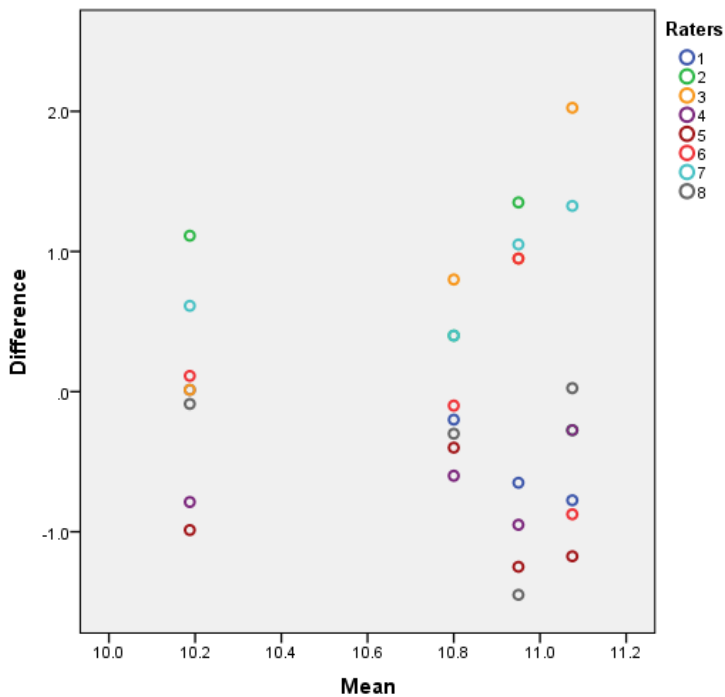


Figure A2.73 Scatterplot of the Mean versus difference of c measurement taken on the calcaneum, on four specimens by 8 raters.

A high spread of the dots along the vertical line can be recognised for measurement c (Fig. A2.73), attesting variability between the raters' scores. In this case, the spread is not influenced by clear outliers. A certain degree of spread is also noticeable for measurement d (Fig. A2.74). Specimens 1, 3 and 4 present almost the same degree of dispersion, while specimen 2 shows a higher degree of scattering.

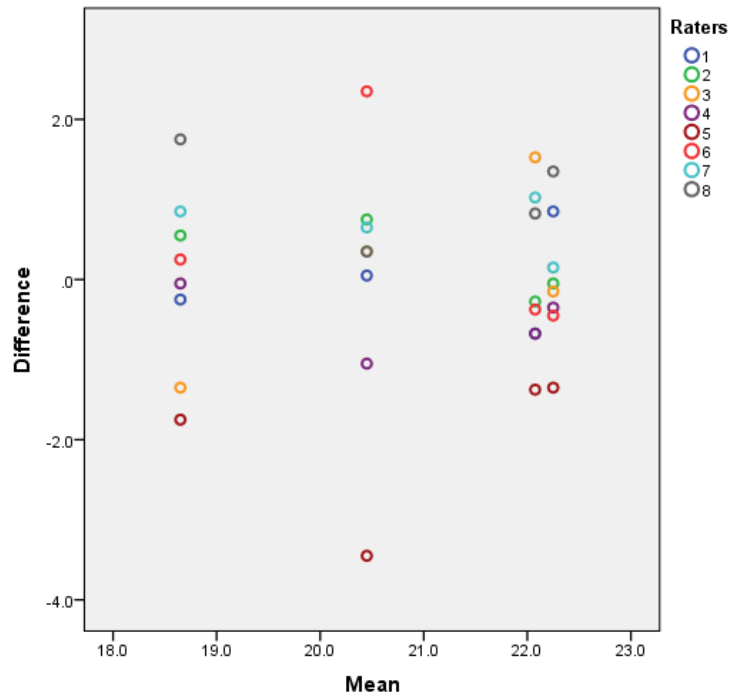


Figure A2.74 Scatterplot of the Mean versus difference of d measurement taken on the calcaneum, on four specimens by 8 raters.

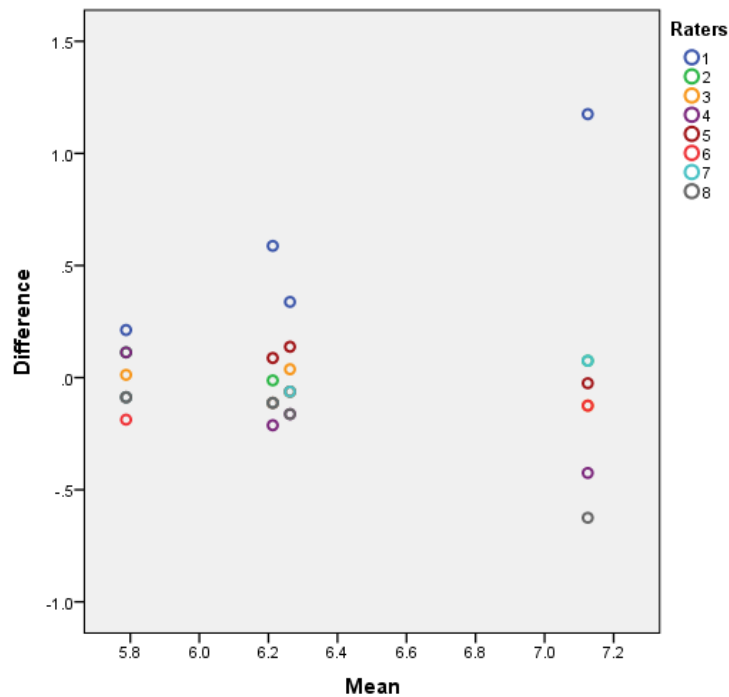


Figure A2.75 Scatterplot of the Mean versus difference of B measurement taken on the calcaneum, on four specimens by 8 raters.

Less spread are the dots for measurement B (Fig. A2.75). Some extreme high difference scores are given by rater 1. Nevertheless, if those are not considered, dots on specimens 1, 2 and 3 seem to be gathered close to 0, attesting agreement among the raters. On the contrary, dots for all the specimens are spread along the vertical line for measurements DS (Fig. A2.76), with some extreme low difference scores given by rater 1. This pattern suggests that low agreement was present among the raters. Apart from some extreme scores (again raters 1 and, to a lesser

extent, rater 8, who gave very high difference scores), the dots fall around the 0 area for measurement Gd (Fig. A2.77), indicating that some agreement among the raters was present.

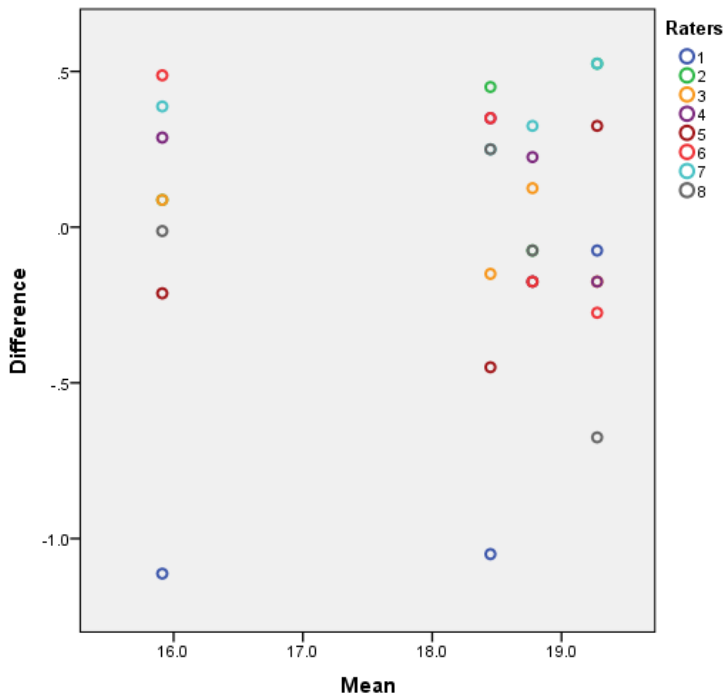


Figure A2.76 Scatterplot of the Mean versus difference of DS measurement taken on the calcaneum, on four specimens by 8 raters.

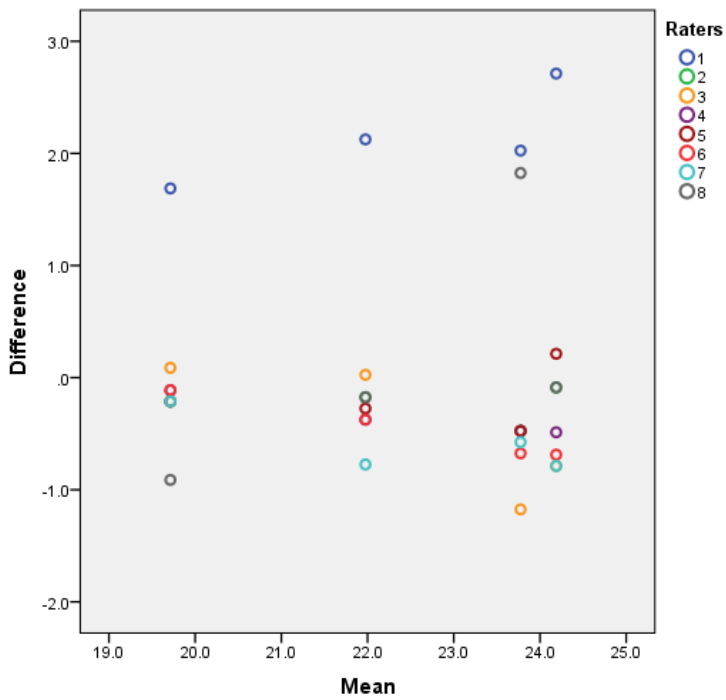


Figure A2.77 Scatterplot of the Mean versus difference of Gd measurement taken on the calcaneum, on four specimens by 8 raters.

Finally, scatterplots A2.78 and A2.79 show the results for the measurements taken on the 3rd phalanx.

Dots representing the raters, for measurement MBS (Fig. A2.79) are more spread along the vertical line than those related to measurement DLS (Fig. A2.78). Thus DLS has been taken more consistently than MBS.

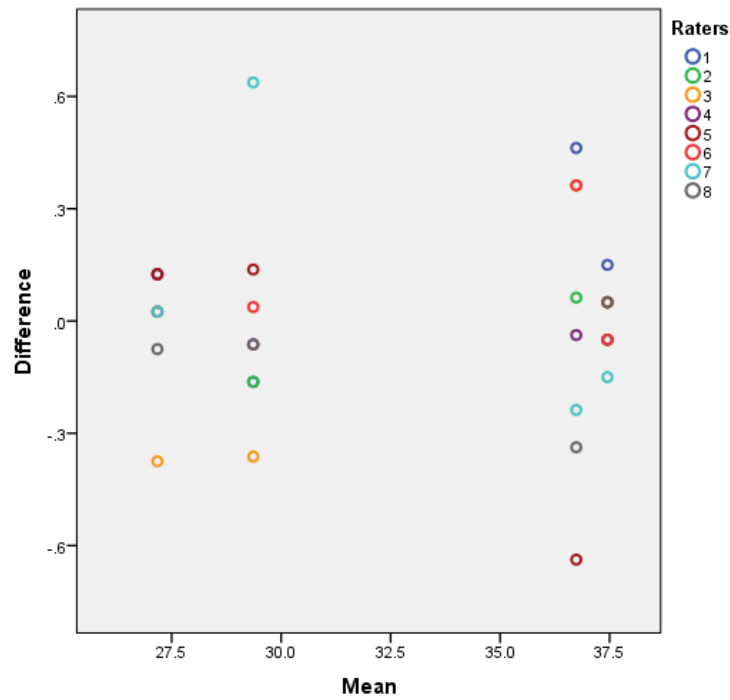


Figure A2.78 Scatterplot of the Mean versus difference of DLS measurement taken on the 3 phalanx, on four specimens by 8 raters.

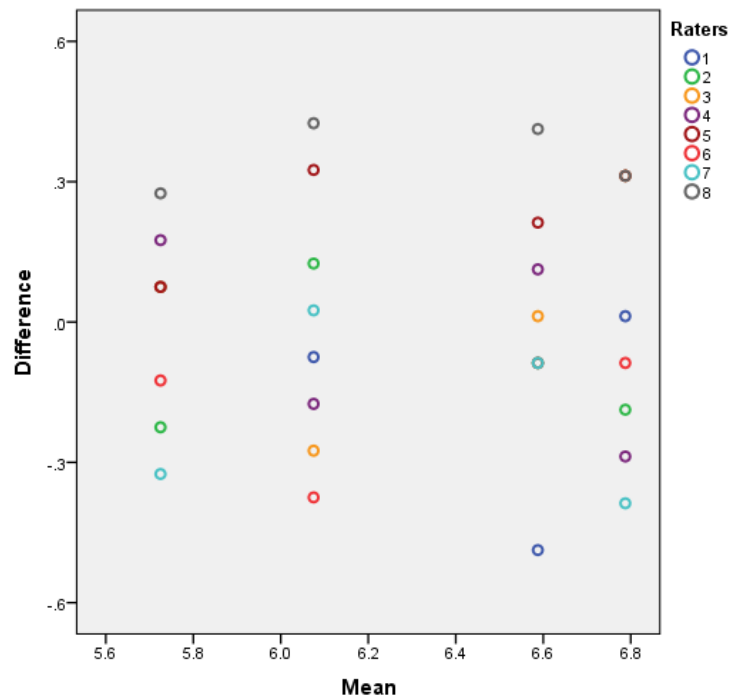


Figure A2.79 Scatterplot of the Mean versus difference of MBS measurement taken on the 3 phalanx, on four specimens by 8 raters.

Appendix III: Descriptive statistics for the modern sheep and goat material

The results of the descriptive statistics of the modern biometrical data are presented here on an element by element basis.

Horncore

Table A3.1 Summary of the sheep and goat modern specimens for each measurement taken on the horncore processed by SPSS.

Case Processing Summary							
	TAXA	Cases					
		Valid		Missing		Total	
		N	Percent	N	Percent	N	Percent
HC (A)	CH	39	49.4%	40	50.6%	79	100.0%
	OA	30	38.5%	48	61.5%	78	100.0%
HC (B)	CH	39	49.4%	40	50.6%	79	100.0%
	OA	30	38.5%	48	61.5%	78	100.0%
HC (C)	CH	36	45.6%	43	54.4%	79	100.0%
	OA	29	37.2%	49	62.8%	78	100.0%
HC (D)	CH	36	45.6%	43	54.4%	79	100.0%
	OA	29	37.2%	49	62.8%	78	100.0%
HC (E)	CH	36	45.6%	43	54.4%	79	100.0%
	OA	28	35.9%	50	64.1%	78	100.0%
HC (F)	CH	35	44.3%	44	55.7%	79	100.0%
	OA	28	35.9%	50	64.1%	78	100.0%

Table A3.2 Descriptive statistics for the modern goat (CH) and sheep (OA) for each measurement taken on the horncore.

Element	Measurement	TAXA	Descriptives			
			Statistic		Std. Error	CV
HC	HC (A)	CH	Mean	35.495	1.9094	33.5945
			Median	30.700		
			Variance	142.190		
			Std. Deviation	11.9244		
			Minimum	18.0		
			Maximum	65.9		
		OA	Mean	35.287	1.8327	28.4475
			Median	32.350		
			Variance	100.767		

Descriptives						
			Std. Deviation	10.0383		
			Minimum	20.7		
			Maximum	57.6		
	HC (B)	CH	Mean	24.013	1.1832	30.7724
			Median	21.000		
			Variance	54.603		
			Std. Deviation	7.3894		
			Minimum	13.1		
			Maximum	42.3		
		OA	Mean	25.090	1.7831	38.9246
			Median	21.200		
			Variance	95.379		
			Std. Deviation	9.7662		
			Minimum	12.7		
			Maximum	45.5		
	HC (C)	CH	Mean	26.450	1.3575	30.7928
			Median	24.600		
			Variance	66.336		
			Std. Deviation	8.1447		
			Minimum	12.9		
			Maximum	44.5		
		OA	Mean	30.079	1.4818	
			Median	27.800		
			Variance	63.679		
			Std. Deviation	7.9799		
			Minimum	16.4		
			Maximum	48.6		
HC (D)	CH	Mean	15.706	.6499	24.8287	
		Median	14.900			
		Variance	15.207			
		Std. Deviation	3.8996			
		Minimum	9.3			
		Maximum	25.9			
	OA	Mean	19.090	1.2875	36.3205	
		Median	16.700			
		Variance	48.075			
		Std. Deviation	6.9336			
		Minimum	10.7			
		Maximum	34.9			
HC (E)	CH	Mean	149.658	10.2342	41.0304	
		Median	137.450			
		Variance	3770.615			
		Std. Deviation	61.4053			

		Descriptives				
		OA	Minimum	78.5		
			Maximum	316.5		
			Mean	99.639	8.0793	42.9063
			Median	85.150		
			Variance	1827.693		
			Std. Deviation	42.7515		
			Minimum	50.0		
			Maximum	192.9		
	HC (F)	CH	Mean	166.580	12.4277	44.1367
			Median	146.000		
			Variance	5405.630		
			Std. Deviation	73.5230		
			Minimum	88.9		
			Maximum	380.0		
OA		Mean	127.821	12.7882	52.9403	
		Median	100.900			
		Variance	4579.086			
		Std. Deviation	67.6689			
		Minimum	55.8			
		Maximum	303.0			

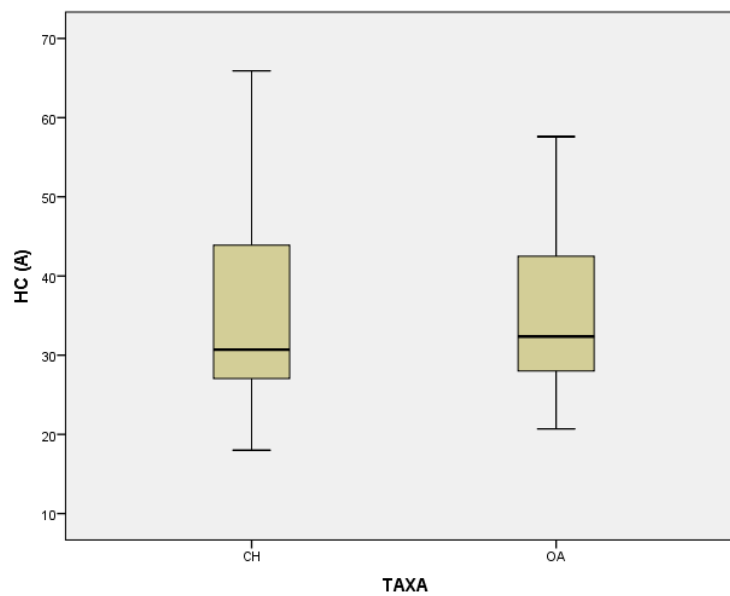


Figure A3.0.1 Horncore. Box plot for the modern sample of goat (CH) and sheep (OA) for measurement A.

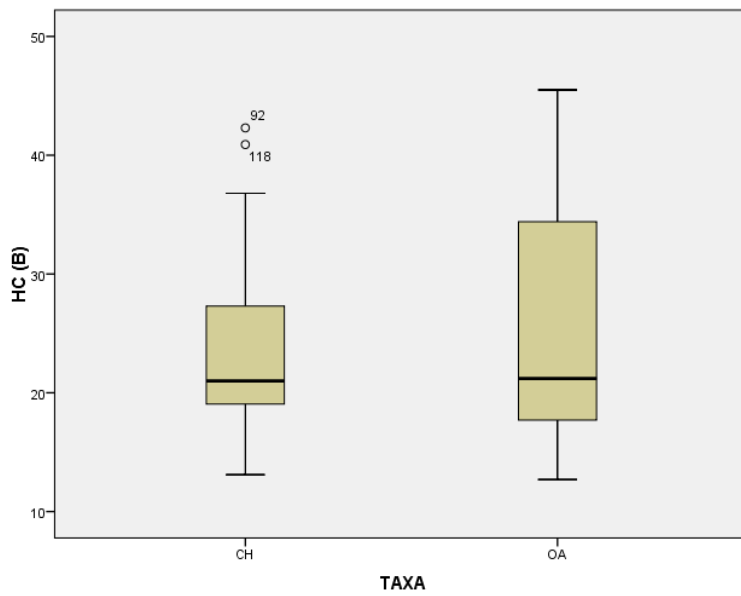


Figure A3.0.2 Horncore. Box plot for the modern sample of goat (CH) and sheep (OA) for measurement B.

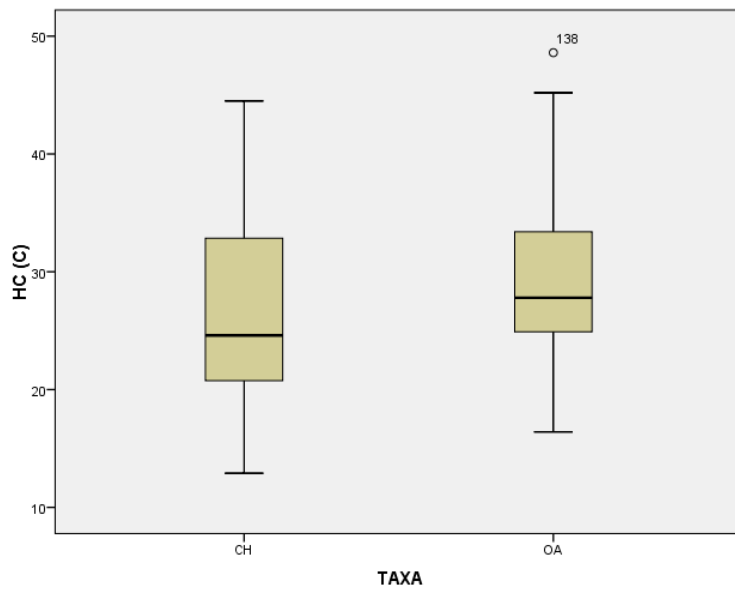


Figure A3.0.3 Horncore. Box plot for the modern sample of goat (CH) and sheep (OA) for measurement C.

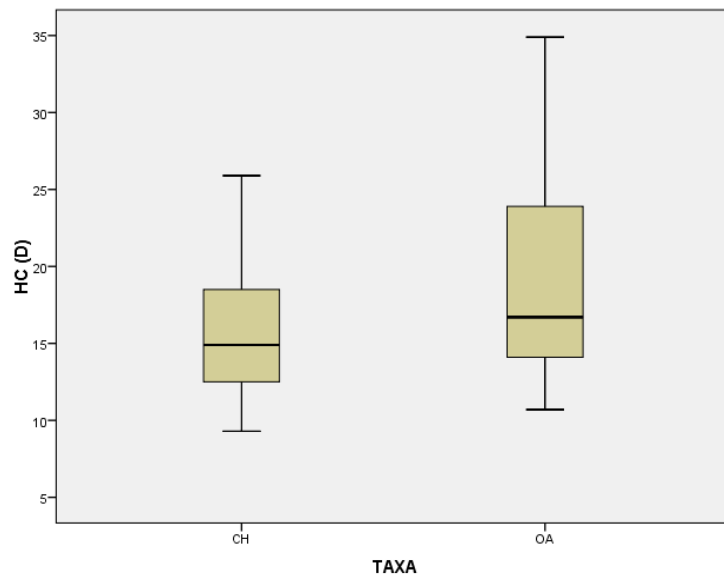


Figure A3.0.4 Horncore. Box plot for the modern sample of goat (CH) and sheep (OA) for measurement D.

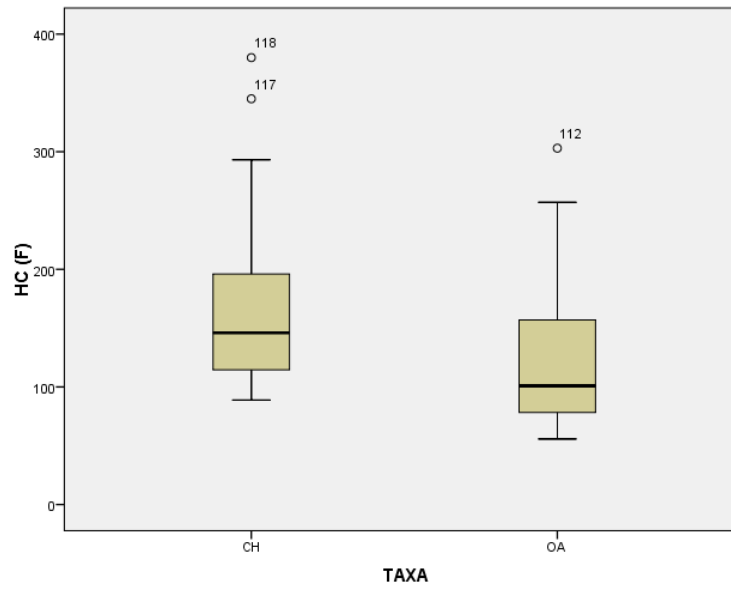


Figure A3.0.5 Horncore. Box plot for the modern sample of goat (CH) and sheep (OA) for measurement F.

Scapula

Table A3.3 Summary of the sheep and goat modern specimens for each measurement taken on the scapula processed by SPSS.

Case Processing Summary							
	TAXA	Cases					
		Valid		Missing		Total	
		N	Percent	N	Percent	N	Percent
BG	CH	73	92.4%	6	7.6%	79	100.0%
	OA	73	93.6%	5	6.4%	78	100.0%
LG	CH	73	92.4%	6	7.6%	79	100.0%
	OA	73	93.6%	5	6.4%	78	100.0%
SLC	CH	73	92.4%	6	7.6%	79	100.0%
	OA	73	93.6%	5	6.4%	78	100.0%
ASG	CH	73	92.4%	6	7.6%	79	100.0%
	OA	73	93.6%	5	6.4%	78	100.0%
GLP	CH	73	92.4%	6	7.6%	79	100.0%
	OA	73	93.6%	5	6.4%	78	100.0%

Table A3.4 Descriptive statistics for the modern goat (CH) and sheep (OA) for each measurement taken on the scapula.

Element	Measurement	TAXA	Descriptives			
			Statistic		Std. Error	CV
Sc	BG	CH	Mean	24.325	.3255	11.4326
			Median	24.300		
			Variance	7.734		
			Std. Deviation	2.7810		
			Minimum	19.4		
			Maximum	32.1		
		OA	Mean	21.062	.2915	11.8265
			Median		20.700	
			Variance		6.205	
			Std. Deviation		2.4909	
			Minimum		16.1	
			Maximum		26.6	
	LG	CH	Mean	28.548	.3883	11.6221
			Median	28.600		
			Variance	11.009		
			Std. Deviation	3.3179		
			Minimum	22.3		
			Maximum	37.1		

		Descriptives				
	OA	Mean	25.811	.3387	11.2130	
		Median	25.900			
		Variance	8.377			
		Std. Deviation	2.8942			
		Minimum	19.3			
		Maximum	33.2			
	SLC	CH	Mean	22.166	.3564	13.7372
			Median	21.500		
			Variance	9.272		
			Std. Deviation	3.0450		
			Minimum	16.8		
			Maximum	30.8		
		OA	Mean	19.762	.2604	11.2564
			Median	19.500		
			Variance	4.949		
			Std. Deviation	2.2245		
			Minimum	15.2		
			Maximum	25.7		
	ASG	CH	Mean	26.142	.3946	12.8976
			Median	25.800		
			Variance	11.368		
			Std. Deviation	3.3717		
			Minimum	19.3		
			Maximum	34.9		
OA		Mean	21.060	.2517	10.2113	
		Median	21.000			
		Variance	4.625			
		Std. Deviation	2.1505			
		Minimum	14.4			
		Maximum	26.5			
GLP	CH	Mean	35.081	.4533	11.0401	
		Median	34.300			
		Variance	15.000			
		Std. Deviation	3.8730			
		Minimum	28.4			
		Maximum	46.1			
	OA	Mean	32.937	.4427	11.4837	
		Median	33.100			
		Variance	14.307			
		Std. Deviation	3.7824			
		Minimum	24.6			
		Maximum	42.8			

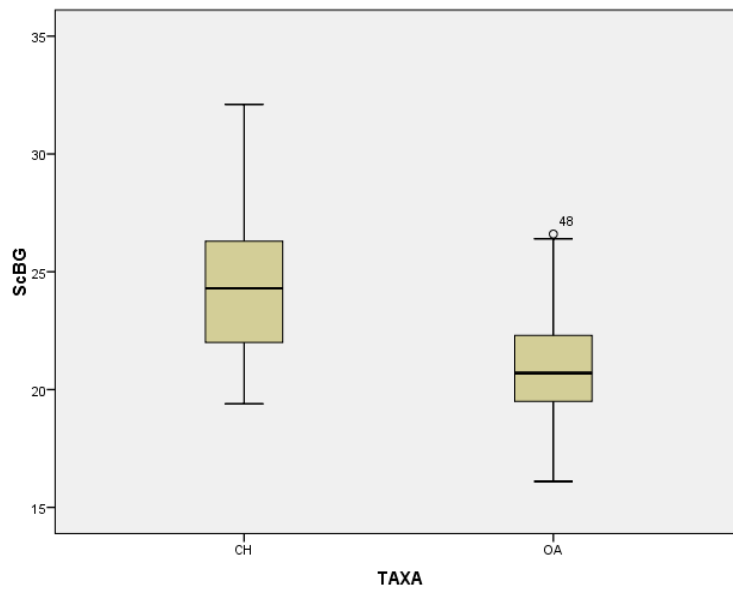


Figure A3.0.6 Scapula. Box plot for the modern sample of goat (CH) and sheep (OA) for measurement BG.

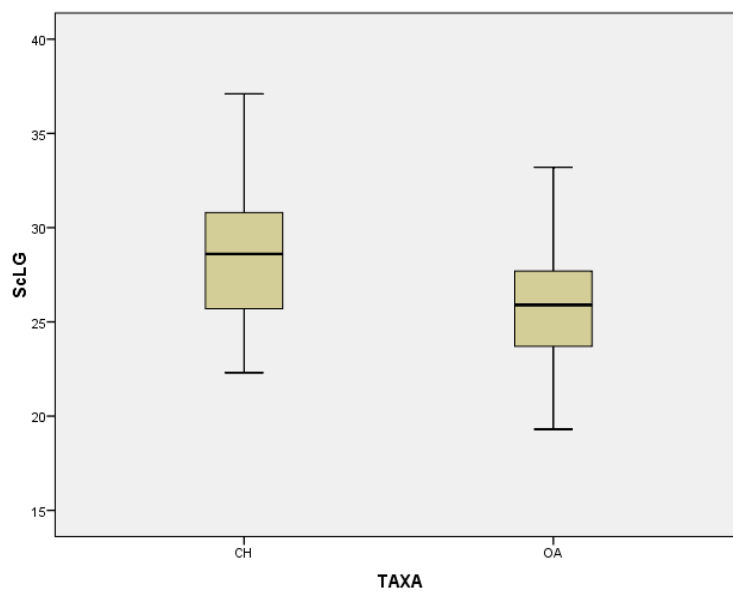


Figure A3.0.7 Scapula. Box plot for the modern sample of goat (CH) and sheep (OA) for measurement LG.

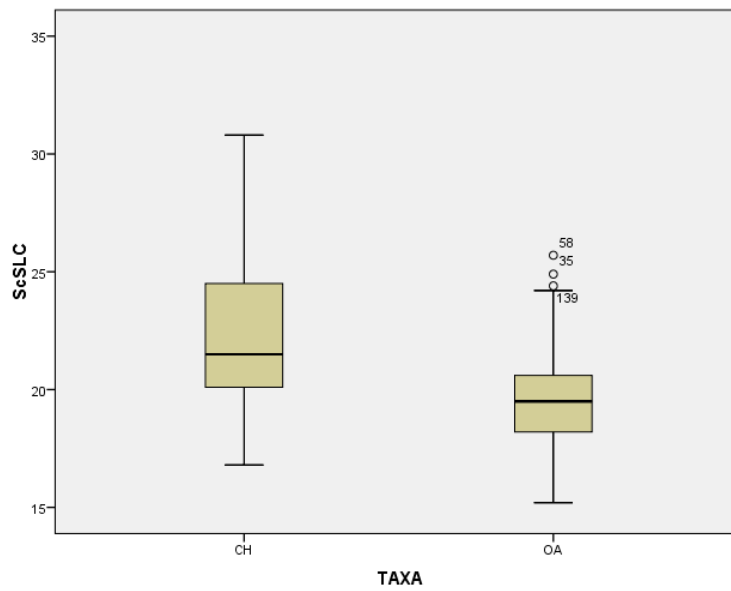


Figure A3.0.8 Scapula. Box plot for the modern sample of goat (CH) and sheep (OA) for measurement SLC.

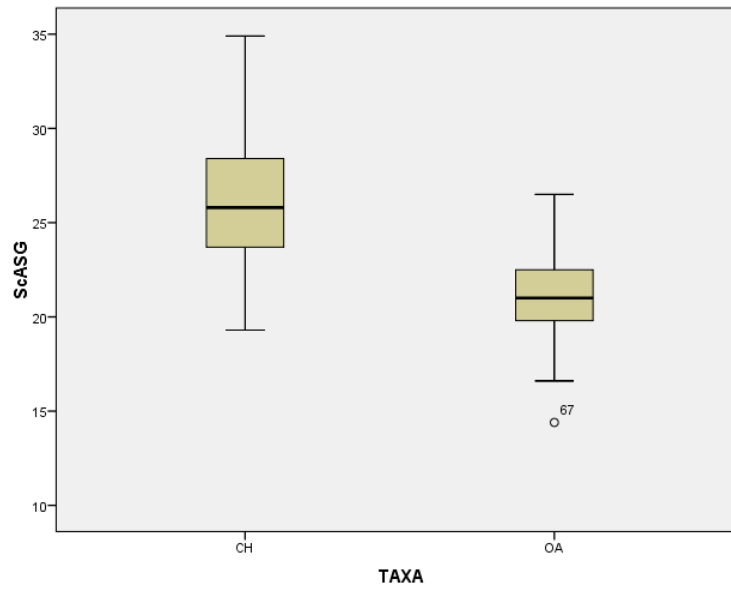


Figure A3.0.9 Scapula. Box plot for the modern sample of goat (CH) and sheep (OA) for measurement ASG.

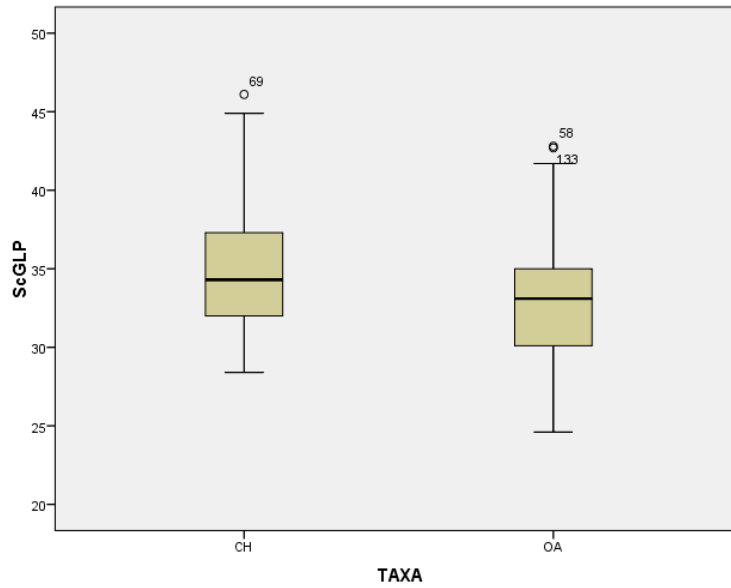


Figure A3.0.10 Scapula. Box plot for the modern sample of goat (CH) and sheep (OA) for measurement GLP.

Humerus

Table A3.5 Summary of the sheep and goat modern specimens for each measurement taken on the humerus processed by SPSS.

Case Processing Summary							
	TAXA	Cases					
		Valid		Missing		Total	
		N	Percent	N	Percent	N	Percent
HuBT	CH	75	94.9%	4	5.1%	79	100.0%
	OA	71	91.0%	7	9.0%	78	100.0%
HuBd	CH	75	94.9%	4	5.1%	79	100.0%
	OA	71	91.0%	7	9.0%	78	100.0%
HuHT	CH	75	94.9%	4	5.1%	79	100.0%
	OA	71	91.0%	7	9.0%	78	100.0%
HuHTC	CH	75	94.9%	4	5.1%	79	100.0%
	OA	71	91.0%	7	9.0%	78	100.0%
HuBE	CH	75	94.9%	4	5.1%	79	100.0%
	OA	71	91.0%	7	9.0%	78	100.0%
HuBEI	CH	75	94.9%	4	5.1%	79	100.0%
	OA	71	91.0%	7	9.0%	78	100.0%
HuDd	CH	75	94.9%	4	5.1%	79	100.0%
	OA	70	89.7%	8	10.3%	78	100.0%

Table A3.6 Descriptive statistics for the modern goat (CH) and sheep (OA) for each measurement taken on the humerus.

Descriptives						
Element	Measurement	TAXA	Statistics		Std. Error	CV
Hu	BT	CH	Mean	32.004	.3516	9.5147
			Median	31.400		
			Variance	9.273		
			Std. Deviation	3.0451		
			Minimum	26.5		
			Maximum	40.8		
		OA	Mean	28.255	.3403	10.1479
			Median	28.700		
			Variance	8.221		
			Std. Deviation	2.8673		
			Minimum	23.1		
			Maximum	35.6		
	Bd	CH	Mean	33.548	.4123	10.6438
			Median	33.000		
			Variance	12.750		
			Std. Deviation	3.5708		
			Minimum	27.6		
			Maximum	44.6		
		OA	Mean	29.518	.3695	10.5464
			Median	29.800		
			Variance	9.692		
			Std. Deviation	3.1131		
			Minimum	23.9		
			Maximum	37.0		
HT	CH	Mean	19.897	.2446	10.6458	
		Median	20.100			
		Variance	4.487			
		Std. Deviation	2.1182			
		Minimum	16.2			
		Maximum	26.6			
	OA	Mean	18.359	.2440	11.1988	
		Median	18.400			
		Variance	4.227			
		Std. Deviation	2.0560			
		Minimum	14.5			
		Maximum	23.6			
HTC	CH	Mean	15.288	.1810	10.2544	
		Median	15.300			
		Variance	2.458			
		Std. Deviation	1.5677			

Descriptives						
		OA	Minimum	10.8		
			Maximum	19.4		
			Mean	14.280	.1974	11.6449
			Median	14.200		
			Variance	2.765		
			Std. Deviation	1.6629		
			Minimum	11.3	.	
			Maximum	19.7		
	BE	CH	Mean	10.209	.1517	12.8670
			Median	10.200		
			Variance	1.725		
			Std. Deviation	1.3136		
			Minimum	7.5		
			Maximum	14.2		
		OA	Mean	8.551	.1255	12.3681
			Median	8.600		
			Variance	1.119		
			Std. Deviation	1.0576		
			Minimum	6.1		
			Maximum	11.2		
	BEI	CH	Mean	6.171	.1237	17.3602
			Median	6.100		
			Variance	1.148		
			Std. Deviation	1.0713		
			Minimum	4.2		
			Maximum	9.0		
		OA	Mean	6.627	.1310	16.6606
			Median	6.500		
Variance			1.219			
Std. Deviation			1.1041			
Minimum			4.8			
Maximum			9.4			
Dd	CH	Mean	27.768	.3341	10.4202	
		Median	27.500			
		Variance	8.372			
		Std. Deviation	2.8935			
		Minimum	21.9			
		Maximum	35.8			
	OA	Mean	24.547	.3450	11.7590	
		Median	24.600			
		Variance	8.332			
		Std. Deviation	2.8865			
		Minimum	19.4			

Descriptives						
			Maximum	32.2		

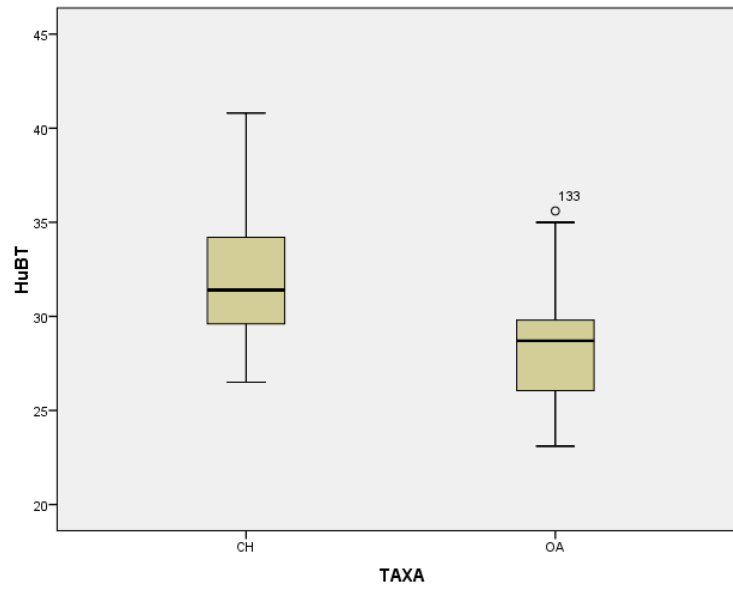


Figure A3.0.11 Humerus. Box plot for the modern sample of goat (CH) and sheep (OA) for measurement BT.

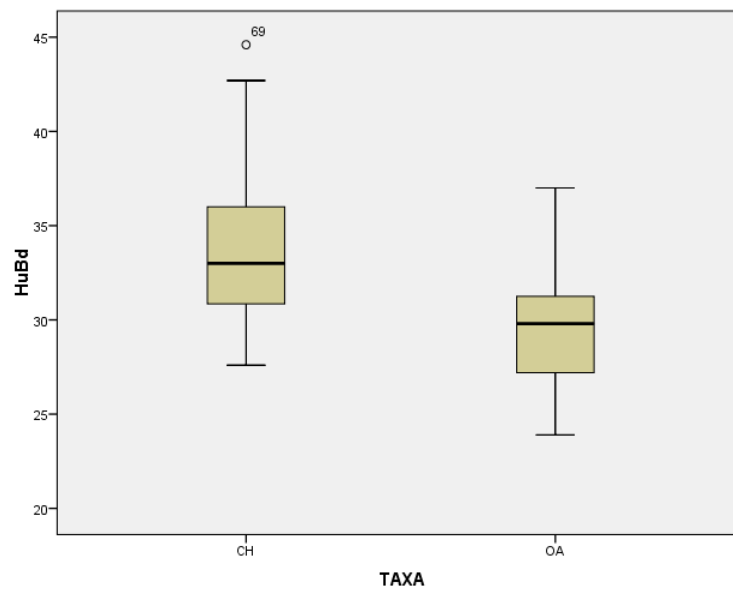


Figure A3.0.12 Humerus. Box plot for the modern sample of goat (CH) and sheep (OA) for measurement Bd.

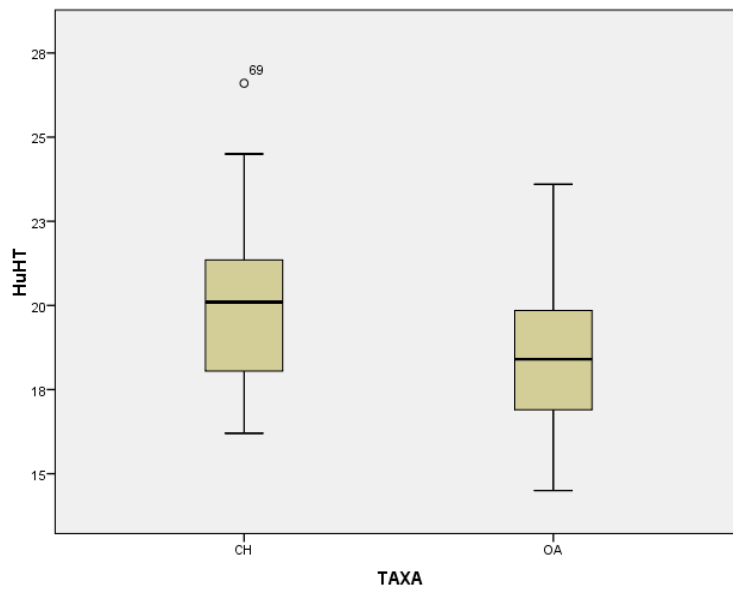


Figure A3.0.13 Humerus. Box plot for the modern sample of goat (CH) and sheep (OA) for measurement HT.

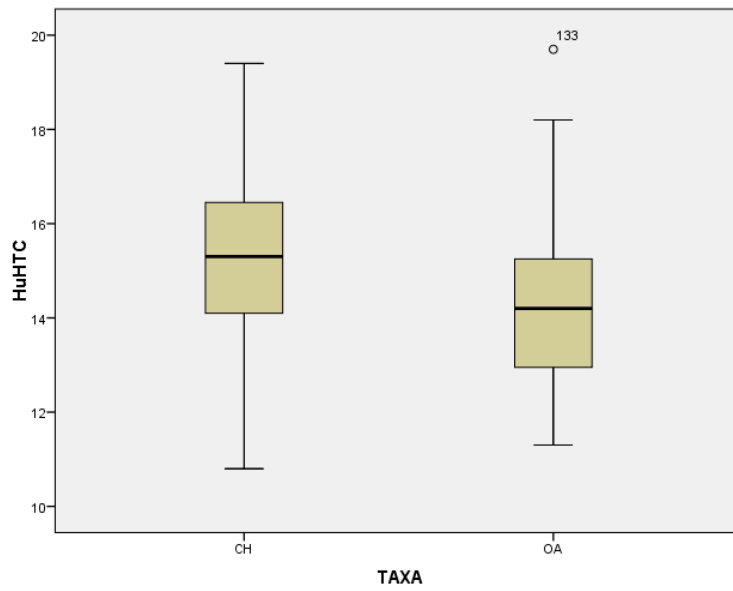


Figure A3.0.14 Humerus. Box plot for the modern sample of goat (CH) and sheep (OA) for measurement HTC.

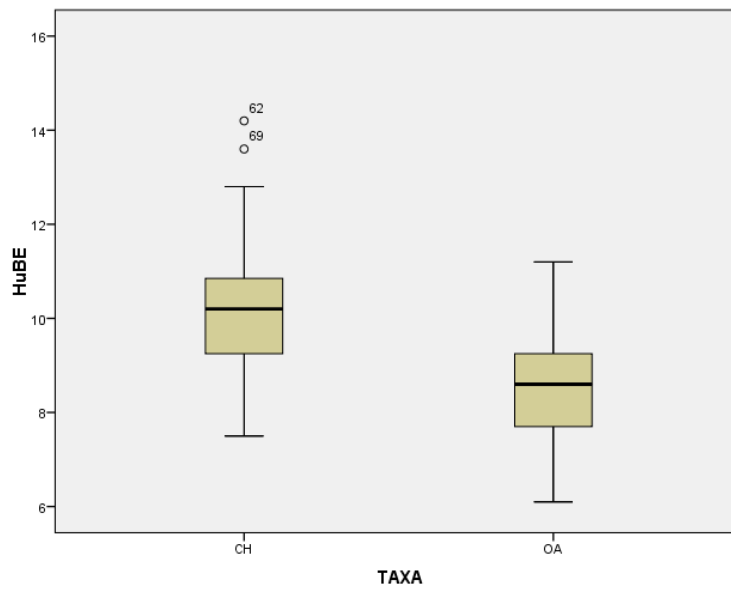


Figure A3.0.15 Humerus. Box plot for the modern sample of goat (CH) and sheep (OA) for measurement BE.

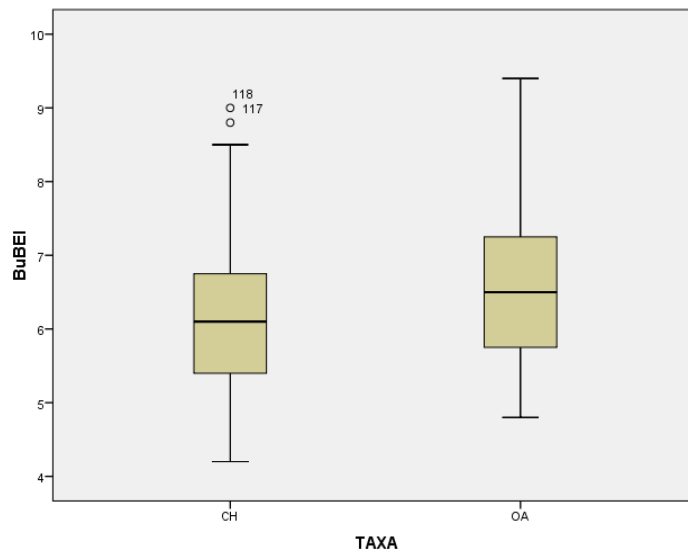


Figure A3.0.16 Humerus. Box plot for the modern sample of goat (CH) and sheep (OA) for measurement BEI.

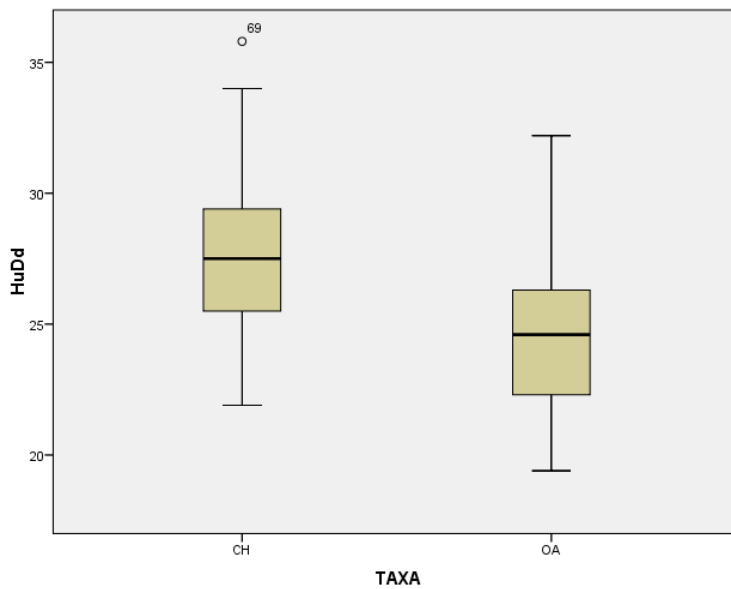


Figure A3.0.17 Humerus. Box plot for the modern sample of goat (CH) and sheep (OA) for measurement Dd.

Radius

Table A3.7 Summary of the sheep and goat modern specimens for each measurement taken on the radius processed by SPSS.

Case Processing Summary							
	TAXA	Cases					
		Valid		Missing		Total	
		N	Percent	N	Percent	N	Percent
RaBp	CH	73	92.4%	6	7.6%	79	100.0%
	OA	72	92.3%	6	7.7%	78	100.0%
RaBFp	CH	73	92.4%	6	7.6%	79	100.0%
	OA	72	92.3%	6	7.7%	78	100.0%
RaDp	CH	73	92.4%	6	7.6%	79	100.0%
	OA	72	92.3%	6	7.7%	78	100.0%
RaGL	CH	55	69.6%	24	30.4%	79	100.0%
	OA	53	67.9%	25	32.1%	78	100.0%
RaSD	CH	72	91.1%	7	8.9%	79	100.0%
	OA	72	92.3%	6	7.7%	78	100.0%

Table A3.8 Descriptive statistics for the modern goat (CH) and sheep (OA) for each measurement taken on the radius.

Descriptives						
Element	Mesurement	TAXA	Statistics		Std. Error	CV
Hu	Bp	CH	Mean	33.115	.3855	9.9471
			5% Trimmed Mean	32.951		
			Median	32.900		
			Variance	10.850		
			Std. Deviation	3.2940		
			Minimum	27.7		
		Maximum	42.4			
		OA	Mean	31.219	.3887	10.5640
			Median	31.000		
			Variance	10.877		
			Std. Deviation	3.2980		
			Minimum	22.8		
	Maximum		38.9			
	BFp	CH	Mean	31.671	.3471	9.3637
			Median	31.300		
			Variance	8.795		
			Std. Deviation	2.9656		
			Minimum	26.2		
			Maximum	40.0		
		OA	Mean	28.575	.3365	9.9919
			Median	28.850		
			Variance	8.152		
			Std. Deviation	2.8552		
			Minimum	23.0		
			Maximum	35.4		
	Dp	CH	Mean	17.156	.2154	10.7291
			Median	16.800		
			Variance	3.388		
			Std. Deviation	1.8407		
			Minimum	13.8		
Maximum			23.7			
OA		Mean	15.861	.2026	10.8366	
		Median	16.000			
		Variance	2.954			
		Std. Deviation	1.7188			
		Minimum	12.6			
		Maximum	20.8			
GL	CH	Mean	172.918	2.0713	8.8833	
		Median	173.800			

Descriptives						
			Variance	235.957		
			Std. Deviation	15.3609		
			Minimum	141.8		
			Maximum	209.7		
		OA	Mean	150.592	1.9609	9.4796
			Median	150.500		
			Variance	203.793		
			Std. Deviation	14.2756		
			Minimum	130.1		
			Maximum	184.3		
	SD	CH	Mean	19.336	.3167	13.8968
			Median	19.100		
			Variance	7.221		
			Std. Deviation	2.6871		
			Minimum	14.8		
			Maximum	26.8		
		OA	Mean	16.846	.2539	12.7870
			Median	16.900		
Variance			4.640			
Std. Deviation			2.1541			
			Minimum	11.6		
			Maximum	21.9		

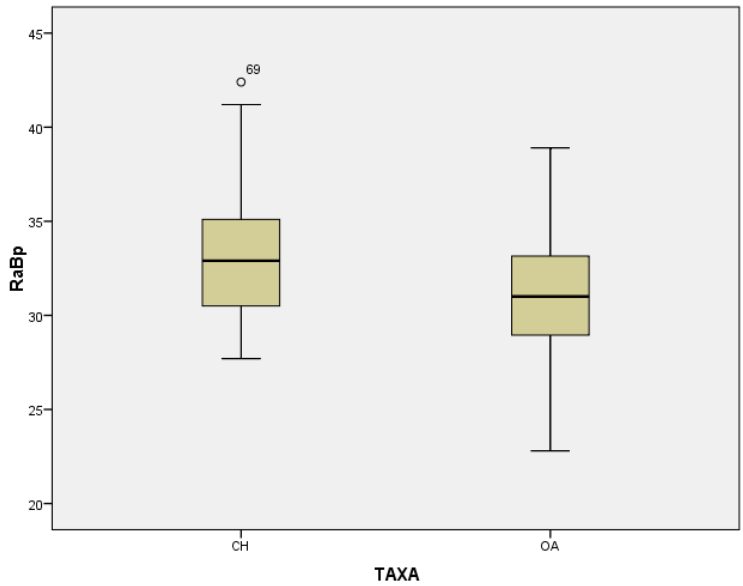


Figure A3.0.18 Radius. Box plot for the modern sample of goat (CH) and sheep (OA) for measurement Bp.

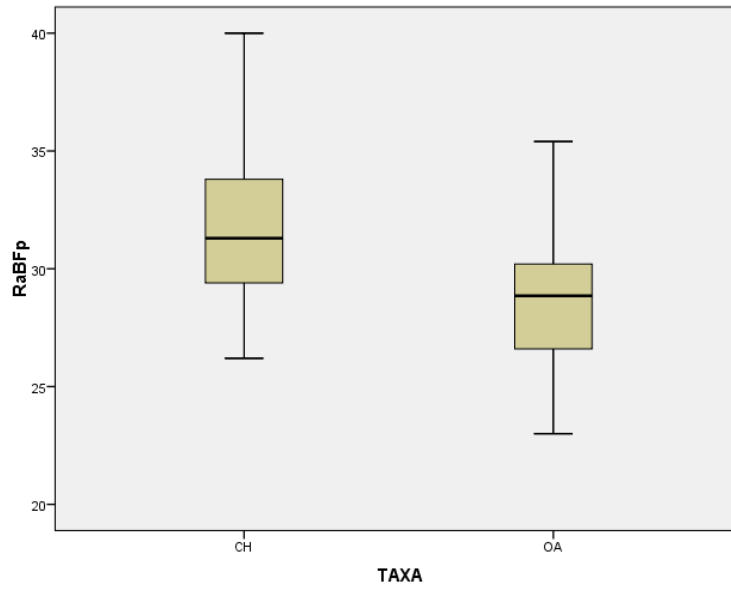


Figure A3.0.19 Radius. Box plot for the modern sample of goat (CH) and sheep (OA) for measurement BFp.

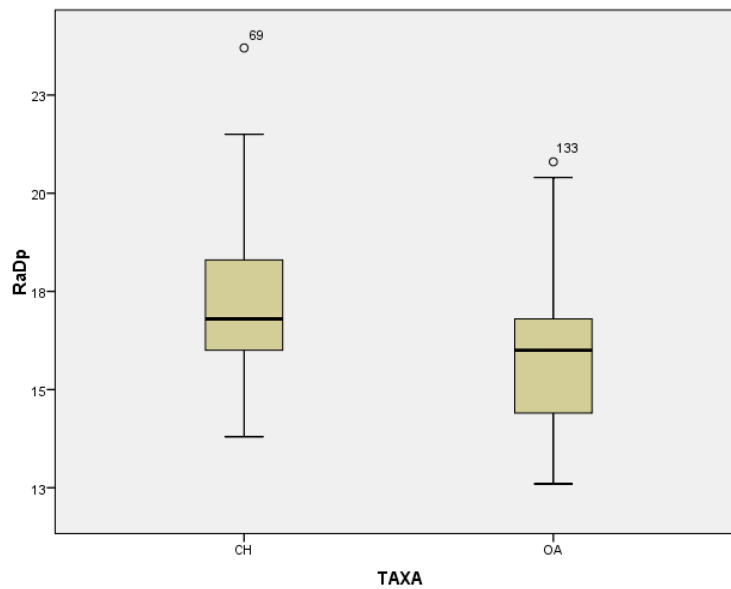


Figure A3.0.20 Radius. Box plot for the modern sample of goat (CH) and sheep (OA) for measurement Dp.

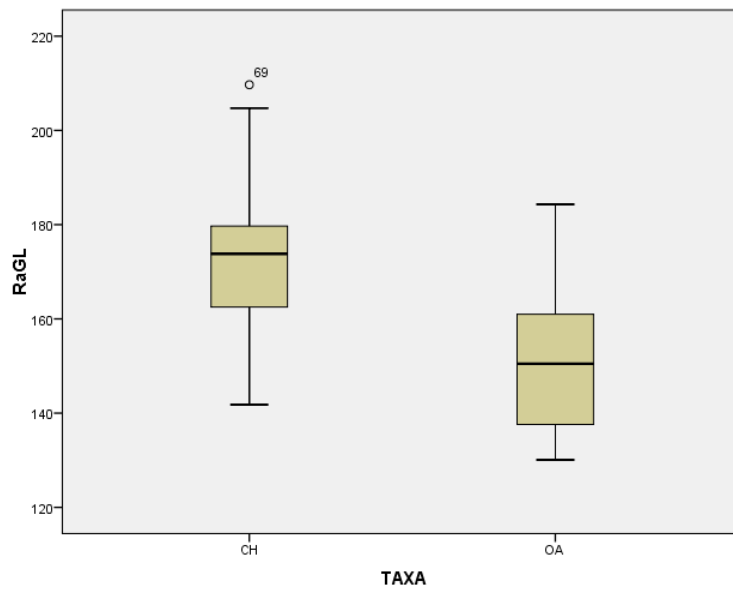


Figure A3.0.21 Radius. Box plot for the modern sample of goat (CH) and sheep (OA) for measurement GL.

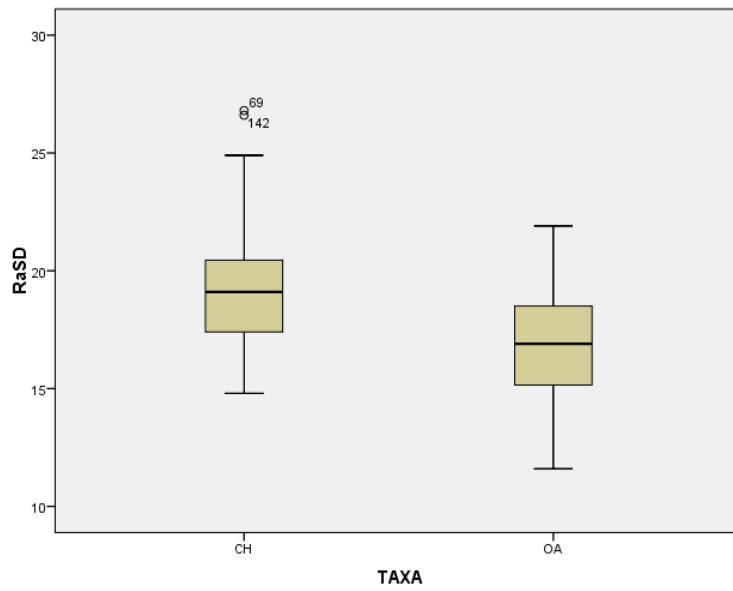


Figure A3.0.22 Radius. Box plot for the modern sample of goat (CH) and sheep (OA) for measurement SD.

Ulna

Table A3.9 Summary of the sheep and goat modern specimens for each measurement taken on the ulna processed by SPSS.

Case Processing Summary							
	TAXA	Cases					
		Valid		Missing		Total	
		N	Percent	N	Percent	N	Percent
UIB	CH	55	69.6%	24	30.4%	79	100.0%
	OA	58	74.4%	20	25.6%	78	100.0%
UIL	CH	55	69.6%	24	30.4%	79	100.0%
	OA	58	74.4%	20	25.6%	78	100.0%
SDO	CH	56	70.9%	23	29.1%	79	100.0%
	OA	58	74.4%	20	25.6%	78	100.0%
DPA	CH	56	70.9%	23	29.1%	79	100.0%
	OA	57	73.1%	21	26.9%	78	100.0%
BPC	CH	56	70.9%	23	29.1%	79	100.0%
	OA	58	74.4%	20	25.6%	78	100.0%

Table A3.10 Descriptive statistics for the modern goat (CH) and sheep (OA) for each measurement taken on the ulna.

Descriptives						
Element	Measurement	TAXA	Statistics		Std. Error	CV
UI	B	CH	Mean	12.165	.1827	11.1409
			Median	12.100		
			Variance	1.837		
			Std. Deviation	1.3553		
			Minimum	9.8		
			Maximum	15.4		
		OA	Mean	10.243	.1762	13.1016
			Median	10.000		
			Variance	1.801		
			Std. Deviation	1.3420		
			Minimum	8.0		
			Maximum	14.7		
	L	CH	Mean	27.273	.4963	13.4968
			Median	26.800		
			Variance	13.550		
			Std. Deviation	3.6810		
			Minimum	20.8		
			Maximum	35.9		
OA	Mean	24.078	.3935	12.4458		
	Median	24.100				
	Variance	8.980				

Descriptives						
	SDO	CH	Std. Deviation	2.9967		
			Minimum	18.3		
			Maximum	31.2		
		Mean	24.821	.3945	11.8931	
		Median	24.650			
		Variance	8.714			
		Std. Deviation	2.9520			
		Minimum	19.0			
		Maximum	30.8			
	OA	Mean	22.024	.3432	11.8679	
		Median	21.850			
		Variance	6.832			
		Std. Deviation	2.6138			
		Minimum	17.4			
		Maximum	28.4			
	DPA	CH	Mean	28.839	.4482	11.6297
			Median	28.400		
			Variance	11.249		
			Std. Deviation	3.3539		
			Minimum	22.9		
			Maximum	36.2		
		OA	Mean	26.612	.3602	10.2179
			Median	26.500		
			Variance	7.394		
			Std. Deviation	2.7192		
			Minimum	21.7		
			Maximum	33.3		
BPC	CH	Mean	25.438	.3945	11.6050	
		Median	25.150			
		Variance	8.715			
		Std. Deviation	2.9521			
		Minimum	17.9			
		Maximum	32.4			
	OA	Mean	19.016	.2994	11.9888	
		Median	18.850			
		Variance	5.197			
		Std. Deviation	2.2798			
		Minimum	15.4			
		Maximum	25.5			

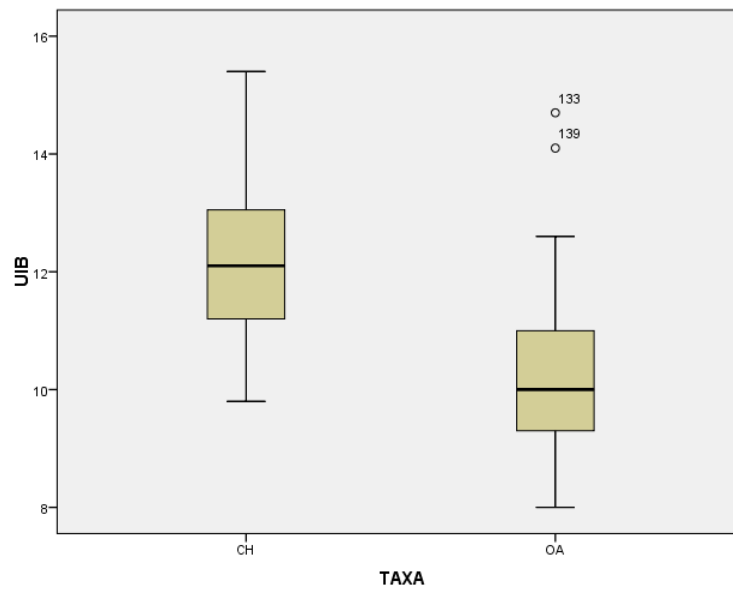


Figure A3.0.23 Ulna. Box plot for the modern sample of goat (CH) and sheep (OA) for measurement B.

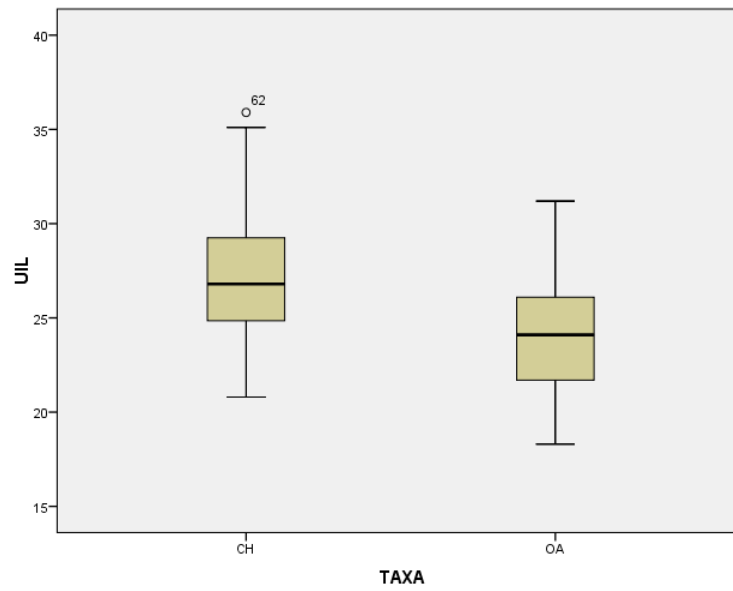


Figure A3.0.24 Ulna. Box plot for the modern sample of goat (CH) and sheep (OA) for measurement L.

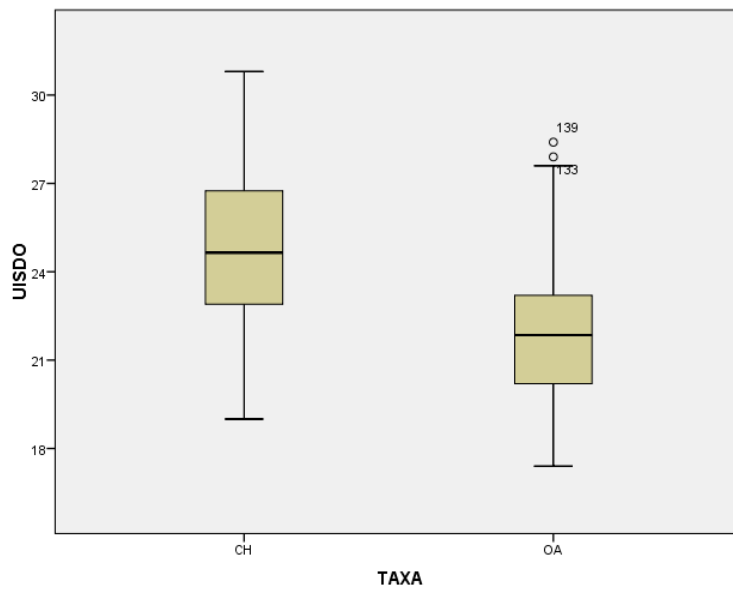


Figure A3.0.25 Ulna. Box plot for the modern sample of goat (CH) and sheep (OA) for measurement SDO.

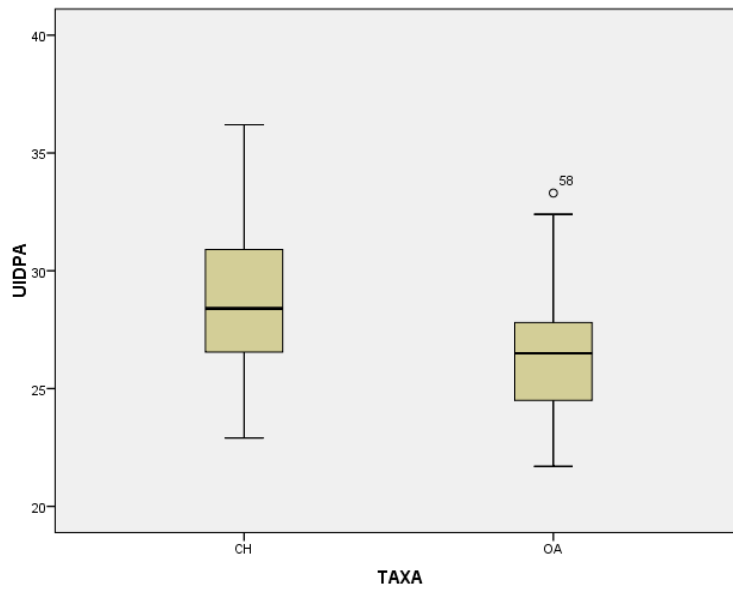


Figure A3.0.26 Ulna. Box plot for the modern sample of goat (CH) and sheep (OA) for measurement DPA.

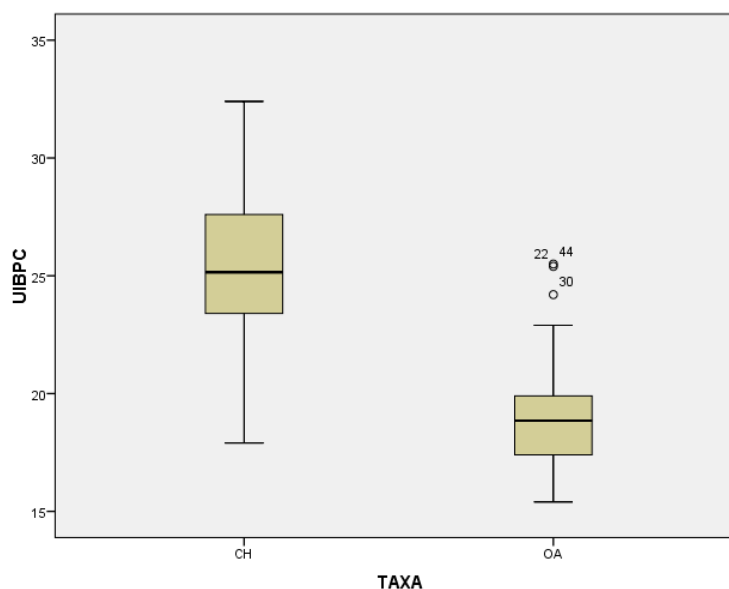


Figure A3.0.27 Ulna. Box plot for the modern sample of goat (CH) and sheep (OA) for measurement BPC.

Metacarpal

Table A3.11 Summary of the sheep and goat modern specimens for each measurement taken on the metacarpal processed by SPSS.

Case Processing Summary							
	TAXA	Cases					
		Valid		Missing		Total	
		N	Percent	N	Percent	N	Percent
McGL	CH	58	73.4%	21	26.6%	79	100.0%
	OA	61	78.2%	17	21.8%	78	100.0%
McSD	CH	58	73.4%	21	26.6%	79	100.0%
	OA	62	79.5%	16	20.5%	78	100.0%
McBFd	CH	58	73.4%	21	26.6%	79	100.0%
	OA	62	79.5%	16	20.5%	78	100.0%
McBatF	CH	58	73.4%	21	26.6%	79	100.0%
	OA	62	79.5%	16	20.5%	78	100.0%
Mca	CH	58	73.4%	21	26.6%	79	100.0%
	OA	62	79.5%	16	20.5%	78	100.0%
Mcb	CH	58	73.4%	21	26.6%	79	100.0%
	OA	62	79.5%	16	20.5%	78	100.0%
Mc1	CH	58	73.4%	21	26.6%	79	100.0%
	OA	62	79.5%	16	20.5%	78	100.0%
Mc2	CH	58	73.4%	21	26.6%	79	100.0%
	OA	62	79.5%	16	20.5%	78	100.0%
Mc4	CH	58	73.4%	21	26.6%	79	100.0%
	OA	62	79.5%	16	20.5%	78	100.0%
Mc5	CH	58	73.4%	21	26.6%	79	100.0%

Case Processing Summary							
	OA	62	79.5%	16	20.5%	78	100.0%
Mc3	CH	58	73.4%	21	26.6%	79	100.0%
	OA	62	79.5%	16	20.5%	78	100.0%
Mc6	CH	58	73.4%	21	26.6%	79	100.0%
	OA	62	79.5%	16	20.5%	78	100.0%

Table A3.12 Descriptive statistics for the modern goat (CH) and sheep (OA) for each measurement taken on the metacarpal.

Descriptives						
Element	Measurement	TAXA	Statistics		Std. Error	CV
Mc	GL	CH	Mean	120.140	1.3311	8.4381
			Median	120.650		
			Variance	102.771		
			Std. Deviation	10.1376		
			Minimum	97.2		
			Maximum	140.9		
		OA	Mean	123.484	1.2654	8.0037
			Median	122.800		
			Variance	97.680		
			Std. Deviation	9.8833		
			Minimum	105.4		
			Maximum	146.5		
	SD	CH	Mean	17.033	.2941	13.1503
			Median	16.800		
			Variance	5.017		
			Std. Deviation	2.2399		
			Minimum	12.7		
			Maximum	22.3		
		OA	Mean	13.987	.1931	10.8686
			Median	14.300		
			Variance	2.311		
			Std. Deviation	1.5202		
			Minimum	11.0		
			Maximum	17.4		
BFd	CH	Mean	29.003	.3366	8.8394	
		Median	28.750			
		Variance	6.573			
		Std. Deviation	2.5637			
		Minimum	24.7			
		Maximum	36.1			
	OA	Mean	24.819	.3047	9.6679	
		Median	25.250			

Descriptives						
			Variance	5.758		
			Std. Deviation	2.3995		
			Minimum	20.0		
			Maximum	30.5		
	BatF	CH	Mean	29.622	.3873	9.9571
			Median	29.350		
			Variance	8.699		
			Std. Deviation	2.9495		
			Minimum	23.9		
			Maximum	37.2		
		OA	Mean	25.958	.3711	11.2562
			Median	25.750		
			Variance	8.537		
			Std. Deviation	2.9219		
			Minimum	20.6		
			Maximum	32.0		
	a	CH	Mean	13.447	.1559	8.8279
			Median	13.400		
			Variance	1.409		
			Std. Deviation	1.1871		
			Minimum	11.3		
			Maximum	16.7		
		OA	Mean	11.534	.1457	9.9488
			Median	11.650		
			Variance	1.317		
			Std. Deviation	1.1475		
			Minimum	9.2		
			Maximum	14.3		
	b	CH	Mean	13.007	.1552	9.0889
			Median	13.000		
			Variance	1.397		
			Std. Deviation	1.1822		
			Minimum	11.0		
			Maximum	16.5		
		OA	Mean	11.148	.1416	10.0026
			Median	11.300		
			Variance	1.244		
			Std. Deviation	1.1151		
			Minimum	8.8		
			Maximum	13.4		
	1	CH	Mean	11.090	.1380	9.4761
			Median	11.000		

Descriptives						
			Variance	1.104		
			Std. Deviation	1.0509		
			Minimum	9.6		
			Maximum	13.8		
		OA	Mean	11.171	.1582	11.1520
			Median	11.150		
			Variance	1.552		
			Std. Deviation	1.2458		
			Minimum	8.8		
			Maximum	14.6		
	2	CH	Mean	17.962	.2079	8.8147
			Median	17.600		
			Variance	2.507		
			Std. Deviation	1.5833		
			Minimum	15.6		
			Maximum	22.5		
		OA	Mean	15.906	.2017	9.9867
			Median	15.750		
			Variance	2.523		
			Std. Deviation	1.5885		
			Minimum	13.3		
			Maximum	21.5		
	4	CH	Mean	10.545	.1315	9.4964
			Median	10.450		
			Variance	1.003		
			Std. Deviation	1.0014		
			Minimum	8.8		
			Maximum	12.6		
		OA	Mean	10.353	.1350	10.2646
			Median	10.300		
			Variance	1.129		
			Std. Deviation	1.0627	.	
			Minimum	8.6		
			Maximum	14.0		
	5	CH	Mean	17.707	.2114	9.0941
			Median	17.500		
			Variance	2.593		
			Std. Deviation	1.6103		
			Minimum	15.1		
			Maximum	22.3		
		OA	Mean	15.368	.1929	9.8848
			Median	15.250		

Descriptives						
			Variance	2.308		
			Std. Deviation	1.5191		
			Minimum	12.8		
			Maximum	20.8		
	3	CH	Mean	14.772	.1663	8.5756
			Median	14.400		
			Variance	1.605		
			Std. Deviation	1.2668		
			Minimum	13.2		
			Maximum	18.3		
		OA	Mean	13.334	.1642	9.6977
			Median	13.200		
			Variance	1.672		
			Std. Deviation	1.2931		
6	CH	Mean	14.941	.1682	8.5737	
		Median	14.600			
		Variance	1.641			
		Std. Deviation	1.2810			
		Minimum	13.3			
		Maximum	18.5			
	OA	Mean	13.447	.1726	10.1063	
		Median	13.300			
		Variance	1.847			
		Std. Deviation	1.3590			
		Minimum	11.0			
		Maximum	17.9			

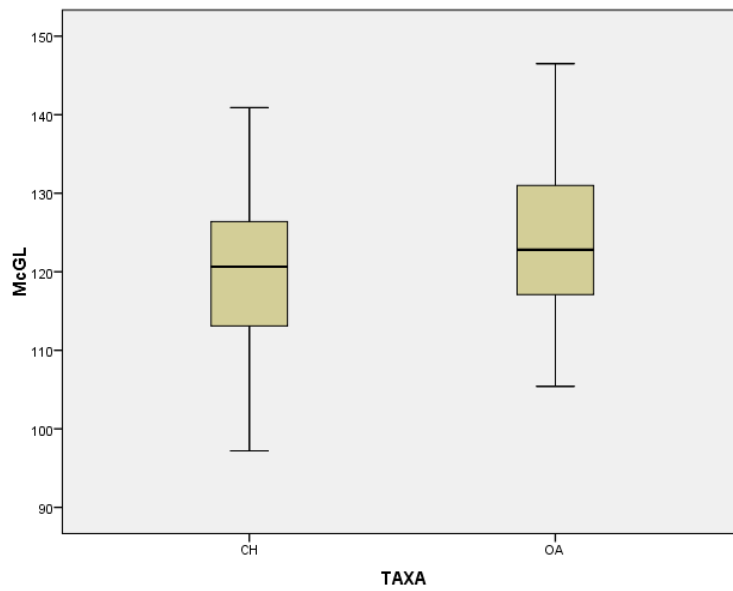


Figure A3.0.28 Metacarpal. Box plot for the modern sample of goat (CH) and sheep (OA) for measurement GL.

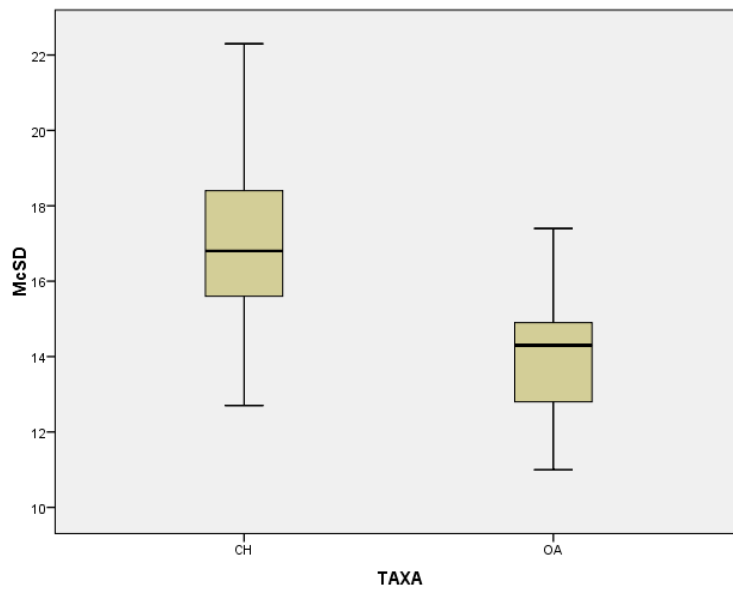


Figure A3.0.29 Metacarpal. Box plot for the modern sample of goat (CH) and sheep (OA) for measurement SD.

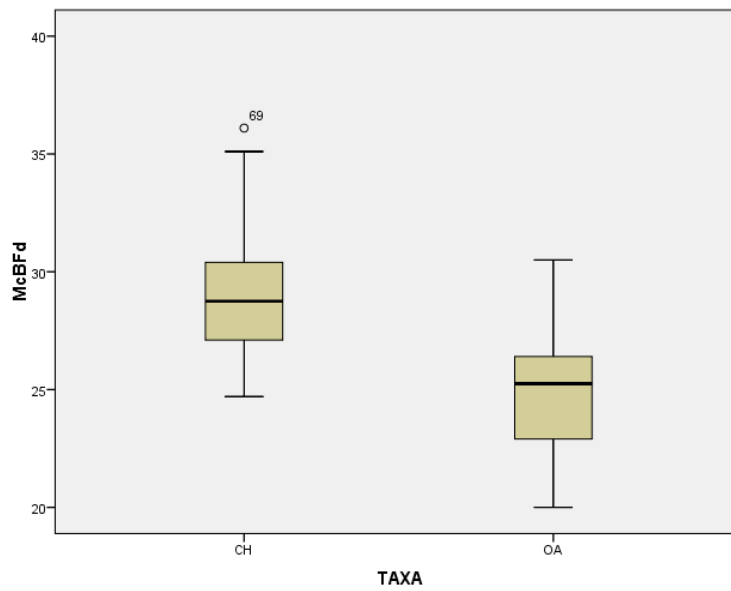


Figure A3.0.30 Metacarpal. Box plot for the modern sample of goat (CH) and sheep (OA) for measurement BFd.

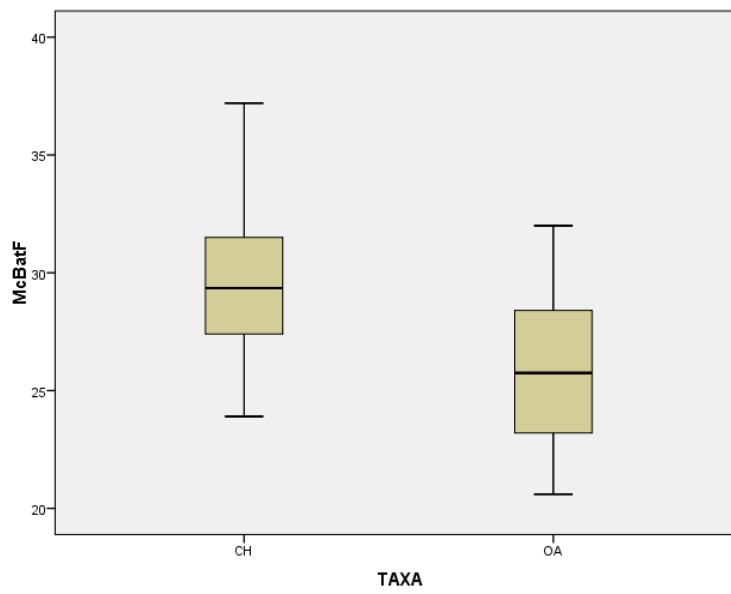


Figure A3.0.31 Metacarpal. Box plot for the modern sample of goat (CH) and sheep (OA) for measurement BatF.

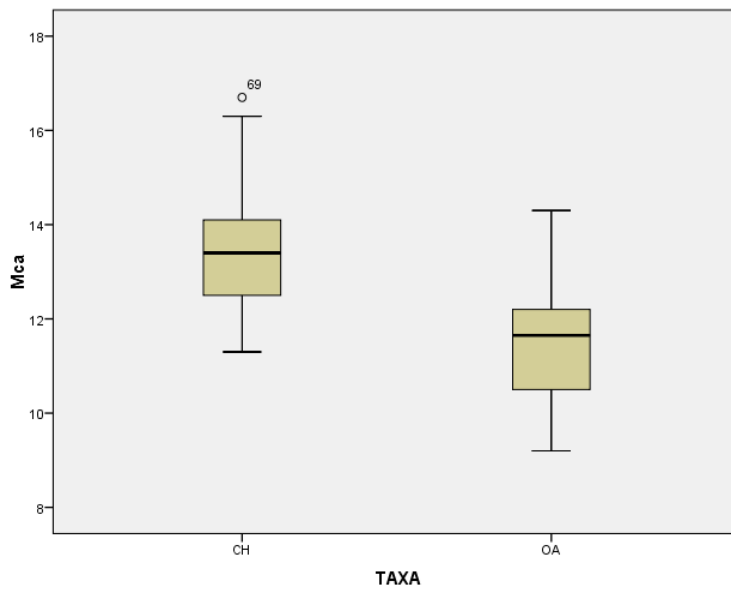


Figure A3.0.32 Metacarpal. Box plot for the modern sample of goat (CH) and sheep (OA) for measurement a.

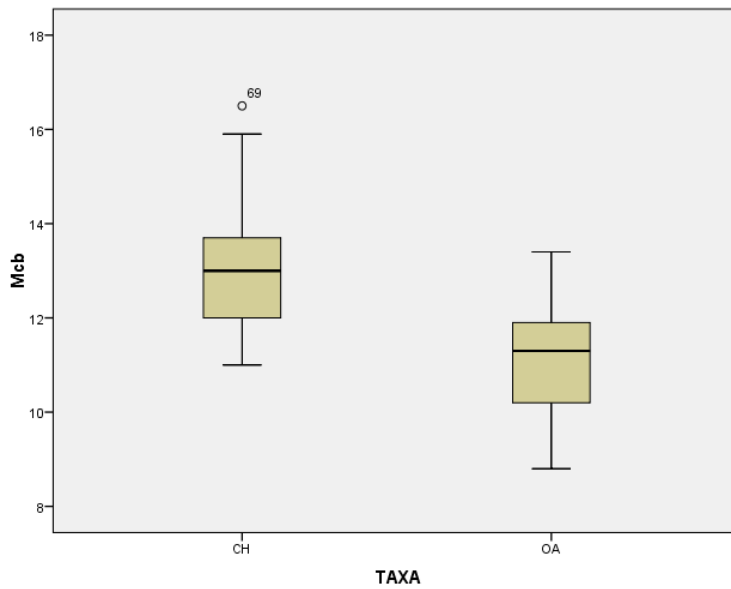


Figure A3.0.33 Metacarpal. Box plot for the modern sample of goat (CH) and sheep (OA) for measurement b.

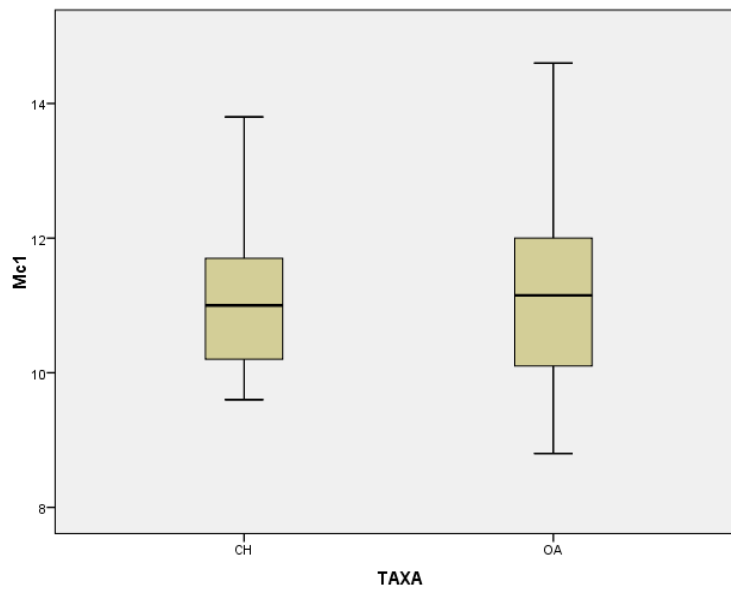


Figure A3.0.34 Metacarpal. Box plot for the modern sample of goat (CH) and sheep (OA) for measurement 1.

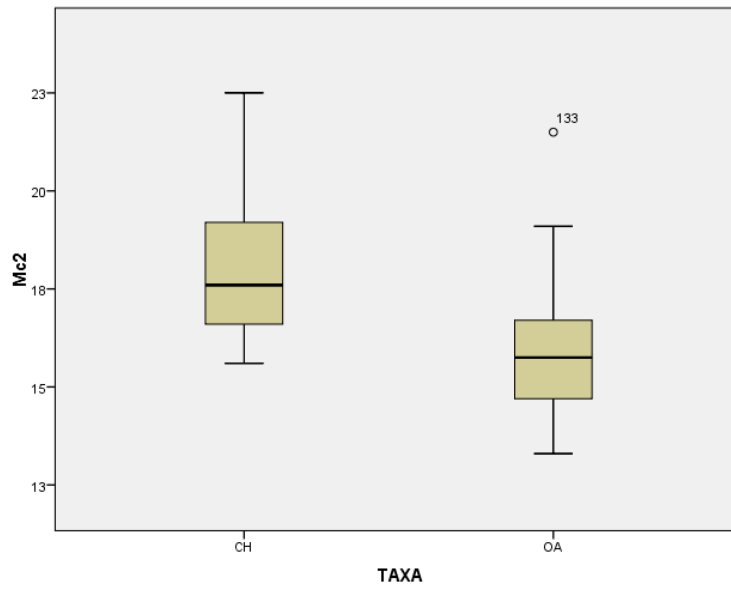


Figure A3.0.35 Metacarpal. Box plot for the modern sample of goat (CH) and sheep (OA) for measurement 2.

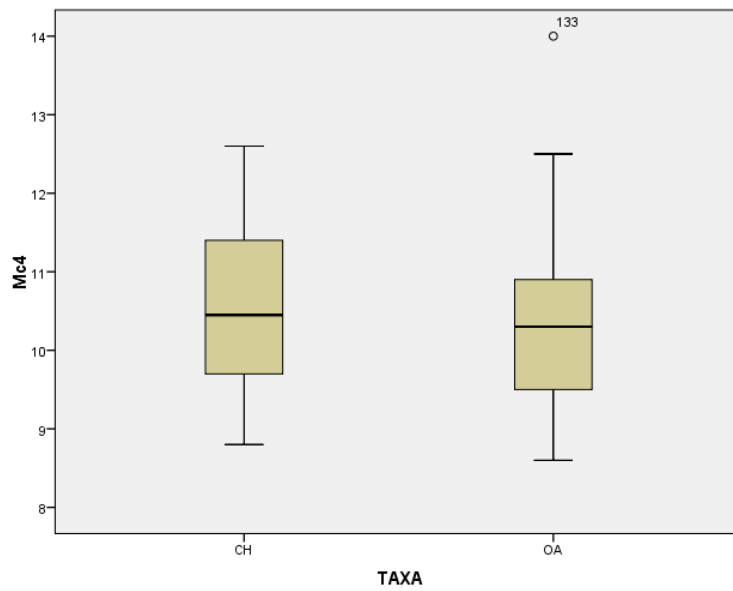


Figure A3.0.36 Metacarpal. Box plot for the modern sample of goat (CH) and sheep (OA) for measurement 4.

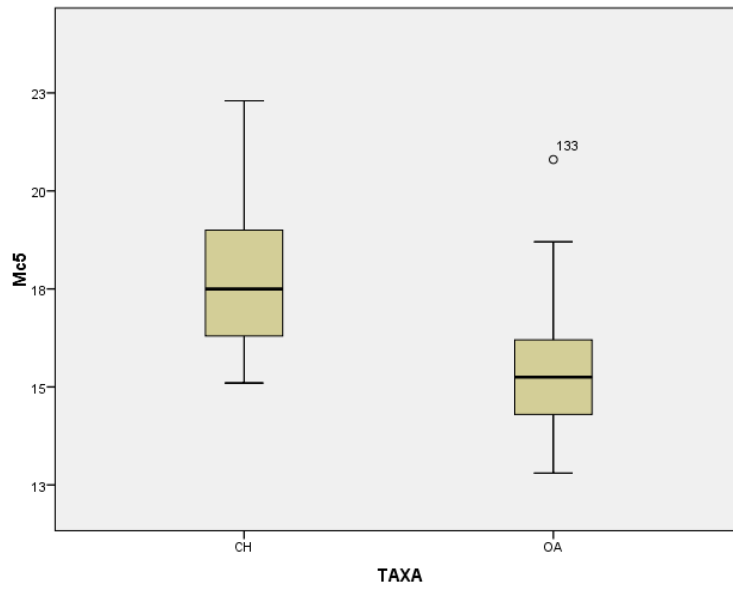


Figure A3.0.37 Metacarpal. Box plot for the modern sample of goat (CH) and sheep (OA) for measurement 5.

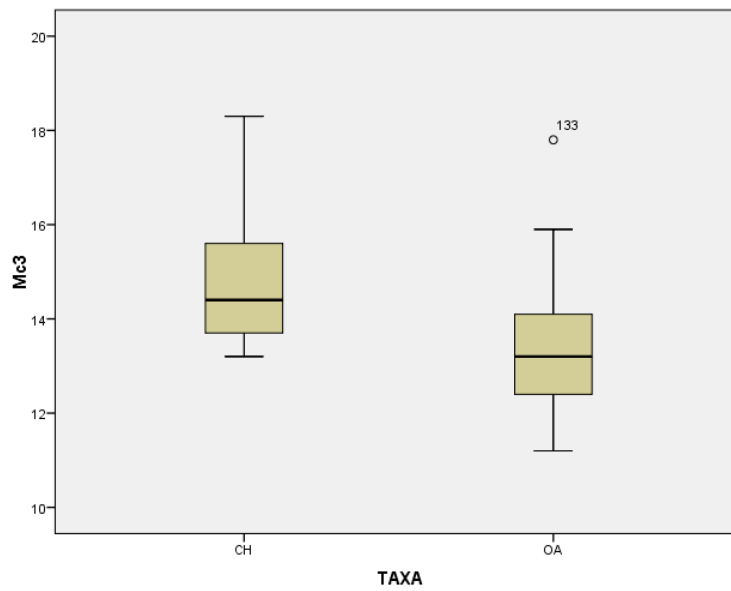


Figure A3.0.38 Metacarpal. Box plot for the modern sample of goat (CH) and sheep (OA) for measurement 3.

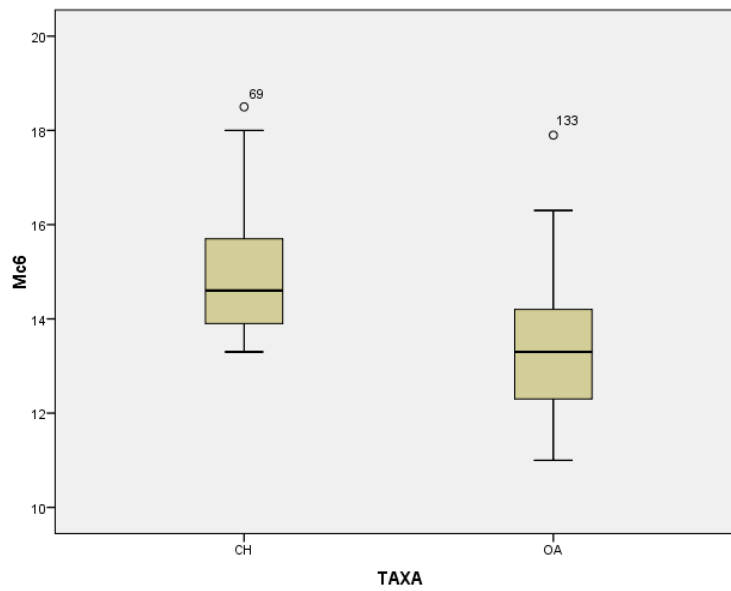


Figure A3.0.39 Metacarpal. Box plot for the modern sample of goat (CH) and sheep (OA) for measurement 6.

Metatarsal

Table A3.13 Summary of the sheep and goat modern specimens for each measurement taken on the metacarsal processed by SPSS.

Case Processing Summary							
	TAXA	Cases					
		Valid		Missing		Total	
		N	Percent	N	Percent	N	Percent
MtGL	CH	62	78.5%	17	21.5%	79	100.0%
	OA	63	80.8%	15	19.2%	78	100.0%
MtSD	CH	62	78.5%	17	21.5%	79	100.0%
	OA	64	82.1%	14	17.9%	78	100.0%
MtBFd	CH	62	78.5%	17	21.5%	79	100.0%
	OA	64	82.1%	14	17.9%	78	100.0%
MtBatF	CH	61	77.2%	18	22.8%	79	100.0%
	OA	64	82.1%	14	17.9%	78	100.0%
Mta	CH	62	78.5%	17	21.5%	79	100.0%
	OA	64	82.1%	14	17.9%	78	100.0%
Mtb	CH	62	78.5%	17	21.5%	79	100.0%
	OA	64	82.1%	14	17.9%	78	100.0%
Mt1	CH	62	78.5%	17	21.5%	79	100.0%
	OA	64	82.1%	14	17.9%	78	100.0%
Mt2	CH	62	78.5%	17	21.5%	79	100.0%
	OA	64	82.1%	14	17.9%	78	100.0%
Mt4	CH	62	78.5%	17	21.5%	79	100.0%
	OA	64	82.1%	14	17.9%	78	100.0%
Mt5	CH	62	78.5%	17	21.5%	79	100.0%
	OA	64	82.1%	14	17.9%	78	100.0%
Mt3	CH	62	78.5%	17	21.5%	79	100.0%
	OA	64	82.1%	14	17.9%	78	100.0%
Mt6	CH	62	78.5%	17	21.5%	79	100.0%
	OA	64	82.1%	14	17.9%	78	100.0%

Table A3.14 Descriptive statistics for the modern goat (CH) and sheep (OA) for each measurement taken on the metatarsal.

Descriptives						
Element	Measurement	TAXA	Statistics		Std. Error	CV
Mt	GL	CH	Mean	128.013	1.3738	8.4503
			Median	128.200		
			Variance	117.018		
			Std. Deviation	10.8175		
			Minimum	105.4		
			Maximum	150.7		
		OA	Mean	133.017	1.3358	7.9705
			Median	131.900		
			Variance	112.408		
			Std. Deviation	10.6022		
			Minimum	111.9		
			Maximum	158.7		
	SD	CH	Mean	13.753	.2231	12.7724
			Median	13.850		
			Variance	3.086		
			Std. Deviation	1.7566		
			Minimum	10.8		
			Maximum	18.2		
		OA	Mean	12.133	.1572	10.3634
			Median	12.150		
			Variance	1.581		
			Std. Deviation	1.2574		
			Minimum	9.8		
			Maximum	15.2		
BFd	CH	Mean	25.779	.2715	8.2927	
		Median	25.700			
		Variance	4.570			
		Std. Deviation	2.1378			
		Minimum	21.9			
		Maximum	31.6			
	OA	Mean	23.453	.2851	9.7254	
		Median	23.750			
		Variance	5.203			
		Std. Deviation	2.2809			
		Minimum	18.9			
		Maximum	29.7			
BatF	CH	Mean	26.305	.3162	9.3898	
		Median	25.900			
		Variance	6.101			

Descriptives						
			Std. Deviation	2.4700		
			Minimum	22.1		
			Maximum	33.1		
		OA	Mean	23.878	.3221	10.7906
			Median	23.800		
			Variance	6.639		
			Std. Deviation	2.5766		
			Minimum	19.2		
			Maximum	30.3		
	a	CH	Mean	12.026	.1302	8.52223
			Median	12.000		
			Variance	1.050		
			Std. Deviation	1.0249		
			Minimum	10.2		
			Maximum	14.6		
		OA	Mean	11.073	.1452	10.4912
			Median	11.200		
			Variance	1.350		
			Std. Deviation	1.1617		
			Minimum	8.9		
			Maximum	14.3		
	b	CH	Mean	11.282	.1203	8.3992
			Median	11.200		
			Variance	.898		
			Std. Deviation	.9476		
			Minimum	9.5		
			Maximum	13.9		
OA		Mean	10.130	.1258	9.9368	
		Median	10.100			
		Variance	1.013			
		Std. Deviation	1.0066			
		Minimum	8.2			
		Maximum	12.9			
1	CH	Mean	10.726	.1296	9.5123	
		Median	10.650			
		Variance	1.041			
		Std. Deviation	1.0203			
		Minimum	9.1			
		Maximum	13.2			
	OA	Mean	10.417	.1444	11.0895	
		Median	10.400			
		Variance	1.334			

Descriptives						
			Std. Deviation	1.1552		
			Minimum	8.2		
			Maximum	14.1		
	2	CH	Mean	17.260	.2025	9.2398
			Median	17.050		
			Variance	2.543		
			Std. Deviation	1.5948		
			Minimum	13.2		
			Maximum	21.5		
			Mean	15.863	.2044	10.3076
		OA	Median	15.800		
			Variance	2.673		
			Std. Deviation	1.6351		
			Minimum	13.1		
			Maximum	21.2		
	4	CH	Mean	10.368	.1231	9.3479
			Median	10.350		
			Variance	.939		
			Std. Deviation	.9692		
			Minimum	8.5		
			Maximum	13.0		
		OA	Mean	9.563	.1323	11.0655
			Median	9.350		
			Variance	1.120		
			Std. Deviation	1.0582		
			Minimum	7.8		
			Maximum	13.5		
5	CH	Mean	16.858	.2018	9.4246	
		Median	16.750			
		Variance	2.524			
		Std. Deviation	1.5888			
		Minimum	13.1			
		Maximum	21.0			
	OA	Mean	14.991	.1915	10.2214	
		Median	14.800			
		Variance	2.348			
		Std. Deviation	1.5323			
		Minimum	12.4			
		Maximum	20.2			
3	CH	Mean	14.316	.1556	8.5610	
		Median	14.050			
		Variance	1.502			

Descriptives						
			Std. Deviation	1.2256		
			Minimum	12.0		
			Maximum	17.2		
		OA	Mean	13.044	.1609	9.8689
			Median	12.900		
			Variance	1.657	.	
			Std. Deviation	1.2873		
			Minimum	10.9		
			Maximum	17.5		
	6	CH	Mean	14.563	.1606	8.6836
			Median	14.450		
			Variance	1.599		
			Std. Deviation	1.2646		
			Minimum	12.1		
			Maximum	17.8		
		OA	Mean	13.102	.1627	9.9374
			Median	12.850		
			Variance	1.695		
			Std. Deviation	1.3020		
			Minimum	11.1		
			Maximum	17.7		

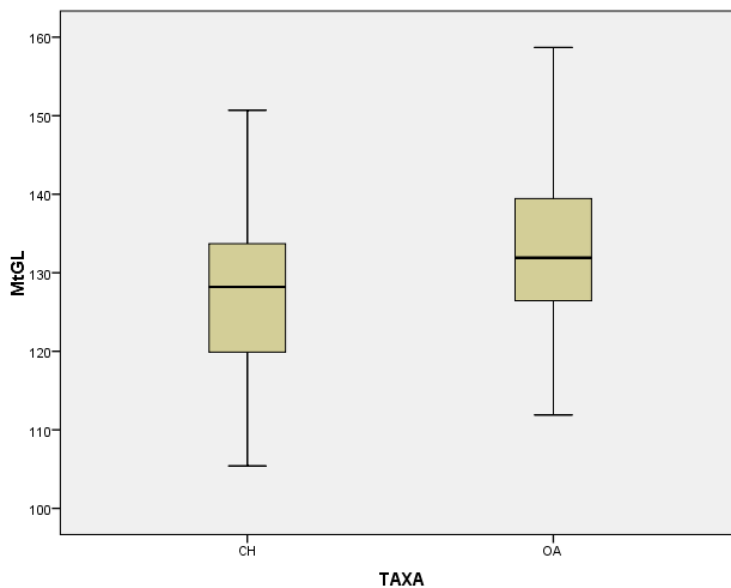


Figure A3.0.40 Metatarsal. Box plot for the modern sample of goat (CH) and sheep (OA) for measurement GL.

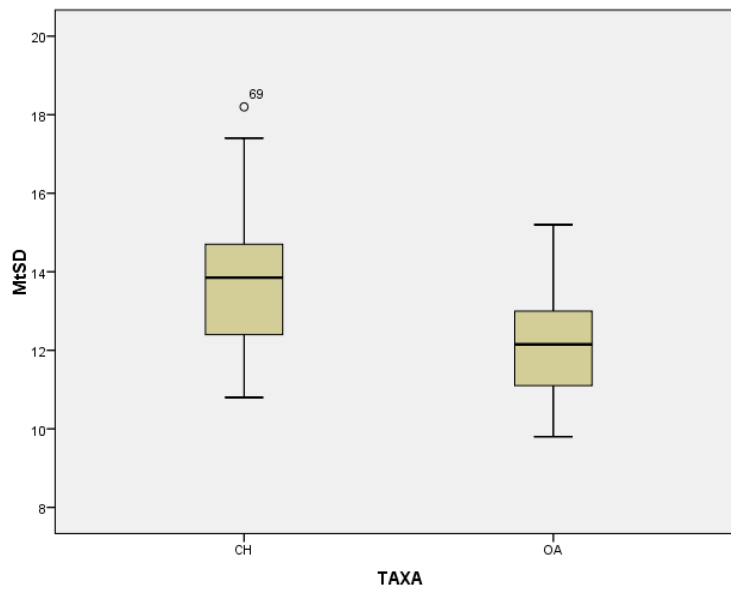


Figure A3.0.41 Metatarsal. Box plot for the modern sample of goat (CH) and sheep (OA) for measurement SD.

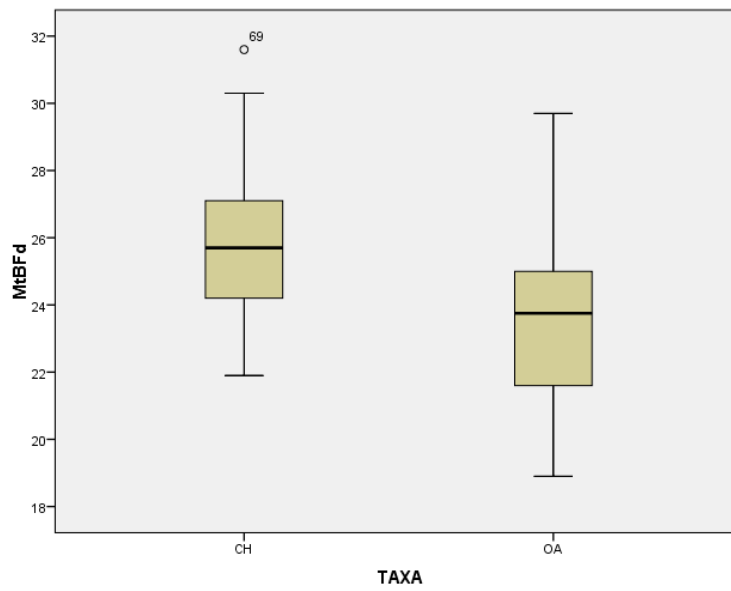


Figure A3.0.42 Metatarsal. Box plot for the modern sample of goat (CH) and sheep (OA) for measurement BFd.

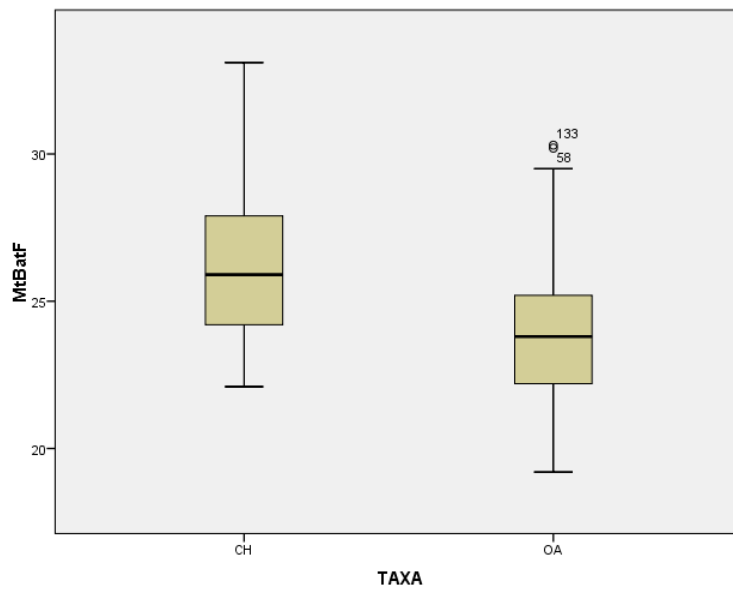


Figure A3.0.43 Metatarsal. Box plot for the modern sample of goat (CH) and sheep (OA) for measurement BatF.

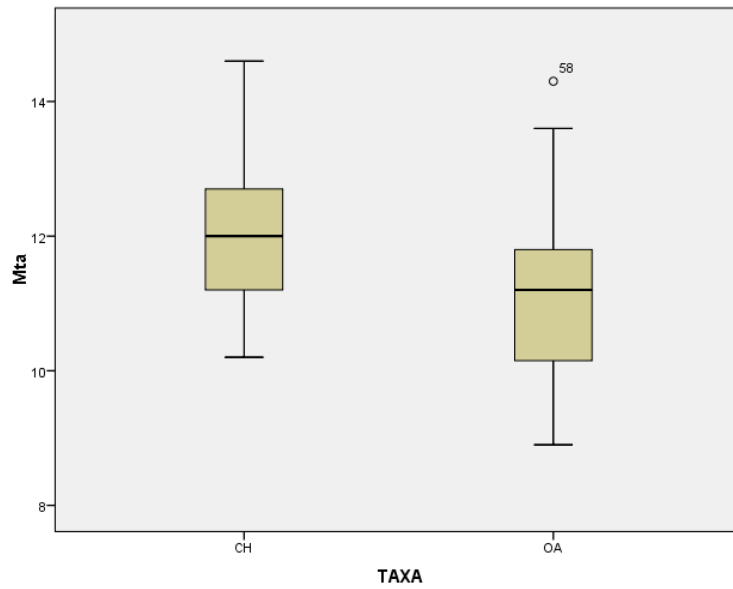


Figure A3.0.44 Metatarsal. Box plot for the modern sample of goat (CH) and sheep (OA) for measurement a.

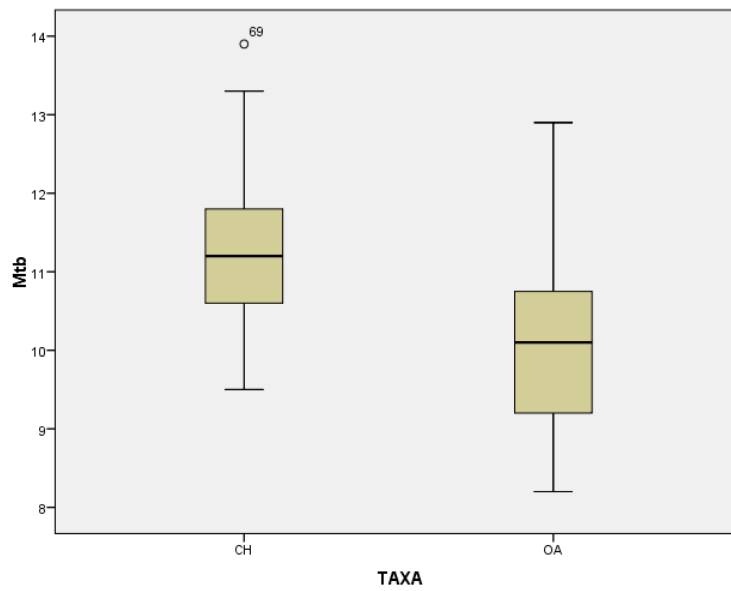


Figure A3.0.45 Metatarsal. Box plot for the modern sample of goat (CH) and sheep (OA) for measurement b.

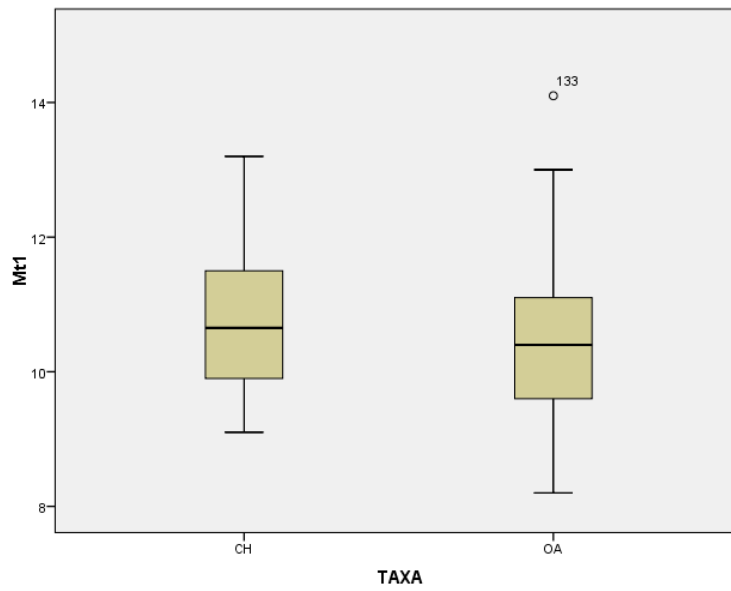


Figure A3.0.46 Metatarsal. Box plot for the modern sample of goat (CH) and sheep (OA) for measurement 1.

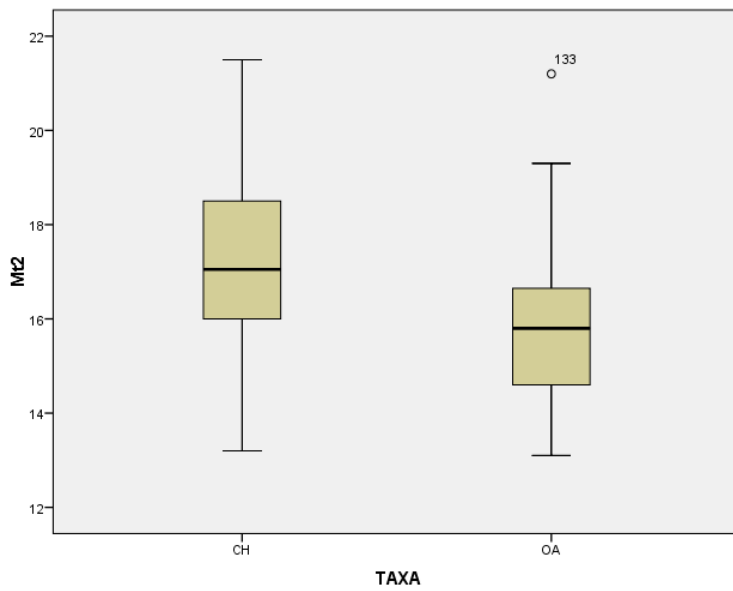


Figure A3.0.47 Metatarsal. Box plot for the modern sample of goat (CH) and sheep (OA) for measurement 2.

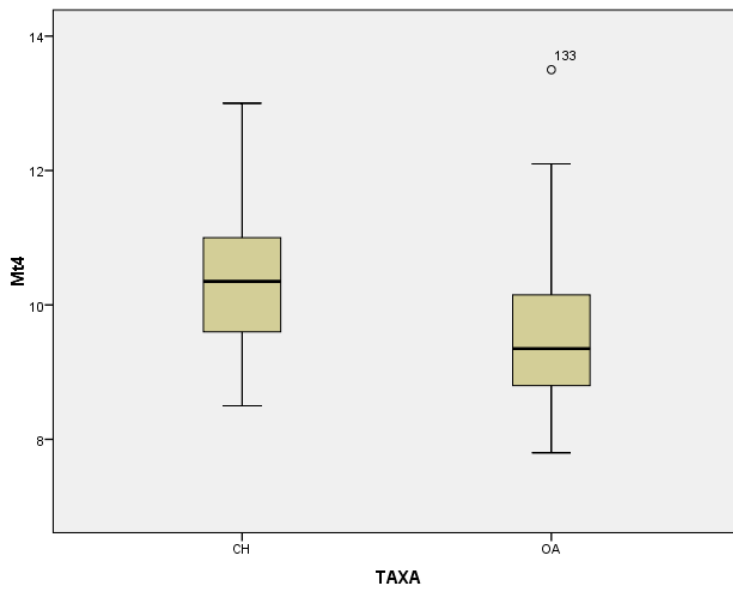


Figure A3.0.48 Metatarsal. Box plot for the modern sample of goat (CH) and sheep (OA) for measurement 4.

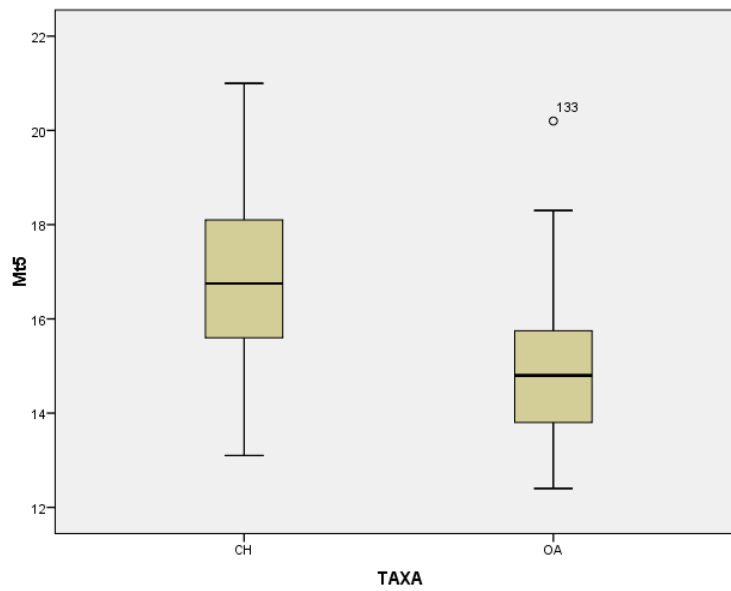


Figure A3.0.49 Metatarsal. Box plot for the modern sample of goat (CH) and sheep (OA) for measurement 5.

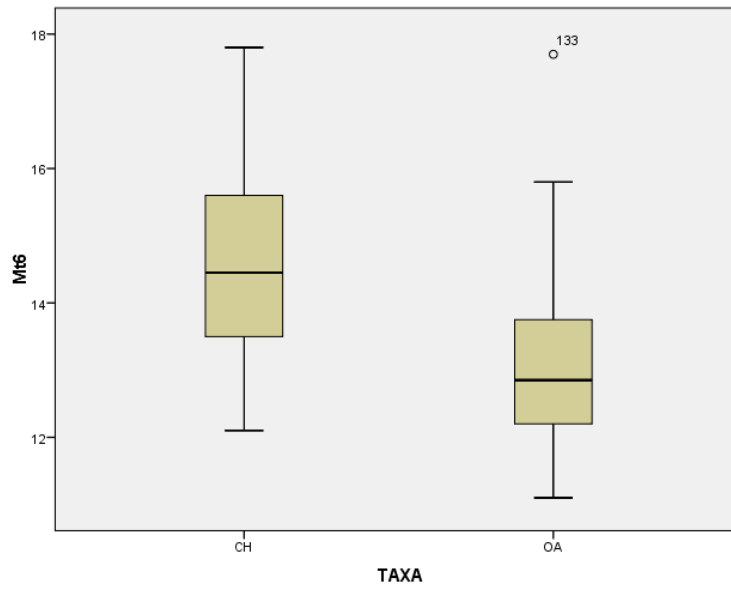


Figure A3.0.50 Metatarsal. Box plot for the modern sample of goat (CH) and sheep (OA) for measurement 6.

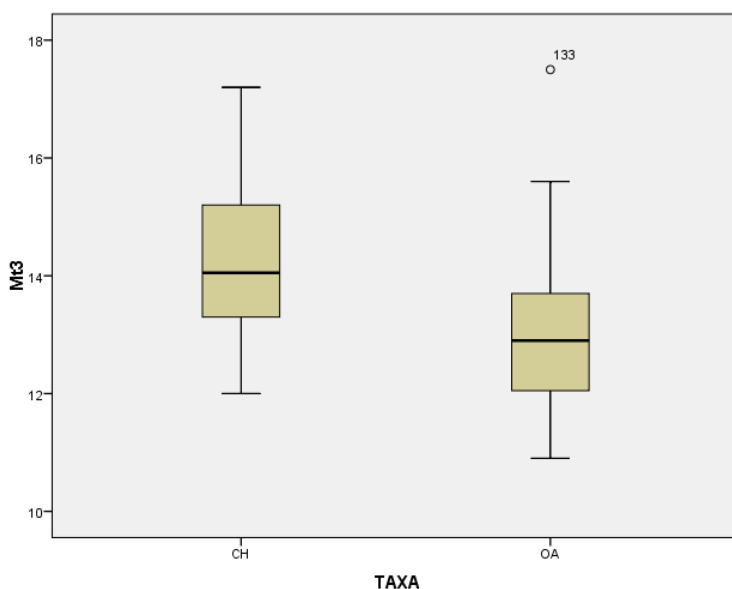


Figure A3.0.51 Metatarsal. Box plot for the modern sample of goat (CH) and sheep (OA) for measurement 3.

Tibia

Table A3.15 Summary of the sheep and goat modern specimens for each measurement taken on the tibia processed by SPSS.

Case Processing Summary							
	TAXA	Cases					
		Valid		Missing		Total	
		N	Percent	N	Percent	N	Percent
TiDda	CH	71	89.9%	8	10.1%	79	100.0%
	OA	69	88.5%	9	11.5%	78	100.0%
TiDd	CH	71	89.9%	8	10.1%	79	100.0%
	OA	69	88.5%	9	11.5%	78	100.0%
TiBd	CH	71	89.9%	8	10.1%	79	100.0%
	OA	69	88.5%	9	11.5%	78	100.0%
TiGL	CH	58	73.4%	21	26.6%	79	100.0%
	OA	52	66.7%	26	33.3%	78	100.0%
TiSD	CH	71	89.9%	8	10.1%	79	100.0%
	OA	68	87.2%	10	12.8%	78	100.0%

Table A3.16 Descriptive statistics for the modern goat (CH) and sheep (OA) for each measurement taken on the tibia.

Descriptives						
Element	Measurement	TAXA	Statistics		Std. Error	CV
Ti	a	CH	Mean	21.090	.2312	9.2380
			Median	21.100		
			Variance	3.796		
			Std. Deviation	1.9483		
			Minimum	16.8		
			Maximum	26.2		
		OA	Mean	20.862	.2603	10.3638
			Median	20.800		
			Variance	4.675		
			Std. Deviation	2.1621		
			Minimum	16.9		
			Maximum	26.7		
	b	CH	Mean	18.545	.2038	9.2585
			Median	18.500		
			Variance	2.948		
			Std. Deviation	1.7170		
			Minimum	15.2		
			Maximum	23.7		
		OA	Mean	17.449	.2269	10.8029
			Median	17.000		
			Variance	3.553		
			Std. Deviation	1.8850		
			Minimum	14.2		
			Maximum	23.2		
Bd	CH	Mean	27.977	.3130	9.4281	
		Median	27.900			
		Variance	6.957			
		Std. Deviation	2.6377			
		Minimum	22.4			
		Maximum	34.9			
	OA	Mean	26.277	.3389	10.7124	
		Median	26.000			
		Variance	7.924			
		Std. Deviation	2.8149			
		Minimum	20.6			
		Maximum	32.9			
GL	CH	Mean	231.069	2.4197	7.9752	
		Median	231.250			
		Variance	339.600			

Descriptives						
			Std. Deviation	18.4283		
			Minimum	188.7		
			Maximum	274.2		
		OA	Mean	203.117	2.8520	10.1253
			Median	200.150		
			Variance	422.976		
			Std. Deviation	20.5664		
			Minimum	171.4		
			Maximum	264.3		
	SD	CH	Mean	15.885	.2451	13.0028
			Median	15.500		
			Variance	4.266		
			Std. Deviation	2.0655		
			Minimum	12.7		
			Maximum	22.1		
		OA	Mean	14.910	.2213	12.2374
			Median	14.800		
			Variance	3.329		
			Std. Deviation	1.8246		
			Minimum	11.5		
			Maximum	19.1		

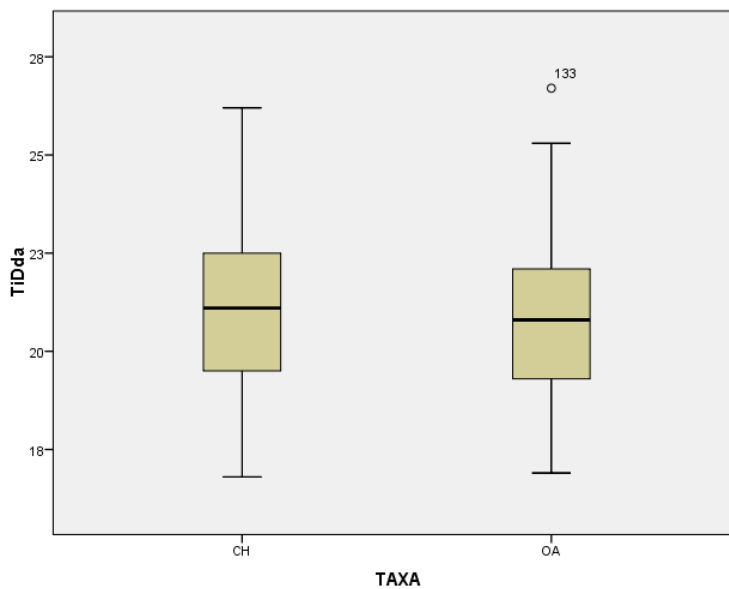


Figure A3.0.52 Tibia. Box plot for the modern sample of goat (CH) and sheep (OA) for measurement Dda.

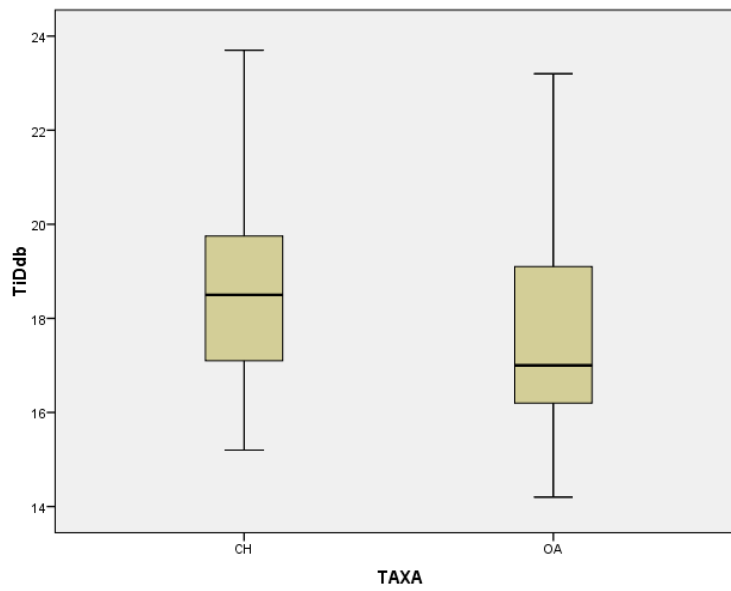


Figure A3.0.53 Tibia. Box plot for the modern sample of goat (CH) and sheep (OA) for measurement Ddb.

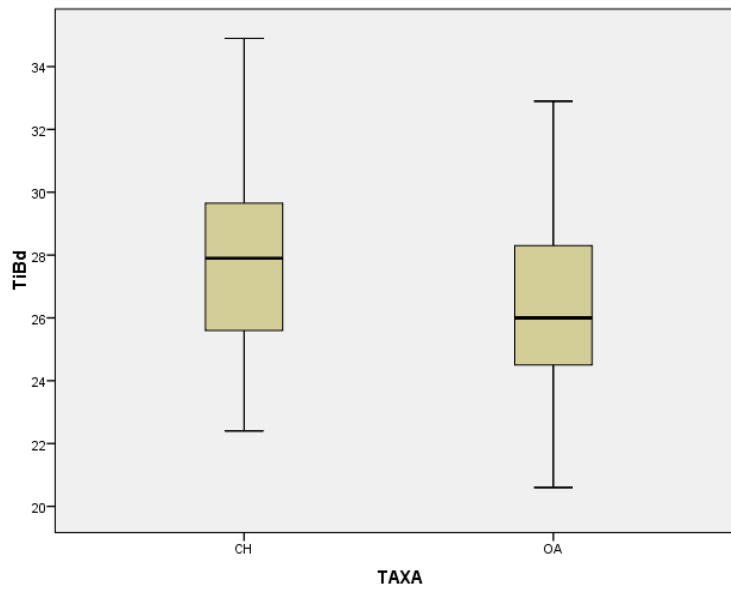


Figure A3.0.54 Tibia. Box plot for the modern sample of goat (CH) and sheep (OA) for measurement Bd.

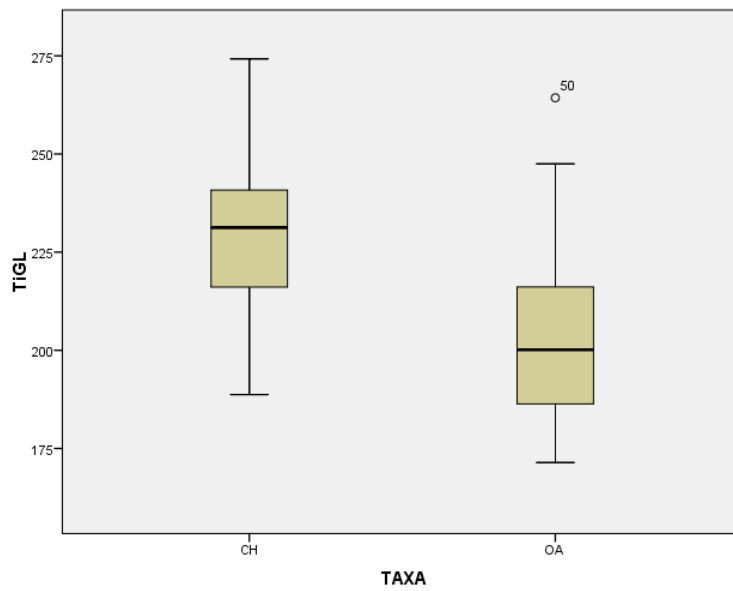


Figure A3.0.55 Tibia. Box plot for the modern sample of goat (CH) and sheep (OA) for measurement GL.

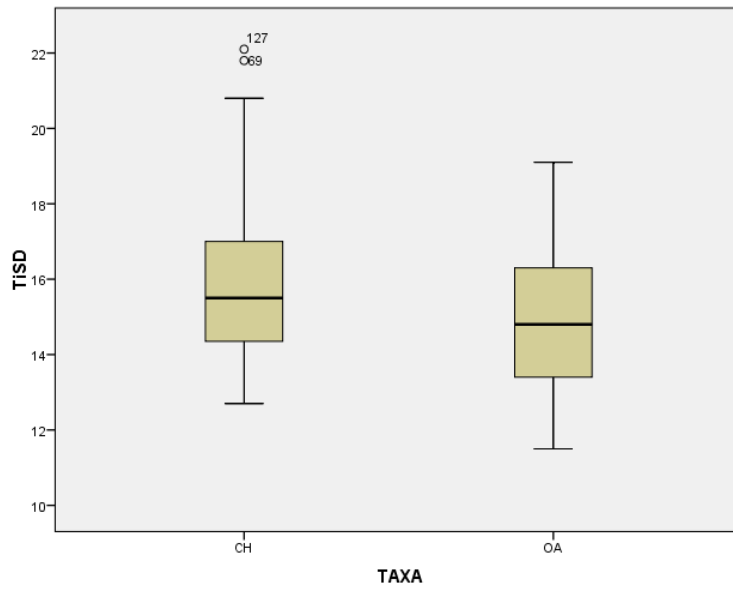


Figure A3.0.56 Tibia. Box plot for the modern sample of goat (CH) and sheep (OA) for measurement SD.

Astragalus

Table A3.17 Summary of the sheep and goat modern specimens for each measurement taken on the astragalus processed by SPSS.

Case Processing Summary							
	TAXA	Cases					
		Valid		Missing		Total	
		N	Percent	N	Percent	N	Percent
TaBd	CH	72	91.1%	7	8.9%	79	100.0%
	OA	73	93.6%	5	6.4%	78	100.0%
TaGLm	CH	72	91.1%	7	8.9%	79	100.0%
	OA	73	93.6%	5	6.4%	78	100.0%
TaGLI	CH	72	91.1%	7	8.9%	79	100.0%
	OA	73	93.6%	5	6.4%	78	100.0%
TaDm	CH	72	91.1%	7	8.9%	79	100.0%
	OA	73	93.6%	5	6.4%	78	100.0%
TaDI	CH	72	91.1%	7	8.9%	79	100.0%
	OA	73	93.6%	5	6.4%	78	100.0%
TaH	CH	72	91.1%	7	8.9%	79	100.0%
	OA	73	93.6%	5	6.4%	78	100.0%
TaBpT	CH	72	91.1%	7	8.9%	79	100.0%
	OA	73	93.6%	5	6.4%	78	100.0%

Table A3.18 Descriptive statistics for the modern goat (CH) and sheep (OA) for each measurement taken on the astragalus.

Descriptives						
Element	Measurement	TAXA	Statistics		Std. Error	CV
Ta	Bd	CH	Mean	19.644	.2187	9.4461
			Median	19.700		
			Variance	3.443		
			Std. Deviation	1.8556		
			Minimum	15.9		
			Maximum	24.6		
		OA	Mean	18.596	.2297	10.5560
			Median	18.900		
			Variance	3.853		
			Std. Deviation	1.9630		
			Minimum	14.5		
			Maximum	22.9		
	GLm	CH	Mean	29.304	.3175	9.1922
			Median	29.300		
Variance			7.256			
Std. Deviation			2.6937			

Descriptives						
		OA	Minimum	21.0		
			Maximum	34.2		
			Mean	26.651	.3197	10.2495
			Median	26.400		
			Variance	7.461		
			Std. Deviation	2.7316		
			Minimum	21.6		
			Maximum	34.9		
	GLI	CH	Mean	31.397	.3327	8.9922
			Median	31.400		
			Variance	7.971		
			Std. Deviation	2.8233		
			Minimum	23.7		
			Maximum	37.5		
		OA	Mean	28.048	.3523	10.7319
			Median	27.900		
			Variance	9.061		
			Std. Deviation	3.0101		
			Minimum	22.3		
			Maximum	36.8		
	Dm	CH	Mean	17.997	.2009	9.4715
			Median	18.050		
			Variance	2.906		
			Std. Deviation	1.7046		
			Minimum	13.8		
			Maximum	22.7		
		OA	Mean	17.018	.2210	11.0935
			Median	16.900		
Variance			3.564			
Std. Deviation			1.8879			
Minimum			13.8			
Maximum			22.8			
DI	CH	Mean	16.450	.1851	9.5489	
		Median	16.400			
		Variance	2.467			
		Std. Deviation	1.5708			
		Minimum	13.2			
		Maximum	20.8			
	OA	Mean	15.588	.1946	10.6633	
		Median	15.400			
		Variance	2.763			
		Std. Deviation	1.6622			
		Minimum	12.6			

Descriptives						
	H	CH	Maximum	20.5		
			Mean	25.597	.2784	9.2272
			Median	25.600		
			Variance	5.579		
			Std. Deviation	2.3619		
			Minimum	18.6		
		OA	Maximum	30.4		
			Mean	22.641	.2794	10.5445
			Median	22.400		
			Variance	5.700		
			Std. Deviation	2.3874		
			Minimum	18.3		
	BpT	CH	Maximum	30.3		
			Mean	14.081	.1390	8.3786
			Median	14.050		
			Variance	1.392		
			Std. Deviation	1.1798		
			Minimum	11.9		
		OA	Maximum	16.7		
			Mean	12.771	.1640	10.9686
			Median	12.600		
			Variance	1.962		
			Std. Deviation	1.4008		
			Minimum	10.2		
			Maximum	16.7		

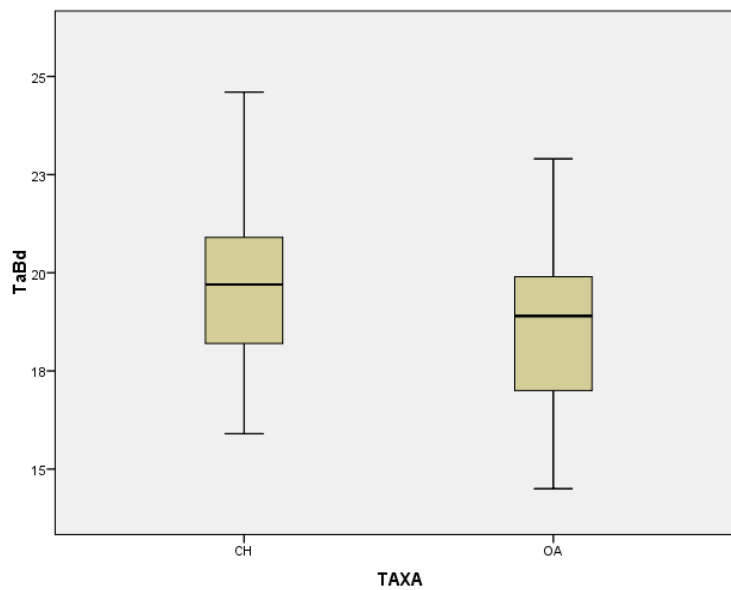


Figure A3.0.57 Astragalus. Box plot for the modern sample of goat (CH) and sheep (OA) for measurement Bd.

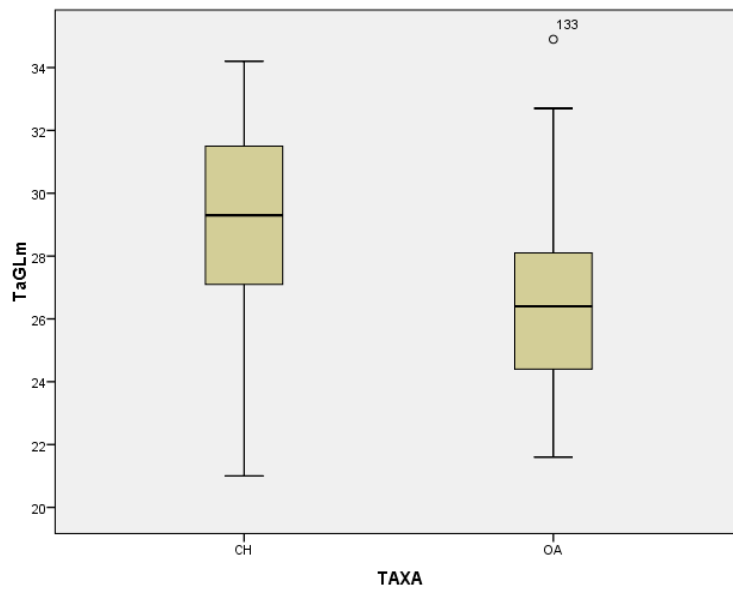


Figure A3.0.58 Astragalus. Box plot for the modern sample of goat (CH) and sheep (OA) for measurement GLm.

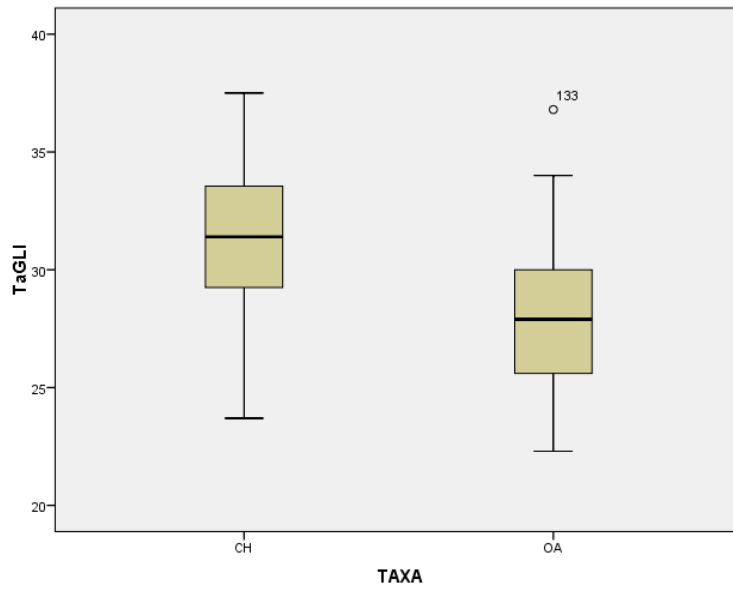


Figure A3.0.59 Astragalus. Box plot for the modern sample of goat (CH) and sheep (OA) for measurement GLI.

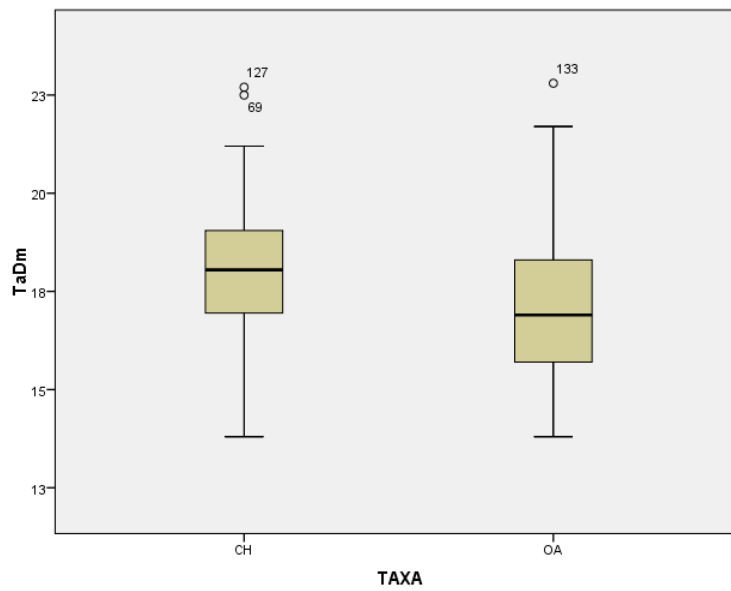


Figure A3.0.60 Astragalus. Box plot for the modern sample of goat (CH) and sheep (OA) for measurement D.

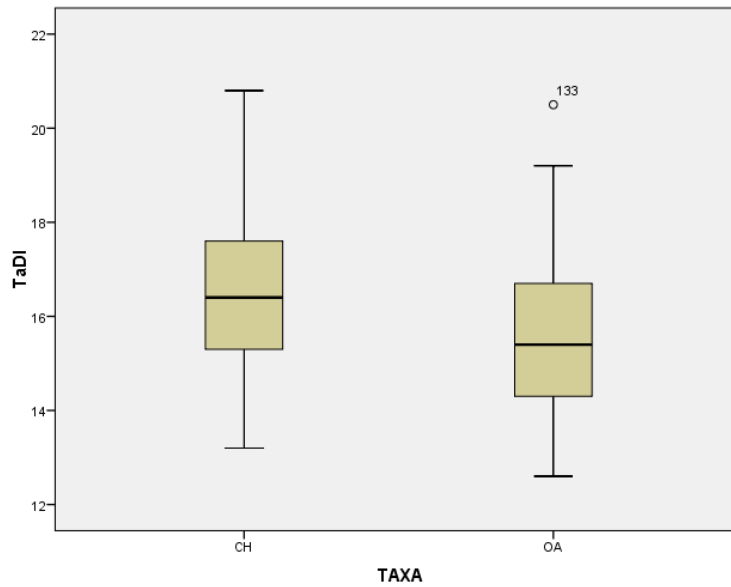


Figure A3.0.61 Astragalus. Box plot for the modern sample of goat (CH) and sheep (OA) for measurement DI.

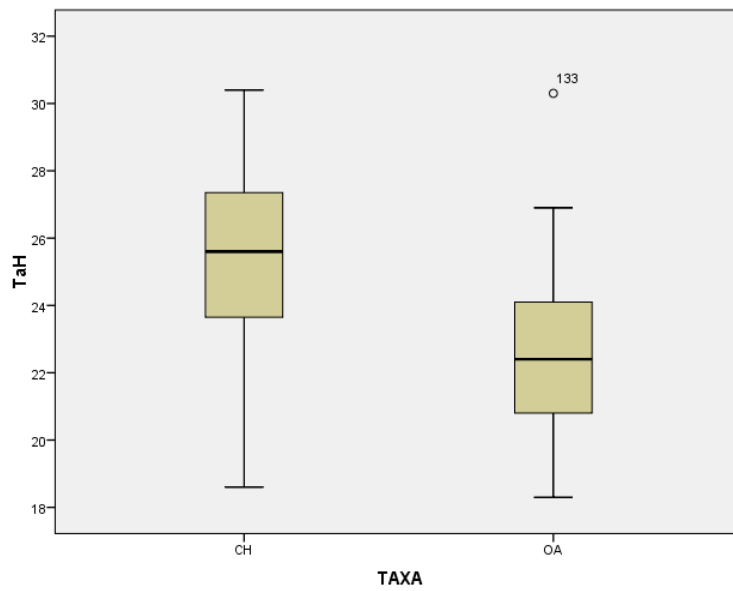


Figure A3.0.62 Astragalus. Box plot for the modern sample of goat (CH) and sheep (OA) for measurement H.

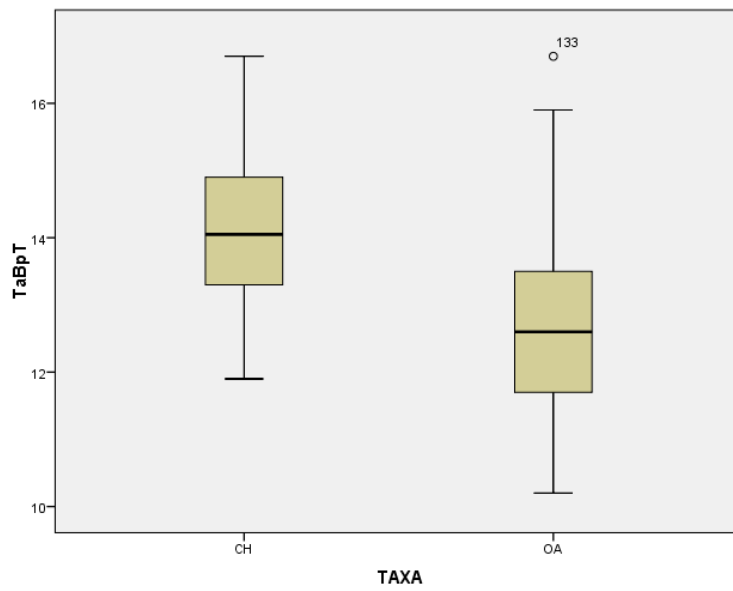


Figure A3.0.63 Astragalus. Box plot for the modern sample of goat (CH) and sheep (OA) for measurement BpT.

Calcaneus

Table A3.19 Summary of the sheep and goat modern specimens for each measurement taken on the calcaneus processed by SPSS.

Case Processing Summary							
	TAXA	Cases					
		Valid		Missing		Total	
		N	Percent	N	Percent	N	Percent
CcSB	CH	60	75.9%	19	24.1%	79	100.0%
	OA	62	79.5%	16	20.5%	78	100.0%
CcGL	CH	60	75.9%	19	24.1%	79	100.0%
	OA	62	79.5%	16	20.5%	78	100.0%
Ccc	CH	60	75.9%	19	24.1%	79	100.0%
	OA	62	79.5%	16	20.5%	78	100.0%
Ccd	CH	60	75.9%	19	24.1%	79	100.0%
	OA	62	79.5%	16	20.5%	78	100.0%
CcB	CH	60	75.9%	19	24.1%	79	100.0%
	OA	62	79.5%	16	20.5%	78	100.0%
CcDS	CH	60	75.9%	19	24.1%	79	100.0%
	OA	62	79.5%	16	20.5%	78	100.0%
CcGd	CH	60	75.9%	19	24.1%	79	100.0%
	OA	62	79.5%	16	20.5%	78	100.0%

Table A3.20 Descriptive statistics for the modern goat (CH) and sheep (OA) for each measurement taken on the calcaneum.

Descriptives						
Element	Measurement	TAXA	Statistics		Std. Error	CV
Cc	SB	CH	Mean	17.707	.2230	9.7532
			Median	17.450		
			Variance	2.983		
			Std. Deviation	1.7270		
			Minimum	15.0		
			Maximum	22.8		
		OA	Mean	16.160	.2156	10.5068
			Median	15.800		
			Variance	2.883		
			Std. Deviation	1.6979		
			Minimum	12.9		
			Maximum	20.4		
	GL	CH	Mean	63.730	.7388	8.9802
			Median	62.600		
Variance			32.753			
Std. Deviation			5.7231			

Descriptives						
		OA	Minimum	52.5		
			Maximum	76.6		
			Mean	56.239	.7408	10.3725
			Median	56.100		
			Variance	34.028		
			Std. Deviation	5.8334		
			Minimum	45.8		
			Maximum	70.4		
	c	CH	Mean	12.408	.1609	10.0467
			Median	12.300		
			Variance	1.554		
			Std. Deviation	1.2466		
			Minimum	9.9		
			Maximum	15.7		
		OA	Mean	13.052	.1980	11.9468
			Median	12.950		
			Variance	2.431		
			Std. Deviation	1.5593		
			Minimum	10.3		
			Maximum	16.4		
	d	CH	Mean	24.223	.2712	8.6731
			Median	24.000		
			Variance	4.414		
			Std. Deviation	2.1009		
			Minimum	19.3		
			Maximum	29.9		
		OA	Mean	22.353	.3136	11.0468
			Median	22.300		
Variance			6.097			
Std. Deviation			2.4693			
Minimum			17.6			
Maximum			29.0			
B	CH	Mean	6.798	.0942	10.7296	
		Median	6.700			
		Variance	.532			
		Std. Deviation	.7294			
		Minimum	5.5			
		Maximum	9.1			
	OA	Mean	6.166	.1054	13.4544	
		Median	6.100			
		Variance	.688			
		Std. Deviation	.8296			
		Minimum	4.6			

Descriptives						
	DS	CH	Maximum	8.8		
			Mean	19.678	.2520	9.9186
			Median	19.350		
			Variance	3.810		
			Std. Deviation	1.9518		
			Minimum	15.6		
		OA	Maximum	24.3		
			Mean	18.465	.2686	11.4524
			Median	18.150		
			Variance	4.472		
	Gd	CH	Maximum	24.4		
			Mean	24.433	.2632	8.3428
			Median	24.400		
			Variance	4.155		
			Std. Deviation	2.0384		
			Minimum	20.1		
		OA	Maximum	28.3		
			Mean	22.247	.3144	11.1282
			Median	21.750		
			Variance	6.129		
			Std. Deviation	2.4757		
			Minimum	17.6		
			Maximum	28.6		

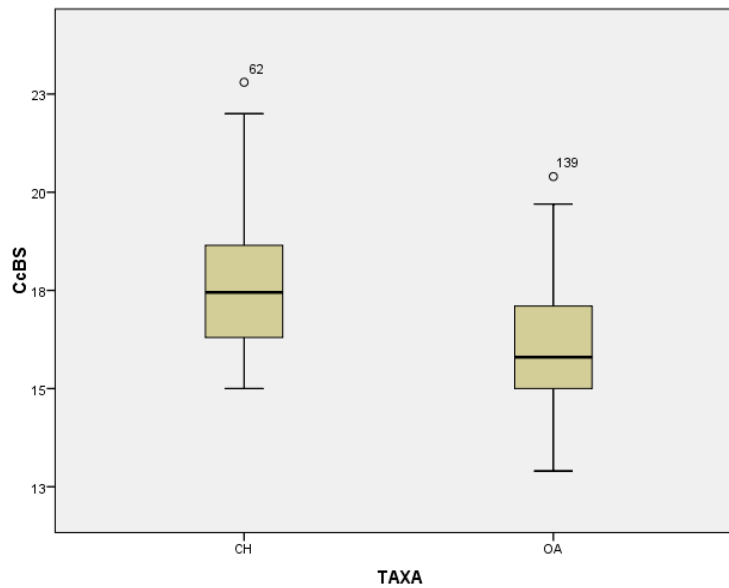


Figure A3.0.64 Calcaneum. Box plot for the modern sample of goat (CH) and sheep (OA) for measurement BS.

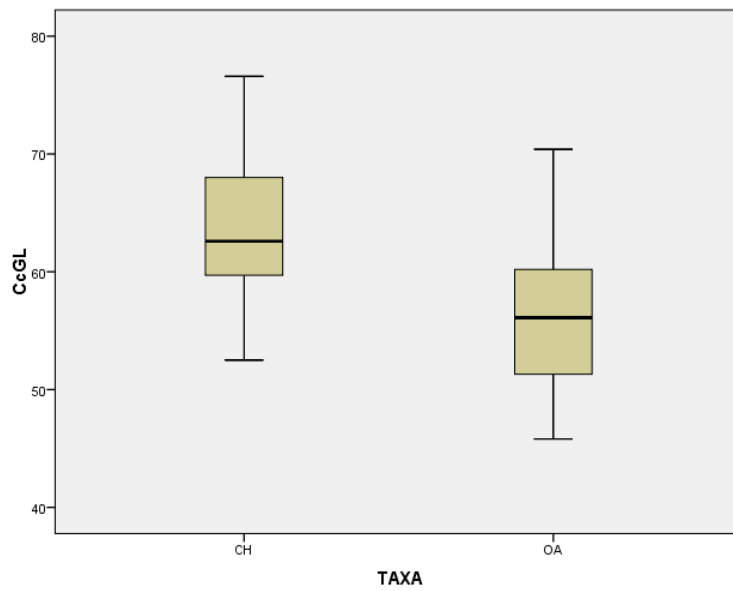


Figure A3.0.65 Calcaneum. Box plot for the modern sample of goat (CH) and sheep (OA) for measurement GL.

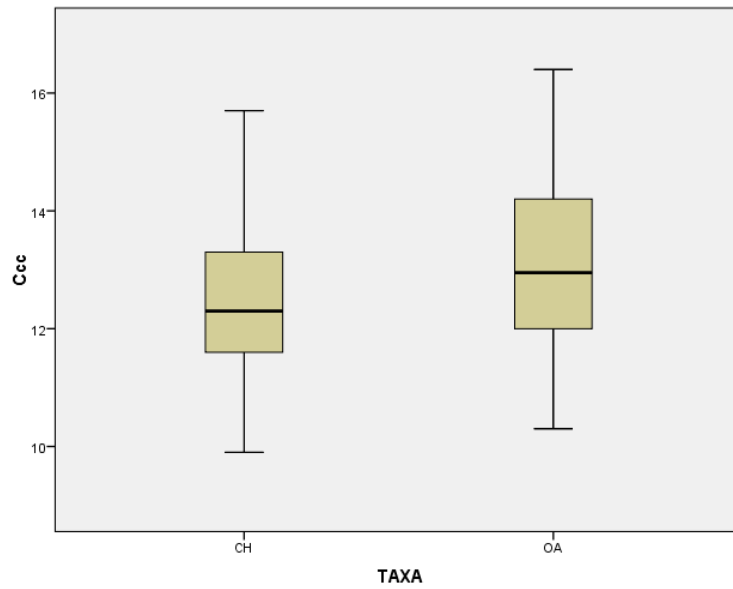


Figure A3.0.66 Calcaneum. Box plot for the modern sample of goat (CH) and sheep (OA) for measurement c.

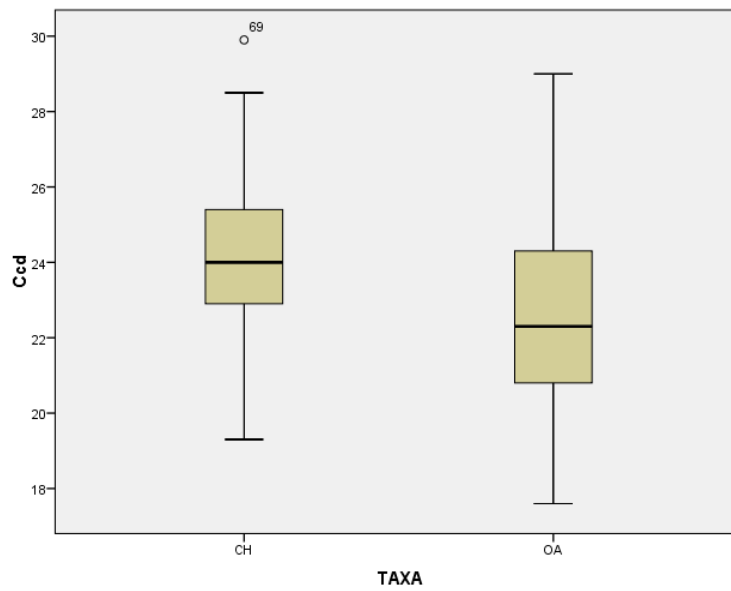


Figure A3.0.67 Calcaneum. Box plot for the modern sample of goat (CH) and sheep (OA) for measurement d.

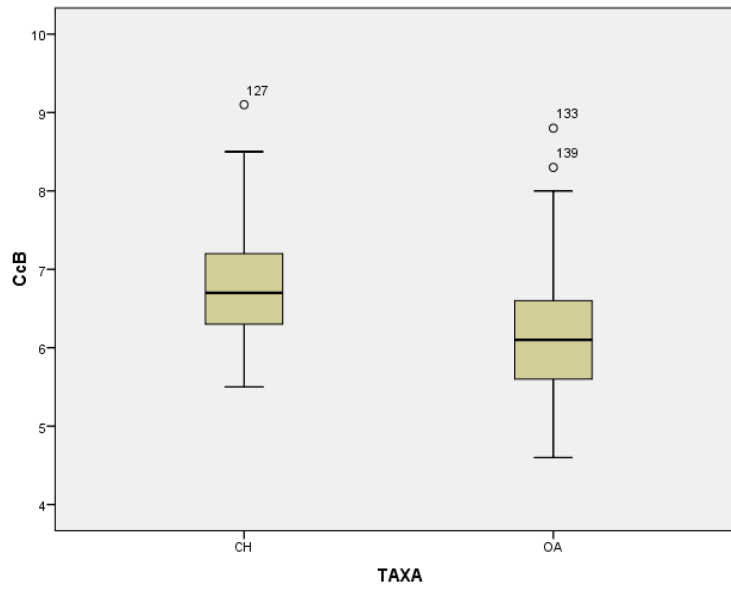


Figure A3.0.68 Calcaneum. Box plot for the modern sample of goat (CH) and sheep (OA) for measurement B.

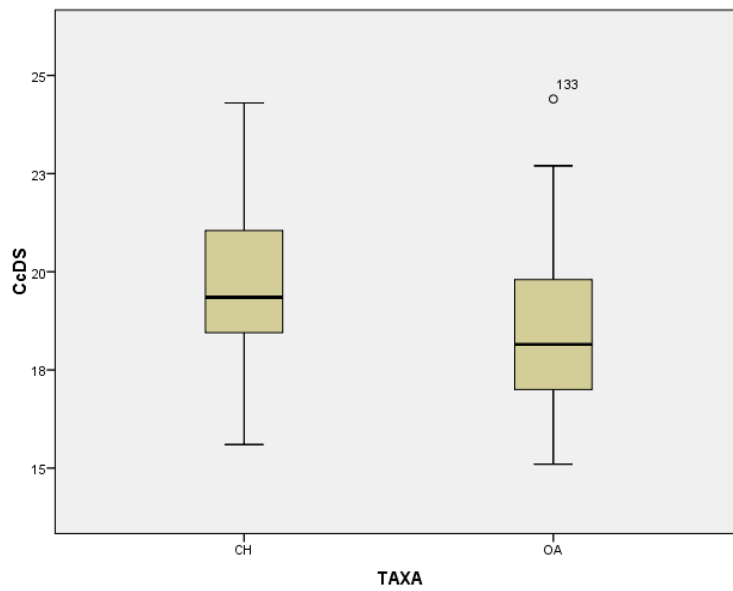


Figure A3.0.69 Calcaneum. Box plot for the modern sample of goat (CH) and sheep (OA) for measurement DS.

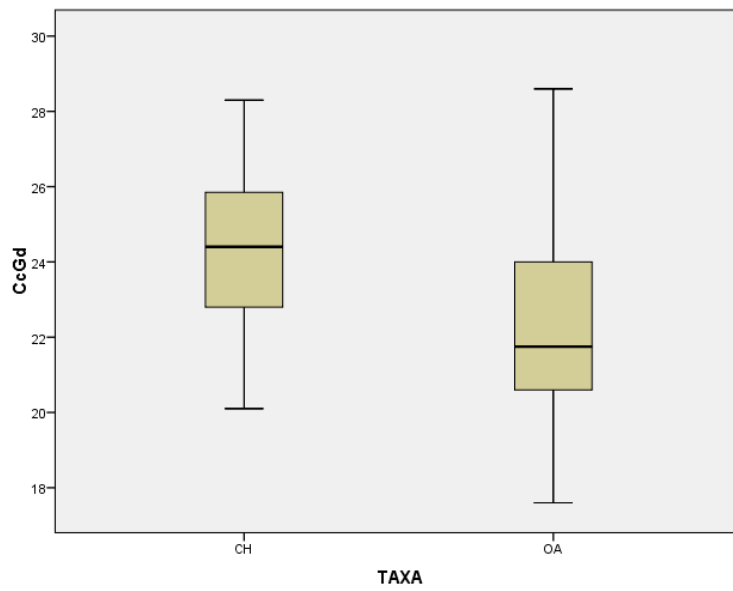


Figure A3.0.70 Calcaneum. Box plot for the modern sample of goat (CH) and sheep (OA) for measurement Gd.

Phalanx 3

Table A3.21 Summary of the sheep and goat modern specimens for each measurement taken on the 3rd phalanx processed by SPSS.

Case Processing Summary							
	TAXA	Cases					
		Valid		Missing		Total	
		N	Percent	N	Percent	N	Percent
Ph3DLS	CH	64	81.0%	15	19.0%	79	100.0%
	OA	69	88.5%	9	11.5%	78	100.0%
Ph3MBS	CH	65	82.3%	14	17.7%	79	100.0%
	OA	69	88.5%	9	11.5%	78	100.0%

Table A3.22 Descriptive statistics for the modern goat (CH) and sheep (OA) for each measurement taken on the 3rd phalanx.

Descriptives						
Element	Measurement	TAXA	Statistics		Std. Error	CV
Ph3	DLS	CH	Mean	33.067	.4897	11.8477
			Median	32.900		
			Variance	15.349		
			Std. Deviation	3.9177		
			Minimum	25.6		
			Maximum	42.2		
		OA	Mean	27.251	.3018	9.1981
			Median	27.200		
			Variance	6.283		
			Std. Deviation	2.5066		
			Minimum	20.8		
			Maximum	33.1		
	MBS	CH	Mean	6.018	.1103	14.6299
			Median	5.800		
Variance			.791			
Std. Deviation			.8895			
Minimum			4.4			
Maximum			8.3			
OA		Mean	6.157	.0885	11.9360	
		Median	6.100			
		Variance	.540			
		Std. Deviation	.7349			
		Minimum	4.2			
		Maximum	8.8			

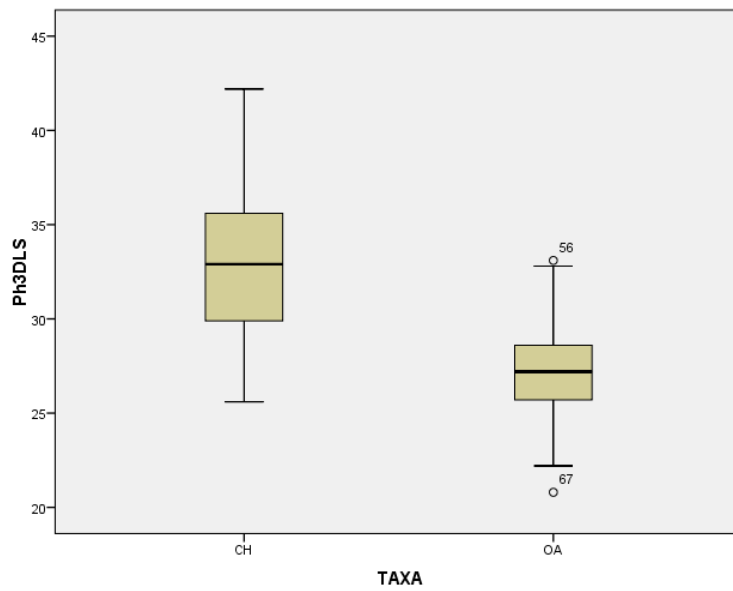


Figure A3.0.71 3rd phalanx. Box plot for the modern sample of goat (CH) and sheep (OA) for measurement DLS.

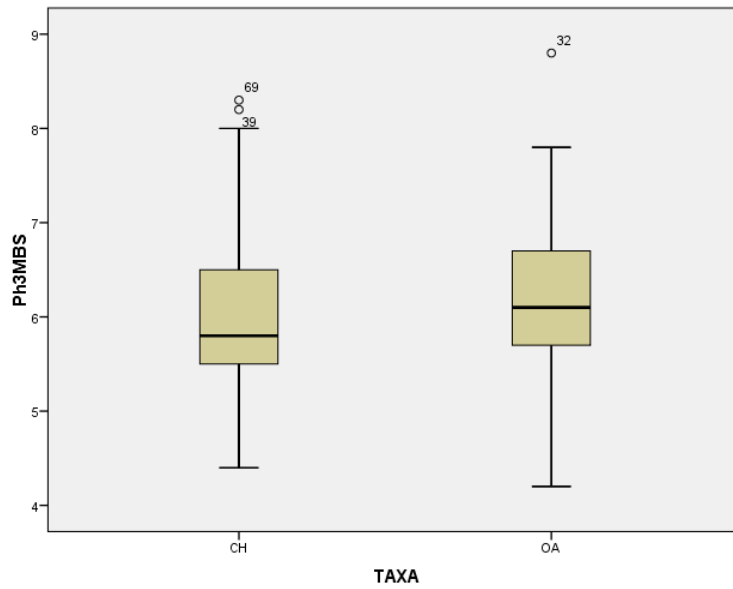


Figure A3.0.72 3rd phalanx. Box plot for the modern sample of goat (CH) and sheep (OA) for measurement MBS.

Appendix IV: Assumptions for Discriminant Analysis and Principal Component Analysis

Before running Discriminant Analysis and Principal Component Analysis, the assumptions of the tests as suggested by Field (2009) and Tabachnick and Fidell (2007) have been considered and, as a consequence, the data have been screened. For the Discriminant Analysis the most important assumptions are the following (as in MANOVA, Tabachnick and Fidell 2007: 381):

- multivariate normality: the assumption is that scores on predictors are independently and randomly sampled from a population and that the sampling distribution of any linear combination of predictors is normally distributed (Tabachnick and Fidell 2007: 382);
- absence of outliers: DA is highly sensitive to the inclusion of outliers (a case with an extreme value on one variable or an unusual combination of scores on two or more variables. Tabachnick and Fidell 2007: 72). Outliers can bias statistics such as the mean, as a consequence, eliminating or transforming the outliers is suggested (Tabachnick and Fidell 2007: 382);
- homogeneity of variance-covariance matrices: this assumption assumes that variances for each dependent variable are the same across groups and that the relationships (covariances) between these dependent variables are roughly equal (Field 2009: 787). As when DA is used for classification purposes the cases tend to be over assigned to the groups with a greater dispersion, the assumption of equality of within-group variance-covariance (dispersion) must be respected (Tabachnick and Fidell 2007: 382-383);
- linearity: DA assumes linear relationships (a model which is based upon a straight line; Field 2007: 789) among all pairs of predictors within each group (Tabachnick and Fidell 2007: 383);
- absence of multicollinearity and singularity: multicollinearity is a situation in which two or more variable are very closely linearly related (Field 2009: 790) while singularity is the term used to describe two variables that are perfectly correlated (Field 2009: 793)

For Principal Component Analysis, the assumptions are:

- sample size: correlation coefficients tend to be less reliable when estimated from small samples, as a consequence, it is important to have an adequate sample size (a guide of sample sizes is given by Comrey and Lee (1992) in Tabachnick and Fidell 2007: 613) for the correlations to be reliably estimated (Tabachnick and Fidell 2007: 613);
- multivariate normality: see above;

- linearity: see above;
- absence of outlier among cases: see above;
- absence of outlier and variables: a variable with a low squared multiple correlation with all other variables and low correlation with all important factors is an outlier among the variables (Tabachnick and Fidell 2007: 615);
- absence of multicollinearity and singularity: see above. Multicollinearity in PCA is not a problem but linearity or extreme multicollinearity is (Tabachnick and Fidell 2007: 614);
- factorability of R : a matrix that is factorable should include several sizable correlations; if no correlation exceed 0.30 the use of PCA is questionable (Tabachnick and Fidell 2007: 614).

Appendix V: Principal Component Analysis: Brief Glossary

Variable: anything that can be measured and can vary across time and entities (Field 2009:795).

Variance: estimate average of the variability or spread of a data set (Field 2009: 796).

Factor/Component: in PCA is an underlying dimension which aspects could be measured by clusters of large correlation coefficients between subsets variables. These clusters can be seen on the correlation matrix (Field 2009: 631). In PCA there are as many components/factors extracted as the variables put into it.

Factor/Component loading (score): in this case Pearson correlation between a factor and a variable; it expresses the relative contribution of a variable to a factor/component (Field 2009: 631).

Matrix: is a group of numbers arranged in columns and rows; the values within it refers to as components or elements. The identity matrix occurred when on a square matrix (same number of rows and columns), the diagonal elements are equal to 1 and the off-diagonal are equal to 0 and it attests the complete independency (or very low correlation) between the variables. It is important in PCA that the matrix is not an identity matrix because the correlation between the variables has to be not too high and not too low for the analysis to be reliable (Field 2009: 647).

KMO: is a sample adequacy test which assesses the adequacy of the sample size; it varies between 0 and 1 so that if the value is close to 0, it attests diffusion in the pattern of correlation (association or relationship between two variables), namely that factor analysis is likely to be inappropriate (Tabachnick and Fidell 2007: 614; Field 2009: 788). If the value is close to 1, it indicates that the pattern of correlation is relatively compact, as a consequence factor analysis could be reliable. As this test is highly dependent on sample size, the solution suggested when a low KMO occurs, is to collect more data (Field 2009: 660).

Bartlett's Test: it measures the null hypothesis that the correlation matrix is an identity matrix. An identity matrix is matrix in which all of the diagonal elements are 1 and all off diagonal elements are 0. This null hypothesis has to be rejected so the results from Bartlett's Test has to be significant which means that p has to be $< .001$. As seen for the matrix, it is important in PCA that the matrix is not an identity matrix (Field 2009: 781; Tabachnick and Fidell 2007: 307).

Rotation: once factors are extracted, it is possible to see to what degree variables load to these factors. Rotation permits to discriminate between factors: as a factor is a classification axis along which variables can be plotted, rotation rotates this axes so that variables are loaded maximally to only one factor and minimized on to the remaining factors. There are two type of rotation, orthogonal, with which factors are kept unrelated, and oblique rotation, with which factors are allowed to correlate (Field 2009: 642; Tabachnick and Fidell 2007: 620). Among the

different options given by SPSS for the orthogonal rotation, the varimax is the most commonly used. It is a variance maximizing procedure which means that it maximises the variance of factor loadings by making high loadings higher and low ones lower for each factor (Tabachnick and Fidell 2007: 620).

Appendix VI: Discriminant Analysis: how to use it to predict new archaeological cases

As Discriminant Analysis (DA) provided better results on the modern material than Principal Component Analysis (PCA), it was decided to use this statistical tool on the sheep/goat assemblage from King's Lynn. This was carried out in order to see if this alternative method could provide further insight in the distinction between sheep and goat.

During the predicting process, SPSS attributes an individual score to each of the new archaeological cases. This score represents the distance of that specimen from the group centroid value for each modern group (i.e. group means of the predictor variables; Field 2009: 620). As a consequence, the program itself will reattribute to species level (prediction) the archaeological specimens on the basis of their individual scores; the group to which the new cases will be attributed is the one from which their distance is smallest (Burns and Burns 2008).

This tool, if shown to provide high reattribution percentages, as it evaluates all metric variables at the same time, has the potential to support or contradict the identifications based on the morphological approach. In addition, it represents an additional aid for attributing the unidentified specimens to species level. Finally it represents a means to predict statistically the taxa of new specimens.

The procedure will be explained step by step, in order to facilitate application by other researchers.

Step one: enter the archaeological data in the same database as the modern material data. (NB the number of measurements/variables must be the same for both datasets). While all metric variables in the database must be 'Numerical', the variable 'Taxa' for each case must be entered as a 'Nominal' variable, e.g. 1= goat and 2 = sheep. When in 'Variable view', by clicking on the field 'Values' a new window will appear and you will be able to input the number associated with the two species. Click then on the field 'Measure' and select 'Nominal'.

Step two: a new variable should be added and categorised as 'Nominal'. This will distinguish the modern cases - which will be used to create the predicting equation - and the archaeological cases - which will have to be assigned to one of the two groups. In 'Variable view', under the field 'Measure', click on 'Nominal'. Click on the field 'Values' and a new window will appear where to specify the values which will represent the two samples; in this case 0= modern material and 1= archaeological material. In this way SPSS will know which is the sample to be used as the model and which are the new cases it will have to attribute (Fig. 3.123).

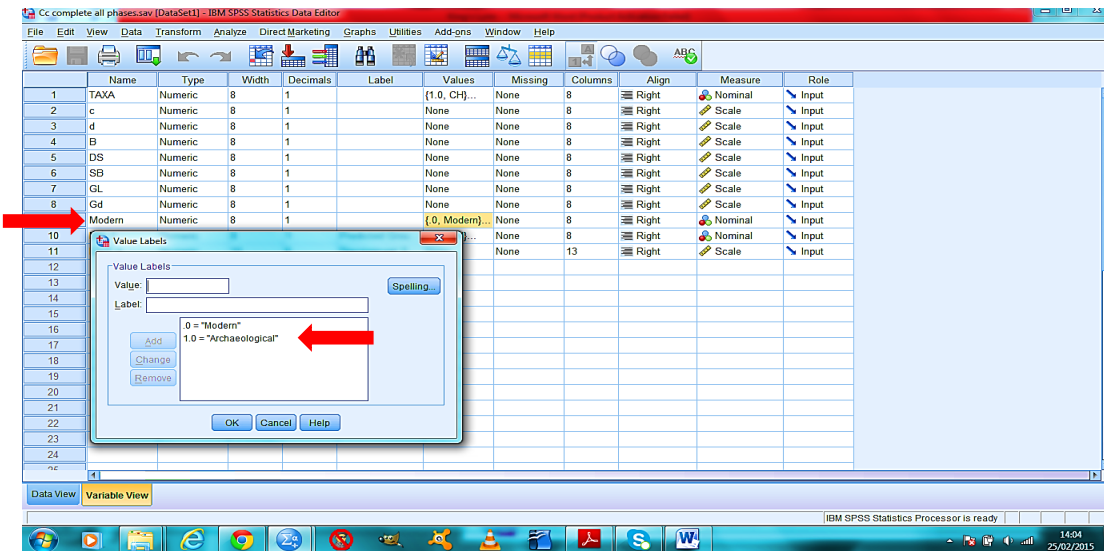


Figure A6.0.1 SPSS in 'Variable view'. When the field 'Values' is chosen, a new window appears in which the numbers corresponding to the samples - in this case 0 = modern material and 1 = archaeological material- can be input. The new variable has to be 'Nominal' as the field 'Measure' shows.

Step three: in 'Data view' click on 'Analyse', 'Classify' and choose 'Discriminant' (Fig. 3.124). A new window will appear in which, as a 'Grouping Variable', the variable 'Taxa' must be selected. Remember to specify, by clicking on 'Define Range', the two species present in the sample, in this case 1 = goat and 2 = sheep (Fig. 3.125).

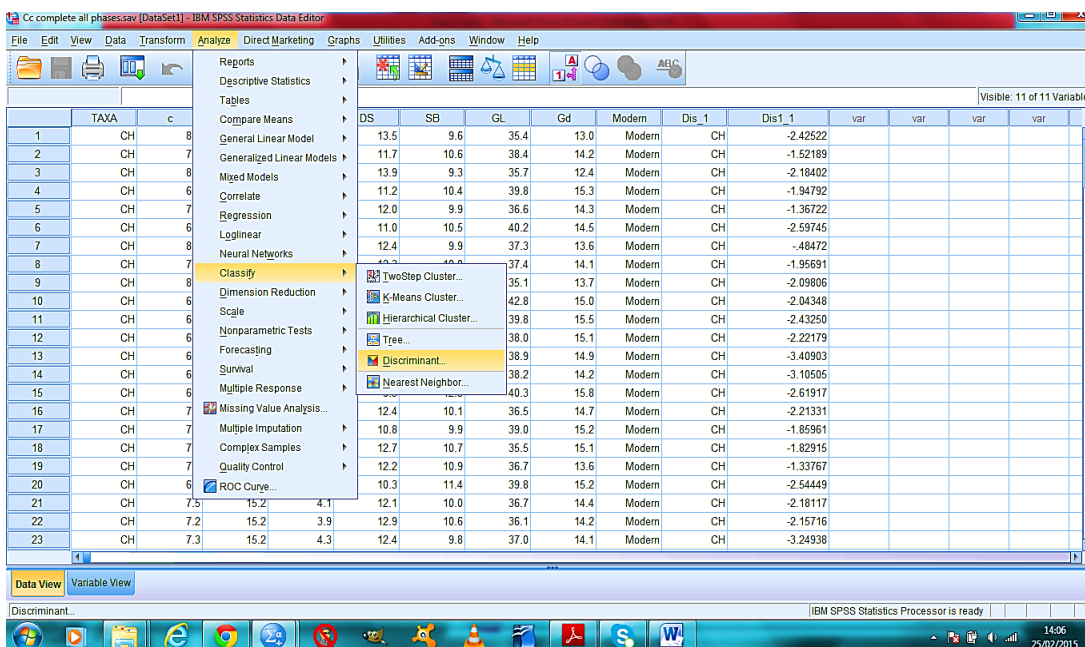


Figure A6.0.2 SPSS in 'Data View'. How to choose and start running a Discriminant Analysis.

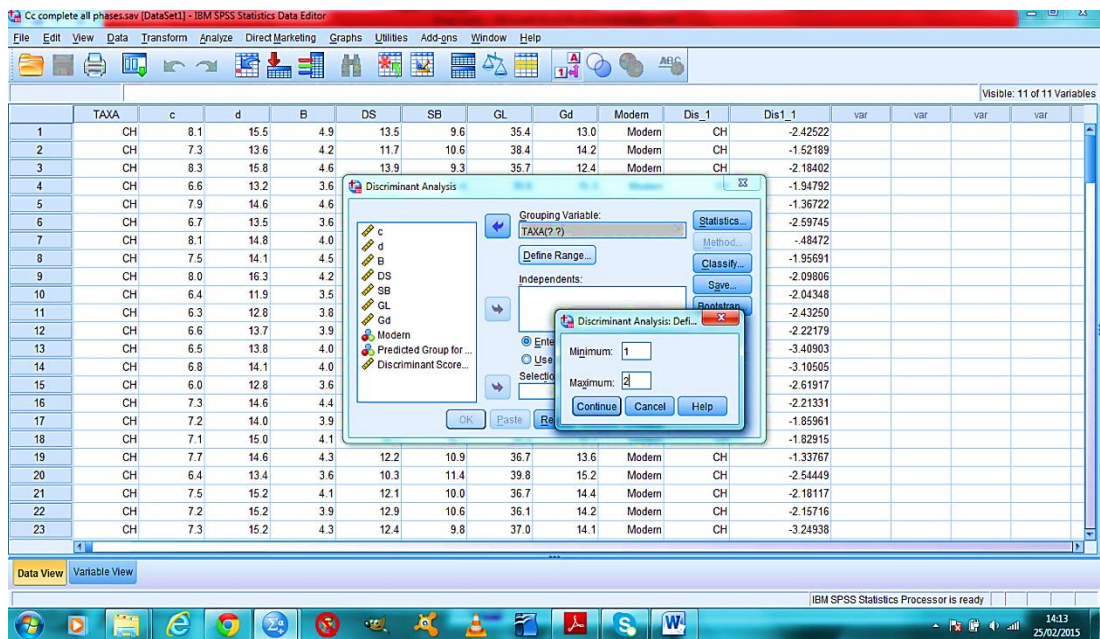


Figure A6.0.3 SPSS in 'Data view'. By clicking on 'Define range' a new window appears where to define the different groups- 1=goat and 2= sheep for the grouping variable 'Taxa'.

Step four: indicate which are the 'Independent Variables', in this case, the measurements we want the program to consider. In the field 'Selection Variable', insert the name given to the new variable we created earlier (Step 2) which discriminates the modern from the archaeological material. Click on 'Value' and type the number chosen as representing the modern material (in this case 0; see Fig. 3.126).

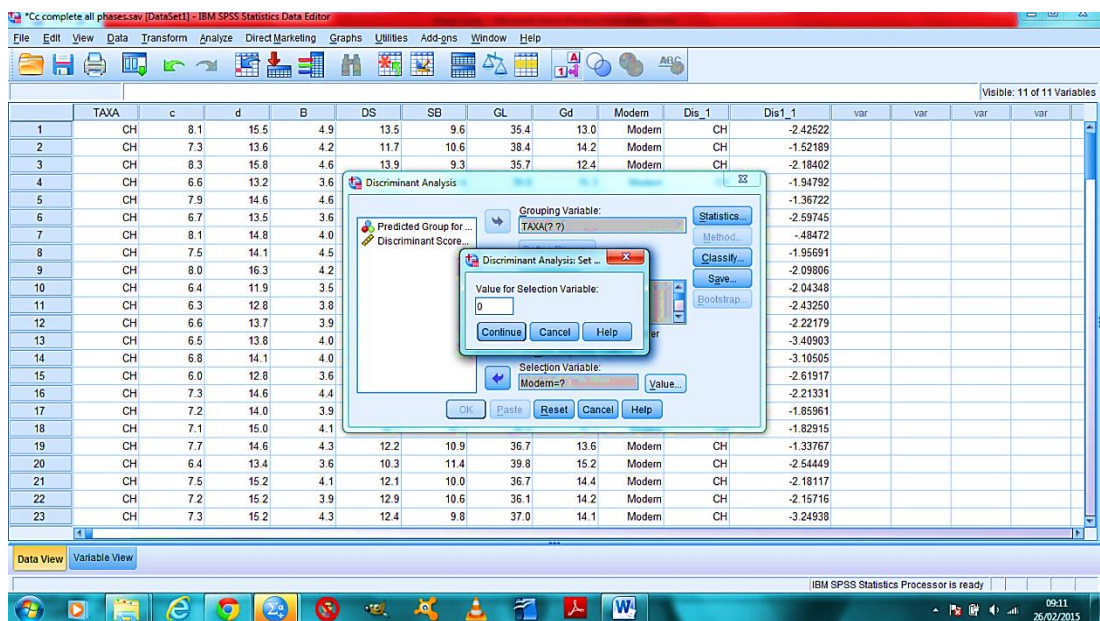


Figure A6.0.4 SPSS in 'Data View'. How to enter the value indicating the modern material when clicking on 'Selection variable'.

Step Five: click on ‘Save’ and tick ‘Predicted Group Membership’ and ‘Discriminant Scores’ so that SPSS will save the new individual score for each of the modern and archaeological cases and the group to which the cases were attributed according to the Discriminant Analysis (Fig. 3.127).

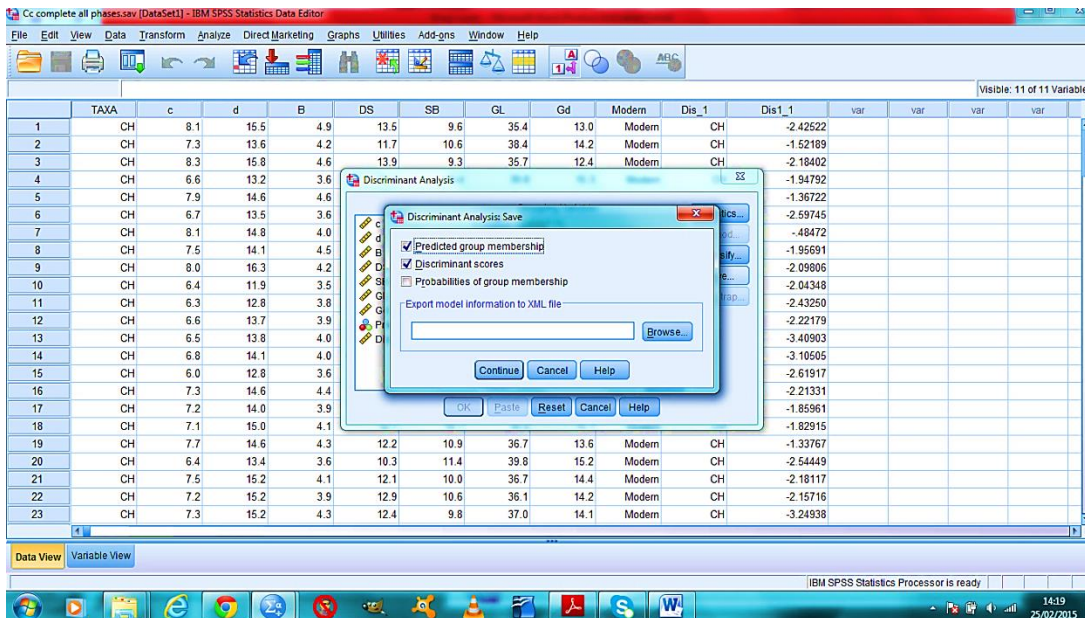


Figure A6.0.5 SPSS in ‘Data View’. Click on the ‘Save’ command and a new window will appear. Tick ‘predicted group Membership’ and ‘Discriminant Scores’.

Step six: you should now have two new columns on your database when in ‘Data View’; one indicating the group attributions the Discriminant Analysis has given to each of the cases in the data set and the other indicating the individual score for each case (Fig. 3.128).

	TAXA	c	d	B	DS	SB	GL	Gd	Modern	Dis_1	Dis1_1	var	var	var	var
1	CH	8.1	15.5	4.9	13.5	9.6	35.4	13.0	Modern	CH	-2.42522				
2	CH	7.3	13.6	4.2	11.7	10.6	38.4	14.2	Modern	CH	-1.52189				
3	CH	8.3	15.8	4.6	13.9	9.3	35.7	12.4	Modern	CH	-2.18402				
4	CH	6.6	13.2	3.6	11.2	10.4	39.8	15.3	Modern	CH	-1.94792				
5	CH	7.9	14.6	4.6	12.0	9.9	36.6	14.3	Modern	CH	-1.36722				
6	CH	6.7	13.5	3.6	11.0	10.5	40.2	14.5	Modern	CH	-2.59745				
7	CH	8.1	14.8	4.0	12.4	9.9	37.3	13.6	Modern	CH	-.48472				
8	CH	7.5	14.1	4.5	12.3	10.0	37.4	14.1	Modern	CH	-1.95691				
9	CH	8.0	16.3	4.2	13.1	9.6	35.1	13.7	Modern	CH	-2.09806				
10	CH	6.4	11.9	3.5	9.8	10.7	42.8	15.0	Modern	CH	-2.04348				
11	CH	6.3	12.8	3.8	10.9	10.9	39.8	15.5	Modern	CH	-2.43250				
12	CH	6.6	13.7	3.9	11.8	11.0	38.0	15.1	Modern	CH	-2.22179				
13	CH	6.5	13.8	4.0	11.2	10.7	38.9	14.9	Modern	CH	-3.40903				
14	CH	6.8	14.1	4.0	12.8	9.9	38.2	14.2	Modern	CH	-3.10505				
15	CH	6.0	12.8	3.6	9.3	12.3	40.3	15.8	Modern	CH	-2.61917				
16	CH	7.3	14.6	4.4	12.4	10.1	36.5	14.7	Modern	CH	-2.21331				
17	CH	7.2	14.0	3.9	10.8	9.9	39.0	15.2	Modern	CH	-1.85961				
18	CH	7.1	15.0	4.1	12.7	10.7	35.5	15.1	Modern	CH	-1.82915				
19	CH	7.7	14.6	4.3	12.2	10.9	36.7	13.6	Modern	CH	-1.33767				
20	CH	6.4	13.4	3.6	10.3	11.4	39.8	15.2	Modern	CH	-2.54449				
21	CH	7.5	15.2	4.1	12.1	10.0	36.7	14.4	Modern	CH	-2.18117				
22	CH	7.2	15.2	3.9	12.9	10.6	36.1	14.2	Modern	CH	-2.15716				
23	CH	7.3	15.2	4.3	12.4	9.8	37.0	14.1	Modern	CH	-3.24938				

Figure A6.0.6 SPSS in 'Data view'. Two new columns are now present on the database, one containing the new attribution for each case and the other containing the individual scores.